

Edited by Didier Astruc
Modern Arene Chemistry

Related Titles from WILEY-VCH

S. Kobayashi, K. A. Jørgensen (Eds.)

Cycloaddition Reactions in Organic Synthesis

XII, 332 pages

2001

Hardcover

ISBN 3-527-30159-3

N. Krause (Ed.)

Modern Organocopper Chemistry

XIV, 373 pages

2002

Hardcover

ISBN 3-527-29773-1

A. Ricci (Ed.)

Modern Amination Methods

XVIII, 267 pages

2000

Hardcover

ISBN 3-527-29976-9

F. Vögtle, J. F. Stoddart, M. Shibasaki (Eds.)

Stimulating Concepts in Chemistry

XVII, 396 pages

2000

Hardcover

ISBN 3-527-29978-5

Modern Arene Chemistry

Edited by Didier Astruc

 WILEY-VCH

Editor

Prof. Didier Astruc

LCOO, UMR CNRS N° 5802
Université Bordeaux I
33405 Talence Cedex
France

■ This book was carefully produced. Nevertheless, editor, authors and publisher do not warrant the information contained therein to be free of errors. Readers are advised to keep in mind that statements, data, illustrations, procedural details or other items may inadvertently be inaccurate.

Library of Congress Card No.: applied for

A catalogue record for this book is available from the British Library.

Die Deutsche Bibliothek – CIP Cataloguing-in-Publication-Data

A catalogue record for this publication is available from Die Deutsche Bibliothek

© 2002 Wiley-VCH Verlag GmbH & KGaA, Weinheim

All rights reserved (including those of translation in other languages). No part of this book may be reproduced in any form – by photoprinting, microfilm, or any other means – nor transmitted or translated into machine language without written permission from the publishers. Registered names, trademarks, etc. used in this book, even when not specifically marked as such, are not to be considered unprotected by law.

Printed in the Federal Republic of Germany.
Printed on acid-free paper.

Typesetting Asco Typesetters, Hong Kong

Printing Strauss Offsetdruck GmbH, Mörlenbach

Bookbinding J. Schäffer GmbH & Co. KG, Grünstadt

ISBN 3-527-30489-4

Contents

List of Contributors *xvi*

Arene Chemistry: From Historical Notes to the State of the Art 1

Didier Astruc

The History of Benzene 1

The History of Aromaticity 5

Some Key Trends Towards Modern Arene Chemistry 9

Aromatic Chemistry: From the 19th Century Industry to the State of the Art 11

Organization of the Book and Content 13

References 16

1 The Synthesis of Tris-Annulated Benzenes by Aldol Trimerization of Cyclic Ketones 20

Margaret M. Boorum and Lawrence T. Scott

Abstract 20

1.1 Introduction 20

1.2 Truxene and Truxone: Venerable Prototypes 21

1.3 Other Examples 23

1.4 Limitations 27

1.4.1 Experimental Observations and a Working Hypothesis 27

1.4.2 Guidance from Calculations 29

1.5 Conclusions 30

References 31

2 Oligounsaturated Five-Membered Carbocycles – Aromatic and Antiaromatic Compounds in the Same Family 32

Rainer Haag and Armin de Meijere

Abstract 32

2.1 Introduction 32

2.2 Cyclopentadienyl Cations 33

2.3 Fulvene and Spiroannelated Cyclopentadiene Derivatives 37

2.4	Polyunsaturated Di-, Tri-, and Oligoquinanes	38
2.4.1	Pentalene, Pentalenediide, and Pentalene Metal Complexes	39
2.4.2	Acepentalene, Acepentalenediide, and Acepentalene Metal Complexes	42
2.4.3	Generation of C ₂₀ -Fullerene	44
	References	50
3	The Suzuki Reaction with Arylboron Compounds in Arene Chemistry	53
	<i>Akira Suzuki</i>	
	Abstract	53
3.1	Introduction	53
3.2	Reactions with Aryl Halides and Triflates: Synthesis of Biaryls	54
3.2.1	Aromatic–Aromatic Coupling	54
3.2.2	Aromatic–Heteroaromatic and Heteroaromatic–Heteroaromatic Couplings	65
3.2.3	Coupling of Arylboron Compounds Bearing Sterically Bulky or Electron-Withdrawing Substituents	76
3.2.4	Modified Catalysts and Ligands	80
3.2.5	Solid-Phase Synthesis (Combinatorial Methodology)	84
3.3	Reactions with 1-Alkenyl Halides and Triflates	88
3.4	Reactions with Aryl Chlorides and Other Organic Electrophiles	93
3.5	Miscellaneous	98
3.6	Applications in Polymer Chemistry	99
	References	102
4	Palladium-Catalyzed Amination of Aryl Halides and Sulfonates	107
	<i>John F. Hartwig</i>	
	Abstract	107
4.1	Introduction	107
4.1.1	Synthetic Considerations	107
4.1.2	Prior C–X Bond-Forming Coupling Chemistry Related to the Amination of Aryl Halides	108
4.1.3	Novel Organometallic Chemistry	109
4.1.4	Organization of the Review	109
4.2	Background	110
4.2.1	Early Palladium-Catalyzed Amination	110
4.2.2	Initial Synthetic Problems to be Solved	111
4.3	Palladium-Catalyzed Amination of Aryl Halides with Amine Substrates	111
4.3.1	Early Work	111
4.3.1.1	Initial Intermolecular Tin-Free Aminations of Aryl Halides	111
4.3.1.2	Initial Intramolecular Amination of Aryl Halides	112
4.3.2	Second Generation Catalysts: Aryl Bis-phosphines	112
4.3.2.1	Amination of Aryl Halides	112
4.3.2.2	Amination of Aryl Triflates	115
4.3.2.3	Amination of Heteroaromatic Halides	116
4.3.2.4	Aminations of Solid-Supported Aryl Halides	119

4.3.2.5	Amination of Polyhalogenated Aromatic Substrates	119
4.3.3	Third-Generation Catalysts with Alkylmonophosphines	119
4.3.3.1	High-Temperature Aminations Involving $P(tBu)_3$ as Ligand	120
4.3.3.2	Use of Sterically Hindered Bis(phosphine) Ligands	120
4.3.3.3	P,N Ligands and Dialkylphosphinobiaryl Ligands	121
4.3.3.4	Phenyl Backbone-Derived P,O Ligands	123
4.3.3.5	Low-Temperature Reactions Employing $P(tBu)_3$ as a Ligand	124
4.3.3.6	Heterocyclic Carbenes as Ligands	124
4.3.3.7	Phosphine Oxide Ligands	128
4.3.4	Heterogeneous Catalysts	129
4.4	Aromatic C–N Bond Formation with Non-Amine Substrates and Ammonia Surrogates	129
4.4.1	Amides, Sulfonamides, and Carbamates	130
4.4.2	Allylamine as an Ammonia Surrogate	131
4.4.3	Imines	132
4.4.4	Protected Hydrazines	132
4.4.5	Azoles	133
4.5	Amination of Base-Sensitive Aryl Halides	135
4.6	Applications of the Amination Chemistry	136
4.6.1	Synthesis of Biologically Active Molecules	136
4.6.1.1	Arylation of Secondary Alkylamines	136
4.6.1.2	Arylation of Primary Alkylamines	138
4.6.2	Applications in Materials Science	141
4.6.2.1	Polymer Synthesis	141
4.6.2.2	Synthesis of Discrete Oligomers	143
4.6.2.3	Synthesis of Azacyclophanes	146
4.6.2.4	Synthesis of Small Molecules for Materials Applications	146
4.6.3	Palladium-Catalyzed Amination in Ligand Synthesis	147
4.7	Mechanism of Aryl Halide Amination and Etheration	149
4.7.1	Oxidative Addition of Aryl Halides to L_2Pd Complexes ($L = P(o\text{-tolyl})_3$, BINAP, DPPF) and its Mechanism	149
4.7.2	Formation of Amido Intermediates	151
4.7.2.1	Mechanism of Palladium Amide Formation from Amines	151
4.7.3	Reductive Eliminations of Amines from $Pd(II)$ Amido Complexes	152
4.7.4	Competing β -Hydrogen Elimination from Amido Complexes	155
4.7.5	Selectivity: Reductive Elimination <i>vs.</i> β -Hydrogen Elimination	156
4.7.6	Overall Catalytic Cycle with Specific Intermediates	158
4.7.6.1	Mechanism for Amination Catalyzed by $P(o\text{-C}_6\text{H}_4\text{Me})_3$ Palladium Complexes	158
4.7.6.2	Mechanism for Amination Catalyzed by Palladium Complexes with Chelating Ligands	159
4.7.6.3	Mechanism of Amination Catalyzed by Palladium Complexes with Sterically Hindered Alkyl Monophosphines	160
4.8	Summary	160
	References	161

5	From Acetylenes to Aromatics: Novel Routes – Novel Products	169
	<i>Henning Hopf</i>	
	Abstract	169
5.1	Introduction	169
5.2	The Aromatization of Hexa-1,3-dien-5-yne to Benzene: Mechanism and Preparative Applications	171
5.3	The Construction of Extended Aromatic Systems from Ethynyl Benzene Derivatives	177
5.4	Bridged Aromatic Hydrocarbons Containing Triple Bonds (Cyclophynes)	187
	References	192
6	Functional Conjugated Materials for Optonics and Electronics by Tetraethynylethene Molecular Scaffolding	196
	<i>Mogens Brøndsted Nielsen and François Diederich</i>	
	Abstract	196
6.1	Introduction	196
6.2	Arylated Tetraethynylethenes	198
6.2.1	Nonlinear Optical Properties	198
6.2.2	Photochemically Controlled <i>cis</i> – <i>trans</i> Isomerization: Molecular Switches	199
6.2.3	Electrochemically Controlled <i>cis</i> – <i>trans</i> Isomerization	201
6.3	Tetraethynylethene Dimers	202
6.4	Two-Dimensional Scaffolding: Expanded Carbon Cores	204
6.4.1	Perethynylated Dehydroannulenes	204
6.4.2	Perethynylated Expanded Radialenes	205
6.4.3	Cyclic Platinum σ -Acetylide Complex of Tetraethynylethene	208
6.5	Linearly π -Conjugated Oligomers and Polymers: Poly(triacetylene)s	209
6.5.1	Lateral Aryl Substitution	210
6.5.2	Aromatic Spacer Units	210
6.5.3	Donor–Donor and Acceptor–Acceptor End-Functionalization	212
6.6	Conclusions	212
	Abbreviations	213
	References	213
7	The ADIMET Reaction: Synthesis and Properties of Poly(dialkylparaphenyleneethynylene)s	217
	<i>Uwe H. F. Bunz</i>	
	Abstract	217
7.1	Introduction	217
7.1.1	Scope and Coverage of this Review	217
7.1.2	Historical Perspective	217
7.2	Syntheses	220
7.2.1	PPEs by Acyclic Diyne Metathesis (ADIMET) Utilizing Schrock's Tungsten Carbyne Complex	220
7.2.2	Synthesis of Diarylalkynes Utilizing the Mori System	221

7.2.3	Cycles	223
7.2.4	Alkyne-Bridged Polymers by ADIMET	225
7.3	Reactivities of PPEs	229
7.4	Solid-State Structures and Liquid-Crystalline Properties of the PPEs	231
7.4.1	Organometallic Poly(aryleneethynylene)s	231
7.4.2	Poly(dialkylparaphenyleneethynylene)s	233
7.5	Spectroscopic Properties of Dialkyl-PPEs	235
7.5.1	UV/vis Spectroscopy of Dialkyl-PPEs	237
7.5.2	Fluorescence Spectroscopy: The Excited State Story	240
7.6	Self-Assembly of PPEs on Surfaces: From Jammed Gel Phases to Nanocables and Nanowires	242
7.7	PPE-Based Organic Light-Emitting Diodes (OLEDs)	244
7.8	Conclusions and Outlook	245
	References	247

8 The Chromium-Templated Carbene Benzannulation Approach to Densely Functionalized Arenes (Dötz Reaction) 250

Karl Heinz Dötz and Joachim Stendel jr.

Abstract 250

8.1	Introduction	250
8.2	Mechanism and Chemoselectivity of the Benzannulation	253
8.2.1	Mechanism	253
8.2.2	Chemoselectivity	255
8.3	Scope and Limitations	257
8.3.1	The Carbene Complex	257
8.3.1.1	Availability	257
8.3.1.2	The Carbene Ligand	259
8.3.1.3	The Chromium Template	263
8.3.2	The Alkyne	264
8.3.3	Regioselectivity	265
8.3.4	Diastereoselectivity	269
8.3.5	Thermal and Photochemical Benzannulation	271
8.3.6	Subsequent Transformations	271
8.4	Typical Experimental Procedure	272
8.5	Synthesis of Specific Arenes	273
8.5.1	Biaryls	273
8.5.2	Cyclophanes	275
8.5.3	Annulenes and Dendritic Molecules	278
8.5.4	Angular, Linear, and Other Fused Polycyclic Arenes	279
8.5.5	Fused Heterocycles	283
8.6	Synthesis of Biologically Active Compounds	285
8.6.1	Vitamins	285
8.6.2	Antibiotics	286
8.6.3	Steroids	289

8.6.4	Alkaloids	290
8.7	Summary and Outlook	291
	References	292
9	Osmium- and Rhenium-Mediated Dearomatization Reactions with Arenes	297
	<i>Mark T. Valahovic, Joseph M. Keane, and W. Dean Harman</i>	
	Abstract	297
9.1	Introduction	297
9.2	$\{\text{Os}(\text{NH}_3)_5\}^{2+}$ – The Pentaammineosmium(II) Fragment	298
9.2.1	Preparation of η^2 -Arene Complexes	298
9.2.2	Binding Selectivity	298
9.2.3	Hydrogenations	299
9.2.4	Benzene and Alkylated Benzenes	300
9.2.4.1	Benzene	300
9.2.4.2	Toluene	301
9.2.4.3	Xylenes	302
9.2.5	Naphthalene	302
9.2.5.1	Tandem Addition Reactions	303
9.2.5.2	Cyclizations	304
9.2.6	Anisole	306
9.2.6.1	Electrophilic Substitutions	306
9.2.6.2	Tandem Additions	306
9.2.6.3	Cyclization Reactions	310
9.2.7	Aniline	315
9.2.7.1	Electrophilic substitution	315
9.2.7.2	4 <i>H</i> -Anilinium Michael Additions	316
9.2.7.3	Electrophilic Addition Reactions	318
9.2.7.4	Michael–Michael–Michael Ring-Closure	318
9.2.8	Phenol	318
9.2.8.1	Electrophilic Substitution Reactions	318
9.2.8.2	Michael Addition Reactions	320
9.2.8.3	<i>o</i> -Quinone Methide Complexes	323
9.3	$\{\text{TpRe}(\text{CO})(\text{L})\}$	323
9.3.1	Introduction	323
9.3.2	Preparation of η^2 -Arene Complexes	324
9.3.3	Quadrant Analysis	324
9.3.4	Naphthalene	324
9.3.5	Cycloadditions	326
9.4	Concluding Remarks	328
	References	328
10	The Directed <i>ortho</i> Metalation Reaction – A Point of Departure for New Synthetic Aromatic Chemistry	330
	<i>Christian G. Hartung and Victor Snieckus</i>	
	Abstract	330

10.1	Introduction	330
	Aims of this Account	330
10.2	The DoM Reaction as a Methodological Tool	332
10.2.1	The <i>N</i> -Cumyl Carboxamide, Sulfonamide, and <i>O</i> -Carbamate DMGs	333
10.2.2	The Lithio Carboxylate and Carboxylate Ester DMGs	334
10.2.3	The Di- <i>tert</i> -Butyl Phosphine Oxide DMG	336
10.3	Heteroaromatic Directed <i>ortho</i> Metalation (HetDoM) in Methodological Practice	337
10.3.1	π -Excessive Heteroaromatic Directed <i>ortho</i> Metalation (HetDoM)	337
10.3.1.1	Furans and Thiophenes	337
10.3.1.2	Indoles	339
10.3.2	π -Deficient Heteroaromatic Directed <i>ortho</i> Metalation (HetDoM)	342
10.3.2.1	Pyridines	342
10.4	The DoM–Transition Metal Catalyzed Aryl–Aryl Cross-Coupling Symbiosis	344
10.4.1	The Suzuki–Miyaura–DoM Link	345
10.4.2	Aryl <i>O</i> -Carbamate and <i>S</i> -Thiocarbamate–Grignard Cross-Coupling Reactions	346
10.4.3	The DoM–Negishi Cross-Coupling Connection	349
10.4.4	DoM–Derived Cross-Coupling Reactions. Synthetic Comparison of Boron, Zinc, and Magnesium Coupling Partners	350
10.5	Beyond DoM: The Directed Remote Metalation (DreM) of Biaryl Amides and <i>O</i> -Carbamates – New Methodologies for Condensed Aromatics and Heteroaromatics	351
10.5.1	Heteroatom-Bridged Biaryl DreM. General Anionic Friedel–Crafts Complements for Several Classes of Heterocycles	356
10.6	Interfacing DoM with Emerging Synthetic Methods	359
10.7	Closing Comments	362
	References	363
11	Arenetricarbonylchromium Complexes: <i>Ips</i>o, <i>Cine</i>, <i>Tele</i> Nucleophilic Aromatic Substitutions	368
	<i>Françoise Rose-Munch and Eric Rose</i>	
	Abstract	368
11.1	Introduction	368
11.1.1	Effects on Arene Reactivity of Cr(CO) ₃ Coordination	368
11.1.2	Coverage and Definitions	369
11.2	<i>Ips</i> o Nucleophilic Aromatic Substitutions	372
11.2.1	Carbon–Oxygen, –Sulfur and –Selenium Bond Formation	372
11.2.2	Carbon–Nitrogen and Carbon–Phosphorus Bond Formation	378
11.2.3	Carbon–Carbon Bond Formation	383
11.2.4	Carbon–Hydrogen and Carbon–Metal Bond Formation	389
11.3	<i>Cine</i> and <i>Tele</i> Nucleophilic Aromatic Substitutions	392
11.3.1	Cleavage of C–F and C–Cl Bonds	392
11.3.2	Cleavage of C–O Bonds	394

11.3.3	Cleavage of C–N Bonds	395
11.4	Concluding Remarks	396
	Abbreviations	396
	References	397
12	Activation of Simple Arenes by the CpFe⁺ Group and Applications to the Synthesis of Dendritic Molecular Batteries	400
	<i>Didier Astruc, Sylvain Nlate, and Jaime Ruiz</i>	
	Abstract	400
12.1	Introduction	400
12.2	General Features of the CpFe ⁺ Activation of Arenes	401
12.2.1	Complexation and Decomplexation	401
12.2.2	Solubility, Stability, and General Reactivity Trends	402
12.2.3	Single-Electron Reduction and Oxidation	403
12.2.4	Deprotonation	403
12.2.5	Reaction of the 19-Electron Fe ^I Complex with O ₂ : Extraordinary Reactivity of Naked Superoxide and its Inhibition	404
12.2.6	Nucleophilic Reactions	405
12.2.7	Heterolytic Cleavage of Aryl Ethers	406
12.3	CpFe ⁺ -Induced Hexafunctionalization of Hexamethylbenzene for the Synthesis of Metallo-Stars	406
12.4	CpFe ⁺ -Induced Octafunctionalization of Durene in the Synthesis of Metallo-dendrimer Precursors	411
12.5	CpFe ⁺ -Induced Triallylation of Toluene and Reactivity of the Triallyl Tripod Towards Transition Metals	413
12.6	Nonaallylation of Mesitylene for the Synthesis of Dendritic Precursors of Large Metallo-dendrimers	414
12.7	CpFe ⁺ -Induced Activation of Ethoxytoluene in the One-Pot Synthesis of a Phenol Dendron by Triple-Branching and Synthesis of Organometallic Dendrons	419
12.8	Convergent and Divergent Syntheses of Large Ferrocenyl Dendrimers with Good Redox Stabilities	421
12.9	Polyferrocenium Dendrimers: Molecular Batteries?	426
12.10	Large Dendrimers Functionalized on their Branches by the Electron-Reservoir [FeCp(η^6 -C ₆ Me ₆)] ⁺ Groups: A Molecular Battery in Action	428
12.11	Conclusion	429
	References	431
13	Charge-Transfer Effects on Arene Structure and Reactivity	435
	<i>Serhiy V. Rosokha and Jay K. Kochi</i>	
	Abstract	435
13.1	Introduction	435
13.2	Mulliken's Quantitative Description of Intermolecular (Charge-Transfer) Complexes	436

13.2.1	Short Theoretical Background	436
13.2.2	Quantitative Evaluation of Arenes as Electron Donors	437
13.2.3	Spectral (UV/vis) Probe for the Formation of CT Complexes	438
13.2.4	IR Spectroscopic Studies of Charge-Transfer Complexation	442
13.2.5	Thermodynamics of Charge-Transfer Complexation	443
13.3	Structural Features of Arene Charge-Transfer Complexes	445
13.3.1	Bonding Distance of the Donor/Acceptor Dyad in Arene Complexes	446
13.3.2	Relationship Between Hapticity and Charge Transfer in Arene Complexes	447
13.3.3	Effect of Charge Transfer on the Structural Features of Coordinated Arenes	448
13.3.3.1	Expansion of the Arene Ring	448
13.3.3.2	π -Bond Localization in the Arene Ring	449
13.3.3.3	Loss of Planarity of the Arene Ring and the Transition from π - to σ -Binding	451
13.4	Charge-Transfer Activation of Coordinated Arenes	452
13.4.1	Carbon-Hydrogen Bond Activation	453
13.4.2	Nucleophilic/Electrophilic Umpolung	455
13.4.3	Modification of the Donor/Acceptor Properties of Coordinated Arene Ligands	457
13.5	CT Complexes as Critical Intermediates in Donor/Acceptor Reactions of Arenes	460
13.5.1	Effects of the Donor/Acceptor Interaction on the ET Dynamics of Arene Donors	461
13.5.1.1	Steric Control of the Inner/Outer-Sphere Electron Transfer	461
13.5.1.2	Thermal and Photochemical ET in Strongly Coupled CT Complexes	463
13.5.2	Electron-Transfer Paradigm for Arene Transformation via CT Complexes	465
13.5.3	Electron-Transfer Activation of Electrophilic Aromatic Substitution	469
13.5.4	Structural Pre-organization of the Reactants in CT Complexes	470
13.5.5	CT Complexes in Aromatic Nitration and Nitrosation	472
13.6	Concluding Summary	475
	References	475
14	Oxidative Aryl-Coupling Reactions in Synthesis	479
	<i>Guillaume Lessene and Ken S. Feldman</i>	
	Abstract	479
14.1	Introduction	479
14.2	Mechanistic Overview	480
14.3	Oxidative Coupling Reactions with Hypervalent Iodine Reagents	484
14.4	Other Reagents for the Oxidative Coupling Reaction	495
14.4.1	Iron(III)	495
14.4.2	Vanadium, Thallium, and Lead	499
14.4.3	Copper(II)	504
14.4.4	Electrochemical Methods	509
14.4.5	Other Metals	510

14.4.6	Non-Metal Mediated Methods	513
14.5	Phase-Supported Oxidants	515
14.5.1	Reagents Supported on Inorganic Materials	515
14.5.2	Polymer-Supported Hypervalent Iodine Reagents	515
14.6	Control of Atropisomerism	517
14.6.1	Transfer of Chiral Information via the Molecular Backbone	518
14.6.2	Oxidative Coupling of Two Chiral Molecules	524
14.6.3	Stoichiometric Chiral Oxidation Reagents	524
14.6.4	Catalytic Enantioselective Oxidative Coupling	527
14.7	Conclusion	534
	References	535
15	Oxidative Conversion of Arenols into <i>ortho</i>-Quinols and <i>ortho</i>-Quinone Monoketals – A Useful Tactic in Organic Synthesis	539
	<i>Stéphane Quideau</i>	
	Abstract	539
15.1	Introduction	539
15.1.1	How to Prepare <i>ortho</i> -Quinols and <i>ortho</i> -Quinone Monoketals	540
15.1.2	Why Bother with <i>ortho</i> -Quinols and <i>ortho</i> -Quinone Monoketals?	542
15.1.2.1	Synthetic Reactivity of <i>ortho</i> -Quinols and <i>ortho</i> -Quinone Monoketals	542
15.1.2.2	Biosynthetic Implications of <i>ortho</i> -Quinols and <i>ortho</i> -Quinone Monoketals	543
15.1.2.3	Biomechanistic Implications of <i>ortho</i> -Quinols and <i>ortho</i> -Quinone Monoketals	545
15.2	Oxidative Dearomatization of <i>ortho</i> -Substituted Arenols	546
15.2.1	Anodic Oxidation	546
15.2.2	Metal-Based Oxidative Activation	548
15.2.3	Halogen-Based Reagents	550
15.3	Synthetic Applications of <i>ortho</i> -Quinols and <i>ortho</i> -Quinone Monoketals	554
15.3.1	Diels–Alder Cycloadditions	554
15.3.2	Photochemical Rearrangements	561
15.3.3	Nucleophilic Substitutions and Additions	563
15.4	Conclusion	568
	References	568
16	Molecular Switches and Machines Using Arene Building Blocks	574
	<i>Hsian-Rong Tseng and J. Fraser Stoddart</i>	
	Abstract	574
16.1	Introduction	574
16.2	From Self-Assembling [2]Catenanes to Electronic Devices	575
16.3	A Hybrid [2]Catenane Switch	580
16.4	A Self-Complexing Molecular Switch	581
16.5	Pseudorotaxane-Based Supramolecular Machines	582
16.6	[2]Rotaxanes and Molecular Shuttles	583
16.7	The Evolution of Photochemically Driven Molecular Switches	589
16.8	Chemically Switchable Pseudorotaxanes	594

16.9	Molecule-Based XOR Logic Gate	596
16.10	Conclusions	597
	References	597
	<i>Index</i>	600

List of Contributors

Didier Astruc
Laboratoire de Chimie Organique et
Organométallique
UMR CNRS No. 5802
Université Bordeaux I
F-33405 Talence Cedex
France

Margaret M. Boorum
Department of Chemistry
Merkert Chemistry Center
Boston College
Chestnut Hill, MA 02467-3860
U.S.A.

Uwe H. F. Bunz
Department of Chemistry and Biochemistry
The University of South Carolina
Columbia, SC 29208
U.S.A.

Armin de Meijere
Institut für Organische Chemie
Georg-August-Universität Göttingen
Tammannstraße 2
D-37077 Göttingen
Germany

François Diederich
Laboratorium für Organische Chemie
ETH Hönggerberg
HCI, G 313
CH-8093 Zürich
Switzerland

Karl Heinz Dötz
Institut für Organische Chemie und Biochemie
Universität Bonn
Gerhard-Domagk-Straße 1
D-53121 Bonn
Germany

Ken S. Feldman
Department of Chemistry
Eberly College of Science
The Pennsylvania State University
152 Davey Laboratory
University Park, PA 16802-6300
U.S.A.

Rainer Haag
Institut für Organische Chemie
Georg-August-Universität Göttingen
Tammannstraße 2
D-37077 Göttingen
Germany

W. Dean Harman
Department of Chemistry
University of Virginia
Charlottesville, VA 22901
U.S.A.

Christian G. Hartung
Department of Chemistry
Queen's University
Kingston, ON
K7L 3N6
Canada

John F. Hartwig
Department of Chemistry
Yale University
P.O. Box 208107
New Haven, CT 06520-8107
U.S.A.

Henning Hopf
Institut für Organische Chemie
Technische Universität Braunschweig
Hagenring 30
D-38106 Braunschweig
Germany

Joseph M. Keane
Department of Chemistry
University of Virginia
Charlottesville, VA 22901
U.S.A.

Jay K. Kochi
Department of Chemistry
University of Houston
University Park
Houston, TX 77204-5003
U.S.A.

Guillaume Lessene
Department of Chemistry
Eberly College of Science
The Pennsylvania State University
152 Davey Laboratory
University Park, PA 16802-6300
U.S.A.

Mogens Brøndsted Nielsen
Laboratorium für Organische Chemie
ETH Hönggerberg
HCI, G 313
CH-8093 Zürich
Switzerland

Sylvain Nlate
Laboratoire de Chimie Organique et
Organométallique
UMR CNRS No. 5802
Université Bordeaux I
F-33405 Talence Cedex
France

Stéphane Quideau
Laboratoire de Chimie des Substances Végétales
Centre de Recherche en Chimie Moléculaire
Université Bordeaux I
351, cours de la Libération
F-33405 Talence Cedex
France

Eric Rose
Laboratoire de Synthèse Organique et
Organométallique
UMR CNRS 7611
Université Pierre et Marie Curie
Boite Postale 181
Tour 44 – 1^{er} étage
4, Place Jussieu
F-75252 Paris Cedex 05
France

Françoise Rose-Munch
Laboratoire de Synthèse Organique et
Organométallique
UMR CNRS 7611
Université Pierre et Marie Curie
Boite Postale 181
Tour 44 – 1^{er} étage
4, Place Jussieu
F-75252 Paris Cedex 05
France

Sergiy V. Rosokha
Department of Chemistry
University of Houston
Houston, TX 77204-5003
U.S.A.

Jaime Ruiz
Laboratoire de Chimie Organique et
Organométallique
UMR CNRS No. 5802
Université Bordeaux I
F-33405 Talence Cedex
France

Lawrence T. Scott
Department of Chemistry
Merkert Chemistry Center
Boston College
Chestnut Hill, MA 02467
U.S.A.

Victor Snieckus
Department of Chemistry
Queen's University
Kingston, Ontario K7L 3N6
Canada

Joachim Stendel Jr.
Institut für Organische Chemie und Biochemie
Universität Bonn
Gerhard-Domagk-Straße 1
D-53121 Bonn
Germany

J. Fraser Stoddart
Department of Chemistry and Biochemistry
University of California, Los Angeles
405 Hilgard Avenue
Los Angeles, CA 90095
U.S.A.

Akira Suzuki
Department of Chemistry and Bioscience
Kurashiki University of Science and the Arts
Kurashiki-shi, 712-8505
Japan

Hsian-Rong Tseng
Department of Chemistry and Biochemistry
University of California,
Los Angeles
405 Hilgard Avenue
Los Angeles, CA 90095
U.S.A.

Mark T. Valahovic
Department of Chemistry
University of Virginia
Charlottesville, VA 22901
U.S.A.

Arene Chemistry: From Historical Notes to the State of the Art

Didier Astruc

The History of Benzene

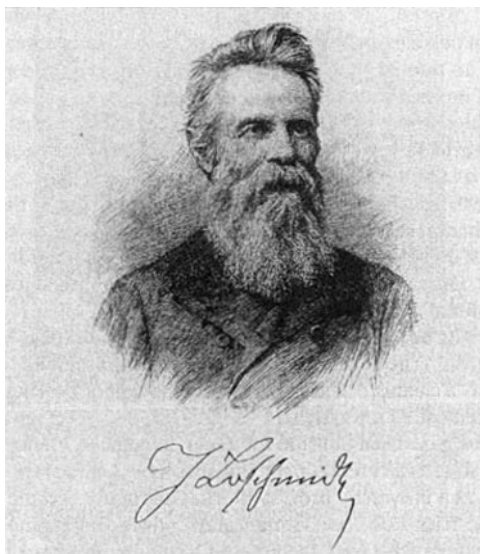
The history of benzene is one of the most intriguing in science. It started in 1825 with the isolation of benzene by Michael Faraday from the condensed phase of pyrolyzed whale oil. Its planar cyclic structure was first proposed in 1861 by the Austrian physicist and physical chemist Johann Josef Loschmidt [1–5]. However, it was only fully understood some 70 years later, around 1930, with the advent of the modern theories of aromaticity, i.e. the theory of molecular orbitals (Hückel's theory) [6–8] and the theory of resonance [9–12].

Loschmidt published the cyclic planar structure of benzene together with those of 121 other arene compounds in a unique 54-page booklet entitled *Konstitution-Formeln der organischen Chemie in geographischer Darstellung*, which constituted a masterpiece of 19th century organic chemistry [1]. An abstract of this book was published by Herman Kopp in *Liebigs Jahresbericht* in 1861 [2]. Crucially, Loschmidt's representation of benzene was very close to the present one.

Four years later, in 1865, August Kekulé proposed another planar cyclic structure, but in which double bonds were alternating with single bonds. In his article published in the *Bull. Soc. Chim. Fr.* [13], Kekulé briefly refers to Loschmidt's formula in a single sentence “Elle me paraît préférable aux modifications proposées par MM. Loschmidt et Crum-Brown.” [10] (It seems to me preferable to the modifications proposed by Loschmidt and Crum-Brown). The strength of Kekulé's structure (original representation below) is that this type of formalism is still in use today for the representation of arenes because it shows the tetravalency of carbon.

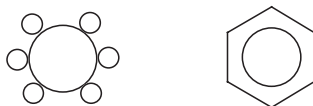
Whereas Loschmidt's work was not much publicized, Kekulé's structure of benzene immediately became well known, criticized, and controversial. Various other structures were proposed as substitution on benzene was shown to be easier than addition, which conflicted with the cyclohexatriene structure. Claus and Dewar proposed alternative structures in 1867, and Claus' formula was adopted by Koener in 1874.

Ladenburg pointed out that the Kekulé structure does not account for the fact that there is only one *ortho*-disubstituted benzene as its fixed double bonds should give rise to two isomers. Thus, Ladenburg suggested a prismatic geometry, for which there would also only be three disubstituted isomers as found experimentally for benzene, whereas Kekulé's cyclohexatriene structure implies four disubstituted isomers. In 1872, Kekulé answered this



Johann Josef Loschmidt (1821–1895) attended Prague University, and then at 21 went to Vienna to study first philosophy and mathematics, and then the natural sciences, physics and chemistry. After industrial ventures making potassium nitrate and oxalic acid among other products, he returned to Vienna as a concierge in the early 1850s, and then became a school teacher. Always attracted by theoretical problems, he is also known for his calculation in 1865 of the number of molecules in one mL of gas (the “Loschmidt number”). In 1866, he became Privatdozent at the University

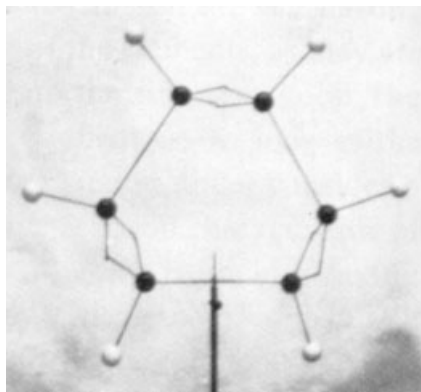
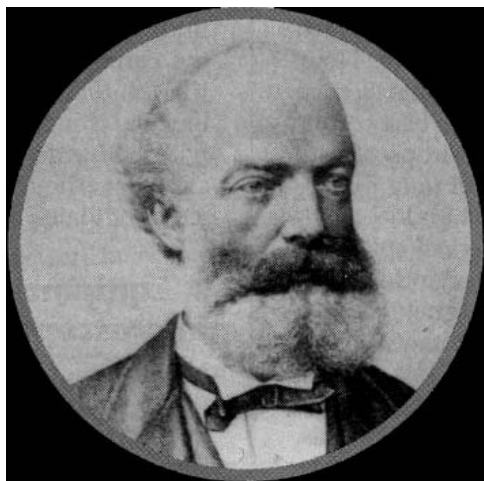
of Vienna, was elected to the Royal Academy of Sciences in 1867, then became Associate Professor and got the honorary degree of Doctor of Philosophy in 1868. He founded the Society of Chemists and Physicists in Vienna (1869), became the Chairman of the Physical Chemistry Institute (1875), Dean of the Faculty of Philosophy (1877), and was elected to the Senate of the faculty (1885). He was a close friend of Josef Stephan and Ludwig Boltzmann, who were the greatest Viennese physicists of their time.



Compare Loschmidt's representation of benzene (left) in 1861, 4 years before Kekule's formula, and the modern representation (right)



Loschmidt's representation of phenol (left), anisole (middle) and toluene (right) among 121 arenes in 1861.



August Kekulé (1829–1892) is well known as one of the pioneers of modern structural theory in organic chemistry. He became interested in chemistry after attending classes of Justus von Liebig, then went to study in Paris with Charles Gerhardt, and became acquainted with Jean-Baptiste Dumas. He enrolled in the University of Heidelberg as a Privatdozent in 1856, then in the

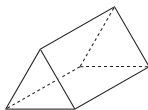
University of Ghent (Belgium) in 1858, and finally in the University of Bonn in 1867. His major contributions to chemistry were reiterating the tetravalency of carbon (first stated by A. S. Cooper), proposing its ability to form chains, and, of course, his drawing of the benzene structure that stimulated much synthetic work in aromatic chemistry.



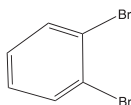
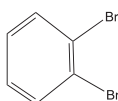
Claus (1867)



Dewar (1867)



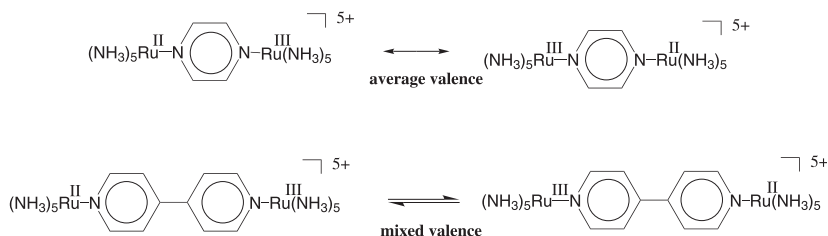
Ladenburg (1869)



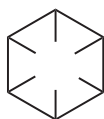
Equilibrium proposed by Kekulé (1872) to explain the unicity of ortho-disubstituted benzene

objection by suggesting that the two isomers of the disubstituted benzene are in rapid equilibrium, i.e. in what we now call a tautomeric equilibrium.

Although first-year students can now recognize Kekulé's confusion, the answer was astute at that time, since the distinction between average valence and mixed valence would only be made a century later in 1969 by Henry Taube and Carol Creutz using Ru(II)-Ru(III) complexes [14]. In the 1930's, Mills and Nixon evaluated this possibility with small rings being attached to benzene (*vide infra*).

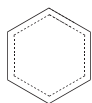


Another serious problem with Kekulé's formula was the fact that cold KMnO_4 and acids leave benzene unreacted whereas alkenes react with these reagents to give addition products. Indeed, Ladenburg showed experimentally in 1874 that the six carbon atoms of benzene are equivalent. After the main chemical properties of benzene had been established, the possible structure types became limited to the hexagon, the triangular prism, and the octahedron. Based on his experimental studies of benzene derivatives, Baeyer concluded that Claus', Dewar's, and Ladenburg's formulae were untenable, and that benzene contained six carbon atoms in a ring, but did not accept Kekulé's formula. He adopted a suggestion of Armstrong (1887) and proposed another hexagonal formula known as the Armstrong–Bayer centric formula, which had already been suggested by L. Meyer in 1865.



Baeyer (1884-92)

It is noteworthy that among the formulae proposed for benzene in the 19th century, only the first one, that of Loschmidt, is not far from being correct. The next acceptable formula only appeared with Thiele's suggestion of fractional carbon–carbon bonds (partial valences) in 1899–1900. This formalism did not explain why cyclooctatetraene is not aromatic, however, as shown experimentally (for historical accounts, see refs. [15, 16]).

The fractional-bond model:
Thiele (1899)Thiele's fractional-bond model
does not work for cyclooctatetraene

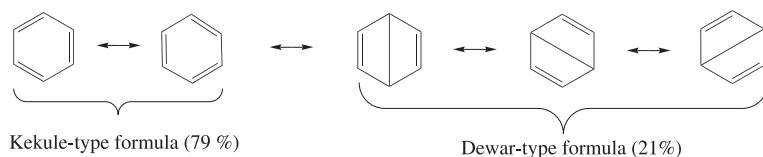
The name “benzene” was disputed in the 19th century. V. Meyer proposed “*benzene*” from “*benzoin*” because the means of preparing pure benzene involved decarboxylation of benzoic acid using sodium hydroxide at high temperature (otherwise, thiophene was an impurity that proved difficult to remove). Benzoic acid was obtained from gum *benzoin* as a white powder. On the other hand, Auguste Laurent, who *inter alia* taught crystallography to Louis

Pasteur in Paris and was one of the pioneers of modern atomic theory, proposed the name “*phene*”. The word *phene* (from the Greek “*phainen*”, to shine) was proposed because benzene burns with a bright flame. Although it was not adopted for benzene, this word is now used in a number of names of arenes, such as phenol, phenanthrene, etc.

The X-ray crystal structure of benzene, proving the equivalence of the six C–C bonds, appeared in 1929 and 1932, and Pauling reported its electron-diffraction data in 1931. Note that several of the structures proposed in the 19th century, such as Dewar benzene (non-planar) and Ladenburg’s prismane, which are valence isomers of benzene, have now actually been prepared from benzene derivatives photochemically. They are kinetically stabilized, since they do not spontaneously revert to benzene or its derivatives [17–20].

The History of Aromaticity [21–32]

At the beginning of the 19th century, the compounds that were said to be “aromatic” were those having an aromatic smell. When the arenes were synthesized or isolated later in that century, the tendency was to distinguish two groups: the aromatic and non-aromatic (aliphatic, etc.) derivatives. The analysis of aromatic compounds showed unsaturation, although these compounds were different from alkenes and alkynes. In 1910, Pascal showed that *aromatic* compounds had exalted diamagnetic susceptibilities, and, in 1925, Armit and Robinson [33] suggested the aromatic sextet. The development of wave mechanics by Schrödinger [34, 35] in 1926 led to molecular orbital theory, application of which led Hückel in 1931 to the fundamental idea of the π -electron molecular orbital and the well-known $(4n + 2)$ rule for aromatics and of anti-aromaticity for planar conjugated rings containing $4n$ π electrons [6, 7]. At about the same time, the theory of resonance, proposed by Slater [9], was based on the combinatorial representation of all the π electrons around the σ skeleton. Thus, for benzene, among all the possible combinations, five were found to provide the best contribution to the real structure, i.e. two Kekulé-type and three Dewar-type structures, which



Canonical valence-bond structures of benzene according to the theory of resonance by Slater (1929)

were termed “canonical” valence-bond structures. This valence-bond approach with its structural representation was exploited by Pauling and became commonly used [11, 36].

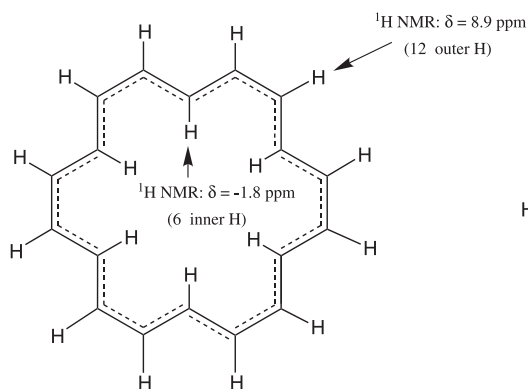
Pauling proposed the theory of ring currents in 1935, i.e. free electron circulation around the benzene ring. In the following year, 1936, London stated that the π -electron circulation is responsible for a diamagnetic contribution to magnetic susceptibility. These ring-current effects on NMR chemical shifts were disclosed by Pople in 1956 [37]. By the end of the 1960s, the development of molecular orbital theory had extended to non-benzenoid compounds [15, 38]. Modern theories taking into account the exaltation and anisotropy of magnetic susceptibility by Dauben and Flygare appeared at the end of the 1960s, and quantum chemical calculations were reported by Kutzelnig in 1980.

The criteria for aromaticity have been numerous and have changed with time. Chemical reactivity was the only criterion of aromaticity at the end of the 19th century, since a good number of electrophilic substitution reactions of arenes were already known. Thus, aromatic systems reacted with bromine to give the substitution product with retention of the aromatic character, whereas non-aromatic unsaturated compounds readily added bromine to form a dibromide. This distinction was used as a guide to define aromatic and non-aromatic compounds. This easy rule-of-thumb criterion for neutral compounds has obviously been very useful owing to its simplicity, and has survived to the present day. It is by no means general, however. For instance, anthracene and phenanthrene add bromine, and the former is used as a diene in Diels–Alder reactions. Ferrocene, a super aromatic, does not react with bromine to give the substitution product, but rather the bromide salt of the oxidized ferrocenium cation [39]. Fullerenes cannot give substitution products upon reaction with bromine, but addition products are readily obtained. Thus, fullerenes show a non-aromatic, olefin-like behavior, yet they are somewhat aromatic, although much less so than planar arenes [40].

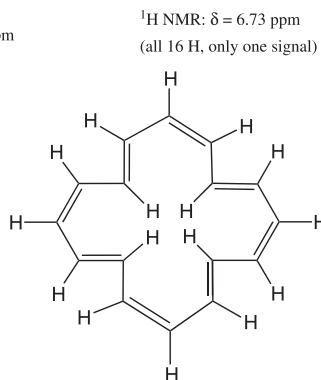
A classical criterion that was frequently mentioned at the beginning of the 20th century was the thermodynamic one. Since ΔH° for the hydrogenation of cyclohexene is 120 kJ mol⁻¹, the hypothetical cyclohexatriene should have a ΔH° of hydrogenation of 360 kJ mol⁻¹. Experimentally, ΔH° for the hydrogenation of benzene amounts to just 210 kJ mol⁻¹, a difference of 150 kJ mol⁻¹, suggesting that benzene is more stable than the hypothetical cyclohexatriene by 150 kJ mol⁻¹. This stabilization energy may be thought of as an approximation of the resonance energy. There are uncertainties associated with the approximation made in the comparisons, however, and theoretical calculation led to an estimate of 40–120 kJ mol⁻¹ for the resonance energy of benzene. Thus, this criterion is not satisfactory, especially if one tries to extend it to other arenes and heteroarenes.

In 1959, Albert suggested that the criterion of aromaticity should be based on bond lengths [38]. Thus, a ring was classed as aromatic if its C–C bond lengths were the same as those in benzene. A refinement was that the molecule was deemed aromatic if its C–C bond lengths were between 1.36 and 1.43 Å, while it was deemed a polyene if it had alternating bond lengths of 1.34 to 1.356 Å for the double bonds and 1.44 to 1.475 Å for single bonds. Another refinement was based on the mean-square deviations of the C–C bond lengths as a quantitative criterion for measuring of aromaticity. This definition was not very convenient because, in most cases, accurate bond lengths were unknown, and it did not apply to heteroatom-containing systems. Also, some well-known aromatics have some long bonds (for instance, the transannular bond of azulene). Thus, this criterion is not generally rigorously applicable. A further example for which it fails is borazine, which, despite equal bond lengths, is not aromatic. The bond lengths in the cyclopentadienyl cation (0.1425 nm, anti-aromatic) and in the cyclopentadienyl anion (0.1414 nm, aromatic) are also almost identical [41]. The magnetic ring current effects constitute the modern criterion of aromaticity that is now considered as the most reliable one. Their experimental effects are (i) the well-known anomalous chemical shifts in ¹H NMR, (ii) large magnetic anisotropies, and (iii) diamagnetic susceptibility exaltation. The mobile electrons are not only π electrons, but can also be σ or mixed, as has long been exemplified by the transition states of electrocyclic reactions. While the high field ¹H NMR chemical shifts found for aromatic protons on the exterior of an aromatic ring offer a straightforward, easy, and popular criterion, there are complications. For instance, with [16] annulene, the inner and outer protons resonate in the

opposite sense from what would be expected based on simple arguments because $[4n]$ annulenes have low-lying excited states leading to a large paramagnetic effect that reverses ring currents [41].



[18] annulene obeys the Hückel rule
(18 π electrons) and is aromatic



[16] annulene does not obey the Hückel rule
(16 π electrons) and is not aromatic (non-planar)

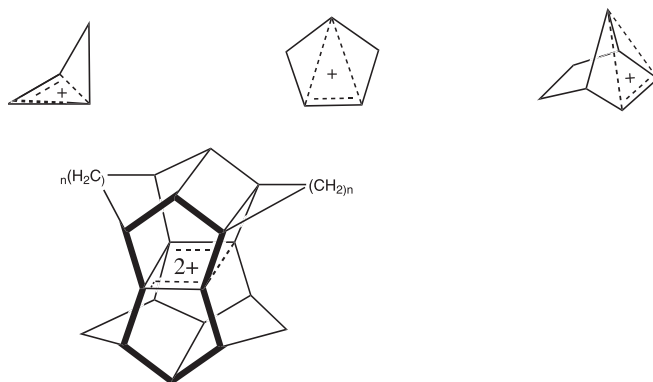
Prototypes of Sondheimer's annulenes (1956–7)

Thus, attempts to make the effect of ring current on $^1\text{H NMR}$ chemical shifts a quantitative criterion have met with serious problems, suggesting that other effects may interfere. The large diamagnetic susceptibility exaltation Δ , however, is uniquely associated with aromaticity, whereas anti-aromatic compounds exhibit paramagnetic exaltation. The diamagnetic susceptibility exaltation Δ is defined as the difference between the bulk magnetic susceptibility χ_M of a compound and the susceptibility $\chi_{M'}$ estimated from an increment system for the structural components such as isomers without cyclic delocalization ($\Delta = \chi_M - \chi_{M'}$). The experimental results have recently been satisfyingly compared with computational data by von Ragué Schleyer [41]. Thus, the definition of aromatic compounds as those exhibiting a significantly exalted diamagnetic susceptibility now appears to be an absolute criterion [37].

Anti-aromaticity was predicted by the Hückel approach for conjugated cyclic planar structures with $4n$ π electrons due to the presence of two electrons in antibonding orbitals, such as in the cyclopropenyl anion, cyclobutadiene, and the cyclopentadienyl cation ($n = 1$), and in the cycloheptatrienyl anion and cyclooctatetraene ($n = 2$). It has been argued that a simple definition of an anti-aromatic molecule is one for which the $^1\text{H NMR}$ shifts reveal a paramagnetic ring current, but the subject is controversial. The power of the Hückel theory indeed resides not only in the aromatic stabilization of cyclic $4n + 2$ electron systems, but also in the destabilization of those with $4n$ electrons [22, 27, 42].

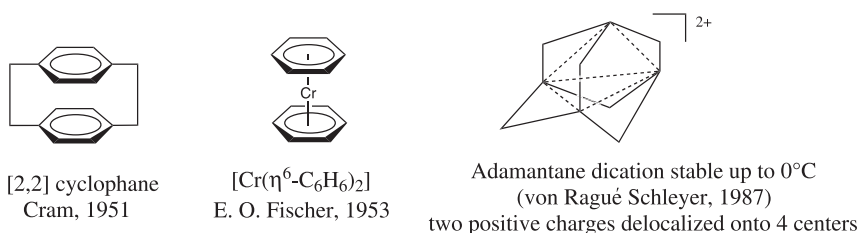
The term homoaromaticity has been coined by Winstein [43, 44]. The rupture of a cyclic conjugation due to the insertion of a saturated fragment such as CH_2 partly preserves the aromatic stabilization of the original aromatic molecule or ion. Winstein suggested that homoaromaticity, a type of aromaticity, is found for cations that have neither the σ -electron

framework of a classical aromatic system nor a parallel π -orbital arrangement, but that have an arrangement resembling the cyclic one with $(4n + 2)$ electrons. For instance, the cyclobutenyl cation is homoaromatic, because it resembles the cyclopropenyl cation. Remarkably, most examples of homoaromaticity are those of cations in which the $p\pi$ atomic orbitals involved are not parallel, the prototype being the norbornenyl cation, which has a “bishomoaromatic” arrangement. Indeed, a key experiment concerning homoaromaticity was the solvolysis of the *anti*-7-norbornenyl tosylate, which was found to be 10^{11} times faster than that of the saturated analogue [24]. Prinzbach's pagodane dications [45] are *inter alia* [44] remarkable examples.



Prinzbach's 4-center 2-electron bis-homoaromatic pagodane dication

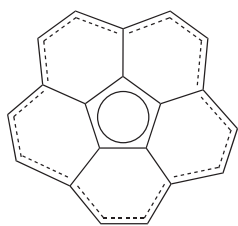
Three-dimensional aromaticity has been demonstrated, for instance in the case of Cram's cyclophane in 1951 [46, 47] and, more recently, for von Ragué Schleyer's adamantane dication [48], half-sandwich carbocations, and *nido*-carboranes. Ferrocene and various other organometallic compounds also are three-dimensional aromatics. “Spherical aromaticity” is exhibited by *closo*-carboranes, borane anions, and, to a lesser extent, C_{60} , although these compounds are isotropic.



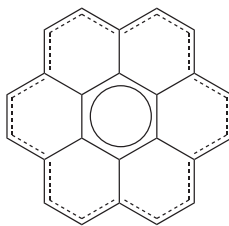
Tridimensional aromaticity

In $[m]$ circulenes, a family of polyaromatic hydrocarbons so named in 1975 by Wynsberg, in which m refers to the number of aromatic rings arranged in a circle, the total number of π electrons does not indicate aromaticity or anti-aromaticity according to the Hückel rule. This rule is strictly only applicable to monocyclic systems. It is adequate, however, to consider the inner and the outer π electrons separately, whose numbers obey the $4n + 2$ Hückel criterion for aromaticity, since both these circuits are monocyclic [49]. Coronene, a flat graphite frag-

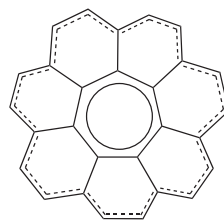
ment of D_{6h} symmetry synthesized in 1932 is the prototype of circulene with $m = 6$ [50]. It would formally be anti-aromatic according to the Hückel rule, since it contains 24 π electrons. The inner and outer sub-circuits contain 6 and 18 π electrons, respectively, however, and these numbers conform to the aromatic $4n + 2$ series. The same situation arises for corannulene ($m = 5$), a bowl-shaped hydrocarbon with D_{5h} symmetry corresponding to one-third of C_{60} , that was first synthesized by Schott and Meyer in 1966 [51]. It has 20 π electrons, which would also correspond to anti-aromaticity. The inner ring can be viewed as an aromatic cyclopentadienyl anion with 6 π electrons, however, leaving 14 electrons for the cationic outer sub-circuit, which also correspond to $4n + 2$ electrons with $n = 3$. Pleiadanulene, the [7] circulene synthesized by Yamamoto in 1983 [52], has a saddle-shaped structure with static C_2 symmetry and dynamic D_{7h} symmetry. It would also formally be anti-aromatic with 28 π electrons ($4n$; $n = 7$). However, the inner cycloheptatrienyl cation (6 π electrons) and outer anion sub-circuit (22 π electrons) can be viewed as aromatic fragments since they obey the $4n + 2$ rule of Hückel. The most popular higher circulene is kekulene, a planar hydrocarbon with D_{6h} symmetry first synthesized in 1978 by Diederich and Staab, which is also called circumcoronene because its inner ring is equivalent to the outer ring of coronene [53].



corannulene (bowl-shaped)
Barth and Lawton, 1966
6 (inner anionic ring) + 14
 π electrons (outer cationic ring)

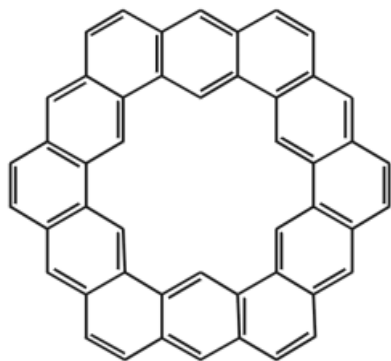


coronene (planar)
Scholl and Meyer, 1932
6 (inner ring) + 18 (outer
ring) π electrons



pleiadannulene
Yamamoto et al., 1983
6 (cationic inner ring) +
22 (anionic outer ring)
 π electrons

[m]-Circulenes viewed with a central aromatic (be) core and an aromatic ($4n + 2e$) annulene outer circuit

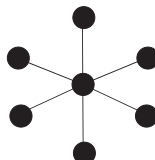
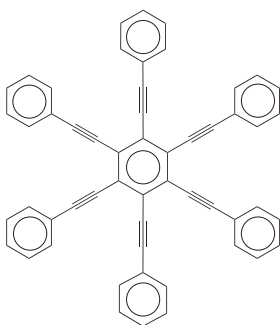


Kekulene (Staab and Diederich, 1978)

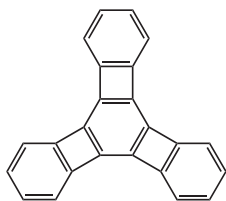
Higher PAHs have also been the subject of theoretical studies, including graph theories [54, 55]. The idea of Loschmidt on the representation of benzene using annotated circles, ascribing elemental character to the ring of six carbons in benzene has been revived by Siegel, who used the point replacement for benzene called the *Loschmidt replacement*. A very large variety of modern arene structures were shown using this representation [56].

Some Key Trends Towards Modern Arene Chemistry

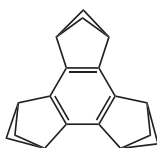
Attempts to localize the double bonds of the benzene ring in a Kekulé-like structure have been made with some success by the groups of Vollhardt [57] and of Frank and Siegel [58]. This was reminiscent of the Mills–Nixon effect predicted in the 1930's, although the partial localization has nothing to do with the tautomeric equilibrium in benzene argued by Kekulé.



“Loschmidt-replacement” representation of hexaalkynylbenzene



K.P.C. Vollhardt's [4] phenylene

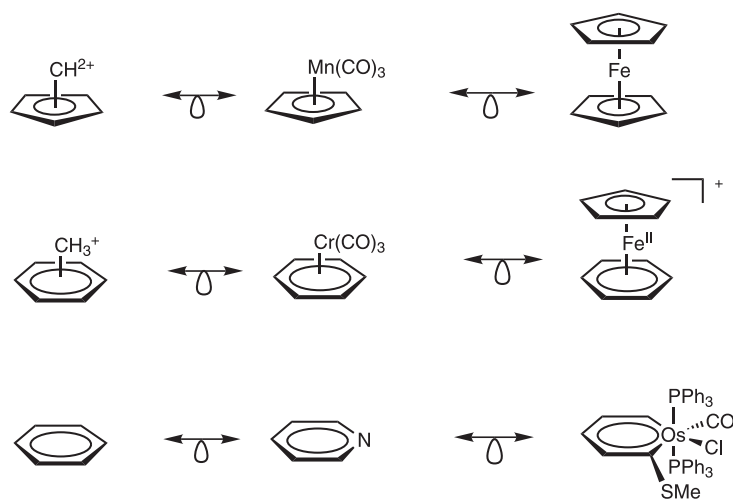


N. Frank and J. Siegel's
tribicyclo[2.1.1] hexabenzene

Threefold-symmetric arene structures synthesized with the aim of localizing the double bonds in the benzene ring

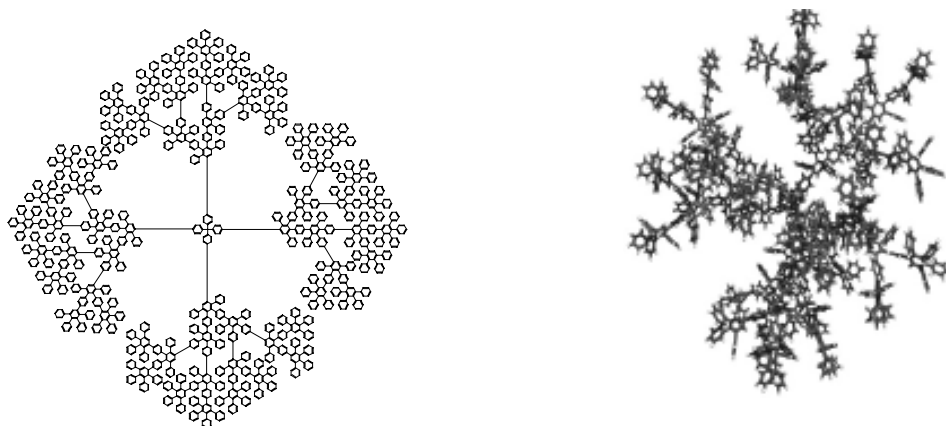
The aromatic families have benefited from Hoffmann's concepts of isolobal analogy that links organic fragments to inorganic ones [59].

Besides these classical aromatics and polyaromatic hydrocarbons, other very important classes of arene molecules are: porphyrins [60, 61], phthalocyanins [61, 62], porphycens [63], calixarenes [64], resorcarenes [64], cyclophanes [47], dendrimers [65], elementa-arenes [66], organometallic arene (hexahapto) [67], benzyne (dihapto), and aryl- and benzyl (monohapto) complexes [68], inorganic pyridine and polypyridine complexes [69], fullerenes [70, 71], and



Isolobal analogy between organic and organometallic arene and cyclopentadienyl fragments and compounds (R. Hoffmann, 1975)

carbon nanotubes [72]. Arene complexes that are not aromatic have the tetrahapto and dihapto coordination modes, and also include trihapto and pentahapto benzyl complexes [68].

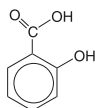


Müllen's fourth generation polyphenylene dendrimer [65]

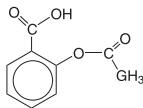
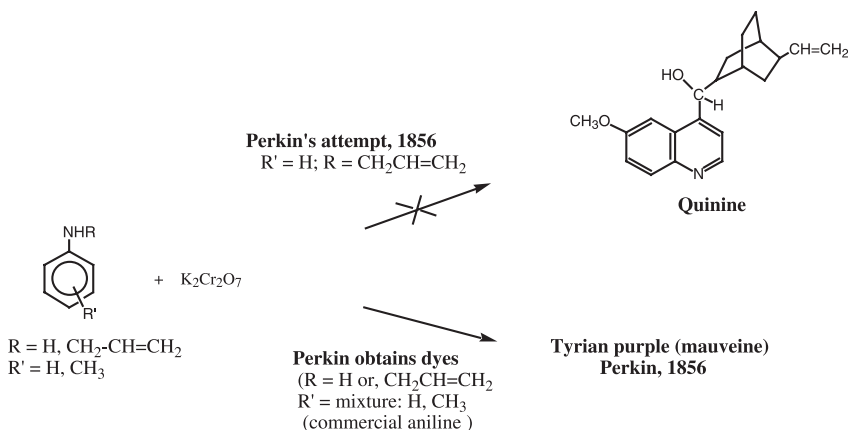
Aromatic Chemistry: From the 19th Century Industry to the State of the Art

From a synthetic standpoint, a historical landmark, after the discovery of electrophilic substitution in the 1860's, was the synthesis of aspirin, acetylsalicylic acid. The earliest known use of the drug can be traced back to the Greek physician Hippocrates in the 5th century BC. He used powder extracted from the bark of willow trees to treat pain and reduce fever. Salicin, the parent of the salicylate drug family that generates salicylic acid *in vivo*, was isolated

in 1829 from willow bark. Sodium salicylate, the predecessor of aspirin was developed in 1875 as a pain reliever. This drug caused stomach irritation, however. In 1897, Felix Hoffman, a German chemist working for Bayer, who had given sodium salicylate to his father to treat arthritis and encountered the same problem, found a new synthesis of a less acidic formula, acetylsalicylic acid (ASA), which was patented in 1899 and commercialized by Bayer in 1900. The effect of aspirin was not understood until 1970 when the British pharmacologist John Vane found that it inhibited the release of prostaglandin. Aspirin regulates blood vessel elasticity and changes the functions of blood platelets, and therefore has also become a popular drug to prevent heart attacks and circulatory troubles.



salicylic acid

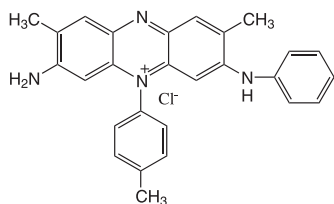
acetylsalicylic acid (ASA)
Aspirin, commercialized by Bayer in 1900.

Perkin finds Tyrian purple (mauveine), and this sets the start of the industrial chemistry with dyes

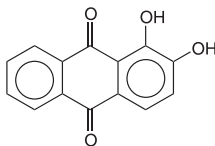
Industrial aromatic chemistry was initiated in the 1850s with the pioneering efforts of William H. Perkin in London, where he started to work as a student of August W. von Hoffmann, himself a bright student of Justus von Liebig [73]. During attempts to synthesize quinine, the only substance known, at that time, to be effective against malaria, he obtained dyes, and started to develop that field pertaining to aromatic chemistry.

With the influence of an artist friend interested in painting and dyes, he started to develop aniline purple (Tyrian purple) production, which he patented in 1856 and set up a factory for. The dyestuff industry soon flourished. In 1859, Emanuel Verguin prepared the important dye fuschine, which was subsequently produced in Basel. In 1869, Perkin patented the synthesis of the natural dye alizarin, at the same time as Caro, Lieberman, and Graebe did so in Germany. Later, moreover, Perkin prepared alizarin from anthracene, which had been

discovered by Jean-Baptiste Dumas and Auguste Laurent in 1832, who obtained it as a high-boiling product at the end of the distillation of coal tar. Besides dyes, Perkin also synthesized coumarin from salicylaldehyde and acetic anhydride [74–77].



Tyrian purple (mauveine)
Perkin, 1856



Alizarin
Perkin, 1869 and
Graebe and Liebermann, 1869

Two major industrial dyes produced by European factories since the middle of the XIXth century

On the academic side, W. H. Perkin made mention of unsuccessful experiments directed towards the preparation of benzocyclobutene in 1888. This compound was eventually prepared by H. Finkelstein, a student of J. Thiele, in 1909, as reported in his long-unknown Ph.D. thesis. Benzocyclobutene and biphenylene were also reported by Lothrop in 1941. Tropylium bromide was synthesized in 1891 by Merling, but its structure was only established in 1954 by Doering and Knox. The isolation and structure determination of the aromatic steroids estrone, estriol, and estradiol arrived only in 1929 (E. A. Doissy, A. Bute-nandt), 1931 (G. F. Marian), and 1935 (E. A. Doissy), respectively, with the advent of X-ray crystallography.

A considerable jump was made possible with the advent of homogeneous catalysis. Reppe prepared kilograms of cyclooctatetraene by the tetramerization of acetylene using nickel cyanide as the catalyst during the Second World War in Germany. Cyclooctatetraene had first been prepared by Willstätter in 1911–13 by a long sequence from an alkaloid. Higher cyclo-oligomers are not available in this way, however, and annulenes were made by starting with the coupling reaction of acetylene in dilute ethanolic solution with oxygen in the presence of copper(I) oxide, a reaction discovered by Glaser in 1865 [78]. In applying this reaction to α,ω -diacetylenes, Sondheimer and his group found, in the late 1950's, that not only linear products, but also cyclic dimers were produced when the two triple bonds were separated by three, four, or five methylene units [79]. Conversion to annulenes was achieved by heating with potassium *tert*-butoxide in *tert*-butanol, which induced prototropic rearrangement, followed by partial catalytic reduction of the remaining triple bonds [80]. More recently, the transition metal catalyzed trimerization of alkynes leading to arenes has been exploited, as best exemplified by Vollhardt's short synthesis of estrone starting from a diyne and a disilylacetylene [81]. Pyridines, bipyridines, and various heterocycles have also been synthesized using this type of catalysis by cobalt complexes. Other popular reactions are the Dötz reaction [82a], reviewed herein, and the cobalt carbonyl catalyzed Pauson–Khand reaction [82b] to form cyclopentenones from an alkyne, an alkene, and carbon monoxide [68, 82]. After Grignard's and subsequent syntheses of masked carbanions allowing the construction of

carbon–element bonds, a considerable improvement in the synthesis of such bonds, in particular C–C bonds, was the use of palladium catalysis. The Tsuji–Trost [83], Heck [84], Suzuki [85], Sonogashira [86], and Stille [87] C–C coupling reactions using palladium catalysis are now part of the organic field. A limitation has been the requirement to use aryl bromide or iodides, because the oxidative addition of aryl chlorides to the palladium center, the limiting step, is difficult [88]. However, the most recent ligands combined with palladium have allowed, in particular, the groups of Hartwig [88a], Buchwald [88b], and Fu [88c] to extend this type of catalysis to aryl chlorides that are of economic interest. As regards the use of stoichiometric organotransition metal groups, the pioneering efforts of Semmelhack concerning the addition of carbanions to arene chromium tricarbonyl complexes to make functional arenes and cyclohexadienes were invaluable [89]. Subsequent works using more powerful yet isolobal transition metal groups, such as CpFe^+ , CpFe^{*+} , CpRu^+ , Cp^*Ru^+ , and $\text{Mn}(\text{CO})_3^+$, have proved very fruitful, providing a type of arene transformation that is more complex than and complementary to that using palladium catalysts [90].

Organization of the Book and Content

Arene chemistry presently constitutes such a large part of overall molecular chemistry that a presentation of the state of the art would require an encyclopedia. Arene groups are indeed key units, in particular, in molecular and crystal engineering, drug design, and molecular electronics and spread among organic, inorganic and organometallic chemistry. Recent references to the various branches of arene chemistry can be found at the end of this historical introduction.

In the preparation of this book, we invited the best-known authors from very distinct areas of “Modern Arene Chemistry”. Gratifyingly, a large majority of them, including the most prestigious ones, have accepted to contribute a chapter, so that the main areas of this broad topic are covered herein.

Lawrence T. Scott, from Boston College, Chestnut Hill, Massachusetts, has been possibly the most successful chemist on the trail of the construction of C_{60} fragments, as illustrated in particular by his recent success in the synthesis of C_{60} [91]. His chapter (No. 1), prepared together with his co-author M. M. Boorum, deals with the synthesis of C_{60} fragments, namely tris-annulated benzenes by aldol trimerization of cyclic ketones.

Rainer Haag and Armin de Meijere, from the University of Göttingen, have produced a chapter (No. 2) devoted to oligounsaturated five-membered carbocycles, including the aromatic and anti-aromatic compounds in the same family. Armin de Meijere, a leader in German organic chemistry, has a long-standing interest in the synthetic and structural chemistry of hydrocarbon compounds, and this inspired chapter covers a broad range of modern odd-aromatic and anti-aromatic molecules, including some excursions into organotransition metal chemistry.

Akira Suzuki, from Kurashiki University, Japan, is one of the great names of arene chemistry due to his outstanding reaction that bears his name. As expected, his chapter (No. 3) deals with the Suzuki reaction with arylboron compounds and its synthetic applications in arene chemistry. The Suzuki reaction is now becoming all the more important as requirements for organic synthesis will necessarily have to take ecological aspects (“green chemistry”) into account and use of a number of toxic metals is phased out.

John Hartwig, from Yale, is not only one of the very leaders of the new generation in organometallic chemistry, but also possibly the best presently known expert in the synthetic and mechanistic aspects of palladium-catalyzed coupling of aryl halides with nucleophiles. His chapter (No. 4) covers the broad area of palladium-catalyzed amination of aryl halides and sulfonates.

Arylalkynes are key building blocks for the covalent construction of molecular architectures with remarkable physical properties, and three chapters are concerned with this field. Henning Hopf, from Braunschweig, is another major German chemist. He recently authored a beautiful book entitled “*Classics in Hydrocarbon Chemistry*” (Wiley-VCH, 2000), and has now authored a chapter (No. 5) on the routes from acetylenes to aromatics that also include cyclophane compounds. A chapter (No. 6) by M. B. Nielsen and F. Diederich (ETA, Zurich), one of the very pioneers of fullerene chemistry, deals with conjugated materials for optonics and electronics prepared by tetraethynylethene molecular scaffolding. In this chapter, the authors show how the physical properties of the materials depend strongly on the presence of arene units. Uwe Bunz, from the University of South Carolina at Columbia, is a gifted young professor, formerly a Ph.D. student with Peter Vollhardt in Berkeley, who has recently greatly developed the field of molecular architectures using arylalkyne segments. His chapter (No. 7) is devoted to the Acyclic Diyne Metathesis (ADIMET) reaction, which is a powerful source of such organic arylalkyne bridged materials.

Heinrich Dötz, from the Kekulé-Institut (a predestined name!) of the University of Bonn, is another famous chemist who has given his name to a reaction. Coming from E. O. Fischer's school, he advantageously exploited his serendipitous discovery of the very rich reactivity of Fischer-type carbene complexes in synthesizing polycyclic arene derivatives. This chromium-templated carbene benzannulation approach to densely functionalized arenes (Dötz reaction) is the subject of the chapter (No. 8) that he has co-authored with J. Stendel Jr.

Dean Harman, from the University of Virginia in Charlottesville, discovered dihapto osmium-arene complexes together with Henry Taube when he was a Ph.D. student of the latter at Stanford. They showed that the protection of one arene double bond by osmium allows selective hydrogenation of the two other double bonds by molecular hydrogen under ambient conditions, and that the anisole complex is transformed into cyclohexenone under these hydrogenation conditions that include trace water. These intriguing findings led Dean Harman to further develop the useful osmium- and rhenium-mediated dearomatizations and functionalizations of arenes that are the subject of the chapter (No. 9) prepared together with his co-authors M. T. Valahovic and J. M. Keane.

Victor Snieckus is well known for having developed powerful methodological tools for the synthesis of polysubstituted aromatics, in particular heteroaromatic directed *ortho*-metalation. Thus, in his chapter (No. 10), prepared with his co-author Christian Hartung, directed *ortho*-metalation is taken as a starting point for new synthetic aromatic chemistry.

Françoise Rose is leading an organotransition metal chemistry group in Jussieu (University Paris VI) dedicated to the activation of arenes using chromium tricarbonyl and manganese tricarbonyl cation, a field in which she has become a master. She has, in particular, discovered the very powerful *ipso*, *cine*, and *tele* nucleophilic aromatic substitution. She has now prepared a chapter (No. 11), together with her husband Eric, in which they start with the general applications of chromium tricarbonyl complexes in arene synthesis before reviewing Cr(CO)₃-mediated nucleophilic substitution reactions and their mechanisms.

I have reviewed, in Chapter No. 12, the activation of arenes by the strongly electron-withdrawing 12-electron fragment CpFe^+ , isolobal to $\text{Cr}(\text{CO})_3$ and $\text{Mn}(\text{CO})_3^+$, and its application to the synthesis of dendritic cores, dendrons, dendrimers, and metallodendrimers, including molecular batteries.

It would have been impossible to produce a book on modern arene chemistry without Jay Kochi's physical organic-organometallic vision of the area. His work on charge transfer involving arenes, inspired by Mulliken's ideas, is unique and deep, and has considerable impact on our understanding of organic and organometallic mechanisms. This is indeed the theme of his chapter (No. 13) prepared with his co-author S. V. Rosokha (Houston).

Finally, the oxidation of arenes is an area of research that is most relevant to the synthesis of natural and biologically active molecules, and is more generally useful in bioorganic synthesis. Two chapters by experts are devoted to this theme. G. Lassene and K. Feldman from Penn State have prepared a chapter (No. 14) dedicated to oxidative aryl coupling reactions that formally involve the loss of two electrons and two protons, the biaryl moiety being found in many active biomolecules. My young colleague Stéphane Quideau from the University Bordeaux I, who was a Ph.D. student of Ken Feldman at Penn State, has focused on the oxidative conversion of arenols into *ortho*-quinols and *ortho*-quinone monoketals. Methods of dearomatizing arenols are reviewed and the applications of this far-reaching tactic to natural product synthesis are detailed in his chapter (No. 15) [92].

Fraser Stoddart, from UCLA, is a master in many fields of organic and supramolecular chemistry and materials science. Arenes are building blocks in many of the molecules synthesized by his research group, in particular his catenanes for the design of molecular machines. He has co-authored a chapter (No. 16) together with Hsian-Rong Tseng on molecular switches and machines.

References

- 1 J. LOSCHMIDT, *Chemische Studien*, A. Konstitution-Formeln der organischen Chemie in geographischer Darstellung, B. Das Mariotte'sche Gesetz, Vienna, 1861.
- 2 H. KOPP, *Liebigs Jahresbericht*, 1861, 1, 335 (abstract of ref. [1]).
- 3 R. ANSCHÜTZ, *J. Loschmidt's Konstitution-Formeln der organischen Chemie in geographischer Darstellung*, W. Engelmann, Leipzig, 1913 (re-publication of Loschmidt's book by one of his students, includes a biography of Loschmidt with many comments about his work), 120 pages.
- 4 M. KOHN, *J. Chem. Ed.* 1945, 381 (article about Loschmidt based on ref. [3]).
- 5 W. J. WISESSER, *Aldrichimica Acta* 1989, 22(1), 17 (brief summary of Loschmidt's work and biography).
- 6 E. HÜCKEL, *Zeitschrift für Physik* 1931, 70, 204–286.
- 7 E. HÜCKEL, *Theoretical Principles of Organic Chemistry*, Elsevier, London, 1955, vol. 1.
- 8 On Erich Hückel's life, theory, and controversy: J. BERSON, *Chemical Creativity*, Wiley-VCH, New York, 1999; *Angew. Chem. Int. Ed. Engl.* 1996, 35, 2750.
- 9 J. C. SLATER, *Phys. Rev.* 1930, 36, 57.
- 10 B. PULLMAN, A. PULLMAN, *Les Théories Electroniques de la Chimie Organique*, Masson, Paris, 1952.
- 11 L. PAULING, *The Nature of the Chemical Bond*, Cornell University Press, Ithaca, New York, 1940; 2nd Edn., 1944; 3rd Edn., 1960.
- 12 a) A. STREITWEISER, JR., *Molecular Orbital Theory for Organic Chemists*, Wiley, New York, 1961; b) L. SALEM, *Molecular Orbital Theory of Conjugated Systems*, Benjamin, New York, 1966.

- 13 A. KEKULÉ, *Bull. Soc. Chim. Fr.* **1865**, 3(2), 100.
- 14 a) C. CREUTZ, H. TAUBE, *J. Am. Chem. Soc.* **1969**, 91, 3988; b) H. TAUBE, *Electron-Transfer Reactions of Complex Ions in Solution*, Academic Press, New York, **1970**.
- 15 a) I. L. FINAR, *Organic Chemistry*, Longmans, London, 5th Edn., Vol. 1, **1967**, p. 537. b) J. P. SNYDER, *Nonbenzenoid Aromatics*, Academic Press, New York, **1969**.
- 16 P. GARRATT, *Aromaticity*, Wiley, New York, **1986**.
- 17 I. HALLER, *J. Am. Chem. Soc.* **1966**, 88, 2070.
- 18 E. E. VAN TAMELEN, S. P. PAPAS, K. L. KIRK, *J. Am. Chem. Soc.* **1971**, 93, 6092.
- 19 M. G. BARLOW, R. N. HASZELDINE, J. G. DINGWALL, *J. Chem. Soc., Perkin Trans. 1* **1973**, 1542.
- 20 J. D. COYLE (Ed.), *Photochemistry in Organic Synthesis*, Royal Society of Chemistry, London, **1986**.
- 21 G. M. BADGER, *Aromatic Character and Aromaticity*, Cambridge University Press, Cambridge, **1969**.
- 22 E. D. BERGMAN, B. PULLMAN (Eds.), *Aromaticity, Pseudo-Aromaticity, Anti-Aromaticity*, Academic Press, New York, **1971**.
- 23 E. CLAR, *The Aromatic Sextet*, Wiley, New York, **1972**.
- 24 J. LEWIS, J. PETERS, *Facts and Theories of Aromaticity*, Macmillan Press, London, **1975**.
- 25 I. GUTMAN, S. J. SYVIN, *Introduction to the Theory of Benzenoid Hydrocarbons*, Springer, Heidelberg, **1989**.
- 26 D. LLOYD, *The Chemistry of Conjugated Cyclic Compounds*, Wiley, Chichester, **1989**.
- 27 V. I. MINKIN, M. N. GLUCKHOVTSSEV, B. YA. SIMKIN, *Aromaticity and Antiaromaticity*, Wiley, New York, **1994**.
- 28 For recent reviews on aromaticity, see: T. M. KRYGOWSKI, M. K. CYRANSKI, *Chem. Rev.* **2001**, 101, 1385 (structural aspects); L. J. SCHAAD, B. A. HESS JR., *Chem. Rev.* **2001**, 101, 1465 (Dewar–Llano resonance energy); K. JUG, P. C. HIBERTY, S. SHAIK, *Chem. Rev.* **2001**, 101, 1477 (σ - π energy separation); S. SHAIK, A. SHURKI, D. DANOVITCH, P. C. HIBERTY, *Chem. Rev.* **2001**, 101, 1501 (π delocalization); S. W. SLAYDEN, J. F. LIEBMAN, *Chem. Rev.* **2001**, 101, 1541 (energetics).
- 29 For a recent review on quantitative measurements of aromaticity, see: A. R. KATRITZKY, K. JUG, D. C. ONICIU, *Chem. Rev.* **2001**, 101, 1421.
- 30 For recent DFT computations of aromaticity, see: F. DE PROFT, P. GEERLINGS, *Chem. Rev.* **2001**, 101, 1451.
- 31 For the spherical aromaticity of polyhedral boranes, see: B. KING, *Chem. Rev.* **2001**, 101, 1119.
- 32 For a recent review of the aromaticity of phosphorus heterocycles, see: L. NYULASZI, *Chem. Rev.* **2001**, 101, 1229.
- 33 J. W. ARMIT, R. ROBINSON, *J. Chem. Soc.* **1925**, 127, 1604.
- 34 E. SCHRÖDINGER, *Ann. Phys.* **1926**, 79, 361 and 489; **1926**, 80, 437, **1926**, 81, 109.
- 35 R. S. MULIKEN, *Phys. Rev.* **1932**, 41, 49.
- 36 L. PAULING, *J. Am. Chem. Soc.* **1931**, 53, 1367 and 3225.
- 37 For recent reviews on aromaticity and ring currents and on the measurement of aromaticity by NMR, see: J. A. N. F. GOMES, R. B. MALLION, *Chem. Rev.* **2001**, 101, 1349; R. H. MITCHELL, *Chem. Rev.* **2001**, 101, 1301; P. LAZERETTI, in *Progress in Nuclear Magnetic Resonance Spectroscopy* (Eds.: J. W. EMSLEY, J. FEENEY, L. SUTCLIFFE), Elsevier, Amsterdam, **2000**, Vol. 36, pp. 1–88.
- 38 A. ALBERT, *Heterocyclic Chemistry*, The Atholone Press, London, **1959**, 201.
- 39 For a modern account of ferrocene chemistry, see *Ferrocenes* (Eds.: A. TOGNI, T. HAYASHI), VCH, Weinheim, **1995**.
- 40 For the spherical aromaticity of fullerenes, see: M. BÜHL, A. HIRSCH, *Chem. Rev.* **2001**, 101, 1153.
- 41 P. VON RAGUÉ SCHLEYER, H. JIAO, *Chemistry International* **1996**, 18(5), 205.
- 42 For recent reviews on anti-aromaticity, see: K. B. WIBERG, *Chem. Rev.* **2001**, 101, 1317; A. A. ALLEN, T. T. TIDWELL, *Chem. Rev.* **2001**, 101, 1348.
- 43 S. WINSTEIN, *J. Am. Chem. Soc.* **1959**, 81, 6524; **1961**, 83, 3235, 3244, 3248; **1963**, 85, 343, 344.
- 44 a) First mention of homoaromaticity: D. E. APPLEQUIST, J. D. ROBERTS, *J. Am. Chem.*

- Soc. **1956**, 78, 4012; b) For a recent review on homoaromaticity, see: R. V. WILLIAMS, *Chem. Rev.* **2001**, 101, 1185.
- 45 H. PRINZBACH, G. GEISCHIEDT, H.-D. MARTIN, R. HERGES, J. HEINZE, G. K. S. PRAKASH, G. A. OLAH, *Pure Appl. Chem.* **1995**, 67, 673.
 - 46 D. J. CRAM, H. STEINBERG, *J. Am. Chem. Soc.* **1951**, 73, 5691.
 - 47 a) For a superb account of cyclophane chemistry, see: F. VÖGTLE, *Cyclophane Chemistry*, Wiley, New York, **1993**; for recent reviews by Vögtle's group on other elaborate arene-containing molecular architectures, see: F. VÖGTLE, O. SAFAROWSKY, C. HEIM, A. AFFELD, O. BRAUN, A. MOHRY, *Pure Appl. Chem.* **1999**, 71, 247; C. REUTER, R. SCHMIEDER, F. VÖGTLE, *Pure Appl. Chem.* **2000**, 72, 2233; b) R. GLEITER, D. KRATZ, *Acc. Chem. Res.* **1993**, 26, 311.
 - 48 a) M. BREMER, P. VON RAGUÉ SCHLEYER, K. SCHÜTZ, M. KAUSCH, M. SCHINDLER, *Angew. Chem. Int. Ed. Engl.* **1987**, 26, 761; b) S. STINSON, *C. fE. News*, April 20, **1987**, p. 60.
 - 49 J. S. SIEGEL, T. J. SEIDERS, *Chemistry in Britain* **1995**, 313.
 - 50 R. SCHOLL, K. MEYER, *Chem. Ber.* **1932**, 65, 902.
 - 51 W. E. BARTH, G. W. LAWTON, *J. Am. Chem. Soc.* **1966**, 88, 380.
 - 52 K. YAMAMOTO, T. HARADA, N. MASAO, *J. Am. Chem. Soc.* **1983**, 105, 7171.
 - 53 H. A. STAAB, F. N. DIEDERICH, *Angew. Chem. Int. Ed. Engl.* **1978**, 17, 372.
 - 54 E. CLAR, *Polyaromatic Hydrocarbons*, Academic Press, London, **1964**.
 - 55 *Advance in the Theory of Hydrocarbons* (Ed.: I. GUTMAN), *Topics in Current Chemistry*, Springer, Heidelberg, **1992**, vol. 162.
 - 56 Y. STRITANA-ANANT, T. J. SEIDERS, J. S. SIEGEL, in *Topics in Current Chemistry* (Ed.: A. DE MEIJERE), Springer, Heidelberg, **1998**, 196, 1.
 - 57 First report of a three-fold symmetric phenylene: K. P. C. VOLLHARDT, *J. Am. Chem. Soc.* **1986**, 108, 3150.
 - 58 Using bicyclic annelation, Natia Franck obtained bond deformation in such a way that double bonds prefer to be exocyclic to strained bicyclic rings: N. FRANK, J. S. SIEGEL, *Angew. Chem. Int. Ed. Engl.* **1995**, 34, 1454.
 - 59 R. HOFFMANN, *Angew. Chem. Int. Ed. Engl.* **1982**, 21, 711.
 - 60 *Porphyryns and Metalloporphyrins* (Ed.: K. M. SMITH), Elsevier, Amsterdam, **1975**.
 - 61 *The Porphyrin Handbook* (Eds.: K. M. KADISH, K. SMITH, R. GUILARD), Academic Press, San Diego, CA, **2000**.
 - 62 F. H. MOSER, A. L. THOMAS, *Phthalocyanine Compounds*, ACS Monograph No. 157, ACS, New York, **1963**.
 - 63 Porphycens: see a) E. VOGEL, M. BRÖRING, S. J. WEGHORN, P. SCHOLZ, R. DEPONTE, J. LEX, H. SCHMICKLER, K. SCHAFFNER, S. E. BRASLAVSKY, M. MÜLLER, S. PÖRTING, C. J. FOWLER, J. L. SESSLER, *Angew. Chem. Int. Ed. Engl.* **1997**, 36, 1651; b) D. O'SULLIVAN, *C. fE. News*, **1986**, June 9, p. 27; S. BORMAN, *C. fE. News*, **1995**, June 26, p. 30.
 - 64 a) C. D. GUTSCHE, *Calixarenes Revisited*, The Royal Society of Chemistry, Cambridge, **1998**; b) J. VICENS, V. BÖHMER (Eds.), *Calixarenes, A Versatile Class of Macrocyclic Compounds*, Kluwer, Dordrecht, **1991**; c) A. G. S. HOBERG, *J. Am. Chem. Soc.* **1980**, 45, 4498.
 - 65 For polyaryl dendrimers, see: M. D. WATSON, A. FECHTENKÖTTER, K. MÜLLEN, *Chem. Rev.* **2001**, 101, 1267.
 - 66 For a recent review on metallabenzenes, see: J. R. BLEEKE, *Chem. Rev.* **2001**, 101, 1205; first metallabenzene (Chart): G. P. ELLIOT, W. R. ROPER, J. M. WATERS, *J. Chem. Soc., Chem. Commun.* **1982**, 811.
 - 67 For arene complexes, see ref. [68] and chapters 8 to 13 of this book.
 - 68 R. H. CRABTREE, *Organometallic Chemistry of the Transition Metals*, 3rd Edn., Wiley, New York, **2000**.
 - 69 A. VICEK, JR., J. HEYROSKY, in *Electron Transfer in Chemistry* (Ed.: V. BALZANI), Vol. II, Wiley-VCH, Weinheim, pp. 804–877.
 - 70 A. HIRSCH, *The Chemistry of Fullerenes*, Thieme, New York, **1994**.
 - 71 R. TAYLOR (Ed.), *The Chemistry of Fullerenes*, World Scientific Publishing, Singapore, **1995**.
 - 72 Carbon nanotubes: a) S. IJIMA, *Nature* **1991**, 354, 776; **1992**, 356, 776; **1993**, 361, 603; b) M. S. DRESSSELHAUS, G. DRESSSELHAUS, P. C. EKLUND, *Science of Fullerenes and Carbon Nanotubes*, Academic Press, San Diego, **1996**.

- 73 F. M. ROWE, "Perkins Centenary Lecture: The Life and Work of Sir William Henry Perkin", *J. Soc. Dyers Colorists* **1938**, *54*, 551.
- 74 W. H. PERKIN, *J. Soc. Arts* **1869**, *17*, 99.
- 75 L. F. FIESER, *J. Chem. Ed.* **1930**, *7*, 2609.
- 76 H.-G. FRANCK, J. W. STADELHOFFER, *Industrial Aromatic Chemistry*, Springer Verlag, Heidelberg, **1988**.
- 77 J. W. STADELHOFFER, H. VIERRATH, O. KRÄTZ, *Chem. Ind.* **1988**, 515 (August 15).
- 78 C. GLASER, *Ber. Dtsch. Chem. Ges.* **1869**, *2*, 422; *Ann. Chem.* **1870**, *154*, 434.
- 79 F. SONDHEIMER, *Pure Appl. Chem.* **1963**, *7*, 363.
- 80 A. T. BALABAN, M. BANCUI, V. CIORBA, *Annulenes, Benzo-, Hetero-, Homo-Derivatives and their Valence Isomers*, CRC Press, Boca Raton, FL, **1987**, Vols. I and II.
- 81 K. P. C. VOLHARDT, *Acc. Chem. Res.* **1977**, *10*, 1; *Angew. Chem. Int. Ed. Engl.* **1984**, *23*, 539.
- 82 a) K. H. DÖTZ, *Angew. Chem. Int. Ed. Engl.* **1984**, *23*, 587; b) S. TAKANO, *Chem. Lett.* **1992**, 443.
- 83 J. TSUJI, *Organic Synthesis with Palladium Compounds*, Springer Verlag, Berlin, **1980**; *Synthesis* **1984**, 369.
- 84 R. F. HECK, *Palladium Reagents in Organic Synthesis*, Academic Press, New York, **1985**.
- 85 a) A. SUZUKI, N. MIYAJIMA, *Chem. Rev.* **1995**, *95*, 2457; *J. Organomet. Chem.* **1999**, *576*, 147; b) Chapter 3 of this book.
- 86 K. SONOGASHIRA, Y. TOHDA, N. HAGIHARA, *Tetrahedron Lett.* **1975**, 4467; *Synthesis* **1980**, 627.
- 87 J. K. STILLE, *J. Am. Chem. Soc.* **1987**, *109*, 2138 and 5478.
- 88 a) J. F. HARTWIG, *Acc. Chem. Res.* **1998**, *31*, 852; b) S. L. BUCHWALD, *Acc. Chem. Res.* **1998**, *31*, 805; c) A. LITKE, G. C. FU, *J. Am. Chem. Soc.* **2000**, *122*, 4020; d) V. V. GRUSHIN, H. ALPER, *Chem. Rev.* **1994**, *94*, 1047.
- 89 M. F. SEMMELHACK, *New York Acad. Sci.* **1977**, 295, 36.
- 90 For π -activation of arenes by 12-electron electron-withdrawing groups, see Chapters 11 and 12 of this book.
- 91 L. T. SCOTT, M. M. BOORUM, B. J. MCMAHON, S. HAGEN, J. MACK, J. BLANK, H. WEGNER, A. DE MEIJERE, *Science* **2002**, 5559, 1500–1502.
- 92 a) I am grateful to Dr. Françoise Chardac for her kind and efficient help in literature search and to my distinguished neighbor and colleague Professor Henri Bouas-Laurent for having shared his passion for and culture in arene chemistry [91b] and for his precious advice on these historical notes; b) for a recent review, see, for instance: H. BOUAS-LAURENT, A. CASTELLAN, J.-P. DESVERGNE, R. LAPOUYADE, *Chem. Soc. Rev.* **2001**, *30*, 248.

1

The Synthesis of Tris-Annulated Benzenes by Aldol Trimerization of Cyclic Ketones

Margaret M. Boorum and Lawrence T. Scott

Abstract

For the synthesis of tris-annulated benzene rings, the aldol trimerization of cyclic ketones has been known as a powerful tool since the 19th century. Why the reaction works so well with some ketones (e.g., indanone) but fails so miserably with others (e.g., tetralone), however, has never been adequately explained. This chapter outlines the development and scrutiny of a hypothesis that says: formation of an α,β -unsaturated (conjugated) dimer from a cyclic ketone is vital to the success of an aldol trimerization reaction for the synthesis of a tris-annulated benzene; the reaction will fail with ketones that form only β,γ -unsaturated (unconjugated) dimers. This hypothesis unifies much experimental chemistry and is supported by theoretical calculations.

1.1

Introduction

The aldol trimerization reaction constitutes a powerful tool in organic chemistry for the synthesis of tris-annulated benzene rings from cyclic ketones (Figure 1). Although the reaction has been known for more than a century, its scope and limitations remain poorly defined. Some ketones give a trimeric product readily and in high yield, while others result predominantly or exclusively in acyclic dimers, higher oligomers, or intractable mixtures of products.

In recent years, C_3 -symmetric condensation products of the sort that are available by this trimerization reaction have taken on a new significance. Many of these trimers map onto the surface of C_{60} and have been seen as potential intermediates for the chemical synthesis of fullerenes [1–10]. A better understanding of the reaction would help to establish the range over which it can be used to synthesize novel polycyclic aromatic hydrocarbons (PAHs), and that is the goal of this chapter. The related trimerizations of methyl ketones to give 1,3,5-trisubstituted benzene rings [11], and of other acyclic ketones to give hexasubstituted benzene rings, will not be discussed here.

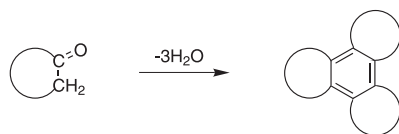


Fig. 1. Generalized synthesis of a tris-annulated benzene by aldol trimerization of a cyclic ketone.

1.2

Truxene and Truxone: Venerable Prototypes

The first thorough investigation of an aldol trimerization to produce a tris-annulated benzene ring from three cyclic ketone monomer units was performed over 100 years ago. It focused on the conversion of “hydrindone” (1, a compound known today as 1-indanone) to “truxene” (2) (Figure 2).

The story appears to have begun in 1877 with Gabriel and Michael’s report [12] on the synthesis of “tribenzoylenebenzene” from phthalylacetic acid (3) (Figure 3). On the basis of the empirical formula of this new compound, $(\text{C}_9\text{H}_4\text{O})_n$, these early pioneers tentatively (but correctly!) assigned the structure as that of the cyclic condensation product 4. Ten years later, Wislicenus succeeded in preparing indane-1,3-dione (5) and noticed its tendency to form condensation products, including “truxone”, a cyclic trimer that turned out to have the same structure as Gabriel and Michael’s “tribenzoylenebenzene” (4, Figure 3) [13]. Since that

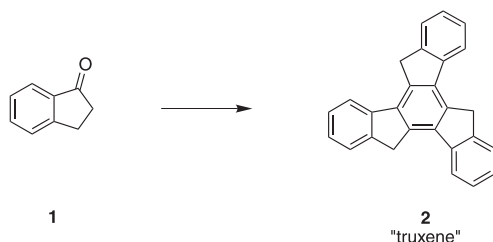


Fig. 2. Aldol trimerization of 1-indanone (1) to “truxene” (2).

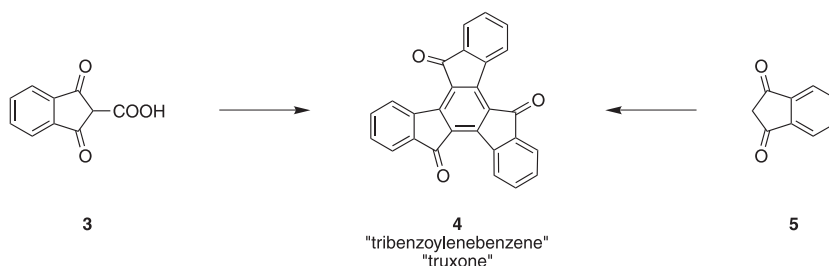


Fig. 3. Gabriel and Michael’s 1877 conversion of phthalylacetic acid (3) to “tribenzoylenebenzene” and Wislicenus’s 1887 synthesis of “truxone” from indane-1,3-dione (5); both products turned out to have the same structure (4).

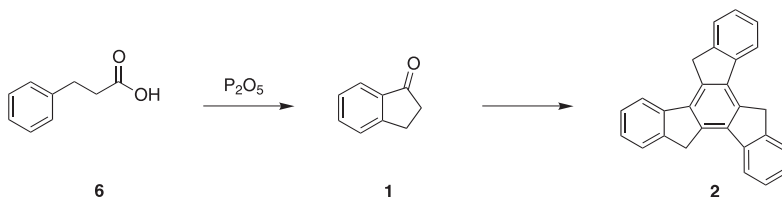


Fig. 4. Hausmann's 1889 discovery of "truxene" (2) while attempting to synthesize 1-indanone (1) from phenylpropionic acid (6).

time, the condensation of 5 to 4 has been observed under both acidic and basic conditions, and it can even be induced by merely heating the ketone in the absence of a solvent. Many reagents have been used to effect this transformation; however, the reaction with concentrated sulfuric acid is clearly superior, giving truxone in an isolated yield of 90 % [14].

In 1889, Hausmann reported [15] the formation of a $(C_9H_6)_n$ hydrocarbon from phenylpropionic acid (6). In those days, it was already known that cyclic ketones could sometimes be obtained from aryl-substituted carboxylic acids by the action of strong dehydrating agents. Hausmann therefore treated 6 with phosphorus pentoxide, expecting to form hydrindone (1). Small amounts of 1 were, in fact, isolated from the reaction mixture, but the major product proved to be a $(C_9H_6)_n$ hydrocarbon that became known as "truxene" (Figure 4). Hausmann performed several chemical tests on the $(C_9H_6)_n$ hydrocarbon, including chromic acid oxidation to a $(C_9H_4O)_n$ derivative ("truxone"). Ultimately, he actually proposed the correct structure for "truxene", but he never managed to prove it.

It was not until 1894 that the tris-annulated benzene structures of truxene and truxone were finally confirmed by Kipping [16]. Molecular weight determinations on both compounds, performed in boiling aniline and boiling phenol solutions, unambiguously established the trimeric structures of the hydrocarbon (2) and its oxidation product (4). Furthermore, by running Hausmann's reaction in dilute solutions of sulfuric acid, Kipping succeeded in isolating the dimeric intermediate 7, and he showed that 7 was converted to 2 upon treatment with phosphorus pentoxide (Figure 5) [17].

Since Hausmann's and Kipping's initial studies, the synthesis of truxene from 1-indanone has been carried out many times under a wide variety of conditions. Reagents that have been reported to promote this trimerization are generally either strong protic acids or Lewis acids and include hydrochloric acid [15], hydroiodic acid [15], phosphorus pentoxide [15], zinc dust [15], sulfuric acid [17], phosphorus pentachloride [17], zinc chloride in acetic acid [18],

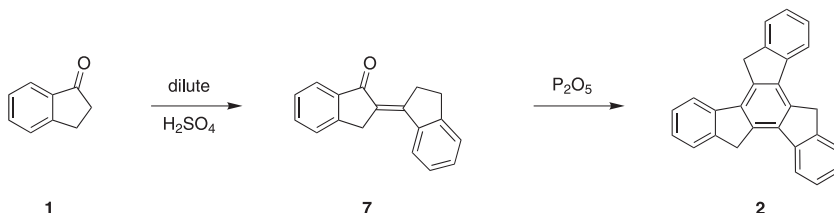


Fig. 5. Kipping's 1894 identification of the aldol dimer 7 as an intermediate in the cyclotrimerization of 1-indanone.

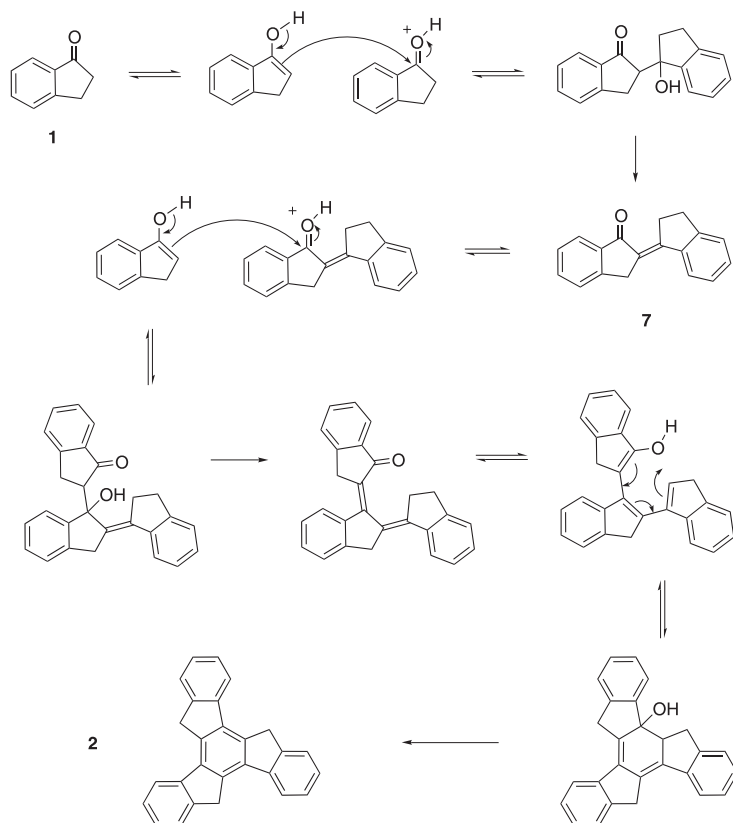


Fig. 6. Mechanism for the acid-catalyzed aldol trimerization of 1-indanone (1) to truxene (2).

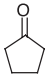
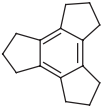
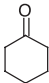
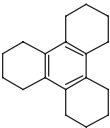
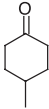
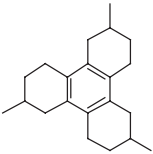
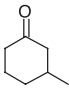
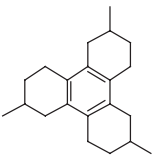
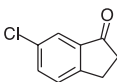
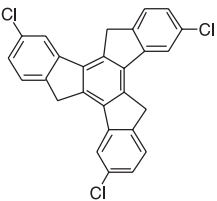
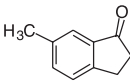
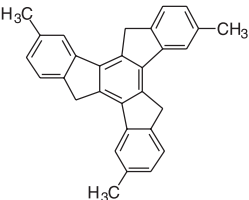
polyphosphoric acid [18], polyphosphate ethyl ester [19], *para*-toluenesulfonic acid [20], and pyridinium hydrochloride [20]. While most of these reactions give truxene in good yield, the best synthesis appears to be that of Dehmlow [14], which is reported to give truxene in 98 % yield by heating 1 in a 2:1 mixture of hydrochloric acid and acetic acid at 100 °C for 16 hours. The mechanism proposed for the acid-catalyzed trimerization of 1-indanone to truxene is outlined in Figure 6.

1.3 Other Examples

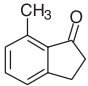
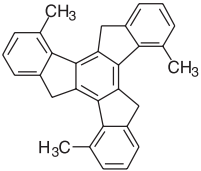
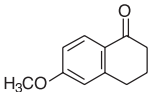
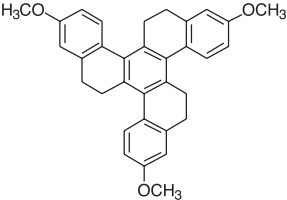
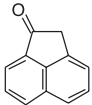
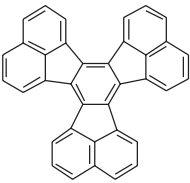
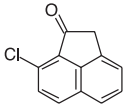
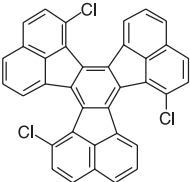
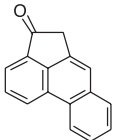
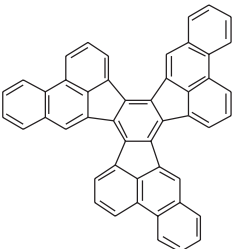
Truxene and truxone were the first members of what is now a large family of tris-annulated benzenes that have been synthesized by aldol trimerizations of cyclic ketones during the past 125 years. Table 1 provides some additional representative examples [6, 10, 21–29].

This list is undoubtedly incomplete; however, some general observations can be made on the basis of just these examples. First, it should be noted that good yields of cyclic trimers

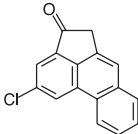
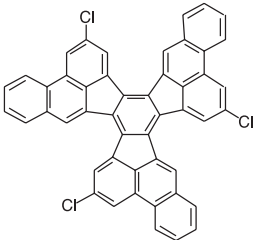
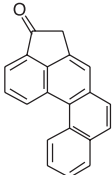
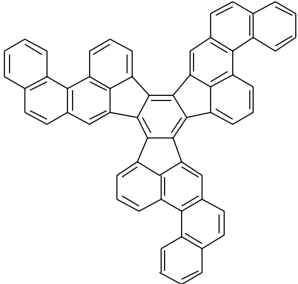
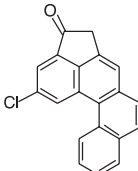
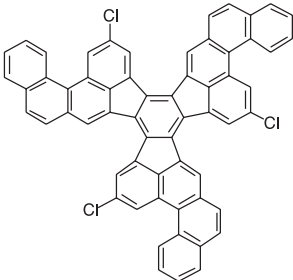
Tab. 1. Other representative cyclic ketones and their trimeric aldol condensation products.

<i>Ketone</i>	<i>Trimer</i>	<i>Reaction Conditions</i>	<i>Yield</i>	<i>Ref.</i>
 8	 9	1. SiCl_4 2. HCl	65 %	21
 10	 11	1. $350\text{ }^\circ\text{C}$, 2 h 2. HOAc , HCl(g)	91 %	22
 12	 13	1. NaOH , $25\text{ }^\circ\text{C}$, 4 d 2. H_2SO_4 , MeOH , 1 h 3. $350\text{ }^\circ\text{C}$, 1 h	64 %	23
 14	 15	1. NaOH , $25\text{ }^\circ\text{C}$, 4 d 2. H_2SO_4 , MeOH , 1 h 3. $350\text{ }^\circ\text{C}$, 1 h	53 %	23
 16	 17	Conc. HCl $100\text{ }^\circ\text{C}$	not given	18
 18	 19	ZnCl_2	not given	18

Tab. 1. (continued)

Ketone	Trimer	Reaction Conditions	Yield	Ref.
 <p>20</p>	 <p>21</p>	TiCl_4 , $\text{Cl}(\text{CH}_2)_4\text{Cl}$ $164\text{ }^\circ\text{C}$, 30 min	14 %	24
 <p>22</p>	 <p>23</p>	1. TiCl_4 , Et_3N , $-5\text{ }^\circ\text{C}$ 2. $25\text{ }^\circ\text{C}$, 17 h	41 %	25
 <p>24</p>	 <p>"decacyclene" 25</p>	anthranilic acid heat	not given	26
 <p>26</p>	 <p>27</p>	TiCl_4 $o\text{-C}_6\text{H}_4\text{Cl}_2$ $180\text{ }^\circ\text{C}$	25 %	6
 <p>28</p>	 <p>29</p>	TiCl_4 $\text{ClCH}_2\text{CH}_2\text{Cl}$ $83\text{ }^\circ\text{C}$, 75 min	95 %	27, 28

Tab. 1. (continued)

Ketone	Trimer	Reaction Conditions	Yield	Ref.
 30	 31	TiCl_4 $o\text{-C}_6\text{H}_4\text{Cl}_2$ $100\text{ }^\circ\text{C}$, 2 h	83 %	28
 32	 33	TiCl_4 $o\text{-C}_6\text{H}_4\text{Cl}_2$ $100\text{ }^\circ\text{C}$, 1 h	80 %	10, 28
 34	 35	TiCl_4 $o\text{-C}_6\text{H}_4\text{Cl}_2$ $100\text{ }^\circ\text{C}$, 2 h	85 %	28, 29

have been obtained not only with five-membered- but also with six-membered ring ketones, at least in some cases (e.g., cyclohexanone, **10**).

It is equally noteworthy that both aliphatic and aromatic ketones undergo the aldol trimerization reaction.

For all but the most symmetrical trimers, two distinct cyclocondensations can be identified as potential synthetic routes starting from two isomeric ketones (e.g., **13** = **15**).

Finally, as one might expect, aldol trimerizations that lead to sterically crowded products generally fail or give the trimer only in modest yield (e.g., **21** and **27**, the quoted yields for which represent optimized values). The high degree of regioselectivity seen in the trimeri-

zation of 3-methylcyclohexanone (**14**) is another manifestation of this same effect. We examine this limitation in more detail below.

1.4

Limitations

1.4.1

Experimental Observations and a Working Hypothesis

The 3,9,15-trichloro derivative of “decacyclene” (**27**, Table 1) has proven to be a superb precursor for the synthesis of “circumtriindene,” a bowl-shaped $C_{36}H_{12}$ PAH (geodesic dome) that constitutes 60 % of C_{60} [6]. Unfortunately, the aldol trimerization of 8-chloroacenaphthenone (**26**, Table 1) gives the tris-annulated benzene **27** in only 25 % yield, even after extensive optimization of the reaction conditions [6]. It appears that the energetic cost of forcing three large chlorine atoms into the crowded fjord regions of the molecule diverts the reaction toward unwanted by-products. The *extra* strain energy contributed by the introduction of these three chlorine atoms to the decacyclene ring system is estimated to be about 17 kcal mol^{-1} on the basis of homodesmotic density functional calculations [30, 31].

This steric effect is even more dramatic in the next higher member of the series. Thus, whereas 4-acephenanthrenone (**28**) trimerizes to tribenzo[*a,l,w*]decacyclene (**29**) in almost quantitative yield under relatively mild conditions [27, 28], the chlorinated derivative **36** gives no more than traces of the cyclic trimer under a wide range of experimental conditions [28]. The only low molecular weight product isolated in the latter case (57 % yield + recovered starting material) is the acyclic aldol dimer **37** (Figure 7). $TiCl_4$ -catalyzed aldol condensation of the bromo analogue of **36** likewise stops after the first step, giving the corresponding dimer in 95 % yield [28].

It did not go unnoticed in the above cases in which the trimerizations failed that the dimers obtained are the β,γ -unsaturated enones and not the conjugated products that one might have expected to be thermodynamically more stable. Similar behavior had previously been observed for α -tetralone (**38**), which also gives a β,γ -unsaturated enone in high yield rather than the cyclic trimer when treated with $TiCl_4$ (Figure 8) [4].

In sharp contrast to these results, we obtained a pair of *E*- and *Z*- α,β -unsaturated ketones when the condensation of **28** was conducted under sufficiently mild conditions [32] such

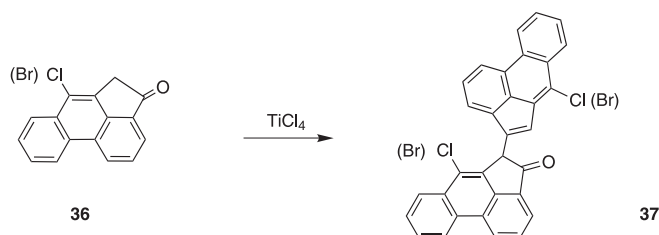


Fig. 7. 6-Chloro-4-acephenanthrenone (**36**) gives the β,γ -unsaturated aldol dimer (**37**), which does not continue on to form the cyclic trimer; 6-bromo-4-acephenanthrenone behaves identically.

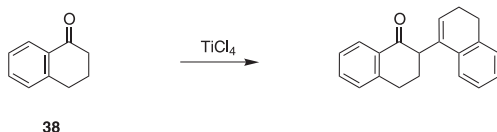


Fig. 8. α -Tetralone (**38**) gives the β,γ -unsaturated aldol dimer, which does not continue on to form the cyclic trimer.

that it terminated at the dimer stage [28]. Furthermore, careful examination of the ^1H NMR spectra recorded during the condensation of **26** showed signals that could be attributed to two stereoisomeric conjugated enone intermediates. On the basis of these admittedly limited observations, we began formulating and scrutinizing the following empirical working hypothesis:

Formation of an α,β -unsaturated (conjugated) dimer from a cyclic ketone is vital to the success of an aldol trimerization reaction for the synthesis of a tris-annulated benzene; the reaction will fail with ketones that form only β,γ -unsaturated (unconjugated) dimers.

In agreement with this hypothesis, α,β -unsaturated aldol dimers have been reported for many of the cyclic ketones discussed above that are known to proceed to tris-annulated benzene rings under appropriate cyclotrimerization conditions. Thus, in addition to the acenaphthenone derivatives **26** and **28** just mentioned, 1-indanone (**2**) and indane-1,3-dione (**5**), the precursors to “truxene” and “truxone” (Figures 2 and 3), have both been reported to give exclusively the α,β -unsaturated aldol dimers when the trimerization is suppressed [33, 34]. Because of symmetry, the latter (**5**) gives a single dimer, whereas the former (**2**) gives a pair of conjugated enones (*E*- and *Z*-isomers). Acenaphthenone itself (**24**) likewise gives only an α,β -unsaturated dimer (stereochemistry not determined) [35]. The aldol condensations of cyclopentanone (**8**) and cyclohexanone (**10**) can also be arrested at the dimer stage, and each of these ketones gives a mixture of both the α,β - and the β,γ -unsaturated aldol dimers, with the conjugated enones dominating under equilibrating conditions [36]. Thus, we were gratified to find a considerable body of experimental data that is consistent with our hypothesis.

Are there any fundamental chemical principles that make this empirical hypothesis mechanistically reasonable? We believe there are. Looking back at Figure 6, one can identify two key bond-forming steps that bring together the three ketone molecules into a single acyclic trimer. Both steps are acid-catalyzed aldol condensation reactions, in which the enol of the starting ketone serves as the nucleophile. The electrophilic partners in these two steps are, respectively, the protonated monomer ketone (**1**) and the protonated dimer ketone (**7**). Obviously, any factor that favors the second of these two reactions (dimer \rightarrow trimer) over the first (monomer \rightarrow dimer) will set the stage for a cyclization and dehydration to the desired tris-annulated benzene. Conversely, if the first aldol step is fast relative to the second one, all of the monomer will be converted to the dimer, but there will then be no more monomer left to serve as the nucleophilic partner for the second aldol step, and the reaction will terminate at the acyclic dimer stage.

Since, at a given concentration of acid [37], a conjugated enone will be more extensively protonated than a ketone that lacks the extra α,β -unsaturation (e.g., $7\cdot\text{H}^+/7$ vs. $1\cdot\text{H}^+/1$), it is mechanistically reasonable that the dimer \rightarrow trimer step should be favorable for cyclic ketones that form α,β -unsaturated (conjugated) dimers. On the other hand, β,γ -unsaturated al-

dol dimers are less likely to make it all the way to the trimer because they are: (1) less fully protonated, and (2) more hindered than the starting ketone with which they must compete for the nucleophile. Thus, both halves of our hypothesis make sense.

To be useful, of course, a hypothesis must have predictive value. Can one predict in advance whether the aldol dimer from a particular ketone will be α,β -unsaturated or β,γ -unsaturated?

1.4.2

Guidance from Calculations

We have performed single-point energy calculations, using density functional theory with AM1 optimized geometries (pBP/DN**//AM1) [31], on many of the ketones discussed above that are known to give tris-annulated benzenes by the aldol trimerization reaction (**1**, **5**, **8**, **10**, **22**, **24**, **26**, and **28**). In agreement with our hypothesis, the α,β -unsaturated aldol dimer is calculated to be more stable than the β,γ -unsaturated isomer in every case, sometimes by as much as 10 kcal mol⁻¹ or more. In those cases in which the α,β -unsaturated aldol dimer can adopt either an *E*- or a *Z*-configuration, the more stable of the two was used for the comparison.

The tris-annulated benzene **40** is a particularly interesting example. As in many cases, one may envisage two ways of assembling this molecule by aldol trimerizations. We have attempted to prepare this obviously strained PAH derivative by subjecting both chloro ketones **36** and **39** to TiCl₄ under a range of conditions [28]. The former gives almost exclusively the β,γ -unsaturated dimer (**37**, Figure 7), with no more than traces of **40** being formed under any of the conditions we examined. The isomeric chloro ketone **39**, on the other hand, gives significant quantities of **40** (Figure 9). Unfortunately, the yield of **40** obtained from the aldol trimerization of **39** is still too low to be synthetically useful, presumably due to steric factors at a later stage in the process. Nevertheless, this pair of reactions serves as an excellent illustration of the predictive power of our working hypothesis coupled with reliable energy calculations. At the pBP/DN**//AM1 level of theory, the most stable aldol dimer of chloro ketone **36** is the β,γ -unsaturated isomer, which our hypothesis predicts will resist further condensation to give **40**, and that is exactly what we observe. Conversely, calculations find the most stable aldol dimer for chloro ketone **39** to be the (*Z*)- α,β -unsaturated isomer, which our hypothesis identifies as a viable intermediate to continue on to **40**, and this chloro ketone does indeed give the tris-annulated benzene **40**.

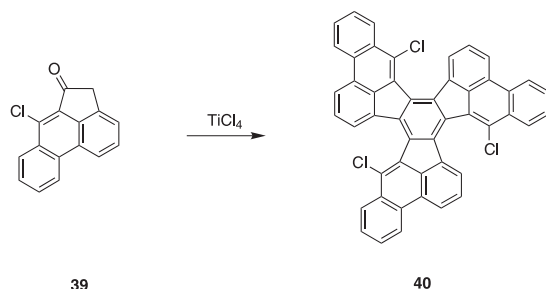


Fig. 9. Aldol trimerization of 6-chloro-5-acephenanthrenone (**39**) to form a tris-annulated benzene. This behavior contrasts sharply with that of the closely related 6-chloro-4-acephenanthrenone (**36**) in Figure 7.

The only exception that we have encountered so far to predictions based on this analysis is the aldol trimerization of α -tetralone (**38**). At the level of theory used above (pBP/DN**//AM1), the most stable aldol dimer is found to be the (*E*)- α,β -unsaturated isomer, which, according to our hypothesis, should condense further and cyclize to the tris-annulated benzene product. Experimentally, however, α -tetralone (**38**) gives a high yield of the β,γ -unsaturated aldol dimer (Figure 8), which was calculated to be one of the less stable isomers. This “failure” must be either a shortcoming of our hypothesis or a shortcoming of the energy calculations. To test the latter possibility, we recalculated the energies of the aldol dimers of α -tetralone (**38**), still at the pBP/DN** level of density functional theory but this time with full geometry optimization at the pBP/DN** level of theory. These calculations required considerably more computer time than the original pBP/DN**//AM1 calculations, which use approximate geometries based on a fast semiempirical method (AM1), but at this higher level of theory the β,γ -unsaturated aldol dimer of α -tetralone is found to be the lowest energy isomer. This lone “failure” can therefore be attributed to erroneous energy calculations, rather than to a flaw in the hypothesis. It is worth noting that, unlike α -tetralone, the 6-methoxy derivative of α -tetralone (**22**, Table 1), *does* yield a tris-annulated benzene (**23**) by the aldol trimerization reaction. In harmony with our hypothesis, the α,β -unsaturated dimer (*E*-isomer) of **22** is calculated to be more stable than the β,γ -unsaturated dimer at the pBP/DN** level of theory.

1.5

Conclusions

The aldol trimerization reaction has proven its value as a tool in organic synthesis. Many large PAHs can be assembled easily in one step from smaller, less complex starting materials by this method. For most unhindered cyclic ketones, there is rarely much difficulty with the first step (self-aldol) in the triple dehydration progression of monomer \rightarrow dimer \rightarrow trimer \rightarrow tris-annulated benzene (Figure 6). Likewise, the third step (cyclization–aromatization) is often very good (Figure 6), although steric impediments will generally lead to diminished yields. For this reaction cascade to succeed, however, the second step (cross-aldol of the monomer ketone with the dimer ketone) must also be kinetically competitive. Herein, we have presented empirical evidence and mechanistic arguments to support the view that this requirement will be met only in those cases that lead to α,β -unsaturated (conjugated) dimers in the initial aldol condensation. Those ketones that give only β,γ -unsaturated (unconjugated) dimers in the initial aldol condensation will not yield tris-annulated benzenes (e.g., Figures 7 and 8).

In an attempt to derive some predictive power from this hypothesis, we have demonstrated how cases that are destined to fail at the second step can be identified in advance by relatively straightforward energy calculations on the isomeric aldol dimers. The number of examples is still limited, so one must use this hypothesis with caution, but we have so far found no exceptions.

Acknowledgements

We thank Stefan Hagen, Brandon J. McMahon, and John P. Amara for their contributions to our understanding of this chemistry and to the NSF for financial support.

References

- 1 D. LOGUERCIO, JR., Ph.D. Dissertation, UCLA, 1988.
- 2 C. FABRE, A. RASSAT, *C. R. Acad. Sci., Ser.* **2 1989**, 308, 1223–1228.
- 3 F. SBROGIO, F. FABRIS, O. DE LUCCHI, *Synlett* **1994**, 761–762.
- 4 S. HAGEN, L. T. SCOTT, *J. Org. Chem.* **1996**, 61, 7198–7199.
- 5 L. T. SCOTT, M. S. BRATCHER, S. HAGEN, *J. Am. Chem. Soc.* **1996**, 118, 8743–8744.
- 6 R. B. M. ANSEMS, L. T. SCOTT, *J. Am. Chem. Soc.* **2000**, 122, 2719–2724.
- 7 G. MEHTA, G. PANDA, P. V. V. S. SARMA, *Tetrahedron Lett.* **1998**, 39, 5835–5836.
- 8 M. SAROBE, R. H. FOKKENS, T. J. CLEIJ, L. W. JENNEKENS, N. M. M. NIBBERING, W. STAS, C. VERSLUIS, *Chem. Phys. Lett.* **1999**, 313, 31.
- 9 B. GOMEZ-LOR, O. DE FRUTOS, A. M. ECHAVARREN, *Chem. Commun.* **1999**, 2431–2432.
- 10 M. M. BOORUM, Y. V. VASIL'EV, T. DREWELLO, L. T. SCOTT, *Science* **2001**, 294, 828–831.
- 11 M. J. PLATER, *Synlett* **1993**, 405–406.
- 12 S. GABRIEL, A. MICHAEL, *Ber. Dtsch. Chem. Ges.* **1877**, 10, 1551–1562.
- 13 W. WISLICENUS, *Ber. Dtsch. Chem. Ges.* **1887**, 20, 589–595.
- 14 E. V. DEHMLOW, T. KELLE, *Synth. Commun.* **1997**, 27, 2021–2031.
- 15 J. HAUSMANN, *Ber. Dtsch. Chem. Ges.* **1889**, 22, 2019–2026.
- 16 F. S. KIPPING, *J. Chem. Soc.* **1894**, 65, 269–289.
- 17 F. S. KIPPING, *J. Chem. Soc.* **1894**, 65, 480–503.
- 18 R. SEKA, W. KELLERMANN, *Ber. Dtsch. Chem. Ges.* **1942**, 75, 1730–1738.
- 19 J. CHENAULT, C. SAINSON, M. G. CHAMPETIER, *Comptes Rendus* **1978**, 287, 545–547.
- 20 T. W. WARMERDAM, R. J. M. NOITE, W. DRENTH, J. C. VAN MILTENBURG, D. FRENKEL, R. J. J. ZIJLSTRA, *Liquid Crystals* **1988**, 3, 1087–1104.
- 21 S. S. ELMORSY, A. PELTER, K. SMITH, *Tetrahedron Lett.* **1991**, 32, 4175–4176.
- 22 S. V. SVETOZARSKII, G. A. RAZUVAEV, E. N. ZIL'BERMAN, G. S. VOLKOV, *J. Gen. Chem. USSR* **1960**, 30, 2023–2027.
- 23 S. V. SVETOZARSKII, E. N. ZIL'BERMAN, G. A. RAZUVAEV, *J. Gen. Chem. USSR* **1959**, 29, 1428–1431.
- 24 S. HAGEN, L. T. SCOTT, unpublished results.
- 25 A. N. PYRKO, *Zh. Org. Khim.* **1992**, 28, 215–216.
- 26 J. MOSZEW, W. ZANKOWSKA-JASINSKA, *Roczniki Chemii* **1958**, 32, 225–233.
- 27 B. J. McMAHON, B.Sc. Thesis, Boston College, 1997.
- 28 M. M. BOORUM, Ph.D. Dissertation, Boston College, 2001.
- 29 L. T. SCOTT, M. M. BOORUM, B. J. McMAHON, S. HAGEN, J. MACK, J. BLANK, H. WEGNER, A. DE MEIJERE, *Science*, **2002**, 295, 1500–1503.
- 30 Homodesmic reaction:
 $25 + 3(\text{C}_6\text{H}_5\text{Cl}) \rightarrow 27 + 3(\text{C}_6\text{H}_6)$.
 Calculation performed at the pBP/DN** level of theory with full geometry optimization using the Spartan collection of programs [31].
- 31 Spartan 5.0, Wavefunction, Inc., Irvine, CA.
- 32 A. G. HOLBA, V. PREMASAGER, B. C. BAROT, E. J. EISENBRAUN, *Tetrahedron Lett.* **1985**, 26, 571–574.
- 33 P. J. WILLIAMS, *J. Chem. Soc., Chem. Commun.* **1967**, 719–720.
- 34 K. JACOB, M. SIGALOV, J. Y. BECKER, A. ELLERN, V. KHODORKOVSKY, *Eur. J. Org. Chem.* **2000**, 2047–2055.
- 35 J. TATSUGI, M. OKUMURA, *Bull. Chem. Soc. Jpn.* **1978**, 51, 1227–1228.
- 36 S. D. MEKHTIEV, M. R. MUSAIEV, A. G. GASANOV, *Azerb. Khim. Zh.* **1971**, 93–97.
- 37 Homodesmic reaction:
 $7 + 1 \cdot \text{H}^+ \rightarrow 7 \cdot \text{H}^+ + 1$ ($\Delta H_{\text{calc}} = -13.5$ kcal mol⁻¹). Calculation performed at the pBP/DN**//AM1 level of theory using the Spartan collection of programs [31].

2

Oligounsaturated Five-Membered Carbocycles – Aromatic and Antiaromatic Compounds in the Same Family

Rainer Haag and Armin de Meijere

Abstract

Most compounds containing oligounsaturated five-membered carbocycles ranging from cyclopentadiene to C_{20} fullerene display interesting electronic and structural properties. This chapter describes recent developments in this area, starting with stabilized cyclopentadienyl cations, then discusses several fulvenes as well as spiroannulated cyclopentadiene derivatives and eventually linearly as well as angularly fused oligocyclic five-membered ring systems. Among these oligounsaturated di-, tri-, and oligoquinanes, the features of the rather unstable pentalene and acepentalene are discussed with respect to their generation and electronic ground states. Structural properties, including those of the stable dilithium diides as well as several metal complexes are presented. Finally, the generation and characterization of the highly unstable C_{20} fullerene, which sets a new benchmark for this class of molecules, are highlighted.

2.1

Introduction

The chemistry of oligounsaturated five-membered carbocycles has fascinated chemists for more than 100 years, since Thiele published the first synthesis of the aromatic cyclopentadienyl (Cp) anion 1^- [1]. In the last couple of decades, knowledge about fully unsaturated oligoquinanes, the class of fused-ring compounds consisting of five-membered rings only, has experienced an exceptional growth (Figure 1) [2, 3]. Only recently has the existence of C_{20} -fullerene **4**, which is the smallest conceivable fullerene and can be considered as the Mount Everest of oligoquinanes, been proved [4]. This and many other new developments in the area of oligounsaturated five-membered carbocyclic compounds are highlighted in this chapter.

Cyclopentadienide (Cp) 1^- is well known as one of the most frequently used ligands in organometallic chemistry. In addition, the cyclopentadienide anion 1^- has always been quoted as a classic example of Hückel aromaticity, to demonstrate along with benzene and the cycloheptatrienyl cation the validity of the $(4n + 2)$ π -electron rule. In contrast, a simple and stable cyclopentadienyl cation of the type 1^+ remains to be elusive [5]. With the highly unstable neutral cyclobutadiene and the cycloheptatrienyl anion, 1^+ shares the character-

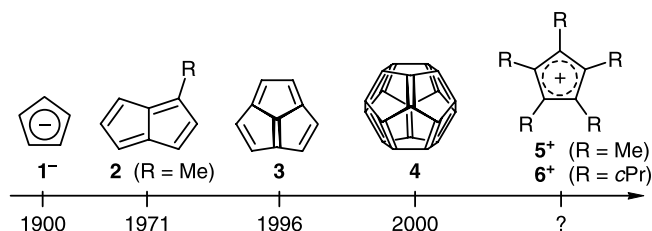


Fig. 1. The non-linear time scale for the development of cyclopentadiene chemistry in the last century.

istics of possessing $4n$ π -electrons, and thus, according to Hückel MO theory, being anti-aromatic. For higher oligoquinanes the situation is more complex, because Hückel theory is strictly valid only for monocyclic systems. Hence, reliable predictions concerning the electronic ground states are possible only on the basis of highest level *ab initio* calculations.

2.2

Cyclopentadienyl Cations

The parent cyclopentadienyl cation 1^+ has been calculated at various levels of theory [6, 7], and has been found to have a triplet ground state. Its existence as a triplet species in an SbF_5 matrix at 75 K had previously been proved by ESR spectroscopy [8]. Prior to that, the pentachlorocyclopentadienyl cation 7^+ (Figure 2) had been generated, also in an SbF_5 matrix at 77 K, and identified as a triplet on the basis of its observable ESR spectrum [9]. The pentarylcyclopentadienyl cations 8^+ [10], especially those with donor-substituted aryl substituents [11], are stable in solution up to 233 K, coexisting as singlet and triplet species due to the small energy difference between them.

About 30 years later, the penta-isopropylcyclopentadienyl cation (9^+) was generated from the corresponding chloride and bromide and proved to be stable in the frozen solution at 115 K, existing as a triplet [12]. Penta-isopropylcyclopentadiene is unique in that it not only forms a stable anion – which is aromatic, just like any other cyclopentadienide – but also a persistent radical that has been characterized by ESR/ENDOR, ^1H NMR spectroscopy, and mass spectrometry, as well as by X-ray crystal structure analysis [12].

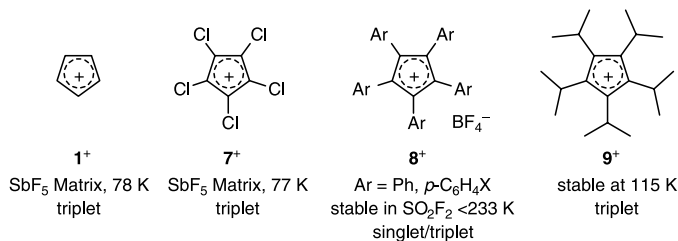
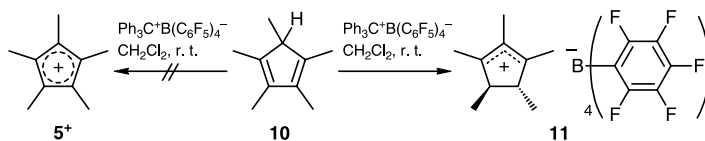


Fig. 2. Previously known cyclopentadienyl cations.

What looked like a breakthrough towards the simple pentamethylcyclopentadienyl (Cp^*) cation 5^+ which was believed to be generated as the tetrakis(pentafluorophenyl)borate salt by hydride abstraction from pentamethylcyclopentadiene (**10**), [5a] soon turned out to be a misinterpretation of the X-ray crystal structure analysis. The observed structural characteristics of the obtained crystals, which were stable at room temperature for weeks, with two pyramidal carbon atoms in the five-membered ring, are simply those of a cyclic trimethylallyl cation **11** bridged by a slightly shortened single bond (1.48 Å). [5b–e] The solid state ^{13}C -NMR spectrum of **11** reflects the nonequivalence of the five ring carbons, with two signals (C2,5) in the cationic region (243 and 250 ppm) and that of C1 at 153 ppm. Thus, rather than undergoing a hydride abstraction to yield 5^+ ($\text{R}=\text{Me}$), **10** had been protonated to give the cyclopentenyl cation **11** (Scheme 1).



Scheme 1.

Since the cyclopropyl group is well known to be a particularly good donor for electron-deficient centers, cyclopropyl-substituted cyclopentadienyl cations ought to be more stable than those with any other alkyl substituent. Indeed, the singlet pentacyclopropylcyclopentadienyl cation 6^+ was predicted by DFT computations at the B3LYP/3-31+G** level of theory to be 19.4 kcal mol $^{-1}$ more stable than the pentaisopropylcyclopentadiene singlet cation 9^+ and 29.3 kcal mol $^{-1}$ more stable than the Cp^* singlet cation 5^+ (Figure 3) [7].

The best potential precursors of the pentacyclopropylcyclopentadienyl cation 6^+ have recently been prepared. The Grignard reagent **13**, which was obtained by hydromagnesiation of easily accessible dicyclopropylacetylene (**12**), gave, upon reaction with butyl formate and

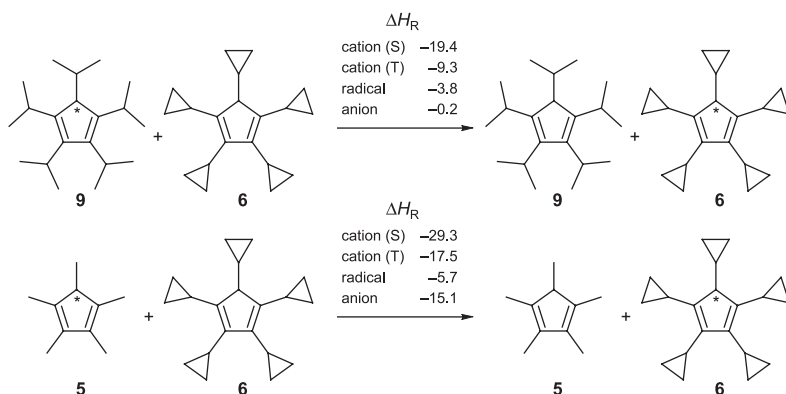
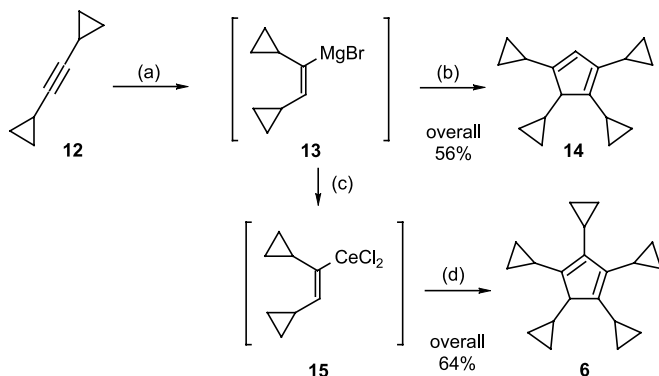


Fig. 3. Isodesmic stabilization energies of pentasubstituted cyclopentadienyl species (all structures fully optimized at the B3LYP/6-31G* level).

methyl cyclopropanecarboxylate – for the latter reaction after prior addition of cerium(III) chloride – tetracyclopropyl- (**14**) and pentacyclopropylcyclopentadiene (**6**), respectively, in good yields (Scheme 2) [13].

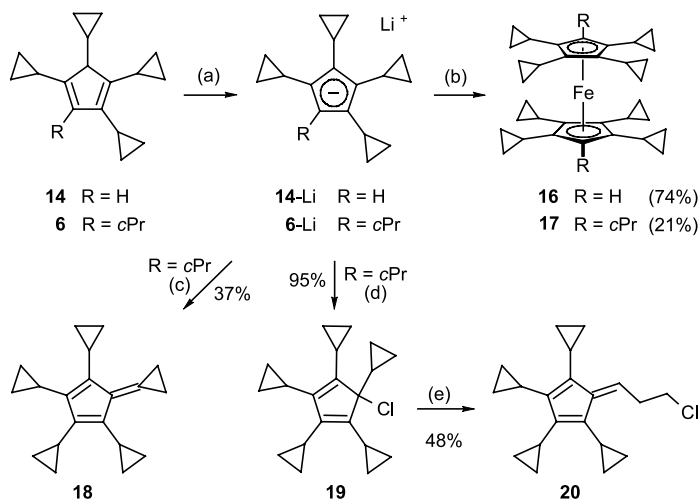


Scheme 2. (a) $i\text{BuMgBr}$ (1 equiv.), Cp_2TiCl_2 (1–2 mol %), Et_2O , 20°C , 30 min. – (b) Add inversely to HCO_2nBu (0.9 equiv.) in THF, 20°C , 1 h. – (c) Add inversely to a suspension of CeCl_3 (1.5 equiv.) in THF, 20°C , 1 h. – (d) 1) Add $c\text{PrCO}_2\text{Me}$ in THF, 20°C , 1 h; 2) $\text{H}_2\text{O}/\text{HOAc}$ (6:1).

Upon treatment with an ethereal solution of methyllithium, both oligocyclopropyl-substituted cyclopentadienes **14** and **6** in tetrahydrofuran were quantitatively deprotonated to the corresponding cyclopentadienides **14-Li** and **6-Li**, respectively, which were characterized by their ^1H and ^{13}C NMR spectra. Treatment of the solutions of **14-Li** and **6-Li** with solutions of iron(II) chloride in tetrahydrofuran yielded the 1,1',2,2',3,3',4,4'-octacyclopropylferrocene (**16**) (74%) and the decacyclopropylferrocene (**17**) (21%). After crystallization from hexane (for **16**) and pentane/dichloromethane (for **17**), the structures of both ferrocenes were established by X-ray crystal structure analyses (Scheme 3). The electron-donating effect of the cyclopropyl substituents on these cyclopentadiene systems is manifested in the oxidation potentials of the ferrocenes **16** and **17**. While the parent ferrocene has an oxidation potential $E_{1/2}$ (*vs.* SCE) = +0.475 V, that of dcamethylferrocene is significantly lower with $E_{1/2} = -0.07$ V, and so are those of **16** ($E_{1/2} = -0.01$ V) and **17** ($E_{1/2} = -0.13$ V) [13].

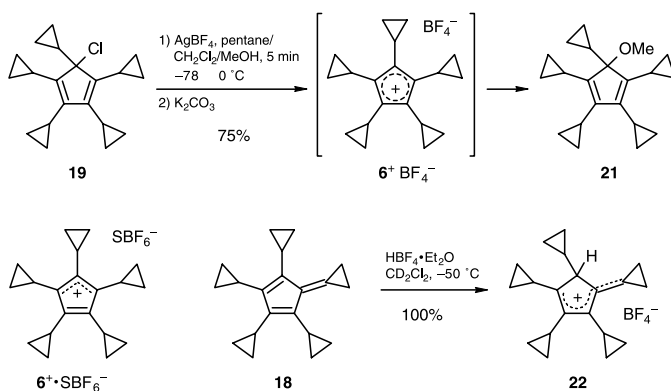
Reaction of the cyclopentadienide **6-Li** with *N*-chlorosuccinimide gave chloropentacyclopropylcyclopentadiene (**19**) in 95% yield. Hydride abstraction from **6-Li** with triphenylmethyl tetrafluoroborate yielded the interesting tetracyclopropylcyclopropylidenecyclopentadiene **18** (37%). While the chloride **19**, an ideal precursor to the cation 6^+ , is stable at ambient temperature in the absence of moisture, it rearranges upon attempted chromatography on silica gel with the opening of one cyclopropyl ring to give the tetracyclopropylfulvene **20**.

This rearrangement must occur by heterolytic cleavage of the carbon–chlorine bond in **19** to yield the intermediate cation 6^+ , which is then attacked by the nucleophilic chloride at one of the partially positively charged cyclopropyl groups. With the less nucleophilic tetrafluoroborate counterion, generated by treating **19** with silver tetrafluoroborate under sol-



Scheme 3. (a) MeLi (1 equiv.) in Et₂O, THF, –78 → 20 °C, 45 min. – (b) Add to FeCl₂·2THF in THF, 0 → 20 °C, reflux, 5 h. – (c) Ph₃CBF₄, THF. – (d) NCS, 0–20 °C, 20 h. – (e) SiO₂, pentane.

volytic conditions (in pentane/CH₂Cl₂/MeOH), $6^+ \cdot \text{BF}_4^-$ survives even at 0 °C and is trapped by methanol to give the methyl ether **21** without rearrangement in 75% yield (Scheme 4). The cation 6^+ does indeed appear to be stable—at least at –115 °C—in a non-nucleophilic solvent such as SO₂ClF/SO₂F₂, when generated with a weakly coordinating counterion, e.g. by treatment of the chloride **19** with an excess of SbF₅ [7]. The observed ¹³C-NMR signals are best interpreted with the singlet structure $6^+ \cdot \text{SbF}_6^-$ (Scheme 4). Quenching the solution with methanol at –196 °C and basic work-up at ambient temperature gave the methyl ether **21** in 40% yield.



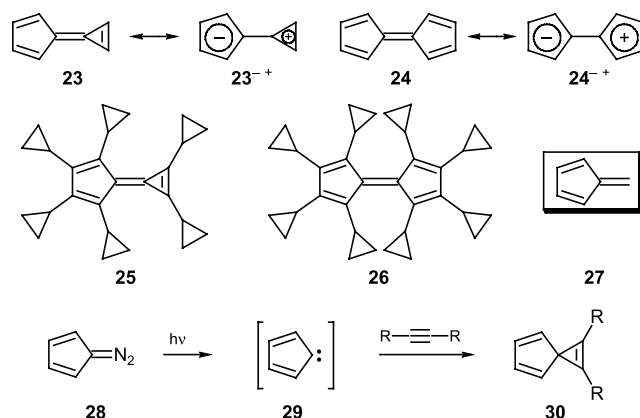
Scheme 4. The relatively stable pentacyclopropylcyclopentadienyl cation $6^+ \cdot \text{SbF}_6^-$ and the related fulvenyl cation $22^+ \cdot \text{BF}_4^-$.

The remarkable stabilizing effect of the cyclopropyl substituents is also illustrated by the fact that the fulvene **18**, upon protonation with tetrafluoroboric acid in dichloromethane, yields the fulvenyl tetrafluoroborate **22**, which is completely stable in solution at $-50\text{ }^{\circ}\text{C}$. Compound **22** could be characterized by NMR spectroscopy (^1H and ^{13}C) and survives at ambient temperature for several days.

2.3

Fulvene and Spiroannellated Cyclopentadiene Derivatives

The chemistry of the so-called calicene **23** and its stable derivatives has recently been reviewed [14, 15], as has that of pentafulvalene **24** and its derivatives [14]. In view of the possible stabilization of at least the cationic moieties in the zwitterionic resonance structures 23^{-+} and 24^{-+} , it would certainly be interesting to prepare the pericyclopropylated hydrocarbons **25** and **26**. The easily accessible tetracyclopropylcyclopentadiene **14** [13] appears to be an appropriate precursor for these target molecules (Scheme 5).

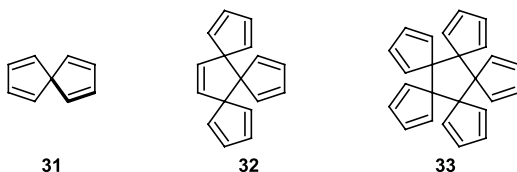


Scheme 5.

Common to these molecules with their cyclopentadiene moieties is the so-called fulvene subunit **27**. The first fulvenes, 6,6-dialkylfulvenes, were prepared as early as 1906 by Thiele et al. from sodium cyclopentadienide and ketones [16]. The parent hydrocarbon **27** and many other derivatives have been thoroughly studied since the 1960s [17–19]. Diazocyclopentadiene (**28**), which is also easily prepared from cyclopentadienide, is a heteroanalogue of fulvene. It has frequently been used as a precursor to other theoretically interesting molecules containing annellated cyclopentadiene moieties, because its irradiation readily generates the cyclopentadienylidene **29**. This carbene has, for example, been trapped with alkynes to form spiro-annellated cyclopentadiene derivatives **30** (Scheme 5) [20]. It has been proved by UV spectroscopy [21] and supported by calculations [22] that these spiro[2.4]heptatrienes (so-called [1.2]spirenes) **30** experience a special kind of electronic

interaction, so-called spiroconjugation, across their central sp^3 carbon atom in spite of the orthogonal orientation of the two π -systems.

As far as purely five-membered carbocyclic systems are concerned, spiro[4.4]nonatetraene (**31**) is the prototypical example of two π -systems experiencing electronic interaction through their common central carbon atom. Based on symmetry considerations, it was proposed that spiroconjugation in molecules such as **31** should result in a splitting of the cyclopentadienyl HOMOs, whereas the LUMOs should be degenerate [22, 23]. As a consequence, the first electronic absorption (EA) band of cyclopentadiene in **31** was predicted to be split into a lower and a higher lying component of quite different absorptivities.



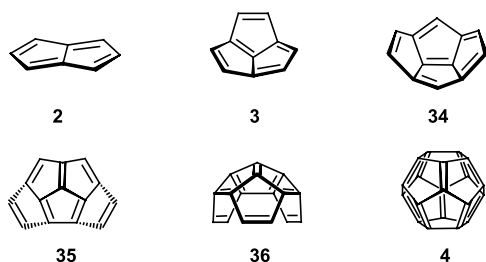
Rather recently, the electronic structure of spiro[4.4]nonatetraene (**31**), as well as those of its radical anion and radical cation, respectively, have been probed by a variety of spectroscopic methods (electron transmission and energy loss in the gas phase, electronic absorption in cryogenic matrices) [24]. The extension of this concept of spiroconjugation to higher analogues of spiro[4.4]nonatetraene **31** would lead to the hydrocarbons **32** and **33**. However, no attempts to prepare these compounds have yet been reported.

2.4

Polyunsaturated Di-, Tri-, and Oligoquinanes

Fully unsaturated fused-ring compounds, consisting only of five-membered rings, contain the most highly strained π -systems conceivable. Such unsaturated di- and triquinanes and higher oligoquinanes are therefore unlikely to be found in natural sources, although saturated linear and angular triquinanes and higher oligoquinanes are known skeletons of naturally occurring sesquiterpenes. In addition to their high strain, these polyenes possess interesting electronic properties [25]. Although several groups have been and still are engaged in efforts to synthesize some of these fully unsaturated oligoquinanes [2], only three members of the series, **2** [26, 27], **3** [28], and **4** [4], have as yet actually been prepared or at least spectroscopically characterized as short-lived transients. Other members of the series have been approached synthetically, but the increasing ring strain in the series from the bicyclic pentalene **2** to C_{20} -fullerene **4** makes the higher members less and less likely to be even observable [2].

Formally, higher oligoquinanes can be derived from fulvene (**27**) by the consecutive addition of etheno bridges. This concept has actually been successfully applied in the synthesis of the antiaromatic pentalene **2** [27], but it is unlikely to be practicable for higher members of this family due to the drastic increase in ring strain. While fulvene (**27**) and pentalene **2** possess almost planar geometries [2], acpentalene (**3**) and higher fully unsaturated oligo-



quinanes **4**, **34–36** have a considerable inherent curvature, which increases with an increasing number of annelated five-membered rings. This is confirmed by high level ab initio calculations (see below). In view of this, it can safely be assumed that **3** and higher vinylogues **4**, **34–36**, if accessible at all, would each have to be made from a precursor that bears close structural resemblance to the desired fully unsaturated oligoquinane.

2.4.1

Pentalene, Pentalenediide, and Pentalene Metal Complexes

Bicyclo[3.3.0]octa-1,3,5,7-tetraene (**2**), trivially called pentalene [26, 27], is the second member in the series of fully unsaturated oligoquinanes. Hückel MO theory predicts that this planar hydrocarbon with its 8π -electron system should be an antiaromatic species [25]. 2-Methylpentalene (**37**) has been generated by a retro-Diels–Alder reaction and deposited as a film at $-196\text{ }^{\circ}\text{C}$ on a NaCl or quartz plate for its spectroscopic characterization. It rapidly dimerized upon warming the cold plates to temperatures above $-140\text{ }^{\circ}\text{C}$ [26]. Only two stable derivatives of pentalene not complexed to a metal [29], the hexaphenyl- (**38**) [30] and 2,4,7-tri-*tert*-butylpentalene (**39**) [31], have hitherto been reported (Figure 4).

The question of aromaticity versus antiaromaticity and delocalized versus localized double bonds in pentalene (**2**) dates back to 1922, when Armit and Robinson compared it with naphthalene and postulated that the former might be similarly aromatic [32, 33]. While the first synthesis of a non-fused hexaphenylpentalene (**38**) [30] provided only some clues as to the non-aromatic reactivity of the pentalene skeleton, the tri-*tert*-butyl derivative **39**, prepared and studied by Hafner et al. in great detail [31], gave a better insight. The ring-proton signals of this alkyl-substituted pentalene **39** are shifted upfield compared to those of fulvene (**27**) and other cyclic polyenes. This observation led to the conclusion that the pentalene derivative **39** should be an antiaromatic species. However, the results did not permit a distinction

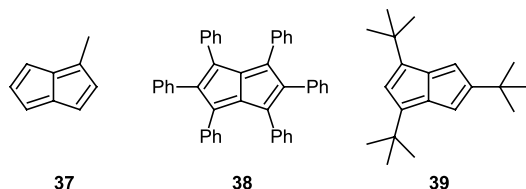
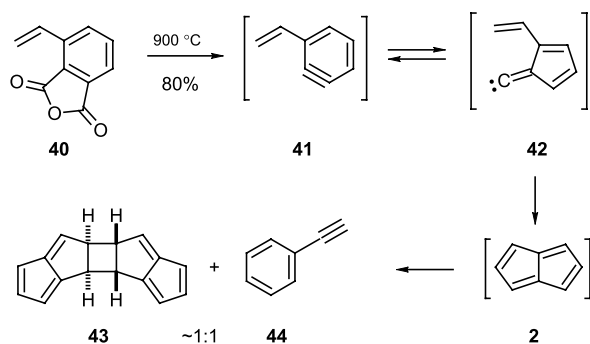


Fig. 4. An unstable and two stable pentalene derivatives that have been observed experimentally.

to be made as to whether the double bonds in **39** are localized or whether they are subject to a rapid bond shift between the two Kekulé structures. An indication that the parent system **2** has alternating bonds has been obtained by comparing the photoelectron (PE) and electronic absorption (UV/vis) data with calculated orbital energies [34]. More recent DFT calculations at the B3LYP/6-311+G*/B3LYP/6-31G* + ZPVE (B3LYP/6-31G*) level of theory have revealed that pentalene (**2**) has a localized antiaromatic π -system with a singlet ground state lying 9.7 kcal mol⁻¹ below the triplet state [35]. The calculated structural parameters of **2** and its dication **2**²⁺ (see Figure 5) appear to be quite reliable as the agreement between calculated and experimental bond lengths for pentalene dianion **2**²⁻ and its dilithium derivative **2**²⁻·2Li⁺ is excellent.

Brown et al. [36] attempted to approach pentalene (**2**) by a thermolytic ring-contraction-cyclization of 3-ethynylbenzyne **41**, which, in turn, was generated by flash vacuum thermolysis of 3-ethynylphthalic anhydride **40**. Indeed, the pentalene dimer **43** (~50%) was formed along with phenylacetylene **44** (~50%) in 80% overall yield (Scheme 6). The failure to detect monomeric pentalene (**2**) is in accord with the observation of de Mayo et al. that 1-methylpentalene (**37**) dimerizes above -140 °C [29]. The formation of phenylacetylene **44** was unexpected, and it is as yet unclear as to whether it arises by migration of two hydrogens in the aryne **41** or the intermediate carbene **42**, or whether it is a secondary product formed from pentalene (**2**).



Scheme 6.

Recently, the neutral pentalene (**2**) has been generated from its dimer **43** by photocleavage in an argon matrix [37]. In this structurally characterized cross-conjugated hydrocarbon **2**, the distortive force of the π -electrons favors a C_{2h} structure with localized single and double bonds, and this effect predominates over that of the σ -electrons, which would drive the molecule towards D_{2h} symmetry (Figure 5).

Both the synthesis [38] and X-ray crystal structure [39] of dilithium pentalenediide **2**²⁻·2Li⁺ have been reported (Scheme 7, Figure 5). Reaction of the dihydropentalene **46** with *n*-butyllithium yielded the crystalline dilithium pentalenediide **2**²⁻·2Li⁺ (Scheme 7). The more recently reported flash vacuum thermolysis of 6-norbornenylfulvene (**45**), initially producing 6-ethynylfulvene, which immediately cyclizes to dihydropentalene (**46**), allows one to prepare this immediate precursor to **2**²⁻ in gram quantities [40]. A similarly convenient

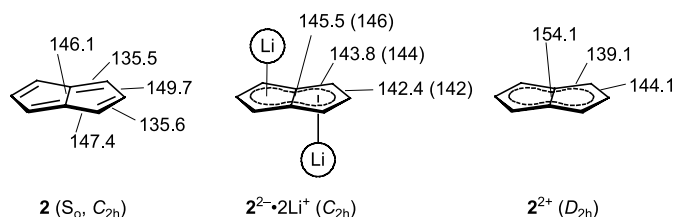
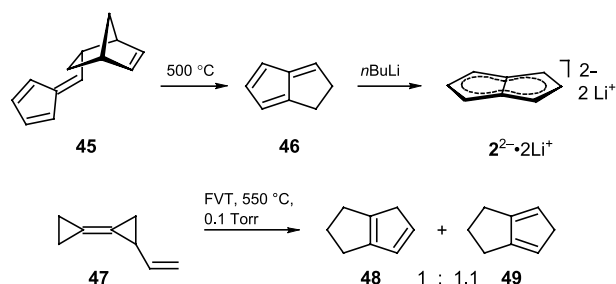


Fig. 5. Calculated structural parameters of pentalene (**2**), pentalene dianion 2^{2-} (experimental values for dilithium pentalenediide $2^{2-} \cdot 2Li^+$ in parentheses [39]), and pentalene dication 2^{2+} .



Scheme 7.

access to the pentalene skeleton is by flash vacuum thermolysis of easily prepared ethylbicyclopopylidene **47**, which yields a 1:1.1 mixture of the tetrahydropentalenes **48** and **49** (90%) [41].

Structural analysis of the dilithium pentalenediide revealed a C_{2h} -symmetric ion triplet with the two lithium cations located on opposite sides of the two fused rings. The structural parameters were extremely well reproduced by *ab initio* calculations [35] (see Figure 5). Both the experimental structural parameters and calculated magnetic susceptibility exaltation classify the 10π -electron species 2^{2-} as an aromatic compound. Apparently, the lithium counterions in $2^{2-} \cdot 2Li^+$ do not exert any significant effect on the bond lengths of the dianion 2^{2-} . On the other hand, the antiaromatic pentalene (**2**) and its aromatic dication 2^{2+} show the characteristic bond length alternation (Figure 5) [35].

The first metal complex (**50**) of unsubstituted pentalene (**2**) was prepared in 1973 by reaction of the pentalene [2+2] dimer **43** with Fe_2CO_9 (Figure 6) [42]. Several other dinuclear complexes of **2** have been prepared from the dilithium pentalenediide $2^{2-} \cdot 2Li^+$ [43]. In all

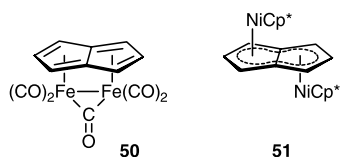
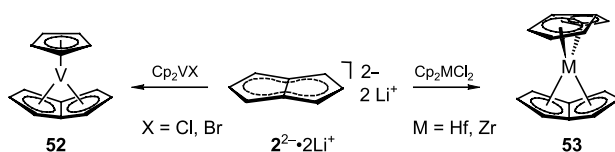


Fig. 6. Dinuclear pentalene complexes.

these complexes, the pentalene ligand is completely planar, and each five-membered ring is coordinated to a different metal atom either as in **50** or as in bis(pentamethylcyclopentadienylnickel)pentalene **51**, which was obtained by reaction of $2^{2-} \cdot 2\text{Li}^+$ with $\text{Cp}^*\text{Ni}(\text{acac})$ [44].

More recently, Jonas et al. presented a new mode of complexation of the pentalene ligand, in which all eight carbon atoms are coordinated to only one metal atom (Scheme 8). Dilithium pentalenediide $2^{2-} \cdot 2\text{Li}^+$ reacts with Cp_2VCl to yield the vanadium pentalene-Cp complex **52** [45]. Reaction with Cp_2ZrCl_2 or Cp_2HfCl_2 gives the bis(pentalene) metal complexes **53** [45b]. In these complexes, all the carbon–metal bonds have similar lengths and the out-of-plane deformation angle of the pentalene skeleton is ca. 43° .



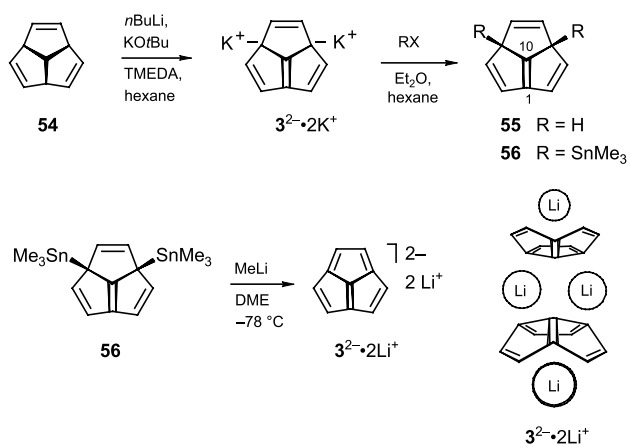
Scheme 8.

2.4.2

Acepentalene, Acepentalenediide, and Acepentalene Metal Complexes

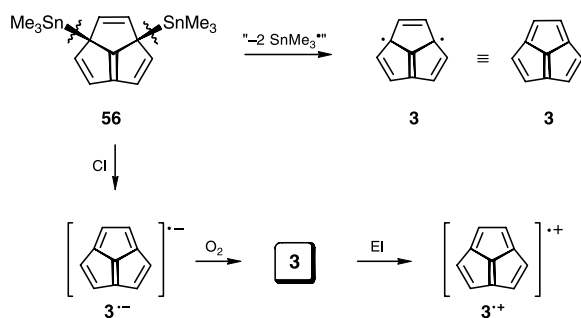
In the series of fully unsaturated oligoquinanes, the tricyclic acepentalene (**3**) is the first member to exhibit a curved molecular surface, and – at least according to its number of carbon atoms – it resembles one hemisphere of the C_{20} -fullerene (**4**). For almost five years this C_{10} -bowl **3** remained the largest fully unsaturated oligoquinane ever observed [28]. According to Hückel MO theory, acepentalene (**3**) should have a triplet ground state [25], but more recently performed ab initio calculations have indicated the singlet state to be more stable by $3.9 \text{ kcal mol}^{-1}$ [28]. The prohibitively high strain in the molecule, which by far exceeds that of pentalene (**2**), renders the isolation of **3** impossible at ambient temperature. As early as 1964, Woodward introduced the idea of using triquinacene **54** as a stable tricyclic precursor of acepentalene (**3**) [46]. However, it took another 30 years to generate acepentalene by the stepwise introduction of double bonds. The breakthrough came with the facile preparation of dipotassium acepentalenediide $3^{2-} \cdot 2\text{K}^+$ [47] and the purification trick of obtaining the pure dilithium derivative $3^{2-} \cdot 2\text{Li}^+$ via the bis(trimethylstannyl)-dihydroacepentalene **56** (Scheme 9) [48]. The dilithium acepentalenediide $3^{2-} \cdot 2\text{Li}^+$ permitted the first X-ray crystal structure determination of a bowl-shaped aromatic dianion; it was found to aggregate as a homodimer held together by two dimethoxyethane-ligated lithium counteranions in the solid state (Scheme 9). The immediate precursor to the dilithio derivative $3^{2-} \cdot 2\text{Li}^+$, the bis(stannyl)dihydroacepentalene derivative **56**, is thermally stable and can be purified by sublimation [49]. However, the unsubstituted dihydroacepentalene **55** readily dimerizes in a [4+2] cycloaddition mode at ambient temperature, and it can only be observed as a monomer at temperatures below -80°C [49, 50].

The bis(stannane) **56** also proved to be a perfect precursor for the generation of the neutral acepentalene **3** [28]. By cleavage of the two labile tin–carbon bonds in **56** a diradical is



Scheme 9.

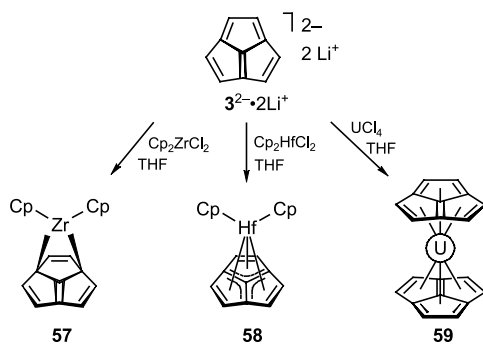
generated, which, in fact, resembles one possible electronic state of **3** (Scheme 10). Initial attempts to perform this bond cleavage in an argon matrix both photolytically as well as thermally were unsuccessful [51]. However, due to the advances in the equipment for ionization–neutralization–reionization mass spectrometry experiments [52], it was possible to generate the neutral molecule **3** and unequivocally prove its short-lived existence in the gas phase. In this experiment, the radical anion $3^{\cdot-}$ generated from **56** by chemical ionization with N_2O , was mass-selected and then neutralized by collision with oxygen to give acenaphthalene (**3**), which was subsequently reionized to $3^{+\cdot}$ [28]. The estimated lifetime of neutral **3** in the field-free zone of the mass spectrometer exceeded 1 μs , and therefore **3** can be considered as an existing species. The experimentally measured electron affinity as well as the fragmentation pattern after reionization of neutral **3** by electron impact agreed well with theoretical predictions [28].



Scheme 10. Cl = chemical ionization; EI = electron-impact ionization.

In view of the high purity and thermal stability of dilithium acenaphthalenediide $3^{2-} \cdot 2\text{Li}^+$ [48], it is the most feasible precursor of other stable acenaphthalene metal derivatives and

transition metal complexes. The reactions of $3^{2-} \cdot 2\text{Li}^+$ with Cp_2ZrCl_2 , Cp_2HfCl_2 , and UCl_4 gave metal complexes **57–59** of different coordination types and structures, as revealed by their NMR spectra [53]. The reaction of $3^{2-} \cdot 2\text{Li}^+$ with Cp_2ZrCl_2 in tetrahydrofuran gave a complex, which, according to its ^1H NMR spectrum, has a C_s -symmetric carbon skeleton and therefore, in analogy to the known bis(pentamethylcyclopentadienylzirconium)-trimethylenemethane complex [54], is best formulated as **57** [55]. The dilithium derivative $3^{2-} \cdot 2\text{Li}^+$ also reacted with Cp_2HfCl_2 to give an oxygen-sensitive complex, the ^1H NMR spectrum of which showed a single line due to the six protons on the acpentalene residue, in accordance with the C_3 -symmetric structure of **58** [55]. The remarkably stable sandwich complex **59** formed from $3^{2-} \cdot 2\text{Li}^+$ and UCl_4 in THF (Scheme 11) closely resembles the uranocene formed from dilithium cyclooctatetraenediide and UCl_4 . The ^1H NMR spectrum of complex **59** shows a very characteristic singlet at $\delta = -21$ ppm, which is close to that observed for the bis(cyclooctatetraenediyl)uranium complex [56].

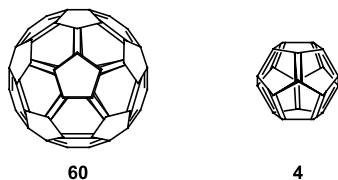


Scheme 11.

2.4.3

Generation of C_{20} -Fullerene

According to the isolated-pentagon rule, each five-membered ring in a spherical structure must be fully surrounded by six-membered rings [57]. Therefore, the C_{60} -fullerene (**60**) has to be the smallest stable fullerene. However, the smallest conceivable spherical fullerene is the C_{20} -fullerene (**4**), consisting exclusively of five-membered rings. C_{20} -fullerene (**4**) exceedingly violates the isolated-pentagon rule and must therefore also be the least stable and most reactive of all fullerenes [58]. Even the less curved C_{36} -fullerene is so reactive that it spontaneously oligomerizes in the solid state [59]. Unlike C_{36} - and higher fullerenes, C_{20} -



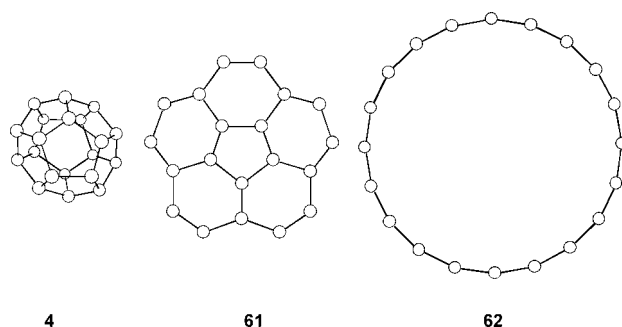
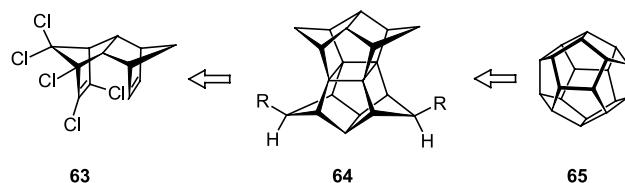


Fig. 7. C_{20} clusters **4**, **61**, and **62**.

fullerene (**4**) has not been observed in carbon vapor condensation or cluster annealing processes [60].

High level calculations identified C_{20} -fullerene (**4**) along with the bowl-shaped isomer decadehydrocorannulene **61** and the monocyclic isomer **62** as relatively low-energy representatives of the family of C_{20} clusters (Figure 7) [58, 61]. To date, only the monocyclic C_{20} **62** has been observed in laser ablation experiments on graphite [60, 62]. Recently, Prinzbach, Scott, von Issendorff et al. reported the first spectroscopic characterization of the other two highly strained C_{20} clusters **4** and **61** [4]. Among these, the most appealing candidate is certainly the C_{20} -fullerene (**4**). It is the carbon transliteration of Plato's universe [53], and it beats **53** and **54** both in symmetry and beauty.

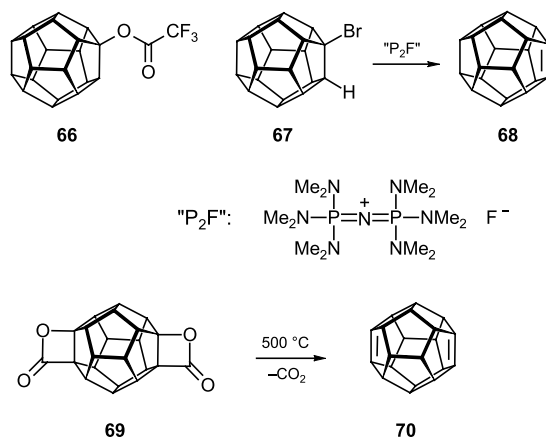
In close analogy to the successful generation of acepentalene (**3**), the best chance of forming C_{20} -fullerene (**4**) would certainly be realized by starting from a stable precursor with exactly the same carbon skeleton as C_{20} . Thus, the ideal starting material is the most highly symmetrical $C_{20}H_{20}$ hydrocarbon, the so-called pentagonododecahedrane (**65**), which also represents the lowest energy structure of all $(CH)_{20}$ isomers. The first synthesis of **65** by Paquette et al. has been a landmark in organic synthesis [64]. In the meantime, Prinzbach et al. have developed several dramatically improved approaches to dodecahedrane (**65**) by the so-called isodrine-pagodane route, i.e. via **63** and **64** (Scheme 12) [65].



Scheme 12.

The stepwise introduction of double bonds into the saturated skeleton of dodecahedrane (**65**) has been pursued for quite some time, since Paquette et al. reported the β -elimination of trifluoroacetic acid from (trifluoroacetoxy)dodecahedrane (**66**) induced by hydroxide and methoxide ions in an ion cyclotron resonance mass spectrometer and inferred indirectly the

existence of dodecahedrene (**68**) in the gas phase (Scheme 13) [66]. Subsequently, Prinzbach et al. systematically developed approaches to several highly strained oligodehydrododecahedranes by β -eliminations on the dodecahedrane skeleton [67]. According to their studies, pure dodecahedrene (**68**) can be isolated upon dehydrobromination of bromododecahedrane (**67**) [68] induced by the strongly basic naked fluoride ion provided by the iminophosphorane base “P₂F” developed by Schwesinger et al. [59] (Scheme 13). The fact that dodecahedrene (**68**), with its highly out-of-plane bent C=C double bond ($\psi = 43.5^\circ$, Figure 8), can be isolated, is quite remarkable on its own, but even more remarkable is the observation that **68** dimerizes only under forcing conditions (around 300 °C) [70]. Such a degree of kinetic stabilization was unexpected, but can be attributed to the efficient steric shielding by four allylic hydrogen atoms, which are all rigidly held in eclipsed orientations adjacent to the double bond on the surface of **68**. The dihydroacepentalene (**55**), with a similarly pyramidalized double bond ($\psi = 37^\circ$, Figure 8) but with only two eclipsed allylic hydrogens protecting it, cannot be isolated or even observed as a monomer at temperatures higher than -80°C (see above) [50].



Scheme 13.

Dodecahedradiene **70** has also been prepared and isolated as a stable compound [68, 71]. The highest yields (up to 70%) were obtained by flash vacuum pyrolysis of the bis(lactone) **69**, which can easily be prepared along the pagodane route (*cf.* Scheme 12) [72]. The calculated degree of pyramidalization of the double bonds in **70** ($\psi = 42.8^\circ$) is slightly smaller than that in dodecahedrene **68** (Figure 8).

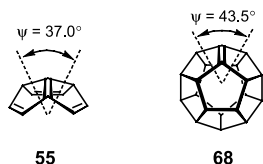
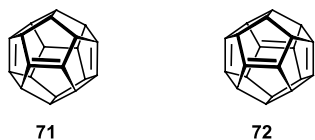
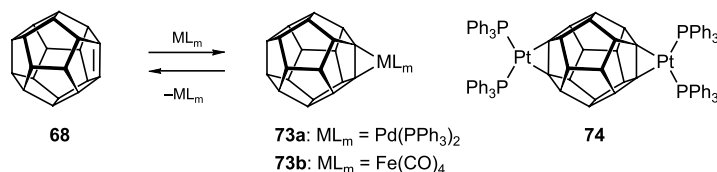


Fig. 8. Structural features of dihydroacepentalene **55** and dodecahedrene **68**.

Oligodehydrododecahedrane derivatives with an even greater degree of unsaturation have also been approached by Prinzbach et al. [67, 68, 70, 73, 74]. While the monoene **68** and diene **70** can be obtained as single regioisomers, the possibility of forming double bond isomers became a serious problem for the characterization of more highly unsaturated structures generated by dehydrobromination of tri- and tetrabromododecahedrane derivatives with the Schwesinger base “P₂F”. In fact, due to the number of regioisomers obtained, no pure triene or tetraene could be isolated. Nevertheless, trapping experiments with dienes in Diels–Alder reactions, as well as extensive mass spectrometric analyses, confirmed the existence of dodecahedratriene and -tetraene isomers **71** and **72**, respectively.



In analogy to acepentalene (**3**) and dihydroacepentalene **55** [75], the extremely strained double bonds in unsaturated dodecahedranes can be protected by metal complexation. Due to the high degree of pyramidalization, the HOMOs are slightly raised and the LUMOs significantly lowered and hence d¹⁰ metals (Pt, Pd, and Ni) are good coordinators for these double bonds. The steric protection of the double bonds by the allylic hydrogen atoms (see above) did not prohibit the formation of these metal complexes, as predicted for such pyramidalized double bonds [76]. Metal coordination of dodecahedrene **68**, e.g. by a Pd(PPh₃)₂ unit, occurred smoothly upon treatment with Pd(PPh₃)₄ at room temperature to give the crystalline air-sensitive complex **73a** (Scheme 14) [77]. The binuclear platinum complex **74** of the diene was characterized by X-ray crystal structure analysis, which revealed an elongation of the double bonds by ca. 0.11 Å and an increase in the pyramidalization by 7°.



Scheme 14.

As a reversible protection measure, complexation with a Fe(CO)₄ moiety appeared to be most promising. The monoene **68** was indeed found to react smoothly with Fe(CO)₅ at room temperature to give the tetracarbonyliron complex **73b** in 75% yield after crystallization. The complex **73b** proved to be stable for days in air as a solid and in solution (CHCl₃, benzene), and its ligand **68** can be conveniently liberated under mild oxidative conditions [Ce(NO₃)₄/MeOH/THF] at room temperature (Scheme 14) [77]. Although the use of metal complexation as a protection method for such compounds with highly pyramidalized double bonds works well for the monoene **68** and the diene **70**, the complexation of more highly unsatu-

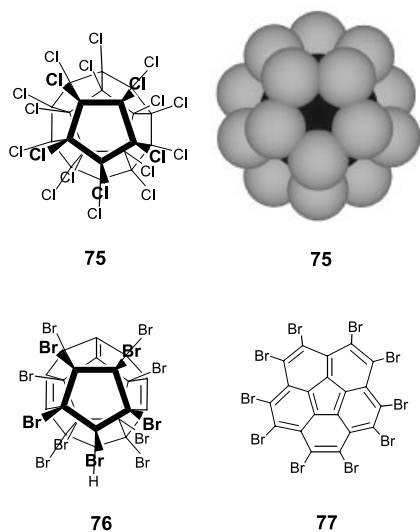


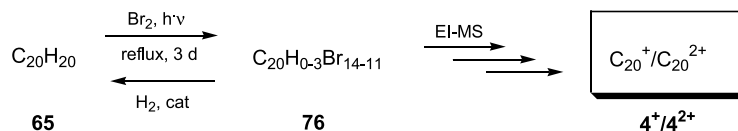
Fig. 9. Perhalogenated derivatives of dodecahedrane **75**, **76**, and corannulene **77**.

rated dehydrododecahedranes is hampered by the occurrence of regioisomers, as in the case of **71** and **72**, and by steric overcrowding on the surface if the metal bears additional bulky ligands.

In order to get from the stable, fully saturated dodecahedrane **65** with the correct connectivity of the carbon skeleton of **4** to the fully unsaturated C_{20} -fullerene, ten (!) double bonds have to be introduced without breaking any of the C–C bonds of the carbon skeleton [70]. The working hypothesis for the transformation of **65** into **4** was to replace most or all of the strongly bound hydrogen atoms by more weakly bound chlorine or bromine atoms. The perhalogenated derivatives of **65** would then be submitted to conditions under which elimination of the halogen atoms could occur, e.g. electron impact in a mass spectrometer. While the perchlorination of dodecahedrane (**65**) could indeed be achieved to give mixtures of compounds with up to 20 chlorine substituents on the C_{20} skeleton, i.e. **75** (Figure 9), subsequent electron impact mass spectrometric investigation in the positive ion mode was not indicative of consecutive elimination of chlorine atoms following ionization, but rather of significant cage fragmentation [73].

Functionalization of **65** with more weakly bound bromine atoms appeared to be the solution to this dilemma. However, due to the increased bulk of the bromine substituents and the resulting steric repulsion on the surface of **65** (compare structure **75**, Figure 9), substitution of all the hydrogen atoms could never be achieved with any of a variety of bromination protocols [78]. Only when a brute force method (neat Br_2 , reflux, and irradiation with a 450 W halogen lamp for 3 d) was applied, could a highly brominated product with an average elemental composition of $C_{20}HBr_{13}$, corresponding to **76**, be reproducibly isolated [4, 70]. Spectroscopic evidence showed that the obtained material consisted of a multitude of isomeric trienes, such as **76**, with a range of compositions $C_{20}H_{0-3}Br_{14-11}$, which, in spite of their highly pyramidalized double bonds ($\psi > 50^\circ$) (cf. Figure 8), proved to be insensitive to oxygen. The three double bonds that were introduced during the bromination process by

spontaneous elimination reactions apparently provide relief from the steric overcrowding at the molecular periphery. Catalytic hydrogenation of the bromination product **76** led back to the fully saturated dodecahedrane (**65**), proving that the cage survived the harsh conditions (Scheme 15) [73].



Scheme 15.

The cationic mode mass spectrum of the $[\text{C}_{20}\text{H}_{0-3}\text{Br}_{14-11}]$ sample showed singly and doubly charged C_{20} ions with up to 14 bromine atoms attached. The remarkably high intensities of the C_{20}^+ and C_{20}^{2+} ion peaks and the very low abundance of smaller fragments attested to a remarkable kinetic stability of the C_{20} cluster **4**. The anionic mode mass spectra obtained from brominated dodecahedrane **76** and perbrominated corannulene **77** resembled those of the cationic mode mass spectra, and again showed a high kinetic stability of the respective C_{20} clusters. Obviously, these mass spectra alone are not sufficient proof for the existence of the C_{20} -fullerene (**4**), nor can they reveal which isomer of the three, i.e. **4**, **61**, or **62**, was actually formed. Therefore, the C_{20} species obtained from three different sources, i.e. from the perbrominated cage **76**, from decabromocorannulene **77** [79], and from laser-ablated graphite, the latter known to yield the monocycle **62**, were converted to their anions and these were examined with a photoelectron (PE) spectrometer that was directly linked to the mass spectrometer [80]. In these experiments, a special ion source was used to generate an ion beam that was stable for several hours even though only a few milligrams of the respective materials were at hand. The PE spectra of the mass-selected $\text{C}_{20}^{\cdot-}$ clusters obtained from these three sources showed significantly different features. While the PE spectrum of the monocycle **62** had previously been assigned in combination with ion mobility experiments [60d], the spectra of the other two isomers **4** and **61** had not been observed before. The monocycle **62** was found to have an electron affinity of $2.44 (\pm 0.03)$ eV and its spectrum exhibited a vibrational progression of $2260 (\pm 100)$ cm^{-1} . The bowl isomer **61** generated from decabromocorannulene **77** showed a significantly lower electron affinity of $2.17 (\pm 0.03)$ eV, but a similar vibrational progression of $2060 (\pm 50)$ cm^{-1} . The cage isomer **4** generated from the oligobrominated dodecahedrane **76** had an electron affinity of $2.25 (\pm 0.03)$ eV and exhibited a vibrational progression of $730 (\pm 79)$ cm^{-1} ; at 0.27 eV above the first ionization threshold, another progression with a spacing of $260 (\pm 40)$ cm^{-1} set in. These observations clearly demonstrate that three different C_{20} clusters were obtained. Similarly to the highly strained acepentalene (**3**), the C_{20} clusters had lifetimes of at least the total flight time (0.4 ms) in the gas phase.

While the PE spectra of the bowl **61** and the monocycle **62** are in good agreement with theoretical predictions, the situation is more complex for the C_{20} -fullerene (**4**). Although the observed 730 cm^{-1} progression is consistent with that expected for a closed “polyolefinic” cage **4**, the theoretical confirmation of the PE spectrum of **4** remains a challenge for quantum mechanical methods. The ground-state symmetry of the neutral C_{20} -fullerene (**4**) is currently disputed in the literature [81], yet it is indispensable for the prediction of the vibrational modes excited upon electron attachment.

Further experimental confirmation of the existence of C₂₀-fullerene **4** might be provided by the endohedral incorporation of small atoms, such as He, into the cage. Such an incorporation is known for C₆₀-fullerene (**60**), and the existence of He@C₆₀ has additionally confirmed the cage structure of these molecules [82]. More recently, Cross, Saunders, and Prinzbach demonstrated that such a helium incorporation is even possible for the much smaller cage of the fully saturated dodecahedrane (**65**) [83]. However, the yield of this process (0.01 % He@C₂₀H₂₀) is as yet too low to enable one to use the product as a precursor for the generation of the fully unsaturated He@C₂₀. The possibility of stabilizing and isolating C₂₀-fullerene as a metal complex, as has been demonstrated for pentalene (**2**) and acepentalene (**3**), will, however, largely depend on the successful synthesis of suitable precursors in the future.

Acknowledgements

The authors are indebted to Stefan Beußhausen, Göttingen, for drawing the figures and schemes, and to Dr. Burkhard Knieriem, Göttingen, for careful proofreading of the final manuscript. R. H. is grateful to the Gottlieb Daimler- and Karl Benz-Stiftung as well as the Fonds der Chemischen Industrie for financial support.

References

- 1 J. THIELE, *Chem. Ber.* **1901**, 34, 68.
- 2 R. HAAG, A. DE MEIJERE, *Top. Curr. Chem.* **1998**, 196, 137, and refs. cited therein.
- 3 A. DE MEIJERE, R. HAAG, F.-M. SCHÜNGEL, S. I. KOZHUSHKOV, I. EMME, *Pure Appl. Chem.* **1999**, 71, 253.
- 4 H. PRINZBACH, A. WEILER, P. LANDENBERGER, F. WAHL, J. WÖRTH, L. T. SCOTT, M. GELMONT, D. OLEVANO, B. VON ISSENDORFF, *Nature* **2000**, 407, 60.
- 5 a) J. B. LAMBERT, L. LIN, V. RASSOLOV, *Angew. Chem.* **2002**, 114, 1487; *Angew. Chem. Int. Ed.* **2002**, 41, 1429; b) M. OTTO, D. SCHESCHKEWITZ, T. KATO, M. M. MIDLAND, J. B. LAMBERT, G. BERTRAND, *Angew. Chem.* **2002**, 114, 2379; *Angew. Chem. Int. Ed.* **2002**, 41, 2275; c) T. MÜLLER, *Angew. Chem.* **2002**, 114, 2380; *Angew. Chem. Int. Ed.* **2002**, 41, 2276; d) J. B. LAMBERT, *Angew. Chem.* **2002**, 114, 2382; *Angew. Chem. Int. Ed.* **2002**, 41, 2278; e) J. N. JONES, A. H. COWLEY, C. L. B. MACDONALD, *Chem. Commun.* **2002**, 1520.
- 6 a) H. JIAO, P. V. R. SCHLEYER, Y. MO, M. A. McALLISTER, T. T. TIDWELL, *J. Am. Chem. Soc.* **1997**, 119, 7075; b) B. REINDL, P. V. R. SCHLEYER, *J. Comp. Chem.* **1998**, 19, 1402.
- 7 A. DE MEIJERE, I. EMME, S. REDLICH, C. FREUDENBERGER, H.-U. SIEHL, P. R. SCHREINER, unpublished results.
- 8 M. SAUNDERS, R. BERGER, A. JAFFE, J. M. MCBRIDE, J. O. NEILL, R. BRESLOW, J. M. HOFFMANN, JR., C. PERCHONOK, E. WASSERMAN, R. S. HUTTON, V. J. KUCK, *J. Am. Chem. Soc.* **1973**, 95, 3017.
- 9 R. BRESLOW, R. HILL, E. WASSERMAN, *J. Am. Chem. Soc.* **1964**, 86, 5349.
- 10 R. BRESLOW, H. W. CHANG, W. A. YAGER, *J. Am. Chem. Soc.* **1963**, 85, 2033.
- 11 W. BROSER, H. KURRECK, P. SIEGLE, *Chem. Ber.* **1967**, 100, 788.
- 12 H. SITZMANN, H. BOCK, R. BOESE, T. DEZEMBER, Z. HAVLAS, W. KAIM, M. MOSCHEROSCH, L. ZANATHY, *J. Am. Chem. Soc.* **1993**, 115, 12003.
- 13 I. EMME, S. REDLICH, T. LABAHN, J. MAGUL, A. DE MEIJERE, *Angew. Chem.* **2002**, 114, 811; *Angew. Chem. Int. Ed.* **2002**, 41, 786.
- 14 H. HOPF, *Classics in Hydrocarbon Chemistry*, Wiley-VCH, Weinheim, 2000, pp. 269–271.
- 15 M. ODA, in *Houben-Weyl, Methods of Organic Chemistry*, Vol. E17a (Ed.: A. DE MEIJERE), Thieme, Stuttgart, 1997, pp. 2966–2972.

- 16 J. THIELE, H. BALHORN, *Justus Liebigs Ann. Chem.* **1906**, 348, 1.
- 17 J. THIEC, J. WIEMANN, *Bull. Soc. Chim. Fr.* **1960**, 1066.
- 18 E. STURM, K. HAFNER, *Angew. Chem.* **1964**, 76, 862; *Angew. Chem. Int. Ed. Engl.* **1964**, 3, 749.
- 19 H. SCHALTEGGER, M. NEUENSCHWANDER, D. MEUCHE, *Helv. Chim. Acta* **1965**, 48, 955.
- 20 H. DÜRR, B. RUGE, *Angew. Chem.* **1972**, 84, 215; *Angew. Chem. Int. Ed. Engl.* **1972**, 11, 225.
- 21 H. DÜRR, B. RUGE, H. SCHMITZ, *Angew. Chem.* **1973**, 85, 616; *Angew. Chem. Int. Ed. Engl.* **1973**, 12, 577.
- 22 H. E. SIMMONS, T. FUKUNAGA, *J. Am. Chem. Soc.* **1967**, 89, 5208.
- 23 R. HOFFMANN, A. IMAMAURA, D. G. ZEISS, *J. Am. Chem. Soc.* **1967**, 89, 5215.
- 24 E. HASELBACH, M. ALLAN, A.-C. SERGENTON, T. BALLY, P. BEDNAREK, A. DE MEIJERE, S. KOZHUSHKOV, S. GRIMME, *Helv. Chim. Acta* **2001**, 84, 1670.
- 25 A. STREITWIESER JR., *Molecular Orbital Theory for Organic Chemists*, Wiley, New York, 1961, and refs. cited therein.
- 26 R. BLOCH, R. A. MARTY, P. DE MAYO, *J. Am. Chem. Soc.* **1971**, 93, 3071.
- 27 K. HAFNER, R. DÖNGES, E. GOEDECKE, R. KAISER, *Angew. Chem.* **1973**, 85, 362; *Angew. Chem. Int. Ed. Engl.* **1973**, 12, 337.
- 28 R. HAAG, D. SCHRÖDER, T. ZYWIETZ, H. JIAO, H. SCHWARZ, P. v. R. SCHLEYER, A. DE MEIJERE, *Angew. Chem.* **1996**, 108, 1413; *Angew. Chem. Int. Ed. Engl.* **1996**, 35, 1317.
- 29 L. A. PAQUETTE, *Top. Curr. Chem.* **1979**, 79, 80.
- 30 E. LEGOFF, *J. Am. Chem. Soc.* **1962**, 84, 3975.
- 31 K. HAFNER, H. U. SÜSS, *Angew. Chem.* **1973**, 85, 626; *Angew. Chem. Int. Ed. Engl.* **1973**, 12, 575.
- 32 J. W. ARMIT, R. ROBINSON, *J. Chem. Soc.* **1922**, 121, 827; **1925**, 127, 1604.
- 33 N. C. BAIRD, R. M. WEST, *J. Am. Chem. Soc.* **1971**, 93, 3072.
- 34 P. BISCHOF, R. GLEITER, K. HAFNER, K. H. KNAUER, J. SPANGET-LARSEN, H. U. SÜSS, *Chem. Ber.* **1978**, 111, 932.
- 35 T. K. ZYWIETZ, H. JIAO, P. v. R. SCHLEYER, A. DE MEIJERE, *J. Org. Chem.* **1997**, 63, 3417, and refs. cited therein.
- 36 R. F. C. BROWN, N. CHOI, F. W. EASTWOOD, *Aust. J. Chem.* **1995**, 48, 185.
- 37 T. BALLY, A. CHAI, M. NEUENSCHWANDER, Z. ZHU, *J. Am. Chem. Soc.* **1997**, 119, 1869.
- 38 T. J. KATZ, M. ROSENBERGER, *J. Am. Chem. Soc.* **1962**, 84, 865.
- 39 J. J. STEZOWSKI, H. HOIER, D. WILHELM, T. CLARK, P. v. R. SCHLEYER, *J. Chem. Soc., Chem. Commun.* **1985**, 1263.
- 40 A. G. GRIESBECK, *J. Org. Chem.* **1989**, 54, 4981.
- 41 A. DE MEIJERE, S. I. KOZHUSHKOV, D. FABER, V. BAGUTSKII, R. BOESE, T. HAUMANN, R. WALSH, *Eur. J. Org. Chem.* **2001**, 3607.
- 42 K. HAFNER, *Angew. Chem.* **1973**, 85, 958; *Angew. Chem. Int. Ed. Engl.* **1973**, 12, 925.
- 43 L. A. PAQUETTE, *Topics Curr. Chem.* **1984**, 119, and refs. cited therein.
- 44 E. E. BUNEL, L. VALLE, N. L. JONES, P. J. CARROLL, C. BARRA, M. GONZALES, N. MUNOZ, G. VISCONTI, A. AIZAMAN, J. M. MANRIWUEZ, *J. Am. Chem. Soc.* **1988**, 110, 6596.
- 45 a) K. JONAS, B. GABOR, R. MYNOTT, K. ANGERMUND, O. HEINEMANN, C. KRÜGER, *Angew. Chem.* **1997**, 109, 1790; *Angew. Chem. Int. Ed. Engl.* **1997**, 36, 1712; b) K. JONAS, P. KOLB, G. KOLLBACH, B. GABOR, R. MYNOTT, K. ANGERMUND, O. HEINEMANN, C. KRÜGER, *Angew. Chem.* **1997**, 109, 1793; *Angew. Chem. Int. Ed. Engl.* **1997**, 36, 1714.
- 46 R. B. WOODWARD, T. FUKUNAGA, R. C. KELLY, *J. Am. Chem. Soc.* **1964**, 86, 3162.
- 47 T. LENDVAI, T. FRIEDEL, H. BUTENSCHÖN, T. CLARK, A. DE MEIJERE, *Angew. Chem.* **1986**, 98, 734; *Angew. Chem. Int. Ed. Engl.* **1986**, 25, 719.
- 48 R. HAAG, R. FLEISCHER, D. STALKE, A. DE MEIJERE, *Angew. Chem.* **1995**, 107, 1642; *Angew. Chem. Int. Ed. Engl.* **1995**, 34, 1492.
- 49 R. HAAG, F.-M. SCHÜNGEL, B. OHLHORST, T. LENDVAI, H. BUTENSCHÖN, T. CLARK, M. NOLTEMEYER, T. HAUMANN, R. BOESE, A. DE MEIJERE, *Chem. Eur. J.* **1998**, 4, 1192.
- 50 a) R. HAAG, B. OHLHORST, A. SCHUSTER, D. KUCK, A. DE MEIJERE, *J. Chem. Soc. Chem. Commun.* **1993**, 1727; b) R. HAAG, B. OHLHORST, M. NOLTEMEYER, R. FLEISCHER, D. STALKE, A. SCHUSTER, D. KUCK, A. DE MEIJERE, *J. Am. Chem. Soc.* **1995**, 117, 10474.

- 51 R. HAAG, H. P. REISENAUER, G. MAIER, A. DE MEIJERE, unpublished results.
- 52 N. GOLDBERG, H. SCHWARZ, *Acc. Chem. Res.* **1994**, 27, 347.
- 53 R. HAAG, *Dissertation*, Universität Göttingen, **1995**.
- 54 G. E. HERBERICH, C. KRUDER, U. ENGLERT, *Angew. Chem.* **1994**, 106, 2589; *Angew. Chem. Int. Ed. Engl.* **1994**, 33, 2465.
- 55 R. HAAG, F.-M. SCHÜNGEL, P. POREMBA, F. EDELMANN, A. DE MEIJERE, unpublished results.
- 56 A. STREITWIESER JR., S. A. KINSLEY, in *Fundamental and Technological Aspects of Organo-element Chemistry* (Eds.: T. J. MARKS, I. L. FRAGALA), Reidel, Dordrecht, NATO ASI Series C, Vol. 155, 1985, p. 77.
- 57 H. W. KROTO, *Nature* **1987**, 329, 529.
- 58 A. VAN ORDEN, R. J. SAYKALLY, *Chem. Rev.* **1998**, 98, 2313, and refs. cited therein.
- 59 a) C. PISKOTI, J. YARGER, A. ZETTL, *Nature* **1998**, 393, 771; b) P. W. FOWLER, T. HEINE, K. M. ROGERS, J. P. B. SANDALL, G. SEIFERT, F. ZERBETTO, *Chem. Phys. Lett.* **1999**, 300, 369; c) A. KOSHIO, M. INAKUMA, T. SUGAI, H. SHINOHARA, *J. Am. Chem. Soc.* **2000**, 122, 398.
- 60 a) S. YANG, K. J. TAYLOR, M. J. CRAYCRAFT, J. CONCEICAO, C. L. PETTITTE, O. CHESHNOVSKY, R. E. SMALLEY, *Chem. Phys. Lett.* **1988**, 144, 431; b) G. VON HELDEN, M. T. HSU, N. G. GOTTS, P. R. KEMPER, M. T. BOWERS, *Chem. Phys. Lett.* **1993**, 204, 15; c) H. HANDSCHUH, *Phys. Rev. Lett.* **1995**, 74, 1095; d) T. WAKABAYASHI, M. KOHNO, Y. ACHIBA, H. SHIRAMARU, T. MOMOSE, T. SHIDA, K. NAEMURA, Y. TOBE, *J. Chem. Phys.* **1997**, 107, 4783.
- 61 G. E. SCUSERIA, *Science* **1996**, 271, 942.
- 62 G. VON HELDEN, N. G. GOTTS, M. T. BOWERS, *Nature* **1993**, 363, 60.
- 63 E. HEILBRONNER, J. D. DUNITZ, in *Reflections on Symmetry*, VCH, Weinheim, 1993.
- 64 L. A. PAQUETTE, *Chem. Rev.* **1989**, 89, 1051.
- 65 M. BERTAU, F. WAHL, A. WEILER, K. SCHEUMANN, J. WÖRTH, M. KELLER, H. PRINZBACH, *Tetrahedron* **1997**, 53, 10029.
- 66 J. P. KIPLINGER, F. R. TOLLENS, A. G. MARSHALL, T. KOBAYASHI, D. R. LAGERWALL, L. A. PAQUETTE, J. E. BARTMESS, *J. Am. Chem. Soc.* **1989**, 111, 6914.
- 67 J. REINBOLD, E. SACKERS, T. OSSWALD, K. WEBER, A. WEILER, T. VOSS, D. HUNKLER, J. WÖRTH, L. KNOTHE, F. SOMMER, M. MORGNER, B. VON ISSENDORFF, H. PRINZBACH, *Chem. Eur. J.* **2002**, 8, 509.
- 68 J.-P. MELDER, K. WEBER, A. WEILER, E. SACKERS, H. FRITZ, D. HUNKLER, H. PRINZBACH, *Res. Chem. Intermed.* **1996**, 22, 667.
- 69 R. SCHWESINGER, J. WILLAREDT, H. SCHLEMPER, M. KELLER, D. SCHMITT, H. FRITZ, *Chem. Ber.* **1994**, 127, 2435.
- 70 H. PRINZBACH, K. WEBER, *Angew. Chem.* **1994**, 106, 2329; *Angew. Chem. Int. Ed. Engl.* **1994**, 33, 2239.
- 71 E. E. B. CAMPBELL, R. TELLGMANN, F. WAHL, H. PRINZBACH, *Int. J. Mass Spec. & Ion Processes* **1994**, 136, 209.
- 72 M. BERTAU, J. LEONHARDT, A. WEILER, K. WEBER, H. PRINZBACH, *Chem. Eur. J.* **1996**, 2, 570.
- 73 a) F. WAHL, J. WÖRTH, H. PRINZBACH, *Angew. Chem.* **1993**, 105, 1788; *Angew. Chem. Int. Ed. Engl.* **1993**, 32, 1722.
- 74 R. PINKAS, J. P. MELDER, K. WEBER, D. HUNKLER, H. PRINZBACH, *J. Am. Chem. Soc.* **1993**, 115, 7173.
- 75 H. BUTENSCHÖN, *Angew. Chem.* **1997**, 109, 1771; *Angew. Chem. Int. Ed.* **1997**, 36, 1695.
- 76 W. T. BORDEN, *Chem. Rev.* **1989**, 89, 1095.
- 77 T. OSWALD, M. KELLER, C. JANIAK, M. KOLM, H. PRINZBACH, *Tetrahedron Lett.* **2000**, 41, 1631.
- 78 J. CIOSLOWSKY, L. EDGINGTON, B. B. STEFANOV, *J. Am. Chem. Soc.* **1995**, 17, 10381.
- 79 L. T. SCOTT, P.-C. CHENG, M. M. HASHEMI, M. S. BRATCHER, D. T. MEYER, H. B. WARREN, *J. Am. Chem. Soc.* **1997**, 119, 10963.
- 80 H. HABERLAND, H. KORNMEIER, C. LUDEWIGT, A. RISCH, M. A. SCHMIDT, *Rev. Sci. Instrum.* **1991**, 62, 2621.
- 81 a) G. GALLI, F. GYGI, J. C. GOLAZ, *Phys. Rev. B* **1998**, 57, 1860; b) G. DUŠKESAS, S. LARSSON, *Theor. Chem. Acc.* **1997**, 97, 110.
- 82 a) M. SAUNDERS, A. JIMÉNEZ-VÁZQUEZ, R. J. CROSS, R. J. POREDA, *Science* **1996**, 259, 1428; b) M. SAUNDERS, R. J. CROSS, H. A. JIMÉNEZ-VÁZQUEZ, R. SHIMSHI, A. KHONG, *Science* **1996**, 271, 1693.
- 83 R. J. CROSS, M. SAUNDERS, H. PRINZBACH, *Org. Lett.* **1999**, 1, 1479.

3

The Suzuki Reaction with Arylboron Compounds in Arene Chemistry

Akira Suzuki

Abstract

Carbon–carbon bond formation reactions are important processes in chemistry, constituting key steps in the building of complex molecules from simple precursors. Recently, such couplings have been realized by cross-coupling reactions between organoboron compounds and organic electrophiles in the presence of a palladium catalyst and a base. This chapter surveys couplings of aryl- or heteroarylboron compounds with aryl or heteroaryl halides, including chlorides and triflates, which selectively afford the corresponding biaryl derivatives in excellent yields. The application of these couplings in polymer chemistry is also mentioned.

3.1

Introduction

Carbon–carbon bond-forming reactions are among the most important processes in chemistry, providing key steps in the building of more complex molecules from simple precursors. Over several decades, reactions enabling carbon–carbon bond formation between molecules with saturated sp^3 C-atoms have been developed. However, there were no simple and general methods for establishing carbon–carbon linkages between unsaturated species such as vinyl, aryl, and alkynyl moieties prior to the discovery and development of metal-mediated cross-coupling reactions in the 1970s.

In the mid-1970s, attempts were made to find a stereo- and regioselective synthetic means of obtaining conjugated alkadienes, which are of great importance in organic chemistry, both in themselves as well as with regard to their utilization in other reactions such as the Diels–Alder reaction. A number of methods for the preparation of conjugated dienes and polyenes were developed utilizing organometallic compounds. Although each of these methods had its own merits, the scope of many of these reactions was limited by the nature of the organometallic involved or the procedure employed. Perhaps the most promising procedure for preparing conjugated dienes or enynes in a selective manner was considered to be that based on the direct cross-coupling reaction of stereodefined haloalkenes or haloalkynes in the presence of a transition metal catalyst with stereodefined alkenylboron compounds, which are readily prepared from alkynes by hydroboration. In spite of efforts by many chemists to find such coupling reactions, there were no successful reports when we started this work.

At the initial stage of our exploration, we surmised that the difficulties encountered in achieving such a coupling stemmed from the following features. The common mechanism of transition metal catalyzed cross-coupling reactions between organometallic compounds and organic halides involves a sequence of: (a) oxidative addition, (b) transmetalation, and (c) reductive elimination [1]. One of the major reasons why 1-alkenylboranes cannot react with 1-alkenyl- or 1-alkynyl halides appears to be step (b), where the transmetalation process between RMX (M = transition metal, X = halogen) and organoboranes does not occur readily because of the weak carbanion character of organic groups in the organoboranes. To overcome this difficulty, we envisaged the use of tetracoordinated organoboron compounds instead of tricoordinated organoboron derivatives. It was observed that the methyl group in tetramethylborate is 5.5 times more electronegative than the methyl groups of trimethylborane [2]. Such speculation is also expected to apply in the case of the reaction of triorganoboranes in the presence of base. Actually, we found that the cross-coupling reaction of vinylic boron compounds with vinylic halides proceeds smoothly in the presence of base and a catalytic amount of a palladium complex to give the expected conjugated alkadienes and alkenynes stereo- and regioselectively in excellent yields [3]. Not only such vinylborane derivatives but also arylboron compounds readily cross-couple with a number of organic electrophiles to selectively provide coupling products in high yields. In this chapter, such cross-coupling reactions of arylboron compounds are described.

3.2

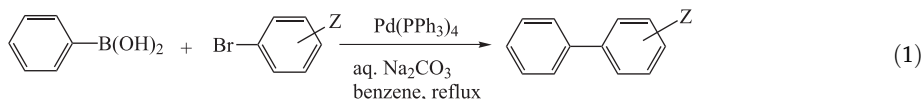
Reactions with Aryl Halides and Triflates: Synthesis of Biaryls

3.2.1

Aromatic–Aromatic Coupling

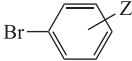
As mentioned in the previous section, it was found that vinylboron compounds (sp^2 carbon–boron bond) readily react with vinylic halides (sp^2 carbon–halogen bond) to stereo- and regioselectively provide the corresponding cross-coupling products, i.e. conjugated alkadienes, in excellent yields. In order to confirm the possibility of cross-coupling between areneboronic acids and aryl halides, both of which possess sp^2 carbons, such coupling reactions were subsequently investigated.

The first observation concerning the preparation of biaryls was reported in 1981 [4]. Thus, the palladium-catalyzed cross-coupling reaction of phenylboronic acid with a number of haloarenes was found to proceed smoothly in the presence of base to selectively afford the corresponding biaryls in high yields (Eq. (1) and Table 1).



Following this discovery, various modifications were made to the reaction conditions. A combination of $\text{Pd(PPh}_3)_4$ or $\text{PdCl}_2(\text{PPh}_3)_2$ and aqueous Na_2CO_3 in dimethoxyethane (DME) was reported to work satisfactorily in most cases [5, 6].

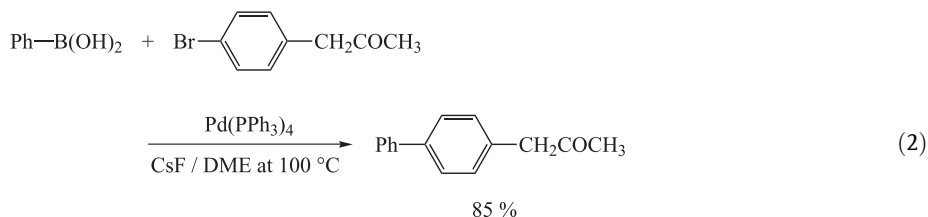
Tab. 1. Synthesis of Biphenyls^a.

	Solvent	Reac. time (h)	Yield of biphenyl (%)
<i>o</i> -MeC ₆ H ₄ Br	benzene	6	94
<i>p</i> -MeC ₆ H ₄ Br	benzene	6	88
<i>o</i> -MeOC ₆ H ₄ Br	benzene	6	99
<i>p</i> -ClC ₆ H ₄ Br	benzene	6	89
<i>p</i> -MeO ₂ CC ₆ H ₄ Br	benzene	6	94 ^b
Mesityl bromide	toluene	17	80 ^b

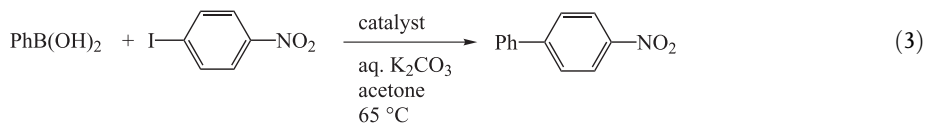
^aThe reaction was carried out by using 10 % excess of phenylboronic acid, Pd(PPh₃)₄ (3 mol %), and 2 M Na₂CO₃·H₂O (2 equiv.) at the reflux temperature of solvent.

^bIsolated yields.

Combinations with other bases, such as Et₃N [7, 8], NaHCO₃ [9], Cs₂CO₃ [10], Tl₂CO₃ [11], and K₃PO₄ [12], with or without Bu₄NCl [13] and 18-crown-6 [10], were also used. The reaction is successful for aryl iodides, bromides, and triflates. Chlorobenzene derivatives are generally quite inert to oxidative addition, but some π -deficient heteroaryl chlorides and related compounds do give coupling products [14]. Most recently, modified conditions effective for aryl chlorides have been proposed (see Section 3.4). The reaction proceeds most rapidly under homogeneous conditions (aqueous base in DME), but reasonable yields are also obtained under heterogeneous conditions. For example, K₂CO₃ suspended in toluene works well for base-sensitive reactants [15]. Although the conditions using such bases are not entirely compatible with the functional groups present in all desired reactants, the extremely mild conditions using CsF or Bu₄NF allow the synthesis of various functionalized biaryls (Eq. (2)) [16].

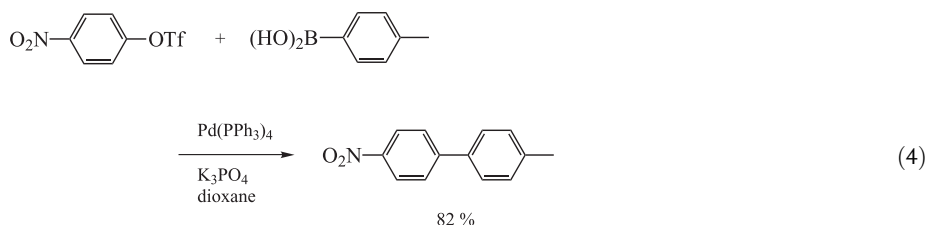


Phosphine-based palladium catalysts are generally used since they are stable to prolonged heating; however, extremely high coupling reaction rates can sometimes be achieved by using palladium catalysts without a phosphine ligand, such as Pd(OAc)₂, [(η^3 -C₃H₅)PdCl]₂, or Pd₂(dba)₃C₆H₆ (Eq. (3)) [17, 18].

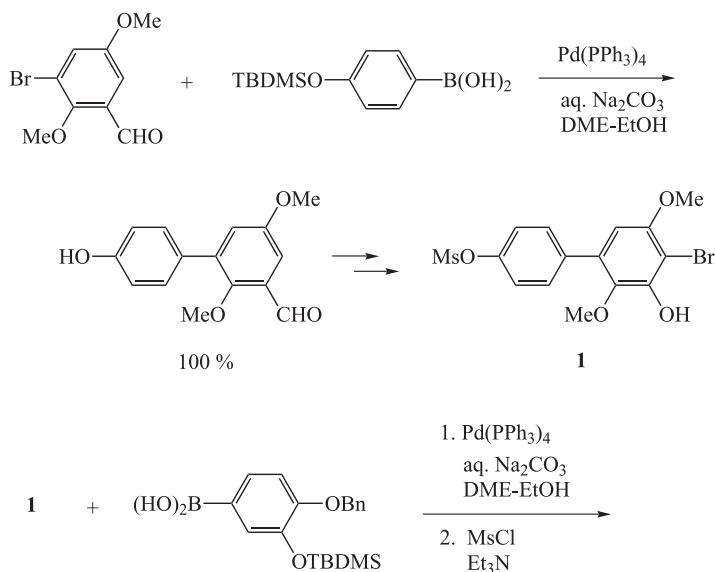


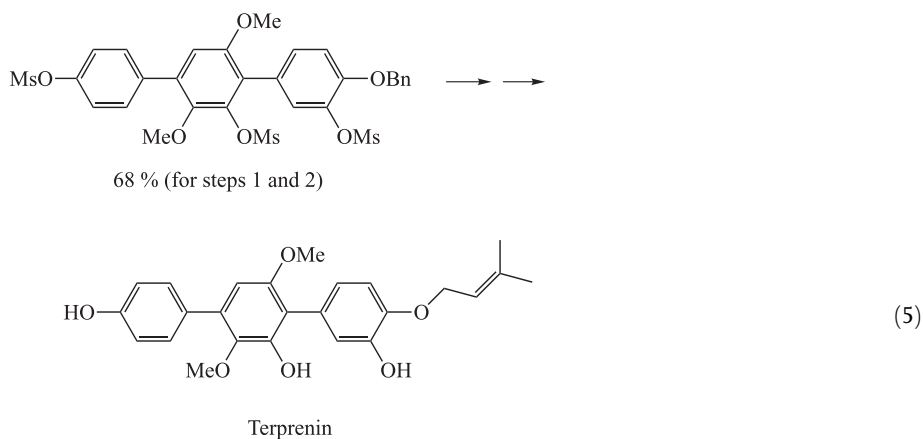
Cross-coupling reactions of areneboronic acids with aryl triflates in the presence of K_3PO_4 and a catalytic amount of $Pd(PPh_3)_4$ or $PdCl_2(dppf)$ in dioxane proceed with high yields. The reaction conditions are sufficiently mild that a variety of functionalized biaryls may readily be obtained (Eq. (4)) [19].

catalyst: $Pd(PPh_3)_4$ (8 h, 23 %); $Pd(OAc)_2$ (0.75 h, 98 %);
 $(\eta^3-C_3H_5)PdCl$ (1 h, 98 %)

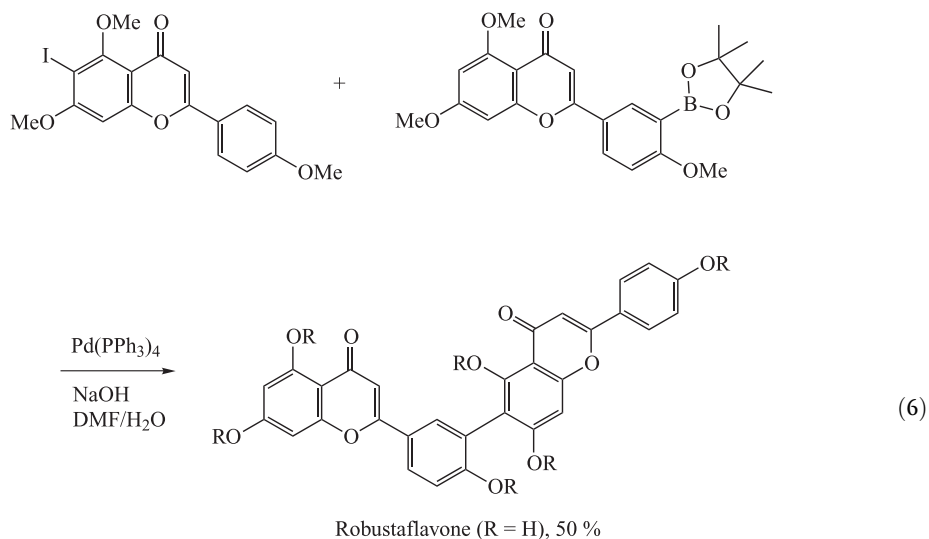


Aromatic–aromatic coupling reactions have been amply applied in syntheses of biologically active chemicals, and of other materials of interest in many scientific and industrial fields. Terpenin was recently discovered in the fermentation broth of *Aspergillus candidus*. The impressive feature of the immunosuppressive activities of terpenin is its highly potent *in vitro* and *in vivo* suppressive effect on immunoglobulin E antibody production without any toxicological signs. The total synthesis of terpenin was reported recently, the key steps of which relied on the Suzuki reaction (Eq. (5)) [20]. The highly efficient and practical production of this important natural product offers promise for the development of a new type of anti-allergic drug.



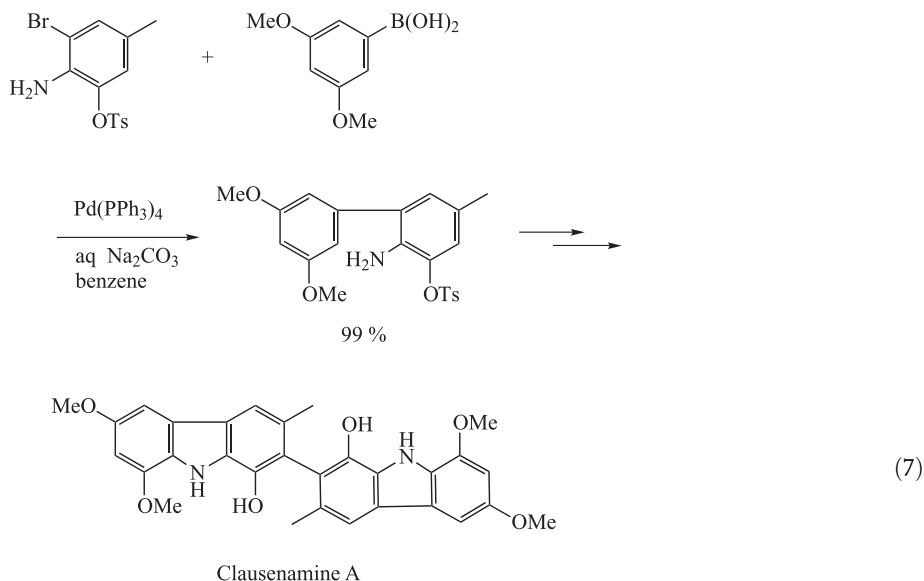


Robustaflavone, a naturally occurring compound, is an inhibitor of hepatitis B virus replication *in vitro*. The natural material was isolated from the seed kernels of *Rhus succedanea*. To provide ready access to sufficient quantities of material for continued biological studies, as well as to provide a general route for the preparation of structural analogues, a total synthesis of robustaflavone was requested, and Zembower recently reported the first total synthesis of this compound using Suzuki coupling as a key step (Eq. (6)) [21].

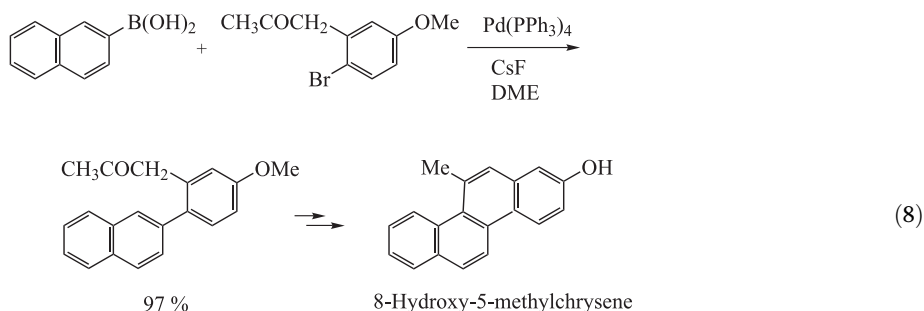


A number of dimeric carbazole alkaloids have been isolated from various natural sources in recent years, which have been found to exhibit various biological activities including anti-tumor, anti-inflammatory, and cytotoxic activities. In 1996, clausenamine A was isolated from the stem and root bark of *Clausena excavata*, which is used in Chinese herbal medicine for detoxification treatment following poisonous snakebites. The first total synthesis of clau-

senamine A has since been developed, which involves Suzuki cross-coupling and an oxidative coupling reaction (Eq. (7)) [22].

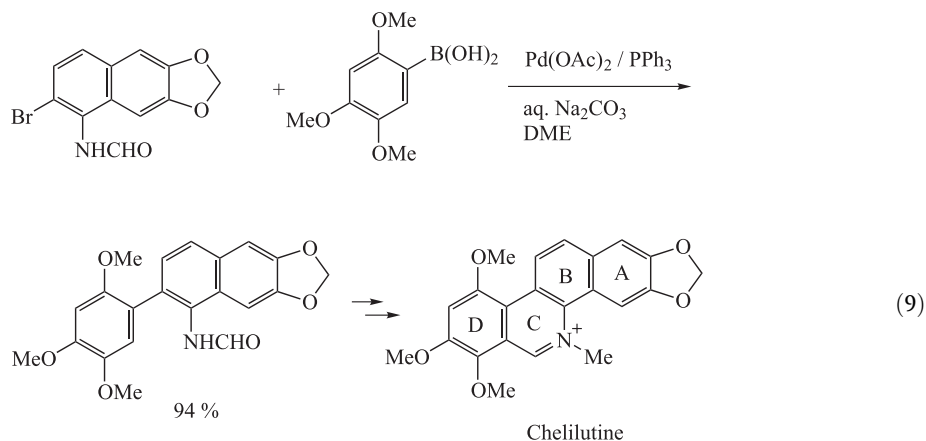


The Suzuki cross-coupling reaction is recognized as a novel, abbreviated method for the synthesis of 2-hydroxychrysene, 2-hydroxy-5-methylchrysene, and 8-hydroxy-5-methylchrysene from easily accessible reactants (Eq. (8)) [23]. These phenolic compounds constitute precursors for the synthesis of dihydrodiol and bay-region diol epoxide derivatives of chrysene and 5-methylchrysene, which are implicated as the active forms of carcinogenic polynuclear aromatic hydrocarbons.



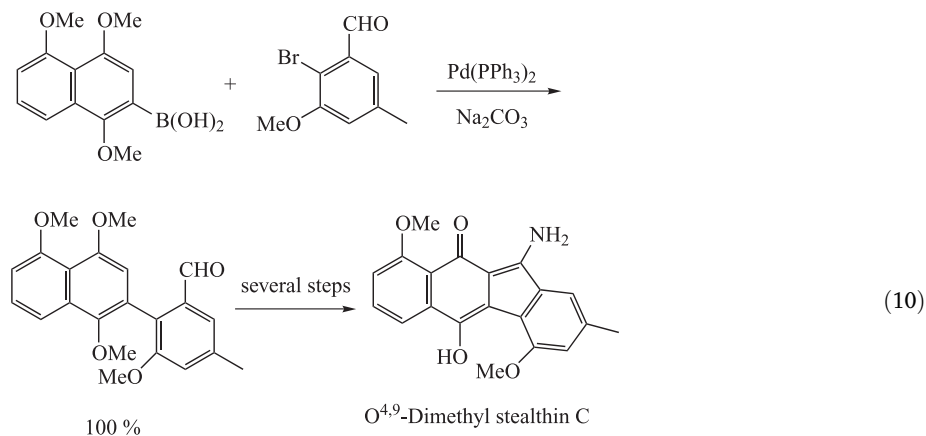
The benzo[*c*]phenanthridines are an important group of isoquinoline alkaloids, many of which show a wide range of pharmacological properties including antitumor and antiviral activities. They have therefore attracted much synthetic interest in the 60 years since Robinson published the first synthesis. Geen et al. reported a synthesis involving a late-stage fusion of the A and D ring components, thereby allowing easy access to a number of benzo[*c*]phenanthridine alkaloids from only a few synthetic intermediates [24]. For example, following the coupling of 2-bromo-1-formamidonaphthalene with 2,4,5-trimethoxyphenyl-

boronic acid to afford the desired coupling product in 94 % yield, chelilutine can readily be obtained after a few more steps (Eq. (9)).

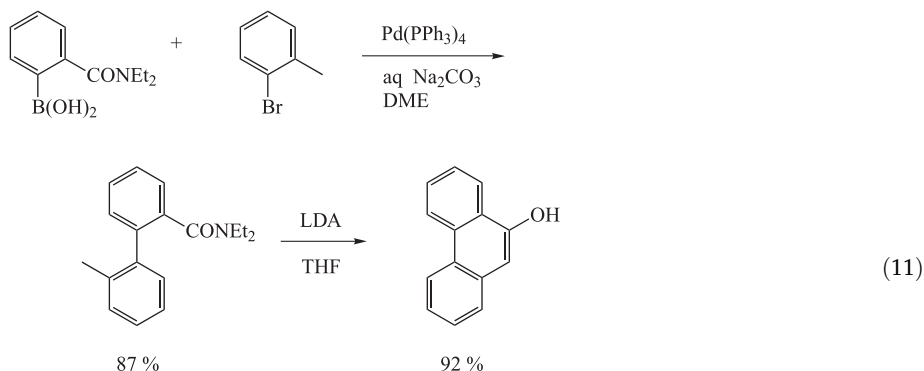


Comins and Green have recently developed a new method for the enantioselective synthesis of 4-substituted phenylalanines based on Pd-catalyzed cross-coupling reactions of a protected boronophenyl alanine with aromatic halides. These reactions proceed with good to excellent yields, and furnish the desired products with high enantiomeric purities [25].

Recently, a growing number of radical scavengers have been isolated from microorganisms. In 1992, for example, Seto et al. reported the isolation of stealthins A and B as potent radical scavengers from *Streptomyces viridochromogenes*, and showed that their radical-scavenging activities were 20–30 times greater than that of vitamin E. Most recently, $O^{4,9}$ -dimethylstealthin C [26a] and O^{12} -acetyl- O^4, O^9 -dimethylstealthin A [26b] have been synthesized using the Suzuki coupling as a key step, as shown in Eq. (10).

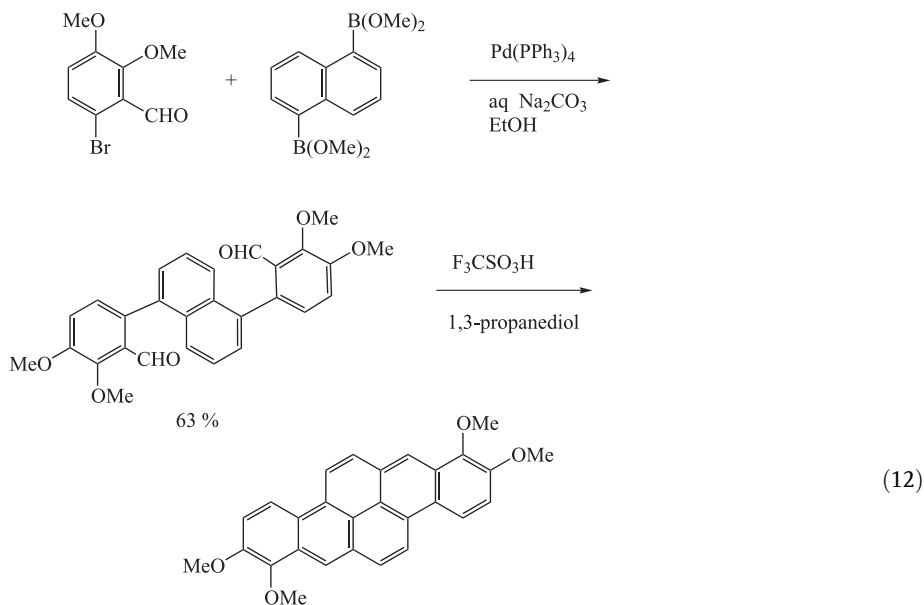


Snieckus and Fu reported a new general and regiospecific synthesis of 9-phenanthrols involving direct *ortho*-metalation, Suzuki cross-coupling, and an LDA-mediated directed remote metalation sequence (Eq. (11)) [27].

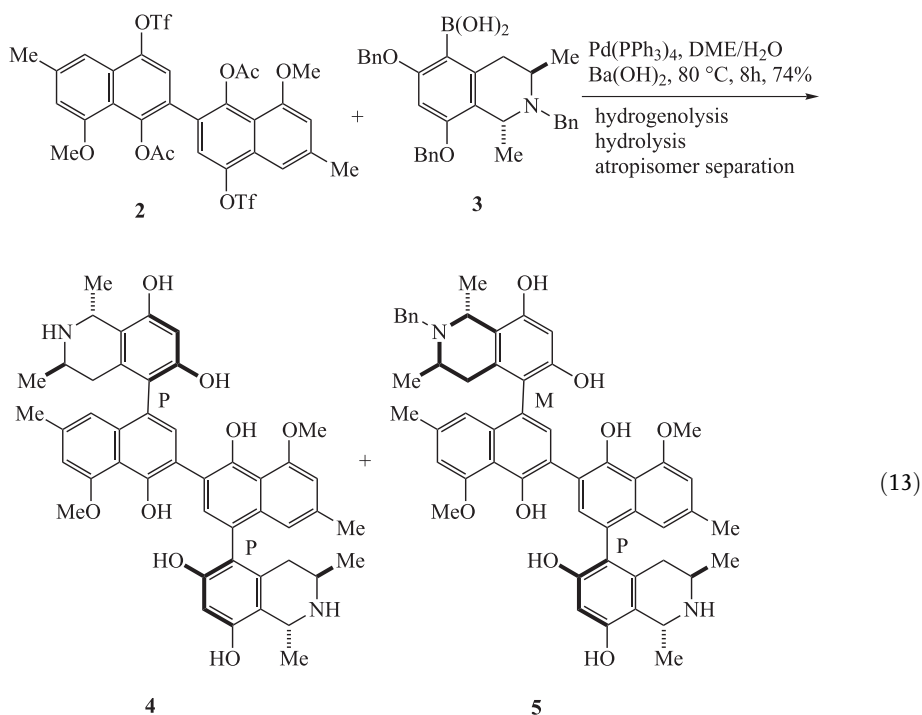


A versatile method for the synthesis of complex, fused polycyclic aromatic systems in high chemical yield has been discovered. Pd-catalyzed Suzuki-type cross-coupling allows the preparation of nonfused skeletal ring systems in high yield. The ring-forming step, which generally proceeds in high yield, utilizes 4-alkoxyphenylethynyl groups and is induced by strong electrophiles such as trifluoroacetic acid and iodonium tetrafluoroborate. The reaction produces phenanthrene moieties, which are integrated into extended polycyclic aromatic structures [28, 29]. Fused polycyclic benzenoids as well as benzenoid/thiophene systems may be prepared utilizing this methodology.

A new synthetic approach to polycyclic aromatic compounds has been developed based on double Suzuki coupling of polycyclic aromatic hydrocarbon bis(boronic acid) derivatives with *o*-bromoaryl aldehydes to furnish aryl dialdehydes. These are then converted to larger polycyclic aromatic ring systems by either: (a) conversion to diolefins by Wittig reaction followed by photocyclization, or (b) reductive cyclization with trifluoromethanesulfonic acid and 1,3-propanediol (Eq. (12)) [30].



Recently, the anti-HIV alkaloids michellamines A (**4**) and B (**5**) have attracted much attention. The tetraaryl skeleton of the michellamines is constructed by first forming the inner (nonstereogenic) biaryl axis and then adding the two other (stereogenic) axes by means of a double Suzuki-type cross-coupling reaction between binaphthalene ditriflate (**2**) and isoquinolineboronic acid (**3**) (Eq. (13)) [31].

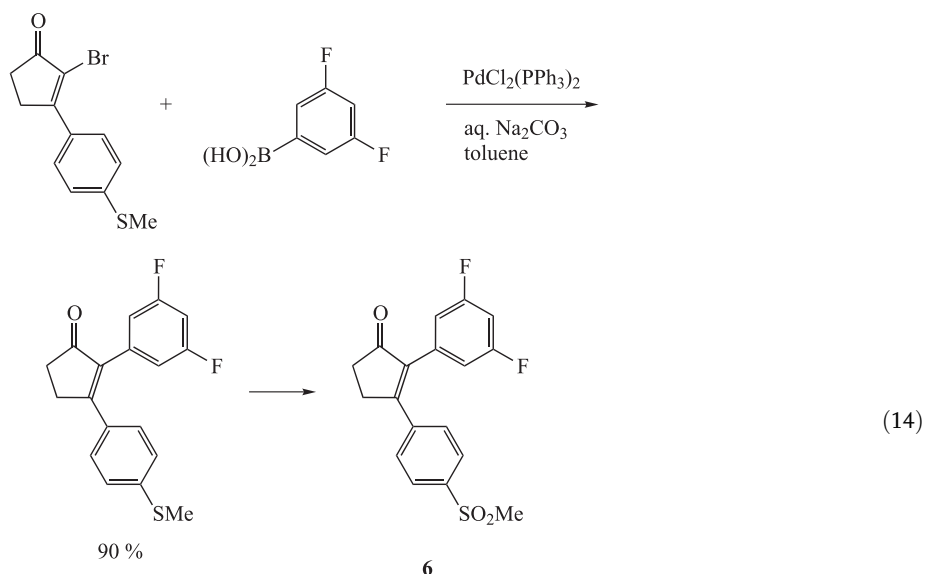


Another total synthesis of michellamines A–C, korupensamines A–D, and ancistrobrevine B has been developed by Hoyer et al. [32], who emphasized that Suzuki coupling of the boronic acid derived from the naphthalene moiety with a THIQ-iodide proved to be the most generally effective method for forming the hindered biaryl bond. A racemic isochromane analogue of michellamines has been synthesized by a similar procedure [33].

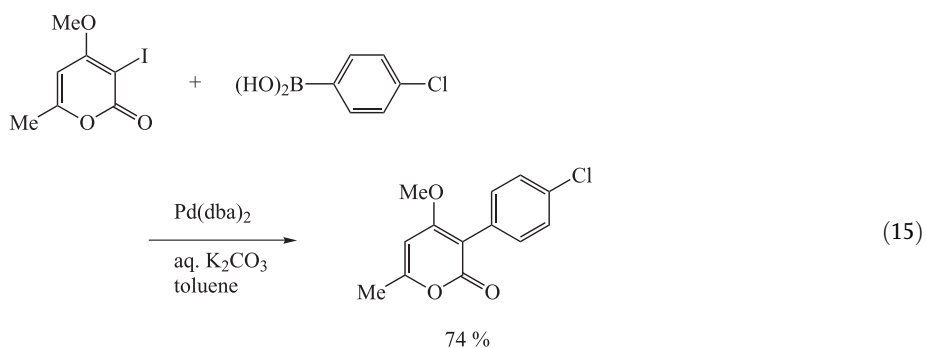
Vancomycin is well-known as the last line of defense against drug-resistant bacteria. Nicolaou and his group reported a Suzuki coupling approach to the AB-COD bicyclic system of vancomycin [34]. The total synthesis of the vancomycin aglycon was subsequently reported by the same workers [35].

It has been demonstrated that 2-(3',5'-difluorophenyl)-3-(4'-methylsulfonylphenyl)-cyclopent-2-enone (**6**), which is synthesized by means of a Suzuki reaction (Eq. (14)), displays high selectivity and potency towards cyclooxygenase [36].

The 4-hydroxy-2H-pyran-2-one moiety is a key structural feature in a recently discovered new class of non-peptidic HIV protease inhibitors. Therefore, the synthetic methodologies were extended to allow the functionalization of commercially available chemicals. Direct arylation of the pyrone ring at the C-3 and C-5 positions had not been reported until the re-

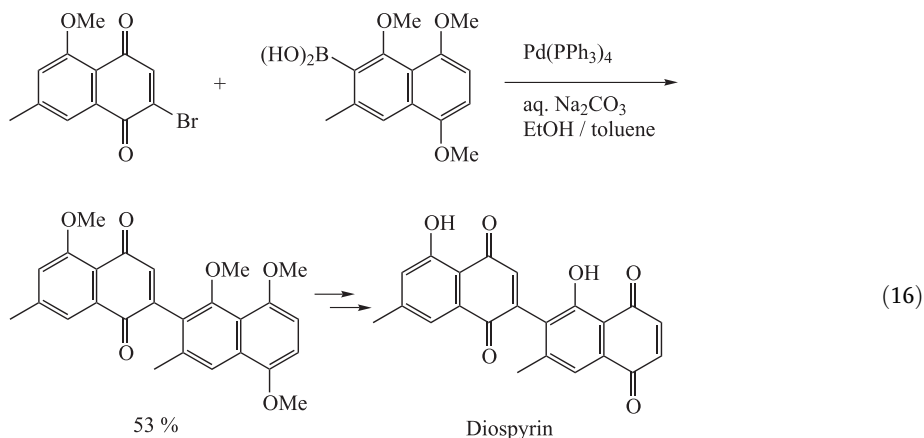


cent publication of the palladium-catalyzed cross-coupling of organozinc derivatives with iodobenzene [37]. Recently, Pleixats et al. demonstrated that 3-arylpyrones and 5-arylpyrones, incorporating the 4-methoxy-2*H*-pyran-2-one moiety, are readily obtained by Suzuki cross-coupling of the corresponding 3-iodo and 5-iodo derivatives with arylboronic acids (Eq. 15) [38].

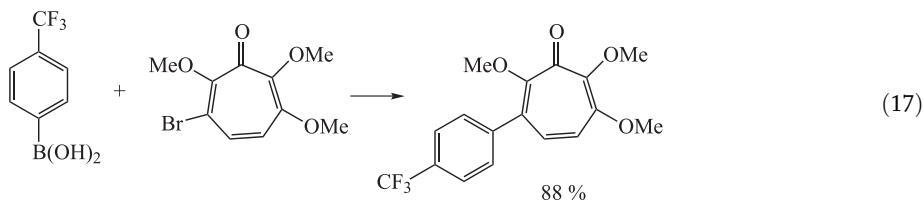


Diospyrin was first isolated in 1961 as an orange-red constituent of *Diospyros montana* Roxb. (*Ebenaceae*) in India. Mori and Yoshida have reported the first synthesis of diospyrin, employing Suzuki coupling as a key reaction enabling connection of the two 7-methyljuglone units (Eq. (16)) [39].

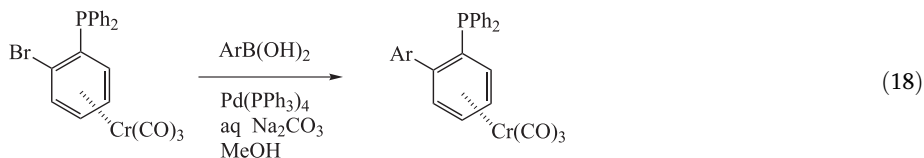
3,7-Dihydroxytropolone derivatives have emerged as the foremost representatives of a new class of potent, competitive inhibitors of inositol monophosphatase. The first successful preparations of mono- and disubstituted 3,7-dihydroxytropolones were accomplished by single or double Suzuki coupling reactions between these permethylated monobromo- and



dibromodihydroxytropolone derivatives and a variety of boronic acids [40]. An example is outlined in Eq. (17). These compounds were found to be potent inhibitors of inositol mono-phosphatase with IC_{50} values in the low-micromolar range.



Under standard Suzuki reaction conditions, the coupling of tricarbonyl[η^6 -(diphenylphosphino)benzene]chromium(0) with typical arylboronic acids has been achieved, giving biaryl complexes in high yield (Eq. (18)). This type of reaction sequence serves to generate product complexes that are not available by other means [41].

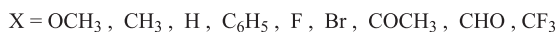
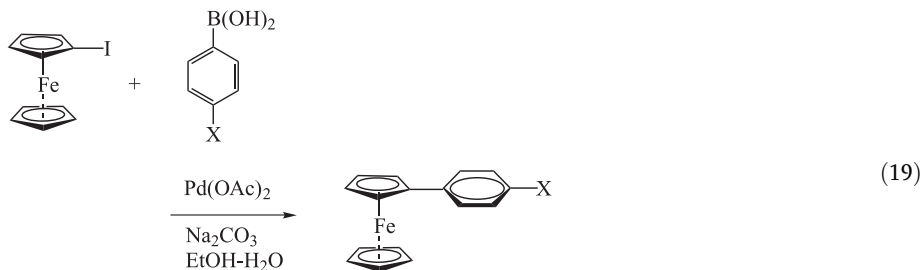


Similar coupling reactions of other chromium(0) complexes with arylboronic acids have also been reported [42, 43].

Uemura and Kamikawa have presented a review on the stereoselective synthesis of axially chiral biaryls utilizing planar chiral (arene)chromium complexes [44].

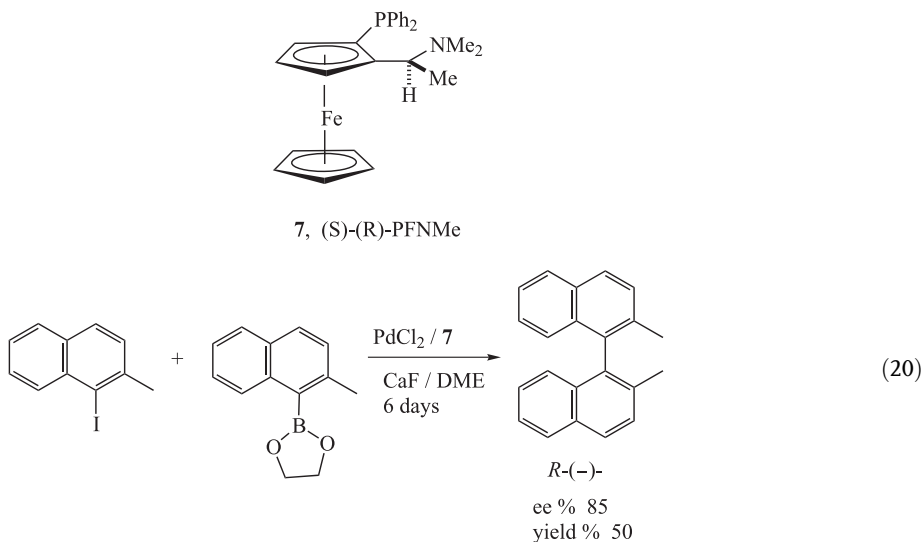
A modification of the Suzuki coupling reaction proved to be a clean and useful method for the preparation of monosubstituted arylferrocenes. Iodoferrocene was reacted with a series of substituted arylboronic acids in the presence of sodium carbonate and palladium acetate in aqueous ethanol at room temperature to produce a range of substituted monoarylferrocenes (Eq. (19)). A systematic investigation undertaken to determine the optimal reaction conditions indicated that scrupulous deoxygenation of the solvent is critical. The use of

stronger bases such as barium hydroxide and potassium carbonate is favorable and gives rise to better yields of monoarylferrocenes. The reactions also proceed efficiently in aqueous DMF, broadening the scope of the process and allowing efficient reactions with boronic acids that show low solubility in organic solvents [45].



Ferrocenyl-substituted aldehydes have also been prepared by a Suzuki reaction [46].

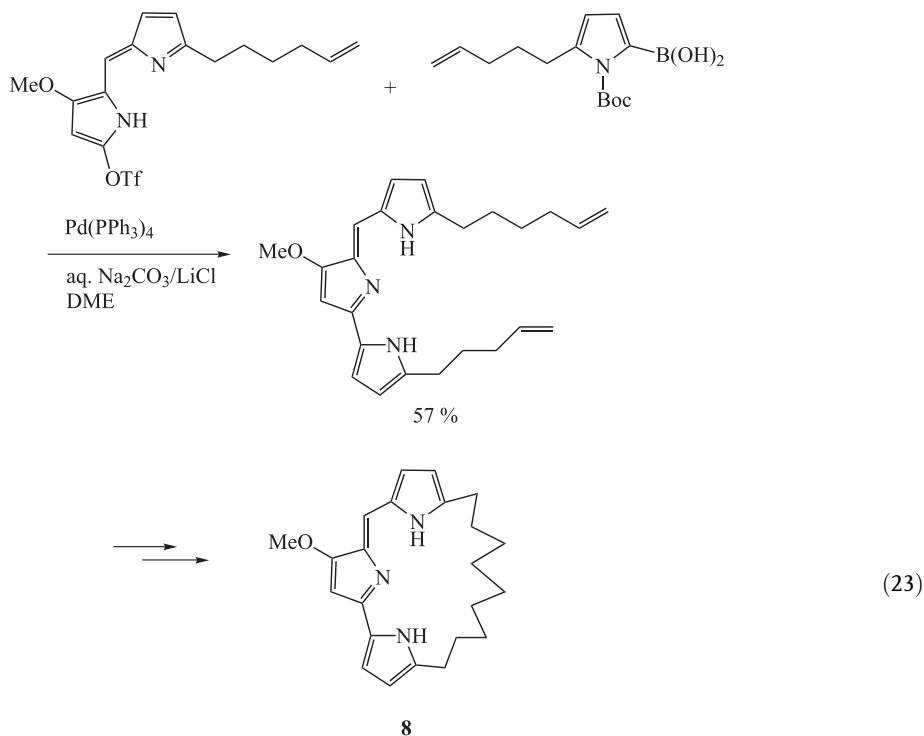
Restricted rotation about the aryl-aryl bond in biaryls can lead to the phenomenon of atropisomerism. Chiral binaphthalenes constitute an important class of such atropisomeric compounds, not least because they are among the most useful chiral ligands and auxiliaries employed in asymmetric synthesis. A small number of asymmetric biaryl syntheses have been reported. However, variable results have been reported depending on the nature of the catalyst used (e.g. Ni or Pd), and in all cases a Grignard reagent has been used as the organometallic component. Recently, Cammidge and Crepy [47] have reported examples of the use of an asymmetric Suzuki coupling protocol for the construction of binaphthalenes. Here, the ligand (**7**) with a tertiary amine moiety was found to lead to the highest selectivity, suggesting that the high *ee* obtained may stem from pre-complexation between the nitrogen in **7** and the boron prior to transmetalation (Eq. (20)).



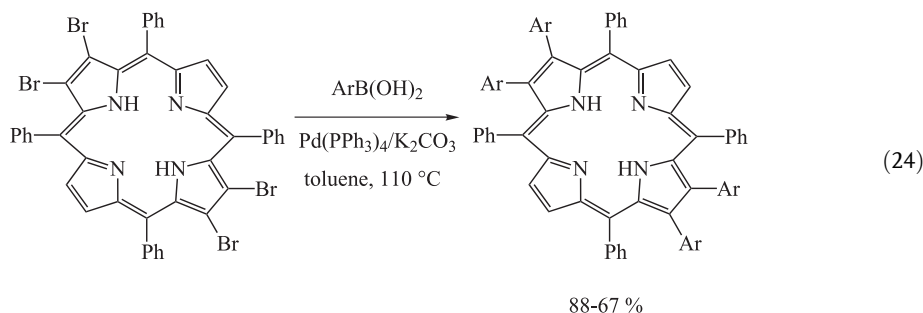
Aromatic–Heteroaromatic and Heteroaromatic–Heteroaromatic Couplings

The deep-red colored prodigiosin alkaloids are endowed with potent antibacterial, cytotoxic, and antimalaria properties. Additionally, in a series of recent reports it has been claimed that this family also displays a significant immunosuppressive activity. This finding is particularly noteworthy since the mechanism of action seems to be distinctly different from that of

cyclosporin or FK-506. Consequently, these alkaloids are viewed as lead structures in the search for new drugs to prevent allograft rejection. Recently, the first total synthesis of the cyclic prodigiosin derivative **8** has been demonstrated (Eq. (23)) [50]. The key steps of this approach comprise a palladium-catalyzed Suzuki cross-coupling reaction of the rather unstable pyrroleboronic acid derivative with the electron-rich pyrrolyl triflate, followed by a ring-closing metathesis reaction.

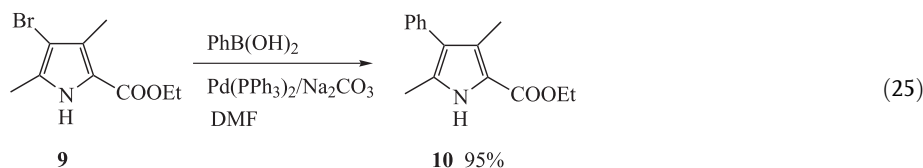


Porphyrin synthesis arouses continuing interest in biological, material, and inorganic chemistry. Substituents at the β -position of porphyrins exert much larger steric and electronic effects on the porphyrin ring than substituents at the *meso*-aryl positions. However, the synthesis of β -substituted porphyrins often requires the relatively inaccessible 3-substituted or 3,4-disubstituted pyrroles for either protic or Lewis acid-catalyzed co-tetramerization with aldehydes. Furthermore, in the preparation of unsymmetrical porphyrins, regioisomeric mixtures requiring difficult and tedious chromatographic purification are often obtained. Since β -brominated porphyrins are easily obtained by the controlled bromination of porphyrins or metalloporphyrins, the transformation of the bromo substituents into other functional groups would provide facile access to β -substituted porphyrins. Chan and co-workers have reported on the synthesis of β -aryl-substituted tetraphenylporphyrins by Suzuki cross-coupling of the corresponding β -bromoporphyrins (Eq. (24)) [51].

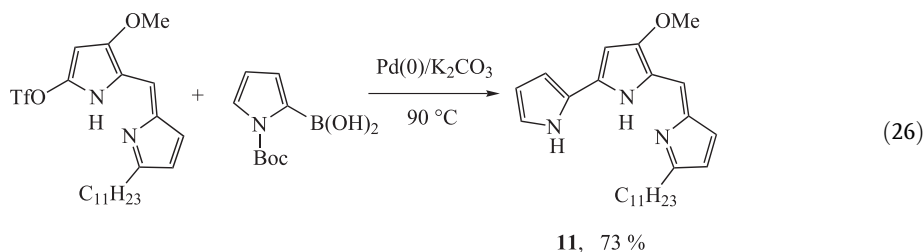


Similarly, a facile synthesis of β -derivatized porphyrins has been reported by Nocera et al. [52].

In connection with such syntheses, Chang and Bag [53] also reported a synthetic route to tetramethyltetraphenylporphyrin from a pyrrole derivative. The required pyrroles were synthesized from bromopyrrole (**9**) and phenylboronic acid by means of a Pd(0)-catalyzed cross-coupling. The reaction proceeded well in DMF to give an essentially quantitative yield of the product **10** (Eq. (25)).

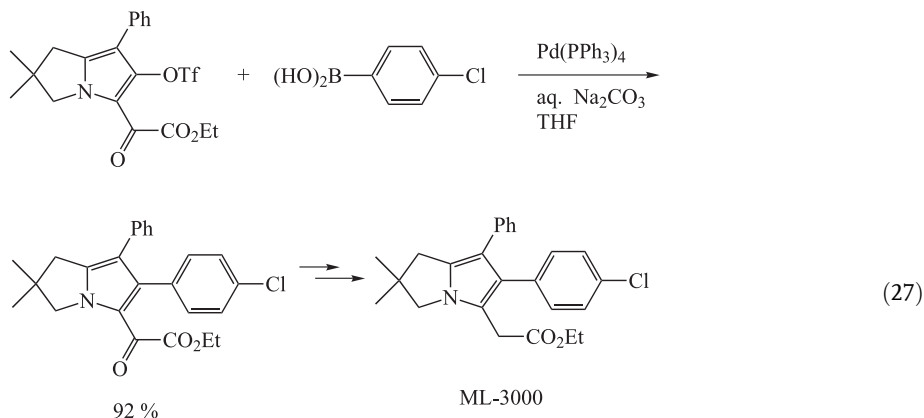


Recently, undecylprodigiosine (**11**) was reported to inhibit T-cell proliferation at doses that are not cytotoxic, which is particularly attractive with regard to its potential clinical application. The hitherto published total syntheses of prodigiosines involve several steps and are not suitable for scale-up in the case of possible lead structure development. D'Alessio and Rossi [54] have devised a new synthetic pathway allowing the reproducible and consistent production of undecylprodigiosine (Eq. (26)).

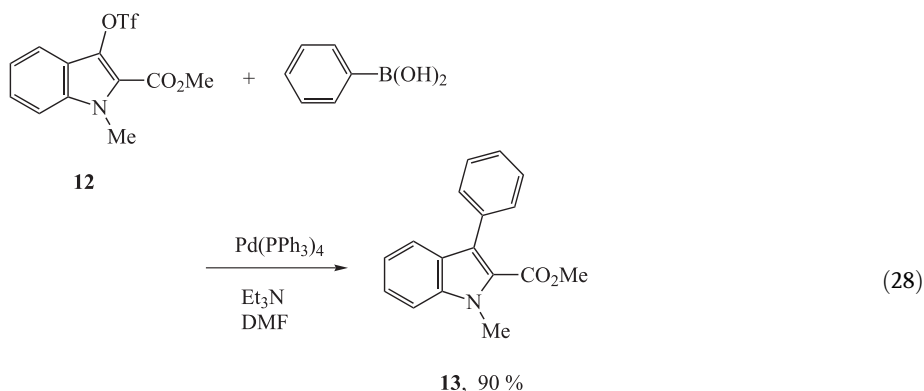


Non-steroidal antiinflammatory drugs (NSAIDs) are the main therapeutic agents for the treatment of the symptoms of arthritis. The drugs seem to inhibit the enzyme cyclooxygenase and consequently the conversion of arachidonic acid into prostaglandins. The main drawbacks of NSAIDs are severe side effects, including gastrointestinal ulceration and

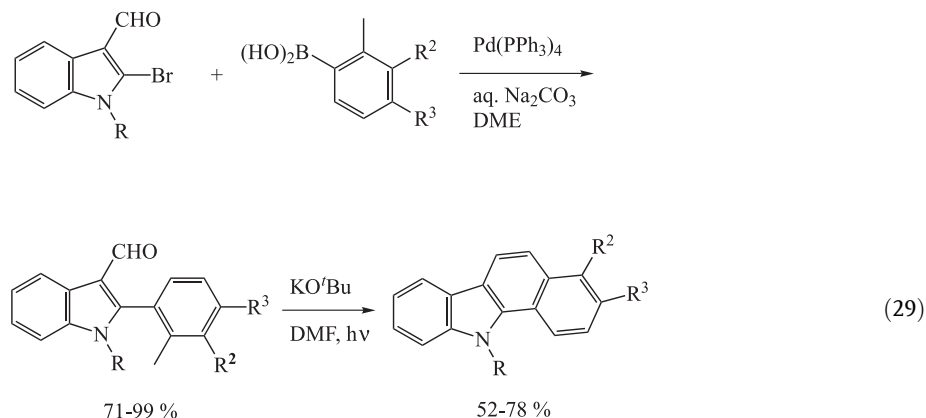
bronchospasm. Recently, 2,3-dihydro-1*H*-pyrrolizine derivatives such as ML-3000 were proven to selectively inhibit the enzymes cyclooxygenase and 5-lipoxygenase. Thus, ML-3000 is one of the most potent and well-balanced dual inhibitors of both enzymes. However, the previous synthesis of ML-3000 proceeds with poor overall yields (<5 %). Most recently, Cossy and Belotti have reported that ML-3000 may be obtained from 1-chloro-3-phenyl-2-propyne in eight steps in an overall yield of 19 %. The key step is a Suzuki cross-coupling reaction between a heteroaryl triflate and (4-chlorophenyl)boronic acid (Eq. (27)) [55].



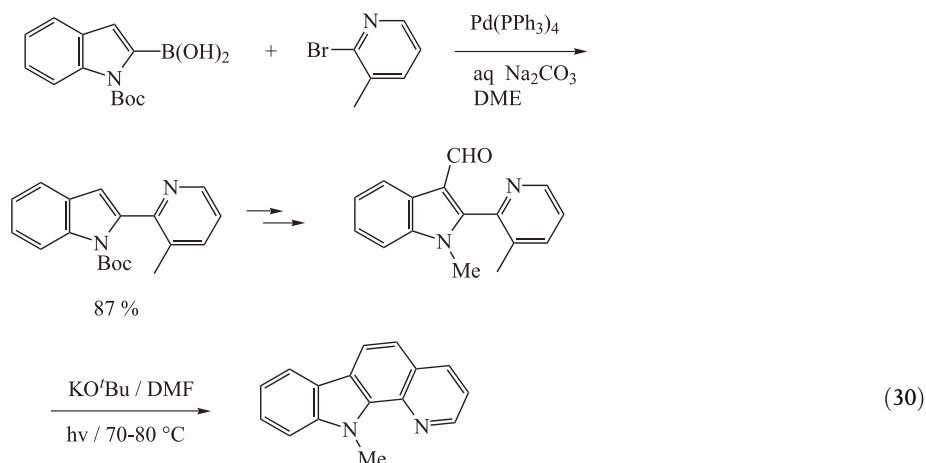
In recent years, palladium(0)-catalyzed Suzuki coupling reactions have been reported in indole chemistry, whereby the indole moiety is usually introduced using an indolylboronic acid [56], but little work has been carried out with 2- or 3-haloindoles. Recently, Malapel-Andrieu and Merour [57] reported such a Suzuki coupling using substituted 3-indolyltriflate and arylboronic acids, which afforded the corresponding 3-substituted indoles. Since 3-phenylindoles have interesting pharmacological structures, resembling endothelin antagonists, these authors have treated the triflate (**12**) with phenylboronic acid to produce the coupling product (**13**) in 90 % yield (Eq. (28)). Although it is well known that inorganic bases are recommended for the Suzuki reaction, organic bases such as triethylamine gave satisfactory results in this reaction.



2-Bromoindole-3-carbaldehyde, or its *N*-methyl analogue, was found to undergo Suzuki coupling with boronic acids in the presence of palladium(0); subsequent treatment of the coupled products with potassium *tert*-butoxide gave the desired carbazoles in good yields (Eq. (29)) [58].

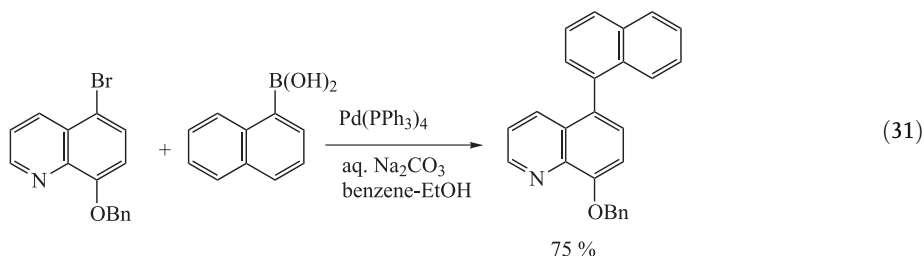


A versatile and convenient method for the synthesis of substituted benzo[*a*]carbazoles and pyrido[2,3-*a*]carbazoles has recently been developed [59]. Treatment of 2-(*o*-tolyl)- or 2-(3-methyl-2-pyridyl)-substituted indole-3-carbaldehydes (obtained by Suzuki reaction) with potassium *tert*-butoxide in DMF at 70–80 °C under irradiation by a 400 W high-pressure mercury lamp afforded benzo[*a*]carbazoles and pyrido[2,3-*a*]carbazoles, respectively, in good yields (Eq. (30)).

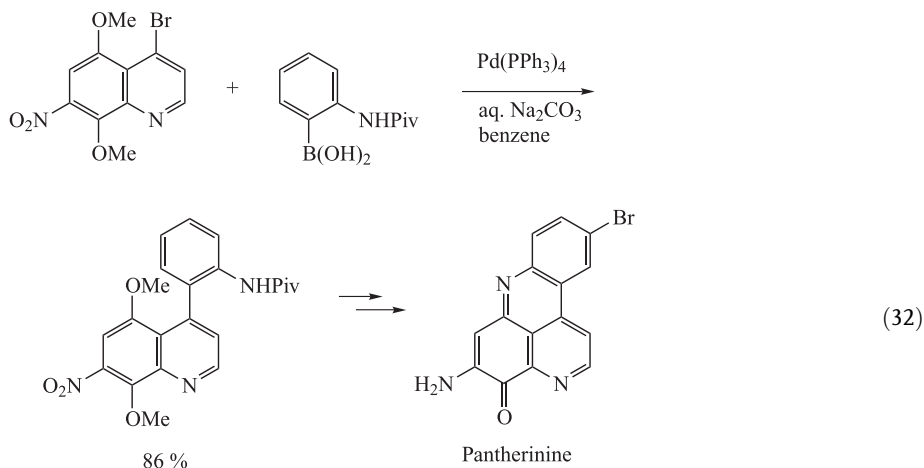


In the course of an investigation on axial chirality in metal chelates [60], 4- and 5-aryl-substituted quinolin-8-ols were required. If, in the case of aryl groups bearing bulky sub-

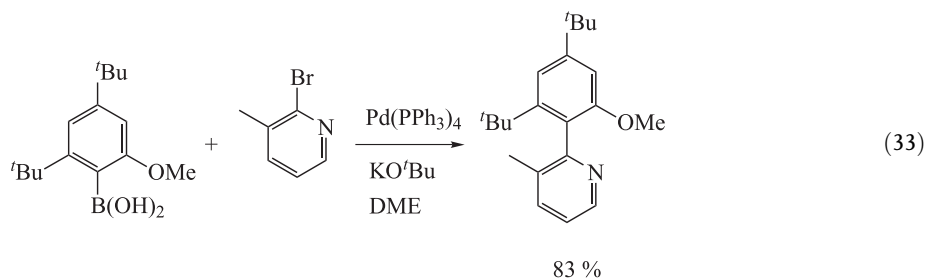
stituents on the quinoline ring, there is a sufficient energy barrier to rotation about the pivotal bond, as in 5-arylquinolin-8-ols, this series of ligands is very fruitful for the development of a new entry to axial chirality based on quinolin-8-ol chelates. Furthermore, considering the applicability of these ligands in analytical science, electronic devices, and pharmaceuticals, they are evidently promising and important in various fields of science. Classically, 5-arylquinolin-8-ols have been prepared by a Skraup synthesis from 2-amino-4-arylphenols and acrolein or its equivalent. If it is possible to directly introduce the required aryl groups at the desired position of quinolin-8-ol, the synthetic route is much more advantageous. Recently, such a direct introduction of aryl groups was reported by Nakano [61], employing a Suzuki coupling reaction (Eq. (31)).



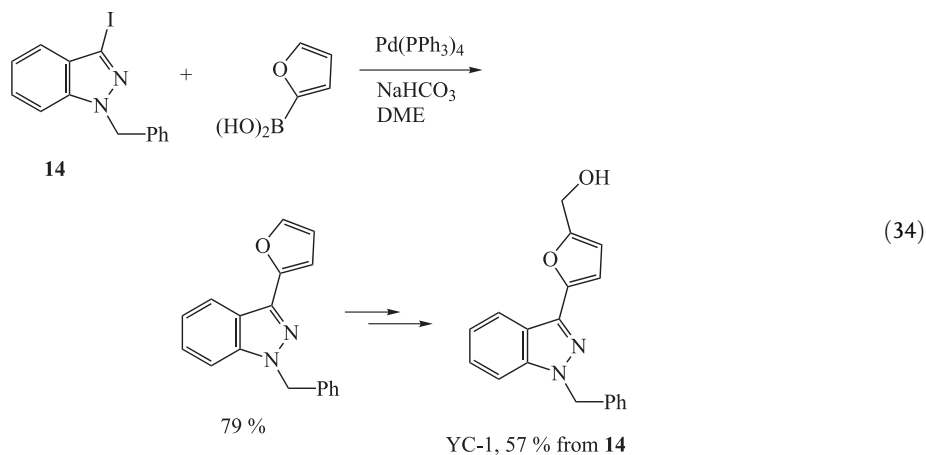
During the last decade a series of structurally fascinating and biologically active fused polycyclic aromatic alkaloids has been isolated from marine sources. One such alkaloid, pantherinine, has recently been synthesized using the Suzuki reaction (Eq. (32)) [62].



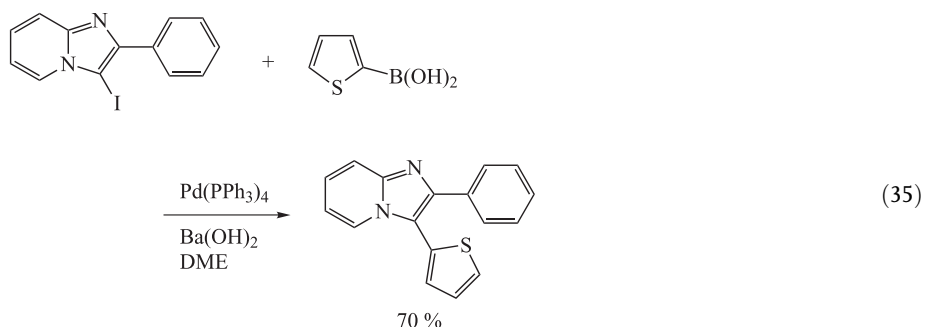
A highly sterically hindered pyridylphenol derivative has been synthesized by means of a Suzuki cross-coupling (Eq. (33)) [63].



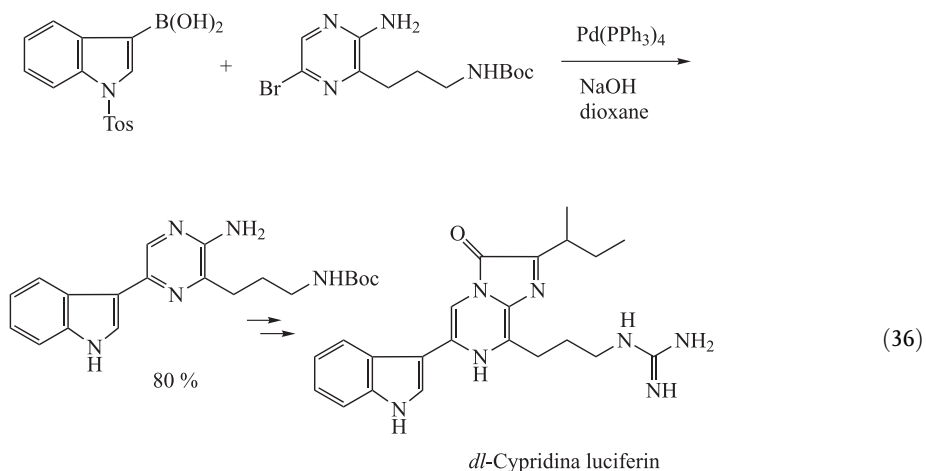
The indazole nucleus is a seldom used but effective pharmacophore in medicinal chemistry, as illustrated by its application in pharmaceutical agents in fields as diverse as CNS disorders, antiinflammatories, and HIV protease inhibition. However, compared to indoles and benzimidazoles, indazole chemistry remains poorly studied due to the limited synthetic approaches to these compounds. Most syntheses of indazoles reported in literature start from benzene derivatives, and the pyrazole moiety is generated by ring-closure starting from isatins, *o*-substituted anilines, or phenyl hydrazines. These traditional synthetic routes do not readily facilitate substitution of at the 3-position with aryl or heteroaryl nuclei. Although YC-1, a pharmacological agent with potential use in the treatment of cardiovascular diseases or erectile dysfunction, was obtained synthetically, its overall yield was only 4 % [64]. Recently, Rault et al. reported a new synthetic method for 3-arylindazoles based on a Suzuki-type coupling reaction of 3-iodoindazoles with aryl- and heteroarylboronic acids, which offered a general and flexible route to 3-arylindazoles, including YC-1, in good yields (Eq. (34)) [65].



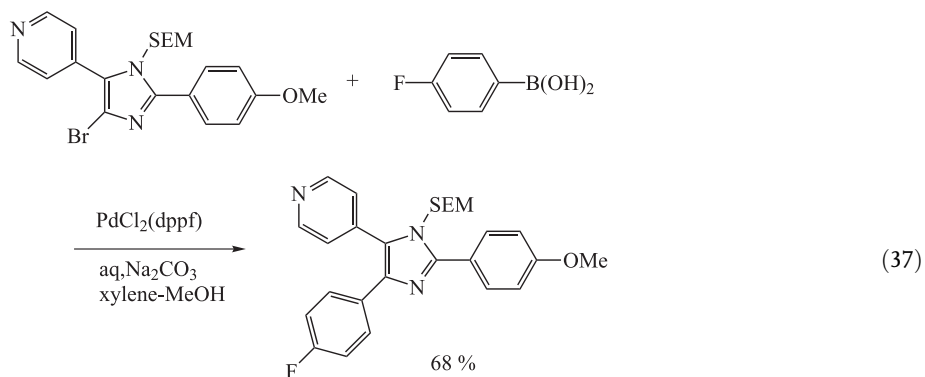
The influence of the base and solvent on Suzuki cross-coupling reactions of various 2-substituted 3-iodoimidazo[1,2-*a*]pyridines has been reported. The reactivity is mainly influenced by the nature of the substituent. Optimized yields and shortened reaction times were achieved using strong bases in DME (Eq. (35)) [66].



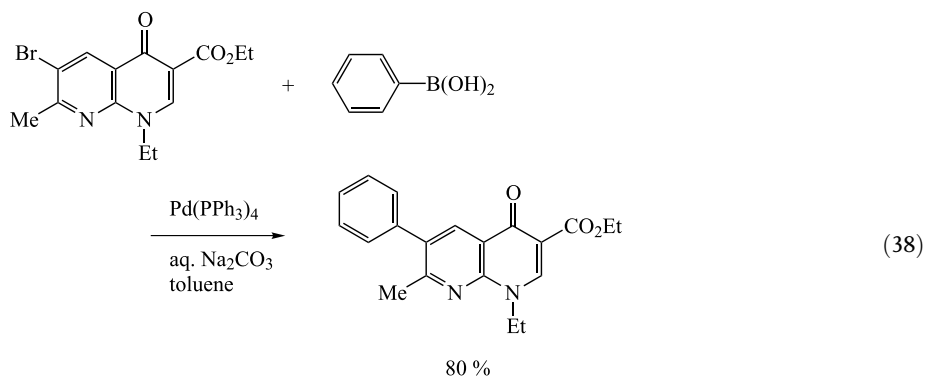
Cypridina luciferin is an imidazopyrazinone involved in the bioluminescence of the crustacean *Cypridina (Vargula) hilgendorfii*. The first total synthesis of this natural product was achieved by Kishi in 1966, which was followed by that of White and Karpetsky in 1971. Most recently, Nakamura et al. developed a convenient, direct procedure for this synthesis, employing Suzuki coupling (Eq. (36)) [67].



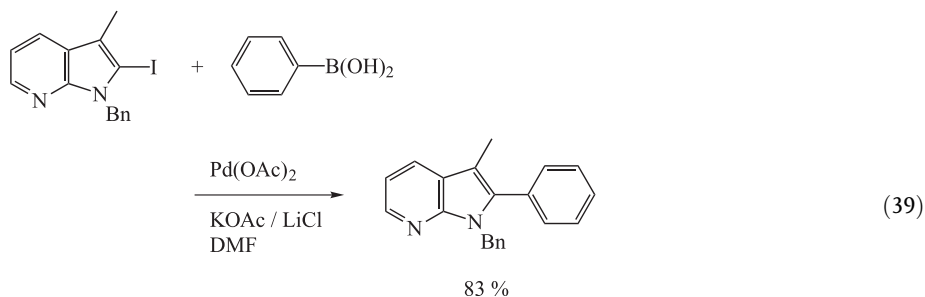
Biologically interesting 4,5-disubstituted and 2,4,5-trisubstituted imidazoles have been prepared by the Suzuki reaction (Eq. (37)) [68].



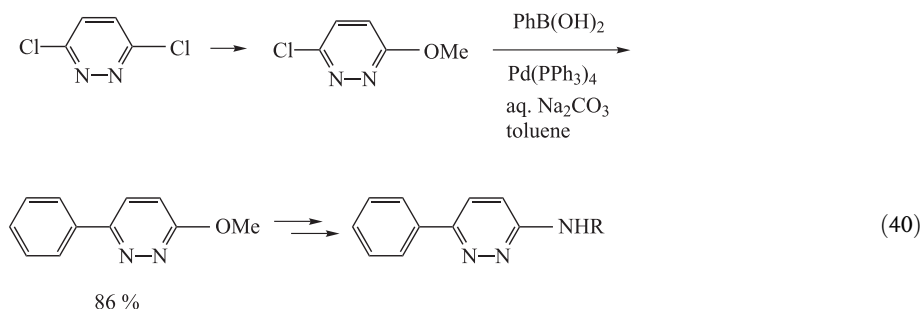
Since the introduction in 1963 of nalidixic acid (*N*-ethyl-7-methyl-4-oxo-1,4-dihydro[1,8]-naphthyridinyl-3-carboxylic acid) as a systemic Gram-negative antibacterial agent, many related derivatives have been synthesized. These types of compounds have received much attention and interest by virtue of their chemical and clinical properties. The methods reported in the chemical literature for preparing C-6- and C-3-substituted 4-oxo[1,8]naphthyridines are somewhat limited. These methods involve the condensation of substituted 2-aminopyridines with suitable 3-ethoxyacrylates, followed by cyclization. Recently, such substituted 4-oxo-1,4-dihydro[1,8]naphthyridines have been obtained using the Suzuki reaction (Eq. (38)) [69].



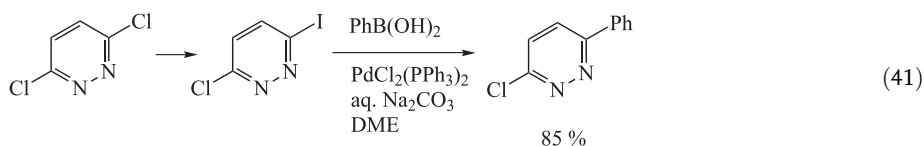
Palladium-catalyzed functionalization at the 2-positions of various 5- and 7-azaindoles has been performed by the Suzuki reaction. The 2-substituted azaindoles were obtained in moderate to high yields by using $\text{Pd}(\text{OAc})_2$, LiCl , and KOAc in DMF at 110 °C (Eq. (39)) [70].



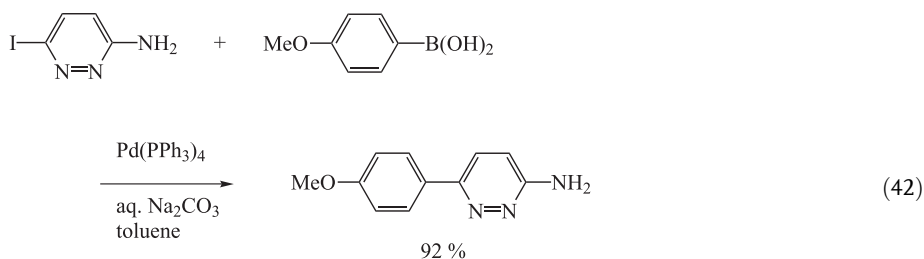
Starting from the commercially available 3,6-dichloropyridazine, 3-amino-6-arylpyridazines, which show acetylcholine esterase inhibiting activities, were prepared in good yields under mild conditions by means of a Suzuki coupling (Eq. (40)) [71].



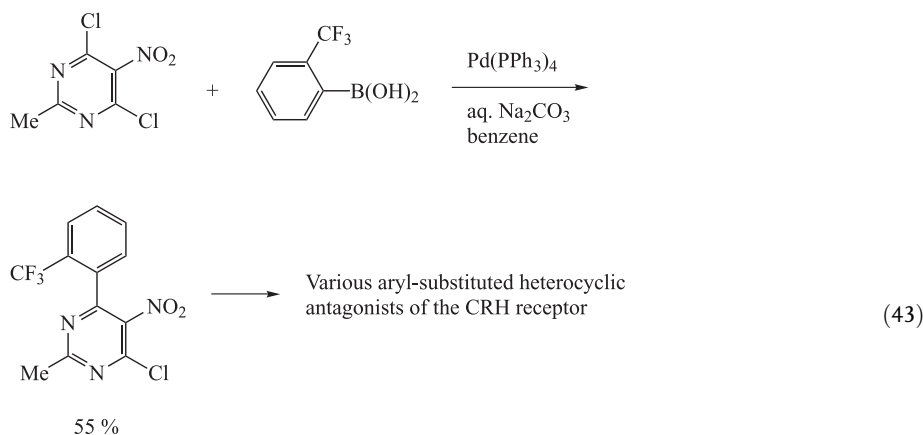
3-Chloro-6-arylpyridazines can also be synthesized in good yields by Suzuki reaction of arylboronic acids with 3-chloro-6-iodopyridazine, the latter being readily accessible from 3,6-dichloropyridazine (Eq. (41)) [72].



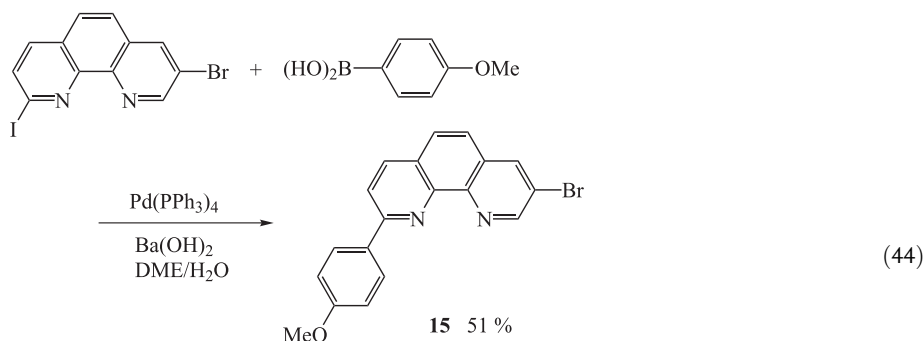
The 3-aminopyridazine skeleton has proved to be interesting from a pharmacological point of view. An interesting group of 3-aminopyridazines are 3-amino-6-(hetero)arylpyridazines as they are intermediates in the synthesis of several pharmacologically active compounds. 6-(Hetero)arylimidazo[1,2-*b*]pyridazines, for instance, have been proposed for the treatment of anxiety and dementia of the Alzheimer type. The 3-amino-6-(hetero)arylpyridazines have hitherto been prepared by a multistep sequence starting from 3(2*H*)-pyridazinones. Recently, a new approach towards the synthesis of 3-amino-6-(hetero)arylpyridazines based on the palladium-catalyzed cross-coupling reaction has been proposed (Eq. (42)) [73].



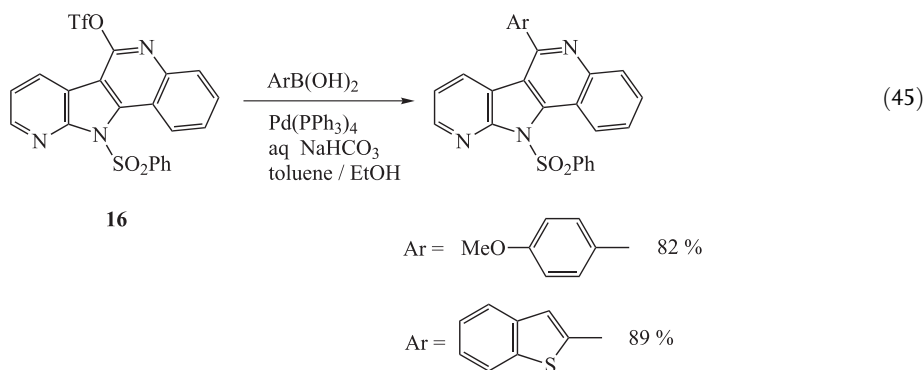
Based on a new substantial body of pharmacological and clinical evidence, it is anticipated that the modulation of the effects of corticotropin releasing hormone or factor (CRH or CRF) may eventually play a role in the treatment of depression or anxiety-related disorders. This interest in CRH as a new important target for drug discovery is clearly evident. Recently, Gilligan et al. [74] have observed that the Suzuki reaction can be used to synthesize a variety of aryl-substituted heterocyclic antagonists of the CRH receptor (Eq. (43)).



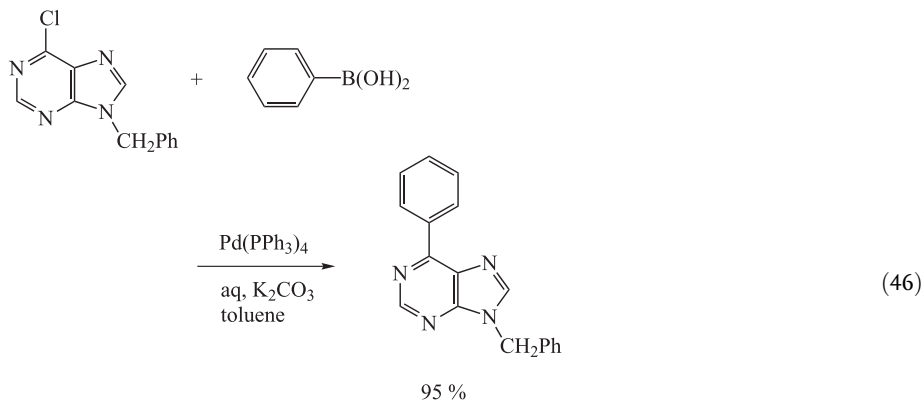
Because of the different reactivities of iodo and bromo substituents in the Suzuki reaction, selective coupling can be realized. For example, 8-bromo-2-(4-methoxyphenyl)-1,10-phenanthroline (**15**) can be prepared by reacting the 4-boronic acid derivative of anisole with bromo(iodo)phenanthroline under Suzuki conditions (Eq. (44)) [75].



Suzuki coupling reactions of **16** with 4-methoxyphenylboronic acid and 2-benzo[*b*]thiophene-2-boronic acid in the presence of $\text{Pd}(\text{PPh}_3)_4$ and aqueous NaHCO_3 as base, in a mixture of toluene/ethanol (5:1) at 90 °C for 2 h, afforded the corresponding coupling products in high yields (Eq. (45)) [76].



Many 6-alkylaminopurine nucleosides are important adenosine receptor antagonists, and acyclic nucleotide analogues derived from 6-dialkylaminopurines are strong antivirals, anti-neoplastic agents, and immunomodulators. Recently, several 6-(arylalkynyl)-, 6-(arylalkenyl)-, and 6-(arylalkyl)purines have been reported to exhibit cytokinine activity. Suzuki cross-coupling reactions of 9-benzyl-6-chloropurine with boronic acids have recently been reported to provide 6-substituted purines in moderate to excellent yields (Eq. (46)) [77].



3.2.3

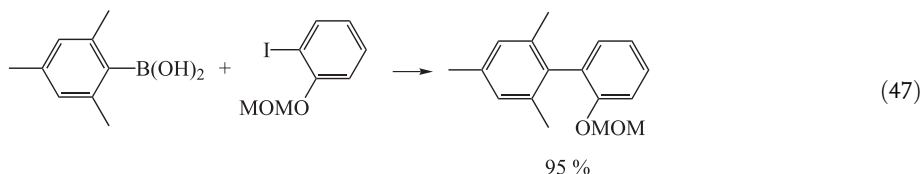
Coupling of Arylboron Compounds Bearing Sterically Bulky or Electron-Withdrawing Substituents

Although steric hindrance of aryl halides is not a major factor in the formation of substituted biaryls, low yields are obtained when *ortho*-disubstituted arylboronic acids are used. For example, the reaction with mesitylboronic acid proceeds only slowly because of steric hindrance during transmetalation to the palladium(II) complex.

The reaction of mesitylboronic acid with iodobenzene at 80 °C in the presence of $\text{Pd}(\text{PPh}_3)_4$ and various bases has been reported [78]. The results are summarized in Table 2.

Aqueous Na_2CO_3 in benzene or DME (dimethoxyethane) is not effective as a base for the coupling of mesitylboronic acid, and the reaction does not reach completion even after 2 days. Although side reactions such as homocoupling occur to a negligible extent, the formation of mesitylene as a result of hydrolytic deboronation increases with increasing reaction time. It is noteworthy that such hydrolytic deboronation is faster in benzene/ H_2O than under the modified conditions using aqueous DME. On the other hand, the addition of stronger bases, such as aqueous NaOH or $\text{Ba}(\text{OH})_2$, both in benzene and DME, has a remarkable accelerating effect on the rate of coupling. By using aqueous $\text{Ba}(\text{OH})_2$ in DME at 80 °C, mesitylboronic acid couples with iodobenzene within 4 h to give the corresponding biaryl in quantitative yield.

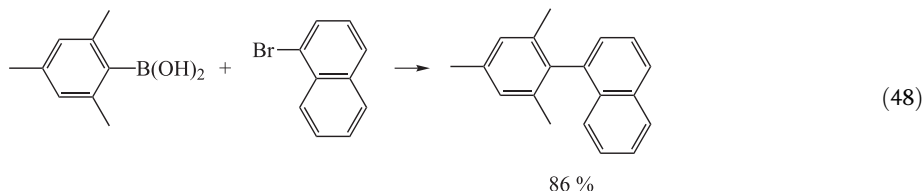
Further coupling reactions of this type are depicted in Eqs. (47) and (48).



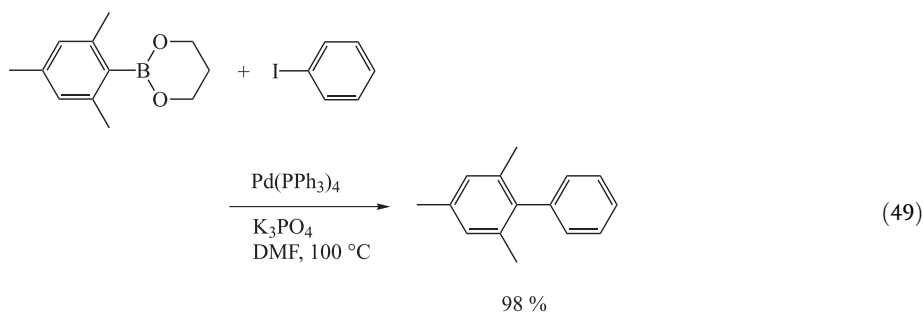
Tab. 2. Reaction of mesitylboronic acid with iodobenzene under different conditions.

Base	Solvent	Temp/°C	Yield/% ^a			
			Time	8 h	24 h	48 h
Na ₂ CO ₃	Benzene/H ₂ O	80		25(6)	77(12)	84(25)
Na ₂ CO ₃	DME/H ₂ O	80		50(1)	66(2)	83(7)
K ₃ PO ₄	DME/H ₂ O	80		70(0)		
NaOH	DME/H ₂ O	80		95(2)		
Ba(OH) ₂	DME/H ₂ O	80		99(2)		

^aGLC yields of the coupling product based on iodobenzene and the yields of mesitylene are shown in the parentheses.

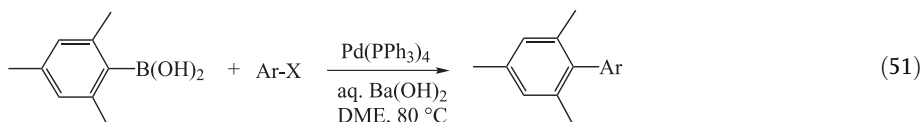
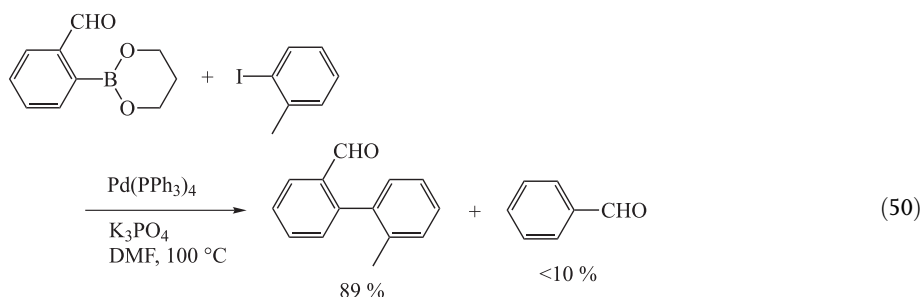


For such sterically hindered boronic acids, an alternative procedure using the esters of boronic acids and an anhydrous base has been developed. Thus, the coupling can readily be achieved by employing the trimethylene glycol ester of mesitylboronic acid and Cs₂CO₃ or K₃PO₄ in DMF at 100 °C, whereby the coupling product is obtained quantitatively (Eq. (49)) [78].

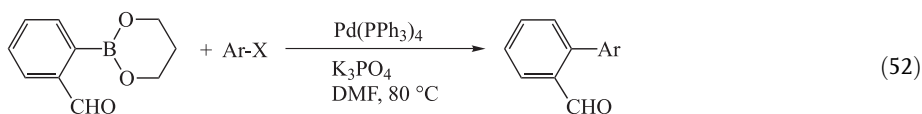


Even if there is no great steric hindrance, the reaction under aqueous conditions is often accompanied by undesirable competitive hydrolytic deboronation [79]. Kinetic studies [80] on the reaction of substituted arylboronic acids indicated that electron-withdrawing substituents accelerate the deboronation. Although there is no great difference between *meta*- and *para*-substituted phenylboronic acids, substituents at the *ortho* position may have a

marked accelerating effect on the rate of deboronation. A 2-formyl group on an arylboronic acid is known to increase the rate of hydrolytic deboronation [80]. Indeed, the coupling of 2-formylphenylboronic acid with 2-iodotoluene at 80 °C using Na_2CO_3 in DME/ H_2O gives only a 54 % yield of the corresponding biaryl, accompanied by benzaldehyde (39 %). Aprotic conditions are desirable for such boronic acids that are sensitive to aqueous base. Thus, the trimethylene glycol ester of 2-formylphenylboronic acid readily couples with iodotoluene at 100 °C in DMF to give the product in 89 % yield, accompanied by less than 10 % of benzaldehyde (Eq. (50)) [78].



ArX: 2-MeOC₆H₄I (80 %), 2-ClC₆H₄I (94%), 2-bromonaphthalene (86 %)



ArX: iodomesitylene (73%), 2-MOMOC₁₀H₆I (85 %)

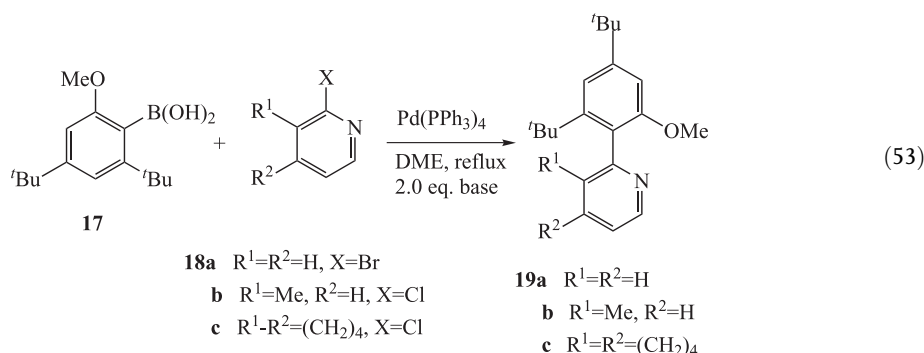
Such modified procedures have been utilized by many chemists [81, 82].

Leadbeater and Griffiths developed palladium catalysts for the Suzuki cross-coupling of aryl halides bearing two *ortho* substituents with phenylboronic acid, and used them in the synthesis of sterically hindered biaryls [83].

Zhang and Chan observed that base has a remarkable accelerating effect on the rate of Suzuki couplings of sterically bulky boronic acids with halopyridines in non-aqueous solvents (Eq. (53)) [84]. For instance, in the reactions of the extremely sterically bulky arylboronic acid **17** with halopyridines **18a–c**, the strong base KO^{*t*}Bu gave the best result among the bases examined (Table 3). During their initial synthetic efforts aimed at obtaining compound **19b**, they did not observe any coupling products under the typical Suzuki reaction conditions using either Na_2CO_3 or NaOEt. Over 70 % of **17** was recovered from the attempted synthesis of **19b** using Na_2CO_3 , while a complex reaction mixture was formed using NaOEt. On increasing the strength of the base, boronic acid **17** underwent a Suzuki cross-coupling with 2-bromo-3-methylpyridine (**18b**), e.g. in the presence of 2.0 equiv. of KO^{*t*}Bu and 5 mol % of Pd(PPh₃)₄ in DME, to produce **19b** in 83 % yield (Table 3).

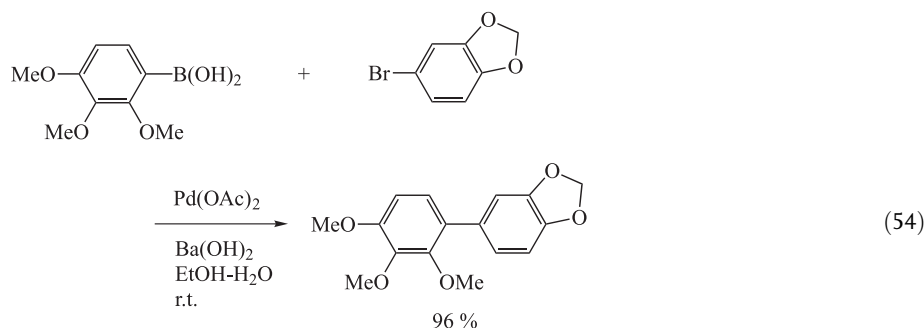
Tab. 3. Base effect on the cross-coupling of arylboronic acid with halopyridines, yield (%) / reaction time (h).

Base	19a	19b	19c
Na ₂ CO ₃	26/90	0/90	0/90
NaOH	40/140	22/24	44/26
NaOEt	74/4	0/12	45/26
KO ^t Bu	86/4	83/16	77/10

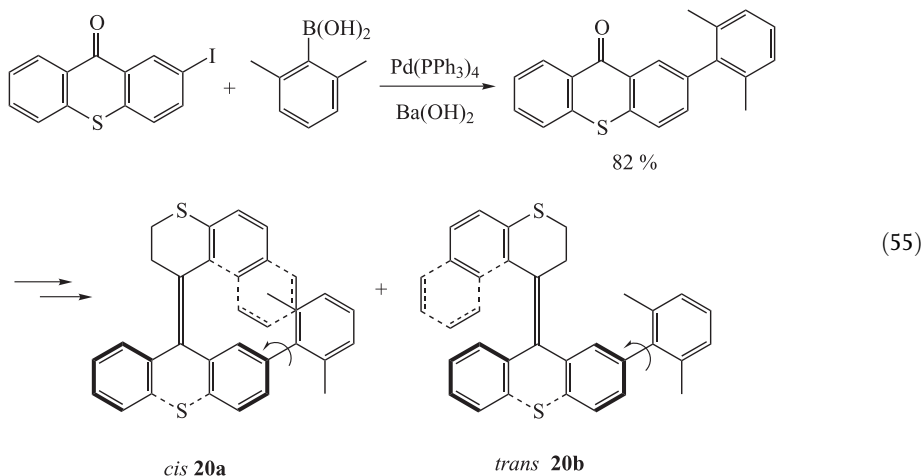


Generally speaking, stronger bases may give such better yields of coupling products, but the relationship between the base strength and product yield or reaction time should be considered more prudentially.

Restricted rotation about the biaryl axis as a result of bulky substituents leads to the existence of atropisomers. Depending upon the degree of steric hindrance due to the *ortho* substituents, three or four substituents are needed to produce a sufficient barrier to rotation at room temperature. This particular form of axial chirality is not generally resistant to heat. To produce acceptable yields of hindered biaryls under Suzuki conditions, high temperatures (60–110 °C) [78, 85] and reaction times of several hours are required. In atropisomer-selective reactions, these conditions would be deleterious to the discrimination between diastereomeric transition states and could racemize the biaryls formed. As a consequence, it is necessary to carry out such Suzuki reactions at ambient temperature. Recently, conditions employing Pd(OAc)₂ and 95 % ethanol were used to generate mono-*ortho*-substituted biaryls at 20 °C (Eq. (54)) [86].



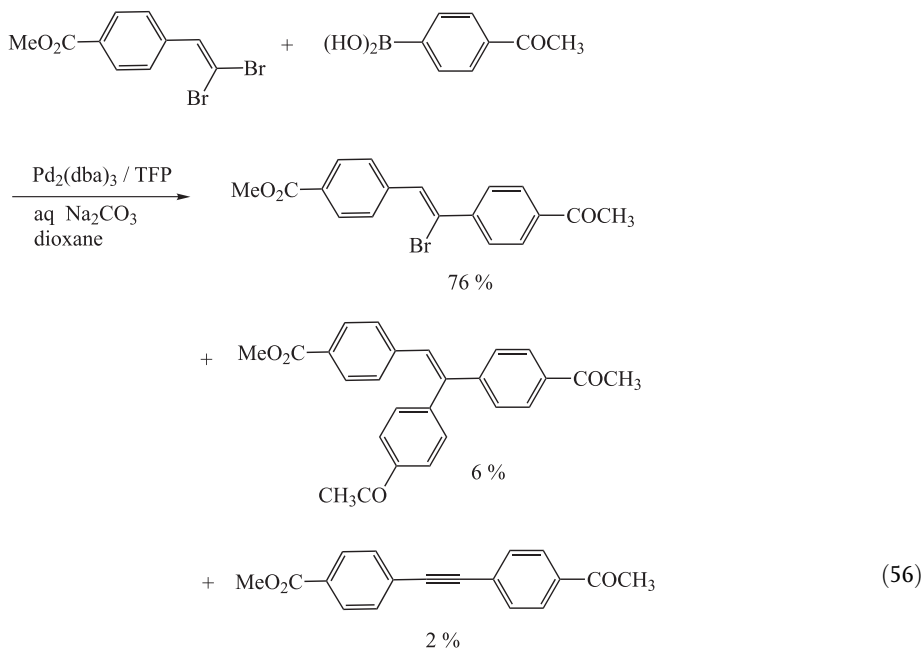
In an approach towards a photochemically bistable molecular rotor, the synthesis of the sterically overcrowded isomeric alkenes *cis*-**20a** and *trans*-**20b**, functionalized with an *o*-xylyl group as a rotor, has been described (Eq. (55)) [87]. The key step in the synthesis was a Suzuki coupling to attach the xylyl moiety.



3.2.4

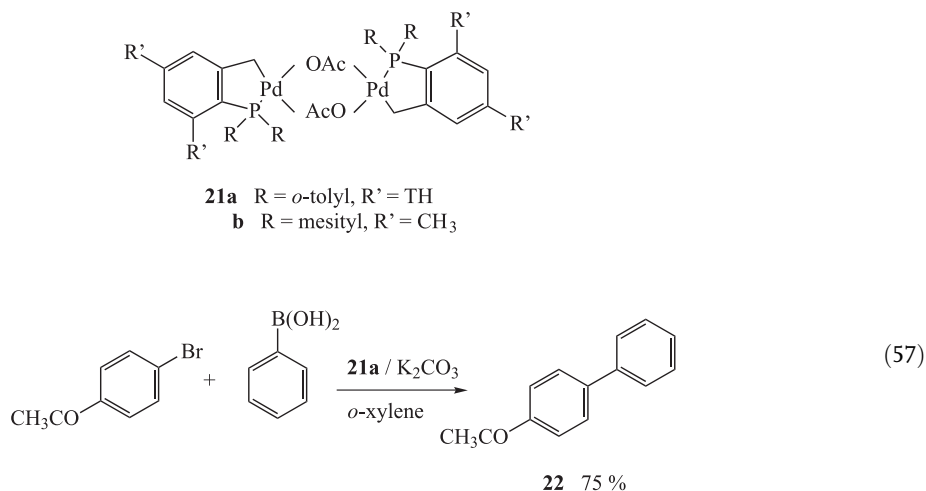
Modified Catalysts and Ligands

The (*E*)-bromides in 1,1-dibromo-1-alkenes can be stereoselectively coupled with aryl- or alkenylboronic acids to give the corresponding (*Z*)-1-aryl(or alkenyl)-1-bromo-1-alkenes. Tris(2-



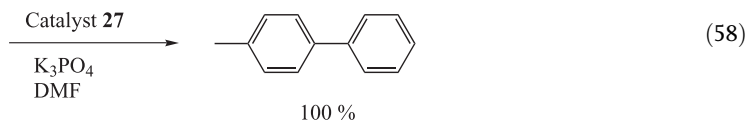
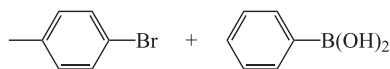
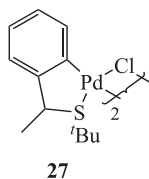
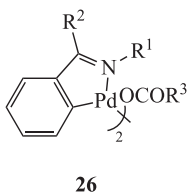
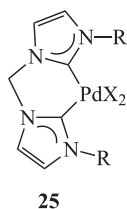
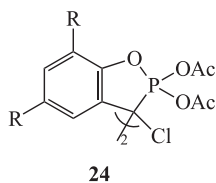
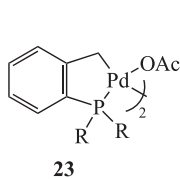
furyl)phosphine (TFP) is used as a ligand for the palladium, and the combination of 1,4-dioxane and aqueous sodium carbonate produces the best results (Eq. (56)) [88]. Depending on the reaction conditions and reactants, some by-products are obtained. This work demonstrates that the soft ligand TFP is effective in the palladium-catalyzed coupling of 1,1-dibromo-1-alkenes with organoboronic acids. These modified Suzuki reaction conditions are advantageous compared to the corresponding Stille reaction [89] and the previously reported Suzuki reaction [90].

In recent years, a large number of palladium-mediated Suzuki syntheses of complex synthetic building blocks, as well as of structurally simple but industrially important intermediate products, have been reported and further developed. However, the quality of the catalysts used is generally not sufficient for industrial demands. As a result of the increasing importance of unsymmetrically substituted biaryl derivatives, for example, as drug intermediates, the transferability of the catalytic properties of the palladacycle complexes (**21a,b**) to the cross-coupling between aryl halides and arylboronic acids was examined [91]. It emerged that palladacycles **21** catalyze this type of reaction with unusual efficiency. When 4-bromoacetophenone is treated with phenylboronic acid under the appropriate conditions [bromoacetophenone (10 mmol), phenylboronic acid (15 mmol), K_2CO_3 (20 mmol), catalyst **21a** (0.001 mol %), *o*-xylene (30 mL), reaction temperature 130 °C], the expected coupling product (**22**) is obtained in 75 % yield, and the turnover number (TON) 75000 is achieved using only 0.001 mol % of **21a** as the catalyst (Eq. (57)).



Najera et al. [92] have reported that for the coupling of aryl halides with organoboronic acids, complexes **23–26** are adequate catalysts, giving TONs between 10^2 and 10^6 . These palladacycles exhibit greater aerial and thermal stability than palladium(0) complexes.

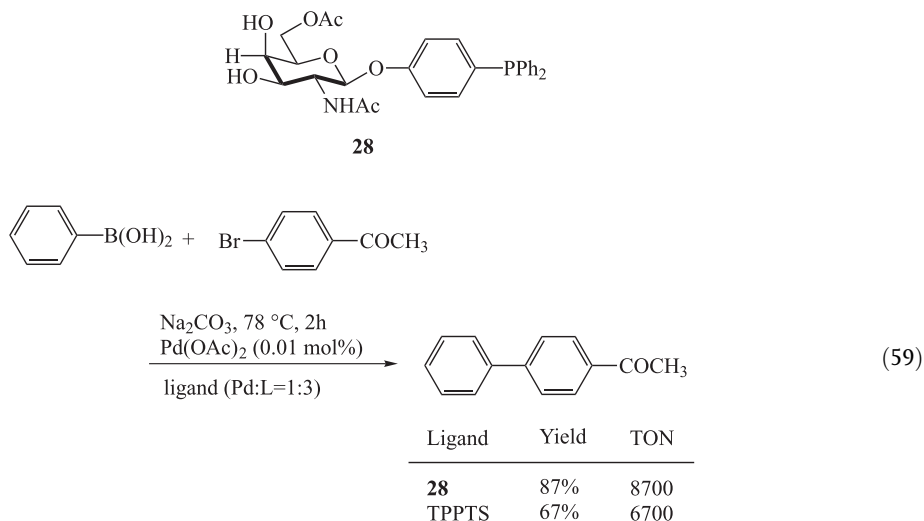
Most recently, Monteiro et al. have reported that cyclopalladated compounds derived from the *ortho*-metalation of benzylic *tert*-butyl thioethers are excellent catalyst precursors for the Suzuki cross-coupling reaction of aryl bromides and chlorides with phenylboronic acid under mild reaction conditions. A broad range of substrates and functional groups are tolerated in this protocol, and high catalytic activity is attained (Eq. (58)) [93].



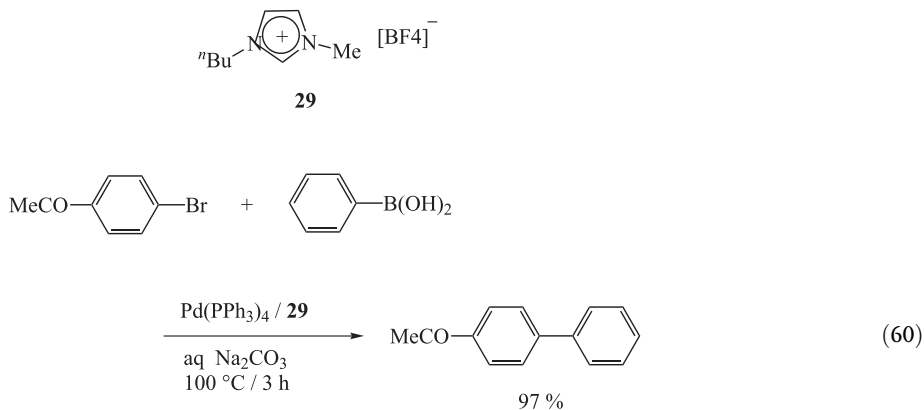
The Suzuki reaction of aryl bromides and chlorides is efficiently catalyzed by palladium/phosphite complexes generated in situ. The influence of the ligand, base, and various additives was examined. The process tolerates various functional groups, and catalyst turnovers of up to 820,000 were obtained, even with deactivated aryl bromides [94].

The two basic problems of homogeneous catalysis, separation and recycling of the catalyst, can be solved by using two-phase catalysis. Here, the catalyst is in a hydrophilic phase, in which the organic products are insoluble. In order to implement this principle, it is necessary to develop new ligands that are soluble in hydrophilic phases. Diphenylphosphinoacetic acid and the TPPTS ligand (TPPTS, trisodium salt of triphenylphosphane trisulfonate) are used on the ton-scale for the most important industrial two-phase processes. To attain sufficient solubility of the ligands in polar media (particularly water), inorganic groups (sulfonic acid and carboxylic acids, quaternary aminoalkyl/aryl groups, and phosphonium salts) are usually used as substituents on the phosphanes. Beller et al. reported a new class of polar, hydrophilic triarylphosphanes for two-phase catalysis, consisting of aryl- β -O-glycosides of

glucose, galactose, and glucosamine [95]. Thus, the ligand **28** shows a high catalytic activity in the Suzuki reaction (Eq. (59)).

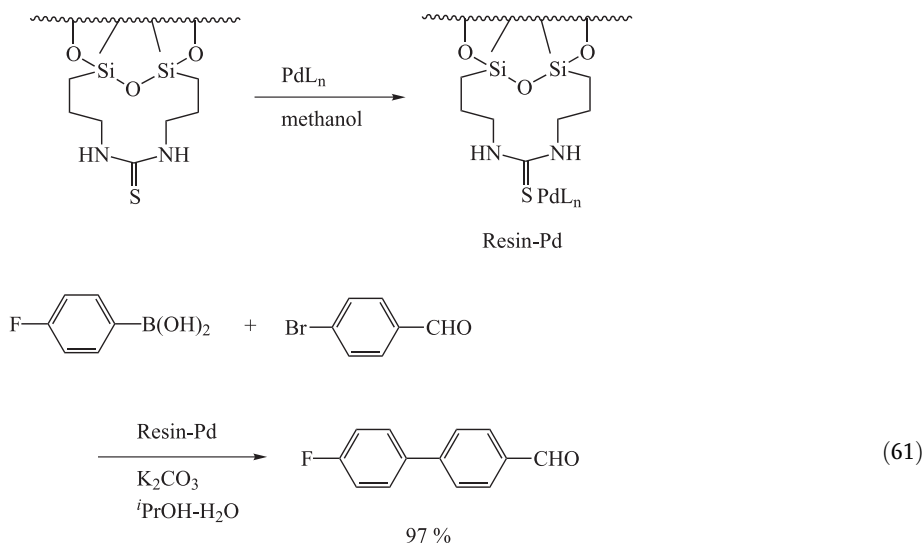


Palladium-catalyzed Suzuki cross-coupling reactions can be conducted in the ambient temperature ionic liquid, 1-butyl-3-methylimidazolium tetrafluoroborate (**29**), in which unprecedented reactivities are witnessed, and which allows easy product isolation and catalyst recycling (Eq. (60)) [96].



Zhang and Allen [97] have recently reported an easily prepared, air- and moisture-stable resin-bound palladium catalyst for the Suzuki coupling reaction. Commercially available resin-bound thiourea, Deloxan THP II [98], was used as the starting material. The resin-bound catalyst was prepared simply by treating the wet Deloxan resin with a solution of $\text{Pd}(\text{OAc})_2$ in methanol. Suzuki coupling reactions were then carried out using the resin at a

level equivalent to 2–3 mol % Pd in a mixture of water and isopropanol (Eq. (61)). The reactions proceeded at a similar rate and gave similar yields to those carried out using conventional homogeneous catalysts such as $\text{Pd}(\text{PPh}_3)_4$.



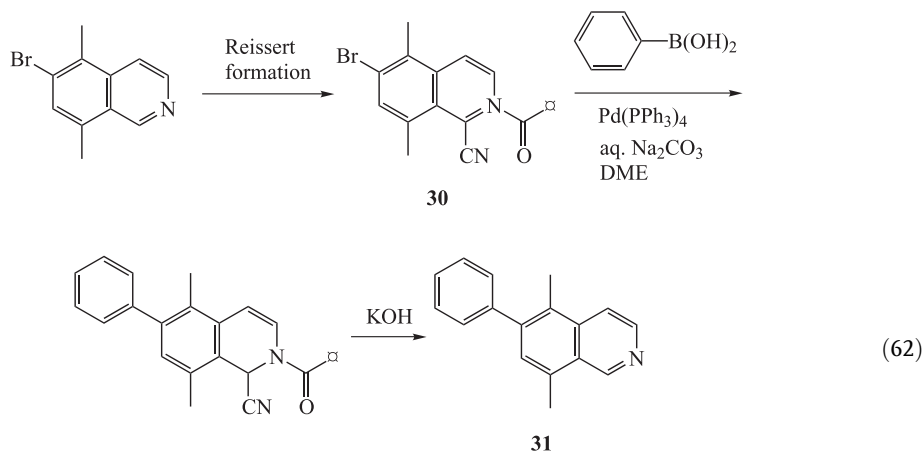
One limitation to the scope of the Suzuki reaction has been its inefficiency when aryl chlorides are employed as substrates. Recently, Buchwald and Fu have discovered the palladium-catalyzed cross-coupling of aryl chlorides with organoboron reagents, employing highly active palladium catalysts mediated by special ligands. These are discussed in Section 3.4.

3.2.5

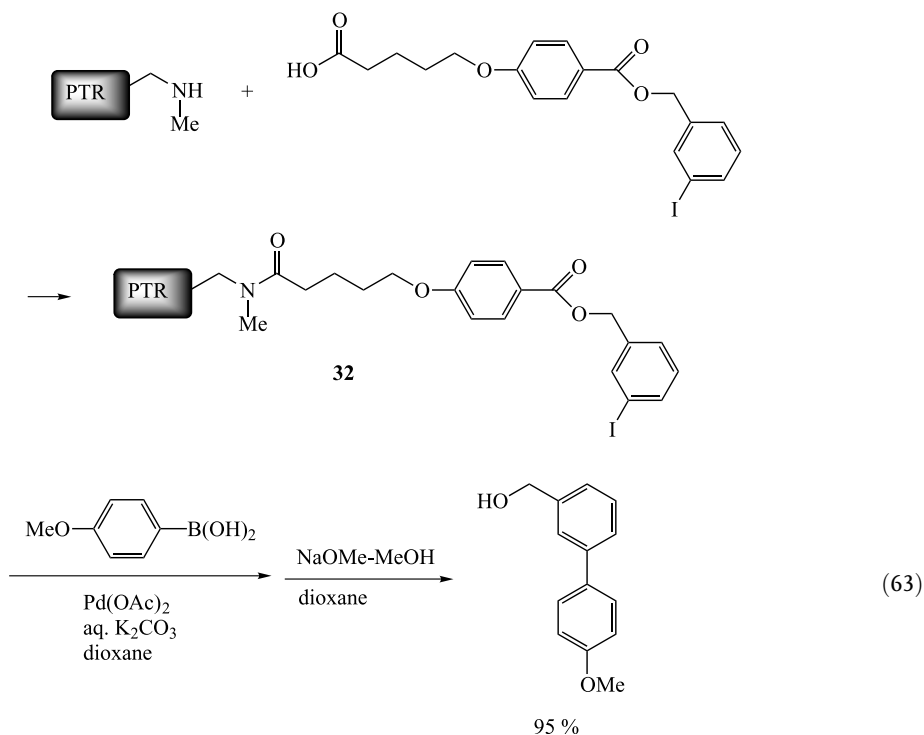
Solid-Phase Synthesis (Combinatorial Methodology)

A traceless solid-phase synthetic strategy has been developed. For example, a solid-phase Suzuki coupling of the Reissert intermediate **30** to **31** has been reported. The process consists of three steps: (a) Solid-phase Reissert formation by the reaction of polymer-supported benzoic acid chloride resin with an isoquinoline, followed by reaction with TMSCN to afford the aryl bromide of Reissert **30**, (b) Suzuki coupling of the solid-phase Reissert **30** with phenylboronic acid to provide the coupling product, and (c) subsequent treatment of the coupling product with aqueous KOH to produce **31** (86% overall yield based on the starting bromide) (Eq. (62)) [99].

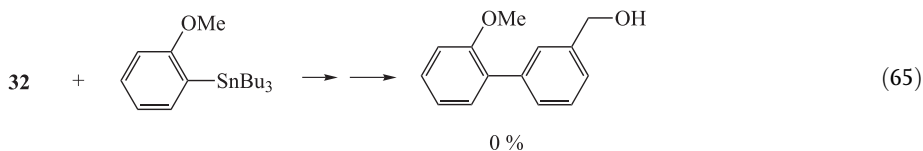
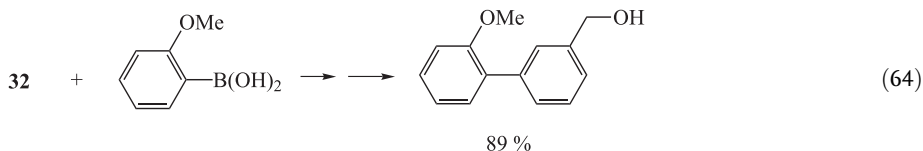
A 9-phenylfluoren-9-yl polystyrene-based resin has been described for the attachment of nitrogen and oxygen nucleophiles. Greater acid stability compared to the standard trityl resins that are widely used in solid-phase peptide synthesis make this solid support an interesting alternative in solid-phase organic synthesis. This resin can be used in Suzuki coupling reactions to furnish biaryls in good yields [100].



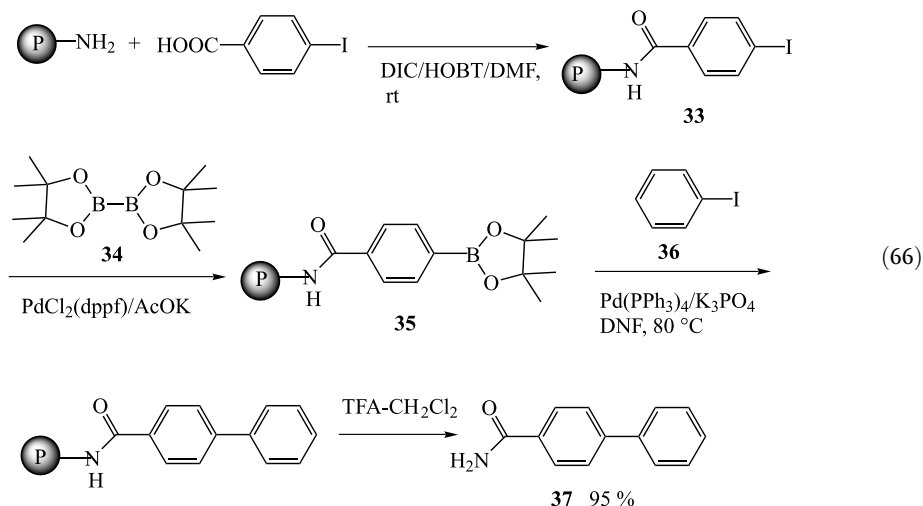
The scope and limitations of Pd(0)-mediated coupling reactions between aromatic halides linked to a polystyrene resin and boronic acid derivatives (Suzuki coupling) or arylstannanes (Stille coupling) have been reported. For all the reactions, the conditions were optimized and evaluated with various reagents. In most cases, products were obtained in excellent yields upon cleavage from the solid support (Eq. (63)) [101].

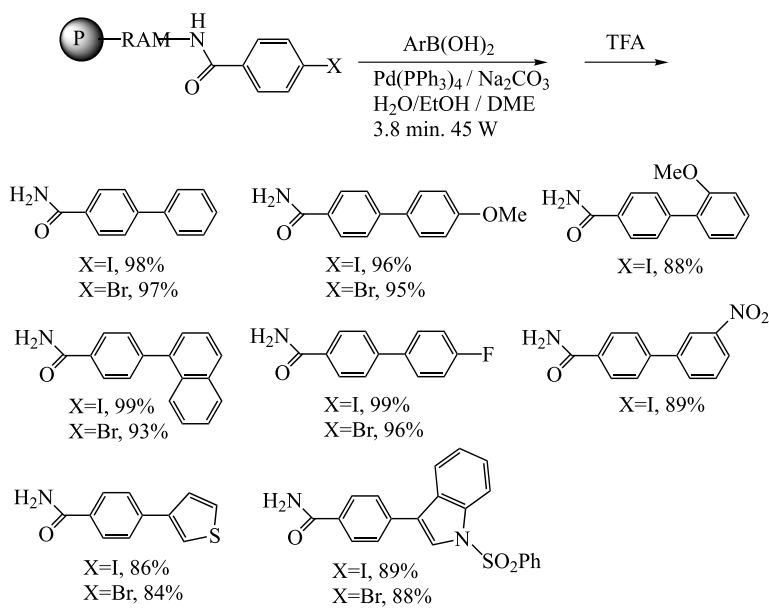


It is worthwhile pointing out that coupling results with electron-rich aryltin derivatives (Eq. (65)) were far inferior to those obtained with the corresponding boronic acids (Eq. (64)) [102].



Constructing libraries of nonpolymeric, small organic molecules by solid-phase techniques has been the recent focus of combinatorial synthesis. While many pharmacologically interesting molecules have been prepared on solid supports in the last few years, most of the linkers (e.g., OH, COOH, NHR) employed in these syntheses were inherited from those used in generating peptide, oligonucleotide, and oligosaccharide libraries. Efforts to prepare boronic acid derivatives on solid-phase using classical methodology have met with little success. Piettre and Baltzer [103] found that application of Miyaura's conditions [pinacol ester of diboron (**34**) (2 equiv.), PdCl₂(dppf) (0.03 equiv.), KOAc (3 equiv.) in DMF at 80 °C for 20 h] to a model polymer-bound *p*-iodobenzamide (**33**) leads to a solid-phase boronate (**35**). Subsequent reaction of **35** with an aryl halide such as **36** in the presence of Pd(PPh₃)₄ (0.02 equiv.)/K₃PO₄ (5 equiv.)/DMF at 80 °C gives **37** in 95 % yield (Eq. (66)) [104].



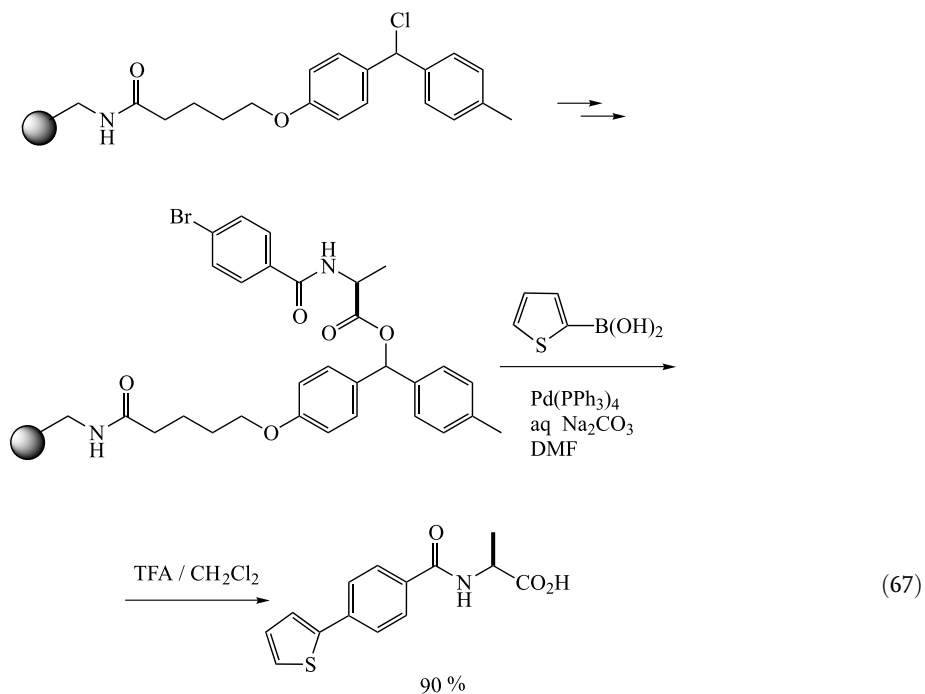
Tab. 4. Suzuki coupling on solid-phase assisted by microwave irradiation.

In combinatorial chemistry, the reaction times and reaction temperatures required are frequently crucial factors. Microwave irradiation is used to enhance reaction rates [105]. Larhed et al. recently reported that microwave-assisted, palladium-catalyzed coupling of aryl and heteroaryl boronic acids with iodo- and bromo-substituted benzoic acids, anchored to Tentagel S RAM, provides coupling products in excellent yields after a reaction time of just 3.8 minutes (45 W) [106]. The preparative results are summarized in Table 4.

Numerous linkers have been developed with the aim of immobilizing substrates on a solid support. Commercially available (\pm)- α -lipoic acid has been employed as a novel, chemically stable linker for the immobilization of ketones. The utility of this thioacetal-based linker in solid-phase synthesis has been demonstrated by the synthesis of several 4-acetylbiphenyls by means of the Suzuki reaction. The products were readily cleaved from the solid support by treatment with [bis(trifluoroacetoxy)iodo]benzene [$\text{PhI}(\text{OCOCF}_3)_2$] [107].

Recently, the Suzuki reaction has been extensively developed for solid-phase organic chemistry as a method allowing the parallel synthesis of potential medicinal compounds [108]. Chan et al. reported a versatile polymer-supported 4-[4-methylphenyl(chloro)methyl]-phenoxy linker for the solid-phase synthesis of pseudopeptides based on the Suzuki coupling (Eq. (67)) [109].

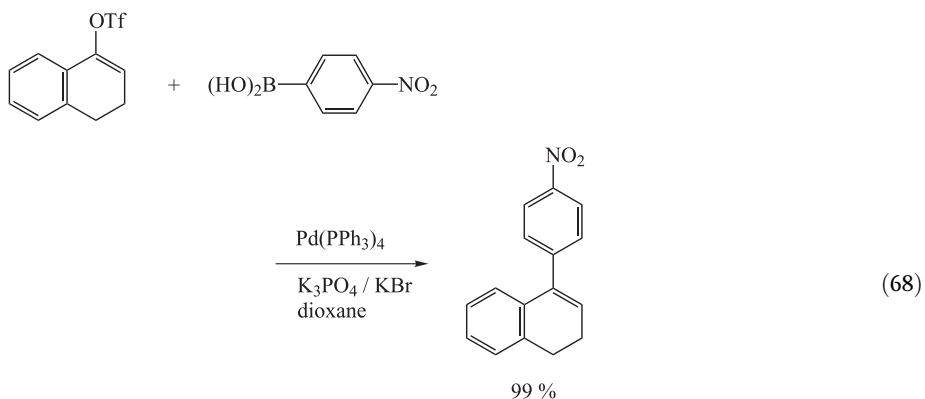
Franzen has recently presented a review on the Suzuki, Heck, and Stille reactions on solid supports [110].



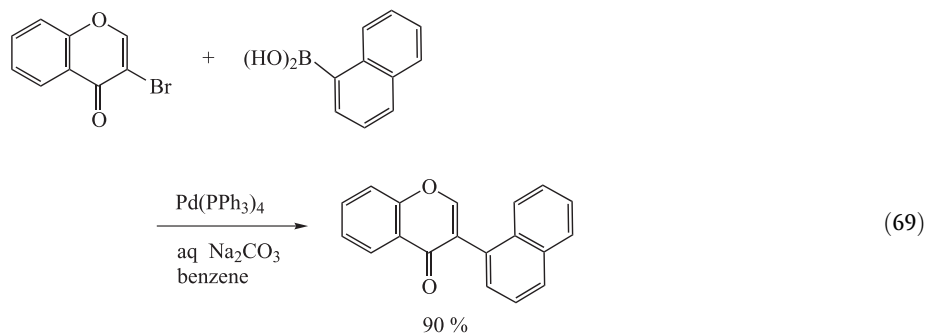
3.3

Reactions with 1-Alkenyl Halides and Triflates

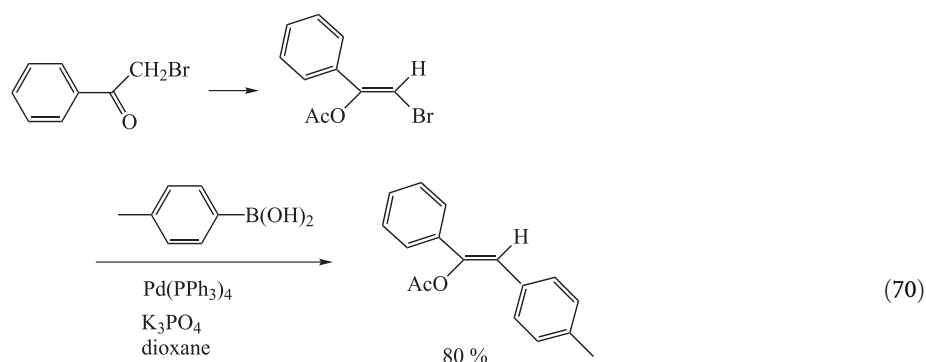
Arylboronic acids are also efficient reagents for the arylation of 1-alkenyl halides and triflates. The first such cross-coupling reactions between arylboronic acids or esters and 1-alkenyl electrophiles were performed in the presence of a palladium catalyst and a base [111].



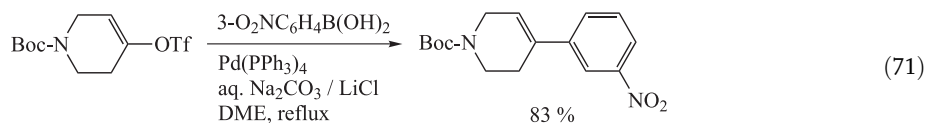
It was further discovered that 3-bromochromones readily react with arylboronic acids or their esters under the Suzuki coupling conditions to provide the corresponding isoflavone derivatives in excellent yields (Eq. (69)) [112].



Stereodefined enol acetates of ketones can readily be synthesized by palladium-catalyzed cross-coupling reactions of arylboron compounds with enol acetates of α -bromo ketones (Eq. (70)) [113].

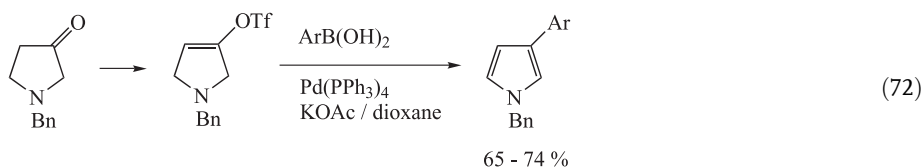


Arylcycloalkenes are prepared by cross-coupling with the corresponding triflates [114]. In the arylation of triflates, higher yields can be obtained in the presence of LiCl or LiBr (Eq. (71)).

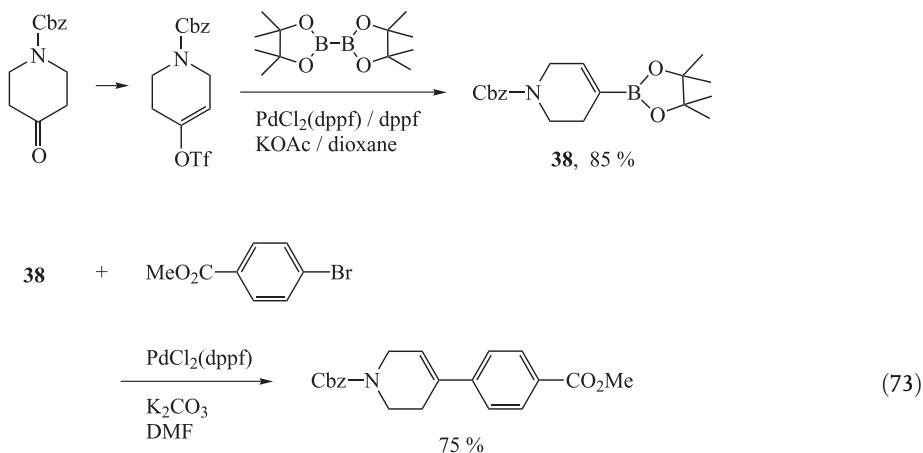


The introduction of substituents at the 3-position of pyrrole has been actively pursued in recent years due to the importance of this class of compound in natural product synthesis. In contrast to the significant number of preparations of polysubstituted 3-arylpyrroles, there have been relatively few syntheses of simple 3-arylpyrroles. A literature survey on the preparation of 3-arylpyrroles showed that the methods reported include the reductive cyclization of 2-arylsuccinonitriles, the base-induced ring-closure of arylvinamidinium salts, and

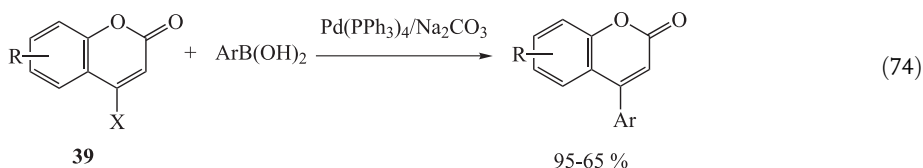
the rhodium-catalyzed hydroformylation of β -alkynylamines with CO/H₂. Recently, a facile synthesis of such 3-arylpyrroles by a tandem Suzuki coupling–dehydrogenation sequence has been reported by Lee and Chung [115]. Thus, the reaction of 1-benzyl-2,5-dihydro-1*H*-pyrrol-3-yl triflate with arylboronic acids in the presence of a palladium catalyst and base leads directly to the formation of 3-arylpyrroles. Apparently, after Suzuki coupling, subsequent dehydrogenation occurs to provide 3-arylpyrroles. Dehydrogenative aromatization can generally be achieved by heating (300–350 °C) hydroaromatic compounds with a catalytic amount of palladium on activated carbon. In the Lee reaction, performed under the Suzuki coupling conditions, the dehydrogenative aromatization of the pyrroline occurs in tandem mode (Eq. (72)).



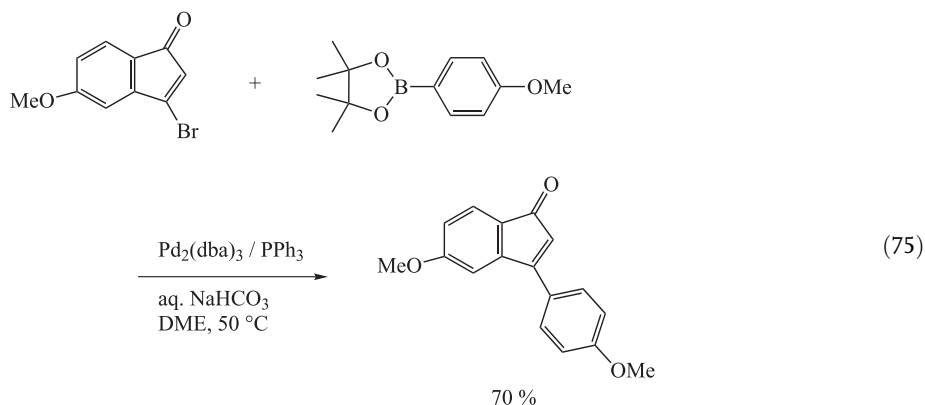
A simple preparation of cyclic vinyl boronates has been achieved from vinyl triflates of *N*-protected tetrahydropyridines. Suzuki coupling of the boronates with aryl bromides, iodides, and triflates proceeds in good yield to give 4-aryl tetrahydropyridines (Eq. (73)) [116].



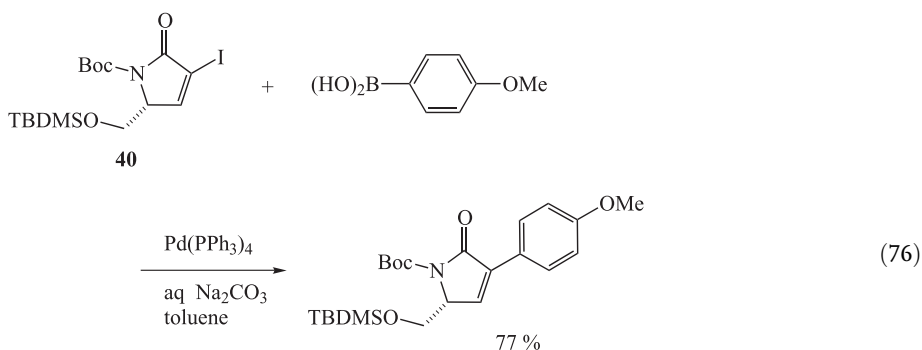
Palladium-catalyzed coupling of the 4-chloro- or 4-bromocoumarins (**39**) with arylboronic acids constitutes an efficient access to 4-arylcoumarins in good yields [117].



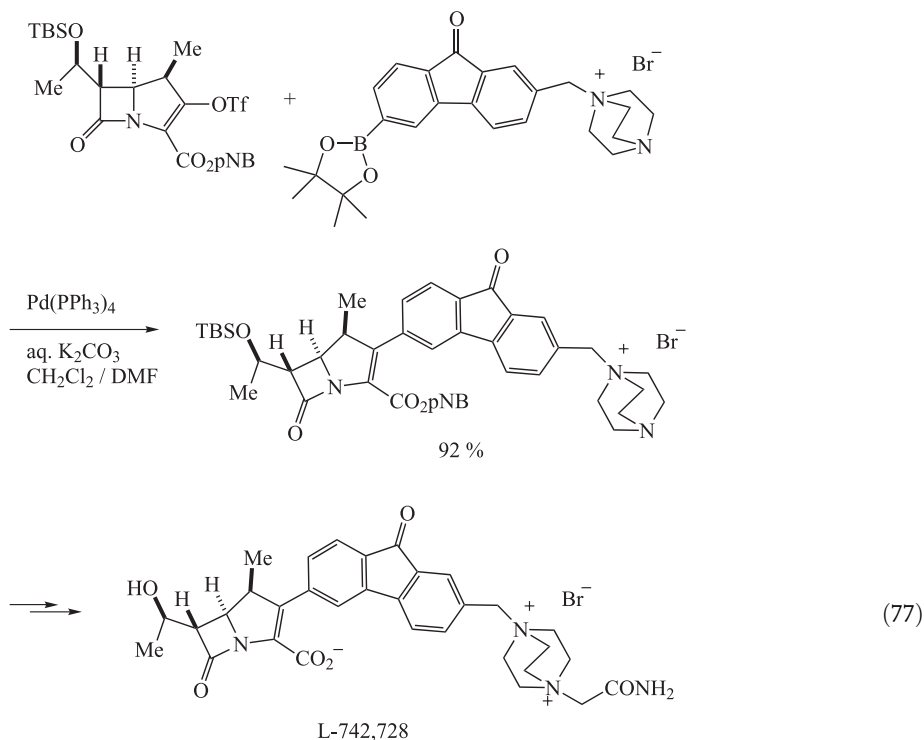
Some 3-aryinden-1-ones can be prepared by the Suzuki reaction of pinacol boronate esters with 3-bromoinden-1-ones. Initially, the Suzuki coupling proved to be difficult due to the base sensitivity of the bromides at elevated temperature. Eventually, it was found that the cross-coupling reaction proceeds well when using aqueous NaHCO_3 and $\text{Pd}_2(\text{dba})_3/\text{PPh}_3$ in DME at 50°C to give the coupling products in relatively good yields (Eq. (75)) [118].



In the course of a study of structure-based design and synthesis of a potent matrix metalloproteinase-13 inhibitor based on a pyrrolidinone scaffold, the Suzuki coupling reaction of α,β -unsaturated γ -lactam iodide (**40**) with 4-methoxyphenylboronic acid was carried out to give the corresponding coupling product in 77 % yield (Eq. (76)) [119].

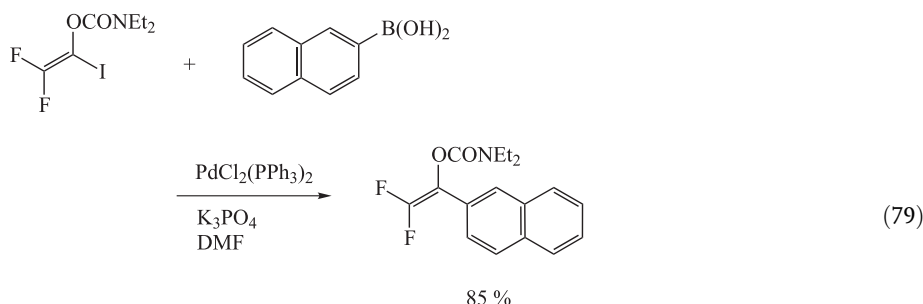
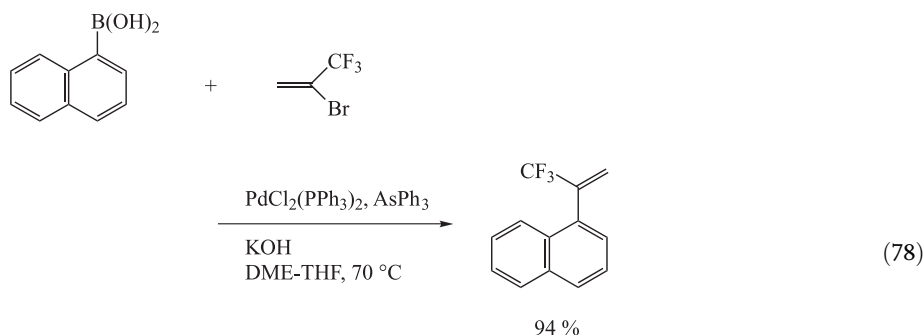


The ubiquitous use of antibiotics for the treatment of infectious disease has resulted in many bacterial strains acquiring resistance to multiple drugs. One of the most serious resistant strains is the methicillin-resistant *Staphylococcus aureus* (MRSA), which has become a worldwide problem, especially in areas where potent antibiotics have been heavily used. Recently, Merck scientists have reported anti-MRSA activity in carbapenems bearing aromatic substituents at the 3-position. The most recent candidate to emerge from this program is L-742,728. This compound was prepared in large quantities using the Suzuki cross-coupling as the key reaction by Yasuda et al. (Eq. (77)) [120].



Trifluoromethylated compounds have become increasingly important for a large number of industrial applications, such as pharmaceuticals, agrochemicals, and polymers. Consequently, there is increasing interest in convenient synthetic methods for such compounds. There are two general ways of introducing the trifluoromethyl group: (a) by direct substitution, e.g. by fluorination, halogen-exchange reaction, etc., at a late stage of the synthesis, and (b) by using trifluoromethyl-substituted building blocks derived from readily available starting materials. As the former route is seldom satisfactory because of low reactivity and low reaction selectivity, the latter is now becoming an important strategy for the preparation of trifluoromethylated molecules because it allows us to obtain these compounds under milder conditions. Deng et al. [121] demonstrated that the Suzuki-type coupling reaction of arylboronic acids with 2-bromo-3,3,3-trifluoropropene in the presence of dichlorobis-(triphenylphosphine)palladium as a catalyst and a base readily gives α -(trifluoromethyl)-styrenes in excellent yields (Eq. (78)).

As mentioned above, palladium-catalyzed couplings of fluoroalkenes are becoming part of the repertoire of organofluorine chemists. However, the range of fluoroalkenes that have been coupled is still very limited and a ubiquitous feature is the presence of a (small) fluorine atom at the α -carbon. Recently, Percy et al. have reported that 1-(*N,N*-diethylcarbamoyloxy)-2,2-difluoro-1-iodoethene undergoes smooth Suzuki coupling (Eq. (79)) [122].



3.4

Reactions with Aryl Chlorides and Other Organic Electrophiles

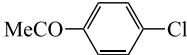
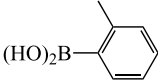
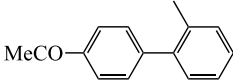
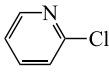
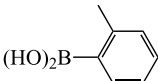
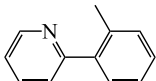
One of the challenges in the Suzuki-type cross-coupling is to extend this reaction from electron-rich aryl iodides, bromides, and triflates to less reactive aryl sulfonates and aryl chlorides, which show poor reactivity in terms of oxidative addition in the catalytic cycle. Aryl mesylates, benzenesulfonates, and tosylates are much less expensive than triflates, and are unreactive toward palladium catalysts. The Ni(0)-catalyzed Suzuki-type cross-coupling reaction of aryl sulfonates, including mesylates, with arylboronic acids in the presence of K_3PO_4 has been reported [123].

One limitation in the scope of the Suzuki reaction has been its inefficiency when aryl chlorides are employed as substrates, although there have been several accounts of the coupling of electron-poor aryl chlorides [124].

The low reactivity of aryl chlorides in cross-coupling reactions is generally ascribed to their reluctance to oxidatively add to $\text{Pd}(0)$. Aryl halides bearing an electron-withdrawing group oxidatively add to $\text{Pd}(0)$ more readily than do the corresponding unactivated aryl halides [125]. In view of the greater availability and lower cost of aryl chlorides relative to aryl bromides, iodides, and triflates, many chemists have shown an interest in new methodologies employing aryl chlorides.

Most recently, Fu and co-workers [126] have reported that the use of $\text{Pd}_2(\text{dba})_3/\text{P}t\text{Bu}_3$ as a catalyst for a wide range of aryl and vinyl halides, including chlorides, facilitates their Suzuki cross-coupling with arylboronic acids, giving the coupled products in very good yield, typi-

Tab. 5. Suzuki couplings of activated aryl chlorides.

$ \begin{array}{c} \text{X} \text{---} \text{C}_6\text{H}_4 \text{---} \text{Cl} + (\text{HO})_2\text{B} \text{---} \text{C}_6\text{H}_4 \text{---} \text{Y} \\ \xrightarrow[\text{THF / r.t.}]{\begin{array}{l} 0.5\% \text{ Pd}_2(\text{dba})_3 \\ 1\% \text{ P}^t\text{Bu}_3 \\ 3.3 \text{ equiv KF} \end{array}} \\ \text{X} \text{---} \text{C}_6\text{H}_4 \text{---} \text{C}_6\text{H}_4 \text{---} \text{Y} \end{array} $			
(Hetero)Aryl Chloride	Boronic Acid	Product	Yield (%)
			99
			97

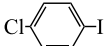
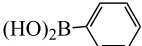
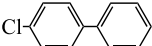

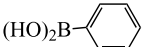
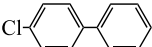
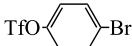
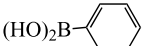
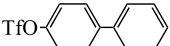
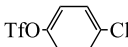

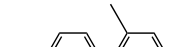
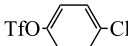

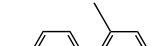
cally at room temperature. Using $\text{Pd}(\text{OAc})_2/\text{Pcy}_3$, a diverse array of aryl and vinyl triflates react cleanly at room temperature. These two catalyst systems cover a broad spectrum of commonly encountered substrates for Suzuki couplings. Furthermore, they display novel reactivity patterns, such as the selective cross-coupling by $\text{Pd}_2(\text{dba})_3/\text{P}^t\text{Bu}_3$ of an aryl chloride in preference to an aryl triflate, and they can be used at low loadings, even for the reactions of aryl chlorides. Some representative results are presented in Tables 5, 6, and 7.

To gain some insight into the $\text{Pd}_2(\text{dba})_3/\text{P}^t\text{Bu}_3$ catalyst system, Fu et al. pursued a series of NMR and reactivity studies, and found that the bis(phosphine) adduct, $\text{Pd}(\text{P}^t\text{Bu}_3)_2$, is favored over the monophosphine and the tris(phosphine) over a wide range of $\text{P}^t\text{Bu}_3:\text{Pd}$ ratios. They monitored the Suzuki coupling of 3-chloropyridine and 2-tolylboronic acid by ^{31}P NMR spectrometry (2.5 % $\text{Pd}_2(\text{dba})_3$, 5 % P^tBu_3 ; $[\text{D}_8]\text{THF}$), and found $\text{Pd}(\text{P}^t\text{Bu}_3)_2$ to be the sole species observed during the course of the reaction. Since the overall $\text{P}^t\text{Bu}_3:\text{Pd}$ ratio is 1:1,

Tab. 6. Suzuki couplings of unactivated aryl chlorides.

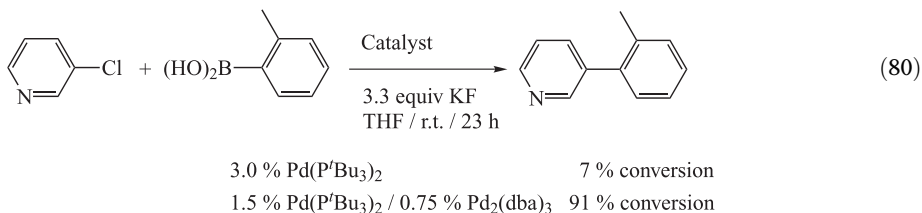
<div><div><div><div><div><div></div><div>X</div></div><div><div></div><div></div><div></div><div></div><div></div><div></div></div><div><div></div><div></div><div></div><div></div><div></div><div></div></div><div><div></div><div></div><div></div><div></div><div></div><div></div></div><div><div></div><div></div><div></div><div></div><div></div><div></div></div><div><div></div><div></div><div></div><div></div><div></div><div></div></div><div><div></div><div></div><div></div><div></div><div></div><div></div></div><div><div></div><div></div><div></div><div></div><div></div><div></div></div><div><div></div><div></div><div></div><div></div><div></div><div></div></div><div><div></div><div></div><div></div><div></div><div></div><div></div></div><div><div></div><div></div><div></div><div></div><div></div><div></div></div><div><div></div><div></div><div></div><div></div><div></div><div></div></div><div><div></div><div></div><div></div><div></div><div></div><div></div></div><div><div></div><div></div><div></div><div></div><div></div><div></div></div><div><div></div><div></div><div></div><div></div><div></div><div></div></div><div><div></div><div></div><div></div><div></div><div></div><div></div></div><div><div></div><div></div><div></div><div></div><div></div><div></div></div><div><div></div><div></div><div></div><div></div><div></div><div></div></div><div><div></div><div></div><div></div><div></div><div></div><div></div></div><div><div></div><div></div><div></div><div></div><div></div><div></div></div><div><div></div><div></div><div></div><div></div><div></div><div></div></div><div><div></div><div></div><div></div><div></div><div></div><div></div></div><div><div></div><div></div><div></div><div></div><div></div><div></div></div><div><div></div><div></div><div></div><div></div><div></div><div></div></div><div><div></div><div></div><div></div><div></div><div></div><div></div></div><div><div></div><div></div><div></div><div></div><div></div><div></div></div><div><div></div><div></div><div></div><div></div><div></div><div></div></div><div><div></div><div></div><div></div><div></div><div></div><div></div></div><div><div></div><div></div><div></div><div></div><div></div><div></div></div><div><div></div><div></div><div></div><div></div><div></div><div></div></div><div><div></div><div></div><div></div><div></div><div></div><div></div></div><div><div></div><div></div><div></div><div></div><div></div><div></div></div><div><div></div><div></div><div></div><div></div><div></div><div></div></div><div><div></div><div></div><div></div><div></div><div></div><div></div></div><div><div></div><div></div><div></div><div></div><div></div><div></div></div><div><div></div><div></div><div></div><div></div><div></div><div></div></div><div><div></div><div></div><div></div><div></div><div></div><div></div></div><div><div></div><div></div><div></div><div></div><div></div><div></div></div><div><div></div><div></div><div></div><div></div><div></div><div></div></div><div><div></div><div></div><div></div><div></div><div></div><div></div></div><div><div></div><div></div><div></div><div></div><div></div><div></div></div><div><div></div><div></div><div></div><div></div><div></div><div></div></div><div><div></div><div></div><div></div><div></div><div></div><div></div></div><div><div></div><div></div><div></div><div></div><div></div><div></div></div><div><div></div><div></div><div></div><div></div><div></div><div></div></div><div><div></div><div></div><div></div><div></div><div></div><div></div></div><div><div></div><div></div><div></div><div></div><div></div><div></div></div><div><div></div><div></div><div></div><div></div><div></div><div></div></div><div><div></div><div></div><div></div><div></div><div></div><div></div></div><div><div></div><div></div><div></div><div></div><div></div><div></div></div><div><div></div><div></div><div></div><div></div><div></div><div></div></div><div><div></div><div></div><div></div><div></div><div></div><div></div></div><div><div></div><div></div><div></div><div></div><div></div><div></div></div><div><div></div><div></div><div></div><div></div><div></div><div></div></div><div><div></div><div></div><div></div><div></div><div></div><div></div></div><div><div></div><div></div><div></div><div></div><div></div><div></div></div><div><div></div><div></div><div></div><div></div><div></div><div></div></div><div><div></div><div></div><div></div><div></div><div></div><div></div></div><div><div></div><div></div><div></div><div></div><div></div><div></div></div><div><div></div><div></div><div></div><div></div><div></div><div></div></div><div><div></div><div></div><div></div><div></div><div></div><div></div></div><div><div></div><div></div><div></div><div></div><div></div><div></div></div><div><div></div><div></div><div></div><div></div><div></div><div></div></div><div><div></div><div></div><div></div><div></div><div></div><div></div></div><div><div></div><div></div><div></div><div></div><div></div><div></div></div><div><div></div><div></div><div></div><div></div><div></div><div></div></div><div><div></div><div></div><div></div><div></div><div></div><div></div></div><div><div></div><div></div><div></div><div></div><div></div><div></div></div><div><div></div><div></div><div></div><div></div><div></div><div></div></div><div><div></div><div></div><div></div><div></div><div></div><div></div></div><div><div></div><div></div><div></div><div></div><div></div><div></div></div><div><div></div><div></div><div></div><div></div><div></div><div></div></div><div><div></div><div></div><div></div><div></div><div></div><div></div></div><div><div></div><div></div><div></div><div></div><div></div><div></div></div><div><div></div><div></div><div></div><div></div><div></div><div></div></div><div><div></div><div></div><div></div><div></div><div></div><div></div></div><div><div></div><div></div><div></div><div></div><div></div><div></div></div><div><div></div><div></div><div></div><div></div><div></div><div></div></div><div><div></div><div></div><div></div><div></div><div></div><div></div></div><div><div></div><div></div><div></div><div></div><div></div><div></div></div><div><div></div><div></div><div></div><div></div><div></div><div></div></div><div><div></div><div></div><div></div><div></div><div></div><div></div></div><div><div></div><div></div><div></div><div></div><div></div><div></div></div><div><div></div><div></div><div></div><div></div><div></div><div></div></div><div><div></div><div></div><div></div><div></div><div></div><div></div></div><div><div></div><div></div><div></div><div></div><div></div><div></div></div><div><div></div><div></div><div></div><div></div><div></div><div></div></div><div><div></div><div></div><div></div><div></div><div></div><div></div></div><div><div></div><div></div><div></div><div></div><div></div><div></div></div><div><div></div><div></div><div></div><div></div><div></div><div></div></div><div><div></div><div></div><div></div><div></div><div></div><div></div></div><div><div></div><div></div><div></div><div></div><div></div><div></div></div><div><div></div><div></div><div></div><div></div><div></div><div></div></div><div><div></div><div></div><div></div><div></div><div></div><div></div></div><div><div></div><div></div><div></div><div></div><div></div><div></div></div><div><div></div><div></div><div></div><div></div><div></div><div></div></div><div><div></div><div></div><div></div><div></div><div></div><div></div></div><div><div></div><div></div><div></div><div></div><div></div><div></div></div><div><div></div><div></div><div></div><div></div><div></div><div></div></div><div><div></div><div></div><div></div><div></div><div></div><div></div></div><div><div></div><div></div><div></div><div></div><div></div><div></div></div><div><div></div><div></div><div></div><div></div><div></div><div></div></div><div><div></div><div></div><div></div><div></div><div></div><div></div></div><div><div></div><div></div><div></div><div></div><div></div><div></div></div><div><div></div><div></div><div></div><div></div><div></div><div></div></div><div><div></div><div></div><div></div><div></div><div></div><div></div></div><div><div></div><div></div><div></div><div></div><div></div><div></div></div><div><div></div><div></div><div></div><div></div><div></div><div></div></div><div><div></div><div></div><div></div><div></div><div></div><div></div></div><div><div></div><div></div><div></div><div></div><div></div><div></div></div><div><div></div><div></div><div></div><div></div><div></div><div></div></div><div><div></div><div></div><div></div><div></div><div></div><div></div></div><div><div></div><div></div><div></div><div></div><div></div><div></div></div><div><div></div><div></div><div></div><div></div><div></div><div></div></div><div><div></div><div></div><div></div><div></div><div></div><div></div></div><div><div></div><div></div><div></div><div></div><div></div><div></div></div><div><div></div><div></div><div></div><div></div><div></div><div></div></div><div><div></div><div></div><div></div><div></div><div></div><div></div></div><div><div></div><div></div><div></div><div></div><div></div><div></div></div><div><div></div><div></div><div></div><div></div><div></div><div></div></div><div><div></div><div></div><div></div><div></div><div></div><div></div></div><div><div></div><div></div><div></div><div></div><div></div><div></div></div><div><div></div><div></div><div></div><div></div><div></div><div></div></div><div><div></div><div></div><div></div><div></div><div></div><div></div></div><div><div></div><div></div><div></div><div></div><div></div><div></div></div><div><div></div><div></div><div></div><div></div><div></div><div></div></div><div><div></div><div></div><div></div><div></div><div></div><div></div></div><div><div></div><div></div><div></div><div></div><div></div><div></div></div><div><div></div><div></div><div></div><div></div><div></div><div></div></div><div><div></div><div></div><div></div><div></div><div></div><div></div></div><div><div></div><div></div><div></div><div></div><div></div><div></div></div><div><div></div><div></div><div></div><div></div><div></div><div></div></div><div><div></div><div></div><div></div><div></div><div></div><div></div></div><div><div></div><div></div><div></div><div></div><div></div><div></div></div><div><div></div><div></div><div></div><div></div><div></div><div></div></div><div><div></div><div></div><div></div><div></div><div></div><div></div></div><div><div></div><div></div><div></div><div></div><div></div><div></div></div><div><div></div><div></div><div></div><div></div><div></div><div></div></div><div><div></div><div></div><div></div><div></div><div></div><div></div></div><div><div></div><div></div><div></div><div></div><div></div><div></div></div><div><div></div><div></div><div></div><div></div><div></div><div></div></div><div><div></div><div></div><div></div><div></div><div></div><div></div></div><div><div></div><div></div><div></div><div></div><div></div><div></div></div><div><div></div><div></div><div></div><div></div><div></div><div></div></div><div><div></div><div></div><div></div><div></div><div></div><div></div></div><div><div></div><div></div><div></div><div></div><div></div><div></div></div><div><div></div><div></div><div></div><div></div><div></div><div></div></div><div><div></div><div></div><div></div><div></div><div></div><div></div></div><div><div></div><div></div><div></div><div></div><div></div><div></div></div><div><div></div><div></div><div></div><div></div><div></div><div></div></div><div><div></div><div></div><div></div><div></div><div></div><div></div></div><div><div></div><div></div><div></div><div></div><div></div><div></div></div><div><div></div><div></div><div></div><div></div><div></div><div></div></div><div><div></div><div></div><div></div><div></div><div></div><div></div></div><div><div></div><div></div><div></div><div></div><div></div><div></div></div><div><div></div><div></div><div></div><div></div><div></div><div></div></div><div><div></div><div></div><div></div><div></div><div></div><div></div></div><div><div></div><div></div><div></div><div></div><div></div><div></div></div><div><div></div><div></div><div></div><div></div><div></div><div></div></div><div><div></div><div></div><div></div><div></div><div></div><div></div></div><div><div></div><div></div><div></div><div></div><div></div><div></div></div><div><div></div><div></div><div></div><div></div><div></div><div></div></div><div><div></div><div></div><div></div><div></div><div></div><div></div></div><div><div></div><div></div><div></div><div></div><div></div><div></div></div><div><div></div><div></div><div></div><div></div><div></div><div></div></div><div><div></div><div></div><div></div><div></div><div></div><div></div></div><div><div></div><div></div><div></div><div></div><div></div><div></div></div></div></div></div></div>				
--	--	--	--	--

Tab. 7. Chemoselective Suzuki couplings.

<i>Aryl Halide</i>	<i>Boronic Acid</i>	<i>Product</i>	<i>Conditions</i>	<i>Yield (%)</i>
			0.5 % Pd ₂ (dba) ₃ 1.2 % P ^t Bu ₃	98
			0.5 % Pd ₂ (dba) ₃ 1.2 % P ^t Bu ₃	97
			0.5 % Pd ₂ (dba) ₃ 1.2 % P ^t Bu ₃	98
			1.5 % Pd ₂ (dba) ₃ 3.0 % P ^t Bu ₃	96
			3.0 % Pd(OAc) ₃ 6.0 % PCy ₃	87

this suggests that one-half of the palladium is in the form of $\text{Pd}(\text{P}t\text{Bu}_3)_2$, while the other half is in the form of a phosphine-free complex.

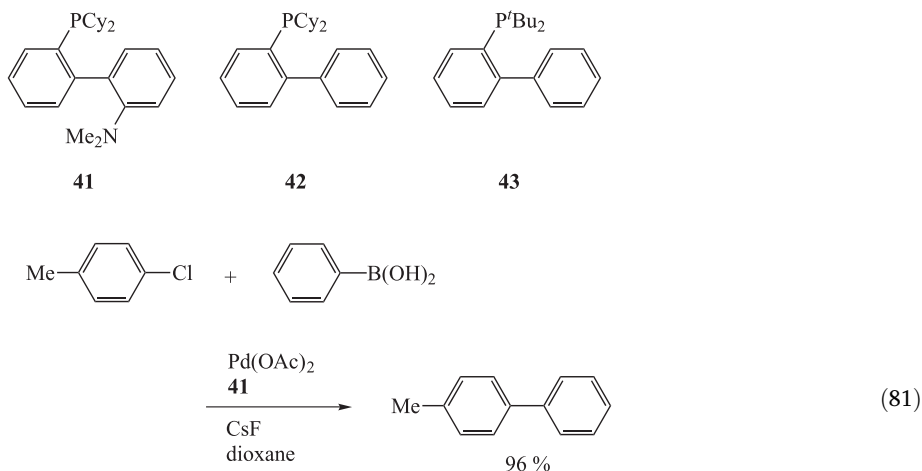
$\text{Pd}(\text{PtBu}_3)_2$ does not appear to be the active catalyst in the Suzuki coupling process under Fu conditions, since the reaction of 3-chloropyridine with 2-tolylboronic acid proceeds sluggishly at room temperature. However, the addition of phosphine-free $\text{Pd}_2(\text{dba})_3$ to the $\text{Pd}(\text{PtBu}_3)_2$ leads to a marked increase in the rate of cross-coupling (Eq. (80)).



These observations suggest that a palladium monophosphine adduct may be the active catalyst in these Suzuki couplings, and that phosphine-free palladium complexes present in the reaction mixture may play an important role by increasing the concentration of the active catalyst. The unusual cross-coupling activity promoted by PtBu_3 may therefore be attributed to both its size and its electron-richness: the steric demand favors dissociation (relative to less bulky phosphines) to a monophosphine complex, which, due to the donating ability of PtBu_3 , readily undergoes oxidative addition.

Buchwald [127] and Lohse [128] have independently reported coupling reactions using aryl chlorides. In order to overcome the sluggish oxidative addition step of aryl chlorides in

their palladium-catalyzed C–N bond-forming reaction, Buchwald et al. have explored the use of electron-rich phosphine ligands. They were finally able to demonstrate that use of the aminophosphine ligand 2-(dimethylamino)-2'-dicyclohexylphosphino-1,1'-biphenyl (**41**) is superior and significantly expands the scope of the palladium-catalyzed amination of unactivated aryl chlorides. They also observed that the reaction conditions using $\text{Pd}(\text{OAc})_2$ /**41**/ CsF are significantly more effective for the Suzuki coupling of unactivated aryl chlorides with arylboronic acids (Eq. (81)).



Thereafter, Buchwald et al. [129] reported that mixtures of palladium acetate and *o*-(di-*tert*-butylphosphino)biphenyl (**43**) (see Table 8) catalyze the room temperature Suzuki coupling

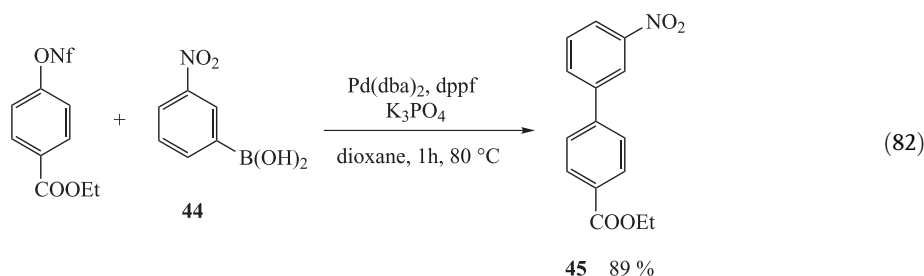
Tab. 8. Suzuki coupling of aryl chlorides under Buchwald's conditions^a.

Chloride	Bopronic Acid	Product	Yield (%)
			95
			98
			93
			94

^a Reaction conditions: catalyst $\text{Pd}(\text{OAc})_2$, ligand **43** (2L/Pd), KF in THF.

of aryl bromides and aryl chlorides at a level of 0.5–1.0 mol % Pd, and that the use of *o*-(dicyclohexylphosphino)biphenyl (**42**) allows Suzuki couplings to be carried out at low catalyst loadings (0.000001–0.02 mol % Pd). The process tolerates a broad range of functional groups and substrate combinations, including the use of sterically hindered substrates. The following conclusions were made. The catalyst systems based on ligands **42** and **43**, which are easily prepared in one step and are commercially available [130], are new, highly active catalysts for the Suzuki coupling of aryl halides. While the use of **43** generally gives faster reaction rates in room temperature Suzuki couplings, **42** is more effective for hindered substrates and operates more efficiently at low catalyst loadings. Of great importance is the fact that using such ligands the rate of oxidative addition is greatly enhanced, while the rates of the other steps of the catalytic cycle are probably also increased. Thus, their use avoids the common pitfall whereby speeding up the rate of one step slows that of another, resulting in little or no increase in the overall rate of the reaction. The authors consider that the success of these ligands is due to a combination of (1) their electron-richness, which enhances the rate of oxidative addition and keeps the palladium in solution, and (2) their steric bulk, which enhances the rate of reductive elimination and maximizes the concentration of L_1Pd complexes, thereby increasing the rate of transmetalation. It is also being considered that (3) the presence of the *o*-biphenyl moiety might be important, helping to confer aerial stability to the ligand, enhancing the rate of reductive elimination, as well as stabilizing the catalyst by interacting with the Pd. However, further mechanistic studies to determine the factors responsible for the high activities of these catalysts are necessary.

Due to the moderate reactivity of aryl triflates and the high cost of the triflate functionality, aryl fluoroalkanesulfonates [$ArOSO_2(CF_2)_nCF_3$] have recently been proposed as an alternative to triflates, because they are easily prepared using commercially available fluoroalkanesulfonic anhydrides or halides. Especially attractive are aryl nonaflates ($ArONf = ArOSO_2(CF_2)_8CF_3$), which are readily prepared and are stable to flash column chromatography. Rottländer and Knochel [131] reported that treatment of the nonaflate with the boronic acid **44** provides, under typical conditions for Suzuki coupling, the expected product (**45**) in 89 % yield (Eq. (82)).



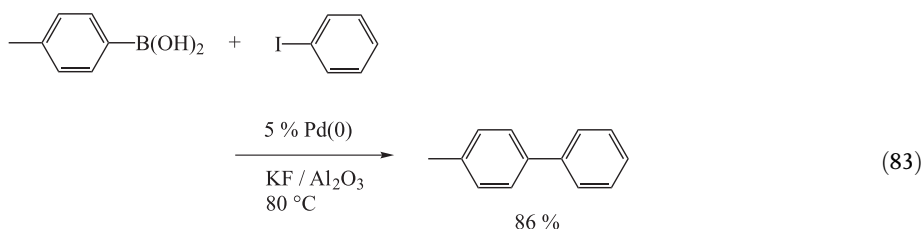
As an alternative to the use of organic electrophiles, Kang et al. employed hypervalent iodonium compounds in cross-couplings with organoboranes [132]. Thereafter, these authors reported on cross-coupling reactions of organoboron compounds with organolead(IV) compounds [133]. Of the catalysts tested, $Pd_2(dba)_3 \cdot CHCl_3$, $Pd(OAc)_2$, and $PdCl_2$,

$\text{Pd}_2(\text{dba})_3 \cdot \text{CHCl}_3$ was generally found to be superior. A solvent system of $\text{CH}_3\text{CN}/\text{DME}$ (1:1) proved to be most suitable. Also, it is noteworthy that CuI (10 mol %) was added as a co-catalyst to avoid homocoupling.

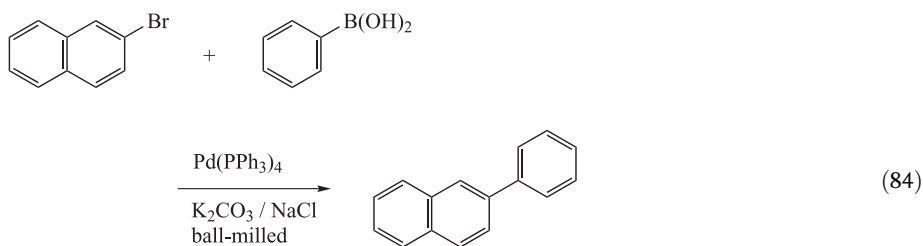
3.5

Miscellaneous

Kabalka et al. have reported a solvent-free Suzuki coupling methodology involving the use of a commercially available potassium fluoride/ γ -alumina mixture, doped with a ligand-free $\text{Pd}(0)$ catalyst (Eq. (83)) [134]. A number of parameters of the reaction were investigated. Suzuki reactions require the presence of a base, which is also true of the solid-state reaction. Both potassium phosphate and potassium fluoride proved effective in inducing the solid-phase coupling reactions. The quantity of palladium was found to be important; a 4–5 % loading of palladium was most effective.



There is currently a great deal of interest in performing chemical reactions under solvent-free conditions, since there are both financial and environmental benefits. One problem associated with performing reactions with solid starting materials is the mixing of the reactants. Another is the difficulty of achieving uniform and controlled heating of large amounts of powdery materials. Such difficulties may be overcome by a ball-milling procedure, and the Suzuki coupling reaction has been attempted under these conditions [135]. A factor that needs to be considered for the ball-mill conditions is the degree of stickiness of the mixture. Peters et al. have observed that the addition of sodium chloride to the reaction mixtures is efficient in making them sufficiently powdery. Sodium chloride has the following favorable characteristics: hard and brittle crystals, chemical inertness, good water solubility, low toxicity, and low price. The order of reactivity is complementary to that of the normal Suzuki reaction (Eq. (84)).

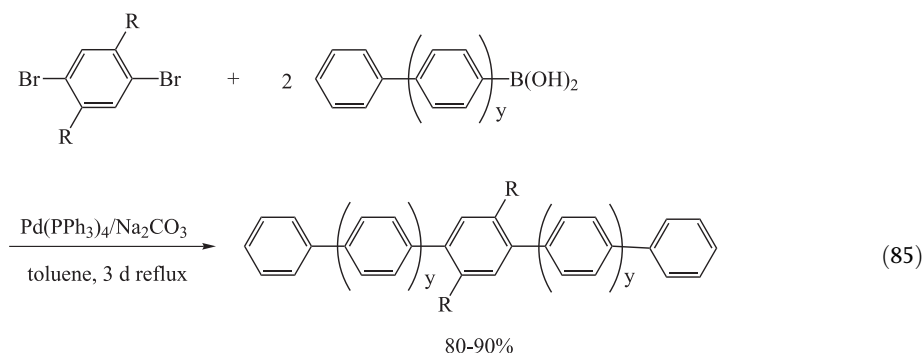


3.6

Applications in Polymer Chemistry

Aromatic, rigid-rod polymers play an important role in a number of diverse technologies, including high-performance engineering materials, conducting polymers, and nonlinear optical materials.

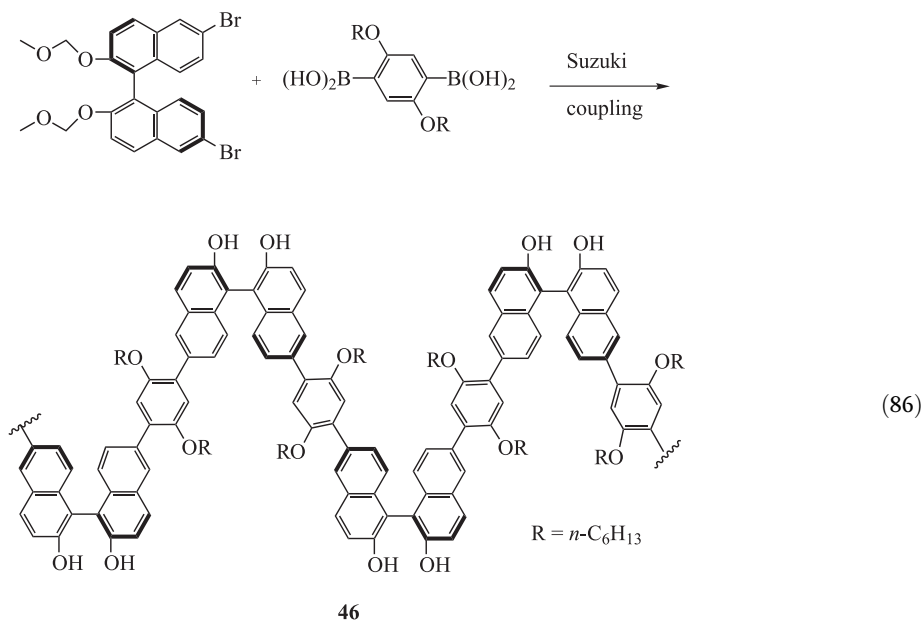
Constitutionally homogeneous oligo-*p*-phenyls are materials of considerable current interest to chemists, physicists, and material scientists because such compounds are excellent model compounds for developing a profound understanding of the spectroscopic and redox properties of polyaromatic systems, and of the thermal phase behavior and solution properties of rod-like liquid-crystalline molecules. Furthermore, functionalized oligo-*p*-phenyls have gained some importance as mainchain-stiffening building blocks in semi-flexible polymers such as aromatic polyesters and polyimides. Despite considerable advantages, parent oligo-*p*-phenyls have a serious drawback, however, with regard to the above applications: their solubility decreases dramatically with increasing number of benzene rings. Fortunately, it is known that the attachment of lateral methyl groups to oligo-*p*-phenyls increases their solubility. Nevertheless, the solubilizing effect of methyl groups is insufficient in the case of longer oligo-*p*-phenyls, and flexible side chains are required to further increase the solubility of rigid-rod molecules such as aromatic polyesters. By taking advantage of this latter concept, Galda and Rehahn [136] applied the Suzuki coupling as the oligomer formation reaction, which was found to furnish the expected oligo-*p*-phenyls in excellent yields (Eq. (85)).



Many poly(*p*-phenylenes) have since been synthesized by such Suzuki reactions [137].

The development of enantioselective polymer catalysts is important with regard to the efficient production of optically pure chiral organic compounds, including drug molecules. The major advantage that a polymer catalyst offers is the ease of recovery and reuse of the expensive catalyst. The use of polymer catalysts may also enable the reactions to be carried out in flow reactors or flow membrane reactors. Recently, a highly enantioselective hetero-Diels–Alder reaction catalyzed by chiral polybinaphthylaluminum complexes was reported [138]. Thus, Jorgensen et al. synthesized the optically active polybinaphthyl **46** as a polymeric ligand by Suzuki coupling of the optically active binaphthyl dibromide and a benzenediboronic acid derivative (Eq. (86)). The polymer **46** reacts with Me₃Al or Me₂AlCl to

generate the corresponding polymeric chiral aluminum catalyst in situ for the hetero Diels–Alder reaction.

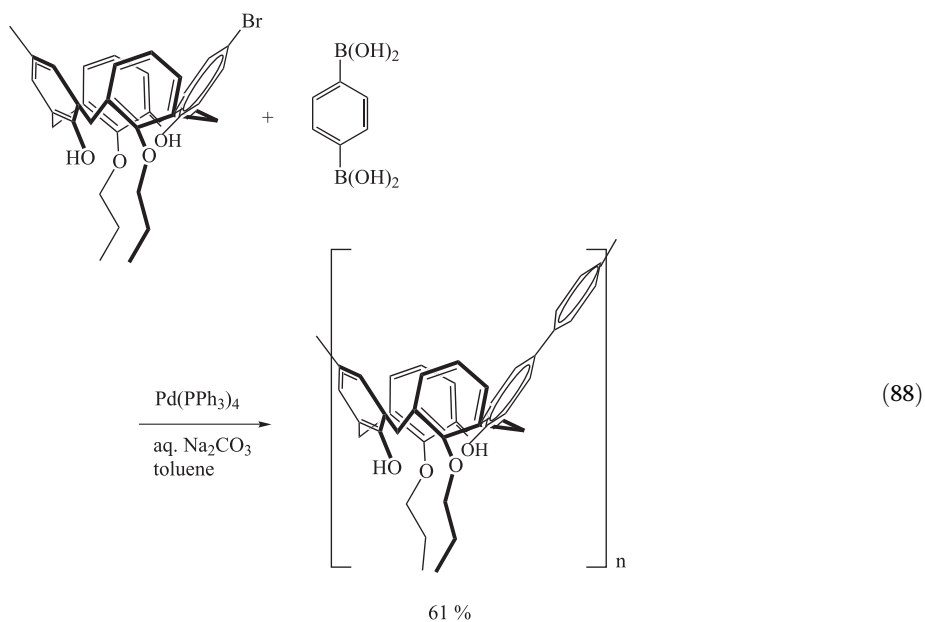
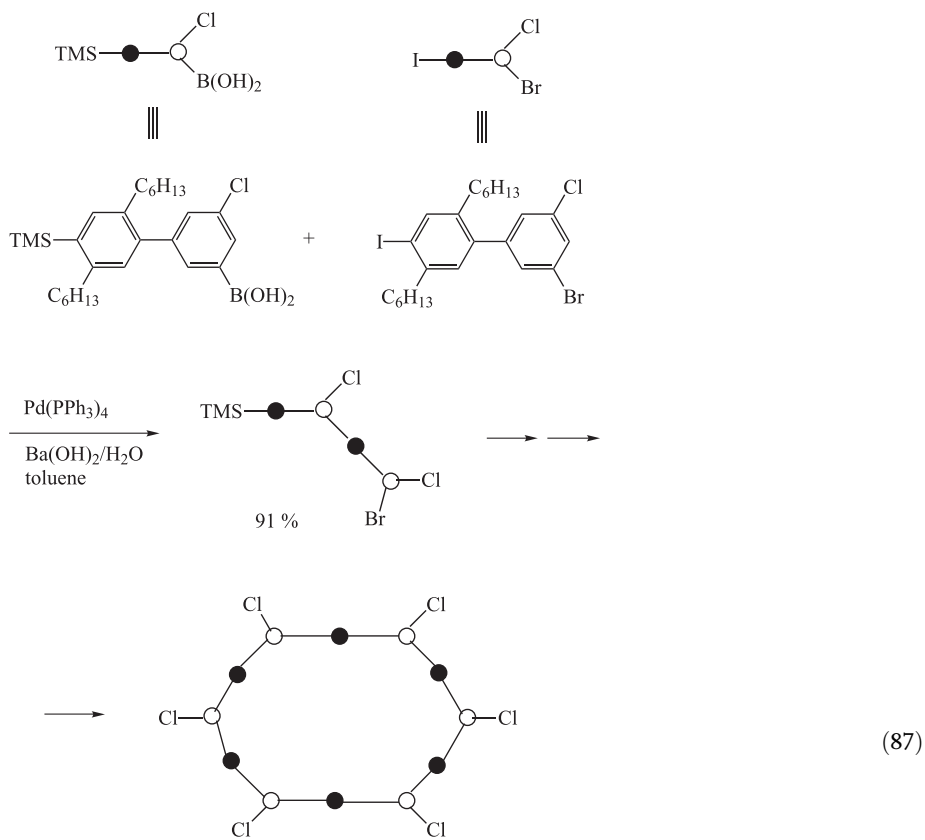


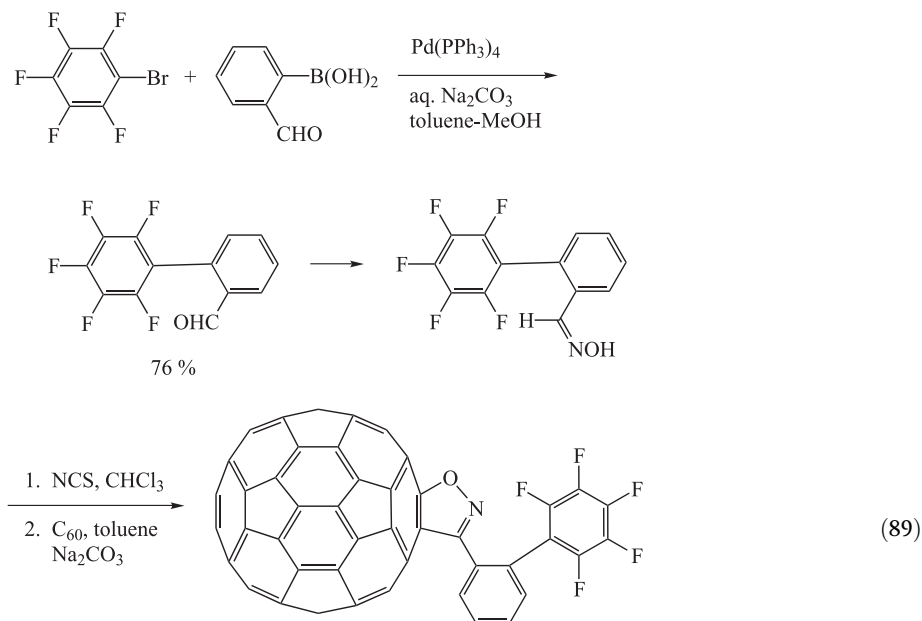
Research on dendrimers was first focused on synthetic aspects concerning this new class of macromolecules, and a broad range of dendrimers is now available, some even commercially. The emphasis of current study has shifted from merely synthetic aspects to questions of practical applications of dendrimers and the ways in which these unique compounds are superior to known systems. Consequently, much more useful synthetic procedures are required. Schlüter et al. have reported the synthesis of dendrimers with poly(*p*-phenylene) (PPP) derived cores using the Suzuki polycondensation [139].

The synthesis of a variety of kinked oligophenylene building blocks has recently been demonstrated. The synthetic strategy is repetitive, utilizes the Suzuki cross-coupling protocol, and involves potentially bifunctional building blocks (modules) that bear one functional group for coupling and another that serves as place holder. After the coupling, the place holder is converted into a coupling functionality for the next growth step. The building blocks also bear chloro substituents, which remain unaffected during each transformation. For one of the large building blocks, it has been shown that it may be cyclized to an oligophenylene macrocycle with a chloro substituent at each corner and a pair of hexyl chains at each side (Eq. (87)) [140].

Dondoni et al. have recently explored the synthesis of oligomers in which 1,3-(distal)-calix[4]arenes are linked to a *p*-phenylene unit by a single carbon–carbon bond emerging from the upper rim of the macrocycle (Eq. (88)) [141].

Investigations concerning the synthesis and electrochemical behavior of a new class of acceptor-substituted isoxazolofullerenes have been reported. In this instance, such fullerene derivatives were synthesized by Suzuki coupling (Eq. (89)) [142].





A novel topological strategy has been examined for designing amorphous molecular solids suitable for optoelectronic applications. In this approach, chromophores were attached to a tetrahedral point of convergence. For instance, stilbenoid units were covalently linked to a tetraphenylmethane core by means of a palladium-catalyzed Suzuki coupling reaction [143]. The optical properties of these compounds were examined.

References

- 1 F. DIEDERICH, P. J. STANG (Eds.), *Metal-Catalyzed Cross-Coupling Reactions*, Wiley-VCH, Weinheim, 1998.
- 2 O. GROPEN, A. HAALAND, *Acta Chim. Scand.* **1973**, 27, 521.
- 3 (a) A. SUZUKI, *Pure Appl. Chem.* **1985**, 57, 1749. (b) A. SUZUKI, *Pure Appl. Chem.* **1994**, 66, 213. (c) N. MIYaura, A. SUZUKI, *Chem. Rev.* **1995**, 95, 2457. (d) A. SUZUKI, in *Metal-Catalyzed Cross-Coupling Reactions* (Ed.: F. DIEDERICH, P. J. STANG), Wiley-VCH, Weinheim, 1998, p. 49. (e) A. SUZUKI, in *Transition Metal Catalyzed Reactions*, A 'Chemistry for the 21st Century' monograph (Eds.: S. MURAHASHI, S. G. DAVIES), IUPAC, Blackwell, Oxford, 1999, p. 441. (f) A. SUZUKI, *J. Organomet. Chem.* **1999**, 576, 147.
- 4 N. MIYaura, T. YANAGI, A. SUZUKI, *Synth. Commun.* **1981**, 11, 513.
- 5 S. GRONOWITZ, V. BOBOSIK, K. LAWITZ, *Chem. Scripta* **1984**, 23, 120.
- 6 B. I. ALO, A. KANDIL, P. A. PATIL, M. J. SHARP, M. A. SIDDIQUI, V. SNIIECKUS, *J. Org. Chem.* **1991**, 56, 3763.
- 7 W. J. THOMPSON, J. GAUDINO, *J. Org. Chem.* **1984**, 49, 5237.
- 8 W. MÜLLER, D. A. LOWE, H. NEIJT, S. URWYLER, P. HERRLING, D. BLASER, D. SEEBACH, *Helv. Chim. Acta* **1992**, 75, 855.
- 9 S. GRONOWITZ, V. BOBOSIK, K. LAWITZ, *Chem. Scripta* **1984**, 23, 120.
- 10 H. E. KATZ, *J. Org. Chem.* **1987**, 52, 3932.
- 11 Y. HOSHINO, N. MIYaura, A. SUZUKI, *Bull. Chem. Soc. Jpn.* **1988**, 61, 3008.
- 12 R. S. COLEMAN, E. B. GRANT, *Tetrahedron Lett.* **1993**, 34, 2225.

- 13 M. ISHIKURA, M. KAMADA, M. TERASHIMA, *Synthesis* **1984**, 936.
- 14 (a) M. B. MITCHELL, P. J. WALLBANK, *Tetrahedron Lett.* **1991**, 32, 2273. (b) N. M. ALI, A. MCKILLOP, M. B. MITCHELL, R. A. REBELO, P. J. WALLBANK, *Tetrahedron* **1992**, 48, 8117. (c) N. W. ALCOCK, J. M. BROWN, D. I. HULMES, *Tetrahedron: Asymmetry* **1993**, 4, 743. (d) D. JANIEZ, M. BAUER, *Synthesis* **1993**, 33. (e) S. ACHAB, M. GUYOT, P. POTIER, *Tetrahedron Lett.* **1993**, 34, 2127.
- 15 W.-C. SHIEH, J. A. CARLSON, *J. Org. Chem.* **1992**, 57, 379.
- 16 S. W. WRIGHT, D. L. HAGEMAN, L. D. MCCLURE, *J. Org. Chem.* **1994**, 59, 6095.
- 17 T. I. WALLOW, B. M. NOVAK, *J. Org. Chem.* **1994**, 59, 5034.
- 18 G. MARCK, A. VILLINGER, R. BUCHECKER, *Tetrahedron Lett.* **1994**, 35, 3277.
- 19 T. OH-E, N. MIYURA, A. SUZUKI, *J. Org. Chem.* **1993**, 58, 2201.
- 20 S. YONEZAWA, T. KOMURASAKI, K. KAWADA, T. TSURI, M. FUJI, A. KUGIMIYA, N. HAGA, S. MITSUMORI, M. INAGAKI, T. NAKATANI, Y. TAMURA, S. TAKECHI, T. TAISHI, M. OHTANI, *J. Org. Chem.* **1998**, 63, 5831.
- 21 D. E. ZEMBOWER, H. ZHANG, *J. Org. Chem.* **1998**, 63, 9300.
- 22 G. LIN, A. ZHANG, *Tetrahedron* **2000**, 56, 7163.
- 23 S. KUMAR, *J. Chem. Soc., Perkin Trans. 1* **1998**, 3157.
- 24 G. R. GEEN, I. S. MANN, M. V. MULLANE, A. MCKILLOP, *Tetrahedron* **1998**, 54, 9875.
- 25 D. L. COMINS, G. M. GREEN, *Tetrahedron Lett.* **1999**, 40, 217.
- 26 (a) H. KOYAMA, T. KAMIKAWA, *Tetrahedron Lett.* **1997**, 38, 3973. (b) H. KOYAMA, T. KAMIKAWA, *J. Chem. Soc., Perkin Trans. 1* **1998**, 203.
- 27 J. FU, V. SNIIECKUS, *Can. J. Chem.* **2000**, 78, 905.
- 28 M. B. GOLDFINGER, K. B. CRAWFORD, T. M. SWAGER, *J. Am. Chem. Soc.* **1997**, 119, 4578.
- 29 M. B. GOLDFINGER, K. B. CRAWFORD, T. M. SWAGER, *J. Org. Chem.* **1998**, 63, 1676.
- 30 F.-J. ZHANG, C. CORTEZ, R. G. HARVEY, *J. Org. Chem.* **2000**, 65, 3952.
- 31 G. BRINGMANN, R. GÖTZ, P. A. KELLER, R. WALTER, M. R. BOYD, F. LANG, A. GARCIA, J. J. WALSH, I. TELLITU, K. V. BHASKAR, T. R. KELLY, *J. Org. Chem.* **1998**, 63, 1090.
- 32 T. R. HOYE, M. CHEN, B. HOANG, L. MI, O. P. PRIEST, *J. Org. Chem.* **1999**, 64, 7184.
- 33 C. B. DE KONING, J. P. MICHAEL, W. A. L. OTTERLO, *Tetrahedron Lett.* **1999**, 40, 3037.
- 34 K. C. NICOLAOU, J. M. RAMANJULU, S. NATARAJAN, S. BRÄSE, H. LI, C. N. C. BODDY, F. RÜBSAM, *J. Chem. Soc., Chem. Commun.* **1997**, 1899.
- 35 (a) K. C. NICOLAOU, H. LI, C. N. C. BODDY, J. M. RAMANJULU, T.-Y. TUE, S. TATARAJAN, X.-J. CHU, S. BRÄSE, *Chem. Eur. J.* **1999**, 5, 2584. (b) K. C. NICOLAOU, C. N. C. BODDY, H. LI, A. E. KOUMBIS, R. HUGHES, S. NATARAJAN, N. F. JAIN, J. M. RAMANJULU, S. BRÄSE, M. E. SOLOMON, *Chem. Eur. J.* **1999**, 5, 2602. (c) K. C. NICOLAOU, A. E. KOUMBIS, M. TAKAYANAGI, S. NATARAJAN, N. F. JAIN, T. BANDO, H. LI, R. HUGHES, *Chem. Eur. J.* **1999**, 5, 2622.
- 36 D. ZHAO, F. XU, C. CHEN, R. D. TILLYER, E. J. J. GRABOWSKI, P. J. REIDER, C. BLACK, N. OUMET, P. PRASIT, *Tetrahedron* **1999**, 55, 6001.
- 37 V. N. KALININ, O. S. SHILOVA, D. S. OKLADNOY, H. SCHMIDHAMMER, *Mendeleev Commun.* **1996**, 244.
- 38 S. CEREZO, M. MORENO-MANAS, R. PLEIXATS, *Tetrahedron* **1998**, 54, 7813.
- 39 M. YOSHIDA, K. MORI, *Eur. J. Org. Chem.* **2000**, 1313.
- 40 S. R. PIETTRE, C. ANDRE, M.-C. CHANAL, J.-B. DUCEP, B. LESUR, F. PIRIOU, P. ROBOISSON, J.-M. RONDEAU, C. SCHELCHER, P. ZIMMERMANN, A. J. GANZHORN, *J. Med. Chem.* **1997**, 40, 4208.
- 41 A. ARIFFIN, A. J. BLAKE, R. A. EWIN, W.-S. LI, N. S. SIMPKINS, *J. Chem. Soc., Perkin Trans. 1* **1999**, 3177.
- 42 K. KAMIKAWA, T. WATANABE, A. DAIMON, M. UEMURA, *Tetrahedron* **2000**, 56, 2325.
- 43 S. G. NELSON, M. A. HILFIKER, *Org. Lett.* **1999**, 1, 1379.
- 44 K. KAMIKAWA, M. UEMURA, *Synlett.* **2000**, 938.
- 45 C. IMRIE, C. LOUBSER, P. ENGELBRECHT, C. W. MCCLELAND, *J. Chem. Soc., Perkin Trans. 1* **1999**, 2513.
- 46 Z. F. PLYTA, D. PRIM, J.-P. TRANCHIER, R. ROSE-MUNCH, E. ROSE, *Tetrahedron Lett.* **1999**, 40, 6769.

- 47 A. N. CAMMIDGE, K. V. L. CREPY, *Chem. Commun.* **2000**, 1723.
- 48 Y. GONG, H. W. PAULS, *Synlett* **2000**, 829.
- 49 C. N. JOHNSON, G. STEMPEL, N. ANAND, S. C. STEPHEN, T. GALLAGHER, *Synlett* **1998**, 1025.
- 50 A. FÜRSTNER, J. GRABOWSKI, C. W. LEHMANN, *J. Org. Chem.* **1999**, *64*, 8275.
- 51 K. S. CHAN, X. ZHOU, M. T. AU, C. Y. TAM, *Tetrahedron* **1995**, *51*, 3129.
- 52 Y. DENG, C. K. CHANG, D. G. NOCERA, *Angew. Chem. Int. Ed.* **2000**, *39*, 1066.
- 53 C. K. CHANG, N. BAG, *J. Org. Chem.* **1995**, *60*, 7030.
- 54 R. D'ALESSIO, A. ROSSI, *Synlett* **1996**, 513.
- 55 J. COSSY, D. BELOTTI, *Tetrahedron* **1999**, *55*, 5145.
- 56 (a) Q. ZHENG, Y. YANG, A. R. MARTIN, *Heterocycles* **1994**, *37*, 1761. (b) I. KAWASAKI, M. YAMASHITA, S. OHTA, *Chem. Pharm. Bull.* **1996**, *44*, 1831.
- 57 B. MALAPEL-ANDRIEU, J.-Y. MEROUR, *Tetrahedron* **1998**, *54*, 11079.
- 58 C. B. DE KONING, J. P. MICHAEL, A. L. ROUSSEAU, *Tetrahedron Lett.* **1998**, *39*, 8725.
- 59 C. B. DE KONING, J. P. MICHAEL, A. L. ROUSSEAU, *J. Chem. Soc., Perkin Trans. 1* **2000**, 1705.
- 60 Y. NAKANO, Y. YOSHIKAWA, H. KONDO, *J. Am. Chem. Soc.* **1986**, *108*, 7630.
- 61 Y. NAKANO, D. IMAI, *Synthesis* **1997**, 1425.
- 62 S. NAKAHARA, J. MATSUI, A. KUBO, *Tetrahedron Lett.* **1998**, *39*, 5521.
- 63 H. ZHANG, F. XUE, T. C. W. MARK, K. S. CHANG, *J. Org. Chem.* **1996**, *61*, 8002.
- 64 K. SHENG-CHU, Y. L. FANG, T. CHE-MING, *Eur. Pat. Appl.* 0667345 A1, **1995** (C.A.: 123: 340113j).
- 65 V. COLLOT, P. DALLEMAGNE, P. R. BOVY, S. RAULT, *Tetrahedron* **1999**, *55*, 6917.
- 66 C. ENGUEHARD, J.-L. RENOU, V. COLLOT, M. HERVET, S. RAULT, A. GUEIFFIER, *J. Org. Chem.* **2000**, *65*, 6572.
- 67 H. NAKAMURA, M. AIZAWA, D. TAKEUCHI, A. MURAI, O. SHIMOURA, *Tetrahedron Lett.* **2000**, *41*, 2185.
- 68 L. REVESZ, F. BONNE, P. MAKAVOU, *Tetrahedron Lett.* **1998**, *39*, 5171.
- 69 C. PLISSON, J. CHENAULT, *Heterocycles* **1999**, *51*, 2627.
- 70 S. M. CHI, J.-K. CHOI, E. K. YUN, D. Y. CHI, *Tetrahedron Lett.* **2000**, *41*, 919.
- 71 I. PARROT, Y. RIVAL, C. G. WERMUTH, *Synthesis* **1999**, 1163.
- 72 A. J. GOODMAN, S. P. STANFORTH, B. TARBIT, *Tetrahedron* **1999**, *55*, 15067.
- 73 B. U. W. MAES, G. L. F. LEMIERE, R. DOMMISSE, K. AUGUSTYNE, A. HAEMERS, *Tetrahedron* **2000**, *56*, 1777.
- 74 A. J. COCUZZA, D. R. CHIDESTER, S. CULP, L. FITZGERALD, P. GILLIGAN, *Biorg. Med. Chem. Lett.* **1999**, *9*, 1063.
- 75 S. TOYOTA, C. R. WOODS, M. BENAGLIA, J. S. SIEGEL, *Tetrahedron Lett.* **1998**, *39*, 2697.
- 76 A. MOUADDIB, B. JOSEPH, A. HASNAOUI, J.-Y. MEROUR, *Synthesis* **2000**, 549.
- 77 M. HAVELKOVA, M. HOCEK, M. CESNEK, D. DVORAK, *Synlett* **1999**, 1145.
- 78 T. WATANABE, N. MIYAJIMA, A. SUZUKI, *Synlett* **1992**, 207.
- 79 (a) D. MULLER, J.-P. FLEURY, *Tetrahedron Lett.* **1991**, *32*, 2229. (b) Y. FUKUYAMA, Y. KIRIYAMA, M. KODAMA, *Tetrahedron Lett.* **1993**, *34*, 7637.
- 80 M. H. ABRAHAM, P. L. GRELLIER, *The Chemistry of the Metal–Carbon Bond* (Eds.: F. R. HARTLEY, S. PATAI), J. Wiley, New York, 1985, Vol. 1, p. 115.
- 81 (a) P. ROCCA, F. MARSAIS, A. GODARD, G. QUEGUINER, *Tetrahedron Lett.* **1993**, *34*, 2937. (b) F. GUILLIER, F. NIVOLIER, A. GODARD, F. MARSAIS, G. QUEGUINER, *Tetrahedron Lett.* **1994**, *35*, 6489.
- 82 T. R. KELLY, A. GARCIA, F. LANG, J. J. WALSH, K. V. BHASKAR, M. R. BOYD, R. GÖTZ, P. A. KELLER, R. WALTER, G. BRINGMANN, *Tetrahedron Lett.* **1994**, *35*, 7621.
- 83 C. GRIFFITHS, N. E. LEADBEATER, *Tetrahedron Lett.* **2000**, *41*, 2487.
- 84 (a) H. ZHANG, K. S. CHAN, *Tetrahedron Lett.* **1996**, *37*, 1043. (b) H. ZHANG, F. Y. KWONG, Y. TIAN, K. S. CHAN, *J. Org. Chem.* **1998**, *63*, 6886.
- 85 J. M. SAA, G. MARTORELL, *J. Org. Chem.* **1993**, *58*, 1963.
- 86 E. M. CEMPI, W. R. JACKSON, S. M. MARUCCIO, C. G. M. NAESLUND, *J. Chem. Soc., Chem. Commun.* **1994**, 2395.
- 87 A. M. SCHOEVAARS, W. KRUIZINGA, R. W. J. ZIJLSTRA, N. VELDMAN, A. L. SPEK, B. L. FERGINGA, *J. Org. Chem.* **1997**, *62*, 4943.
- 88 W. SHEN, *Synlett* **2000**, 737.
- 89 W. SHEN, L. WANG, *J. Org. Chem.* **1999**, *64*, 8873.
- 90 W. R. ROUSH, M. L. REILLY, K. KAYAMA, B. B. BROWN, *J. Org. Chem.* **1997**, *62*, 8708.

- 91 M. BELLER, H. FISCHER, W. A. HERRMANN, K. ÖFELE, C. BROSSMER, *Angew. Chem. Int. Ed. Engl.* **1995**, *34*, 1848.
- 92 D. A. ALONSO, C. NAJERA, M. A. C. PACHECO, *Org. Lett.* **2000**, *2*, 1823.
- 93 D. ZIM, A. S. GRUBER, G. EBELING, J. DUPONT, A. L. MONTEIRO, *Org. Lett.* **2000**, *2*, 2881.
- 94 A. ZAPF, M. BELLER, *Chem. Eur. J.* **2000**, *6*, 1830.
- 95 M. BELLER, J. G. E. KRAUTER, A. ZAPF, *Angew. Chem. Int. Ed. Engl.* **1997**, *36*, 772.
- 96 C. J. MATHEWS, P. J. SMITH, T. WELTON, *Chem. Commun.* **2000**, 1249.
- 97 T. Y. ZHANG, M. J. ALLEN, *Tetrahedron Lett.* **1999**, *40*, 5813.
- 98 Deloxan THP II can be purchased from Degussa AG.
- 99 B. A. LORSBACH, J. T. BAGDANOFF, R. B. MILLER, M. J. KURTH, *J. Org. Chem.* **1998**, *63*, 2244.
- 100 K. H. BLEICHER, J. R. WAREING, *Tetrahedron Lett.* **1998**, *39*, 4587.
- 101 S. WENDEBORN, S. BERTEINA, W. K.-D. BRILL, A. DE MESMAEKER, *Synlett.* **1998**, 671.
- 102 See ref. 101 and refs. cited therein.
- 103 T. ISHIYAMA, M. MURATA, N. MIYaura, *J. Org. Chem.* **1995**, *60*, 7508.
- 104 S. R. PIETTRE, S. BALTZER, *Tetrahedron Lett.* **1997**, *38*, 1197.
- 105 (a) C. R. STRAUSS, R. W. TRAINOR, *Aust. J. Chem.* **1995**, *48*, 1665. (b) S. CADDICK, *Tetrahedron* **1995**, *51*, 10403.
- 106 (a) M. LARHED, G. LINDERBERG, A. HALLBERG, *Tetrahedron Lett.* **1996**, *37*, 8219. (b) M. LARHED, A. HALLBERG, *J. Org. Chem.* **1996**, *61*, 9582.
- 107 C. M. HUWE, H. KÜNZER, *Tetrahedron Lett.* **1999**, *40*, 683.
- 108 In addition to those references cited above, see: (a) B. J. BACKES, J. A. ELLAM, *J. Am. Chem. Soc.* **1994**, *116*, 11171. (b) B. RUHLAND, A. BOMBRUN, M. A. GALLOP, *J. Org. Chem.* **1997**, *62*, 7820. (c) R. FRENETTE, R. W. FRIESEN, *Tetrahedron Lett.* **1994**, *35*, 9177. (d) Y. HAN, A. GIROUX, C. LEPINE, F. LALIBERTE, Z. HUANG, H. PERRIER, C. I. BAYLY, R. N. YOUNG, *Tetrahedron* **1999**, *55*, 11669.
- 109 G. E. ATKINSON, P. M. FISCHER, W. C. CHAN, *J. Org. Chem.* **2000**, *65*, 5048.
- 110 R. FRANZEN, *Can. J. Chem.* **2000**, *78*, 957.
- 111 (a) T. OH-E, N. MIYaura, A. SUZUKI, *Synlett.* **1990**, 221. (b) T. OH-E, N. MIYaura, A. SUZUKI, *J. Org. Chem.* **1993**, *58*, 2201.
- 112 Y. HOSHINO, N. MIYaura, A. SUZUKI, *Bull. Chem. Soc. Jpn.* **1988**, *61*, 3008.
- 113 S. ABE, N. MIYaura, A. SUZUKI, *Bull. Chem. Soc. Jpn.* **1992**, *65*, 2863.
- 114 Q. ZHENG, Y. YANG, A. R. MARTIN, *Tetrahedron Lett.* **1993**, *34*, 2235.
- 115 C.-W. LEE, Y. J. CHUNG, *Tetrahedron Lett.* **2000**, *41*, 3423.
- 116 P. R. EASTWOOD, *Tetrahedron Lett.* **2000**, *41*, 3705.
- 117 G. M. BOLAND, D. M. X. DANNELLY, J.-P. FINET, M. D. REA, *J. Chem. Soc., Perkin Trans. I* **1996**, 2591.
- 118 W. M. CLARK, A. J. KASSICK, M. A. PLOTKIN, A. E. ELDRIDGE, I. LANTOS, *Org. Lett.* **1999**, *1*, 1839.
- 119 R. P. ROBINSON, E. R. LAIRD, J. F. BLAKE, J. BORDNER, K. M. DONAHUE, L. L. LOPRESTI-MORROW, P. G. MITCHELL, M. R. REESE, L. M. REEVES, E. J. STAM, S. A. YOCUM, *J. Med. Chem.* **2000**, *43*, 2293.
- 120 N. YASUDA, M. A. HUFFMAN, G.-J. HO, L. C. XAVIER, C. YANG, K. M. EMERSON, F.-R. TSAY, Y. LI, M. H. KRESS, D. L. RIEGER, S. KARADY, P. SOHAR, N. L. ABRAMSON, A. E. DECAMP, D. J. MATHRE, A. W. DOUGLAS, H.-H. DOLLING, E. J. J. GRABOWSKI, P. J. REIDER, *J. Org. Chem.* **1998**, *63*, 5438.
- 121 R.-Q. PAN, X.-X. LIU, M.-Z. DENG, *J. Fluorine Chem.* **1999**, *95*, 167.
- 122 G. A. DEBOOS, J. J. FULLBROOK, W. M. OWTON, J. M. PERCY, A. C. THOMAS, *Synlett* **2000**, 963.
- 123 V. PERCEC, J.-Y. BAE, D. H. HILL, *J. Org. Chem.* **1995**, *69*, 1060.
- 124 (a) S. GRONOWITZ, A.-B. HÖRNFELDT, V. KRISTJANSSON, T. MUSIL, *Chem. Scripta* **1986**, *26*, 305. (b) W. J. THOMPSON, J. H. JONES, P. A. LYLE, J. E. THIES, *J. Org. Chem.* **1988**, *53*, 2052. (c) M. B. MITCHELL, P. J. WALLBANK, *Tetrahedron Lett.* **1991**, *32*, 2273. (d) M. UEMURA, H. NISHIMURA, K. KAMIKAWA, K. NAKAYAMA, Y. HAYASHI, *Tetrahedron Lett.* **1994**, *35*, 1909. S. SAITO, M. SAKAI, N. MIYaura, *Tetrahedron Lett.* **1996**, *37*, 2993. (g) W. SHEN, *Tetrahedron Lett.* **1997**, *38*, 5575. (h) W. A. HERRMANN, C.-P. REISINGER, M. SPIEGLER, *J. Organomet. Chem.* **1998**, *557*, 93. (i) F.

- FIROOZANIA, C. GUDE, K. CHAN, Y. SATOH, *Tetrahedron Lett.* **1998**, 39, 3985.
- 125 (a) V. V. GRUSHIN, H. ALPER, *Chem. Rev.* **1994**, 94, 1047. (b) N. MIYaura, A. SUZUKI, *Chem. Rev.* **1995**, 95, 2457.
- 126 (a) A. F. LITKE, G. C. FU, *Angew. Chem. Int. Ed.* **1998**, 37, 3387. (b) A. F. LITKE, C. DAI, G. C. FU, *J. Am. Chem. Soc.* **2000**, 122, 4020.
- 127 D. W. OLD, J. P. WOLFE, S. L. BUCHWALD, *J. Am. Chem. Soc.* **1998**, 120, 9722.
- 128 O. LOHSE, P. THEVENIN, E. WALDVOGEL, *Synlett* **1999**, 45.
- 129 (a) J. P. WOLFE, R. A. SINGER, B. H. YANG, S. L. BUCHWALD, *J. Am. Chem. Soc.* **1999**, 121, 9550. (b) J. P. WOLFE, S. L. BUCHWALD, *Angew. Chem. Int. Ed. Engl.* **1999**, 38, 2413.
- 130 Ligands **42** and **43** are now commercially available from Strem Chemical Co.
- 131 M. ROTTLÄNDER, P. KNOCHEL, *J. Org. Chem.* **1998**, 63, 203.
- 132 S.-K. KANG, H.-W. LEE, S.-B. JANG, P.-S. HO, *J. Org. Chem.* **1996**, 61, 4720.
- 133 S.-K. KANG, H.-C. RYU, H.-J. SON, *Synlett* **1998**, 771.
- 134 G. W. KABALKA, R. M. PAGNI, C. M. HAIR, *Org. Lett.* **1999**, 1, 1423.
- 135 S. F. NIELSEN, D. PETERS, O. AXELSSON, *Synth. Commun.* **2000**, 30, 3501.
- 136 P. GALDA, M. REHAHN, *Synthesis*, **1996**, 614.
- 137 (a) M. REMMERS, B. MÜLLER, K. MARTIN, H.-J. RÄDER, W. KÖHLER, *Macromolecules* **1999**, 32, 1073. (b) J. BAUR, M. F. RUBNER, D. BOILS, *Macromolecules* **1998**, 31, 964. (c) W.-L. YU, J. PEI, Y. CAO, W. HUANG, A. J. HEEGER, *Chem. Commun.* **1999**, 1837. (d) M. RANGER, M. LECLERC, *Can. J. Chem.* **1998**, 76, 1571. (e) A. DONAT-BOUILLUD, I. LEVESQUE, Y. TAO, M. D'IORIO, S. BEAUPRE, P. BLONDIN, M. RANGER, J. BOUCHARD, M. LECLERC, *Chem. Mater.* **2000**, 12, 1931. (f) D.-C. SHIN, J.-H. AHN, Y.-H. KIM, A.-K. KWON, *J. Polym. Sci. Part A* **2000**, 38, 3086. (g) S. HOTTA, H. KIMURA, S. A. LEE, T. TAMAKI, *J. Heterocycl. Chem.* **2000**, 37, 281. (h) A. IZUMI, M. TERAGUCHI, R. NOMURA, T. MASUDA, *Macromolecules* **2000**, 33, 5347.
- 138 M. JOHANNSEN, K. A. JORGENSEN, X.-F. ZHENG, Q.-S. HU, L. PU, *J. Org. Chem.* **1999**, 64, 299.
- 139 B. KARAKAYA, W. CLAUSSEN, K. GESSLER, W. SAENGER, A. D. SCHLÜTER, *J. Am. Chem. Soc.* **1997**, 119, 3296.
- 140 (a) V. HENSEL, A. D. SCHLÜTER, *Eur. J. Org. Chem.* **1999**, 451. (b) V. HENSEL, A. D. SCHLÜTER, *Chem. Eur. J.* **1999**, 421.
- 141 A. DONDONI, C. CHIGLIONE, A. MARRA, M. SCOPONI, *J. Org. Chem.* **1998**, 63, 9535.
- 142 H. IRNGARTINGER, T. ESCHER, *Tetrahedron* **1999**, 55, 10753.
- 143 S. WANG, W. J. OLDHAM JR., R. A. HUDACK JR., G. C. BAZAN, *J. Am. Chem. Soc.* **2000**, 122, 5695.

4

Palladium-Catalyzed Amination of Aryl Halides and Sulfonates*John F. Hartwig***Abstract**

The transition metal catalyzed synthesis of arylamines by the reaction of aryl halides or triflates with primary or secondary amines has become a valuable synthetic tool for many applications. This process forms monoalkyl or dialkyl anilines, mixed diarylamines or mixed triarylamines, as well as *N*-arylimines, carbamates, hydrazones, amides, and tosylamides. The mechanism of the process involves several new organometallic reactions. For example, the C–N bond is formed by reductive elimination of amine, and the metal amido complexes that undergo reductive elimination are formed in the catalytic cycle in some cases by N–H activation. Side products are formed by β -hydrogen elimination from amides, examples of which have recently been observed directly. An overview that covers the development of synthetic methods to form arylamines by this palladium-catalyzed chemistry is presented. In addition to the synthetic information, a description of the pertinent mechanistic data on the overall catalytic cycle, on each elementary reaction that comprises the catalytic cycle, and on competing side reactions is presented. The review covers manuscripts that appeared in press before June 1, 2001. This chapter is based on a review covering the literature up to September 1, 1999. However, roughly one-hundred papers on this topic have appeared since that time, requiring an updated review.

4.1**Introduction****4.1.1****Synthetic Considerations**

Arylamines are commonplace. They are part of molecules with medically important properties, of molecules with structurally interesting properties, of materials with important electronic properties, and of transition metal complexes with catalytic activity. An aryl–nitrogen linkage is present in nitrogen heterocycles such as indoles [1, 2] and benzopyrazoles, conjugated polymers such as polyanilines [3–9], and readily oxidizable triarylamines used in electronic applications [10–13]. The ability of aryl halides and triflates to form arylamines allows a single group to be used as a synthetic intermediate in aromatic carbon–

carbon cross-coupling and amination reactions during structure–activity studies or library synthesis in drug development.

Despite the simplicity of the arylamine moiety, synthesis of these materials is often difficult. Procedures involving nitration, reduction, and substitution are incompatible with many functional groups and often require protection and deprotection steps. Reductive amination provides a convenient route to some alkyl arylamines, but this procedure requires a pre-existing aromatic C–N bond [14–17]. The addition of amines or alcohols to benzyne intermediates leads to variable regiochemistry [18, 19], and direct nucleophilic substitution of aryl halides typically requires a large excess of reagent, a highly polar solvent, and either high reaction temperatures or highly activated aryl halides [20, 21]. Alternatively, transition metal arene complexes have been used to accelerate substitution of the aryl halide. In this case, stoichiometric amounts of the transition metal complex are required [22, 23]. Thus, the new, mild, general catalytic method for the replacement of aryl halogen or sulfonate with amine provides an invaluable route to arylamines.

The procedure that is most competitive with the palladium chemistry is the traditional copper-mediated (Ullmann) substitution. Some recent progress has been made toward increasing the scope of these reactions and reducing the reaction temperatures [24, 25]. However, the reactions still typically require elevated temperatures [26–29], often precluding chemistry with sensitive functionalities. Further, these reactions often give products arising from diarylation of primary arylamine substrates. The Ullmann couplings are also substrate-specific. Reactions of primary alkylamines and even dialkylamines give lower yields than do reactions of more acidic substrates such as arylamines, amides, and azoles. Reactions that form aromatic carbon–nitrogen bonds with weakly nucleophilic nitrogen substrates such as imidazoles and amides have been recently accomplished by a different copper-catalyzed process: coupling of arylboronic acids with the nitrogen nucleophile [30–39]. This chemistry is mild, but requires two steps from an aryl halide because of the intermediacy of the boronic acid.

Prior to the development of palladium-catalyzed amination chemistry, palladium-catalyzed coupling had been a powerful method of forming new C–C bonds starting from aryl halides or triflates [40–46]. A variety of main group and transition metal reagents have been used as the source of the carbon nucleophile. Tin and boron are most commonly used, but aluminum, zinc, magnesium, and silicon reagents are also effective in this “cross-coupling” chemistry. Nickel and palladium complexes are now the most common catalysts. The cross-coupling chemistry has been reviewed a number of times, and several review articles are cited in the aforementioned references.

4.1.2

Prior C–X Bond-Forming Coupling Chemistry Related to the Amination of Aryl Halides

There is a substantial body of literature on the palladium- and nickel-catalyzed formation of aryl sulfides, selenides, and phosphines from aromatic and heteroaromatic halides. Progress on these reactions has continued with several recent contributions [47–50]. A review in 1997 covered the types of transformations that can be conducted and the types of catalysts used [51]. Particularly useful examples are the conversions of binaphthol to binaphthylphosphines

via the triflate intermediate in the presence of palladium and nickel catalysts [52, 53]. The soft, nucleophilic character of thiolates and phosphides favors formation of the palladium thiolate or phosphide complexes and reductive elimination [54] of phosphine and sulfide.

4.1.3

Novel Organometallic Chemistry

Reductive elimination to form C–C and C–H bonds [55] generates the organic product in cross-coupling processes, as well as many other transition metal catalyzed reactions. Reductive elimination reactions comprise an early chapter in any organometallic text. Similarly, the cleavage of C–H bonds by oxidative addition, including the C–H bond in methane, is now known [56]. Even some remarkably mild C–C cleavage reactions have now been observed with soluble transition metal complexes [57–62].

In contrast, examples of complexes that undergo reductive elimination to form the C–N bond in amines have been uncovered only recently [63–68]. These reductive eliminations are the crucial C–N bond-forming steps of the aryl halide and triflate amination chemistry discussed in this review. Information on how these reactions occur and what types of complexes favor this process has been crucial to the understanding and development of new amination catalysts [64].

The cleavage of alkylamine N–H bonds by late transition metals to form metal amido complexes is also rare [69, 70]. When the transition metal is a low valent, late metal, the resulting amido complexes are highly reactive [71, 72]. It appears that the amination of aryl halides can involve an unusual N–H activation process by a palladium alkoxide to form a highly reactive palladium amide [65, 73].

In general, catalytic organometallic chemistry that forms carbon–heteroatom bonds is less developed than that which forms C–C bonds, although the Wacker process is classic catalytic organometallic chemistry [74, 75]. Other processes that form carbon–heteroatom bonds by homogeneous catalysis include oxidative carbonylations of amines and alcohols [75]. Non-oxidative carbonylation includes the reaction between an aryl halide, CO, and an alcohol or amine to form esters or amides [75], but these reactions may not involve alkoxo or amido intermediates. The amination and aquation of alkenes could form the C–X bonds in alcohols or amines, but an efficient, intermolecular aquation or hydroamination of alkenes is a highly sought-after process that remains rare [76]. Some interesting intramolecular examples [77–79] and some slow intermolecular examples [80, 81] are known. Thus, the selectivities, deactivation mechanisms, and potential transformations of alkoxo and amido intermediates in catalytic chemistry are not well understood.

4.1.4

Organization of the Review

This review covers palladium-catalyzed amination of aryl halides and sulfonates. The nickel-catalyzed process [82–85] requires much higher catalyst loads and has a narrower substrate scope. Thus, it is not reviewed. Sections 4.2 to 4.5 cover the development of different palladium catalysts for the synthesis of arylamines and related structures. This work has

stemmed from Kosugi's initial finding [86, 87] that palladium complexes catalyze the formation of arylamines from tin amides and aryl halides. Section 4.6 covers the various arenas in which the palladium chemistry has been applied. Finally, Section 4.7 presents current mechanistic data concerning these processes with different catalysts.

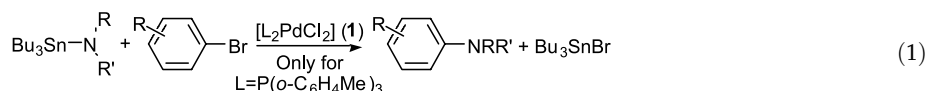
4.2

Background

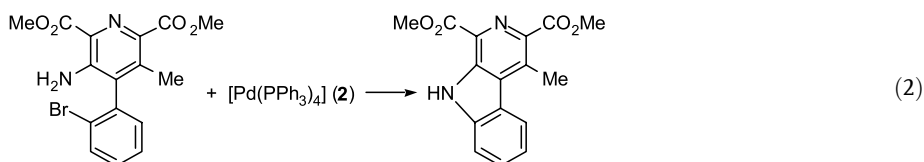
4.2.1

Early Palladium-Catalyzed Amination

In the 1980s, a few results suggested that a general metal-catalyzed method of forming arylamines from aryl halides would be possible. In 1983, Kosugi, Kameyama, and Migita published a short paper on the reaction of tributyltin amides with aryl bromides catalyzed by $[P(o\text{-C}_6\text{H}_4\text{Me})_3]_2\text{PdCl}_2$ (**1**), as shown in Eq. (1) [86, 87].

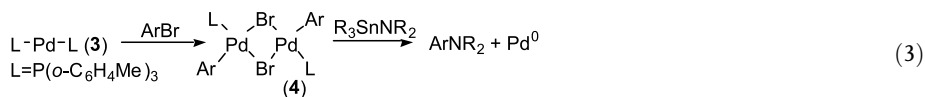


The scope of this reaction appeared to be limited to dialkylamides and electron-neutral aryl halides. For example, nitro-, acyl-, methoxy-, and dimethylamino-substituted aryl halides gave poor yields upon palladium-catalyzed reaction with tributyltin diethylamide. Further, aryl bromides were the only aryl halides to give any reaction product. Vinyl bromides gave modest yields of enamines in some cases. Only unhindered dialkyl tin amides gave substantial amounts of amination product. The mechanism did not appear to involve radicals or benzyne intermediates.



Boger reported studies on palladium-mediated cyclization to form the CDE ring system of lavendamycin, as shown in Eq. (2) [88–90]. These reactions were conducted with stoichiometric amounts of $[\text{Pd}(\text{PPh}_3)_4]$ (**2**). When used in a 1 mol % quantity, **2** failed to catalyze these reactions, presumably because of the absence of a base. Until almost ten years later, no palladium-catalyzed amination chemistry was reported, and there were few citations of the early amination chemistry.

In 1994, Paul, Patt, and Hartwig showed that the $\text{Pd}(0)$ catalyst in Kosugi's process was $\{[\text{Pd}[\text{P}(o\text{-C}_6\text{H}_4\text{Me})_3]_2]\}$ (**3**), which underwent oxidative addition of aryl halides to give dimeric aryl halide complexes (**4**) [91]. These aryl halide complexes reacted directly with tin amides to form arylamine products (Eq. (3)). Thus, this chemistry could formally be viewed as being roughly parallel to Stille coupling.



In the same year, Guram and Buchwald showed that the use of *in situ* derived tin amides extended this chemistry beyond just electron-neutral aryl halides [92]. However, reactions that gave yields of 80 % or more were still limited to tin amides derived from secondary amines.

4.2.2

Initial Synthetic Problems to be Solved

The initial results concerning aryl halide amination and related results in chemistry forming aryl sulfides [93–96] and phosphines [97] strongly suggested that a mild, convenient route to arylamines from aryl halides could be developed. However, the source of the amido group had to be less toxic, more thermally stable, and less air-sensitive than a tin amide. The type of aryl halide amenable to this reaction had to be extended beyond electron-neutral aryl halides. Aryl chlorides and iodides, along with aryl triflates and less reactive, but more convenient, sulfonates needed to be included in the substrates capable of undergoing amination. Of course, heteroaromatic amines and halides are also important substrates and also needed to be included. Perhaps most importantly, reactions of primary amines needed to be developed. Finally, the rates and turnover numbers provided by the catalysts had to be much higher than those in the Kosugi and Migita chemistry and in Boger's stoichiometric cyclization reaction. Faster rates would allow for the use of weaker bases and lower reaction temperatures. Over the past seven years, each of these goals has been achieved.

4.3

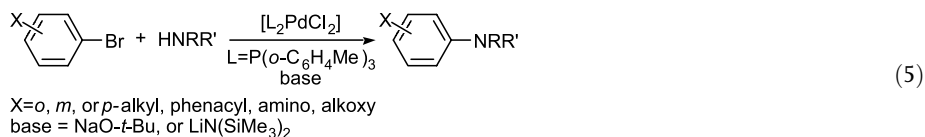
Palladium-Catalyzed Amination of Aryl Halides with Amine Substrates

4.3.1

Early Work

4.3.1.1 Initial Intermolecular Tin-Free Aminations of Aryl Halides

In 1995, Hartwig and Buchwald published concurrently their respective groups' results on tin-free amination of aryl halides [98, 99]. Instead of isolating or generating a tin amide *in situ*, the amination reactions were conducted by allowing an aryl halide to react with a combination of an amine and either an alkoxide or silylamide base (Eq. (5)).

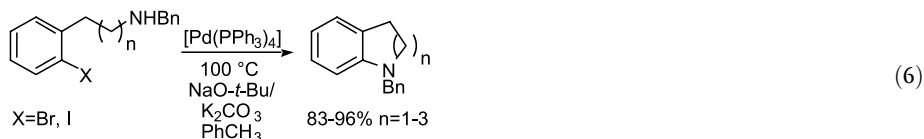


These reactions were typically conducted between 80 and 100 °C in toluene solution. The catalysts used initially were **1**, **3**, or a combination of [Pd₂(dba)₃] (**5a**) (dba = *trans,trans*-

dibenzylidene acetone) and $P(o\text{-C}_6\text{H}_4\text{CH}_3)_3$. Catalysts used subsequently will be described below. Secondary amines were viable substrates, but primary amines gave substantial yields only with electron-poor aryl halides.

4.3.1.2 Initial Intramolecular Amination of Aryl Halides

Intramolecular aryl halide aminations were also conducted with the original catalysts [99]. For example, the reactions in Eq. (6) proceeded with yields in excess of 80 %. In this case, the halide could be iodide or bromide, and $[Pd(PPh_3)_4]$ proved to be a more effective catalyst than $\{Pd[P(o\text{-C}_6\text{H}_4\text{Me})_3]_2Cl_2\}$.



Buchwald later provided an extensive account of the intramolecular amination reactions [100]. Catalysts and conditions were optimized using triaryl and chelating phosphines, but the catalysts discussed in Section 4.4, developed after this work was published, would most probably provide milder conditions for these reactions. Screening of a variety of combinations of phosphine ligands and palladium precursors showed that chelating ligands such as $\text{Ph}_2\text{P}(\text{CH}_2)_n\text{PPh}_2$ ($n = 2-4$) or 1,1'-bis(diphenylphosphino)ferrocene (DPPF) gave good yields of cyclized product, as did a combination of $\text{Pd}_2(\text{dba})_3$ and $\text{P}(2\text{-furyl})_3$, but none were better than $[Pd(PPh_3)_4]$.

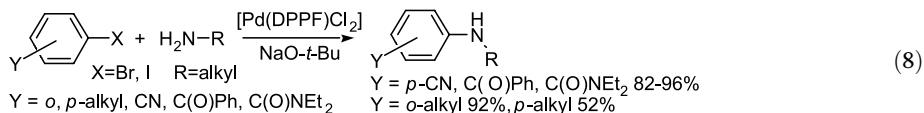
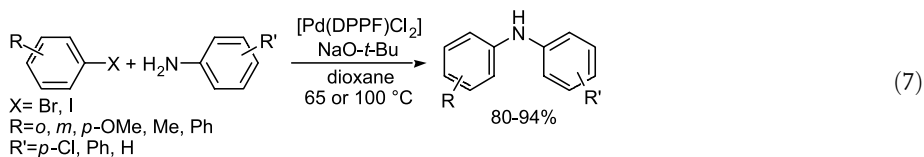
4.3.2

Second Generation Catalysts: Aryl Bis-phosphines

4.3.2.1 Amination of Aryl Halides

With the exception of the intramolecular amination reactions, all of the chemistry described above involved reactions catalyzed by palladium complexes containing the sterically hindered $P(o\text{-C}_6\text{H}_4\text{Me})_3$. Mechanistic studies, as described below, showed that the catalytic cycle involved exclusively mono-phosphine intermediates. However, stoichiometric studies on reductive elimination from PPh_3 -ligated palladium amides [63, 101] and on β -hydrogen elimination from related d^8 square-planar iridium amides [102] suggested that palladium complexes with chelating ligands would be particularly effective catalysts for the amination chemistry. In fact, many of the reasons why such complexes should be effective for this amination process parallel the reasons why they are effective for cross-coupling of aryl halides with main group alkyl reagents [103].

In papers published back-to-back in 1996, Hartwig and Buchwald reported amination chemistry with palladium complexes of DPPF and BINAP as catalysts [64, 104]. These palladium complexes facilitated aminations of aryl bromides and iodides with primary alkyl amines, with cyclic secondary amines, and with anilines. It is ironic that the amination chemistry was first discovered by using a particularly labile phosphine, but was dramatically improved by the use of tightly bound chelating ligands.

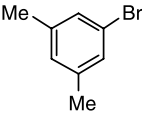
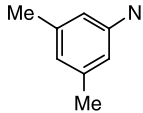
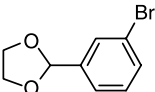
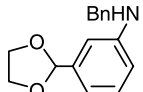
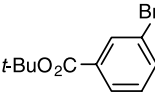
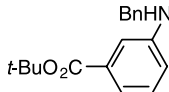
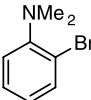
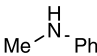
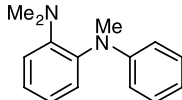
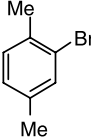
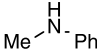
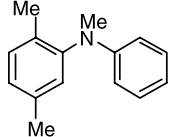


DPPF-ligated palladium provided nearly quantitative yields for the amination of aryl halides with anilines (Eq. (7)). Electron-rich, electron-poor, hindered or unhindered aryl bromides or iodides all participated in the amination chemistry with only a few exceptions. Nitro haloarenes gave no amination product with aniline substrates. Aryl halides with carbonyl groups bearing enolizable hydrogens gave poor yields, and esters were converted to the *tert*-butyl ester by the *tert*-butoxide base. These groups have since been shown to be amenable to amination processes with Cs_2CO_3 as the base [105]. DPPF-ligated palladium also gave good yields of mixed alkyl arylamines with a variety of substrates (Eq. (8)). With electron-poor aryl halides, excellent yields of *N*-alkyl anilines were obtained. With electron-neutral aryl halides, 60–92 % yields were obtained, depending on the positions of the alkyl substituents [64, 106]. In the cases of unhindered and electron-neutral aryl halides coupled with unhindered primary amines, diarylation can occur. In these cases, excess amine suppressed the formation of diarylation products [107]. For most of these reactions, 5 mol % catalyst was employed, although 1 mol % can be used in most cases.

A full account of the palladium-catalyzed amination reactions involving BINAP complexes was published in 2000 [108]. BINAP-ligated palladium provides higher yields than DPPF in the case of electron-neutral aryl halides and primary alkyl amines, as shown in Table 1. The increased yields result largely from the lack of diarylation products. Slightly less reduction product is also observed, although the amount of arene formed when using BINAP or DPPF is low in both cases. Further, in favorable cases, it was shown that 0.05 mol % of the BINAP-ligated catalyst may be used. Racemic and resolved BINAP give identical results. Again, aryl iodides are suitable substrates. A subtle but sometimes important advantage of the chelating ligands is their ability to prevent racemization of amines that possess a stereogenic center α to nitrogen. Reactions of optically active amines have been evaluated; the racemization that sometimes occurs with the original $\text{P}(\text{o-tolyl})_3$ catalyst system does not occur when *rac*-BINAP is used as a ligand [109].

In general, BINAP-ligated palladium is exquisitely selective for the monoarylation of primary amines and is the preferred catalyst for reactions of primarily alkylamine substrates. This result is mutually exclusive with mild, high-yielding reactions of secondary amines with aryl halides to form tertiary amines. Thus, reactions of secondary amines with aryl halides catalyzed by BINAP-ligated palladium are less reliable. For example, reactions of morpholine gave good yields, but those of piperidine and of acyclic secondary amines gave low to modest yields. Exceptions to this rule include reactions of *N*-methyl aniline, of *ortho*-substituted aryl bromides, and of electron-poor aryl bromides. In fact, a particularly favorable case is the re-

Tab. 4.1. Selected aryl bromide aminations catalyzed by BINAP/ $\text{Pd}_2(\text{dba})_3$

	Halide	Amine	Product	Cat. (%)	t (h)	Isolated Yield (%)
1		RNH_2		R = hexyl 0.5 R = Bn 0.5 0.05	2 4 7	88 79 79
2		H_2NBn		0.5	2	81
3		H_2NBn		0.5	3.5	71
4				1.0	39	66
5				0.5	36	94

action of 2-bromo-*p*-xylene with *N*-methyl piperazine, which requires only 0.05 mol % catalyst. Reactions of primary and secondary amines with electron-poor aryl halides were also conducted with weak bases, as outlined in Section 4.5.

Related bis(phosphine) ligands and some additional aryl bis(phosphine)s and hemilabile arylphosphines have been used in the amination chemistry and may be valuable for certain aryl halide aminations (Figure 1). For example, PHANEPHOS has been shown to give good yields in the specific case of the resolution of 2,2'-dibromo[2,2]paracyclophane [110]. More extensive studies have not been reported. Buchwald has reported that reactions with DPEphos [bis(2,2'-diphenylphosphino)diphenyl ether] gave higher yields in the formation of certain diarylamines than did reactions with BINAP or DPPF as ligand [111]. As described in more detail below, solutions to the problem of coupling acyclic dialkylamines and the employment of milder bases began with the use of Kumada's phosphino ether ligand **6** [105, 112]. In addition, Uemura has reported the amination of aryl bromides in the presence of arene-chromium complexes **7a,b** as phosphino ether and phosphino amine analogues of Kumada's ferrocene-based ligands. Good yields were observed for reactions of cyclic and acyclic secondary amines [113]. Finally, Boche has used a sulfonated BISBI ligand **8** to conduct aminations in a two-phase aqueous solution containing water/methanol, water/methanol/

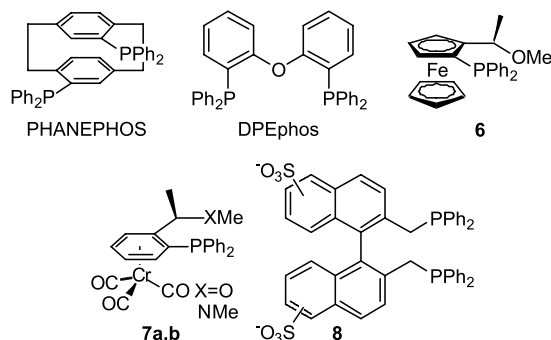
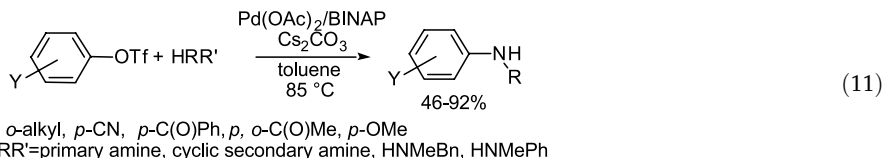
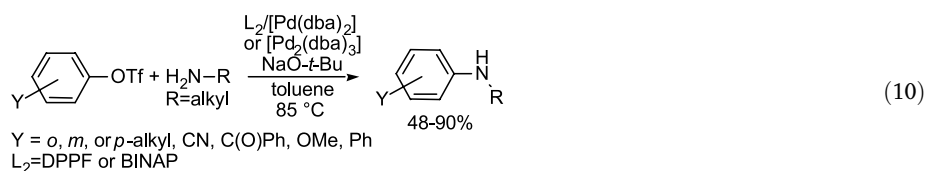
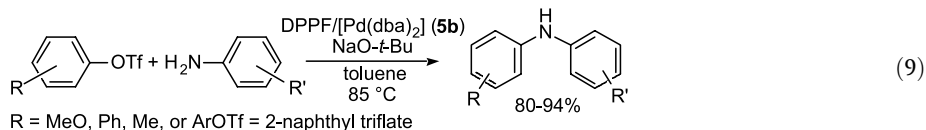


Fig. 1. Chelating and hemilabile ligands used in palladium-catalyzed amination of aryl halides.

toluene, or water/2-butanol. Electron-poor aryl halides reacted with aniline under these aqueous palladium-catalyzed conditions to give diarylamines [114].

In general, the fastest rates for the amination of aryl bromides with bis(phosphine) ligands are seen when sodium *tert*-butoxide is used as the base. However, Prashad has recently reported that bases containing β -hydrogens may be used, and, in some cases, reactions with sodium methoxide as the base occurred in higher yields than those with sodium *tert*-butoxide [115]. The improvement in reaction yield was first observed for a coupling of benzophenone imine with a pendant carbamate. However, this study showed high yields for reactions of primary and secondary amines, including anilines, when using BINAP as the ligand and methoxide or isopropoxide as the base.



4.3.2.2 Amination of Aryl Triflates

Palladium(0) complexes containing P(*o*-C₆H₄Me)₃ as a ligand show low reactivity toward aryl triflates [116, 117]. Thus, the original catalyst is not effective for the amination of aryl tri-

flates. However, palladium complexes with the chelating phosphines DPPF and BINAP are effective [118, 119]. Selected aminations of aryl triflates by aniline are shown in Eq. (9), and selected aminations of aryl triflates by alkylamines are shown in Eq. (10). As in the case of the amination of aryl halides, DPPF is an effective ligand for amination reactions involving anilines or aminations involving electron-poor aryl triflates. The yields for formation of mixed diarylamines have exceeded 90 % in all the examples explored [118]. Reactions of electron-neutral aryl halides with alkylamines gave yields in the range 42–75 % when DPPF was the ligand. This combination of substrates gave yields in the range 54–77 % when BINAP or Tol-BINAP was the ligand; several examples, particularly the triflate derived from the *p*-OMe-substituted phenol, showed higher yields in reactions conducted with BINAP as the ligand than in those conducted with DPPF.

The reactions of electron-poor aryl triflates were plagued by triflate cleavage to form phenol, presumably due to the stable phenolate that initially results from cleavage. In some cases, this problem could be overcome by slow addition of the triflate, whereby high-yielding amination could be achieved [118]. The problem of triflate cleavage was reduced in a more general fashion by using Cs_2CO_3 as the base, as shown in Eq. (11) [120]. Under these conditions, primary and secondary amines reacted in high yields with both electron-poor and electron-rich aryl triflates in the presence of BINAP-ligated palladium as the catalyst. However, no reactions of unhindered, unactivated aryl triflates with primary amines were reported with Cs_2CO_3 as the base, and this combination gave modest yields of 47–65 % when NaOtBu was the base. Reactions performed in toluene solution gave higher yields than those performed in THF, although good yields were obtained in THF in some cases.

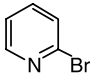
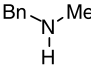
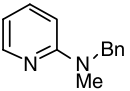
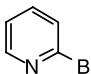
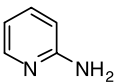
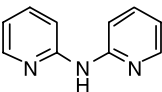
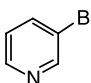
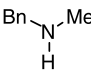
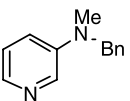
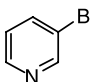
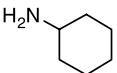
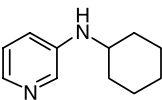
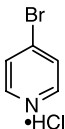
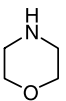
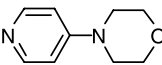
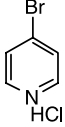
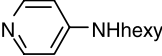
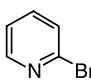
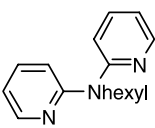
Recently, Torisawa reported that the addition of 18-crown-6 promotes the reactions of aryl triflates when Cs_2CO_3 is used as the base [121]. This study focused on the reactions of *N*-Boc piperazine. In the absence of the crown ether, bis-*N*-Boc piperazine was produced as a by-product, and reaction times were long. Yields for the reaction of 3,4-dichlorophenyl triflate with *N*-Boc piperazine were 35 % and 65 %, respectively, in the absence and presence of the crown ether. A similar effect was also observed for the reaction of the analogous dichloro bromoarene.

4.3.2.3 Amination of Heteroaromatic Halides

Many nitrogen heterocycles bind strongly to late transition metals. As a result, heteroaromatic halides with basic nitrogens can displace weakly binding ligands such as $\text{P}(o\text{-C}_6\text{H}_4\text{Me})_3$. The original catalyst system containing $\text{P}(o\text{-C}_6\text{H}_4\text{Me})_3$ as ligand was consequently ineffective for aminations of heteroaromatic substrates that could bind to palladium. Indeed, pyridine displaces $\text{P}(o\text{-C}_6\text{H}_4\text{Me})_3$ from isolated palladium complexes to form pyridine-ligated species [122]. Chelating phosphines are less readily displaced by pyridines. Thus, the advent of amination reactions conducted with chelating ligands allowed the amination of pyridyl halides [123]. However, studies discussed below on third-generation catalysts show that chelating ligands are not required for the amination of pyridines.

Results on the amination of pyridyl halides conducted with two phosphine ligands and two different palladium precursors have been published (Table 2) [123]. The most general palladium precursor proved to be palladium acetate. Again, BINAP was found to be generally effective for amination with either primary or secondary amines. However, yields were lower with unbranched primary amines than those with branched amines, such as cyclo-

Tab. 4.2. Palladium-catalyzed amination of pyridyl halides.

	<i>halopyridine</i>	<i>Amine</i>	<i>product</i>	<i>catalyst</i>	<i>yield (%)</i>
1				$\text{Pd}_2(\text{dba})_3/\text{DPPP}$	86
2				$\text{Pd}_2(\text{dba})_3/\text{DPPP}$	87
3				$\text{Pd}_2(\text{dba})_3/(\pm)\text{BINAP}$	77
4				$\text{Pd}_2(\text{dba})_3/(\pm)\text{BINAP}$	82
5				$\text{Pd}_3(\text{OAc})_6/\text{DPPP}$	91
6		H_2Nhexyl		$\text{Pd}_3(\text{OAc})_6/(\pm)\text{BINAP}$	67
7	2equiv. 	H_2Nhexyl		$\text{Pd}_3(\text{OAc})_6/(\pm)\text{BINAP}$	71

hexylamine. DPPP [bis(diphenylphosphine)propane], which is less expensive than BINAP, in combination with either **5a** or $\text{Pd}(\text{OAc})_2$ (**9**), acted as an effective catalyst system for the amination of pyridyl bromides by secondary amines or amines lacking hydrogens α to the nitrogen. As was the case for aminations of aryl halides conducted with DPPF and BINAP as ligand, acyclic secondary amines gave only low yields of the amino pyridines.

Hydrazinopyridines are important in the preparation of triazines and as intermediates in the production of agrochemicals and pharmaceuticals. Thus, Arterburn et al. investigated the reaction between hydrazine derivatives and pyridyl halides and triflates [124]. These workers found that 2-bromo- and 2-chloropyridine reacted with benzophenone hydrazone

(see Section 4.4.5 for the use of hydrazones) to give good yields of the coupled product. However, pyridines with ester functionalities in the 5-position gave lower yields unless the pyridyl triflate was used. These reactions were conducted with BINAP as the ligand and NaOtBu as the base. In addition, these authors investigated the reactions of *tert*-butyl carbazate (*tert*-butylOC(O)NHNH₂) with 2-bromopyridine. Using DPPF as the ligand and Cs₂CO₃ as the base, they obtained a 45 % yield of the pyridylhydrazine after acidic work-up. Reactions of 2-bromo- and 2-chloropyridine with di-*tert*-butyl hydrazodiformate (*t*BuOC(O)NHNHC(O)OtBu) gave the coupled product in 45–85 % yield when this ligand and base were used. These reactions are surprising if one considers the potential for reduction of palladium by hydrazines. Pd(PPh₃)₄ is generally prepared using Pd(II) precursors and hydrazine as a reducing agent [125].

Aminations of five-membered heterocyclic halides, such as furans and thiophenes, are limited. These substrates are particularly electron-rich. As a result, oxidative addition of the heteroaryl halide and reductive elimination of the amine are slower than for simple aryl halides (see Sections 4.7.1 and 4.7.3). In addition, the amine products can be air-sensitive and require special conditions for their isolation. Nevertheless, Watanabe has reported examples of successful couplings between diarylamines and bromothiophenes [126]. Triaryl-amines are important for materials applications because of their redox properties, and these particular triaryl-amines should be especially susceptible to electrochemical oxidation. Chart 1 shows the products formed from the amination of bromothiophenes and the associated yields. As can be seen, 3-bromothiophene reacted in higher yields than 2-bromothiophene, but the yields were more variable with substituted bromothiophenes. In some cases, acceptable yields for double additions to dibromothiophenes were achieved. These reactions all employed a third-generation catalyst (*vide infra*), containing a combination of Pd(OAc)₂ and P(*t*Bu)₃. The yields for reactions of these substrates were much higher in the presence of this catalyst than they were in the presence of arylphosphine ligands.

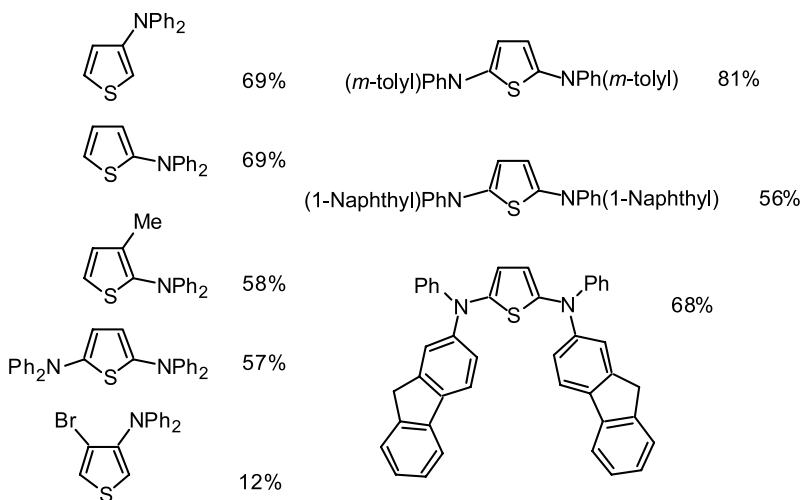


Chart 1

4.3.2.4 Aminations of Solid-Supported Aryl Halides

Two groups [127, 128] have reported results on the solid-phase amination of aryl halides using both $P(o\text{-C}_6\text{H}_4\text{Me})_3$ and chelating ligands. It has been shown that Stille and Suzuki reactions are reliable, high-yielding processes for substrates loaded on solid supports [129]. Thus, supported aryl halides can now be used to form new C–C and C–N bonds, and presumably C–S, C–P, and C–O bonds as well.

Both Farina and Ward [127] at Boehringer Ingelheim and Willoughby and Chapman [128] at Merck have reported successful amination reactions of aryl halides supported on polystyrene Rink and Rapp TentaGel S RAM resin. The results closely parallel those obtained in the solution phase. Secondary amines were successfully coupled with solid-supported aryl halides in high yields with $P(o\text{-C}_6\text{H}_4\text{Me})_3$ as the ligand on palladium. Primary amines required either BINAP or DPPF for successful coupling with the aryl halides, and similar results were obtained with either ligand. N–H groups for which no arylation chemistry had been reported in the solution phase were likewise unreactive on the solid supports. For example, nitroanilines, aminotriazine, 5-aminouracil, 6-diaminoanthraquinone, histidine, 2-aminobenzimidazole, imidazole, and pyrazole gave no products of C–N bond formation in attempted solid-phase reactions in the presence of $P(o\text{-C}_6\text{H}_4\text{Me})_3$, DPPF, or BINAP-ligated palladium.

4.3.2.5 Amination of Polyhalogenated Aromatic Substrates

Multiple arylations of polybromobenzenes have been conducted to generate electron-rich arylamines. Tris(4-bromophenyl)amine and 1,3,5-tribromobenzene both react cleanly with *N*-aryl piperazines in the presence of either $P(o\text{-tolyl})_3$ or BINAP-ligated catalysts to form hexamine products [130]. Reactions of other polyhalogenated arenes have also been reported with DPPF as the ligand [131, 132]. Competition between aryl bromides and iodides or aryl bromides and chlorides has been investigated in relation to the formation of aryl ethers [133], and similar selectivity should presumably be observed for the amination. In this case, bromochloroarenes reacted preferentially at the aryl bromide position. Sowa showed complete selectivity for amination of aryl-chloro, -bromo, or -iodo linkages over aryl-fluoro linkages [134]. This selectivity contrasts the faster fluoride substitution in uncatalyzed aromatic substitutions.

4.3.3

Third-Generation Catalysts with Alkylmonophosphines

Until recently, alkylphosphines had been used less often than arylphosphines in cross-coupling chemistry. However, several studies pointed to the potential of such ligands in the palladium-catalyzed amination of aryl halides. Alkylphosphines in combination with palladium catalyst precursors have now been shown to allow milder conditions for the amination of aryl bromides, to improve yields with acyclic secondary amines, to give high turnover numbers, and to induce mild aminations of inexpensive aryl chlorides and tosylates.

As discussed in more detail in Section 4.7, which reviews studies on the reaction mechanism, the major product that competes with the arylamine is the arene resulting from hydrodehalogenation of the aryl halide. Hartwig showed that steric hindrance was crucial to minimize formation of this side product when monophosphines are used [135]. A second side product from reaction of a primary amine is diaryl alkyl tertiary amine, resulting from

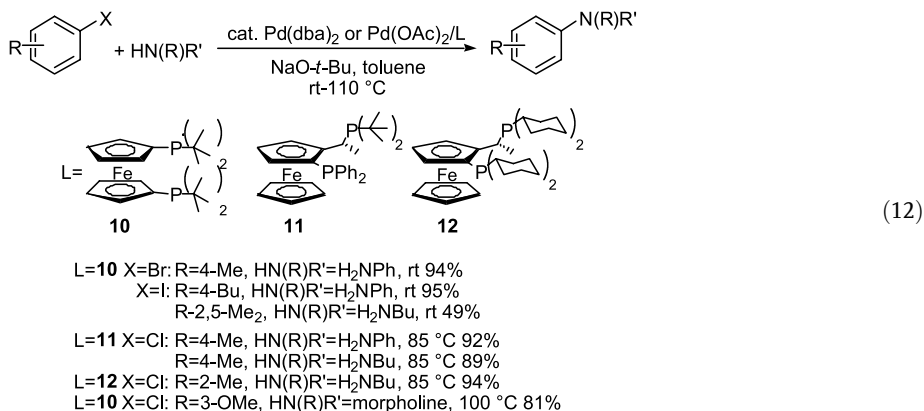
arylation of the secondary amine product. Buchwald showed that chelating ligands such as BINAP minimize the formation of this product, presumably because of the increased steric demand at the metal center created by the four-coordinate amido intermediate containing a bis(phosphine) [104].

4.3.3.1 High-Temperature Aminations Conducted with $P(tBu)_3$ as Ligand

Subsequent to these mechanistic and synthetic findings, Yamamoto, Nishiyama, and Koie at Tosoh Corporation reported high yield formation of aryl piperazines with turnover numbers as high as 7000 when $P(tBu)_3$ was used as a ligand for palladium at high temperatures [136]. They found that unprotected piperazine reacted with aryl bromides at 120 °C to form good yields of the monoarylated piperazines, which are useful pharmaceutical intermediates. The high turnover numbers demonstrate that the amination chemistry may be industrially feasible on a large scale for even the less expensive of specialty chemicals. In a subsequent paper, these authors showed that triarylaminines, which are useful as components of light-emitting diodes, can be prepared from aryl halides and diamines with the same catalyst system with turnover numbers of 4000 [137]. These studies suggested that sterically hindered alkylphosphines can generate highly active catalysts for cross-coupling reactions.

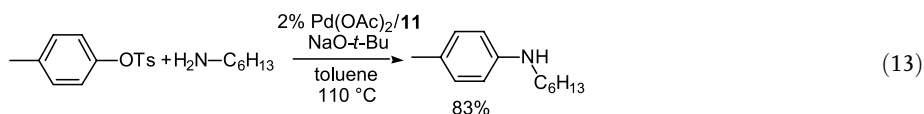
4.3.3.2 Use of Sterically Hindered Bis(phosphine) Ligands

Amination of aryl bromides and chlorides: Hartwig first reported the high yielding amination of unactivated aryl chlorides under mild conditions by using D⁺BPF bis(di-*tert*-butylphosphino)ferrocene [138, 139] and similar sterically hindered bis(phosphine) ligands developed by Spindler, Togni, and Bläser for asymmetric hydrogenations [140–142]. Activated aryl chlorides react much like unactivated aryl bromides, and reactions of these substrates with the original catalyst based on tri-*ortho*-tolyl phosphine were reported [143]. Nickel complexes are also known to react readily with aryl chlorides in cross-coupling chemistry [144–149], and they have also been used in the catalyzed amination of aryl chlorides [82, 83]. In general, the nickel-catalyzed chemistry occurs with lower turnover numbers and has a narrower substrate scope than the palladium-catalyzed reactions with third-generation ligands. For example, primary alkylamines are not suitable substrates for unhindered aryl halides when the nickel catalysts are used, although cyclic secondary amines and anilines can give good yields. Thus, the palladium, rather than nickel, chemistry will be described in detail.



Motivated by the mechanistic and synthetic studies with hindered monophosphines described in the previous paragraph and by the benefits of chelating ligands in controlling the selectivity in reactions with primary amines, Hartwig and Hamann employed the three sterically hindered alkyl bis(phosphine) ligands in Eq. (12) for the amination chemistry [150]. Reactions conducted with D'BPF (**10**) as the ligand gave high yields of amination products under mild conditions (80–100 °C) with unactivated aryl halides and either anilines or cyclic secondary amines. Reactions of aryl bromides were remarkably fast and, for the first time, could be carried out at room temperature. However, this ligand did not give the anticipated high yields in reactions with primary amines. This result and additional results on the use of this ligand in ketone arylation and in the formation of diaryl ethers from aryl halides suggest that D'BPF acts as a monodentate ligand during the catalytic cycle.

Thus, commercially available sterically hindered bis(phosphine)s were tested for their selectivity with primary amines. The ligands **11** and **12** in Eq. (12) [142] are more constrained to a geometry that ensures chelation and may improve selectivity. Indeed, reactions of primary amines with unactivated aryl chlorides gave high yields of the coupled product with high selectivity for C–N coupling over hydrodehalogenation and for monoarylation of the primary amine. These ligands generate catalysts that provide the most favorable combination of monoarylation over diarylation, amination over hydrodehalogenation, and mild activation of aryl chlorides.

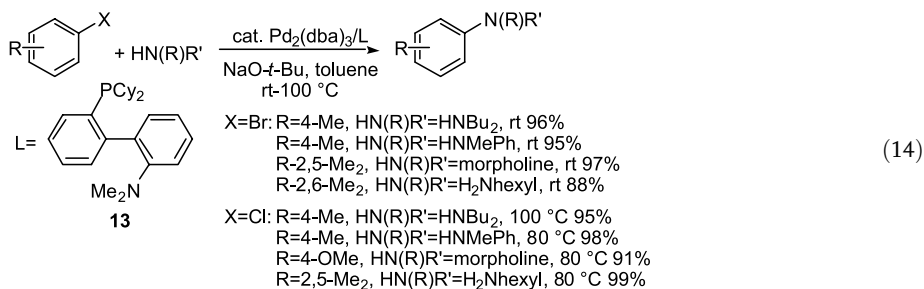


Amination of aryl tosylates: Aryl tosylates are, of course, more convenient to prepare and are more stable reagents than aryl triflates, and they are generated from phenols using a cheaper sulfonating agent. However, the palladium-catalyzed coupling of aryl tosylates is rare. Only one paper has contained palladium-catalyzed coupling with arene sulfonates, and this work involved an electron-deficient aryl fluoroarene sulfonate [151]. One report of the carbonylation of an activated aryl tosylate has appeared [152]. Thus, it was remarkable that the complexes derived from ligand **11** were found to catalyze the amination of aryl tosylates as shown in Eq. (13). These reactions required 110 °C for unactivated aryl tosylates, but the yields were high. Because of the tight chelation of these ligands, high selectivity is observed for reactions of primary amines with the unhindered and unactivated *p*-tolyl tosylate.

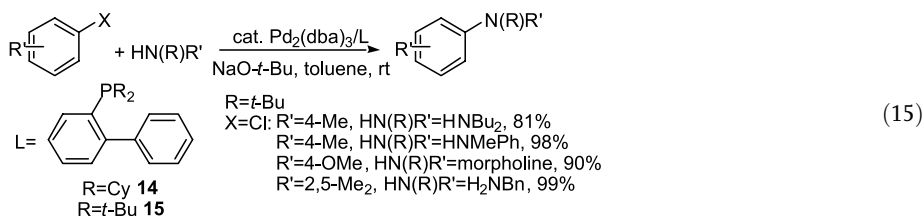
4.3.3.3 P,N Ligands and Dialkylphosphinobiaryl Ligands

Buchwald's group showed that phosphino ether ligands developed by Kumada and Hayashi for asymmetric cross-coupling [153, 154] gave high yields in the formation of tertiary amines from aryl bromides and acyclic secondary amines [112]. Kocovsky showed that complexes of MAP, an amino analogue of MOP that is based on a binaphthyl structure, gives fast rates in the arylation of anilines [155]. To convert palladium complexes of these ligands into catalysts suitable for amination of aryl chlorides, Buchwald's group prepared cyclohexyl analogues of MAP and of BINAP, one of which (ligand **13**) is shown in Eq. (14) [156]. These ligands generate catalysts for high-yielding aminations of unhindered aryl bromides with secondary

amines and of *ortho*-substituted aryl bromides with primary amines at room temperature. The catalysts bearing these ligands also allow the amination of activated aryl chlorides at room temperature and of unactivated aryl chlorides at 80–100 °C. The cyclohexyl MAP analogue **13** is generally more suitable for reactions of secondary amines than primary amines, but it does permit mild coupling chemistry of primary amines and *ortho*-substituted aryl halides.



Although the P,O and P,N structures and their potential hemilability were part of the design and selection of these ligands [157], the nitrogen substituent proved to detract from rather than enhance the catalytic performance of palladium complexes of these ligands. Thus, their desamino analogues, dialkylphosphino-2-biphenyl ligands **14** and **15** in Eq. (15) generated more active catalysts and are simpler to prepare [156]. The dicyclohexylphosphino-2-biphenyl and di-*tert*-butylphosphino-2-biphenyl ligands allow room temperature amination of aryl chlorides in selected cases. For example, reactions that required elevated temperatures when the cyclohexylphosphino P,N ligand was used could be performed at room temperature with the 2-di-*tert*-butylphosphinobiphenyl ligand.



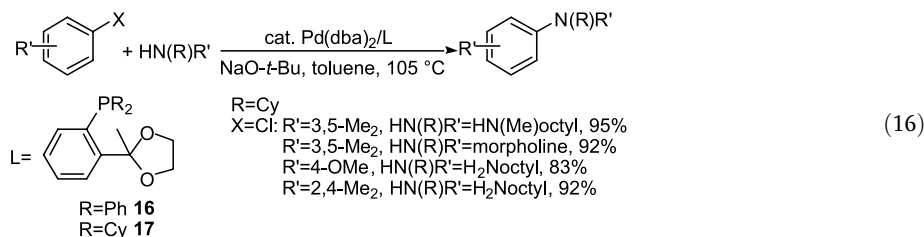
A full account of the scope and limitations of the amination chemistry of these ligands has recently appeared [158]. With ligand **15**, a number of aminations were conducted at room temperature. In the absence of an *ortho* substituent, couplings of primary amines with unactivated aryl chlorides at room temperature required 5 mol % catalyst. However, a variety of secondary amines, both cyclic and acyclic, reacted with activated or deactivated aryl chlorides at room temperature. Thirteen examples were demonstrated. The scope of this process was broader, however, when reactions were conducted at 80 or 110 °C. Under these conditions, unactivated aryl chlorides reacted with a variety of amines in high yields. In favorable cases, such as reactions of aryl chlorides bearing one *ortho* methyl group, reactions of *N*-methyl

aniline, or reactions of morpholine with chlorotoluene, catalyst loadings of 0.05 % gave complete conversion and high yields. As for hindered monodentate ligands discussed below, reactions of chloropyridines with amines occurred, thus demonstrating that chelation is not necessary for coupling of this class of electrophile. However, reaction temperatures of 110 °C, which are significantly higher than those needed for aryl chlorides, were necessary for reaction of these heterocyclic substrates. Finally, these ligands generated catalysts that induced clean chemistry with substrates containing base-sensitive groups. For these substrates and this ligand system, K_3PO_4 was an effective base.

A variety of aryl bromides also reacted with amines at room temperature. Nevertheless, reactions at 80 °C were generally the most suitable for catalyst loadings of 0.5 mol %. In general, reactions of secondary amines or of primary amines with *ortho*-substituted bromoarenes were most favorable. The two examples of primary alkylamines reacting with unhindered aryl halides required long reaction times or higher catalyst loadings. Reaction of benzylamine with 3,5-dimethylbromobenzene required a reaction time of 42 h, while reaction of butylamine with bromobenzonitrile required 3 mol % catalyst and 22 h. In this case, small amounts of the diarylamine were also formed. Aryl triflates were also suitable substrates and reacted with similar scope. Reactions at room temperature were conducted with NaOtBu as the base, while reactions at 80 °C were conducted with K_3PO_4 . Most recently, conditions have been optimized for reactions of aryl iodides. In this case, the dicyclohexyl ligands **13** and **14**, as well as Xantphos [159], provided the best yields between room temperature and 100 °C [160]. Despite some remaining limitations, these studies showed the broad scope of reactivity generated by catalysts with sterically hindered alkylphosphine ligands.

4.3.3.4 Phenyl Backbone-Derived P,O Ligands

A related set of ligands was discovered from a screening study conducted at Symyx Technologies by Guram et al. They found that phenyl backbone-derived P,O and P,N ligands were effective for amination chemistry and that a cyclohexylphosphino version of these ligands, **17**, gave high yields in the amination of aryl chlorides with secondary amines at 105 °C [161, 162]. The ligand **16** in Eq. (16) provided good yields of tertiary amines from aryl bromides and acyclic secondary amines. Simply replacing the diphenylphosphino group with a dicyclohexylphosphino group, as in ligand **17**, generated catalysts that are similar in activity to those bearing the cyclohexylphosphino biphenyl ligands **13** and **14**. Unactivated aryl chlorides reacted with secondary cyclic or acyclic amines in good yields, and unactivated *ortho*-substituted aryl chlorides reacted with primary aryl- or alkylamines in good yields when this ligand was used in combination with $Pd(dba)_2$. Reactions of primary amines with unhindered aryl halides were not reported.



4.3.3.5 Low-Temperature Reactions Conducted with $P(tBu)_3$ as a Ligand

As discussed above, the group at Tosoh reported high turnover numbers for the arylation of piperazine at high temperatures when an excess of $P(tBu)_3$ was used. During preliminary kinetic studies on this process, it was discovered that the reactions occurred under much milder conditions when the isolated $Pd(0)$ complex was used as catalyst and under even milder conditions when a 1:1 ratio of ligand to $Pd(dba)_2$ was used [163]. Moreover, this catalyst system gave essentially quantitative yields with all secondary amines tested, including acyclic dialkylamines. Aryl chlorides were also suitable substrates, and in all cases this catalyst system provided high yields at 70 °C for reactions of secondary amines or anilines. Primary amines reacted at 100–110 °C [164]. In some cases, including an example of an unactivated aryl halide, room temperature reactions were observed with aryl chlorides. The 1:1 ratio of ligand to palladium, low molecular weight of the ligand, and simple structure (and therefore cost) make this catalyst system an economical one for large-scale synthesis. This ligand is more air-sensitive than the biphenyl ligands **13–15**, but is available as a 10 % solution in hexanes in a Sure/Seal bottle from Strem. Several examples of coupling reactions conducted with this ligand are shown in Table 3.

4.3.3.6 Heterocyclic Carbenes as Ligands

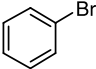
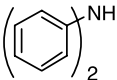
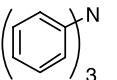
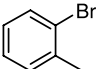
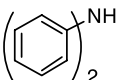
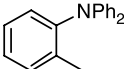
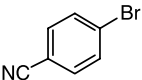
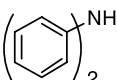
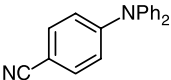
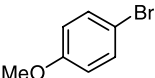
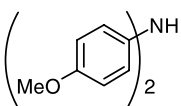
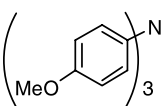
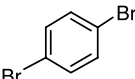
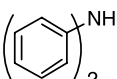
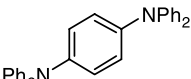
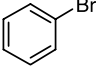
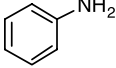
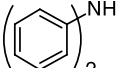
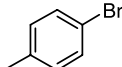
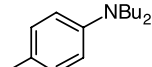
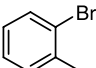
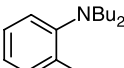
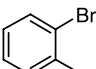
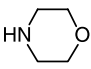
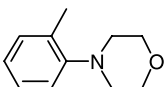
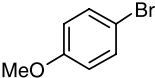
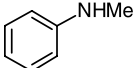
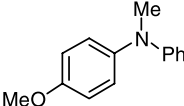
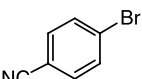
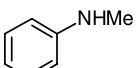
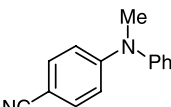
A large body of literature has recently emerged on the use of heterocyclic carbenes as ligands for many catalytic processes, and amination is no exception. These compounds can be made in a sterically hindered form, and they are strongly electron-donating. Chart 2 shows several ligand structures that have been used for palladium-catalyzed amination. In general, these ligands are added to the reaction mixture in their air-stable protonated form, and the base present in the system leads to deprotonation and subsequent coordination of the neutral carbene to palladium. These ligands are commercially available as the protonated precursors. For the amination of aryl halides, the 2,6-diisopropylphenyl-substituted carbene with a saturated backbone (**18**) is the most active.

Nolan reported the use of the 2,6-diisopropylphenyl imidazolium carbene precursor, which contains an unsaturated backbone, for the reaction of aryl chlorides with a variety of amines at 100 °C [165, 166]. This temperature is lower than those conventionally used for reactions of aryl chlorides, but is higher than those used with $P(tBu)_3$ or the 2-biphenyl di-*tert*-butylphosphines. Reaction yields were high when 2 mol % palladium was used. Reactions of primary amines occurred in good yield, even when unhindered aryl halides were used. The monoarylamine was obtained in 86 % yield, and only a 5 % yield of the diarylamine by-product was isolated. Notably, reactions of both aryl bromides and iodides proceeded at room temperature.

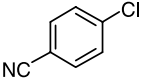
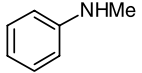
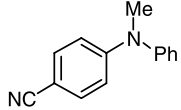
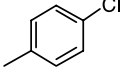

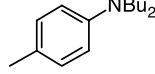
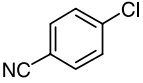

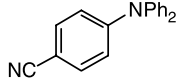
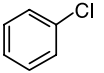


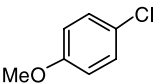

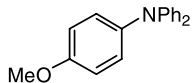
Subsequently, as part of an effort to analyze ligand libraries in a high-throughput fashion, Hartwig and co-workers showed that the carbene precursor with 2,6-diisopropylphenyl groups and a saturated backbone **18** generated complexes that catalyzed the reactions of aryl chlorides at room temperature and with high turnover numbers at elevated temperatures [167]. As for the catalysts formed from imidazolium salts, the ligand precursor is stable to air, simple to prepare, and is now available from Strem. In fact, complete conversion was observed for a reaction conducted without degassing the toluene solvent. These reactions are summarized in Table 4.

In general, reactions of secondary amines and of anilines occurred in high yields with

Tab. 4.3. Reactions of aryl bromides and chlorides with amines catalyzed by Pd(0)/P(*t*-Bu)₃

Entry	Aryl Bromide	Amine	Product	Cond. ^a	Yield ^b (%)
1				RT 1 % Pd 1 h	91
2				RT 1 % Pd 4 h	97
3				RT 1 % Pd 1 h	97
4				RT 1 % Pd 1 h	94
5				RT 1 % Pd 1 h	85
6				RT 1 % Pd 1 h	87
7		HNBu ₂		RT 1 % Pd 4 h	90
8		HNBu ₂		RT 2 % Pd ^c 6 h	81
9				RT 1 % Pd ^c 6 h	96
10				RT 1 % Pd 6 h	99
11				RT 1 % Pd 5 h	95

Tab. 4.3. (continued)

Entry	Aryl Bromide	Amine	Product	Cond. ^a	Yield ^b (%)
12				1 % Pd RT 12 h	90
13				1 % Pd 70 °C 12 h	88
14				1 % Pd RT 5.5 h	89
15				5 % Pd RT 25 h	75
16				4 % Pd 70 °C 16 h	80

^a Reactions run with 1 mmol of aryl halide in 1–2 mL of toluene at room temperature. Pd(dba)₂ used in combination with 0.8 equiv of ligand/Pd.

^b Isolated yields are an average of at least two runs.

^c Pd(OAc)₂ used in place of Pd(dba)₂.

1 mol % palladium. Even electron-rich substrates such as 4-chloroanisole gave nearly quantitative yields. As mentioned in Section 4.3.2.3, pyridyl halides can behave differently to aryl halides because of their ability to coordinate to palladium and displace the phosphine ligands. However, the high binding energy of these heterocyclic carbene ligands [168] apparently prevents displacement of the ligand in the active form of the catalyst. Both 2- and 3-chloropyridine give complete conversion. Reactions at 100 °C provide high turnover num-

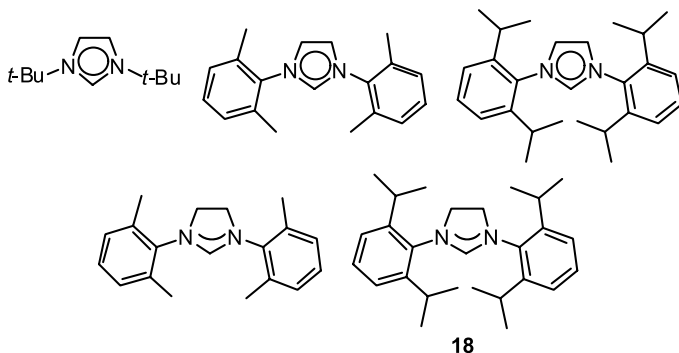
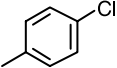
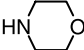
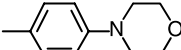
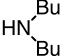
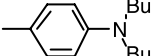
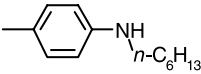
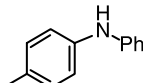
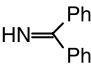
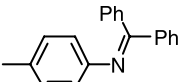
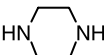
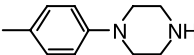
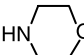
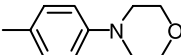
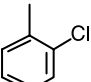
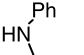
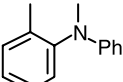
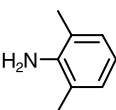
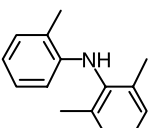
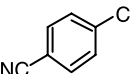
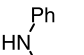
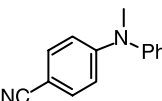
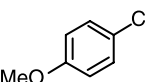
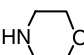
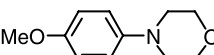
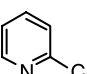
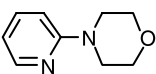
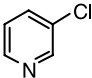
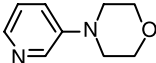


Chart 2

Tab. 4.4.

$\text{ArCl} + \text{NHRR}' \xrightarrow[1.5 \text{ eq NaOt-Bu, DME}]{\text{Pd(dba)}_2/18} \text{Ar-NRR}'$ 1.0 mmol 1.2 mmol						
entry	ArCl	amine	product	T/°C	time	yield ^b
1				rt	3 h	quant.
2				rt	20 h	86 % ^c
3		NH ₂ - <i>n</i> -C ₆ H ₁₃		70	8 h	40 % ^c
4		H ₂ N-Ph		rt	18 h	82 % ^{c,d}
5				55	18 h	94 % ^c
6				100	3 h	71 % ^{c,e}
7				100	7 h	quant. ^f
8				rt	16 h	97 % ^c
9				rt	4 h	88 %
10				rt	3 h	97 %
11				rt	5 h	96 %
12				rt	3 h	98 %

Tab. 4.4. (continued)

entry	ArCl	amine	product	T/ μ C	time	yield ^b
13				rt	20 h	93 % ^c

^aperformed at 1 mol % Pd/2 (1/1) and 1.0 M unless indicated otherwise; see [22] for further details.

^bisolated yields are average of at least two runs; products > 95 % pure as judged by ¹H NMR and GC.

^c2 mol % Pd/2.

^dsubstrate conc. 2.0 M.

^e4 equiv of amine.

^fsubstrate conc. 2.9 M, 0.02 mol % Pd and 0.08 mol % ligand 2.

bers. Morpholine reacts with 4-chlorotoluene in quantitative yield when using 0.02 mol % catalyst. These 5000 turnover numbers are equal to the highest obtained for the amination of aryl chlorides. Piperazine, however, reacts more sluggishly, and a temperature of 100 °C was necessary even when 2 mol % of catalyst was used. Reactions of primary amines were slower than those of secondary amines, and low conversions were observed at room temperature. In addition, Caddick and Cloke [169] have recently reported the use of isolated bis(1,3-di-*N*-*tert*-butylimidazol-2-ylidene)palladium(0) (see Chart 2) as a catalyst for the reactions of 4-chlorotoluene with morpholine and piperidine to give yields of 95 % and 70 %, respectively, at 100 °C.

4.3.3.7 Phosphine Oxide Ligands

A clever ligand design that makes use of phosphine oxides and their tautomeric phosphinous acids has recently been reported by Li at DuPont [170, 171]. As shown in Chart 3, the coordinated di-*tert*-butylphosphinous acid becomes a strongly donating ligand when deprotonated, and the ligand is air-stable when free in solution. This strategy generated catalysts for a variety of cross-coupling reactions, including aryl halide amination. Although the substrate scope was not demonstrated to be particularly broad, and substrates that cannot be tackled effectively with other ligands were not studied, the approach to ligand design was a significant departure from conventional systems.

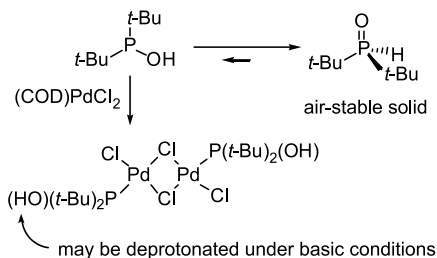


Chart 3

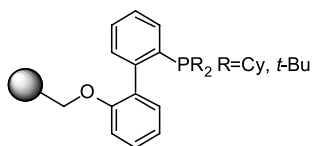


Chart 4

4.3.4

Heterogeneous Catalysts

Three papers have appeared in the past two years on catalysts that are either supported on polymers or are heterogeneous. Djakovitch first reported amination reactions catalyzed by palladium particles immobilized on metal oxide supports, as well as by palladium complexes contained in NaY zeolites [172]. In most cases, these reactions were conducted at high temperatures, generally 135 °C. When NaOtBu was used as the base, competing amination through a benzyne intermediate was observed. Thus, *para:meta* regioselectivity was not high, and reaction yields were modest.

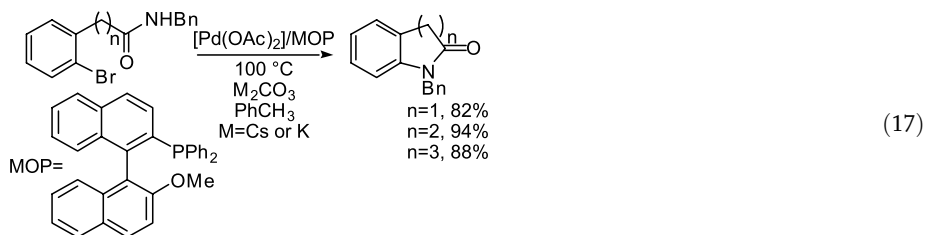
Lipshutz has reported nickel on carbon catalysts for the amination of aryl chlorides [173]. The reactions were conducted with added DPPF as the ligand. The scope of the process is similar to that seen with homogeneous nickel species. Secondary amines provide good yields with electron-poor or electron-rich aryl chlorides, and anilines are suitable for coupling with a range of aryl chlorides.

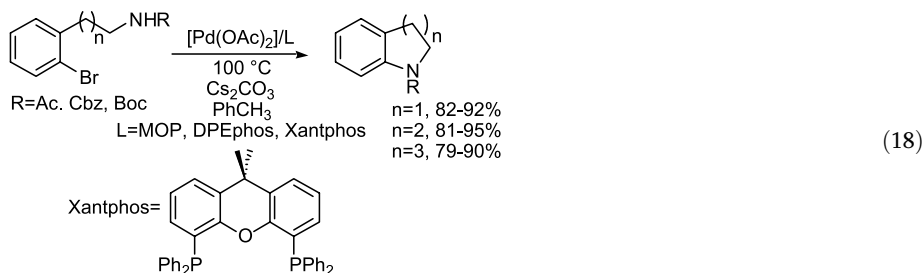
In addition, Buchwald has reported polymer-bound versions of the biphenyl dialkylphosphines. As shown in Chart 4, the ligand is tethered to Merrifield resin through a 2'-OH on the biphenyl group. The scope for reactions was similar to that of homogeneous catalysts bearing these types of ligands. Catalysts were recycled four times starting with 2 mol % catalyst, and they largely retained their activity.

4.4

Aromatic C–N Bond Formation with Non-Amine Substrates and Ammonia Surrogates

The scope of the aromatic C–N bond formation extends beyond simple amine substrates. For example, selected imines, sulfoximines, hydrazines, lactams, azoles, carbamates, and amides all give useful products following aromatic C–N bond formation. In addition, allylamine undergoes arylation, providing an alternative to the ammonia surrogates benzylamine, *tert*-butyl carbamate, and benzophenone imine. Although it is an amine substrate, the reaction of this reagent is included here because of its special purpose.

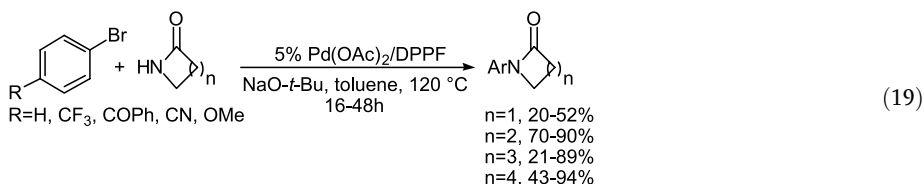




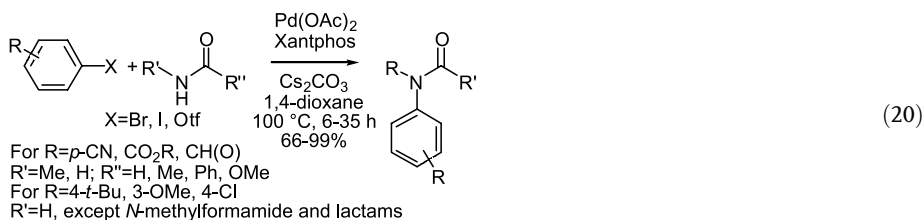
4.4.1

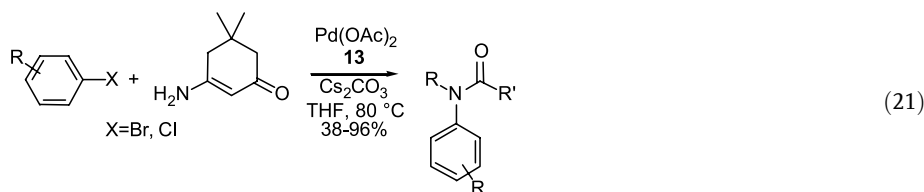
Amides, Sulfonamides, and Carbamates

The initial reports on the arylation of amides and sulfonamides involved intramolecular examples and monodentate triarylphosphine ligands [100]. A paper has recently appeared that reports improved yields for intramolecular reactions when are used MOP, DPEphos, or Xantphos are used as the ligand [174] (Eqs. (17) and (18)). In general, Cs_2CO_3 was used for the cyclization of acetamides and carbamates, but K_2CO_3 proved to be the best base for the cyclization of benzamides. In the initial report, $\text{P}(\text{furyl})_3$ and $\text{P}(o\text{-C}_6\text{H}_4\text{Me})_3$ were the ligands that gave the most effective catalysts. Five- and six-membered rings, but not seven-membered rings, could be formed with acceptable yields. The more recent report improved upon the original procedures, extended the chemistry to carbamates, and included the formation of five-, six-, and seven-membered rings with benzamides, acetamide, *N*-carbobenzyloxy, and *tert*-butyl carbamate substituents tethered to aryl halides, as shown in Eq. (18). The optimal ligand depended on the particular substrate.

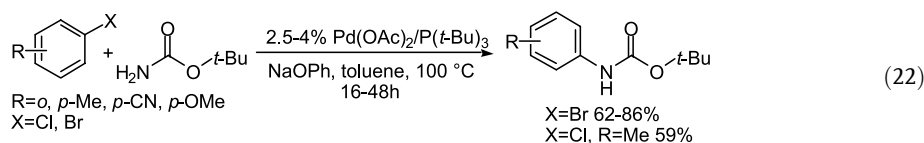


In addition, the coupling of lactams with aryl halides has been conducted in certain cases using arylphosphines, in this case DPPF. Shakespeare showed that a combination of $\text{Pd}(\text{OAc})_2$ and DPPF formed *N*-aryl lactams in good yields from five-membered lactams (Eq. (19)) [175]. Reactions involving electron-neutral aryl halides required long reaction times, but did proceed in good yield. Four-, six-, and seven-membered lactams gave poor yields with unactivated aryl halides, but good yields with electron-poor aryl halides. No reaction was, of course, observed in the absence of catalyst.





Most recently, significant improvements have been made with regard to the reaction of aryl halides with amides, sulfonamides, and carbamates (Eq. (20)) [176]. Yin and Buchwald reported that palladium complexes containing Xantphos as a ligand gave good yields in a number of reactions between aryl bromides and these nucleophiles. The scope of the reaction remains narrower than that for amine substrates, but a variety of benzamides, acetamides, formamides, sulfonamides, and carbamates reacted with electron-poor aryl bromides to form good yields of the respective products. In addition, unactivated aryl bromides, iodides, and triflates reacted with benzamides, acetamides, *N*-methylformamide, and four-, five-, and six-membered ring lactams. Aryl chlorides, *ortho*-substituted aryl bromides, and *N*-alkyl acetamides were not suitable substrates. Moreover, the reactions were highly sensitive to temperature, as outlined in a footnote. Reactions performed at 100 °C for 16 h led to full conversion, but those performed at 120 °C, even with higher catalyst loadings, gave only low conversions. In addition, Edmundson reported the reaction of aryl halides with vinylogous amides using P,N ligand **13** (Eq. (21)) [177].



Prior to the recent paper by Buchwald, an intermolecular version of the arylation of carbamates was published by Hartwig et al. (Eq. (22)) [163]. His group showed that reactions catalyzed by a combination of $\text{Pd}(\text{OAc})_2$ and $\text{P}(\text{tBu})_3$ formed *N*-aryl carbamates from aryl bromides or chlorides and *tert*-butyl carbamate, but that this system was inactive for reactions of amides or sulfonamides. Again, the reaction conditions were not as mild as those used for amination, but they were similar to those employed in the reactions with Xantphos. For the intermolecular reactions, the use of sodium phenoxide as base was crucial.

4.4.2

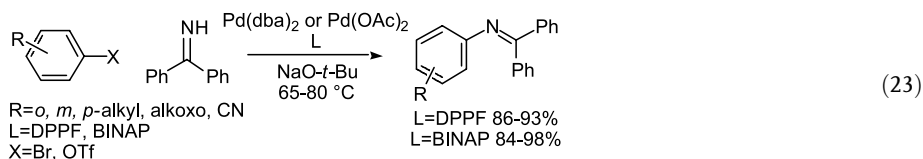
Allylamine as an Ammonia Surrogate

Allylamine can serve as an ammonia surrogate [178]. In the presence of palladium catalysts ligated by $\text{P}(\text{o-tolyl})_3$, diallylamine reacts with aryl bromides in modest yields. Reactions of allylamine with aryl and heteroaryl bromides catalyzed by $(\text{DPPF})\text{PdCl}_2$ give higher yields. Presumably, these reactions can be conducted in a more general fashion with the improved catalysts described above. Cleavage of the allyl group to give the parent arylamine was achieved using methanesulfonic acid and Pd/C .

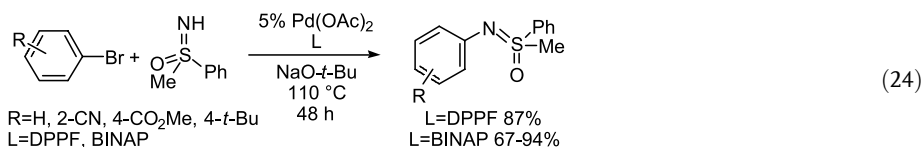
4.4.3

Imines

Benzophenone imine is commercially available and serves as an ammonia surrogate that reacts with aryl halides in high yields under standard palladium-catalyzed conditions. Catalysts based on both DPPF- and BINAP-ligated palladium give essentially quantitative yields in reactions with aryl bromides (Eq. (23)). These reactions can be conducted with either Cs_2CO_3 or NaOtBu as the base [179, 180]. The products are readily isolated by chromatographic techniques or by crystallization. Alternatively, they can be cleaved to the parent aniline by addition of hydroxylamine, acid, or Pd/C [180].



Sulfoximines have also proven to be suitable substrates for palladium-catalyzed C–N bond formation, as shown in Eq. (24), but the chemistry is less general than that with benzophenone imine [181]. Instead of serving as protected anilines, the products may be used as ligands for asymmetric catalysis. *S*-Methyl-*S*-phenyl sulfoximine was coupled with aryl bromides using $\text{P}(o\text{-tolyl})_3$, BINAP-, and DPPF-ligated palladium catalysts and alkoxide or carbonate as the base. Reaction times were long, but good yields were obtained in the case of electron-deficient aryl halides when either BINAP or DPPF was used as the ligand. Reactions of unactivated aryl halides gave good yields when an excess of the aryl halide was used or when the sulfoximine was added slowly. A full account of this work, including the synthesis of unsymmetrical, non-racemic, chiral N,N ligands, has recently appeared [182].



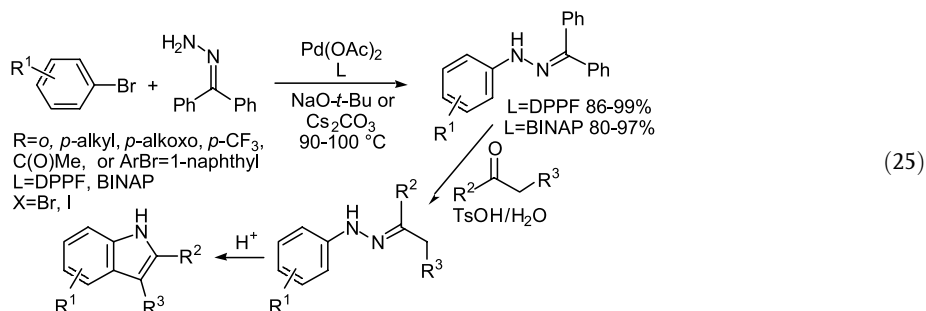
4.4.4

Protected Hydrazines

Azoles can be produced from the products of palladium-catalyzed hydrazone arylation and can themselves serve as substrates for arylation reactions to produce *N*-aryl azoles by the Fischer indole synthesis. *N*-Aryl pyrazoles and related heterocycles can also be prepared after obtaining *N*-aryl hydrazines by palladium-catalyzed procedures. Benzophenone hydrazone was first found by both the Yale and MIT groups to be a particularly effective substrate for palladium-catalyzed reactions, as summarized in Eq. (25) [183, 184]. Reactions of benzophenone hydrazone with either aryl bromides or iodides occur in high yields in the presence of either DPPF- or BINAP-ligated palladium. These reactions are general and proceed with electron-rich, electron-poor, hindered, or unhindered aryl halides. The products of these re-

actions can be converted to hydrazones that bear enolizable hydrogens and that are suitable for indole synthesis in the presence of an acid and a ketone [183].

Most recently, Wagaw, Yang, and Buchwald published a full account of the synthesis of indoles using the palladium-catalyzed amination process [185]. From the standpoint of catalysis, new results included improved turnover numbers and rates when Xantphos was used as ligand. Moreover, this ligand allowed diarylation of the hydrazone, including a one-pot sequential diarylation to provide mixed diaryl hydrazones. A procedure for the alkylation of *N*-aryl hydrazones was also reported. These procedures allow the formation of *N*-aryl and *N*-alkyl indoles after subjecting the products to Fischer conditions for indole synthesis.



An addition to the literature on the arylation of protected hydrazines was recently contributed by Skerlj et al. [186]. In addition to the reactions of halopyridines with *tert*-butyl carbazate (H_2NNHBoc) discussed in Section 4.3.2.3, these authors have reported the reaction of electron-deficient aryl bromides with this substrate. Reactions occurred when using DPPF or the ferrocenyl **11** as the ligand along with Cs_2CO_3 as the base at temperatures of 100–110 °C.

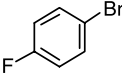
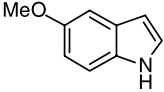
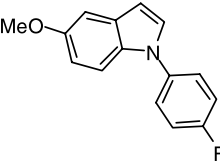
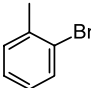
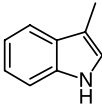
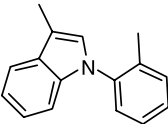
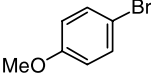
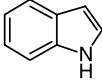
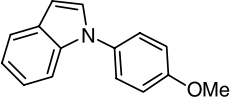
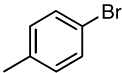
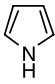
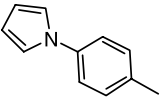
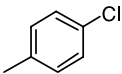
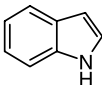
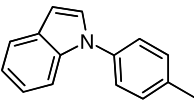
4.4.5

Azoles

Indoles, pyrroles, and carbazoles are themselves suitable substrates for palladium-catalyzed amination. An initial study of this reaction using DPPF-ligated palladium as the catalyst showed that these reactions occurred readily with electron-poor aryl halides. With unactivated aryl bromides, reactions with pyrrole or indole resulted in good yields, but reaction times were long and a temperature of 120 °C was required. Thus, an improved catalyst system was necessary to make the reaction more general and amenable to temperature- or base-sensitive substrates.

Sterically hindered alkylmonophosphines provided improved catalyst systems (Table 5) [163]. In this case, reactions occurred within 8 h at 100 °C for both activated and deactivated aryl bromides and with electron-poor or electron-neutral aryl chlorides. Reactions of *ortho*-substituted aryl halides were unusual, providing a mixture of 1- and 3-substituted indoles, but these aryl halides were suitable substrates when the 3-position of the indole was also substituted. The origin of this *C*- vs. *N*-arylation is unknown. The Tosoh group has also used this catalyst system for the arylation of the parent pyrrole, indole, and carbazole. They observed that Rb_2CO_3 was a particularly effective base [187].

Tab. 4.5. Reactions of aryl halides with azoles catalyzed by Pd(0)/P(*t*-Bu)₃

Entry	Aryl Halide	Azole	Product	Cond. ^a	Yield ^b (%)
1				4 % Pd 12 h	72
2				3 % Pd 12 h	88
4				3 % Pd 6 h	83
5				3 % Pd 6 h	77
6				5 % Pd 12 h	64

^a Reactions were run with 1 mmol of azole in 1–2 mL of toluene at 100 °C. Pd(dba)₂ used in combination with 0.8–1.0 equiv. of ligand/Pd.

^b Isolated yields are an average of at least two runs.

Old, Harris, and Buchwald most recently reported the use of their 2-biphenyl ligands for the arylation of indoles [188]. Similar problems of multiple and non-regiospecific arylation were observed, but some of the ligands alleviated these problems. NaOtBu was the most useful base with these ligands, but K₃PO₄ could also be used with base-sensitive functionalities. Pd₂(dba)₃ proved to be superior to Pd(OAc)₂ as precursor. The ligands in Chart 5 proved most effective for these reactions. Ligands **19** and **20** gave the highest rates, and ligand **21** was most effective in generating the *N*-aryl indole rather than the products of C3-arylation in reactions of 2- and 7-substituted indoles.

Beletskaya has shown that the reaction of benzotriazoles with aryl halides catalyzed by a

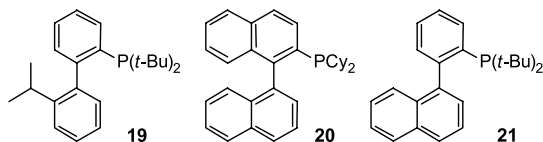
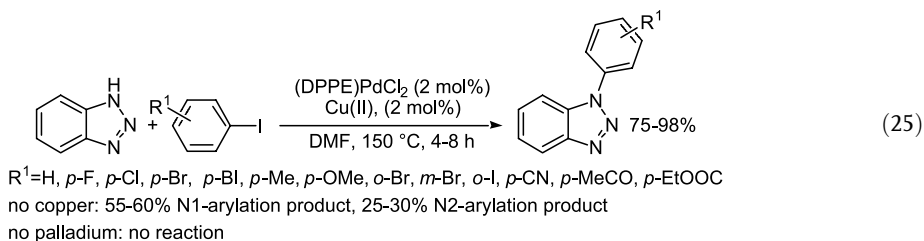
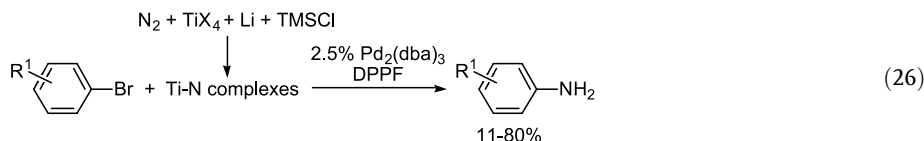


Chart 5

mixture of dppe (bis(diphenylphosphino)ethane) and copper(I) iodide or copper(II) carboxylates proceeds in good yield in DMF solution with a phase-transfer catalyst [189]. The mechanism of these reactions is unknown, although copper is known to catalyze them. However, it was shown that both copper and palladium are required for these reactions to occur at the *N*-1 position in high yields. Similar results were observed in aqueous solution with arylodonium salts as electrophiles [131].



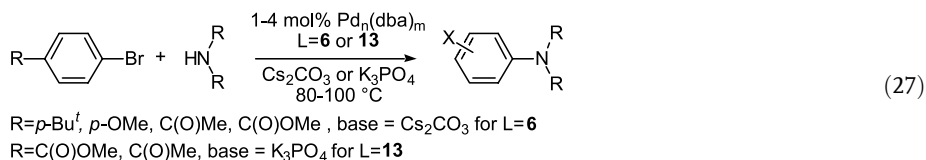
A remarkable process was recently reported by Mori in which dinitrogen is the source of the nucleophile to form anilines, as shown in Eq. (26) [190]. In this chemistry, dinitrogen is used to generate “titanium nitrogen fixation complexes” by reactions of titanium tetrachloride or tetraisopropoxide, lithium metal, trimethylsilyl chloride, and dinitrogen. These complexes are then allowed to react with the aryl halide and a palladium catalyst to generate a mixture of the aryl- and diarylamine. In general, palladium ligated by DPPF gave higher yields of the arylamine product, which were as high as 77 % when using 4-biphenyl bromide and 80 % when using 1-naphthyl triflate.



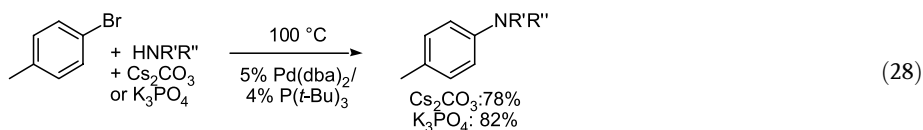
4.5

Amination of Base-Sensitive Aryl Halides

The use of a strong base in the palladium-catalyzed amination of aryl halides precludes the use of many substrates, such as those with aromatic nitro groups or enolizable hydrogens, esters other than *tert*-butyl esters, and many substrates with base-sensitive stereochemistry such as some protected amino acids and heterocyclic substrates [191]. Thus, conditions that employ milder bases are required. A solution that involves reaction temperatures as low as those used for reactions conducted with sodium *tert*-butoxide has not been developed. However, carbonate and phosphate bases can be used with certain catalysts at reaction temperatures comparable to those of reactions involving the first- and second-generation catalysts.



As discussed above, the reactions of amines with aryl triflates instead of aryl halides allow the use of Cs_2CO_3 as the base. Further, reactions of activated aryl halides and some heteroaryl halides can be conducted with Cs_2CO_3 as the base instead of *tert*-butoxide, without requiring a change of catalyst [105, 191]. However, reactions of unactivated aryl halides with this weaker base require a different catalyst. A solution to the problem of coupling unactivated aryl halides in the presence of base-sensitive functionalities began with the use of one of Kumada's phosphino ether ligands (Eq. (27)) [105, 112]. Catalysts containing Kumada's P,O ligand allowed aminations of unactivated aryl halides in the presence of Cs_2CO_3 as base. More recently, Buchwald has used the biaryl ligands **13**–**15** for the amination of aryl halides with Cs_2CO_3 and the less expensive and less toxic K_3PO_4 [156]. The catalyst containing commercially available $\text{P}(\text{tBu})_3$ also allows the reaction of unactivated aryl halides with secondary amines in the presence of Cs_2CO_3 or K_3PO_4 as the base, as shown in Eq. (28) [163]. Thus, simple *tert*-butyl monophosphines appear to generate active catalysts for reactions involving weaker bases, albeit at temperatures in the range 85–100 °C. Presumably the amine can coordinate to the three-coordinate, 14-electron, monophosphine intermediate formed after oxidative addition of aryl halides to complexes with hindered monophosphines [122, 192].



4.6

Applications of the Amination Chemistry

Studies on the applications of the amination chemistry have begun to emerge. The results demonstrate the utility of the amination in the construction of complex, biologically active molecules, in the synthesis of electronically important structures, and in the synthesis of ligands for other catalytic chemistry.

4.6.1

Synthesis of Biologically Active Molecules

Stoichiometric, palladium-mediated cyclization was used in natural product synthesis by Boger a number of years ago, as was noted in the introduction. More recently, an intramolecular palladium-catalyzed amination of a heteroaromatic halide has been used as a step in the synthesis of an α -carboline natural product analogue [193]. As discussed above, the diphenylhydrazone arylation can also be used for nitrogen heterocycle synthesis [183].

4.6.1.1 Arylation of Secondary Alkylamines

N-Arylpiperazines are common substructures of molecules that influence various biological processes and, therefore, the arylation of monoprotected and the single arylation of unprotected piperazines has been studied. As discussed above, the monoarylation of piperazines

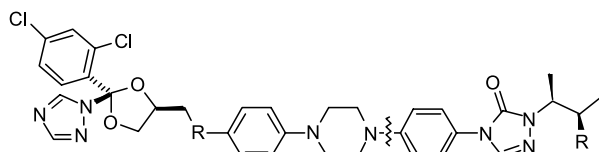
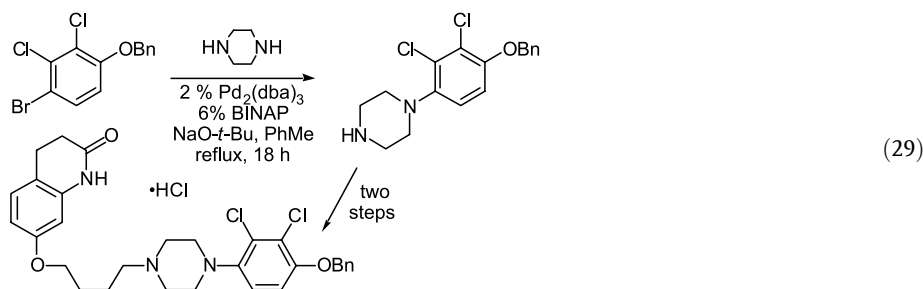
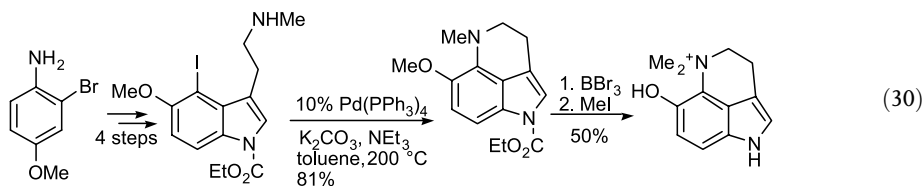


Fig. 2. The disconnection used to form hydroxyitraconazole.

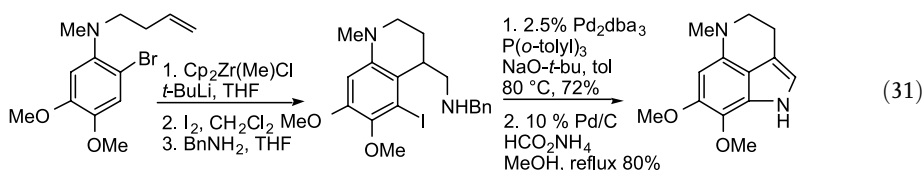
was the reaction for which Nishiyama, Koie, et al. initially applied catalysts bearing $P(tBu)_3$ as a ligand to obtain high turnover numbers at high temperatures [136]. Two other reports of piperazine arylation have appeared, one of a Boc-protected piperazine [194] and one of an unprotected piperazine (the original $P(o\text{-tolyl})_3/Pd(0)$ catalyst system) [195]. Morita has used the arylation of piperazines as a crucial step in the synthesis of a metabolite of aripiprazole, as shown in Eq. (29) [196]. This reaction involved the use of a tetrasubstituted dichlorobromoarene as substrate to give a product that could be readily converted to the final target. Researchers at Sepracor have conducted the amination of an *N*-aryl aryl triazolone with a piperazine to generate the two enantiomeric versions of hydroxyitraconazole (Figure 2) [197]. Finally, Schmid reported the use of a piperidine or morpholine group installed by palladium chemistry as a directing and then leaving group in a concise synthesis of raloxifene. Reaction of the cyclic secondary amines with 2-bromobenzo[*b*]thiophene generated a structure that could be acylated and then reacted at the amino position to deliver an aryl Grignard for synthesis of a 2-aryl benzothiophene [198].



Buchwald has used the intramolecular reaction of acyclic secondary amines with an aryl halide in the total synthesis or the formal total synthesis of a series of tetrahydropyrroloquinolines using palladium-catalyzed amination [199]. A brief description of the methods employed is provided in Eqs. (30) and (31). The approach in Eq. (30) involves formation of the six-membered ring system by means of a palladium-catalyzed intramolecular amination. The reaction conditions contained K_2CO_3 as the base for the cyclization and involved high temperatures. However, the use of $NaOtBu$, which might have allowed reaction at lower temperatures, led to cleavage of the carbamate. The cleavage products apparently inhibited catalyst activity.

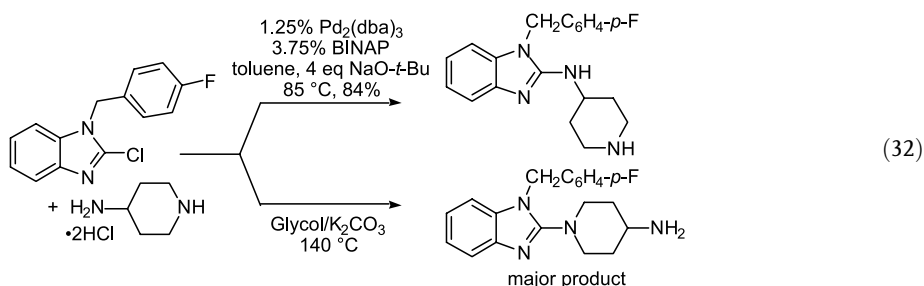


A second approach involved formation of the indole five-membered ring by amination chemistry and the six-membered ring by Zr-benzyne chemistry (Eq. (31)). In this case, the optimal cyclization conditions could be employed, and the reaction temperature was lower. The product of the cyclization is an intermediate in the previous total syntheses of makaluvamine C and of damirone A and B.



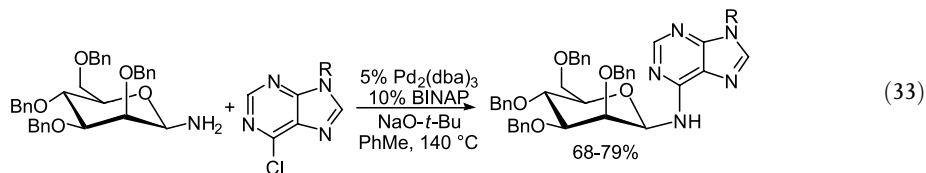
4.6.1.2 Arylation of Primary Alkylamines

Several reports on the application of the intermolecular arylation of primary alkylamines have appeared. For example, the reaction of primary amines with chloro-1,3-azoles has been used to produce the H-1-antihistaminic norastemizole [200]. As shown in Eq. (32), the selectivity of the palladium chemistry is controlled by the steric properties of the amines. This property creates selectivity that complements the thermal chemistry, which is dictated by the amine nucleophilicity. The same researchers have also shown that this high selectivity for arylation of primary over secondary amines with catalysts containing BINAP as ligand allows the rapid assembly of other multiamino-based structures [201].



Chida has coupled glycosylamines with 6-chloropurines to prepare models of spicamycin and septacidin, two *Streptomyces* metabolites that show antitumor activity [202]. As shown in Eq. (33), 5 mol % catalyst was used, and the reaction temperature was high (140 °C). Nevertheless, good yields of the desired *N*-aryl glycosylamine were obtained when BINAP was used as the ligand, NaOtBu as the base, and either MPM or SEM as the N9 protective group.

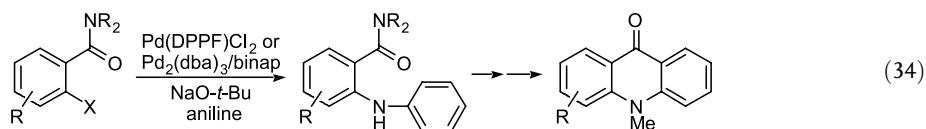
The gluco isomer was also amenable to the palladium-catalyzed arylation, although two anomers were obtained as products.



Recently, the arylation of several specific primary amines have been studied because of the potential biological relevance of the products or products further downstream in a synthetic sequence. For example, cyclopropylamine was shown to be a viable substrate for the coupling under standard conditions [203]. Reactions of 7-azabicyclo[2.2.1]heptane have also been conducted [204] under relatively standard conditions, but with bis(imidazol-2-ylidene) as ligand. Complexes of this ligand and DPPF showed similar catalytic activities, which proved to be superior to those of most bis(phosphine)s. *ortho*-Halo anilines were also studied, in this case to provide access to carbolines after use of the halogen as a means of effecting cyclizations by an electrophilic or reductive C–C bond formation with the other *N*-aryl group [205].

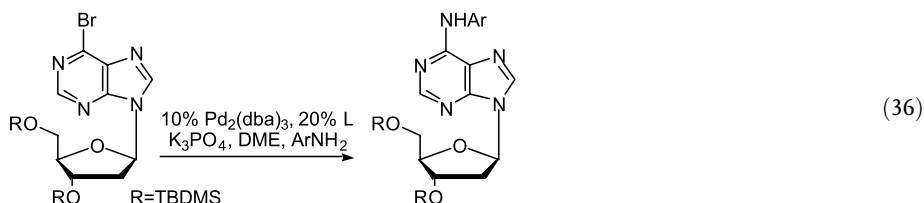
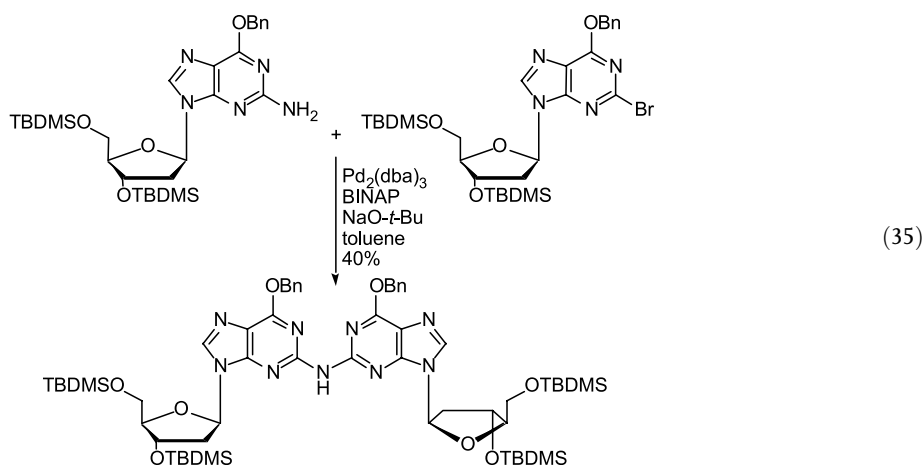
In other cases, unusual aryl halides have been used. Reactions of morpholine and aminopyridine with iodoarylporphyrins have been reported [206]. These reactions take advantage of the ability of chelating ligands to provide activity and were conducted with either DPPF or BINAP as the ligand, depending on the amine substrate. Protected benzimidazoles have been used to prepare (benzimidazolyl)piperazines that show affinity for the 5-HT_{1A} receptor. Yields varied with the amine, but catalysts bearing DPPF or BINAP gave sufficient product for biological evaluation [207, 208].

The palladium-catalyzed formation of diarylamines has been used in several contexts to form molecules of biological relevance. The ability to prepare haloarenes selectively by an *ortho*-metalation–halogenation sequence allows the selective delivery of an amino group to a substituted aromatic structure. Snieckus has used directed metalation to form aryl halides that were subsequently allowed to react with anilines to form diarylamines (Eq. (34)) [209]. Frost and Mendonça have reported an iterative strategy to prepare, by the palladium-catalyzed chemistry, amides and sulfonamides that may act as peptidomimetics. Diarylamine units were constructed using the DPPF-ligated palladium catalysts, and the products were then acylated or sulfonated with 4-bromobenzoyl or arylsulfonyl chlorides [210]. Lemi re has coupled primary arylamines with 4-chloro-3(2*H*)-pyridazinones to form compounds with possible analgesic and antiinflammatory properties.



Several recent papers have reported the palladium-catalyzed formation of diarylamines to prepare nucleosides of damaged DNA. Sigurdsson, Hopkins et al. reported the formation of

a precursor to an interstrand cross-link by the reaction in Eq. (35) [211]. Improved yields were reported by De Riccardis and Johnson when using Cs_2CO_3 . Lakshman reported the reaction of bromonucleosides with amines shown in Eq. (36) as a route to the DNA adducts of carcinogenic aminobiphenyls [212]. In this case, a number of different reaction conditions were investigated, and those involving K_3PO_4 and the P,N ligand **13** proved most effective for the transformation, albeit with high catalyst loadings. Johnson et al. have also recently reported several preparations of carcinogenic amine adducts of 2'-deoxyguanosine and 2'-deoxyadenosine. In one case, they allowed protected derivatives of dG or dA to react with *o*-nitroaryl bromides or triflates, and in another case they coupled 2'-deoxy-2-bromoinosine with several different amines. The latter method offered more flexibility because of the greater generality of the procedures involving the reaction of amines with electron-deficient aryl halides [213, 214]. This general strategy was also followed by Wang and Rizzo [215]. An 8-bromo-2'-deoxyguanosine derivative was coupled to the food mutagen 2-amino-3-methylimidazo[4,5-*f*]quinoline (IQ). To obtain satisfactory yields, they used hexamethyldisilazide as the base and BINAP as the ligand. Several other arylamines and benzylamine were successfully coupled to this guanosine. Finally, Arterburn et al. have recently reported the nickel-catalyzed amination of a nucleobase [216]. They conducted a series of reactions that coupled amino heterocycles and amines tethered to piperazine and piperidine in the presence of a nickel catalyst bearing DPPF as the ligand.



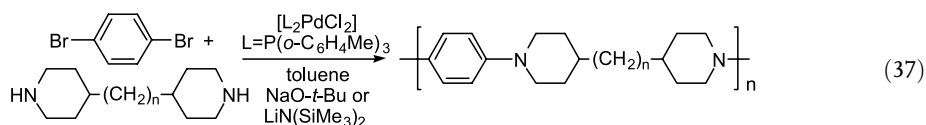
An interesting application of the amination in carbohydrate chemistry has been reported by Buchwald and Seeburger [217]. In this work, the amination chemistry was used as a de-

protection method for 4-halo benzyl ethers. After the amination, a Lewis or protic acid will readily induce cleavage of the benzyl group. The differential reactivity of aryl chlorides, bromides, and iodides allows each of the halobenzyl groups to be deprotected selectively. The iodobenzyl protective group reacts with amines more readily than the other halides and, therefore, can be deprotected first. The bromobenzyl group is the next most reactive toward coupling with amine and subsequent deprotection, and the chlorobenzyl group is the least reactive. The halobenzyl substituents, therefore, serve as orthogonal protective groups to PMB, TIPS, acetyl, and simple benzyl substituents.

4.6.2

Applications in Materials Science

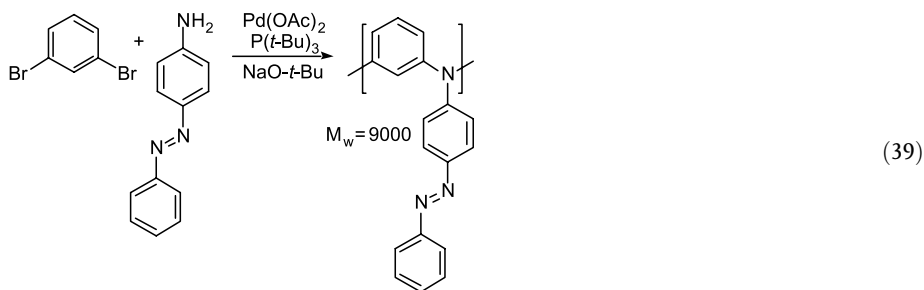
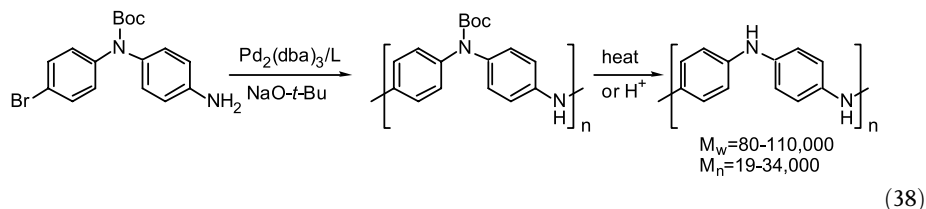
Arylamines display electronic properties that are favorable for materials science. In particular, they are readily oxidized to the aminium form, and this oxidation leads to conductivity in polyanilines, hole-transport properties in triarylamines, stable polyradicals with low-energy or ground-state high-spin states, and the potential to conduct electrochemical sensing. The high yields of the palladium-catalyzed formation of di- and triarylamines has allowed ready access to these materials as both small molecules and discrete oligomeric or polymeric macromolecules.



4.6.2.1 Polymer Synthesis

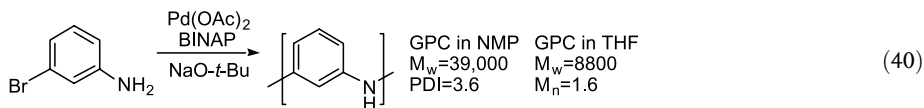
Several reports on the synthesis of polymeric arylamines by palladium-catalyzed chemistry have appeared. One group used the initial amination of aryl halides with dialkylamines to prepare arylamine polymers [218] by coupling a bifunctional diamine and a dihaloarene, as shown in Eq. (37). The highest molecular weights achieved were in the range 5000–6000, indicating an average of 20 monomers each in a chain. Subsequent to this paper, the same group published work with BINAP and $\text{P}(t\text{Bu})_3$ as ligands instead of $\text{P}(\text{o-tolyl})_3$. Several surprising results were obtained, including higher molecular weights when using $\text{P}(\text{o-tolyl})_3$ than when using $\text{P}(t\text{Bu})_3$, despite the higher yields for the formation of triarylamines in small molecule studies on triarylamine synthesis when using $\text{P}(t\text{Bu})_3$ [137, 163, 219]. The molecular compositions of these materials were not characterized in detail. Branching and end-capping as a result of phosphine incorporation [220], molecular weight limiting cyclization [219], and precipitation of the polymer may account for these results.

More recently, Buchwald has reported the polymerization of the monomer in Eq. (38) [220]. This monomer was polymerized at 80 °C for 24 h in the presence of a catalyst comprised of $\text{Pd}_2(\text{dba})_3$ and ligand **14**. The polymers generated from this monomer bearing a Boc group are soluble in THF and chloroform with the aid of sonication. After isolation, the Boc group could be removed by thermolysis at 185 °C or by protonolysis in air. Emeraldine or the emeraldine salt forms of polyaniline result.



Polymers containing chromophores such as acridine and azobenzene have also been prepared by palladium-catalyzed amination according to two approaches [222–224]. The first approach involved the polymerization of monomers containing the chromophore. For example, 4-aminoazobenzene was condensed with 1,3-dibromobenzene (Eq. (39)) or 4,4'-dibromobiphenyl ether to form polymeric materials with M_w values of 9.0×10^3 and 19×10^3 , respectively. Alternatively, polymers prepared by polymerization of 4-bromostyrene or copolymerization of styrene and 4-bromostyrene were coupled with *N*-phenyl-4-amino azobenzene. Substitution of the aryl bromides by the amino azobenzene unit was essentially quantitative when using $P(tBu)_3$ as the ligand.

A related approach to the formation of triarylamine-containing polymers involves synthesis of a monomer containing the triarylamine unit and a second functional group that is amenable to polymerization. Grubbs, Marder et al. reported the synthesis of norbornene monomers containing a tethered triarylamine, using DPPF-ligated palladium as a catalyst to form the triarylamine unit. Ruthenium-catalyzed ring-opening metathesis polymerization then forms the triarylamine-containing polymer [225–226].



Poly(*m*-aniline) has been prepared by palladium-catalyzed condensation of 1,3-dibromobenzene and 1,3-phenylene diamine by two different research groups (Eq. (40)) [227, 228]. In this case, reactions with BINAP as the ligand gave the highest molecular weights. Kanbara has reported M_w and M_n values in formamide solution of 42,400 and 20,100. Meyer has carefully analyzed the products of these reactions, and these results cast doubt on the molecular weight data obtained by Kanbara, as shown in Eq. (40). First, studies on the reaction yields using small molecules suggest that an M_n value near 7000 should be obtained. Sec-

ond, M_w values in NMP and THF solutions are dramatically different: 24,000–39,000 in NMP and 6300–8200 in THF. Thus, the values in THF would appear to be more realistic. Some incorporation of the BINAP ligand into the polymer product was also observed. A small degree of cross-linking may also be present, although small molecule studies showed only a 0.05 % yield of triarylamine. In addition to the linear poly(*m*-aniline), a hyper-branched version of this polymer was prepared [227].

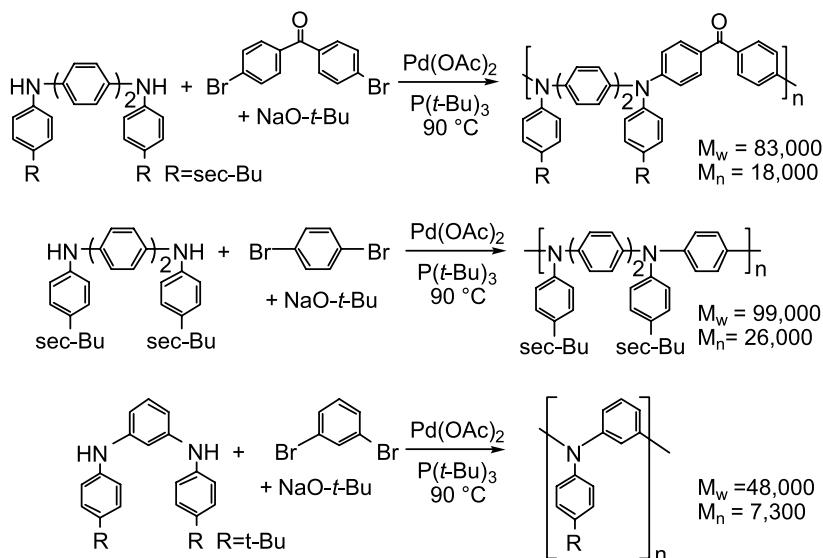
Kanbara has since generated a family of poly(iminoarene)s by reaction of 1,3-dibromobenzene, 4,4-dibromodiphenyl ether, 2,6- and 3,5-dibromopyridines, 2,4-dibromothiophene, and 1,1'-dibromoferrocene with a variety of bifunctional arylamines [229]. In many cases, no polymer was obtained, but for polymerizations involving dibromobenzene and 2,6-dibromopyridine, materials with M_n values of over 10,000 were obtained. Spectral data were provided for poly(2,6-aminopyridine) and a polymer made from dibromobenzene and a diarylamino sulfone. These authors have also investigated nickel catalysts for the polymerization of diamines with dichloroarenes, but the materials generated had molecular weights below 10,000 in most cases [230].

Triarylamine polymers that possess oxetane rings for subsequent cross-linking have been generated [231]. *N,N*-Diphenyl diaminobiphenyl was copolymerized with a dibromo monomer containing the pendant oxetane. Using a catalyst comprised of $\text{Pd}_2(\text{dba})_3$ and $\text{P}(t\text{Bu})_3$ at 97 °C for 5 d, Braig et al. generated materials with M_n values of 7300–9400 and T_g values of 66–79 °C. Films of the polymers were deposited onto indium tin oxide with a photochemically active acid. The materials were then cross-linked under UV irradiation at elevated temperatures and were investigated by UV/vis spectroscopy before and after washing with THF. After heating at 150 °C under irradiation, the polymers became insoluble.

Detailed chemical studies on the formation of triarylamine polymers based on an early communication [232] have now appeared [219]. Goodson, Hauck, and Hartwig reported the use of improved catalysts and synthetic strategies to prepare pure, soluble, linear triarylamine polymers with high molecular weights (Scheme 1). A large number of ligands were prepared and tested for their ability to catalyze the formation of triarylamines in quantitative yields. A phosphino ether ligand and $\text{P}(t\text{Bu})_3$ were shown to be the most effective. True polymeric *N*-aryl versions of poly(*p*-anilines), poly(*m*-anilines), alternating poly(*m*- and *p*-aniline)s, and alternating donor–acceptor copolymers were all prepared. In the case of polymerizations of substrates with *meta*-linkages, cyclization to form tetraazacyclophanes occurred in competition with polymerization. The polymerization of oligomeric fragments and/or the separation of the macrocycles from the polymer by size-exclusion chromatography provided purely linear material. Incorporation of phosphine into the polymer by P–C bond cleavage or ligand metalation processes is common in the formation of polymers by palladium-catalyzed cross-coupling [233, 234]. The materials formed with $\text{P}(t\text{Bu})_3$ as the catalyst contained no phosphorus, as determined by long ^{31}P NMR spectroscopic acquisitions and by ^1H NMR spectroscopy. Thus, the use of $\text{P}(t\text{Bu})_3$ as the ligand is important to observe coupling in yields that are high enough to generate a polymer, to employ low catalyst loads, and to prevent metalation or P–C cleavage reactions of the phosphine ligand.

4.6.2.2 Synthesis of Discrete Oligomers

Buchwald's and Hartwig's groups have both used exponential growth strategies to prepare discrete arylamine materials. Buchwald, Sadighi, and Singer prepared oligomers based on

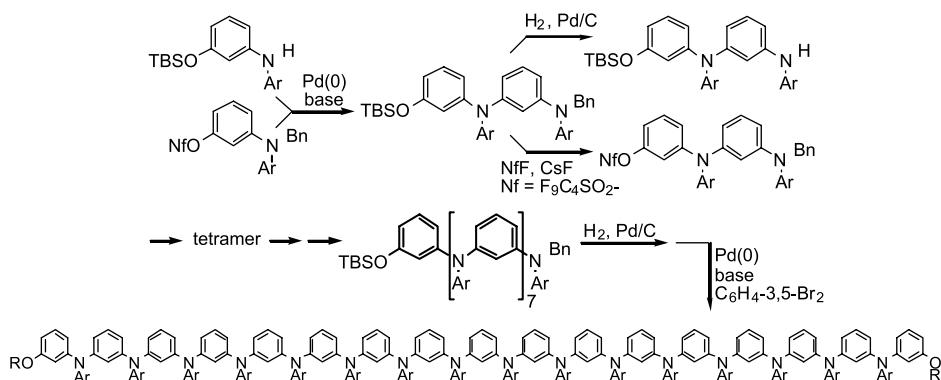


Scheme 1

diarylamine structures [235, 236], while Hartwig and Louie prepared discrete triarylamine oligomers [237]. Janssen has since prepared *N*-methyl versions of alternating *meta,para*-diarylamine octamers without exponential growth by coupling dibromobenzene with two tetramers containing amino termini [238]. These materials generate high-spin structures after oxidation. The exponential growth strategy used by Buchwald and Hartwig to generate the larger oligomers relies on orthogonal protection of two functional groups at the termini of the oligomers. Buchwald's group used *N*-aryl benzophenone imines as protected anilines and trimethylsilylarenes as masked aryl halides. In addition, Boc groups were used to protect internal diarylamine nitrogens in the monomer units. This protection served to solubilize the materials and to make them less susceptible to air or chemical oxidation. BINAP-ligated palladium complexes were used to conduct the couplings to form the diarylamine linkages. Deprotection of the Boc group and the end-functionalized termini produced materials suitable for studies on the electronic properties of polyanilines with variable chain lengths.

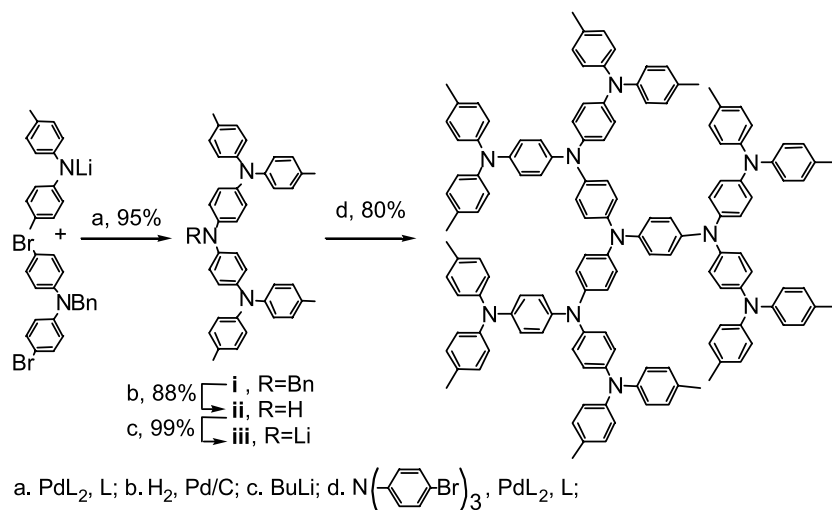
Triarylamine materials of variable chain length [237] were synthesized by using palladium chemistry to couple diarylamines with aryl nonaflates as shown in Scheme 2. The diarylamines were protected with an *N*-benzyl group, and the aryl nonaflate was masked as a TBS-protected phenol. The TBS-protected phenol was directly converted to the nonaflate by CsF and $\text{FSO}_2\text{C}_4\text{F}_9$, and the benzyl group was, of course, removed by hydrogenolysis. The building blocks were prepared prior to the use of $\text{P}(\text{tBu})_3$ for this chemistry. The C–N bonds of the chain were, therefore, constructed using a complex containing DPPF as ligand; a bromide additive appeared to increase reaction yields, but it is unclear as to how large an effect this additive had on this amination process. The materials produced were soluble in organic solvents by virtue of the methoxy substituents on the pendant *N*-aryl groups.

Hyperbranched triarylamine materials have also been prepared by the amination chemistry, as shown in Scheme 3. The material contains exclusively *p*-phenylene diamine linkages



Scheme 2

and triarylamines. The triarylamines were constructed with a combination of benzyl-protected 4,4'-dibromodiarylamines and lithium diarylamides. The formation of the triarylamine linkage with aryl bromides and lithium diarylamides proceeded in >90 % yield under mild conditions in the presence of tris(*o*-tolyl)phosphine-ligated palladium as the catalyst. These materials were characterized by conventional spectroscopic means, as well as by microanalysis. Each carbon was resolved in the ^{13}C NMR spectrum, and a molecular ion was observed by mass spectrometry. The electrochemical behavior of the three-fold symmetric dendrimer was complex and showed a large number of reversible electrochemical waves. The radical cation was generated in solution, which proved to be stable and could be observed by ESR spectroscopy. This material also shows a high glass-transition temperature.



Scheme 3. Synthesis of triarylamine dendrimers.

Multiple arylations of polybromobenzenes have also been conducted to generate electron-rich arylamines. Tris(4-bromophenyl)amine and 1,3,5-tribromobenzene both react cleanly with *N*-aryl piperazines with either $P(o\text{-tolyl})_3$ or BINAP-ligated catalysts to form hexamine products [130]. Reactions of other polyhalogenated arenes have also been reported [189].

4.6.2.3 Synthesis of Azacyclophanes

In 1998 and 1999, two groups reported macrocyclizations to form tri- and tetraazacyclophanes [239–242]. These classes of arylamine have more defined structures than the linear oligomers. Tanaka has prepared cyclic, *meta*-linked trimers of *N*-methylaniline. Both Tanaka and Hartwig have prepared alternating *meta,para,meta,para*-tetraazacyclophanes. Tanaka's structures bear *N*-methyl groups, while Hartwig's bear *N*-aryl groups of varying electronic structure. Both research groups showed that the high-spin state of the dication is the ground state or is energetically low lying relative to the singlet state. The *N*-methyl cyclophanes generated dications that were unstable except at well below room temperature. The *N*-aryl cyclophanes were stable for hours at room temperature. The most recently developed catalysts bearing $P(t\text{Bu})_3$ as the ligand have led to high yields of the *N*-aryl tetraazacyclophanes in the last cyclization step and yields of 20–30 % from a one-pot synthesis. The *N*-methyl materials were produced in less than 5 % yield.

4.6.2.4 Synthesis of Small Molecules for Materials Applications

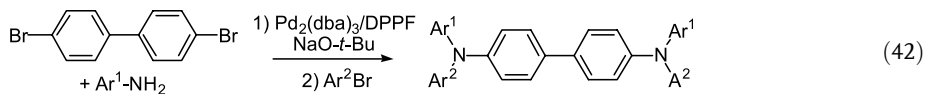
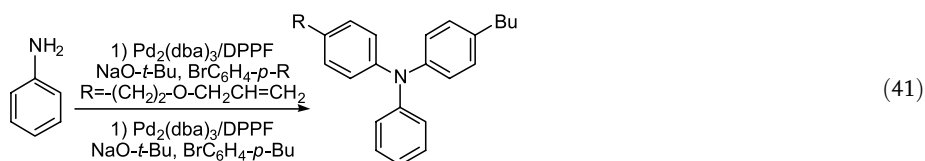
Palladium-catalyzed amination has also been used to prepare small arylamines that can function as sensors, nonlinear optical materials, magnetic materials, electrode modifiers, hole-transport materials, and dyestuffs. *N*-Arylpolyamines that have the potential for multiple applications have also been prepared.

Azacrown ethers with chromophores bound to the nitrogen for metal cation selective detection systems have been prepared by several groups. Aza-18-crown-6 reacts in modest yields with 9-bromoanthracene in the presence of palladium catalysts to form the *N*-aryl azacrown [243]. Among reactions conducted with the four ligands $P(o\text{-tolyl})_3$, BINAP, DPPP, and DPPF (DPPP = 1,3-diphenylphosphinopropane), the DPPF as one with ligand furnished the highest yield, 29 %. Improved yields have recently been reported with electron-poor aryl bromides, such as bromobenzonitrile, bromobenzophenone, 2-bromopyridine, and dibromo analogues of the latter two substrates [244]. For these substrates, $P(o\text{-tolyl})_3$ and PPh_3 were used as ligands. In addition, Witulski et al. prepared an alkali metal chemosensor by an amination to form a 10-cyano-9-*N*-anthryl-azacrown ether. The nitrogen donor and cyano acceptor create a material showing intramolecular charge transfer that allows spectroscopic detection of metal ions [245]. Concurrently, Zhang and Buchwald employed dialkyl biphenylphosphines in the synthesis of *N*-aryl azacrowns. They showed that ligand **13** generates catalysts with improved activity, relative to those generated from $P(o\text{-tolyl})_3$ or PPh_3 , for the coupling with azacrown ethers. Beletskaya has used the DPPF-ligated palladium system to conduct selective monoarylation of ethylene diamine, diethylene triamine, triethylene tetraamines, and 2,2-dimethylbutane-1,3-diamine [246]. These polyamines could also be used for ion sensing by attaching chromophoric aryl groups to the polyamine.

A number of groups have used the palladium chemistry to prepare triaryl amines that are relevant to electronic materials. Barlow and Marder showed that *N,N*-diarylaminofereocenes can be prepared by this methodology. Aminofereocene [247] was allowed to react with 4-bromotoluene under rigorously anaerobic palladium-catalyzed conditions with DPPF as the

ligand to produce *N,N*-di-*p*-tolylferrocene in 58 % yield [248]. This material is readily oxidized to the radical cation. The radical resides predominantly on the ferrocene, but the metal–ligand charge-transfer band is red-shifted. Lin, Tao and co-workers have generated green light-emitting carbazole derivatives using the palladium-catalyzed amination [249]. Using catalysts generated from $P(tBu)_3$ and $Pd(dba)_2$ in a 1:1 ratio, they prepared *N*-phenyl carbazole and, after bromination, a structure with two diarylamino groups on the carbazole. One of the *N*-aryl substituents of each diarylamino group was a pyrenyl group, while the other was a phenyl, tolyl, or anisyl group.

Marder et al. were the first to show that unsymmetrical triarylamines could be prepared, as shown in Eqs. (41) and (42), by sequentially reacting aniline with two different aryl halides, or by reacting 4,4'-dibromobiphenyl with an arylamine and then a second aryl halide with DPPF-ligated palladium as the catalyst [250]. Buchwald subsequently published similar results on the formation of mixed alkyl diarylamines starting from a primary alkylamine [251] or a primary arylamine [252]. With ligand **15**, good yields were obtained in one-pot syntheses of triarylamines. Meerholz used DPPF to prepare TPD analogues containing cross-linkable groups analogous to those used to generate the triarylamine polymers discussed above [253].



The amination chemistry has also been applied to dyes. Ipaktschi and Sharifi reported the palladium-catalyzed synthesis of 2,7-diaminofluorenones by two indirect routes due to the base sensitivity of fluorenones [254]. In the first, 2,7-dibromofluorene was initially treated with secondary amines, and subsequent oxidation of the product formed the diamino-fluorenone. Alternatively, reaction of aminostannanes derived from secondary amines with 2,7-dibromofluorene gave yields of the fluorenone ranging from 42–58 %. Most recently, Mullen et al. have prepared thermotropic perylene dyes [255]. Using benzophenone imine as an ammonia surrogate and palladium-BINAP catalysts, they generated an amino-substituted perylene dye from the corresponding brominated dye. After acid-mediated hydrolysis of the benzophenone imine and the introduction of two Boc groups on the nitrogen, the dye changes from one color at low temperature to a second at higher temperature due to release of the Boc groups and regeneration of the free arylamine.

4.6.3

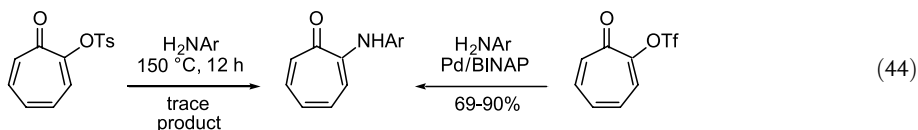
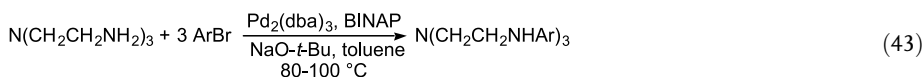
Palladium-Catalyzed Amination in Ligand Synthesis

Amido compounds are gaining increasing importance in early transition metal chemistry as supporting ligands, and structures with both phosphorus and nitrogen donor atoms are

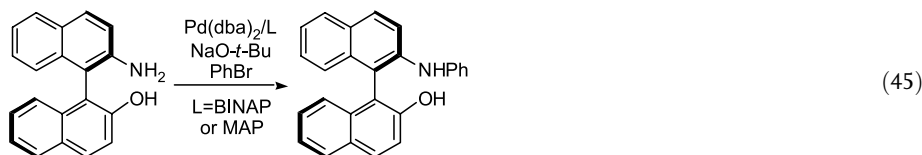
finding increased use as non- C_2 symmetric ligands for asymmetric catalysis. Thus, the amination chemistry can provide a useful method for ligand synthesis. In the past few years, the number of ligands that have been generated using this chemistry has increased rapidly.

Schrock reported a palladium-catalyzed synthesis of triamido ligands that are useful for performing α -olefin polymerization chemistry with Group IV metals (Eq. (43)) [256]. For Schrock's group, this reaction has become a mainstay for the synthesis of related ligands for early transition metal chemistry. Arylation and subsequent alkylation of diethylene triamine led to a set of diamido amine ligands with terminal mesityl groups and an internal tertiary amine [257]. In addition, a diamido ether ligand was prepared with *N*-mesityl groups by the arylation of *o,o'*-diamino diphenyl ether [258]. The coordination, organometallic, and polymerization chemistry of these Group IV complexes has been studied in depth.

An interesting approach to generating ligands for late transition metal polymerization catalysts has recently been reported by Hicks and Brookhart [259]. A series of 2-anilino tropones was prepared by the amination of a pseudoaromatic triflate. This reaction features a novel substrate for the amination process. As shown in Eq. (44), the uncatalyzed reaction of 2-tosyloxytropone with aniline gave low yields of the desired anilino tropone, but the palladium-catalyzed amination of the corresponding triflate with a variety of anilines gave high yields of the desired material.



A number of nonracemic, chiral ligands have also been prepared using the aromatic amination process. A small library of C_2 -symmetric *N,N'*-diaryldiamine ligands was prepared using BINAP-ligated palladium as the catalyst. A variety of chiral diamines were coupled with a variety of aryl bromides to give the *N,N'*-diaryldiamines in modest to excellent yields [260–262]. Some of these ligands have been used for Lewis acid-catalyzed reactions [260, 261] and others for transfer hydrogenations [262]. Kocovsky has treated his NOBIN aminoalcohol (Eq. (45)) with bromobenzene to modify this basic ligand structure [155, 263, 264]. Use of the P,N ligand MAP led to significant rate enhancements. Buchwald and Singer have also conducted palladium-catalyzed amination on binaphthyl ligand substructures. They coupled benzophenone imine with the triflate formed from optically pure binaphthol to prepare similar N,O ligands without a need for resolution [265]. Finally, Diver et al. targeted a different type of ligand that contained a phenylene backbone and chiral *N*-alkyl groups [266]. They prepared this ligand by the reaction of dibromobenzene with enantiopure phenethylamine. The highest yields were obtained with ligand **13**, and the enantiopurity of the starting phenethylamine was retained in the coupled product.



4.7

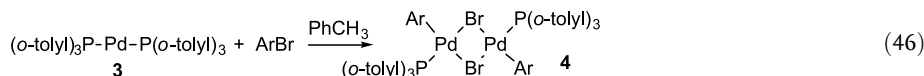
Mechanism of Aryl Halide Amination

The previous sections described synthetic methods involving palladium- and nickel-catalyzed additions of amines to aryl halides and triflates. The development of procedures and catalysts for these processes has occurred hand in hand with mechanistic analysis of the amination chemistry. The following section describes the current understanding of the mechanistic origin of the effectiveness of these procedures and catalysts and how this understanding has led to some of the breakthroughs described above.

4.7.1

Oxidative Addition of Aryl Halides to L_2Pd Complexes ($L = P(o\text{-tolyl})_3$, BINAP, DPPF) and its Mechanism

$L_2Pd(0)$ complexes bearing the three ligands $P(o\text{-tolyl})_3$, BINAP, and DPPF are the resting states of the catalyst when the isolated $Pd(0)$ complex is used as the catalyst in mechanistic studies and when $Pd(OAc)_2$ is used as a catalyst precursor in more synthetically convenient procedures [98, 150]. $Pd(0)$ ligated by dba and BINAP [267] in combination with the $L_2Pd(0)$ complex is the resting state of reactions catalyzed by BINAP and $Pd_n(dba)_m$ complexes [268]. Thus, oxidative addition is the turnover-limiting step with these catalyst systems, and the mechanism and rate of these reactions determines the generation of arylamine products.



$\{Pd[P(o\text{-tolyl})_3]_2\}$ undergoes oxidative addition of aryl halides to provide the unusual dimeric aryl halide complexes $\{Pd[P(o\text{-tolyl})_3](Ar)(Br)\}_2$ (Eq. (46)) [91, 122]. These complexes remain dimeric in solution, as determined by solution molecular weight measurements, but react as the monomers.

These oxidative addition products have been used as precursors to aryl halide complexes containing several of the P,O and P,N ligands discussed in Section 4.3.3. In these cases, monomeric complexes with or without O- or N-coordination are observed. With these systems, it is difficult to determine whether the heteroatom is coordinated in the complex that lies on the reaction pathway or whether the observed complexes are simply the most stable structures; coordination and dissociation of the heteroatom are generally kinetically undetectable. The three structures obtained are shown in Figure 3. Both Kumada's [112] and Guram's [161] ligand systems derived from *o*-acetyl phosphines generate monomeric, monophosphine structures. Guram's ligand derived from the *o*-formyl phosphine forms

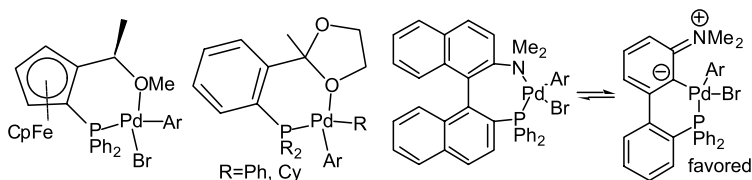


Fig. 3. Structures of various aryl halide complexes containing P,O and P,N ligands used in the amination of aryl halides.

standard monomeric, bis(phosphine) aryl halide complexes. Kocovsky has shown that MAP adopts an unusual conformation involving Pd–C coordination [269], which is observed in some binaphthol complexes [270] as part of a complex equilibrium between the expected P,N ligation mode and a third binding mode without C or N coordination.

The mechanism of the oxidative addition of aryl bromides to the bis-P(*o*-tolyl)₃ Pd(0) complex **3** was surprising [271]. It has been well established that aryl halides undergo oxidative addition to L₂Pd fragments [272–275]. Thus, one would expect oxidative addition of the aryl halide to occur directly to **3** and ligand dissociation and dimerization to occur subsequently. Instead, the addition of the aryl halide to {Pd[P(*o*-tolyl)₃]₂} occurs after phosphine dissociation, as shown by an inverse first-order dependence of the reaction rate on the phosphine concentration and the absence of any tris(phosphine) complex in solution [271].

A similar mechanism presumably operates for the oxidative addition of aryl halides to Pd(0) complexes coordinated by two P(*t*Bu)₃ ligands, but the thermodynamics of this oxidative addition is unusual. Roy and Hartwig obtained the unexpected result that oxidative addition to Pd[P(*t*Bu)₃]₂, and presumably to related, highly hindered bis(phosphine) palladium(0) complexes as well, is close to thermoneutral or is endoergic [276]. Reaction with aryl chlorides is even less favorable than addition of aryl bromides, which is less favorable than addition of aryl iodides. Although oxidative addition is generally rate-limiting with these systems and the thermodynamics is less favorable for addition to these Pd(0) complexes than for addition to more conventional palladium-phosphine complexes, the rates of addition are sufficiently fast to allow room temperature reaction of aryl bromides and chlorides in some cases.

Alcazar-Roman and Hartwig have conducted kinetic studies on the oxidative addition of aryl halides to L₂Pd(0) complexes ligated by BINAP and DPPF [268]. It was shown that full dissociation of the chelating ligand occurs to generate an LPd(0) (L = DPPF or BINAP) species prior to oxidative addition of the aryl halide. The relative rates for reassociation of the ligand and addition of aryl halide were depended on the ligand and altered the kinetic behavior of the systems. Thus, the LPd(0) fragment with L = BINAP reacts faster with aryl bromide than with BINAP when the aryl bromide concentration is high. The reactions are zero order in aryl bromide under these conditions. If the (BINAP)₂Pd(0) complex is part of the catalytic cycle, this result implies that the catalytic cycle will be zero order in all reagents because the aryl bromide concentration is much higher than the free ligand concentration in synthetic reactions. Under these conditions, ligand dissociation from (BINAP)₂Pd is the turnover-limiting step. For complexes of DPPF, ligand reassociation to LPd(0) is faster than aryl bromide addition, making the stoichiometric oxidative addition reversible

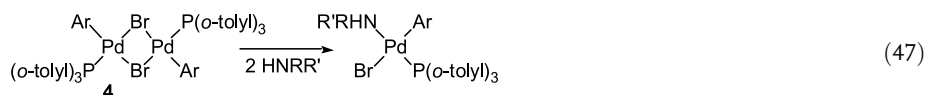
and, therefore, the catalytic cycle first order in aryl bromide and inverse first order in free ligand.

4.7.2

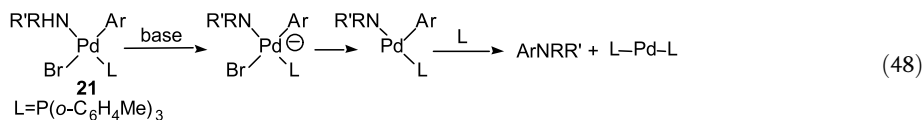
Formation of Amido Intermediates

4.7.2.1 Mechanism of Palladium Amide Formation from Amines

In the original process conducted with tin amides, transmetalation formed the amido intermediate. However, this synthetic method is outdated and the transfer of amides from tin to palladium will not be discussed here. In the tin-free processes, reaction of a palladium aryl halide complex with an amine and a base generates a palladium amide intermediate. One pathway for the generation of the amido complex from an amine and a base would be reaction of the metal complex with the small concentration of amide that is present in the reaction mixtures. However, this pathway seems unlikely considering the two directly observed alternative pathways discussed below and the absence of benzyne and radical nucleophilic aromatic substitution products that would be generated from the reaction of an alkali amide with an aryl halide.



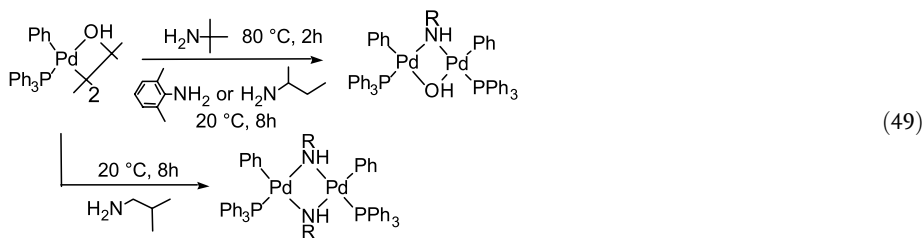
Paul, Patt, and Hartwig showed that the dimeric aryl halide complexes $\{\text{Pd}[\text{P}(\text{o-C}_6\text{H}_4\text{Me})_3](\text{Ar})(\text{Br})\}_2$ react with a variety of amines to form the monometallic, amine-ligated aryl halide complexes $\{\text{Pd}[\text{P}(\text{o-C}_6\text{H}_4\text{Me})_3](\text{amine})(\text{Ar})(\text{Br})\}$ in Eq. (47) [122]. Buchwald and Widenhoeffer subsequently published similar results and showed that primary amines can even displace the phosphine ligand [192, 277, 278]. It is likely that similar amine-ligated monophosphine complexes are formed when other hindered phosphines are employed, such as the *tert*-butyl- and cyclohexylphosphine ligands discussed in Section 4.3.3. These amine complexes are important in the catalytic cycle because the acidity of the N–H bond is enhanced upon coordination of the amine to the metal.



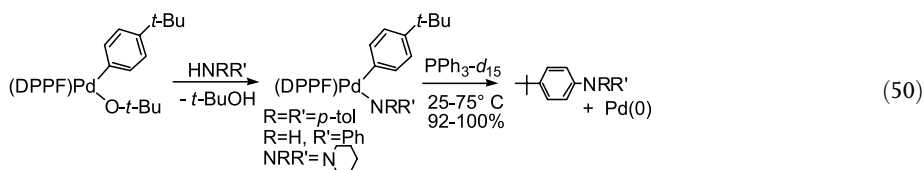
The amine-ligated aryl halide complexes react with alkoxide or silylamide bases to form arylamine products (Eq. (48)) [279]. The reaction of $\{\text{Pd}[\text{P}(\text{o-C}_6\text{H}_4\text{Me})_3](\text{HNEt}_2)(\text{p-Bu}^n)(\text{Br})\}$ and $\text{LiN}(\text{SiMe}_3)_2$ occurred immediately at room temperature to form the arylamine in greater than 90 % yield. Low-temperature reactions conducted in the NMR spectrometer probe allowed direct observation of the anionic halo amido complex $\{\text{Pd}[\text{P}(\text{o-C}_6\text{H}_4\text{Me})_3](\text{NEt}_2)(\text{Ar})(\text{Br})\}^-$ [279]. Thus, one experimentally supported mechanism for gen-

eration of the amido aryl intermediate is coordination of the amine to form a square-planar 16-electron complex that reacts with the base.

An alternative pathway when soluble alkoxide or silylamido bases are used involves reaction of an arylpalladium halide complex with the alkoxide or silylamide to form an intermediate alkoxide or amide. These complexes can react with amines to form the required amido aryl intermediates. The reaction of $\{\text{Pd}(\text{PPh}_3)(\text{Ph})(\mu\text{-OH})\}_2$ with primary alkylamines to generate palladium amido complexes and water (Eq. (49)) [70, 280] gave an early indication that the conversion of an alkoxide to an amide could be occurring during the catalytic cycle. These reactions are reversible, but the equilibrium favors the amido complex.



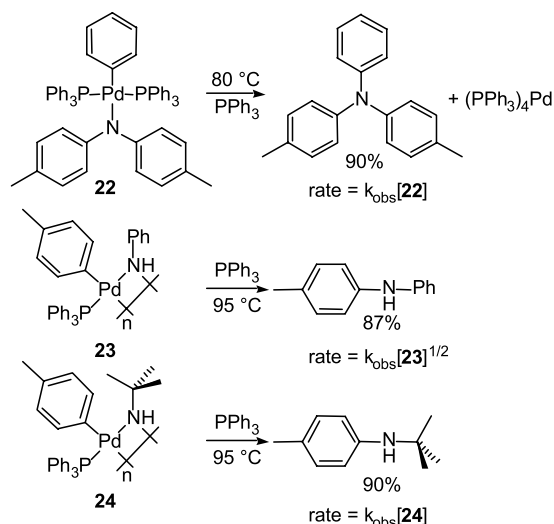
Alkoxo intermediates may be formed when monophosphines are used, but the stability of the amine complexes favors the mechanism involving deprotonation of the coordinated amine. Instead, the alkoxo complexes are likely to be important in catalytic systems involving chelating ligands [65]. Indeed, the DPPF complex $\{\text{Pd}(\text{DPPF})(p\text{-Bu}^t\text{C}_6\text{H}_4)(\text{O}^t\text{Bu})\}$ reacted with diphenylamine, aniline, and piperidine, as shown in Eq. (50) to give, in each case, the product of amine arylation in high yield [65]. Since no alkali metal is present in this stoichiometric reaction, the palladium amide is formed by a mechanism that cannot involve external deprotonation by an alkali metal base. Of course, reactions involving the carbonate and phosphate bases, which are insoluble and would act as poor ligands, are more likely to occur by a coordination and deprotonation mechanism even when chelating ligands are used.



4.7.3

Reductive Eliminations of Amines from Pd(II) Amido Complexes

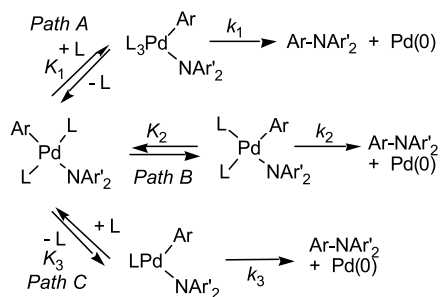
Reductive elimination of amines is the key bond-forming step in the catalytic amination processes. These reactions were unknown a couple of years ago. There are now several examples of this reaction, and the factors that control the rates of this process are beginning to be understood. The identity of the intermediates in some of these reductive elimination reactions has recently been uncovered.



Scheme 4. Reductive elimination of arylamines from PPh_3 -ligated Pd^{II} amido complexes.

The best-understood examples of reductive eliminations that form the C–N bond in amines involve palladium complexes. Both Boncella et al. [66] and Hartwig et al. [63, 64, 101] have observed these reactions with palladium amido aryl complexes. Hartwig's group has studied the mechanism of this process in detail [101, 280]. Although monomeric and dimeric amido complexes have been isolated, the monomeric species undergoes reductive elimination. For complexes with monodentate ligands, kinetic studies have indicated that the actual C–N bond formation occurs simultaneously from both three- and four-coordinate intermediates. With chelating phosphines, therefore, the chemistry is likely to occur directly from the four-coordinate complexes observed in solution. The reductive elimination of arylamines is favored by increasing nucleophilicity of the amido group and by increasing electrophilicity of the aryl group.

The mechanisms of the reductive eliminations shown in Scheme 4 have been studied [101, 280]. Potential pathways for reductive elimination are shown in Scheme 5. The reduc-



Scheme 5. Potential mechanisms for reductive elimination of arylamines from PPh_3 -ligated Pd^{II} amido complexes.

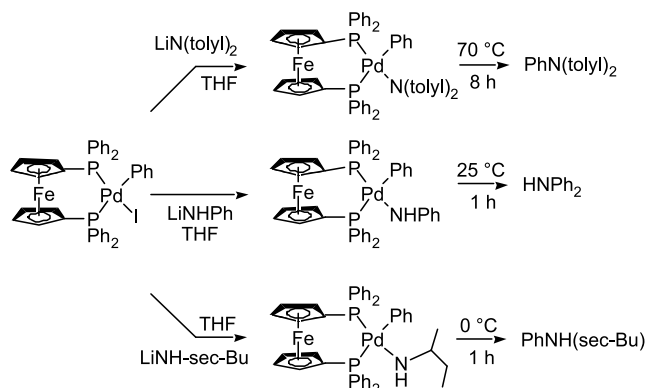
tive eliminations from the monomeric diarylamido aryl complex **23** illustrate two important points concerning the elimination reactions. First, these reactions were found to be first order, demonstrating that the actual C–N bond formation occurred from a monomeric complex. Second, the observed rate constant for the elimination reaction contained two terms (Eq. (51)), corresponding to the two concurrent mechanisms, Path B and Path C in Scheme 5. One of these mechanisms involves initial, reversible phosphine dissociation followed by C–N bond formation from the resulting 14-electron, three-coordinate intermediate. The second mechanism involves reductive elimination from a 16-electron, four-coordinate intermediate, presumably after *trans*-to-*cis* isomerization. The dimeric amido complexes undergo reductive elimination after cleavage to form two monomeric, three-coordinate, 14-electron amido complexes.

$$-d[\mathbf{22}]/dt = k_{\text{obs}}[\mathbf{22}]$$

$$k_{\text{obs}} = K_2k_2 + \frac{K_3k_3}{[PPh_3]} \quad (51)$$

The observation that the reductive elimination process involves a pathway proceeding via four-coordinate, presumably *cis*, monomeric amido aryl complexes led to the preparation of palladium amido complexes with chelating ligands [64]. Results with these complexes confirmed this conclusion and led to the development in our laboratory of second-generation catalysts based on palladium complexes with chelating ligands [281]. The DPPF-ligated palladium amido aryl complexes in Scheme 6 were found to undergo reductive elimination of arylamines in high yields [64, 101]. The rates of these reactions were first order in palladium and zero order in the trapping ligand. Thus, the data on the reductive elimination reactions are consistent with a direct, concerted formation of the C–N bond from the *cis*, four-coordinate DPPF complex.

Because the reductive elimination from DPPF-ligated palladium does not involve geometric rearrangements or changes in coordination number before the rate-determining step, the DPPF complexes allowed an assessment to be made of the electronic properties of the transition state in this reaction. The relative rates for elimination from amido groups were found



Scheme 6. Reductive elimination of arylamines from DPPF-ligated palladium amido complexes.

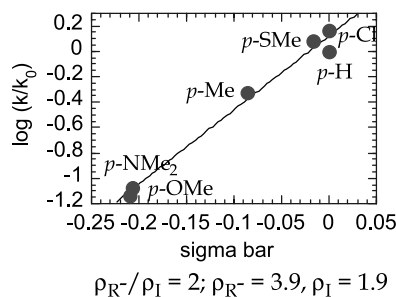


Fig. 4. Electronic analysis using a combination of σ_I , and σ_R for the reductive elimination of aryl arylamines.

to decrease in the order alkylamido > arylamido > diarylamido. This trend implies that the more nucleophilic the amido group, the faster the elimination process. Variation of the aryl group led to similar results as those seen in an extensive study of the electronic aspects of C–S bond-forming eliminations of sulfides [54]. The data for electronic effects on sulfide and amine eliminations (Figure 4) show that electron-withdrawing groups accelerate the reductive elimination process and that substituents with large σ_R values affect the reaction rates more than substituents with large σ_I values. Resonance effects are stronger than inductive effects, perhaps due to arene coordination during the reaction. In a more rough sense, the amido group acts as a nucleophile and the aryl group as the electrophile.

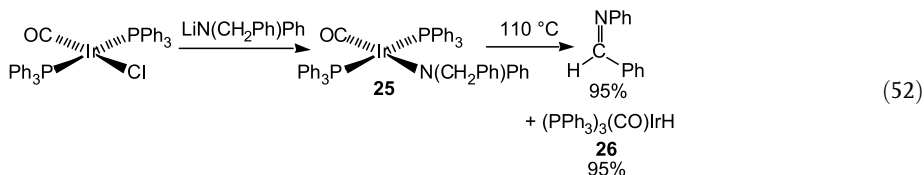
Although it focused on the reductive elimination of ethers and not amines, a recent study revealed the importance of steric hindrance in accelerating the reductive elimination process. Until recently, reductive elimination of acyclic aryl ethers had only been achieved from palladium complexes containing highly electron-poor palladium-bound aryl groups [65]. The lower nucleophilicity of alkoxides and aryl oxides, relative to amides, makes the elimination process sufficiently slow that reactions occur only with palladium complexes bearing strongly electrophilic aryl groups. However, the use of ligands with demanding steric properties was found to accelerate this reaction to the point that reductive elimination was observed from complexes containing electron-neutral aryl groups bound to palladium [282]. The dimeric phenoxide complex $\{\text{Pd}[\text{FcP}(\text{tBu})_2](\text{o-tolyl})(\text{OC}_6\text{H}_4\text{-4-OMe})\}_2$ gave diaryl ether at 70 °C in roughly 20 % yield. Addition of $\text{P}(\text{tBu})_3$ to this complex led to some phosphine exchange that ultimately provided the diaryl ether in close to quantitative yield. Thus, the strong electron-donating property of alkylphosphines is dominated by the steric demands, and this steric demand appears to have a large accelerating affect on the rate of reductive elimination.

4.7.4

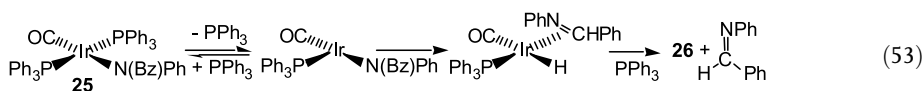
Competing β -Hydrogen Elimination from Amido Complexes

The amination chemistry depends on preventing irreversible β -hydrogen elimination from the amido complexes before reductive elimination of the amine. At the early stages of the development of the amination chemistry, it was remarkable that the unknown reductive elimination of arylamines could be faster than the presumed rapid [71, 72] β -hydrogen

elimination from late transition metal amides. In fact, directly observed β -hydrogen elimination from late transition metal amido complexes was rare ADDIN and there were no known examples of its irreversible occurrence from a simple monomeric amido species [283].



Recently, Hartwig prepared 16-electron, square-planar amido complexes that undergo irreversible β -hydrogen elimination [102]. This observation allowed the beginning of a mechanistic understanding of this process and highlighted the unfounded assumption that this β -hydrogen elimination process is typically rapid. The *N*-benzyl anilide **25** in Eq. (52) produced the stable imine and iridium hydride **26** in nearly quantitative yields. β -Hydrogen elimination from **25** required temperatures of 100 °C or above, while elimination from an alkyl-amide required 70 °C. In contrast, Schwartz showed that the analogous alkyl complexes underwent β -hydrogen elimination below room temperature [284, 285].



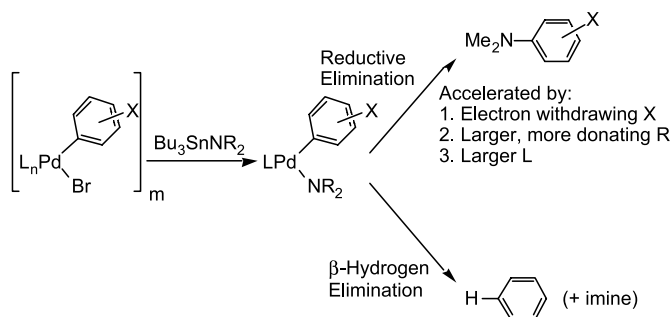
The intermediate that underwent C–H bond cleavage was a 14-electron, three-coordinate complex that formed by reversible phosphine dissociation (Eq. (53)). Importantly, there was no detectable competing β -hydrogen elimination from a 16-electron, four-coordinate complex. The mechanism for β -hydrogen elimination from a 14-electron intermediate parallels that for β -hydrogen elimination from square-planar alkyl complexes [286, 287]. β -Hydrogen elimination from analogous alkoxides has been studied by Zhao, Hesslink, and Hartwig [288]. β -Hydrogen elimination from the alkoxide complexes occurs at similar rates to that from the amides. Detailed mechanistic studies have shown that alkoxide β -hydrogen elimination is reversible and that the irreversible step is the displacement of the resulting aldehyde or ketone from the metal center by free phosphine.

4.7.5

Selectivity: Reductive Elimination vs. β -Hydrogen Elimination

Two studies have been conducted that outline the effects of the steric and electronic properties of the ligand on the relative rates for reductive elimination of amine and β -hydrogen elimination from amides. One study focused on the amination chemistry catalyzed by $\text{P}(o\text{-C}_6\text{H}_4\text{Me})_3$ palladium complexes [135], while the second focused on the chemistry catalyzed by complexes containing chelating ligands [106].

Studies of aryl halide amination with secondary aminostannanes and palladium catalysts bearing $\text{P}(o\text{-C}_6\text{H}_4\text{Me})_3$ ligands are summarized in Scheme 7. These studies revealed four



Scheme 7. Factors controlling selectivity for amination vs. hydrodehalogenation of aryl halides.

factors that control the amount of product formed from aryl halide hydrodehalogenation *vs.* the amount formed by amination. First, aryl halides bearing electron-withdrawing groups on the aryl ring gave more amination product and less hydrodehalogenation product than did those bearing electron-donating groups. This result is consistent with the faster reductive elimination of amines from complexes with electron-poor aromatic groups discussed above. Second, reactions of *N*-alkyl arylamides gave more hydrodehalogenation product than did those of dialkylamides, consistent with reductive elimination from complexes of arylamides being slower than that from complexes of dialkylamides. Third, deuterium-labeling experiments showed that the majority of the dehalogenation product after catalyst initiation came from β -hydrogen elimination from the amido group.

The final point concerns the steric effects of the phosphine aryl groups on the relative amounts of arene and arylamine products. Careful monitoring of the products formed from both stoichiometric and catalytic reactions of palladium complexes containing $\text{P}(o\text{-C}_6\text{H}_4\text{Me})_3$, $\text{P}(o\text{-C}_6\text{H}_4\text{Me})_2\text{Ph}$, $\text{P}(o\text{-C}_6\text{H}_4\text{Me})\text{Ph}_2$, and PPh_3 showed steadily decreasing ratios of amine to arene as the size of the ligand was decreased. Thus, larger phosphine ligands enhance the rate of reductive elimination of amines relative to the rate of β -hydrogen elimination. Reductive amine elimination decreases the coordination number of the metal, whereas β -hydrogen elimination from an amide either increases the coordination number of the metal because of the formation of a coordinated imine along with the hydride, or leaves it unchanged if imine is extruded without coordination. Large groups on the phosphine ligand enhance the rates of reactions that decrease the coordination number, and will, therefore, increase the rate of reductive elimination [289] of amines relative to the rate of β -hydrogen elimination. This study foreshadowed the ability of even larger *tert*-butylphosphine ligands to drive the amido intermediate toward reductive elimination to form the arylamine instead of undergoing β -hydrogen elimination, even when sterically undemanding primary amines are used as substrates [164, 290].

Results obtained with chelating ligands displaying varied steric properties contrasted those obtained with monodentate ligands [106]. Large, chelating phosphine ligands such as bis-1,1'-(di-*o*-tolylphosphino)ferrocene gave more hydrodehalogenation product than did DPPF. Reactions catalyzed by complexes of electron-poor DPPF derivatives, which should generate a more electron-poor metal and favor reductive elimination of amine, gave more arene than did those catalyzed by complexes of electron-rich DPPF derivatives. Further, ligands with large bite angles gave more arene than those with small bite angles, in contrast to what

would be expected from previous studies that showed an increase in the rate of C–C bond-forming reductive elimination with increasing bite angle [291]. Surprisingly, the arene product produced by these substrates contained no deuterium when formed from reactions catalyzed by complexes of many chelating phosphines. The source of hydrogen remains unclear, but these results demonstrated that much of the arene generated in reactions conducted with DPPF or BINAP as ligand does not form by a simple β -hydrogen elimination and C–H bond-forming reductive elimination sequence.

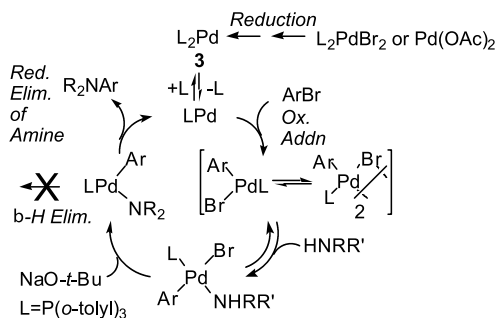
4.7.6

Overall Catalytic Cycle with Specific Intermediates

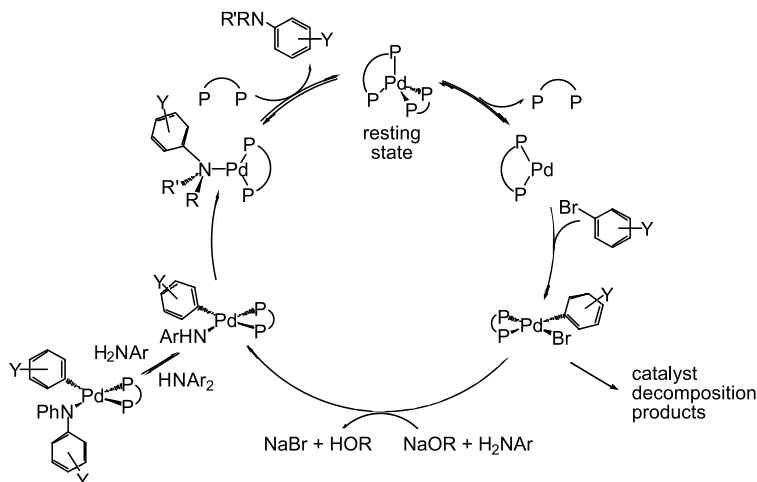
At this time, one can combine the results on reductive elimination and oxidative addition to construct a mechanism for the amination chemistry catalyzed by palladium complexes containing several types of both monodentate and chelating ligands. These catalytic cycles differ in the coordination number and charge of the palladium complexes that lie on the catalytic cycle, the factors that control amination *vs.* aryl halide reduction, and the role of base in inducing rapid oxidative addition. It has been shown that the catalytic cycle for the amination of aryl halides catalyzed by $P(o\text{-C}_6\text{H}_4\text{Me})_3$ involves exclusively intermediates with a single phosphine ligand. In contrast, the chemistry catalyzed by DPPF or BINAP palladium complexes involves bis(phosphine) complexes as a result of ligand chelation

4.7.6.1 Mechanism for Amination Catalyzed by $P(o\text{-C}_6\text{H}_4\text{Me})_3$ Palladium Complexes

Scheme 8 shows an experimentally supported mechanism for amination catalyzed by $P(o\text{-C}_6\text{H}_4\text{Me})_3$ phosphine complexes. The Pd^0 complex is a 14-electron, two-coordinate species, from which one of the phosphine ligands dissociates before aryl halide oxidative addition. The aryl halide complexes react with an amine to generate amine-ligated aryl halide complexes either by reaction with the monomer or by an associative reaction with dimeric **4**. Reactions of these amine complexes with base generate three-coordinate amido species, which undergo rapid reductive elimination. In the case of reactions catalyzed by complexes containing monodentate ligands, large phosphines accelerate the overall rate by favoring monophosphine complexes and provide good selectivity by accelerating reductive elimination relative to β -hydrogen elimination.



Scheme 8. Overall mechanism for aryl halide amination catalyzed by $P(o\text{-C}_6\text{H}_4\text{Me})_3$ -ligated palladium complexes.



Scheme 9. Overall mechanism for aryl halide amination catalyzed by bis(phosphine)-ligated palladium complexes.

4.7.6.2 Mechanism for Amination Catalyzed by Palladium Complexes with Chelating Ligands

Scheme 9 shows a mechanism for the amination of aryl halides catalyzed by DPPF- or BINAP-ligated palladium complexes, and a similar mechanism is presumably followed by reactions catalyzed by structurally related bis(phosphine) complexes. As discussed in the section on oxidative addition of aryl halides, the monochelate Pd(0) complex is formed by dissociation of BINAP or DPPF, and these 14-electron intermediates add aryl halide. The monochelate complex containing DPPF as the ligand undergoes recoordination of phosphine faster than oxidative addition of aryl halide, while the monochelate complex containing BINAP adds aryl bromide faster than it recoordinates ligand when an excess of aryl bromide is present. The amido complex is generated by either deprotonation of coordinated amine or by reaction of amine with an intermediate alkoxide complex [65]. When aryl sulfonates are used as substrates, a third pathway for amide generation is possible. The triflate ligand can be displaced by amine to generate a cationic amine complex. The coordinated amine in this species would then be deprotonated by even weak phosphate or carbonate base.

The resulting amido aryl complexes undergo reductive elimination directly from the 16-electron, four-coordinate complex, rather than from the three-coordinate, 14-electron, monophosphine complex generated when catalysts bearing sterically hindered monophosphines are used. For reactions involving chelating phosphines, the selectivity for reductive elimination, rather than β -hydrogen elimination, results from chelation, which blocks phosphine dissociation and accompanying pathways for β -hydrogen elimination from 14-electron, three-coordinate species. Many mechanistic questions remain poorly understood at this point, but these results provide a general, experimentally supported pathway for reactions catalyzed by complexes with monodentate and chelating phosphines.

As described in the section on catalyst development, Xantphos is an effective ligand for certain aryl halide aminations. This ligand has a particularly large bite angle and a central

oxygen that can coordinate to the metal center. Van Leeuwen et al. have recently studied the mechanism of the reaction catalyzed by palladium Xantphos complexes [292]. Several interesting results were found. First, aryl triflate complexes with this ligand are cationic and the central oxygen of the ligand is coordinated to the metal. Second, the reaction of the aryl halide or triflate complexes with amine and base to generate the amido complex is rate-limiting. Oxidative addition is faster than generation of the amido intermediate. These authors deduced that the cationic arylpalladium complexes react by coordination of amine and subsequent deprotonation by the alkoxide base. For reactions proceeding through the neutral arylpalladium bromide complexes with this type of ligand, the mechanism is more complex. Reaction of alkoxide appears to be rate-limiting, and this rate behavior can be attributed to slow reaction of a palladium alkoxide complex with amine to generate the amido species. An accelerating effect of bromide is observed for this system at low bromide concentrations, and this effect has been attributed to activation of the alkoxide base by the generation of a less tightly bound ion pair. Alternatively, these authors suggested that higher ionic strength might favor reaction of the arylpalladium halide complex with the alkoxide. At high bromide concentrations, this accelerating effect was attenuated.

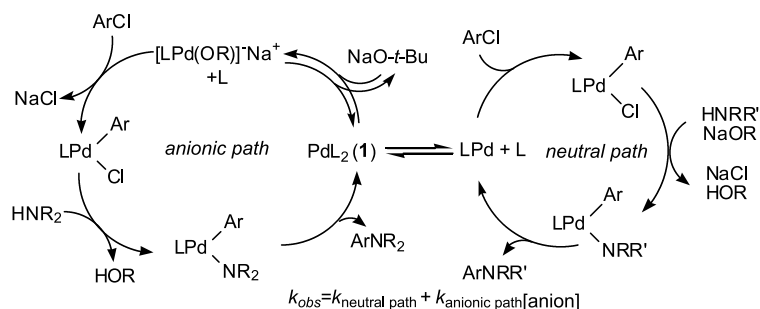
4.7.6.3 Mechanism of Amination Catalyzed by Palladium Complexes with Sterically Hindered Alkyl Monophosphines

Most recently, Alcazar-Roman and Hartwig have evaluated the amination of aryl chlorides catalyzed by palladium complexes with $P(tBu)_3$ as the ligand [293]. In particular, they were interested in evaluating why couplings of aryl chlorides in the presence of different bases occurred at different rates when oxidative addition is generally believed to be turnover-limiting. Their results suggested that the base is intimately involved in the oxidative addition step, most likely by direct coordination of the metal to generate an anionic $Pd(0)$ species. Rate equations were consistent with reaction in the presence of $NaOtBu$ occurring by two mechanisms, one being zero-order- and the other first-order in base.

Amatore and Jutand have shown that reactions of aryl bromides and iodides are accelerated by added halide, and have observed direct coordination of the halide to form an anionic $Pd(0)$ species that undergoes oxidative addition [294, 295]. Thus, the one mechanism that is consistent with the observed first-order behavior in alkoxide and that is consistent with Amatore and Jutand's studies involves initial displacement of phosphine by *tert*-butoxide to form an anionic $Pd(0)$ species $\{Pd[P(tBu)_3](OtBu)\}^-$. Oxidative addition of the aryl chloride would then occur to this anionic species. These concurrent mechanisms are shown in Scheme 10.

4.8 Summary

The amination of aryl halides and triflates catalyzed by palladium complexes is suitable for use in complex synthetic problems. Many amines couple with a variety of aryl halides and sulfonates to produce high yields of mixed arylamines with at least one of the existing catalyst systems. Nevertheless, there are many combinations of substrates for which the amination chemistry may be substantially improved. For the most part, these reactions involve nitrogen centers, such as those in pyrroles, indoles, amides, pyrazoles, and other heterocyclic groups that are less basic than those in standard alkylamines. Although mild reaction con-



Scheme 10. Two concurrent mechanisms for the amination of aryl chlorides catalyzed by $P(tBu)_3$ complexes of palladium.

ditions have been developed for many substrates, the harsh conditions used in many of the applications indicate that continued studies on developing milder conditions are warranted. Further, turnover numbers must be improved for the use of this reaction in many industrial applications. In particular, high turnover numbers for reactions conducted with less expensive and weaker bases need to be developed. Finally, mechanistic information is emerging with some of the second-generation catalysts, but data on the most recent catalysts is sparse. Data on reactions of substrates more complicated than simple amines and aryl halides is not presently available.

Acknowledgements

Portions of my groups' contributions to this work have been supported by the NIH (R29-GM55382 and RO1-GM55382) and DOE. We also gratefully acknowledge support from a DuPont Young Professor Award, a Union Carbide Innovative Recognition Award, a National Science Foundation Young Investigator Award, a Dreyfus Foundation New Faculty Award, and a Camille Dreyfus Teacher-Scholar Award for support of this work at its early stages. The author is a fellow of the Alfred P. Sloan Foundation. We also thank Johnson-Matthey Alpha/Aesar for donations of palladium chloride. Finally, I am deeply indebted to the graduate students, postdoctoral associates, and undergraduates in my laboratory, whose names appear in the references and whose experimental and intellectual input led to our contributions.

References

- 1 R. A. GLENNON, *J. Med. Chem.* **1987**, *30*, 1–12.
- 2 H. HUGEL, D. J. KENNAWAY, *Org. Prep. Proc. Int.* **1995**, *27*, 1–31.
- 3 A. KITANI, M. KAYA, J. YANO, K. YOSHIKAWA, K. SASAKI, *Synth. Metals* **1987**, *18*, 341.
- 4 F.-L. LU, F. WUDL, M. NOWAK, A. J. HEEGER, *J. Am. Chem. Soc.* **1986**, *108*, 8311–8313.
- 5 A. G. MACDIARMID, J. C. CHIANG, A. F. RICHTER, A. J. EPSTEIN, *Synth. Metals* **1987**, *18*, 285–290.
- 6 A. G. MACDIARMID, A. J. EPSTEIN, *Faraday Discuss. Chem. Soc.* **1989**, *88*, 317–332.
- 7 A. G. MACDIARMID, A. J. EPSTEIN, in *Science and Applications of Conducting Polymers* (Eds.: W. R. SALANECK, D. T. CLARK, E. J. SAMUELSEN), Adam Hilger, New York, 1991, pp 117.

- 8 A. RAY, A. F. RICHTER, D. L. KERSHNER, A. J. EPSTEIN, *Synth. Metals* **1989**, 29, E141–E150.
- 9 D. VACHON, R. O. ANGUS, F. L. LU, M. NOWAK, Z. X. LIU, H. SCHAFER, F. WUDL, A. J. HEEGER, *Synth. Metals* **1987**, 18, 297–302.
- 10 M. STOLKA, J. F. YANUS, D. M. PAI, *J. Phys. Chem.* **1984**, 88, 4707–4714.
- 11 E. UETA, H. NAKANO, Y. SHIROTA, *Chem. Lett.* **1994**, 2397.
- 12 Y. KUWABARA, H. OGAWA, H. INADA, N. NOMA, Y. SHIROTA, *Adv. Mater.* **1994**, 6, 677–679.
- 13 M. STRUKELJ, R. H. JORDAN, A. DODABALAPUR, *J. Am. Chem. Soc.* **1996**, 118, 1213.
- 14 J. MARCH, *Advanced Organic Chemistry*; 3rd ed.; John Wiley and Sons, New York, 1985.
- 15 G. W. GRIBBLE, P. D. LORD, J. SKOTNICKI, S. E. DIETZ, J. T. EATON, J. L. JOHNSON, *J. Am. Chem. Soc.* **1974**, 96, 7812–7814.
- 16 P. MARCHINI, G. LISO, A. REHO, *J. Org. Chem.* **1975**, 40, 3453–3456.
- 17 C. F. LANE, *Synthesis* **1975**, 135–146.
- 18 H. HEANEY, *Chem. Rev.* **1962**, 62, 81–97.
- 19 M. BELLER, C. BREINDL, T. H. RIERMEIER, A. TILLACK, *J. Org. Chem.* **2001**, 66, 1403–1412.
- 20 R. ROSSI, R. H. DE ROSSI, *Aromatic Substitution by the $S_{RN}1$ Mechanism*; American Chemical Society, Washington DC, 1983; Vol. 178.
- 21 J. E. SHAW, D. C. KUNERTH, S. B. SWANSON, *J. Org. Chem.* **1976**, 41, 732–733.
- 22 A. J. PEARSON, J. G. PARK, S. H. YANG, Y.-H. CHUANG, *J. Chem. Soc., Chem. Commun.* **1989**, 1363–1364.
- 23 J. P. COLLMAN, L. S. HEGEDUS, J. R. NORTON, R. G. FINKE, *Principles and Applications of Organotransition Metal Chemistry*, University Science Books, Mill Valley, CA, 1987.
- 24 A. KLAPARS, J. C. ANTILLA, X. HUANG, S. L. BUCHWALD, *J. Am. Chem. Soc.* **2001**, 123, 7727–7729.
- 25 R. GUJADHUR, D. VENKATARAMAN, J. T. KINTIGH, *Tetrahedron Lett.* **2001**, 42, 4791–4793.
- 26 J. LINDLEY, *Tetrahedron* **1984**, 40, 1433–1456.
- 27 H. L. AALTEN, G. VAN KOTEN, D. M. GROVE, *Tetrahedron* **1989**, 45, 5565–5578.
- 28 A. J. PAINE, *J. Am. Chem. Soc.* **1987**, 109, 1496–1502.
- 29 H. WEINGARTEN, *J. Org. Chem.* **1964**, 29, 977–978.
- 30 D. M. T. CHAN, K. L. MONACO, R.-P. WANG, M. P. WINTERS, *Tetrahedron Lett.* **1998**, 39, 2933–2936.
- 31 P. Y. S. LAM, S. DEUDON, E. HAUPTMAN, C. G. CLARK, *Tetrahedron Lett.* **2001**, 42, 2427–2429.
- 32 P. Y. S. LAM, G. VINCENT, C. G. CLARK, S. DEUDON, P. K. JADHAV, *Tetrahedron Lett.* **2001**, 42, 3415–3418.
- 33 S. K. KANG, S. H. LEE, D. LEE, *Synlett* **2000**, 1022–1024.
- 34 D. J. CUNDY, S. A. FORSYTH, *Tetrahedron Lett.* **1998**, 39, 7979–7982.
- 35 A. P. COMBS, M. RAFALSKI, *J. Comb. Chem.* **2000**, 2, 29–32.
- 36 A. P. COMBS, S. SAUBERN, M. RAFALSKI, P. Y. S. LAM, *Tetrahedron Lett.* **1999**, 40, 1623–1626.
- 37 P. S. LAM, S. DEUDON, K. M. AVERILL, R. LI, M. Y. HE, P. DESHONG, C. G. CLARK, *J. Am. Chem. Soc.* **2000**, 122, 7600–7601.
- 38 W. W. K. R. MEDERSKI, M. LEFORT, M. GERMANN, D. KUX, *Tetrahedron* **1999**, 55, 12757–12770.
- 39 J. P. COLLMAN, M. ZHONG, *Org. Lett.* **2000**, 1233–1236.
- 40 J. K. STILLE, *Angew. Chem. Int. Ed. Engl.* **1986**, 25, 508–524.
- 41 J. K. STILLE, *Pure Appl. Chem.* **1985**, 57, 1771–1780.
- 42 A. SUZUKI, *Pure Appl. Chem.* **1994**, 66, 213–222.
- 43 N. MIYAUURA, A. SUZUKI, *Chem. Rev.* **1995**, 95, 2457–2483.
- 44 E. NEGISHI, *Acc. Chem. Res.* **1982**, 15, 340–348.
- 45 T. HAYASHI, Y. HAGIHARA, Y. KATSURO, M. KUMADA, *Bull. Chem. Soc. Jpn.* **1983**, 56, 363–364.
- 46 T. N. MITCHELL, *Synthesis* **1992**, 803–815.
- 47 U. SCHOPFER, A. SCHLAPBACH, *Tetrahedron* **2001**, 57, 3069–3073.
- 48 N. ZHENG, J. C. MCWILLIAMS, F. J. FLEITZ, J. D. ARMSTRONG, R. P. VOLANTE, *J. Org. Chem.* **1998**, 63, 9606–9607.
- 49 R. ROSSI, F. BELLINA, L. MANNINA, *Tetrahedron* **1997**, 53, 1025–1044.
- 50 T. ISHIYAMA, M. MORI, A. SUZUKI, N. MIYAUURA, *J. Organomet. Chem.* **1996**, 525, 225–231.

- 51 D. BARAÑANO, G. MANN, J. F. HARTWIG, *Curr. Org. Chem.* **1997**, *1*, 287–325.
- 52 D. CAI, J. F. PAYACK, D. R. BENDER, D. L. HUGHES, T. R. VERHOEVEN, P. J. REIDER, *J. Org. Chem.* **1994**, *59*, 7180.
- 53 Y. UOZUMI, N. SUZUKI, A. OGIWARA, T. HAYASHI, *Tetrahedron* **1994**, *50*, 4293–4302.
- 54 D. BARAÑANO, J. F. HARTWIG, *J. Am. Chem. Soc.* **1995**, *117*, 2937–2938.
- 55 J. P. COLLMAN, L. S. HEGEDUS, J. R. NORTON, R. G. FINKE, in *Principles and Applications of Organotransition Metal Chemistry*, 2nd ed., University Science Books, Mill Valley, 1987, pp 279–354.
- 56 R. H. CRABTREE, *Chem. Rev.* **1995**, *95*, 987–1007.
- 57 S.-Y. LIOU, M. GOZIN, D. MILSTEIN, *J. Am. Chem. Soc.* **1995**, *117*, 9774–9775 and references therein.
- 58 S. Y. LIOU, M. GOZIN, D. MILSTEIN, *J. Chem. Soc., Chem. Commun.* **1995**, 1965–1966.
- 59 J. J. GARCIA, W. D. JONES, *Organometallics* **2000**, *19*, 5544–5545.
- 60 B. L. EDELBACH, R. J. LACHICOTTE, W. D. JONES, *Organometallics* **1999**, *18*, 4660–4668.
- 61 B. L. EDELBACH, R. J. LACHICOTTE, W. D. JONES, *Organometallics* **1999**, *18*, 4040–4049.
- 62 B. L. EDELBACH, D. A. VICIC, R. J. LACHICOTTE, W. D. JONES, *Organometallics* **1998**, *17*, 4784–4794.
- 63 M. S. DRIVER, J. F. HARTWIG, *J. Am. Chem. Soc.* **1995**, *117*, 4708–4709.
- 64 M. S. DRIVER, J. F. HARTWIG, *J. Am. Chem. Soc.* **1996**, *118*, 7217–7218.
- 65 G. MANN, J. F. HARTWIG, *J. Am. Chem. Soc.* **1996**, *118*, 13109–13110.
- 66 L. A. VILLANUEVA, K. A. ABOUD, J. M. BONCELLA, *Organometallics* **1994**, *13*, 3921–3931.
- 67 K. KOO, G. L. HILLHOUSE, *Organometallics* **1995**, *14*, 4421–4423.
- 68 P. T. MATSUNAGA, J. C. MAVROPOULOS, G. L. HILLHOUSE, *Polyhedron* **1995**, *14*, 175–185.
- 69 E. G. BRYAN, B. F. G. JOHNSON, J. LEWIS, *J. Chem. Soc., Dalton Trans.* **1977**, 1328–1330.
- 70 M. S. DRIVER, J. F. HARTWIG, *J. Am. Chem. Soc.* **1996**, *118*, 4206–4207.
- 71 M. D. FRYZUK, C. D. MONTGOMERY, *Coord. Chem. Rev.* **1989**, *95*, 1–40.
- 72 H. BRYNDZA, W. TAM, *Chem. Rev.* **1988**, *88*, 1163–1188.
- 73 L. M. ALCAZAR-ROMAN, J. F. HARTWIG, **2001**, unpublished results.
- 74 P. M. HENRY, *Palladium-Catalyzed Oxidation of Hydrocarbons*, D. Reidel Publ. Co., Boston, 1980, Vol. 2.
- 75 B. CORNILS, W. A. HERRMANN (Eds.), *Applied Homogeneous Catalysis with Organometallic Compounds: A Comprehensive Handbook in Two Volumes*, VCH, New York, 1996.
- 76 M. KAWATSURA, J. F. HARTWIG, *J. Am. Chem. Soc.* **2000**, *122*, 9546–9547.
- 77 M. R. GAGNÉ, T. J. MARKS, *J. Am. Chem. Soc.* **1989**, *111*, 4108–4109.
- 78 M. R. GAGNÉ, S. P. NOLAN, T. J. MARKS, *Organometallics* **1990**, *9*, 1716–1718.
- 79 V. M. ARREDONDO, S. TIAN, F. E. McDONALD, T. J. MARKS, *J. Am. Chem. Soc.* **1999**, *121*, 3633–3639.
- 80 A. L. CASALNUOVO, J. C. CALABRESE, D. MILSTEIN, *J. Am. Chem. Soc.* **1988**, *110*, 6738–6744.
- 81 R. DORTA, P. EGLI, F. ZURCHER, A. TOGNI, *J. Am. Chem. Soc.* **1997**, *119*, 10857–10858.
- 82 J. P. WOLFE, S. L. BUCHWALD, *J. Am. Chem. Soc.* **1997**, *119*, 6054–6058.
- 83 E. BRENNER, Y. FORT, *Tetrahedron Lett.* **1998**, *39*, 5359–5362.
- 84 E. BRENNER, R. SCHNEIDER, Y. FORT, *Tetrahedron Lett.* **2000**, *41*, 2881–2884.
- 85 C. DESMARETS, R. SCHNEIDER, Y. FORT, *Tetrahedron Lett.* **2000**, *41*, 2875–2879.
- 86 M. KOSUGI, M. KAMEYAMA, T. MIGITA, *Chem. Lett.* **1983**, 927–928.
- 87 M. KOSUGI, M. KAMEYAMA, H. SANO, T. MIGITA, *Nippon Kagaku Kaishi* **1985**, *3*, 547–551.
- 88 D. L. BOGER, J. S. PANEK, *Tetrahedron Lett.* **1984**, *25*, 3175–3178.
- 89 D. L. BOGER, S. R. DUFF, J. S. PANEK, M. YASUDA, *J. Org. Chem.* **1985**, *50*, 5782–5789.
- 90 D. L. BOGER, S. R. DUFF, J. S. PANEK, M. YASUDA, *J. Org. Chem.* **1985**, *50*, 5790–5795.
- 91 F. PAUL, J. PATT, J. F. HARTWIG, *J. Am. Chem. Soc.* **1994**, *116*, 5969–5970.
- 92 A. S. GURAM, S. L. BUCHWALD, *J. Am. Chem. Soc.* **1994**, *116*, 7901–7902.
- 93 M. KOSUGI, T. OGATA, M. TERADA, H. SANO, T. MIGITA, *Bull. Chem. Soc. Jpn.* **1985**, *58*, 3657–3658.

- 94 A. CARPITA, R. ROSSI, B. SCAMUZZI, *Tetrahedron Lett.* **1989**, 30, 2699–2702.
- 95 S. I. MURAHASHI, M. YAMAMURA, K. YANAGISAWA, N. MITA, K. KONDO, *J. Org. Chem.* **1979**, 44, 2408–2417.
- 96 T. MIGITA, T. SHIMIZU, Y. ASAMI, J. SHIOBARA, Y. KATO, M. KOSUGI, *Bull. Chem. Soc. Jpn.* **1980**, 53, 1385.
- 97 S. E. TUNNEY, J. K. STILLE, *J. Org. Chem.* **1987**, 52, 748–753.
- 98 J. LOUIE, J. F. HARTWIG, *Tetrahedron Lett.* **1995**, 36, 3609–3612.
- 99 A. S. GURAM, R. A. RENNELS, S. L. BUCHWALD, *Angew. Chem. Int. Ed. Engl.* **1995**, 34, 1348–1350.
- 100 J. P. WOLFE, R. A. RENNELS, S. L. BUCHWALD, *Tetrahedron* **1996**, 52, 7525–7546.
- 101 M. S. DRIVER, J. F. HARTWIG, *J. Am. Chem. Soc.* **1997**, 119, 8232–8245.
- 102 J. F. HARTWIG, *J. Am. Chem. Soc.* **1996**, 118, 7010–7011.
- 103 T. HAYASHI, M. KONOSHI, Y. KOBORI, M. KUMADA, T. HIGUCHI, K. HIROTSU, *J. Am. Chem. Soc.* **1984**, 106, 158–163.
- 104 J. P. WOLFE, S. WAGAW, S. L. BUCHWALD, *J. Am. Chem. Soc.* **1996**, 118, 7215–7216.
- 105 J. P. WOLFE, S. L. BUCHWALD, *Tetrahedron Lett.* **1997**, 38, 6359–6362.
- 106 B. C. HAMANN, J. F. HARTWIG, *J. Am. Chem. Soc.* **1997**, 119, 12382–12383.
- 107 B. C. HAMANN, J. F. HARTWIG, *J. Am. Chem. Soc.* **1998**, 120, 3694–3703.
- 108 J. P. WOLFE, S. L. BUCHWALD, *J. Org. Chem.* **2000**, 65, 1144–1157.
- 109 S. WAGAW, R. A. RENNELS, S. L. BUCHWALD, *J. Am. Chem. Soc.* **1997**, 119, 8451–8458.
- 110 K. ROSSEN, P. J. PYE, A. MALIAKAL, R. P. VOLANTE, *J. Org. Chem.* **1997**, 62, 6462–6463.
- 111 J. P. SADIGHI, M. C. HARRIS, S. L. BUCHWALD, *Tetrahedron Lett.* **1998**, 39, 5327–5330.
- 112 J.-F. MARCOUX, S. WAGAW, S. L. BUCHWALD, *J. Org. Chem.* **1997**, 62, 1568–1569.
- 113 K. KAMIKAWA, S. SUGIMOTO, M. UEMURA, *J. Org. Chem.* **1998**, 63, 8407–8410.
- 114 G. WÜLLNER, H. JANSCH, S. KANNENBERG, F. SCHUBERT, G. BOCHE, *Chem. Commun.* **1998**, 1509–1510.
- 115 M. PRASHAD, B. HU, Y. LU, R. DRAPER, D. HAR, O. REPIC, T. J. BLACKLOCK, *J. Org. Chem.* **2000**, 65, 2612–2614.
- 116 K. TAKAGI, Y. SAKAKIBARA, *Chem. Lett.* **1989**, 1957–1958.
- 117 S. CACCHI, P. G. CIATTINI, E. MORERA, G. ORTAR, *Tetrahedron Lett.* **1986**, 27, 3931–3934.
- 118 J. LOUIE, M. S. DRIVER, B. C. HAMANN, J. F. HARTWIG, *J. Org. Chem.* **1997**, 62, 1268–1273.
- 119 J. P. WOLFE, S. L. BUCHWALD, *J. Org. Chem.* **1997**, 62, 1264–1267.
- 120 J. AHMAN, S. L. BUCHWALD, *Tetrahedron Lett.* **1997**, 38, 6363–6366.
- 121 Y. TORISAWA, T. NISHI, J. MINAMIKAWA, *Bioorg. Med. Chem. Lett.* **2000**, 10, 2489–2491.
- 122 F. PAUL, J. PATT, J. F. HARTWIG, *Organometallics* **1995**, 14, 3030–3039.
- 123 S. WAGAW, S. L. BUCHWALD, *J. Org. Chem.* **1996**, 61, 7240–7241.
- 124 J. B. ARTERBURN, K. V. RAO, R. RAMDAS, B. R. DIBLE, *Org. Lett.* **2001**, 3, 1351–1354.
- 125 D. R. COULSON, *Inorg. Synth.* **1990**, 28, 107–109.
- 126 M. WATANABE, T. YAMAMOTO, M. NISHIYAMA, *Chem. Commun.* **2000**, 133–134.
- 127 Y. D. WARD, V. FARINA, *Tetrahedron Lett.* **1996**, 37, 6993–6996.
- 128 C. A. WILLOUGHBY, K. T. CHAPMAN, *Tetrahedron Lett.* **1996**, 37, 7181–7184.
- 129 P. H. H. HERMKENS, H. C. J. OTTENHEIJM, D. REES, *Tetrahedron* **1997**, 52, 4527–4554.
- 130 B. WITULSKI, S. SENFT, A. THUM, *Synlett* **1998**, 504–505.
- 131 I. P. BELETSKAYA, D. V. DAVYDOV, M. MORENOMANAS, *Tetrahedron Lett.* **1998**, 39, 5621–5622.
- 132 I. BELETSKAYA, A. BESSMERTNYKH, R. GUILARD, *Synlett* **1999**, 9, 1459–1461.
- 133 M. PALUCKI, J. P. WOLFE, S. L. BUCHWALD, *J. Am. Chem. Soc.* **1997**, 119, 3395–3396.
- 134 S. HAYDEN, J. R. J. SOWA, *Proc. Catal. Org. React.* **1998**, 627–632.
- 135 J. F. HARTWIG, S. RICHARDS, D. BARAÑANO, F. PAUL, *J. Am. Chem. Soc.* **1996**, 118, 3626–3633.
- 136 M. NISHIYAMA, T. YAMAMOTO, Y. KOIE, *Tetrahedron Lett.* **1998**, 39, 617–620.
- 137 T. YAMAMOTO, M. NISHIYAMA, Y. KOIE, *Tetrahedron Lett.* **1998**, 39, 2367–2370.
- 138 I. R. BUTLER, W. R. CULLEN, T. J. KIM, S. J. RETTIG, J. TROTTER, *Organometallics* **1985**, 4, 972–980.

- 139 W. R. CULLEN, T. J. KIM, F. W. B. EINHSTEIN, T. JONES, *Organometallics* **1983**, *2*, 714–719.
- 140 H. BLASER, F. SPINDLER, *Chimia* **1997**, *51*, 297–299.
- 141 A. TOGNI, C. BREUTEL, M. C. SOARES, N. ZANETTI, T. GERFIN, V. GRAMLICH, F. SPINDLER, G. RIHS, *Inorg. Chim. Acta* **1994**, *222*, 213–224.
- 142 A. TOGNI, C. BREUTEL, A. SCHNYDER, F. SPINDLER, H. LANDERT, A. TIJANI, *J. Am. Chem. Soc.* **1994**, *116*, 4062–4066.
- 143 M. BELLER, T. H. REIRMEIER, C. REISINGER, W. A. HERRMAN, *Tetrahedron Lett.* **1997**, *38*, 2073–2074.
- 144 S. SAITO, M. SAKAI, N. MIYaura, *Tetrahedron Lett.* **1996**, *37*, 2993–2996.
- 145 A. F. INDOLESE, *Tetrahedron Lett.* **1997**, *38*, 3513–3516.
- 146 S. SAITO, S. OH-TANI, N. MIYaura, *J. Org. Chem.* **1997**, *62*, 8024–8030.
- 147 J. MILLER, R. FARRELL, *Tetrahedron Lett.* **1998**, 6441–6444.
- 148 J.-C. GALLAND, M. SAVIGNAC, J.-P. GENËT, *Tetrahedron Lett.* **1999**, *40*, 2323–2326.
- 149 B. H. LIPSHUTZ, P. A. BLOMGREN, *J. Am. Chem. Soc.* **1999**, *121*, 5819–5820.
- 150 B. C. HAMANN, J. F. HARTWIG, *J. Am. Chem. Soc.* **1998**, *120*, 7369–7370.
- 151 D. BADONE, R. CECCHI, U. GUZZI, *J. Org. Chem.* **1992**, *57*, 6321–6323.
- 152 Y. KUBOTA, S. NAKADA, Y. SUGI, *Synlett* **1998**, 183–185.
- 153 T. HAYASHI, T. MISE, M. FUKISHIMA, M. KAGOTANI, N. NAGASHIMA, Y. HAMADA, A. MATSUMOTO, S. KAWAKAMI, M. KONOSHI, K. YAMAMOTO, M. KUMADA, *Bull. Chem. Soc. Jpn.* **1980**, *53*, 1138–1151.
- 154 T. HAYASHI, M. KONOSHI, M. FUKUSHIMA, T. MISE, M. KAGOTANI, M. TAJIKA, M. KUMADA, *J. Am. Chem. Soc.* **1982**, *104*, 180–186.
- 155 S. VYSKOCIL, M. SMRCINA, P. KOCOVSKY, *Tetrahedron Lett.* **1998**, *39*, 9289–9292.
- 156 D. W. OLD, J. P. WOLFE, S. L. BUCHWALD, *J. Am. Chem. Soc.* **1998**, *120*, 9722–9723.
- 157 J. P. WOLFE, S. WAGAW, J.-F. MARCOUX, S. L. BUCHWALD, *Acc. Chem. Res.* **1998**, *31*, 805–818.
- 158 J. P. WOLFE, H. TOMORI, J. P. SADIGHI, J. J. YIN, S. L. BUCHWALD, *J. Org. Chem.* **2000**, *65*, 1158–1174.
- 159 M. KRANENBURG, Y. E. M. VAN DER BURGT, P. C. J. KAMER, P. W. N. M. VAN LEEUWEN, K. GOUBITZ, J. FRAANJE, *Organometallics* **1995**, *14*, 3081–3089.
- 160 M. H. ALI, S. L. BUCHWALD, *J. Org. Chem.* **2001**, *66*, 2560–2565.
- 161 X. BEI, T. UNO, J. NORRIS, H. W. TURNER, W. H. WEINBERG, A. S. GURAM, *Organometallics* **1999**, *18*, 1840–1853.
- 162 X. BEI, A. S. GURAM, H. W. TURNER, W. H. WEINBERG, *Tetrahedron Lett.* **1999**, *40*, 1237–1240.
- 163 J. F. HARTWIG, M. KAWATSURA, S. I. HAUCK, K. H. SHAUGHNESSY, L. M. ALCAZAR-ROMAN, *J. Org. Chem.* **1999**, *64*, 5575–5580.
- 164 S. I. HAUCK, J. F. HARTWIG, unpublished results.
- 165 J. HUANG, G. GRASA, S. P. NOLAN, *Org. Lett.* **1999**, *1*, 1307–1309.
- 166 G. A. GRASA, M. S. VICIU, J. K. HUANG, S. P. NOLAN, *J. Org. Chem.* **2001**, *66*, 7729–7737.
- 167 S. STAUFFER, S. I. HAUCK, S. LEE, J. STAMBULI, J. F. HARTWIG, *Org. Lett.* **2000**, *2*, 1423–1426.
- 168 J. K. HUANG, H. J. SCHANZ, E. D. STEVENS, S. P. NOLAN, *Organometallics* **1999**, *18*, 2370–2375.
- 169 S. CADDICK, F. G. N. CLOKE, G. K. B. CLENTSMITH, P. B. HITCHCOCK, D. MCKERRACHER, L. R. TITCOMB, M. R. V. WILLIAMS, *J. Organomet. Chem.* **2001**, *617*–*618*, 635–639.
- 170 G. Y. LI, *Angew. Chem. Int. Ed.* **2001**, *40*, 1513–1516.
- 171 G. Y. LI, G. ZHENG, A. F. NOONAN, *J. Org. Chem.* **2001**, *66*, 8677–8681.
- 172 L. DJAKOVITCH, M. WAGNER, K. KOHLER, *J. Organomet. Chem.* **1999**, *592*, 225–234.
- 173 B. H. LIPSHUTZ, H. UEDA, *Angew. Chem. Int. Ed.* **2000**, *39*, 4492–4494.
- 174 B. H. YANG, S. L. BUCHWALD, *Org. Lett.* **1999**, *1*, 35–37.
- 175 W. SHAKESPEARE, *Tetrahedron Lett.* **1999**, *40*, 2035–2038.
- 176 J. YIN, S. L. BUCHWALD, *Org. Lett.* **2000**, *2*, 1101–1104.
- 177 S. D. EDMONDSON, A. MASTRACCHIO, E. R. PARMEE, *Org. Lett.* **2000**, *2*, 1109–1112.
- 178 S. JAIME-FIGUEROA, Y. LIU, J. M. MUCHOWSKI, D. G. PUTMAN, *Tetrahedron Lett.* **1998**, *39*, 1313–1316.
- 179 G. MANN, D. BARAÑANO, J. F. HARTWIG, A. L. RHEINGOLD, I. A. GUZEI, *J. Am. Chem. Soc.* **1998**, *120*, 9205–9219.

- 180 J. P. WOLFE, J. ÅHMAN, J. P. SADIGHI, R. A. SINGER, S. L. BUCHWALD, *Tetrahedron Lett.* **1997**, 38, 6367–6370.
- 181 C. BOLM, *Angew. Chem. Int. Ed. Engl.* **1993**, 32, 232–233.
- 182 C. BOLM, J. P. HILDEBRAND, *J. Org. Chem.* **2000**, 65, 169–175.
- 183 S. WAGAW, B. H. YANG, S. L. BUCHWALD, *J. Am. Chem. Soc.* **1998**, 120, 6621–6622.
- 184 J. F. HARTWIG, *Angew. Chem. Int. Ed.* **1998**, 37, 2090–2093.
- 185 S. WAGAW, B. YANG, S. L. BUCHWALD, *J. Am. Chem. Soc.* **1999**, 121, 10251–10263.
- 186 Z. WANG, R. T. SKERLJ, G. J. BRIDGER, *Tetrahedron Lett.* **1999**, 40, 3543–3546.
- 187 M. WATANABE, M. NISHIYAMA, T. YAMAMOTO, Y. KOIE, *Tetrahedron Lett.* **2000**, 41, 481–483.
- 188 D. W. OLD, M. C. HARRIS, S. L. BUCHWALD, *Org. Lett.* **2000**, 2, 1403–1406.
- 189 I. P. BELETSKAYA, D. V. DAVYDOV, M. MORENOMANAS, *Tetrahedron Lett.* **1998**, 39, 5617–5620.
- 190 K. HORI, M. MORI, *J. Am. Chem. Soc.* **1998**, 120, 7651–7652.
- 191 J. KOSMRLJ, B. U. W. MAES, G. L. F. LEMIERE, A. HAEMERS, *Synlett* **2000**, 1581–1584.
- 192 R. A. WIDENHOEFER, S. L. BUCHWALD, *Organometallics* **1996**, 15, 2755–2763.
- 193 A. ABOUABDELLAH, R. DODD, *Tetrahedron Lett.* **1998**, 39, 2119–2122.
- 194 F. KERRIGAN, C. MARTIN, G. H. THOMAS, *Tetrahedron Lett.* **1998**, 39, 2219–2222.
- 195 S. ZHAO, A. K. MILLER, J. BERGER, L. A. FLIPPIN, *Tetrahedron Lett.* **1996**, 37, 4463–4466.
- 196 S. MORITA, K. KITANO, J. MATSUBARA, T. OHTANI, Y. KAWANO, K. OTSUBO, M. UCHIDA, *Tetrahedron* **1998**, 54, 4811–4818.
- 197 G. J. TANOURY, C. H. SENANAYAKE, R. HETT, A. M. KUHN, D. W. KESSLER, S. A. WALD, *Tetrahedron Lett.* **1998**, 39, 6845–6848.
- 198 D. A. BRADLEY, A. G. GODFREY, C. R. SCHMID, *Tetrahedron Lett.* **1999**, 40, 5155–5159.
- 199 A. J. PEAT, S. L. BUCHWALD, *J. Am. Chem. Soc.* **1996**, 118, 1028–1030.
- 200 Y. P. HONG, G. J. TANOURY, H. S. WILKINSON, R. P. BAKALE, S. A. WALD, C. H. SENANAYAKE, *Tetrahedron Lett.* **1997**, 38, 5663–5666.
- 201 Y. P. HONG, C. H. SENANAYAKE, T. J. XIANG, C. P. VANDENBOSSCHE, G. J. TANOURY, R. P. BAKALE, S. A. WALD, *Tetrahedron Lett.* **1998**, 39, 3121–3124.
- 202 N. CHIDA, T. SUZUKI, S. TANAKA, I. YAMADA, *Tetrahedron Lett.* **1999**, 40, 2573–2576.
- 203 W. CUI, R. N. LOEPPKY, *Tetrahedron* **2001**, 57, 2953–2956.
- 204 J. CHENG, M. L. TRUDELL, *Org. Lett.* **2001**, 3, 1371–1374.
- 205 T. IWAKI, Y. AKITO, T. SAKAMOTO, *J. Chem. Soc., Perkin Trans. 1* **1999**, 1505–1510.
- 206 M. M. KHAN, H. ALI, J. E. VAN LIER, *Tetrahedron Lett.* **2001**, 42, 1615–1617.
- 207 M. L. LOPEZ-RODRIGUEZ, A. VISO, B. BENHAMU, J. L. ROMINGUERA, M. MURCIA, *Bioorg. Med. Chem. Lett.* **1999**, 9, 2339–2342.
- 208 M. L. LOPEZ-RODRIGUEZ, B. BENHAMU, D. AYALA, J. L. ROMINGUERA, M. MURCIA, J. A. RAMOS, A. VISO, *Tetrahedron* **2000**, 56, 3245–3253.
- 209 S. L. MACNEIL, M. GRAY, L. E. BRIGGS, J. J. LI, V. SNIIECKUS, *Synlett* **1998**, 419–421.
- 210 C. G. FROST, P. MENDONÇA, *Chem. Lett.* **1997**, 1159–1160.
- 211 E. A. HARWOOD, S. T. SIGURDSSON, N. B. F. EDFELDT, B. R. REID, P. B. HOPKINS, *J. Am. Chem. Soc.* **1999**, 121, 5081–5082.
- 212 M. K. LAKSHMAN, J. C. KEELER, J. H. HILMER, J. Q. MARTIN, *J. Am. Chem. Soc.* **1999**, 121, 6090–6091.
- 213 R. R. BONALA, I. G. SHISHKINA, F. JOHNSON, *Tetrahedron Lett.* **2000**, 41, 7281–7284.
- 214 F. DE RICCARDIS, R. BONALA, F. JOHNSON, *J. Am. Chem. Soc.* **1999**, 121, 10453–10460.
- 215 Z. W. WANG, C. J. RIZZO, *Org. Lett.* **2001**, 3, 565–568.
- 216 J. B. ARTERBURN, M. PANNALA, A. M. GONZALEZ, *Tetrahedron Lett.* **2001**, 42, 1475–1477.
- 217 O. J. PLANTE, S. L. BUCHWALD, P. H. SEEBERGER, *J. Am. Chem. Soc.* **2000**, 122, 7148–7149.
- 218 T. KANBARA, A. HONMA, K. HASEGAWA, *Chem. Lett.* **1996**, 1135–1136.
- 219 F. E. GOODSON, S. I. HAUCK, J. F. HARTWIG, *J. Am. Chem. Soc.* **1999**, 121, 7527–7539.
- 220 X. X. ZHANG, J. P. SADIGHI, T. W. MACKEWITZ, S. L. BUCHWALD, *J. Am. Chem. Soc.* **2000**, 122, 7606–7607.

- 221 T. I. WALLOW, B. M. NOVAK, *Polym. Prepr.* **1993**, 34, 1009.
- 222 T. KANBARA, T. IMAYASU, K. HASEGAWA, *Chem. Lett.* **1998**, 709–710.
- 223 T. KANBARA, M. OSHIMA, K. HASEGAWA, *J. Polym. Sci. Polym. Chem.* **1998**, 36, 2155–2160.
- 224 T. KANBARA, M. OSHIMA, T. IMAYASU, K. HASEGAWA, *Macromolecules* **1998**, 31, 8725–8730.
- 225 R. H. GRUBBS, W. TUMAS, *Science* **1989**, 243, 907.
- 226 P. SCHWAB, R. H. GRUBBS, J. W. ZILLER, *J. Am. Chem. Soc.* **1996**, 118, 100.
- 227 N. SPETSERIS, R. E. WARD, T. Y. MEYER, *Macromolecules* **1998**, 31, 3158–3161.
- 228 T. KANBARA, K. IZUMI, Y. NAKADANI, T. NARISE, K. HASEGAWA, *Chem. Lett.* **1997**, 1185–1186.
- 229 T. KANBARA, Y. NAKADANI, K. HASEGAWA, *Polym. J.* **1999**, 31, 206–209.
- 230 T. KANBARA, Y. MIYAZAKI, K. HASEGAWA, T. YAMAMOTO, *J. Polym. Sci. Polym. Chem.* **2000**, 38, 4194–4199.
- 231 T. BRAIG, D. C. MULLER, M. GROSS, K. MEERHOLZ, O. NUYKEN, *Macromol. Rapid Commun.* **2000**, 21, 583–589.
- 232 F. E. GOODSON, J. F. HARTWIG, *Macromolecules* **1998**, 31, 1700–1703.
- 233 F. E. GOODSON, T. I. WALLOW, B. M. NOVAK, *Macromolecules* **1998**, 31, 2047–2056.
- 234 F. E. GOODSON, T. I. WALLOW, B. M. NOVAK, *J. Am. Chem. Soc.* **1997**, 119, 12441–12453.
- 235 R. A. SINGER, J. P. SADIGHI, S. L. BUCHWALD, *J. Am. Chem. Soc.* **1998**, 120, 213–214.
- 236 J. P. SADIGHI, R. A. SINGER, S. L. BUCHWALD, *J. Am. Chem. Soc.* **1998**, 120, 4960–4976.
- 237 J. LOUIE, J. F. HARTWIG, *Macromolecules* **1998**, 31, 6737–6739.
- 238 M. P. STRUIJK, R. A. JANSSEN, *Synth. Metals* **1999**, 103, 2287–2290.
- 239 A. ITO, Y. ONO, K. TANAKA, *New J. Chem.* **1998**, 22, 779–781.
- 240 A. ITO, Y. ONO, K. TANAKA, *J. Org. Chem.* **1999**, 64, 8236–8241.
- 241 A. ITO, Y. ONO, K. TANAKA, *Angew. Chem. Int. Ed.* **2000**, 39, 1072–1075.
- 242 S. I. HAUCK, K. V. LAKSHMI, J. F. HARTWIG, *Org. Lett.* **1999**, 1, 2057–2060.
- 243 B. WITULSKI, Y. ZIMMERMANN, V. DARCO, J. P. DESVERGNE, D. M. BASSANI, H. BOUAS-LAURENT, *Tetrahedron Lett.* **1998**, 39, 4807–4808.
- 244 B. WITULSKI, *Synlett* **1999**, 8, 1223–1226.
- 245 B. WITULSKI, M. WEBER, U. BERGSTRASSER, J. P. DESVERGNE, D. M. BASSANI, H. BOUAS-LAURENT, *Org. Lett.* **2001**, 3, 1467–1470.
- 246 I. P. BELETSKAYA, A. G. BESSERMERTNYKH, R. GUILLARD, *Tetrahedron Lett.* **1997**, 38, 2287–2290.
- 247 N. MONTSERRAT, A. W. PARKINS, A. R. TOMKINS, *J. Chem. Res., Synop.* **1995**, 336–337.
- 248 A. MENDIRATTA, S. BARLOW, M. W. DAY, S. R. MARDER, *Organometallics* **1999**, 18, 454–456.
- 249 K. R. J. THOMAS, J. T. LIN, Y. T. TAO, C. W. KO, *Adv. Mater.* **2000**, 12, 1949.
- 250 S. THAYUMANAVAN, S. BARLOW, S. R. MARDER, *Chem. Mater.* **1997**, 9, 3231–3235.
- 251 M. C. HARRIS, O. GEIS, S. L. BUCHWALD, *J. Org. Chem.* **1999**, 64, 6019–6022.
- 252 M. C. HARRIS, S. L. BUCHWALD, *J. Org. Chem.* **2000**, 65, 5327–5333.
- 253 M. S. BAYERL, T. BRAIG, O. NUYKEN, D. C. MULLER, M. GROSS, K. MEERHOLZ, *Macromol. Rapid Commun.* **1999**, 20, 224–228.
- 254 J. IPAKTSCHI, A. SHARIFI, *Monatsh. Chem.* **1998**, 129, 915–920.
- 255 S. BECKER, A. BOHM, K. MULLEN, *Chem. Eur. J.* **2000**, 6, 3984–3990.
- 256 G. E. GRECO, A. I. POPA, R. R. SCHROCK, *Organometallics* **1998**, 17, 5591–5593.
- 257 R. R. SCHROCK, A. L. CASADO, J. T. GOODMAN, L. C. LIANG, P. J. BONITATEBUS, W. M. DAVIS, *Organometallics* **2000**, 19, 5325–5341.
- 258 L. C. LIANG, R. R. SCHROCK, W. M. DAVIS, *Organometallics* **2000**, 19, 2526–2531.
- 259 F. A. HICKS, M. BROOKHART, *Org. Lett.* **2000**, 2, 219–221.
- 260 I. CABANAL-DUVILLARD, P. MANGENEX, *Tetrahedron Lett.* **1999**, 40, 3877–3880.
- 261 S. E. DENMARK, X. SU, Y. NISHIGAICHI, D. M. COE, K.-T. WONG, S. B. D. WINTER, J. Y. CHOI, *J. Org. Chem.* **1999**, 64, 1958–1967.
- 262 C. G. FROST, P. MENDONÇA, *Tetrahedron: Asymmetry* **1999**, 10, 1831–1834.
- 263 S. VYSKOCIL, M. SMRCINA, P. KOCOVSKY, *Collect. Czech. Chem. Commun.* **1998**, 63, 515–519.

- 264 S. VYSKOCIL, S. JARACZ, M. SMRCINA, M. STICHA, V. HANUS, M. POLASEK, P. KOCOVSKY, *J. Org. Chem.* **1998**, *63*, 7727–7737.
- 265 R. A. SINGER, S. L. BUCHWALD, *Tetrahedron Lett.* **1999**, *40*, 1095–1098.
- 266 F. M. RIVAS, U. RIAZ, S. T. DIVER, *Tetrahedron: Asymmetry* **2000**, *11*, 1703–1707.
- 267 C. AMATORE, G. BROEKER, A. JUTAND, F. KHALIL, *J. Am. Chem. Soc.* **1997**, *119*, 5176–5185.
- 268 L. M. ALCAZAR-ROMAN, J. F. HARTWIG, A. L. RHEINGOLD, L. M. LIABLE-SANDS, I. A. GUZEI, *J. Am. Chem. Soc.* **2000**, *122*, 4618–4630.
- 269 P. KOCOVSKY, S. VYSKOCIL, I. CISAROVA, J. SEJBAL, I. TICLEROVÁ, M. SMRCINA, G. C. LLOYD-JONES, S. C. STEPHEN, C. P. BUTTS, M. MURRAY, V. LANGER, *J. Am. Chem. Soc.* **1999**, *121*, 7714–7715.
- 270 N. M. BRUNKAN, P. S. WHITE, M. R. GAGNE, *J. Am. Chem. Soc.* **1998**, *120*, 11002–11003.
- 271 J. F. HARTWIG, F. PAUL, *J. Am. Chem. Soc.* **1995**, *117*, 5373–5374.
- 272 E. NEGISHI, T. TAKAHASHI, K. AKIYOSHI, *J. Chem. Soc., Chem. Commun.* **1986**, 1338.
- 273 C. AMATORE, F. FLUGER, *Organometallics* **1990**, *9*, 2276–2282.
- 274 C. AMATORE, A. JUTAND, A. SUAREZ, *J. Am. Chem. Soc.* **1993**, *115*, 9531–9541.
- 275 J. K. STILLE, K. S. Y. LAU, *Acc. Chem. Res.* **1977**, *10*, 434–442.
- 276 A. ROY, J. F. HARTWIG, *J. Am. Chem. Soc.* **2001**, *123*, 1232–1233.
- 277 R. A. WIDENHOEFER, S. L. BUCHWALD, *Organometallics* **1996**, *15*, 3534–3542.
- 278 R. A. WIDENHOEFER, H. A. ZHONG, S. L. BUCHWALD, *Organometallics* **1996**, *15*, 2745–2754.
- 279 J. LOUIE, F. PAUL, J. F. HARTWIG, *Organometallics* **1996**, *15*, 2794–2805.
- 280 M. S. DRIVER, J. F. HARTWIG, *Organometallics* **1997**, *16*, 5706–5715.
- 281 The use of BINAP in Buchwald's laboratory was initiated by studies on the kinetic resolution of chiral amines.
- 282 G. MANN, C. INCARVITO, A. L. RHEINGOLD, J. F. HARTWIG, *J. Am. Chem. Soc.* **1999**, *121*, 3224–3225.
- 283 M. D. FRYZUK, W. E. PIERS, *Organometallics* **1990**, *9*, 986–98.
- 284 J. B. CANNON, J. SCHWARTZ, *J. Am. Chem. Soc.* **1974**, *96*, 2276–2278.
- 285 J. EVANS, J. SCHWARTZ, P. W. URQUHART, *J. Organomet. Chem.* **1974**, *81*, C37–C39.
- 286 R. J. CROSS, in *The Chemistry of the Metal–Carbon Bond* (Eds.: F. R. HARTLEY, S. PATAI), John Wiley, New York, 1985, Vol. 2, pp 559.
- 287 G. M. WHITESIDES, J. F. GAASCH, E. R. STEDRONSKY, *J. Am. Chem. Soc.* **1972**, *94*, 5258–5270.
- 288 J. ZHAO, H. HESSLINK, J. F. HARTWIG, *J. Am. Chem. Soc.* **2001**, *123*, 7220–7227.
- 289 W. D. JONES, V. L. KUYKENDALL, *Inorg. Chem.* **1991**, *30*, 2615–2622.
- 290 J. P. WOLFE, S. L. BUCHWALD, *Angew. Chem. Int. Ed.* **1999**, *38*, 2413–2416.
- 291 J. M. BROWN, P. J. GUIRY, *Inorg. Chim. Acta* **1994**, *220*, 249–259.
- 292 Y. GUARI, G. P. F. VAN STRIJDONCK, M. D. BOELE, J. N. H. REEK, P. C. J. KAMER, P. W. N. M. VAN LEEUWEN, *Chem. Eur. J.* **2001**, *7*, 475–482.
- 293 L. M. ALCAZAR-ROMAN, J. F. HARTWIG, *J. Am. Chem. Soc.* **2001**, *123*, 12905–12906.
- 294 C. AMATORE, A. JUTAND, A. SUAREZ, *J. Am. Chem. Soc.* **1993**, *115*, 9531–9541.
- 295 C. AMATORE, A. JUTAND, *J. Organomet. Chem.* **1999**, *576*, 254–278.

5

From Acetylenes to Aromatics: Novel Routes – Novel Products

Henning Hopf

Abstract

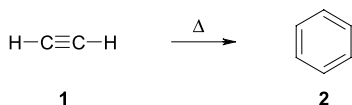
Alkynes have been used as precursors for aromatic compounds since Berthelot converted acetylene to benzene in 1867. The review presents new evidence on the mechanism of this first total synthesis of an aromatic compound. Presumably, its last step involves the thermocyclization of hexa-1,3-dien-5-yne to benzene. Trapping experiments as well as the study of derivatives of this highly unsaturated hydrocarbon show that the reaction takes place via isobenzene intermediates (1,2,4-cyclohexatrienes) at lower temperatures. Under high temperature pyrolysis conditions, carbenes as well as radical routes compete with the pericyclic process. In another recent application of acetylenes in the synthesis of aromatic compounds, the use of the isomeric diethynylbenzenes is discussed, which, depending on the actual substitution pattern, may be used for the construction of long extended π -systems or cyclic derivatives. When the number of triple bond substituents at the aromatic core is increased, subsystems of novel carbon allotropes become available ("graphyne"). Cyclooligomerization of acetylenes in the presence of cobalt catalysts leads to phenylenes, a class of condensed aromatic compounds hitherto available only with difficulty. Debromination of bis(propargyl bromide)-substituted aromatics provides highly reactive intermediates, which cyclodimerize to cyclophanes possessing unsaturated molecular bridges (cyclophynes). Cyclophynes are not only of interest for structural and stereochemical reasons but also as precursors of novel fullerene derivatives.

5.1

Introduction

Based on earlier studies on the total synthesis of benzene (**2**), which he called the "keystone of the total aromatic edifice", Berthelot in 1867 carried out a remarkable experiment: heating acetylene (**1**) – which he had prepared from the elements – in a "bent bell-jar at a temperature where the glass began to soften", he noticed the formation of "polymeric substances". When these were subjected to fractional distillation, benzene, styrene, and other aromatic hydrocarbons could be isolated, with **2** constituting approximately half of the product mixture (Scheme 1) [1].

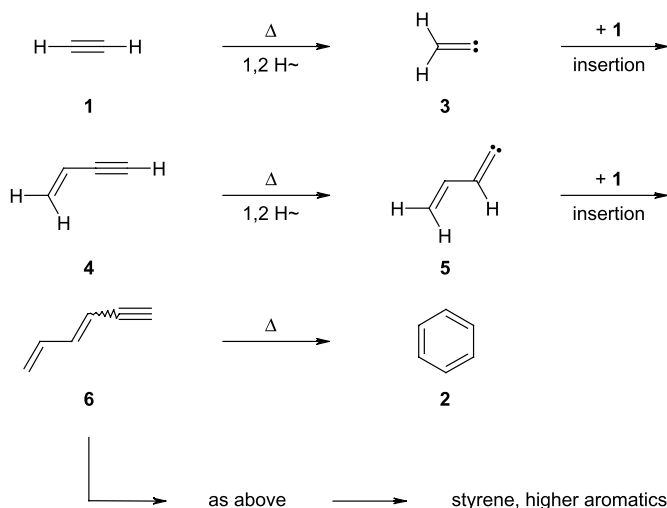
In the long period following Berthelot's courageous efforts, not only was the thermal tri-



Scheme 1. Berthelot's benzene synthesis.

merization of **1** and many of its derivatives repeated many times (under safer conditions), but it was also shown that this ring-generating oligomerization could be brought about by irradiation with ultraviolet light as well as catalytically in the presence of metals, metal salts, and – in particular – metal π -complexes, notably those of nickel, iron, cobalt, rhodium, and many others [2]. Many of these metal-mediated transformations, which became of great value for the industrial and academic synthesis of aromatic compounds, go back to Reppe's celebrated studies on the use of **1** in synthetic organic chemistry [3].

Although the Berthelot benzene synthesis must obviously be a multi-step process, its detailed mechanism surprisingly remains unknown to the present day. Being interested in the actual ring-producing step (see below), several years ago we postulated [4] that the overall process might be initiated by the isomerization of **1** to vinylidene carbene (**3**), a reaction that has been studied in detail by Brown and co-workers (Scheme 2) [5]:



Scheme 2. Berthelot's benzene synthesis: a possible mechanism.

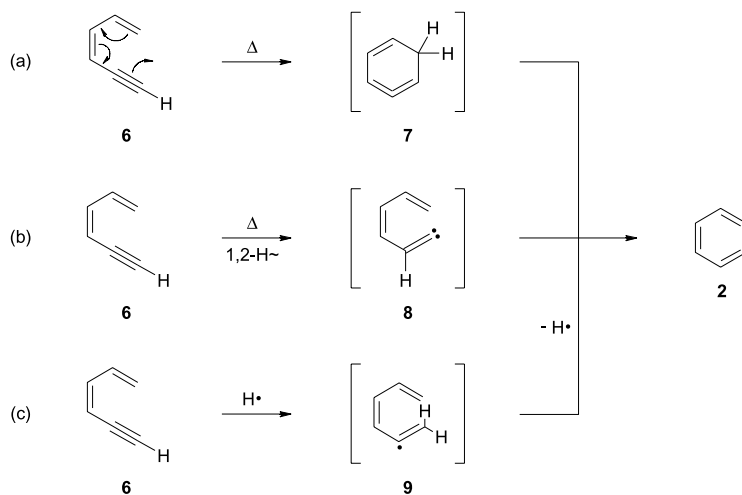
In the next step, **3** could insert into one of the C–H bonds of **1** to provide vinylacetylene (**4**, butenyne), a compound that is indeed generated when **1** is pyrolyzed. Repetition of the carbene formation step could then produce **5**, which, by another insertion step, would lead to hexa-1,3-dien-5-yne (**6**, mixture of isomers). This is already an isomer of benzene, and that it can cyclize to **2** was shown by us many years ago [6]. Obviously, **6** could also be a precursor of styrene and other oligomers of **1**. The mechanism proposed in Scheme 2 could also be of importance in connection with soot formation from smaller hydrocarbon fragments, and account for the formation of **2** in interstellar space.

This chapter first addresses the mechanism and preparative uses of the $6 \rightarrow 2$ cyclization in modern aromatic chemistry, and then proceeds to the construction of larger aromatic systems (“carbon networks” incorporating benzene rings), acetylenes serving as starting materials in both cases. In a third and final section, devoted to the construction of novel bridged aromatics (cyclophanes) from acetylenes, it is shown that substrates containing triple bonds have lost little of their importance and fascination since Berthelot’s days, and that highly topical problems of synthetic aromatic chemistry can be solved starting from alkynes. Clearly, in a chapter for a monograph like the present one, the author’s own contributions to this field of hydrocarbon chemistry will dominate the discussion.

5.2

The Aromatization of Hexa-1,3-dien-5-yne to Benzene: Mechanism and Preparative Applications

Formally, the aromatization of **6** is the dihydro variant of the Bergman cyclization [7]; however, compared to the latter process, the ring-closure of **6** does not require additional (“external”) hydrogen atoms to proceed. Whereas the mechanism of the Bergman cyclization, involving a benzene-1,4-diyl intermediate, is comparatively clear-cut [8], the aromatization of **6** is more complex and at least three different mechanisms are presently discussed for the process (Scheme 3) [9].

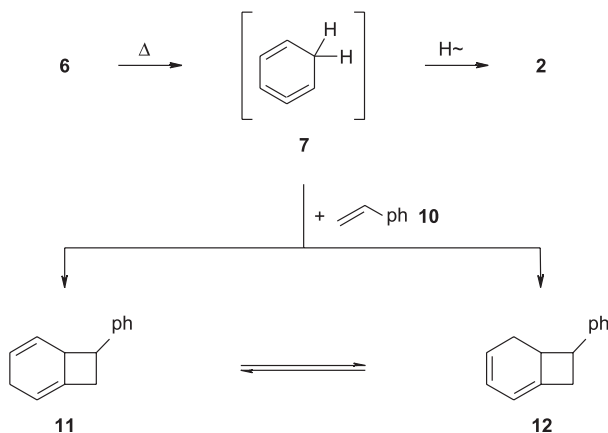


Scheme 3. Three routes from hexa-1,3-dien-5-yne (**6**) to benzene (**2**).

In alternative (a), ring-formation takes place electrocyclically and leads to isobenzene (**7**; 1,2,4-cyclohexatriene) as the primary reaction intermediate [10]. This highly strained cycloallene subsequently aromatizes to **2** by hydrogen migration. In the second route, pathway (b), reversible generation of a vinylidene carbene (**8**; see above) constitutes the first step, and is followed by 1,6-carbon hydrogen insertion. Finally, in pathway (c), vinyl radicals of type **9**

are produced by hydrogen atom addition to the triple bond. Cyclization is again achieved by a pericyclic step, and **2** is ultimately produced by the splitting off of a chain-carrying hydrogen atom. Because of their different activation energies [8, 9], these three mechanisms show a different response to an increase in temperature. Whereas up to ca. 550 °C, the cycloaromatization preferentially follows route (a), beyond this temperature the other alternatives become increasingly competitive. At 625 °C, the radical route dominates the aromatization reaction, and at 750 °C the process is almost exclusively governed by the carbene mechanism.

That isobenzene (**7**) is indeed produced as a reactive intermediate during the **6** → **2** cyclization was demonstrated by pyrolyzing acetylene in the presence of styrene (**10**) at 200 °C (Scheme 4) [11]:



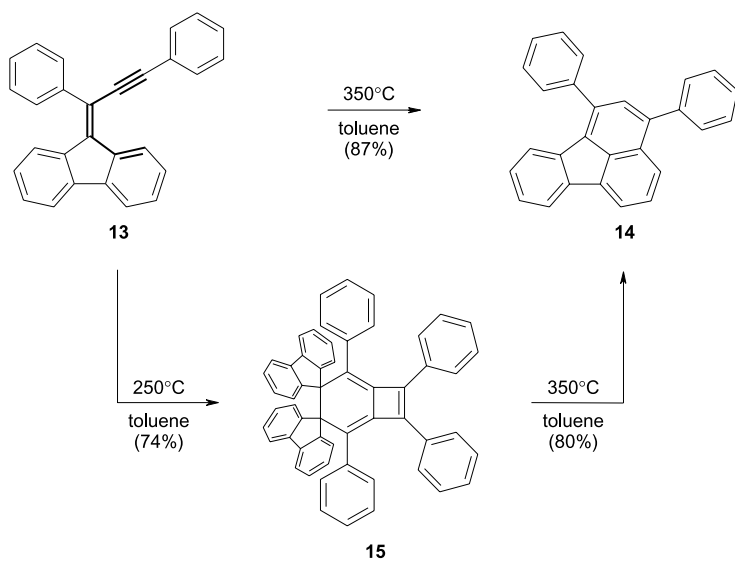
Scheme 4. The trapping of isobenzene (**7**).

Besides other homo and hetero dimers and trimers of **6**, the trapping products **11** and **12** were obtained, with the conjugated diene **12** presumed to be a secondary product formed by thermal equilibration of the [2+2] cycloadduct **11** of **7** and **10**.

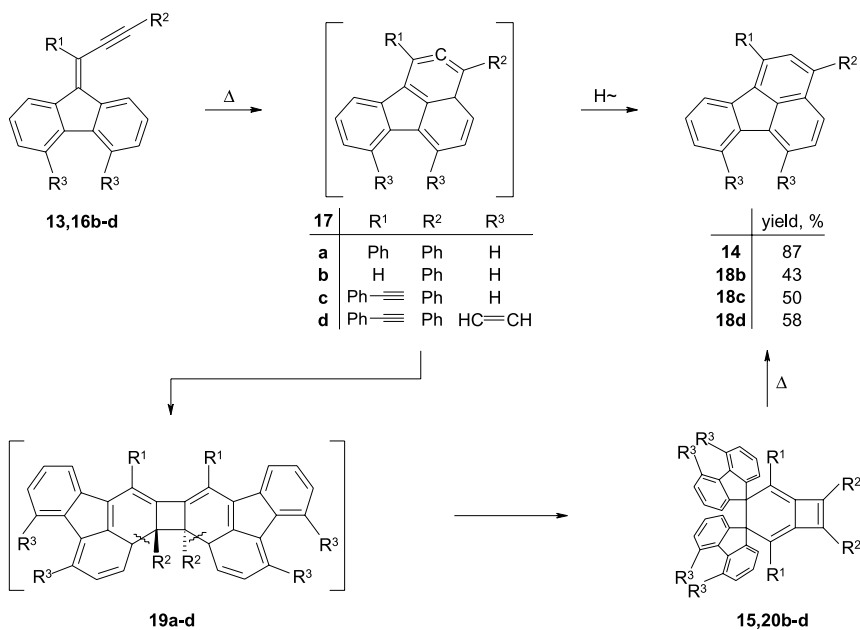
Preparatively important applications of the isobenzene route to aromatics were discovered by thermolysis of the dibenzofulvene derivative **13** (Scheme 5). When this hydrocarbon, which incorporates the hexa-1,3-dien-5-yne unit as a subsystem, is heated in toluene in a sealed ampoule at 350 °C, the condensed aromatic hydrocarbon **14** is produced in excellent yield (87 %) [11].

Repeating the cycloaromatization at lower temperatures (250 °C, toluene) leads to formation of the highly crowded dispiro compound **15**, which is again produced in good yield (74 %) and represents a formal dimer of **13**. Taking authentic **15** to the original temperature again provides **14**, also in good yield (80 %).

To account for this novel route to condensed aromatic systems, which – as the examples in Scheme 6 illustrate – can apparently be generalized, it has been suggested [9, 11, 12] that the isobenzene derivatives **17** are initially produced from their acetylenic precursors **16** by electrocyclization (Scheme 6).



Scheme 5. A new route to condensed aromatic hydrocarbons.

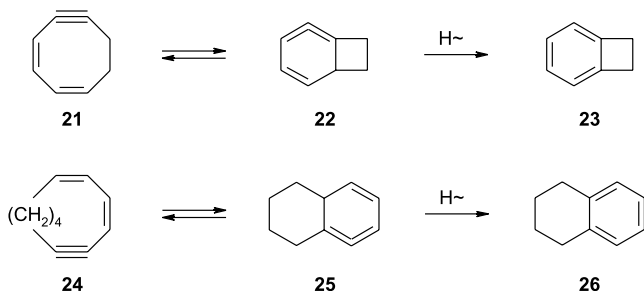


Scheme 6. The dimerization of an isobenzene intermediate.

As in the case of the parent molecule **6**, **17** can subsequently stabilize itself to **18** by hydrogen migration or, as a highly reactive cycloallene, participate in a [2+2]cycloaddition. This process, which can only be observed at lower isomerization temperatures, leads to the bis(methylene)cyclobutane intermediate **19** [13]. Cleavage of its weakest bonds (see wavy lines) could subsequently generate a resonance stabilized diradical, which, by reformation of a carbon–carbon single bond, would furnish **20**, with the generation of two fluorene moieties and a bis(methylene)cyclobutene core providing the driving force. Whether a reversal of these steps takes place at higher temperatures or the intermediate **20** finds an alternative route to the final product **18** is an open question at present. The yields have been satisfactory in all cases studied so far, and the substitution pattern can presumably be varied over a considerable range. The starting acetylenes are easily available in good yield [11, 12] by Wittig or Peterson olefination of the appropriate mono and diacetylenic aldehydes and ketones.

So far, only the cycloaromatization of precursors possessing an acyclic hexadienyne unit has been discussed. That this route probably also has considerable potential as a cyclic variant has been shown by the thermal ring-closure of the cyclic dienyynes **21** and **24** (Scheme 7).

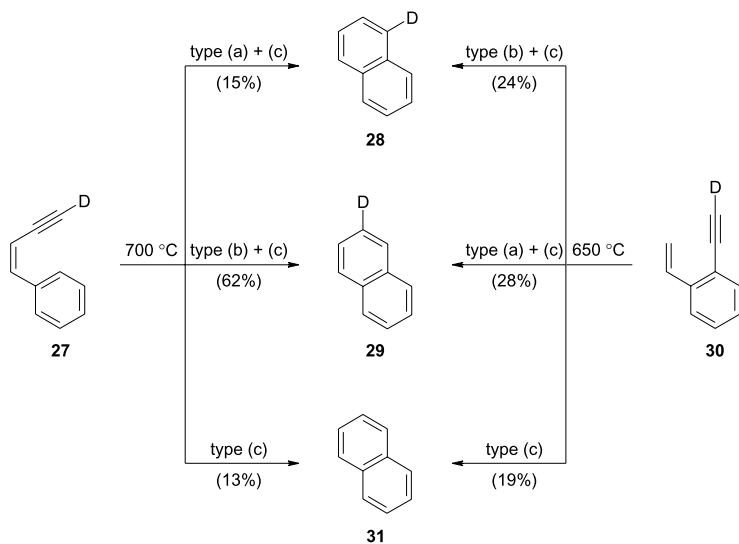
Hydrocarbon **21**, a highly reactive cyclic acetylene has only been generated in situ and rearranges immediately to **23**, presumably via the bicyclic isobenzene **22** [14]. The “tetramethylene-bridged” *cis*-hexadienyne **24** can be characterized, but cyclizes to tetralin (**26**) even at room temperature [15]. When the length of the oligomethylene bridge is extended, the thermal stability of the starting acetylene is strongly increased [15].



Scheme 7. Thermal cyclization of cyclic hexa-1,3-dien-5-ynes.

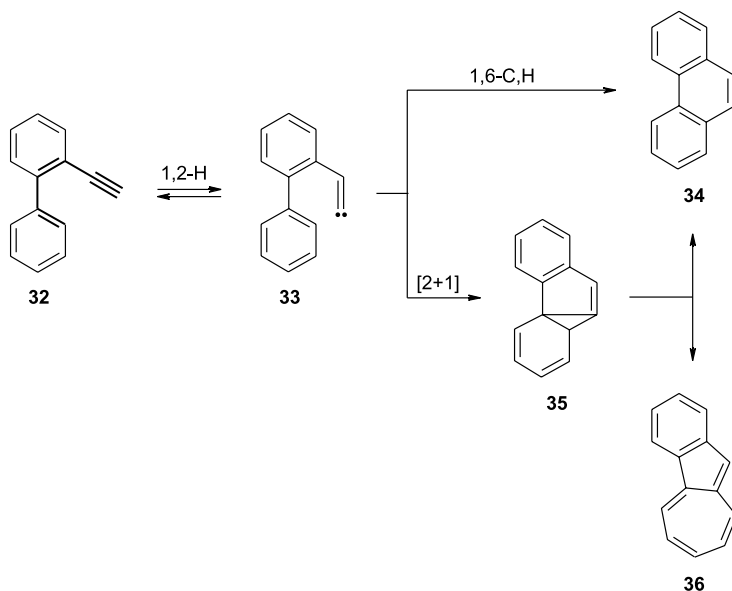
The most thorough analysis of the relative contributions of the three competing pathways (see Scheme 3) is due to Zimmermann and co-workers, who have addressed this problem by studying the thermocyclization of various substituted and D-labeled dienyynes, in which, *inter alia*, one of the double bonds was part of a benzene ring. As summarized in Scheme 8 for the two acetylenes **27** and **30**, which cycloaromatize to naphthalene (**31**) and its two mono-deuterio derivatives **28** and **29** on flash vacuum pyrolysis, the radical route (pathway (c)) plays a significant role in the formation of all these aromatization products [9, 16].

The carbene insertion route (pathway (b)) has most frequently been implied to explain the thermal cyclizations of various ethynyl-substituted aromatic precursors. Although the other two alternatives cannot be excluded at present, since in many cases (see below) no careful mechanistic studies have been undertaken, the carbene hypothesis has the advantage of



Scheme 8. Three different routes from 1-phenyl-buten-3-yne to biphenyl.

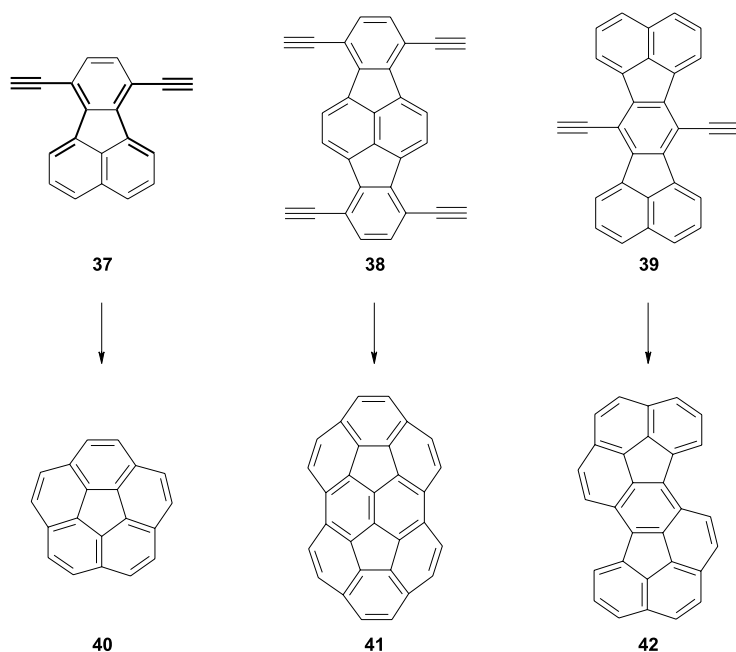
greater simplicity and hence will also be employed here. The prototypical experiment here is Brown's famous cyclization of 2-ethynylbiphenyl (**32**) to yield a mixture of phenanthrene (**34**) and 1,2-benzazulene (**36**; total yield 99 % at 700 °C, 0.2 Torr; product ratio 2.6:1) [17] (Scheme 9):



Scheme 9. The thermal cyclization of 2-ethynylbiphenyl (**32**) to phenanthrene (**34**) and 1,2-benzazulene (**36**).

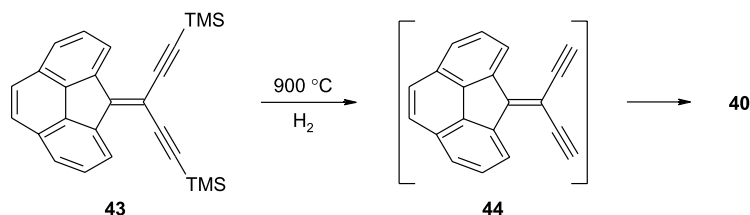
The initially generated vinylidene carbene intermediate **33** has two options for further reaction: it can either undergo 1,6-carbon hydrogen insertion to give **34** or participate in a carbene addition to the phenyl substituent. The latter process leads to the formation of the highly strained norcaradiene derivative **35**, which is ring-opened to give **36** under the reaction conditions. If this process occurred in a stepwise manner, the intermediately produced diradical could also participate in a hydrogen-shift process, opening up a second pathway to phenanthrene (**34**).

The importance of this cycloaromatization in modern aromatic chemistry only became obvious when it was realized that it constitutes an optimal route to bowl-shaped aromatics and fullerene partial structures [9, 18, 19]. The key experiment, Scott's synthesis of corannulene (**40**) from 7,10-diethynylfluoranthene (**37**) [20], was quickly adapted to more extended systems, the examples **38** → **41** [21] and **39** → **42** [22] in Scheme 10 being just two of many:



Scheme 10. Bowl-shaped aromatics by high temperature pyrolysis of acetylenes.

In many of these applications, the ethynyl group is present in the starting material only in latent form, e.g. as a chlorovinyl substituent, from which it is liberated during the pyrolysis step. That even non-terminal acetylenes can be employed in these cycloaromatizations is illustrated by the protected cross-conjugated diacetylene **43** in Scheme 11. When this was subjected to hydropyrolysis at 900 °C, the diacetylene **44** was generated in situ and double-cyclized to corannulene (**40**) immediately [23].



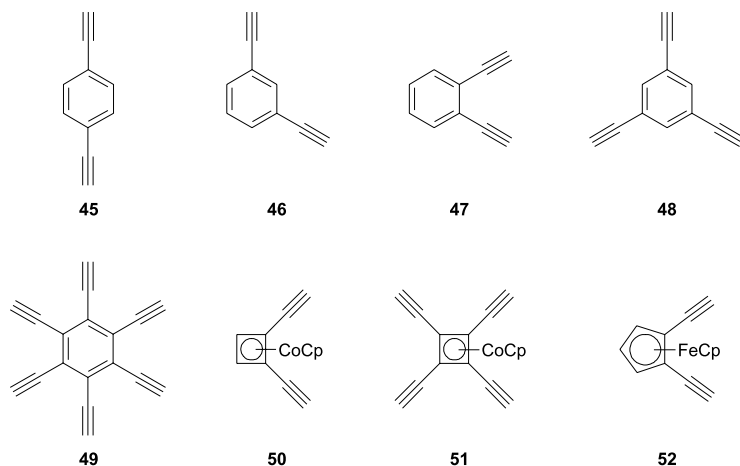
Scheme 11. Corannulene (**40**) from a cross-conjugated enediyne precursor.

5.3

The Construction of Extended Aromatic Systems from Ethynyl Benzene Derivatives

In the examples described so far, the acetylene unit ended up as an integral part of an aromatic system. There is, however, a vast and structurally very varied area of modern aromatic chemistry in which acetylenes that already contain an aromatic system – very often a benzene ring – are used to construct extended aromatic hydrocarbons of sometimes very large dimensions and high structural complexity. In these cases, the acetylene unit(s) is (are) used for connectivity purposes only, and it (they) remain(s) intact and recognizable in the product. Over the years, numerous coupling protocols to achieve these synthetic ends have been developed. At least one of these is as old as Berthelot's work on the thermal trimerization of acetylene (**1**) to benzene (**2**), namely the oxidative dimerization of terminal acetylenes discovered by Glaser in 1869 [24]. Over the years, acetylene coupling reactions have not only steadily been improved (*inter alia* Eglinton [25] and Hay variations [26] of the Glaser coupling, Cadiot–Chodkiewicz coupling [27], Stephens–Castro coupling [28]), but the arrival of the Heck [29], the Sonogashira [30, 31], and many other metal-mediated coupling reactions [31] have made it possible to construct practically any desired acetylene-containing aromatic framework, whether the coupling reactions are carried out in a symmetrical or unsymmetrical fashion. Acetylenic coupling reactions are the current methods of choice for the preparation of novel oligomers of ethynylbenzene, of dehydroannulene systems, and of new cyclic and polycyclic hydrocarbons containing aromatic rings and triple bonds simultaneously. These compounds are of interest for the study of aromaticity problems, as model compounds for molecular electronics, as subunits of novel allotropes of carbon, and as guest molecules with large cavities. Rather than attempting to cover the vast literature, the discussion here will concentrate on the fundamental aspects of this building block approach to new aromatic hydrocarbons, present a selection of important building units, and show how they are coupled to form greater aggregates. Some of the frequently used building blocks are depicted in Scheme 12.

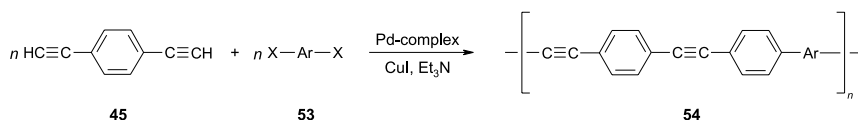
Beginning with diethynylbenzene derivatives, it is obvious that the *para*-isomer **45** could lead to rod-like hydrocarbons, whereas the *meta*- (**46**) and the *ortho*-isomers (**47**), respectively, could provide angular and circular structures. Of course, an increase in the number of ethynyl groups results in an increased number of coupling possibilities. 1,3,5-Triethynylbenzene (**48**), for example, is of interest since it can be used for the construction of bicyclic hydrocarbons – it constitutes a “blown-up” version of a bridgehead. Clearly, hexaethynylbenzene (**49**) [32] can function as a “tile” for the preparation of novel forms of



Scheme 12. A selection of building blocks for the preparation of large aromatic systems containing triple bonds.

graphite, and the three transition metal complexes **50–52** are shown here not only because they will be used for the building purposes described below, but also since they illustrate that the aromatic core unit may be replaced by metal complexes of anti-aromatic and non-benzenoid aromatic systems. Furthermore, if one bears in mind that the role of the center unit can also be played by a heteroaromatic system, the structural variability becomes almost endless.

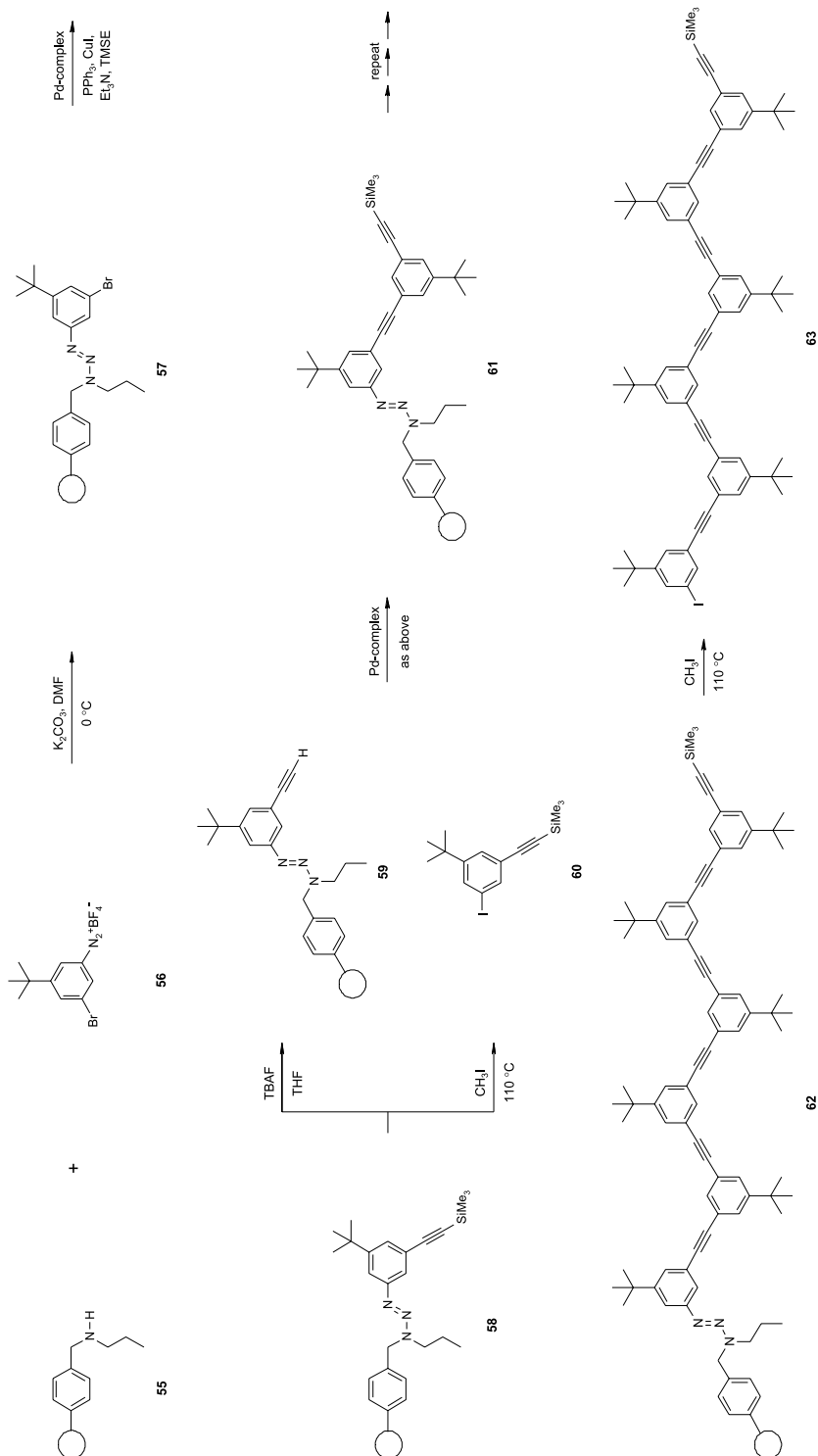
Rod-shaped systems such as **54**, extended versions of the widely studied poly(phenylene)s, are available by coupling the *para*-isomer **45** with a *para*-dihaloaromatic unit in the presence of a palladium catalyst [33] (Scheme 13):



Scheme 13. The synthesis of rod-like oligomers and polymers of 1,4-diethynylbenzene (**45**).

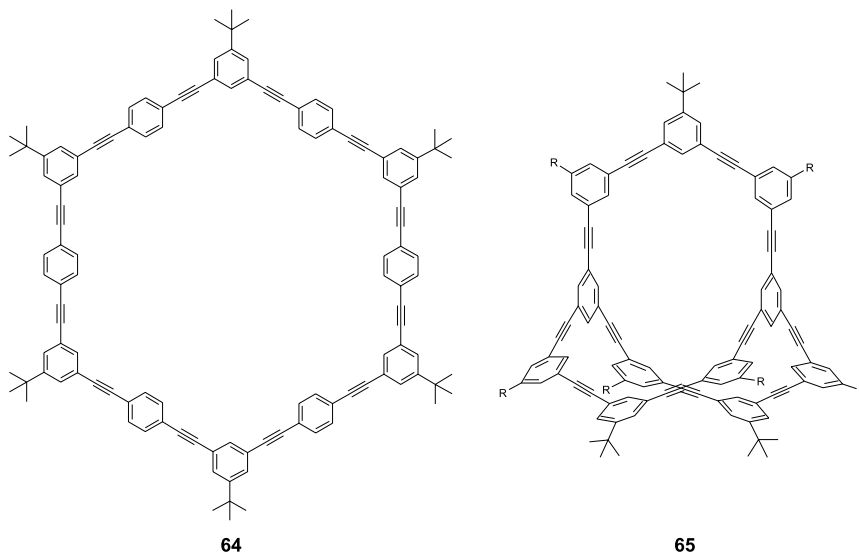
Another coupling strategy, often used in this area of aromatic chemistry, has been widely applied by Moore and co-workers for the preparation of shape-persistent molecular architectures of nanoscale dimensions [34]. Thus, as illustrated in Scheme 14, coupling of the Merrifield resin **55** with the diazonium salt **56** provided the triazene **57**, with the *tert*-butyl groups serving as solubilizing substituents in the higher oligomers. The ethynyl group was then introduced by Pd-catalyzed reaction of **57** with trimethylsilylethyne, and the resulting **58** could either be desilylated to give (the still resin-bound) **59** or treated with methyl iodide to give the bisfunctional coupling component **60**. In this latter step, the triazene group functions as a diazonium equivalent.

The two units **59** and **60** could then be coupled to give **61** and, by repetition of this sequence, oligomers such as **62** were obtained, which, in the terminating step to yield **63**, were



Scheme 14. The synthesis of 1,3-diethynylbenzene (46) derived hydrocarbons: open oligomers.

removed from the solid support by methyl iodide treatment. Using this methodology, not only could discrete oligomers with up to 32 monomer units be obtained, but also cyclic systems such as **64** and the bicyclic derivative **65**, the latter illustrating the aforementioned use of **48** as an enlarged bridgehead (Scheme 15).



Scheme 15. Cyclic oligomers based on **46**.

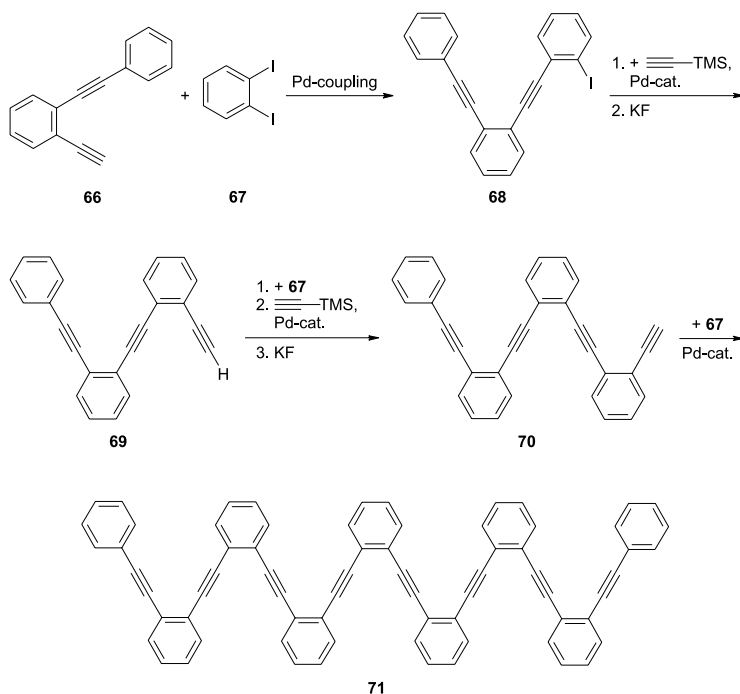
The *ortho*-diethynylbenzene motif **47** can be recognized in countless novel aromatic hydrocarbons, whether these are acyclic or cyclic.

A prototypical acyclic oligomer of **47** is the oligo[1,2-phenylene(2,1-ethynediyl)] derivative **71** prepared by Grubbs and co-workers [35] by the sequence described in Scheme 16. Heck-type coupling of 2-ethynyltolane (**66**) – itself readily available by Heck reaction from *ortho*-dibromobenzene – with *ortho*-diiodobenzene (**67**) initially provided the *ortho*-diethynylbenzene derivative **68**. This was ethynylated to give the terminal acetylene **69**, which, on coupling with **67** and another ethynylation/deprotection step, furnished **70**. To obtain the phenylacetylene octamer **71** from **70**, this latter building block was finally coupled with the diiodide **67**.

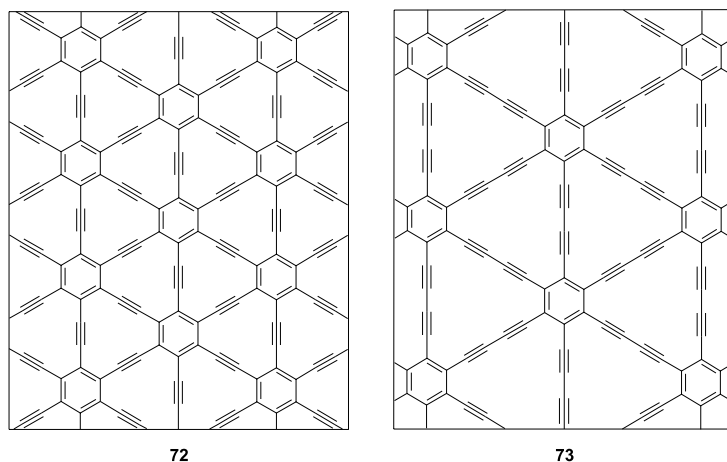
Interest in preparing cyclic oligomers of **47** has been high not only because these dehydrobenzoannulenes are important model compounds for the study of aromaticity phenomena, but also because they can be regarded as subsystems of two planar carbon allotropes: graphyne (**72**) and graphdiyne (**73**). As can be recognized in Scheme 17, these two carbon sheets can be deconstructed in countless ways to give various subsystems: hexaethynylbenzene (**49**) [32] and hexa(butadiynyl)benzene [36, 37], *ortho*-diethynylbenzene (**47**), tetraethynylbenzene, etc.

Whether **72** and **73** can be prepared in a stepwise (“rational”) synthesis is extremely unlikely, but the preparation of “highly evolved” subunits is a goal that has been realized by several groups in recent years.

Subjecting **47** and some of its derivatives to copper-mediated oligomerization leads to the

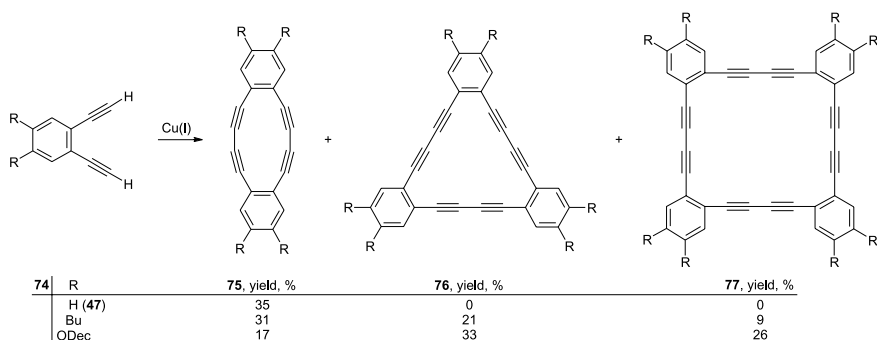


Scheme 16. The synthesis of acyclic oligomers of 1,2-diethynylbenzene (47).



Scheme 17. Graphyne (72) and graphdiyne (73): novel allotropes of carbon.

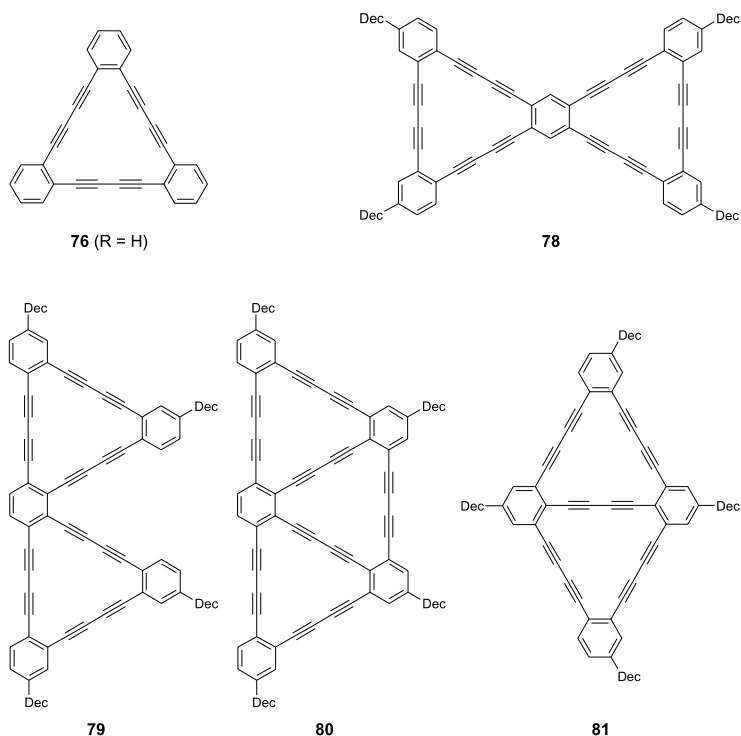
results shown in Scheme 18. Whereas in the case of the parent system 47 only the dimer 75 is produced [38], the derivatives 74 with R = butyl or *O*-decyl also give rise to trimer (76) and tetramer (77) formation [39]. Whereas the trimers 76 represent a substructure of graphdiyne, the tetramers 77 possess an unusual box-like structure.



Scheme 18. Cyclooligomerization of 1,2-diethynylbenzene (**47**) and some of its derivatives.

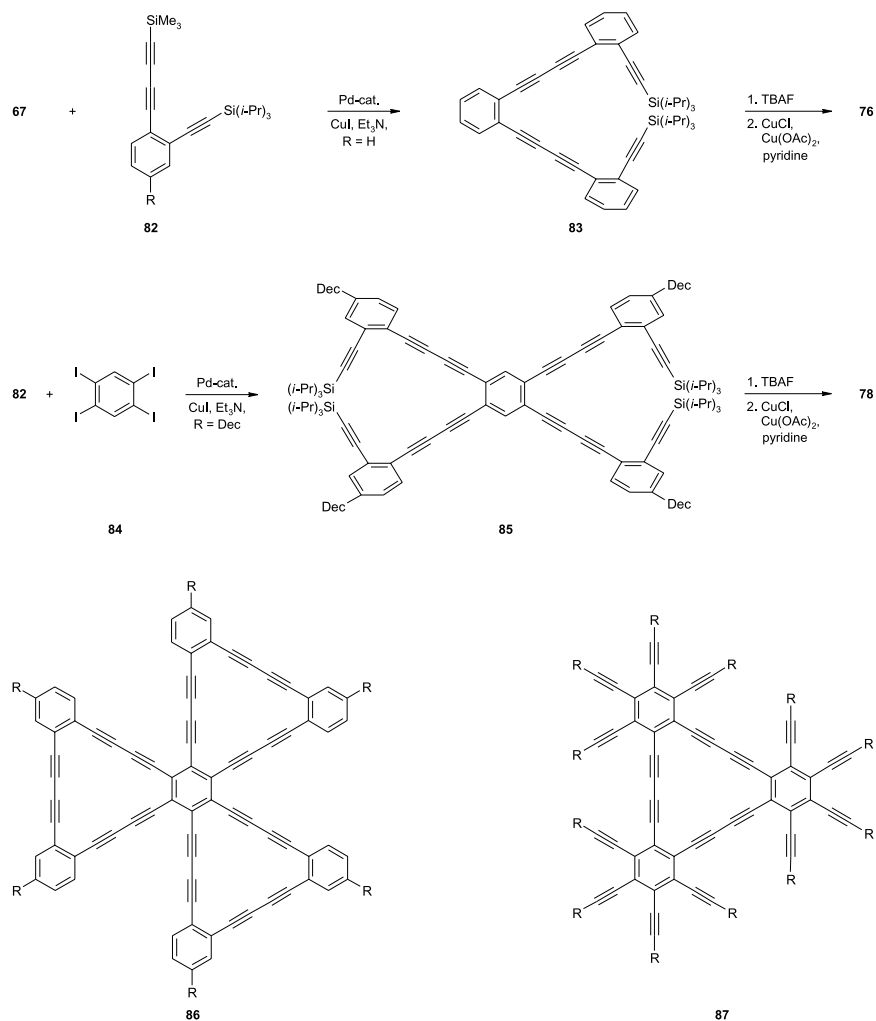
Haley and co-workers in particular have been successful in preparing graphyne and graphdiyne substructures and have synthesized numerous hydrocarbons such as **76** and **78–81** during the last few years (Scheme 19) [40, 41].

To demonstrate their approach, the preparation of the parent system **76** and the so-called bow-type hydrocarbon **78** is discussed here [42]. To prepare the trimer of **47** (which was not among the oxidative dimerization products, see above), the triyne **82** was coupled with *ortho*-



Scheme 19. A selection of graphdiyne substructures.

diiodobenzene (**67**) in a modified Sonogashira coupling. The resulting **83** was subsequently deprotected by treatment with tetrabutylammonium fluoride (TBAF) and the hexayne thus formed was ring-closed by Eglinton coupling to give **76** (Scheme 20).



Scheme 20. The synthesis of several graphdiyne substructures.

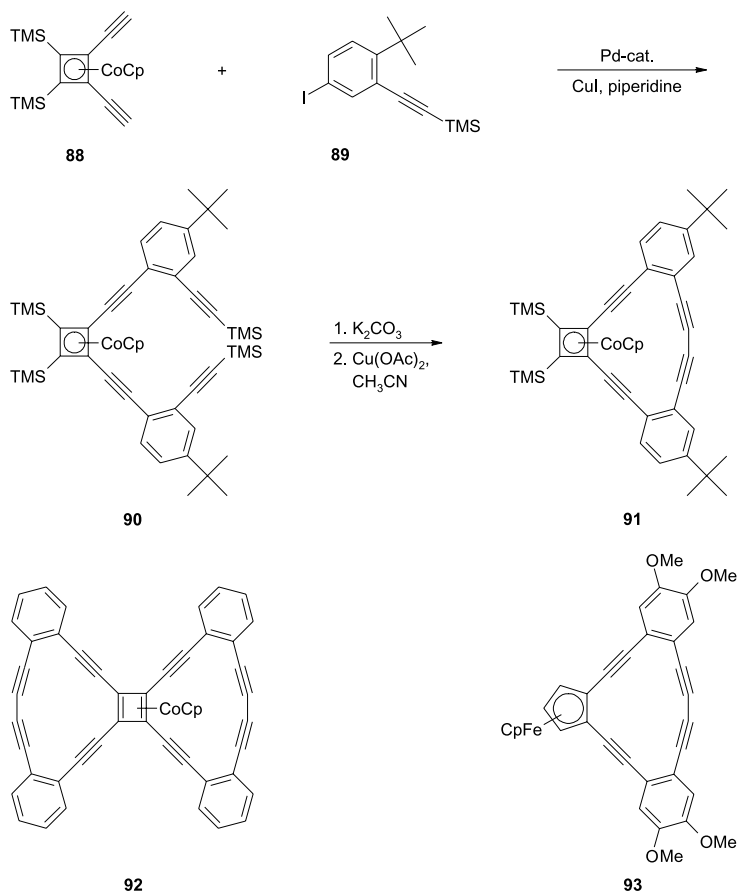
Analogously, **82** (R = Dec) was coupled with the tetraiodide **84** to give the polyacetylene **85**, which, after desilylation, could be oxidized to the desired **78** [42]. The largest subsections of graphdiyne reported to date have been the hydrocarbons **86** (R = *tert*-Bu and Dec) [43] and **87** (R = *tert*-Bu) [44] (Scheme 20).

To study the aromatic character of dehydrobenzoannulenes by ^1H NMR spectroscopy, it is desirable to replace one or more of the benzene rings in the above and related hydrocarbons

by double bonds, and many of the respective model compounds have been prepared by coupling reactions similar to those presented so far [45]. Derivatives of several of the above hydrocarbons bearing polarizing functional groups have also been reported [46], as has the preparation of several derivatives in which the benzene ring has been replaced by a thiophene ring [47].

Compared to the purely organic dehydroannulenes, much less is known about systems that incorporate metal organic fragments. Nevertheless, due to the efforts of Bunz and co-workers, there has been steady progress in this area as well, and again interest in these compounds stems from their spectroscopic properties (especially their NMR behavior) and their potential uses in material science, one attractive goal being the preparation of metal-containing nanostructures. The preparation of the cyclobutadiene complex **91** is typical (Scheme 21).

Coupling of the cyclobutadiene complex **88** [48] with the protected acetylene **89** furnished the tetrayne **90**, copper-mediated coupling of which, after removal of its acetylenic trimethylsilyl groups, yielded the organometallic complex **91** [49]. ^1H NMR analysis of this

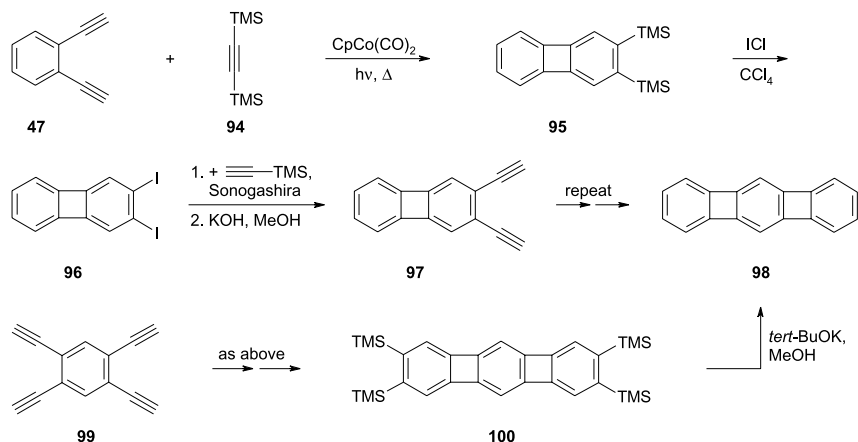


Scheme 21. The preparation of dehydrobenzannulenes containing metal organic fragments.

and related dehydro[14]annulenes incorporating the bis(trimethylsilyl)cyclobutadiene-(cyclopentadienyl-cobalt) moiety suggest that the aromaticity of the fused cyclobutadiene complex might be stronger than that of benzene according to the ring-current criterion. The butterfly complex **92** [50] and the ferrocene derivative **93** [51] (Scheme 21) were synthesized by comparable coupling routes, starting from the building blocks **51** and **52**, respectively. According to X-ray structural analysis, complexes such as **92** possess a concave structure and are of interest since the tetraethynylcyclobutadiene motif has been suggested to play an important role in the formation of fullerenes such as C_{60} [52].

The central role of *ortho*-diethynylbenzene (**47**) as a construction unit in modern aromatic chemistry is also demonstrated by two other developments.

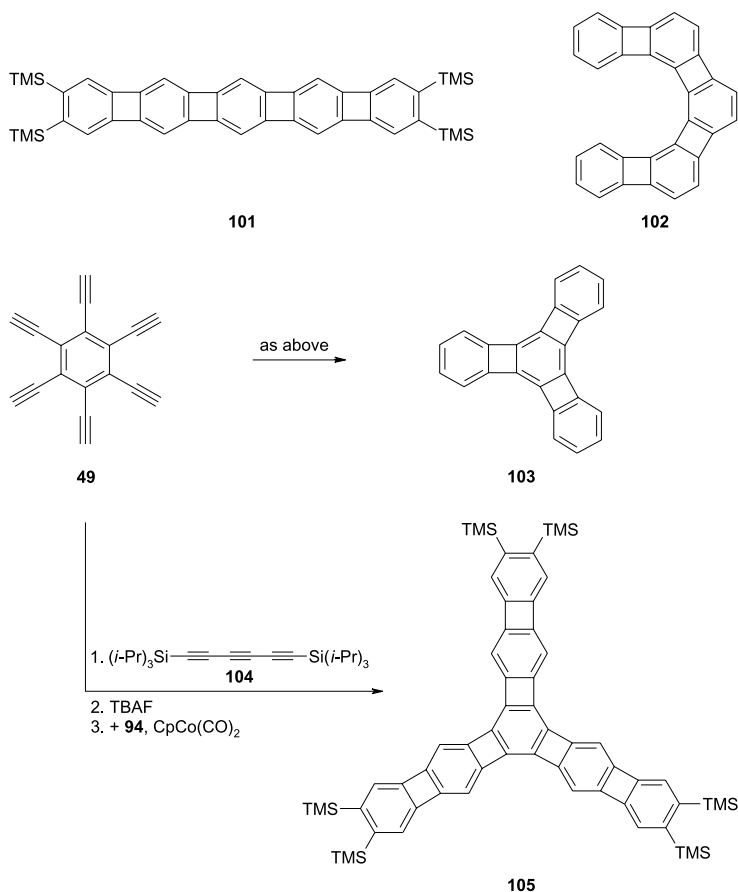
In 1982, Vollhardt and co-workers made a discovery that turned out to be of major importance with regard to the synthesis of numerous natural and non-natural products: addition of bis(trimethylsilyl)ethyne (**94**) to **47** in the presence of a Co catalyst led to the biphenylene derivative **95** in practically quantitative yield [53]. In fact, because of the steric bulk of the TMS substituents, self-trimerization of **94** does not take place, and it can be used as a solvent for the reaction. For the preparation of the [*n*]phenylenes, of which biphenylene is the smallest member, this conversion of acetylene units into aromatic rings remains the only general known protocol [54]. For example, when **95** was iododesilylated, the resulting diiodide **96** could be coupled with trimethylsilyl ethyne to give the bis(acetylene) **97**, which, by repeating the addition step with **94** and removal of the protecting groups, was transformed into [3]phenylene (**98**, Scheme 22).



Scheme 22. A general route to linear [*n*]phenylenes.

When **47** was replaced by the tetraacetylene **99**, the route to **98** could even be shortened: cycloaddition as described above provided the [3]phenylene derivative **100**, which was desilylated to give **98** by treatment with potassium *tert*-butoxide in methanol [55].

The vast scope of this annelation sequence [54] has not only been demonstrated by the preparation of further linear [*n*]phenylenes such as **101**, but also by the synthesis of angular representatives such as **102** and triangular systems such as **103** and **105** (Scheme 23) [56].

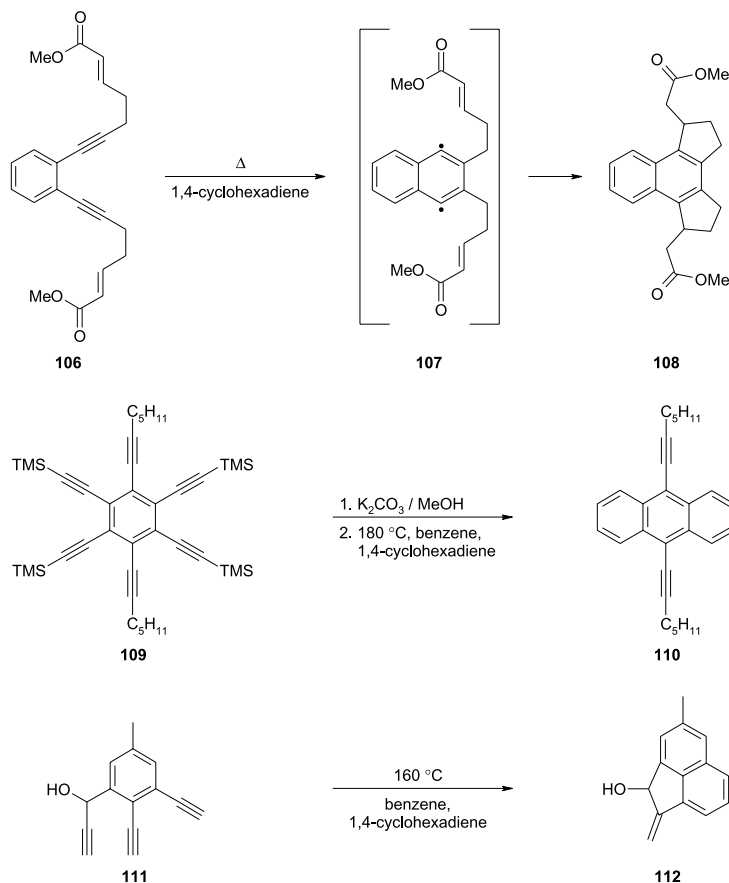


Scheme 23. Linear, angular, and triangular $[n]$ phenylenes.

These latter aromatic compounds are of interest for the study of structural and bonding issues, since some of them show extreme bond alternation, suggesting the presence of discrete double and single bonds in aromatic rings [57].

In another recent development in aromatic synthesis, the Bergman cyclization [7] is beginning to be exploited for preparative purposes. This process has been studied for many years because of its importance with regard to the biological action of several marine anti-tumor antibiotics such as calicheamicin [58] and because of its interesting reaction mechanism [8]. Now, more and more synthetic applications are beginning to be reported in the literature [59].

A case in point, again involving a derivative of **47**, is illustrated by the cycloaromatization of **106**, a starting material that has two in-built radical traps. After the diradical **107** has been generated by the Bergman process, the 1,4-diyl is intercepted by the two α,β -unsaturated ester groups and the tetracyclic product **108** is formed (Scheme 24) [60].



Scheme 24. Using the Bergman cyclization for preparative purposes.

In another example, the hexaalkyne **109** – after deprotection with potassium carbonate in methanol – is subjected to typical Bergman trapping conditions, resulting in the formation of the anthracene derivative **110** [61]. As a third, more complex illustration, the aromatization of the trialkyne **111** may be considered. Here, the 1,4-diradical intermediate faces another triple bond as an internal trap, and, after hydrogen transfer from 1,4-cyclohexadiene, the tricyclic allylic alcohol **112** is produced [61].

5.4

Bridged Aromatic Hydrocarbons Containing Triple Bonds (Cyclophynes)

Ever since Cram started his systematic efforts to study bridged aromatic hydrocarbons and their derivatives half a century ago [62, 63], this field has had a strong influence on the development of aromatic chemistry [64–67]. In fact, after a period during which numerous cyclophane hydrocarbons were prepared and their chemical and structural properties were studied, their derivatives are now enjoying growing attention as chiral ligands in reagents

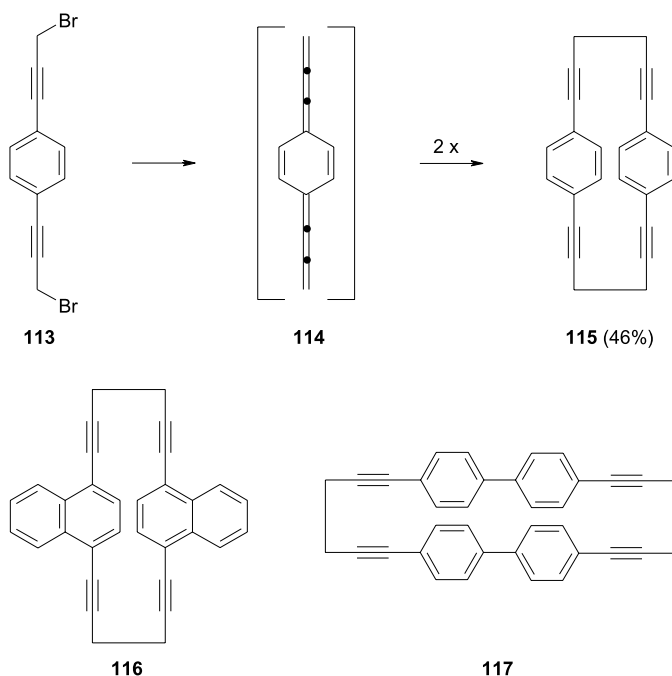
used for asymmetric synthesis [68], as novel liquid crystalline materials [69], and as monomers in polymer chemistry [70], to name but a few recent applications. However, as in any active field, there is a strong need for the development of new synthetic methods providing these interesting aromatic compounds in ever increasing variety.

As found a few years ago [71], acetylenes that can be traced back to the diethynylbenzenes **45** and **47** are useful starting materials for the preparation of cyclophanes that possess triple bonds and triple-bond derived functionalities in their molecular bridges. Compared to cyclophanes bearing functional groups in benzene ring positions, relatively little is known about bridge-functionalized cyclophanes. That these – and especially acetylenic derivatives – have considerable potential in synthetic aromatic chemistry will be shown below.

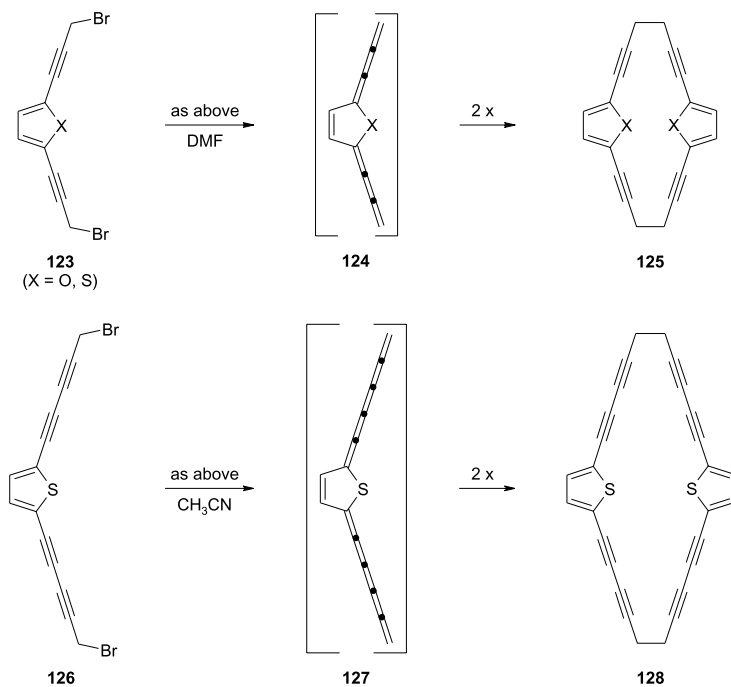
Treating **113** (easily available from **45** by reaction of its dilithio derivative with formaldehyde and treatment of the resulting diol with phosphorus dibromide) with the so-called Mori reagent [72], a trimethylsilyl(tri-*n*-butyl)stannane/cesium fluoride combination that has been used very successfully in many debromination reactions [73], results in the production of the [6.6]paracyclophane **115** in acceptable yield. Since *p*-xylylene (*p*-quinodimethane) is known to dimerize to [2.2]paracyclophane, it may well be that the bis(cumulene) **114** is formed as an intermediate in this reaction. Since a stepwise process is also conceivable, further clarification of the mechanism is obviously desirable (Scheme 25).

Analogously, **116** and **117** have been prepared from the corresponding dibromides [74].

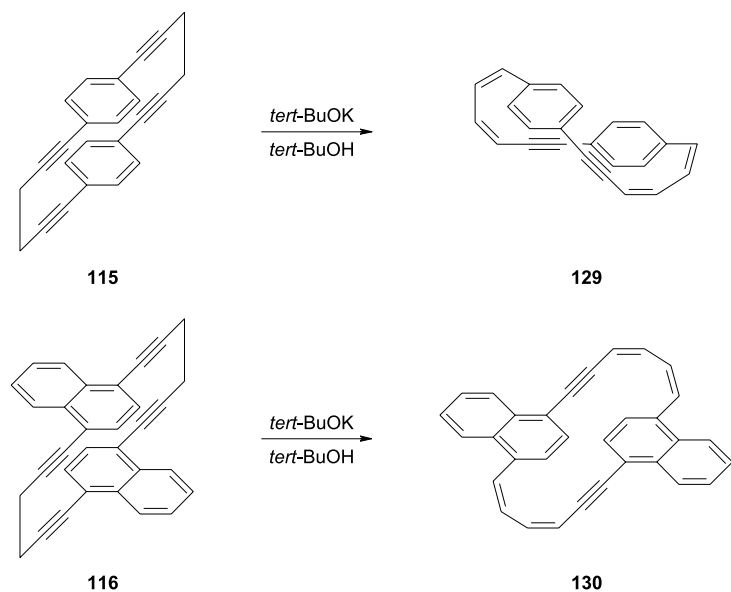
Applying the elimination protocol to the *ortho*-isomer of **113**, the dibromide **118**, results in the formation of the “orthocyclophane” **120**, i.e. in this case no dimerization of a reactive



Scheme 25. A new route to cyclophanes with bridges containing triple bonds.



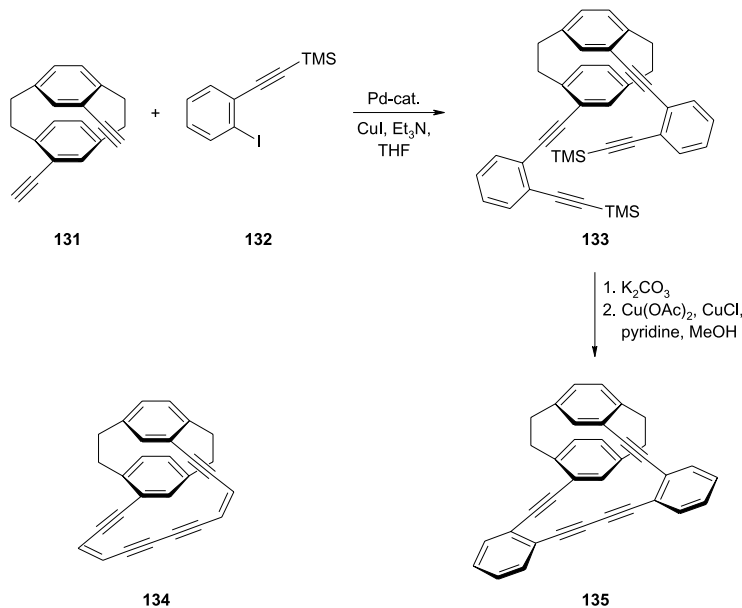
Scheme 27. Heterophanes with bridges containing triple bonds.



Scheme 28. The preparation of the three-dimensional annulenes **129** and **130**.

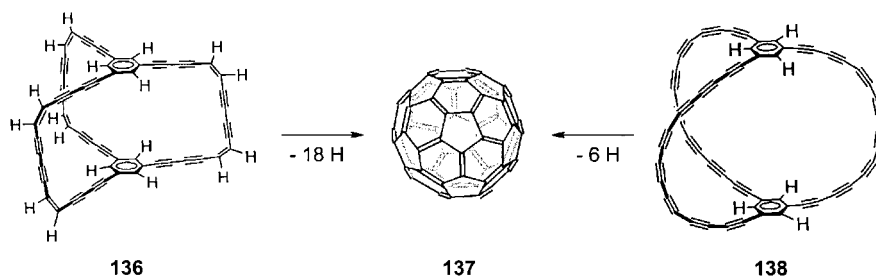
carbons **129** and **130** have a figure-8 structure (as indicated for **129**), and are hence chiral [74].

Another type of chiral cyclophyne was obtained by applying the coupling methods developed by Haley to the chiral *pseudo-ortho* diacetylene **131** [76]. When this was connected to 2-(trimethylsilylethynyl)iodobenzene (**132**) the open tetraacetylene **133** resulted, which, after deprotection, was oxidatively closed to give **135**. By a similar route, the non-benzo variant **134** was prepared, which could be characterized by X-ray structural analysis (Scheme 29) [76].



Scheme 29. Chiral paracyclophane/dehydrobenzannulene hybrids.

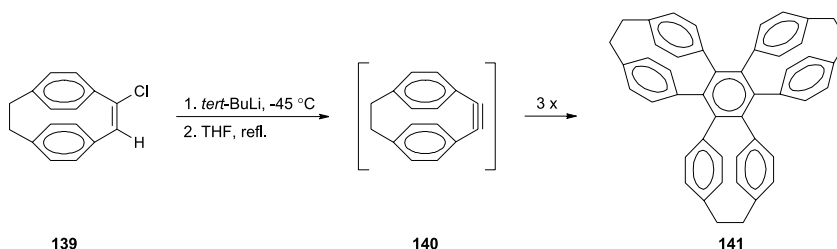
Hydrocarbons such as **134** and **135**, so-called [2.2]paracyclophane/dehydrobenzoannulene hybrids (PC/DBAs), are not only of interest because of their stereochemical properties. Their electronic absorption spectra indicate that there must be electron delocalization through their open circuits. With their high degree of unsaturation, these layered hydrocarbons are also a step on the way to the triply-bridged cyclophane polyyne **136** and **138**, generated *in situ* by Rubin [77] and by Tobe [78] by laser desorption time-of-flight mass spectrometry from appropriate precursor systems (these, in turn, produced by coupling reactions of various acetylenic building blocks). In the ICR mass spectrum (operating in the negative mode) of **136**, partial dehydrogenation down to $C_{60}H_{16}^-$ was observed, suggesting the possibility of complete dehydrogenation to C_{60} (**137**). In the negative mode laser desorption mass spectrum of **138**, the polyyne anion $C_{60}H_6^-$ was detected. Size-selective formation of C_{60}^+ and C_{60}^- was also observed, indicating a possible polyyne cyclization to the fullerene cage (Scheme 30).



Scheme 30. Multibridged cyclophynes as precursors for C₆₀ (137)?

Although representing rational syntheses of 137 – compared to the mode of formation of this parent fullerene from graphite [79] – it should be mentioned that these approaches do not provide isolable and spectroscopically characterizable amounts of the precursor systems 136 and 138. Thus, it appears that for the time being the directed synthesis of these intermediates based on organochemical transformations is out of reach.

The first cyclophynane, incidentally, for which this name was also coined, was 1-cyclophynane (140), generated as a highly reactive intermediate from the vinyl chloride 139 by treatment with *tert*-butyllithium and heating of the resulting organolithio intermediate. Not surprisingly, 140 is unstable under the reaction conditions and trimerizes (*inter alia*) to trifoliaphane (141, Scheme 31) [80].



Scheme 31. A modern version of Berthelot's benzene synthesis: trifoliaphane (141) from [2.2]paracyclophynane (140).

Although chemistry has clearly come a long way since the days of Berthelot – once again an acetylene has been converted into an aromatic ring.

Acknowledgement

I thank Cornelia Mlynek for drawing the reaction schemes.

References

- 1 M. BERTHELOT, *Ann. Chem. Pharmacie* 1867, 141, 177–184. This journal later became *Liebigs Annalen der Chemie*, which,

in due course, became one of the founding journals of the *European Journal of Organic Chemistry*.

- 2 For a review, see: H. FIEGE, K.-D. GUNDERMANN, C. GRUNDMANN, in Houben-Weyl-Müller, *Methoden der Organischen Chemie*, Vol. V/2b, *Arene und Arine*, Thieme Verlag, Stuttgart, 1981, pp. 41–87.
- 3 W. REPPE, W. J. SCHWECKENDIECK, *Liebigs Ann. Chem.* **1948**, 560, 104–116; cf. W. REPPE, *Neue Entwicklungen auf dem Gebiet des Acetylens und Kohlenoxids*, Springer Verlag, Heidelberg, 1949, and W. REPPE, *Experientia* **1949**, 5, 93–110.
- 4 H. HOPF, plenary lecture at the International Symposium of Novel Aromatic Systems (ISNA-9), Hong Kong, 1998.
- 5 For a summary, see: R. F. C. BROWN, *Pyrolytic Methods in Organic Chemistry*, Academic Press, New York, 1980; cf. R. F. C. BROWN, *Eur. J. Org. Chem.* **1999**, 3211–3222, and refs. cited therein.
- 6 H. HOPF, H. MUSSO, *Angew. Chem.* **1969**, 81, 704; *Angew. Chem. Int. Ed. Engl.* **1969**, 8, 680.
- 7 R. G. BERGMAN, *Acc. Chem. Res.* **1973**, 6, 25–31.
- 8 For the determination of the activation parameters of the Bergman and related processes, see W. R. ROTH, H. HOPF, C. HORN, *Chem. Ber.* **1994**, 127, 1765–1779.
- 9 For a recent review, see: G. ZIMMERMANN, *Eur. J. Org. Chem.* **2001**, 457–471.
- 10 For the first preparation of isobenzene, see: M. CHRISTL, M. BRAUN, G. MÜLLER, *Angew. Chem.* **1992**, 104, 471–473; *Angew. Chem. Int. Ed. Engl.* **1992**, 31, 473–475; cf. M. CHRISTL, S. GROETSCH, *Eur. J. Org. Chem.* **2000**, 1871–1874.
- 11 H. HOPF, H. BERGER, G. ZIMMERMANN, U. NÜCHTER, P. G. JONES, I. DIX, *Angew. Chem.* **1997**, 109, 1236–1238; *Angew. Chem. Int. Ed. Engl.* **1997**, 36, 1187–1190.
- 12 H. BERGER, planned Ph.D. dissertation, Braunschweig, 2002.
- 13 1,2-Bismethylenecyclobutanes are commonly observed dimerization products of acyclic and cyclic allenes: H. HOPF, in *The Chemistry of the Allenes* (Ed.: S. R. LANDOR) Academic Press, London, 1982, pp. 525–562.
- 14 H. MEIER, N. HANOLD, H. KOLSHORN, *Angew. Chem.* **1982**, 94, 67–68; *Angew. Chem. Int. Ed. Engl.* **1982**, 21, 66–67; cf. N. HANOLD, H. MEIER, *Chem. Ber.* **1985**, 118, 198–209.
- 15 H. HOPF, A. KRÜGER, *Chem. Eur. J.* **2001**, 7, 4378–4385; cf. M. PRALL, H. HOPF, P. SCHREINER, A. KRÜGER, *Chem. Eur. J.* **2001**, 7, 4386–4394.
- 16 J. HOFMANN, K. SCHULZ, A. ALTMAN, M. FINDEISEN, G. ZIMMERMANN, *Liebigs Ann./Recueil* **1997**, 2541–2548; cf. K. SCHULZ, J. HOFMANN, G. ZIMMERMANN, *Eur. J. Org. Chem.* **1998**, 2135–2142.
- 17 R. F. C. BROWN, F. W. EASTWOOD, K. J. HARRINGTON, G. L. McMULLEN, *Aust. J. Chem.* **1974**, 27, 2393–2402; cf. R. F. C. BROWN, F. W. EASTWOOD, G. P. JACKMAN, *Aust. J. Chem.* **1977**, 30, 1757–1767.
- 18 For a recent summary of the extensive literature, see H. HOPF, *Classics in Hydrocarbon Chemistry*, Wiley-VCH, Weinheim, 2000, Ch. 12.2, pp. 330–336.
- 19 S. HAGEN, H. HOPF, *Top. Curr. Chem.* **1998**, 196, 45–89.
- 20 L. T. SCOTT, M. M. HASHEMI, D. T. MEYER, H. B. WARREN, *J. Am. Chem. Soc.* **1991**, 113, 7082–7084; cf. L. T. SCOTT, *Pure Appl. Chem.* **1996**, 68, 291–300 and refs. cited therein.
- 21 P. W. RABIDEAU, A. H. ABDOURAZAK, H. E. FOLSOM, Z. MARZINOW, A. SYGULA, R. J. SYGULA, *J. Am. Chem. Soc.* **1994**, 116, 7891–7892.
- 22 M. MATSUDA, H. MATSUBARA, M. SATO, S. OKAMOTO, K. YAMAMOTO, *Chem. Lett.* **1996**, 157–158.
- 23 G. ZIMMERMANN, U. NÜCHTER, S. HAGEN, M. NÜCHTER, *Tetrahedron Lett.* **1994**, 35, 4747–4750.
- 24 C. GLASER, *Ber. Dtsch. Chem. Ges.* **1869**, 2, 422–424.
- 25 G. EGLINTON, A. R. GALBRAITH, *Chem. Ind. (London)* **1956**, 737–738; cf. G. EGLINTON, A. R. GALBRAITH, *J. Chem. Soc.* **1959**, 889–896.
- 26 A. S. HAY, *J. Org. Chem.* **1962**, 27, 3320–3321.
- 27 W. CHODKIEWICZ, P. CADIOT, *Compt. Rend.* **1955**, 241, 1055; cf. W. CHODKIEWICZ, *Ann. Chim.* **1957**, 2, 819–869 and P. CADIOT, W. CHODKIEWICZ, in *The Chemistry of Acetylenes* (Ed.: H. G. VIEHE), Marcel Dekker, New York, 1969, Chapter 9, pp. 597–647.
- 28 C. E. STEPHENS, R. D. CASTRO, *J. Org. Chem.* **1963**, 28, 2163; for a review, see A. M. SLADKOV, I. R. GOL'DING, *Russ. Chem. Rev.* **1979**, 48, 868–896.

- 29 For a recent review, see: A. DE MEIJERE, F. E. MEYER, *Angew. Chem.* **1994**, 106, 2473–2506; *Angew. Chem. Int. Ed. Engl.* **1994**, 33, 1943–1962.
- 30 K. SONOGASHIRA, Y. TOHDA, N. HAGIHARA, *Tetrahedron Lett.* **1975**, 4467–4470; cf. K. SONOGASHIRA, *Comprehensive Organic Synthesis*, Vol. 3, Pergamon Press, Oxford, **1990**, pp. 521–549, and K. MÜLLEN, S. VALIYAVEETIL, V. FRANCKE, V. S. IYER, in *Molecular Wires*, NATO-AST Series, Kluwer Int. Press, **1997**.
- 31 F. DIEDERICH, P. J. STANG (Eds.), *Metal-Catalyzed Cross-Coupling Reactions*, Wiley-VCH, Weinheim, **1998**.
- 32 R. DIERCKS, J. D. ARMSTRONG, R. BOESE, K. P. C. VOLLHARDT, *Angew. Chem.* **1986**, 98, 270–271; *Angew. Chem. Int. Ed. Engl.* **1986**, 25, 268–269.
- 33 K. SANESHIKA, T. YAMAMOTO, A. YAMAMOTO, *Bull. Chem. Soc. Jpn.* **1984**, 57, 752–755; cf. M. E. WRIGHT, *Macromolecules* **1989**, 22, 3256–3259.
- 34 Reviews: J. K. YOUNG, J. S. MOORE, in *Modern Acetylene Chemistry* (Eds.: P. J. STANG, F. DIEDERICH), VCH Verlagsgesellschaft, Weinheim, **1995**, pp. 415–442; J. F. MOORE, *Acc. Chem. Res.* **1997**, 30, 402–413.
- 35 R. H. GRUBBS, D. KRATZ, *Chem. Ber.* **1993**, 126, 149–157.
- 36 R. BOESE, J. R. GREEN, J. MITTENDORF, D. L. MOHLER, K. P. C. VOLLHARDT, *Angew. Chem.* **1992**, 104, 1643–1645; *Angew. Chem. Int. Ed. Engl.* **1992**, 31, 1643–1645.
- 37 M. M. HALEY, J. J. PAK, S. C. BRAND, *Top. Curr. Chem.* **1999**, 201, 81–130.
- 38 G. EGLINTON, A. R. GALBRAITH, *Proc. Chem. Soc.* **1957**, 350; cf. O. M. BEHR, G. EGLINTON, A. R. GALBRAITH, R. A. RAPHAEL, *J. Chem. Soc.* **1960**, 3614–3625.
- 39 Q. ZHOU, P. J. CARROLL, T. M. SWAGER, *J. Org. Chem.* **1994**, 59, 1294–1301.
- 40 M. M. HALEY, W. B. WAN, in *Advances in Strained and Interesting Organic Molecules* (Ed.: B. HALTON), JAI Press, Inc., Stamford, CT, **2000**, pp. 1–41.
- 41 M. L. BELL, R. C. CHIECHI, C. A. JOHNSON, D. B. KIMBALL, A. J. MATZGER, W. B. WAN, T. J. R. WEAKLEY, M. M. HALEY, *Tetrahedron* **2001**, 57, 3507–3520.
- 42 W. B. WAN, S. C. BRAND, J. J. PAK, M. M. HALEY, *Chem. Eur. J.* **2000**, 6, 2044–2052.
- 43 W. B. WAN, M. M. HALEY, *J. Org. Chem.* **2001**, 66, 3893–3901.
- 44 J. D. TOVAR, N. JUX, T. JARROSSON, S. I. KHAN, Y. RUBIN, *J. Org. Chem.* **1997**, 62, 3422–3433.
- 45 W. B. WAN, R. C. CHIECHI, T. J. R. WEAKLEY, M. M. HALEY, *Eur. J. Org. Chem.* **2001**, 3487–3490; cf. A. J. BOYDSTON, M. M. HALEY, *Org. Lett.* **2001**, 3, 3599–3601.
- 46 J. J. PAK, T. J. R. WEAKLEY, M. M. HALEY, *J. Am. Chem. Soc.* **1999**, 121, 8182–8192.
- 47 A. SARKAR, M. M. HALEY, *Chem. Commun.* **2000**, 1733–1734.
- 48 J. R. FRITCH, K. P. C. VOLLHARDT, *Organometallics* **1982**, 1, 590–602.
- 49 M. LASKOSKI, M. D. SMITH, J. G. M. MORTON, U. H. F. BUNZ, *J. Org. Chem.* **2001**, 66, 5174–5181.
- 50 M. LASKOSKI, G. ROIDL, M. D. SMITH, U. H. F. BUNZ, *Angew. Chem.* **2001**, 113, 1508–1511; *Angew. Chem. Int. Ed.* **2001**, 1460–1463.
- 51 M. LASKOSKI, W. STEFFEN, M. D. SMITH, U. H. F. BUNZ, *Chem. Commun.* **2001**, 691–692.
- 52 J. M. HUNTER, J. L. FYE, E. J. ROSKAMP, M. F. JARROLD, *J. Phys. Chem.* **1994**, 98, 1810–1818.
- 53 K. P. C. VOLLHARDT, *Angew. Chem.* **1984**, 96, 525–541; *Angew. Chem. Int. Ed. Engl.* **1984**, 23, 539–555; cf. N. E. SCHORE, *Chem. Rev.* **1988**, 88, 1081–1119.
- 54 K. P. C. VOLLHARDT, D. L. MOHLER, in *Advances in Strain in Organic Chemistry* (Ed.: B. HALTON), JAI Press, Inc., Greenwich, CT, Vol. V, **1996**, 121–160.
- 55 B. C. BERRIS, G. H. HOVAKEEMIAN, Y.-H. LAI, H. MESTDAGH, K. P. C. VOLLHARDT, *J. Am. Chem. Soc.* **1985**, 107, 5670–5687; cf. R. L. FUNK, K. P. C. VOLLHARDT, *J. Am. Chem. Soc.* **1980**, 102, 5253–5261.
- 56 R. BOESE, A. J. MATZGER, D. L. MOHLER, K. P. C. VOLLHARDT, *Angew. Chem.* **1995**, 107, 1630–1633; *Angew. Chem. Int. Ed. Engl.* **1995**, 34, 1478–1481 and refs. cited therein.
- 57 N. L. FRANK, K. K. BALDRIDGE, J. J. SIEGEL, *J. Am. Chem. Soc.* **1995**, 117, 2102–2103.
- 58 Review: K. C. NICOLAOU, A. L. SMITH, in *Modern Acetylene Chemistry* (Eds.: P. J. STANG, F. DIEDERICH), VCH Verlagsgesellschaft, Weinheim, **1995**, pp. 203–283.

- 59 K. K. WANG, *Chem. Rev.* **1996**, 96, 207–222.
- 60 J. W. GRISSOM, G. U. GUNAWARDENA, D. KLINGBERG, D. H. HUANG, *Tetrahedron* **1996**, 52, 6453–6518.
- 61 D. M. BOWLES, G. J. PALMER, C. A. LANDIS, J. L. SCOTT, J. E. ANTHONY, *Tetrahedron* **2001**, 57, 3753–3760.
- 62 D. J. CRAM, J. M. CRAM, *Acc. Chem. Res.* **1971**, 4, 204–213.
- 63 D. J. CRAM, J. M. CRAM, *Container Molecules and Their Guests*, Royal Society of Chemistry, London, **1992**.
- 64 P. M. KEEHN, S. M. ROSENFELD (Eds.), *Cyclophanes I and II*, Academic Press, New York, N.Y., **1983**.
- 65 F. DIEDERICH, *Cyclophanes*, Royal Society of Chemistry, London, **1991**.
- 66 F. VÖGTLE, *Cyclophane Chemistry*, J. Wiley and Sons, Chichester, **1993**.
- 67 G. J. BODWELL, *Angew. Chem.* **1996**, 108, 2221–2224; *Angew. Chem. Int. Ed. Engl.* **1996**, 35, 2085–2088; cf. A. DE MEIJERE, B. KÖNIG, *Synlett* **1997**, 1221–1232.
- 68 For a recent summary of pertinent references, see: V. ROZENBERG, T. DANILOVA, E. SERGEEVA, E. VORONTSOV, Z. STARIKOVA, A. KORLYUKOV, H. HOPF, *Eur. J. Org. Chem.* **2002**, 468–477.
- 69 H. HOPF, V. ROZENBERG, L. POPOVA, *Helv. Chim. Acta* **2002**, 85, 431–441.
- 70 J. LAHANN, H. HÖCKER, R. LANGER, *Angew. Chem.* **2001**, 113, 746–749, *Angew. Chem. Int. Ed.* **2001**, 40, 726–728; cf. J. LAHANN, D. KLEE, H. HÖCKER, *Macromol. Rapid Commun.* **1998**, 19, 441–444.
- 71 H. HOPF, C. WERNER, P. G. JONES, P. BUBENITSCHKE, *Angew. Chem.* **1995**, 107, 2592–2594; *Angew. Chem. Int. Ed. Engl.* **1995**, 34, 2367–2368.
- 72 H. SATO, N. ISONO, K. OKAMURA, T. DATE, M. MORI, *Tetrahedron Lett.* **1994**, 35, 2035–2038.
- 73 Review: M. MORI, N. ISONO, H. WAKAMATSU, *Synlett* **1999**, 269–280.
- 74 H. HOPF, CHR. WERNER, *Eur. J. Org. Chem.*, in preparation.
- 75 F. SONDHEIMER, R. WOLOVSKY, *J. Am. Chem. Soc.* **1962**, 84, 260–269; cf. F. SONDHEIMER, *Acc. Chem. Res.* **1972**, 5, 81–91.
- 76 A. J. BOYDSTON, L. BONDARENKO, I. DIX, T. J. R. WEAKLEY, H. HOPF, M. M. HALEY, *Angew. Chem.* **2001**, 113, 3074–3077; *Angew. Chem. Int. Ed.* **2001**, 40, 2986–2989.
- 77 Y. RUBIN, T. C. PARKER, S. I. KHAN, C. L. HOLLIMAN, S. W. McELVANY, *J. Am. Chem. Soc.* **1996**, 118, 5308–5309; cf. Y. RUBIN, *Chem. Eur. J.* **1997**, 3, 1009–1016.
- 78 Y. TOBE, N. NAKAGAWA, J. KISHI, M. SONODA, K. NAEMURA, T. WAKABAYASHI, T. SHIDA, Y. ACHIBA, *Tetrahedron* **2001**, 57, 3629–3636.
- 79 W. KRÄTSCHMER, L. D. LAMB, K. FOSTIROPOLOUS, R. D. HUFFMAN, *Nature* **1990**, 347, 354–358.
- 80 H. HOPF, M. PSIORZ, *Angew. Chem.* **1982**, 94, 639–640; *Angew. Chem. Int. Ed. Engl.* **1982**, 21, 623–624.

6

Functional Conjugated Materials for Optonics and Electronics by Tetraethynylethene Molecular Scaffolding

Mogens Brøndsted Nielsen and François Diederich

Abstract

The physical properties of scaffolds based on tetraethynylethene (TEE; 3,4-diethynylhex-3-ene-1,5-diyne) are strongly enhanced by arylation. Indeed, owing to the coplanarity of anilino-substituted TEE scaffolds, very high third-order optical nonlinearities are obtained. Moreover, arylated TEEs are able to undergo photochemically induced *cis-trans* isomerization, paving the way for applications as light-driven molecular switches in optoelectronic devices. Suitably functionalized TEE modules are readily incorporated into linear and cyclic π -conjugated scaffolds, employing stepwise acetylenic coupling protocols. Thus, TEE molecular scaffolding has provided access to large, macrocyclic, all-carbon cores and long poly(triacetylene) (PTA) oligomers.

6.1

Introduction

Acetylenic scaffolding [1] of derivatized tetraethynylethenes (TEE; 3,4-diethynylhex-3-ene-1,5-diyne; Figure 1) has provided access to advanced materials for electronic and photonic applications, such as chromophores with high second- and third-order optical nonlinearities, molecular photochemical switches, large two-dimensional carbon cores, and linearly π -conjugated molecular rods [2]. The physical properties of these materials rely strongly on the presence of arene units. Indeed, the six potential two-dimensional conjugation pathways (Figure 1) within the TEE unit can be controlled by arylation, hence providing the functional properties of the molecules.

In this chapter, we demonstrate how aryl groups, of either electron-donating or -accepting nature, determine the properties of a number of linear and cyclic scaffolds based on TEE. These scaffolds have been assembled by employing a number of metal-catalyzed coupling reactions. Thus, arylated TEEs are readily prepared by Pd-catalyzed cross-coupling of arylacetylenes with vinylic dibromides under Sonogashira [3] conditions (Scheme 1). Synthetic strategies developed during the last ten years have allowed access to TEEs with almost any desired substitution pattern about the central ten-carbon core. These methods have been covered in some recent review articles [4].

The construction of conjugated advanced materials based on functionalized TEE mono-

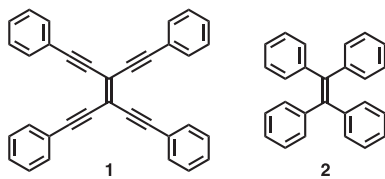


Fig. 2. The phenyl-substituted TEE **1** is planar in contrast to **2** [9, 10].

6.2

Arylated Tetraethynylethenes

The unique TEE framework facilitates π -conjugation with pendant aromatic substituents by allowing coplanar orientation throughout the molecular core, as was first witnessed in the X-ray crystal structure of tetrakis(phenylethynyl)ethene **1** determined by Hopf and co-workers [9]. In contrast, coplanarity is prevented by steric interactions in molecules such as *cis*-stilbenes or tetraphenylethene **2** [10] (Figure 2). The planarity makes it possible for **1** to form highly ordered 1:2 stoichiometric donor–acceptor π -complexes in the solid state with electron-deficient molecules such as 2,4,7-trinitrofluoren-9-one and (2,4,7-trinitrofluoren-9-ylidene)malonitrile [11]. In solution, relatively weak 1:1 complexes with each of these two acceptors are formed, with association constants of 7.9 M^{-1} and 31.5 M^{-1} , respectively, at 300 K in CDCl_3 .

The coplanarity has endowed arylated TEEs with some of the highest known third-order optical nonlinearities and, in the case of acentricity, also very large second-order nonlinear optical effects. Furthermore, the strain-free planarity allows *cis*- and *trans*-arylated TEEs to interconvert upon photochemical excitation without competition from undesirable thermal isomerization.

6.2.1

Nonlinear Optical Properties

The development of highly active third-order nonlinear optical (NLO) materials is important for all-optical signal processing. A comprehensive study by Günter, Bosshard, and co-workers [12] on the NLO properties of derivatized TEEs established useful structure–property relationships and provided insight into routes leading to desired optical nonlinearities. The following fundamental conclusions were drawn by comparison of compounds **3**–**11** depicted in Figure 3: (i) Donor substitution (e.g. with *N,N*-dimethylanilino) gives higher second hyperpolarizabilities (γ) than acceptor substitution (4-nitrophenyl) (*trans*-**6** versus *trans*-**4**), and the magnitude of γ increases with donor strength (**7** versus **5**). Similar increases in γ as a result of increased electron density have been observed in one-dimensional systems such as stilbenes [13], polyenes [14], as well as various carotenoid systems [15]. (ii) Acentricity leads to larger γ values (*trans*-**9** versus *trans*-**8**). The significance of asymmetry in third-order NLO chromophores was initially postulated by Garito *et al.* [16], and this prediction has been confirmed experimentally for other linearly conjugated molecules [14, 17]. (iii) TEEs with donor and acceptor groups in *trans* or *cis* configurations exhibit much higher nonlinearities on account of favorable linear donor–acceptor conjugation (routes *a* and *b* in Figure 1) than TEEs with substituents in a geminal configuration, in

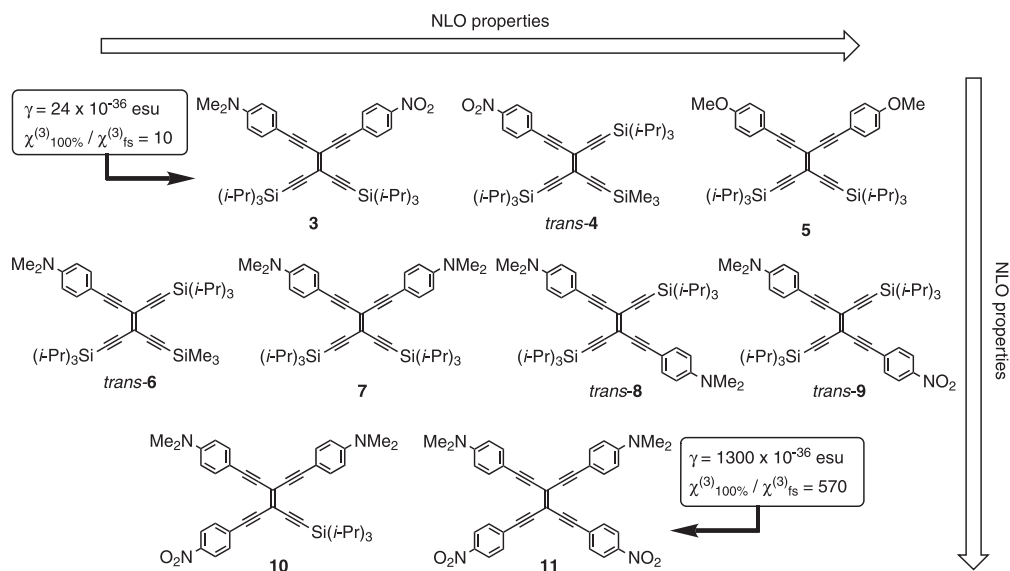


Fig. 3. The second hyperpolarizability γ and third-order nonlinear optical susceptibility $\chi^{(3)}_{100\%}$ increase in the sequence from **3** to **11** [12a]. The values given for **3** and **11** were determined under non-resonant conditions by third-harmonic genera-

tion experiments at a laser wavelength of 1.907 μm (third-harmonic wavelength 636 nm). $\chi^{(3)}_{100\%}$ was measured relative to $\chi^{(3)}$ of fused silica (fs) [12g], for which a value of $\chi^{(3)}_{\text{fs}} = 1.16 \times 10^{-14}$ esu was used (adjusted value relative to ref. [12a]).

which only the weaker cross-conjugation is effective (route *c* in Figure 1) (*trans*-**8** versus **7**, *trans*-**9** versus **3**). (iv) A substantial increase in γ is observed upon extending the conjugation length (as in TEE dimers, *vide infra*). (v) Full, two-dimensional conjugation with as many as six conjugation pathways leads to very large γ values (**11**).

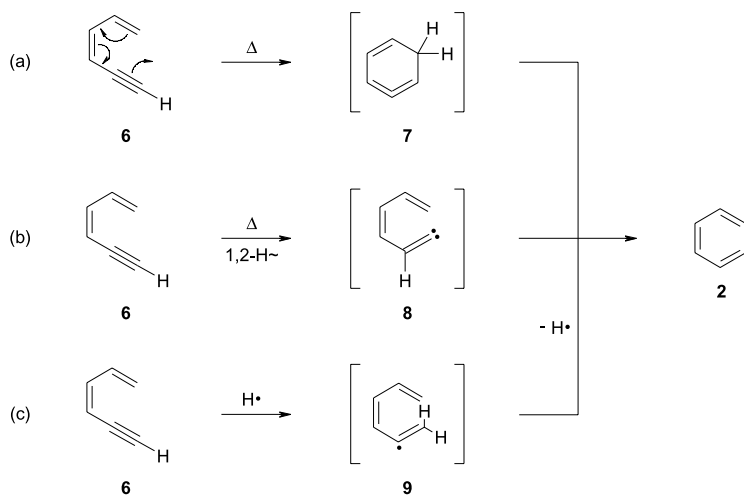
Since benzenoid aromaticity is reduced in thiophene as compared to benzene, thiophene exhibits an increased capacity to transmit linear π -electron conjugation, which can lead to an enhanced NLO response. This capacity has been demonstrated theoretically [18] and experimentally for both second- [19] and third-order [20] NLO effects. Replacement of one 4-nitrophenyl ring in **11** by a 5-nitro-2-thienyl moiety leads to an increase in γ by a factor of 1.3, as revealed by third-harmonic generation measurements at a laser wavelength of 2.1 μm (third-harmonic wavelength 700 nm) [12e]. However, this enhancement is more a result of the lowered molecular symmetry than of the nitrothienyl group itself, since substituting both nitrophenyl groups only increases γ by a factor of 1.1. Thus, within the uncertainty of the measurements, γ remains essentially unchanged when both nitrophenyl groups in **11** are replaced.

6.2.2

Photochemically Controlled *cis-trans* Isomerization: Molecular Switches

One very interesting property of arylated TEEs is their ability to undergo reversible, photochemical *cis-trans* isomerization [21], a property that is not exhibited by the non-arylated derivatives. The *trans*-to-*cis* isomerization is of preparative use for the synthesis of *cis*-TEEs that

are otherwise difficult to prepare. For example, *trans*-**9** is converted to its *cis* isomer (37 % yield) by irradiation at 366 nm [22]. Moreover, the isomerization process has been employed for the construction of light-driven molecular switches [23]. Recently, the complex, highly programmed system *trans*-**12a** (Scheme 3) was developed, combining the *cis/trans*-isomerizable TEE unit with two other addressable subunits, a photoswitchable dihydroazulene (DHA)/vinylheptafulvene (VHF) moiety, and a proton-sensitive dimethylaniline (DMA) group [23a, 23c]. This three-way chromophoric molecular switch is, in principle, able to perform individual, reversible switching cycles between as many as eight states. DHA derivatives are known to undergo, upon light irradiation, a 10-electron retro-electrocyclization to the isomeric VHF compounds [24], which, in turn, undergo a thermal cyclization back to the DHA forms. However, this switching capacity of the DHA chromophore is affected when it is incorporated into the TEE derivative *trans*-**12a**. Thus, irradiation of *trans*-**12a** results only in reversible *trans*–*cis* isomerization of the TEE core, leaving the DHA moiety unchanged. On the other hand, protonation of the third subunit, the DMA substituent, triggers the DHA → VHF photoreaction. Indeed, irradiation of the protonated species *trans*-**12b** causes retro-electrocyclization to *trans*-**12c**, which can thermally cyclize back to *trans*-**12b**. Clean isobestic points in the UV/vis spectra imply that only this DHF/VHF equilibrium is operative, which can be explained by the fact that the TEE *trans*–*cis* isomerization process is much



Scheme 3. “Three-dimensional” switching diagram of TEE-DHA-DMA hybrid derivative *trans*-**12a**, a three-way chromophoric molecular switch. Six out of eight possible states can be attained [23c].

slower. Deprotonation of *trans*-**12c** by triethylamine does not offer a route to *trans*-**12d**, but is accompanied by retro-electrocyclization to *trans*-**12a**. Thus, the non-protonated VHF-containing conjugate *trans*-**12d** (as well as the VHF isomer *cis*-**12d**) cannot be reached in the three-dimensional switching diagram. Consequently, of the eight potential states of **12**, six are accessible and can be individually addressed by the various switching modes.

The failure of photochemical DHA \rightarrow VHF isomerization in *trans*-**12a** was rationalized through a joint experimental and computational study by Lüthi and co-workers [25]. The neutral conjugate showed a strong fluorescence emission that almost completely disappeared after protonation to *trans*-**12b**. The maximum of this intense emission was found to be strongly dependent on solvent polarity, and in hexane a dual fluorescence ($\lambda_{\text{max}} = 505$ and 541 nm; $\lambda_{\text{exc}} = 420$ nm) was observed. In more polar solvents, such as CH_2Cl_2 , the emission spectrum featured only a single, strongly red-shifted band ($\lambda_{\text{max}} = 602$ nm). Time-dependent density functional calculations on the excited state of related DMA-substituted TEEs suggested that the DHA \rightarrow VHF isomerization channel is quenched in *trans*-**12a** by an efficient relaxation of the vertically excited singlet state to an emitting twisted intramolecular charge-transfer (TICT) state [26], which would explain the experimentally observed dual fluorescence. In this lower-energy TICT state, either the dimethylamino group is twisted into an orthogonal position with respect to the planar arylated TEE moiety or the entire DMA group adopts an orthogonal orientation with respect to the TEE moiety. The calculations suggested that the twist of the dimethylamino group is more probable.

6.2.3

Electrochemically Controlled *cis*–*trans* Isomerization

A combined computational and electrochemical investigation revealed that arylated TEEs may also have potential as electrochemically driven molecular switches [27]. The electrochemical studies showed that the first reduction potentials of mono- and bis(4-nitrophenyl)-substituted TEEs occur at similar values (around -1.35 to -1.38 V versus the ferrocene/ferricinium couple, Fc/Fc^+) on steps involving one and two electrons, respectively. Moreover, the first reduction potential of nitrophenyl-substituted TEEs is hardly affected by the presence of other aryl substituents, such as the DMA donor groups, attached to the TEE frame. These findings suggest that the nitrophenyl redox centers behave as independent redox centers. However, *ab initio* calculations on singly-reduced *trans*-**13** (Figure 4)

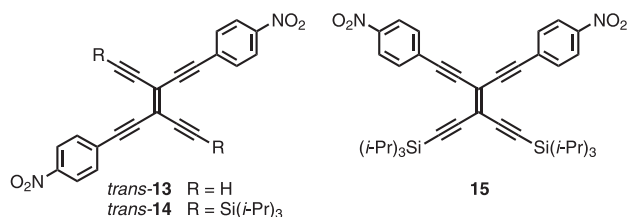
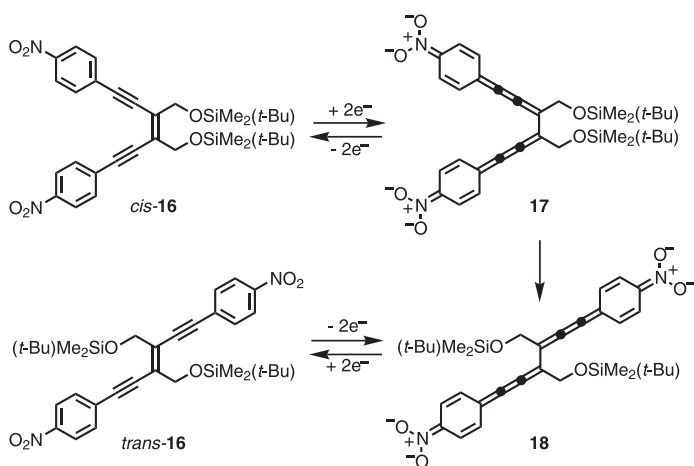


Fig. 4. Bis(4-nitrophenyl)-substituted TEEs. The linear conjugation pathway between the two nitrophenyl groups makes the second one-electron reduction of *trans*-**14**, generating the trianion, more difficult (by ~ 80 mV) than for the geminally substituted **15** [27].

suggested that the charge is actually localized on the TEE core. Indeed, the second reduction of the Si(*i*Pr)₃-protected derivative of *trans*-**13**, that is *trans*-**14**, in which the two nitrophenyl groups are linearly conjugated, was found to be more difficult (by ~80 mV) than that of the geminally substituted, cross-conjugated TEE **15**. Thus, charge delocalization into the TEE core of dianionic *trans*-**14** augments the energetic requirements for the second reduction step forming the trianion. For the generated dianion of *trans*-**14**, linear delocalization results in a cumulenenic/quinoind structure, in which the central TEE bond acquires significant single-bond character. This structure allows rotation about this central bond and hence isomerization. Spectroelectrochemical experiments on the *cis*-enediynes *cis*-**16** offered support for this theoretically predicted cumulenenic-type intermediate, since it was found to isomerize irreversibly, via **17** and **18**, to its *trans* isomer (Scheme 4). However, *cis*-**16** can be photochemically regenerated, although the photoequilibrium only slightly favors it relative to *trans*-**16** ($K_{\text{photo}} = [\textit{cis}]/[\textit{trans}] = 1.2$ in *n*-hexane, 27 °C, $\lambda_{\text{exc}} = 360$ nm) [28]. Accordingly, *cis*/*trans*-**16** behaves as a molecular switch that is turned on (*trans*) by electrons and off (*cis*/*trans* mixture) by light. The quantum yield for the *trans* → *cis* conversion is $\phi_{\text{trans} \rightarrow \textit{cis}} = 0.14$, and for the opposite conversion it is $\phi_{\textit{cis} \rightarrow \textit{trans}} = 0.27$ ($\lambda_{\text{exc}} = 360$ nm). Replacing one 4-nitrophenyl acceptor group in *cis*-**16** with a DMA donor group has a substantial impact on both the photoequilibrium constant and the quantum yields: $K_{\text{photo}} = 33.5$, $\phi_{\textit{trans} \rightarrow \textit{cis}} = 0.080$, $\phi_{\textit{cis} \rightarrow \textit{trans}} = 0.0080$ ($\lambda_{\text{exc}} = 405$ nm) [28].

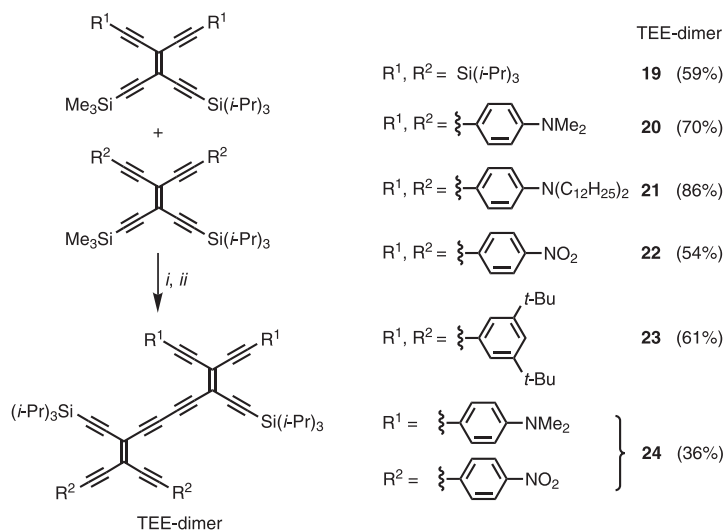


Scheme 4. Proposed mechanism for electrochemical *cis*-*trans* isomerization of enediyne **16** [27].

6.3

Tetraethynylethene Dimers

The simplest scaffolding with TEE is the linking of two ten-carbon cores by a C(sp)–C(sp) single bond under oxidative conditions. By selective deprotection of the trimethylsilyl group with K₂CO₃ in MeOH/THF, leaving the triisopropylsilyl group unreacted, followed by an oxidative Eglinton or Hay coupling, a selection of TEE dimers (**19**–**24**) was prepared (Scheme 5) [29].



Scheme 5. Synthesis of TEE dimers by selective desilylation-oxidative coupling methodology [29]. i) K_2CO_3 , MeOH, THF; ii) anhydrous $\text{Cu}(\text{OAc})_2$, pyridine, air (for **19**) or CuCl , TMEDA, CH_2Cl_2 , air (for **20–24**). TMEDA = *N,N,N',N'*-tetramethylethylenediamine.

The electronic properties of these dimers were studied by UV/vis spectrophotometry. The absorption spectra of the anilino-substituted compounds **20**, **21**, and **24** display broad absorption shoulders at low energy (λ_{max} in the range 550–580 nm), with end-absorptions extending to 600 nm and beyond. These bands were assigned to charge-transfer (CT) transitions; this was confirmed by protonation with conc. aqueous HCl of the electron-donating anilino groups, which resulted in complete loss of the CT transition [29d]. From these studies it was inferred that the central conjugated C_{20} core in the TEE dimers, with its 16 C(sp) atoms, is a strong electron-acceptor and that the electron-accepting properties are only weakly enhanced by the two 4-nitrophenyl substituents in the donor–acceptor push–pull system **24**. Indeed, this strong acceptor property is not surprising, taking into account the ability of nitrophenyl-substituted TEEs to convey a negative charge from the nitrophenyl group into the carbon framework, as described in the previous paragraph. Moreover, absorption spectra of anilino-substituted TEE monomers reveal a CT transition that is lost upon protonation [12b, 22]. For both the TEE monomers and dimers, this quenching proved to be reversible: treatment of the protonated forms with NaOH regenerated the neutral species, and the UV/vis spectra became virtually identical to those measured before acid treatment. In addition, the first reduction of **20** ($E^\circ = -1.61$ V versus Fc/Fc^+ in CH_2Cl_2 [29d]) is cathodically shifted relative to that of **19** ($E^\circ = -1.52$ V versus Fc/Fc^+ in THF [29b]) as a result of electron donation from the anilino groups into the carbon core of **20**. The anilino groups of **20** are oxidized in two reversible two-electron steps at +0.37 and +0.54 V.

Further extension of the chromophores in **25**, by two anilinoethynyl groups (Figure 5), leads to a significant bathochromic shift of the longest-wavelength absorption band ($\lambda_{\text{max}} = 616$ nm (shoulder), end-absorption ~ 750 nm). Thus, the chromophoric properties of

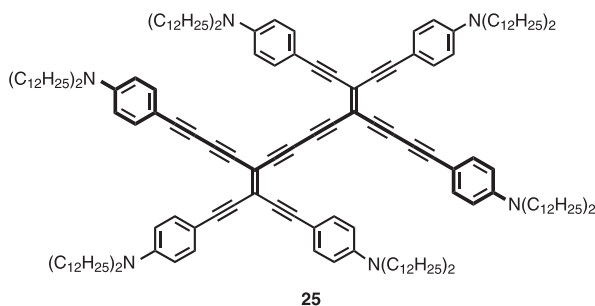


Fig. 5. Extended TEE dimer, containing a long linear conjugation path (shown in bold) [29d].

TEE dimers are readily tunable upon aryl substitution, extending the absorption range into the near-IR region [29d].

The long linear conjugation in TEE dimers **20** and **24** causes almost a doubling of the second hyperpolarizabilities relative to that of TEE monomer **11** (Figure 3), containing the same number of aryl groups [29d]: $\gamma = 2036 \times 10^{-36}$ esu for **20**, $\gamma = 2243 \times 10^{-36}$ esu for **24**, measured by third-harmonic generation experiments at a wavelength of 1.907 μm (third-harmonic wavelength: 636 nm). However, it is important to note that this increase in γ corresponds to an increase in the molecular weight, leaving the macroscopic nonlinearities almost unaltered: $\chi^{(3)}_{100\%}/\chi^{(3)}_{\text{fs}} = 519$ for **20**, $\chi^{(3)}_{100\%}/\chi^{(3)}_{\text{fs}} = 570$ for **24** (fs = fused silica: $\chi^{(3)}_{\text{fs}} = 1.16 \times 10^{-14}$ esu).

6.4

Two-Dimensional Scaffolding: Expanded Carbon Cores

Based on either *cis*-substituted or geminally substituted TEE derivatives, two families of macrocycles have been constructed, namely perethynylated dehydroannulenes and expanded radialenes.

6.4.1

Perethynylated Dehydroannulenes

Glaser–Hay macrocyclization of *cis*-bis(trialkylsilyl)-protected TEEs generated the perethynylated octadehydro[12]annulenes **26a,b** and dodecahydro[18]annulenes **27a,b** (Figure 6) with fully planar π -conjugated carbon cores as evidenced by X-ray crystallography [30]. The $4n + 2$ ($n = 4$) π electron cycles **27a,b** possess a large HOMO-LUMO gap (2.57 eV in pentane) and are aromatic, as is the parent, unsubstituted dodecahydro[18]annulene prepared by Okamura and Sondheimer in 1967 [31]. In contrast, the $4n$ ($n = 3$) π electron cycles **26a,b** possess a small HOMO-LUMO gap (1.87 eV) and are anti-aromatic like the parent, unsubstituted octadehydro[12]annulene that was synthesized simultaneously by two different groups in 1966 [32, 33]. Electrochemical studies [29b, 30b] showed that [12]annulene **26b** is more readily reduced than [18]annulene **27b** ($E^\circ = -0.99$ and -1.46 V for **26b**, $E^\circ = -1.12$, -1.52 , and -1.91 V for **27b**, versus Fc/Fc^+ , in THF). Indeed, **27b** loses its

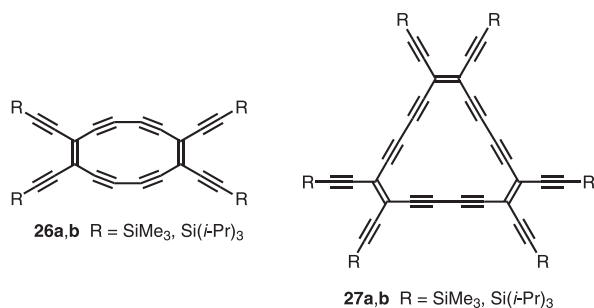


Fig. 6. Planar, perethynylated aromatic (27a,b) and anti-aromatic (26a,b) dehydroannulenes [30].

Hückel aromaticity upon reduction, whereas 26b gains aromaticity ($4n + 2$, $n = 3$) when converted to its dianion. The effect of substituting the peripheral silyl groups by aromatic groups still needs to be explored for these perethynylated dehydroannulenes.

6.4.2

Perethynylated Expanded Radialenes

Expanded radialenes are a family of macrocycles derived from radialenes [34] by the formal insertion of ethynediyl or buta-1,3-diynediyl moieties into the cyclic framework between each pair of vicinal *exo* methylene units. Geminally substituted TEEs, as well as TEE dimers, are perfect building blocks for the construction of perethynylated expanded radialenes. Thus, by bis-deprotection of a suitable bis-silylated TEE precursor, followed by oxidative coupling under high-dilution conditions, the expanded $[n]$ radialenes 28a–c ($n = 3–5$) were prepared (Figure 7) [29]. The expanded [6]radialene 28d, as well as the expanded $[n]$ radialenes 29a,c ($n = 4, 6$) and 30a–c ($n = 4, 6, 8$) were prepared in a similar manner by cyclization of TEE dimers 21, 19, and 23, respectively, after their desilylation by treatment with tetrabutylammonium fluoride. The expanded [5]radialene 29b was obtained by cyclizing dimer 19, after bis-deprotection, with a related TEE trimer. A study of the electronic properties of these three differently substituted series of expanded radialenes (R = Si(*i*Pr)₃, 3,5-di(*t*Bu)Ph, or *p*-(C₁₂H₂₅)₂NPh) provided fundamental information regarding π -electron delocalization in cyclic systems, where both linear and cross-conjugative pathways can be operational [29d].

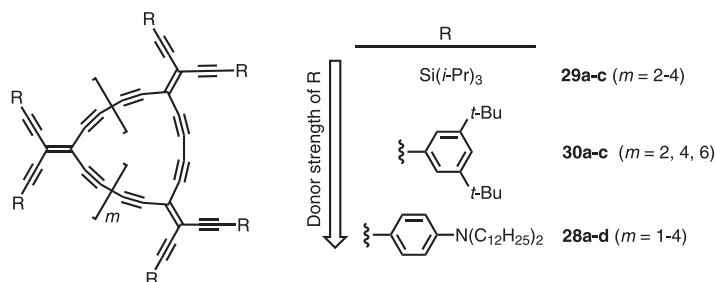


Fig. 7. Expanded radialenes bearing peripheral substituents of different electron-donating strengths [29].

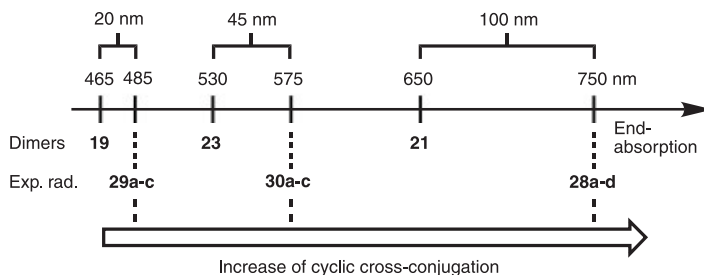


Fig. 8. Comparison of the end-absorptions of TEE dimers and expanded radialenes reveals that the degree of cyclic cross-conjugation in the radialenes increases with increasing donor strength of the peripheral substituents [29d].

The absorption spectra of the expanded radialenes were compared to those of their related TEE dimers, which serve as models for the longest linearly conjugated π -electron fragment in the macrocycles. Within each radialene series, the optical end-absorption remained almost constant, and hence was independent of the ring size. For the per(silylethynylated) expanded radialenes **29a–c**, this end-absorption was seen to be bathochromically shifted by only ~ 20 nm compared to that of dimer **19**. However, the introduction of aryl substituents results in dramatic spectral changes (Figure 8). Thus, for the series **30a–c** versus **23**, a bathochromic shift of ~ 45 nm is observed, and for the series **28a–d** versus **21**, the shift is as much as 100 nm. These large bathochromic shifts are interpreted as resulting from a high degree of macrocyclic cross-conjugation in the arylated macrocycles **28a–d** and **30a–c**. Thus, it transpires that arylation is of major importance for inducing macrocyclic cross-conjugation, which becomes increasingly efficient with increasing donor strength of the substituents.

Another interesting property of expanded radialenes is their strong ability to accommodate electrons upon reduction, as revealed by an electrochemical study by Gross, Gisselbrecht, and Boudon [29d]. Thus, in all three series, the first reduction occurred at anodically shifted potentials relative to the reference TEE dimers; the following shifts were observed: +170–440 mV for **29a–c** relative to **19**, +210–330 mV for **30a,b** relative to **23**, and +240–320 mV for **28a–c** relative to **21** (Figure 9). Thus, the radical anions of expanded radialenes are very stable, particularly those of the expanded [3]- and [4]radialenes, whatever the nature of the substituents.

Donor-substituted expanded radialenes also display huge nonlinear optical coefficients: **28a**: $\gamma = 18000 \times 10^{-36}$ esu, $\chi^{(3)}_{100\%}/\chi^{(3)}_{fs} = 2700$; **28b**: $\gamma = 7000 \times 10^{-36}$ esu, $\chi^{(3)}_{100\%}/\chi^{(3)}_{fs} = 800$ ($\chi^{(3)}_{fs} = 1.16 \times 10^{-14}$ esu). These values are, however, to some extent resonance-enhanced owing to absorption at the third-harmonic wavelength of 700 nm (laser wavelength: 2.1 μm) [29c, 29d].

Interestingly, the perethynylated core of an expanded [6]radialene contains 60 carbon atoms and can therefore be viewed as an isomer of Buckminsterfullerene C_{60} . X-ray crystal structure analysis of **30b** (Figure 10) revealed that the cyclic core adopts a non-planar, “chair-like” conformation, with an average torsional angle of 57.2° [29d]. Each buta-1,3-diynediyl moiety only deviates slightly from linearity. Thus, the corresponding bond angles vary from 174 to 180° . The six individual TEE units are almost planar, with deviations of no more than 0.03 \AA from the mean plane.

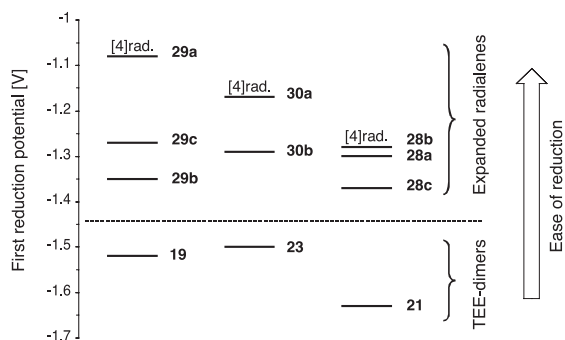


Fig. 9. Comparison of first reduction potentials (vs. Fc/Fc^+) for the three differently substituted series of TEE dimers/expanded radialenes [29d]. Solvent: THF for **19**, **29a–c**; CH_2Cl_2 for **21**, **23**, **28a–c**, and **30a,b**.

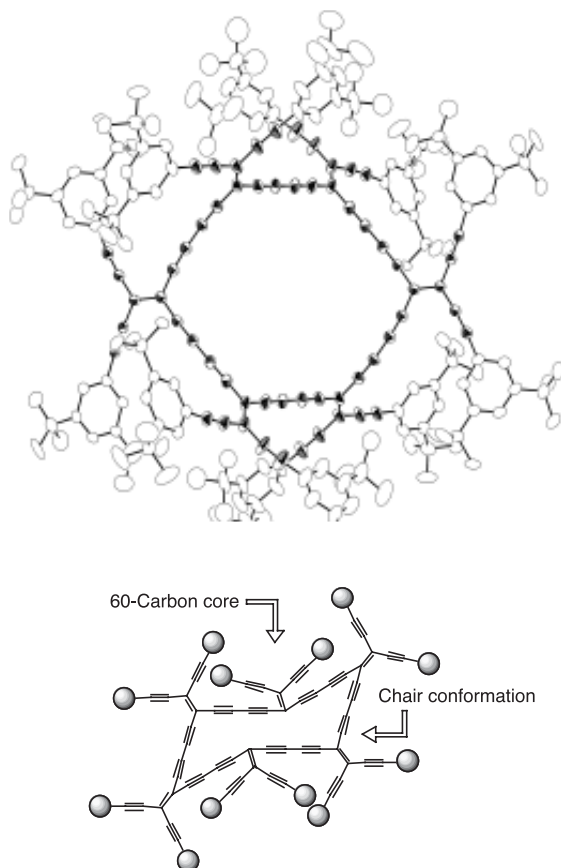


Fig. 10. X-ray crystal structure of expanded [6]radialene **30b**; H-atoms have been omitted for clarity. Atomic displacement parameters at 203 K are drawn at the 20 % probability level. The perethynylated C_{60} -core is highlighted in bold; it adopts a chair-like conformation [29d].

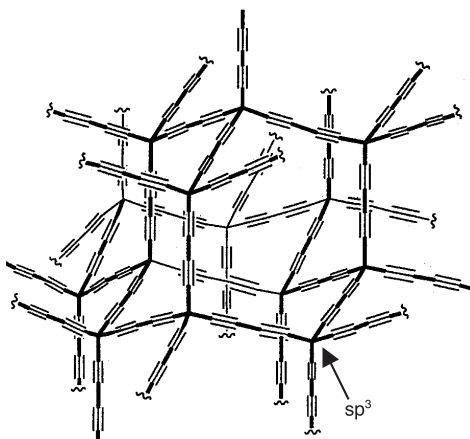


Fig. 11. “Superdiamond” network, an elusive allotrope of carbon.

The synthesis of all-carbon networks, representing artificial counterparts of the two naturally occurring allotropes, graphite and diamond, has attracted considerable interest in recent years [1c]. A fascinating allotrope, still elusive, is the “superdiamond” network depicted in Figure 11. It is tempting to compare this network with an expanded [6]radialene, recognizing that they contain chair-form cyclic parts of the same size, the only difference being the hybridization of the corner carbon atoms, sp^3 *versus* sp^2 . In this context, the class of perspirocyclopropanated macrocyclic oligo(diacetylene)s, $[n]$ rotanes, should be mentioned. These macrocycles are structurally similar to the expanded radialenes, but have insulating sp^3 carbon centers separating the buta-1,3-diynediyl fragments. Indeed, [6]rotanes also adopt chair-like conformations [35].

6.4.3

Cyclic Platinum σ -Acetylide Complex of Tetraethynylethene

By Pt-TEE scaffolding, the macrocyclic complex **31** (Figure 12) was prepared by deprotection and Hay coupling of dimer **32** [36]. This macrocycle can be envisaged as an expanded

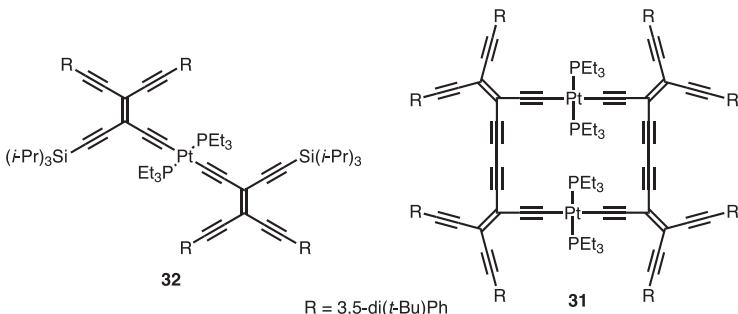


Fig. 12. Linear and cyclic Pt-TEE complexes [36].

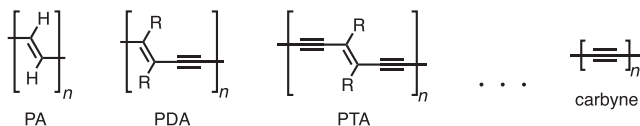


Fig. 13. Progression of linearly π -conjugated all-carbon backbones from *trans*-polyacetylene (PA) through *trans*-poly(diacetylene) (PDA), *trans*-poly(triacetylene) (PTA), to carbyne.

[4]radialene containing two platinum centers as an integral part of the cyclic core. The end-absorption of **31** is bathochromically shifted relative to that of the dimer **32** and extends well beyond 500 nm to about the same onset as observed for **30a**. Thus, it seems that there is electronic communication along the rectangular perimeter of **31**.

6.5

Linearly π -Conjugated Oligomers and Polymers: Poly(triacetylene)s

Polyacetylene (PA) is the simplest conjugated polymer [37] with an all-carbon backbone not composed of aromatic rings (Figure 13), and has been extensively exploited for its electrical conductivity upon doping [38]. The poly(diacetylene)s (PDAs) and poly(triacetylene)s (PTAs) are the next representatives in a progression that ultimately leads to carbyne. PTAs were first synthesized in 1994 [39], after suitable monomeric tetraethynylethene and *trans*-1,2-diethynylethene (DEE) building blocks had become available [40]. The π -electron conjugation in the PTA backbone is best described as cylindrical and is maintained upon rotation about C(sp)–C(sp²) and C(sp)–C(sp) single bonds, since UV/vis studies on PTA oligomers **33a–e**, **34a–c**, and **35a,b**, dendritically encapsulated by shells of Fréchet-type dendrons [41], demonstrated that the electronic properties were not altered upon distorting the backbone out of planarity as a result of steric compression of the bulky dendritic wedges (Figure 14) [42].

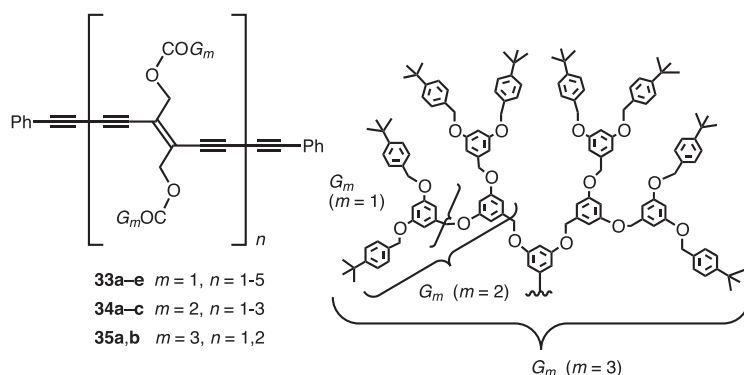


Fig. 14. Dendritic PTA oligomers with the linearly π -conjugated all-carbon backbone encapsulated by dendrons of first to third generation [42].

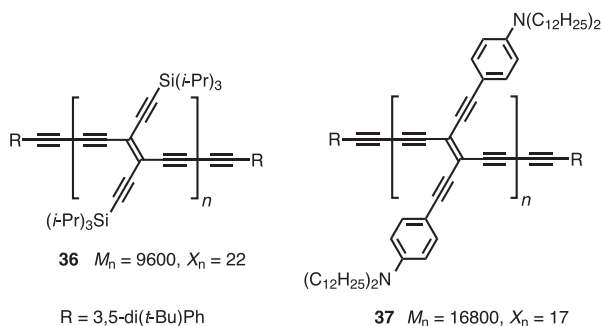


Fig. 15. PTAs containing lateral silyl [39] or anilino [29c] groups. M_n = average molecular weight; X_n = average number of TEE monomer units.

The question that needs to be addressed is how the physical properties of PTAs are influenced by aryl groups, in either the lateral positions or within the carbon backbone, or by donor–donor or acceptor–acceptor substitution in the end groups.

6.5.1

Lateral Aryl Substitution

The effect of lateral aryl donor functionalization can be understood by comparing the two PTAs **36** [39] and **37** [29c], the first containing lateral silyl groups and the second lateral anilino groups (Figure 15). They were readily obtained by oxidative Glaser–Hay polymerization of *trans*-bis-deprotected TEEs in the presence of the end-capping reagent 3,5-di(*tert*-butyl)phenylacetylene. By ^1H NMR signal integration, the average molecular weight M_n and the degree of polymerization X_n were determined. Comparison of their physical properties reveals a significant enhancement upon lateral donor functionalization. Thus, the solution-state optical gap of **37** ($E_g = 1.6$ eV) is substantially reduced relative to that of **36** ($E_g = 2.0$ eV). The PTA **37** only showed one irreversible reduction at -1.28 V (*versus* Fc/Fc^+ , in CH_2Cl_2), this being anodically shifted by $+350$ mV relative to the first reduction of TEE dimer **21**. Thus, the longer linear conjugation length in **37** facilitates the first reduction relative to that in **21**. Moreover, as is generally observed for anilino-substituted TEE scaffolds, **37** undergoes reversible oxidation centered on the anilino groups ($E^\circ = +0.45$ V *versus* Fc/Fc^+ in CH_2Cl_2).

6.5.2

Aromatic Spacer Units

The modulation of the electronic properties of PTA oligomers by π -electron-deficient and -rich aromatic and heteroaromatic spacer units was first tested in DEE dimers **38a–j** and **39a,b** (Figure 16) [43]. The insertion of such spacers was found to have a profound influence on the molecular properties, such as the fluorescence behavior. Thus, whereas the quantum yields of compounds **39a,b** and hybrid trimer **38j** were below 5 % in chloroform ($\lambda_{\text{exc}} = 356$ nm), hybrid derivatives **38a**, **38e**, **38g**, and **38i** exhibited quantum yields between 20 and

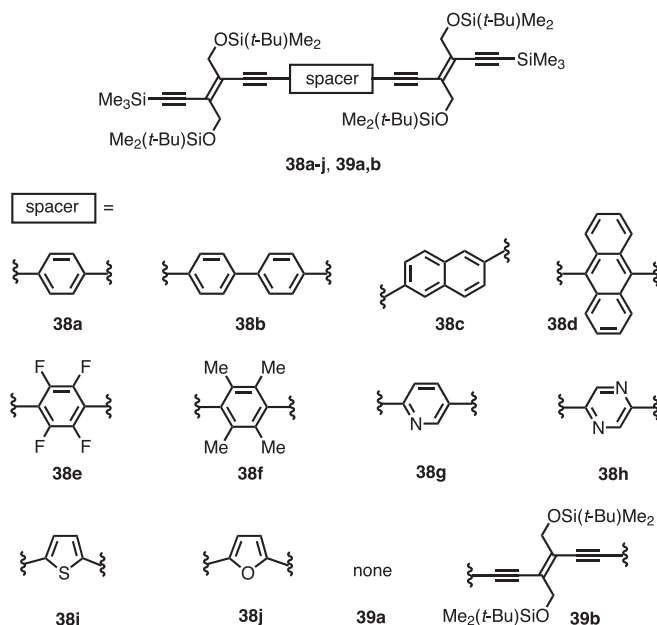


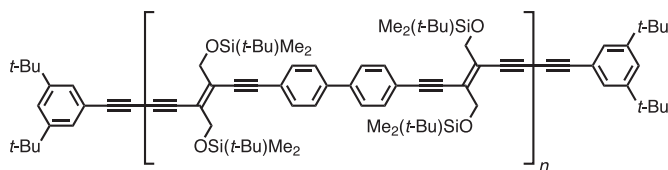
Fig. 16. Dimers of *trans*-1,2-diethynylethene (DEE) containing aromatic spacer units [43].

50 %. The quantum yields were even increased above 50 % in hybrid trimers **38b–d**, **38f**, and **38h**.

Whereas DEE trimer **39b** experiences a large bathochromic shift of the longest-wavelength absorption maximum relative to that of DEE dimer **39a** ($\lambda_{\text{max}} = 407$ nm, shoulder (**39b**), $\lambda_{\text{max}} = 376$ nm (**39a**)), hybrid trimers **38a–c** display about the same longest-wavelength absorption maxima, as well as end-absorptions, as **39a**. Thus, benzenoid spacers are less effective in transmitting π -electron delocalization along the oligomeric backbone. In contrast, introduction of the anthracene spacer in **38d** produces a remarkable red-shift of all the bands in the UV/vis spectrum. Insertion of electron-rich heterocyclic spacers, as in thiophene derivative **38i** and furan derivative **38j**, results in very efficient π -electron delocalization, shifting the longest wavelength absorption maximum to 404 nm (shoulder) and 398 nm (shoulder), respectively. While a pyridine spacer (in **38g**) does not produce a bathochromic shift, the pyrazine-spaced compound **38h** exhibits a longest-wavelength absorption at $\lambda_{\text{max}} = 392$ nm (shoulder). Indeed, the benzenoid aromaticity is more pronounced in pyridine than in pyrazine. Pyridine derivative **38g** represents an interesting example of a molecular system in which both the electron absorption and emission characteristics can be reversibly switched as a function of pH. Thus, protonation results in a large bathochromic shift of the most intense electronic absorption band from $\lambda_{\text{max}} = 337$ to 380 nm and a decrease in the fluorescence quantum yield from 40 % to 7 % ($\lambda_{\text{exc}} = 356$ nm) [43c].

Based on the biphenyl spacer, a long-chain oligomer (**40**) was prepared (Figure 17) [43d]. This PTA retained the strong emission behavior of **38b**, displaying a quantum yield of 44 % in chloroform. Its potential in light-emitting diodes is currently under investigation.

Recently, Pt-TEE molecular scaffolding yielded PTA oligomers with $[\text{Pt}(\text{PEt}_3)_2]$ as spacer units [44]. Both the linear and nonlinear optical properties of these compounds revealed an



40 $M_n = 16900$, $X_n = 19$

Fig. 17. PTA comprised of biphenyl-spaced DEE units [43d].

almost complete lack of π -electron conjugation along the backbones, that is, the Pt groups act as insulating centers in these linear systems. This insulating behavior of the $[\text{Pt}(\text{PET}_3)_2]$ spacer units is in contrast to their ability to convey, at least to some extent, π -electron delocalization in the macrocyclic complex **31**.

6.5.3

Donor–Donor and Acceptor–Acceptor End-Functionalization

The PTA mono-, di-, tri-, tetra-, penta-, and hexamers **41a–f** and **42a–f** (Figure 18) provide useful information regarding the influence of donor–donor (D–D) and acceptor–acceptor (A–A) substitution in the end groups of PTAs based on the *trans*-1,2-diethynylethene repeat unit [45]. As reference points for the infinitely long polymers, compounds **41g** and **42g** (~ 18 and 12 DEE units) were studied. From the longest-wavelength absorption maxima of the compounds in each of these two series, the effective conjugation length (ECL) was estimated. The ECL indicates the number of repeat units required to furnish size-independent properties in a conjugated polymer. The electronic properties of the end caps were found to have a strong bearing on the ECL. Thus, the ECL of the A–A PTA oligomer **42g** was determined to be $n = 10$, this being of the same length as found for silyl group end-capped PTA oligomers. However, the D–D PTA oligomer **41g** exhibits a much shorter ECL of only $n = 4$. This decrease in ECL is probably explained by the appearance of strong CT bands that dominate the absorption properties. Raman scattering measurements suggested an even smaller value of $n = 3$ for this PTA.

6.6

Conclusions

Tetraethynylethene molecular scaffolding has provided conjugated materials with properties that are greatly enhanced upon incorporating functional arene units. Indeed, third-order nonlinear optical properties are increased by aryl groups; photochemical *cis-trans* isomer-

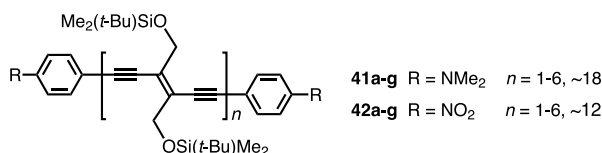


Fig. 18. PTAs containing either donor or acceptor end-caps [45].

ization can be controlled, providing molecular photoswitches; absorptions up to the near-IR region are obtained upon extending the linear conjugation, cyclic cross-conjugation in expanded radialenes is enforced by donor groups; the optical gap of PTA oligomers is decreased; strong fluorescence behavior can be introduced in PTAs, and the effective conjugation length in PTAs can be adjusted by changing the donor strength of the end groups.

Abbreviations

A	acceptor
Ac	acetyl
Bu	butyl
CT	charge-transfer
D	donor
DEE	<i>trans</i> -1,2-diethynylethene
DHA	dihydroazulene
DMA	dimethylaniline
ECL	effective conjugation length
Et	ethyl
Fc	ferrocene
fs	fused silica
IR	infrared
Me	methyl
NLO	nonlinear optics
PA	polyacetylene
Ph	phenyl
PDA	poly(diacetylene)
Pr	propyl
PTA	poly(triacetylene)
TEE	tetraethynylethene
UV	ultraviolet
TICT	twisted intramolecular charge-transfer
TMEDA	<i>N,N,N',N'</i> -tetramethylethylenediamine
VHF	vinylheptafulvene
vis	visible

References

- 1 For reviews on acetylenic molecular scaffolding, see: a) F. DIEDERICH, *Nature* **1994**, 369, 199–207; b) L. T. SCOTT, M. J. COONEY, in *Modern Acetylene Chemistry* (Eds.: P. J. STANG, F. DIEDERICH), VCH, Weinheim, **1995**, pp. 321–351; c) U. H. F. BUNZ, Y. RUBIN, Y. TOBE, *Chem. Soc. Rev.* **1999**, 28, 107–119; d) U. H. F. BUNZ, *Top. Curr. Chem.* **1999**, 201, 131–161; e) F. DIEDERICH, L. GOBBI, *Top. Curr. Chem.* **1999**, 201, 43–79; f) P. SIEMSEN, R. C. LIVINGSTON, F. DIEDERICH, *Angew. Chem. Ed.* **2000**, 112, 2740–2767; *Angew. Chem. Int. Ed.* **2000**, 39, 2632–2657.
- 2 F. DIEDERICH, *Chem. Commun.* **2001**, 219–227.

- 3 K. SONOGASHIRA, in *Metal-Catalyzed Cross-Coupling Reactions* (Eds.: F. DIEDERICH, P. J. STANG), Wiley-VCH, Weinheim, **1998**, pp. 203–229.
- 4 Recent reviews: a) R. R. TYKWINSKI, F. DIEDERICH, *Liebigs Ann./Recueil* **1997**, 649–661; b) M. B. NIELSEN, F. DIEDERICH, *Synlett* **2002**, 544–552.
- 5 C. GLASER, *Ber. Dtsch. Chem. Ges.* **1869**, 2, 422–424.
- 6 G. EGLINTON, A. R. GALBRAITH, *Chem. Ind. (London)* **1956**, 737–738.
- 7 A. S. HAY, *J. Org. Chem.* **1962**, 27, 3320–3321.
- 8 a) W. CHODKIEWICZ, P. CADIOT, C. R. *Hebld. Seances Acad. Sci.* **1955**, 241, 1055–1057; b) W. CHODKIEWICZ, *Ann. Chim. (Paris)* **1957**, 2, 819–869.
- 9 H. HOPF, M. KREUTZER, P. G. JONES, *Chem. Ber.* **1991**, 124, 1471–1475.
- 10 A. HOEKSTRA, A. VOS, *Acta Cryst. B* **1975**, 31, 1716–1721.
- 11 D. PHILP, V. GRAMLICH, P. SEILER, F. DIEDERICH, *J. Chem. Soc., Perkin Trans. 2* **1995**, 875–886.
- 12 a) C. BOSSHARD, R. SPREITER, P. GÜNTER, R. R. TYKWINSKI, M. SCHREIBER, F. DIEDERICH, *Adv. Mater.* **1996**, 8, 231–234; b) R. R. TYKWINSKI, M. SCHREIBER, V. GRAMLICH, P. SEILER, F. DIEDERICH, *Adv. Mater.* **1996**, 8, 226–231; c) R. SPREITER, C. BOSSHARD, G. KNÖPFLE, P. GÜNTER, R. R. TYKWINSKI, M. SCHREIBER, F. DIEDERICH, *J. Phys. Chem. B* **1998**, 102, 4451–4465; d) R. R. TYKWINSKI, U. GUBLER, R. E. MARTIN, F. DIEDERICH, C. BOSSHARD, P. GÜNTER, *J. Phys. Chem. B* **1998**, 102, 4451–4465; e) U. GUBLER, R. SPREITER, C. BOSSHARD, P. GÜNTER, R. R. TYKWINSKI, F. DIEDERICH, *Appl. Phys. Lett.* **1998**, 73, 2396–2398; f) C. BOSSHARD, in *Non-linear Optical Effects and Materials* (Ed.: P. GÜNTER), Springer Verlag, Berlin, **2000**, pp. 7–161; g) U. GUBLER, C. BOSSHARD, *Phys. Rev. B* **2000**, 61, 10702–10710.
- 13 L.-T. CHENG, W. TAM, S. R. MARDER, A. E. STIEGMAN, G. RIKKEN, C. W. SPANGLER, *J. Phys. Chem.* **1991**, 95, 10643–10652.
- 14 C. W. SPANGLER, K. O. HAVELKA, M. W. BECKER, T. A. KELLEHER, L.-T. CHENG, *Proc. SPIE – Int. Soc. Opt. Eng.* **1991**, 1560, 139–147.
- 15 a) J. MESSIER, F. KAJZAR, C. SENTEIN, M. BARZOUKAS, J. ZYSS, M. BLANCHARD-DESCE, J.-M. LEHN, *Nonlinear Opt.* **1992**, 2, 53–70; b) G. PUCCETTI, M. BLANCHARD-DESCE, I. LEDOUX, J.-M. LEHN, J. ZYSS, *J. Phys. Chem.* **1993**, 97, 9385–9391; c) M. BLANCHARD-DESCE, J.-M. LEHN, M. BARZOUKAS, C. RUNSER, A. FORT, G. PUCCETTI, I. LEDOUX, J. ZYSS, *Nonlinear Opt.* **1995**, 10, 23–36.
- 16 a) A. F. GARITO, J. R. HEFLIN, K. Y. WONG, O. ZAMANI-KHAMIRI, in *Organic Materials for Nonlinear Optics* (Eds.: R. A. HANN, D. BLOOR), The Royal Society of Chemistry, London, **1989**, pp. 16–27; b) J. W. WU, J. R. HEFLIN, R. A. NORWOOD, K. Y. WONG, O. ZAMANI-KHAMIRI, A. F. GARITO, P. KALYANARAMAN, J. SOUNIK, *J. Opt. Soc. Am. B* **1989**, 6, 707–720.
- 17 S. R. MARDER, W. E. TORRUELLAS, M. BLANCHARD-DESCE, V. RICCI, G. I. STEGEMAN, S. GILMOUR, J.-L. BRÉDAS, J. LI, G. U. BUBLITZ, S. G. BOXER, *Science (Washington D.C.)* **1997**, 276, 1233–1236.
- 18 a) I. D. L. ALBERT, J. O. MORLEY, D. PUGH, *J. Phys. Chem.* **1995**, 99, 8024–8032; b) V. KESHARI, W. WIJEKON, P. N. PRASAD, S. P. KARNA, *J. Phys. Chem.* **1995**, 99, 9045–9050; c) P. R. VARANASI, A. K.-Y. JEN, J. CHANDRASEKHAR, I. N. N. NAMBOOTHIRI, A. RATHNA, *J. Am. Chem. Soc.* **1996**, 118, 12443–12448; d) I. D. L. ALBERT, T. J. MARKS, M. A. RATNER, *J. Am. Chem. Soc.* **1997**, 119, 6575–6582.
- 19 a) L.-T. CHENG, W. TAM, S. R. MARDER, A. E. STIEGMAN, G. RIKKEN, C. W. SPANGLER, *J. Phys. Chem.* **1991**, 95, 10643–10652; b) S. P. KARNA, Y. ZHANG, M. SAMOC, P. N. PRASAD, B. A. REINHARDT, A. G. DILLARD, *J. Chem. Phys.* **1993**, 99, 9984–9993; c) V. P. RAO, A. K.-Y. JEN, K. Y. WONG, K. J. DROST, *J. Chem. Soc., Chem. Commun.* **1993**, 1118–1120; d) A. K.-Y. JEN, V. P. RAO, K. Y. WONG, K. J. DROST, *J. Chem. Soc., Chem. Commun.* **1993**, 90–92; e) K. Y. WONG, A. K.-Y. JEN, V. P. RAO, K. J. DROST, *J. Chem. Phys.* **1994**, 100, 6818–6825; f) V. P. RAO, K. Y. WONG, A. K.-Y. JEN, K. J. DROST, *Chem. Mater.* **1994**, 6, 2210–2212; g) P. BOLDT, G. BOURHILL, C. BRÄUCHLE, Y. JIM, R. KAMMLER, C. MÜLLER, J. RASE, J. WICHERN, *Chem. Commun.* **1996**, 793–795; h) S.-S. P. CHOU, D.-J. SUN, H.-C. LIN, P.-K. YANG, *Chem. Commun.* **1996**,

- 1045–1046; i) V. P. RAO, A. K.-Y. JEN, Y. CAI, *Chem. Commun.* **1996**, 1237–1238; j) C. Z. CAI, I. LIKATAS, M.-S. WONG, M. BÖSCH, C. BOSSHARD, P. GÜNTER, S. CONCILIO, N. TIRELLI, U. W. SUTER, *Org. Lett.* **1999**, 1, 1847–1849.
- 20 a) M.-T. ZHAO, B. P. SINGH, P. N. PRASAD, *J. Chem. Phys.* **1988**, 89, 5535–5541; b) V. P. RAO, A. K.-Y. JEN, K. Y. WONG, K. J. DROST, *Tetrahedron Lett.* **1993**, 34, 1747–1750; c) K. Y. WONG, A. K.-Y. JEN, V. P. RAO, *Phys. Rev. A* **1994**, 49, 3077–3080.
- 21 For examples of other *cis-trans* photoisomerizations about a central carbon–carbon double bond, see: a) D. SCHULTE-FROHLINDE, H. GÖRNER, *Pure Appl. Chem.* **1979**, 51, 279–297; b) D. H. WALDECK, *Chem. Rev.* **1991**, 91, 415–436; c) H. MEIER, *Angew. Chem.* **1992**, 104, 1425–1446; *Angew. Chem. Int. Ed. Engl.* **1992**, 31, 1399–1420; c) B. L. FERGINGA, W. F. JAGER, B. DE LANGE, *Tetrahedron* **1993**, 49, 8267–8310; d) W. F. JAGER, J. C. DE JONG, B. DE LANGE, N. P. M. HUCK, A. MEETSMA, B. L. FERGINGA, *Angew. Chem.* **1995**, 107, 346–349; *Angew. Chem. Int. Ed. Engl.* **1995**, 34, 348–350; e) B. L. FERGINGA, N. P. M. HUCK, A. M. SCHOEVAARS, *Adv. Mater.* **1996**, 8, 681–684; f) R. BALLARDINI, V. BALZANI, J. BECHER, A. DI FABIO, M. T. GANDOLFI, G. MATTERSTEIG, M. B. NIELSEN, F. M. RAYMO, S. J. ROWAN, J. F. STODDART, A. J. P. WHITE, D. J. WILLIAMS, *J. Org. Chem.* **2000**, 65, 4120–4126.
- 22 R. R. TYKWINSKI, M. SCHREIBER, R. P. CARLÓN, F. DIEDERICH, V. GRAMLICH, *Helv. Chim. Acta* **1996**, 79, 2249–2281.
- 23 a) L. GOBBI, P. SEILER, F. DIEDERICH, *Angew. Chem.* **1999**, 111, 737–740; *Angew. Chem. Int. Ed.* **1999**, 38, 674–678; b) L. GOBBI, P. SEILER, F. DIEDERICH, V. GRAMLICH, *Helv. Chim. Acta* **2000**, 83, 1711–1723; c) L. GOBBI, P. SEILER, F. DIEDERICH, V. GRAMLICH, C. BOUDON, J.-P. GISSELBRECHT, M. GROSS, *Helv. Chim. Acta* **2001**, 84, 743–777.
- 24 S. GIERISCH, J. DAUB, *Chem. Ber.* **1989**, 122, 69–75.
- 25 L. GOBBI, N. ELMACI, H. P. LÜTHI, F. DIEDERICH, *ChemPhysChem* **2001**, 2, 423–433.
- 26 a) K. ROTKIEWICZ, K. H. GRELLMANN, Z. R. GRABOWSKI, *Chem. Phys. Lett.* **1973**, 19, 315–318; b) K. ROTKIEWICZ, Z. R. GRABOWSKI, A. KRWOCZYNSKI, W. KÜHNLE, *J. Lumin.* **1976**, 12/13, 877–885; c) Z. R. GRABOWSKI, K. ROTKIEWICZ, A. SIEMIARCZUK, *J. Lumin.* **1979**, 18/19, 420–424; d) Z. R. GRABOWSKI, K. ROTKIEWICZ, A. SIEMIARCZUK, D. J. COWLEY, W. BAUMANN, *Nouv. J. Chim.* **1979**, 3, 443–454.
- 27 A. HILGER, J. P. GISSELBRECHT, R. R. TYKWINSKI, C. BOUDON, M. SCHREIBER, R. E. MARTIN, H. P. LÜTHI, M. GROSS, F. DIEDERICH, *J. Am. Chem. Soc.* **1997**, 119, 2069–2078.
- 28 R. E. MARTIN, J. BARTEK, F. DIEDERICH, R. R. TYKWINSKI, E. C. MEISTER, A. HILGER, H. P. LÜTHI, *J. Chem. Soc., Perkin Trans. 2* **1998**, 233–241.
- 29 a) A. M. BOLDI, F. DIEDERICH, *Angew. Chem.* **1994**, 106, 482–485; *Angew. Chem. Int. Ed. Engl.* **1994**, 33, 468–471; b) J. ANTHONY, A. M. BOLDI, C. BOUDON, J.-P. GISSELBRECHT, M. GROSS, P. SEILER, C. B. KNOBLER, F. DIEDERICH, *Helv. Chim. Acta* **1995**, 78, 797–817; c) M. SCHREIBER, R. R. TYKWINSKI, F. DIEDERICH, R. SPREITER, U. GÜBLER, C. BOSSHARD, I. POBERAJ, P. GÜNTER, C. BOUDON, J.-P. GISSELBRECHT, M. GROSS, U. JONAS, H. RINGSDORF, *Adv. Mater.* **1997**, 9, 339–343; d) M. B. NIELSEN, M. SCHREIBER, Y. G. BAEK, P. SEILER, S. LECOMTE, C. BOUDON, R. R. TYKWINSKI, J.-P. GISSELBRECHT, V. GRAMLICH, P. J. SKINNER, C. BOSSHARD, P. GÜNTER, M. GROSS, F. DIEDERICH, *Chem. Eur. J.* **2001**, 7, 3263–3280.
- 30 a) J. ANTHONY, C. B. KNOBLER, F. DIEDERICH, *Angew. Chem.* **1993**, 105, 437–440; *Angew. Chem. Int. Ed. Engl.* **1993**, 32, 406–409; b) C. BOUDON, J.-P. GISSELBRECHT, M. GROSS, J. ANTHONY, A. M. BOLDI, R. FAUST, T. LANGE, D. PHILP, J.-D. VAN LOON, F. DIEDERICH, *J. Electroanal. Chem.* **1995**, 394, 187–197.
- 31 W. H. OKAMURA, F. SONDHEIMER, *J. Am. Chem. Soc.* **1967**, 89, 5991–5992.
- 32 a) R. WOLOVSKY, F. SONDHEIMER, *J. Am. Chem. Soc.* **1965**, 87, 5720–5727; b) F. SONDHEIMER, R. WOLOVSKY, P. J. GARRATT, I. C. CALDER, *J. Am. Chem. Soc.* **1966**, 88, 2610.
- 33 K. G. UNTCH, D. C. WYSOCKI, *J. Am. Chem. Soc.* **1966**, 88, 2608–2610.
- 34 For a review on radialenes, see: H. HOPF, G. MAAS, *Angew. Chem.* **1992**, 104, 953–

- 977; *Angew. Chem. Int. Ed. Engl.* **1992**, *31*, 931–954.
- 35 a) A. DE MEIJERE, S. KOZHUSHKOV, T. HAUMANN, R. BOESE, C. PULS, M. J. COONEY, L. T. SCOTT, *Chem. Eur. J.* **1995**, *1*, 124–131; b) M. BRAKE, V. ENKELMANN, U. H. F. BUNZ, *J. Org. Chem.* **1996**, *61*, 1190–1191.
- 36 R. FAUST, F. DIEDERICH, V. GRAMLICH, P. SEILER, *Chem. Eur. J.* **1995**, *1*, 111–117.
- 37 a) D. T. MCQUADE, A. E. PULLEN, T. M. SWAGER, *Chem. Rev.* **2000**, *100*, 2537–2574; b) U. H. F. BUNZ, *Chem. Rev.* **2000**, *100*, 1605–1644.
- 38 a) C. K. CHIANG, C. R. FINCHER, JR., Y. W. PARK, A. J. HEEGER, H. SHIRAKAWA, E. J. LOUIS, S. C. GAU, A. G. MACDIARMID, *Phys. Rev. Lett.* **1977**, *39*, 1098–1101; b) H. SHIRAKAWA, *Angew. Chem.* **2001**, *113*, 2642–2648; *Angew. Chem. Int. Ed.* **2001**, *40*, 2574–2580; c) A. G. MACDIARMID, *Angew. Chem.* **2001**, *113*, 2649–2659; *Angew. Chem. Int. Ed.* **2001**, *40*, 2581–2590; d) A. J. HEEGER, *Angew. Chem.* **2001**, *113*, 2660–2682; *Angew. Chem. Int. Ed.* **2001**, *40*, 2591–2611.
- 39 M. SCHREIBER, J. ANTHONY, F. DIEDERICH, M. E. SPAHR, R. NESPER, M. HUBRICH, F. BOMMELI, L. DEGIORGI, P. WACHTER, P. KAATZ, C. BOSSHARD, P. GÜNTER, M. COLUSSI, U. W. SUTER, C. BOUDON, J.-P. GISSELBRECHT, M. GROSS, *Adv. Mater.* **1994**, *6*, 786–790.
- 40 Recently, Fowler and co-workers reported a very elegant PTA synthesis by topologically controlled polymerization of hexa-1,3,5-triynes in the crystal: J. XIAO, M. YANG, J. W. LAUHER, F. W. FOWLER, *Angew. Chem.* **2000**, *112*, 2216–2219; *Angew. Chem. Int. Ed.* **2000**, *39*, 2132–2135.
- 41 C. J. HAWKER, J. M. J. FRÉCHET, *J. Am. Chem. Soc.* **1990**, *112*, 7638–7647.
- 42 A. P. H. J. SCHENNING, J.-D. ARNDT, M. ITO, A. STODDART, M. SCHREIBER, P. SIEMSEN, R. E. MARTIN, C. BOUDON, J.-P. GISSELBRECHT, M. GROSS, V. GRAMLICH, F. DIEDERICH, *Helv. Chim. Acta* **2001**, *84*, 296–334.
- 43 a) J. WYTKO, V. BERL, M. McLAUGHLIN, R. R. TYKWINSKI, M. SCHREIBER, F. DIEDERICH, C. BOUDON, J.-P. GISSELBRECHT, M. GROSS, *Helv. Chim. Acta* **1998**, *81*, 1964–1977; b) E. M. MAYA, P. VAZQUEZ, T. TORRES, L. GOBBI, F. DIEDERICH, S. PYO, L. ECHEGUYEN, *J. Org. Chem.* **2000**, *65*, 823–830; c) R. E. MARTIN, J. A. WYTKO, F. DIEDERICH, C. BOUDON, J.-P. GISSELBRECHT, M. GROSS, *Helv. Chim. Acta* **1999**, *82*, 1470–1485; d) M. J. EDELMANN, S. ODERMATT, F. DIEDERICH, *Chimia* **2001**, *55*, 1–11.
- 44 P. SIEMSEN, U. GÜBLER, C. BOSSHARD, P. GÜNTER, F. DIEDERICH, *Chem. Eur. J.* **2001**, *7*, 1333–1341.
- 45 R. E. MARTIN, U. GÜBLER, C. BOUDON, C. BOSSHARD, J.-P. GISSELBRECHT, P. GÜNTER, M. GROSS, F. DIEDERICH, *Chem. Eur. J.* **2000**, *6*, 4400–4412.

7

The ADIMET Reaction: Synthesis and Properties of Poly(dialkylparaphenyleneethynylene)s

Uwe H. F. Bunz

Abstract

A mixture of molybdenum hexacarbonyl and 4-chlorophenol is effective in performing alkyne metathesis of dipropynylated dialkylbenzenes. Alkyne metathesis of these precursors leads to the clean formation of dialkyl poly(*paraphenyleneethynylene*)s (PPEs) in high yield and with high molecular weights. This facile yet effective access to the PPEs has allowed study of their spectroscopic, structural, and thermal properties. While PPEs have been made before, the dialkyl-PPEs turned out to have particularly interesting optical and liquid-crystalline properties that can be explained in terms of the conformation of the main chains. The PPEs have also been utilized to construct light-emitting diodes and other semiconductor devices. This chapter discusses the interplay of structure, chromicity, and electronic properties of the dialkyl-PPEs.

7.1

Introduction

7.1.1

Scope and Coverage of this Review

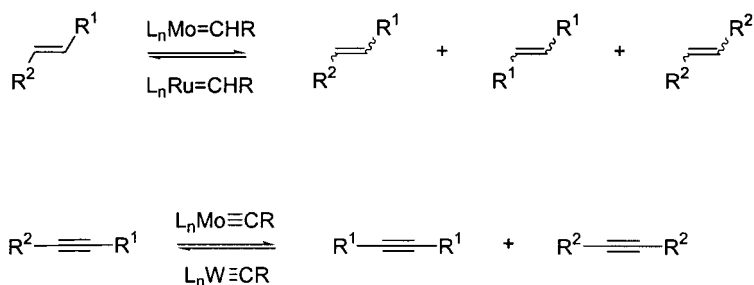
This contribution describes the synthesis and properties of organic alkyne-bridged materials that have been made by alkyne metathesis or by *Acyclic Diyne Metathesis* (ADIMET). This review covers mostly poly(aryleneethynylene)s made at the author's laboratory in South Carolina. A comprehensive review covering poly(aryleneethynylene)s listing important contributions in adjacent areas has appeared [1, 2]. This chapter discusses the synthesis and properties of dialkyl-poly(*paraphenyleneethynylene*)s (dialkyl-PPEs) in relation to the concept of ADIMET with simple catalyst systems.

7.1.2

Historical Perspective

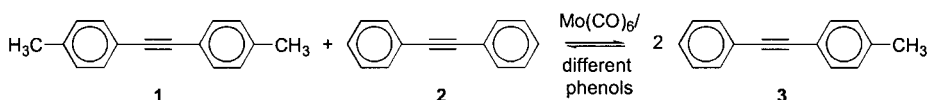
The metathesis of carbon–carbon multiple bonds has “exploded” in the last ten years. In particular, alkene metathesis, that is the transition metal promoted 1,2-permutation of

substituents in alkenes (Scheme 1), has made great strides since the commercialization of Grubbs' and Schrock's ruthenium and molybdenum alkylidenes. Herrmann discovered that imidazolium ligands boost the reactivity of the Grubbs catalysts. Alkene metathesis has been applied in all fields of organic and materials chemistry, and has been covered by excellent review articles [3, 4].



Scheme 1

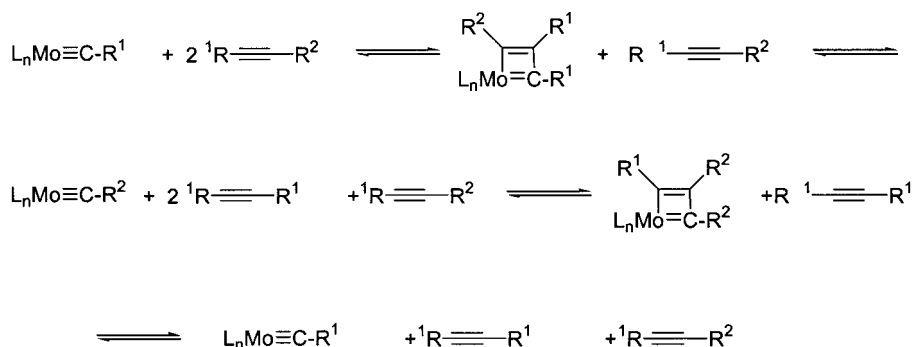
On the other hand, alkyne metathesis (Scheme 1, 2), is the permutation of substituents in alkynes in a process that involves the transition metal catalyzed scission of the carbon-carbon triple bond [5]. The first example of this reaction in homogeneous solution was found by Mortreux [6]; when he heated a mixture of diphenylacetylene, ditolylacetylene, $\text{Mo}(\text{CO})_6$, and catechol in a high-pressure reactor, he observed the formation of the mixed phenyltolylacetylene **3** in the reaction mixture (Scheme 2). Although this reaction set-up is simple, Mortreux did not exploit this attractive system for the preparation of organic target molecules. He did not address the question of the catalytically active species, even though several more interesting papers covering the topic appeared in the literature [5].



Scheme 2

In the early 1980s, Schrock prepared a series of tungsten- and molybdenum-based carbyne complexes, and demonstrated that they are viable catalysts for performing stoichiometric and catalytic alkyne metathesis [7]. With the defined carbyne complexes, he laid the foundation for the mechanistic understanding of alkyne metathesis, and was the first to demonstrate that vinyl-substituted carbyne complexes are stable [8] and that alkyne metathesis could be performed in the presence of C=C double bonds.

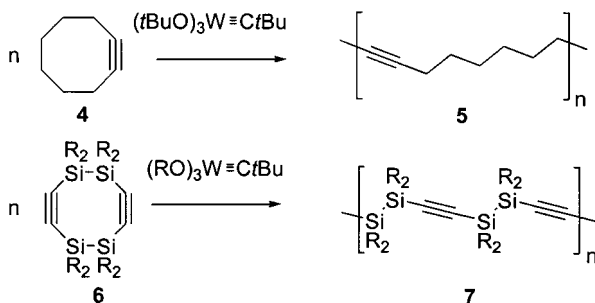
From a mechanistic point of view (Scheme 3), a transition metal carbyne undergoes a [2+2] cycloaddition with an alkyne to form a metallacyclobutadiene as an intermediate, or possibly as a transition state. The four-membered ring then cycloreverts, expelling a di-substituted alkyne with regeneration of a catalytically active carbyne complex. In a subsequent



Scheme 3

reaction, another [2+2] cycloaddition to give a metallacyclobutadiene occurs. Cycloreversion again regenerates the catalytically active species, and ejects the final product of the metathesis.

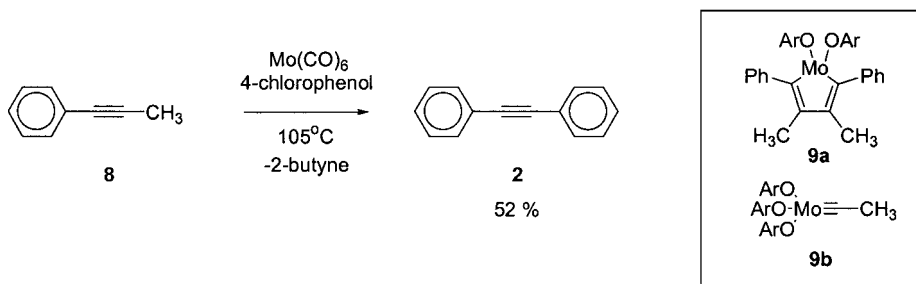
Schrock and Krouse utilized alkyne metathesis to ring-open cyclooctyne **4** [9]. They obtained a polycyclooctynamer **5**. This ROMP is the first known application of a carbyne complex in polymer science. Bazan showed in 1994 elegantly that alkyne metathesis of silicon-containing diynes **6** with tungsten carbynes of the Schrock-type furnishes conjugated polymers **7** [10]. However, while both of these seminal papers were of high importance and exciting, the results lacked their well-deserved impact (Scheme 4).



Scheme 4

Further interest in the use of alkyne metathesis in polymer science arose through a collaborative effort of Bunz and Müllen, exploring the synthesis of poly(*para*phenyleneethynylene)s (PPEs) by Pd-catalyzed couplings [11]. The PPEs that were isolated were of relatively low molecular weight and had a significant amount of defects, a consequence inherent to the Pd methodology. The presence of diyne units, the occurrence of phosphonium end groups, and dehalogenation generally plague this – *per se* valuable and generally applicable – synthetic approach. Alkyne metathesis is proposed as an alternative route to PPEs that may circumvent the problems associated with Pd catalysis.

In 1995, Mori revived alkyne metathesis with simple Mo(CO)_6 -based catalyst systems, and successfully prepared a series of diaryl- and arylalkylacetylenes (Scheme 5) [12]. The yields of the dimerization reactions were not particularly high. The simplicity of the method utilizing off-the-shelf catalyst precursors in combination with technical quality solvents made these systems potentially valuable for the synthesis of novel aromatic oligomers and polymers (Scheme 5). Mori offered an alternative mechanistic picture as to how alkyne metathesis might work in these simple catalyst systems, which invoked a transient molybdenacyclopentadiene **9a**; the classic interpretation of alkyne metathesis according to Schrock involves an intermediate **9b** as shown in Scheme 5.



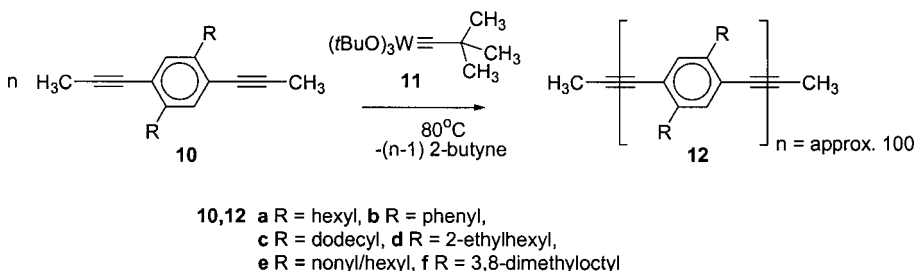
Scheme 5

7.2 Syntheses

7.2.1

PPEs by Acyclic Diyne Metathesis (ADIMET) Utilizing Schrock's Tungsten Carbyne Complex 11

The first conjugated polymer to be made by the ADIMET process was dihexyl-PPE (**12a**) [13]. Reaction of 1,4-dipropynyl-2,5-dihexylbenzene (**10a**) with $(t\text{BuO})_3\text{W}\equiv\text{C}t\text{Bu}$ (**11**) at 80°C in vacuo in a high boiling solvent furnished dihexyl-PPE **12a** as a yellow powder in 80 % yield and with a degree of polymerization (P_n) of 94 repeat units (Scheme 6). The material was characterized by NMR spectroscopy, and did not show any defects that could be attributed to



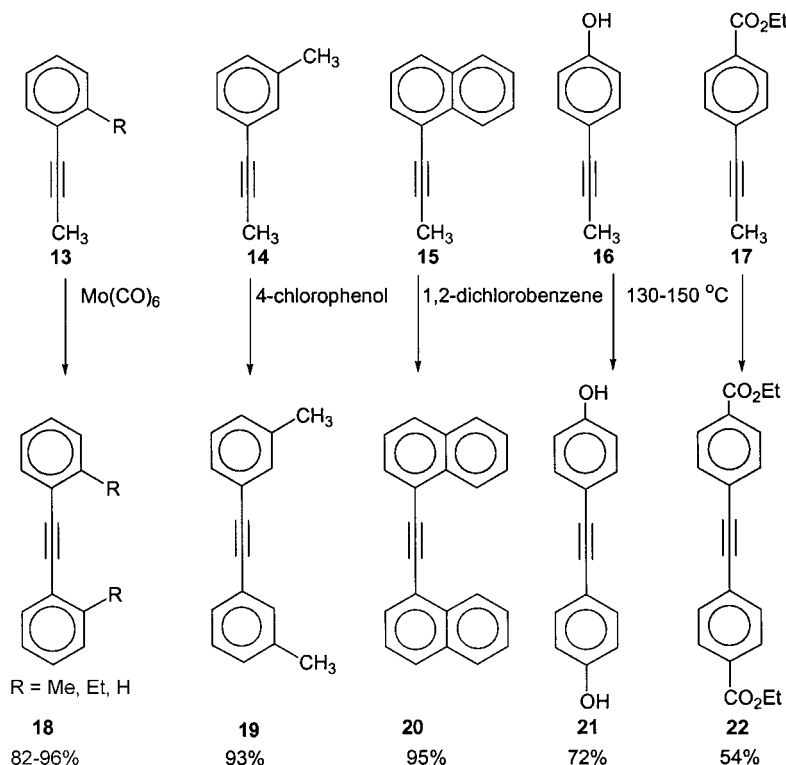
Scheme 6

cross-linking, electrophilic addition of aryl oxides, or partial reduction. In an extension of this approach, 1,4-dipropynyl-2,5-diphenylbenzene **10b** and 1,3-dipropynylbenzene were metathesized to give poly(aryleneethynylene)s in good yields but with a relatively low degree of polymerization. The successful performance of alkyne metathesis inspired Fürstner [14] to utilize ADIMET to close large rings in a clever exploitation of alkyne metathesis in natural product synthesis. While the defined carbyne complex **11** is successful in the synthesis of PPEs, this alkylidyne is not commercially available. It has to be synthesized in a multistep procedure utilizing glove-box techniques, a task that the preparative by working organic chemist wants to avoid! As a consequence, it was of great importance to explore whether the simple in situ catalysts formed from Mo(CO)_6 and 4-chlorophenol could be used for the synthesis of PPEs **12** and other target molecules.

7.2.2

Synthesis of Diarylalkynes Utilizing the Mori System

The low yields of the Mori dimerization presented a challenge for the utilization of the simple catalyst systems [12]: optimization by increasing the reaction temperature from 105 to 130–150 °C combined with the slow introduction of N_2 into the reaction mixture increased the isolated yield of **8** from 52 % to 82 % (Scheme 7). If the propynylated aromatics (**13**, **14**)

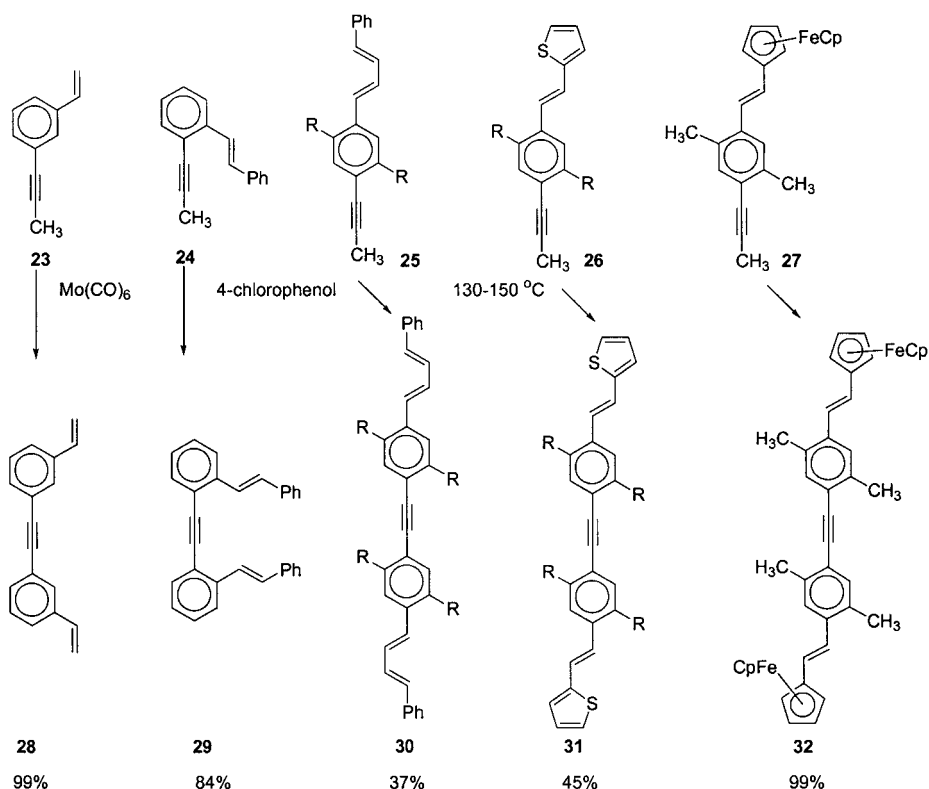


Scheme 7

bear an alkyl group in a position *ortho* or *meta* to the propyne group, the yield (after crystallization and chromatography) of the dimers **18** or **19** exceeds 90 %, suggesting that their formation is quantitative.

Propynylnaphthalene **15** furnishes dinaphthylacetylene **20** in near quantitative yield. On the other hand, the Mori system performs somewhat less well if heteroatoms are present in the substrates, suggesting that the catalytic system is poisoned by the presence of the heteroatom through complexation and/or chelation of the active molybdenum center. Cyano groups and bromides/iodides inhibit the reactivity of the catalyst system. However, both propynylated phenols (**16**) and esters (**17**) give satisfactory dimerization results (**21**, **22**).

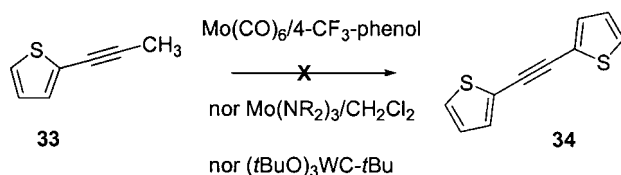
Grubbs and Zuercher [15] have shown that alkene metathesis in the presence of alkynes leads to the transformation of the alkynes into alkenes in the final product. Thus, it was of importance to check if the reverse was true for alkyne metathesis utilizing the simple Mori system. Subjecting a series of propynylated styrenes and stilbenes **23–27** to the “shake-and-bake” catalysts led to the isolation of the dimers **28–32** in good to excellent yields after their precipitation from methanol (Scheme 8) [16]. It is noteworthy that unsupported double bonds are tolerated in the metathesis process forming divinyltolane **28** in good yields. Likewise, butadiene (**25**) and thiophene (**26**) containing substrates are dimerized, providing that the heteroatom or large π -system is far enough away from the reactive metathesis center.



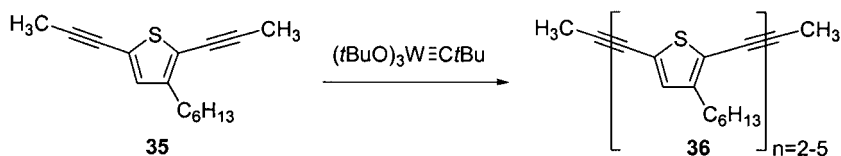
Scheme 8

The yields are lower in these more difficult cases. It was demonstrated that the metathesis conditions do not exert any oxidative stress on the substrates. Dimerization of **27** furnished spectroscopically pure **32** in 99 % yield after precipitation from methanol. Under oxidative stress, the ferrocene nucleus would have been oxidized and paramagnetic material would have been isolated.

While butadiene units and thiophenes are tolerated in ADIMET with simple catalyst systems, the thiophene nucleus has to be relatively far away from the reacting propyne group (Scheme 8); 2-propynylthiophene **33** did not undergo ADIMET with simple catalyst systems (Scheme 9). Fürstner [14] reported a highly active catalyst system that was formed from Cummins' tris(amide) $[\text{Mo}(\text{NHR})_3]$ [17] and dichloromethane in situ. According to the authors, this is the most active and heteroatom-tolerant catalyst available to date. Attempts to dimerize **33** with Fürstner's catalyst failed (Scheme 9), although co-metathesis with a second alkyne proceeded smoothly. Weiss [18] reacted 2,5-dipropynylthiophene **35** with **11**, whereby small thiophenyleneethynylene oligomers **36** formed in moderate yields (Scheme 10).



Scheme 9

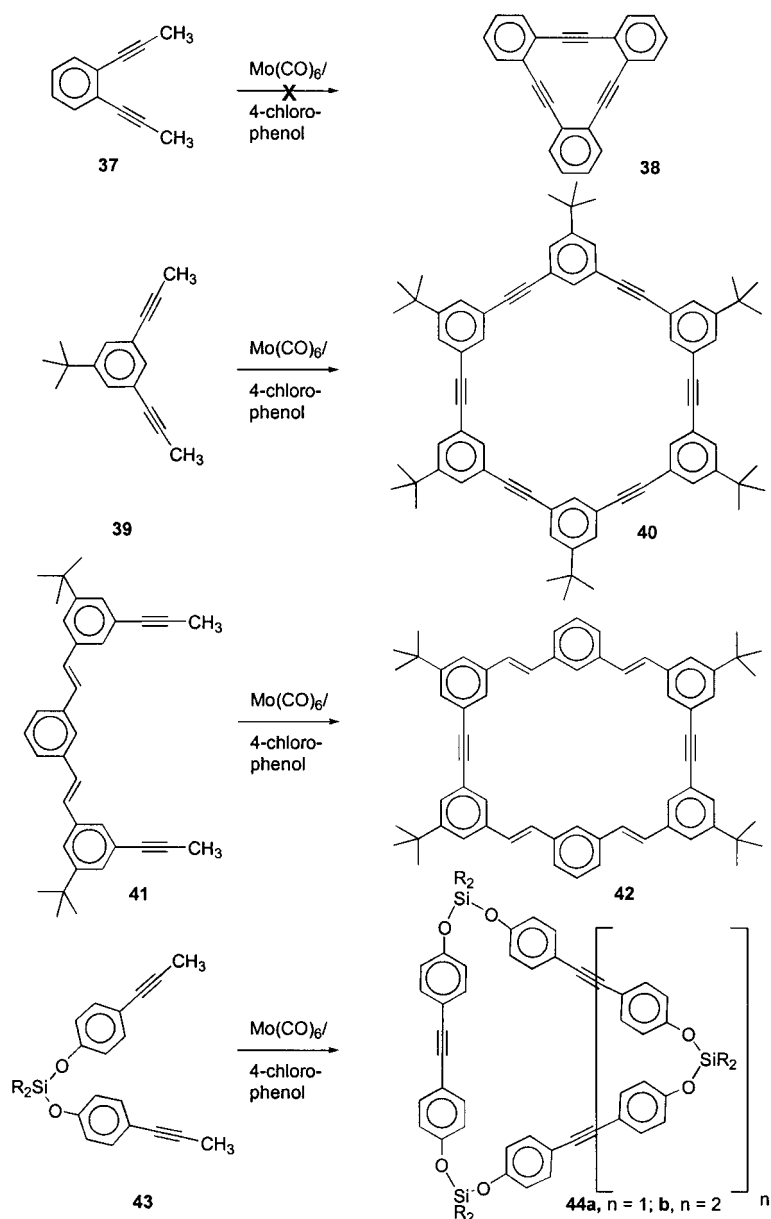


Scheme 10

7.2.3

Cycles

Having demonstrated that the dimerization of propynylated substrates works well, it was important to explore ring-forming metathesis (RCM) [14]. The first experiments utilizing 1,2-dipropynylbenzene **37** were unsuccessful, and led to the isolation of unreacted starting material along with a small amount of an infusible and intractable dark solid. Perhaps the second alkyne group in **37** chelates the molybdenum center and prevents metathesis activity. More successfully, subjecting 1,3-dipropynyl-5-*tert*-butylbenzene **39** to RCM conditions provided the cyclohexameric phenyleneethynylene **40** in an isolated yield of 8 % after repeated chromatography. According to mass spectrometry, the heptameric and octameric cycles are also formed, albeit in much lower yields. The other identified product of this reaction is a poly(*meta*phenyleneethynylene) of relatively low molecular weight [19]. To confirm the structure of **40**, Adams, Bunz, and Herrmann performed a single-crystal X-ray



Scheme 11

structure analysis [19]. The geometry of the ring is hexagonal, although the packing of the cycles is of more interest. Moore has recently described a packing motif of a hexaphenolic phenyleneethynylene cycle. This macrocycle forms extended channels, and the rings are packed in a coplanar fashion [20] on top of one another. In the simpler hydrocarbon system

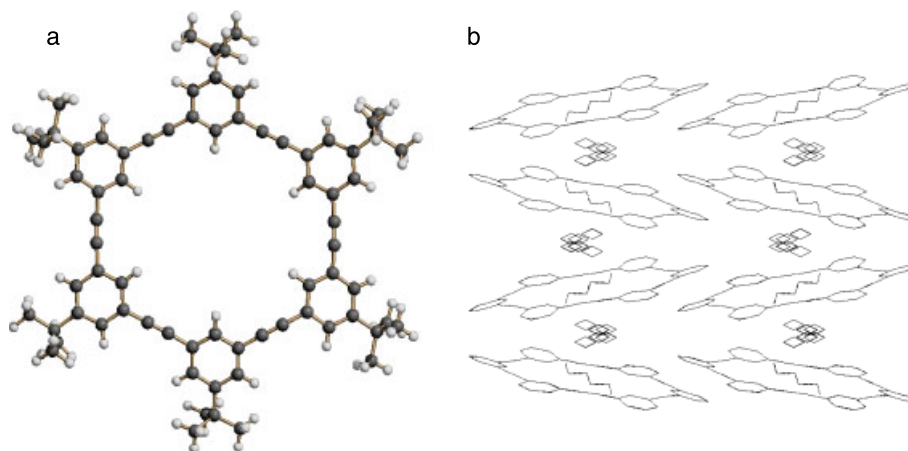


Fig. 1. (a) Ball-and-stick plot of **40**, (b) packing diagram of **40**. The *tert*-butyl groups and the hydrogens are omitted for clarity. The squares indicate highly disordered solvent, probably hexanes.

40, a related packing motif is observed, but stacks of the rings that form channels are mutually arranged in a herringbone pattern. This would be expected for large aromatic molecules where only van der Waals and electrostatic forces play a role.

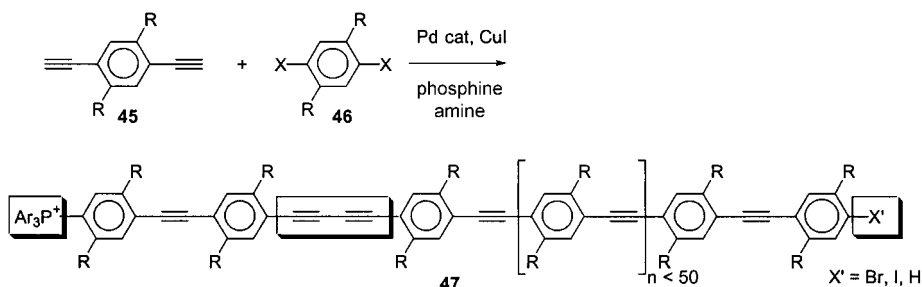
To explore other ring-forming metatheses, the trimeric precursor **41** was subjected to ADIMET, which produced a small percentage of the cycle **42** in addition to large amounts of a weakly fluorescent but not very soluble polymer. The substrate that proved most ideal for ring-forming ADIMET was **43**, which, upon metathesis, furnished the trimeric cycle **44a** ($n = 1$) in 14 % and the tetrameric cycle **44b** ($n = 2$) in 18 % isolated yield after chromatography and crystallization. While larger ring sizes could be detected by mass spectrometry, it was not possible to isolate these rings by column chromatography [21].

7.2.4

Alkyne-Bridged Polymers by ADIMET

Conjugated polymers are organic semiconductors, and as such they are of great importance in the fabrication of organic semiconductor devices. These devices include, but are not restricted to, light-emitting diodes (LEDs), thin-film transistors, photovoltaic cells, and plastic lasers. The most important polymers in this field are the PPVs, despite their moderate stability, delicate processing requirements, and less than ideal photophysical properties [22]. The dehydrogenated congeners of the PPVs, the PPEs (**12**), show considerably higher stability, are more easily processible, and have superior photophysical properties in solution compared to those of the PPVs [1]. The PPEs have attracted much less attention in device fabrication, even though they have been popularized by Swager [23] as sensory materials and by Tour [24] as “molecular wires”.

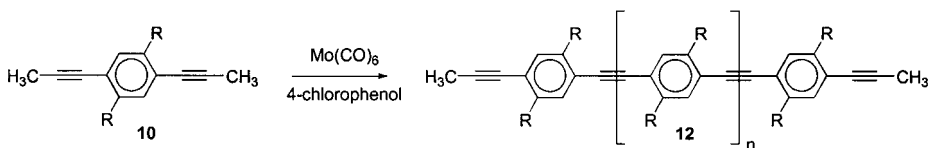
The classic synthesis of PPEs is the Pd/Cu-catalyzed coupling of diethynylbenzenes **45** with diiodo- or dibromobenzenes **46** [1]. This coupling reaction is widely applicable, quite



Scheme 12

general in scope, and was first utilized by Giesa and Schulz to prepare soluble PPEs [25]. However, the method is not without its problems, and the polymers **47** contain numerous defects, including diyne groupings. This is due to oxidative dimerization (by traces of oxygen or other oxidants in the reaction mixture) of the bis(alkyne) component. In addition, the end-groups of Pd-made PPEs are not well defined because of dehalogenation or phosphonium salt formation [26]. The reaction is a classic polycondensation, and is quite sensitive to imbalances in the stoichiometry. Furthermore, the degree of polymerization of the Pd-made PPEs is not very high ($P_n < 50$ repeating units) [1] unless acceptor-substituted dihalides are utilized [27]. The best polymers made by this method were described by Swager [28], who reacted diiodo aromatic coupling partners and a Pd(0) catalyst to minimize side reactions.

Because of the problems associated with Pd-catalyzed polycondensations, it became necessary to develop an independent, simple synthetic access that was not based on the Pd methodology. Alkyne metathesis was deemed appropriate, and with optimization of the simple “shake and bake” catalysts it was expected that it would be well-suited for forming PPEs [29]. The high yields obtained in the dimerization reactions of propynylated arenes (Schemes 7 and 8) strongly supported this notion, and from the work of Bunz, Müllen, and Weiss it was clear that PPEs **12** could be made by ADIMET, at least if Schrock’s tungsten carbyne complex **11** was employed [13]. A reaction mixture containing dihexyldipropynylbenzene **10a** and the “shake and bake” catalyst $\text{Mo}(\text{CO})_6/4\text{-chlorophenol}$ became strongly fluorescent after approximately 1 h at a reaction temperature of 130 °C, suggesting that productive metathesis had commenced (Scheme 13).



Scheme 13

Work-up furnished dihexyl-PPE **12a** in an almost quantitative yield with a degree of polymerization (P_n) of approximately 100. It was noticed that **12a** was only sparingly soluble in hot 1,2-dichlorobenzene. Dodecyl-, 2-ethylhexyl-, and bis(3,8-dimethyloctyl)dipropynylben-

Tab. 1. Substituent pattern and molecular weights for representative PPEs **12**.

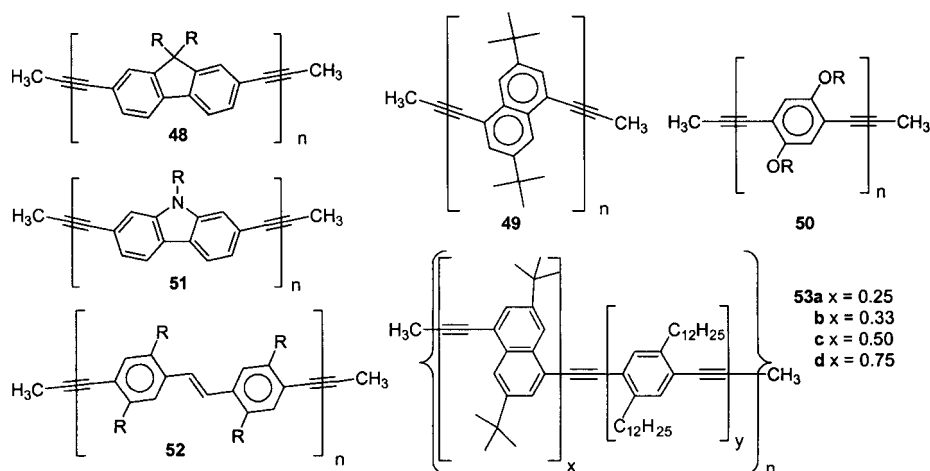
Substituent	Hexyl <i>a</i>	Hexyl <i>a</i>	Hexyl <i>a</i>	2-Ethylbutyl <i>e</i>	2-Ethylhexyl <i>d</i>	Dodecyl <i>c</i>
Temp. (°C)	120	170	150	150	150	150
Co-catalyst	4-Cl-phenol	4-Cl-phenol	4-CF ₃ -phenol	4-CF ₃ -phenol	4-CF ₃ -phenol	4-Cl-phenol
Yield	70	76	99	80	99	96
<i>P_n</i> (GPC)	22	10	94	insoluble	510	770

zenes **10c,d,f** were prepared by standard Pd-catalyzed reactions to improve the solubility and molecular weight. The ADIMET of **10c,d,f** with the Mo(CO)₆/4-chlorophenol mixture gave polymers **12c,d,f** of higher molecular weight. The samples showed a degree of polymerization in the range $P_n = 200\text{--}700$ [30, 31], as estimated by gel permeation chromatography (GPC). In rare cases, the P_n values exceeded 1000 repeat units. The degree of polymerization increases with the scale of the reaction and the purity of the monomers. An interesting point is the temperature window in which these reactions are successful. At 120 °C, these polymerizations give low molecular weight oligomers, as is also the case above 160 °C. From the data collected in South Carolina, the optimum conditions for ADIMET with Mori catalysts are 135–150 °C, an excess of phenol, and a small amount of solvent. 4-Chlorophenol is not the only potent co-catalyst; 4-(trifluoromethyl)phenol/Mo(CO)₆ is likewise effective in promoting ADIMET.

The PPEs are isolated by precipitation from methanol after washing with acid and base to remove Mo-containing residues. The polymers are obtained as light-yellow to bright-yellow powders (branched side chains give paler polymers), flakes, or rubbery fibrous materials depending upon the nature of the side chain and the degree of polymerization. After 16 h, ADIMET gives materials of substantial molecular weight, and the reaction is finished after approximately 24–30 h, beyond which no increase in molecular weight is observed [31]. After 30 h, the concentration of reactive end-groups is very low, and it may be that the catalytic system slowly decomposes under these conditions. The reaction can be scaled-up; 10 g of PPE was prepared in a 250 mL Schlenk flask, suggesting that industrial scale synthesis of PPEs will be facile.

The ¹³C NMR spectra of dialkyl-PPEs (**12**) feature three signals in the aromatic region and one signal due to the alkyne units. No other resonances are detected in the region $\delta = 80\text{--}200$, excluding cross-linking by formation of networked PPV-type structures.

The synthetic utility of the ADIMET process with simple catalyst systems would be restricted if only PPE (albeit very pure and in high yields) could be made. Fortunately, this is not the case, and a series of different propynylated aromatics underwent ADIMET to give the polymers **48**, **49**, and **51–53** in good to excellent yields with respectable P_n values [32–35]. Most of these polymers were not known (**49**, **52**, **53**) or had never been appropriately characterized (**48**, **51**). The PPVEs **52** are hybrids of PPEs and PPVs that have not been described previously. They may combine the stability of the PPEs with the exciting properties of the PPVs. Utilizing a series of dipropynylated stilbene derivatives accessible by a Horner–Wittig approach, alkyl-substituted PPVEs **52** of high molecular weight (P_n up to 400 aryleneethynylene units) and purity were obtained by ADIMET as stable, deep-yellow



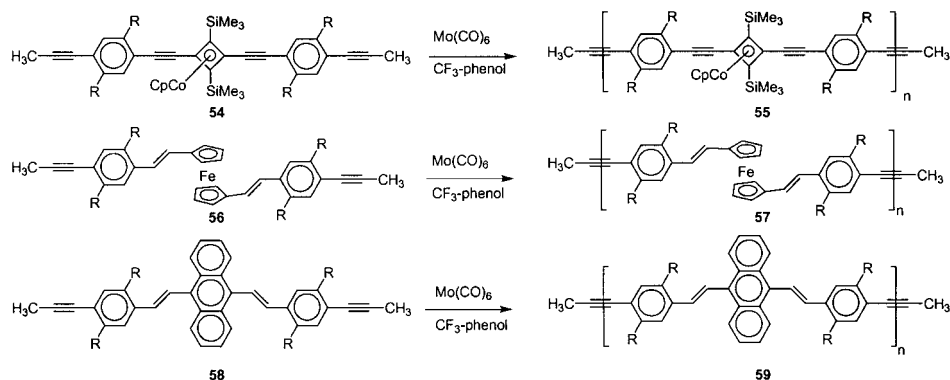
Scheme 14

or greenish emitting materials. PPVEs are of interest as active materials in organic light-emitting diodes [16].

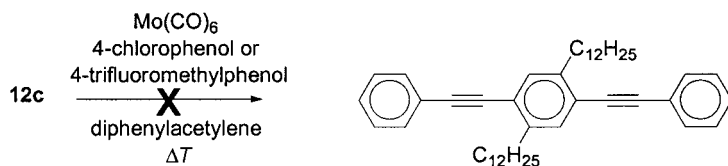
Heteroatoms are tolerated in these polymerization reactions as long as they are spatially separated from the reacting propyne groups. An excellent example is the poly(carbazyleneethynylene) **51**, which is made by ADIMET from *N*-alkyldipropynylcarbazoles [32]. The presence of oxygen functionalities is likewise tolerated, but the formation of dialkoxy-PPE **50** gives polymers of relatively low molecular weight, even though it proceeds in high yields. Polymer **50** is only formed when the active co-catalyst 4-(trifluoromethyl)phenol is employed. ADIMET allows the synthesis of copolymers, as exemplified by the formation of poly(naphthyleneethynylene)/PPE hybrid **53** when dipropynyldialkylbenzenes **10** and dipropynyldi-*tert*-butylnaphthalene are co-metathesized. Typically, P_n values of 50–100 are achieved, and the polymers are formed in high yields. The copolymers are, like the poly(fluorenyleneethynylene)s **48**, strongly solid-state blue-fluorescent emitting, and have been utilized in the fabrication of PPE-based OLEDs (*vide infra*). ADIMET-made poly(dialkylfluorenyleneethynylene)s **48** are now commercially available and are marketed by Aldrich.

ADIMET is not restricted to the synthesis of simple poly(aryleneethynylene)s. If somewhat more complex monomers (**54**, **56**, **58**) are employed, organometallic and arylenevinylene-containing modules can be embedded into the polymer backbone. The introduction of electroactive and other modules of interest is possible whenever propynylbenzene groups can be attached to the target core. The polymers **55**, **57**, **59** are stable under the reaction conditions, and the $\equiv[-A\equiv-A\equiv-B\equiv]_n$ sequence is not disturbed according to ^{13}C NMR spectroscopy. That is to say, no scrambling of the arene units is observed under ADIMET conditions. By the same token, it was not possible to degrade **12c** by the Mori catalysts in the presence of an excess of either dodecyne or diphenylacetylene (Scheme 16).

Overall, the most difficult part of the ADIMET process is the synthesis of the monomers. Monomer synthesis can be a challenge, considering that the necessary aromatic diiodides



Scheme 15



Scheme 16

are often either not described in the literature or are difficult to prepare. Given the absence of chelating heteroatoms, most monomers bearing two propyne groups will be polymerizable by ADIMET with simple catalyst systems to give high molecular weight polymers in good yields and with high purity.

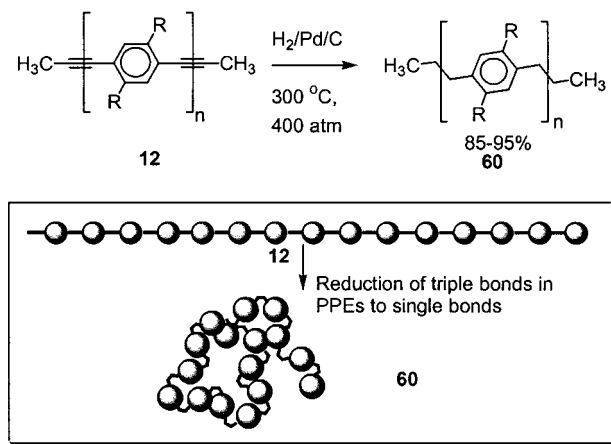
7.3

Reactivities of PPEs

The determination of the absolute molecular weights of rigid rods by GPC is problematic, because molecular weight standards for GPC are almost all (for an exception, see ref. [36]) based on polystyrene. Polystyrene is coiled and much more flexible than PPE. PPEs behave like tough rods with a persistence length of several tens of nm, as reported by Cotts and Swager [37]. Numerical values of by how much GPC overestimates the molecular weight of PPEs are difficult to determine, but Tour reported that the GPC values for phenyleneethynylene oligomers overestimate their real molecular weights by roughly a factor of two [38]. An interesting situation would arise if the PPEs could be transformed from rigid-rod polymers into flexible coils. Thus, a rigid rod could be compared to a flexible coil with the same polydispersity and the same molecular weight. PPEs should be uniquely suited for this purpose because catalytic hydrogenation of their triple bonds should lead to a coiled polymer with only a slightly increased molecular weight. The hydrogenated PPE would be an isomeric polystyrene **60** [39], in which the polymer connection is made through the 1,4-positions of the benzene ring instead of the benzene units substituting a polyethylene chain.

The polymer **60** is expected to be coiled and thus better amenable to reliable molecular weight determination by GPC using polystyrene standards.

Attempts to reduce PPEs **12** under moderate pressures (2–3 bar H_2) at temperatures of around 70–80 °C were unsuccessful. PPEs seem to be very stable *chemically*, and only when the reduction was performed in an autoclave under drastic conditions successful hydrogenation was observed. Hydrogen pressures of 300–500 bar at temperatures of around 300 °C are necessary for complete reduction of the PPE to the hydrogenated polymer **60** [40]. The yield of **60** is high; the aromatic rings are not affected under these conditions and side products are not detected in the colorless materials formed. Attempts to use shorter reaction times, lower temperatures, or lower hydrogen pressures failed, and partially reacted material of undefined structure resulted.

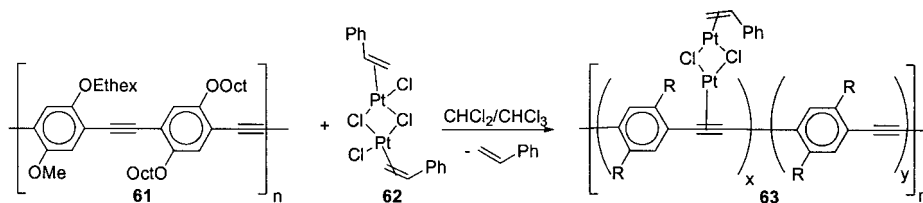


Scheme 17

The hydrogenation of several low to medium molecular weight PPEs showed that the molecular weights of the PPEs and their hydrogenated congeners **60** can differ by a factor ranging from 1.1 to 1.6 depending upon the side chain. Further experiments are necessary to evaluate the relationship between the molecular weights of the rods and the corresponding coils.

Generally, the reactivity of PPEs is not well established. Weder has recently reported an interesting means of functionalizing PPEs via an organometallic route. Thus, treatment of PPE **61** with the styrene complex of platinum dichloride (**62**) furnished the polymeric PPE complexes **63**, in which the content of the organometallic units could be controlled by the amount of Pt complex added. The labile styrene ligand in the platinated polymer **63** may be removed at a later stage to give three-dimensionally conjugated organometallic PPE-heterostructures [41].

PPEs should offer a potent platform for polymer-analogous reactions, and a family of new materials should be accessible by either complexation or cycloaddition via their bridging triple bonds. A difficulty is the relatively low reactivity of the alkyne units in PPEs. Steric shielding by the adjacent alkyl or alkoxy groups, as well as electronic effects, reduce the re-



Scheme 18

activity of the alkynes in the highly conjugated polymer and present formidable obstacles to the exploitation of this concept.

7.4

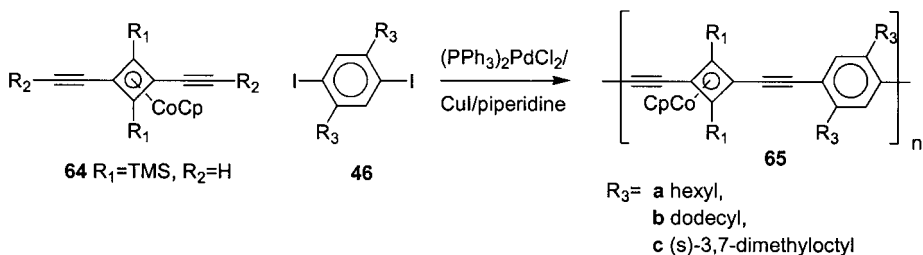
Solid-State Structures and Liquid-Crystalline Properties of the PPEs

PPEs are formally linear and rigid molecular rods with a high molecular anisotropy. As a result, PPEs have a large aspect ratio (aspect = length/width). In the early contributions that dealt with the synthesis of dialkoxy-PPEs, it was claimed that PPEs were liquid crystalline [1]. However, no convincing proof was obtained. Optical micrographs showed shear-induced birefringence, but no identifiable liquid-crystalline textures pointed to a smectic or nematic phase [42]. In addition, the dialkoxy-PPEs are not thermally robust and they do not generally give a stable isotropic melt but decompose at temperatures above 120 °C. Swager, Weder, and Wrighton [43], and Le Moigne [42] observed the lamellar packing of the PPEs by powder diffraction analysis, which provided evidence of a smectic ordering in these materials. In 1997, Weder [44] demonstrated that dialkoxy-PPEs form lyotropic-nematic liquid-crystalline phases in highly concentrated solutions in 1,2-dichlorobenzene. However, there have been no reported cases of thermotropic dialkoxy-PPEs in the literature.

7.4.1

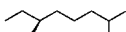
Organometallic Poly(aryleneethynylene)s

The first reported thermotropic and lyotropic liquid-crystalline poly(aryleneethynylene)s were not parent PPEs, but organometallic derivatives **65** made by the Pd-catalyzed condensation of Vollhardt's diethynyl **64** with diiodobenzenes **46** [45]. The polymers were isolated in good to excellent yields as amorphous tan or red powders with moderate P_n values of



Scheme 19

Tab. 2. Substituent pattern, yield, molecular weight, and polydispersities of 65a–c.

65	R ₁	R ₃	Yield (%)	M _n (10 ³)	P _n	M _w /M _n
a	SiMe ₃	Hexyl	74	5.1	18	2.6
b	SiMe ₃	Dodecyl	79	4.9	12	4.1
c	SiMe ₃		80	21	29	3.0
		(S)-3,7-dimethyloctyl				

12–30 repeating units. The thermal and phase behaviors of **65a** and **65c** were investigated in detail. Both **65a** and **65c** form lyotropic nematic phases, as was evident from polarizing microscopy and powder diffraction analyses.

However, only **65a** exhibits thermotropic nematic behavior if amorphous thin films are heated to 155 °C, at which a Schlieren texture develops. The material decomposes above

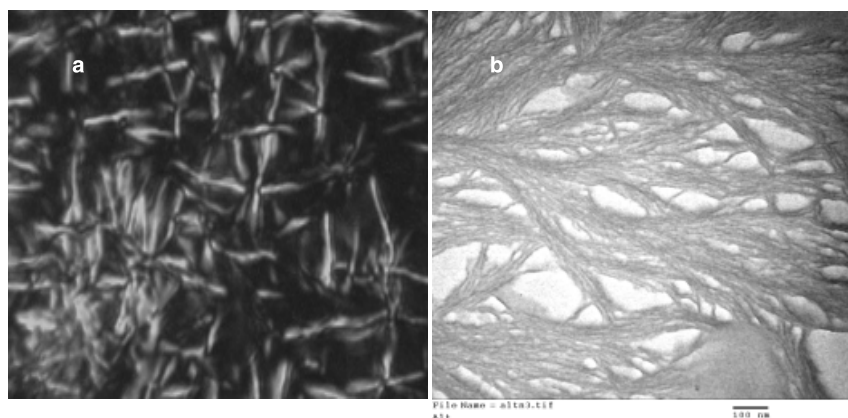
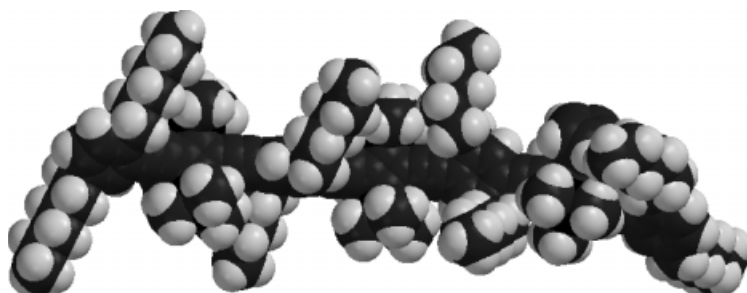
Fig. 2. a) Polarizing micrograph of **65c**. b) Transmission electron micrograph of **65a**.

Fig. 3. Single chain geometry of a segment of the organometallic PPE derivative **65a**. Planarization of the backbone in these materials is not favorable due to the added-on cyclopentadienylcobalt fragments that bulk up the main chain.

170 °C without attaining the isotropic phase. At room temperature, both polymers show a higher than nematic order, as is evident from their polarizing micrographs. The textures (Figure 2a) suggest an ordering of the lamellar smectic type. This ordering is unusual because the organometallic main chains cannot form a planar board-like structure. Investigation of the organometallic polymer **65a** by transmission electron microscopy (TEM) revealed an ordered lamellar superstructure with a lamellar width of approximately 18 nm. The lamellae are several hundred nm long. The extended length of the polymer chain **65a** is 18 nm. This result was based on the P_n value obtained by gel permeation chromatography, with the extended length of the macromolecule and the width of the lamellae conforming. The extended length of **65c** is 21 nm, while the observed lamellae are 24 nm wide by TEM. According to powder and electron diffraction data, the polymer chains must be aligned perpendicularly to the axis of the lamellae and are responsible for their width. These polymers show a highly ordered lamellar phase, although their ordering principle is fundamentally different to that observed for the dialkyl-PPEs (*vide infra*, Figure 4b).

7.4.2

Poly(dialkylparaphenyleneethynylene)s **12**

High molecular weight PPEs obtained by ADIMET are stable and do not decompose up to 250 °C in air and up to 300 °C under nitrogen. The high stability is a testimony to both their

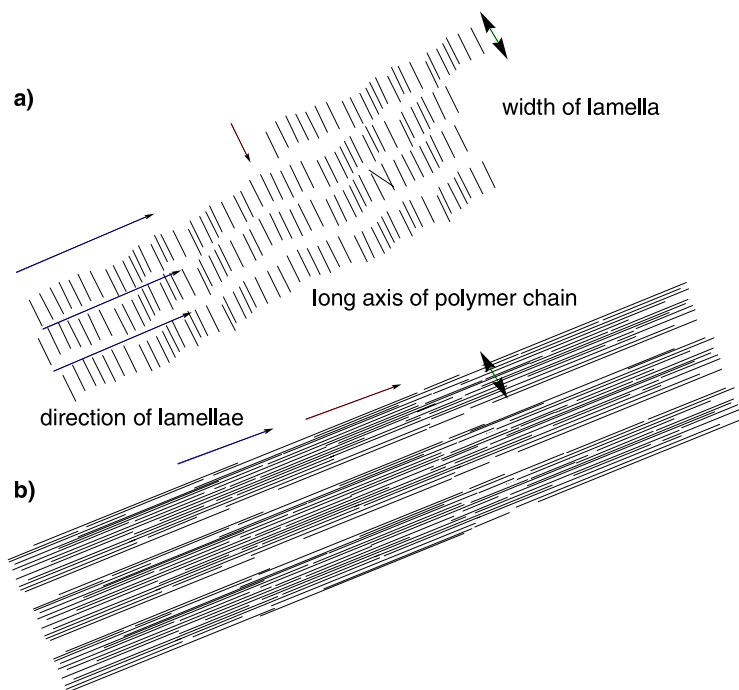


Fig. 4. Supramolecular arrangements of organometallic (**65**) and organic poly(aryleneethynylene)s (**12**) in the solid state.

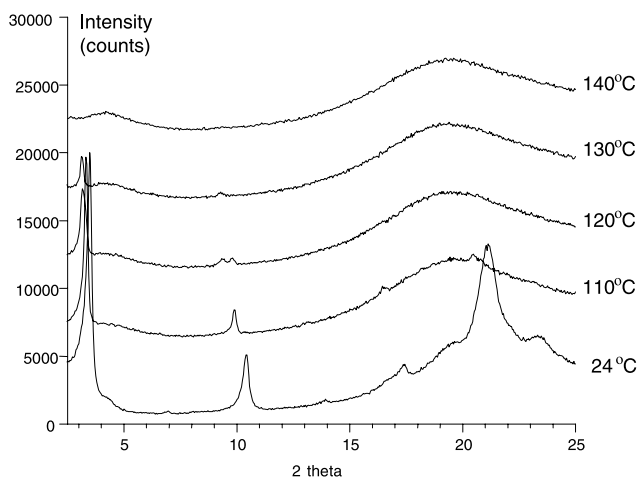


Fig. 5. Variable-temperature powder X-ray diffraction of didodecyl-PPE **12c**.

defect-free structure and the absence of electron-releasing oxygen substituents, which make the dialkoxy-PPEs so prone to oxidative decomposition at elevated temperatures. As a consequence of their high thermal stabilities, most ADIMET-made dialkyl-PPEs (didodecyl-, bis(ethylhexyl)-, and bis(3,7-dimethyloctyl)-substituted) **12c–f** melt reversibly without decomposition. They attain the isotropic phase at temperatures in the range 100–250 °C depending upon their P_n and the nature of their side chain. Increasing P_n and decreasing the length of the side chains raises the melting point [46, 47]. For example, dihexyl-PPE **12a** with a P_n of 100 cannot be melted, but decomposes above 270 °C with darkening.

The favorable stability of the ADIMET PPEs allowed a determination of their temperature-dependent X-ray diffraction and optical microscopy data. Didodecyl-PPE **12c** is crystalline at

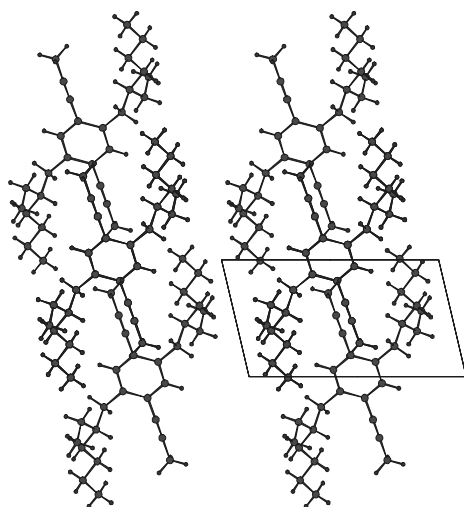


Fig. 6. Single-crystal X-ray diffraction analysis of 2,5-bis(ethylhexyl)-1,4-dipropynylbenzene **10d** [48].

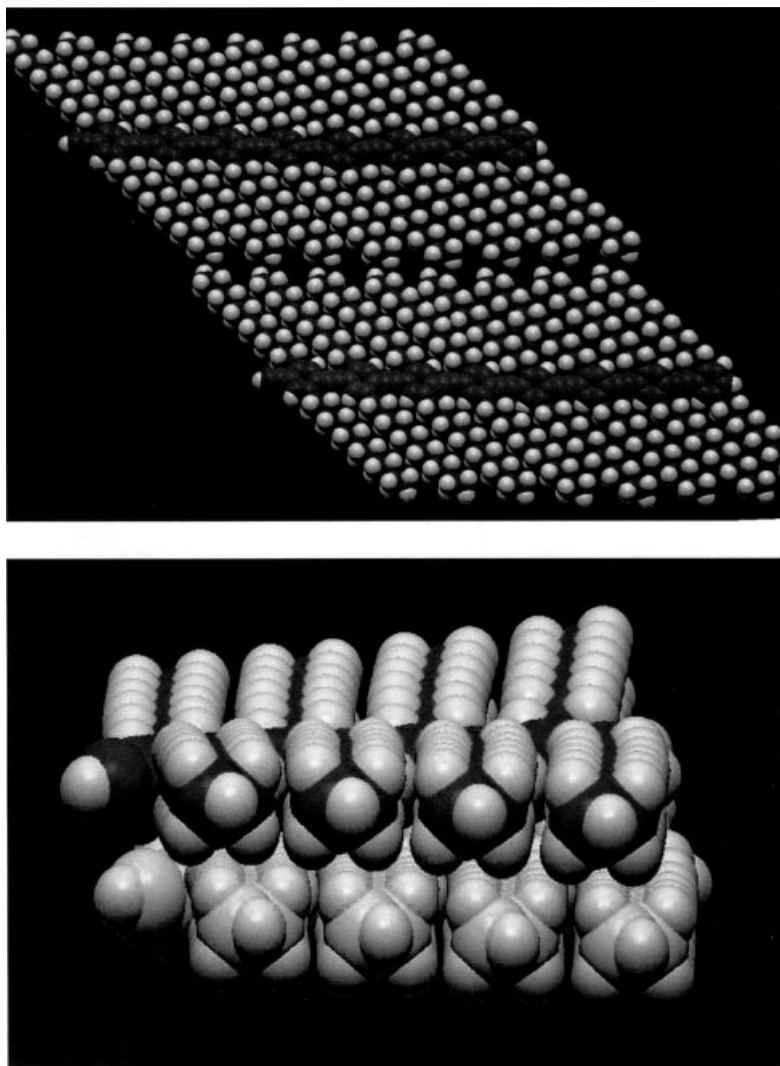


Fig. 7. Packing model of didodecyl PPE **12c** in the solid state. The packing was derived from single-molecule MM2 calculations utilizing powder diffraction and electron diffraction data obtained for the PPEs.

room temperature and shows diffraction peaks in both the small-angle and wide-angle regions of the powder diffraction spectrum (Figure 5). At 110 °C, all of the wide angle peaks have disappeared and only the intense small-angle peak at $d = 25.0 \text{ \AA}$ remains. This suggests the transition into the smectic liquid-crystalline state. At 140 °C, *all* of the diffraction peaks have disappeared, an isotropic melt has formed, and samples of **12c** appear black under crossed polarizers in optical microscopy. Differential scanning calorimetry (DSC) confirms

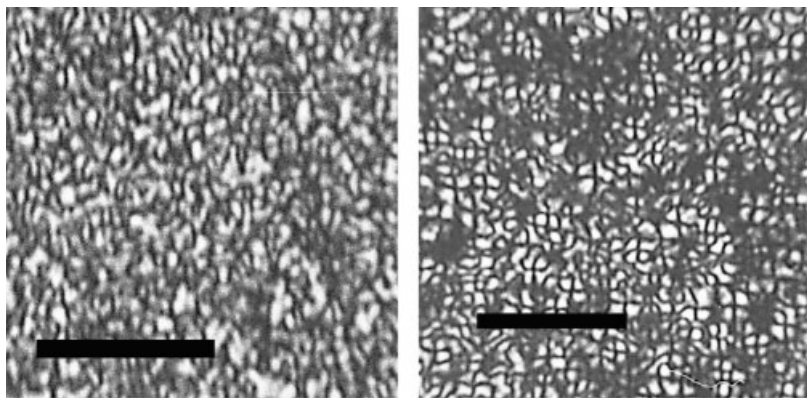


Fig. 8. Liquid-crystalline textures of didodecyl-PPE **12c**. Bars represent 20 microns. These PPEs form homeotropic smectic phases; the textures are typical for an edge-on view of lamellae that show apparent nematic ordering in this projection [46].

the phase transitions. From X-ray/electron diffraction data and single-crystal structures of a series of dipropynyldialkylbenzenes **10** (Figure 6), a valid packing model of PPEs (**12**) at ambient temperatures was developed. This is a refined version of the models suggested by Wrighton [43] and by Le Moigne [42]. Dialkyl-PPEs **12** form a doubly lamellar structure in the solid state [48]. The optimum space filling of the long alkyl chains forces the PPE backbone into planarity, and enables the packing of their backbones on top of one another. The polymer chains pack in an AB pattern, in which the positions of the vertically adjacent polymer chains are displaced by 3.5 Å to accommodate the spatial requirements of the side chain and to ensure optimum electrostatic interaction of the main chains as shown in Figure 7.

Above 110 °C, this arrangement becomes mobile, and a smectic C liquid-crystalline phase is entered. Samples cooled down from the isotropic melt (140 °C) show Schlieren and banded textures when viewed under crossed polarizers (Figure 8). These textures *look* similar to nematic Schlieren textures, but from the X-ray diffraction data it is clear that **12c** forms a homeotropically oriented smectic C phase. In a nematic phase, the small-angle diffraction peak would be absent, and a broad scattering feature, a “nematic streak”, would be observed. Polymer **12c** was the first example of a PPE derivative for which three states of matter, i.e. crystalline, thermotropic liquid crystalline, and a highly viscous isotropic liquid, were accessible [46].

7.5

Spectroscopic Properties of Dialkyl-PPEs **12** [47–49]

An important point in the science of conjugated polymers is the dependence of their optical properties as a response to their physical state (solution, aggregated, liquid crystalline, solid state, thermal treatment) [50]. Processable PPEs, particularly dialkoxy-PPEs, have been known since the early 1990s [1], and their spectroscopic behavior has been studied both in

good solvents (chloroform) and in the solid state. Early on, it was noticed by Wrighton, Weder, and Swager [43] that the absorptions of PPEs in the solid state were red-shifted from those observed in solution. Annealing of thin dialkoxy-PPE films at elevated temperatures led to a further red shift of the primary absorption band [43]. The underlying reason for this phenomenon was not well explained nor examined in depth [1]. The dialkoxy-PPEs are not well-behaved with respect to aggregation-induced changes in their optical properties and might not be the best examples for studying aggregation behavior by electronic spectroscopy. However, Swager has recently re-examined these issues utilizing self-assembled monolayers at the air–water interface (Langmuir–Blodgett technique) in order to gain a better understanding of the electronic properties of dialkoxy-PPEs [51].

There has also been discussion about the origin of the spectroscopic signature of *dialkyl*-PPEs upon aggregation, both in absorption and emission. It is clear for PPEs that excimer and aggregate formation have a substantial influence on their emission properties in the solid state. However, the contribution of multichain phenomena to the UV/vis spectra of the aggregated phases of dialkyl-PPEs is not clear. For the dialkyl-PPEs **12**, a strong case can be made for conformational changes of single polymer chains inducing the “aggregation band” observed at 439–445 nm (Figure 9).

7.5.1

UV/vis Spectroscopy of Dialkyl-PPEs 12

The UV/vis spectra of **12** are broad and featureless in chloroform, showing an absorption maximum at 388 nm. If methanol is added, the colorless and purplish-emitting solutions turn yellow and almost non-emissive, but remain clear (Figure 9) [48, 49]. Similarly, thin films of **12e** (Figure 10) form highly viscous melts above 190 °C, which are almost colorless and their UV/vis spectra resemble those obtained for PPEs in chloroform solution at ambient temperatures.

Addition of methanol to a solution of **12c** gives rise to a new band at 442 nm and a resolution of the high energy features into three bands at 416, 407, and 382 nm (Figure 9). The spacing between the 442 nm band and the other bands is 3554, 1928, and 1414 cm^{-1} , which is not readily interpretable in terms of defined molecular vibrations. The energetic separa-

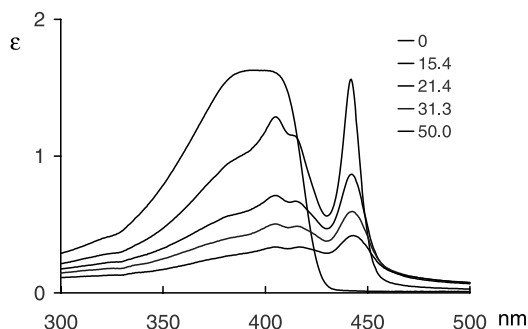


Fig. 9. Solvatochromic behavior of didodecyl-PPE **12c** upon addition of methanol.

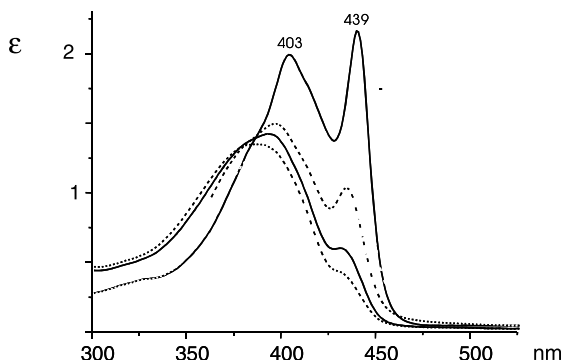


Fig. 10. Thermochromicity of a co-hexyl-dodecyl-PPE **12e**.

tion of the high energy features translates into vibronic spacings of 2140 cm^{-1} ($382 \rightarrow 416\text{ nm}$) and 1608 cm^{-1} ($407 \rightarrow 382\text{ nm}$), respectively, which can be interpreted as vibronic fine structure resulting from the C–C triple bond stretching (2140 cm^{-1}) and an aromatic stretching (1608 cm^{-1}) vibration.

What is the underlying reason for the the sharp and red-shifted band observed for dialkyl-PPEs **12** at 439–442 nm upon aggregation and in the solid state? This band could have several different origins: it could be (i) of strictly intramolecular nature, due to conformational processes of single polymer chains, (ii) of intermolecular nature, i.e. true aggregate formation between two or more polymer chains in a process that is similar to the formation of J-aggregates in the cyanines, (iii) a mixture of inter- and intramolecular processes, or (iv) a property of a single chain that is nevertheless elicited by aggregation and involves several chains resulting in a conformational change of single chains. The 439 nm band would then be an aggregate-induced band.

To explain the optical properties of the PPEs, comparison of their behavior with that of other conjugated polymers was helpful. The poly(3-alkylthiophene)s **66** show a similar spectral behavior (but in a more bathochromic regimen) as the PPEs. Thus, on entering the aggregated phase or on forming thin films, a substantial red shift of λ_{max} and a significant sharpening of the bands is seen for **66**. Wudl and Heeger [52] explained the spectroscopic changes in the poly(3-alkylthiophene)s **66** in terms of single chain planarization.

To confirm the qualitative agreement between the spectra of the polythiophenes and those of the PPEs, temperature-dependent UV/vis spectra of **12e** were measured (Figure 10). The UV/vis spectrum recorded at ambient temperature shows the typical solid-state feature at

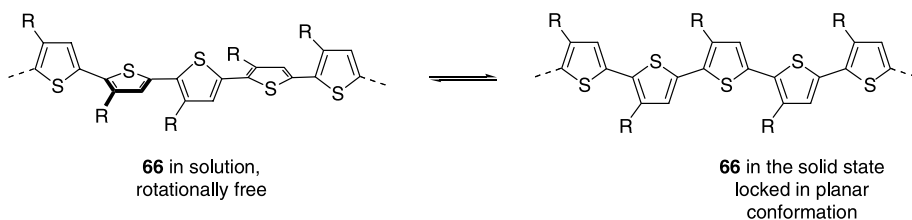


Fig. 11. Conformational preference of the poly(alkylthiophene)s according to Wudl et al. [51].

439 nm. When the film of **12e** was heated, the band at 439 nm slowly diminished and completely disappeared at temperatures above 185 °C, at which point the spectrum resembled those obtained in dilute chloroform solution. A variable-temperature powder diffraction study showed that **12e** loses all its ability to diffract or scatter X-rays at temperatures above 190 °C. Under crossed polarizers, films of **12e** appear “black” above 190 °C, indicating that this PPE transits from the liquid-crystalline form to the isotropic melt at this temperature.

To understand the implication of this experiment, knowledge of the conformational preference of diphenylacetylene in solution and in the solid state is necessary. According to Wudl, “we chemists are married to the concept of rotational invariance of modules connected by alkynes” [53]. This holds true in solutions of phenyleneethynylene oligomers and polymers, for which the barrier to rotation about the triple bonds is small (≤ 1 kcal mol⁻¹) according to quantum chemical calculations [54] and photoacoustic measurements [55]. However, this picture is no longer correct for solid PEs, where full planarization occurs even in the case of diphenylacetylene [56]. While the difference between the planar and twisted conformations is too miniscule to prohibit deplanarization of PE oligomers in solution, the small energy difference is sufficient in the solid state to force them to adopt structures in which they have planar backbones. This effect is more pronounced in the case of alkyl-substituted PEs, where the accommodation of the side chains reinforces and “freezes” the coplanar packing of the conjugated backbones.

While deplanarization has a small effect on the *total* energy of the phenyleneethynylenes, its influence on the frontier orbitals (HOMO and LUMO), which are mostly responsible for the optical properties of conjugated molecules, is much more dramatic. Semiempirical calculations on an octameric phenyleneethynylene model compound, utilizing the AM1 and PM3 methods, revealed a significant increase in the band gap on going from the fully planar form to the more twisted forms (Figure 12). The band gap was calculated to be largest when all adjacent benzene units were twisted by 90°. In collaboration with Garcia-Garibay [57], a phenyleneethynylene model trimer was carefully analyzed, revealing a small band gap in the solid state and a larger gap in solution. A semiempirical calculation including configuration interaction supported the experimental evidence that planarization leads to an increased λ_{max} in the UV/vis spectrum of phenyleneethynylenes.

A self-consistent picture arises, in which the optical changes of the PPEs upon thin-film formation can be attributed to an aggregation-induced planarization of single polymer chains. While the aggregation process involves many chains that enforce their mutual pla-

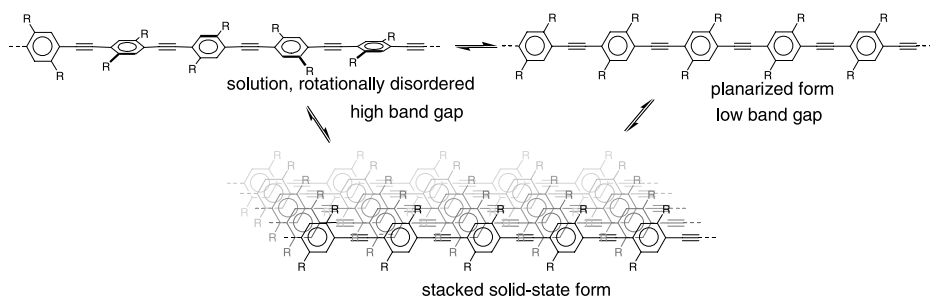


Fig. 12. Conformational preferences of dialkyl-PPEs **12** in solution and in the solid state.

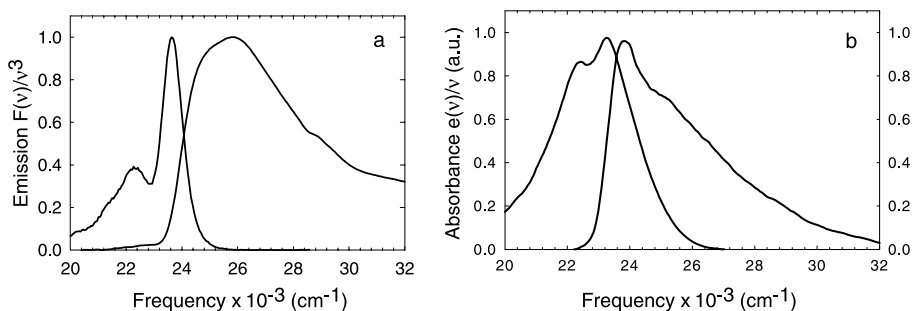


Fig. 13. (a) Overlay of absorption and emission spectra of **67** in chloroform at room temperature. (b) Overlay of absorption and emission spectra of **67** in low molecular weight polystyrene at 77 K.

narization invoking Ockham's razor, the spectroscopic changes of dialkyl-PPEs **12** can be explained in terms of conformational changes of *single* polymer chains (Figure 12). However, interchain interactions may also play a minor role. PPEs bearing donor and/or acceptor substituents are fundamentally different because charge-transfer effects will enhance their interchain interactions, and the influence of these on their optical properties will be more significant [50].

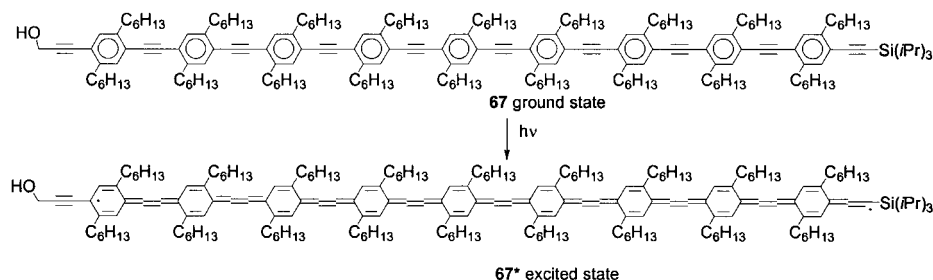
7.5.2

Fluorescence Spectroscopy: The Excited State Story [58]

The UV/vis spectra of **67** and **12a–f** are sharp in the solid state, but broad and featureless in good solvents. This is due to the fact that the rotation of the PE units about the $C\equiv C-Ar$ single bonds is unrestricted, and deviation of planarity between PE units in single chains increases the HOMO-LUMO gap [47]. The emission spectra of **12** and **67** are narrow and show a well-resolved shoulder (Figure 13a). For rigid molecules such as **67**, one would expect approximate mirror symmetry of absorption and fluorescence with a relatively small Stokes' shift. Thus, the question arises as to why this is not the case.

The optical and emissive properties of **12** and **67** are almost identical, confirming that **67** has reached the convergence length of PPEs and is thus a good model for **12**. The use of **67** avoids issues of energy migration along single polymer chains, chain entanglement, energy transfer between multiple chains, and excimer formation. The optical behavior of PPEs may therefore be explained by investigating **67**. When a solution of **67** in polystyrene is cooled to 77 K, its absorption spectrum narrows slightly. However, significant changes are seen in the *emission* spectrum (Figure 13b), which, according to Berg et al. [58], is broadened towards the blue side. In a time-resolved fluorescence experiment (Figure 15; 297 K, chloroform), the blue component of the emission decreases over time and the narrow fluorescence spectrum is reconstituted.

These experiments are consistently interpretable. The ground state of **67** features a shallow potential energy profile with respect to rotation about the PE units ($CHCl_3$ solution at 297 K; Figures 13 and 14). In the excited state, this may not be the case. The spectroscopic data can be explained if the potential energy profile of **67*** (Scheme 20) is much steeper than that of **67**, and symmetric with respect to rotation (Figure 13a). This makes sense: in a va-



Scheme 20

lence bond picture, the excited state of **67** has a diradicaloid/cumulenoid character and rotation about the PE units is *not* facile anymore because the allenic structure has a strong preference for planarity of the conjugated backbone, eliminating the twisted double bonds.

In good solvents at ambient temperature, the excited state (**67***) will quickly relax to the planar form, so that only the 0–0 emission from S_1 is detected in steady-state emission. If the same experiment is performed at low temperature and in a viscous solvent, the molecular torsion of **67*** in attaining its planar form is hampered by the medium, and planarization is slow on the timescale of the fluorescence lifetime (355 ps). Emission will not only occur from the potential minimum of the lowest excited state, but from virtually all frozen rotamers resulting in a broad and blue-shifted spectrum. Only after planarization of **67*** is complete narrow emission from the lowest excited-state conformation will reoccur. Consequently, planarization of the excited state rather than energy migration is likely to govern the emission behavior in PPEs such as **12**.

In linear coupling models, the lowest-energy configuration is different in the ground and excited states, but the restoring forces are identical. The strong torsional coupling between the ground and excited states of **67** features a restoring force that is much stronger in the excited state than in the ground state, although the lowest-energy configuration is very similar. This situation is called quadratic coupling [58]. Quadratic coupling mimics spectroscopic effects in PPEs that have been attributed to energy migration, mode mixing, and other processes. It may be important but unrecognized in other conjugated polymers [52].

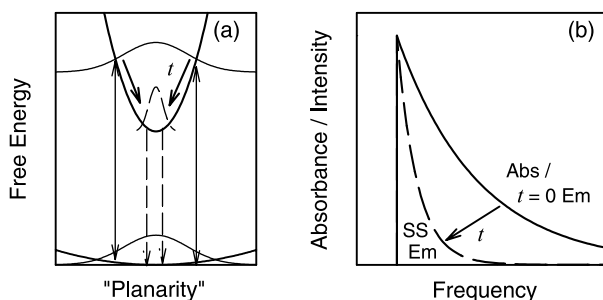


Fig. 14. (a) Potential energy profile of **67** in the excited state with respect to the torsional angle about the $sp-sp^2$ single bond. Note that the excited state has a much steeper torsional profile than the ground state. (b) Expected time-dependence of the emission in a system for which quadratic coupling is significant.

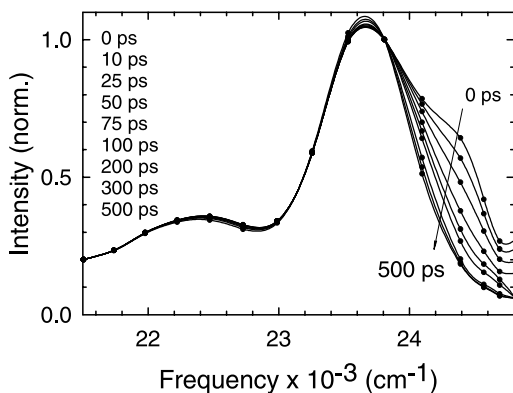


Fig. 15. Time-resolved spectrum of the emission of **67** in chloroform at 298 K.

7.6

Self-Assembly of PPEs on Surfaces: From Jammed Gel Phases to Nanocables and Nanowires

PPEs **12** are rigid and linear conjugated organic polymers, and it is expected that due to their shape anisotropy, self-assembly processes of PPEs will be facile. In bulk PPE samples, solid-state organization leads to lamellar phases with high order, whereas in thin films additional supramolecular features may be possible. Casting a dilute yellow solution of PPE in toluene onto a silicon wafer followed by slow evaporation of the aromatic solvent led to thin films that were investigated by atomic force microscopy (AFM). AFM showed two different self-assembly modes in these thin films. One is on the 1–2 nm, i.e. molecular scale and corresponds to the lamellae observed by powder diffraction analysis. The second features are much larger in their dimensions (Figure 16a). Long, cable-like structures form, that are approximately 30 nm in diameter and between 700 nm and 2 μm in length. Samori, Müllen, and Rabe [59] had earlier observed that PPEs **12a** display a rich self-assembly, and these authors demonstrated that depending on the conditions under which these films were grown

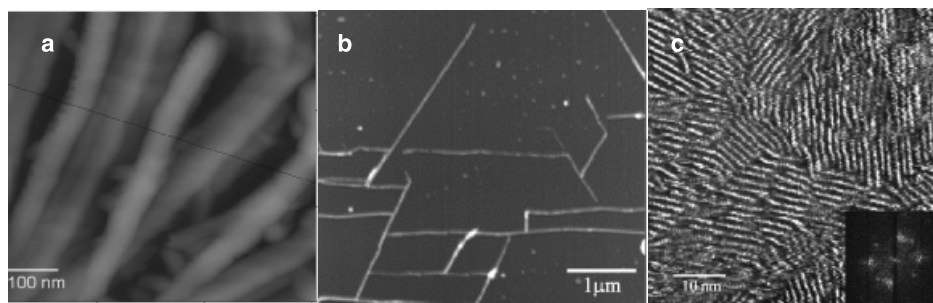


Fig. 16. (a) Nanocable arrangement of didodecyl-PPE **12c** on a silicon wafer [60]. The observed superstructure exceeds the size of single lamellae. (b) Nanowires and (c) nanoribbons of PPEs **12a** as observed by Samori, Müllen, and Rabe [59]. Single polymer chains are visible in (c).

(solvent, evaporation rate, support), either nanowires (Figure 16b) or nanoribbons (Figure 16c) could be formed. The Müllen–Rabe wires are 3–5 microns long and 30–40 nm wide. They correspond to the features observed by Perahia et al. [60, 61]. Using more concentrated solutions, Müllen and Rabe observed the formation of these structures on a smaller scale, and dense nanoribbons were observed by a combination of transmission electron microscopy and AFM. These features are approximately 1 nm wide and several hundred nm long, and represent single polymer lamellae in which the “wing span” of **12a** dictates the width of the lamellae. In simple terms, each of the structures in Figure 16c would represent one or several polymer chains stacked on top of one another.

While the formation of the nanoribbons can be explained in terms of a crystallization process that leads to these structures on solid surfaces, the formation of the nanocables and nanowires is not so straightforward. The origin of the cable-like structures thus became a topic of interest. They could either arise by a crystallization process when a homogeneous solution of **12** is dried on a surface, or these superstructures could be preformed in solution and act as seeds for the subsequent growth of cables.

It was observed early on that solutions of PPEs in toluene are colorless at temperatures above 35 °C, while they turn yellow at room temperature. Almost all PPE samples prepared for ^{13}C NMR spectroscopy show gel-like behavior at concentrations exceeding 5 % weight. Perahia et al. [61] investigated the behavior of the yellow/colorless toluene solutions of PPEs. At elevated temperatures, colorless PPEs form molecular solutions in which the rigid PPE chains are almost fully extended. On cooling these solutions below 30 °C, a slightly exothermic phase transition ($0.02 \text{ kcal mol}^{-1} (\text{repeating unit})^{-1}$) occurs, accompanied by a color change to yellow. In these yellow solutions, neutron scattering is enhanced by a factor of 40–50, indicative of the presence of large superstructures. Computational fitting of the scattering data suggests the formation of a jammed gel phase in these yellow solutions (Figure 17). This gel phase has not been described, and consists of aggregates that are approximately 7 nm in diameter and several μm long (Figure 17). Due to their size, the flat aggregates cannot flow freely, restrict the movement of the solvent, and form a gel. Upon casting onto surfaces, these nanocylinders seed the growth of the nanocables observed in thin solid films. The nanostructures observed in thin films must be preformed in solution. Several of these cylinders (from their dimensions, approximately 10–15) aggregate to form nanocables (Figure 16a). Schnablegger et al. [62] reported similar behavior for a different PPE derivative. *However, their polymer was a highly carboxylated polyelectrolyte*, in which strong intermolecular interactions are expected due to the preminent electrostatic forces between charged particles. The dialkyl-PPEs **12** are devoid of any strong intermolecular forces, and so only van der Waals interactions and π – π stacking interactions need to be considered. The principles

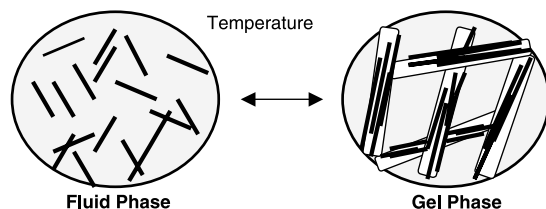


Fig. 17. Formation of gel phases upon cooling solutions of dialkyl-PPEs **12** in toluene.

that guide the size and the shape of these fascinating intermolecular complexes must be subtle and are under investigation by Perahia et al.

7.7

PPE-Based Organic Light-Emitting Diodes (OLEDs)

Conjugated polymers are superb candidates for applications as active emissive layers in light-emitting diodes [63]. Flexibility in synthesis and processing allows the fabrication of large-area devices by spin-coating and doctor-blade techniques, while their electronic and mechanical properties can be easily modified by selection of the appropriate substituent pattern and polymer backbone. Until recently, the conjugated polymer that has found the most widespread application in OLEDs is PPV, either as the unsubstituted parent or as dialkoxy-PPV. PPVs possess well-balanced properties for applications in OLEDs. PPV multilayer LEDs with hole-blocking and/or electron-injecting layers combine long lifetimes with high brightness of more than 2000 Cd m^{-2} at reasonable turn-on voltages [64].

Despite the overall excellent profile of the PPVs, they have delicate processing requirements and are not particularly stable under ambient conditions. This leads to the formation of photo-oxidized products and device degradation. In addition, the band gap of PPVs is relatively small so that only green, yellow, orange, and red emitters can be realized; for organic blue emitters other backbone structures have to be employed [64]. PPEs are easily prepared in large quantities, are stable, and show emission in the solid state that can range from bluish-green to yellow depending on the side chain and the solid-state ordering of the sample.

First attempts by Barton and Shinar [65] to utilize PPE types as active emitter layers were somewhat disappointing, and the fabricated devices performed poorly. Subsequently, Weder [66, 67] and Neher and Bunz [68] reinvestigated PPEs as active emitter layers in OLEDs. According to both groups, there are big differences between PPEs and PPVs, and one reason for the poorer performance of the PPEs is the unsatisfactory hole injection. The presence of alkyne groups instead of vinyl groups in the backbone leads to an increased band gap with a considerably lowered HOMO and LUMO. The lowered HOMO stifles hole injection, but the lowered LUMO has the advantage that electron injection from the cathode is less difficult than in the case of PPVs. As a positive consequence of the decreased LUMO, aluminum works considerably better as a cathode material than calcium does in PPE-based light-emitting devices. This gives testimony to the facilitated electron injection into the lower-lying LUMO of the PPEs. To increase the performance of PPEs, Neher et al. [67] fabricated multilayer diodes. The known problems with hole injection were overcome by adding a hole-injecting layer, Baytron P (a water-soluble mixture of polystyrene sulfonate and oxidized poly(ethylenedioxythiophene); PEDOT), onto the indium tin oxide (ITO) substrate. To increase the emissive intensity of the PPE-types in the solid state, as well as the band gap, a copolymer **53** was utilized in which 25–75 % of the phenyl rings were replaced by naphthalene units (**53a** 25 %; **b** 33 %; **c** 50 %; **d** 75 % naphthyl units). Increasing naphthalene content increased the solid-state quantum yield and led to a hypsochromic shift of the solid-state emission. Figure 18 shows the solid-state emission spectra of **53a–d**, and Figure 19 displays a typical OLED architecture that was utilized for **53**. The organic emitter layer is capped with an evaporated layer of LiF, upon which Al is sublimed in a high vacuum metal evaporator.

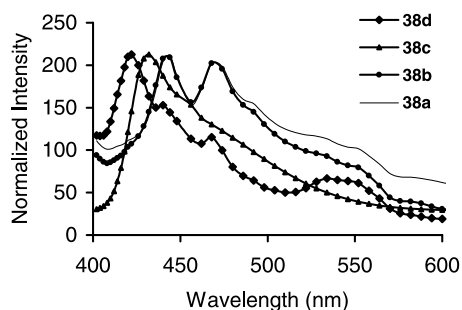


Fig. 18. Solid-state emission of copolymers **53a–d**.

On charging, the sandwich emits blue or blue-green light depending upon the naphthalene content in **53**. The higher the naphthalene content the more blue-shifted the emission. The brightest diodes (see Figure 20), up to 100 Cd m^{-2} at 10 V, were obtained for a PPE copolymer that contained 33 % naphthyl units. The electroluminescence spectrum of this diode is shown in Figure 20. The pure blue emitter **53b** shows peak brightness values of 20 Cd m^{-2} at a driving bias of 18 V.

Recently, Weder [67] demonstrated that PPEs can show a device brightness of up to 300 Cd m^{-2} in OLEDs if Alq_3 is utilized as a hole-injecting and emissive layer. At the moment, it is not clear as to what limits the efficiency and brightness of PPEs in OLED applications because charge transport does not seem to be a problem. The exploration of different hole-injecting layers combined with other cathode materials, interspersed inorganic nanoparticles, or carbon nanotubes would be directions worth exploring when optimizing PPE-based device architectures.

7.8

Conclusions and Outlook

Alkyne metathesis is an exciting method that furnishes small molecules, oligomers, and cycles in excellent yields, and at the same time ADIMET makes conjugated alkyne-bridged polymers of high molecular weight available. A series of different catalysts for alkyne metathesis and ADIMET is available; these range from the sophisticated but sensitive defined tungsten and molybdenum carbynes of the Schrock, Cummins, and Fürstner types to sim-

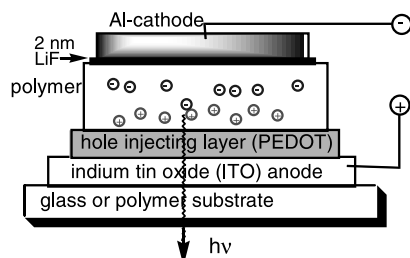


Fig. 19. OLED architecture used for **53b,c**.

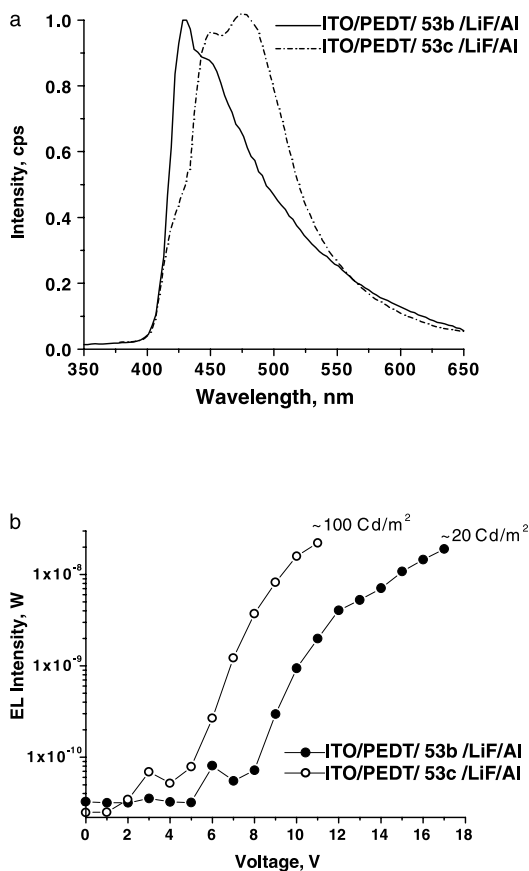
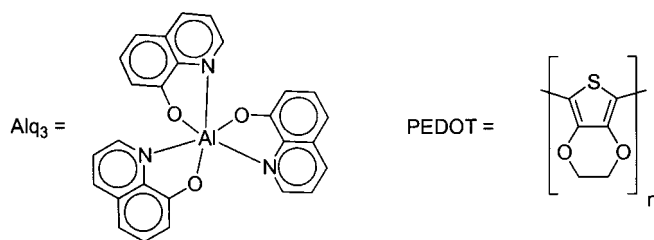


Fig. 20. (a) Normalized electroluminescence (EL) spectra of devices with **53b** and **53c** as emissive layers. (b) Spectrally integrated EL intensity vs. voltage characteristics for multilayer devices made from **53b** and **53c**.



Scheme 21

ple but robust “shake-and-bake” catalysts formed *in situ*. The *in situ* catalysts give excellent results in the formation of polymers and oligomers, and most of the described targets have been made utilizing this reliable “low-tech” approach.

The main thrust of this contribution has been to present results obtained for PPEs. While processible PPEs have been known for more than a decade, many of their fundamental properties, including liquid crystallinity, aggregation and emission behavior, as well as thermo- and solvatochromicity, have been explored only recently. Although the PPEs represent the dehydrogenated congeners of the PPVs, their physical and spectroscopic properties are more different than one might expect from the small changes in chemical structure. The facile access to large amounts of PPEs of high molecular weight and purity by ADIMET has been the key to the discovery of most of the interesting properties of these unusual polymers. The simplicity and ease of scale-up make the ADIMET process with mixtures of $\text{Mo}(\text{CO})_6$ and phenols valuable for industrial applications. At the same time, this process is useful in an academic environment as a tool for the discovery and synthesis of novel alkyne-bridged polymers due to its simplicity, reliability, and low cost. Many future developments are anticipated, and so far we have only scratched the surface of the possibilities offered by this powerful and exciting reaction and these fascinating structures.

Acknowledgements

This work has been supported by the National Science Foundation (CHE-9814118, CHE 0138-659). The Petroleum Research Funds, the Camille and Henry Dreyfus Foundation (UB is Camille Dreyfus Teacher Scholar 2000–2004), the Research Corporation, the Commission of Higher Education of the State of South Carolina, and the University of South Carolina are acknowledged for generous funding of this project. I am very much indebted to my co-workers Dr. Lioba Kloppenburg, Dr. Neil G. Pschirer, Dr. Winfried Steffen, Dr. Ping-Hua Ge, Dr. Paul M. Windscheif, Glen Brizius, Carlito G. Bangcuyo, James Wilson, Dschun Song, Alan R. Marshall, Steve Kroth, Liam Palmer, and Rhonda Roberts. My thanks as well to the invaluable collaborators (and friends), Prof. Dr. Dieter Neher; Prof. Dr. Ulli Scherf; Prof. Mark A. Berg, Ph.D.; Prof. Michael L. Myrick, Ph.D.; Prof. Cathy J. Murphy, Ph.D.; Prof. Dvora Perahia, Ph.D.; and Prof. Miguel Garcia-Garibay, Ph.D., who have all helped to develop the physical understanding of the PPEs.

References

- 1 U. H. F. BUNZ, *Chem. Rev.* **2000**, *100*, 1605. U. H. F. BUNZ, *Acc. Chem. Res.* **2001**, *34*, December issue, ASAP article.
- 2 U. H. F. BUNZ, L. KLOPPENBURG, *Angew. Chem. Int. Ed.* **1999**, *38*, 478.
- 3 T. M. TRNKA, R. H. GRUBBS, *Acc. Chem. Res.* **2001**, *34*, 18. R. H. GRUBBS, S. J. MILLER, G. C. FU, *Acc. Chem. Res.* **1995**, *28*, 446. T. WESKAMP, W. C. SCHATTENMANN, M. SPIEGLER, W. A. HERRMANN, *Angew. Chem. Int. Ed.* **1998**, *37*, 2490. T. WESKAMP, F. J. KOHL, W. A. HERRMANN, *J. Organomet. Chem.* **1999**, *582*, 362.
- 4 M. SCHUSTER, S. BLECHERT, *Angew. Chem. Int. Ed.* **1997**, *36*, 2037. A. FÜRSTNER, *Angew. Chem. Int. Ed.* **2000**, *39*, 3013. A. FÜRSTNER, L. ACKERMANN, B. GABOR, R. GODDARD, C. W. LEHMANN, R. MYNOTT, F. STELZER, O. R. THIEL, *Chem. Eur. J.* **2001**, *7*, 3236.
- 5 R. R. SCHROCK, *J. Chem. Soc. Dalton Trans.* **2001**, 2541.

- 6 A. MORTREUX, M. BLANCHARD, *J. Chem. Soc., Chem. Commun.* **1974**, 786. A. BENCHEIK, M. PETIT, A. MORTREUX, F. PETIT, *J. Mol. Cat.* **1982**, 15, 93. D. VILLEMEN, P. CADIOT, *Tetrahedron Lett.* **1982**, 23, 5139.
- 7 R. R. SCHROCK, D. N. CLARK, J. SANCHE, J. H. WENGROVIUS, S. M. ROCKIAGE, S. F. PEDERSEN, *Organometallics* **1982**, 1, 1645. M. H. CHISHOLM, *Acc. Chem. Res.* **1990**, 23, 419.
- 8 M. L. LISTEMANN, R. R. SCHROCK, *Organometallics* **1985**, 4, 74.
- 9 S. A. KROUSE, R. R. SCHROCK, *Macromolecules* **1989**, 22, 2569.
- 10 X.-P. ZHANG, G. C. BAZAN, *Macromolecules* **1994**, 27, 4627.
- 11 T. MANGEL, A. EBERHARDT, U. SCHERF, U. H. F. BUNZ, K. MÜLLEN, *Macromol. Rapid Commun.* **1995**, 16, 571.
- 12 N. KANETA, K. HIKICHI, M. MORI, *Chem. Lett.* **1995**, 1055. N. KANETA, T. HIRAI, M. MORI, *Chem. Lett.* **1995**, 8627.
- 13 K. WEISS, A. MICHEL, E. M. AUTH, U. H. F. BUNZ, T. MANGEL, K. MÜLLEN, *Angew. Chem. Int. Ed.* **1997**, 36, 506.
- 14 A. FÜRSTNER, C. MATHES, C. W. LEHMANN, *J. Am. Chem. Soc.* **1999**, 121, 9453. A. FÜRSTNER, C. MATHES, *Org. Lett.* **2001**, 3, 221.
- 15 W. J. ZUERCHER, M. SCHOLL, R. H. GRUBBS, *J. Org. Chem.* **1998**, 63, 4291. S. H. KIM, W. J. ZUERCHER, N. B. BOWDEN, R. H. GRUBBS, *J. Org. Chem.* **1996**, 61, 1073. From Schrock's earlier work it was known that alkyne metathesis with defined catalysts proceeds in the presence of double bonds. See ref. [8].
- 16 G. BRIZIUS, N. G. PSCHIRER, W. STEFFEN, K. STITZER, H.-C. ZUR LOYE, U. H. F. BUNZ, *J. Am. Chem. Soc.* **2000**, 122, 12435.
- 17 Y. C. TSAI, P. L. DIACONESCU, C. C. CUMMINS, *Organometallics* **2000**, 19, 5260. C. C. CUMMINS, *Chem. Commun.* **1998**, 1777.
- 18 K. WEISS, U. H. F. BUNZ, unpublished results.
- 19 P. H. GE, W. FU, C. CAMPANA, E. HERDTWECK, W. A. HERMANN, R. D. ADAMS, U. H. F. BUNZ, *Angew. Chem. Int. Ed.* **2000**, 39, 3607.
- 20 D. VENKATARAMAN, S. LEE, J. S. ZHANG, J. S. MOORE, *Nature* **1994**, 371, 591. J. S. MOORE, *Acc. Chem. Res.* **1997**, 30, 402.
- 21 N. G. PSCHIRER, W. FU, R. D. ADAMS, U. H. F. BUNZ, *Chem. Commun.* **2000**, 87.
- 22 U. SCHERF, *Top. Curr. Chem.* **1999**, 201, 163. L. GONZALEZ-RONDA, D. C. MARTIN, J. I. NANOS, J. K. POLITIS, M. D. CURTIS, *Macromolecules* **1999**, 32, 4558. J. I. NANOS, J. W. KAMPF, M. D. CURTIS, L. GONZALEZ, D. C. MARTIN, *Chem. Mater.* **1995**, 7, 2232. M. D. CURTIS, H. CHENG, J. I. NANOS, G.-A. NAZRI, *Macromolecules* **1998**, 31, 205. J. K. POLITIS, M. D. CURTIS, L. GONZALEZ, D. C. MARTIN, Y. HE, J. KANICKI, *Chem. Mater.* **1998**, 10, 1713. *Photovoltaic cells*: G. YU, J. GAO, J. C. HUMMELEN, F. WUDL, A. J. HEEGER, *Science* **1995**, 270, 1789. J. M. HALLS, C. A. WALSH, N. C. GREENHAM, E. A. MARSEGIA, R. H. FRIEND, S. V. MORATTI, A. B. HOLMES, *Nature* **1995**, 376, 498.
- 23 J. YANG, T. M. SWAGER, *J. Am. Chem. Soc.* **1998**, 120, 11864. T. M. SWAGER, *Acc. Chem. Res.* **1998**, 31, 201.
- 24 J. M. TOUR, *Chem. Rev.* **1996**, 96, 537.
- 25 R. GIESA, R. C. SCHULZ, *Makromol. Chem.* **1990**, 191, 857.
- 26 F. E. GOODSON, T. I. WALLOW, B. M. NOVAK, *J. Am. Chem. Soc.* **1997**, 119, 12441.
- 27 V. A. SOLOMIN, W. HEITZ, *Macromol. Chem. Phys.* **1994**, 195, 303.
- 28 Q. ZHOU, T. M. SWAGER, *J. Am. Chem. Soc.* **1995**, 117, 12593.
- 29 N. G. PSCHIRER, U. H. F. BUNZ, *Tetrahedron Lett.* **1999**, 40, 2481.
- 30 L. KLOPPENBURG, D. SONG, U. H. F. BUNZ, *J. Am. Chem. Soc.* **1998**, 120, 7973.
- 31 L. KLOPPENBURG, D. JONES, U. H. F. BUNZ, *Macromolecules* **1999**, 32, 4194.
- 32 G. BRIZIUS, S. KROTH, U. H. F. BUNZ, *Macromolecules*, **2002**, 35, 5317.
- 33 N. G. PSCHIRER, U. H. F. BUNZ, *Macromolecules* **2000**, 33, 3961.
- 34 N. G. PSCHIRER, A. R. MARSHALL, C. STANLEY, H. W. BECKHAM, U. H. F. BUNZ, *Macromol. Rapid. Commun.* **2000**, 21, 493.
- 35 W. STEFFEN, B. KÖHLER, M. ALTMANN, U. SCHERF, K. STITZER, H.-C. ZUR LOYE, U. H. F. BUNZ, *Chem. Eur. J.* **2001**, 7, 117.
- 36 M. REMMERS, B. MÜLLER, K. MARTIN, H. J. RÄDER, W. KÖHLER, *Macromolecules* **1999**, 32, 1073.
- 37 P. M. COTTS, T. M. SWAGER, Q. ZHOU, *Macromolecules* **1996**, 29, 7323.

- 38 S. L. HUANG, J. M. TOUR, *J. Am. Chem. Soc.* **1999**, *121*, 4908, and references cited therein.
- 39 D. STEIGER, T. TERVOORT, C. WEDER, P. SMITH, *Macromol. Rapid. Commun.* **2000**, *21*, 405.
- 40 A. R. MARSHALL, U. H. F. BUNZ, *Macromolecules* **2001**, *34*, 4688.
- 41 C. HUBER, F. BANGERTER, W. R. CASERI, C. WEDER, *J. Am. Chem. Soc.* **2001**, *123*, 3857.
- 42 P. WAUTELET, M. MORONI, L. OSWALD, J. LEMOIGNE, A. PHAM, J.-Y. BIGOT, S. LUZATTI, *Macromolecules* **1996**, *29*, 446.
- 43 C. WEDER, M. S. WRIGHTON, P. GUNTER, *J. Phys. Chem.* **1996**, *100*, 8931. C. WEDER, M. S. WRIGHTON, *Macromolecules* **1996**, *29*, 5157. M. S. WRIGHTON, D. OFER, T. M. SWAGER, *Chem. Mater.* **1995**, *7*, 418. T. M. SWAGER, C. J. GIL, M. S. WRIGHTON, *J. Phys. Chem.* **1995**, *99*, 4886.
- 44 D. STEIGER, P. SMITH, C. WEDER, *Macromol. Rapid Commun.* **1997**, *18*, 643.
- 45 M. ALTMANN, U. H. F. BUNZ, *Angew. Chem. Int. Ed. Engl.* **1995**, *34*, 569.
- 46 L. KLOPPENBURG, D. JONES, J. B. CLARIDGE, H.-C. ZUR LOYE, U. H. F. BUNZ, *Macromolecules* **1999**, *32*, 4460.
- 47 T. MITEVA, L. PALMER, L. KLOPPENBURG, D. NEHER, U. H. F. BUNZ, *Macromolecules* **2000**, *33*, 652.
- 48 U. H. F. BUNZ, V. ENKELMANN, L. KLOPPENBURG, D. JONES, K. D. SHIMIZU, J. B. CLARIDGE, H.-C. ZUR LOYE, G. LIESER, *Chem. Mater.* **1999**, *11*, 1416.
- 49 C. E. HALKYARD, M. E. RAMPEY, L. KLOPPENBURG, S. L. STUDER-MARTINEZ, U. H. F. BUNZ, *Macromolecules* **1998**, *31*, 8655.
- 50 D. NEHER, *Adv. Mater.* **1995**, *7*, 691. D. J. SANDMAN, *Trends Polym. Sci.* **1994**, *2*, 44. A. B. KOREN, M. D. CURTIS, J. W. KAMPE, *Chem. Mater.* **2000**, *12*, 1519.
- 51 J. S. KIM, T. M. SWAGER, *Nature* **2001**, *411*, 1030.
- 52 S. D. D. V. RUGHOPUT, S. HOTTA, A. J. HEEGER, F. WUDL, *J. Polym. Sci. B* **1987**, *25*, 1071. A. O. PATIL, A. J. HEEGER, F. WUDL, *Chem. Rev.* **1988**, *88*, 183–200.
- 53 F. WUDL, personal communication.
- 54 J. M. SEMINARIO, A. G. ZACARIAS, J. M. TOUR, *J. Am. Chem. Soc.* **1998**, *120*, 3970.
- 55 K. OKUYAMA, T. HASEGAWA, M. ITO, N. MIKAMI, *J. Phys. Chem.* **1984**, *88*, 1711.
- 56 H. LI, D. R. POWELL, R. K. HAYASHI, R. WEST, *Macromolecules* **1998**, *31*, 52.
- 57 M. LEVITUS, K. SCHMIEDER, H. L. RICKS, K. D. SHIMIZU, U. H. F. BUNZ, M. A. GARCIA-GARIBAY, *J. Am. Chem. Soc.* **2001**, *123*, 4259.
- 58 M. I. SLUCH, A. GODT, U. H. F. BUNZ, M. A. BERG, *J. Am. Chem. Soc.* **2001**, *123*, 6447.
- 59 P. SAMORI, V. FRANCKE, K. MÜLLEN, J. P. RABE, *Chem. Eur. J.* **1999**, *5*, 2312. P. SAMORI, N. SEVERIN, K. MÜLLEN, J. P. RABE, *Adv. Mater.* **2000**, *12*, 579. P. SAMORI, V. FRANCKE, K. MÜLLEN, J. P. RABE, *Thin Solid Films* **1998**, *336*, 13.
- 60 D. PERAHIA, R. TRAIPOH, U. H. F. BUNZ, *Macromolecules* **2001**, *34*, 151.
- 61 D. PERAHIA, R. TRAIPOH, U. H. F. BUNZ, *J. Chem. Phys.*, submitted.
- 62 H. SCHNABLEGGER, M. ANTONIETTI, C. GÖLTNER, J. HARTMANN, H. CÖLFEN, P. SAMORI, J. P. RABE, H. HÄGER, W. HEITZ, *J. Colloid Interfac. Sci.* **1999**, *212*, 24.
- 63 A. KRAFT, A. C. GRIMSDALE, A. B. HOLMES, *Angew. Chem. Int. Ed.* **1998**, *37*, 402–428.
- 64 M. T. BERNIUS, M. INBASEKARAN, J. O'BRIEN, W. WU, *Adv. Mater.* **2000**, *12*, 1737.
- 65 L. S. SWANSON, J. SHINAR, Y. W. DING, T. J. BARTON, *Synth. Metals* **1993**, *55*, 1. W. CHEN, S. IJADA-MAGHSOODI, T. J. BARTON, T. CERKVENIK, J. SHINAR, *Polym. Preprints* **1995**, *36*, 495.
- 66 For PPE-based LEDs, Weder noticed that hole injection is a problem, while electron injection is quite efficient for PPEs having a low-lying LUMO: A. MONTALI, P. SMITH, C. WEDER, *Synth. Metals* **1998**, *97*, 123.
- 67 C. SCHMITZ, P. PÖSCH, M. THELAKKAT, H. W. SCHMIDT, A. MONTALI, K. FELDMAN, P. SMITH, C. WEDER, *Adv. Funct. Mater.* **2001**, *11*, 41.
- 68 N. G. PSCHIRER, T. MITEVA, U. EVANS, R. S. ROBERTS, A. R. MARSHALL, D. NEHER, M. L. MYRICK, U. H. F. BUNZ, *Chem. Mater.* **2001**, *13*, 2691.

8

The Chromium-Templated Carbene Benzannulation Approach to Densely Functionalized Arenes (Dötz Reaction)

Karl Heinz Dötz and Joachim Stendel jr.

Abstract

The benzannulation of readily accessible aryl- or vinylcarbene chromium complexes by alkynes provides a straightforward synthesis of densely functionalized benzenoid and fused arenes selectively labeled with a $\text{Cr}(\text{CO})_3$ fragment. The reaction occurs under mild conditions, is regioselective, and tolerates a variety of functional groups both on the alkyne and on the carbene ligand. The chromium fragment undergoes a haptotropic metal migration controlled by the substitution pattern of the arene; moreover, it activates the coordinated benzene ring towards selective nucleophilic addition and aromatic substitution. Final decomplexation occurs upon ligand exchange or oxidation reactions. Chiral information imposed on either the carbene ligand or the alkyne allows for a diastereoselective benzannulation providing optically active arene- $\text{Cr}(\text{CO})_3$ complexes.

8.1

Introduction

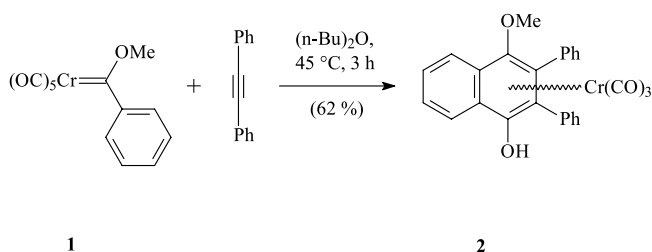
The regiospecific preparation of polyfunctionalized aromatic compounds still represents a major challenge. Aiming at the realization of complex substitution patterns, conventional synthetic methodologies starting from a given aromatic starting material, such as electrophilic or nucleophilic substitutions, coupling reactions, and metalation–functionalization reactions, are often inconvenient. This inconvenience is caused by the (linear) multistep reaction sequence needed, the different activating or deactivating and orientating effects of the substituents, and the difficulties associated with the regioselective introduction of a specific substitution pattern (especially in the case of polycyclic compounds).

As a consequence, new methodologies have been designed to overcome these bottlenecks. In this context, strategies that simultaneously construct the aromatic skeleton and the target substitution pattern are both elegant and powerful solutions to the problem because only a few steps are required and the formation of regioisomeric mixtures can be avoided in most cases. Reppe's research [1] with nickel catalysts in the 1940s initiated the development of the alkyne cyclotrimerization with organometallic compounds leading to benzene derivatives. An elegant result of this development has been the work by the Vollhardt group [2] in

applying cobalt templates to the synthesis of natural products such as steroids [2a] and strained polycyclic compounds such as oligophenylenes [2b].

Another attractive route to densely substituted arenes is based on transition metal carbene chemistry. In Fischer-type carbene complexes, the carbene carbon atom is linked by a formal double bond to a metal carbonyl fragment incorporating a low-valent metal of Groups VI to VIII [3]. The electron-deficient carbene carbon typically bears at least one stabilizing heteroatom π -donor substituent. The second carbene substituent may be either a saturated or an unsaturated hydrocarbon chain. The metal center is coordinated by π -acceptors such as carbon monoxide, phosphines, or cyclopentadienyl ligands. Reactions of carbene complexes [4] may either proceed at the metal center or occur within the carbene ligand. The metal carbene fragment represents a potent electron-acceptor moiety, which activates adjacent C=C and C \equiv C bonds towards the addition of nucleophiles or cycloaddition reactions; moreover, it considerably enhances the C–H acidity of α -hydrogen atoms, which allows for C–C coupling reactions via metal carbene anions.

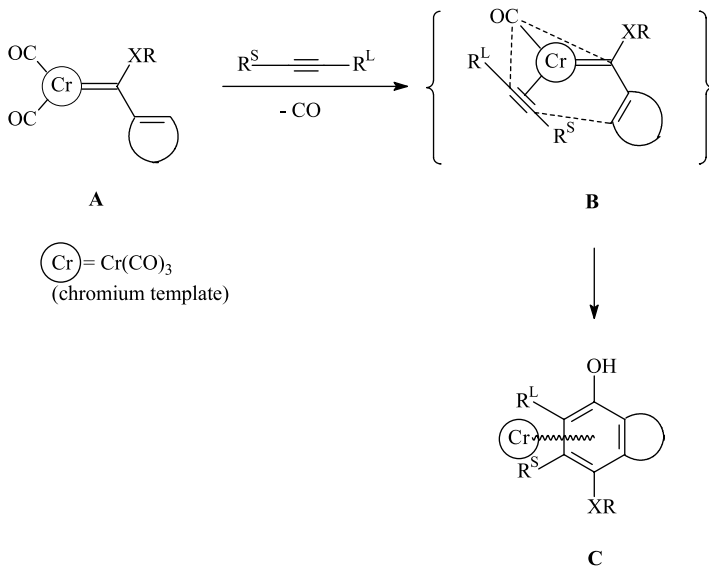
On the other hand, as demonstrated by early examples, carbene complexes may serve as stable carbene equivalents and undergo [2+1] cycloaddition with alkenes to give cyclopropanes [5]. However, no indication of a free carbene intermediate has yet been obtained; in contrast, the principal reaction mechanism involves a carbene transfer within the coordination sphere of the metal, which acts as a “template”. In an early extension of this idea, when pentacarbonyl(α -methoxybenzylidene)chromium was reacted with tolane, our aim was the in situ generation of an alkyne–carbene–carbonyl complex in which the carbonyl chromium “template” keeps these three different ligands in a facial configuration favorable for subsequent interligand coupling. The experimental result was quite exciting: We did not observe any type of two-ligand (alkyne/carbene, alkyne/CO, or carbene/CO) coupling to give cyclopropene or ketene derivatives; instead, a three-ligand coupling of the alkyne, phenyl-carbene, and carbonyl ligand to afford a naphthohydroquinone skeleton had occurred at the Cr(CO)₃ template, which remained η^6 -coordinated to the benzannulation product (Scheme 1) [6].



Scheme 1. Reaction of pentacarbonyl(α -methoxybenzylidene)chromium with diphenylethyne: the first example of benzannulation.

The benzannulation product may be viewed as a formal [3+2+1] cycloaddition product, in which the alkyne (C₂ synthon) is connected to the carbon monoxide ligand (C₁ unit) and the carbene carbon atom of the unsaturated carbene ligand (C₃ building block), the β -carbon

atom of which, in turn, is further coupled to the carbon monoxide ligand. However, a closer insight into the mechanism of this reaction, as discussed in Section 8.2, indicates a stepwise carbon–carbon bond formation starting from the alkyne–carbene–carbonyl complex **B** as the key intermediate, formed in a decarbonylation equilibrium from the pentacarbonyl carbene complex **A** and the alkyne (Scheme 2). The $\text{Cr}(\text{CO})_3$ template assists the interligand coupling and remains coordinated to the newly formed arene ring **C**.



Scheme 2. Connectivity in the chromium-templated benzannulation reaction.

Chromium(0) in an octahedral configuration is the metal of choice for this type of reaction. There have been a few examples in which metals other than chromium, such as tungsten and molybdenum [7a], manganese [7b, 7c], and iron [7d] have been reported as alternative templates, but all of them turned out to be far less efficient and general.

The benzannulation of α,β -unsaturated chromium carbene complexes with alkynes, sometimes referred to as the “Dötz reaction” [8], has stimulated organic synthesis along the borderline of organometallic and synthetic organic chemistry. Since the end of the 1970s, the reaction has been applied to the synthesis of biologically active compounds by Dötz, Semmelhack, and Wulff and their groups, in order to define its scope. In the early 1980s, Dötz and co-workers started to elucidate the mechanism of the reaction. At the end of the 1980s, the research temporarily shifted to amino chromium carbene complexes in order to determine the factors that control the competitive formation of benzannulation and pentannulation products. In the 1990s, related additional and useful benzannulation procedures employing chromium carbene complexes, such as the photochemical benzannulation methodology of Merlic, were developed. More recently, part of the focus has been shifted to strained arenes and to the chiral plane present in the benzannulation products, and efforts

to control the diastereoselectivity of the reaction have met with considerable success. Altogether, after more than two decades, the benzannulation of α,β -unsaturated chromium carbene complexes with alkynes has been developed to a versatile and widely used strategy for the synthesis of densely functionalized mono- and polycyclic benzenoid arenes.

The present overview deals with the application of Fischer chromium carbene complexes in the benzannulation reaction for the preparation of highly substituted aromatic compounds. Before focussing on specific arenes (Section 8.5), details of the mechanism are given (Section 8.2), and the scope and limitations of the reaction are defined (Section 8.3). A short description of the experimental procedure is given thereafter (Section 8.4). Finally, the contribution deals with the application of the chromium carbene benzannulation to natural compounds and molecules with biological activity (Section 8.6).

8.2

Mechanism and Chemoselectivity of the Benzannulation

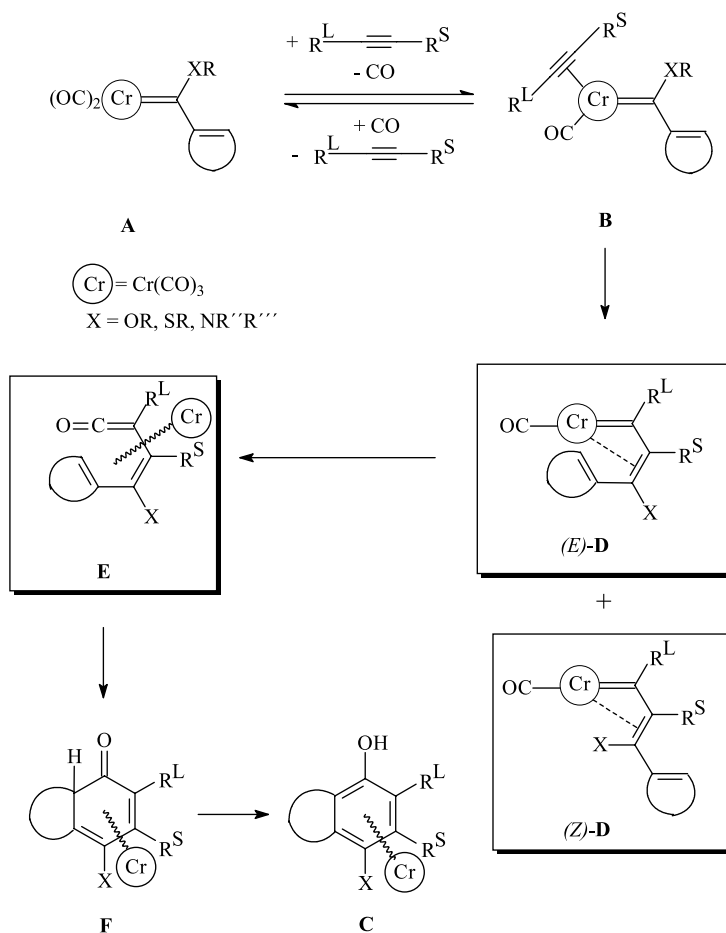
8.2.1

Mechanism

The mechanism of the benzannulation reaction involves the stepwise construction of the aromatic ring within the coordination sphere of the chromium template (Scheme 3). This idea is strongly supported by experimental evidence for model intermediates and by theoretical calculations [9] highlighting the course of the reaction (see below).

Starting from carbene complex **A**, ligand exchange of one *cis*-carbonyl ligand by the alkyne leads to the η^2 -alkyne complex intermediate **B**. The equilibrium between **A** and **B** is supported by kinetic and inhibition studies under CO atmosphere [10] and has been shown to be the rate-determining step of the benzannulation process. In the course of the decarbonylative ligand exchange, the coordinatively unsaturated 16-electron tetracarbonyl carbene intermediate may be stabilized by the solvent. Recently, based on DFT calculations, an alkyne coordination prior to decarbonylation has been proposed [11a], although this idea is in severe conflict with overwhelming experimental evidence supporting CO dissociation as the first step [11b]. Analogues of intermediate **B** (linking the alkyne and carbene moieties by a rigid *C*₂-*ortho*-phenylene) have been isolated as stable alkyne–carbene chromium chelates and structurally characterized by X-ray diffraction analysis, which indicated a weak alkyne–metal interaction in complexes of type **3** (Scheme 4) [12]. This finding is in agreement with Extended Hückel MO studies [13].

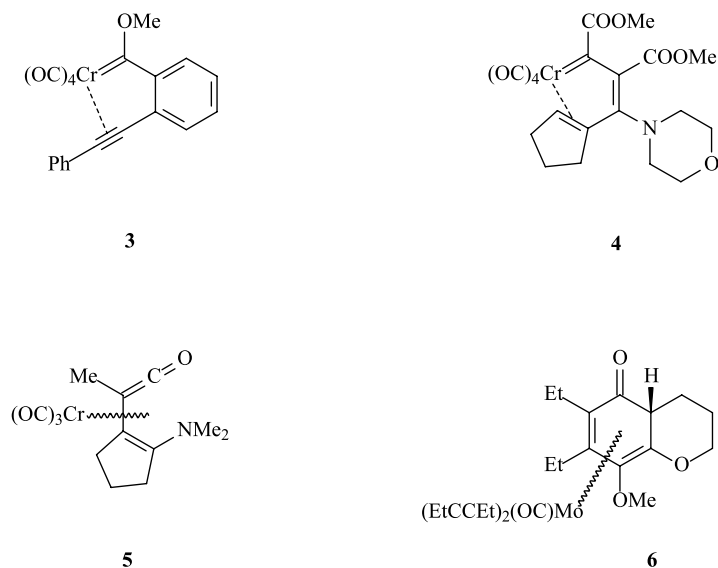
Insertion of the alkyne into the chromium carbene bond in intermediate **B** affords vinyl carbene complex **D**, in which the C=C double bond may be either (*Z*) or (*E*). A putative chromacyclobutene intermediate resulting from a [2+2] cycloaddition of the alkyne across the metal–carbene bond on the way to chromium vinylcarbene **D**, as was sometimes suggested in early mechanistic discussions, has been characterized as a high energy species on the basis of theoretical calculations [9c]. Its formation and ring-opening cannot compete with the direct insertion path of the alkyne into the chromium–carbene bond. An example of an (*E*)-**D** alkyne insertion product has been isolated as the decarbonylation product of a tetracarbonyl chromahexatriene (**4**, Scheme 4) [14], and has been characterized by NMR spectroscopy and X-ray analysis.



Scheme 3. Mechanism of the benzannulation reaction (intermediates (E)- and (Z)-D and E serve as branch points, from which side products originate, see Section 8.2.2 for further discussion).

Intramolecular insertion of carbon monoxide into the metal–carbene bond of the (E)-isomer of **D** leads to the η^4 -vinyl ketene complex intermediate **E**. Experimental support for this type of intermediate has been provided by the isolation of $\text{Cr}(\text{CO})_3$ -coordinated dieny ketenes related to **5** (Scheme 4) [15a], and by trapping the vinyl ketene intermediates as vinyl lactone derivatives in the course of the reaction of chromium carbene complexes with 1-alkynols [15b].

Electrocyclization of **E** is expected to give cyclohexadienone complex **F**; a related molybdenum complex **6** (Scheme 4), in which two carbonyl ligands have been replaced by alkyne ligands, has been isolated from the reaction of a vinyl molybdenum carbene complex with 3-



Scheme 4. Isolated analogues of intermediates in the benzannulation reaction.

hexyne [16]. If substituents such as $R = H, SiR_3$ are present in one of the positions adjacent to the carbonyl group in **F** allowing a 1,3-shift, the cyclohexadienone undergoes tautomerization to phenol **C** as the final product of the benzannulation sequence. DFT calculations reveal that the C–C bond-forming steps are characterized by rather low activation barriers ($10\text{--}25\text{ kJ mol}^{-1}$) and that the thermodynamic driving force for the benzannulation results from the aromatization energy in the final step (ca. 175 kJ mol^{-1}). The tautomerization can be blocked in the presence of *ortho*-alkyl substituents, and the reaction stops at the cyclohexadienone [17].

The stepwise coupling of two *cis* ligands as depicted in Scheme 3 has been verified as involving a sequence of three discrete steps at low temperatures, allowing the isolation of the relevant intermediates as individual compounds [18]. When a chelated tetracarbonyl amino-vinyl carbene complex (chelated analogue of intermediate **B** in Scheme 3) was reacted with an electron-deficient alkyne under controlled conditions, a 1,4,5- η^3 -dienylcarbene tetracarbonyl chromium complex (corresponding to intermediate **D** in Scheme 3) was formed. It underwent thermal decomposition to give phenol derivatives as the final products.

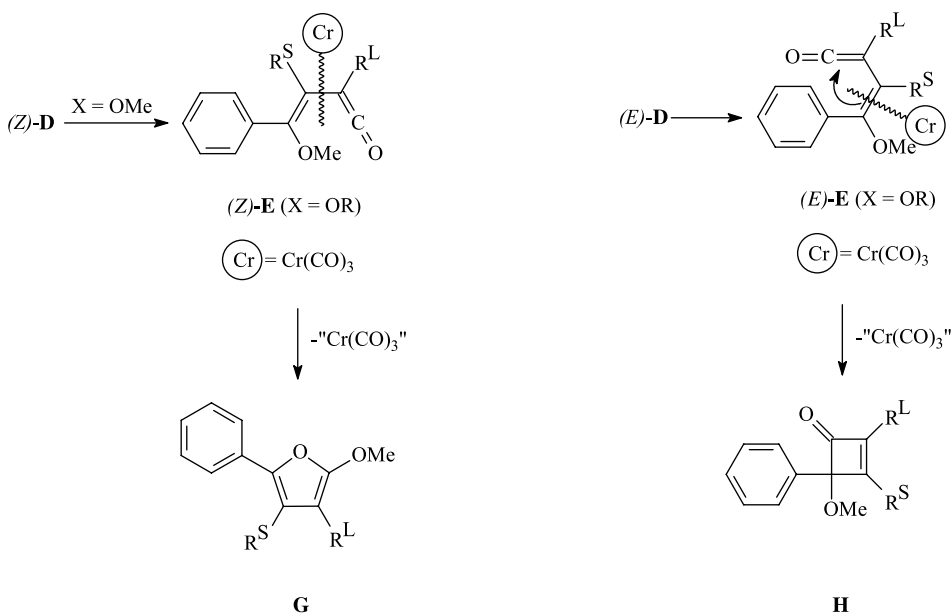
8.2.2

Chemoselectivity

The intermediate **D** in Scheme 3 represents a branching point in the benzannulation mechanism, from which side products may arise. Their formation depends on the solvent and on the substitution pattern within the carbene ligand and the alkyne.

The intermediate **D** resulting from alkyne insertion may be formed in either the (*Z*)- or

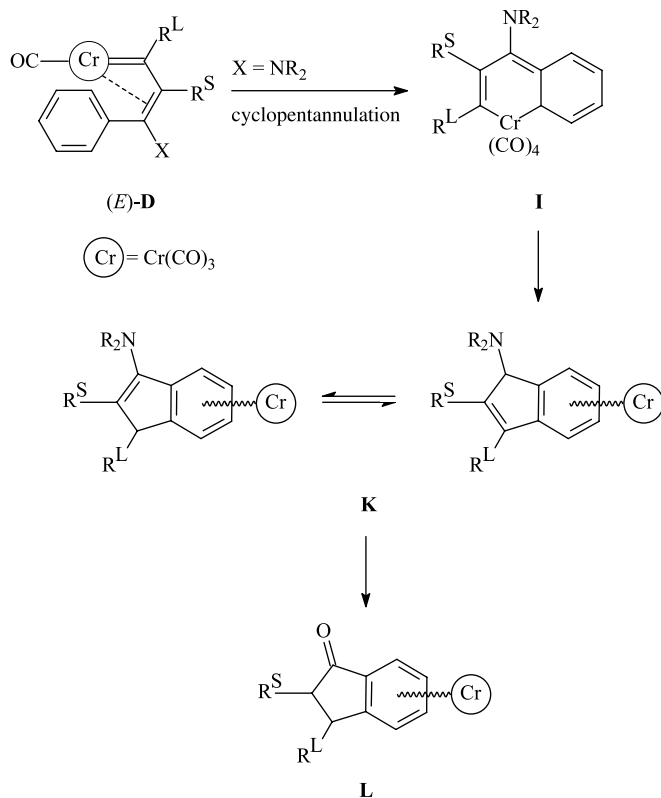
(*E*)-configuration, which will be retained in the course of subsequent carbonylation to give vinyl ketene complexes (*Z*)-**E** or (*E*)-**E**. Vinyl ketenes (*E*)-**E** provide the appropriate geometry for the 6π -electrocyclization leading to benzannulation. An alternative 4π -electrocyclization, which is favored by internal chelation, strongly coordinating solvents, and *o,o'*-aryl disubstitution, affords cyclobutenones **H**. (*Z*)-Vinyl ketenes (*Z*)-**E** are presumed to be the precursors of furans **G**, which are believed to result from a cyclization/alkyl migration sequence (Scheme 5) [19].



Scheme 5. Potential side reactions of the benzannulation leading to furans **G** and cyclobutenones **H**.

Replacing the alkoxy carbene substituent by a better electron-donating amino group stabilizes the metal carbonyl bond. As a result, CO insertion in vinyl carbene **D** is hampered; instead, cyclopentannulation via the chromacyclohexadiene **I** leads to aminoindenes **K**, which are readily hydrolyzed to indanones **L** (Scheme 6) [20].

The formation of side products depends on the choice of substituents and solvent [21]. The role of the solvent is illustrated by the reaction of phenyl carbene complex **1** with diphenylethyne (Scheme 7). An ethereal solvent such as THF leads exclusively to the benzannulation product isolated as quinone **7** after oxidative work-up, while use of the non-coordinating solvent hexane results in comparable amounts of cyclobenzannulation and cyclopentannulation products **7** and **8a**. Strongly coordinating acetonitrile suppresses benzannulation product **7** in favor of the cyclobutenone **9**, which is accompanied by minor amounts of cyclopentannulation products **8a** and **8b**. Indene **8a** is obtained exclusively if the polar solvent DMF is employed.



Scheme 6. Cyclopentannulation of amino carbene complexes.

8.3

Scope and Limitations

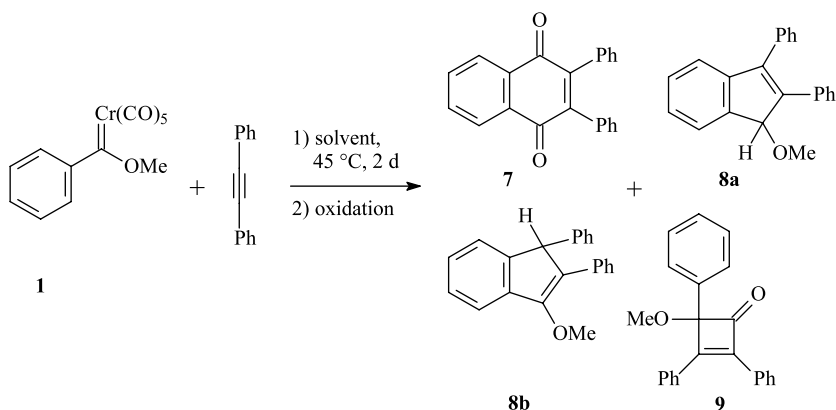
8.3.1

The Carbene Complex

8.3.1.1 Availability

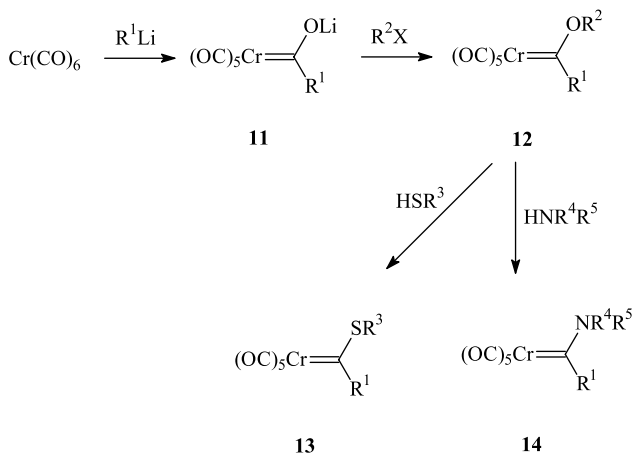
Although not yet commercially available, Fischer carbene complexes are readily accessible by well-elaborated synthetic methods.

The most general access to Fischer-type metal carbenes ("Fischer route") is based on sequential addition of a carbon nucleophile and a carbon electrophile across a metal-coordinated carbon monoxide ligand (Scheme 8) [22]. Addition of an organolithium reagent to hexacarbonyl chromium affords acyl metalate **11**, which undergoes in situ *O*-alkylation by hard alkylating reagents such as trialkyloxonium tetrafluoroborates or alkyl fluorosulfonates to give alkoxycarbene complex **12** in typical yields of 60–90 % [23, 24]. Alkylation of the acyl metalate has also been performed with methyl iodide under phase-transfer catalysis [25].



Solvent	7 (%)	8a (%)	8b (%)	9 (%)
THF	59	0	0	0
Hexane	41	38	0	0
MeCN	0	4	15	51
DMF	0	83	0	0

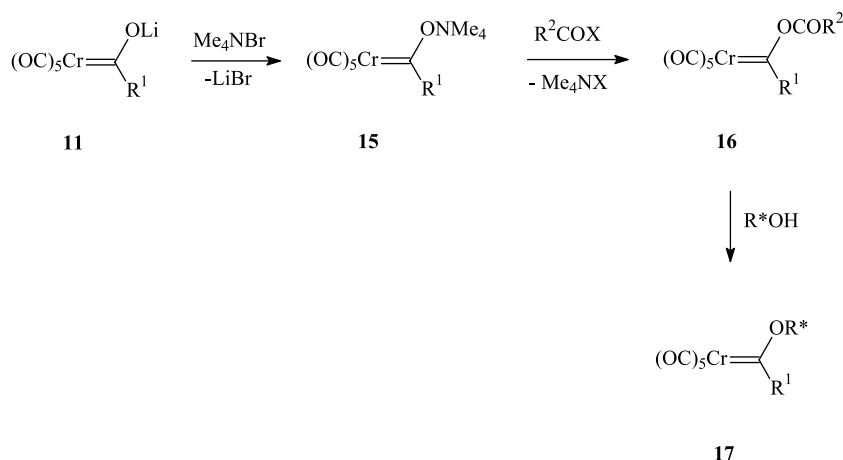
Scheme 7. Influence of the solvent on the competition of cyclobenzannulation, cyclopentannulation, and cyclobutenone formation.



Scheme 8. The Fischer route to chromium carbene complexes.

The alkoxy substituent in **12** may be replaced by thio or amino groups upon treatment with thiols and amines to give thiocarbene **13** and aminocarbene complexes **14**, respectively.

Alternatively, alkoxy carbene complexes are formed upon alcoholysis of strongly electrophilic acyloxy carbene complexes **16** [26] generated by in situ acylation of tetraalkylammonium acyl metalates **15**. These compounds are obtained from lithium precursors **11** and can be stored in a refrigerator for months. This is the method of choice for the synthesis of chiral metal carbenes **17** bearing terpene or sugar auxiliaries (Scheme 9).

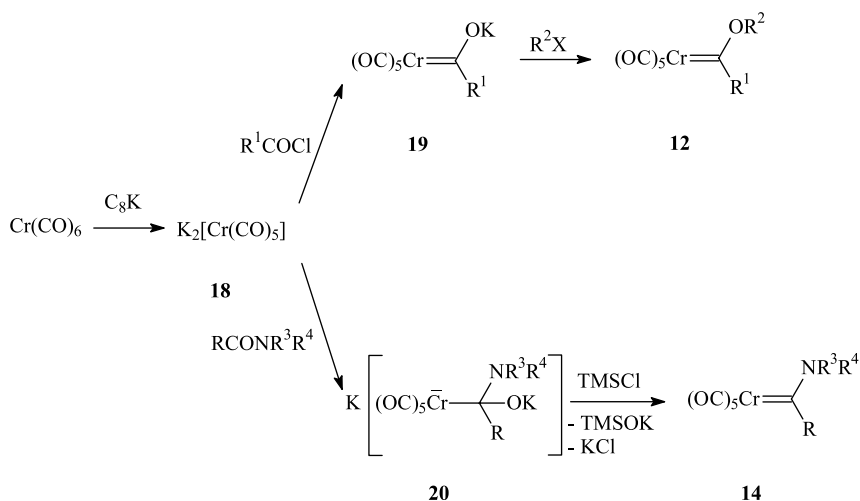


Scheme 9. Chiral alkoxy carbene complexes from the alcoholysis of acyloxy carbene complexes.

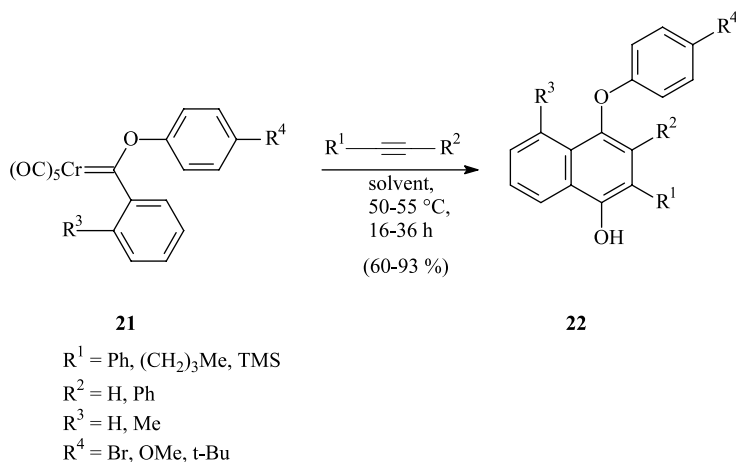
A complementary access to alkoxy- and aminocarbene complexes (“Semmelhack–Hegedus route”) involves the addition of the pentacarbonylchromate dianion **18** (obtained from the reduction of hexacarbonylchromium with C_8K) to carboxylic acid chlorides and amides [27] (Scheme 10). While alkylation of acyl chromate **19** leads to alkoxy carbene complexes **12**, addition of chromate dianion **18** to carboxylic amides generates the tetrahedral intermediates **20**, which are deoxygenated by trimethylsilyl chloride to give amino carbene complexes **14**.

8.3.1.2 The Carbene Ligand

Although mostly alkoxy carbene complexes have been benzannulated, other types of carbene complexes are equally well suited. These include aryloxy carbene complexes as well as acylamino and thioalkylidene complexes, and even complexes with no heteroatoms, such as diaryl carbene complexes, are suitable (see below). Besides the commonly used methoxy and ethoxy carbene complexes, alkoxy carbene complexes with a longer alkyl chain have also been successfully reacted. The benzannulation of aryloxy carbene complexes has recently been studied to probe electronic effects [28a]. Aryloxy alkylidene complexes of type **21** have been used to prepare diaryl ethers **22**, which constitute a common substructure in many important types of natural products [28b]. The benzannulation methodology provides an access to phenyl naphthyl ethers in yields of 60–93 % under mild conditions (Scheme 11).



Scheme 10. Semmelhack–Hegedus route to alkoxy and amino carbene complexes.

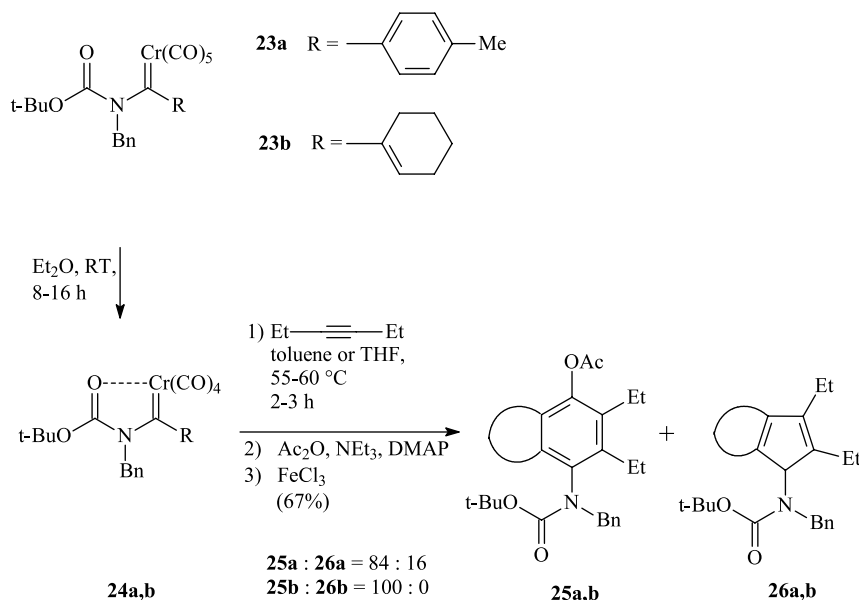


Scheme 11. Benzannulation of aryloxy carbene complexes affording diaryl ethers.

Besides alkoxy carbene complexes, acyloxy carbene complexes have also been proven to be effective in the benzannulation reaction. For example, Yamashita and Ohishi have reported the synthesis of various naphthoquinones in yields of 47–71 % using acetyloxy phenyl chromium carbene complex and terminal alkynes with different alkyl chain lengths [29].

Even Lewis acid adducts of the acyl metalate **11** (Section 8.3.1.1, Scheme 8) proved effective in generating benzannulation products. The reaction of a trimethylsilyloxy chromium carbene complex with 3-hexyne to give the respective semi-silylated hydroquinone tricarbonylchromium complex in 35 % yield [30a] and the use of titanoxycarbene complexes [30b] constitute such examples. Thiocarbene complexes form hydrothioquinones in a Lewis acid supported benzannulation reaction [32].

As discussed above, dialkylamino carbene complexes result in the formation of indenenes due to the increased donor ability of the nitrogen compared to the oxygen heteroatom. The formation of benzannulation products is favored, however, if the electron density at nitrogen is lowered by substitution with electron-withdrawing acyl groups [33]. The example in Scheme 12 demonstrates the effect.



Scheme 12. Acylamino carbene complexes as amino carbene complex synthons for the benzannulation process.

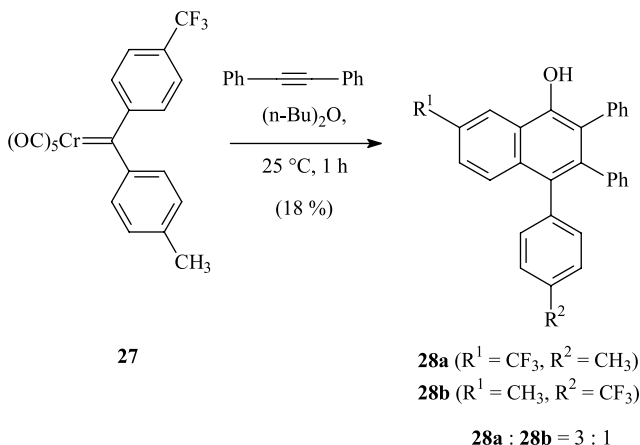
The facile decarbonylation of pentacarbonyl complexes **23a** and **23b** results in tetracarbonyl carbene complex intermediates **24a** and **24b**, respectively. Their annulation can produce benzene and/or cyclopentadiene derivatives **25** and/or **26**. In the case of aryl acylamino complex **23a**, the reaction course is shifted towards the benzannulation reaction (**25a** : **26a** = 84 : 16). With the vinyl carbene complex **23b**, the benzannulation product **25b** (**25b** : **26b** = 100 : 0) is produced exclusively.

Recently, Barluenga et al. have introduced some electron-deficient *dialkylamino* carbene complexes that bear a carboxylic functionality at the vinyl moiety and undergo exclusively the benzannulation process [34].

The benzannulation reaction tolerates phenyl carbene complexes bearing both electron-donating [35a] and -withdrawing [35b] substituents. Additionally, carbene complexes containing condensed systems such as naphthalene and other carbocyclic hydrocarbons as well as heterocycles have also been successfully submitted to the reaction (see Section 8.5).

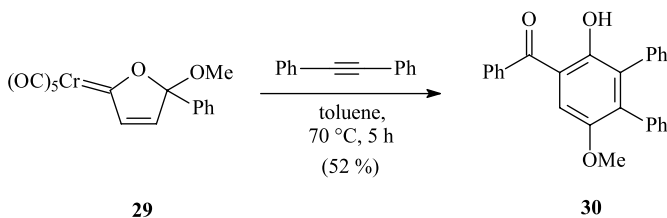
Representatives of Fischer carbene complexes possessing no heteroatom at the carbene carbon are diaryl chromium carbene complexes. Due to the lack of π -stabilization, they react more readily than the heteroatom-functionalized carbene complexes (already at ambient

temperature). Diaryl carbene complexes are interesting candidates for synthesizing arenes bearing an extended carbocyclic skeleton [28a, 36]. Scheme 12 shows one example of such a benzannulation [28a, 36a] involving the annulation of a carbene complex bearing two aryl substituents of different electron densities. Reaction of compound **27** with diphenylethyne provides a mixture of two regioisomeric benzannulation products **28a** and **28b** in a 3:1 ratio in a modest yield of 18 % (Scheme 13). Remarkably, the benzannulation occurs preferentially at the aromatic ring having the lower electron density.



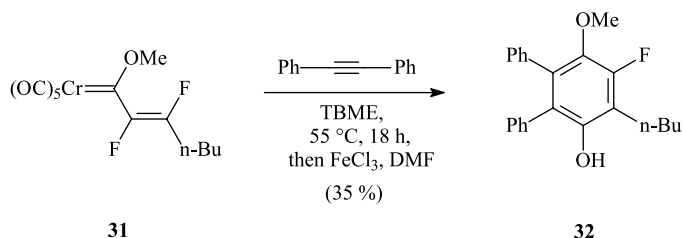
Scheme 13. Benzannulation of diaryl chromium carbene complexes.

In contrast to aryl carbene complexes, vinyl carbene complexes are known to yield only the benzannulation products [37]. For instance, carbohydrates [38], tetramethyl ketals of quinones [39], heterocycles, and oxacycloalkenylidene carbene complexes [40] have been used as part of a (cyclic) vinyl carbene complex. For example, complex **29** and diphenylethyne were converted to the acyl hydroquinone **30**. Thus, **29** serves as a synthon for the (electron-poor) benzoyl vinyl carbene complex (Scheme 14) [40].



Scheme 14. Complex **29** acting as an acyl vinyl carbene complex synthon in the benzannulation reaction.

The only example of a vinyl carbene complex bearing fluoro substituents that has been benzannulated is presented in Scheme 15 [41]. Carbene complex **31** was reacted with diphenylethyne to give hydroquinone **32**. Interestingly, one of the fluoro substituents in the educt is lost in the reaction.



TBME = *t*-BuOMe

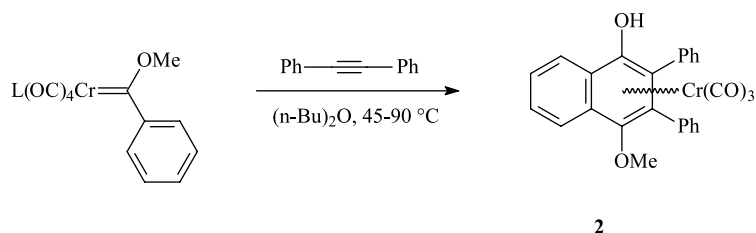
Scheme 15. Benzannulation of a fluorovinyl carbene complex.

8.3.1.3 The Chromium Template

The overwhelming majority of benzannulations with chromium carbene complexes involve compounds in which the metal bears only carbonyl ligands. However, phosphine ligands may also be present in the chromium coordination sphere.

The effect of phosphine ligands differing in their donor–acceptor properties on the benzannulation reaction has been studied with chromium carbenes (**33a,b**) (Scheme 16) [36a]. The yield of the tricarbonylchromium complex **2** starting from the pentacarbonyl carbene complex **1** (62 %) was essentially unchanged at a slightly higher reaction temperature (60 °C for **33a** compared to 45 °C for **1**) when a *cis*-CO ligand was replaced by tris(*p*-fluorophenyl)phosphine (**33a**). In contrast, the yield significantly dropped and the reaction temperature had to be increased to 90 °C when the tris(*n*-butyl)phosphine complex **33b** was subjected to the benzannulation reaction.

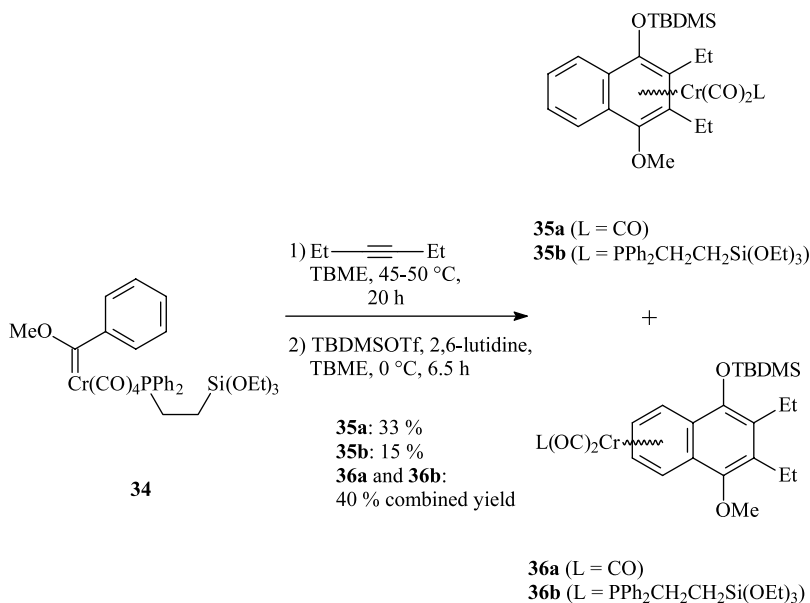
Very recently, the benzannulation has been applied to chromium(phosphine)carbonyl complex **34**, which is suited for subsequent immobilization by sol-gel methodology; the tri-



Compound	Ligand L	Yield
1	CO	62 %
33a	P(<i>p</i> -C ₆ H ₄ F) ₃	61 %
33b	P(<i>n</i> -Bu) ₃	11 %

Scheme 16. Effect of phosphine ligands on the benzannulation of methoxy phenyl carbene complexes with diphenylethyne.

carbonylchromium complexes **35a** (33 %) and **35b** (15 %) were obtained, along with the dicarbonyl(phosphine)chromium complexes **36a** and **36b** (inseparable mixture in 40 % combined yield) (Scheme 17) [42].



Scheme 17. Synthesis of dicarbonyl(phosphine)carbene complexes by means of the benzannulation reaction.

Finally, the α,β -unsaturated carbene complex may be generated in situ by alkyne insertion into a chromium–carbene bond of a saturated chromium carbene leading to a chromium vinyl carbene (equivalent to intermediate (*E*)-**D** in the mechanism of the benzannulation reaction, see Section 8.2.1, Scheme 3), which may undergo subsequent benzannulation with a second equivalent of the alkyne [43a]. This strategy was subsequently applied to the synthesis of (*Z*)-enediynes and related compounds [43b], and to that of substituted benzofurans (see also Section 8.5) [43c, 43d].

8.3.2

The Alkyne

The benzannulation reaction tolerates a range of alkyl and aryl alkynes, which may bear additional functionalities. The simultaneous presence of two bulky substituents directly attached to the $\text{C}\equiv\text{C}$ bond, as for example in bis(trimethylsilyl)ethyne, however, blocks the final electrocyclization and causes the reaction to stop at the vinyl ketene stage [44]. Neither very electron-rich nor very electron-poor alkynes can undergo benzannulation. Strongly electron-deficient alkynes such as hexafluorobut-2-yne cannot adequately compete with car-

bon monoxide in the initial ligand-exchange process. On the other hand, strongly electron-rich alkynes, especially those having a polarized $\text{C}\equiv\text{C}$ bond such as ynamines, tend to preferentially add to the carbene carbon atom and subsequently insert into the metal–carbene bond. The insertion products may undergo cyclopentannulation at elevated temperatures [45].

Few examples are known in which acetylenic ethers have been incorporated into benzannulation products [46]. Propargyl ethers have been reported to afford variable amounts of indenenes and furans depending on the carbon chain [47]. Other heteroatoms that support the benzannulation reaction when adjacent to the $\text{C}\equiv\text{C}$ bond in the alkyne are boron (see Section 8.3.6), silicon, and tin (see Section 8.3.3). Haloalkynes give only inseparable product mixtures.

Furthermore, the successful $[3+2+1]$ cycloaddition of alkynes bearing a cyclopropane ring and a carbene complex unit has been reported. These benzannulations result in the formation of bimetallic naphthohydroquinone chromium tricarbonyl complexes [48]. Additionally, (non-strained) cyclic alkynes are potent reaction partners in the cycloaddition of chromium carbene complexes [49].

The $\text{C}\equiv\text{C}$ bond is distinctly more reactive towards the metal carbene than the $\text{C}=\text{C}$ bond [50]. This distinction allows a benzannulation approach to vitamins K and E (see Section 8.6.1). Bis(alkynes) have been shown to participate in the $[3+2+1]$ cycloaddition with either one or both of their triple bonds (see Section 8.5).

The benzannulation approach has been applied to aromatic molecules of biological interest. Alkynes bearing porphyrin (for example **37**) [51a, 51b], ferrocene (for example **39**) [51c], and carbohydrate functionalities [51d, 51e] have been incorporated into the (hydro)quinone skeleton, as demonstrated for porphyrinyl and ferrocenyl naphthoquinones **38** and **40** (Scheme 18).

tert-Butylphosphaethyne **42** is the only heteraalkyne known to be amenable to benzannulation [52]. In a competitive experiment, it was demonstrated [52c] that this phosphaalkyne is about six times more reactive than the corresponding *tert*-butylethyne. This is due to the higher electron density in *tert*-butylphosphaethyne.

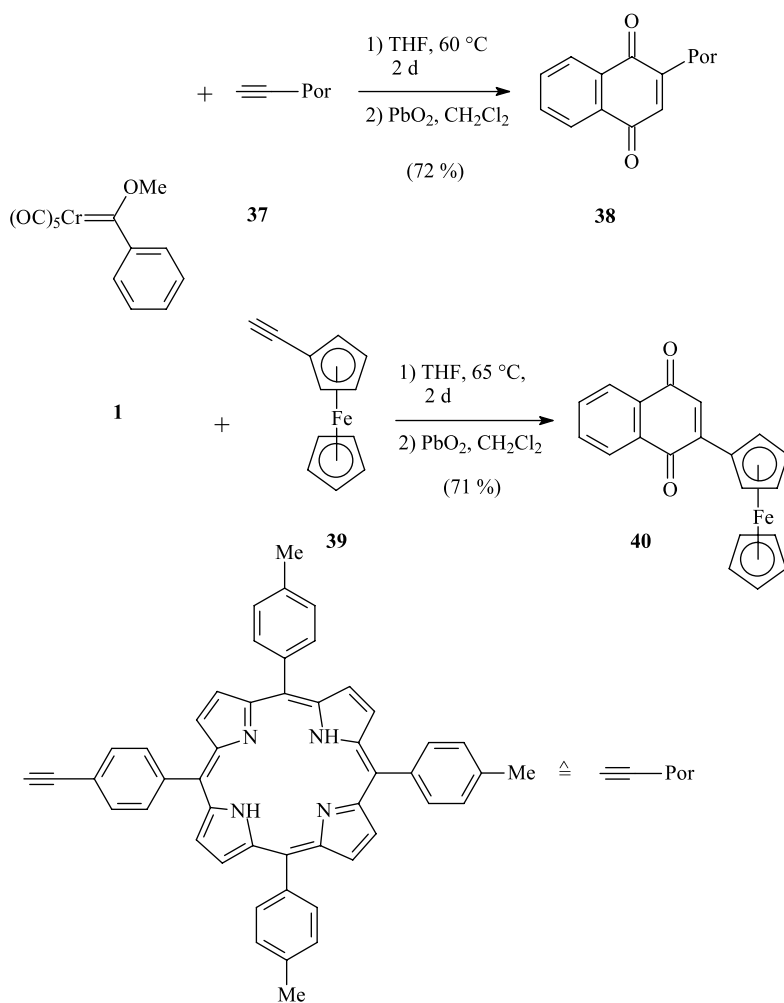
A benzannulation was carried out with **42** and carbene complex **41** to give phosphaphenanthrene **43** in high yield (Scheme 19), whereas yields of phosphabenzenes were only marginal [52].

8.3.3

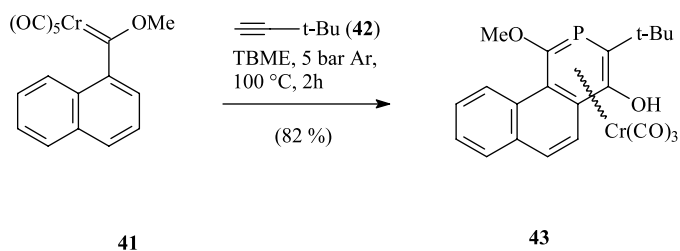
Regioselectivity

One of the main features of the benzannulation reaction of Fischer carbene complexes is the regiochemistry of the incorporation of alkynes into the assembled hydroquinone [53]. While terminal alkynes are incorporated with high regioselectivity (regardless of alkyl and aryl substituents), internal alkynes are prone to much poorer regioselectivity. Regioselectivity is virtually lost in the case of diarylacetylenes.

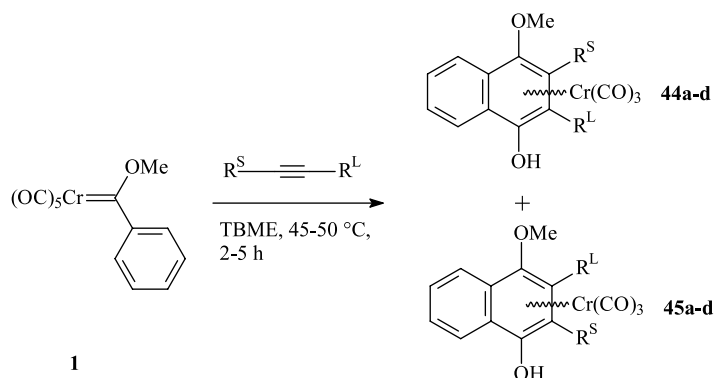
Scheme 20 presents the regiochemical outcome of some benzannulations with both terminal and internal alkynes. With similar alkyl substituents attached to the triple bond, the regioselectivity in favor of **44** gradually drops on going from 1-pentyne (entry A; exclusive formation of **44**) through 2,2-dimethyl-3-pentyne (entry B; **44**:**45** = 90:10) to 3-pentyne



Scheme 18. Applications of ferrocenyl and porphyrinyl alkynes in the benzannulation reaction.



Scheme 19. Synthesis of a phosphaphenanthrene via the benzannulation path.



Entry	R ^S	R ^L	Ratio 44 : 45
A	H	<i>n</i> -Pr	100 : 0
B	Me	<i>t</i> -Bu	90 : 10
C	Me	Et	70 : 30
D	Ph	<i>p</i> -Me-C ₆ H ₄	54 : 46

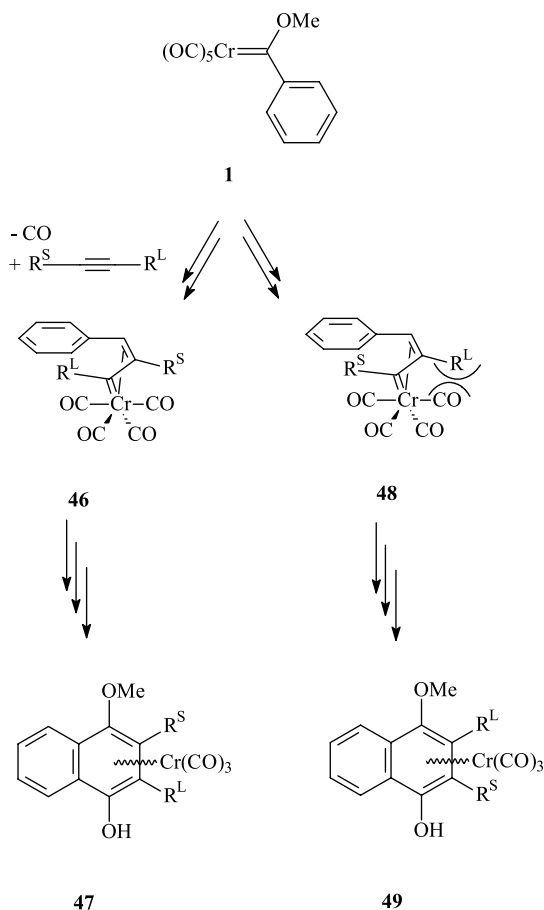
Scheme 20. Regioselective incorporation of terminal and internal alkynes in the benzannulation reaction.

(entry C; **44**:**45** = 70:30), but incorporation of the larger alkyl substituent next to the phenolic hydroxy group remains favored. Entry D shows the poor selectivity observed when two similar aryl substituents are attached to the acetylene moiety; here, isomers **44** and **45** are obtained in comparable quantities.

The regioselectivity is mainly governed by the steric demands of the two alkyne substituents (Scheme 21). The discrimination between the two possible regioisomers is supposed to occur at the stage of the vinyl carbene intermediates **46** and **48**, respectively. While **48** suffers from steric repulsion between the apical carbonyl ligand and the larger R^L substituent, this unfavorable interaction does not occur in regioisomer **46**; as a result, regioisomer **47** generally prevails over **49**.

The incorporation of alkynes bearing substituents of similar steric bulk next to the triple bond results in only poor regioselectivity. This restriction may be overcome by an intramolecular version of the benzannulation, in which the alkyne and the carbene complex are linked by a suitable spacer that may be detached upon oxidation [31, 54].

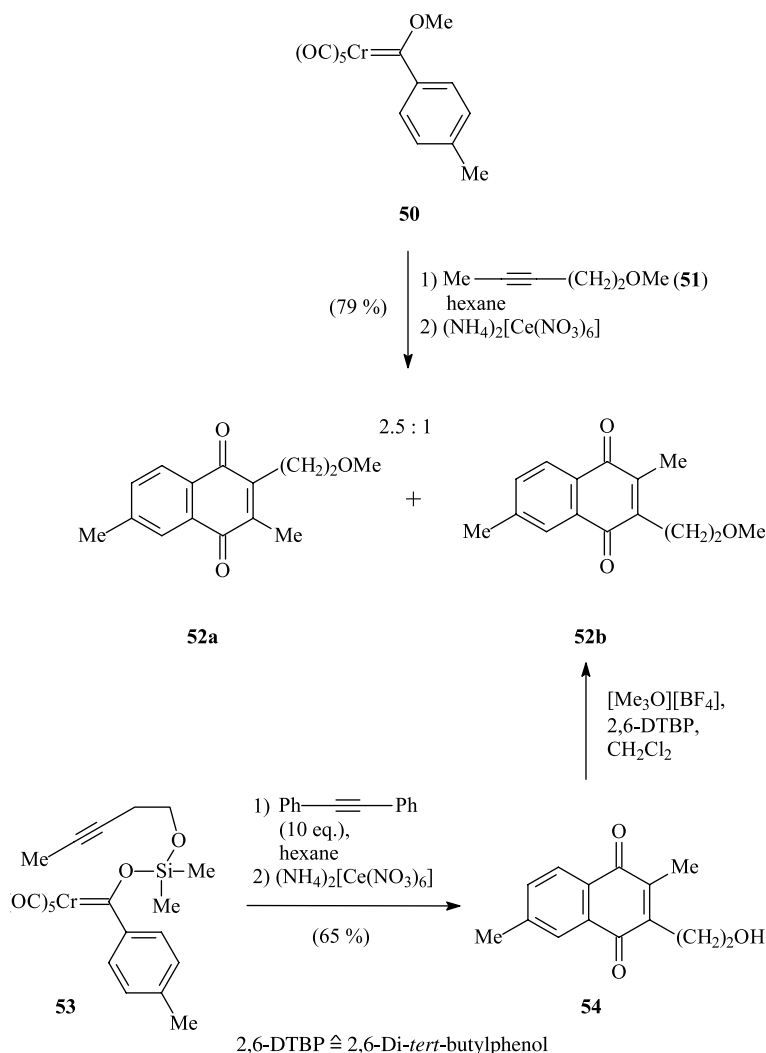
An advanced approach used a silyloxyethylene linker as in complex **53** (Scheme 22) [31]. Benzannulation in the presence of an excess of diphenylethyne (“xenochemical effect”) gave naphthoquinone **54**, which was subjected to oxidative cleavage and demetalation to afford regioisomer **52b** exclusively. The complementary intermolecular benzannulation protocol



Scheme 21. Origin of the regioselectivity of alkyne incorporation in benzannulation reactions.

involving chromium carbene **50** and alkyne **51** resulted in a 2.5:1 preference for the other naphthoquinone regioisomer **52a**.

The regiochemistry of the intermolecular benzannulation can be reversed to some extent by an appropriate substitution pattern of the alkyne. While incorporation of silylacetylene occurs with the expected regiopreference in favor of the 2-silylphenols, the homologous stannylacetylene gives the reverse regiochemistry [55]. The origin of this reversal is not quite clear; it has been attributed to a stabilizing interaction between the tin and the adjacent apical carbon monoxide ligand at chromium in intermediate **48** (see Scheme 21) [55a]. A similar reversal of regiochemistry in the benzannulation product results from the ring-opening of arylcyclopropanes in the presence of hexacarbonylchromium [55b]. This rearrangement is believed to involve a metal-coordinated vinylcarbene intermediate, and thus parallels the benzannulation methodology of carbene complexes with alkynes.



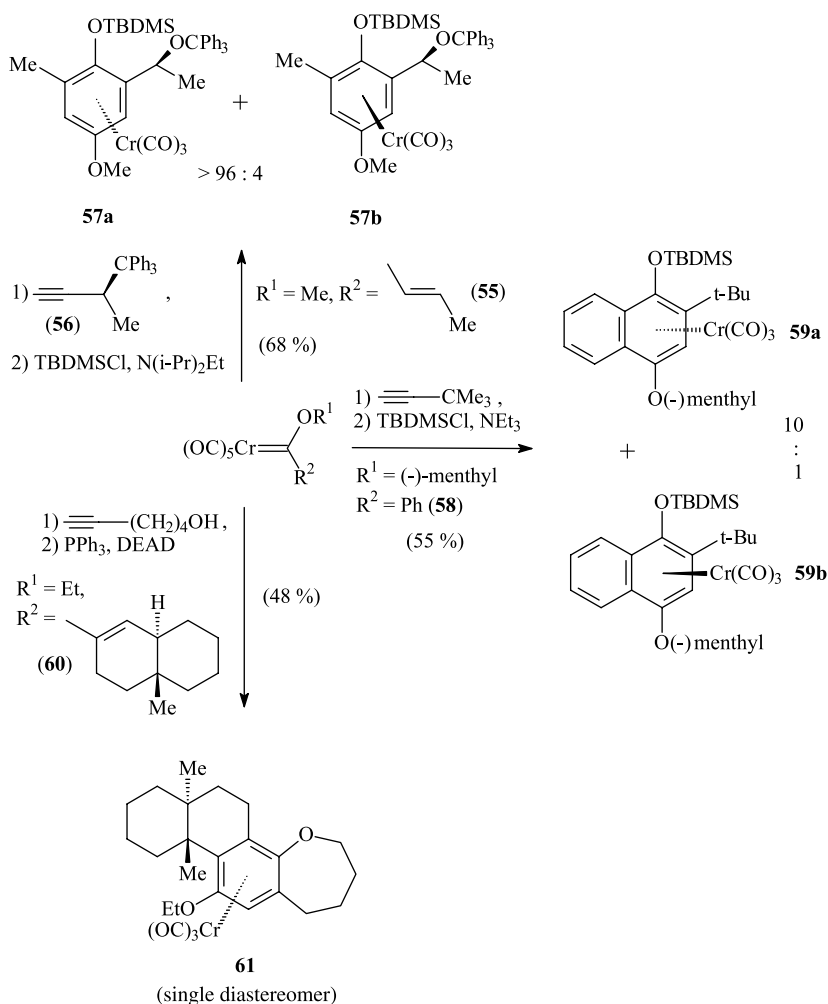
Scheme 22. Improved regioselectivity by intramolecular benzannulations.

8.3.4

Diastereoselectivity

The benzannulation affords arene-Cr(CO)₃ complexes possessing a plane of chirality resulting from the unsymmetrical arene substitution pattern. This aspect is relevant to stereoselective synthesis, in which enantiopure arene tricarbonyl chromium complexes play a major role [56]. The benzannulation reaction avoids both harsh conditions incompatible with the retention of chiral information and the cumbersome separation of enantiomers, and is thus attractive for the diastereo- and enantioselective synthesis of arene complexes [17b, 57].

Three different strategies have been envisaged. The chiral information can either be incorporated into the alkyne or linked to the heteroatom or to the α,β -unsaturated substituent at the carbene complex carbene carbon. High diastereoselectivities (**57a:57b** > 96:4) have been observed in reactions of vinyl carbene complex **55** with the chiral propargylic ether **56** bearing the bulky trityloxy substituent [57a]. A more general approach is based on chiral alcohols incorporated into the alkoxy-carbene complex. Upon benzannulation with *tert*-butylethyne, the menthyloxy carbene complex **58** gave a diastereoselectivity of 10:1 in favor of the naphthalene tricarbonylchromium complex **59a** [57c, 57d]. Finally, the tandem benzannulation–Mitsunobu reaction of optically active carbene complex **60** with 5-hexyn-1-ol afforded the *anti*-benzoxepine complex **61** as the only diastereomer (Scheme 23) [57b].



Scheme 23. Diastereoselective benzannulation of vinyl and phenyl carbene complexes.

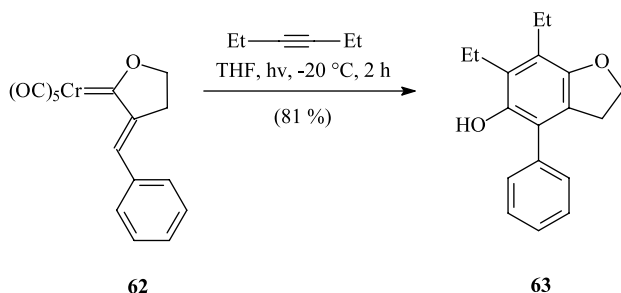
8.3.5

Thermal and Photochemical Benzannulation

The benzannulation reaction is usually performed in ethereal solvents under mild conditions of gentle warming. Modifications of this general protocol involve the use of ultrasound or a dry-state adsorption (DSA) methodology, which involves the adsorption of the reactants onto silica gel, which may speed up the reaction and simplify the work-up procedure in some cases [58a, 58b]. Similarly, photoirradiation of the reaction mixture with light from a xenon lamp has been employed to produce the uncoordinated phenol derivatives without subsequent oxidative work-up [58c].

Stimulated by the photochemical generation of chromium-coordinated ketenes [59d], which have been used in *in situ* nucleophilic additions and cycloadditions, efforts have been directed towards photoinduced benzannulation. Based on earlier observations of photodecarbonylation processes [59a–c], a photobenzannulation was performed starting from a pre-assembled $\alpha,\beta,\gamma,\delta$ -dienyl alkoxy carbene complex [60]. Reacting the alkoxy carbene complex with carbon monoxide, *o*-methoxyphenols [60a, 60d] were obtained, thus complementing the thermal benzannulation route to *p*-methoxyphenols. This approach has been extended to the generation of *o*-aminophenols by reacting dienyl alkoxy carbene complexes with isonitriles [60b, 60c], and dienyl amino carbene complexes with carbon monoxide [60b, 60e]. Examples of this strategy are given in Sections 8.5 and 8.6. Thermal intramolecular benzannulation of dienyl carbene complexes of chromium and tungsten leads to tri- and tetracyclic benzene derivatives [60f]. These carbene complexes react with alkynes to give eight-membered carbocycles via 8π -electrocyclization. Benzannulation, however, occurs if the terminal double bond is part of a benzene ring [60g].

The photochemical protocol may be the method of choice in cases where the thermal reaction fails. This is true for *exo*-alkylidene oxacyclopentylidene chromium complexes such as **62**, which are inert under thermal conditions but undergo a photoinduced benzannulation with, for example, 3-hexyne to give benzofuran **63** (Scheme 24) [61].



Scheme 24. Photochemical benzannulation of an *exo*-alkylidene-oxacyclopentylidene chromium complex.

8.3.6

Subsequent Transformations

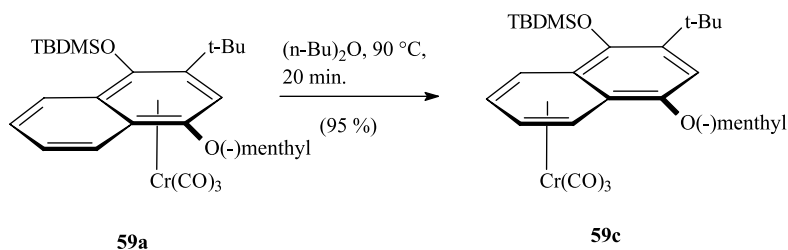
The benzannulation products may be modified by subsequent transformations, by demetalation or by oxidation. To stabilize the coordination of the $\text{Cr}(\text{CO})_3$ fragment and thus to re-

tain both the stereochemical information based on the plane of chirality and the activation of the arene towards the addition of nucleophiles, it is recommended that the phenolic hydroxy group is protected by silylation or esterification to prevent degradation by oxidation [57c, 57d, 62].

The scope and value of the benzannulation reaction is further increased by the substitution pattern of the arene ring, which can be modified by the incorporation of alkynes bearing additional functional groups such as silyl, stannyl, or boryl substituents. These functional groups have been used in various palladium-catalyzed (cross)-coupling reactions [63, 64]. Further structural elaboration may be based on benzannulation followed by nucleophilic aromatic addition [63b].

A special type of reaction, in which the organometallic moiety changes its coordination to the aromatic π -system, is haptotropic metal migration in polycyclic arene chromium tricarbonyl complexes. The reaction feature is best known for naphthalene chromium tricarbonyl complexes [65]. Since the benzannulation allows a regioselective complexation of polycyclic arenes, the benzannulation products are ideal starting materials for studies of the haptotropic migration. Upon warming the primary (kinetic) benzannulation products, in which the metal fragment is coordinated to the hydroquinoid ring, the metal migrates to the less substituted arene ring to give the thermodynamic regioisomer.

A special application of the haptotropic rearrangement is the reaction of diastereopure complex **59a** (Section 8.3.4, Scheme 23). Upon warming to 90 °C in di-*n*-butyl ether, haptotropic migration of the chromium tripod occurs intramolecularly along the same face of the naphthalene system to produce pure diastereomer **59c** (Scheme 25) [57d].



Scheme 25. Stereoselective haptotropic rearrangement in naphthalene tricarbonylchromium complexes.

Demetalation of the benzannulation product can be achieved by careful oxidation in air or, more elegantly, by ligand exchange with acetonitrile or carbon monoxide under pressure to give the uncoordinated hydroquinone.

More vigorous oxidation leads directly to quinones. This approach has been employed in a regioselective synthesis of polysubstituted quinones based on benzannulation with trimethylsilyl alkynes followed by oxidation, iododesilylation, and cross-coupling [66].

8.4

Typical Experimental Procedure

The thermal benzannulation is a well-elaborated synthetic technique that provides direct access to $\text{Cr}(\text{CO})_3$ -activated, densely substituted arenes. While it is possible to obtain the free

arene upon careful oxidation [67], most examples include an oxidative work-up of the reaction mixture and thus afford the corresponding quinones. The reactions are typically performed in an ethereal solvent such as *tert*-butyl methyl ether or THF in the temperature range 45–70 °C to induce the primary decarbonylation. Reflux conditions are beneficial in order to remove the carbon monoxide evolved. The reaction can be conveniently monitored by either thin-layer chromatography or infrared spectroscopy, which allows selection of the appropriate reaction time and temperature and prevents undesired decomposition of the arene tricarbonyl chromium. Most benzannulations are accompanied by a color change from red to orange or yellow. After consumption of the starting material, the reaction mixture is cooled to ambient temperature, and the benzannulation product may then be subjected to a protection protocol (for example, *tert*-butyldimethylsilyl chloride/triethylamine or *tert*-butyldimethylsilyl triflate/2,6-lutidine) in order to increase its stability towards oxidation. Alternatively, in situ protection can be carried out in the course of the benzannulation reaction. Demetalation of the benzannulation product may be achieved by substitution of the arene ligand by typical two-electron ligands such as acetonitrile, triphenylphosphine, or carbon monoxide; the latter, applied at a pressure of 40 bar, is especially attractive since it is a clean process that allows the recovery of hexacarbonyl chromium, which serves as starting material for the carbene complex. Oxidative cleavage of the chromium–arene bond is usually effected by CAN (cerium(IV) ammonium nitrate) or, more selectively, by silver(I) oxide.

8.5

Synthesis of Specific Arenes

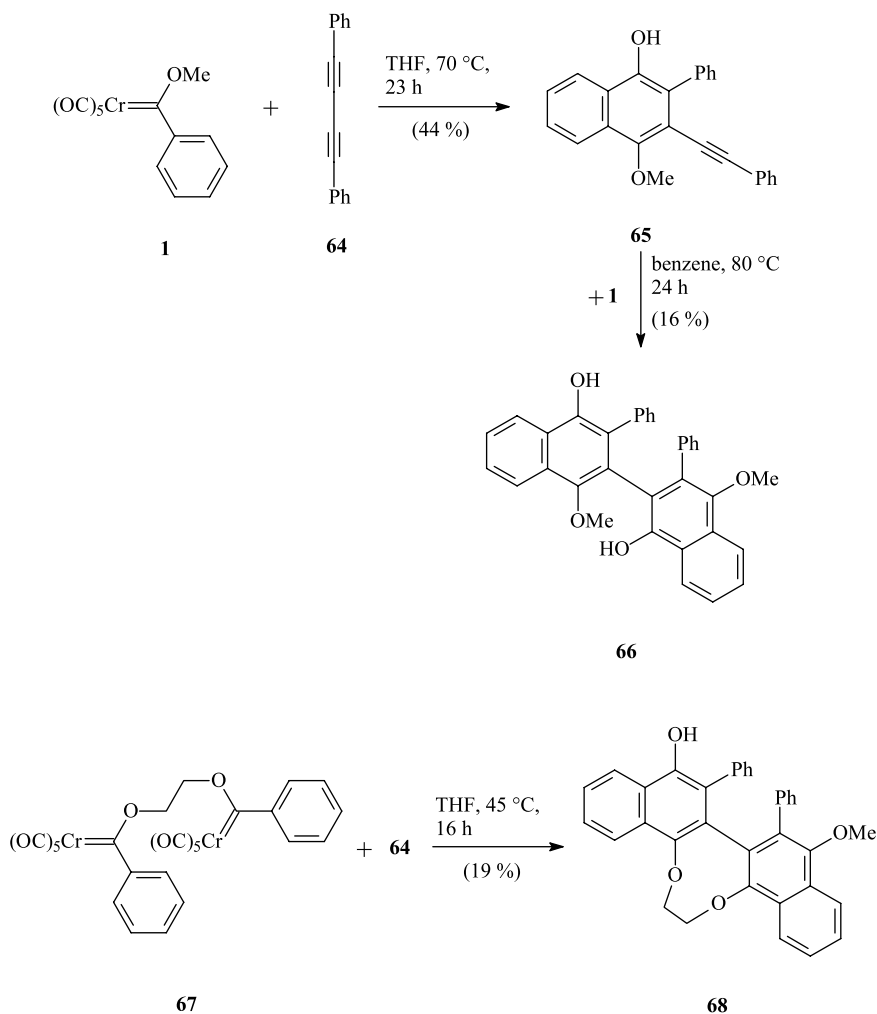
8.5.1

Biaryls

Biaryls merit special interest due to their axial element of chirality and are among the most widely used ligands in enantioselective synthesis and catalysis. Their coordination by a tricarbonyl chromium fragment following benzannulation provides an additional stereogenic element in terms of a chiral plane to the molecule [68]. Biaryl quinones are similarly relevant to natural product synthesis and enantioselective catalysis.

The binaphthohydroquinone skeleton is accessible by a double benzannulation of a bi-phenylbis(carbene) complex using two equivalents of alkyne. Application of one alkyne equivalent affords the mono-benzannulated product; the second benzannulation step proceeds with distinctly lower yield [68a]. A complementary approach to biaryls is based on 1,3-dialkynes (for example, **64**) which undergo a stepwise benzannulation sequence (for example, yielding **65** and **66**) (Scheme 26) [68c]. A one-step protocol starting from the ethylene-bridged bis-carbene complex **67** affords the conformationally less flexible biaryl **68**, albeit in only moderate yield.

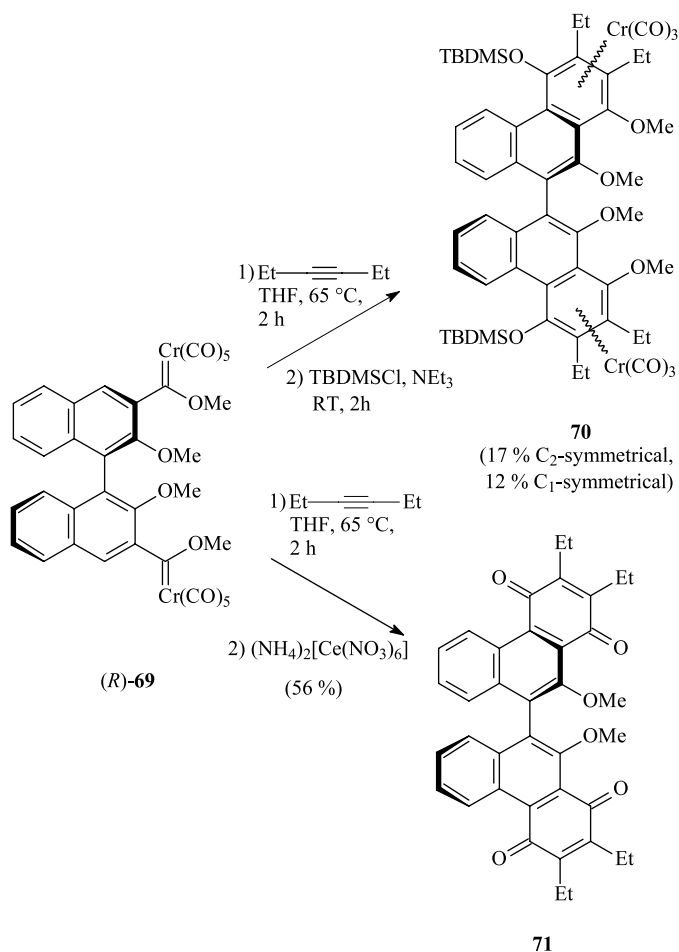
A bidirectional benzannulation strategy allows the extension of an existing biaryl skeleton. The BINOL-derived bis-carbene complex **69**, accessible through a sequence of regioselective double *ortho*-lithiation/Fischer carbene complex synthesis, undergoes bidirectional benzannulation to give the dinuclear biphenanthrene complex **70**. The optical induction exerted by the binaphthyl core is, however, only moderate; a mixture of C_2 - and C_1 -symmetrical bis(phenanthrohydroquinone) bis-chromium complexes is formed, in which the C_2 -



Scheme 26. Inter- and intramolecular approaches to binaphthyls.

symmetrical diastereomer predominates [68e]. The in situ benzannulation/oxidation sequence affords the bis(phenanthroquinone) **71** in higher yield and in enantiopure form (Scheme 27).

The benzannulation reaction further allows the concomitant generation of an axial and chiral plane in a single reaction step (Scheme 28) [68f]. The diastereomeric ratio of the benzannulation products depends on the protocol used for phenol protection. Thus, in situ protection gives the kinetic ratio of **74a**:**74b** = 11:89, whereas a two-step benzannulation/protection sequence results in thermodynamic control to give a ratio of **74a**:**74b** > 99:1. These results can be explained in terms of a possible or arrested rotation around the biaryl axis in the benzannulation product before protection to give either **74a** or **74b**.



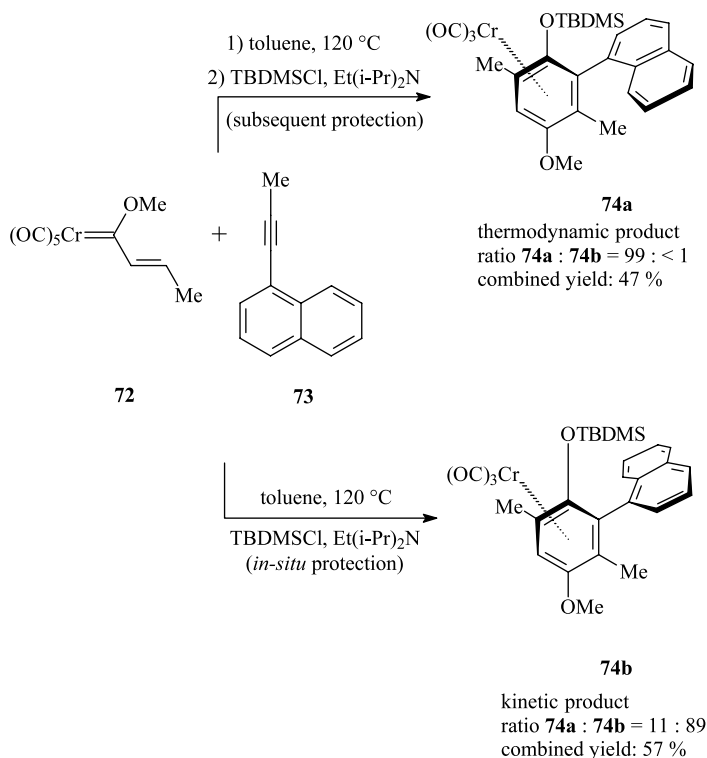
Scheme 27. Synthesis of bis(phenanthroquinones) and -(hydroquinones).

8.5.2

Cyclophanes

Coordinated and uncoordinated cyclophanes receive considerable interest due to the influence of strain on aromaticity [69]. Benzannulation adds a mild synthetic strategy to the known synthetic methods for their production, especially for coordinated cyclophanes, which have been mostly synthesized by the harsher direct coordination of pre-assembled cyclophanes.

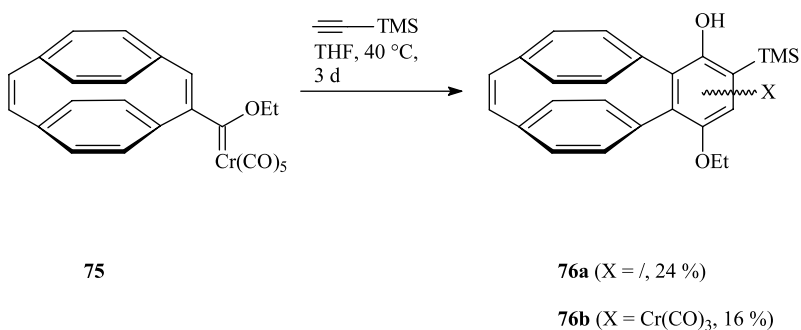
Benzannulation is compatible with the construction of non-planar or strained aromatic rings. This is demonstrated by both the annulation of boat-like arene decks in [2.2]metacyclophanes and by an intramolecular benzannulation to form a hydroquinone deck itself. The first effort concentrated on the annulation of the strained ethene bridge in the [2.2]para-



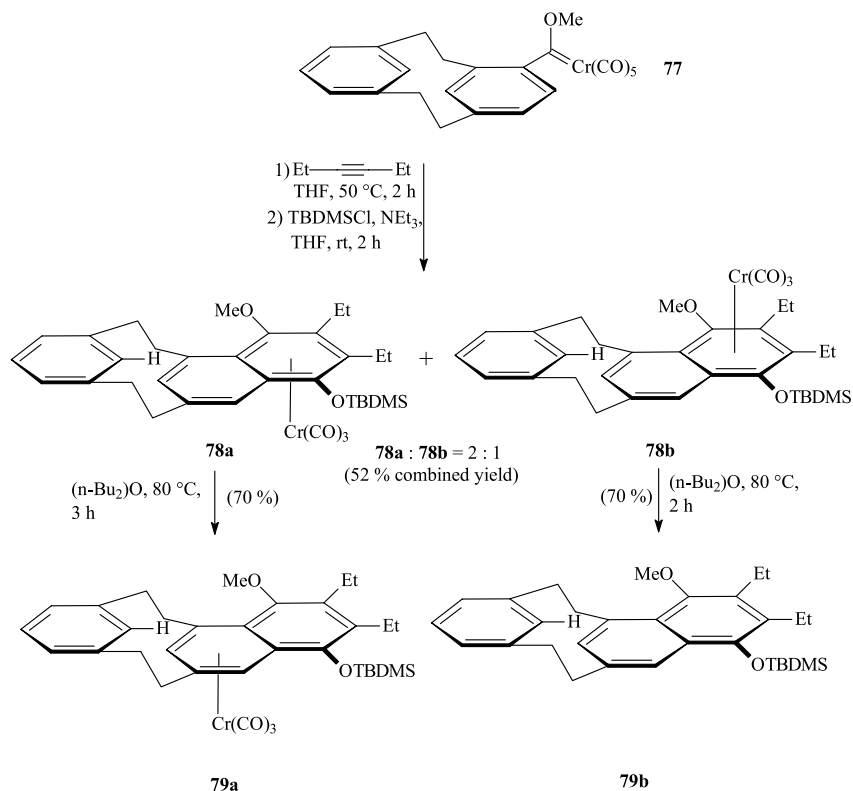
Scheme 28. Concomitant generation of a chiral axis and a planar axis.

cyclophane-based carbene complex **75**, which resulted in a combined 40 % yield of hydroquinone derivatives **76a** and **76b** (Scheme 29) [70].

The non-planar boat-like arene deck in the [2.2]metacyclophane carbene complex **77** undergoes benzannulation to give a diastereomeric mixture of naphthalenophanes **78a** and **78b**; reflecting the steric shielding by the unaffected benzene deck, the *anti*-diastereomer **78a** is formed preferentially to the *syn*-diastereomer **78b** (combined yield: 52 %) (Scheme 30) [71]. The steric influence of the benzene deck is further evident from a study of the hapto-



Scheme 29. Benzannulation of the ethene bridge in [2.2]paracyclophanes.

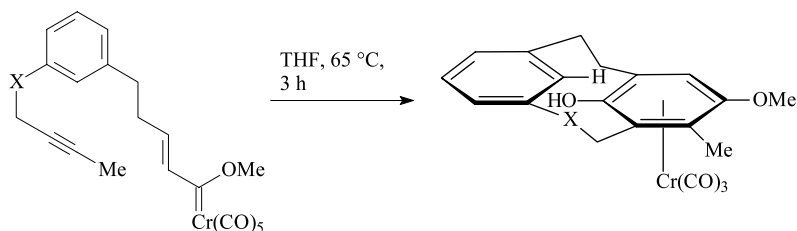


Scheme 30. Synthesis and haptotropic rearrangement of *meta*-benzonaphthohydroquinonophane tricarbonylchromium complexes.

tropic migration of the chromium fragment along the naphthalene π -system. Whereas the *anti*-diastereoisomer **78a** rearranges upon warming to 80 °C to give **79a**, the metal migration to the inner naphthalene ring in the *syn*-diastereomer **78b** is hampered by the combined steric repulsion between the $\text{Cr}(\text{CO})_3$ fragment, the inner hydrogen of the benzene deck, and the benzylic hydrogen atoms of the ethylene bridges. Instead, demetalation occurs under identical conditions to give the uncoordinated naphthalenophane **79b**. The benzannulation methodology provides a regiodefined access to chromium-labeled cyclophanes and is complementary to the complexation protocol using traditional chromium-transfer reagents such as $\text{Cr}(\text{CO})_3(\text{NH}_3)_3$ [72].

Even the distorted boat-like deck in [2.2]metacyclophanes can be constructed by an intramolecular version of the benzannulation. A suitable precursor bears a chromium vinylcarbene and an alkyne moiety linked to a *meta*-phenylene core by two-atom bridges, as shown for complexes **80**. Benzannulation under the typical conditions affords hydroquinonophanes **81** in fair yields (Scheme 31) [73]. Interestingly, the intramolecular benzannulation approach even tolerates heteroatom bridges, which impose both additional strain and helicity on the cyclophane skeleton [73b].

Another independent intramolecular approach to cyclophanes was based on a macrocyclization [74].

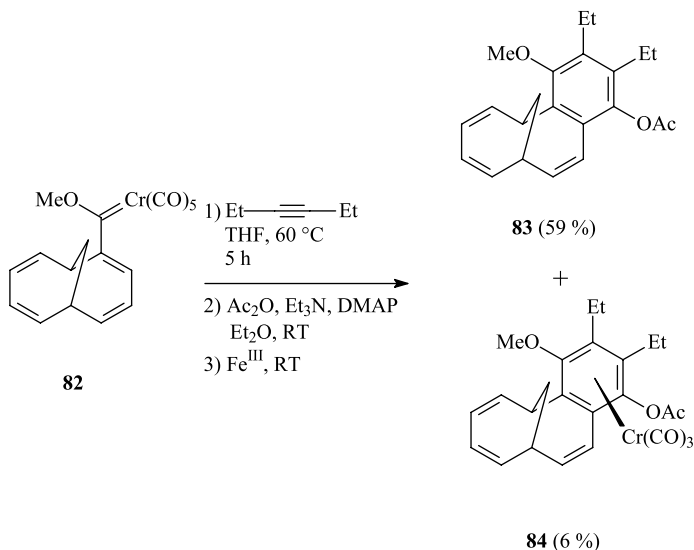
**80a** (X = CH₂)**80b** (X = O)**80c** (X = NMe)**81a** (X = CH₂, 38 %)**81b** (X = O, 25 %)**81c** (X = NMe, 20 %)

Scheme 31. An intramolecular benzannulation approach to [2.2]meta- and [2.2](hetera)metacyclophanes.

8.5.3

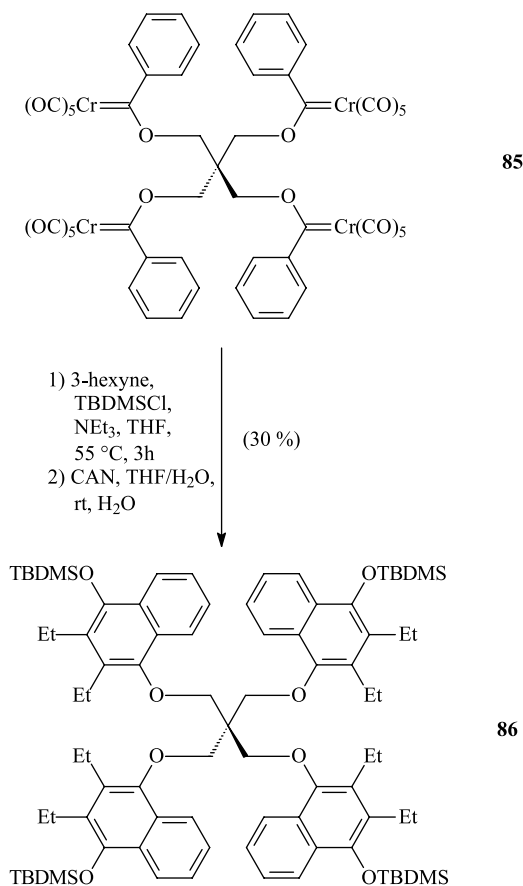
Annulenes and Dendritic Molecules

The benzannulation technique is also applicable to the benzene homologation and functionalization of annulenes, as well to a quadruple arene modification of dendritic cores. The reaction of chromium carbene functionalized 1,6-methano[10]annulene **82** with 3-hexyne under standard conditions afforded a fair yield of the benzannulation product **83** after protection and oxidative work-up (Scheme 32) [75]. The chromium complex **84** evidently partly survived the oxidation conditions using Fe^{III}; a *syn*-stereochemistry with respect to the Cr(CO)₃ fragment and the methano bridge was suggested on the basis of NMR data, which is in contrast to the preferred formation of *anti*-annulation products bearing cyclophane skeletons [75b].



Scheme 32. Benzannulation of chromium [10]annulene carbenes.

The tetrafunctional alcohol pentaerythritol is a popular core in dendrimer chemistry; it has been modified into a tetrakis chromium phenylcarbene **85**, which underwent a quadruple benzannulation upon reaction with 3-hexyne. The reaction proceeded with only moderate diastereoselectivity in terms of the planes of chirality formed; demetalation by mild oxidative work-up gave the tetrakis-hydroquinone derivative **86** (Scheme 33) [76].

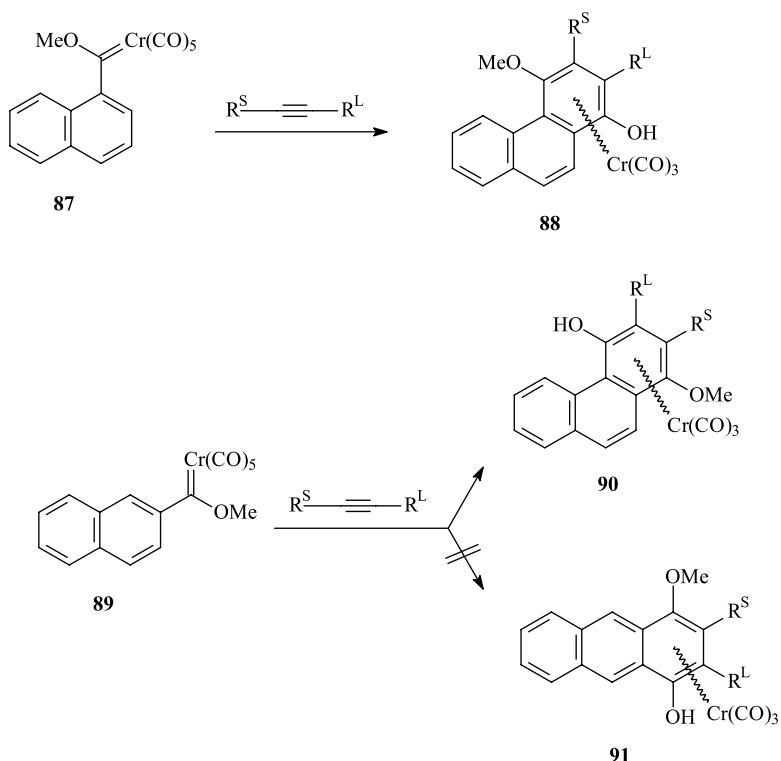


Scheme 33. Quadruple benzannulation of chromium carbenes with a dendritic core.

8.5.4

Angular, Linear, and Other Fused Polycyclic Arenes

The benzannulation of naphthyl carbene complexes may be used as a direct route to functionalized phenanthrenes (Scheme 34) [37a]. While it is obvious that 1-naphthyl carbene complexes such as **87** lead to phenanthrenes **88** (see also Section 8.3.2, Scheme 19), chromium 2-naphthylcarbenes **89** offer two alternatives for annulation, giving either phenanthrene or anthracene derivatives. Generally, angular benzannulation affording phenanthrenes **90** is favored over linear benzannulation to give anthracene derivatives **91**. A rationale for this regiopreference is the higher electron density at C-1 compared with that at



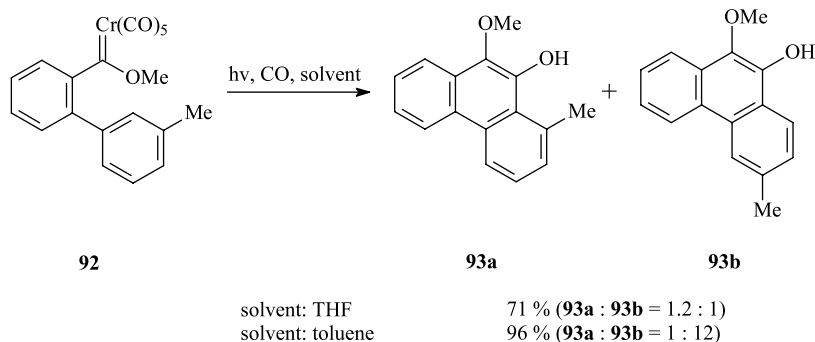
Scheme 34. Benzannulation of 1- and 2-naphthyl carbene complexes.

C-3 of the naphthalene nucleus that controls the electrophilic ring-closure of the vinyl ketene intermediate; moreover, the degree of aromaticity of the angular rings in the phenanthrene skeleton exceeds that in the anthracene analogues. This regioselectivity observed in the benzannulation of chromium carbenes is paralleled by results observed for 2-naphthyl cyclobutenones [77] and for the palladium-catalyzed cyclocarbonylation of 2-naphthyl allyl acetates [78].

To date, reports of linear benzannulation are very limited [55b, 79]. One example referred to the annulation of a 2-naphthohydroquinoid chromium carbene, which was employed in the synthesis of anthracycline (see Section 8.6.2) [79]. Later, a complementary approach in this area started from 2-naphthylcyclopropenes which, in the presence of hexacarbonylmolybdenum, served as precursors for the vinyl ketenes required for linear annulation [55b].

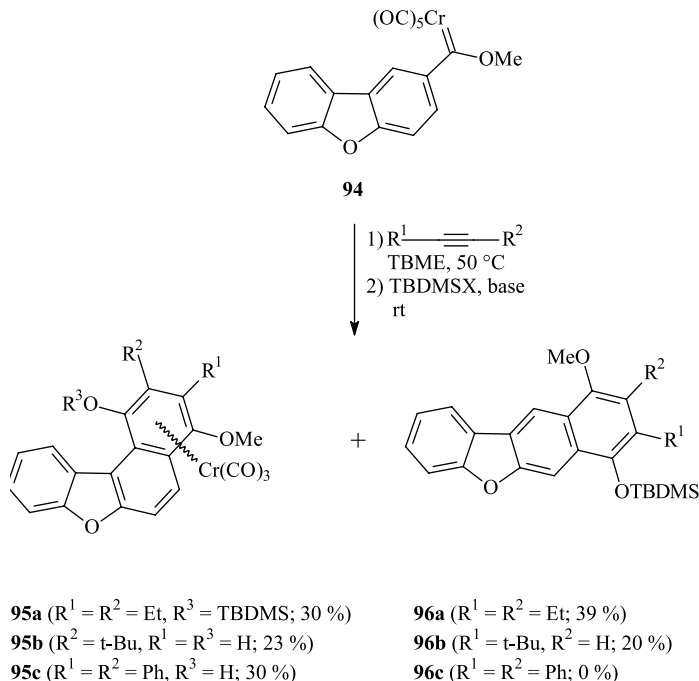
The cycloaddition of naphthyl carbene complexes has found application in the synthesis of biphenanthryl derivatives (see Section 8.5.1) [68c, 68d].

An alternative route to oxygenated phenanthrenes is based on a photocyclization protocol; starting from chromium biphenylcarbene **92**, methoxyphenanthrols **93a** and **93b** are obtained (Scheme 35) [60d]. The regioselectivity of the cyclization depends on the solvent used; while in THF the *ortho* product **93a** is slightly favored, a marked 12:1 preference for *para* annulation is observed in toluene, giving **93b** as the major isomer.



Scheme 35. Regioselective phenanthrene formation via photobenzannulation.

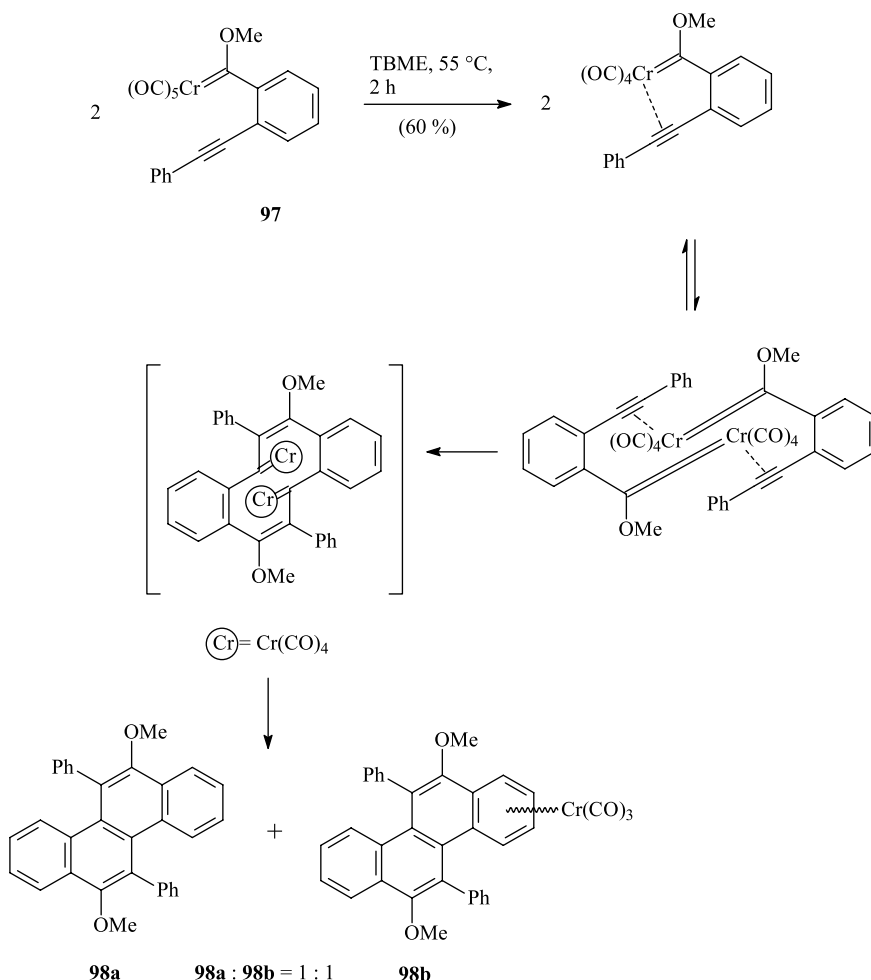
A similar competition of angular *versus* linear benzannulation has recently been observed in the dibenzofuran series (Scheme 36) [80]. The results obtained for carbene complex **94** suggest that the regiochemistry depends on the substitution pattern of the alkyne and, moreover, that this has an influence on whether or not the chromium fragment remains coordinated to the annulation product. When internal alkynes such as 3-hexyne or terminal alkynes bearing bulky alkyl substituents were used, the formation of angular-fused benzo[*b*]naphtho[1,2-*d*]furan tricarboxyl chromium complexes (**95a**, **95b**) was accompanied by that of comparable amounts of uncoordinated benzo[*b*]naphtho[2,3-*d*]furans (**96a**, **96b**) as linear annulation products. Diarylethyne such as tolane, however, gave exclusively the an-



Scheme 36. Angular *versus* linear benzannulations of dibenzofurylcarbene complex **94**.

gular annulation product **95c** in moderate yield. Angular benzannulation may also hamper phenol protection with a bulky silyl group.

Apart from the construction of phenanthrenes, carbene complexes have also been used for the synthesis of more extended polycyclic arenes. An unusual dimerization of chromium coordinated *ortho*-ethynyl aryl carbenes results in the formation of chrysenes (Scheme 37) [81]. This unusual reaction course is presumably due to the rigid C₂ bridge that links the carbene and alkyne moieties, and thus prevents a subsequent intramolecular alkyne insertion into the metal–carbene bond. Instead, a double intermolecular alkyne insertion favored by the weak chromium–alkyne bond is believed to occur forming a central ten-membered ring that may then rearrange to the fused arene system. For example, under typical benzannulation conditions, carbene complex **97** affords an equimolar mixture of chrysene **98a** and its monochromium complex **98b**. The *peri*-interactions between the former alkyne substituent (in the 5- and 11-positions) and the aryl hydrogen induce helicity in the chrysene skeleton.



Scheme 37. Chromium-assisted dimerization of *ortho*-alkynylarylcarbene ligands to chrysenes.

Whereas the torsion angle across the central arene C=C bond is small ($< 6^\circ$) for 5,11-dialkyl substitution, it increases with diaryl substitution and terminal $\text{Cr}(\text{CO})_3$ coordination to $> 30^\circ$ for 5,11-diphenylchrysene-6,12-dione, obtained from **98a** upon careful ether cleavage and oxidation.

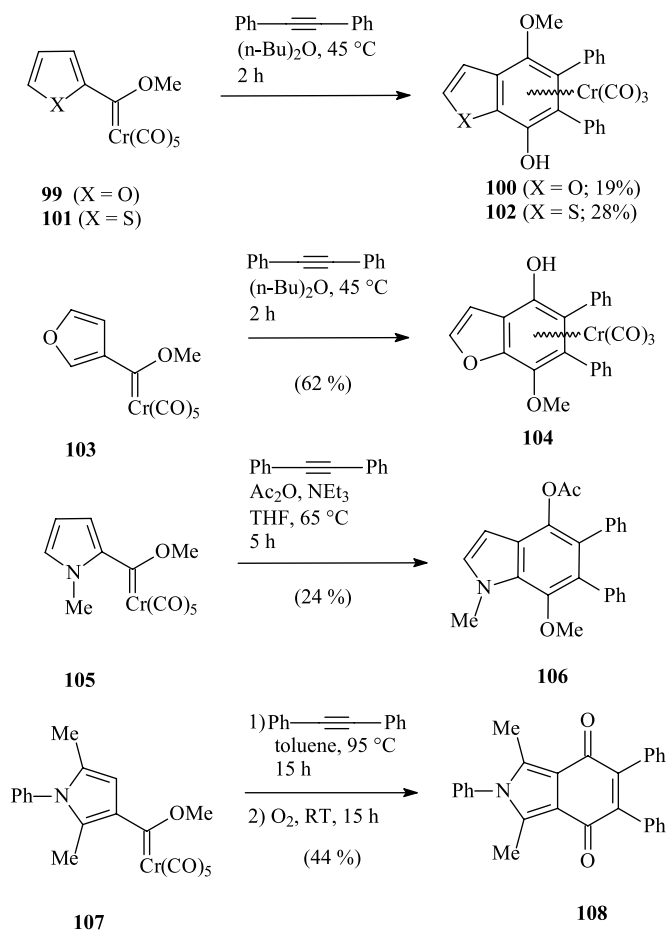
Another route to chrysenes was based on the benzannulation of bis(chromium carbenes) of 1,6-methano[10]annulenes [75b].

A series of other polycyclic hydrocarbons has been synthesized in moderate to good yields by benzannulation of tricyclic diarylcarbene complexes [36b].

8.5.5

Fused Heterocycles

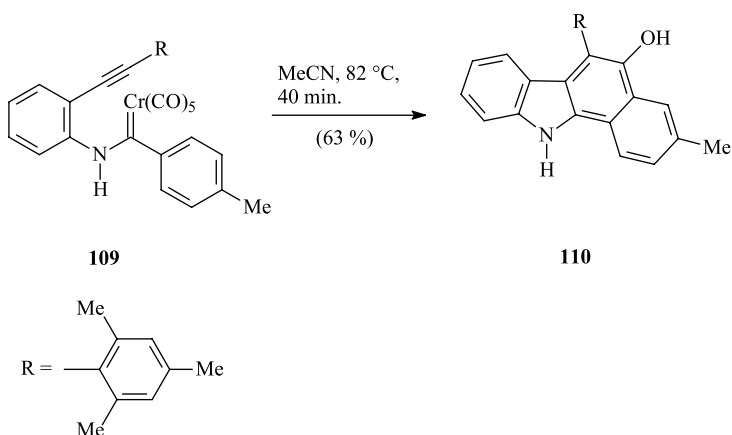
Benzannulated five-membered heterocycles have been synthesized starting from furyl-, thienyl-, and pyrrolylcarbene complexes. With the exception of thiophene (for example, the transformation of **101** into **102**), the corresponding 2- and 3-heteroarylcarbene complexes have been prepared and subjected to the benzannulation reaction (Scheme 38) [35a, 82].



Scheme 38. Benzannulation of furyl-, thienyl-, and pyrrolylcarbene complexes.

While both 2- and 3-furylcarbene complexes **99** and **103** gave $[b]$ -annulated benzofurans (**100** and **104**), only the 2-pyrrolyl carbene complex **105** afforded the aromatic indole skeleton (**106**). In contrast, annulation of the 2,5-dimethylated 3-pyrrolylcarbene complex **107** occurred at the 4-position to give isoindole quinone **108** after oxidative work-up [82g].

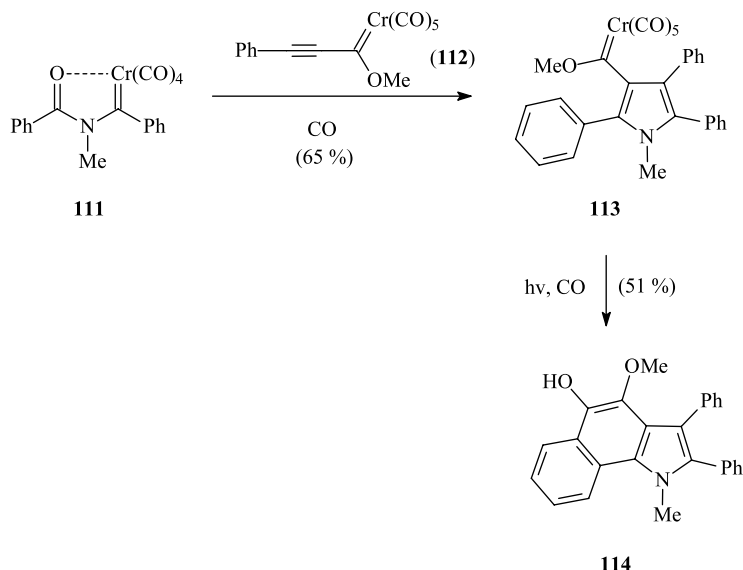
A complementary access to extended indole and carbazole systems is based on the thermal intramolecular benzannulation of *ortho*-alkynylanilinocarbene complexes or on a photo-induced benzannulation of phenylpyrrolylcarbene complexes. The first example involves an intramolecular access to the carbazole skeleton. Refluxing a solution of *ortho*-alkynylphenyl amino carbene complex **109** in acetonitrile gave a 63 % yield of benzocarbazole **110**. Less strongly coordinating solvents (TBME, THF, or di-*n*-butyl ether) or other substituents less bulky than 2,4,6-trimethylphenyl (for example, phenyl or 4-methylphenyl) led to a considerably reduced yield (Scheme 39) [83].



Scheme 39. Fused carbazoles by intramolecular benzannulation.

Benzoindole **114** has been synthesized by a remarkable sequence, in which the benzannulation precursor **113** is pre-assembled starting from two different chromium carbenes. It is formed in a $[3+2]$ cycloaddition, in which the acylamino carbene complex **111** acts as the dipolar component and the alkynylcarbene complex **112** serves as the dipolarophile. The resulting 3-pyrrolylcarbene complex **113** undergoes a photoinduced intramolecular benzannulation to give the benzoindole **114** [84a]. This strategy complements an approach towards carbazoles [84b]. Isoindolines and 1,2,3,4-tetrahydroisoquinolines are accessible from the reaction of pentacarbonyl (α -methoxyethylidene) chromium with π,ω -dialkynes bearing a nitrogen atom in the carbon ether [84c].

Pyrzoyl- [85], dihydropyridyl- [86], and pyrrolizinylicarbene complexes [87] have also been subjected to the benzannulation to give the respective oxygenated benzo-*N*-heterocycles. Finally, $\alpha,\beta,\gamma,\delta$ -dienyl carbene complexes containing a heterocycle at the internal double bond have been utilized to prepare 2,3-dihydro-1,2-benzisoxazoles and indazoles by intramolecular benzannulation [60h].



Scheme 40. Tandem cycloaddition/photobenzannulation approach to benzoindoles.

8.6

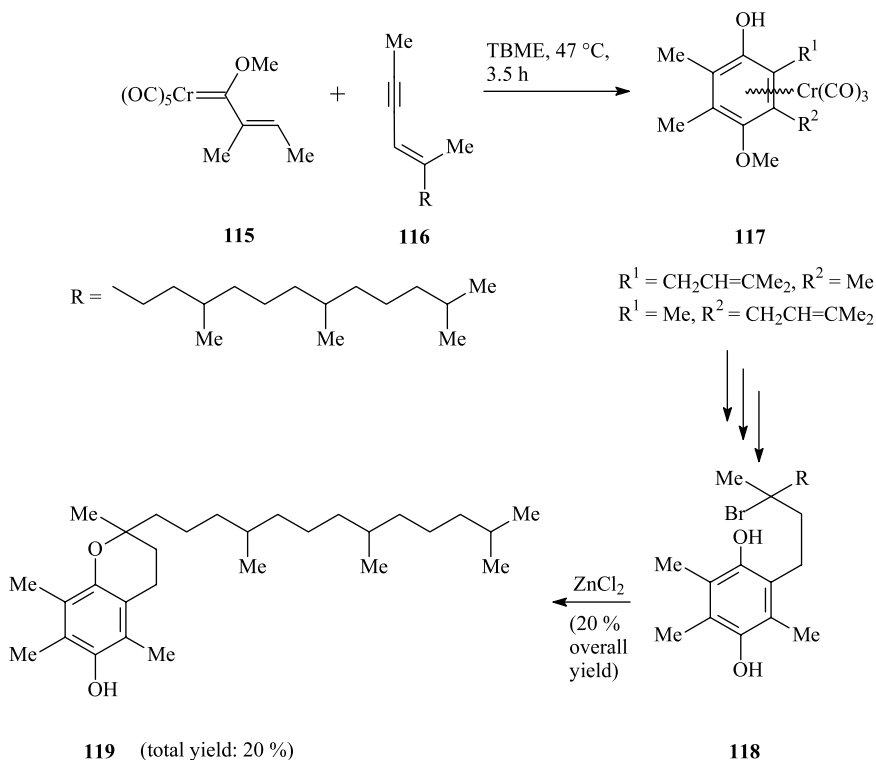
Synthesis of Biologically Active Compounds

Due to its versatility with respect to the scope and substitution pattern, both in terms of the chromium carbene and the alkyne, the benzannulation reaction has been recognized as a valuable methodology for the synthesis of complex biologically active compounds.

8.6.1

Vitamins

Soon after its discovery, the benzannulation reaction was applied to an organometallic synthetic approach to vitamins of the K and E series in order to test its scope [88]. The route leading to vitamin K1(20) has been optimized; its key step, the benzannulation involving chromium phenylcarbene **1** and enyne **116** finally gave a 92 % yield of a 2 : 1 regioisomeric mixture (both regioisomers ultimately afford the identical naphthoquinone (vitamin K) upon oxidation) of the Cr(CO)_3 -coordinated hydroquinone monomethyl ether after chromatographic work-up. Since this method avoids the acidic conditions typically required for the attachment of the allylic terpenoid side chain to the arene nucleus, no undesired (*E*)/(*Z*)-equilibration in the alkene part occurs, which is known to hamper the biological activity of vitamin K [88b]. The related synthesis of vitamin E is outlined in Scheme 41. Starting from (*E*)-2-butenylcarbene complex **115** and enyne **116**, it afforded a 36 % non-optimized yield of hydroquinone complex **117** as a mixture of two regioisomers. Demetalation under CO atmosphere, ether cleavage, and ZnCl_2 -promoted cyclization afforded vitamin E **119** in an overall yield of 20 %.



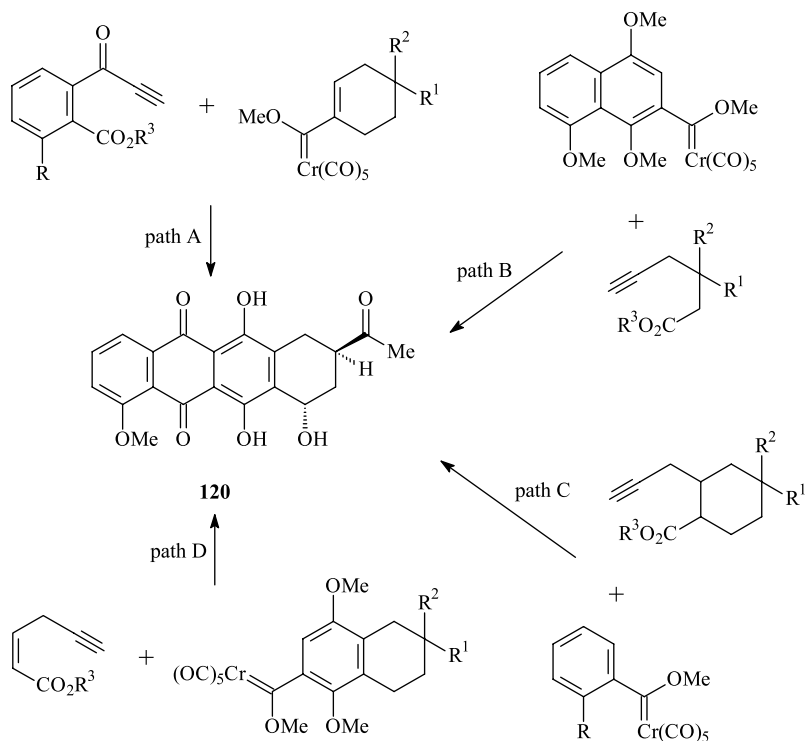
Scheme 41. Total synthesis of vitamin E involving a benzannulation.

8.6.2

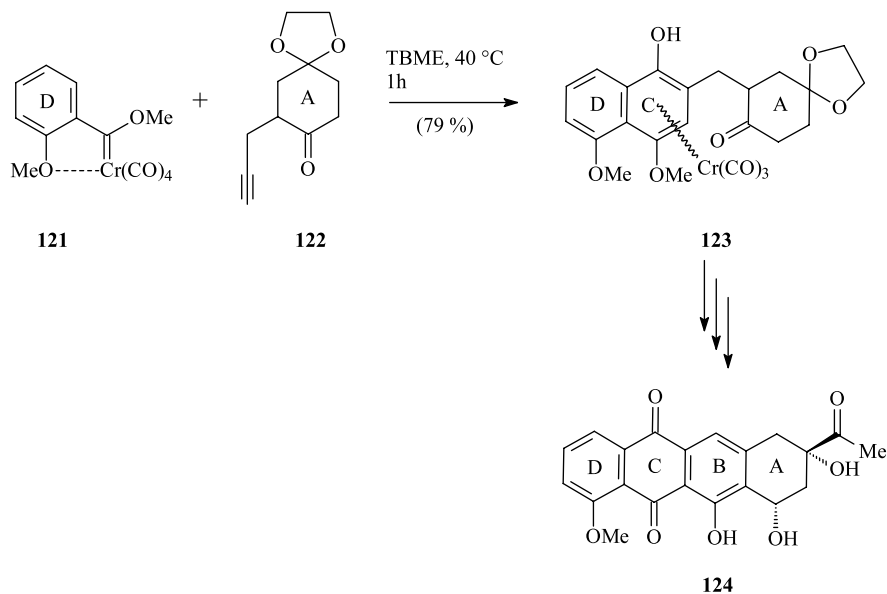
Antibiotics

There are several classes of antibiotics that contain adjacent quinone and hydroquinone moieties. Since both functionalities are directly accessible by chromium carbene benzannulation, this organometallic methodology offers an attractive strategy towards targets of this type. Special attention has been paid to antitumor agents having naphthoquinone and anthraquinone skeletons, such as anthracyclins, which contain a sugar moiety attached to the anthracyclinone [79, 89]. Depending on whether quinone ring C or hydroquinone ring D is to be constructed by benzannulation, there is a choice of complementary key steps combining the appropriate chromium carbene and alkyne precursors, as illustrated for daunomycinone **120** in Scheme 42 [89c, 90].

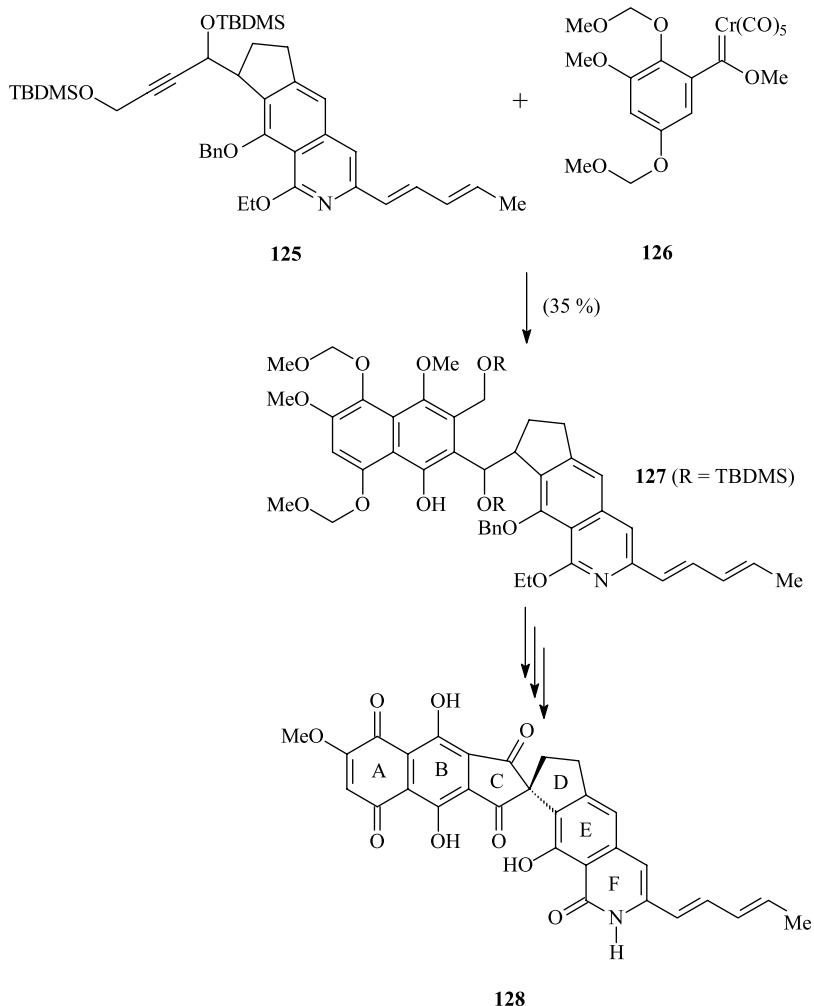
The route for the assembly of the C ring of 11-deoxydaunomycinone **124** is shown in Scheme 43 and corresponds to path C in Scheme 42. Reacting tetracarbonyl carbene complex **121** (available in quantitative yield by heating the corresponding pentacarbonyl carbene complex in boiling *tert*-butyl methyl ether) with the propargylic A-ring synthon **122** forms ring C in the tricarbonylchromium complex **123**. Subsequent demetalation, C_1 -homologation of the ketone to the carboxylic acid, and Friedel–Crafts-type cyclization leads to ring B, and final functionalization of ring A completes the total synthesis of 11-deoxydaunomycinone **124**.



Scheme 42. Synthetic strategies towards the anthracyclinone daunomycinone.



Scheme 43. A chromium carbene route to 11-deoxydaunomycinone.



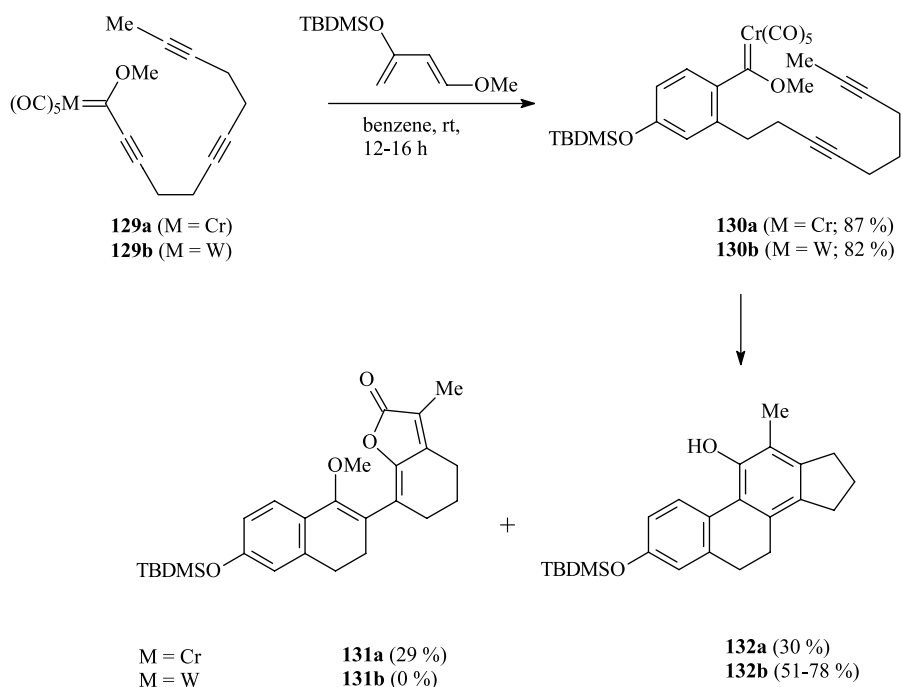
Scheme 44. Total synthesis of fredericamycin A.

Apart from anthraquinone antibiotics, the benzannulation approach has also been applied to naphthoquinone antibiotics, as demonstrated for the antitumor agent fredericamycin A **128** [91]. This hexacyclic compound has a significant degree of complexity, including a series of functional groups and a stereogenic spirocenter. Its total synthesis relied on a regio-specific intermolecular benzannulation to form ring B as the final key step (Scheme 44) [91c, 92]. This involved assembly of the relatively simple chromium carbene **126** and the densely functionalized bulky alkyne **125** to give the desired regioisomer **127** in 35 % yield after oxidative demetalation. The final C/D-spirocyclization completed the total synthesis of fredericamycin A.

8.6.3

Steroids

A less common “two-alkyne” benzannulation approach (a formal [2+2+1+1] cycloaddition involving two alkyne, one carbon, and one carbonyl synthon [15a]) has been exploited in a tandem Diels–Alder benzannulation sequence leading to the tetracyclic steroid skeleton (Scheme 46) [93]. The triynylcarbene complex precursors **129a** and **129b** were first subjected to an intermolecular Diels–Alder reaction with the Danishefsky diene, which occurred at the activated C≡C bond adjacent to the metal carbene fragment and generated the D-ring in the diynylarylcene complex **130** (87 % yield for the Diels–Alder reaction giving the chromium complex **130a** and 82 % for that giving the tungsten complex **130b**). The remaining rings A–C were constructed by a two-alkyne benzannulation affording ring B attached to a central six-membered and a terminal five-membered ring in a *meta* connectivity. Whereas the cyclization of the chromium carbene complex **130a** was accompanied by competing formation of lactone **131a**, the tungsten analogue **130b** selectively afforded the desired steroid skeleton **132b** in 51–78 % yield depending on the solvent used [93]. The influence of the metal is determined by the sequence of carbene carbonylation and insertion of the second alkyne into the metal–carbene bond; the more reactive chromium carbonyl bond has been suggested to favor both ketene formation prior to alkyne insertion and a final carbonylation to give lactone **131a**.



Scheme 45. The “two-alkyne” benzannulation sequence as applied to steroids.

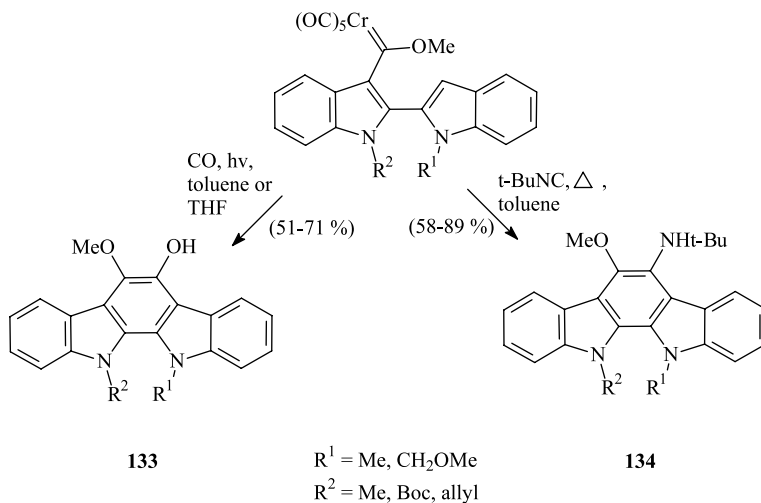
The benzannulation approach has also been used to generate a steroid D ring bearing both a tunable donor (ferrocenyl substituent) and an acceptor site (benzoquinone functionality), which allows for modification of the electron-transfer properties [94].

Another application aimed at the synthesis of novel steroidal systems, for example heterosteroids such as oxasteroids [95].

8.6.4

Alkaloids

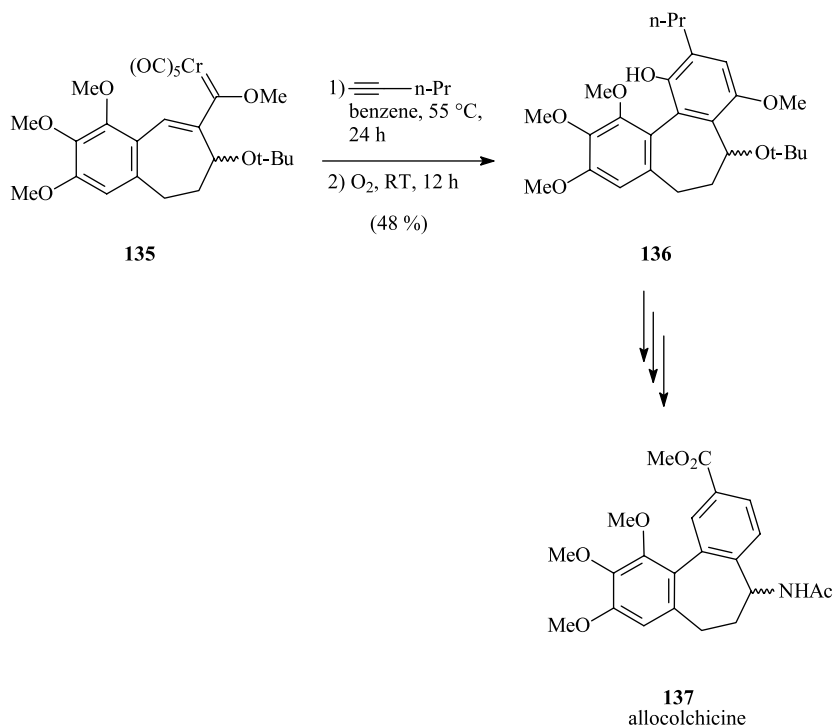
Some selected alkaloids are readily accessible via the corresponding chromium carbenes. A versatile synthesis of indolocarbazoles **133** and **134**, bioactive natural products with interesting protein kinase C inhibiting properties, is based on photobenzannulation. Depending on the nature of the C₁-synthon, dioxy and oxyamino derivatives have been synthesized in good to very good yields (Scheme 46) [96].



Scheme 46. Synthetic approach towards bioactive indolocarbazoles.

The benzannulation allows a facile incorporation of a hydrogen-bonding functionality, which complements the pharmacophore in naturally occurring indolocarbazoles. Orthogonally protected indolocarbazole nitrogen atoms allow a concise and selective glycoside formation en route to synthetic indolocarbazoles as natural product analogues.

A model compound from a second group of alkaloids related to colchicine (alcolchicinoid **137**) has been synthesized by benzannulation of racemic benzocycloheptenyl carbene complex **135** with 1-pentyne; the annulation product **136** was obtained in 48 % yield after oxidative demetalation (Scheme 47) [97].



Scheme 47. Formation of the allocolchicinoid C ring by benzannulation.

8.7

Summary and Outlook

The chromium-templated benzannulation of Fischer carbene complexes with alkynes provides a flexible synthetic tool for a wide range of both natural and theoretically interesting compounds. The key features of this [3+2+1] cycloaddition are the regioselective and (in the presence of a chiral auxiliary) diastereoselective, mild, one-pot assembly of the alkyne, the carbene ligand, and one carbonyl ligand, as assisted by the template effect of the transition metal, to give densely functionalized $\text{Cr}(\text{CO})_3$ -labeled arenes. Beyond the traditional strategy for preparing arene tricarbonylchromium complexes by $\text{Cr}(\text{CO})_3$ -transfer onto a pre-assembled arene, the benzannulation allows a regioselective complexation of polycyclic hydrocarbons under mild conditions. The regioselectivity is virtually complete with terminal alkynes, and can be accomplished for internal alkynes by the intramolecular version of the reaction. The resulting hydroquinone tricarbonylchromium complexes are valuable building blocks possessing a plane of chirality; they can be demetalated to give either densely substituted arenes or, after oxidative work-up, the corresponding quinones. Moreover, the tricarbonylchromium fragment can be exploited in further arene functionalization by stereocontrolled nucleophilic addition or substitution. Finally, the $\text{Cr}(\text{CO})_3$ fragment *per se* incorporated into polycyclic arenes by benzannulation provides a label that can be shifted

along the aromatic π -face in a haptotropic metal migration, and may thus serve as a movable functional group.

References

- 1 W. REPPE, W. J. SCHWECKENDIECK, *Liebigs Ann. Chem.* **1948**, 560, 104–116.
- 2 a) K. P. C. VOLLHARDT, *Angew. Chem. Int. Ed. Engl.* **1984**, 23, 539–555; *Angew. Chem.* **1984**, 96, 525–541; b) D. L. MOHLER, K. P. C. VOLLHARDT, in *Advances in Strain in Organic Chemistry*, Vol. 5 (Ed.: B. HALTON), JAI Press, London, **1995**, pp. 121–160.
- 3 a) E. O. FISCHER, *Angew. Chem.* **1974**, 86, 651–663; b) E. O. FISCHER, *Adv. Organomet. Chem.* **1976**, 14, 1–32.
- 4 a) Recent reviews: K. H. DÖTZ, J. PFEIFFER, in *Transition Metals for Organic Synthesis*, Vol. 1 (Eds.: M. BELLER, C. BOLM), Wiley-VCH, New York, **1998**, pp. 335–360; b) K. H. DÖTZ, H. C. JAHR, in *Transition Metal Complexes of Carbenes and Related Species in 2000* (Ed. G. BERTRAND), *J. Organomet. Chem.* **2001**, 617/618, 1–754; c) K. H. DÖTZ, H. C. JAHR, in *Carbene Chemistry—From Fleeting Intermediates to Powerful Reagents*, (Ed. G. BERTRAND), Fontis Media, Lansanne, **2002**, pp. 231–269.
- 5 a) E. O. FISCHER, K. H. DÖTZ, *Chem. Ber.* **1970**, 103, 1273–1278; b) K. H. DÖTZ, E. O. FISCHER, *Chem. Ber.* **1972**, 105, 1356–1367; c) E. O. FISCHER, K. H. DÖTZ, *Chem. Ber.* **1972**, 105, 3966–3972; d) M. BUCHERT, M. HOFFMANN, H.-U. REISSIG, *Chem. Ber.* **1995**, 128, 605–614; e) J. PFEIFFER, M. NIEGER, K. H. DÖTZ, *Eur. J. Org. Chem.* **1998**, 1011–1022; f) J. BARLUENGA, S. LÓPEZ, A. A. TRABANCO, A. FERNÁNDEZ-ACEBES, J. FLÓREZ, *J. Am. Chem. Soc.* **2000**, 122, 8145–8154.
- 6 K. H. DÖTZ, *Angew. Chem. Int. Ed. Engl.* **1975**, 14, 644–645; *Angew. Chem.* **1975**, 87, 672–673.
- 7 a) K. H. DÖTZ, H. LARBIG, *Bull. Soc. Chim. Fr.* **1992**, 129, 579–584; b) B. L. BALZER, M. CAZANOUE, M. SABAT, M. G. FINN, *Organometallics* **1992**, 11, 1759–1761; c) B. L. BALZER, M. CAZANOUE, M. G. FINN, *J. Am. Chem. Soc.* **1992**, 114, 8735–8736; d) ATIQ-UR-RAHMAN, W. F. K. SCHNATTER, N. MANOLACHE, *J. Am. Chem. Soc.* **1993**, 115, 9848–9849.
- 8 Reviews: a) K. H. DÖTZ, *Angew. Chem. Int. Ed. Engl.* **1984**, 23, 587–608, *Angew. Chem.* **1984**, 96, 573–594; b) W. D. WULFF, in *Comprehensive Organometallic Chemistry*, Vol. 12 (Eds.: E. W. ABEL, F. G. A. STONE, G. WILKINSON), Pergamon Press, Oxford, **1995**, pp. 469–547; b) K. H. DÖTZ, P. TOMUSCHAT, *Chem. Soc. Rev.* **1998**, 28, 187–198; c) A. DE MEIJERE, H. SCHIRMER, M. DUETSCH, *Angew. Chem. Int. Ed. Engl.* **2000**, 39, 3964–4002; *Angew. Chem.* **2000**, 112, 4124–4162.
- 9 M. M. GLEICHMANN, K. H. DÖTZ, B. A. HESS, *J. Am. Chem. Soc.* **1996**, 118, 10551–10560; b) J. MÖLLMANN, K. H. DÖTZ, G. FRENKING, unpublished results; c) P. HOFMANN, M. HÄMMERLE, *Angew. Chem. Int. Ed. Engl.* **1989**, 28, 908–910; *Angew. Chem.* **1989**, 101, 940–942.
- 10 H. FISCHER, J. MÜHLEMEIER, R. MÄRKL, K. H. DÖTZ, *Chem. Ber.* **1982**, 115, 1355–1362.
- 11 a) M. TORRENT, M. DURAN, M. SOLÁ, *Organometallics* **1998**, 17, 1492–1501; b) H. FISCHER, P. HOFMANN, *Organometallics* **1999**, 18, 2590–2592.
- 12 K. H. DÖTZ, T. SCHÄFER, F. KROLL, K. HARMS, *Angew. Chem. Int. Ed. Engl.* **1992**, 30, 1236–1238; *Angew. Chem.* **1992**, 104, 1257–1259.
- 13 P. HOFMANN, M. HÄMMERLE, G. UNFRIED, *New J. Chem.* **1991**, 15, 769–789.
- 14 a) J. BARLUENGA, F. AZNAR, A. MARTÍN, S. GARCÍA-GRANDA, E. PÉREZ-CARREÑO, *J. Am. Chem. Soc.* **1994**, 116, 11191–11192; b) E. CHELAIN, A. PARLIER, H. RUDLER, J. C. DARAN, J. VAISSERMANN, *J. Organomet. Chem.* **1991**, 419, C5–C9.
- 15 a) B. A. ANDERSON, W. D. WULFF, A. L. RHEINGOLD, *J. Am. Chem. Soc.* **1990**, 112, 8615–8617; b) K. H. DÖTZ, W. STURM, *J. Organomet. Chem.* **1985**, 285, 205–211.
- 16 W. D. WULFF, B. M. BAX, T. A. BRANDVOLD, K. S. CHAN, A. M. GILBERT, R. P. HSUNG, J. MITCHELL, J. CLARDY, *Organometallics* **1994**, 13, 102–126.
- 17 a) P.-C. TANG, W. D. WULFF, *J. Am. Chem.*

- Soc. **1984**, 106, 1132–1133; b) R. P. HSUNG, W. D. WULFF, C. A. CHALLENGER, *Synthesis* **1996**, 773–789.
- 18 J. BARLUENGA, F. AZNAR, I. GUTIÉRREZ, A. MARTÍN, S. GARCÍA-GRANDA, M. A. LLORCA-BARAGAÑO, *J. Am. Chem. Soc.* **2000**, 122, 1314–1324.
 - 19 J. S. MCCALLUM, F. A. KUNNG, S. R. GILBERTSON, W. D. WULFF, *Organometallics* **1988**, 7, 2346–2360.
 - 20 A. YAMASHITA, *Tetrahedron Lett.* **1986**, 27, 5915–5918.
 - 21 K. S. CHAN, G. A. PETERSON, T. A. BRANDVOLD, K. L. FARON, C. A. CHALLENGER, C. HYLDAHL, W. D. WULFF, *J. Organomet. Chem.* **1987**, 334, 9–56.
 - 22 a) E. O. FISCHER, A. MAASBÖL, *Angew. Chem. Int. Ed. Engl.* **1964**, 3, 580; *Angew. Chem.* **1964**, 76, 645; b) E. O. FISCHER, A. MAASBÖL, *Chem. Ber.* **1967**, 100, 2445–2456.
 - 23 E. O. FISCHER, R. AUMANN, *Chem. Ber.* **1968**, 101, 954–962.
 - 24 L. S. HEGEDUS, M. A. MCGUIRE, L. M. SCHULTZE, *Org. Synth.* **1987**, 65, 216–219.
 - 25 a) T. R. HOYE, K. CHEN, J. R. VYVYAN, *Organometallics* **1993**, 12, 2806–2809; b) Q.-H. ZHENG, J. SU, *Synth. Commun.* **2000**, 30, 177–185.
 - 26 E. O. FISCHER, T. SELMAYR, F. R. KREISSL, *Chem. Ber.* **1977**, 110, 2947–2955.
 - 27 a) M. F. SEMMELHACK, S. R. LEE, *Organometallics* **1987**, 6, 1839–1844; b) R. IMWINKELRIED, L. S. HEGEDUS, *Organometallics* **1988**, 7, 702–706; c) M. A. SCHWINDT, T. LEJON, L. S. HEGEDUS, *Organometallics* **1990**, 9, 2814–2819.
 - 28 a) M. L. WATERS, T. A. BRANDVOLD, L. ISAACS, W. D. WULFF, A. L. RHEINGOLD, *Organometallics* **1998**, 17, 4298–4308; b) S. R. PULLEY, S. SEN, A. VOROGUSHIN, E. SWANSON, *Org. Lett.* **1999**, 1, 1721–1723.
 - 29 M. YAMASHITA, T. OHISHI, *Bull. Chem. Soc. Jpn.* **1993**, 66, 1187–1190.
 - 30 a) K. H. DÖTZ, C. STINNER, unpublished results; b) M. F. GROSS, M. G. FINN, unpublished results as cited in footnote [41b] in ref. [31].
 - 31 M. F. GROSS, M. G. FINN, *J. Am. Chem. Soc.* **1994**, 116, 10921–10933.
 - 32 a) A. YAMASHITA, A. TOY, N. B. GHAZAL, C. R. MUCHMORE, *J. Org. Chem.* **1989**, 54, 4481–4483; b) K. H. DÖTZ, V. LEUE, *J. Organomet. Chem.* **1991**, 407, 337–351.
 - 33 a) K. H. DÖTZ, D. GROTHJAHN, K. HARMS, *Angew. Chem. Int. Ed. Engl.* **1989**, 28, 1384–1386; *Angew. Chem.* **1989**, 101, 1425–1427; b) D. B. GROTHJAHN, K. H. DÖTZ, *Synlett* **1991**, 381–390; c) D. B. GROTHJAHN, F. E. K. KROLL, T. SCHÄFER, K. HARMS, K. H. DÖTZ, *Organometallics* **1992**, 11, 298–310.
 - 34 a) J. BARLUENGA, L. A. LÓPEZ, S. MARTÍNEZ, M. TOMÁS, *J. Org. Chem.* **1998**, 63, 7588–7589; b) J. BARLUENGA, L. A. LÓPEZ, S. MARTÍNEZ, M. TOMÁS, *Tetrahedron* **2000**, 56, 4967–4975.
 - 35 a) M. E. BOS, W. D. WULFF, R. A. MILLER, S. CHAMBERLIN, T. A. BRANDVOLD, *J. Am. Chem. Soc.* **1991**, 113, 9293–9319; b) V. P. LIPTAK, W. D. WULFF, *Tetrahedron* **2000**, 56, 10229–10247.
 - 36 a) K. H. DÖTZ, R. DIETZ, *Chem. Ber.* **1978**, 111, 2517–2526; b) J. PFEIFFER, M. NIEGER, K. H. DÖTZ, *Chem. Eur. J.* **1998**, 4, 1843–1851.
 - 37 a) K. H. DÖTZ, R. DIETZ, *Chem. Ber.* **1977**, 110, 1555–1563; b) W. D. WULFF, K.-S. CHAN, *J. Org. Chem.* **1984**, 49, 2293–2295; c) B. A. ANDERSON, J. BAO, T. A. BRANDVOLD, C. A. CHALLENGER, W. D. WULFF, Y.-C. XU, A. L. RHEINGOLD, *J. Am. Chem. Soc.* **1993**, 115, 10671–10687.
 - 38 a) K. H. DÖTZ, R. EHLENZ, D. PAETSCH, *Angew. Chem. Int. Ed. Engl.* **1997**, 36, 2376–2378; *Angew. Chem.* **1997**, 109, 2473–2475; b) K. H. DÖTZ, R. EHLENZ, *Chem. Eur. J.* **1997**, 3, 1751–1756; d) M. R. HALLET, J. E. PAINTER, P. QUAYLE, D. RICKETTS, P. PATEL, *Tetrahedron Lett.* **1998**, 39, 2851–2852; e) K. H. DÖTZ, F. OTTO, M. NIEGER, *J. Organomet. Chem.* **2001**, 621, 77–88.
 - 39 a) K. H. DÖTZ, M. POPALL, G. MÜLLER, K. ACKERMANN, *Angew. Chem. Int. Ed. Engl.* **1986**, 25, 911–912; *Angew. Chem.* **1986**, 98, 909–910; b) K. H. DÖTZ, M. POPALL, G. MÜLLER, K. ACKERMANN, *J. Organomet. Chem.* **1990**, 383, 93–111.
 - 40 a) J. CHRISTOFFERS, K. H. DÖTZ, *J. Chem. Soc., Chem. Commun.* **1993**, 1811–1812; b) J. CHRISTOFFERS, K. H. DÖTZ, *Chem. Ber.* **1995**, 128, 157–161.
 - 41 K. H. DÖTZ, J. GLÄNZER, *J. Chem. Soc., Chem. Commun.* **1993**, 1036–1037.
 - 42 K. H. DÖTZ, S. KLAPDOHR, unpublished results.
 - 43 a) R. DIETZ, K. H. DÖTZ, D. NEUGEBAUER,

- Nouv. J. Chim. **1977**, 2, 59–61; b) J. W. HERNDON, A. HAYFORD, *Organometallics* **1995**, 14, 1556–1558; c) J. W. HERNDON, H. WANG, *J. Org. Chem.* **1998**, 63, 4562–4563; d) Y. ZHANG, J. W. HERNDON, *Tetrahedron* **2000**, 56, 2175–2182.
- 44 K. H. DÖTZ, B. FÜGEN-KÖSTER, *Chem. Ber.* **1980**, 113, 1449–1457.
- 45 a) K. H. DÖTZ, I. PRUSKIL, *Chem. Ber.* **1978**, 111, 2059–2063; b) K. H. DÖTZ, D. NEUGEBAUER, *Angew. Chem. Int. Ed. Engl.* **1978**, 17, 851–852; *Angew. Chem.* **1978**, 90, 898–899.
- 46 See, for example: J. KING, P. QUAYLE, J. F. MALONE, *Tetrahedron Lett.* **1990**, 31, 5221–5224.
- 47 M. F. SEMMELHACK, N. JEONG, G. R. LEE, *Tetrahedron Lett.* **1990**, 31, 609–610.
- 48 O. KRETSCHIK, M. NIEGER, K. H. DÖTZ, *Organometallics* **1996**, 15, 3625–3629.
- 49 a) D. M. GORDON, S. J. DANISHEFSKY, G. K. SCHULTE, *J. Org. Chem.* **1992**, 57, 7052–7055; b) R. ZIMMER, H.-U. REISSIG, *J. Prakt. Chem.* **1998**, 340, 755–756.
- 50 K. H. DÖTZ, I. PRUSKIL, *Chem. Ber.* **1980**, 113, 2876–2883.
- 51 a) C.-S. CHAN, C. C. MAK, K.-S. CHAN, *Tetrahedron Lett.* **1993**, 34, 5125–5126; b) C.-S. CHAN, A. K.-S. TSE, K. S. CHAN, *J. Org. Chem.* **1994**, 59, 6084–6089; c) K. S. CHAN, H. ZHANG, *Synth. Commun.* **1995**, 25, 635–639; d) S. R. PULLEY, J. P. CAREY, *J. Org. Chem.* **1998**, 63, 5275–5279; e) D. PAETSCH, K. H. DÖTZ, *Tetrahedron Lett.* **1999**, 40, 487–488.
- 52 a) K. H. DÖTZ, A. TIRILIOMIS, K. HARMS, M. REGITZ, U. ANNEN, *Angew. Chem. Int. Ed. Engl.* **1988**, 27, 713–715; *Angew. Chem.* **1988**, 100, 725–727; b) K. H. DÖTZ, A. TIRILIOMIS, K. HARMS, *J. Chem. Soc., Chem. Commun.* **1989**, 788–790; c) K. H. DÖTZ, A. TIRILIOMIS, K. HARMS, *Tetrahedron* **1993**, 49, 5577–5597.
- 53 a) W. D. WULFF, P.-C. TANG, J. S. MCCALLUM, *J. Am. Chem. Soc.* **1981**, 103, 7677–7678; b) K. H. DÖTZ, J. MÜHLEMEIER, U. SCHUBERT, O. ORAMA, *J. Organomet. Chem.* **1983**, 247, 187–201; c) A. YAMASHITA, A. TOY, *Tetrahedron Lett.* **1986**, 27, 3471–3474.
- 54 a) M. F. SEMMELHACK, J. J. BOZELL, *Tetrahedron Lett.* **1982**, 23, 2931–2934; b) M. F. SEMMELHACK, J. J. BOZELL, L. KELLER, T. SATO, E. J. SPIESS, W. WULFF, A. ZASK, *Tetrahedron* **1985**, 41, 5803–5812.
- 55 a) S. CHAMBERLIN, M. L. WATERS, W. D. WULFF, *J. Am. Chem. Soc.* **1994**, 116, 3113–3114; b) M. F. SEMMELHACK, S. HO, D. COHEN, M. STEIGERWALD, M. C. LEE, G. LEE, A. M. GILBERT, W. D. WULFF, R. G. BALL, *J. Am. Chem. Soc.* **1994**, 116, 7108–7122.
- 56 G. SCHMALZ, S. SIEGEL, in *Transition Metals for Organic Synthesis*, Vol. 1 (Ed.: M. BELLER, C. BOLM), Wiley-VCH, Weinheim, **1998**, pp. 550–559.
- 57 a) R. P. HSUNG, W. D. WULFF, A. L. RHEINGOLD, *J. Am. Chem. Soc.* **1994**, 116, 6449–6450; b) R. L. BEDDOES, J. D. KING, P. QUAYLE, *Tetrahedron Lett.* **1995**, 36, 3027–3028; c) K. H. DÖTZ, C. STINNER, M. NIEGER, *J. Chem. Soc., Chem. Commun.* **1995**, 2535–2536; d) K. H. DÖTZ, C. STINNER, *Tetrahedron: Asymmetry* **1997**, 8, 1751–1765; e) R. P. HSUNG, W. D. WULFF, S. CHAMBERLIN, Y. LIU, R.-Y. LIU, H. WANG, J. F. QUINN, S. L. B. WANG, A. L. RHEINGOLD, *Synthesis* **2000**, 200–220.
- 58 a) J. P. A. HARRITY, W. J. KERR, D. MIDDLEMISS, *Tetrahedron Lett.* **1993**, 34, 2995–2998; b) J. P. A. HARRITY, W. J. KERR, D. MIDDLEMISS, *Tetrahedron* **1993**, 49, 5565–5576; c) Y. H. CHOI, K. S. RHEE, K. S. KIM, G. C. SHIN, S. C. CHIN, *Tetrahedron Lett.* **1995**, 36, 1871–1874.
- 59 a) E. O. FISCHER, H. FISCHER, *Chem. Ber.* **1974**, 107, 657–672; b) E. O. FISCHER, H. FISCHER, *Chem. Ber.* **1974**, 107, 673–679; c) J. R. KNORR, T. L. BROWN, *Organometallics* **1994**, 13, 2178–2185; d) L. S. HEGEDUS, *Tetrahedron* **1997**, 53, 4105–4128.
- 60 a) C. A. MERLIC, D. XU, *J. Am. Chem. Soc.* **1991**, 113, 7418–7420; b) C. A. MERLIC, E. E. BURNS, D. XU, S. Y. CHEN, *J. Am. Chem. Soc.* **1992**, 114, 8722–8724; c) C. A. MERLIC, E. E. BURNS, *Tetrahedron Lett.* **1993**, 34, 5401–5404; d) C. A. MERLIC, W. M. ROBERTS, *Tetrahedron Lett.* **1993**, 34, 7379–7382; e) C. A. MERLIC, D. XU, B. G. GLADSTONE, *J. Org. Chem.* **1993**, 58, 538–545; f) J. BARLUENGA, F. AZNAR, M. A. PALOMERO, S. BARLUENGA, *Org. Lett.* **1999**, 1, 541–543; g) J. BARLUENGA, F. AZNAR, M. A. PALOMERO, *Angew. Chem. Int. Ed. Engl.* **2000**, 39, 4346–4348; *Angew. Chem.* **2000**, 112, 4514–4516; h) J. BARLUENGA,

- F. AZNAR, M. A. PALOMERO, *Chem. Eur. J.* **2001**, 7, 5318–5324.
- 61 a) B. WEYERSHAUSEN, K. H. DÖTZ, *Eur. J. Org. Chem.* **1998**, 1739–1742; b) B. WEYERSHAUSEN, K. H. DÖTZ, *Synlett* **1999**, 231–233.
- 62 a) S. CHAMBERLIN, W. D. WULFF, B. BAX, *Tetrahedron* **1993**, 49, 5531–5547; for a recent example of *in situ* protection, see: b) W. H. MOSER, L. SUN, J. C. HUFFMAN, *Org. Lett.* **2001**, 3, 3389–3391.
- 63 a) A. M. GILBERT, W. D. WULFF, *J. Am. Chem. Soc.* **1994**, 116, 7449–7450; b) S. CHAMBERLIN, W. D. WULFF, *J. Am. Chem. Soc.* **1992**, 114, 10667–10669.
- 64 a) M. W. DAVIES, C. N. JOHNSON, J. P. A. HARRITY, *Chem. Commun.* **1999**, 2107–2108; b) M. W. DAVIES, C. N. JOHNSON, J. P. A. HARRITY, *J. Org. Chem.* **2001**, 66, 3525–3532.
- 65 a) Y. F. OPRUNENKO, N. G. AKHMEDOV, D. N. ROZNYAKOVSKY, Y. A. USTYNYUK, N. A. USTYNYUK, *J. Organomet. Chem.* **1999**, 583, 136–145; b) Y. OPRUNENKO, S. MALYUGINA, P. NESTERENKO, D. MITYUK, O. MALYSHEV, *J. Organomet. Chem.* **2000**, 597, 42–47; c) K. H. DÖTZ, N. SZESNI, M. NIEGER, K. NÄTTINEN, submitted for publication.
- 66 K. S. CHAN, C. C. MAK, *Tetrahedron* **1994**, 50, 2003–2016.
- 67 J. M. TIMKO, A. YAMASHITA, *Org. Synth.* **1993**, 71, 72–76.
- 68 a) N. HOA TRAN HUY, P. LEFLOCH, *J. Organomet. Chem.* **1988**, 344, 303–311; b) K. A. PARKER, C. A. COBURN, *J. Org. Chem.* **1991**, 56, 1666–1668; c) J. BAO, W. D. WULFF, M. J. FUMO, E. B. GRANT, D. P. HELLER, M. C. WHITCOMB, S.-M. YEUNG, *J. Am. Chem. Soc.* **1996**, 118, 2166–2181; d) J. BAO, W. D. WULFF, J. B. DOMINY, M. J. FUMO, E. B. GRANT, A. C. ROB, M. C. WHITCOMB, S.-M. YEUNG, R. L. OSTRANDER, A. L. RHEINGOLD, *J. Am. Chem. Soc.* **1996**, 118, 3392–3405; e) P. TOMUSCHAT, L. KRÖNER, E. STECKHAN, M. NIEGER, K. H. DÖTZ, *Chem. Eur. J.* **1999**, 5, 700–707; f) L. FOGEL, R. P. HSUNG, W. D. WULFF, R. G. SOMMER, A. L. RHEINGOLD, *J. Am. Chem. Soc.* **2001**, 123, 5580–5581.
- 69 a) A. DE MEIJERE, O. REISER, M. STÖBBE, J. KOPF, G. ADIWIDJAJA, V. SINNEWELL, S. I. KHAN, *Acta Chem. Scand.* **1988**, A42, 611–615; b) J. SCHULZ, F. VÖGTLE, *Top. Curr. Chem.* **1994**, 72, 42–89.
- 70 A. DE MEIJERE, J. HÖFFER, unpublished results, as cited in ref. [8c].
- 71 A. LONGEN, M. NIEGER, K. AIROLA, K. H. DÖTZ, *Organometallics* **1998**, 17, 1538–1545.
- 72 J. SCHULZ, M. NIEGER, F. VÖGTLE, *Chem. Ber.* **1991**, 124, 2797–2810.
- 73 a) K. H. DÖTZ, A. GERHARDT, *J. Organomet. Chem.* **1999**, 578, 223–228; b) K. H. DÖTZ, S. MITTENZWEY, *Eur. J. Org. Chem.* **2002**, 39–47.
- 74 a) H. WANG, W. D. WULFF, *J. Am. Chem. Soc.* **1998**, 120, 10573–10574; b) H. WANG, W. D. WULFF, A. L. RHEINGOLD, *J. Am. Chem. Soc.* **2000**, 122, 9862–9863.
- 75 a) R. NEIDLEIN, P. J. ROSYK, W. KRAMER, H. SUSCHITZKY, *Synthesis* **1991**, 123–125; b) R. NEIDLEIN, S. GÜRTLER, C. KRIEGER, *Helv. Chim. Acta* **1994**, 77, 2303–2322; c) R. NEIDLEIN, J. TEICHMANN, unpublished results.
- 76 L. QUAST, M. NIEGER, K. H. DÖTZ, *Organometallics* **2000**, 19, 2179–2183.
- 77 a) J. M. HEERDING, H. W. MOORE, *J. Org. Chem.* **1991**, 56, 4048–4050; b) S. KOO, L. S. LIEBESKIND, *J. Am. Chem. Soc.* **1995**, 117, 3389–3404.
- 78 a) M. IWASAKI, H. MATSUZAKA, Y. HIROE, Y. ISHII, Y. KOYASU, M. HIDAI, *Chem. Lett.* **1988**, 1159–1162; b) M. IWASAKI, Y. ISHII, M. HIDAI, *J. Organomet. Chem.* **1991**, 415, 435–442.
- 79 K. H. DÖTZ, M. POPALL, *Tetrahedron* **1985**, 41, 5797–5802.
- 80 H. C. JAHR, M. NIEGER, K. H. DÖTZ, *J. Organomet. Chem.* **2002**, 641, 185–194.
- 81 a) K. H. DÖTZ, S. SIEMONEIT, F. HOHMANN, M. NIEGER, *J. Organomet. Chem.* **1997**, 541, 285–290; b) F. HOHMANN, S. SIEMONEIT, M. NIEGER, K. H. DÖTZ, *Chem. Eur. J.* **1997**, 3, 853–859.
- 82 a) A. YAMASHITA, T. A. SCAHILL, C. G. CHIDESTER, *Tetrahedron Lett.* **1985**, 26, 1159–1162; b) A. YAMASHITA, T. A. SCAHILL, A. TOY, *Tetrahedron Lett.* **1985**, 26, 2969–2972; c) A. YAMASHITA, J. M. TIMKO, W. WATT, *Tetrahedron Lett.* **1988**, 29, 2513–2516; d) W. D. WULFF, J. S. MCCALLUM, F.-A. KUNNG, *J. Am. Chem. Soc.* **1988**, 110, 7419–7434; e) A. YAMASHITA, A. TOY, T. A. SCAHILL, *J. Org. Chem.* **1989**, 54, 3625–3634; f) A.

- YAMASHITA, R. G. SCHAUB, M. K. BACH, G. J. WHITE, A. TOY, N. B. GHAZAL, M. D. BURDICK, J. R. BRASHLER, M. S. HOLM, *J. Med. Chem.* **1990**, 33, 775–781; g) K. H. DÖTZ, J. GLÄNZER, *Z. Naturforsch.* **1993**, 48b, 2969–2972.
- 83 a) T. LEESE, K. H. DÖTZ, *Chem. Ber.* **1996**, 129, 623–631; b) K. H. DÖTZ, T. LEESE, *Bull. Soc. Chim. Fr.* **1997**, 134, 503–515.
- 84 a) C. A. MERLIC, A. BAUR, C. C. ALDRICH, *J. Am. Chem. Soc.* **2000**, 122, 7398–7399; b) W. E. BAUTA, W. D. WULFF, S. F. PAVKOVIC, E. J. ZALUZEC, *J. Org. Chem.* **1989**, 54, 3249–3252; c) M. MORI, K. KURIYAMA, N. OCHIFUJI, S. WATANUKI, *Chem. Lett.* **1995**, 615–616.
- 85 K. S. CHAN, W. D. WULFF, *J. Am. Chem. Soc.* **1986**, 108, 5229–5236.
- 86 G. A. PETERSON, W. D. WULFF, *Tetrahedron Lett.* **1997**, 38, 5587–5590.
- 87 W. FLITSCH, J. LAUTERWEIN, W. MICKE, *Tetrahedron Lett.* **1989**, 30, 1633–1636.
- 88 a) K. H. DÖTZ, I. PRUSKIL, J. MÜHLEMEIER, *Chem. Ber.* **1982**, 115, 1278–1285; b) K. H. DÖTZ, W. KUHN, *Angew. Chem. Int. Ed. Engl.* **1983**, 22, 732; *Angew. Chem.* **1983**, 95, 750–751; *Angew. Chem. Suppl.* **1983**, 1045–1052.
- 89 a) W. D. WULFF, P.-C. TANG, *J. Am. Chem. Soc.* **1984**, 106, 434–436; b) W. D. WULFF, P.-C. TANG, K.-S. CHAN, J. S. MCCALLUM, D. C. YANG, S. R. GILBERTSON, *Tetrahedron* **1985**, 41, 5813–5832; c) K. H. DÖTZ, M. POPALL, *Chem. Ber.* **1988**, 121, 665–672; d) W. D. WULFF, Y.-C. XU, *J. Am. Chem. Soc.* **1988**, 110, 2312–2314; e) J. SU, W. D. WULFF, R. G. BALL, *J. Org. Chem.* **1998**, 63, 8440–8447; f) W. D. WULFF, J. SU, P.-C. TANG, Y.-C. XU, *Synthesis* **1999**, 415–422.
- 90 For a review of synthetic strategies towards daunomycinone, see: P. J. HARRINGTON, *Transition Metals in Total Synthesis*, Wiley, New York, **1990**, pp. 346–399.
- 91 a) M. F. SEMMELHACK, J. J. BOZELL, T. SATO, W. WULFF, E. SPIESS, A. ZASK, *J. Am. Chem. Soc.* **1982**, 104, 5850–5852; b) K. H. DÖTZ, M. POPALL, G. MÜLLER, *J. Organomet. Chem.* **1987**, 334, 57–75; c) D. BOGER, I. C. JACOBSON, *J. Org. Chem.* **1991**, 56, 2115–2122; d) K. H. DÖTZ, W. A. DONALDSON, W. STURM, *Synth. Commun.* **2000**, 30, 3775–3784; e) X. XIE, M. C. KOZŁOWSKI, *Org. Lett.* **2001**, 3, 2661–2663.
- 92 a) D. L. BOGER, I. C. JACOBSON, *Tetrahedron Lett.* **1989**, 30, 2037–2040; b) D. L. BOGER, I. C. JACOBSON, *J. Org. Chem.* **1990**, 55, 1919–1928; c) D. L. BOGER, O. HÜTER, K. MBIYA, M. ZHANG, *J. Am. Chem. Soc.* **1995**, 117, 11839–11849.
- 93 a) J. BAO, V. DRAGISICH, S. WENGLOWSKY, W. D. WULFF, *J. Am. Chem. Soc.* **1991**, 113, 9873–9875; b) J. BAO, W. D. WULFF, V. DRAGISICH, S. WENGLOWSKY, R. G. BALL, *J. Am. Chem. Soc.* **1994**, 116, 7616–7630.
- 94 P. D. WOODGATE, H. S. SUTHERLAND, C. E. F. RICKARD, *J. Organomet. Chem.* **2001**, 627, 206–220.
- 95 J. D. KING, P. QUAYLE, *Tetrahedron Lett.* **1991**, 32, 7759–7762.
- 96 a) C. A. MERLIC, D. M. MEINNES, Y. YOU, *Tetrahedron Lett.* **1997**, 38, 6787–6790; b) C. A. MERLIC, Y. YOU, D. M. INNES, A. L. ZECHMAN, M. M. MILLER, Q. DENG, *Tetrahedron* **2001**, 57, 5199–5212.
- 97 A. V. VOROGUSHIN, W. D. WULFF, H.-J. HANSEN, *Org. Lett.* **2001**, 3, 2641–2644.

9

Osmium- and Rhenium-Mediated Dearomatization Reactions with Arenes

Mark T. Valahovic, Joseph M. Keane, and W. Dean Harman

Abstract

The fragments $\{\text{Os}(\text{NH}_3)_5\}^{2+}$ and $\{\text{TpRe}(\text{CO})(\text{L})\}$ (where L = 1-methylimidazole, pyridine, PMe_3 , or *tert*-butylisocyanide) form stable η^2 -coordinate complexes with a wide variety of arenes. The act of coordination greatly reduces the aromatic character of these ligands and, as a consequence, activates them towards various organic reactions. In particular, the addition of carbon-based electrophiles to arenes is notably enhanced relative to the free aromatic molecules. The resulting arenium intermediates are stabilized by metal backbonding to the point that they may be isolated and subsequently subjected to a variety of carbon-based nucleophiles. The overall vicinal difunctionalization of two ring carbons may be accomplished with excellent stereo- and regiocontrol.

9.1

Introduction

Arenes are attractive building blocks for the synthesis of complex carbocyclic species. In addition to being inexpensive and available in a variety of substitution patterns, they possess ring structures composed entirely of unsaturated carbons. Because of this unsaturation, they have the potential for extensive functionalization. However, the realization of this potential requires synthetic methods that overcome the energetic barrier associated with aromatic stabilization.

Transition metals continue to be enticing reagents for the dearomatization of aromatic molecules [1]. Not only do they allow transformations to be performed on the dearomatized species at (sub)ambient temperatures, but they also serve to stabilize the reaction intermediates. This latter facet allows a much broader range of manipulations than those accessible through the typical electrophilic/nucleophilic aromatic substitution pathways.

During the past 40 years, two complementary general methodologies for transition metal based dearomatization have been developed. The $\{\text{Cr}(\text{CO})_3\}$ fragment [2, 3] and related cationic fragments ($\{\text{Mn}(\text{CO})_3\}^+$ [3–7], $\{\text{CpRu}\}^+$ [8, 9], and $\{\text{CpFe}\}^+$ [10]) are coordinated by aromatic molecules in a hexahapto fashion and have been shown to behave like electron-withdrawing groups. The coordinated arene is rendered electron-deficient and susceptible to nucleophilic attack. The resulting cyclohexadienyl anion is stabilized by the withdrawal of electron density from the metal fragment (Figure 1).

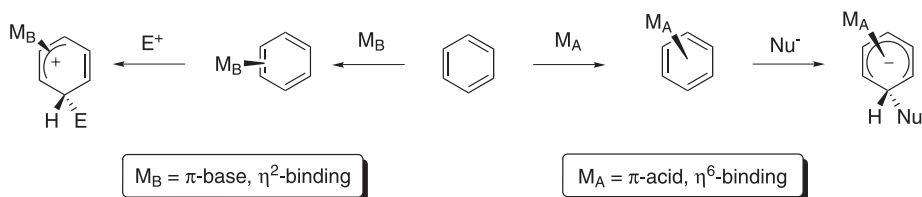


Fig. 1. Transition metal dearomatization methodologies.

Alternatively, the $\{\text{Os}(\text{NH}_3)_5\}^{2+}$ fragment (hereafter abbreviated as [Os]) and the electronically similar $\{\text{TpRe}(\text{CO})(\text{L})\}$ fragment (Tp = hydridotris(pyrazolyl)borate, L = a strongly σ -donating ligand) are coordinated by aromatic molecules in a dihapto fashion. Despite the 2+ charge on the Os and the π -acidic CO on the Re, these fragments are electron-rich and donate π -electron density into the π -system of the aromatic ligand, thereby increasing its nucleophilicity. Reactions of the bound aromatics with electrophiles result in cyclohexadienyl cations that are stabilized by the donation of electron density from the metal fragment. These intermediates can be either further elaborated or rearomatized, and removal of the metal fragment releases the modified organic molecule.

9.2

$\{\text{Os}(\text{NH}_3)_5\}^{2+}$ – The Pentaammineosmium(II) Fragment

9.2.1

Preparation of η^2 -Arene Complexes

The precursor to η^2 -complexes of pentaammineosmium(II), $[\text{Os}(\text{NH}_3)_5(\text{OTf})](\text{OTf})_2$ (OTf = trifluoromethanesulfonate), is commercially available from Aldrich and can be prepared in three steps from OsO_4 (92 % overall yield) [11]. Thermally stable complexes of benzenes, naphthalenes, anisoles, anilines, and phenols can be prepared in yields >90 % by reducing this osmium(III) salt in an excess of the aromatic compound. Typically, the reductions are performed under a dinitrogen atmosphere using either Mg^0 in a DMA/DME mixture (DMA = *N,N*-dimethylacetamide; DME = 1,2-dimethoxyethane) or Zn/Hg in methanol. The η^2 -complexes are isolated by removing the reductant by filtration and precipitating the osmium salt from a solution in diethyl ether/dichloromethane. Excess ligand can be recovered from the resulting filtrate and recycled. Dihapto-coordinated arene complexes of [Os] are stable in solution under an inert atmosphere, and alkene complexes that result from dearomatization are stable to oxygen.

9.2.2

Binding Selectivity

Almost all η^2 -arene complexes of [Os] are amenable to both intrafacial (i.e., ring-walk) and interfacial (i.e., face-flip) isomerization mechanisms, which allow the metal to coordinate to the most thermodynamically favorable position (Figure 2). Aromatic molecules bearing a π -donor group (e.g., anisole, aniline, phenol) tend to place the metal across C5–C6 in order to

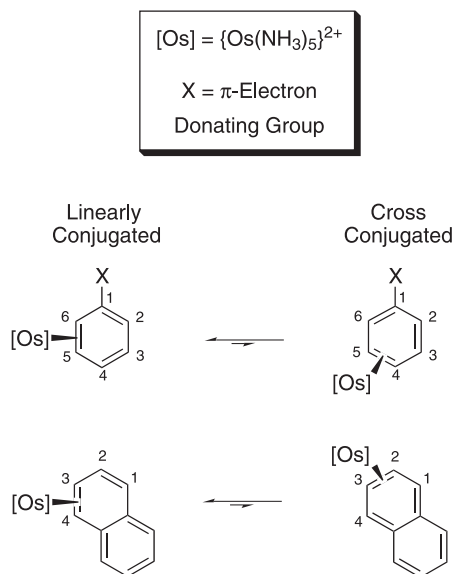


Fig. 2. Binding selectivities of $[\text{Os}]$ -arene complexes.

maintain linear conjugation of the donor group and the uncoordinated diene. (Coordination of the metal across C4–C5 sets up a cross-conjugated relationship between the donor group and the diene.) Naphthalene, having no electron donors, tends to place the metal across C3–C4 instead of C2–C3. In this way, the aromaticity of the unbound ring is maintained (Figure 2).

9.2.3

Hydrogenations

The coordination of an arene to $[\text{Os}]$ serves to protect one double bond while rendering the remaining unsaturated carbons of the pendant ring more susceptible to hydrogenation than those of the corresponding free arene. While arene hydrogenations typically require harsh conditions and often lead to complete saturation, the partial hydrogenation of complexed benzene (**1**) proceeds in 15 h at 30 °C under 1 atm. of H_2 to give complexed cyclohexene (**2**) in 89 % yield (Figure 3) [12]. Likewise, complexed naphthalene (**3**) yields complexed 1,2-dihydronaphthalene (**4**), leaving the uncomplexed and therefore unactivated ring intact.

Steric arguments suggest that the addition of dihydrogen to $[\text{Os}]$ -arenes should occur on the arene face opposite that of metal coordination. This theory is supported by the generation of **2-*d*₄** upon the partial deuteration of **1**. Furthermore, the hydrogenation of complexed anisole (**5**) under anhydrous conditions yields complexed 3-methoxycyclohexene (**6**), in which the methoxy group is syn to the metal. It was found, however, a trace of water in the reaction mixture results in the formation of complexed cyclohexenone (**7**), presumably from the attack of water on the dihydroanisole intermediate [13].

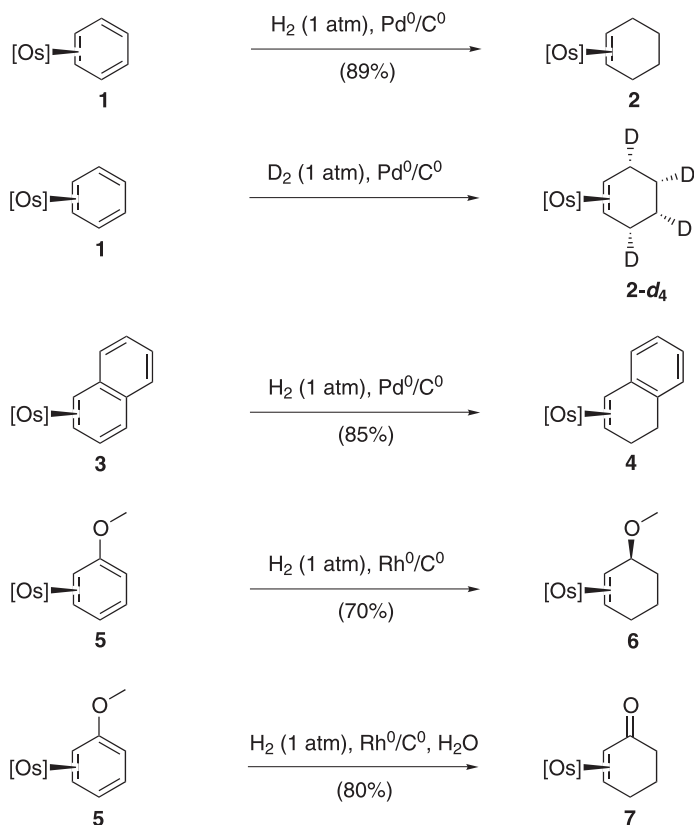


Fig. 3. Hydrogenations of [Os]-arenes.

9.2.4

Benzene and Alkylated Benzenes

The dearomatization of benzene requires that a resonance energy estimated at 36 kcal mol^{-1} be overcome [14]. For this reason, when benzene attacks an electrophile, the end result is typically a substitution product rather than an addition product. The initial cyclohexadienyl cation is unstable to deprotonation by even extremely poor bases, and it therefore loses a proton and returns to an aromatic state.

9.2.4.1 Benzene

Through a significant π -backbonding interaction, the coordination of benzene to [Os] (1) serves both to activate the arene toward the electrophilic addition of dimethoxymethane (Table 1, entries 1–4) or 3-penten-2-one (entry 5) and to stabilize the resulting benzenium intermediate **8**. If manipulated at low temperature (-40°C), **8** can be trapped with either a silyl ketene acetal (entries 1, 4, and 5), 2-trimethylsiloxypyrone (entry 2), or phenyllithium (entry 3) to yield the substituted 1,4-cyclohexadiene complex **9** [15]. This species can be oxi-

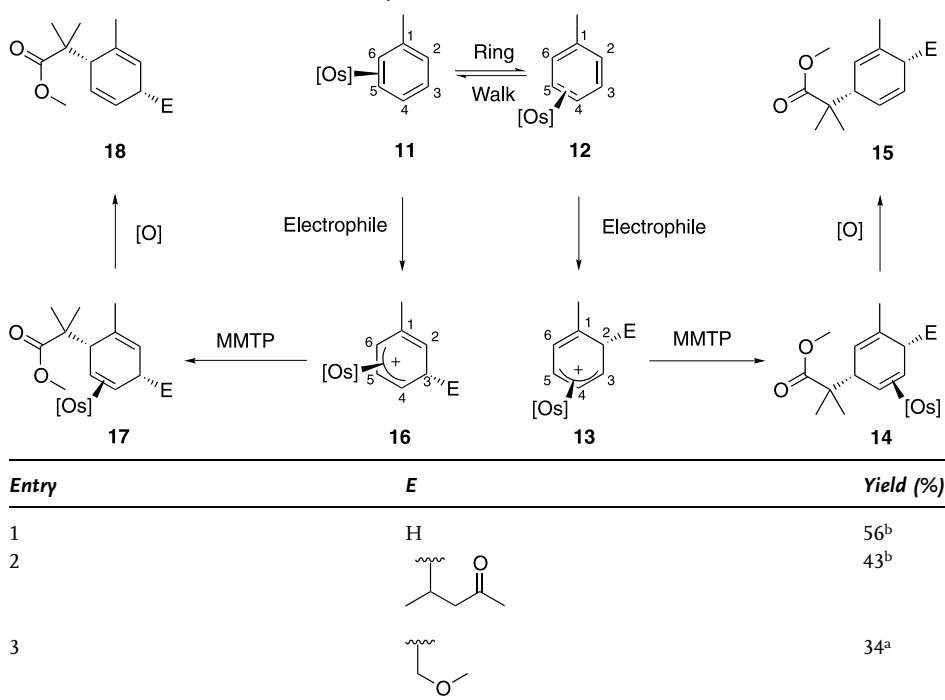
Tab. 1. Tandem additions to the benzene complex **1**.

Entry	E	Nu	Yield (%)
1			82
2			23
3		Ph	16
4			31
5			27

dized to yield the dearomatized organic product **10**. The nucleophile and electrophile add in a *syn* fashion, consistent with approach to the arene face opposite to that involved in metal coordination.

9.2.4.2 Toluene

Alkylated benzenes behave similarly to benzene with respect to the stereochemistry and regiochemistry of tandem additions, but the mechanistic pathway of such additions becomes more complicated with the introduction of a methyl group. The toluene complex exists in solution as a 3:2 mixture of interconverting linkage isomers, with the C4–C5 bound arene (**12**) being favored over the C5–C6 bound arene (**11**) (Table 2). The addition of either trifluoromethanesulfonic acid (HOTf) (entry 1) or 3-penten-2-one (entry 2) at C2 of the bound toluene generates the η^3 -allyl complex **13**. This complex can be trapped with 1-methoxy-2-methyl-1-trimethylsilyloxypropene (MMTP), resulting in a single regioisomer, **14**. Upon oxidation of **14** with AgOTf, the diene **15** is released in moderate overall yield [15]. The tandem addition of dimethoxymethane and MMTP to $[\text{Os}]$ -toluene (entry 3) leads to a mixture of **15** and **18** after demetalation. If the tandem addition is performed at -40°C , the **15**:**18** ratio is 3:1. If it is performed at -70°C , the **15**:**18** ratio is 8:1. Although the origin of this selectivity

Tab. 2. Tandem additions to toluene complexes **11** and **12**.

^a = 3:1 ratio of **15**:**18** at $-40\text{ }^{\circ}\text{C}$; 8:1 ratio of **15**:**18** at $-70\text{ }^{\circ}\text{C}$; ^b = only **15** observed.

is unknown, Table 2 displays two possible pathways. Complex **11** can add an electrophile at C3 to generate **16**, and complex **12** can add an electrophile at C2 to generate **13**. It is thought that stabilization due to hyperconjugation of the methyl group in **13** favors the C2 addition pathway over the C3 addition pathway.

9.2.4.3 Xylenes

Contrary to what is observed during tandem addition reactions to [Os]-toluene (*vide supra*), electrophilic additions to [Os]-bound *ortho*- and *meta*-xylenes result in regioselective attack at C6 (Table 3). A coordination isomer having the metal across C4–C5 (**19**) is the only isomer observed for both *ortho*- and *meta*-xylene. Electrophilic addition of HOTf (entry 1) or dithoxymethane (entries 2 and 3) at C6 generates the complexed allyl cation **20**, which can be trapped with MMTP to form the complexed diene **21**. Demetalation using AgOTf releases the free diene **22**, which potentially possesses two adjacent quaternary centers (entry 3) [15].

9.2.5

Naphthalene

A one-pot tandem addition/oxidative decomplexation methodology has been developed, which yields substituted dihydronaphthalenes from [Os]-naphthalenes. The process involves

Tab. 3. Tandem additions to xylene complexes of [Os].

The reaction scheme shows the conversion of complex 19 to 22. Complex 19 is a naphthalene derivative with an osmium atom coordinated at C5. It has substituents R₁ at C1 and R₂ at C3. An electrophile (E) adds to C4 at -40 °C to form intermediate 20, which is a 1,4-dihydronaphthalene derivative with a positive charge at C4. Intermediate 20 then reacts with MMTP (methyl malonate) at -40 °C to form intermediate 21, where MMTP is attached to C2. Finally, oxidation [O] of 21 yields the final product 22, a cis-1,4-dihydronaphthalene derivative with E at C4 and MMTP at C2.

Entry	R ₁	R ₂	E	Yield (%)
1	CH ₃	H	H	67
2	CH ₃	H		28
3	H	CH ₃		32

the regio- and stereospecific addition of an electrophile and a nucleophile to generate a *cis*-1,4-dihydronaphthalene complex. When the nucleophile is tethered to the electrophile, an intramolecular cyclization occurs with the nucleophile now attacking at C2 to generate a hydrophenanthrone core after oxidative decomplexation.

9.2.5.1 Tandem Addition Reactions

The naphthalene complex of [Os] (**3**) reacts with triflic acid to form a η^3 -1*H*-naphthalenium species, which has been characterized at -40°C [16]. Unfortunately, most nucleophiles react as bases with this species and return the naphthalene complex. However, MMTP and the mild hydride donor triethylsilane (Table 4, entries 1 and 2) both add to C4 of the complex and yield 1,4-dihydronaphthalenes in moderate overall yield following decomplexation [17].

Methyl vinyl ketone (entry 3) and the *tert*-butyl cation (entry 4) are also reactive toward complex **3**. The naphthalenium complexes resulting from the addition of these electrophiles will add the conjugate base of dimethyl malonate (generated *in situ* from a combination of dimethyl malonate (DMM) and diisopropylethylamine (DIEA)) to complete the tandem additions. Oxidation of the resulting complexes yields *cis*-1,4-dihydronaphthalenes. The entire sequence of complexation, tandem addition, and demetalation employed for all entries in Table 4 can be performed using bench-top conditions (i.e., a non-inert atmosphere).

As mentioned in the introduction, one of the major advantages of using transition metals for dearomatization is that they allow the isolation of reaction intermediates and, consequently, broaden the range of accessible manipulations. For example, when the naphthalene complex of [Os] (**3**) is treated with dimethoxymethane in the presence of HOTf, the resulting η^3 -1*H*-naphthalenium species **23** can be isolated in 88 % yield and stored for days at room temperature (Table 5). The electrophile adds anti to the face involved in metal coordination and pushes the proton at C1 toward the metal, which prevents spontaneous rearomatization. As shown in Table 5, **23** reacts with MMTP, the conjugate base of dimethyl malonate, 2-trimethylsiloxypropene, tetrabutylammonium cyanoborohydride (TBAC), dime-

Tab. 4. Overall yields for tandem additions to naphthalene.

Entry	Electrophile	E	Nucleophile	Nu	Overall Yield
1	HOTf	H			77 %
2	HOTf	H	HSiEt ₃	H	56 %
3					41 % ^b
4	<i>t</i> -BuOH ^a				25 % ^b

^a = *t*-BuOH added in the presence of HOTf; ^b = Nucleophile premixed with DIEA.

thylzinc, and phenyllithium. Demetalation with AgOTf liberates the *cis*-1,4-dihydronaphthalenes in moderate overall yields [17]. An interesting stereochemical consequence is observed when PhLi is used as the nucleophile. When the phenyl group adds to C4, a doubly benzylic carbon is generated and the ¹H NMR spectrum of the demetalated material reveals the presence of two diastereomers, presumably due to racemization of the doubly benzylic position.

Tandem additions to [Os]-naphthalene could yield either a 1,2- or a 1,4-addition product, but remarkably, the 1,4-pathway is the only one observed. This outcome is theorized to be the result of C4 having a greater partial positive charge because of its overlap/delocalization with the adjacent unbound ring [17].

9.2.5.2 Cyclizations

An alternative mode of reactivity is observed for [Os]-naphthalene when the nucleophile for the tandem addition is built into the electrophile. The normal mode of reactivity results in the formation of *cis*-1,4-dihydronaphthalenes (*vide supra*), but when a solution of the methyl vinyl ketone Michael addition product **24** in methanol (Table 6, entry 1) and a catalytic amount of triflic acid are allowed to react, the complexed hydrophenanthrenone **25** is isolated in 89 % yield [18]. This reactivity results from the pendant ketone undergoing a tautomerization to form an enol, which can then attack the allyl cation at C2. The stereochemistry of the nucleophilic addition is still anti to the face involved in the metal coordination, but the

Tab. 5. Nucleophilic addition reactions of the η^3 -1H-naphthalenium complex **23**.

Nucleophile	R	Overall Yield ^a
		65 %
		54 % ^b
		69 %
Bu ₄ NBH ₃ CN	H	45 %
Zn(CH ₃) ₂	CH ₃	40 % ^c
PhLi	Ph	40 % ^d

^a = Calculated with respect to naphthalene; ^b = Nucleophile premixed with DIEA;^c = Reaction run with Cu(OTf); ^d = Reaction run with Cu(CN).

regiochemistry now favors addition at C2. This change in regiochemistry is likewise observed when the Michael acceptor is either ethyl vinyl ketone (EVK, entry 2) or isopropyl vinyl ketone (IVK, entry 3). Decomplexation using AgOTf releases the hydrophenanthrenones **26** in moderate to low yields [18].

Tab. 6. Hydrophenanthrenone synthesis from complex **3**.

Entry	R ¹	R ²	Yield	Yield	Yield
1	H	H	90 %	89 %	40 %
2	CH ₃	H	99 %	91 %	40 %
3	CH ₃	CH ₃	97 %	65 %	35 %

9.2.6

Anisole

Anisole and its derivatives have thus far demonstrated the widest variety of [Os]-mediated dearomatization reactions. These transformations have included substitutions, asymmetric tandem addition sequences, and a variety of cyclizations.

9.2.6.1 **Electrophilic Substitutions**

As with [Os] complexes of benzene and naphthalene, a significant π -backbonding interaction renders anisole complexes far more nucleophilic than the free arenes [19]. As a result, they are reactive towards weaker electrophiles than those typically used in electrophilic aromatic substitutions. In the presence of HOTf at -40°C , the anisole complex (**5**) attacks a wide variety of electrophiles, including Michael acceptors (Table 7, entries 1–8) and acetals (entries 9 and 10). The additions occur exclusively at C4 of the anisole complex, and this fact can be rationalized in terms of both the methoxy group effectively blocking C2 and a thermodynamic preference for more conjugation in the uncoordinated portion of the resulting anisolium species **27**. This complex is observable at -40°C , but has only been isolated when an arene starting material containing an additional π -donor group has been utilized (e.g., 1,3-dimethoxybenzene). The addition of an amine base results in deprotonation of the anisolium species at C4 to yield a substituted anisole complex. The substitution product **28** can be liberated in high yield by oxidation or on heating [20].

9.2.6.2 **Tandem Additions**

Racemic tandem additions Mild carbon nucleophiles add to the [Os]-anisolium complex **27** exclusively at C3 to afford substituted 1,3-cyclohexadiene complexes **29–32** in moderate to high yields (Table 8) [21]. Nucleophiles that have been utilized in this manner include MMTP (**29** and **30**), *N*-methylpyrrole (**31**), and 2-trimethylsilyloxyfuran (**32**). As with other tandem additions to [Os] complexes, both the nucleophile and the electrophile add to the arene face opposite to that involved in metal coordination, such that the products are those of syn addition.

The cyclohexadiene complex **29** has been further elaborated to afford either the cyclohexenone **34** or the cyclohexene **36** in moderate yields (Scheme 1) [21]. The addition of HOTf to **29** generates the oxonium species **33**, which can be hydrolyzed and treated with cerium(IV) ammonium nitrate (CAN) to release the cyclohexanone **34** in 43 % yield from **29**. Alternatively, hydride reduction of **33** followed by treatment with acid eliminates methanol to generate the η^3 -allyl complex **35**. This species can be trapped by the conjugate base of dimethyl malonate to afford a cyclohexene complex. Oxidative decomplexation of this species using silver trifluoromethanesulfonate liberates the cyclohexene **36** in 57 % overall yield (based on **29**).

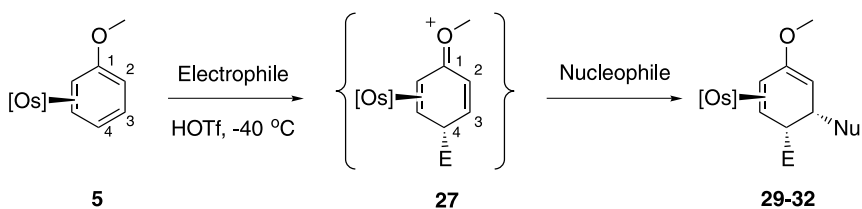
Asymmetric tandem additions In order to further take advantage of the high degree of stereoselectivity observed in tandem additions to [Os]-arene complexes, a chiral anisole derivative has been prepared, which has demonstrated high coordination diastereoselectivity

Tab. 7. Electrophilic substitutions of complex 5.

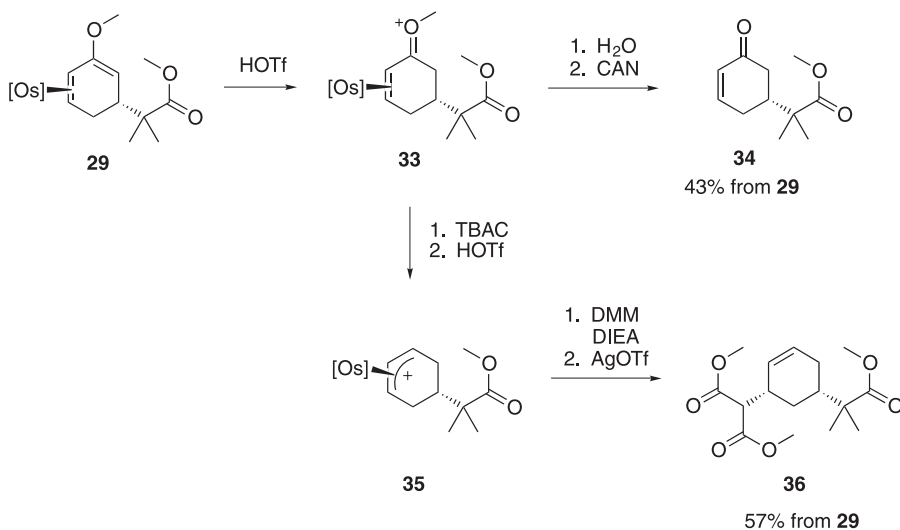
Entry	E	R ₁	R ₂	Yield (%)
1		H	H	84
2	"	H	CH ₃	93
3	"	CH ₃	CH ₃	79
4	"	H	Ph	70
5		–	–	59
6		H	H	94
7	"	CH ₃	CH ₃	85
8		–	–	81
9		–	–	90
10		–	–	95

(>9:1) upon complexation [22]. Complex **37** can be prepared in 83 % yield and >90 % *de* by a two-step sequence involving the coupling of phenol and (*S*)-(-)-methyl lactate followed by complexation (Scheme 2). In addition to the η^2 -bond common to other [Os]-arene complexes, NMR studies of **37** provided evidence of a hydrogen-bonding interaction between the acidic ammine ligands [13] and the ester carbonyl group (Figure 4) [23]. The result of these interactions is a thermodynamic differentiation of the arene faces. It is thought that if the metal binds to the *re* face of the arene, the methyl group adjacent to the methine group is

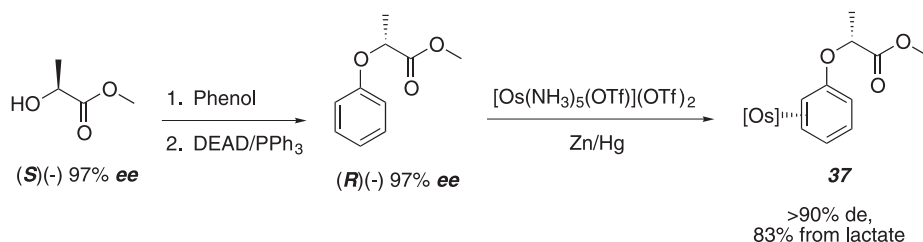
Tab. 8. Tandem additions to [Os]-bound anisole.



Complex	E	Nu	Yield (%)
29	H		92
30			50
31	H		92
32	H		42



Scheme 1. Elaborations of [Os]-anisole tandem addition product 29.



Scheme 2. Synthesis of the asymmetric anisole complex **37**.

forced into a sterically disfavored position near an *ortho* ring proton. If the metal binds to the *si* face of the arene, the proton of the methine group is forced into the same position. As a smaller steric repulsion results in this second situation, it is thermodynamically preferred, and so the metal binds preferentially to the *si* face.

The chiral anisole derivative **37** has been used in the synthesis of several asymmetric functionalized cyclohexenes (Table 9) [22]. In a reaction sequence similar to that employed with racemic anisole complexes, **37** adds an electrophile and a nucleophile across C4 and C3, respectively, to form the cyclohexadiene complex **38**. The vinyl ether group of **38** can then be reduced by the tandem addition of a proton and hydride to C2 and C1, respectively, affording the alkene complex **39**. Direct oxidation of **39** liberates cyclohexenes **40** and **41**, in which the initial asymmetric auxiliary is still intact. Alternatively, the auxiliary may be cleaved under acidic conditions to afford η^3 -allyl complexes, which can be regioselectively attacked by another nucleophile at C1. Oxidative decomplexation liberates the cyclohexenes **42–44**. HPLC analysis revealed high *ee* values for the organic products isolated both with and without the initial asymmetric group.

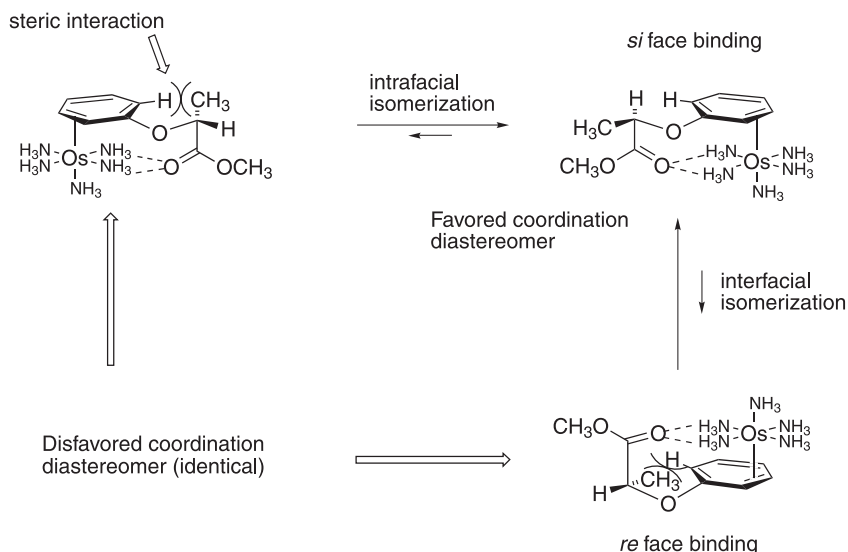


Fig. 4. Interactions responsible for the diastereoselectivity observed in complex **37**.

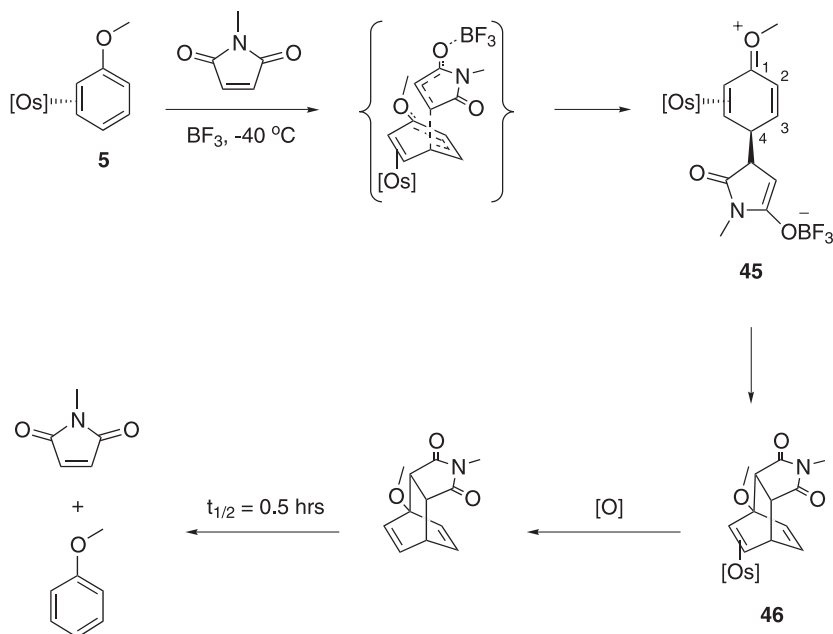
Tab. 9. Tandem additions to Complex 37.

Compound	<i>E</i>	<i>Nu</i> ₁	<i>Nu</i> ₂	% Yield from 37	<i>ee</i> (%)
40	H		—	46	97
41			—	41	97
42				33	81
43				28	90
44		H		19	93

9.2.6.3 Cyclization Reactions

One of the most versatile applications of [Os]-anisole chemistry is the efficient generation of complex polycyclic systems. Through the application of a variety of methodologies, anisole complexes have been used to generate a number of cyclic arrangements, including a bicyclo[2.2.2]octadiene, decalins, tetralins, and tricyclic arrays.

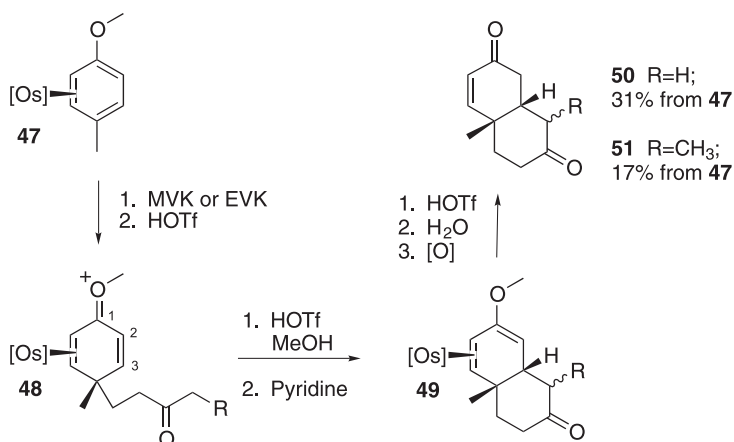
Cycloaddition reactions The anisole complex **5** undergoes a cyclization reaction with *N*-methylmaleimide under Lewis acidic conditions to afford the bicyclo[2.2.2]octadiene complex **46**, a formal [4+2] process (Scheme 3) [24]. Mechanistic studies have suggested that this reaction occurs not as a concerted process but rather through an initial Michael addition at C4 to generate **45**, which then cyclizes by an intramolecular nucleophilic attack at C1. Despite this stepwise pathway, a high degree of diastereoselectivity is observed in the reaction. The succinimide ring is oriented endo with respect to the unbound portion of the former arene. This observation is consistent with the Michael addition proceeding through an ordered Diels–Alder-like transition state. The metal-bound bicyclo[2.2.2]octene can be decomplexed in 25 % yield (based on **5**) by means of low-temperature oxidation, but the resulting organic compound is unstable with respect to cycloreversion ($t_{1/2} = 0.5$ h at 20 °C).



Scheme 3. The formal [4+2] cyclization of [Os]-anisole and *N*-methylmaleimide.

Michael–Michael ring-closures In a variation of the tandem addition reaction discussed previously, the anisolium species **48** generated from the Michael addition of MVK or EVK to the *p*-methyl anisole complex **47** cyclizes in acidic methanol (Scheme 4) [21]. The enol form of the pendant ketone acts as an intramolecular nucleophile, attacking the electrophilic C3 position of the ring and generating the *cis*-decalin complex **49**. Following protonation and hydrolysis of the resulting vinyl ether, the free organic product can be liberated by oxidation of the metal fragment. In this way, the diketones **50** and **51** can be produced in yields of 31 % and 17 %, respectively (based on **47**).

Michael–aldol ring-closures In another variant, the addition of an amine base to the 3,4-dimethyl anisolium species **52** results in deprotonation at the benzylic C3 methyl group,



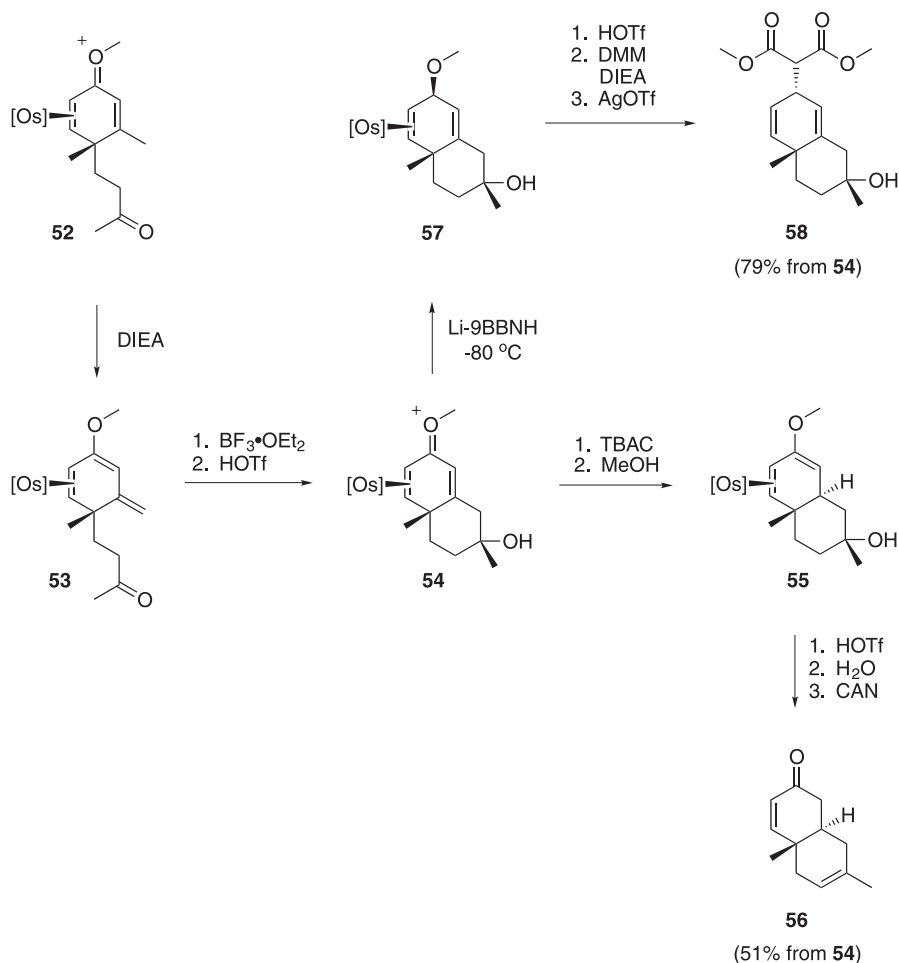
Scheme 4. The synthesis of the decalin system by means of a Michael–Michael ring-closure sequence.

generating the extended vinyl ether **53** (Scheme 5) [25]. Under Lewis acidic conditions, this group acts as an intramolecular nucleophile, attacking the pendant ketone to form an additional six-membered ring. The resulting oxonium species **54** can be further modified to ultimately yield the enone **56** or the diene **58** (Scheme 5). Treatment of **54** with TBAC leads to regioselective reduction of the oxonium species in a 1,4-fashion to form the vinyl ether complex **55**. Protonation and hydrolysis of the vinyl ether generates an enone complex, from which **56** can be liberated by oxidative decomplexation in 51 % yield (based on **54**). Alternatively, with Li-9BBNH the oxonium species **54** is regioselectively reduced in a 1,2-fashion to form the diene complex **57**. Treatment of **57** with HOTf eliminates methanol to generate an η^3 -allyl complex, which can be trapped by the conjugate base of dimethyl malonate. Oxidative decomplexation using silver trifluoromethanesulfonate liberates **58** in 79 % yield (based on **54**).

When the anisolium complex generated by the addition of MVK to the 2-methoxytetrahydronaphthalene complex **59** is utilized in the above cyclization sequence, the tricyclic oxonium complex **61** is generated (Scheme 6). Deprotonation of **59** with pyridine forms the extended vinyl ether complex **60**, which cyclizes and eliminates water to form **61** when exposed to TBSOTf. Hydrolysis of **61**, followed by oxidation of the metal fragment, yields the dienone **62** in 15 % yield (based on **59**).

If an [Os]-anisolium complex bears a proton at C4 (**63**, Scheme 7), exposure to DIEA at low temperature results in a kinetic deprotonation of the benzylic carbon attached to C3 generating the extended vinyl ether **64**. This complex cyclizes under Lewis acidic conditions to generate an anisolium ion, which can then be deprotonated at C4 to generate a tetralin complex [25]. Heating this species liberates the tetralin **65** in 39 % yield (based on **63**).

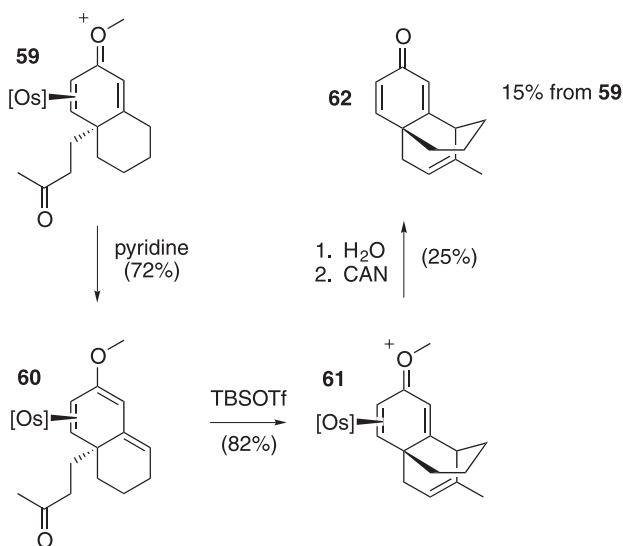
4-Methoxystyrenes The Diels–Alder cyclization of the 4-methoxystyrene complex **67** and a dienophile provides a direct route to substituted decalin systems. Unfortunately, direct complexation of 4-methoxystyrene to [Os] results in the formation of a significant amount of the vinyl-bound coordination isomer. However, the ring-bound form, **67**, can be synthesized



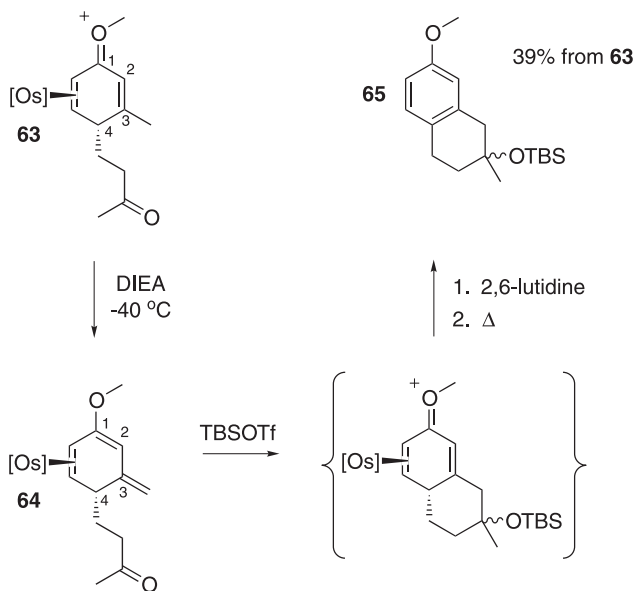
Scheme 5. The synthesis of substituted decalins by means of a Michael-aldol ring-closure sequence.

from [Os]-anisole (**5**) in two steps and 84 % yield (Scheme 8). Acetal substitution at C4 affords **66**, from which a net elimination of ethanol generates **67**.

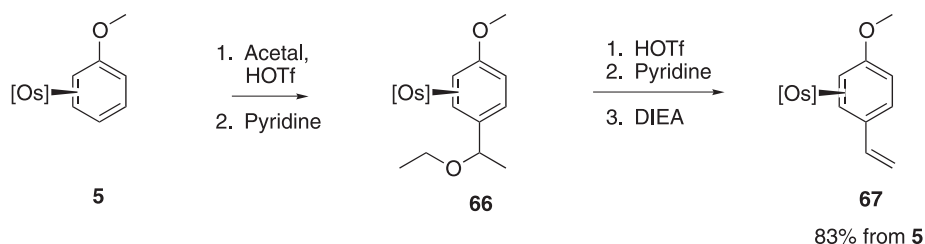
Complex **67** undergoes Diels-Alder reactions with a variety of dienophiles to afford bicyclic (**68** and **69**) or tricyclic (**70** and **71**) vinyl ether complexes (Table 10) [26]. The *N*-methylmaleimide adduct **71** has been elaborated in a number of ways prior to decomplexation (Scheme 9). Oxidation of **71** with AgOTf produces the re-aromatized species **72** and **73** in yields of 35 % and 18 %, respectively. Oxidation following hydrolysis of the vinyl ether group in **71** generates the enone **74** in 42 % yield. Oxidation following the net reduction of the vinyl ether group in **71** generates the 1,3-diene **75** in 28 % yield. Finally, a series of two hydride reductions performed on **71** generates a diene complex, from which **76** can be liberated in 25 % yield by oxidative decomplexation. The cyclopentenone adduct **70**



Scheme 6. The synthesis of a bridged tricyclic system by means of a Michael–aldol ring-closure sequence.

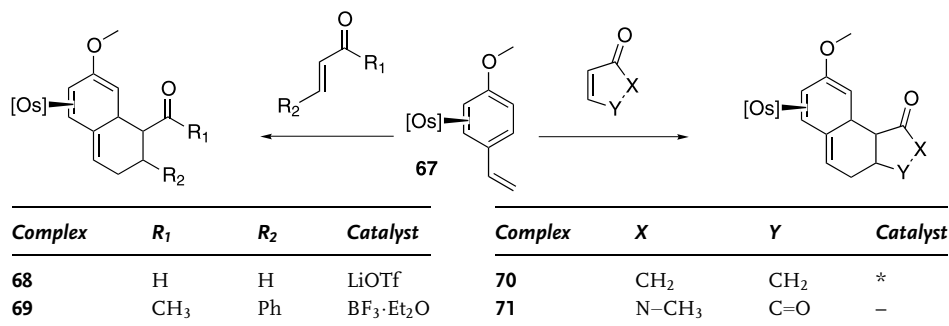


Scheme 7. The synthesis of a tetralin by means of a Michael–aldol ring-closure sequence.



Scheme 8. Synthesis of the 4-methoxystyrene complex 57.

Tab. 10. Diels-Alder reactions with complex 67.



* Reaction performed in H₂O.

(Table 10) may also be elaborated through a hydrolysis sequence to afford a tricyclic dienone similar to 74 in 40 % yield from 67.

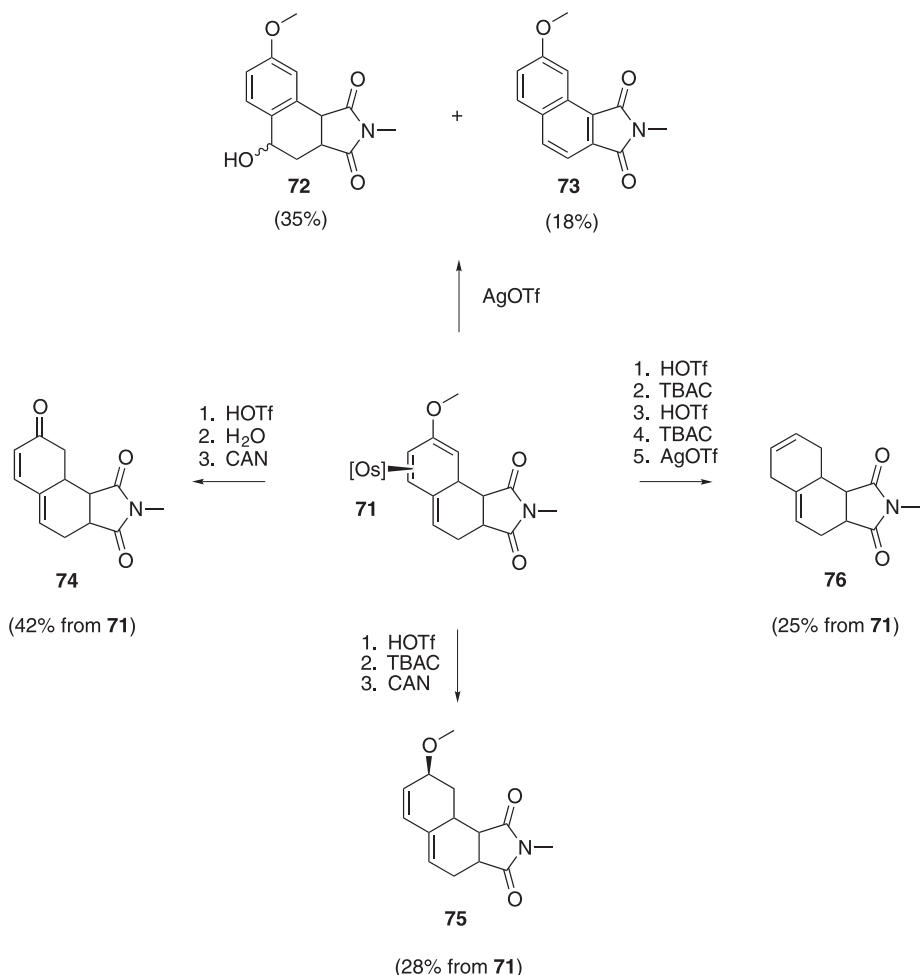
9.2.7

Aniline

Aniline complexes of [Os] are more reactive toward electrophiles than their anisole analogues, presumably because of the less electronegative/more electron-releasing nature of the nitrogen atom. Unfortunately, nucleophilic addition to the resulting anilinium intermediates is difficult and this fact limits the use of this methodology for aniline dearomatization. Nevertheless, [Os]-aniline chemistry has been successfully used in a number of substitution and addition reactions, including an efficient one-pot sequence that generates a di-spiro tetracyclin core through a Michael–Michael–Michael ring-closure.

9.2.7.1 Electrophilic substitution

Aniline complexes are unique in [Os] chemistry in that η^2 -arene coordination competes with η^1 -nitrogen coordination. However, η^2 -coordination becomes favored when the nitrogen is substituted. For example, the *N*-ethyl aniline complex 77 is isolated solely in its ring-bound form (Table 11). Without Lewis acid promotion, 77 will undergo regioselective addition of



Scheme 9. Elaborations of the complexed Diels–Alder cycloaddition product **71**.

Michael acceptors exclusively at C4 to ultimately generate substitution products in high yields [27]. Reaction with acetic anhydride (entry 3) yields the C4-acylated complex. Decomplexed anilines are obtained by heating the substituted complexes at 70 °C in a coordinating solvent such as CH₃CN. For example, the MVK product (entry 1) can be isolated in 74 % yield [27].

9.2.7.2 4*H*-Anilinium Michael Additions

As stated above, the isolation of ring-bound [Os]-aniline is difficult because the nitrogen-bound form competes with the ring-bound form. However, if the nitrogen is first protected with a TMS group, complexation at the ring proceeds cleanly to yield **78** (Table 12). Deprotection and C4-protonation using HOTf forms the 4*H*-anilinium complex **79**. This com-

Tab. 11. Electrophilic substitution reactions of the *N*-ethylaniline complex **77**.

Entry	Electrophile	Solvent(s)	E	Yield (%)
1		MeOH		94
2		MeOH		89
3		CH ₃ CN/DMSO		87 ^a

^a = Reaction run in the presence of DMAP.**Tab. 12.** Michael addition reactions to the 4*H*-anilinium complex **79**.

78	79	80	
Entry	Michael Acceptor	E	Yield (%)
1			83
2			75
3*			86

* = i. DIEA, CH₃CN @ –40 °C; ii. TBSOTf, CH₃CN @ –40 °C; iii. H₂O.

pound will add Michael acceptors (entries 1–3) anti to the face involved in metal coordination and regioselectively at C4 to afford 4*H*-anilinium adducts (**80**) in high yields (Table 12) [27].

9.2.7.3 Electrophilic Addition Reactions

In the presence of Lewis acids, *N*-substituted aniline complexes of [Os] also add electrophiles at C4, again at the arene face opposite to that involved in metal coordination. This reaction has been shown to be general for a broader range of Michael acceptors than may be utilized with anisole complexes of [Os]. The *N*-ethyl aniline complex, for example, adds Michael acceptors and acetals in yields ranging from 53–95 % (Table 13, entries 1–6) [27]. The *N,N*-dimethyl aniline complex (entries 7–9) also adds Michael acceptors to C4 in moderate to high yields (Table 13) and adds to the δ -carbon of an $\alpha,\beta,\gamma,\delta$ -unsaturated ester (entry 3).

9.2.7.4 Michael–Michael–Michael Ring-Closure

The *N,N*-dimethyl aniline complex **81** undergoes a Michael–Michael–Michael ring-closure in the presence of excess α -methylene- γ -butyrolactone (Scheme 10). In this sequence, the intermediate enolate **82** intercepts another molecule of the Michael acceptor, which then closes at C3 to generate the di-*spiro* tetracyclic complex **83**. The tetracyclic adduct is generated as a single diastereomer, and its structure has been confirmed by X-ray diffraction analysis. This molecule undergoes reduction of the enamine through protonation at C2 followed by a stereochemically anomalous hydride reduction at C1. Oxidation of the metal fragment liberates **84** in 77 % yield (based on **83**) [28].

9.2.8

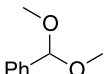
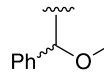
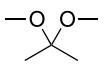
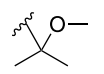
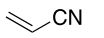
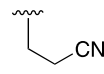
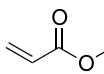
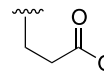
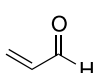
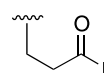
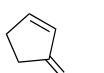
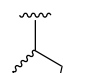
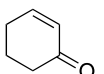
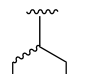
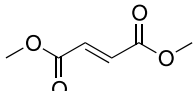
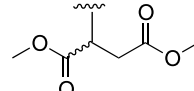
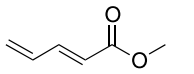
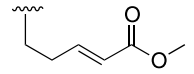
Phenol

Phenol complexes of [Os] display pronounced reactivity toward Michael acceptors under very mild conditions. The reactivity is due, in part, to the acidity of the hydroxyl proton, which can be easily removed to generate an extended enolate. Reactions of [Os]-phenol complexes are therefore typically catalyzed using amine bases rather than Lewis acids. The regiochemistry of addition to C4-substituted phenol complexes is dependent upon the reaction conditions. Reactions that proceed under kinetic control typically lead to addition of the electrophile at C4. In reactions that are under thermodynamic control, the electrophile is added at C2. These C2-selective reactions have, in some cases, allowed the isolation of *o*-quinone methide complexes. As with other [Os] systems, electrophilic additions to phenol complexes occur anti to the face involved in metal coordination.

9.2.8.1 Electrophilic Substitution Reactions

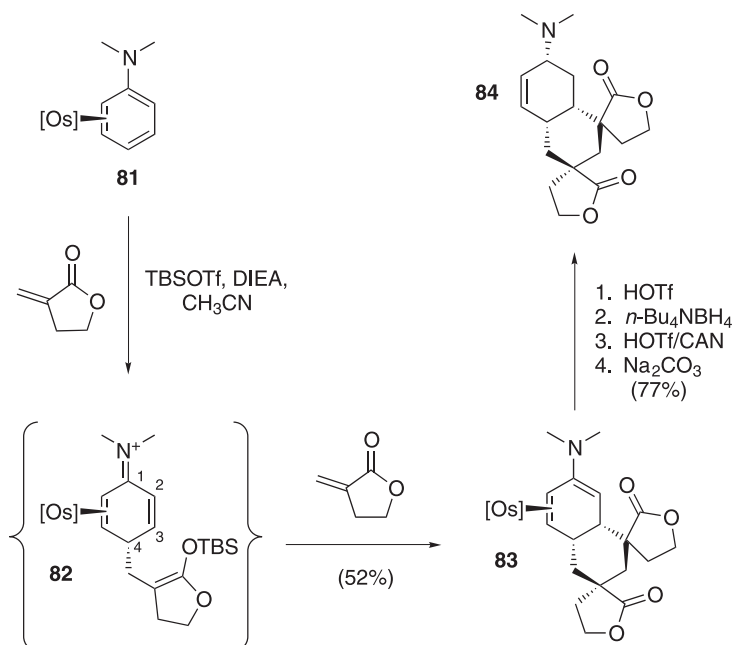
When the parent phenol complex of [Os] **85** is combined with MVK and pyridine in acetonitrile, a Michael addition occurs to give the 4*H*-phenol complex **86** in 91 % yield (Scheme 11). This complex is remarkably stable and resists rearomatization even when allowed to stand in an acidic solution of acetonitrile for 24 h. However, addition of an amine base induces rearomatization to yield complex **87**. This complex may be heated to afford the demetalated substitution product **88** (raspberry ketone) in 71 % yield (based on **85**) [29].

Tab. 13. Scope of electrophilic additions for *N*-substituted aniline complexes.

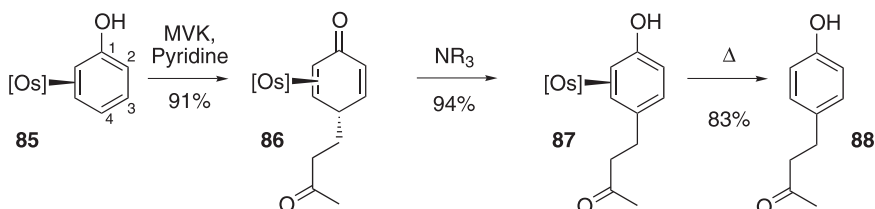
<div style="display: flex; align-items: center; justify-content: center;"> <div style="text-align: center; margin-right: 10px;"> </div> </div>						
Entry	R ¹	R ²	Electrophile	E	Isomers ^a	Yield (%) ^b
1	H	Et			1:1	53
2	H	Et			–	82
3	H	Et			–	95
4	H	Et			–	86 ^c
5	H	Et			–	81 ^d
6	H	Et			4:1	77 ^e
7	Me	Me			6:1	80
8	Me	Me			2:1	63
9	Me	Me			–	73

^a Isomer ratio for asymmetric carbon located on R. This ratio is based on the relative heights of ¹³C NMR resonances and is thus approximate. ^b Unoptimized yields. ^c Reaction performed at –40 °C.

^d = 1. HOTf (1 eq.), 2. H₂O. ^e = 1. HOTf (1 eq.), 2. MeOH.



Scheme 10. A Michael–Michael–Michael ring-closure reaction sequence with complex **81**.



Scheme 11. The osmium(II)-promoted C4 alkylation of phenol with MVK.

9.2.8.2 Michael Addition Reactions

Base-catalyzed The parent phenol complex **85** undergoes a variety of base-catalyzed Michael addition reactions at room temperature to generate *4H*-phenol complexes in yields in the range 79–99 % (Table 14) [29]. Michael additions with MVK, methyl acrylate, acrylonitrile, *N*-methylmaleimide, cyclopentenone, and crotonaldehyde (entries 1–6, respectively) proceed with high regio- and stereocontrol. Demetalation and isolation of the dienone is typically accompanied by tautomerization to the aromatic substitution product.

Estradiol A notable application of phenol activation by [Os] is the C10 alkylation of estradiol **89** (Figure 5). The metal fragment preferentially binds to the α face of the steroid (to form **90**) and thus promotes the addition of MVK to the β face. This forms a quaternary

Tab. 14. Conjugate addition reactions with the η^2 -phenol complex **85** and various Michael acceptors.

Reaction scheme: η^2 -phenol complex **85** + Michael acceptor, NR_3 in CH_3CN yields a product with a Michael adduct at position 4.

Entry	Michael Acceptor	E	Yield (%)
1			91
2			81 ^a
3			99 ^a
4			98
5			79
6			83 ^b

^a = Reaction run with $\text{Zn}(\text{OTf})_2$ as co-catalyst.^b = Reaction run with BF_3 instead of NR_3 .

center at C10 (**91**), and demetalation releases the steroid **92** in 69 % yield (based on **89**). This process results in a steroid that has the C10 stereochemistry of androgens and, consequently, suggests a method for converting estrogen cores to androgen cores in a three-step sequence [30].

Regiocontrol Although Michael additions to $[\text{Os}]$ -phenol occur selectively at C4, addition at C2 is thermodynamically favored for phenol complexes that are substituted at C4. For C4-substituted phenol complexes, the regiochemistry can be controlled by varying the time, temperature, and catalyst (Figure 6) [29]. Additions of MVK to the estradiol complex **90** and the *p*-cresol **94** at -40°C in the presence of an amine base catalyst result in regioselective C4 alkylation in high yields (**91** and **95**). However, when this reaction is performed at room temperature in the presence of a Zn^{2+} co-catalyst, the Michael acceptor adds at C2 to afford

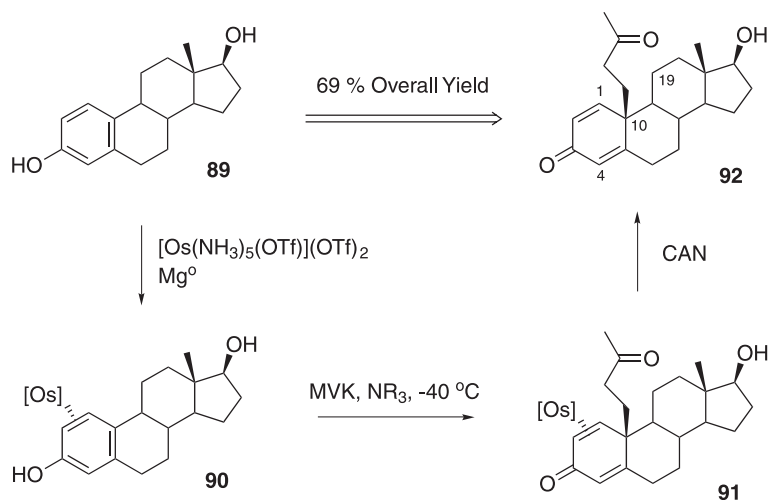


Fig. 5. The C(10) alkylation of β -estradiol using osmium(II) to dearomatize the A ring.

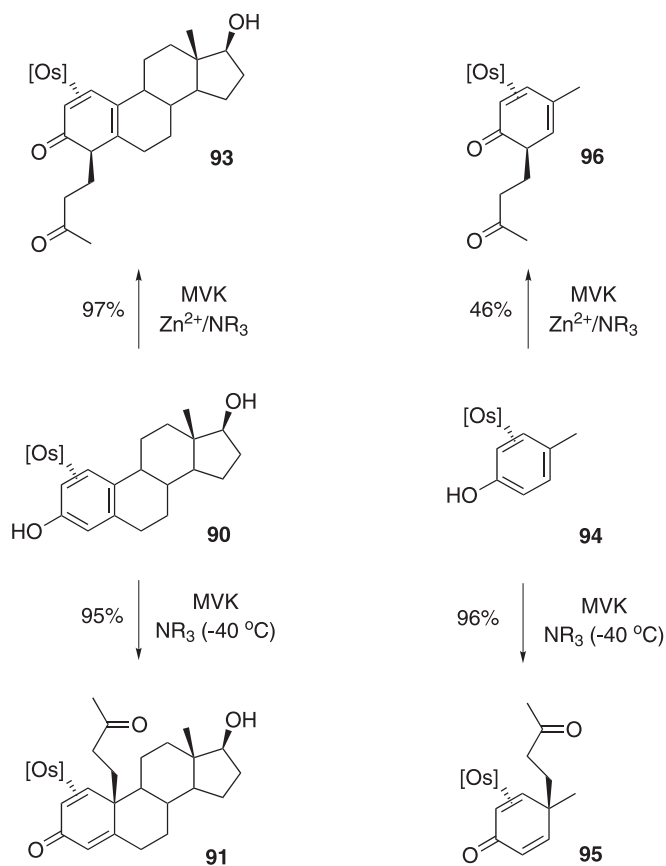


Fig. 6. Regiocontrol of the electrophilic addition reaction of MVK to complexes **90** and **94**.

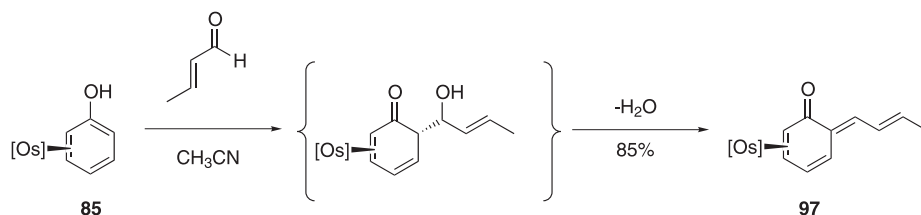


Fig. 7. Formation of an η^2 -o-quinone methide complex from an aldol condensation of crotonaldehyde and the η^2 -phenol complex **85**.

93 and **96**, respectively. Although isolated examples of C2 addition have been observed for complexes of 2-methyl anisole [20] and *N*-ethyl aniline [27], C2 alkylation of [Os]-arenes is primarily a reactivity pattern unique to phenols.

9.2.8.3 *o*-Quinone Methide Complexes

Another example of C2 alkylation is the generation of *o*-quinone methide complexes from [Os]-phenol and crotonaldehyde. When these reagents are combined in the presence of $\text{BF}_3 \cdot \text{OEt}_2$, addition occurs at C4 (Table 14). In the absence of a catalyst, an aldol condensation occurs at C2 to generate the *o*-quinone methide complex **97** in 85 % yield (Figure 7) [29]. This reaction appears to be general for aldehydes and η^2 -phenol complexes, even when the phenol is not substituted at C4.

9.3

{TpRe(CO)(L)}

9.3.1

Introduction

The [Os] fragment is a powerful tool for the dearomatization and activation of aromatic molecules. For more than a decade, however, alternative dearomatizing agents have been sought because of inherent limitations associated with the [Os] system. The metal fragment is achiral and therefore cannot discriminate between enantiofaces upon binding. Unfortunately, changes to the ligand set about the metal completely nullify its ability to coordinate aromatic molecules [31]. Consequently, the achiral nature of the metal center as well as the electronic and steric properties of the system cannot be adjusted. In addition, the dicationic charge of the [Os] complexes limits the solvent environments and purification techniques that may be utilized.

Investigations of cationic rhenium(I) complexes with varying ligand sets showed that the inclusion of a single π -acid in the ligand set was necessary in order to approximate the electronic characteristics of the [Os] fragment [32]. The rhenium(I) fragment *fac*-{Re(dien)(PPh₃)(CO)}⁺ (dien = diethylenetriamine) was successfully bound to furan in an η^2 -fashion. However, it could not be made to bind arenes, with the large PPh₃ ligand in the coordination sphere presumably causing a significant steric hindrance.

Ultimately, it was the Tp ligand, a strong σ -donor ($\text{L} = \text{PMe}_3$), and the π -acid (CO) that proved to possess the right combination of steric and electronic properties to facilitate the η^2 -binding of a variety of aromatic molecules to an Re(I) center [33, 34]. Further studies led to

a series of Re(I) dearomatization fragments having the general formula $\{\text{TpRe}(\text{CO})(\text{L})\}$ ($\text{L} = \text{tert-butyl isonitrile (tBuNC)}$, PMe_3 , pyridine (py), N,N -dimethylaminopyridine (DMAP), N -methylimidazole (MeIm), or NH_3). These fragments not only allow the adjustment of the steric and electronic properties through variation of L , but also have the potential for enantiofacial discrimination of bound prochiral aromatic molecules.

9.3.2

Preparation of η^2 -Arene Complexes

Metal fragments of the form $\{\text{TpRe}(\text{CO})(\text{L})\}$, in which $\text{L} = \text{MeIm}$ or NH_3 , have the ability to bind substituted benzenes in an η^2 -fashion. The fragment having $\text{L} = \text{MeIm}$ has seen more application because of difficulties associated with the synthesis and isolation of aromatic complexes having $\text{L} = \text{NH}_3$. Anisoles, phenols, and naphthalenes all form thermally stable η^2 -complexes when stirred in excess (10–25 equiv.) with $\text{TpRe}(\text{CO})(\text{MeIm})(\eta^2\text{-benzene})$ in THF. The complexes are typically isolated by precipitation from hexanes. The benzene complex can be prepared by direct reduction of the Re(III) precursor, $\text{TpRe}(\text{MeIm})(\text{Br})_2$, with Na^0 in benzene under one atmosphere of CO [35].

Naphthalene forms stable η^2 complexes with $\{\text{TpRe}(\text{CO})(\text{L})\}$ when $\text{L} = \text{tBuNC}$, PMe_3 , py , DMAP , or MeIm . In toluene and an excess of naphthalene, direct reduction of $\text{TpRe}(\text{L})\text{Br}_2$ ($\text{L} = \text{py}$ or DMAP) with Na^0 under CO atmosphere generates the py or DMAP naphthalene complexes in ~40 % yield [36, 37]. Generation of the Re(I) PMe_3 and tBuNC naphthalene systems is not as straightforward. They are synthesized by oxidation of the corresponding Re(I) alkene complexes to Re(II), liberation of the alkene by heating, and reduction of the Re(II) species in the presence of naphthalene [36].

9.3.3

Quadrant Analysis

Upon complexation to the $\{\text{TpRe}(\text{CO})(\text{L})\}$ fragment, a coordinated double bond becomes oriented orthogonally to the Re–CO bond and approximately parallel to the Re–L bond. Such an orientation is thought to maximize overlap between the d orbitals of the metal and the π^* orbitals of the CO and the η^2 -bound species [34]. This arrangement limits the number of coordination diastereomers to two, each of which exists as one dominant rotamer. Typically, the bound arene projects into quadrants **a** and **d** (Figure 8) in order to minimize steric interactions with the scorpionate ligand [34]. The proton labeled H_A on the pyrazolyl ring trans to the CO is directed forward from the quadrant plane, as indicated in Figure 8, and inhibits the placement of any substituents in quadrants **b** or **c**. A study of the binding selectivities of substituted alkenes and ketones with $\text{L} = \text{MeIm}$ suggested that quadrant **c** is the most sterically congested and that quadrant **d** is the least sterically congested [38, 39]. Thus, only one rotamer is typically observed for each coordination diastereomer (*vide infra*).

9.3.4

Naphthalene

In solution, naphthalene complexes of the form $\text{TpRe}(\text{CO})(\text{L})(\eta^2\text{-naphthalene})$ exist as mixtures of diastereomers **A** and **B** (Table 15). Only when $\text{L} = \text{PMe}_3$ (entry 1) does the unbound ring of the naphthalene show a thermodynamic preference for quadrant **a** (**98A**). For all

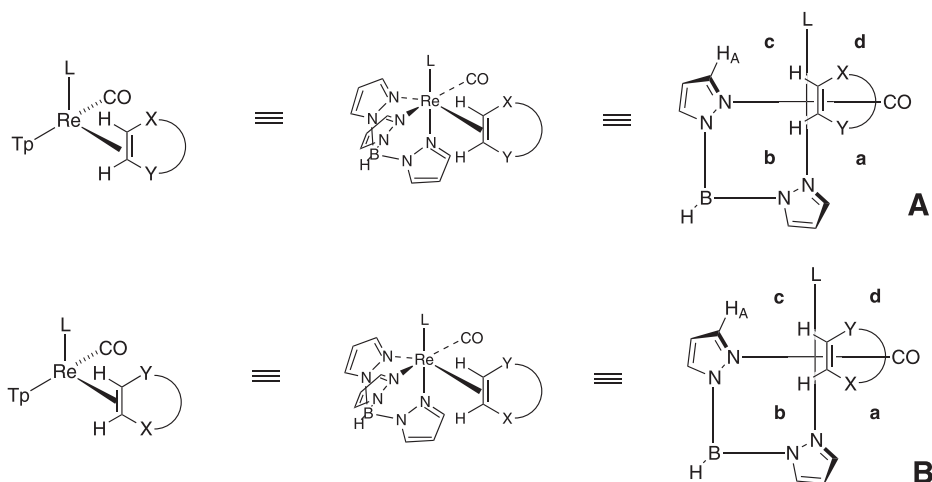
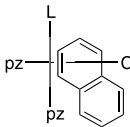
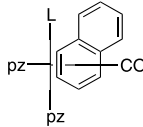
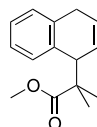
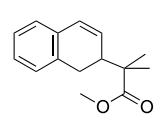


Fig. 8. Quadrant analysis of {TpRe(CO)(L)} fragments.

other L's, the preference is for the unbound ring to lie in quadrant **d** (**98B**) (*vide supra*). When exposed to a solution of HOTf in acetonitrile followed by MMTP, complex **98** undergoes tandem electrophilic/nucleophilic addition reactions with a high degree of regiocontrol. Oxidative decomplexation with AgOTf at room temperature liberates the dihydronaphthalenes

Tab. 15. Regioisomeric ratios and yields of dihydronaphthalenes.

							
98A		98B		99		100	
Entry	L	T (°C)	98A:98B	Method A*		Method B**	
				99:100	Yield	99:100	Yield
1	PMe ₃	{ 0	–	–	–	13:1	29 %
		{ 20	10:1	12:1	52 %	12:1	24 %
2	Pyridine	{ –40	–	1:15	63 %	–	–
		{ 0	–	–	–	1:7	80 %
3	DMAP	{ 20	1:3	1:8	89 %	1:7	66 %
		{ –40	–	1:25	19 %	–	–
4	Melm	{ 20	1:1.5	1:10	50 %	–	–
		{ 0	–	–	–	1:25	55 %
5	NH ₃	{ 20	1:5	1:23	83 %	1:16	63 %
		{ –40	–	1:7	~25 %	–	–
		{ 20	1:4	–	–	–	–

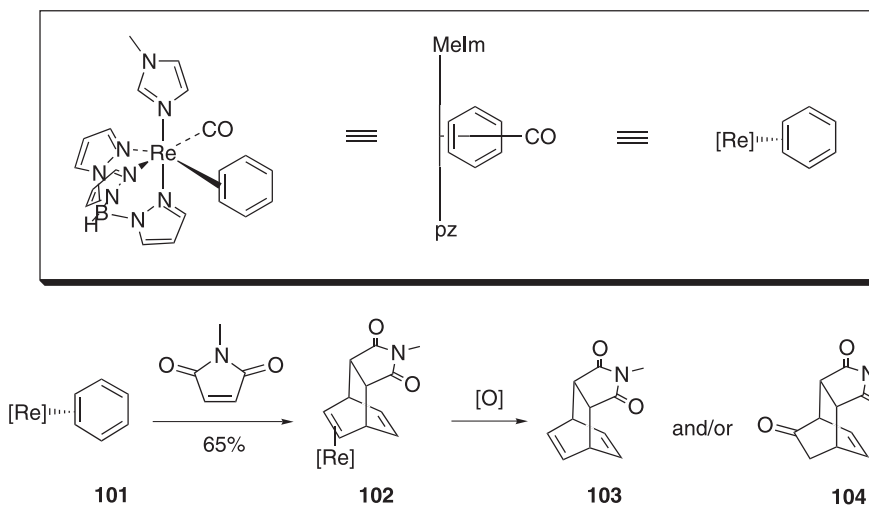
* = Reaction sequence performed in inert atmosphere. ** = Reaction sequence performed on benchtop, with ~500 mg of metal complex, and blanketed under dinitrogen.

99 and **100**. When $L = \text{PMe}_3$ (entry 1), the reaction favors the 1,4-addition product (**99**), a result similar to that observed with $[\text{Os}]$ -bound naphthalene. Complexes that do not have $L = \text{PMe}_3$ (entries 2–5) generate the 1,2-addition product (**100**) with different degrees of selectivity [37]. The regioselectivity of the addition is highest for $L = \text{MeIm}$ (25:1), but the overall yield is highest for $L = \text{py}$ (89 %). Notably, these reactions do not require a glove-box and can be performed with ~ 500 mg of metal complex (Method B). A high degree of stereocontrol has also been demonstrated in these reactions, with both the electrophile and the nucleophile adding anti to the face involved in metal coordination. Furthermore, despite the initial presence of two coordination diastereomers, a single coordination diastereomer can be isolated from each reaction prior to oxidation of the metal center. This result indicates a potential for the synthesis of enantioenriched dihydronaphthalenes through the use of resolved metal complexes [39].

9.3.5

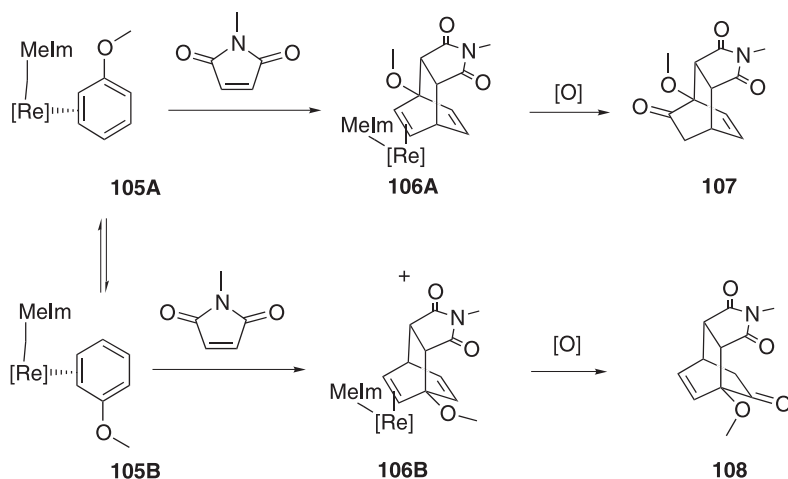
Cycloadditions

Another early success of the $\{\text{TpRe}(\text{CO})(\text{MeIm})\}$ fragment was the promotion of Diels–Alder cycloaddition reactions with benzene and anisole. Complex **101** $[\text{TpRe}(\text{CO})(\text{MeIm})(\eta^2\text{-benzene})]$ undergoes an endo-selective Diels–Alder reaction with *N*-methylmaleimide to afford the bound bicyclo[2.2.2]octadiene complex **102** in 65 % yield (Scheme 12) [40]. Oxidation of **102** yields the bicyclo[2.2.2]octadiene **103** and/or the bicyclo[2.2.2]octenone **104** depending upon the choice of oxidation conditions.



Scheme 12. The $\{\text{TpRe}(\text{CO})(\text{MeIm})\}$ -promoted Diels–Alder reaction of benzene.

The more activated $\text{TpRe}(\text{CO})(\text{MeIm})(\eta^2\text{-anisole})$ complex has demonstrated a slightly broader range of reactivity by undergoing cycloadditions with both *N*-methylmaleimide (Scheme 13) and dimethylacetylene dicarboxylate (DMAD) (Scheme 14). Analysis of these reactions is complicated by the fact that the initial anisole complex exists as a 3:1 mixture of

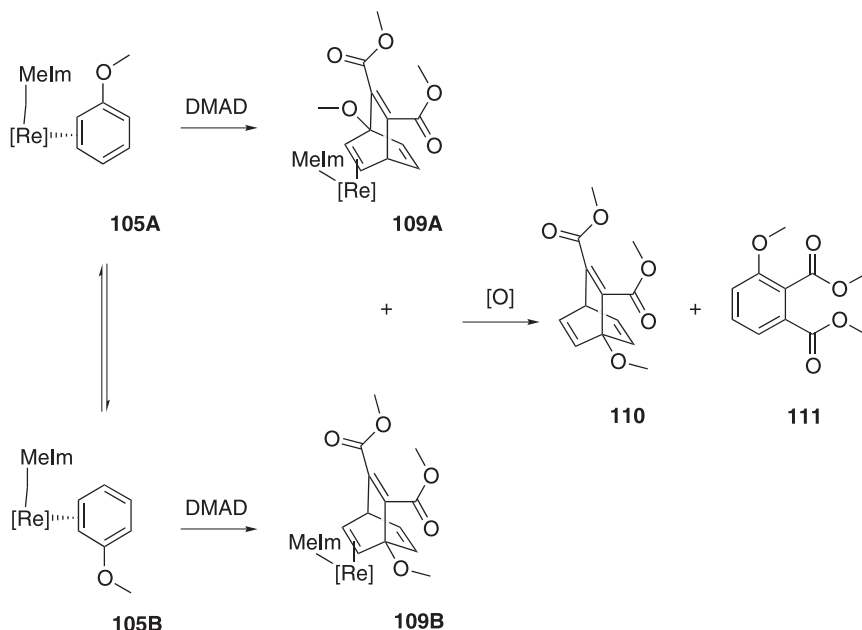


105A : 105B = 3 : 1

106A : 106B = 1 : 1

Scheme 13. A {TpRe(CO)(MeIm)}-promoted Diels-Alder reaction of anisole and *N*-methylmaleimide.

coordination diastereomers (Scheme 13). The major diastereomer **105A** has the methoxy group of the anisole ring directed toward the MeIm ligand, while the minor diastereomer **105B** has the methoxy group directed away from the MeIm ligand. The *N*-methylmaleimide cycloadducts **106A** and **106B** are formed in a diastereomeric ratio of 1:1. They can be sepa-



Scheme 14. A {TpRe(CO)(MeIm)}-promoted Diels-Alder reaction of anisole and DMAD.

rated by chromatography and are far less stable to cycloreversion than the corresponding benzene cycloadduct ($t_{1/2} = 1$ h for **106A**; $t_{1/2} = 0.5$ h for **106B**). Interestingly, initial studies indicate that the decomplexation of these two adducts yields two different oxygen insertion products (**107** and **108**). Oxidation of complex **106A** leads to oxygen insertion into the *exo*-alkene (**107**), while oxidation of complex **106B** leads to oxygen insertion into the *endo*-alkene (**108**).

Complex **105** cyclizes with DMAD to give the diastereomeric bound bicyclo[2.2.2]octatrienes **109A** and **109B** in a 1:1 ratio (Scheme 14). Oxidation of these complexes liberates the corresponding triene **110** as well as the disubstituted anisole **111**, presumably generated with acetylene from the cycloreversion of **110**.

9.4

Concluding Remarks

While more than a decade has passed since the first reports of reactions with η^2 -bound aromatic molecules, this field is still in its infancy compared to the more established field of η^6 -arene chemistry. Nevertheless, the general strategy of using a transition metal to render a conjugated π -system more electron-rich is now firmly established. The next phase of development will be marked by a greater focus on practical issues such as less expensive π -basic metal systems, efficient control of absolute stereochemistry, and standardization of procedures that allow for easier reagent handling.

Acknowledgement

Thanks are due to the many fine graduate, postgraduate, and undergraduate students whose labors have made this account possible.

References

- 1 J. P. COLLMAN, L. S. HEGEDUS, J. R. NORTON, R. G. FINKE, *Principles and Applications of Organotransition metal Chemistry*, University Science Books, Mill Valley, CA, 1987, p. 409–415.
- 2 M. F. SEMMELHACK, in *Comprehensive Organic Synthesis*, Vol. 4 (Eds.: B. M. TROST, I. FLEMING, M. F. SEMMELHACK), Pergamon Press, Oxford, **1990**, p. 517.
- 3 A. R. PAPE, K. P. KALIAPPAN, E. P. KUNDIG, *Chem. Rev.* **2000**, *100*, 2917.
- 4 A. J. PEARSON, M. C. MILLETTI, P. Y. ZHU, *J. Chem. Soc., Chem. Commun.* **1995**, 1309.
- 5 A. J. PEARSON, P. Y. ZHU, *J. Am. Chem. Soc.* **1993**, *115*, 10376.
- 6 A. J. PEARSON, P. R. BRUHN, *J. Org. Chem.* **1991**, *56*, 7092.
- 7 W. H. MILES, P. M. SMILEY, H. R. BRINKMAN, *J. Chem. Soc., Chem. Commun.* **1989**, 659.
- 8 JUNG-NYOUNG HEO, *Org. Lett.* **2002**, *2*, 2987.
- 9 A. J. PEARSON, J. G. PARK, *J. Org. Chem.* **1992**, *57*, 1744.
- 10 D. ASTRUC, *Tetrahedron* **1983**, *39*, 4027.
- 11 P. A. LAY, R. H. MAGNUSON, H. TAUBE, *Inorg. Synth.* **1986**, *24*, 269.
- 12 W. D. HARMAN, H. TAUBE, *J. Am. Chem. Soc.* **1988**, *110*, 7906.
- 13 W. D. HARMAN, H. TAUBE, *J. Am. Chem. Soc.* **1989**, *112*, 2261.
- 14 D. W. ROGERS, F. J. MCCLAFFERTY, *J. Org. Chem.* **2001**, *66*, 1157.
- 15 F. H. DING, W. D. HARMAN, unpublished results (2002).

- 16 M. D. WINEMILLER, M. E. KOPACH, W. D. HARMAN, *J. Am. Chem. Soc.* **1997**, *119*, 2096.
- 17 M. D. WINEMILLER, W. D. HARMAN, *J. Am. Chem. Soc.* **1998**, *120*, 7835.
- 18 M. D. WINEMILLER, *J. Org. Chem.* **2000**, *65*, 1249.
- 19 W. D. HARMAN, *Chem. Rev.* **1997**, *97*, 1953.
- 20 S. P. KOLIS, M. E. KOPACH, R. LIU, W. D. HARMAN, *J. Org. Chem.* **1997**, *62*, 130.
- 21 M. E. KOPACH, S. P. KOLIS, R. LIU, J. W. ROBERTSON, M. D. CHORDIA, W. D. HARMAN, *J. Am. Chem. Soc.* **1998**, *120*, 6199.
- 22 M. D. CHORDIA, W. D. HARMAN, *J. Am. Chem. Soc.* **2000**, *122*, 2725.
- 23 M. D. CHORDIA, W. D. HARMAN, *J. Am. Chem. Soc.* **1998**, *120*, 5637.
- 24 M. E. KOPACH, W. D. HARMAN, *J. Org. Chem.* **1994**, *59*, 6506.
- 25 S. P. KOLIS, M. E. KOPACH, R. LIU, W. D. HARMAN, *J. Am. Chem. Soc.* **1998**, *120*, 6205.
- 26 S. P. KOLIS, M. D. CHORDIA, R. LIU, M. E. KOPACH, W. D. HARMAN, *J. Am. Chem. Soc.* **1998**, *120*, 2218.
- 27 S. P. KOLIS, J. GONZALEZ, L. M. BRIGHT, W. D. HARMAN, *Organometallics* **1996**, *15*, 245.
- 28 J. GONZALEZ, M. SABAT, W. D. HARMAN, *J. Am. Chem. Soc.* **1993**, *115*, 8857.
- 29 M. E. KOPACH, W. D. HARMAN, *J. Am. Chem. Soc.* **1994**, *116*, 6581.
- 30 M. E. KOPACH, L. P. KELSH, K. STORK, W. D. HARMAN, *J. Am. Chem. Soc.* **1993**, *115*, 5322.
- 31 J. BARRERA, S. D. ORTH, W. D. HARMAN, *J. Am. Chem. Soc.* **1992**, *114*, 7316.
- 32 B. C. BROOKS, R. M. CHIN, W. D. HARMAN, *Organometallics* **1998**, *17*, 4716.
- 33 T. B. GUNNOE, M. SABAT, W. D. HARMAN, *J. Am. Chem. Soc.* **1999**, *121*, 6499.
- 34 T. B. GUNNOE, M. SABAT, W. D. HARMAN, *Organometallics* **2000**, *19*, 728.
- 35 S. H. MEIERE, B. C. BROOKS, T. B. GUNNOE, M. SABAT, W. D. HARMAN, *Organometallics* **2001**, *20*, 1038.
- 36 S. H. MEIERE, B. C. BROOKS, T. B. GUNNOE, E. H. CARRIG, M. SABAT, W. D. HARMAN, *Organometallics* **2001**, *20*, 3661.
- 37 M. T. VALAHOVIC, M. SABAT, W. D. HARMAN, *J. Am. Chem. Soc.* **2001**, *123*, 10756.
- 38 S. H. MEIERE, W. D. HARMAN, *Organometallics* **2001**, *20*, 3876.
- 39 S. H. MEIERE, W. D. HARMAN, unpublished results (2001).
- 40 M. D. CHORDIA, P. L. SMITH, S. H. MEIERE, M. SABAT, W. D. HARMAN, *J. Am. Chem. Soc.* **2001**, *123*, 10756.

10

The Directed *ortho* Metalation Reaction – A Point of Departure for New Synthetic Aromatic Chemistry

Christian G. Hartung and Victor Snieckus

Abstract

After a brief allusion to the current status of synthetic aromatic chemistry, a tour based on the Directed *ortho* Metalation (DoM) strategy is provided with selections from recent literature which highlight a) the use of DoM for the regiospecific preparation of polysubstituted aromatics and heteroaromatics; b) the valuable symbiosis of DoM with transition metal catalyzed Ar–Ar cross-coupling protocols; c) the extension of DoM to the Directed remote Metalation (DreM) concept in biaryls, which provides methodologies for the construction of condensed aromatics (fluorenones, phenanthrols) and heterocyclics (thioxanthenes, xanthenes, acridones, dibenzphosphorinones, dibenzthiepinone dioxides, dibenzoxepinones, dibenzazepinones, dibenzphosphinones); and d) the evolving links of DoM to other modern methodologies with a note on the DoM–Grubbs ring-closing metathesis connection. The presentation is solely methodologically rather than total synthesis oriented; dependable directed metalation groups (DMGs = CONR_2 , OCONR_2 , SONR_2 , NHBoc), new and renewed, are emphasized; π -excessive (furan, thiophene, indole) and π -deficient (pyridine) heterocycle HetDoM chemistry is delineated. While definitely not comprehensive, this account attempts to give a flavor of current anionic aromatic chemistry in synthesis.

10.1

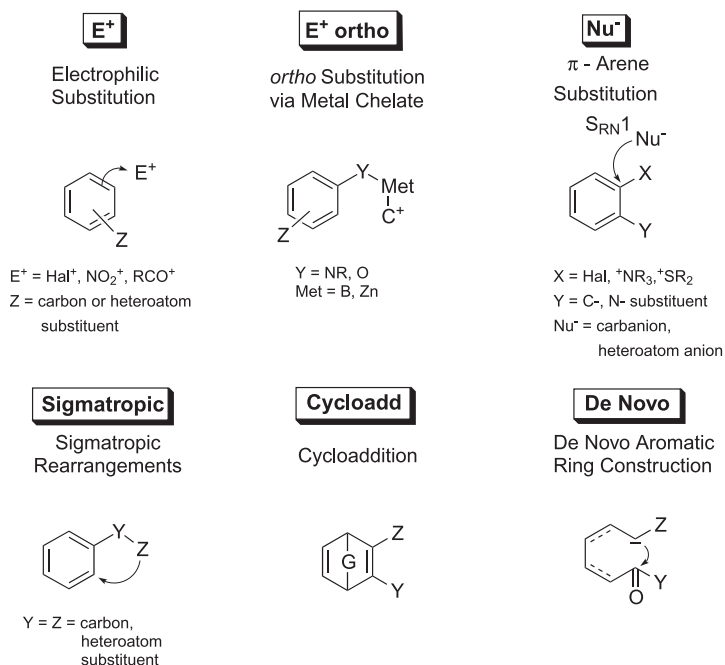
Introduction

“The most common reaction of aromatic compounds is electrophilic aromatic substitution. Many different substituents can be introduced ... Starting from only a few simple materials, we can prepare many thousands of substituted aromatic compounds.” J. McMurry, *Organic Chemistry*, 5th Ed., Brooks/Cole, Pacific Grove, CA, 2000, p. 592.

The study of the structure, synthesis, and reactivity of aromatic compounds has been one of the cornerstones of the teaching of organic chemistry. An account of the historical and sometimes disputed dream of Kekulé [1] is followed by the beautiful logic of electrophilic aromatic substitution rules [2], which allows students to predict syntheses of sparsely substituted aromatics. Aside from a brief diversion into reactions of halonitrobenzenes with nucleophiles [3], this topic constitutes a large chapter in our 1st year organic education but by the time we teach upper year organic majors and graduate students, aromatic chemistry

receives the label “classical”, a certainty for further disregard and/or sparse coverage [4]. Although the preparation and simple reactions of PhMgX or PhLi are taught, aromatic carbanionic chemistry receives no mention in undergraduate texts; similarly, in advanced synthesis courses, with some exceptions [5], students are not familiarized with this subject.

Invariably, the first problem the fresh M.Sc. or Ph.D. student faces upon joining a pharmaceutical company is the construction of a complex, densely substituted aromatic or, even more commonly, heteroaromatic molecule *as a starting material*. The response is, let's buy it [6]. Since, also invariably, this fails, the SciFinderTM or equivalent data base produces (hopefully) a number of hits based on familiar tactics which include (Scheme 1): E^+ substitution [2], Nu^- substitution (including $\text{S}_{\text{RN}}1$ processes) [3], cycloaddition (usually Diels–Alder) [7], and *de novo* ring construction [8], which are familiar but not always fully appreciated. While also not accepted pedagogically, efforts by numerous groups over the past 25 years have added the Directed *ortho* Metalation (DoM) reaction to the armamentarium of the synthetic chemist as a general, regioselective, and effective strategy for the rational construction of polysubstituted aromatic and heteroaromatic substances [9]. While examination of alternative routes is undeniable, the approach to the construction of a key aromatic starting material or intermediate by DoM is, with greater frequency, used for small-scale syntheses by the academic and medicinal chemist and is also increasingly accepted for multi-kg and higher scale process routes to drug candidates and commercial pharmaceuticals and agrochemicals.



Scheme 1. Synthetic approaches to substituted aromatics.

Aims of this Account

This account aims to document, both conceptually and technically, the impact of DoM on the traditional practices of synthetic aromatic chemistry, and is partitioned into the following arbitrary modes from mainly recent research of various laboratories, including our own:

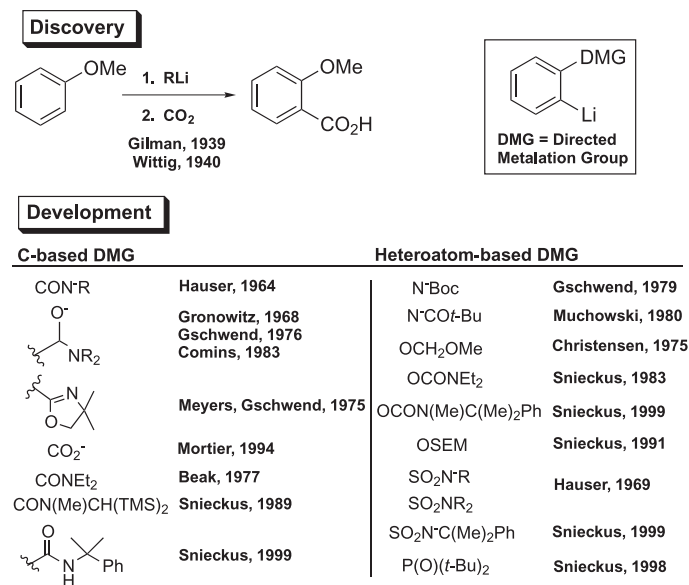
- DoM as a methodological tool for the synthesis of polysubstituted aromatics;
- Heteroaromatic Directed *ortho* Metalation (HetDoM) in synthetic methodology;
- DoM–transition metal catalyzed aryl–aryl cross coupling symbiosis;
- Directed remote Metalation (DreM) in aromatics and heteroaromatics;
- Evolving DoM connections to modern synthetic reactions (Sonogashira, Ullmann, Buchwald–Hartwig, Grubbs metathesis).

10.2

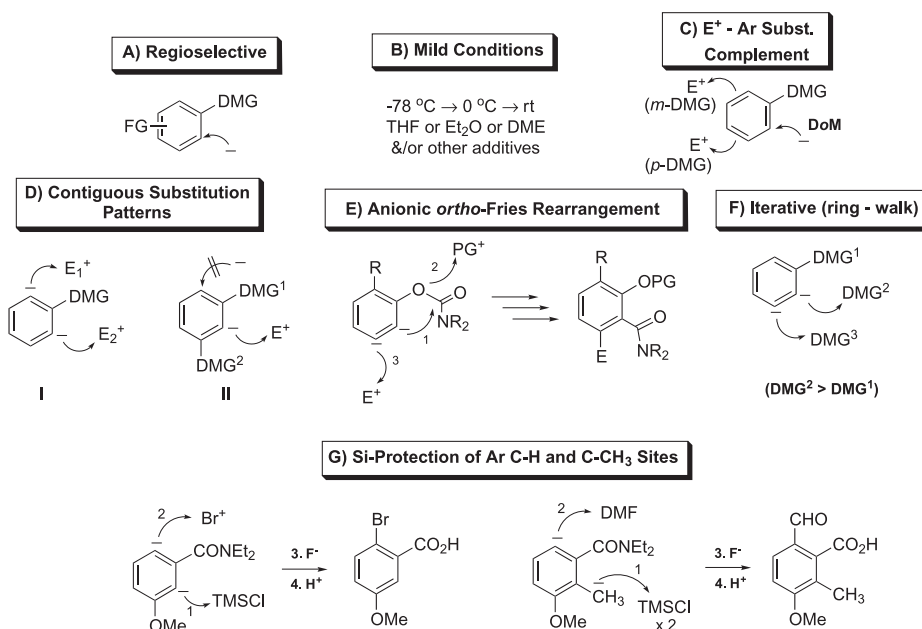
The DoM Reaction as a Methodological Tool

The concurrent and independent discovery of DoM by Wittig and Gilman over sixty years ago set the stage for the systematic work of Hauser, which was pursued in a number of laboratories in the late 1970s and has led to the current status of Directed Metalation Groups (DMGs), which allow the regioselective *ortho* introduction of a host of electrophiles (Scheme 2) [9a–c].

While the mechanism of DoM is an active and controversial field of study [10], a number of synthetic principles have emerged and are commonly practiced (Scheme 3). The con-



Scheme 2. Directed *ortho* Metalation: discovery and development.



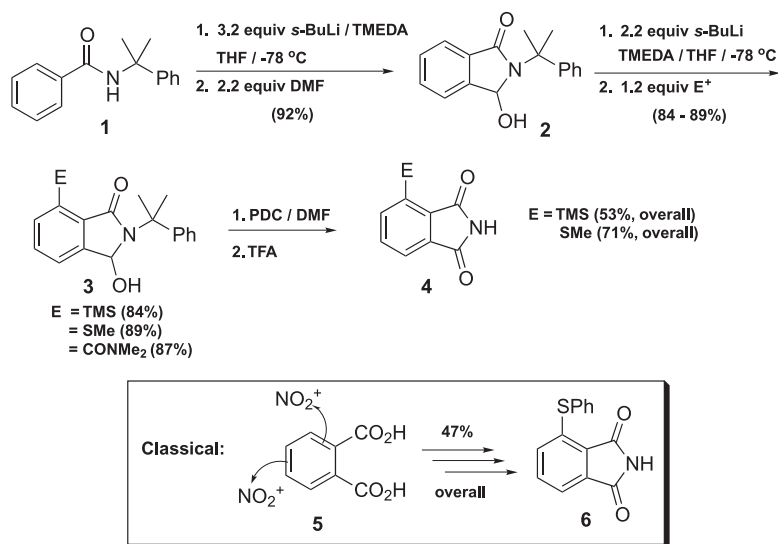
Scheme 3. DoM chemistry generalizations.

ditions for metalation chemistry **B** follow *chacun à son goût* principles: the chemist interested in small-scale reactions refers to them as mild, while the process chemist is concerned about the engineering difficulties and energy demands of anhydrous, low temperature reactions. The complementarity of DoM to aromatic E⁺ substitution **C** is reinforced by the normally harsh, Lewis-acid mediated conditions, and the non-regioselective nature of various reaction types, which complicate separation and isolation procedures. Many DMGs are conducive to sequential *ortho,ortho'*-metalation **DI**, thereby allowing the establishment of 1,2,3-substitution patterns. Alternatively, this pattern may be established by taking advantage of the synergism of two DMGs to in-between metalation **DII** or by the anionic *ortho*-Fries rearrangement **E**. Iterative DoM sequences **F** are also possible, sometimes in one-pot, which offer unique solutions to the introduction of difficult aryl substitution patterns. Unusually substituted systems may also be derived by silicon protection tactics of both aromatic and tolyl C–H acidic sites **G** [9a].

10.2.1

The *N*-Cumyl Carboxamide, Sulfonamide, and *O*-Carbamate DMGs

The stalwart diethyl carboxamide, while a powerful DMG, suffers from treacherous hydrolytic stability, a consequence which has recently been overcome by the development of the *N*-cumyl carboxamide (Scheme 4) [11]. Thus, the readily available **1** undergoes smooth metalation and acceptance of a variety of electrophiles; if DMF is used, the intermediate hydroxyphthalimidine **2** may be further metalated and subjected to electrophile quench to af-



Scheme 4. Synthetic utility of the *N*-cumyl carboxamide DMG.

ford 4-substituted products **3**, conversion of which into **4** establishes a new route to such apparently rare systems, which are normally obtained by classical, non-regioselective E⁺ substitution routes, **5** → **6**.

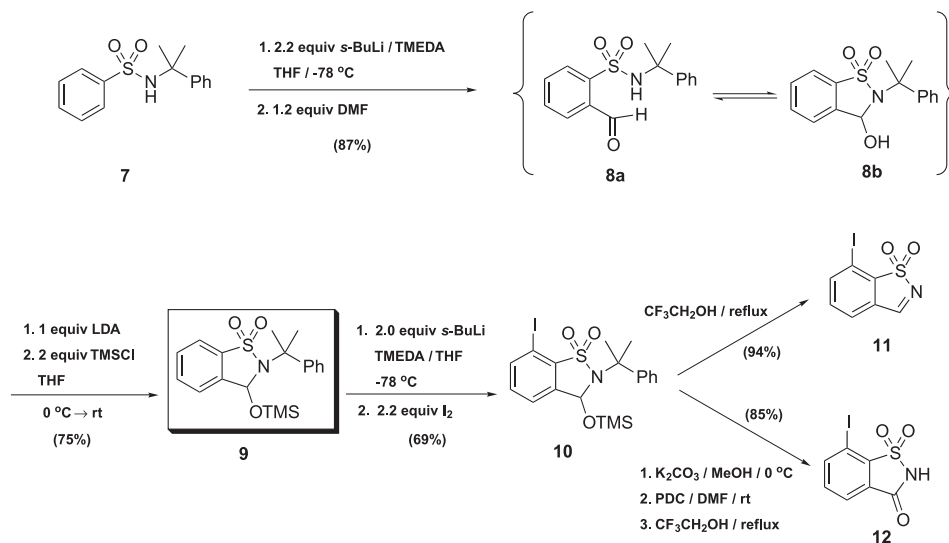
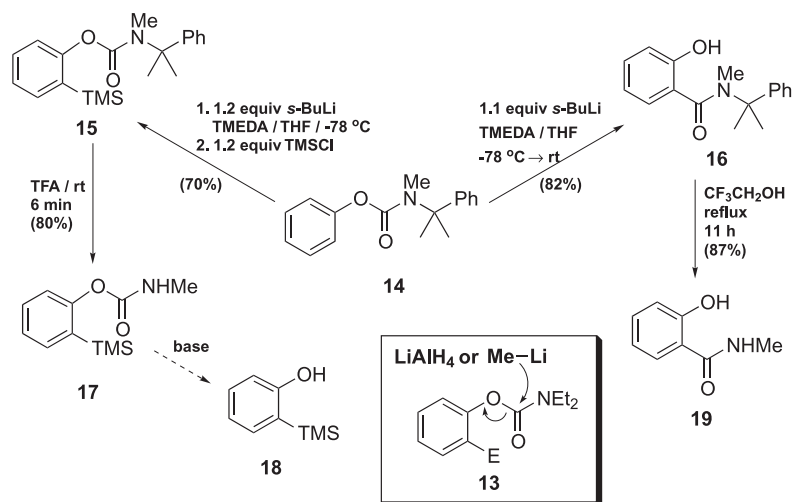
Similarly, the *N*-cumyl benzene sulfonamide **7** (Scheme 5) undergoes metalation–diverse electrophile quench reactions; its quenching with DMF leads to **8**, which, after OTMS protection, may be further metalated and quenched with iodine to give **10**; the latter is transformed under mild conditions into new benzothiazole derivatives **11** and **12** [12].

The *O*-carbamate, the most powerful of DMGs in competition experiments [13], is similarly plagued by stability as the *N,N*-diethyl derivative **13** (Scheme 6). However, the *N*-cumyl-*N*-methyl counterpart **14** undergoes unproblematic metalation–electrophile quench to give **15** and anionic Fries rearrangement (**16**) reactions. The very mild conditions for hydrolysis to **17**, and hence to **18**, as well as to **19** bode well for further useful chemistry of the *N*-cumyl DMG in context of more substituted aromatics [14].

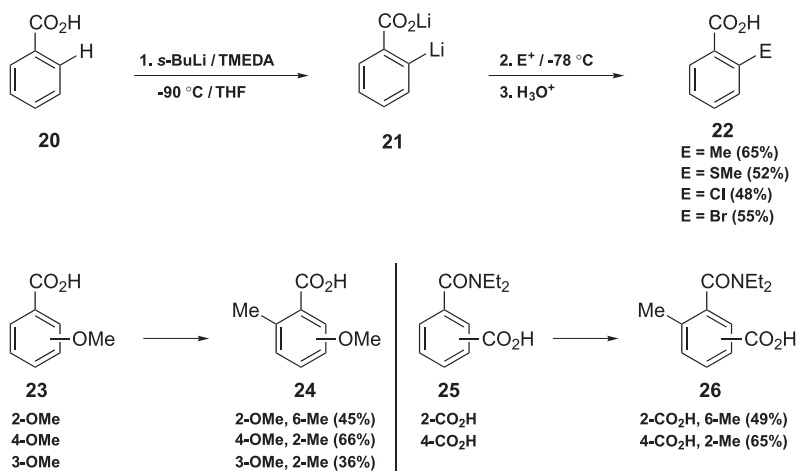
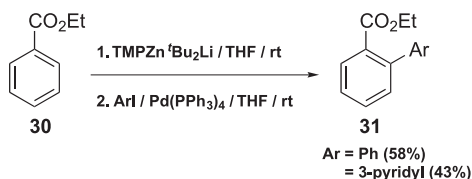
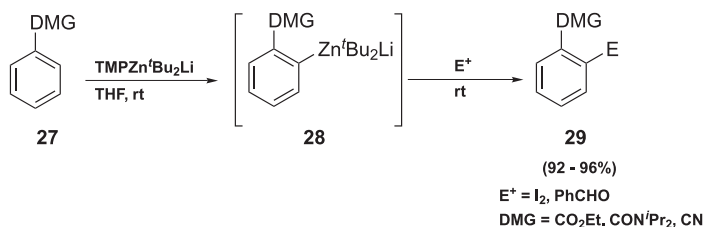
10.2.2

The Lithio Carboxylate and Carboxylate Ester DMGs

Recent results from the laboratories of Mortier offer the potential of the carboxylate DMG as the simplest solution for the preparation of benzoic acid derivatives (Scheme 7) [15]. In order to minimize the expected ketonic products, the metalation **20** → **21** must be carried out at -90 °C, but thus leads to useful yields of products **22**. Based on experiments on *meta*-interrelated DMG systems and competition with other DMGs, **23**–**26** also offer application possibilities. Of similar synthetic potential is the work of Kondo (Scheme 8) [16], which

Scheme 5. The *N*-cumyl sulfonamide DMG.Scheme 6. The *N*-cumyl carbamate DMG.

demonstrates DoM chemistry $27 \rightarrow 28$ using TMP-zincate bases for not only amide but also ester and nitrile DMGs to give high yields of, as yet few, products 29. Negishi cross-coupling chemistry $30 \rightarrow 31$ has also been achieved. Combined *in situ* LiTMP/borate and LiTMP/silane base-electrophile species may be similarly used for DoM chemistry of ester DMG systems [17].

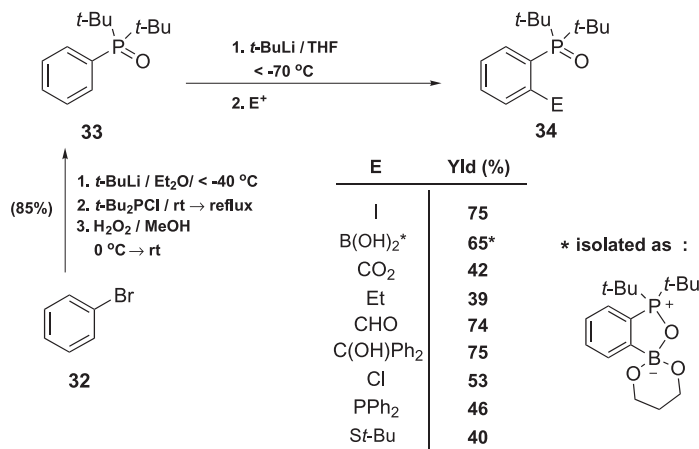
Scheme 7. The COO⁻ DMG.

Scheme 8. DoM chemistry with TMP-zincate as base.

10.2.3

The Di-*tert*-Butyl Phosphine Oxide DMG

The current activity in the area of enantioselective organometallic catalysis using phosphorus-based DMGs stimulated activity to improve the existing repertoire of P-DMGs. Phenyl di-*tert*-butyl phosphine oxide **33** (Scheme 9), chosen for its stability to alkylolithiums and readily prepared from **32**, shows excellent metalation traits to give, after electrophile quench, a variety of interesting aromatic phosphorus derivatives **34**, including di-phosphorus and boron-phosphorus compounds [18]. The difficulty of DMG removal plagues this methodology, a factor that also surfaces in its use in heterocyclic DoM chemistry (Scheme 16), and thus should prompt further studies.



Scheme 9. The di-*tert*-butyl phosphine oxide DMG.

10.3

Heteroaromatic Directed *ortho* Metalation (HetDoM) in Methodological Practice

The routine requirement of substituted heteroaromatics, varying from the traditionally defined π -excessive (furans, thiophenes, pyrroles, and their benzo analogues) and π -deficient (pyridines and benzo analogues) and their multitudes of di- and higher-heteroatom containing relatives, prompts continuing intense studies to explore the scope and limitations of HetDoM chemistries. Although the former derivatives are electrophilically active, their sensitivity to further decomposition pathways as a result of excessive reactivity, at times, limits such chemistry. In contrast, the pyridines, quinolines, and related π -deficient systems are, of course, recalcitrant to electrophilic substitution, a fact which causes either modification of substituted commercial products by classical reactions or *de novo* ring synthesis approaches to obtain polysubstituted systems. While numerous workers have contributed to DoM chemistry of π -excessives [19], the Quéguiner school [9e, 9f] has been the major force in contributions to DoM in the pyridine and diazine areas, which will have a major impact in devising new routes to substituted derivatives that are not readily prepared by conventional means.

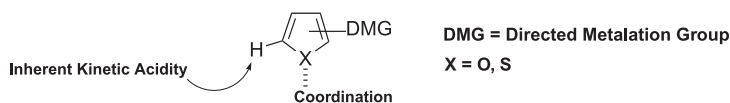
10.3.1

π -Excessive Heteroaromatic Directed *ortho* Metalation (HetDoM)

10.3.1.1 Furans and Thiophenes

In metalation of the π -excessive furans and thiophenes, consideration must be given to not only the DMG effect but also the inherent acidity of the 2-, (5-)hydrogens (Scheme 10) [19, 20].

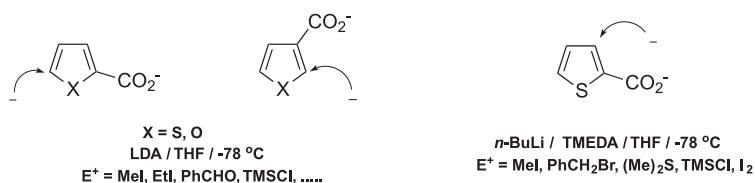
While the standard carbon-based DMGs have received substantial application in these systems, the heteroatom-based groups have enjoyed limited use with the exception of the extensive studies on sulfonamides (Scheme 13). Although amide and oxazoline DMGs have



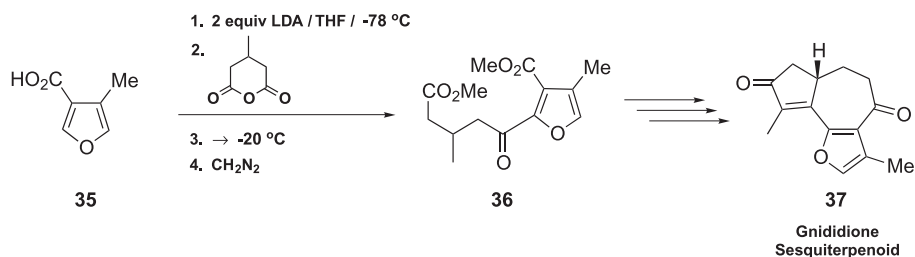
Carbon-based DMGs	Heteroatom-based DMGs
CONR	OR
CONR ₂	OP(NMe ₂) ₂
	SR
CO ₂ ⁻	SO ₂ N ⁻ R
	S(O) _n R n = 1,2
CH ₂ OR	N ⁻ COt-Bu
CH ₂ O ⁻	

Scheme 10. DoM reactivity of furans and thiophenes.

found considerable application, the carboxylic acid DMG in furans and thiophenes and their benzo analogues are arguably the most useful for further manipulation (Scheme 11) [21]. An instructive illustration is the use of furan carboxylic acid **35** in the synthesis of sesquiterpenoid **37** via the diester **36**, which is prepared by condensation of an anhydride with dianion of **35**, the basic character of which appears to have minimal detrimental effects (Scheme 12) [22].



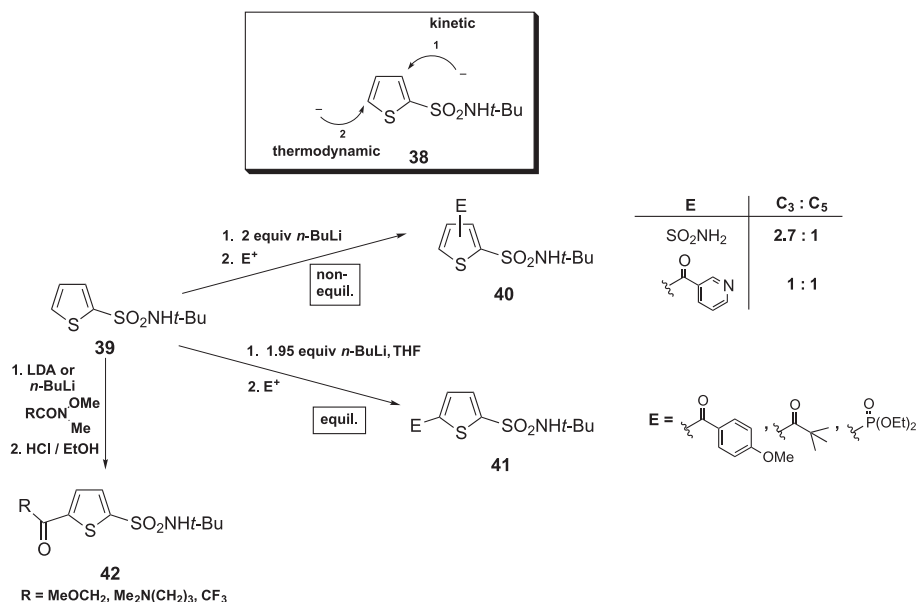
Scheme 11. The COO⁻ DMG in furans and thiophenes.



Scheme 12. Application of the COO⁻ DMG in furans.

Thiophene sulfonamide DoM chemistry is by far the most highly explored in view of the agrochemical significance of the sulfonylurea herbicides [23]. Potential for regioselective deprotonation as a function of kinetic or thermodynamic control **38** may lead to 3- or 5-

substituted products **39** → **40** or **41**, which can be further manipulated hydrolytically at the *tert*-butyl sulfonamide function (Scheme 13) [24]. C-5 functionalization via Weinreb amides to **42** is also feasible.

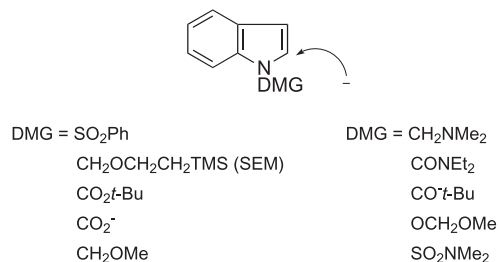


Scheme 13. DoM reactivity of the SO₂N[−]R DMG in thiophenes.

10.3.1.2 Indoles

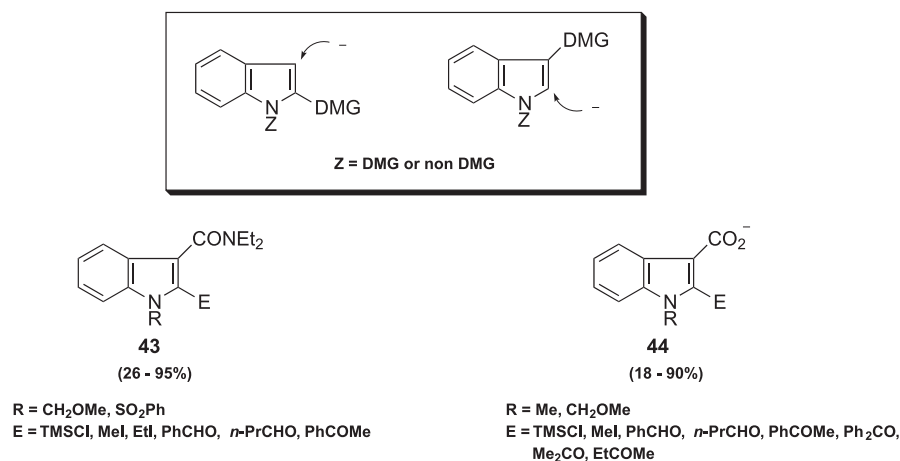
While pyrrole DoM chemistry is still a relatively unexplored area [25], the corresponding indoles, especially with respect to *N*-DMGs (Scheme 14), constitute a rich area of metalation exploitation [26].

The introduction of a 2-DMG or the presence of a 3-DMG allows further metalation chemistry at the respective alternative positions on the pyrrole ring (Scheme 15). The chemistry of the 3-amides and 3-carboxylic acids **43** and **44** is illustrative of the potential for

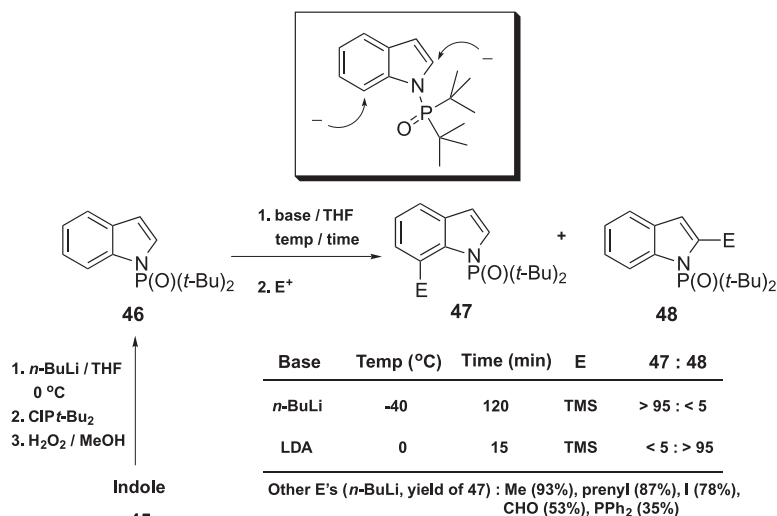


Scheme 14. *N*-DMGs for DoM of indoles.

formation of indole 2,3-substituted products (Scheme 15) [27]. Access to 7-substituted indoles via metalation chemistry has been achieved via indolines [28] and, more recently, specially designed *N*-DMGs such as *N*-COC(Et)₃ [29], and *N*-P(O)(*t*Bu)₂ (Scheme 16) [30]. In the last example, although the starting material **46** is easily prepared from indole (**45**) and highly regioselective 2- (**48**) or 7- (**47**) deprotonation can be achieved by judicious choice of conditions, the difficulty of removing the phosphite group remains.

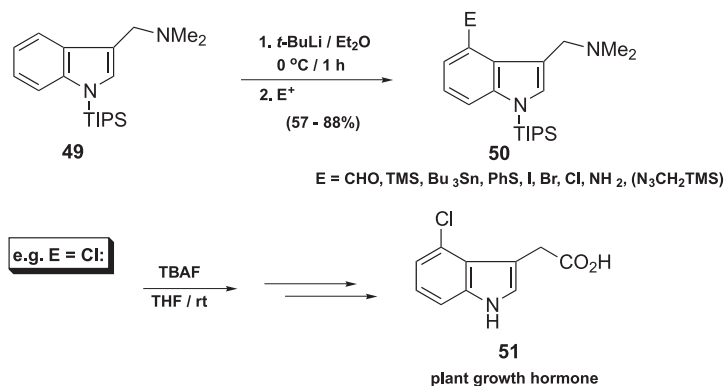


Scheme 15. 3-Amides and 3-carboxylic acids as DMGs in DoM of indoles for the synthesis of 2,3-substituted indoles.



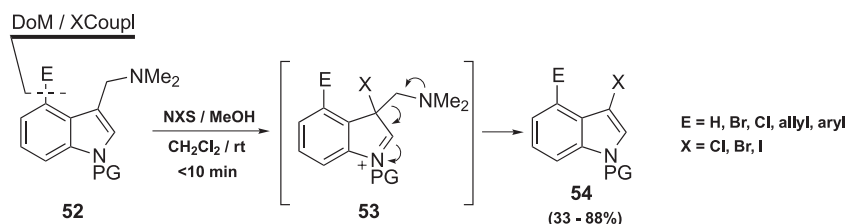
Scheme 16. The *N*-P(O)(*t*-Bu)₂ DMG for the synthesis of 7-substituted indoles.

The discovery by Iwao that gramine bearing the large *N*-silicon functionality TIPS, **49**, undergoes 4-deprotonation to give, after electrophile quench, products **50** (Scheme 17) [31] is of great synthetic consequence for the preparation of difficult to access 4-substituted indoles, e.g. **51**.

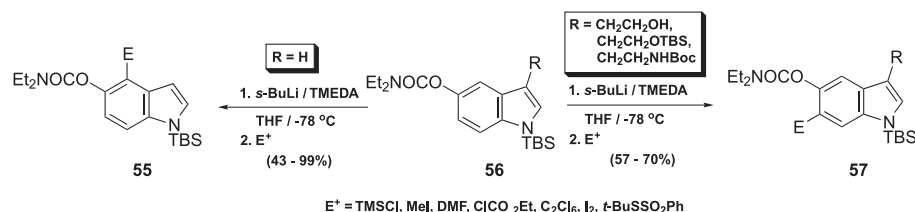


Scheme 17. 4-Deprotonation of gramine bearing a bulky *N*-silyl functionality.

Furthermore, the vintage observation [32] of retro-Mannich reactivity of gramines has allowed the development of a new route to 3,4-disubstituted indoles, especially dihalogenated derivatives **52** \rightarrow **53** \rightarrow **54** (Scheme 18) [33]. In order to open the door to DoM reactivity studies in the benzo ring component of indoles, the 5-*O*-carbamate **56** has recently been systematically studied (Scheme 19) [34]. The absence or presence of 3-substitution, no matter what size, allows, respectively, 4- (**55**) and 6- (**57**) derivatization of indoles, including tryptophols and tryptamines [35].



Scheme 18. 3,4-Substituted indoles via DoM-retro Mannich sequence.



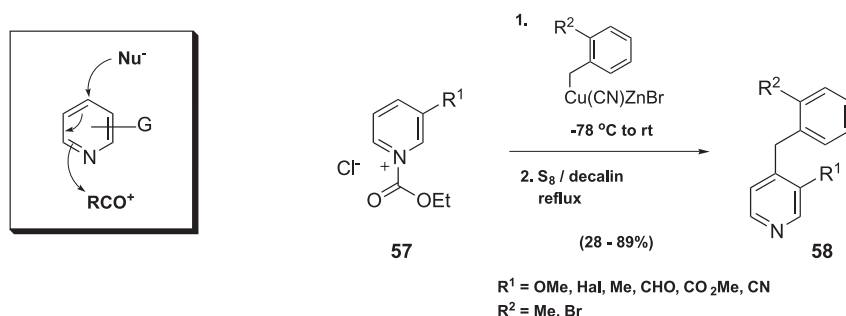
Scheme 19. DoM benzenoid ring functionalization of indole 5-*O*-carbamate.

10.3.2

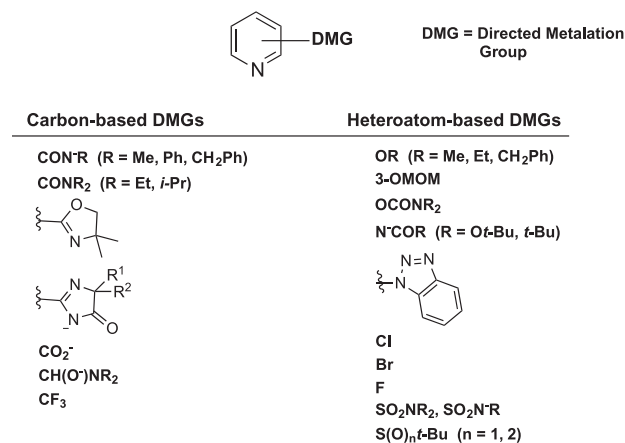
 π -Deficient Heteroaromatic Directed *ortho* Metalation (HetDoM)

10.3.2.1 Pyridines

DoM of pyridines may be compromised by coordinatively driven addition of RLi and LiNR₂ reagents. The synthetic value of such reactivity for substituted pyridines **57** \rightarrow **58** is undeniable (Scheme 20) [36] and may be considered at times complementary to HetDoM (Scheme 21) [9d, 9e, 20d, 37]. As evidenced from methodological use as well as in total synthesis endeavors [9d, 9e], amide and halogen DMGs are most valuable for substituted pyridine synthesis. The recent addition of the CO₂[−] DMG may have future impact [38].

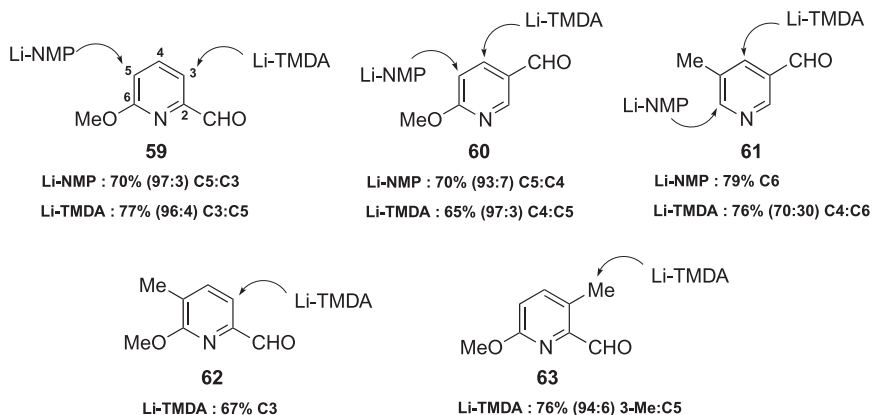


Scheme 20. Nucleophilic addition to pyridines.

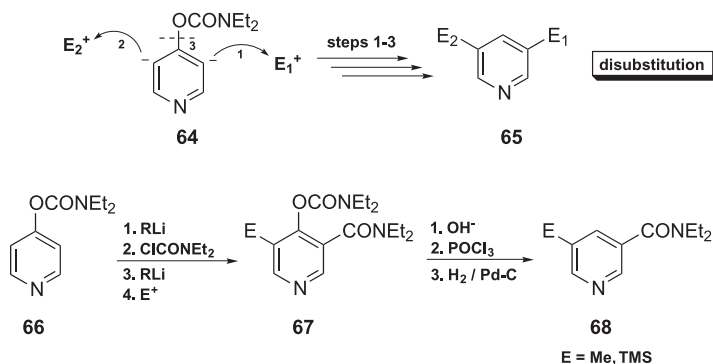


Scheme 21. DMGs in DoM chemistry of pyridines.

Among the methodological studies [9d, 9e, 20d], the rich chemistry of carbinolamine alkoxide DMGs **59**–**63** (Scheme 22) [39], while not explored with regard to the scope of electrophile introduction, predicts access to highly functionalized systems. Similarly as yet unexplored but of foreseeable value for 3,5-disubstituted patterns is the use of the *O*-carbamate DMG, **64** \rightarrow **65** (Scheme 23) [40]. Thus, in a prototype sequence, metalation–electrophile

**Standard Conditions**

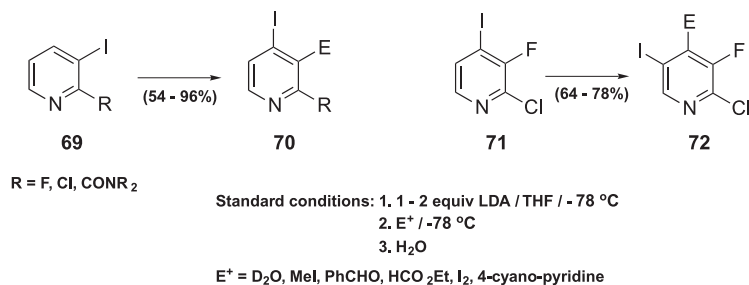
- a) 1.2 equiv Li base / THF / -78 °C
 b) 2.0 equiv *n*-BuLi / -78 °C → -42 °C
 c) MeI / -78 °C → rt

Li-TMDA : Lithium *N,N,N'*-trimethylethylenediamineLi-NMP : Lithium *N*-methylpiperazine**Scheme 22.** The DoM chemistry of carbinolamine alkoxide DMGs in pyridines.**Scheme 23.** The *O*-carbamate DMG in DoM of pyridines.

quencher, **66** → **67**, followed by base hydrolysis, conversion to the 4-chloropyridine, and hydrogenolysis leads to two derivatives **68**.

In contrast to the well known metal-halogen exchange of bromo and iodo aromatics, commercially available halopyridines are amenable, for all halogens, to DoM chemistry of considerable synthetic value [9d]. Recent results [9d, 41], have pointed to the additional feature of the “halogen dance” as a tool for the construction of unusually substituted pyridines. Illustrative are the conversion of **69** into 2,3,4-substituted pyridines **70** and, more interestingly, of **71** into the tetrasubstituted **72** bearing all but one of the theoretically possible halogens (Scheme 24) [42].

Among the few quinolines and isoquinolines that have been tested for DoM reactivity [9e], utility is compromised by RLi addition reactions and unusual behavior [9d, 43].

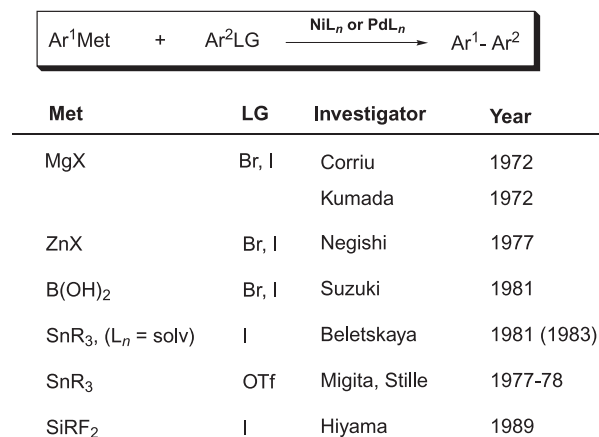


Scheme 24. Tandem DoM/halogen dance reactions of iodopyridines.

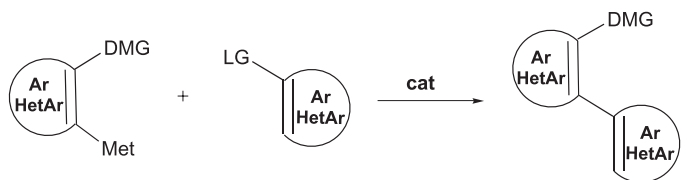
10.4

The DoM–Transition Metal Catalyzed Aryl–Aryl Cross-Coupling Symbiosis

The changing face of synthetic methodology has been fueled by dramatic discoveries of new reactions in transition metal catalyzed processes over the past thirty years. In the area of aryl–aryl bond formation, Corriu–Kumada–Tamao, Suzuki–Miyaura, Negishi, and Stille, in addition to others with preceded and interspersed contributions, have provided the synthetic community with effective cross-coupling methods for biaryl and higher order aryl ring combination constructs (Scheme 25) [44]. The rational connection of these methods to DoM provides, by metal-metal exchange, latitude for the preparation of substituted biaryls and heterobiaryls whose origins may be based on the versatility of DoM and whose new C–C bond regiochemistry is dictated by a variety of carbon- and heteroatom-based DMGs (Scheme 26) [45].



Scheme 25. Transition metal catalyzed cross-coupling reactions for the synthesis of aryl–aryl bonds.



Met	LG	Cat	Xcoupl
B(OR) ₂	I > Br > OTf	Pd	Suzuki
MgX	OTf > OCONeEt ₂ SCONeEt ₂	Ni	Kumada–Corriu
ZnX	Hal, OTf	Ni	Negishi
SnR ₃	Hal, OTf	Pd	Stille

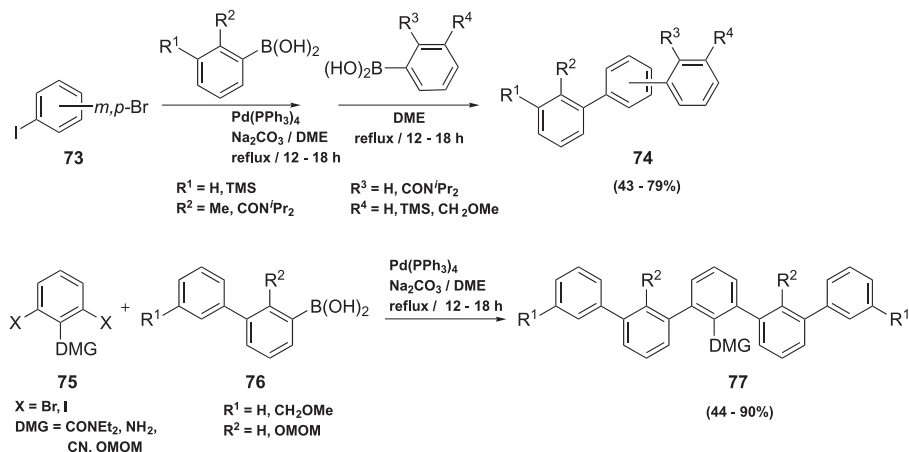
DMG = CONeEt₂, OCONeEt₂, OMOM, NHBoc, SO₂t-Bu

Scheme 26. The DoM–cross-coupling nexus.

10.4.1

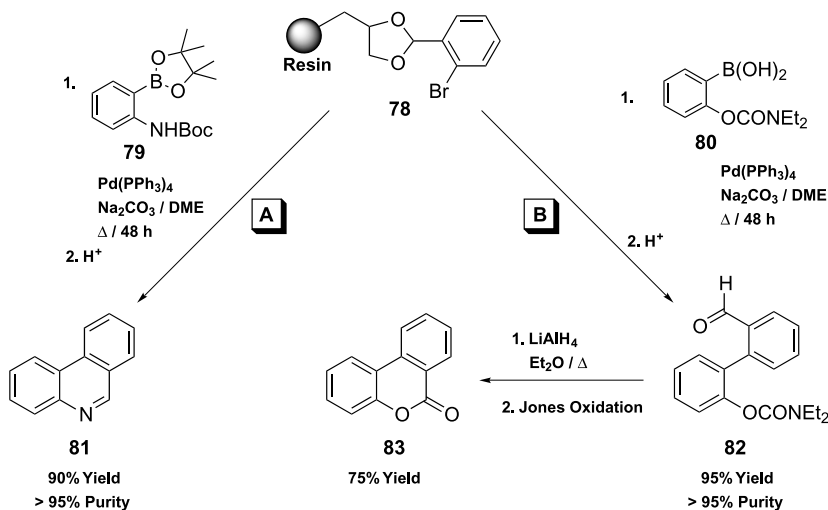
The Suzuki–Miyaura–DoM Link

The connection of the Suzuki–Miyaura strategy [46] with DoM offers a dependable and general route for the synthesis of biaryls and heterobiaryls. While mechanistic knowledge is still lacking [46, 47] and reasons for homocoupling and deboronation are not fully understood [48], this process constitutes a dependable replacement for alternative classical methods [49], as was demonstrated early in sequential **73** → **74** and 2:1 **75** + **76** → **77** cross-coupling modes (Scheme 27) [50]. Similar processes are increasingly being used for the construction of polyaryls of interest in material science areas [51].



Scheme 27. DoM-initiated sequential and 2:1 Suzuki–Miyaura cross-coupling.

The Suzuki–Miyaura tactic carried out on solid support (Scheme 28) [52] provides routes to small libraries of condensed heterocycles. Thus, Merrifield resin with the Leznoff-linked bromobenzene derivative **78** undergoes cross-coupling under normal solution-phase conditions with boron pinacolate **79** or boronic acid **80**, prepared by DoM, to afford phenanthridines **81** or, via **82** and some manipulation, dibenzopyranones **83** in good yields and with high purities. The Stille solid-support reaction has also been successfully executed [53].

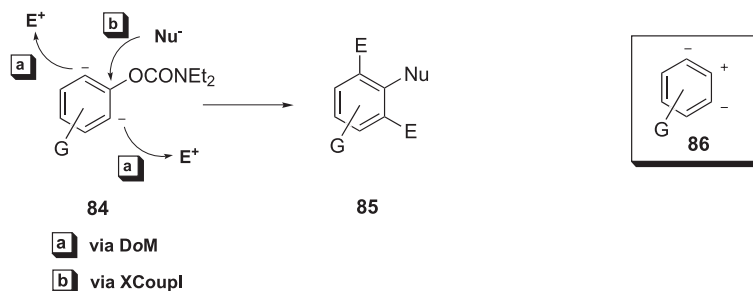


Scheme 28. Solution-phase DoM-initiated Suzuki–Miyaura cross-coupling on solid support.

10.4.2

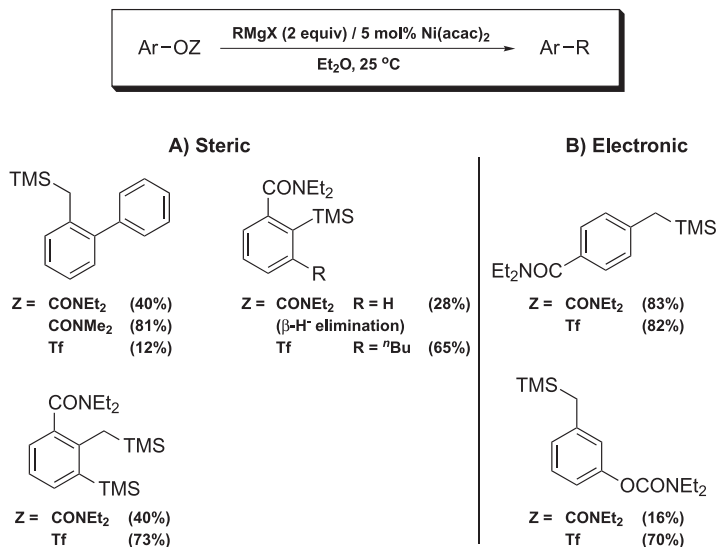
Aryl O-Carbamate and S-Thiocarbamate–Grignard Cross-Coupling Reactions

The discovery that the most powerful OCONEt_2 DMG also acts as a coupling partner with Grignard reagents under nickel-catalyzed conditions [54] opened the doors to new methodology whose potential, **84** \rightarrow **85** (Scheme 29) allows, in theory, the construction of contiguous electrophile-nucleophile-electrophile substitution patterns on an aromatic ring, i.e. the charged equivalency **86**.



Scheme 29. O-Carbamate DoM-cross-coupling connection.

Even in the brief methodological studies so far undertaken (Scheme 30) [54], steric and electronic effects (**A** and **B**) and a rapid route to benzyl silanes using commercially available Grignards have been established.

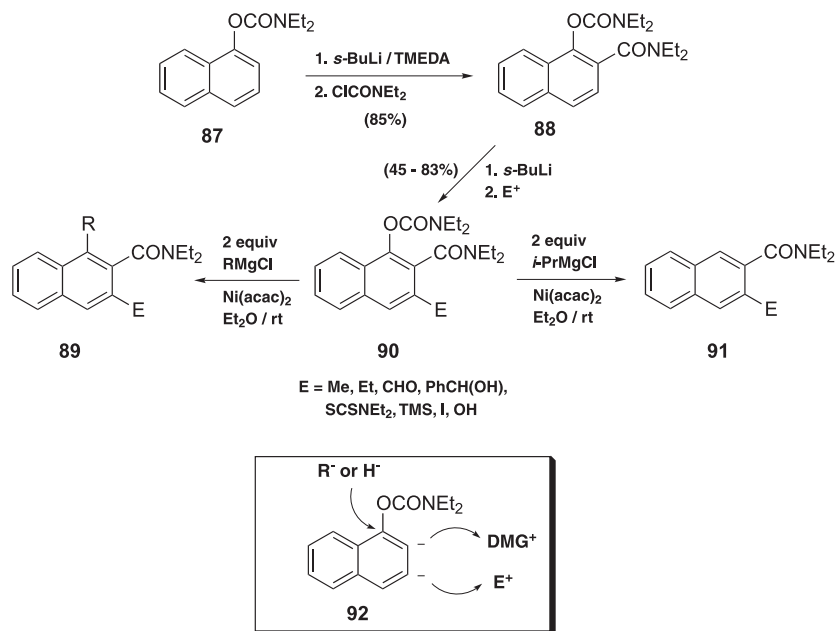


Scheme 30. Nickel-catalyzed cross-coupling of *O*-aryl carbamates and triflates with Grignards; electronic and steric effects.

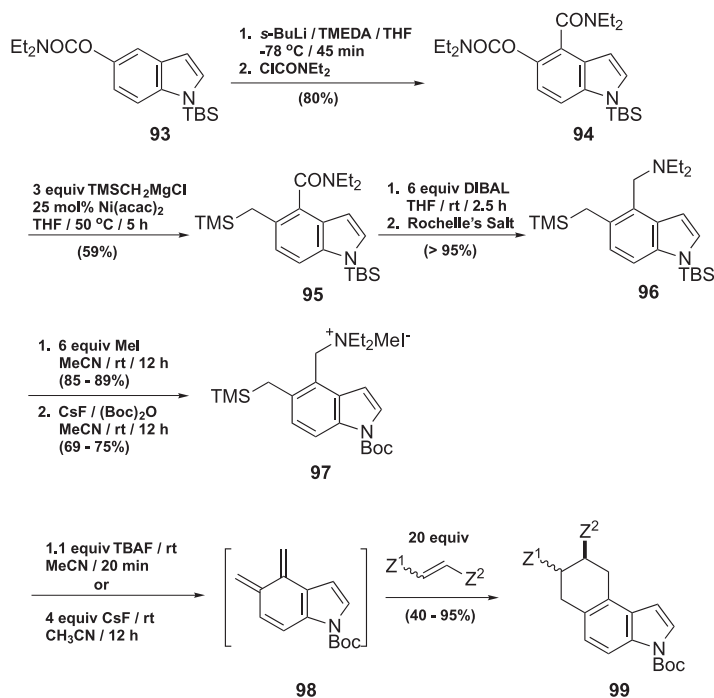
Of perhaps greater value is the utility of this carbamate variation of the Corriu–Kumada–Tamao reaction in the formulation of substitution patterns on simple aromatics that cannot be purchased nor easily constructed. In a demonstration of this point, the naphthyl *O*-carbamate **87** (Scheme 31) [54, 55] is converted into **88**, which, when subjected to a second DoM and various electrophile quenches, leads to **90**. The latter may be elaborated in two directions: by nickel-catalyzed coupling with RMgX reagents (R = Ar, vinyl, Me, TMSCH₂) [56] to 1,2,3-substituted naphthalenes **89** or, by taking advantage of the β-hydride donor properties of *i*PrMgCl, into the 2,3-substituted derivatives **91**. With the proviso that the E substituent is unreactive or protected from RMgX attack, the conceptual framework (**92**) may be of further value in simpler condensed aromatic and heteroaromatic molecules.

The methodological exploration of *O*-carbamate–Grignard cross-coupling in heterocyclic systems may also prove profitable, as suggested by the initial work on the indole 5-*O*-carbamate **93** (Scheme 32) [57]. Thus, the intermediate amide **94** obtained by standard DoM chemistry, when subjected to coupling with an excess of the commercially available TMSCH₂MgX reagent, provides **95** in reasonable yield. Further conversion leads, via **96**, to **97**, a precursor of the indolo 4,5-quinodimethide intermediate **98**, which undergoes cycloaddition with a variety of dienophiles to give new annelated products **99**.

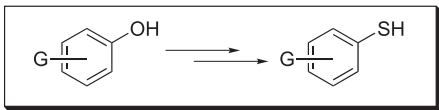
A logical progression of *O*-carbamate DoM chemistry, to metalate *S*-thiocarbamates **103**, E = H, proved unsuccessful, but turning attention to the corresponding *O*-thiocarbamates



Scheme 31. Nickel-catalyzed O-aryl carbamate Grignard cross-coupling; regiospecific access to 1,2,3- and 2,3-substituted naphthalenes.



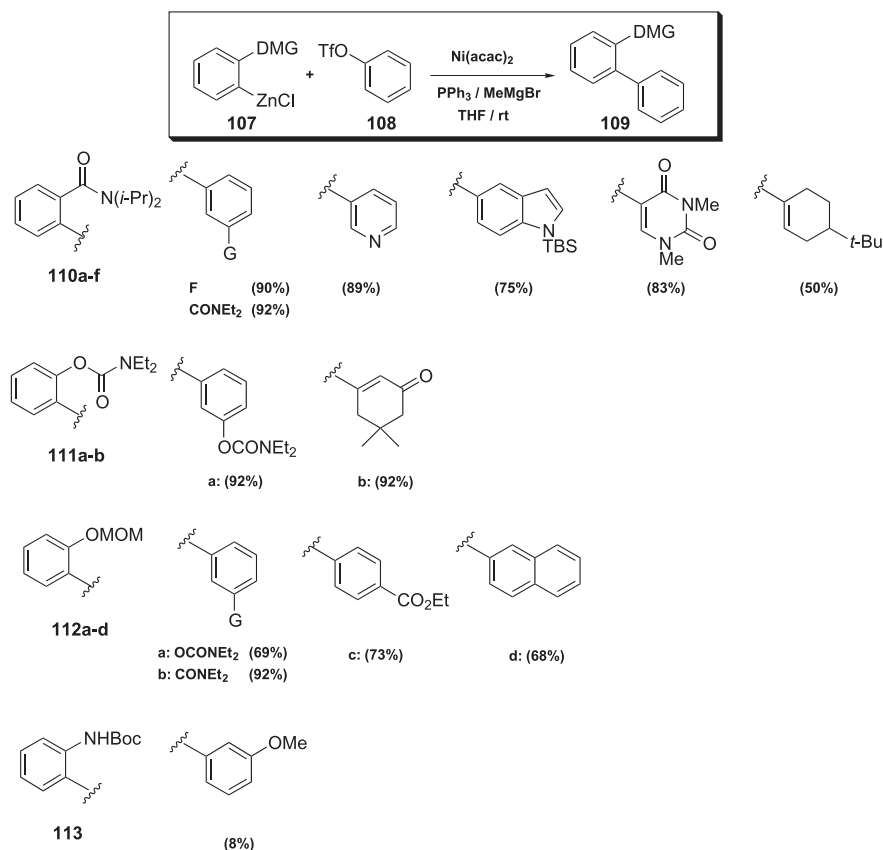
Scheme 32. Indole 5-O-carbamate-Grignard cross-coupling; annelation via indole 4,5-quinodimethide.



100 and using 2 equivalents of alkyllithium (obligatory) resulted in the development of this new DMG not only *per se* (**101**) but also, via Newman–Kwart rearrangement (**102**), as a precursor to the S-thiocarbamates **103** (Scheme 33). Systems **103**, upon hydrolysis, lead to *ortho*-substituted thiophenols **104** that are not easily accessible by electrophilic substitution reactions [55, 58]. While the O-thiocarbamate **100** could not be persuaded to cross-couple with RMgX reagents, the S-thiocarbamate **105** successfully undergoes coupling with Grignards to give **106**. The further development of this O-thiocarbamate–S-thiocarbamate connection may lead to its advantageous use in overcoming the poor DMG qualities of other sulfur groups (SH, SR), the cross-coupling chemistry of which has already been defined by the extensive work of Wenkert [59].

The DoM–Negishi Cross-Coupling Connection

A most important advantage of organozinc over organomagnesium reagents is the compatibility of the former with a variety of functional groups: CHO, COR, CN, NO₂, CO₂R, CONR₂. Thus, the DoM–Negishi cross-coupling reaction with aryl triflates, **107** + **108** → **109**, provides a rich array of aromatic and heteroaromatic products (Scheme 34) [60]. The selected cases illustrate unreactivity of O-carbamates, thus providing opportunity for tuning in the RMgX cross-coupling partner subsequent to the triflate-RZnX coupling (**111a**); the preparation of a number of products which are predisposed for further DoM chemistry (e.g. **111a**, **112a**); compatibility of the ester functionality (**112c**), and the difficulty of *ortho*-N-



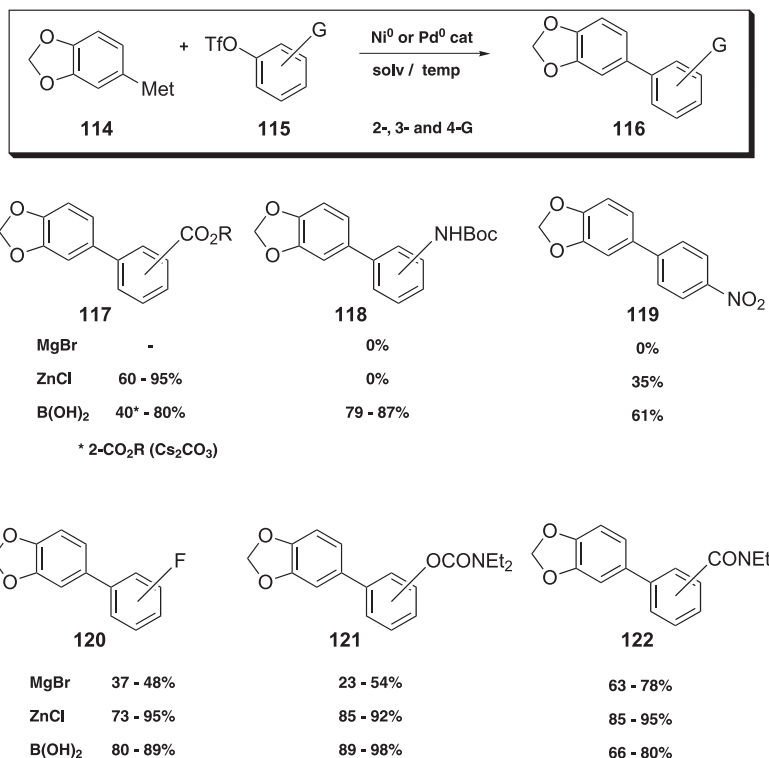
Scheme 34. The DoM–Negishi cross-coupling connection.

Boc organozinc coupling (**113**) presumably due to stability of the incipient *ortho*-zinc intermediate.

10.4.4

DoM–Derived Cross-Coupling Reactions. Synthetic Comparison of Boron, Zinc, and Magnesium Coupling Partners

The literature explosion of new methodologies demand comparisons for the purpose of application and further exploitation. For the Suzuki–Miyaura, Corriu–Kumada, and Negishi processes, qualitative comparison of synthetic value (Scheme 35) [60b] suggests synthetic advantage of the Suzuki–Miyaura and Negishi processes. Thus, in a prototype study, **114** + **115** → **116**, even outside of the context of DoM chemistry, the coupling of triflates bearing esters (**117**), *N*-Boc (**118**), and nitro (**119**) groups fail with Grignard partners and give modest yields with fluoro (**120**) and *O*-carbamate (**121**) aromatics. On the other hand, arylzincs and arylboronic acids provide good to excellent yields of biaryls with two exceptions:



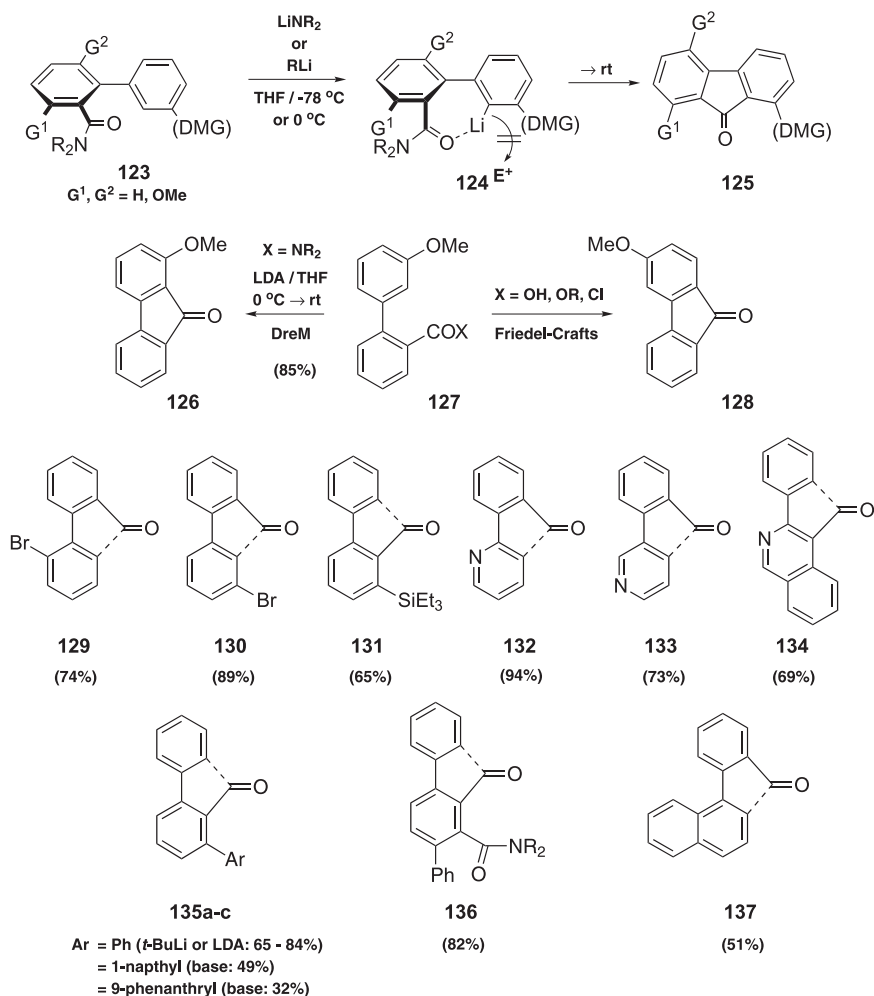
Scheme 35. Qualitative comparison of the Suzuki–Miyaura, Corriu–Kumada, and Negishi processes.

in Negishi couplings, the triflate from *N*-Boc aniline fails (**118**), possibly due to the presence of acidic N–H in the coupling partner, and that derived from the nitrobenzene derivative (**119**) is modestly successful, probably due to the incompatibility of zinc reagents with nitro groups; in the case of Suzuki–Miyaura coupling of triflate of a benzoate (**117**), the use of Cs₂CO₃ rather than Na₂CO₃ avoids ester hydrolysis, an apparently detrimental aspect in obtaining good yields in this coupling reaction.

10.5

Beyond DoM: The Directed Remote Metalation (DreM) of Biaryl Amides and O-Carbamates – New Methodologies for Condensed Aromatics and Heteroaromatics

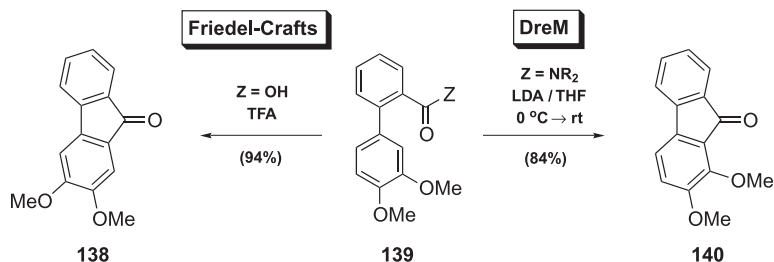
The Complex-Induced Proximity Effect (CIPE), suggested over 15 years ago [61, 62] to rationalize significant effects of strong coordination of donor substituents with organometallic reagents in enhancement of acidity at remote, non-thermodynamic sites, was the concept responsible for the discovery of DreM reactivity in biaryl amides (Scheme 36). A general reaction was developed in which biaryl amide **123**, upon treatment with LDA, in spite of availability of *ortho* hydrogens, G¹ = H, underwent deprotonation on the alternate ring to generate a species (**124**) that could not be trapped by external electrophiles, but led to fluo-



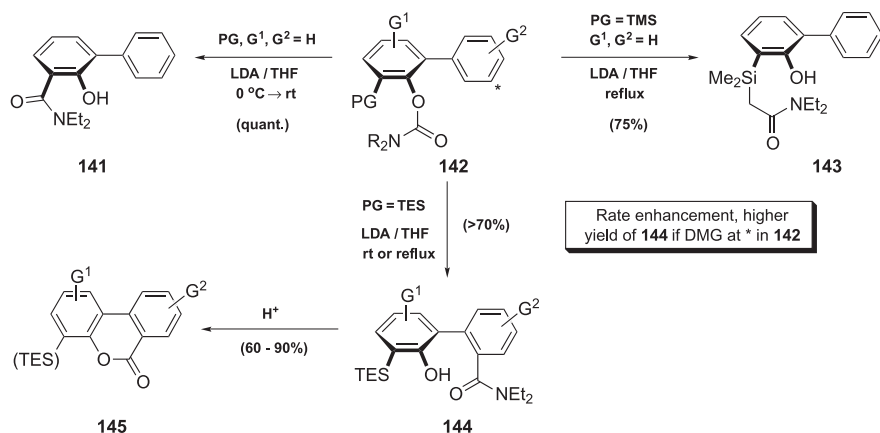
Scheme 36. Biaryl amide DreM. Versatile anionic Friedel–Crafts complements for assemblage of fluorenones and azafluorenones.

renone **125** (Scheme 36) [62, 63]. The scope of the reaction (**129–137**), its regioselectivity dictated by DMGs, and its complementarity to the classical Friedel–Crafts reaction on a small scale ($126 \leftarrow 127 \rightarrow 128$) and in industrial practice for the preparation of protein kinase inhibitors $138 \rightarrow 139 \rightarrow 140$ (Scheme 37) [64] are indicative of the further potential of this DreM process. The ready availability of precursor biaryls via Suzuki–Miyaura chemistry is a further advantage of this “beyond DoM” reaction.

The similarly and equally accessible biaryl O-carbamate **142** (Scheme 38) requires *ortho* substitution (PG = OMe) or protection (PG = SiEt₃) to avoid anionic *ortho* Fries rearrangement (**141**) and to launch a DreM pathway leading to **144** using LDA under vigorous conditions [65]. For PG = TMS, carbamoyl migration to the incipient α -silylmethyl anion occurs



Scheme 37. Friedel–Crafts/DreM complementarity. Synthesis of protein kinase inhibitors.

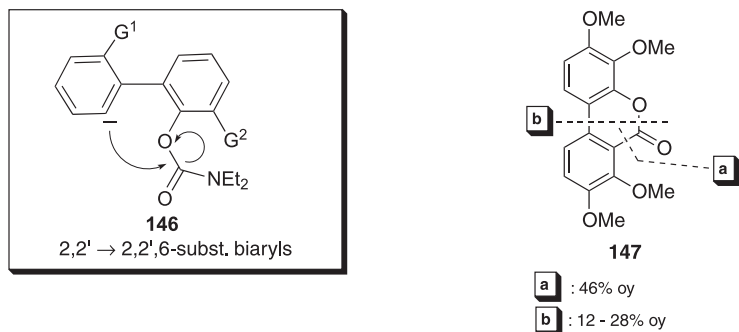


Scheme 38. Biaryl O-carbamate DreM. Ring-to-ring carbamoyl transfer. Synthesis of dibenzo[*b,d*]pyran-6-ones.

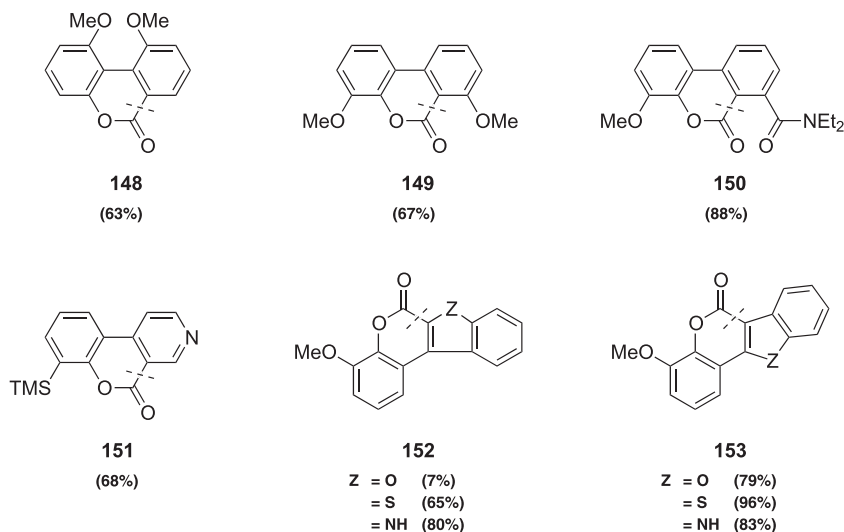
in good yield to give **143**, an observation also rationalized by CIPE [61, 62]. Acid-catalyzed cyclization of **144** leads to dibenzo[*b,d*]pyran-6-ones **145**, constituting a new route to this class of heterocycles.

This anionic remote Fries rearrangement provides a general route to highly substituted biaryls **146** which, due to steric effects, may be difficult to prepare directly by Suzuki–Miyaura cross-coupling, as evidenced in the comparison with the synthesis of dibenzopyranones **147** (Scheme 39) [66]. The efficient acid-catalyzed cyclization to dibenzopyranones shows broad scope both for unusually substituted (**148–150**, Scheme 40) and various heterocyclic analogues (**151–153**, Scheme 40) [65, 67].

A rational extension of *ortho*-tolyl benzamide metalation [68], part of the broadly encompassing lateral metalation protocol [69] that can be DoM-connected, is the DreM equivalent, **154** → **155** (Scheme 41), which provides a general regioselective route to 9-phenanthrols (**156**, **157**, **158**) [70] and may be extended to diaryl nitriles, hydroxylamine ethers, and hydrazones **160**, which provide the corresponding 9-amino derivatives **161** of similar generality **162–165** (Scheme 42), as may also be applied in natural product synthesis [71]. Further opportunities for DoM–cross-coupling and reduction/oxidation chemistry (**159**) have also been demonstrated [70a].



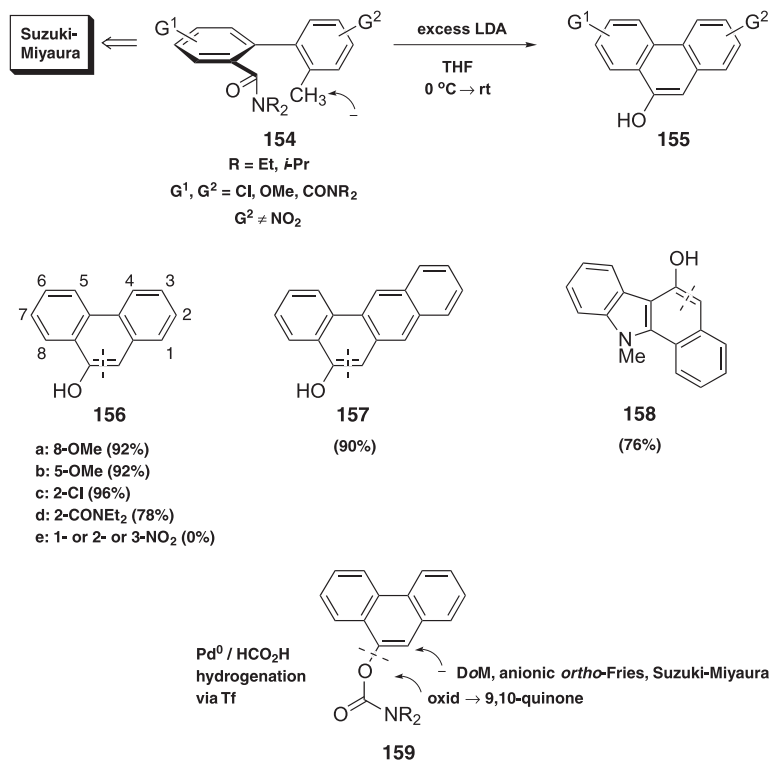
Scheme 39. Biaryl *O*-carbamate anionic remote Fries rearrangement. Conquering steric encumbrance in direct Suzuki–Miyaura cross-coupling.



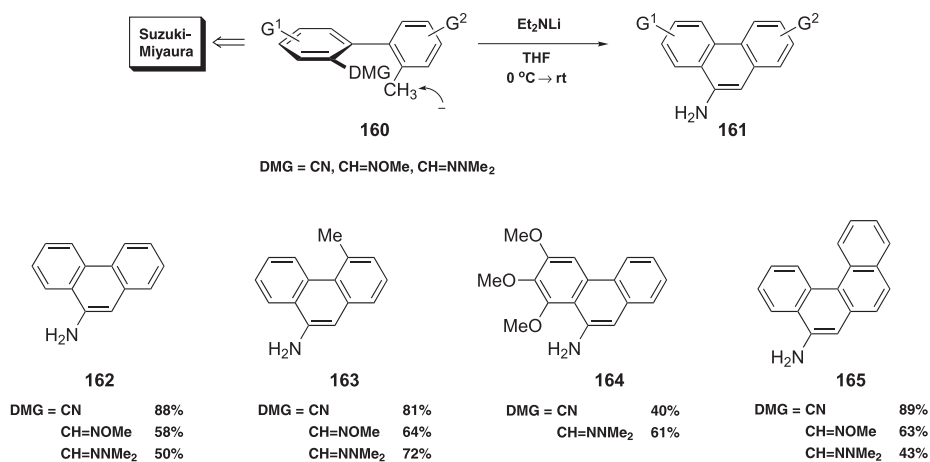
Scheme 40. Dibenzopyranones and heterocyclic analogues by anionic remote Fries rearrangement.

Are the above DreM tactics feasible in tandem? A preliminary but affirmative answer is possible. Thus, the biaryl *O*-carbamate migration–amide cyclization sequence **166** \rightarrow **167** \rightarrow **168** (Scheme 43), which conceptually constitutes a reaction of a biaryl 2,2'-dianion with a carbonyl dication equivalent (**169**), has found application in natural product synthesis [65, 72].

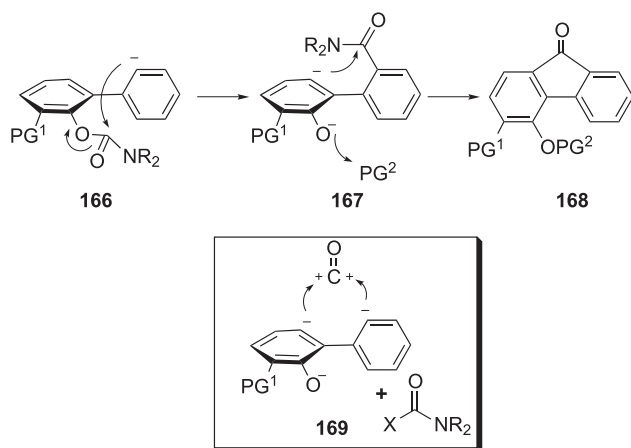
A different sequential DreM pathway involving *O*-carbamate ring switch–vinylogous tolyl amide cyclization, **170** \rightarrow **171** \rightarrow **172** (Scheme 44), a formal bridging of a 2,2'-methyl diaryl dicarbanion with a carbonyl dication equivalent (**173**) has been affirmed in a model study (**174** \rightarrow **175**, Scheme 45) [73] and applied in natural product total synthesis [73, 74].



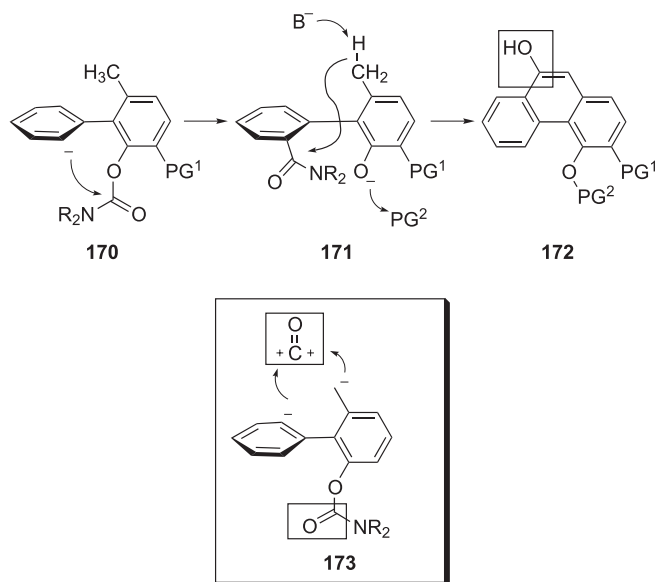
Scheme 41. Synthesis of 9-phenanthrols by DreM chemistry.



Scheme 42. Synthesis of 9-amino phenanthrenes by DreM.



Scheme 43. Synthesis of fluorenones by tandem remote metalation–amide DMG translocation.

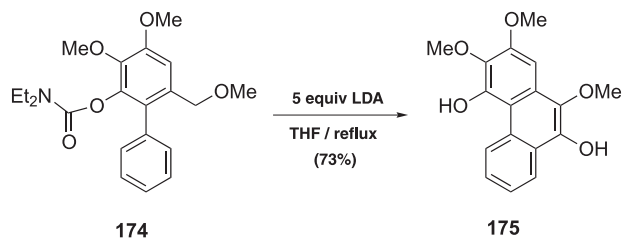


Scheme 44. Synthesis of 9-phenanthrols by tandem remote metalation–amide DMG ring-to-ring translocation.

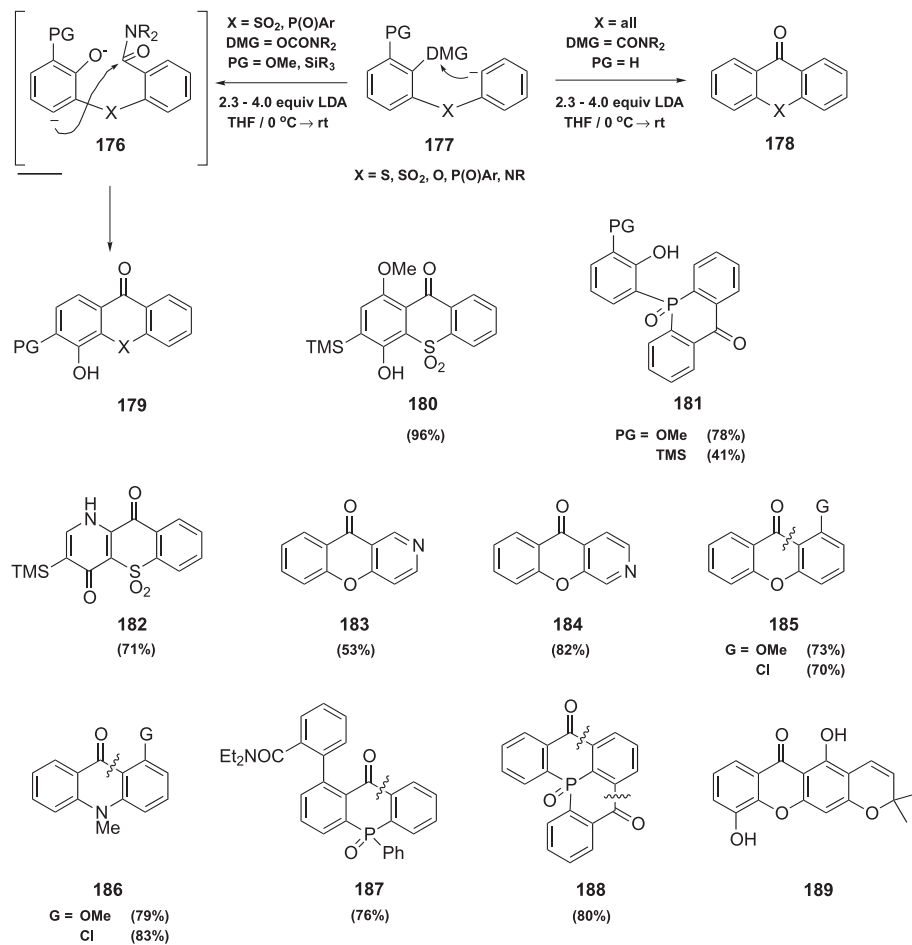
10.5.1

Heteroatom-Bridged Biaryl DreM. General Anionic Friedel–Crafts Complements for Several Classes of Heterocycles

The mental insertion of a heteroatom X into the biaryl motif **177** also provokes questions of DreM-mediated chemistry (Scheme 46). In response, treatment of all heteroatom X de-



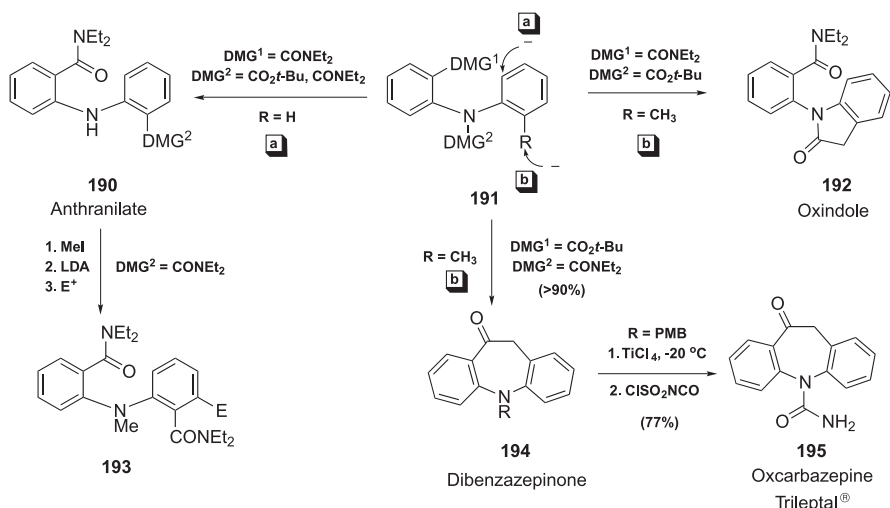
Scheme 45. Sequential remote metalation amide DMG translocation. A model study.



Scheme 46. Heteroatom-bridged diaryl DreM routes to heterocycles.

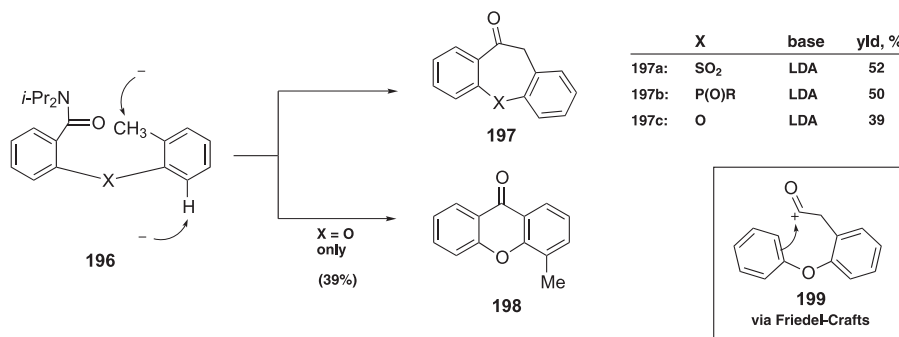
rivatives **177**, without *ortho* protection, with excess LDA provides routes to thioxanthenes, xanthenes, acridones, and dibenzophosphorinones **178**, while the application of very similar conditions to diaryl sulfone and diaryl phosphite systems **177**, X = SO₂ and X = P(O)Ph, with appropriate protection PG = OMe, SiR₃, results in ring-to-ring carbamoyl migration *and*, via **176**, anionic ring-closure to more highly functionalized dibenzophosphorinones and thioxanthenes **179**, e.g. **180** and **181** [75]. A plethora of heterocycles in all series are thus readily derived with useful and unusual features: following phenol protection, the thioxanthone **180** undergoes *ipso*-iododesilylation to give a derivative poised for coupling chemistry; the new heterocycle azathioxanthone **182** is available; azaxanthenes, for example **183** and **184**, are rapidly prepared from readily available starting materials; consistently, Friedel–Crafts complementarity is observed for product xanthenes **185** and acridones **186** obtained from precursors bearing DMGs *ortho* to the incipient anionic site; in the P-heteroatom series, preferred phosphorinone over fluorenone (**187**) and double DreM cyclization (**188**) pathways are observed. The availability of precursors by DoM (diaryl sulfones, diaryl phosphites) and DoM–Buchwald–Hartwig and Ullmann Pd-catalyzed coupling reactions (diaryl amines, diaryl ethers) reinforces the convenience of the synthetic pathways to these heterocycles, including natural products [47, 75b, 75c], e.g. 9-deoxyjacarubein (**189**).

In the diaryl amine series **191** (Scheme 47), additional, synthetically valuable, anionic pathways provide routes to anthranilates **190**, oxindoles **192**, and dibenzazepinones **194**. Although not explored in terms of its scope [75c], the lateral metalation–cyclization, **191** → **192**, is extensively precedented [69] but harbors intriguing potential for subsequent DreM chemistry. The rearrangement **191** → **190** is an *N* → *ortho* C anionic Fries equivalent of the aryl *O*-carbamate migration (Scheme 3E) [75c] and after *N*-methylation, **190** may be transformed into 1,2,3-trisubstituted systems **193** [76]. In another appealing manifestation of CIPE, the efficient conversion of **191** into dibenzazepinone **194** has been applied in an effective synthesis of the antiepileptic drug oxcarbazepine (Trileptal®) **195** [77] and may also be



Scheme 47. Anionic pathways to oxindoles, anthranilates, and dibenzazepinones.

extended regioselectively, with one exception (**196** → **197c** + **198**), to the formation of dibenzthiepinone dioxide **197a** and dibenzophosphorinone **197b** (Scheme 48) [75b–d]. The complementarity to Friedel–Crafts technology (e.g. **199**) is thus also established for these tricyclics, some of which have long-standing biological interest.

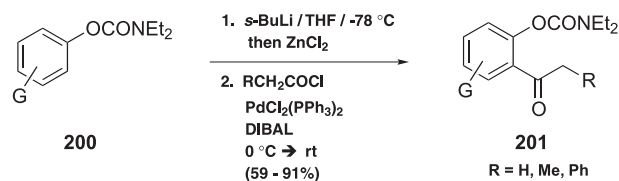


Scheme 48. Synthesis of dibenzthiepinone dioxide, dibenzoxepinone, and dibenzphosphorinone.

10.6

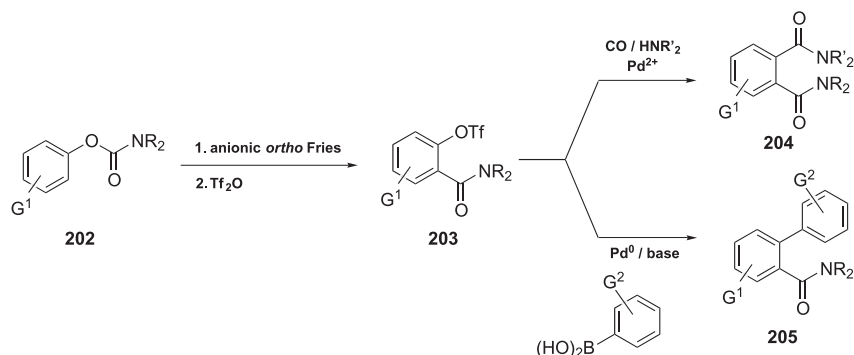
Interfacing DoM with Emerging Synthetic Methods

In the last quarter-century, the practice and art of organic synthesis has been revolutionized by the discovery of transition metal catalyzed organic transformations, “at a rate that would make the discoverer of islands in the St. Lawrence Seaway envious” [78]. Aside from the demonstrated DoM–Ar–Ar cross-coupling connection above and the initial promise of acylative, **200** → **201** (Scheme 49) [79] and carbonylative, **202** → **203** → **204** or Suzuki–Miyaura, **203** → **205** (Scheme 50) [80] coupling, the establishment of potential DoM links to the literature-visible, already reliable, but not yet mature Heck, Sonogashira, and Grubbs metatheses will undoubtedly reap benefits for synthetic aromatic and heteroaromatic chemistry.

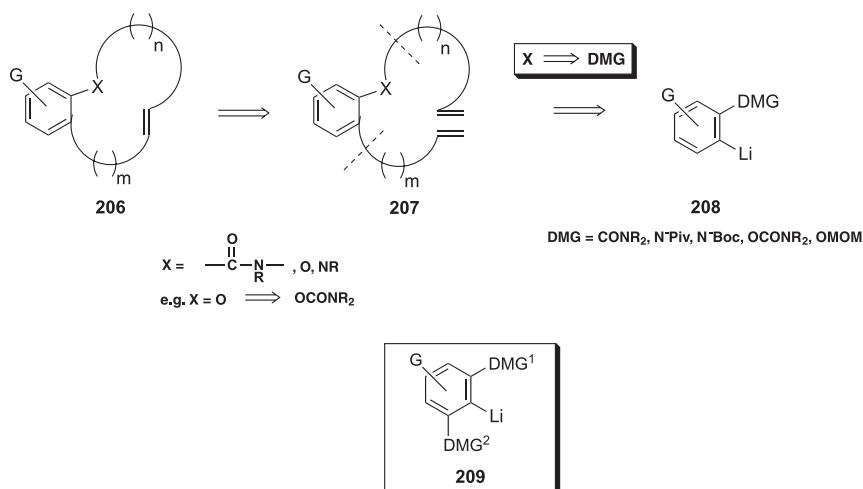


Scheme 49. DoM-acylative Negishi cross-coupling of aryl O-carbamates.

In this context, to tempt the synthetic practitioner’s palate, a general Grubbs ring-closing metathesis (RCM) retrosynthetic analysis may be envisaged for aromatic ring-annulated targets **206** (Scheme 51), which cascades, via **207**, to simple *ortho*-lithiated species **208**. Such starting points offer diverse DMG potential to be either directly or, with modification, incorporated into **206** and the tactic may lend itself to consideration of synergistic effects of double-DMG containing precursors **209**.

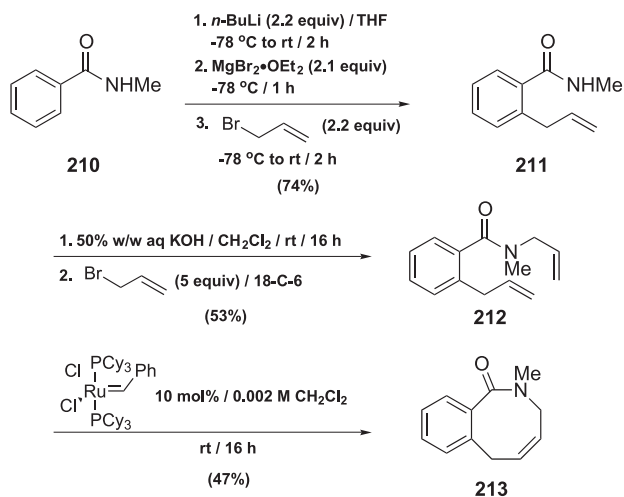


Scheme 50. DoM–amidocarbonylation and Suzuki–Miyaura cross-coupling connections.

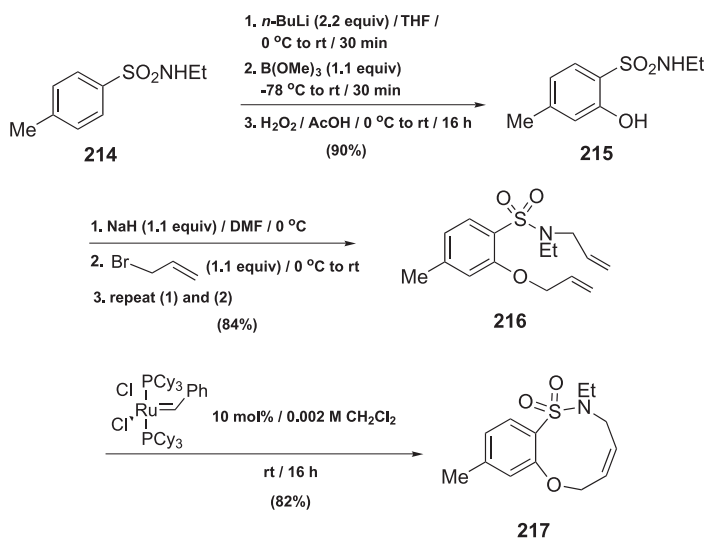


Scheme 51. DoM–Grubbs ring-closing metathesis connections.

Towards these ends, aside from the demonstration of use of the DoM–RCM strategy in natural product synthesis [81], prototype sequences leading to benzazocinone **213** (Scheme 52), macrocyclic ether sulfonamide **217** (Scheme 53), and thiazepine **222** (Scheme 54) have been accomplished [82]. Thus, in the first series, **210** is subjected to DoM–transmetalation, which allows efficient allylation of the incipient Grignard reagent to give **211**. *N*-Allylation to **212** followed by RCM using the popular Grubbs Ru-carbene catalyst affords **213**. In the second sequence, *para*-tolyl sulfonamide **214** metalation followed by the boronation–oxidation sequence to introduce an OH^+ synthetic equivalent leads to **215**, which, by double allylation to give **216** and RCM affords the new heterocyclic system **217**. In the third but undoubtedly not last series, Sonogashira coupling of the DoM-derived sulfonamide **218** furnishes **219**, which, after desilylation (**220**) and allylation gives **221**. Grubbs metathesis of **221**, constitut-

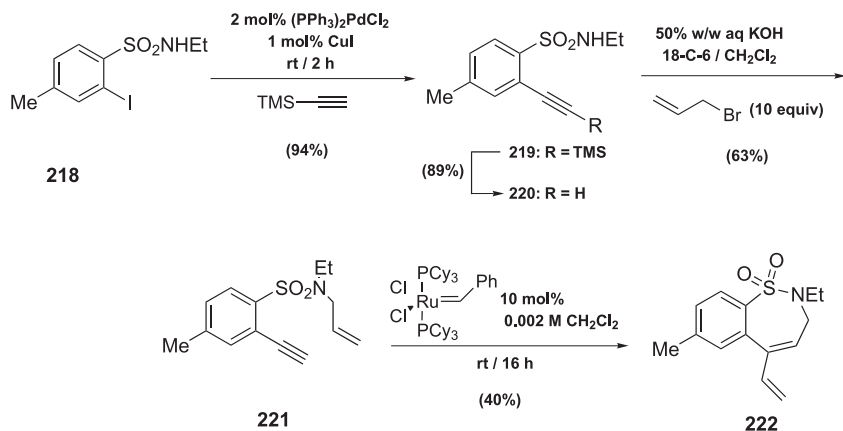


Scheme 52. Benzoazocine system via DoM–Grubbs ring-closing metathesis (RCM) connections.



Scheme 53. Macrocyclic sulfonamide via DoM–RCM.

ing an example of the still relatively unexplored ene–yne RCM, gives **222** in modest yield. The ease with which simple ring systems (**213**), classical syntheses of which appear not to have been described, and bizarre systems (**217**) are available, and the fact that some derived products are obviously useful for venerable follow-up reactions (**222**), offers invitations for further methodological studies, which may lead to opportunities that are greater than their individual sum.



Scheme 54. Benzthiazepine dioxides via DoM–RCM.

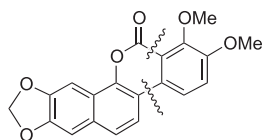
10.7

Closing Comments

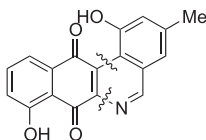
Although the DoM strategy has undergone remarkable development and unexpected industrial application since the systematic work of Hauser [83], it continues in unbridled evolution. This account has attempted to show a) the value of the *ortho*-lithiated DMG species for the regiospecific preparation of polysubstituted aromatics and heteroaromatics, b) the transition metal catalyzed cross-coupling–DoM symbiosis, c) with the availability of biaryls, the extension of DoM to the DreM tactic with the ensuing benefits for the construction of condensed aromatics, and d) the early indications of DoM links to other modern methodologies of synthetic significance. The decision to concentrate on methods and processes prevented discussion of total syntheses endeavors in which the DoM–DreM–cross-coupling trio plays, to various extents, a key role (Scheme 55). While convenience and reasonable temperatures in large-scale DoM remain to be established, mechanistic insight is advancing [10, 62a], new DMGs are being uncovered and, perhaps most significantly, reactions of other aryl metals species (B, Zn, Mg, Sn), derived by transmetalation from Li and with potential for catalytic processes, appear to be rapidly growing [84]. Although written prognosis is dangerous [85], DoM chemistry continues to offer routes to polysubstituted aromatics and heteroaromatics which, at times, are complementary, at other times, highly advantageous, and often unique compared to classical and previous methodologies. There is no defined rubric for organic synthesis and the DoM-derived chemistry waiting to be discovered will be as useful as the eye and experience of the practitioner.

Acknowledgements

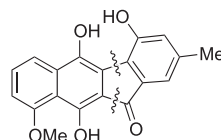
Since the transition from the University of Waterloo to Queen's (350 km = 219 miles), synthetic chemistry according to DoM continues apace in our laboratories due to a group of lively and dedicated students and postdoctoral fellows. They make going to the lab each day

**Arnottin I**

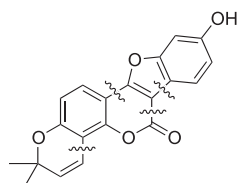
James, C. *Ph.D. Thesis* **1998**
University of Waterloo, Canada

**Phenanthroviridin**

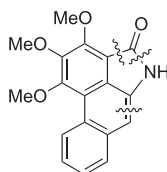
J. Org. Chem. **1997**, 7072

**Kinafluorenone**

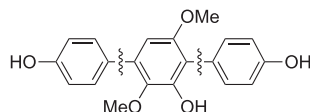
J. Org. Chem. **1997**, 7072

**Plicadin**

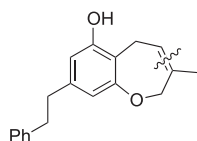
Angew. Chem. **1999**, 1435

**Piperolactam C**

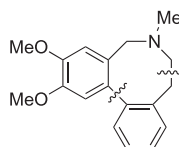
Tetrahedron Lett. **1998**, 4175

**Terphenyllin**

Campbell, M. *Ph.D. Thesis* **1996**
University of Waterloo, Canada

**Radulanin A**

J. Org. Chem. **1997**, 7072

**Buflavine**

Tetrahedron Lett. **1998**, 1325

Scheme 55. Some natural products recently conquered by combined DoM–DreM–cross-coupling strategies.

an exciting prospect and NSERC Canada and CSC Consortium (Combinatorial Chemistry), through support of fundamental synthetic work, make it feasible. C. G. H. thanks the Alexander von Humboldt Foundation for a Feodor Lynen Fellowship.

References

- 1 a) O. T. BENTLEY, *From Vital Force to Structural Formulas*, Houghton Mifflin Co., Boston, **1964**, p. 101 ff; b) M. J. McBRIDE, *Tetrahedron* **1974**, 30, 2009–2035.
- 2 a) L. M. STOCK, *Aromatic Substitution Reactions*, Prentice-Hall Inc., Englewood Cliffs, New York, **1968**; b) R. TAYLOR, in *Electrophilic Aromatic Substitution*, Wiley, New York, **1990**, p. 236.
- 3 a) F. TERRIER, *Nucleophilic Aromatic Displacement – Organic Nitro Chemistry*, John Wiley & Sons, New York, **1991**; b) R. A. ROSSI, R. H. ROSSI, *Aromatic Substitution by $S_{RN}1$ Mechanism*, American Chemical Society, Oxford University Press, New York, **1983**.
- 4 a) S. WARREN, *Organic Synthesis: The Disconnection Approach*, Wiley, New York, **1982**, p. 6–15; b) R. O. C. NORMAN, *Principles of Organic Synthesis*, 2nd Ed., Chapman and Hall, London, **1993**, p. 367–453; c) however, for an enlightening, textual “retrosynthetic” treatment before the term was coined, see J. B. HEDRICK-

- SON, D. J. CRAM, G. S. HAMMOND, *Organic Chemistry*, 3rd Ed., McGraw-Hill, New York, 1970, p. 683 ff.
- 5 a) M. B. SMITH, *Organic Synthesis*, 2nd Ed., McGraw-Hill, Columbus, OH, 2001; b) D. T. DAVIES, *Aromatic Heterocyclic Chemistry*, Oxford University Press, New York, 1997, p. 17–18; c) M. SAINSBURY, *Aromatic Chemistry*, Oxford University Press, New York, 1992, p. 45–46.
 - 6 The 1995 Aldrich catalogue lists 875 monosubstituted benzenes (44 with an alkyl carbon atom and 831 with a carbon other than alkyl or a heteroatom as the direct link); 407 1,2-disubstituted, 243 1,2,3-trisubstituted, and 65 1,2,3,4-tetra-substituted benzenes. We thank Dr. S. J. Branca, Aldrich Chemical Co., for this information.
 - 7 F. FRINGUELLI, A. TATICCHI, *The Diels–Alder Reaction*, John Wiley & Sons, New York, 2002.
 - 8 P. BAMFIELD, P. F. GORDON, *Chem. Soc. Rev.* 1984, 13, 441–488.
 - 9 For selective reviews, see: a) V. SNIIECKUS, *Chem. Rev.* 1990, 90, 879–933; b) L. GREEN, B. CHAUDER, V. SNIIECKUS, *J. Heterocycl. Chem.* 1999, 36, 1453–1468; c) A. LARKIN, V. SNIIECKUS, *FMC LithiumLink* 2000, Winter; d) F. MONGIN, G. QUÉGUINER, *Tetrahedron* 2001, 57, 4059–4090; e) A. TURCK, N. PIE, F. MONGIN, G. QUÉGUINER, *Tetrahedron* 2001, 57, 4489–4506; f) T. R. ELWORTHY, A. I. MEYERS, *Tetrahedron* 1994, 50, 6089–6096; g) for practical aspects, see L. BRANDSMA, in *Houben-Weyl, Methoden der Organischen Chemie*, Vol. E19d (Ed.: M. HANACK), Thieme Verlag, Stuttgart, 1993, p. 369–447.
 - 10 S. T. CHADWICK, R. A. RENNELS, J. L. RUTHERFORD, D. B. COLLUM, *J. Am. Chem. Soc.* 2000, 122, 8640–8647 and references cited therein.
 - 11 C. METALLINOS, S. NERDINGER, V. SNIIECKUS, *Org. Lett.* 1999, 1, 1183–1186.
 - 12 For other transformations of secondary and tertiary sulfonamide DMG systems which undoubtedly would be beneficially transferred to the *N*-cumyl sulfonamide DMG, see: S. L. MACNEIL, O. B. FAMILONI, V. SNIIECKUS, *J. Org. Chem.* 2001, 66, 3662–3670.
 - 13 a) P. BEAK, A. TSE, J. HAWKINS, C.-W. CHEN, S. MILLS, *Tetrahedron* 1983, 39, 1983–1989; b) C. QUESNELLE, T. IIHAMA, T. AUBERT, H. PERRIER, V. SNIIECKUS, *Tetrahedron Lett.* 1992, 33, 2625–2628.
 - 14 *N*-Cumyl planar chiral ferrocenes, also prepared by DoM chemistry, lead to useful new ferrocenyl derivatives: C. METALLINOS, V. SNIIECKUS, in preparation.
 - 15 a) B. BENNETAU, J. MORTIER, J. MOYROUD, J.-L. GUESNET, *J. Chem. Soc., Perkin Trans. 1* 1995, 1265–1272; b) J. MOYROUD, J.-L. GUESNET, B. BENNETAU, J. MORTIER, *Tetrahedron Lett.* 1995, 36, 881–884; c) J. MORTIER, J. MOYROUD, B. BENNETAU, P. A. CAIN, *J. Org. Chem.* 1994, 59, 4042–4044.
 - 16 Y. KONDO, M. SHILAI, M. UCHIYAMA, T. SAKAMOTO, *J. Am. Chem. Soc.* 1999, 121, 3539–3540.
 - 17 a) J. M. HAWKINS, *J. Org. Chem.* 1998, 63, 2054–2055; b) A. L. GREEN, *M.Sc. Thesis*, Queen's University of Kingston, Canada, 2001; c) J. KRISTENSEN, M. LYSÉN, P. VEDS, M. BEGTRUP, *Org. Lett.* 2001, 3, 1435–1437.
 - 18 M. GRAY, B. J. CHAPPELL, J. FELDING, N. J. TAYLOR, V. SNIIECKUS, *Synlett* 1998, 422–424.
 - 19 J. A. JOULE, K. MILLS, *Heterocyclic Chemistry*, 4th Ed., Blackwell Science, Oxford, 2000.
 - 20 a) H. W. GSCHWEND, H. R. RODRIGUEZ, *Org. React.* 1979, 26, 1–360; b) B. L. FERINGA, R. HULST, R. RIKERS, L. BRANDSMA, *Synthesis* 1988, 316–318; c) F. M. DEAN, *Adv. Heterocyclic Chem.* 1982, 30, 167–238; d) F. M. DEAN, *Adv. Heterocyclic Chem.* 1982, 31, 237–344; e) G. W. NEWCASTLE, A. R. KATRITZKY, *Adv. Heterocyclic Chem.* 1993, 56, 155–302.
 - 21 a) D. W. KNIGHT, A. P. NOTT, *Tetrahedron Lett.* 1980, 21, 5051–5054; b) D. W. KNIGHT, A. P. NOTT, *J. Chem. Soc., Perkin Trans. 1* 1981, 1125–1131; c) D. W. KNIGHT, A. P. NOTT, *J. Chem. Soc., Perkin Trans. 1* 1983, 791–794; d) A. J. CARPENTER, D. J. CHADWICK, *Tetrahedron Lett.* 1985, 26, 1777–1780; e) A. J. CARPENTER, D. J. CHADWICK, *Tetrahedron Lett.* 1985, 26, 5335–5338.
 - 22 C. P. DELL, D. W. KNIGHT, *J. Chem. Soc., Chem. Commun.* 1987, 349–50.
 - 23 J. CUOMO, S. K. GEE, S. C. HARTZELL, in *Synthesis and Chemistry of Agrochemicals II*

- (Eds.: D. R. BAKER, J. G. FEYNES, W. K. MOBERG.), ACS Symposium Series No. 443, ACS, Washington D.C., 1990.
- 24 S. L. GRAHAM, T. H. SCHOLZ, *J. Org. Chem.* **1991**, 56, 4260–4263.
 - 25 a) A. R. KATRITZKY, J. N. LAM, S. SENGUPTA, G. W. REWCASTLE, in *Progress in Heterocyclic Chemistry*, Vol. 1 (Eds.: H. SUSCHITZKY, E. F. V. SCRIVEN), Pergamon Press, Oxford, **1989**, p. 1–29; b) A. R. KATRITZKY, C. W. REES, E. F. V. SCRIVEN, *Comprehensive Heterocyclic Chemistry II*, Pergamon Press, Oxford, **1996**; c) A. R. KATRITZKY, K. AKUTAGAWA, *Org. Prep. Proc. Int.* **1988**, 20, 585–590; d) W. CHEN, M. P. CAVA, *Tetrahedron Lett.* **1987**, 28, 6025–6026; e) M. P. EDWARDS, A. M. DOHERTY, S. V. LEY, H. M. ORGAN, *Tetrahedron* **1986**, 42, 3723–3730; f) D. J. CHADWICK, D. S. ENNIS, *Tetrahedron* **1991**, 47, 9901–9914; g) M. NAKAMURA, K. HARA, G. SAKATA, E. NAKAMURA, *Org. Lett.* **1999**, 1, 1505–1507; h) J.-H. LIU, Q.-C. YANG, T. C. W. MAK, H. N. C. WONG, *J. Org. Chem.* **2000**, 65, 3587–3595; i) T. GRIMALDI, M. ROMERO, M. D. PUJOL, *Synlett* **2000**, 1788–1792; j) D. J. CHADWICK, D. S. ENNIS, *Tetrahedron* **1991**, 47, 9901–9914; k) D. L. COMINS, M. O. KILLPACK, *J. Org. Chem.* **1987**, 52, 104–109.
 - 26 a) R. J. SUNDBERG, *Indoles*, 2nd Ed., Academic Press, San Diego, CA, **1996**; b) G. W. GRIBBLE, in *Adv. Heterocyclic Nat. Prod. Synthesis*, Vol. 1 (Ed.: W. H. PEARSON), JAI Press, Greenwich, CT, **1990**, p. 43–94; c) G. W. GRIBBLE, *Synlett* **1991**, 289–300; d) D. L. COMINS, *Synlett* **1992**, 615–625.
 - 27 C. D. BUTTERY, R. G. JONES, D. W. KNIGHT, *Synlett* **1991**, 315–316.
 - 28 M. IWAO, *Heterocycles* **1993**, 36, 29–32.
 - 29 T. FUKUDA, R. MAEDA, M. IWAO, *Tetrahedron* **1999**, 55, 9151–9162.
 - 30 B. J. CHAPEL, V. SNIIECKUS, unpublished results.
 - 31 M. IWAO, T. KURAISHI, *Heterocycles* **1992**, 34, 1031–1038.
 - 32 K. S. BHANDARI, V. SNIIECKUS, *Synthesis* **1971**, 327.
 - 33 B. CHAUDER, A. LARKIN, V. SNIIECKUS, *Org. Lett.* **2002**, in press.
 - 34 E. J. GRIFFEN, D. G. ROE, V. SNIIECKUS, *J. Org. Chem.* **1995**, 60, 1484–1485.
 - 35 E. J. GRIFFEN, D. G. ROE, V. SNIIECKUS, unpublished results.
 - 36 a) T.-L. SHING, W.-L. CHIA, M.-J. SHIAO, T.-Y. CHAU, *Synthesis* **1991**, 849–850 and references cited therein; b) D. L. COMINS, S. O'CONNOR, *Adv. Heterocyclic Chem.* **1988**, 44, 199–267.
 - 37 D. SPITZNER, in *Houben-Weyl, Methoden der Organischen Chemie*, Vol. E7b (Ed.: R. P. KREHER), Thieme Verlag, Stuttgart, **1992**, p. 286–686, especially p. 595.
 - 38 F. MONGIN, F. TRÉCOURT, G. QUÉGUINER, *Tetrahedron Lett.* **1999**, 40, 5483–5486.
 - 39 D. L. COMINS, M. O. KILLPACK, *J. Org. Chem.* **1990**, 55, 69–73.
 - 40 M. A. J. MIAH, V. SNIIECKUS, *J. Org. Chem.* **1985**, 50, 5436–5438.
 - 41 J. FRÖLICH, in *Progress in Heterocyclic Chemistry*, Vol. 6 (Eds.: H. SUSCHITZKY, E. F. V. SCRIVEN), Pergamon Press, Oxford, **1994**, p. 1–35.
 - 42 a) C. COCHENNEC, P. ROCCA, F. MARSAIS, A. GODARD, G. QUÉGUINER, *Synthesis* **1995**, 321–324; b) P. ROCCA, C. COCHENNEC, F. MARSAIS, L. THOMAS-DIT-DUMONT, M. MALLET, A. GODARD, G. QUÉGUINER, *J. Org. Chem.* **1993**, 58, 7832–7838; c) F. GUILLIER, F. NIVOLIER, A. GODARD, F. MARSAIS, G. QUÉGUINER, *Tetrahedron Lett.* **1994**, 35, 6489–6492.
 - 43 See, *inter alia*, a) J. M. JACQUELIN, Y. ROBIN, A. GODARD, G. QUÉGUINER, *Can. J. Chem.* **1988**, 66, 1135–1140; b) J. M. JACQUELIN, F. MARSAIS, A. GODARD, G. QUÉGUINER, *Synthesis* **1986**, 670–672; c) A. GODARD, J.-M. JACQUELIN, G. QUÉGUINER, *J. Organomet. Chem.* **1988**, 354, 273–286.
 - 44 F. DIEDERICH, P. J. STANG, *Metal-Catalyzed Cross-Coupling Reactions*, Wiley-VCH, Weinheim, **1998**.
 - 45 E. J.-G. ANCTIL, V. SNIIECKUS, *J. Organomet. Chem.* **2002**, in press.
 - 46 A. SUZUKI, *J. Organomet. Chem.* **1999**, 576, 147–168.
 - 47 Review: S. L. MACNEIL, *Ph.D. Thesis*, Queen's University of Kingston, Canada, **2001**.
 - 48 a) J. YIN, M. P. RAINKA, X.-X. ZHANG, S. L. BUCHWALD, *J. Am. Chem. Soc.* **2002**, 124, 1162–1163; b) A. F. LITKE, C. DAI, G. C. FU, *J. Am. Chem. Soc.* **2000**, 122, 4020–4028; c) H. TOMORI, J. M. FOX, S. L. BUCHWALD, *J. Org. Chem.* **2000**, 65, 5334–5341.

- 49 Among which, the Pschorr, Ullmann, Meerwein, and Gomberg–Bachmann reactions were dominant, see, by name: *March's Advanced Organic Chemistry* (Eds.: M. B. SMITH, J. MARCH), 5th Ed., Wiley-Interscience, New York, 2001.
- 50 a) M. G. CAMPBELL, *Ph.D. Thesis*, University of Waterloo, Canada, 1996; b) C. M. UNRAU, M. G. CAMPBELL, V. SNIIECKUS, *Tetrahedron Lett.* 1992, 33, 2773–2776.
- 51 a) C. MODRAKOWSKI, S. C. FLORES, M. BEINHOFF, A. D. SCHLÜTER, *Synthesis* 2001, 2143–2155; b) P. BLANCHARD, A. CAPPON, E. LEVILLAIN, Y. NICOLAS, P. FRÈRE, J. RONCALI, *Org. Lett.* 2002, 4, 607–609.
- 52 S. CHAMOIN, S. HOULDSWORTH, C. G. KRUSSE, W. IWEMA BAKKER, V. SNIIECKUS, *Tetrahedron Lett.* 1998, 39, 4179–4182.
- 53 S. CHAMOIN, S. HOULDSWORTH, V. SNIIECKUS, *Tetrahedron Lett.* 1998, 39, 4175–4178.
- 54 S. SENGUPTA, M. LEITE, D. SOARES RASIAN, C. QUESNELLE, V. SNIIECKUS, *J. Org. Chem.* 1992, 57, 4066–4068.
- 55 K. A. PUUMALA, *M.Sc. Thesis*, University of Waterloo, Canada, 1997.
- 56 S. SENGUPTA, V. SNIIECKUS, unpublished results.
- 57 A. C. KINSMAN, V. SNIIECKUS, *Tetrahedron Lett.* 1999, 40, 2453–2456.
- 58 F. BEAULIEU, V. SNIIECKUS, *Synthesis* 1992, 112–118.
- 59 E. WENKERT, T. W. FERREIRA, E. MICHELOTTI, *J. Chem. Soc., Chem. Commun.* 1979, 637 and references cited therein.
- 60 a) C. A. QUESNELLE, O. B. FAMILONI, V. SNIIECKUS, *Synlett* 1994, 349; b) C. A. QUESNELLE, *Ph.D. Thesis*, University of Waterloo, Canada, 1996.
- 61 a) P. BEAK, A. I. MEYERS, *Acc. Chem. Res.* 1986, 19, 356–363; b) G. W. KLUMPP, *Recl. Trav. Chim. Pays-Bas* 1986, 105, 1–21.
- 62 For mechanistic and synthetic developments, see P. BEAK, M. WHISTLER, S. MACNEIL, V. SNIIECKUS, *Angew. Chem.* 2002, submitted.
- 63 J.-m. FU, B.-p. ZHAO, M. J. SHARP, V. SNIIECKUS, *J. Org. Chem.* 1991, 56, 1683–1685.
- 64 a) F. L. CISKE, W. D. JONES JR., *Synthesis* 1998, 1195–1198; b) W. D. JONES JR., F. L. CISKE, *J. Org. Chem.* 1996, 61, 3920–3922.
- 65 W. WANG, V. SNIIECKUS, *J. Org. Chem.* 1992, 57, 424–426.
- 66 B. I. ALO, A. KANDIL, P. A. PATIL, M. J. SHARP, M. A. SIDDIQUI, V. SNIIECKUS, *J. Org. Chem.* 1991, 56, 3763–3768.
- 67 C. JAMES, V. SNIIECKUS, unpublished results.
- 68 a) R. J. MILLS, V. SNIIECKUS, *J. Org. Chem.* 1989, 54, 4386–4390; b) R. J. MILLS, N. J. TAYLOR, V. SNIIECKUS, *J. Org. Chem.* 1989, 54, 4372–4385.
- 69 R. D. CLARK, A. JAHANGIR, *Org. React.* 1995, 47, 1–314.
- 70 a) J.-m. FU, V. SNIIECKUS, *Can. J. Chem.* 2000, 78, 905–919; b) J.-m. FU, M. J. SHARP, V. SNIIECKUS, *Tetrahedron Lett.* 1988, 29, 5459–5462.
- 71 L. BENESCH, P. BURY, D. GUILLANEUX, S. HOULDSWORTH, X. WANG, V. SNIIECKUS, *Tetrahedron Lett.* 1998, 39, 961–964.
- 72 S.-i. MOHRI, M. STEFINOVIC, V. SNIIECKUS, *J. Org. Chem.* 1997, 62, 7072–7073.
- 73 X. WANG, V. SNIIECKUS, *Tetrahedron Lett.* 1991, 32, 4879–4882.
- 74 X. WANG, V. SNIIECKUS, *Tetrahedron Lett.* 1991, 32, 4883–4884.
- 75 a) Thioxanthenes: F. BEAULIEU, V. SNIIECKUS, *J. Org. Chem.* 1994, 59, 6508–6509; b) Xanthenes: O. B. FAMILONI, I. IONICA, J. F. BOWER, V. SNIIECKUS, *Synlett* 1997, 1081–1083; c) Acridones: S. L. MACNEIL, M. GRAY, L. E. BRIGGS, J. J. LI, V. SNIIECKUS, *Synlett* 1998, 419–421; d) Phosphorinones: M. GRAY, B. J. CHAPEL, N. J. TAYLOR, V. SNIIECKUS, *Angew. Chem.* 1996, 108, 1609–1611; *Angew. Chem., Int. Ed. Engl.* 1996, 35, 1558–1560; e) for DreM routes to xanthenes and thioxanthenes via benzamide η^5 -cyclopentadienyl iron salts, see: J. P. STORM, R. D. IONESCU, D. MARTINSSON, C.-M. ANDERSSON, *Synlett* 2000, 975–978.
- 76 B. WILSON, *M.Sc. Thesis*, Queen's University, Canada, 2002, to be submitted.
- 77 O. LOHSE, U. BEUTLER, P. FÜNFSCILLING, P. FURET, J. FRANCE, D. KAUFMANN, G. PENN, W. ZAUGG, *Tetrahedron Lett.* 2001, 42, 385–389.
- 78 Stated with reference to the discovery of alkaloids in the early days by the eminent chemist R. H. F. Manske, see D. B. MACLEAN, V. SNIIECKUS, in *The Alkaloids* (Ed.: G. A. CORDELL), Academic Press, London, 1998, p. 3–59.

- 79 A. V. KALININ, A. J. M. DA SILVA, C. C. LOPES, R. S. C. LOPES, V. SNIIECKUS, *Tetrahedron Lett.* **1998**, 39, 4995–4998.
- 80 X. CAI, V. SNIIECKUS, unpublished results.
- 81 M. STEFINOVIC, V. SNIIECKUS, *J. Org. Chem.* **1998**, 63, 2808–2809.
- 82 C. LANE, V. SNIIECKUS, *Synlett* **2000**, 1294–1296.
- 83 Review: E. M. KAISER, D. W. SLOCUM, in *Organic Reactive Intermediates* (Ed.: S. P. McMANUS), Academic Press, New York, **1973**, p. 337ff.
- 84 a) T. ISHIYAMA, J. TAKAGI, K. ISHIDA, N. MIYAURA, N. R. ANASTASI, J. F. HARTWIG, *J. Am. Chem. Soc.* **2002**, 124, 390–391; b) N. MIYAURA, A. SUZUKI, *Chem. Rev.* **1995**, 95, 2457–2483; c) M. LAUTENS, A. ROY, K. FUKUOKA, K. FAGNOU, B. MARTÍN-MATUTE, *J. Am. Chem. Soc.* **2001**, 123, 5358–5359; d) J.-Y. CHO, M. K. TSE, D. HOLMES, R. E. MALECZKA JR., M. R. SMITH III, *Science* **2002**, 295, 305–308; (e) E. J. FARRINGTON, J. M. BROWN, C. F. J. BARNARD, E. ROWSELL, *Angew. Chem.* **2002**, 114, 177–179; *Angew. Chem. Int. Ed.* **2002**, 41, 169–171.
- 85 “Most if not all of the known types of organic derivatives of silicon have been considered ... the prospect of any immediate and important advances in this section of organic chemistry does not seem to be very hopeful.” F. S. KIPPING, *Proc. Royal Soc. A* **1937**, 159, 139.

11

Arenetricarbonylchromium Complexes: *Ips*o, *Cine*, *Tele* Nucleophilic Aromatic Substitutions

Françoise Rose-Munch and Eric Rose

Abstract

The complexation of an arene C_6H_5X to the tricarbonylchromium unit promotes addition of nucleophiles to the arene ring due to the strong electron-withdrawing ability of the $Cr(CO)_3$ group. If addition of the nucleophile Nu occurs at the carbon bearing the leaving group X, this is an overall *ipso* nucleophilic aromatic substitution S_NAr . If addition of the nucleophile takes place on another carbon, the anionic η^5 -X-cyclohexadienyltricarbonylchromium intermediates can be treated with acid giving η^4 -X-cyclohexadiene derivatives via chromium hydride intermediates. The driving force of these reactions is the elimination of HX. These reactions are called *cine* and *tele* S_NAr . In this chapter, an overview of these S_NAr substitutions is presented as well as recent developments relating to organic synthesis.

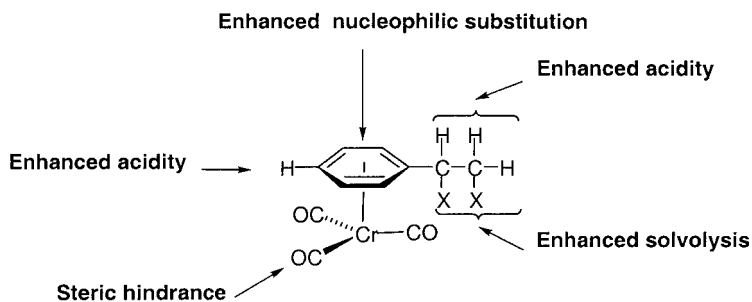
11.1

Introduction

11.1.1

Effects on Arene Reactivity of $Cr(CO)_3$ Coordination

The complexation of an arene to the tricarbonylchromium unit promotes the addition of nucleophiles to the arene ring due to the strong electron-withdrawing ability of the $Cr(CO)_3$ group. Other effects of the coordination of the metal on the reactivity of the arene ligand have been well-documented in the literature [1] and concern (Scheme 1): (i) the stabilization



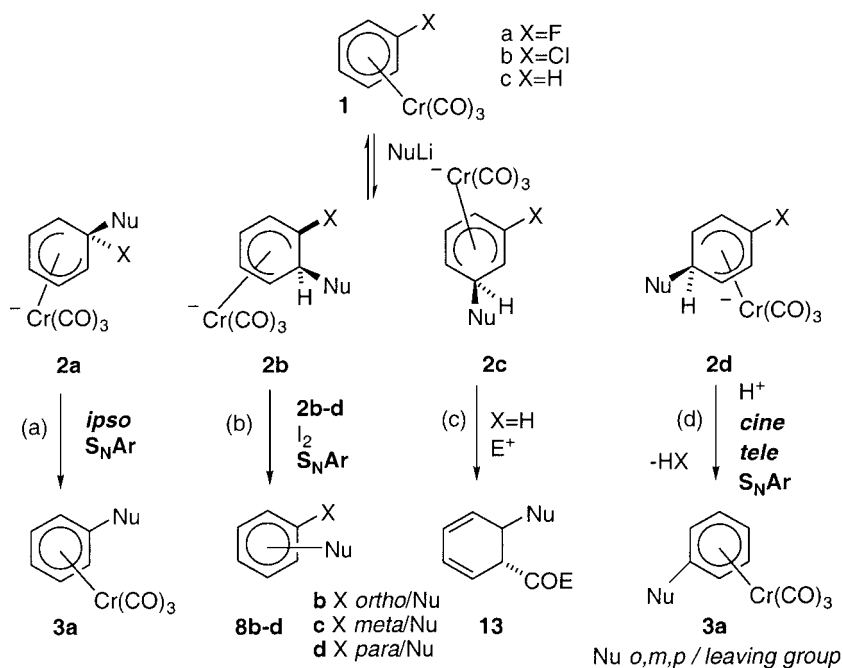
Scheme 1. Effects of the $Cr(CO)_3$ entity on the arene ring.

of negative or positive charges in a side-chain position, (ii) the acidification of the ring protons, which facilitates easy lithiation, and (iii) the large steric effect of the $\text{Cr}(\text{CO})_3$ entity, which blocks one face of the arene and directs incoming reagents to the uncomplexed face of the cycle. The purpose of this chapter is to specifically cover nucleophilic reactions on the activated ring that do not disturb the coordination of the chromium to the arene, namely *ipso*, *cine*, and *tele* nucleophilic aromatic substitutions, and, therefore, open the way to possible double functionalizations that may offer rapid access to interesting synthetic building blocks.

11.1.2

Coverage and Definitions

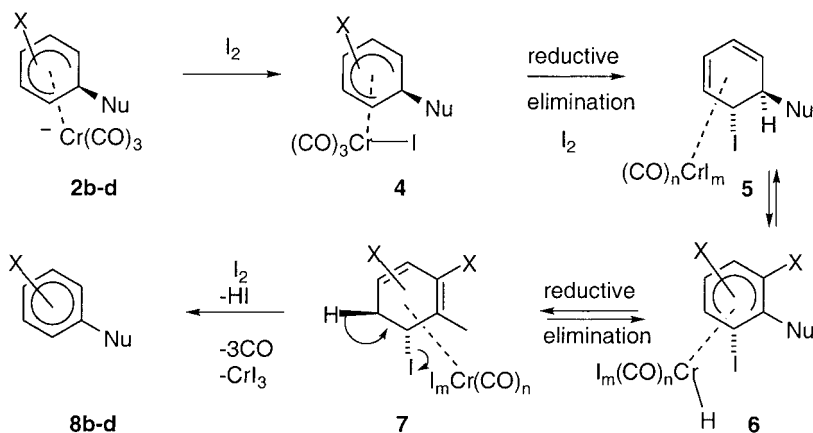
Reactions in which coordination of the tricarbonylchromium unit to the π -system of an arene cycle **1** activates the ring towards addition of nucleophiles to give η^5 -cyclohexadienyltricarbonylchromium anionic species **2a–d** are classified according to the regioselectivity of this addition. If the addition of the nucleophile occurs at the carbon bearing the leaving group, complex **2a** can eliminate X^- leading to an overall *ipso* nucleophilic aromatic substitution, $\text{S}_{\text{N}}\text{Ar}$, affording complex **3a** (Scheme 2, path a).



Scheme 2. Addition of a nucleophile to arenetricarbonylchromium complexes.

If the addition of the nucleophile takes place at another carbon, the intermediates **2b–d** can be oxidized to give the free disubstituted arenes **8b–d** (Scheme 2, path b). No detailed mechanistic study of this oxidation has been reported in the literature, but it has been

pointed out that an excess of I_2 is necessary to realize this decooordination. Thus, we suggest a plausible mechanism involving trapping of the intermediates **2b–d** with I_2 to give the chromium(II) iodide complex **4** (Scheme 3). A reductive elimination could generate an η^4 -cyclohexadiene complex **5**, $n = 3$, $m = 0$ or $n = m = 2$, in equilibrium with another cyclohexadiene **7** (the oxidation number of the Cr atom being II if $m = 2$ or 0 if $m = 0$), via the chromium hydride complex **6**. Adding a third equivalent of iodide to the chromium atom and elimination of HI might liberate the free arene **8b–d**, CO, CrI_3 , and HI. Of course, a mechanism involving direct H_{endo} abstraction or direct oxidation of the metal cannot be ruled out.

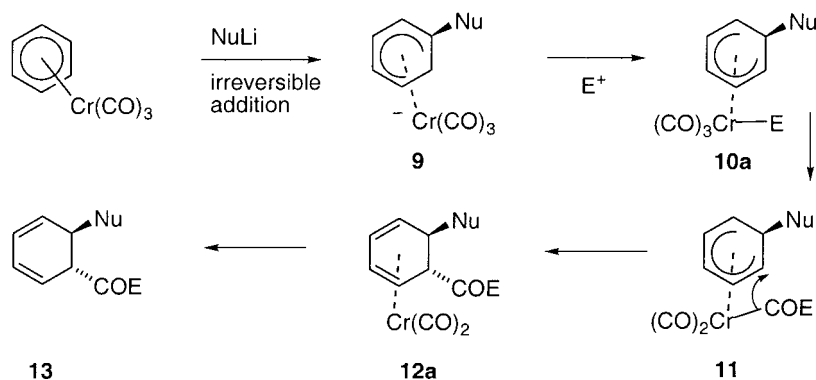


Scheme 3. Oxidation of the η^5 -cyclohexadienyl intermediate: suggested mechanism.

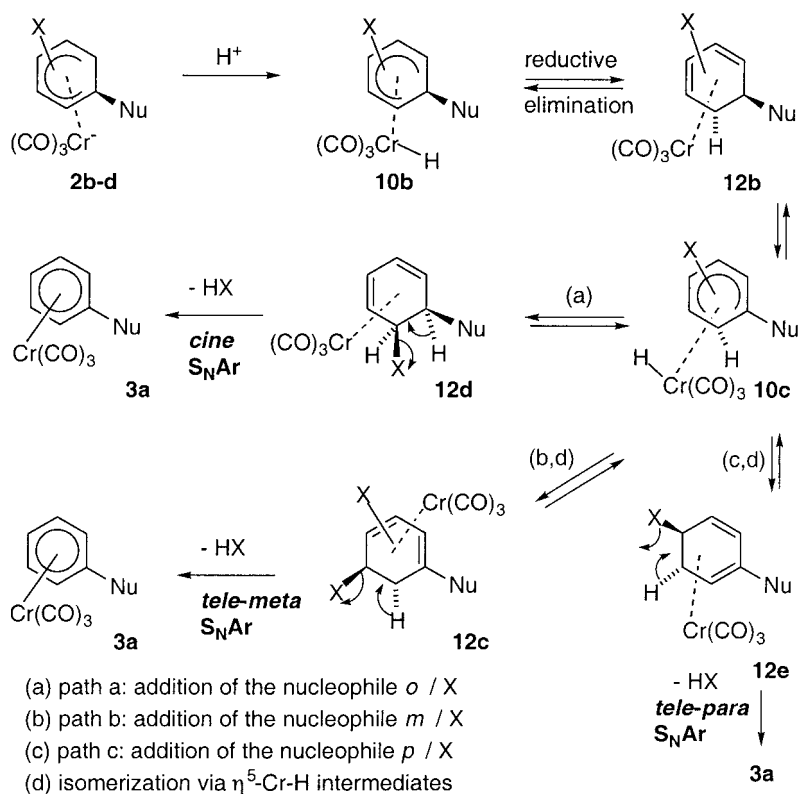
Reaction of the intermediate **2c**, $X = H$, with electrophiles E^+ can give interesting cyclohexadienes **13** (Scheme 2, path c). Indeed, if addition of the nucleophile is irreversible, carbon monoxide can be incorporated into the product, resulting in dearomatization accompanied by the introduction of an acyl group (Scheme 4). For example, complex **9** reacts with an electrophile E^+ to give the $18e^-$ complex **10a**, which can insert CO. A reductive elimination then affords the η^4 -cyclohexadiene **12a**, which liberates the free cyclohexadiene **13** [1i].

Treatment of the intermediates **2b–d** with acid also yields Cr(II) complexes **10b** (Scheme 5). A reductive elimination can generate η^4 -(cyclohexadiene)Cr(0) **12b**, then **12c**, **12d**, or **12e** via the chromium hydride **10c**. Subsequent elimination of HX yields complex **3a**. These reactions are referred to as *cine* and *tele* S_NAr . Indeed, *cine* S_NAr , in accordance with IUPAC recommendations is a reaction in which the incoming group takes up a position at the carbon *ortho* to the leaving group. The term *tele* is used to denote reactions in which the entering group takes up a position more than one atom away from the atom to which the leaving group is attached (Scheme 2, path d, and Scheme 5) [1f, 1k].

Procedures that follow paths b and c (Scheme 2) result in loss of the tricarbonylchromium entity. It is noteworthy that in the case of paths a and d, however (Scheme 2), **the $Cr(CO)_3$ unit is not lost**, and arene tricarbonylchromium complexes are recovered. These can then be reacted with another nucleophile or be decoordinated under CO atmosphere, which affords the free arene and $Cr(CO)_6$, which can be used to prepare the starting complex.



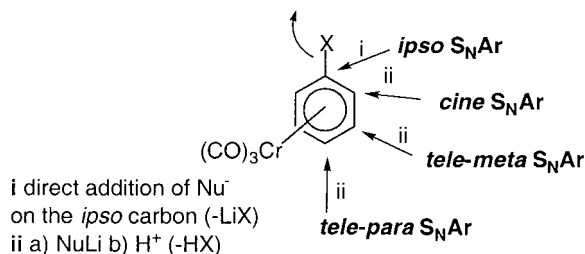
Scheme 4. Chromium-mediated dearomatization reactions.



Scheme 5. Mechanism of *cine* and *tele* nucleophilic aromatic substitutions.

General reviews have appeared in the literature [1, 2] concerning arene chromium complexes as well as iron [2] and manganese [3,4] complexes, and nucleophilic additions followed by iodine oxidation and loss of the metal have been well reported, for example by Semmelhack [1c] and by Morris in 1995 [1e]. The purpose of this chapter is to focus only on *ipso*,

cine, and *tele* nucleophilic aromatic substitutions, S_NAr , of arene- $Cr(CO)_3$ complexes, which have the great advantage of proceeding with retention of the coordinated $Cr(CO)_3$ unit on the arene ring (Scheme 6).



Scheme 6. *Ipso*, *cine*, and *tele* S_NAr regioselectivity.

Unlike many arene complexes, with the exception of manganese complexes which are beginning to show more and more applications [1g], arenechromium complexes possess all the attributes needed for easy synthetic utilization. They are easily formed by direct reaction with $Cr(CO)_6$ in a mixture of THF and di-*n*-butyl ether [5], they readily undergo nucleophilic aromatic substitutions, and the metal is easily removed by mild oxidation with I_2 or by exposure to sunlight and air. In Section 11.2, we describe *ipso* nucleophilic aromatic substitutions in the case of arenes bearing a good leaving group according to the nature of the newly created bonds, these reactions creating C–O, C–S, C–Se, C–N, C–P, C–C, C–H, and C–metal bonds. We point out the pioneering results as well as the main extensions reported in the literature in recent years. In Section 11.3, we describe *cine* and *tele* nucleophilic aromatic substitutions according to the nature of the leaving groups: F^- , Cl^- , ^-OR , and $^-NR_2$.

11.2

Ipso Nucleophilic Aromatic Substitutions

11.2.1

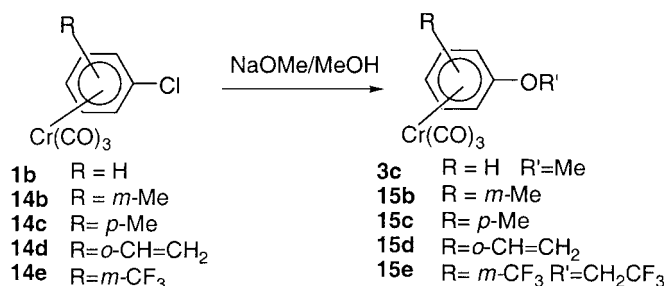
Carbon–Oxygen, –Sulfur and –Selenium Bond Formation (Table 1)

The first description of classical S_NAr at an arenetricarbonylchromium species was reported in 1959, when chlorobenzenetricarbonylchromium **1b** ($X = Cl$) was treated with $NaOH$ and $MeOH$ at $65^\circ C$ for 24 h [6]. Thus, it was recognized that the electron deficiency of the arene promotes *ipso* addition of MeO^- to the carbon bearing the Cl atom, thereby yielding arenetricarbonylchromium **3c** ($R = H$) in 90 % yield (Scheme 7). The temperature and the nature of the nucleophile are important because the kinetic site of addition is not usually at the carbon bearing the chloride atom, but rather at a carbon bearing a hydrogen. Thus, according to the anion, this reaction requires either a reversible or a direct addition of the nucleophile to the *ipso* C– X carbon.

The reaction of MeO^- involves direct *ipso* substitution, as shown by the reactions of *meta*- and *para*-chlorotoluenetricarbonylchromiums **14b** and **14c**, which give *meta*- and *para*-anisole derivatives **15b** and **15c**, respectively. It is interesting at this stage to point out that

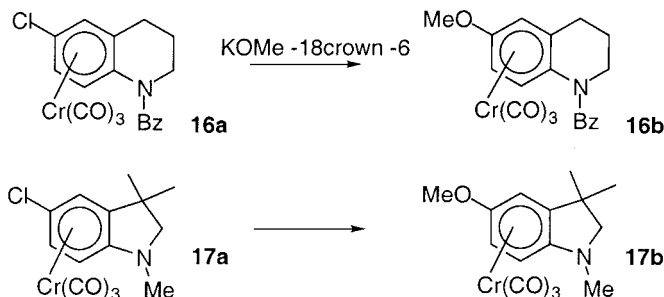
Tab. 1. *Ips*o nucleophilic aromatic substitution of arenetricarbonylchromium complexes: C–O, C–S and C–Se bond formation.

Entry	Arene	Nucleophile	Ref., Year
1	PhCl	MeOH, NaOH	6, 1959
2	<i>m</i> - <i>p</i> -MeC ₆ H ₄ Cl	MeOH, NaOH	7a, 1964
3	Tetrahydroquinoline	MeOK	8, 1977
4	PhF	Lactone	20, 1979
5	<i>o</i> -FC ₆ H ₄ (CH ₂ CH ₂ CH ₂ OH)	<i>t</i> BuOK, DMSO	18, 1980
6	R = C ₆ H ₄ F	F [−] /OSi	21, 1985
7	<i>o</i> , <i>m</i> , <i>p</i> -C ₆ H ₄ Cl ₂	MeOH, <i>i</i> PrOH, KOH	9, 1985
8	<i>o</i> -C ₆ H ₄ Cl ₂	NaO(CH ₂) ₂ O(CH ₂) ₂ ONa	19, 1985
9	<i>o</i> , <i>m</i> , <i>p</i> -MeC ₆ H ₄ F	Me ₂ C=N–OH, KOH	12, 1985
10	RC ₆ H ₄ F, RC ₆ H ₄ Cl	NaOMe	10, 1986
11	<i>p</i> -C ₆ H ₄ Cl ₂	Me ₂ C=N–OH, KOH	13, 1987
12	PhCl	HONHCO ₂ <i>t</i> Bu	14, 1988
13	<i>p</i> -MeOC ₆ H ₄ F	PhONa	17, 1988
14	<i>p</i> -CF ₃ C ₆ H ₄ Cl	CF ₃ CH ₂ ONa	11, 1993
15	<i>o</i> -CH ₂ =CH–C ₆ H ₄ Cl	MeOH, NaOH	7b, 1994
16	<i>p</i> -MeC ₆ H ₄ F	<i>n</i> -C ₄ H ₉ OLi, THF, HMPA	16, 1996
17	2-F-1,3-diOMeC ₆ H ₃	primary, secondary alkoxides	15, 1999
18	<i>o</i> , <i>m</i> , <i>p</i> -C ₆ H ₄ Cl ₂	NaSR	22, 1983
19	<i>o</i> -C ₆ H ₄ Cl ₂	NaSR	23, 1988
20	RC ₆ H ₄ F, RC ₆ H ₄ Cl	NaSMe	24, 1991
21	<i>m</i> -MeOC ₆ H ₄ Cl	ArSeSeAr	25, 1999

**Scheme 7.** *Ips*o S_NAr: C–O bond formation.

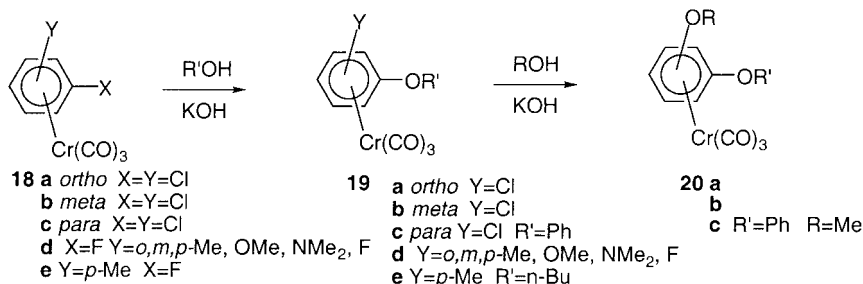
the authors mentioned the formation of very minor products, that probably corresponded to *cine* derivatives! Indeed, they observed the presence of *para*-methoxytoluene-Cr(CO)₃ in 0.1 % yield starting from *m*-chlorotoluene-Cr(CO)₃ **14b**, and the presence of *m*-methoxytoluene Cr(CO)₃ in 0.2 % yield starting from the *p*-chlorotoluene-Cr(CO)₃ complex **14c** [7a]. Similarly, treatment of (–)-(o-chlorostyrene)tricarbonylchromium complex **14d** with MeONa in refluxing MeOH for 18 h gives the (–)-(o-methoxystyrene) complex **15d** in 50 % yield [7b]. The absolute configuration of the chloro complexes was shown to be (1*S*,2*R*).

6-Methoxytetrahydroquinoline and 5-methoxy-3,3-dimethyldihydroindole derivatives **16b** and **17b** are prepared in the same way by adding KOMe in the presence of 18-crown-6 ether to complexes **16a** and **17a**, respectively (Scheme 8) [8].



Scheme 8. Ipso S_NAr : C–O bond formation.

o- and *p*-Dichlorobenzenetricarbonylchromium complexes **18a** and **18c** react with ROH (R = Me, *i*Pr) in the presence of KOH under phase-transfer conditions to give the mono alkoxy products **19a** and **19c**. The *meta* isomer **18b** also gives the disubstitution product **20b** [9]. In DMSO, all three isomers of **18** afford the dialkoxy derivatives **20** with ROH. These results were discussed in terms of different conformations of the tricarbonylchromium tripod (Scheme 9).

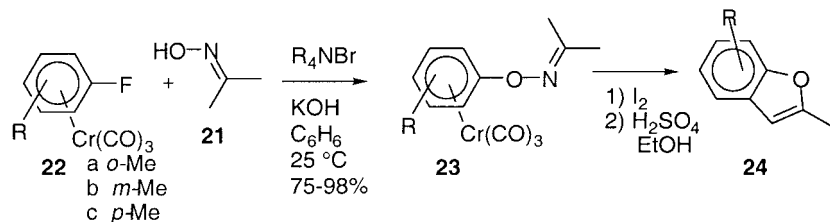


Scheme 9. Ipso S_NAr : C–O bond formation.

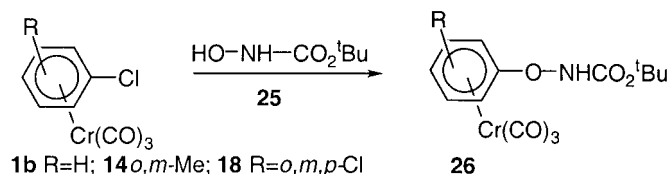
Various substituted fluoroarenetricarbonylchromium complexes **18d** react with MeONa in refluxing MeOH to yield the ipso S_NAr type products **19d** (Scheme 9) [10]. Even a poor nucleophile such as sodium 2,2,2-trifluoroethoxide reacts with *m*-(trifluoromethyl)chlorobenzenetricarbonylchromium complex **14e** at 50 °C in THF/TMEDA to afford the ether **15e** in 97 % yield (Scheme 7) [11]. This reaction is greatly facilitated by the presence of the electron-withdrawing CF_3 group.

A series of *o*-arylhydroxylamines, which are interesting intermediates for the preparation of benzofurans, hydroxybiphenyls, and catechols, have been synthesized starting from $Cr(CO)_3$ -activated fluoroarenes. Oxime **21** reacts with *m*-fluorotoluenetricarbonylchromium

complex **22b** to yield the *m*-aryloxime **23** (Scheme 10) [12]. This oxime can be converted to benzofuran derivatives **24** by oxidation with I_2 and treatment of the free arene with H_2SO_4 [13]. Reactions of complexes **1b**, **14**, and **18** with hydroxylamine **25** afford the *ipso* complex **26** in 90–95 % yield (Scheme 11) [14].

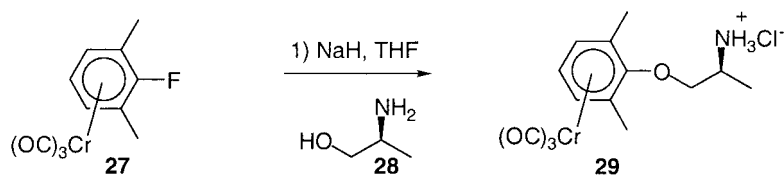


Scheme 10. *Ipsso* S_NAr : C–O bond formation.



Scheme 11. *Ipsso* S_NAr : C–O bond formation.

As part of a program aimed at discovering new sodium channel blockers, authentic samples of both enantiomers of the class I-B antiarrhythmic agent mexiletine are required. Thus, for this purpose, a variety of primary and secondary alkoxides bearing unprotected primary, secondary, and tertiary amino functionalities have been used to displace the fluoride from the sterically demanding 1,3-dimethyl-2-fluorobenzenetricarbonylchromium complex **27**. The corresponding ether **29** (Scheme 12) obtained with (*S*)-(+)-2-amino-1-propanol **28** represents the mexiletinetricarbonylchromium complex with an enantiomeric purity of ≥ 99 % *ee* [15]. A similar sequence, using (*R*)-(-)-2-amino-1-propanol, provides the (*R*)-mexiletine hydrochloride complex.



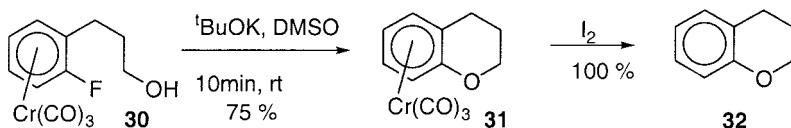
Scheme 12. *Ipsso* S_NAr : C–O bond formation.

An unexpected reaction occurs when *p*-fluorotoluenetricarbonylchromium complex **18e** is treated with lithium phenylacetylide (generated from *n*BuLi and phenylacetylene) in THF

and HMPA, furnishing (η^6 -4-butyloxytoluene)tricarbonylchromium complex **19e** in 44 % yield. The authors rationalized this reaction by suggesting that $n\text{BuOLi}$ might be formed, arising from either aerial oxidation of $n\text{BuLi}$ or ring-opening of THF by $n\text{BuLi}$ [16].

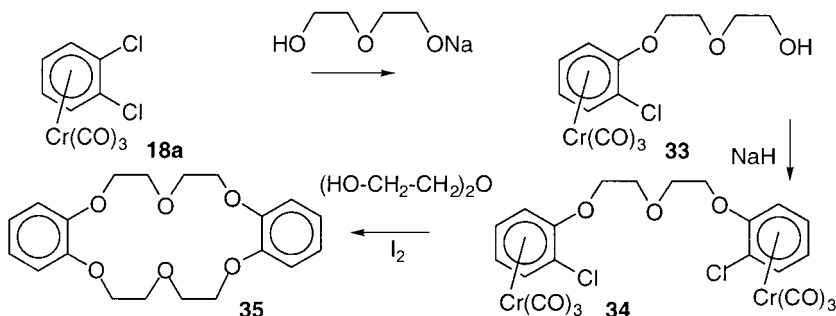
It is worthy of note that treatment of *p*-fluoroanisoletricarbonylchromium complex with 5 equivalents of PhONa in DMSO at 100 °C does not lead to an *ipso* $\text{S}_{\text{N}}\text{Ar}$ reaction [17]! It had been envisaged that the lack of reactivity in this case could be overcome by the use of the 1,4-dichlorobenzene complex. However, *p*-dichlorobenzenetricarbonylchromium complex **18c** reacts smoothly with PhONa in DMSO at room temperature to give the mono *ipso* adduct **19c**, $\text{R}' = \text{Ph}$ [17]. Treatment of this complex with MeONa in DMSO gives **20c** ($\text{R} = \text{Ph}$, $\text{R}' = \text{Me}$) in 52 % yield (Scheme 9). This process represents an interesting sequential replacement of chloride from the *p*-dichlorobenzene complex.

The intramolecular version of the substitution of chloride or fluoride has also been studied. For example, reaction of 3-(2-fluorophenyl)-1-propanol tricarbonylchromium **30** with excess $t\text{BuOK}$ for 3 h at 25 °C gives the chromane complex **31** (Scheme 13) in 75 % yield, from which the free chromane **32** can be obtained by oxidation with I_2 [18].



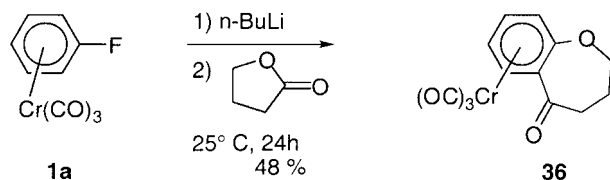
Scheme 13. Intramolecular *ipso* $\text{S}_{\text{N}}\text{Ar}$: C–O bond formation.

Both activation by $\text{Cr}(\text{CO})_3$ complexation and the use of phase-transfer conditions are necessary for success in the following synthesis. A cyclic bis-ether can easily be obtained from the *o*-dichlorobenzene complex **18a** (Scheme 14). Indeed, reaction of **18a** with $\text{Na}[\text{O}(\text{CH}_2)_2]_2\text{OH}$ in $(\text{MeOCH}_2)_2\text{O}$ and with Bu_4NBr as a phase-transfer catalyst at 50 °C for 8 h, followed by decomplexation with I_2 directly affords dibenzo-18-crown-6 **35** in 27 % yield. Compound **34**, which can also be converted into **35**, can be obtained in 84 % yield by heating **18a**, NaH , and diethylene glycol for 24 h in DME at 50 °C [19]. The authors demonstrated the potential of this synthesis by preparing different crown ethers with various heteroatoms.



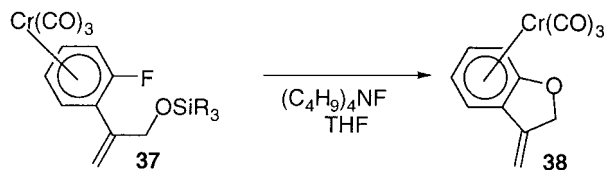
Scheme 14. Intramolecular *ipso* $\text{S}_{\text{N}}\text{Ar}$: C–O bond formation.

Cyclization can also occur through halide displacement after initial metalation. For example, acylation of *o*-lithiofluorobenzenetricarbonylchromium with γ -butyrolactone at 25 °C for 24 h is followed by spontaneous fluoride displacement to give complex **36**. Oxidation with excess iodine liberates the lactone in 48 % overall yield (Scheme 15) [20].



Scheme 15. Intramolecular *ipso* $S_N\text{Ar}$: C–O bond formation.

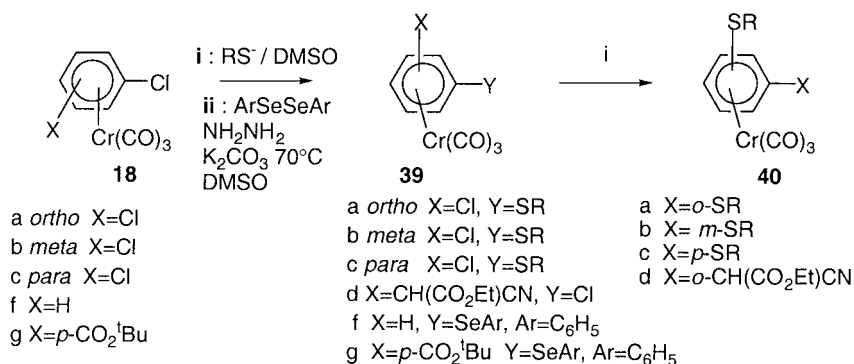
Another intramolecular substitution has been used for the synthesis of an intermediate in a proposed route to 3-substituted benzofurans. A β -methylene-dihydrobenzofuran complex **37** was obtained upon fluoride-induced removal of the SiR_3 protecting group from complex **37** (Scheme 16) in an *ipso* $S_N\text{Ar}$ process. Desilylation resulted in spontaneous cyclization to the stable methylene complex **38** in 89 % yield. No isomerization occurred and the 3-methyl benzofuran complex was not detected [21].



Scheme 16. Intramolecular *ipso* $S_N\text{Ar}$: C–O bond formation.

The reactivity of complexed haloarenes toward thiolates has been studied, and it has been reported that *o*-, *m*-, and *p*-dichlorobenzenetricarbonylchromium complexes **18a–c** react with thiolates (RS^- ; $\text{R} = \text{Me}$, *n*Bu, *t*Bu Scheme 17, path i) under phase-transfer conditions or in DMSO to give **39** and **40a–c**. The *ortho*- and *para*-complexes **18a** and **18c** undergo stepwise substitution of the two Cl atoms in a reaction sequence that can be easily controlled by the amount of added thiolate. The *meta* complex **18b** shows a lower selectivity and gives a mixture of mono- and disubstituted products even in the presence of substoichiometric amounts of thiolate (Scheme 17) [22]. Similarly, $\text{LiCH}(\text{CO}_2\text{Et})\text{CN}$ and BuSH react with the *o*-dichlorobenzene complex **18a** to give complex **39d** and then disubstituted arene **40d**, showing that this substitution can be performed with two different nucleophiles (Scheme 17) [23]. Phase-transfer catalysis has also been applied to fluoroarene- $\text{Cr}(\text{CO})_3$ complexes, which are more reactive toward thiolates than are the corresponding chloro derivatives [22].

Other approaches to Cr-mediated aromatic thiation have been studied [24], and quenching of lithiated arenetricarbonylchromium complexes by electrophilic sulfur has been compared to halogen displacement by nucleophilic sulfur.



Scheme 17. *Ipso* S_NAr: C–S bond formation.

Unsymmetrical diaryl selenides can be prepared by nucleophilic displacement of chloride from chloroarene-Cr(CO)₃ complexes with areneselenolate complexes in DMSO at 70 °C. Selenolates can be generated *in situ* by reduction of the corresponding diselenides with hydrazine in DMSO in the presence of potassium carbonate (Scheme 17, path ii). Thus, chloroarene complexes **18a** and **18f** yield diaryl selenides in moderate to good yields [25]. Product yields are increased with increasing reactivity of the complex and with increasing nucleophilicity of the selenolate reagent. 4-*tert*-Butyloxycarbonylchlorobenzene-Cr(CO)₃ **18g** is particularly reactive, affording the substitution product **39g** at room temperature. 4-Dimethylaminoselenolate reacts more efficiently than 4-chloroselenolate (Scheme 17) [25].

11.2.2

Carbon–Nitrogen and Carbon–Phosphorus Bond Formation (Table 2)

Reaction of (*η*⁶-fluorobenzene)tricarbonylchromium **1a** with primary and secondary amines proceeds rapidly at 25 °C. The formation of (*η*⁵-cyclohexadienyl)complex **2a** (X = F, NuH = NHR₂) has been postulated on the basis of kinetic data. A rate-determining loss of fluoride from the *endo* side of the ring affords the aniline derivative **3j** (Scheme 18) [26].

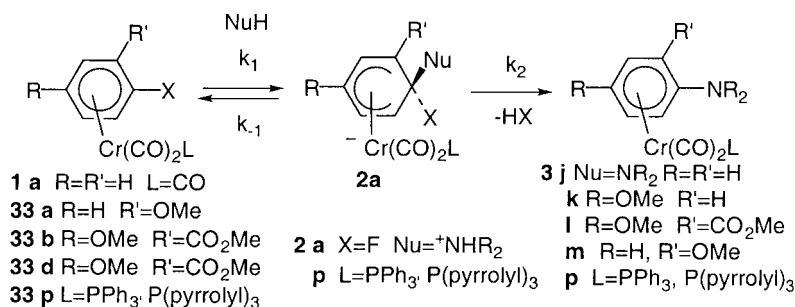
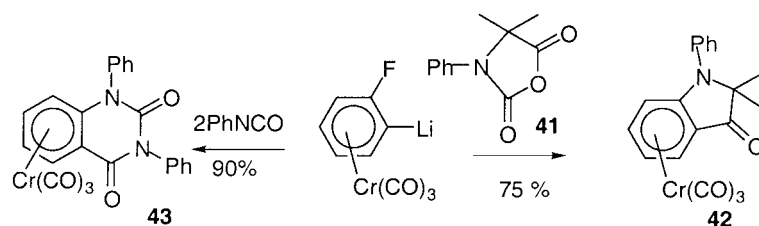
Nucleophilic substitution of the fluoride of fluorobenzenetricarbonylchromium by morpholine leads to phenylation of the nitrogen (Scheme 18) [27]. However, in the case of imidazole, substitution is effected only with the anion of the nitrogen base.

Other aminations of more substituted arene complexes allow the regiospecific synthesis of polysubstituted aromatics. For example, *p*-fluoroanisoletricarbonylchromium complex can first be lithiated and quenched with chloroformate to give **33b** (R = OMe, R' = CO₂Me). After substitution of the fluoride by pyrrolidine, complex **3l** is obtained in 89 % yield (Scheme 18) [29].

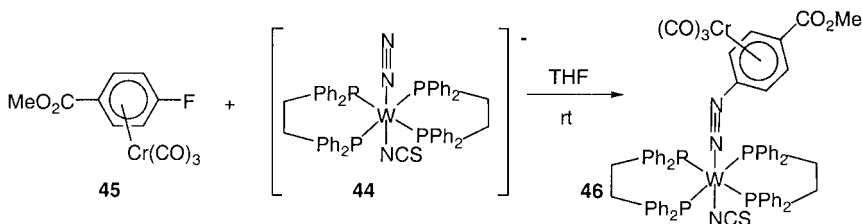
o-Lithiated fluorobenzenetricarbonylchromium complex can be trapped by bifunctional electrophiles such as dimethyl-*N*-carboxy anhydride **41** to give the five-membered ring **42** after spontaneous decarboxylation and displacement of fluoride (Scheme 19) [28]. With two equivalents of phenyl isocyanate, PhNCO, the six-membered heterocycle **43** is recovered. This process has also been extended to seven-membered benzo-fused heterocycles.

Tab. 2. *Ipso* nucleophilic aromatic substitution of arenetricarbonylchromium complexes: C–N and C–P bond formation.

Entry	Arene	Nucleophile	Remarks	Ref., Year
1	C ₆ H ₅ F	R ₂ NH	aniline	26a, 1967–68
2	C ₆ H ₅ F	R ₂ NH	aniline	26b, 1971
3	C ₆ H ₅ F	R ₂ NH	morpholine	27, 1979
4	C ₆ H ₅ F	R ₂ NH	benzo-fused	28, 1979
5	C ₆ H ₅ F	R ₂ NH	heterocycles	28, 1986
6	RC ₆ H ₄ F	R ₂ NH	pyrrolidine	29, 1986
7	<i>p</i> -CO ₂ MeC ₆ H ₄ F	[W–N≡N]	arylation of nitrogen	30, 1992
8	RC ₆ H ₄ Cl	NaH, NH ₂ COCF ₃	aniline	31, 1992
9	CF ₃ C ₆ H ₄ Cl	NaNH ₂ /NH ₃	aniline	32, 1993
10	C ₆ H ₅ OCH ₂ CH ₂ NH ₂	RNH ₂	Smiles reaction	33, 1995
11	RC ₆ H ₄ F	piperazine	aryl piperazine	35, 1996
12	RC ₆ H ₄ F	amines	rate of S _N Ar	36, 1998
13	RC ₆ H ₄ F	LiNR ₂	<i>N</i> -aryl indoles	38, 1998
14	RC ₆ H ₄ OCON(<i>i</i> Pr) ₂	PPh ₂ Li	arylphosphines	39, 1999
15	RC ₆ H ₄ F	pyrrolidine, piperidine	polymer-haloarene	40, 2000
16	RC ₆ H ₄ F	NH ₂ NH ₂ , H ₂ O	indazole	42, 2000

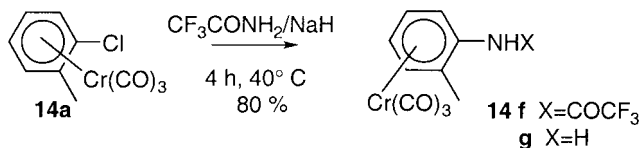
**Scheme 18.** *Ipso* S_NAr: C–N bond formation.**Scheme 19.** Intramolecular *ipso* S_NAr: C–N bond formation.

A reaction corresponding to a novel arylation of molecular nitrogen through bimetallic activation has been reported. Thus, reaction of $[n\text{Bu}_4\text{N}][\text{W}(\text{NCS})(\text{N}_2)(\text{dpe})_2]$ (**44**) with *p*-fluorobenzoic ester complex **45** in THF at room temperature gave complex **46** as a result of an *ipso* $\text{S}_{\text{N}}\text{Ar}$ process [30] (Scheme 20), showing the effectiveness of this method for the direct arylation of coordinated nitrogen.



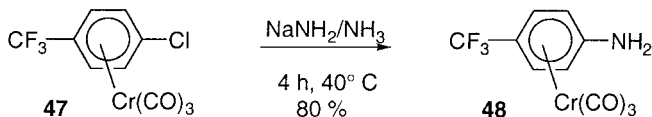
Scheme 20. *Ipso* $\text{S}_{\text{N}}\text{Ar}$: C–N bond formation.

Trifluoroacetamide may be successfully employed as a nucleophile in the synthesis of aniline complexes. The formation of aniline derivatives **14g** can be realized by adding the “in situ” generated trifluoroacetamide anion CF_3CONH^- to the *o*-chlorotoluenetricarbonylchromium complex **14a** followed by KOH treatment (Scheme 21) [31].



Scheme 21. *Ipso* $\text{S}_{\text{N}}\text{Ar}$: C–N bond formation.

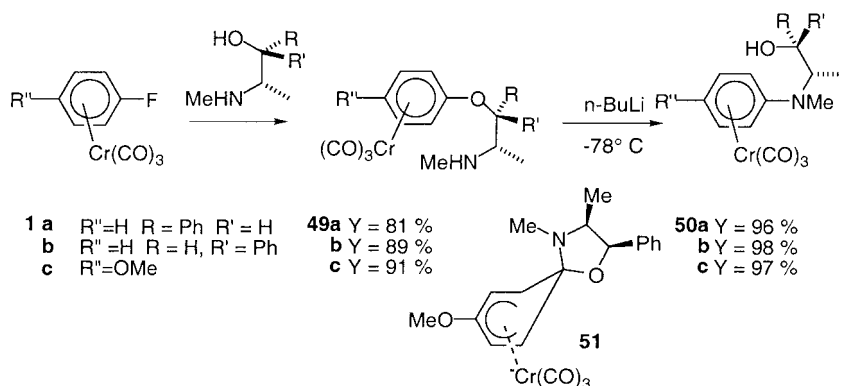
The synthesis of aniline derivatives can also be realized by direct addition of the NH_2 unit, if the arene ring is made more electrophilic through activation by a trifluoromethyl group. For example, in the case of *p*-trifluoromethylchlorobenzenetricarbonylchromium complex **47**, the aniline derivative **48** can be obtained in 32 % yield using $\text{NaNH}_2/\text{NH}_3$ in HMPT (Scheme 22) [11].



Scheme 22. *Ipso* $\text{S}_{\text{N}}\text{Ar}$: C–N bond formation.

The tricarbonylchromium entity promotes *ipso*-Smiles rearrangement of the *O*-phenyl derivatives of ephedrine and pseudoephedrine to the *N*-phenyl derivatives [32]. Indeed, treatment of the sodium alkoxide derived from (1*R*,2*S*)-ephedrine with fluorobenzene complex

1a generates the required phenyl ether **49a** in good yield. Upon treatment with *n*BuLi in THF at -78°C , complex **49a** smoothly undergoes the Smiles rearrangement to liberate the phenylamine **50a** in 96 % yield. Treatment of 4-fluoroanisole complex **1c** with the alkoxide derived from (1*S*,2*S*)-ephedrine yields complex **49c** in 91 % yield, and complex **50c** in 97 % yield upon treatment with *n*BuLi at -78°C . The *ipso* regioselectivity of these reactions is evident from the aromatic AB system in the ^1H NMR spectrum of **50**, which is diagnostic of 1,4-substitution. Thus, the *spiro* intermediate **51** can be postulated, and it would be interesting to trap it, e.g. with ClSnPh_3 [33] (Scheme 23).



Scheme 23. *Ipsso* $\text{S}_{\text{N}}\text{Ar}$: C–N bond formation.

Arylpiperazines can be prepared in a one-pot procedure by *ipso* $\text{S}_{\text{N}}\text{Ar}$ of piperazine derivatives with η^6 -fluoroarene complexes **1a**, **33a**, **b**, **d**. Indeed, piperazine derivatives react with fluorobenzene derivatives in DMSO in the presence of K_2CO_3 at 80°C to give, after 2.5 h, complexes **3m** and **3k** (Nu = piperazine) in good yields (Scheme 18) [34]. Piperazine itself may be used as a nucleophile and gives the monoarylpiperazine derivative uncontaminated by any symmetrical *N,N'*-bis(aryl)piperazine, allowing the direct preparation of unprotected compounds.

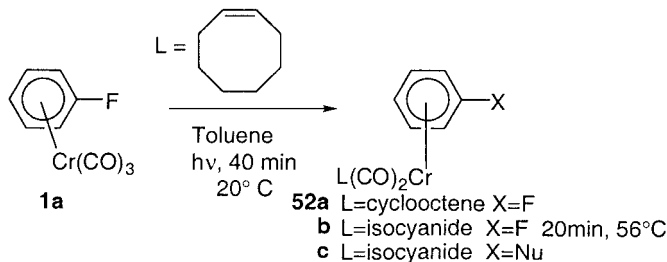
Fluoroarene- $\text{Cr}(\text{CO})_2\text{L}$ complexes **33p** [$\text{L} = \text{CO}$, PPh_3 , $\text{P}(\text{OPh})_3$, $\text{P}(\text{pyrrolyl})_3$, $\text{P}(\text{pyrolyl})_2 \cdot (\text{NMeBn})$], where *L* is a potential linker ligand for solid-phase synthesis, have been evaluated with regard to the rates of nucleophilic substitution by amines [35]. The preparative and kinetic results indicate that $\text{S}_{\text{N}}\text{Ar}$ reactions on tris(pyrrolyl)phosphine-modified fluoroarenechromium complexes proceed rapidly and with high efficiency, and are thus appropriate for the development of solid-phase versions for use in combinatorial synthesis (Scheme 18).

The authors set out to ascertain whether the addition of pyrrolidine (k_1 ; Scheme 18) to give complex **2p** or the loss of fluoride (k_2) to give complex **3p** was the rate-determining step. The reverse of nucleophile addition, k_{-1} , was assumed to be faster than the addition. All the results of a series of kinetic determinations in DMF at 25°C by ^{19}F NMR spectroscopy were consistent with k_1 relating to the rate-determining step (half-lives: 67–180 s). Unlike simple aminophosphines, tris(pyrrolyl)phosphine is relatively stable toward cleavage of the N–P bond and shows a relatively strong electron-withdrawing effect, nearly comparable to that of

CO [36]. This is consistent with a half-life of 91 s, only 1.4 times longer than that of the parent fluorobenzene-Cr(CO)₃ complex.

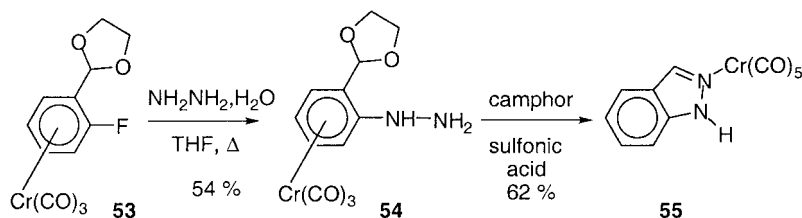
Mild N-arylations of indoles can be achieved in good yields by nucleophilic substitution reactions of the sodium salt of indole on various haloarenetricarbonylchromium complexes. Thus, *o*-fluoroanisole-Cr(CO)₃ **33a** reacts with the indole N anion within 0.75 h at 0 °C to give complex **3m** (Nu = indolyl) in 83 % yield. The chloro derivatives require longer reaction times and higher temperatures (Scheme 18) [37]. The authors were able to extend this procedure to the introduction of two indole rings on the same aromatic nucleus.

New polymer-bound haloarene chromiumdicarbonyl isocyanide complexes have been prepared and used in solid-phase chemistry to react with nitrogen nucleophiles according to an *ipso* S_NAr mechanism [38]. Polymer-bound isocyanides have proved to be valuable ligands for anchoring haloarene-Cr(CO)₃ complexes by means of their substitution of a CO group. It is known from solution chemistry that the coordination of a phosphine group to the chromium atom greatly reduces the reactivity of the aromatic ring to nucleophilic attack, except in particular cases [36]. Thus, the isocyanide ligand is used, the electronic properties of which are similar to those of the CO group. Irradiation of the fluoroarene complex **1a** at room temperature in the presence of cyclooctene gives complex **52a**, treatment of which with the appropriate isocyanide (L = RNC) for 20 min at 55 °C, affords the stable complex **52b**. Different nucleophiles can react in DMF at room temperature (Nu = pyrrolidine, piperidine, benzyl thiolate, methoxide anion) to give the corresponding complexes **52c**, showing that the aromatic ring is only slightly affected by modification of the ligands. The problem of preparing arene complexes bound to appropriate isocyanide resins has been solved. Indeed, fluorobenzene-Cr(CO)₃ can be supported on the resin by direct photochemical irradiation for 1 h to form **52b** (L = isocyanide resin). The resin reacts at room temperature in DMF, for example with pyrrolidine, to give in 80 % yield a resin showing no ¹⁹F NMR signal, as befits an *ipso* S_NAr displacement of the fluoride by the nitrogen nucleophile (Scheme 24).



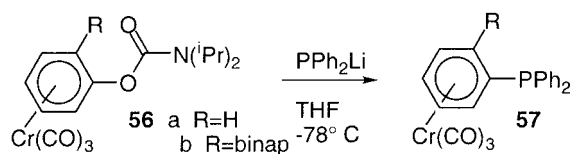
Scheme 24. Ligand exchange.

The formation of these C–N bonds is interesting, because it is not easy to create them in the case of non-coordinated arenes [40]. Very often, another form of activation is necessary [41]. The last example of a C–N bond formation is represented by the recent preparation of the indazole σ -chromium complex **55**, which was obtained by cyclization of η^6 -2-(2'-phenylhydrazine)-1,3-dioxolane-Cr(CO)₃ (**54**) under acidic conditions. The *ipso* S_NAr was achieved by refluxing with 2.5 equivalents of hydrazine and one equivalent of 2-(2'-fluorophenyl)-1,3-dioxolane-Cr(CO)₃ (**53**) for 2 days [39].



Scheme 25. *Ipsso* $S_N\text{Ar}$: C–N bond formation.

Optically active Cr-complexed arylphosphines **57** can be prepared in three steps from achiral arene- Cr(CO)_3 precursors **56**. A successful addition of PPh_2Li to the complex **56a** with concomitant carbamate displacement has been suggested, giving rise to the desired phosphine complex **57a** as an air-stable crystalline solid in 96 % yield ($R = \text{H}$) (Scheme 26). Therefore, efficient C–P bond construction can be achieved by reacting, for example, the biaryl complex **56b** with PPh_2Li , providing the optically active monophosphine ligand **57b** in 87 % yield, which has been used in Pd-catalyzed allylic alkylation reactions (Scheme 26) [42].



Scheme 26. *Ipsso* $S_N\text{Ar}$: C–P bond formation.

11.2.3

Carbon–Carbon Bond Formation (Table 3)

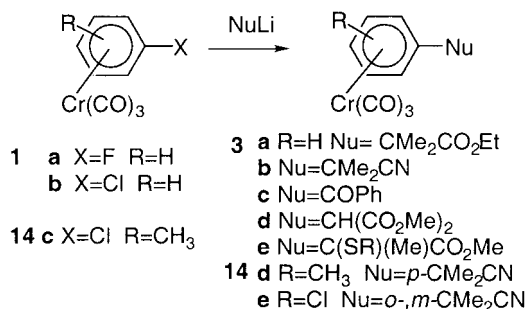
In this section, we examine *ipso* substitutions of leaving groups such as halides, phenoxides, and alkoxides by carbanions. They are presented in chronological order in accordance with Table 3.

Highly stabilized carbanions (e.g., α -cyano, α -alkoxycarbonyl carbanions, etc.) react with fluoro- or chlorobenzenetricarbonylchromium derivatives by substitution of the halides, even at room temperature [1c]. The authors excluded a pathway involving a transient aryne because the reaction of isobutyronitrile carbanion with *p*-chlorotoluenetricarbonylchromium complex **14c** produces a single *p*-tolylisobutyronitrile complex **14d** (Scheme 27). The same conclusion has been reported for the reactions of the chlorobenzene complex with O and N nucleophiles [43, 44]. Thus, additions of tertiary carbanions of ethylisobutyric ester, isobutyronitrile, and cyanohydrin to chlorobenzenetricarbonylchromium complex **1b** afford the corresponding *ipso* complexes **3a–c** in good yields. These can be oxidized by iodine to produce the free arenes substituted by the nucleophile Nu ($\text{Nu} = -\text{CMe}_2\text{CO}_2\text{Et}$, $-\text{CMe}_2\text{CN}$, $-\text{COPh}$) in yields of 85 %, 71 %, and 88 %, respectively. Additions of $\text{LiCH}(\text{CO}_2\text{Me})_2$ and $\text{LiC}(\text{SR})(\text{CH}_3)\text{CO}_2\text{Me}$ to the fluorobenzene complex **1a** yield the *ipso* adducts **3d** and **3e**, respectively, in yields of 95 % and 94 % [45] (Scheme 27). It is worthy of note that several car-

Tab. 3. *Ipso* nucleophilic aromatic substitution of arenetricarbonylchromium complexes: C–C bond formation.

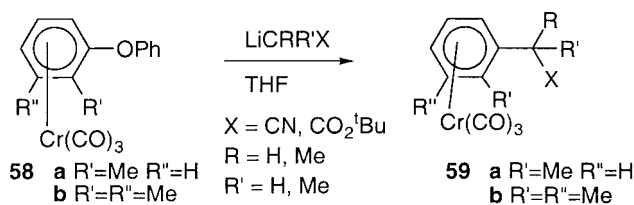
Entry	Arene	Nucleophile	Ref., Year
1	C ₆ H ₅ F, Cl	O, N nucleophiles	43, 1966
2	<i>p</i> -MeC ₆ H ₄ Cl	O, N nucleophiles	44, 1968
3	C ₆ H ₅ F, Cl	LiCMe ₂ CO ₂ Et Stabilized carbanions	45, 1974
4	C ₆ H ₅ OPh	LiCMe ₂ CN, LiCMe ₂ CO ₂ <i>t</i> Bu	46, 1987
5	1,2-C ₆ H ₄ Cl ₂	Stabilized carbanions Phase-transfer conditions	23, 1988
6	methoxy-estra-1,3,5(10)-triene	LiCH ₂ CN	47, 1988
7	C ₆ H ₅ F	Cyclopentadienylanion	48, 1989
8	C ₆ H ₅ F	Imino esters	49, 1989
9	<i>o,m,p</i> -MeC ₆ H ₄ F	Imino nitriles, esters	51, 1990
10	C ₆ H ₅ F	Imino esters	50, 1991
11	<i>o,m,p</i> -MeC ₆ H ₄ F	Imino nitriles, esters	52, 1991
12	<i>p</i> -Me-C ₆ H ₄ F	LiCMe ₂ CN, double nucleophilic substitutions	54, 1991
13	<i>p</i> -C ₆ H ₄ F ₂	LiC ₂ B ₁₀ H ₁₀ Me	54, 1992
14	veratrole derivative	ArMgX	56a, 1996
15	<i>p</i> -MeC ₆ H ₄ X	Cyclopentadienyl anion	57, 1997
16	1,2,3-trimethoxybenzene	LiCMe ₂ CN	58, 1997
17	C ₆ H ₅ Cl	<i>N,N</i> -dimethylhydrazone	59, 1997
18	<i>o</i> -CF ₃ C ₆ H ₄ Cl	PhCH(CN)Li	60, 1999
19	veratrole derivative	ArMgX	56b, 2000

banions fail to react with halogeno complexes. Indeed, LiCH₂CMe₂CO₂Me, LiCH₂COCMe₃, LiCH₂CN, LiCCH, and 2-lithio-1,3-dithiane effectively give complexes **2b–d**, but isomerization to **2a** is difficult due to a high associated energy barrier (Scheme 2). Indirect evidence of this has been obtained by adding I₂ to a mixture of isobutyronitrile carbanion and chlorobenzene complex at 0 °C; no chlorobenzene was detected, in good agreement with a complete conversion of complex **1b**. Free arenes corresponding to *o*- and *m*-chlorophenylisobutyronitriles **14e** were isolated in yields of 2 % and 56 %, respectively [45b]. The *ipso* complex **3b** was recovered in 19 % yield (Scheme 27). Thus, the initial attack of the nucleophile at low temperature occurs preferentially at the *meta* position, and then the course of the reaction depends on the reversibility of the initial addition, which, in turn, depends on the reactivity of the carbanion. For example, NaCH(CO₂Et)₂ adds reversibly, whereas the more reactive carbanions 2-methyl-1,3-dithianyl and CH₂CN add irreversibly at the *ortho* and *meta* positions; *ipso* substitution no longer occurs. It is shown below that there is a possibility of losing the halide by protonation of the η⁵-cyclohexadienyl anionic intermediate, which promotes the elimination of HX.



Scheme 27. *Ipsso* S_NAr: C–C bond formation.

Treatment of the *o*-methyl diphenyl ether complex **58a** with isobutyronitrile carbanion at -78°C and then allowing the reaction mixture to warm up to room temperature affords the *ipso* complex **59a** almost quantitatively. *Ipsso* S_NAr of the phenoxy group also occurs with acetonitrile, propionitrile, and alkoxy carbonyl carbanions (Scheme 28) [46]. Similarly, addition of isobutyronitrile carbanion to 2,3-dimethyl diphenyl ether complex **58b** gives exclusively complex **59b** under the same experimental conditions.

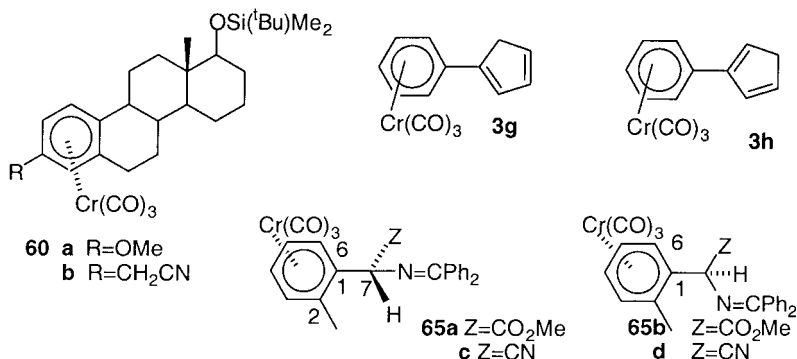


Scheme 28. *Ipsso* S_NAr: C–C bond formation.

The *o*-, *m*-, and *p*-dichlorobenzenetricarbonylchromium complexes **18a–c** react with stabilized carbanions LiCHRR₁ (R = Ph, CO₂Et; R₁ = CN, CO₂Et) both under phase-transfer conditions and in DMSO solution. Only one chloro substituent is replaced by the carbanion. In all cases, the intermediates are not isolated but are directly oxidized with iodine. Shorter reaction times and/or lower reaction temperatures are required in DMSO. It is possible to replace the second chloro substituent of the *o*- and *p*-dichloro regioisomers with a different nucleophile such as *n*BuS[−] or [−]CH(CN)CO₂Et [23].

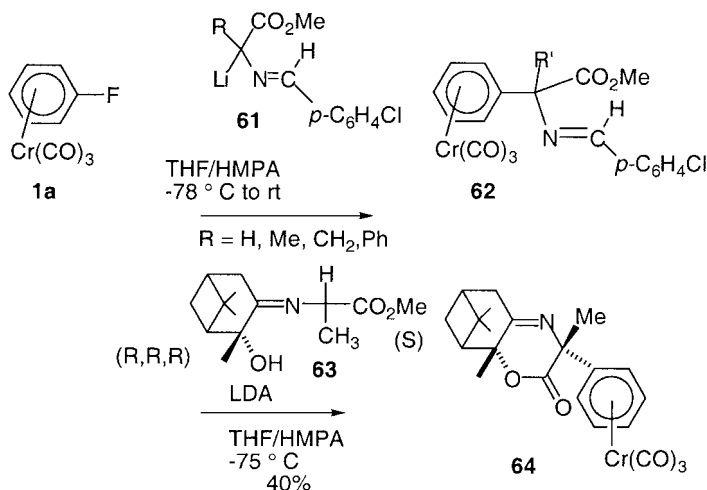
Nucleophilic attack by the lithium anion of acetonitrile has been extended to Cr complexes of ring A aromatic steroids, thereby allowing access to more elaborate derivatives. For example, the diastereomeric tricarbonylchromium complexes of 17β-(*tert*-butyldimethylsilyloxy)-3-methoxyestra-1,3,5-triene **60a** give the corresponding *ipso* 3-cyanomethyl complexes **60b** after displacement of the methoxide group. The free arene was obtained in 46 % yield after I₂ oxidation (Scheme 29) [47].

Cyclic anions, such as the cyclopentadienyl anion, in ethereal solvents at 0°C , can substitute the fluoride of fluorobenzenetricarbonylchromium complex **1a**, thereby generating

Scheme 29. *Ipso* S_NAr: C–C bond formation.

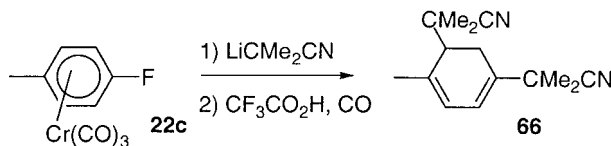
phenylcyclopentadiene complexes **3g** and **3h** in good yields [48] (Scheme 29). Phenylation of indenyl, fluorenyl, 2,4-dimethyl-1,3-pentadienyl, and 1,1',5,5'-tetramethyl-1,3-pentadienyl carbanions can be similarly achieved in an *ipso* S_NAr fashion.

A synthesis of α -aryl amino acids has been reported using Schiff-base anions **61** derived from amino esters, which are arylated with fluorobenzene complex **1a** to give α -aryl imino esters **62** in 48–76 % yield (R = H, Me, CH₂Ph) [49]. Using the same procedure, these authors reported a convenient synthesis of optically pure α -aryl amino acid precursors **64** by enantioselective substitution of fluorobenzene complex **1a** using the Schiff base of L-alanine methyl ester with (1R,2R,5R)-2-hydroxy-3-pinanone **63** in the presence of LDA (Scheme 30) [50].

Scheme 30. *Ipso* S_NAr: C–C bond formation.

Similarly, the addition of α -imino esters or nitriles to *o*-, *m*-, and *p*-fluorotoluene complexes **22a–c** gives α -substituted arylimino esters or nitriles by fluoride displacement. For example, addition of the Schiff-base anions $\text{LiCH}(\text{N}=\text{CPh}_2)\text{Y}$ ($\text{Y} = \text{CO}_2\text{Me}$, CN) in THF containing HMPA (5 equiv.) to a solution of the *o*-fluorotoluene complex **22a** at -78°C , followed by allowing the mixture to warm to room temperature for 24 h, gives complexes **65a,b** and **65c,d** in 45 % yield (Scheme 29). ^1H NMR data indicate that the two diastereomers **65a** (1*S*,7*S*) and **65b** (1*S*,7*R*) are obtained in a 1:1 ratio [51]. It is worthy of note that these diastereomers can be separated by column chromatography on silica gel. The X-ray structure of complex **65a** L couple [(1*S*)(7*S*), (1*R*)(7*R*)] shows that the H_6 proton is almost eclipsed by a $\text{Cr}-\text{CO}$ bond [52]. In solution, ^1H NMR data of this (1*S*)(7*S*) diastereomer indicate that the H_6 proton resonates at low field ($\delta = 6.4$), indicating a similar conformation in solution and in the solid state [53]. The H_6 proton of the U couple resonates at higher field, at $\delta = 5.93$. The addition of 2-methyl iminoester ($\text{Z} = \text{Me}$) also gives a mixture of two diastereomers, in the ratio L:U = 80:20. In this case, the chemical shift difference between the two H_6 protons amounts to 0.91 ppm!

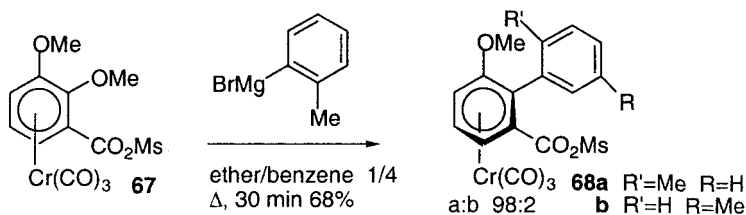
The addition of two nucleophiles to a coordinated η^6 -arene is a synthetically important goal. A “one-pot” synthesis of 1,3-disubstituted cyclohexadienes involving an initial *ipso* addition to fluoroarene complexes is possible. Indeed, *p*-fluorotoluenetricarbonylchromium complex **22c** reacts with isobutyronitrile carbanion (2 equiv.) in THF to give, after 5 days at -30°C and acidic treatment under CO atmosphere, the cyclohexadiene **66** in 47 % yield (Scheme 31) [53]; the yield can reach 75 % after several weeks! Carbon monoxide was used in order to decoordinate the η^4 -cyclohexadiene intermediate and to recover $\text{Cr}(\text{CO})_6$ needed for the preparation of the starting material [54].



Scheme 31. Double functionalization of an arene.

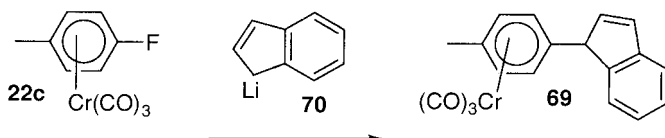
Carbon–boron clusters (“carboranes”) have been shown to react with Cr-coordinated haloarenes. For example, reaction of 2 equiv. of $\text{LiC}_2\text{B}_{10}\text{H}_{10}(\text{CH}_3)$ with *para*-difluorobenzene-tricarbonylchromium complex in refluxing THF results in the displacement of both fluoride substituents from the arene ring to yield the *para*-phenylene compound, albeit in just 9 % yield owing to the effect of the steric bulk of the carborane [55].

Axially chiral biaryls have been diastereoselectively synthesized by means of *ipso* substitution of the methoxide group of 2,4,6-trimethylphenyl-2-methoxybenzoatetricarbonylchromium complex with aryl Grignard reagents [56]. Thus, the reaction of veratrole derivative **67** with *o*-tolylmagnesium bromide leads to a diastereomeric mixture of anisole complexes **68a** and **68b** in 68 % yield and in a 98:2 ratio (Scheme 32). The most plausible reaction mechanism accounting for the high diastereoselectivity would require predominant Grignard approach from the *exo* side with respect to the $\text{Cr}(\text{CO})_3$ tripod [56].



Scheme 32. *Ipso* S_NAr: C–C bond formation.

The complex 3-[(η^6 -4-toluene)tricarbochromium]indene (**69**) is obtained in 69 % yield from the *ipso* nucleophilic substitution of (η^6 -*p*-fluorotoluene)tricarbochromium complex **22c** with indenyllithium (**70**) [57]. A 1,3-shift of the benzylic proton probably takes place after the *ipso* addition of indenyllithium (Scheme 33).

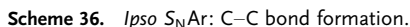
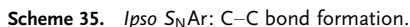


Scheme 33. *Ipso* S_NAr: C–C bond formation.

The following examples show interesting reactions in which C–C bonds are simultaneously created by both *ipso* and *tele-meta* substitutions (the latter is discussed in Section 11.3). Treatment of (η^6 -1,2,3-trimethoxybenzene) (**71**) with the acetonitrile carbanion in THF and then with trifluoroacetic acid leads to a mixture of complexes **72** and **73** in yields of 42 % and 22 %, respectively. The expected formation of complex **72** involves a *tele-meta* substitution of the MeO[−] group, whereas complex **73** is formed irreversibly, even at −78 °C, through an *ipso* S_NAr at the eclipsed C3 carbon, which is somewhat unexpected under these experimental conditions. Treatment of complex **71** with *n*BuLi in THF at −78 °C for 30 min, and then with CF₃CO₂D, affords not only the mono- and di-deuterated complexes **74** and **75**, but also the 3-butyl-4,6-dideuterioveratroletricarbochromium **76** as a minor by-product. Its formation can easily be explained in terms of a surprising *ipso* addition of *n*BuLi to one of the carbons bearing a methoxy group (Scheme 34) [58]. This is indicative of the electrophilic character of the eclipsed carbon C1 of complex **71**.

Arylation of *N,N*-dimethylhydrazone **77** with (η^6 -chlorobenzene)tricarbochromium complex **1b** can be achieved in 64 % yield. The copper lithium azaenolate **78** is trapped with the chromium complex at 70 °C to give α -phenyl ketone **80** as a result of an *ipso* substitution (Scheme 35) [59]. This represents an easy access to α -aryl carbonyl compounds, some of which may exhibit anti-inflammatory properties.

A final example of a carbon–carbon bond formation relates to the reaction of *o*-chlorotrifluoromethylbenzenetricarbonylchromium complex **81** with “in situ” generated phenylacetonitrile carbanion, which, under phase-transfer catalysis (TBAB, toluene, 50 % aqueous NaOH), quantitatively affords two diastereomeric products **82**, decomplexation of which yields α -phenyl- α -[2-(trifluoromethyl)phenyl]acetonitrile (Scheme 36) [60]. Activation of this



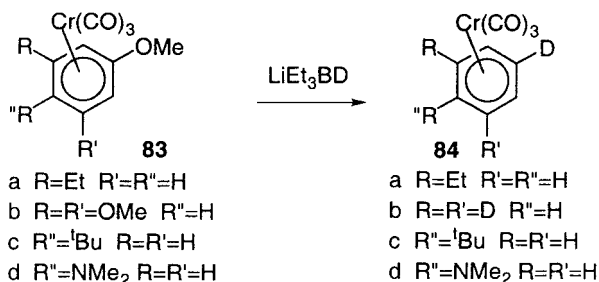
11.2.4

It has been reported that hydrides can be used as nucleophiles towards chromium complexes, and that treatment of 3-ethyl-anisoletricarboxylchromium **83a** with LiEt₃BD in refluxing THF for 2 h quantitatively affords 3-deuterio-ethylbenzenetricarboxylchromium **84a**.

Tab. 4. *Ipso* nucleophilic aromatic substitution of arenetricarbonylchromium complexes: C–H and C–metal bond formation.

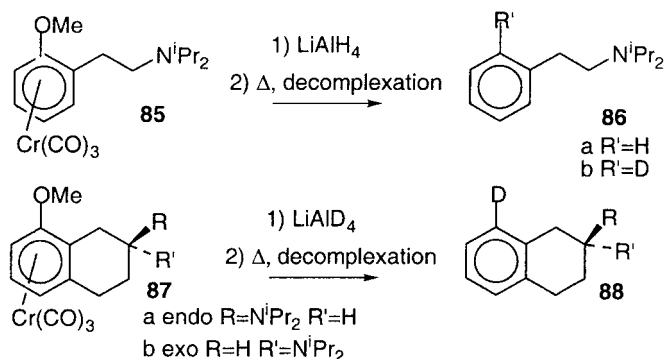
Entry	Arene	Nucleophile	Remarks	Ref., Year
1	C ₆ H ₅ Cl	KCpFe(CO) ₂	C–Fe bond formation	65, 1988
2	C ₆ H ₅ Cl	Na ₂ Fe(CO) ₄	C–Fe bond formation	64, 1988
3	1,4-C ₆ H ₄ XF	NaC ₅ H ₅ Fe(CO) ₂ , Na ₂ M(CO) ₅	C–Cr, C–W, C–Fe	67, 1989
4	anisole derivatives	LiEt ₃ BH(D)	C–H bond formation	60, 1990
5	tetralin	LiAlH ₄	C–H bond formation	61, 1991
6	dibenzofuran	LiEt ₃ BH	C–H bond formation	62, 1992
7	C ₆ H ₅ F	Na(C ₅ H ₄ Me)Fe(CO) ₂	C–Fe bond formation	68, 1992
8	1,3,5-trimethoxybenzene	LiAlH ₄	C–H bond formation	63, 1995

with no other isomer being detected. The three methoxide groups of 1,3,5-trimethoxybenzenetricarbonylchromium **83b** can be displaced by deuteride in a one-pot reaction to quantitatively afford 1,3,5-trideuteriobenzene tricarbonylchromium **84b**. These reactions represent the first hydro-(deuterio)-dealkoxylations reported for alkoxyarenechromium complexes (Scheme 37) [61].

**Scheme 37.** *Ipso* S_NAr: C–D bond formation.

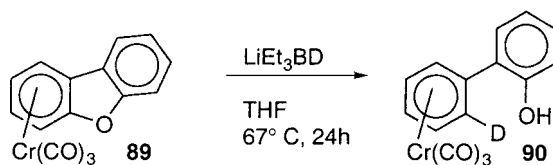
Treatment of 2-(2-methoxyphenyl)-*N,N*-diisopropylethylaminetricarbonylchromium **85** with LiAlH₄ gives an almost quantitative yield of demethoxylated product **86** after decomplexation. If LiAlD₄ is used, the deuteride replaces the methoxy group in a regiospecific manner through an *ipso* substitution (Scheme 38) [62]. Similarly, LiAlD₄ reacts with complexes **87a,b** to give complexes **88a,b**. This reaction occurs more rapidly with the *endo* than with the *exo* isomer, suggesting that a substituent located *syn* to the Cr(CO)₃ unit promotes the demethoxylation (Scheme 38). This could be the result of an eclipsed conformation of the tripod with respect to the OMe group.

Phenoxide group displacement by a hydride or a deuteride takes place in the case of the dibenzofuran complex. Indeed, on treating the dibenzofuran complex **89** with LiEt₃BD, ring-



Scheme 38. *Ips*o $\text{S}_{\text{N}}\text{Ar}$: C–H bond formation.

opening to the diphenyl complex **90** occurs in 75 % yield (Scheme 39). The C–O bond is cleaved in an *ipso* $\text{S}_{\text{N}}\text{Ar}$ of phenoxide group by deuteride, the mechanism of which has been clearly established by isolating one of the reaction intermediates [33].

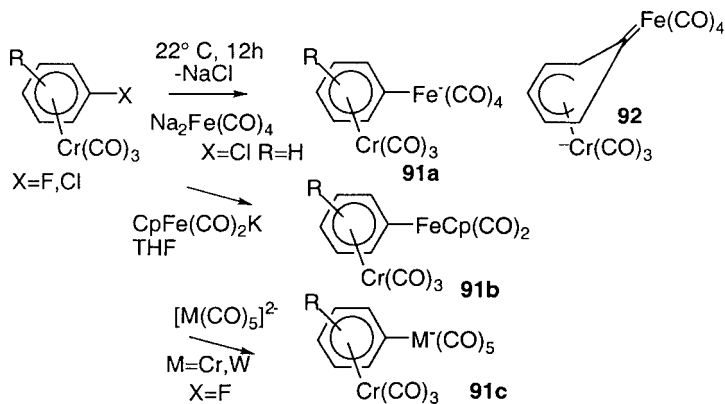


Scheme 39. *Ips*o $\text{S}_{\text{N}}\text{Ar}$: C–D bond formation.

Deuterio-dealkoxylation also occurs on treating 4-*tert*-butyl-anisoletricarboxylchromium complex **83c** with LiEt_3BD , giving *p-tert*-butyl-deuteriobenzene complex **84c**. Carbon–nitrogen bonds can be similarly cleaved by hydride: *p*-dimethylamino anisole complex **83d** affords, under the same experimental conditions, complex **84d** in 24 % yield (Scheme 37) [63].

Metal-based nucleophiles may react with activated haloarenechromium complexes leading to substitution of the halides. The reaction of Collman's reagent $\text{Na}_2[\text{Fe}(\text{CO})_4]$ with chloroarenetricarbonylchromium complexes in THF/*N*-methylpyrrolidinone produces the yellow anionic dinuclear complexes **91a** in 45 % yield (Scheme 40) as a result of an *ipso* $\text{S}_{\text{N}}\text{Ar}$ [64]. Spectroscopic data suggest that complex **91a** adopts the η^6 structure as opposed to the alternative η^5 -cyclohexadienyl carbene structure **92**. Similarly, it has been reported by the same group that the potassium salt of $[\text{CpFe}(\text{CO})_2]^-$ participates in *ipso* nucleophilic attack on chloroarenechromium substrates, producing dinuclear complexes **91b** in 92 % yield (Scheme 40) [65].

Organometallic dianions $[\text{M}(\text{CO})_5]^{2-}$ ($\text{M} = \text{Cr}, \text{W}$) also react with chlorobenzene-tricarboxylchromium in THF at 0°C to form anionic complexes **91c** in yields of 33 % and 11 %, respectively [66].



Scheme 40. *Ipso* S_NAr : C–M bond formation.

The reaction of $\text{Na}(\text{C}_5\text{H}_5)\text{Fe}(\text{CO})_2$ with $(\eta^6\text{-1,4-C}_6\text{H}_4\text{XR})\text{Cr}(\text{CO})_3$ chloro derivatives produces the bimetallic products **91b** in 32 % yield (Scheme 40) [67]. Similarly, reaction of $\text{NaCpFe}(\text{CO})_2$ ($\text{Cp} = \text{C}_5\text{H}_4\text{Me}$, indenyl, C_5H_5) with fluorobenzenetricarbonylchromium affords the respective complexes $[\text{C}_6\text{H}_5\text{Cr}(\text{CO})_3]\text{Fe}(\text{CO})_2\text{Cp}$ **91b**, for which X-ray structures have been obtained. They each display nonplanar benzene rings, with the iron atoms and the *ipso* carbon atoms to which they are bound being substantially bent away from the $\text{Cr}(\text{CO})_3$ tripod. This is due primarily to the π -electron donation from the iron centers to the aromatic rings, rather than to the steric bulk of the iron-containing substituents [68].

11.3

Cine and *Tele* Nucleophilic Aromatic Substitutions (Table 5)

11.3.1

Cleavage of C–F and C–Cl Bonds

Ipso nucleophilic aromatic substitutions represent the main substitution processes known in the case of arenetricarbonylchromium complexes bearing a fluoro or a chloro group. Another procedure involves the initial addition of a nucleophile to the *ortho*, *meta*, or *para* positions of the $\text{C}_6\text{H}_5\text{X}$ ring ($\text{X} = \text{F}$, Cl), followed by the addition of a strong acid (usually $\text{CF}_3\text{CO}_2\text{H}$). 1,5-Hydrogen migration in the $(\eta^4\text{-cyclohexadiene})$ intermediate allows rearomatization by loss of HX (Scheme 5). The result is a substitution in which the nucleophile occupies a site *ortho*, *meta*, or *para* to the leaving group. These reactions are called *cine*, *tele-meta*, and *tele-para* S_NAr (Scheme 6).

The regiochemical course of these *cine* and *para-tele* reactions can be conveniently followed by using deuterated trifluoroacetic acid [69]. Thus, addition of $\text{Li}(\text{CMe}_2)\text{CN}$ and $\text{CF}_3\text{CO}_2\text{D}$ to *p*-chlorotoluenetricarbonylchromium complex **14c** gives the *cine* deuterated complex **93a** and cyclohexadienes **94a** in yields of 42 % and 20 %, respectively (Scheme 41) [69a, 69c]. The chloro substituent is *o*-directing and the methyl substituent is *m*-directing. $\text{LiC}(\text{Ph})[\text{S}(\text{CH}_2)_3\text{S}]$ reacts with the same complex to give, after $\text{CF}_3\text{CO}_2\text{H}$ treatment,

Tab. 5. Cine and tele nucleophilic aromatic substitution of arenetricarbonylchromium complexes.

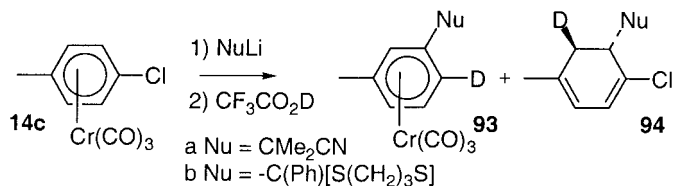
Entry	Arene	Nucleophile	Ref., Year
1	Diphenyl ether	LiCMe ₂ CN, LiCMe ₂ CO ₂ R	75, 1985–86/89
2	<i>p</i> -MeC ₆ H ₄ Cl	LiCMe ₂ CN	69a,e, 1986–89
3	2,6-diMe-C ₆ H ₃ X; X = F, Cl	LiC(CH ₃)[S(CH ₂) ₃ S], LiCMe ₂ CN LiC(Ph)[S(CH ₂) ₃ S]	72, 1987–89
4	<i>m</i> -MeC ₆ H ₄ Cl	LiCMe ₂ CN, LiC(Ph)[S(CH ₂) ₃ S]	69e, 1989
5	<i>o</i> -MeC ₆ H ₄ Cl	ArSO ₂ CH ₂ Li	71, 1990–94
6	<i>o</i> -Me ₃ SiC ₆ H ₄ X	LiEt ₃ BD	69f, 1991
7	<i>o</i> -Me ₃ SiC ₆ H ₄ OPh	LiEt ₃ BD	69f, 1991
8	<i>o</i> -Me ₃ SiC ₆ H ₄ NMe ₂	LiEt ₃ BD	73, 1991
9	methoxyarene	<i>n</i> BuLi	58, 1997
10	veratrole	LiCR ₂ CN	58, 77, 1997, 1989
11	1,3,5-trimethoxybenzene	LiCR ₂ CN	74, 2000

For *cine* S_NAr, see refs. [16, 69a, 71a, 71b, 73, 75b, 77].

For *tele-meta* S_NAr, see refs. [16, 57, 58, 69b–d, 70, 73, 74, 75a, 75b, 76].

For *tele-para* S_NAr, see: [72a, 72b].

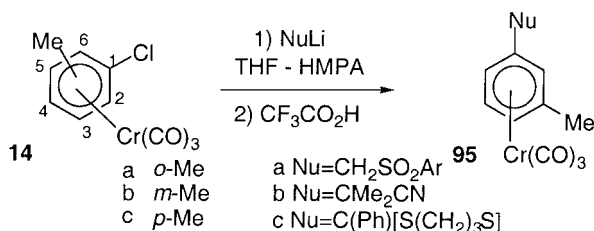
1-methyl-4-chloro-5-(2'-phenyl-1',3'-dithiane)-1,3-cyclohexadiene **94b** as the sole cyclohexadiene isomer, which has been characterized by X-ray crystallography [69b]. This study not only shows that the nucleophile adds *ortho* to the chloro substituent, but also that isomerization of the η^4 -cyclohexadiene **94** coordinated to Cr(CO)₃ does not occur for steric reasons, thus avoiding elimination of HX.



Scheme 41. Cine and tele-*meta* S_NAr: C–Cl bond cleavage.

Addition of ArSO₂CH₂Li to *o*-chlorobenzenetricarbonylchromium complex **14a** gives, after CF₃CO₂H treatment, the *meta*-disubstituted complex **95a** in 72 % yield at 0 °C under thermodynamic control (*cine* S_NAr). Addition of the nucleophile, even at –10 °C, occurs initially at the carbons C3 and C6 (Scheme 42) [71].

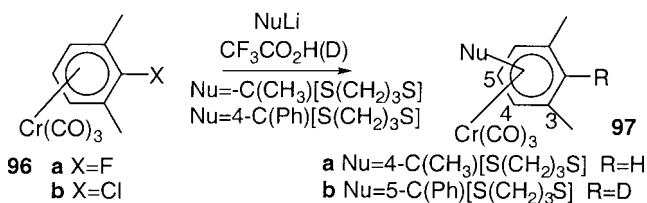
Addition of two equivalents of LiCMe₂CN or LiC(Ph)[S(CH₂)₃S] to *m*-chlorotoluene-Cr(CO)₃ complex **14b**, followed by acid treatment, gives the *tele-meta* complexes **95b** and **95c** in yields of 62 % and 58 %, respectively. No incorporation of deuterium is observed, in good agreement with the mechanism described above (Scheme 5). This *meta* regioselectivity can



Scheme 42. *Cine* and *tele-meta* S_NAr: C–Cl bond cleavage.

be explained in terms of preferential addition of the stabilized carbanion to the carbon eclipsed by a Cr–CO bond in the most stable conformer [69e]. This *tele-meta* regioselectivity is also observed on adding LiEt₃BD to *o*-chloro- or *o*-fluorotrialkylsilylbenzenetricarbonylchromium complexes having an *anti*-eclipsed conformation with respect to the SiR₃ group, giving *p*-deuterated trialkylsilylbenzenetricarbonylchromium complexes [69d].

The effect of the nature of the leaving group has been delineated in the case of 2,6-dimethylfluoro and chloro complexes. Complex **96a** reacts with LiC(CH₃)[S(CH₂)₃S] and CF₃CO₂D to give exclusively complex **97a** by a *tele-meta* S_NAr [70], whereas complex **96b** reacts with LiC(Ph)[S(CH₂)₃S] and CF₃CO₂D to give deuterated complex **97b** by a *tele-para* S_NAr [72].

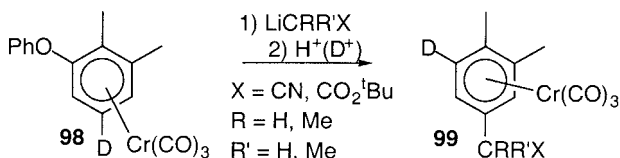


Scheme 43. *Tele-meta* and *tele-para* S_NAr: C–Cl bond cleavage.

11.3.2

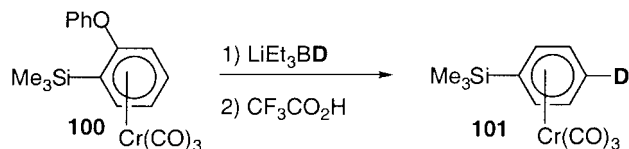
Cleavage of C–O Bonds

Reaction of NuLi (Nu = CMe₂CN, CHMeCN, CH₂CN, etc.) with 5-deuterio-2,3-dimethyldiphenylethertricarboxylchromium complex **98** yields, after CF₃CO₂H(D) treatment, the deuterated complex **99**. This reaction has been shown to involve a 1,5-deuteride migration from the C5 carbon to the C1 carbon (Scheme 44) [75a, 75b].



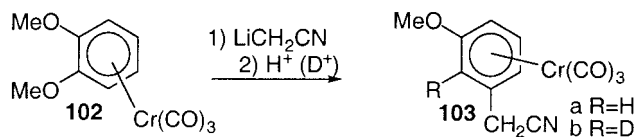
Scheme 44. *Tele-meta* S_NAr: C–O bond cleavage.

Reaction of LiEt_3BD and $\text{CF}_3\text{CO}_2\text{H}$ with *o*-trimethylsilyldiphenylethertricarboxylchromium complex **100** gives the *tele-meta* complex **101** in 77 % yield (Scheme 45) [69d].



Scheme 45. *Tele-meta* $S_N\text{Ar}$: C–O bond cleavage.

Treatment of veratroletricarboxylchromium complex **102** with LiCH_2CN in THF at -40°C for 30 min and then with acid leads to the formation of (3-methoxyphenyl)acetonitrile complex **103a** in 47 % yield (Scheme 46). From this experiment, it cannot be ascertained whether the carbanion adds to the carbon *ortho* to the methoxy group (*cine* $S_N\text{Ar}$) or to the carbon *para* to the methoxy group (*tele-para* $S_N\text{Ar}$) because in each case a *meta*-disubstituted complex is formed. Consequently, $\text{CF}_3\text{CO}_2\text{D}$ is used, whereupon complex **103b** deuterated at the C2 carbon is obtained, as befits a *cine* $S_N\text{Ar}$. When the positions *ortho* to the MeO groups are substituted, *tele* regioselectivity is observed [76]. The same reaction with 1,2,3-trimethoxybenzenetricarboxylchromium complex **71** affords complex **72** by a *tele-meta* $S_N\text{Ar}$ as the major product (42 % yield), contaminated by the *ipso* complex **73** (22 % yield) (*vide supra*; Scheme 34) [58, 74].

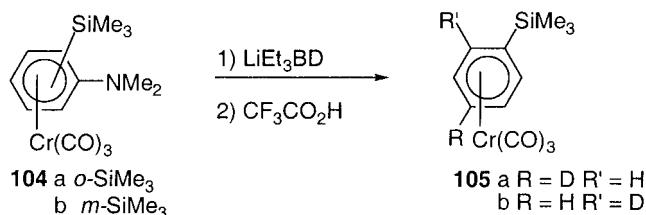


Scheme 46. *Cine* $S_N\text{Ar}$: C–O bond cleavage.

11.3.3

Cleavage of C–N Bonds

An unprecedented cleavage of a carbon–nitrogen bond of a tertiary amine is observed on treating *o*-trimethylsilyldimethylaniline tricarboxylchromium complex **104a** with LiEt_3BD and then with $\text{CF}_3\text{CO}_2\text{H}$. Complexes **105a** and **105b** (ratio 20:80) are recovered as a result of *tele-meta* $S_N\text{Ar}$ (20:80 ratio; 55 % yield; Scheme 47) [73]. When the same experiment is



Scheme 47. *Cine* and *tele* $S_N\text{Ar}$: C–N bond cleavage.

carried out with the *meta* isomer **104b**, complex **105a** is formed, which can be explained in terms of a *cine* mechanism after incorporation of a second deuterium at the *meta* position relative to the SiMe₃ group if CF₃CO₂D is used.

11.4

Concluding Remarks

Methods are available using arenetricarbonylchromium complexes that allow the substitution of hydrogen, halogen, alkoxy, aryloxy, and amino groups by nucleophiles under very mild conditions without decoordination of the Cr(CO)₃ unit. In the light of the results presented herein, three new S_NAr processes, namely the *cine*, *tele-meta*, and *tele-para* S_NAr, have been discovered in our laboratory, which broaden the scope of the applications of these complexes in organic chemistry. These reactions are possible by treating an arenetricarbonylchromium complex substituted by a good leaving group first with a nucleophile and then with an acid. This represents an alternative to the well-known *ipso* S_NAr, which corresponds to a direct addition of a nucleophile to the carbon bearing a leaving group. Knowing that Cr(CO)₆ can be recovered by treating these (η^6 -arene) complexes under CO atmosphere, it is possible to recover the free arene as well as Cr(CO)₆ necessary to prepare the chromium complex. This is the first step of a “pseudo catalytic” cycle. Further work will focus on the possibility of transforming these stoichiometric reactions into catalytic reactions. The main challenge at the present time is to find a general process whereby these fantastic creations of C–O, C–N, and C–C bonds can be made catalytic in the metal. It is also fascinating to know that it is now possible to predict the regioselectivity of the addition of a nucleophile, provided that the reaction is under kinetic control at low temperature. This sheds light on the fundamental role of the Cr(CO)₃ conformation in solution, because addition of the nucleophile occurs preferentially at a carbon eclipsed by a Cr–CO bond. Knowing that the Friedel–Crafts reaction is widely used in arene chemistry to add an electrophile to a ring, it is clear that addition of a nucleophile represents a complementary tool for the functionalization of an arene ring, for which the regioselectivity is now predictable. *Ipso*, *cine*, *tele-meta*, and *tele-para* S_NAr are reactions that keep the Cr(CO)₃ entity still coordinated to the arene ring, and thus a second nucleophile can react to give new disubstituted cycles.

Abbreviations

Cp	cyclopentadienyl
DMSO	dimethyl sulfoxide
HMPA	hexamethylphosphoramide
LDA	lithium diisopropylamide
S _N Ar	nucleophilic aromatic substitution
TBAB	tetrabutylammonium bromide
THF	tetrahydrofuran
TMEDA	tetramethylethylenediamine

Acknowledgements

For the published and unpublished work from our group, we gratefully acknowledge our collaborators whose names appear in the cited references. We thank the CNRS and the EU training and mobility of researchers programme, contract ERBFMR XCT-CT98-0166, for financial support.

References

- 1 For reviews, see: a) L. BALAS, D. JHURRY, L. LATXAGUE, S. GRELIER, Y. MOREL, M. HAMDANI, D. ASTRUC, *Bull. Soc. Chim. Fr.* **1990**, 127, 401; b) F. J. MCQUILLIN, D. G. N. PARKER, G. R. STEPHENSON, *Transition Metals in Organic Synthesis*, Cambridge University Press, Cambridge, **1991**; c) M. F. SEMMELHACK, in: *Comprehensive Organometallic Chemistry II*, vol. 12 (Eds.: E. W. ABEL, F. G. A. STONE, G. WILKINSON), Pergamon, Oxford, **1995**, p. 979; d) S. G. DAVIES, T. D. MCCARTHY, in *Comprehensive Organometallic Chemistry II*, vol. 12 (Ed.: E. W. ABEL, F. G. A. STONE, G. WILKINSON), Pergamon, Oxford, **1995**, p. 1039; e) M. J. MORRIS, in *Comprehensive Organometallic Chemistry II*, Vol. 5 (Eds.: E. W. ABEL, F. G. A. STONE, G. WILKINSON; Volume Eds.: J. A. LABINGER, M. J. WINTER), Pergamon, Oxford, **1995**; f) F. ROSE-MUNCH, V. GAGLIARDINI, C. RENARD, E. ROSE, *Coord. Chem. Rev.* **1998**, 178, 249; g) F. ROSE-MUNCH, E. ROSE, *Curr. Org. Chem.* **1999**, 3, 445; h) F. ROSE-MUNCH, E. ROSE, J. P. DJUKIC, J. VAISSER-MANN, *Eur. J. Inorg. Chem.* **2000**, 1295; i) A. R. PAGE, K. P. KALIAPPAN, E. P. KÜNDIG, *Chem. Rev.* **2000**, 100, 2917; j) D. ASTRUC, in *Chimie Organométallique*, EDP Sciences, Les Ulis, France, **2000**; Chapters 3–6, p. 87; k) F. ROSE-MUNCH, E. ROSE, *Eur. J. Inorg. Chem.* **2002**, 1269.
- 2 D. ASTRUC, *Top. Curr. Chem.* **1992**, 160, 47.
- 3 L. A. P. KANE-MAGUIRE, E. D. HONIG, D. A. SWEIGART, *Chem. Rev.* **1984**, 84, 525.
- 4 R. D. PIKE, D. A. SWEIGART, *Synlett.* **1990**, 565.
- 5 C. A. L. MAHAFFY, P. L. PAUSON, *Inorg. Synth.* **1979**, 19, 154.
- 6 B. NICHOLLS, M. C. WHITING, *J. Chem. Soc.* **1959**, 551.
- 7 a) S. I. ROSCA, S. ROSCA, *Revista de Chemie (Bucharest)* **1964**, 25, 461; b) M. UEMURA, H. NISHIMURA, T. HAYASHI, *J. Organomet. Chem.* **1994**, 473, 129.
- 8 T. OISHI, M. FUKUI, Y. ENDO, *Heterocycles* **1977**, 7, 947.
- 9 A. ALEMAGNA, C. BALDOLI, P. DEL BUTTERO, E. LICANDRO, S. MAIORANA, *Gazz. Chim. Ital.* **1985**, 115, 555.
- 10 J. HAMILTON, C. A. L. MAHAFFY, *Synth. React. Inorg. Met.-Org. Chem.* **1986**, 116, 66.
- 11 F. ROSE-MUNCH, R. KHOURZOM, J.-P. DJUKIC, E. ROSE, *J. Organomet. Chem.* **1993**, 456, C8.
- 12 A. ALEMAGNA, C. BALDOLI, P. DEL BUTTERO, E. LICANDRO, S. MAIORANA, *J. Chem. Soc., Chem. Commun.* **1985**, 417.
- 13 A. ALEMAGNA, C. BALDOLI, P. DEL BUTTERO, E. LICANDRO, S. MAIORANA, *Synthesis* **1987**, 192.
- 14 C. BALDOLI, P. DEL BUTTERO, E. LICANDRO, S. MAIORANA, *Synthesis* **1988**, 344.
- 15 D. G. LOUGHHEAD, L. A. FLIPPIN, R. J. WEIKERT, *J. Org. Chem.* **1999**, 64, 3373.
- 16 F.-E. HONG, S.-C. LO, M.-W. LIU, Y.-T. CHANG, C.-C. LIN, *J. Organomet. Chem.* **1996**, 506, 101.
- 17 F. HOSSNER, M. VOYLE, *J. Organomet. Chem.* **1988**, 347, 365.
- 18 a) R. P. HOUGHTON, M. VOYLE, *J. Chem. Soc., Chem. Commun.* **1980**, 884; b) R. P. HOUGHTON, M. VOYLE, R. PRICE, *J. Organomet. Chem.* **1983**, 259, 183.
- 19 C. BALDOLI, P. DEL BUTTERO, S. MAIORANA, A. PAPAGNI, *J. Chem. Soc., Chem. Commun.* **1985**, 1181.
- 20 M. F. SEMMELHACK, J. BISABA, M. CZARNY, *J. Am. Chem. Soc.* **1979**, 101, 768.
- 21 P. J. BESWICK, D. A. WIDDOWSON, *Synthesis* **1985**, 492.

- 22 a) A. ALEMAGNA, P. DEL BUTTERO, C. GORINI, D. LANDINI, E. LICANDRO, S. MAIORANA, *J. Org. Chem.* **1983**, 48, 605; b) A. ALEMAGNA, P. CREMONESI, P. DEL BUTTERO, E. LICANDRO, S. MAIORANA, *J. Org. Chem.* **1983**, 48, 3114.
- 23 C. BALDOLI, P. DEL BUTTERO, E. LICANDRO, S. MAIORANA, *Gazz. Chim. Ital.* **1988**, 118, 409.
- 24 M. J. DICKENS, J. P. GILDAY, T. J. MOWLEM, D. A. WIDDOWSON, *Tetrahedron* **1991**, 47, 8621.
- 25 A. A. VASIL'EV, L. ENGMAN, J. P. STORM, C.-M. ANDERSON, *Organometallics* **1999**, 18, 1318.
- 26 a) A. N. NESMEYANOV, N. A. VOL'KENAU, I. N. BOLESEVA, *Dokl. Akad. Nauk. SSSR* **1967**, 175, 1606 and **1968**, 183, 834; b) J. F. BUNNET, H. HERMANN, *J. Org. Chem.* **1971**, 36, 4081.
- 27 C. A. L. MAHAFFY, P. L. PAUSON, *J. Chem. Res.* **1979**, 128.
- 28 a) M. GHAVSHOU, D. A. WIDDOWSON, *J. Chem. Soc., Perkin Trans. 1* **1983**, 3065; b) J. P. GILDAY, D. A. WIDDOWSON, *J. Chem. Soc., Chem. Commun.* **1986**, 1235.
- 29 J. P. GILDAY, D. A. WIDDOWSON, *Tetrahedron Lett.* **1986**, 27, 5525.
- 30 Y. ISHII, Y. ISHINO, T. AOKI, M. HIDAI, *J. Am. Chem. Soc.* **1992**, 114, 5429.
- 31 C. BALDOLI, P. DEL BUTTERO, S. MAIORANA, *Tetrahedron. Lett.* **1992**, 33, 4049.
- 32 S. G. DAVIES, W. E. HUME, *Tetrahedron Lett.* **1995**, 36, 2673.
- 33 J. P. DJUKIC, F. ROSE-MUNCH, E. ROSE, Y. DROMZEE, *J. Am. Chem. Soc.* **1993**, 115, 6434.
- 34 M. PEREZ, P. POTIER, S. HALAZY, *Tetrahedron Lett.* **1996**, 37, 8487.
- 35 M. F. SEMMELHACK, G. HILT, J. H. COLLEY, *Tetrahedron Lett.* **1998**, 39, 7683; see also refs. [27, 29].
- 36 K. G. MOLAY, J. L. PETERSEN, *J. Am. Chem. Soc.* **1995**, 117, 7696.
- 37 S. MAIORANA, C. BALDOLI, P. DEL BUTTERO, M. DI CIOLO, A. PAPAGNI, *Synthesis* **1998**, 5, 735.
- 38 S. MAIORANA, C. BALDOLI, E. LICANDRO, L. CASIRAGHI, E. DE MAGISTRIS, A. PAIO, S. PROVERA, P. SERRECI, *Tetrahedron Lett.* **2000**, 41, 7271.
- 39 M. R. G. DA COSTA, M. J. M. CURTO, S. G. DAVIES, M. T. DUARTE, C. RESENDE, F. C. TEIXEIRA, *J. Organomet. Chem.* **2000**, 604, 157.
- 40 a) G. R. BROWN, A. J. FOUBISTER, P. D. RATCLIFFE, *Tetrahedron Lett.* **1999**, 40, 1219; b) A. J. BELFIELD, G. R. BROWN, A. J. FOUBISTER, P. D. RATCLIFFE, *Tetrahedron* **1999**, 50, 1328; c) M. KIDWAI, P. SAPRA, B. DAVE, *Synth. Commun.* **2000**, 30, 4479.
- 41 Pd: a) A. S. GURAM, S. L. BUCHWALD, *J. Am. Chem. Soc.* **1994**, 116, 7901; b) F. PAUL, J. PATT, J. F. HARTWIG, *J. Am. Chem. Soc.* **1994**, 116, 5969; c) L. M. ALCAZAR-ROMAN, J. F. HARTWIG, A. L. RHEINGOLD, L. M. LIABLE-SANDS, I. A. GUZEI, *J. Amer. Chem. Soc.* **2000**, 122, 4618; d) F. A. HICKS, M. BROOKHART, *Org. Lett.* **2000**, 219; e) J. P. WOLFE, S. L. BUCHWALD, *J. Org. Chem.* **2000**, 65, 1144; f) S. R. STAUFFER, S. LEE, J. P. STAMBULI, S. I. HAUCK, J. F. HARTWIG, *Org. Lett.* **2000**, 2, 1423; Ni: g) C. DESMARETS, R. SCHNEIDER, Y. FORT, *Tetrahedron Lett.* **2001**, 42, 247; h) E. BRENNER, R. SCHNEIDER, Y. FORT, *Tetrahedron Lett.* **2000**, 41, 2881; i) A. J. BELFIELD, *Tetrahedron* **1999**, 50, 1328; Cu: j) R. K. GUJADHUR, C. G. BATES, D. VENKATARAMAN, *Org. Lett.* **2001**, 3, 4315; without metal activation, see ref. [40].
- 42 S. G. NELSON, M. A. HILFIKER, *Org. Lett.* **1999**, 1, 1379.
- 43 D. BROWN, J. R. RAJU, *J. Chem. Soc., A* **1966**, 40 and 1617.
- 44 I. U. KHAND, P. L. PAUSON, W. E. WATTS, *J. Chem. Soc., C* **1968**, 2257.
- 45 a) M. F. SEMMELHACK, H. T. HALL, *J. Am. Chem. Soc.* **1974**, 96, 7091; b) M. F. SEMMELHACK, H. T. HALL, *J. Am. Chem. Soc.* **1974**, 96, 7092; c) M. F. SEMMELHACK, H. T. HALL, M. YOSHIFUJI, G. CLARK, *J. Am. Chem. Soc.* **1975**, 97, 1247.
- 46 J. C. BOUTONNET, F. ROSE-MUNCH, E. ROSE, A. SEMRA, *Bull. Soc. Chim. Fr* **1987**, 640.
- 47 H. KÜNZER, M. THIEL, *Tetrahedron Lett.* **1988**, 29, 1135.
- 48 A. CECCON, A. GAMBARO, F. GOTTARDI, F. MANOLI, A. VENZO, *J. Organomet. Chem.* **1989**, 363, 91.
- 49 M. CHAARI, J.-P. LAVERGNE, P. VIALLEFONT, *Synth. Commun.* **1989**, 19, 1211.
- 50 M. CHAARI, A. JENKI, J.-P. LAVERGNE, PH. VIALLEFONT, *J. Organomet. Chem.* **1991**, 401, C10.

- 51 F. ROSE-MUNCH, K. ANISS, E. ROSE, J. *Organomet. Chem.* **1990**, 385, C1.
- 52 F. ROSE-MUNCH, K. ANISS, E. ROSE, J. VAISSEMMANN, J. *Organomet. Chem.* **1991**, 415, 223.
- 53 J.-C. BOUTONNET, O. LE MARTRET, L. MORDENTI, G. PRECIGOUX, E. ROSE, J. *Organomet. Chem.* **1981**, 221, 47.
- 54 F. ROSE-MUNCH, L. MIGNON, J.-P. SOUCHEZ, *Tetrahedron Lett.* **1991**, 32, 6323.
- 55 T. J. HENLY, C. B. KNOBLER, M. F. HAWTHORNE, *Organometallics* **1992**, 11, 2313.
- 56 a) K. KAMIKAWA, M. UEMURA, *Tetrahedron Lett.* **1996**, 37, 6359; b) K. KAMIKAWA, M. UEMURA, *Synlett* **2000**, 7, 938.
- 57 F.-E. HONG, Y.-C. YONG, S.-C. LO, C.-C. LIN, *Polyhedron* **1997**, 16, 2005.
- 58 V. GAGLIARDINI, V. ONNIKIAN, F. ROSE-MUNCH, E. ROSE, *Inorg. Chim. Acta* **1997**, 259, 265.
- 59 T. MINO, T. MATSUDA, K. MARUHASHI, M. YAMASHITA, *Organometallics* **1997**, 16, 3241.
- 60 S. VARELA CALAFAT, E. N. DURANTINI, J. J. SILBER, S. M. CHIACCHIERA, *Organometallics* **1999**, 18, 2727.
- 61 F. ROSE-MUNCH, J.-P. DJUKIC, E. ROSE, *Tetrahedron Lett.* **1990**, 31, 2589.
- 62 M. PERSSON, U. HACKSELL, I. CSOREGH, J. *Chem. Soc., Perkin Trans. 1* **1991**, 1453.
- 63 J.-P. DJUKIC, F. ROSE-MUNCH, E. ROSE, *Organometallics* **1995**, 14, 2027.
- 64 J. A. HEPPERT, M. E. THOMAS-MILLER, P. E. SWESTON, M. W. EXTINE, J. *Chem. Soc., Chem. Commun.* **1988**, 280.
- 65 J. A. HEPPERT, M. A. MORGENSTERN, D. M. SCHERUBEL, F. TAKUSAGAWA, M. R. SHAKER, *Organometallics* **1988**, 7, 1715.
- 66 J. A. HEPPERT, M. E. THOMAS-MILLER, D. M. SCHERUBEL, F. TAKUSAGAWA, M. A. MORGENSTERN, M. R. SHAKER, *Organometallics* **1989**, 8, 1199.
- 67 G. B. RICHTER-ADDO, A. D. HUNTER, N. WICHROWSKA, *Can. J. Chem.* **1990**, 68, 41.
- 68 J. LI, A. D. HUNTER, R. McDONALD, B. D. SANTARSIERO, S. G. BOTT, J. L. ATWOOD, *Organometallics* **1992**, 11, 3050.
- 69 a) F. ROSE-MUNCH, E. ROSE, A. SEMRA, J. *Chem. Soc., Chem. Commun.* **1986**, 1551; b) F. ROSE-MUNCH, E. ROSE, A. SEMRA, Y. JEANNIN, F. ROBERT, J. *Organomet. Chem.* **1988**, 353, 53; c) F. ROSE-MUNCH, E. ROSE, A. SEMRA, C. BOIS, J. *Organomet. Chem.* **1989**, 363, 103; d) J.-P. DJUKIC, P. GEYSERMANS, F. ROSE-MUNCH, E. ROSE, *Tetrahedron Lett.* **1991**, 32, 6703.
- 70 F. ROSE-MUNCH, E. ROSE, A. SEMRA, L. MIGNON, J. GARCIA-ORICAIN, C. KNOBLER, J. *Organomet. Chem.* **1989**, 363, 297.
- 71 a) F. ROSE-MUNCH, J.-P. DJUKIC, E. ROSE, *Tetrahedron Lett.* **1990**, 31, 2011; b) F. ROSE-MUNCH, R. KHOURZOM, J.-P. DJUKIC, A. PERROTEY, E. ROSE, J. BROCARD, J. *Organomet. Chem.* **1994**, 467, 195.
- 72 a) F. ROSE-MUNCH, E. ROSE, A. SEMRA, M. PHILOCHE-LEVISALLES, J. *Organomet. Chem.* **1989**, 363, 123; b) F. ROSE-MUNCH, E. ROSE, A. SEMRA, J. *Chem. Soc., Chem. Commun.* **1987**, 942.
- 73 J.-P. DJUKIC, F. ROSE-MUNCH, E. ROSE, J. *Chem. Soc., Chem. Commun.* **1991**, 22, 1634.
- 74 F. ROSE-MUNCH, R. CHAVIGNON, J.-P. TRANCHIER, V. GAGLIARDINI, E. ROSE, *Inorg. Chim. Acta* **2000**, 300–302, 693.
- 75 a) J.-C. BOUTONNET, F. ROSE-MUNCH, E. ROSE, *Tetrahedron Lett.* **1985**, 26, 3989; b) F. ROSE-MUNCH, E. ROSE, A. SEMRA, J. *Chem. Soc., Chem. Commun.* **1986**, 1108; see also refs. [16, 76, 77].
- 76 a) H.-G. SCHMALZ, M. ARNOLD, J. HOLLANDE, J. W. BATS, *Angew. Chem. Int. Ed. Engl.* **1994**, 33, 109; b) H.-G. SCHMALZ, K. SCHELLHAAS, *Tetrahedron Lett.* **1995**, 36, 5511; c) H.-G. SCHMALZ, K. SCHELLHAAS, *Angew. Chem. Int. Ed. Engl.* **1996**, 35, 2146; d) H.-G. SCHMALZ, T. VOLK, D. BERNICKE, S. HUNECK, *Tetrahedron* **1997**, 53, 9219.
- 77 F. ROSE-MUNCH, E. ROSE, A. SEMRA, J. *Organomet. Chem.* **1989**, 377, C9.

12

Activation of Simple Arenes by the CpFe^+ Group and Applications to the Synthesis of Dendritic Molecular Batteries

Didier Astruc, Sylvain Nlate, and Jaime Ruiz

Abstract

The CpFe^+ -induced polyfunctionalization of polymethylbenzenes under ambient conditions gives virtually quantitative yields of $\text{CpFe}^+(\eta^6\text{-arene})$ -centered stars and dendritic cores on a large scale. From the chlorotoluene complex, mild nucleophilic reaction with ethanol in the presence of K_2CO_3 followed by mild reaction with allyl bromide in the presence of $t\text{BuOK}$ gives a 60 % yield of the triallyl phenol dendron $p\text{-HOC}_6\text{H}_4\text{C(allyl)}_3$. This dendron and its functionalized derivatives have been used as building blocks for the divergent synthesis of large dendrimers and for the convergent synthesis of nonafunctional dendrons including dendrons bearing ferrocenylsilyl termini on their branches. The various dendrimers, with branch numbers of up to 243 in theory, have been decorated with ferrocenyl groups, and polyaminodendrimers have been functionalized with ferrocenyl, cobaltocenyl, and CpFe^+ -arene moieties. The generation or isolation of two redox states of these metallodendrimers and electron-transfer reactions illustrate their function as molecular electron reservoirs or molecular batteries.

12.1

Introduction

Molecular batteries should be useful as part of nanoscopic molecular electronic devices [1–4]. Ideally, nanoscopic assemblies containing a large number of redox centers, for which both redox forms are stable and which operate at the same redox potential, should be able to deliver or accept a large number of electrons at once at this redox potential. Such an assembly constitutes a battery – a molecular battery or a molecular electron reservoir if it is a molecular assembly. Metallodendrimers [5–14] are excellent candidates for such a function when at least two of their redox states are stable [15]. This property is realized with some late transition metal metallocenes and analogous sandwich systems. We describe herein the synthesis and properties of such nanoscopic metallo-assemblies that can be considered as molecular batteries. These syntheses are largely based on the activation of simple arenes by the electron-withdrawing group CpFe^+ [16]. This metal group is thus useful for both

dendritic construction and redox activity [5]. Below are summarized the main properties of the $[\text{CpFe}^+(\eta^6\text{-arene})]$ complexes [17], with emphasis on those relevant to the dendritic syntheses and dendritic redox function.

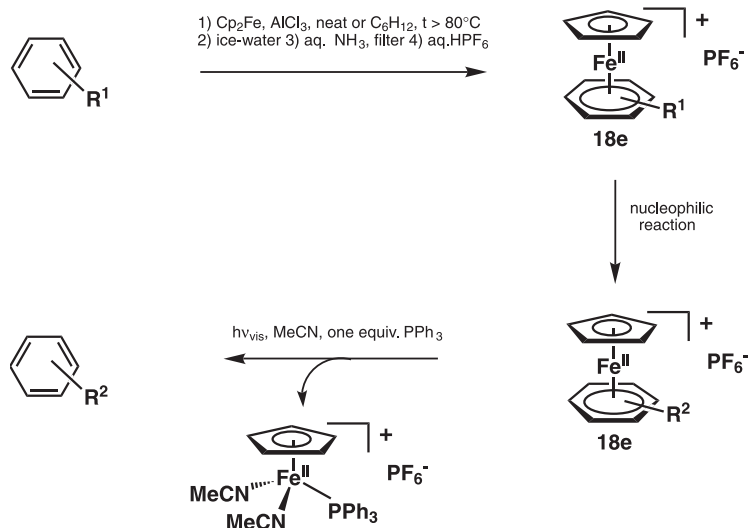
12.2

General Features of the CpFe^+ Activation of Arenes

12.2.1

Complexation and Decomplexation

The CpFe^+ group is an extremely powerful and useful activator of simple arenes [16–19]. It can be easily introduced on a large number of arenes either by reaction with ferrocene in the presence of aluminum chloride [20] or by photolytic arene exchange with another $\text{CpFe}^+(\eta^6\text{-arene})$ complex in dichloromethane in the presence of visible light [18]. Following CpFe^+ -activation of the desired reaction, the CpFe^+ group can be easily removed by photolysis with visible light [21] in acetonitrile solution containing one equivalent of PPh_3 , and then the free arene can be extracted into pentane or diethyl ether (Scheme 1) [16]. Thus, although it is possible to work with organic solutions of these salts in daylight, prolonged exposure to light (especially sunlight) should be avoided if the purpose is not decomplexation. The $\text{CpFe}^+(\eta^6\text{-aniline})$ -type complexes are resistant to decomplexation using this procedure, however, and decomplexation is best achieved by single-electron reduction to the unstable Fe^{I} complex using a rather strong reductant (with E° more negative than 2 V *vs.* FeCp_2) [22].

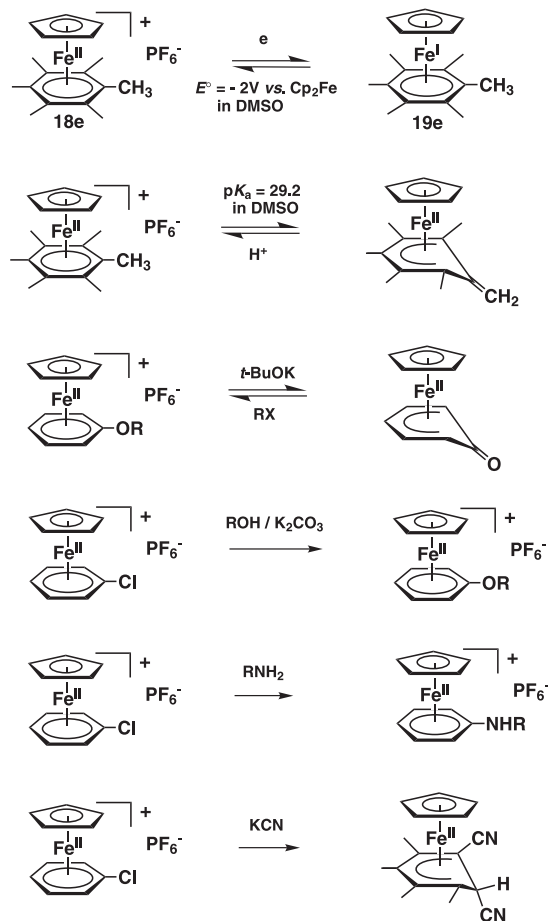


Scheme 1. Principle and general steps of the CpFe^+ -induced activation of arenes by temporary complexation.

12.2.2

Solubility, Stability, and General Reactivity Trends

The yellow $\text{CpFe}^+(\eta^6\text{-arene})$ salts (most commonly BF_4^- or PF_6^-) are usually stable up to at least 200 °C, are stable in concentrated sulfuric acid, and are very resistant towards oxidation (until recently, it was believed that they could not be oxidized [23]; *vide infra*). They are not easy to reduce either [23] (*vide infra*). The chloride salts $[\text{CpFe}^+(\eta^6\text{-arene})] \text{Cl}^-$ are water-soluble; they are formed upon hydrolysis following ligand-exchange reactions between ferrocene and the arene in the presence of aluminum chloride [21]. Such aqueous solutions may sometimes be directly used for nucleophilic reactions [22] (*vide infra*). The BF_4^- salts are also sometimes quite soluble in water, but the PF_6^- salts are much less so. Electrophilic reactions that are readily undergone by the free arenes, such as Friedel–Crafts reactions, are no longer possible on the $\text{CpFe}^+(\eta^6\text{-arene})$ complexes [19, 23]. On the other hand, a range of nucleophilic reactions that are impossible or very difficult to carry out with free arenes become possible under ambient or mild conditions with the $\text{CpFe}^+(\eta^6\text{-arene})$ complexes (Scheme 2) [16–20].



Scheme 2. Main reactions of the $[\text{CpFe}^+(\eta^6\text{-arene})]^+$ complexes.

12.2.3

Single-Electron Reduction and Oxidation

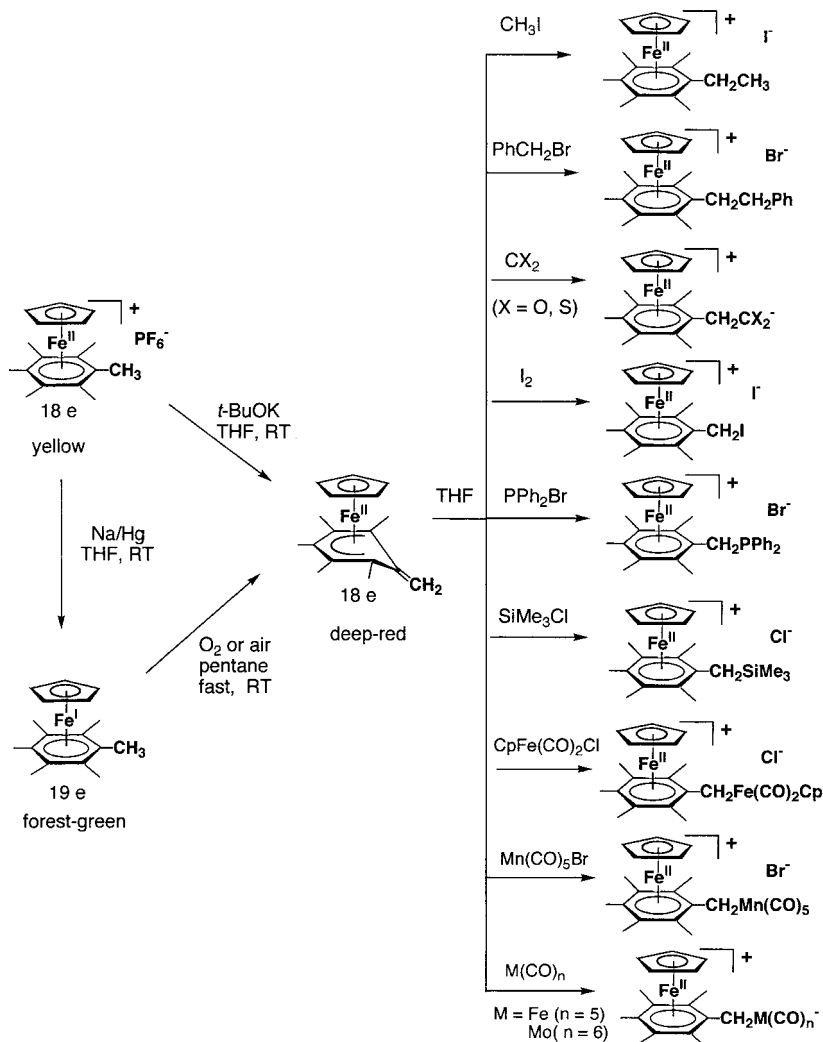
Whatever the arene, single-electron reduction is usually reversible on the classic time scale of cyclic voltammetry [24a]. With benzene or a mono- or polyalkyl benzene ligand, it is possible to generate the green 19-electron neutral complex by one-electron reduction of the yellow 18-electron BF_4^- or PF_6^- precursor salt [24b]. In such cases, it is also possible to isolate the Fe^{I} complexes under careful conditions at low temperature, typically -10°C to 0°C . The CpFe^{I} complexes are thermally stable at room temperature with hexamethylbenzene [25a], hexaethylbenzene [25a], and tris(*tert*-butyl)benzene (Scheme 2). The prototype complex $\text{CpFe}^{\text{I}}(\eta^6\text{-C}_6\text{Me}_6)$ is thermally stable up to 100°C , and has been characterized by a variety of physical techniques [25], including X-ray crystal structure analysis [25b]. EPR and Mössbauer spectra of the Fe^{I} family of complexes show the dynamic rhombic distortion of these Jahn–Teller-active d^7 species [25c] and He(I) photoelectron spectroscopy showed that their ionization potentials are among the lowest known, as low as those of alkali metals [25d]. Thus, these complexes are the most electron-rich molecules known, and $\text{CpFe}^{\text{I}}(\eta^6\text{-C}_6\text{Me}_6)$, an excellent electron reservoir, is extensively used as a strong reductant ($E^\circ = -2\text{ V}$ vs. $\text{Cp}_2\text{Fe}^{0/+}$, i.e. almost one volt more negative than cobaltocene) [25e]. In their monocationic form, these $\text{CpFe}^+(\eta^6\text{-arene})$ complexes are isolobal with ferrocene. The 17-electron dication $\text{Cp}^*\text{Fe}^{2+}(\eta^6\text{-C}_6\text{Me}_6)$, isolobal with ferrocenium, is thermally stable, and is a much stronger oxidant than ferrocenium, the difference being about one volt due to the additional positive charge ($\text{Cp}^* = \eta^5\text{-C}_5\text{Me}_5$, $E^\circ = 1\text{ V}$ vs. $\text{Cp}_2\text{Fe}^{0/+}$). Thus, this latter complex is thermally stable in three redox forms, the 19-e Fe^{I} and 17-e Fe^{III} forms being strongly reducing and oxidizing, respectively [26].

12.2.4

Deprotonation

Deprotonation of benzylic groups on the arene ligand of the $\text{CpFe}^+(\eta^6\text{-arene})$ complexes is rather easy and can be achieved using, for instance, *t*BuOK (Scheme 2) [27]. This is again due to the positively charged iron group, which enhances the acidity of the arene ligand by about 15 $\text{p}K_{\text{a}}$ units in DMSO ($\text{p}K_{\text{a}}$: $\text{Cp}^*\text{Fe}^+(\eta^6\text{-C}_6\text{Me}_6)$: 28.2; C_6Me_6 : 43) [27b]. The X-ray crystal structure of the deep-red deprotonated complex shows a dihedral angle of 32° , which indicates some overlap between the π orbitals of the cyclohexadienyl ligand and those of the exocyclic double bond [27c]. The complex is soluble in pentane, which confirms that it is not zwitterionic. It shows a smooth nucleophilic reactivity with a large variety of electrophiles, however, which is useful for creating many C–heteroatom bonds (Scheme 3) [27d].

Although other deprotonated complexes are sometimes not as stable as $[\text{CpFe}(\eta^5\text{-C}_6\text{Me}_5\text{CH}_2)]$, they can be generated and used at low temperature to form the desired bonds [27e]. Using the base and electrophile in excess, the reactions can be carried out at room temperature because the deprotonated species immediately reacts with the electrophile *in situ*. This kind of deprotonation/alkylation sequence underpins the star and dendrimer construction described herein (*vide infra*). In this way, the complexes $[\text{FeCp}(\eta^6\text{-arene})][\text{PF}_6]$ also act as proton reservoirs [33].



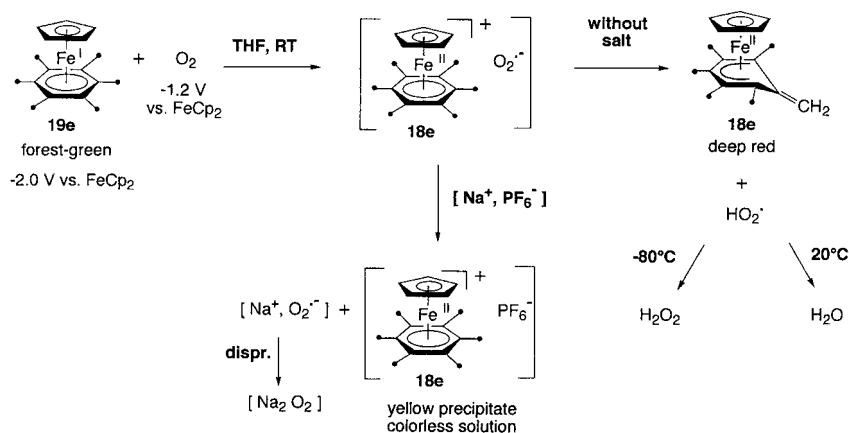
Scheme 3. Benzylation activation of arenes by the 12-electron CpFe^+ and the 13-electron CpFe groups (see also Scheme 4).

12.2.5

Reaction of the 19-Electron Fe^I Complex with O_2 : Extraordinary Reactivity of Naked Superoxide and its Inhibition

The 19-electron Fe^I complex reacts rapidly with O_2 at low temperature ($1/2 \text{ O}_2$ giving $1/2 \text{ H}_2\text{O}_2$) or at ambient temperature ($1/4 \text{ O}_2$ giving $1/2 \text{ H}_2\text{O}$) to yield what is seemingly the product of C–H abstraction, $[\text{CpFe}(\eta^5\text{-C}_6\text{Me}_5\text{CH}_2)]$, nearly quantitatively. The reaction actually proceeds via the ion pair $[\text{CpFe}^+(\eta^6\text{-C}_6\text{Me}_6), \text{O}_2^-]$, however [27a, 27d]. The superoxide

radical anion intermediate is generated by an electron-transfer step that is exergonic by almost one volt (Scheme 4).



Scheme 4. Fast C–H activation reaction in the 19-electron complex $[\text{CpFe}^{\text{I}}(\eta^6\text{-C}_6\text{Me}_6)]$ with O_2 and “quantitative” salt effect of Na^+PF_6^- in THF.

It was characterized by its EPR spectra. The reaction of KO_2 with $[\text{FeCp}(\eta^6\text{-C}_6\text{Me}_6)][\text{PF}_6]$ in DMSO also gives the deprotonated complex $[\text{CpFe}(\eta^5\text{-C}_6\text{Me}_5\text{CH}_2)]$ [27d]. Thus, the basic and nucleophilic properties of the anion are enhanced in the ion pair due to the absence of other interactive counteranions and to the subsequent disproportionation to peroxide and dioxygen. These properties are dramatically inhibited by the presence of one equivalent of NaPF_6 , which quantitatively changes the course of the reactions of the Fe^{I} complexes with O_2 in THF, giving sodium peroxide and $[\text{FeCp}(\eta^6\text{-C}_6\text{Me}_6)][\text{PF}_6]$ instead of deprotonation or nucleophilic reaction (nucleophilic addition of $\text{O}_2^{\cdot-}$ to the arene ligand is observed in the absence of a benzylic proton) [28a]. Thus, a simple sodium salt efficiently plays the same role as the superoxide dismutase enzymes in the aerobic biological systems [28b].

12.2.6

Nucleophilic Reactions

Nucleophilic substitution of halides in the CpFe^+ complexes of halogenoarenes proceeds very easily under mild conditions [16–20, 23]. In the absence of other functional groups, chloroarenes, which are the least expensive of the halogeno derivatives, are readily complexed to the CpFe^+ group upon reaction with ferrocene in the presence of aluminum chloride. In contrast to the $\text{Cr}(\text{CO})_3$ -chloroarene complexes (see the comparison of nucleophilic reactivities in Scheme 4), they undergo facile nucleophilic substitution [19, 29] upon treatment with alcohols and thiols in the presence of Na_2CO_3 or K_2CO_3 , and with amines even under mild aqueous conditions [22]. Likewise, *o*-dichlorobenzene complexes lead to various (O, N, S) heterocycles through double substitution [30]. Reactions with hard carbanions yield

cyclohexadienyl complexes, even in the case of the chlorobenzene complex, whereby the carbanion attack occurs at the *ortho* arene carbon. With stabilized carbanions, however, the reaction starts similarly, and then the incoming group migrates from the *ortho* to the *ipso* position, which is followed by elimination of chloride to provide the substituted arene complex. The reaction can continue by a second attack at the *ortho* position in the case of CN^- , which finally yields a metal-free *ortho*-dicyanoarene after decomplexation of the cyano-cyclohexadienyl complex using an appropriate single-electron oxidant [31]. Nucleophilic substitution of chloride in these cationic chloroarene iron complexes by a variety of anions (azide, amides, alkoxides, thiolates, stabilized carbanions, etc.) is thus also possible under mild conditions.

12.2.7

Heterolytic Cleavage of Aryl Ethers

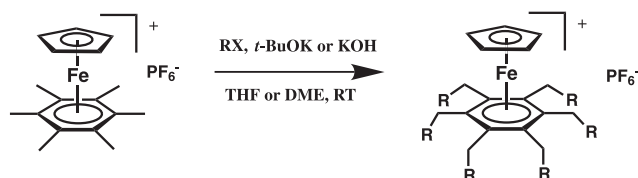
A particularly useful type of nucleophilic reaction is that of the aryl ether complexes $[\text{FeCp}(\eta^6\text{-PhOR})][\text{PF}_6]$, which are readily cleaved in a heterolytic manner to give the phenolate complex $[\text{Fe}^+\text{Cp}(\eta^6\text{-PhO}^-)]$ [32]. The latter is best described as a cyclohexadienyloxo complex $[\text{FeCp}(\eta^5\text{-C}_6\text{H}_5=\text{O})]$ isolobal with the cyclohexadienylmethylene complex $[\text{FeCp}(\eta^5\text{-C}_6\text{H}_5=\text{CH}_2)]$ obtained by deprotonation of the cationic toluene complex. With the stabilizing Cp^* ligand, the same cleavage reaction of $[\text{FeCp}^*(\eta^6\text{-PhOEt})][\text{PF}_6]$ gives the cleavage product $[\text{FeCp}^*(\eta^5\text{-C}_6\text{H}_5=\text{O})]$, the X-ray crystal structure of which reveals the H-bonding ability of this cyclohexadienyloxo ligand. The reverse reaction, alkylation of the phenolate or cyclohexadienyloxo complex using an alkyl iodide, is possible under ambient conditions in the presence of a salt, ideally NaPF_6 , the “magic salt” for efficient salt effects. Thus, the complexes $[\text{FeCp}(\eta^6\text{-PhOR})][\text{PF}_6]$ and $[\text{Fe}^+\text{Cp}(\eta^6\text{-PhO}^-)]$ represent the two stable forms of an alkyl reservoir system. This cleavage reaction is used for the synthesis of our phenol dendron (*vide infra*).

12.3

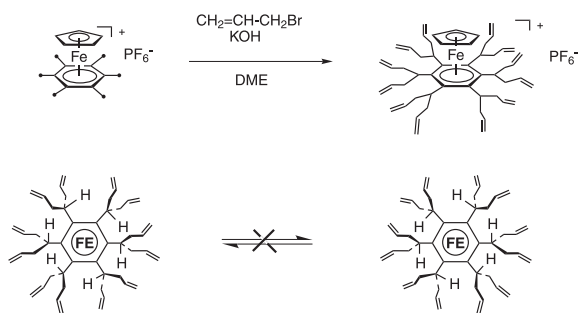
CpFe^+ -Induced Hexafunctionalization of Hexamethylbenzene for the Synthesis of Metallo-Stars

Reaction of $[\text{FeCp}(\text{C}_6\text{Me}_6)][\text{PF}_6]$ [33–35] with excess KOH (or $t\text{BuOK}$) in THF or DME and excess alkyl iodide, allyl bromide, or benzyl bromide leads to one-pot hexasubstitution (Scheme 5a) [36–38]. With allyl bromide (or iodide) in DME, the hexaallylated complex has been isolated and its X-ray crystal structure determined, but the extremely bulky dodeca-allylation [52] product can also be reached when the reaction time is extended to two weeks at 40 °C. The chains are fixed in a directionality such that conversion to the enantiomer is not possible, thus making the metal complex chiral (Scheme 5b).

With alkyl iodides, the reaction using $t\text{BuOK}$ leads only to dehalogenation of the alkyl iodide giving the terminal alkene. Thus, one must use KOH , and the reactions with various alkyl iodides (even long-chain ones) have been shown to work very well with this reagent to give the hexaalkylated Fe^{II} -centered complexes. The yellow 18-electron complexes can be reduced to the dark-green 19-electron complexes (Scheme 6), but the stabilities of these organoiron radicals decrease as the chain length of the alkyl group is increased. Nevertheless, it



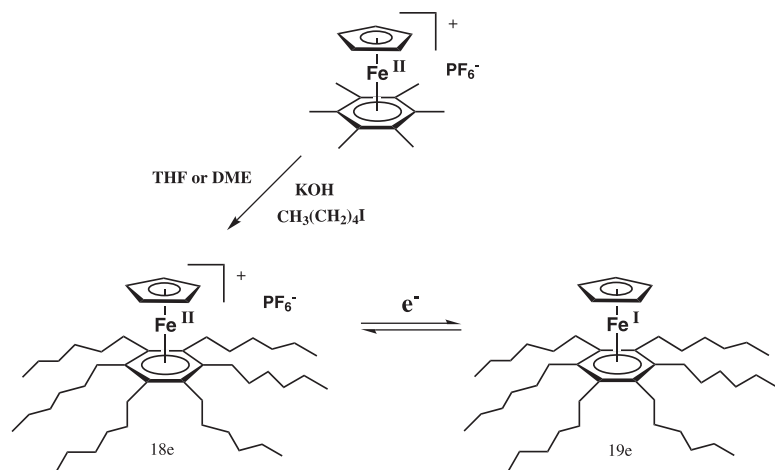
$\text{R} = \text{CH}_3, (\text{CH}_2)_n\text{CH}_3, (\text{CH}_2)_4\text{Fe} \text{ (X = I)}, \text{CH}_2\text{Ph}, p\text{-CH}_2\text{PhOR}', \text{CH}_2\text{CH}=\text{CH}_2 \text{ (X = Br)}$



$\text{FE} = \eta^5\text{-C}_5\text{H}_5\text{Fe}^+$

Scheme 5. The peralkylation or perfunctionalization reaction: this reaction is made possible by the proton-reservoir property of the starting organometallic cation (see Schemes 2 and 3) and is spontaneously reproduced by iteration many times until a steric limit is reached: a) hexa-substitution compounds are formed with methyl

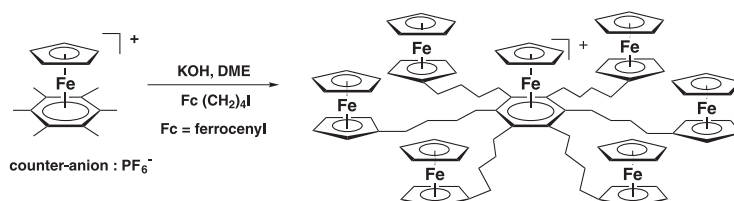
and alkyl iodides and benzyl halides. With allyl bromide, the room temperature reaction can be stopped at the stage of the hexabutenyl derivative or b) can be continued under prolonged heating conditions (40 °C) to give the (chiral) dodecaallyl compound that has a sterically blocked directionality.



Scheme 6. High-yielding, large-scale synthesis of metal-centered stars with tentacles: application of the peralkylation reaction to long-chain alkyl iodides under mild conditions and redox activity.

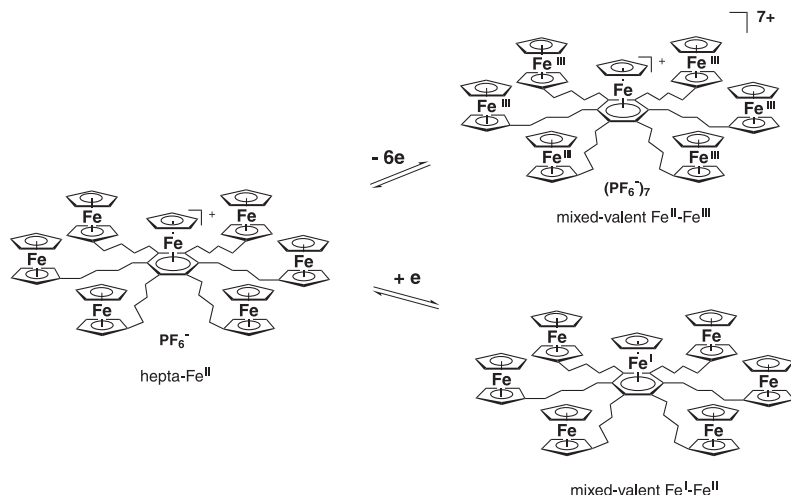
was possible to isolate the 19-electron complexes up to the hexahexylbenzene complex at low temperature and to record their temperature-dependent Mössbauer spectra between 4.2 and 200 K. The rhombic distortion, observed initially for $[\text{FeCp}(\text{C}_6\text{Me}_6)]$ and due to the Jahn–Teller effect, is weaker and milder in these complexes [39].

The hexaalkylation was also performed with alkyl iodides containing functional groups at the alkyl chain termini. For instance, alkyl iodides bearing methoxy [36] or olefinic end-groups [40] were prepared. Finally, 1-ferrocenylbutyl iodide reacts nicely to give the hexaferrocene star containing the CpFe^+ center (Scheme 7).



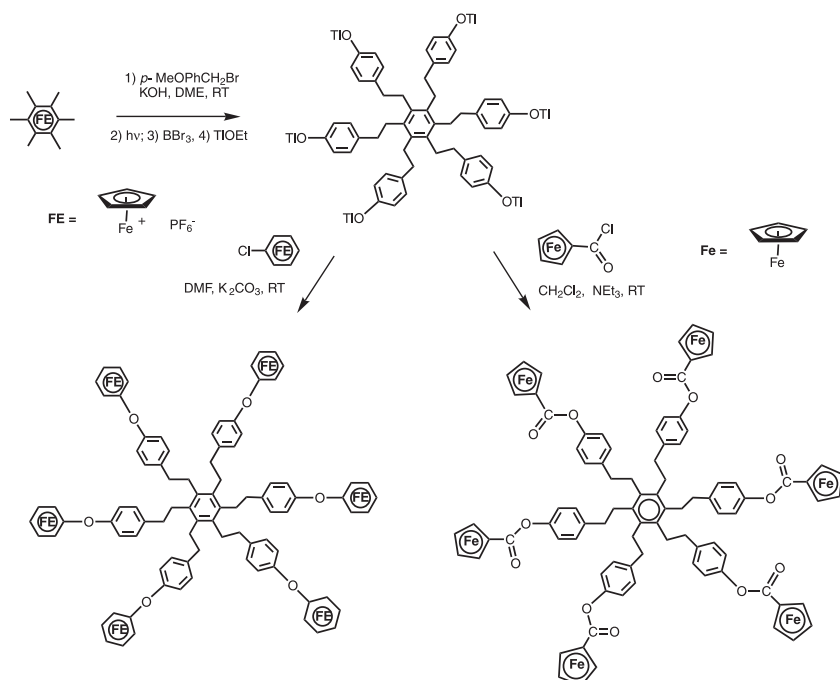
Scheme 7. Branching out: synthesis of hexaferrocenylalkyl metal-centered redox stars.

This heptanuclear complex is of interest because of its various redox states. The six ferrocenyl units are independent, as evidenced by a single cyclic voltammetry wave. They could be oxidized to give the mixed-valence heptacation, in which the central iron group withstands oxidation and retains its Fe^{II} state, because it is protected by the positive charge [41a] (this protection can be estimated to be approximately 1.5 V) [41b]. The central iron serves as an internal reference to count the number of peripheral ferrocenes by comparing intensity ratios in either the cyclic voltammogram or the Mössbauer spectrum of the oxidized $\text{Fe}^{\text{II}}/\text{Fe}^{\text{III}}$ complex (Scheme 8) [41a].



Scheme 8. Oxidation or reduction of metallo-stars to localized mixed-valence complexes. Fe centers for which the oxidation state is not indicated in the scheme are Fe^{II} .

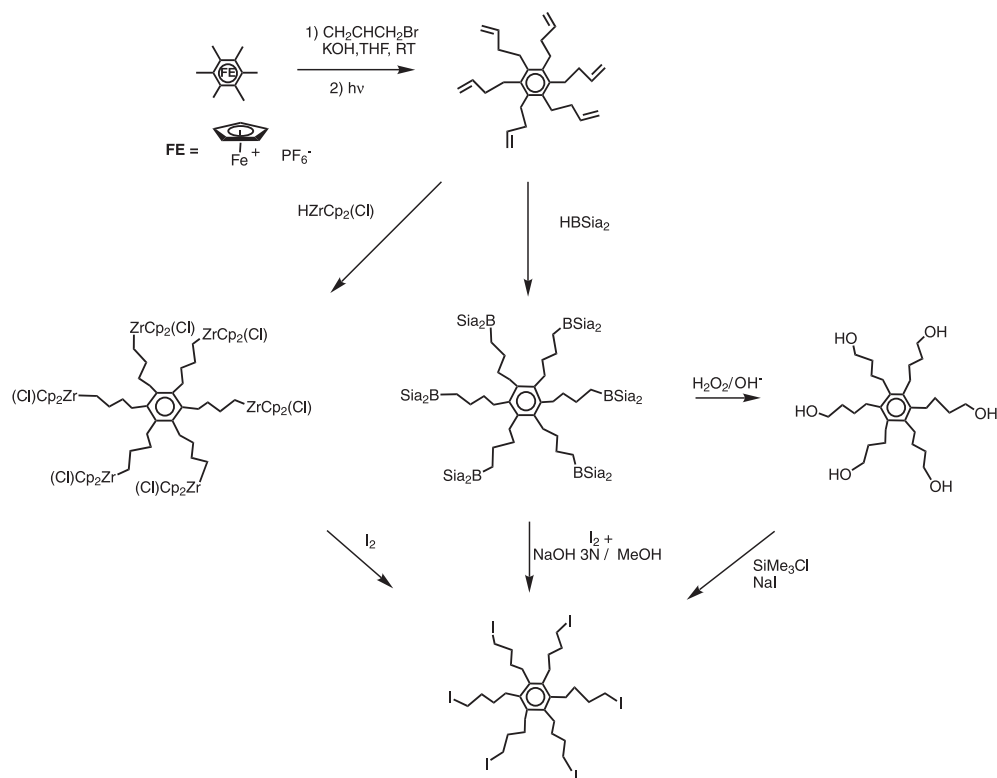
Both the hexa- and dodecaallylation reactions are readily controllable. On the other hand, the reactions with excess benzyl bromide [42] or *p*-alkoxybenzyl bromide [43, 44] give only the hexabenzylated or hexaalkoxybenzylated complexes as the ultimate reaction products. Cleavage of the methyl group from the *p*-methoxybenzyl derivatives synthesized in this way yielded hexaphenolate stars, which could be combined with halogen-containing Fe-sandwich electrophilic compounds such as chlorocarbonylferrocene or $[\text{FeCp}(\eta^6\text{-C}_6\text{H}_5\text{Cl})][\text{PF}_6]$ (Scheme 9) [43, 44].



Scheme 9. Synthesis of metallo-stars starting with the CpFe^+ -induced hexaalkoxybenzylation of hexamethylbenzene. Examples of redox-active hexametallic stars synthesized by reactions of metal-free hexaphenolate with organometallic

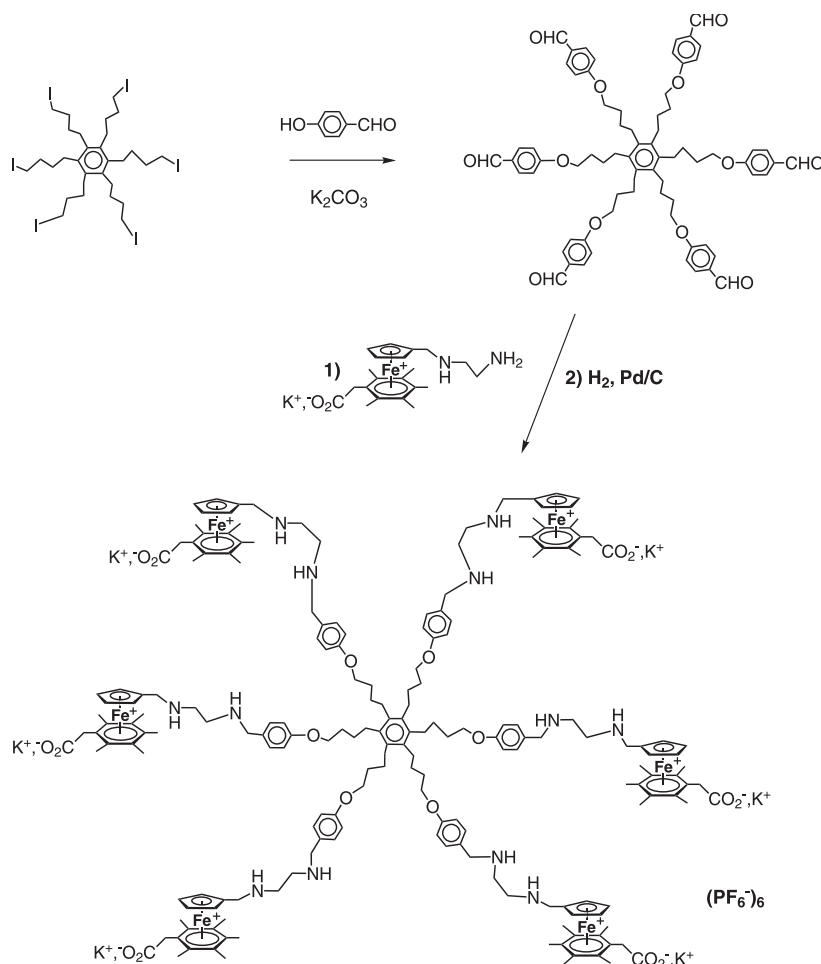
electrophiles such as ferrocenoyl chloride or $[\text{FeCp}(\eta^6\text{-}p\text{-CH}_3\text{C}_6\text{H}_4\text{F})][\text{PF}_6]$. The hepta-iron complex consisting of the $[\text{CpFe}(\eta^6\text{-C}_6\text{R}_6)]^+$ -centered hexaferrocene star was obtained in a same way by omitting the decomplexation step 2).

Alkynyl halides cannot be used in the CpFe^+ -induced hexafunctionalization reaction, but alkynyl substituents can be introduced via the hexaalkene derivative by bromination followed by dehydrohalogenation of the dodecabromo compound [45]. The hexaalkene is also an excellent starting point for further syntheses, especially using hydroelementation reactions. Hydrosilylation reactions catalyzed by Speir's reagent led to long-chain hexasilanes [46], and hydrozirconation has also been achieved using $[\text{Cp}_2\text{Zr}(\text{H})(\text{Cl})]$ [47]. The hexazirconium compound thus obtained is an intermediate for the synthesis of the hexaiodo derivative (Scheme 10) [47].



Scheme 10. Hydroelementation reactions in the functionalization of hexa-olefin stars: hydrosilylation, hydrozirconation, and hydroboration.

One of the most useful hydroelementation reactions is hydroboration, leading to the hexaborane, which can then be oxidized to the hexaol using H_2O_2 under basic conditions [37]. This chemistry can be carried out on the iron complex or, alternatively, on the free hexa-alkene, which may be liberated from the metal by photolysis in CH_2Cl_2 or MeCN using visible light [36]. The polyol stars and dendrimers can be transformed into mesylates and iodo derivatives, which are useful for further functionalization. The hexaol is indeed the best source of the hexaiodo derivative, using either HI in acetic acid or, even better, by trimethylsilylation using Me_3SiCl followed by iodination using NaI [50]. Williamson coupling reactions of the hexaol with 4-bromomethylpyridine or -polypyridine led to the hexapyridine and hexapolypyridine, and thence to their ruthenium complexes [48, 49]. This hexaiodo star was also condensed with *p*-hydroxybenzaldehyde to give a hexabenzaldehyde star, which could be further reacted with substrates bearing a primary amino group. Indeed, this reaction yielded a water-soluble hexametallic redox catalyst, which proved to be active in the electroreduction of nitrate and nitrite to ammonia on a Hg cathode in basic aqueous solution, *vide infra* (Scheme 11) [51].



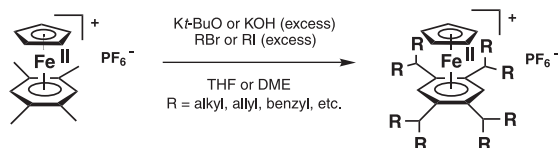
Scheme 11. Hexafunctionalization of aromatic stars with the heterodifunctional, water-soluble organometallic redox catalyst (bottom) for the cathodic reduction of nitrates and nitrites to ammonia in water.

12.4

CpFe⁺-Induced Octafunctionalization of Durene in the Synthesis of Metallo dendrimer Precursors

In the same way as the hexafunctionalization of hexamethylbenzene leads to stars, the octafunctionalization of durene leads to dendritic cores (Scheme 12).

The first of these octaalkylation reactions was reported as early as 1982, and led to a primitive dendritic core containing a metal-sandwich unit [36]. Thus, like the hexafunctionalization, this reaction is very specific. Two hydrogen atoms of each methyl group are re-



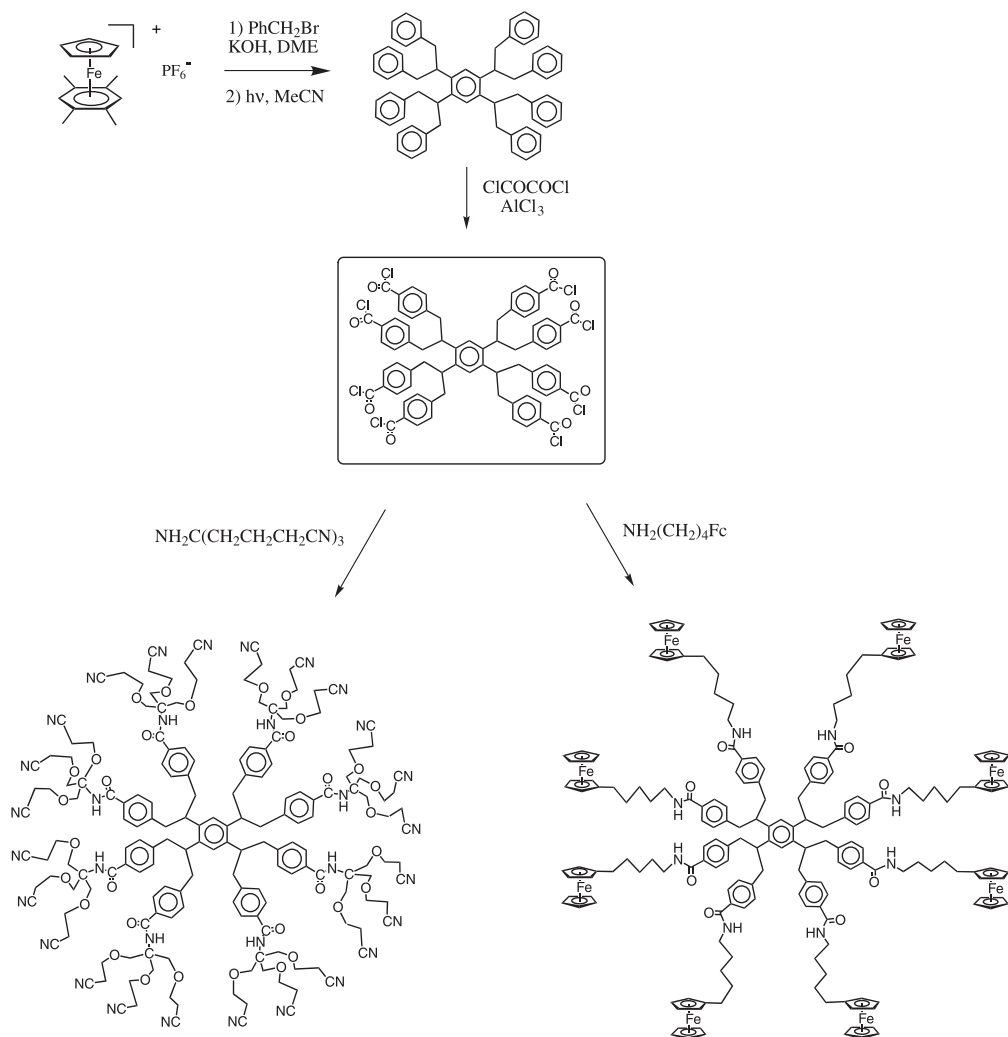
Scheme 12. Octa-alkylation, -allylation, or -benzylation of durene in high yields by a series of eight deprotonation/alkylation (or allylation or benzylation) sequences induced by the 12-electron activating group CpFe^+ in a one-pot reaction under mild conditions.

placed by two methyl, allyl, or benzyl groups [52]. This is due to the fact that each methyl group has only one methyl neighbor in durene instead of two such neighbors in hexamethylbenzene. It is remarkable that the consequence of this difference is so clear-cut. We believe that this is due to the respective rates of the organometallic reaction and the reaction between the base and the halide. The octabenzylation reaction has since been used for further dendritic construction. Indeed, the *p*-chlorocarbonylation of the octabenzyl core is remarkably regioselective and has been used to facilitate reactions with amines of interest such as Newkome's tripodal amine terminated by nitrile groups [53]. This reaction provides a rapid route to the 24-nitrile dendrimer [54]. Another reaction of interest in the present context is that of the octachlorocarbonylbenzyl core with 1-ferrocenylpentylamine, which provides the expected octaferrocenyl compound (Scheme 13) [55].

The reaction of the octaiodomethylbenzyl core with $[\text{Fe}(\eta^5\text{-C}_5\text{H}_5)(\eta^5\text{-C}_6\text{Me}_5\text{CH}_2)]$, i.e. the deprotonated form of $[\text{Fe}(\eta^5\text{-C}_5\text{H}_5)(\eta^6\text{-C}_6\text{Me}_6)]\text{PF}_6$, led to the yellow octa-sandwich $\text{C}_6\text{H}_2\text{-1,2,4,5-}[\text{CH}(\text{CH}_2\text{CH}_2\text{-}p\text{-C}_6\text{H}_4\text{CH}_2\text{CH}_2\text{-}\eta^6\text{-C}_6\text{Me}_5\text{FeCp}^+\text{I}^-)_2]_4$, which proved to be almost insoluble (Scheme 14). Its structure was indicated by the yellow color and the Mössbauer spectrum, both being characteristic of the $\text{FeCp}(\text{arene})^+$ frame [55].

A very interesting series of dendrimers containing 24 transition metal sandwich units has been synthesized from the 24-nitrile dendrimer by reduction of the nitrile groups to primary amines followed by reaction of the 24-amine dendrimer with chlorocarbonylferrocene or with $[\text{Fe}(\eta^5\text{-C}_5\text{Me}_5)(\eta^6\text{-C}_6\text{H}_5\text{F})]\text{PF}_6$ (Scheme 15) [54]. Both 24-branch metallodendrimers proved very useful and complementary for molecular recognition, as will be discussed later in this chapter.

Double branching, i.e. the replacement by two groups of two of the three hydrogen atoms on each methyl substituent of an aromatic ligand coordinated to an activating cationic group CpM^+ in an 18-electron complex is not restricted to the case of durene. It is also encountered in the *o*-xylene ligand [36, 52], in the pentamethylcyclopentadienyl ligand (in pentamethyl cobaltocenium [56] and in penta- [57] and decamethylrhodocenium [58]), and even in the hexamethylbenzene ligand. As mentioned above, with this latter ligand, only allyl groups could be introduced in a double branching arrangement, this reaction requiring two weeks at 40 °C [52] whereas single branching was complete after only one day at this temperature. The extremely bulky dodecaallyl complex formed is chiral, but its directionality is completely blocked (no interconversion between the clockwise and counterclockwise directionalities) [37], in contrast to the directionality of decafunctionalized ligands coordinated to CpCo^+ or CpRh^+ , the interconversion of which could be observed by ^1H NMR (at least for the



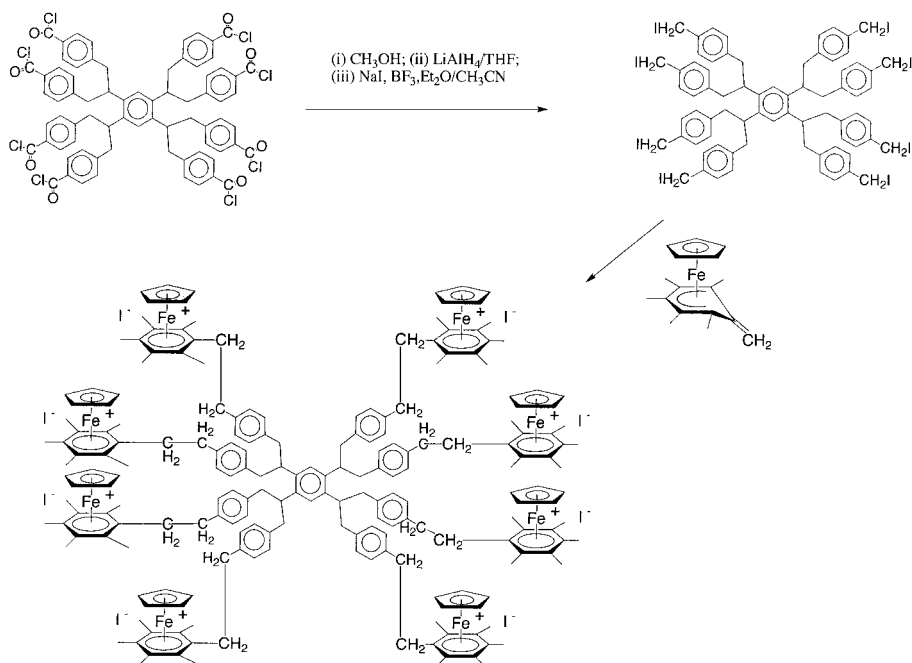
Scheme 13. Synthetic scheme for 24-CN and octa-ferrocenyl dendrimers.

decaisopropyl- and decaisopentyl cyclopentadienyl cobalt and rhodium complexes [56–58]) (Schemes 16 and 17).

12.5

CpFe^+ -Induced Triallylation of Toluene and Reactivity of the Triallyl Tripod Towards Transition Metals

In all of the above examples, the polybranching reaction of arene ligands was limited by the steric bulk. In the toluene and mesitylene ligands, however, the deprotonation–allylation re-



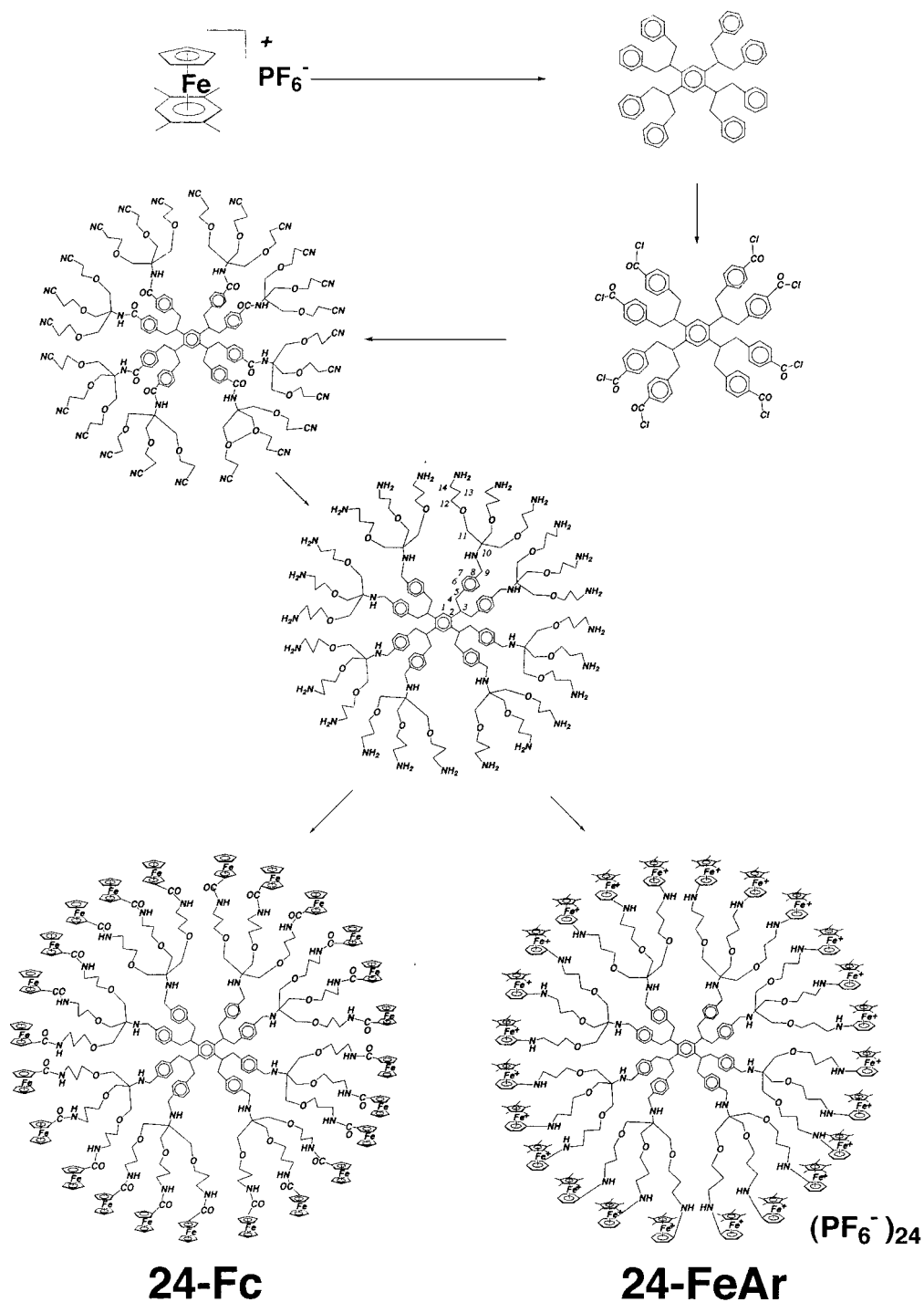
Scheme 14. Synthesis of a small dendrimer terminated by eight CpFe^+ (η^6 -pentamethylbenzene) moieties starting from CpFe^+ (η^6 -1,2,4,5-tetramethylbenzene). The octanuclear compound obtained is almost insoluble in all solvents.

actions are no longer restricted by the neighborhood of other alkyl groups. All of the benzylic protons, i.e. three per benzylic carbon, can be replaced by methyl or allyl groups in the one-pot iterative methylation or allylation reactions. Thus, the toluene complex can be triallylated and the resulting tripod can be desymmetrized by stoichiometric or catalytic reactions with transition metals, as shown in Scheme 18.

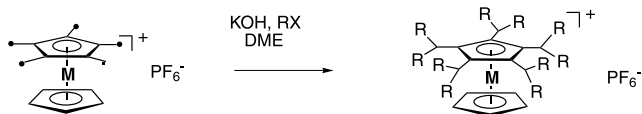
12.6

Nonaallylation of Mesitylene for the Synthesis of Dendritic Precursors of Large Metallodendrimers

The mesitylene complex can be nonaallylated, the reaction proceeding smoothly at room temperature in the presence of excess KOH and allyl bromide (Scheme 19). The nonaallyl complex was photolyzed using visible light to remove the metal group CpFe^+ , then hydroborated using 9-BBN, and the nonaborane was oxidized to the nonaol using $\text{H}_2\text{O}_2/\text{OH}^-$. Reaction of this nonaol with $[\text{FeCp}(\eta^6\text{-}p\text{-MeC}_6\text{H}_4\text{F})][\text{PF}_6]$ in the presence of K_2CO_3 in DMF yielded the nona-sandwich complex as a result of CpFe^+ -induced nucleophilic substitution of the halogen by the alkoxy branch, and the metallodendrimer was subsequently purified by column chromatography (Scheme 19). The cyclic voltammogram of this complex shows that



Scheme 15. Construction of dendrimers with 24 ferrocenyl or cationic iron-sandwich groups.

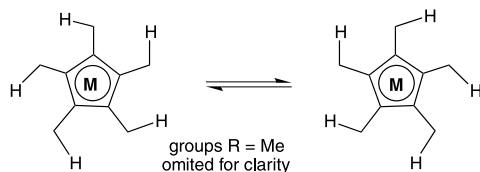


M = Co, Rh

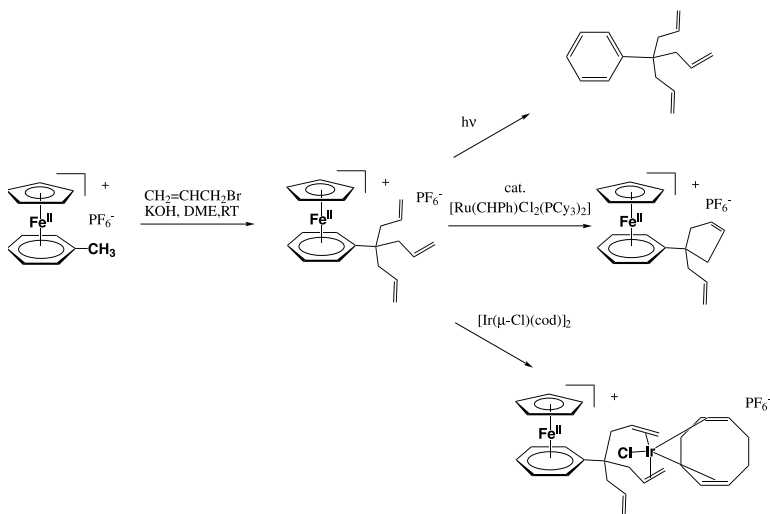
R = Me, Et, CH₂Ph,
CH₂-CH=CH₂

Scheme 16. Deca-alkylation, -allylation, or -benzylation of 1,2,3,4,5-pentamethylcobaltocenium or 1,2,3,4,5-pentamethylrhodocenium in a one-pot reaction consisting of ten deprotonation-alkylation

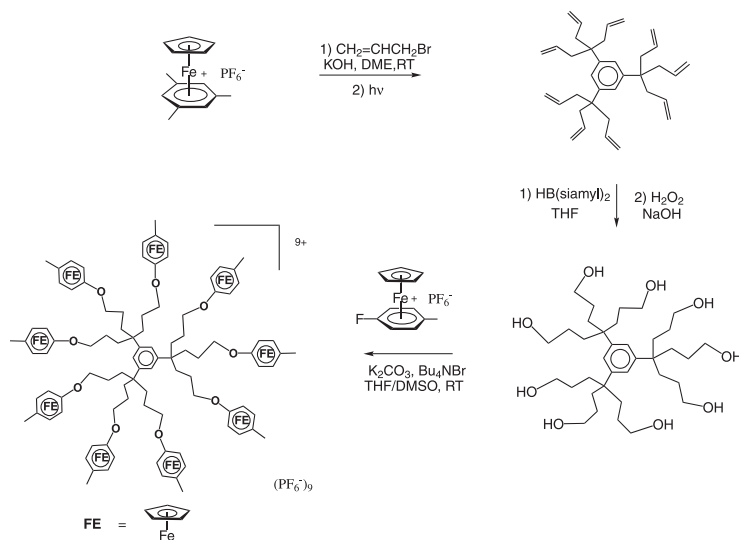
sequences. Steric constraints inhibit further reaction, and the ten groups introduced are self-organized according to a single directionality (see Scheme 17).

M = Co, $\Delta G^\circ = 71.13 \text{ kJ.mol}^{-1}$ ($17.0 \pm 0.2 \text{ kcal.mol}^{-1}$)Rh, $\Delta G^\circ = 70.21 \text{ kJ.mol}^{-1}$ ($16.8 \pm 0.2 \text{ kcal.mol}^{-1}$)

Scheme 17. Interconversion between the clockwise and counterclockwise directionalities of the decaalkylated or decafunctionalized 18-electron cationic metallocenes (from the reactions in Scheme 11) as observed by ¹H NMR. The coalescence temperature increases with increasing size of the introduced R group.



Scheme 18. One-pot CpFe⁺-induced triallylation of toluene and reactions of transition metal complexes with the triallylated complex [59, 95].

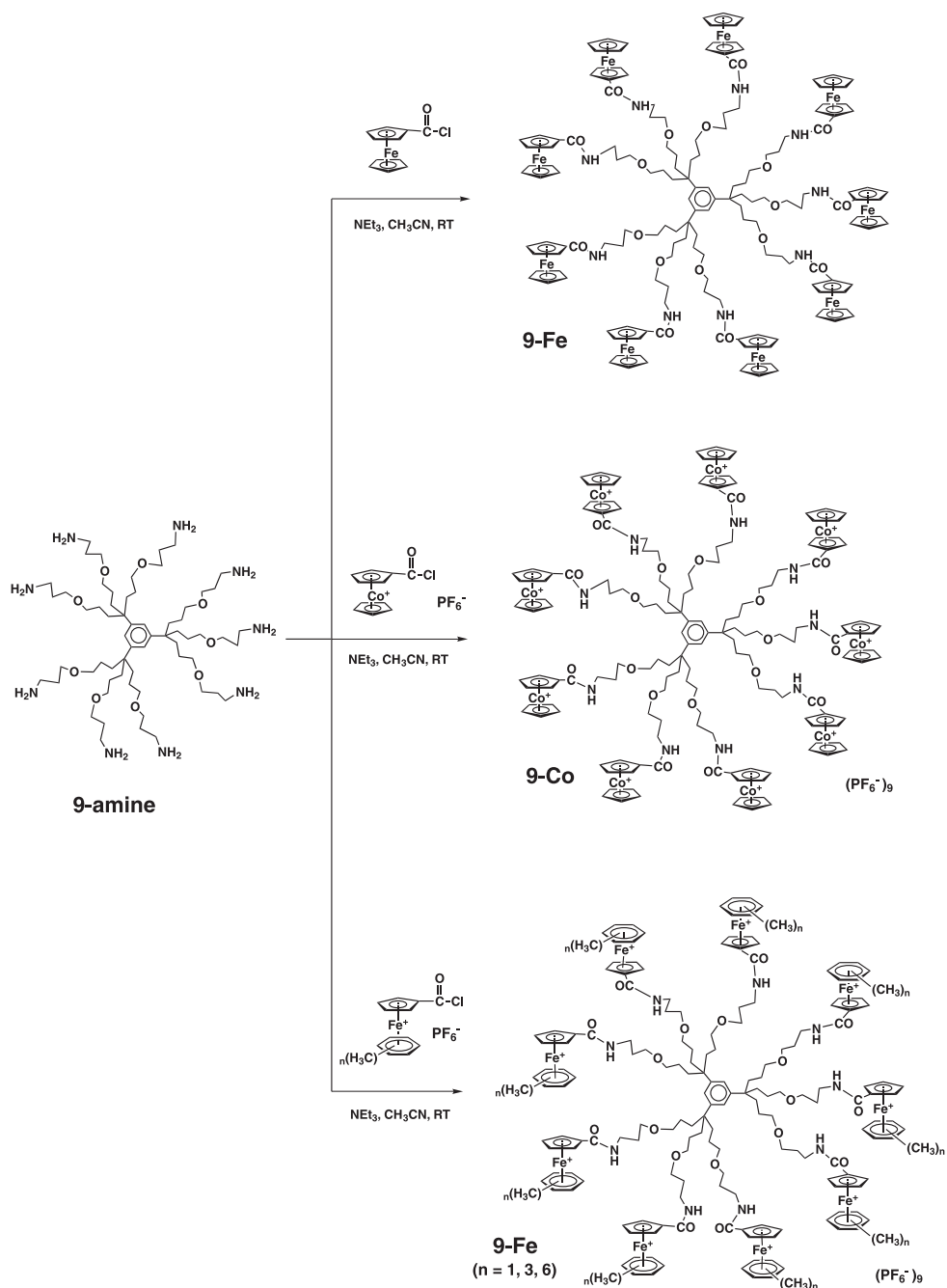


Scheme 19. One-pot, large-scale, high-yielding CpFe^+ -induced nonaallylation of mesitylene and subsequent functionalization of the olefinic branches leading to redox-active nonametallodendrimers.

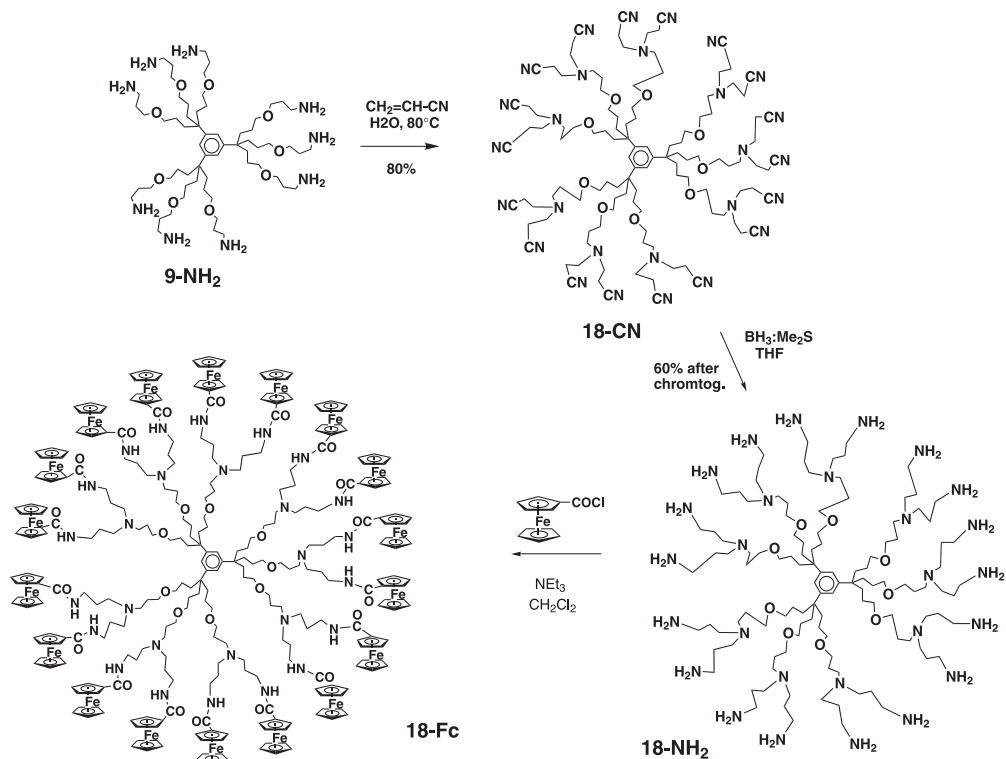
the nine redox Fe^{II} centers are seemingly reduced at the same potential. At -30°C , this wave is reversible and the number of redox centers is found to be 8 ± 1 using the Bard–Anson formula [59, 60].

Alternatively, Michael reaction of the nonaol with acrylonitrile yields a nonanitrile, which can be reduced to the nonaamine. This nonaamine was allowed to react with chlorocarbonylmetallocenes and other chlorocarbonyl sandwich complexes to yield nonaamido-metallocenes [61–63] and nonaamido-sandwich compounds [63] (Scheme 20). These metallodendrimers also give rise to only one cyclic voltammetry wave, the intensity of which corresponds to approximately nine electrons using the technique indicated above (the solvent was CH_2Cl_2 for the nonaamidoferrocene and MeCN for the polycationic dendrimers). Chemical reversibility was observed at room temperature, although some adsorption was noted.

The nonaamine was the starting point for the construction of dendrimers according to the iterative procedure first reported by Vögtle, and then developed by the groups of Meijer [64] and Mülhaupt [65]. Thus, reaction of the nonaamine with acrylonitrile gave an 18-nitrile dendrimer, which was reduced to the 18-amine dendrimer. The dendritic construction was continued in this way until the 144-nitrile dendrimer was reached. Purification of these polynitrile dendrimers was achieved at each generation by column chromatography [66]. Each polyamine dendrimer reacted with chlorocarbonylferrocene, but the 36- and 72-amidoferrocene dendrimers obtained were found to be insoluble in all solvents tested. The last soluble amidoferrocene dendrimer of this series is the 18-amidoferrocene (Scheme 21). This dendrimer subsequently proved very efficient for anionic recognition [61, 62].



Scheme 20. Synthesis of nonaamidometallocenyl dendrimers using the core created by the CpFe^+ -induced nonaallylation of mesitylene.



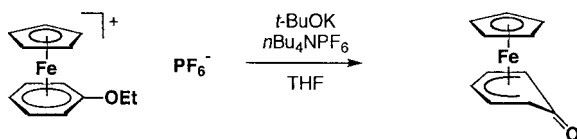
Scheme 21. Syntheses of cationic nonaamido-sandwich complexes of iron and cobalt (18-electron forms) using the same core as that used in Scheme 20.

12.7

CpFe^+ -Induced Activation of Ethoxytoluene in the One-Pot Synthesis of a Phenol Dendron by Triple-Branching and Synthesis of Organometallic Dendrons

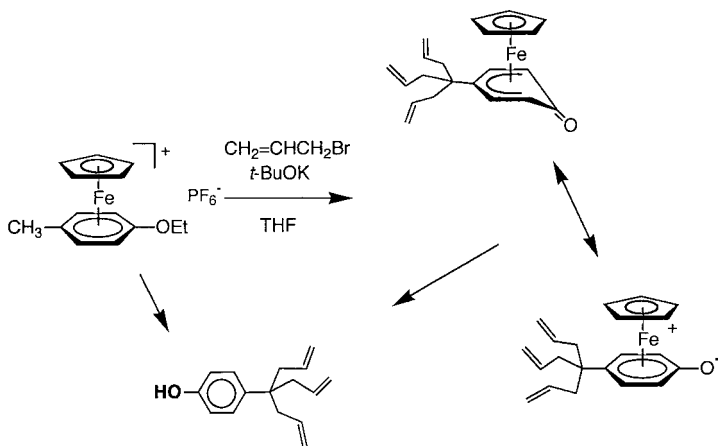
As the triple-branching reaction shown in Scheme 18 is very straightforward, we sought a more sophisticated version compatible with a functional group in the *para* position of the tripod in order to provide access to a functional dendron. Serendipitously, we found that KOH or $t\text{BuOK}$ under very mild conditions easily cleaved the iron complexes of aromatic ethers. The activating CpFe^+ group again induces this reaction, which is very general for a variety of aromatic ether complexes (Scheme 22) [67, 68].

Since this cleavage reaction is carried out with the same reagent and solvent as those used in the trialkylation reaction (ideally $t\text{BuOK}$ in THF), we attempted to perform both reactions in a well-defined order (trialkylation before ether cleavage) in a one-pot reaction. Indeed, this worked out well, and the Fe^+ complex of the phenol tripod was prepared in 60 % yield in this way. This complex could be photolyzed in the usual way using visible light, yielding the free phenol tripod. However, we also investigated the possibility of cleaving the arene ligand



Scheme 22. Heterolytic C–O cleavage reaction in aryl ether complexes by *t*BuOK or KOH, induced by the activating 12-electron fragment CpFe^+ . This reaction is very useful and has been applied to the convenient one-pot synthesis of the phenol-triallyl dendron (see Scheme 23).

in situ at the end of the phenol tripod construction. *t*BuOK is a reductant when it cannot perform other reactions. Since the two important reactions had been completed, it was envisaged that the third role of *t*BuOK, as a single-electron reductant, would come into play. This reasoning turned out to be correct. The cleavage of the arene intervenes rapidly at the 19-electron stage, because 19-electron complexes of this kind are not stable with a heteroatom located in an exocyclic position (most probably because the heteroatom coordinates to the metal of the labile 19-electron structure). After optimizing the reaction conditions, a 50 % yield of the free phenol dendron could be reproducibly obtained from the ethoxytoluene complex [50, 69], and this reaction is now regularly used in our laboratory to synthesize this very useful dendron as a starting material (Scheme 23).



Scheme 23. One-pot syntheses of the phenol-triallyl iron complex and metal-free dendron by variation of the experimental conditions. The iron complex can be demetallated by visible-light photolysis; the metal-free phenol-triallyl dendron can be obtained more rapidly direct from the *p*-ethoxytoluene-iron complex.

Functionalization of the three allyl chains of the phenol dendron could be achieved by hydrosilylation, as catalyzed by the Karstedt catalyst [70]. Indeed, it is very interesting that there is no need to protect the phenol group before performing these reactions. For instance, catalyzed hydrosilylation using ferrocenyldimethylsilane gives a high yield of the triferro-

cenyl dendron HO-*p*-C₆H₄C(CH₂CH₂CH₂SiMe₂Fc)₃, which can easily be purified by column chromatography [70, 71].

12.8

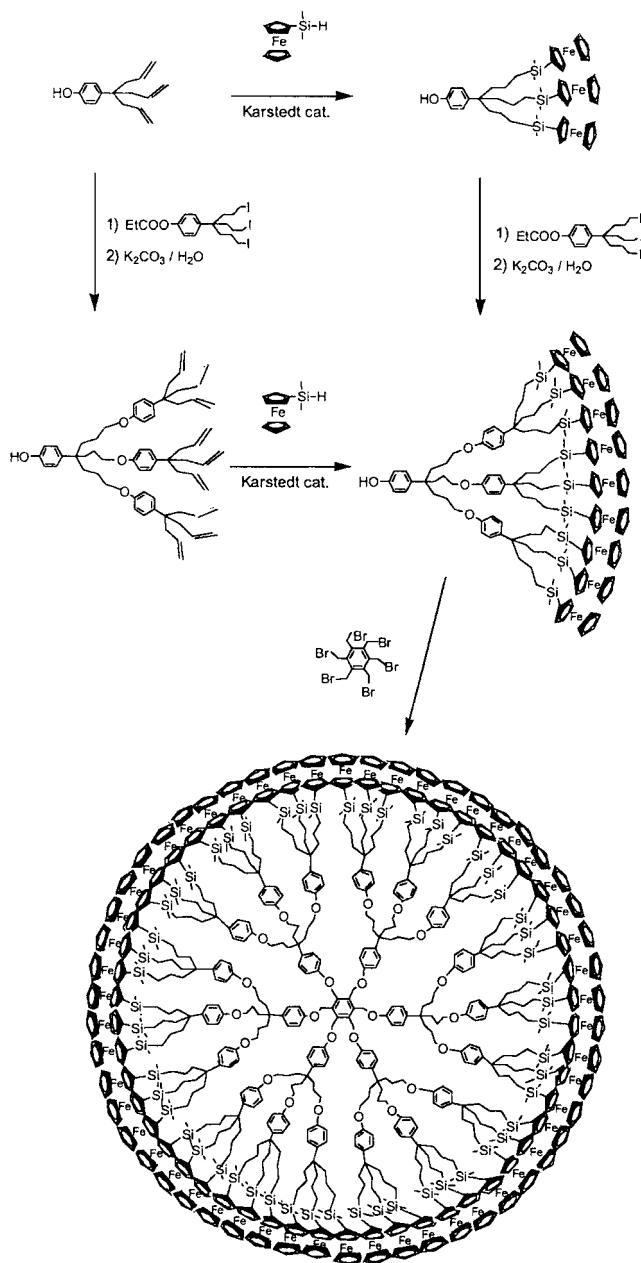
Convergent and Divergent Syntheses of Large Ferrocenyl Dendrimers with Good Redox Stabilities

Protection of the phenol dendron using propionyl iodide gave the phenolate ester, which was hydroborated, and then oxidation of the triborane using H₂O₂/OH[−] gave the triol. Reaction with Me₃SiCl gave the tris-silyl derivative, treatment of which with NaI yielded the triiodo compound, and reaction of the latter with the triferrocenyl dendron provided the nonaferrocenyl dendron, which was deprotected using K₂CO₃ in DMF. The nonaferrocenyl dendron was allowed to react with hexakis(bromomethyl)benzene, which gave the 54-ferrocenyl dendrimer. This convergent synthesis proceeded cleanly and the 54-ferrocenyl dendrimer gave correct analytical data, although a mass spectrum could not be obtained (Scheme 24).

This approach is somewhat limited, however, since larger dendrons that one might like to synthesize in this way cannot be made because dehydrohalogenation becomes faster than nucleophilic substitution of the iodo by phenolate in the bulkier higher-generation dendrons. Although this problem might be overcome by modifying the iodo branch in such a way that there are no hydrogens in the β -positions, the condensation of higher dendrons onto a core would become tedious or impossible for steric reasons. This well-known inconvenience is intrinsic to the convergent dendritic synthesis. On the other hand, divergent syntheses are not marred by such a problem since additional generations and terminal groups are added at the periphery of the dendrimer. The limit is that indicated by De Gennes, i.e. the steric congestion encountered at the generation at which the peripheral branches can no longer be divided. Another obvious limitation arises if the molecular objects added onto the termini of the branches are large and interfere with one another. We have developed a divergent synthesis of polyallyl dendrimers, as indicated in Scheme 20, whereby each generation is created by a sequence of hydroboration, oxidation of the borane to the alcohol, formation of the mesylate, and reaction of the phenol dendron with the mesylate. This strategy has allowed us to synthesize dendrimers of generations 0, 1, 2, and 3 with 9 (G₀), 27 (G₁), 81 (G₂), and 243 branches (G₃), respectively (Scheme 25 and Chart 1).

The MALDI-TOF mass spectrum of the 27-allyl dendrimer shows only the molecular peak and traces of a side product. That of the 81-allyl dendrimer shows a dominant molecular peak, but also peaks due to significant amounts of side products resulting from incomplete branching. That of the 243-allyl dendrimer could not be obtained, possibly signifying that this dendrimer is polydisperse (correct ¹H and ¹³C NMR spectra were nevertheless obtained, indicating that the ultimate reactions had proceeded to completion). This dendrimer proved to be soluble, indicating that this generation is not the last one that might be reached. Ferrocenylsilylation of all these polyallyl dendrimers was accomplished using ferrocenyldimethylsilane, as catalyzed by the Karstedt catalyst [72] at room temperature or 40 °C. The reactions were complete after a day, except in the case of the ferrocenylsilylation of the 243-allyl dendrimer, which required a reaction time of two weeks indicating some degree of steric congestion (Schemes 26 and 27).

The ¹H and ¹³C NMR spectra indicate the absence of regioisomers. Solubility in pentane



Scheme 24. Convergent strategy for the clean synthesis of a 54-ferrocenyl dendrimer. This scheme also illustrates the ability of such large ferrocenyl dendrimers to serve as molecular batteries. The deep-blue ferrocenium form can be synthesized

quantitatively, characterized, and reduced back to the orange ferrocenyl dendrimer. The overall cycle proceeds without any decomposition with all these silylferrocenyl dendrimers, including the 243-ferrocenyl dendrimer.

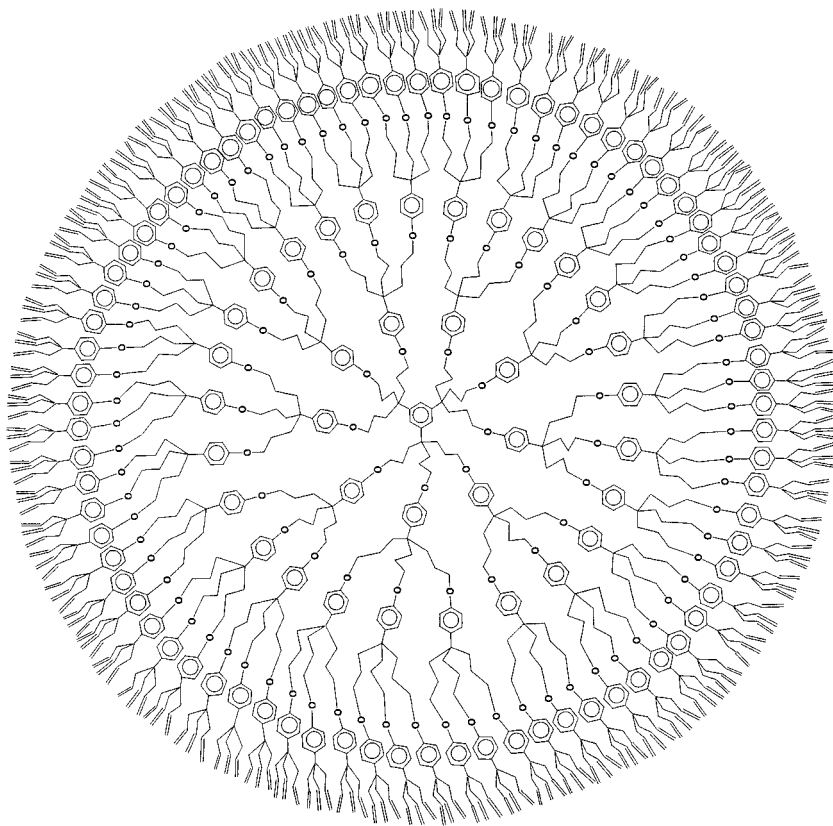
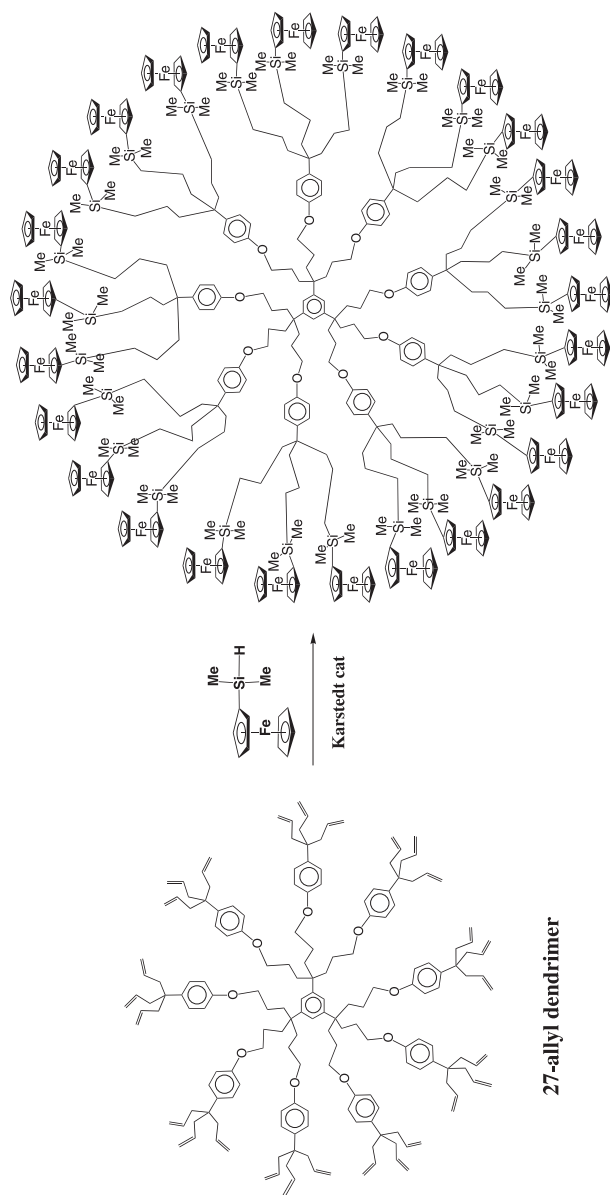


Chart 1. Third-generation polyallyl dendrimer with a theoretical number of 243 allyl branches synthesized according to Scheme 20. This “243-allyl” dendrimer (like the 9-allyl, 27-allyl, and 81-allyl dendrimers of generations 0, 1, and 2, respectively)

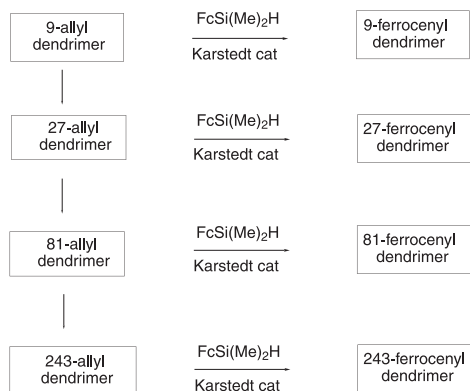
was hydrosilylated using dimethylferrocenylsilane $\text{Fc}(\text{Me})_2\text{SiH}$ to “243-Fc”, a molecular battery dendrimer with a theoretical number of 243 peripheral ferrocenyl units.

This silane, reported by Pannel and Sharma [73], was later used by Jutzi [74] to synthesize the decaferrocenyl dendrimer $[\text{Fe}(\text{CCH}_2\text{CH}_2\text{SiMe}_2\text{Fc})_{10}]$ (Fc = ferrocenyl) from decaallyl-ferrocene.

Cyclic voltammetry of all the ferrocenyl dendrimers on a Pt anode showed all the ferrocenyl centers to be equivalent as only one wave was observed. It was possible to avoid adsorption even using CH_2Cl_2 for the small ferrocenyl dendrimers, but the use of MeCN was necessary for the medium-sized ones (27-Fc, 54-Fc, and 81-Fc). Finally, adsorption could not be avoided even with MeCN for the “243-Fc” dendrimer. From the intensity of the wave, the number of ferrocenyl units could be estimated using the Anson–Bard equation [75], and the numbers found were within 5 % of the branch numbers except in the case of the “243-Fc” dendrimer, for which the experimental number was too high (250) because of the adsorption.



Scheme 26. Divergent construction of ferrocenyl dendrimers from the 9-allyl, 27-allyl, 81-allyl and 243-allyl dendrimers.



Scheme 27. Schematic strategy for the divergent construction of ferrocenyl dendrimers exemplified in Schemes 23.

12.9

Polyferrocenium Dendrimers: Molecular Batteries?

The first polyferrocenium dendrimers reported by our group in 1994 and characterized *inter alia* by Mössbauer spectroscopy (a “quantitative” technique) were mixed-valence $\text{Fe}^{\text{II}}/\text{Fe}^{\text{III}}$ complexes [41]. Since then, we have been seeking larger ferrocenyl dendrimers that could also withstand oxidation to their ferrocenium analogues. Syntheses of amidoferrocene dendrimers were simultaneously reported five years ago by our group [60, 61] and by the Madrid group using different cores [62]. In our reports, we were able to demonstrate the use of these metallo dendrimers as redox sensors for the recognition of oxo anions, with remarkable positive dendritic effects being seen when the generation was increased. The amidoferrocenyl dendrimers are not the best candidates for showing stable redox activity on a synthetic scale, however, and are even less well-suited for molecular batteries. Indeed, although they give fully reversible cyclic voltammetry waves, it is known that ferrocenium derivatives bearing an electron-withdrawing substituent are at best fragile, if stable at all. This inconvenience is probably exacerbated in the dendritic structures because of the steric constraints that force the ferrocenium groups to encounter one another more easily than as monomers. Thus, we oxidized our silylferrocenyl dendrimers using $[\text{NO}^+][\text{PF}_6^-]$ in CH_2Cl_2 and obtained stable polyferrocenium dendrimers as dark-blue precipitates, as expected from the known characteristic color of ferrocenium itself. These polyferrocenium dendrimers could be reduced back to soluble orange polyferrocenyl dendrimers using decamethylferrocene as the reductant [76]. No decomposition was observed in either the oxidation or the reduction reaction, and this redox cycle could be cleanly achieved in quantitative yield even with the 243-ferrocenyl dendrimer. The zero-field Mössbauer spectrum of the 243-ferrocenium dendrimer showed a single line corresponding to the expected spectrum known for ferrocenium itself [77], confirming its electronic structure. Thus, these polyferrocenyl dendrimers are stable electron-reservoir systems. Indeed, despite their size, they transfer a very large number of electrons rapidly and “simultaneously” within the electrode. By “simultaneously”, we mean that, vi-

sually, the cyclic voltammogram looks as if it were that of a monoelectronic wave. One must question the notion of the isopotential for the many ferrocenyl units at the periphery of a dendrimer. In theory, all the standard potentials of the n ferrocenyl units of a single dendrimer are distinct, even if all of them are equivalent and independent. This situation arises since the charge of the overall dendrimer molecule increases by one unit every time one of its ferrocenyl units is oxidized to ferrocenium. The next single-electron oxidation is more difficult than the preceding one since, as the dendritic molecule has one more unit of positive charge, it is more difficult to oxidize because of the increased electrostatic factor. Thus, the potentials of the n redox units are statistically distributed around an average standard potential centered at the average potential (Gaussian distribution) [75]. In practice, the situation is complicated by the fact that the dendritic molecule, despite its large size, is rotating much more rapidly than the usual electrochemical time scales [78, 79]. Under these conditions, all the potentials are probably averaged. The fast rotation is also responsible for the fact that all the ferrocenyl units come close to the electrode within the electrochemical time scale. Consequently, there is no slowing down of the electron-transfer due to distance from the electrode, even in large dendrimers. Indeed, the waves of the ferrocenyl dendrimers always appear fully electrochemically reversible, indicating fast electron transfer.

The ferrocenyl dendrimers are also readily adsorbed on electrodes, a phenomenon already well known with various kinds of polymers [80]. When the polymers contain redox centers, the adsorbed systems have long been shown to give rise to a redox wave for which the cathodic and anodic waves are located at exactly the same potential, and for which the intensity of each wave is proportional to the scan rate. Continuous cycling shows the stability of the adsorption of the electrode modified in this way. As expected, the ferrocenyl dendrimers described here show this phenomenon. The stability of the modified electrode produced by soaking a Pt electrode in a solution in CH_2Cl_2 containing the ferrocenyl dendrimer and cyclic scanning between the ferrocenyl and ferrocenium regions is even better as the ferrocenyl dendrimer is larger. For instance, in the case of the 9-ferrocenyl dendrimer, scanning twenty times is necessary in order to obtain a constant intensity, and this intensity is weak. With the 27-, 54-, 81-, and 243-ferrocenyl dendrimers, only approximately ten cyclic scans are necessary in order to obtain a constant wave, and the intensity is much larger. When such derivatized electrodes are washed with CH_2Cl_2 and re-used with a fresh, dendrimer-free CH_2Cl_2 solution, the cyclic voltammogram obtained shows $\Delta E_p = 0$. Other characteristic features are the linear relationship between the intensity and scan rate and the constant stability after cycling many times with no sign of diminished intensity.

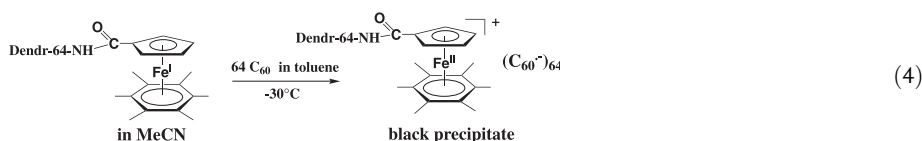
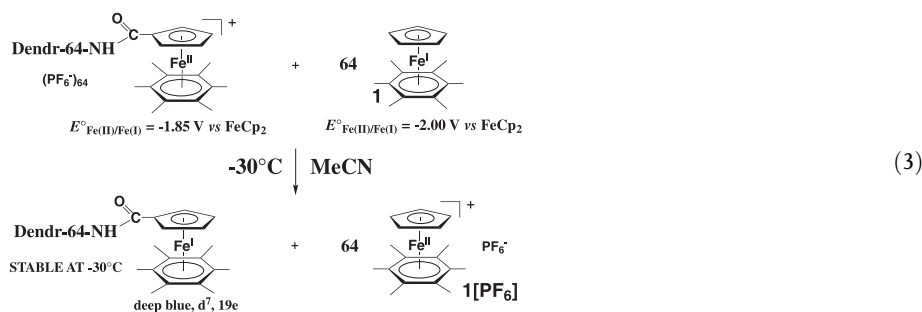
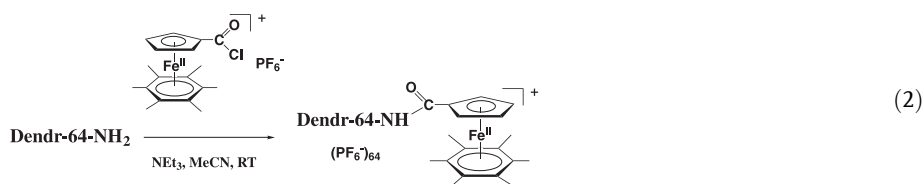
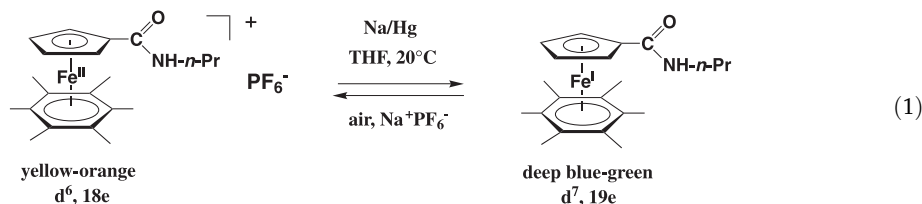
Under these conditions, one may note that the argument of the fast rotation of the dendritic molecule being responsible for bringing all the redox centers in turn close to the electrode does not hold for modified electrodes. Some redox centers must be close to the electrode and some must be far away. It is probable that a hopping mechanism in the solid state is responsible for fast electron transfer and for averaging all the potentials of the different ferrocenyl groups of a single dendritic molecule around a mean value. The proximity of the ferrocenyl groups at the periphery of the dendrimer is a key factor in facilitating this hopping since it is known that electron transfer with redox sites that are remote or buried inside a molecular framework is slow, if observable at all [81–87].

12.10

Large Dendrimers Functionalized on their Branches by the Electron-Reservoir [FeCp(η^6 -C₆Me₆)]⁺ Groups: A Molecular Battery in Action

Ferrocenes and ferrocenyl dendrimers are poor reductants. On the other hand, the complexes $[\text{Fe}(\eta^5\text{-C}_5\text{R}_5)(\eta^6\text{-C}_6\text{Me}_6)]^{2+/+0}$ (R = H or Me) have been shown to be efficient for various stoichiometric and catalytic electron-transfer reactions [26b]. Branching of this sandwich complex by means of a chlorocarbonyl substituent on the Cp ligand leads, upon reaction with dendritic polyamines, to soluble Fe^{II} metallodendrimers. Moreover, these Fe^{II} metallodendrimers can be reduced to Fe^I using $[\text{Fe}^{\text{I}}\text{Cp}(\eta^6\text{-C}_6\text{Me}_6)]$ (1). Reduction of the monomeric model $[\text{Fe}^{\text{II}}(\eta^5\text{-C}_5\text{H}_4\text{CONH}n\text{Pr})(\eta^6\text{-C}_6\text{Me}_6)][\text{PF}_6]$ with Na/Hg in THF at room temp. gives the deep-blue-green, thermally stable 19-electron complex $[\text{Fe}^{\text{I}}(\eta^5\text{-C}_5\text{H}_4\text{CONH}n\text{Pr})(\eta^6\text{-C}_6\text{Me}_6)]$ (Eq. (1)), which shows the classic rhombic distortion of the Fe^I sandwich family, as evidenced by EPR in frozen THF at 77 K (3 g values around 2) [8f]. In view of this stability, we carried out the same reaction of $[\text{Fe}^{\text{II}}(\eta^5\text{-C}_5\text{H}_4\text{COCl})(\eta^6\text{-C}_6\text{Me}_6)][\text{PF}_6]$ with the commercial polypropyleneimine dendrimer of generation five (64 amino termini) in MeCN/CH₂Cl₂ (2:1) in the presence of NEt₃. The polycationic metallodendrimer DAB *dendr*-64-NHCOCpFe^{II}(η^6 -C₆Me₆) was obtained as its PF₆[−] salt, and was found to be soluble in MeCN and DMF (Eq. (2)). This dendritic complex was characterized by ¹H and ¹³C NMR and IR spectroscopies, and by cyclic voltammetry (a single reversible wave in DMF at $E_{1/2} = -1.84$ V *vs.* FeCp₂^{0/+}; $\Delta E = 70$ mV). Attempts to reduce it with the classic reductants that reduce monomeric complexes $[\text{Fe}^{\text{II}}(\eta^5\text{-Cp})(\eta^6\text{-arene})][\text{PF}_6]$, such as Na/sand, Na/Hg, or LiAlH₄ in THF or DME, failed due to the insolubility of both the metallodendrimer and the reductant in the required solvents. The only successful reductant was the parent 19-electron complex $[\text{Fe}^{\text{I}}\text{Cp}(\eta^6\text{-C}_6\text{Me}_6)]$ (in pentane or THF), which reduced the metallodendrimer in MeCN at −30 °C to the neutral, deep-green-blue 19-electron Fe^I dendrimer **6** in a few minutes (Eq. (3)). The exoergonicity of this electron-transfer reaction is 0.16 V; this is due to the electron-withdrawing effect of the juxta-cyclic carbonyl group on the Cp ring, which lowers the reduction potential of the metallodendrimer as compared to that of $[\text{Fe}^{\text{I}}\text{Cp}(\eta^6\text{-C}_6\text{Me}_6)]$. Although the Fe^I dendrimer decomposes at 0 °C, it could also be characterized by its EPR spectrum at 10 K, which confirmed, as the deep-blue-green color, the Fe^I-sandwich structure analogous to that of the monomeric model. In contrast to the case of $[\text{Fe}^{\text{I}}\text{Cp}(\eta^6\text{-C}_6\text{Me}_6)]$, however, it was not possible to record the EPR spectrum of the solution of the Fe^I dendrimer above 10 K. This was presumably due to intramolecular relaxation among the peripheral Fe^I sandwich units. The intermolecular version of this relaxation effect is known to preclude observation of the spectrum of monomeric Fe^I sandwich complexes in the solid state above 4 K and in solution above 77 K [24e]. This solution of the 64-Fe^I dendrimer in acetonitrile was used for the reaction with C₆₀, the Fe^I/C₆₀ stoichiometry being 1:1 (64 C₆₀ per dendrimer). Upon reaction with a solution of C₆₀ in toluene, the deep-blue-green color of the Fe^I dendrimer disappeared, leaving a yellow solution that contained $[\text{Fe}^{\text{II}}\text{Cp}(\eta^6\text{-C}_6\text{Me}_6)][\text{PF}_6]$ and a black precipitate (Eq. (4)). Tentative extraction of this precipitate with toluene yielded a colorless solution, which indicated that no C₆₀ was present. The Mössbauer spectrum of this black solid at 298 K showed parameters indicative of the presence of an Fe^{II} sandwich complex of the same family as $[\text{Fe}^{\text{II}}\text{Cp}(\eta^6\text{-C}_6\text{Me}_6)]^+$ [25a, 25c]. Its EPR spectrum recorded at 77 K was identical to that of $[\text{Fe}^{\text{II}}\text{Cp}(\eta^6\text{-C}_6\text{Me}_6)]^+$

C_{60}^- [88]. It could thus be concluded that C_{60} had been reduced to its monoanion, as befits a process that is exergonic by 0.9 V [89]. The $[\text{dendr-Fe}^{\text{II}}]^+ C_{60}^-$ units, being very large, must be located at the dendrimer periphery, presumably in rather tight ion pairs, although the number of fullerene layers and overall molecular size are unknown (Figure 1).



12.11 Conclusion

CpFe^+ -activation of simple aromatics leads to clean, high-yielding benzylic perfunctionalization reactions. This family of reactions, which can be carried out on a large scale under ambient conditions with a variety of arene ligands, gives stars and dendritic cores and can be applied to the one-pot synthesis of the dendron $p\text{-HOC}_6\text{H}_4\text{C(allyl)}_3$. These building blocks could be assembled to synthesize large polyallyl dendrimers and metallodendrimers containing various redox centers at the extremities of the branches. We have chosen ferrocenyl,

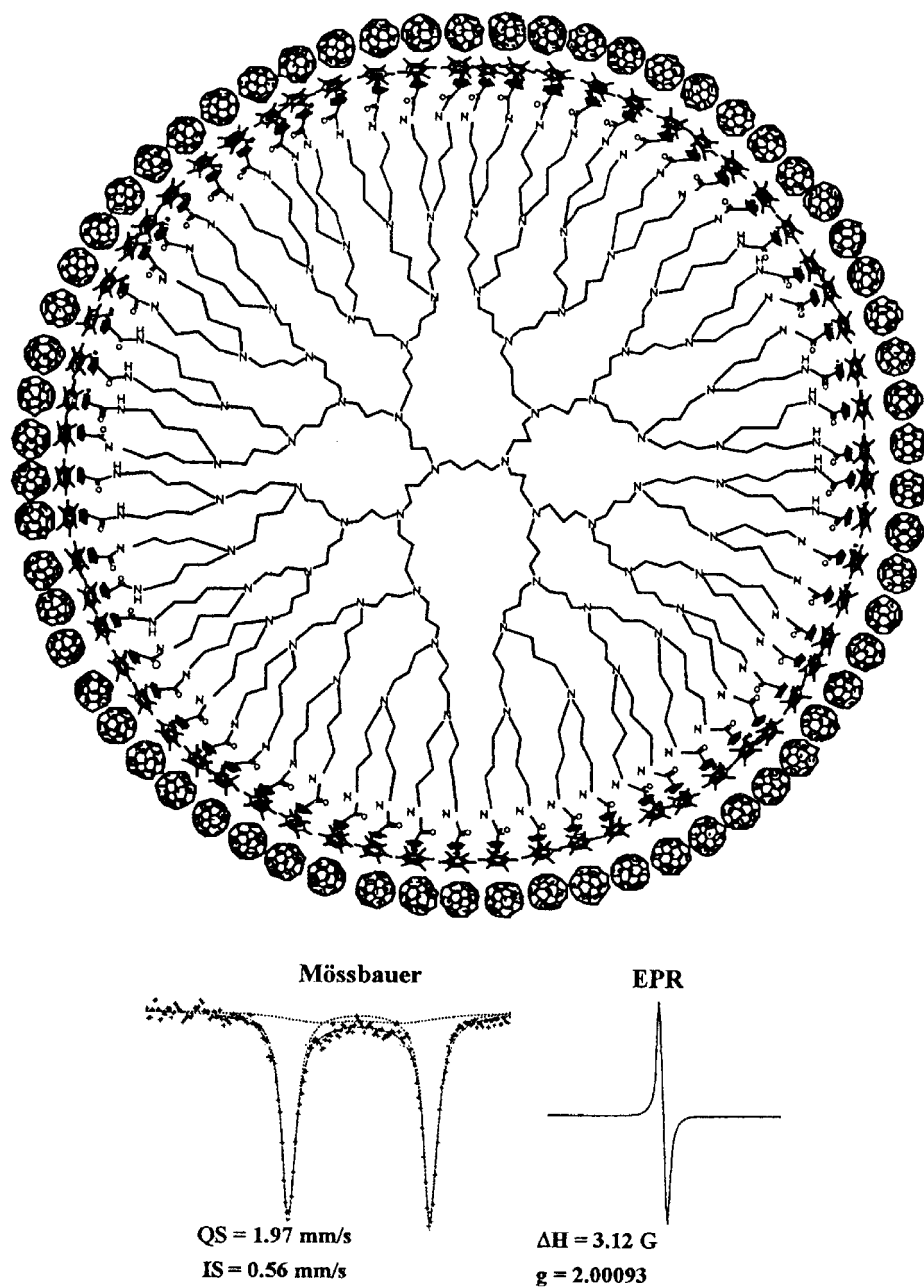


Fig. 1. Dendr-64-NHCOCpFe(C₆Me₆)⁶⁴⁺, 64 C₆₀^{•−} resulting from the reaction of **6** with C₆₀ in MeCN/toluene at −30 °C, along with its EPR spectrum (bottom, right) in MeCN at 10 K and Mössbauer spectrum at 77 K (bottom, left).

cobaltocenyl, and $[\text{FeCp}(\eta^6\text{-C}_6\text{Me}_6)]^+$ redox centers to give stable redox systems. The resulting redox properties are redox recognition (sensors showing a dendritic effect), redox catalysis (as efficient as using monometallic systems with the same driving force), and very efficient derivatization of electrodes (towards more practical sensors). Finally, we have succeeded in using a metallodendrimer containing 64 $[\text{Fe}^{\text{I}}\text{Cp}(\eta^6\text{-C}_6\text{Me}_6)]$ units at the branch termini in a synthetic electron-transfer reaction with C_{60} to give an outer shell of 64 ion pairs $[\text{Fe}^+\text{Cp}(\eta^6\text{-C}_6\text{Me}_6)][\text{C}_{60}^{\cdot-}]$ at the periphery of the dendrimer. This latter reaction shows that the metallodendrimer can behave as an electron reservoir, exemplifying the possibilities of a molecular battery operating at a given potential. Redox-stable metallocene dendrimers [90] offer a spectrum of possibilities [91, 92] in connection with electron-transfer processes in nanoscopic devices [93, 94] that will be further exploited in the future.

Acknowledgement

We are grateful to the students, collaborators, and colleagues cited in the references, in particular Jean-Claude Blais (MALDI-TOF mass spectrometry, University Paris VI) and François Varret (Mössbauer spectroscopy, University of Versailles) for their invaluable contributions to the ideas and experimental efforts that have led to the results presented herein. Financial support from the Institut Universitaire de France (DA), the CNRS, the Universities Bordeaux I and Paris VI, the Ministère de l'Enseignement et de la Recherche Scientifique, and the Région Aquitaine is also gratefully acknowledged.

References

- 1 J.-M. LEHN, *Supramolecular Chemistry: Concepts and Perspectives*, VCH, Weinheim, **1995**.
- 2 M. MAJOR, J.-M. LEHN, *J. Am. Chem. Soc.* **1999**, *121*, 11231.
- 3 V. BALZANI, F. SCANDOLA, *Supramolecular Chemistry*, Ellis Horwood, New York, **1991**.
- 4 V. BALZANI (Ed.), *Electron Transfer in Chemistry*, Vol. II, Wiley-VCH, Weinheim, **2001**.
- 5 N. ARDOIN, D. ASTRUC, *Bull. Soc. Chim. Fr.* **1995**, *132*, 875.
- 6 V. BALZANI, S. CAMPANA, G. DENTI, A. JURIS, S. SERRONI, M. VENTURI, *Acc. Chem. Res.* **1998**, *31*, 26.
- 7 M. VENTURI, S. SERRONI, A. JURIS, S. CAMPANA, V. BALZANI, *Top. Curr. Chem.* **1998**, *197*, 193.
- 8 G. R. NEWKOME, E. HE, C. N. MOOREFIELD, *Chem. Rev.* **1999**, *99*, 1689.
- 9 a) I. CUADRADO, M. MORÁN, C. M. CASADO, B. ALONSO, J. LOSADA, *Coord. Chem. Rev.* **1999**, *189*, 123; b) C. CASADO, I. CUADRADO, M. MORÁN, B. ALONSO, M. BARRANCO, J. LOSADA, *Appl. Organomet. Chem.* **1999**, *14*, 245; c) For a review on ferrocene dendrimers, see: C. M. CASADO, I. CUADRADO, M. MORÁN, B. ALONSO, J. LOSADA, *Coord. Chem. Rev.* **1999**, *185–186*, 53.
- 10 M. A. HEARSHAW, J. R. MOSS, In *Advances in Macromolecules* (Ed.: G. NEWKOME), JAI Press Inc., Stamford, CT, **1999**, Vol. 4, pp. 1–60.
- 11 M. A. HEARSHAW, J. R. MOSS, *Chem. Commun.* **1999**, 1.
- 12 G. R. NEWKOME, C. N. MOOREFIELD, F. VÖGTLE, *Dendrimers and Dendrons. Concepts, Synthesis, Applications*, Wiley-VCH, Weinheim, **2001**.
- 13 G. E. OOSTEROM, J. N. H. REEK, P. C. J. KAMER, P. W. N. M. VAN LEEUWEN, *Angew. Chem. Int. Ed.* **2001**, *40*, 1828.
- 14 D. ASTRUC, F. CHARDAC, *Chem. Rev.* **2001**, *101*, 2991.
- 15 D. ASTRUC, *Electron Transfer and Radical Processes in Transition Metal Chemistry*, VCH, New York, **1995**.
- 16 a) D. ASTRUC, *Topics Curr. Chem.* (Ed.: W. A. HERRMANN), Springer Verlag, Berlin, **1991**, *160*, 47; b) D. ASTRUC, J.-C. BLAIS,

- E. CLOUTET, L. DJAKOVITCH, S. RIGAUT, J. RUIZ, V. SARTOR, C. VALÉRIO, *Topics Curr. Chem.*, Dendrimers II (Ed.: F. VÖGTLE), Springer Verlag, Berlin, **2000**, 210, 229.
- 17 D. ASTRUC, In *The Chemistry of the Metal–Carbon Bond* (Ed.: F. R. HARTLEY), Vol. 4, Wiley, New York, **1987**, pp. 625–731.
 - 18 D. ASTRUC, *Tetrahedron Report N° 157*, *Tetrahedron* **1983**, 39, 4027.
 - 19 L. BALAS, D. JHURRY, L. LATXAGUE, S. GRELIER, Y. MOREL, M. HAMDANI, N. ARDOIN, D. ASTRUC, *Bull. Soc. Chim. Fr.* **1990**, 127, 401.
 - 20 A. N. NESMEYANOV, N. A. VOL'KENAU, I. N. BOLESOVA, *Tetrahedron Lett.* **1963**, 1725.
 - 21 T. P. GILL, K. R. MANN, *Inorg. Chem.* **1980**, 19, 3007.
 - 22 F. MOULINES, M. KALAM-ALAMI, V. MARTINEZ, D. ASTRUC, *J. Organomet. Chem.* **2001**, 125, 643–644. (special issue dedicated to F. Mathey).
 - 23 A. N. NESMEYANOV, *Adv. Organomet. Chem.* **1972**, 10, 1.
 - 24 a) R. E. DESSY, F. E. STARY, R. B. KING, M. WALDROP, *J. Am. Chem. Soc.* **1966**, 88, 471; b) A. N. NESMEYANOV, N. A. VOL'KENAU, L. S. SHILOVSTSEVA, V. A. PETRAKOVA, *J. Organomet. Chem.* **1973**, 61, 329.
 - 25 a) J.-R. HAMON, D. ASTRUC, P. MICHAUD, *J. Am. Chem. Soc.* **1981**, 103, 758; b) J.-R. HAMON, G. ALTHOFF, E. ROMÁN, P. BATAIL, P. MICHAUD, J.-P. MARIOT, F. VARRET, D. ASTRUC, D. COZAK, *J. Am. Chem. Soc.* **1979**, 101, 5445; c) M. V. RAJASEKHARAN, S. GIEZYNSKI, J. H. AMMETER, J.-R. HAMON, P. MICHAUD, D. ASTRUC, *J. Am. Chem. Soc.* **1982**, 104, 2400; d) J. C. GREEN, M. R. KELLY, M. P. PAYNE, E. A. SEDDON, D. ASTRUC, J.-R. HAMON, P. MICHAUD, *Organometallics* **1983**, 2, 211; e) D. ASTRUC, *Acc. Chem. Res.* **1986**, 19, 377.
 - 26 a) J. RUIZ, F. OGLIARO, J.-Y. SAILLARD, J.-F. HALET, F. VARRET, D. ASTRUC, *J. Am. Chem. Soc.* **1998**, 120, 11693; b) D. ASTRUC, *Acc. Chem. Res.* **2000**, 33, 287.
 - 27 a) D. ASTRUC, E. ROMÁN, J.-R. HAMON, P. BATAIL, *J. Am. Chem. Soc.* **1979**, 101, 2240; b) H. J. TRUJILLO, C. M. CASADO, J. RUIZ, D. ASTRUC, *J. Am. Chem. Soc.* **1999**, 121, 5674.
 - 28 a) J.-R. HAMON, D. ASTRUC, *J. Am. Chem. Soc.* **1983**, 105, 5951; b) I. FRIDOVITCH, *Free Radicals in Biology* (Ed.: W. A. PRIOR), Academic Press, New York, **1976**, p. 239.
 - 29 A. N. NESMEYANOV, N. A. VOL'KENAU, I. N. BOLESOVA, *Dokl. Akad. Nauk SSSR* **1967**, 175, 606.
 - 30 C. C. LEE, A. S. ABD EL AZIZ, R. L. CHOWDHURRY, U. S. GILL, A. PIORKO, R. G. SUTHERLAND, *J. Organomet. Chem.* **1986**, 315, 79.
 - 31 R. G. SUTHERLAND, C. H. ZHANG, A. PIORKO, C. C. LEE, *J. Org. Chem.* **1989**, 67, 137.
 - 32 See refs. [67–69] and L. DJAKOVITCH, Ph.D. Thesis, University Bordeaux I, 1994.
 - 33 For the synthesis of [Fe^{II}Cp(η⁶-C₆Me₆)](PF₆), see refs. [25, 34, 35, 51c, p. 792].
 - 34 P. L. PAUSON, W. E. WATTS, *J. Chem. Soc.* **1963**, 2990.
 - 35 D. ASTRUC, J.-R. HAMON, M. LACOSTE, M.-H. DESBOIS, E. ROMÁN, *Organometallic Synthesis* (Ed.: R. B. KING), **1988**, Vol. IV, p. 172.
 - 36 J.-R. HAMON, J.-Y. SAILLARD, A. LE BEUZE, M. MCGLINCHAY, D. ASTRUC, *J. Am. Chem. Soc.* **1982**, 104, 3755.
 - 37 F. MOULINES, D. ASTRUC, *Angew. Chem. Int. Ed. Engl.* **1988**, 27, 1347.
 - 38 F. MOULINES, D. ASTRUC, *J. Chem. Soc., Chem. Commun.* **1989**, 614.
 - 39 J.-R. HAMON, P. HAMON, K. BOUKHEDDADEN, J. LINARÈS, F. VARRET, D. ASTRUC, *Inorg. Chim. Acta* **1995**, 240, 105.
 - 40 E. ALONSO, D. ASTRUC, unpublished work.
 - 41 J.-L. FILLAUT, J. LINARÈS, D. ASTRUC, *Angew. Chem. Int. Ed. Engl.* **1994**, 33, 2460.
 - 42 C. VALÉRIO, B. GIOAGUEN, J.-L. FILLAUT, D. ASTRUC, *Bull. Soc. Chim. Fr.* **1996**, 133, 101.
 - 43 J.-L. FILLAUT, R. BOESE, D. ASTRUC, *Synlett* **1992**, 55.
 - 44 J.-L. FILLAUT, D. ASTRUC, *New J. Chem.* **1996**, 20, 945.
 - 45 H. W. MARX, F. MOULINES, T. WAGNER, D. ASTRUC, *Angew. Chem. Int. Ed. Engl.* **1996**, 35, 1701.
 - 46 J. RUIZ, E. ALONSO, J. GUITTARD, J.-C. BLAIS, D. ASTRUC, *J. Organomet. Chem.* **1999**, 582/1, 139.
 - 47 F. MOULINES, L. DJAKOVITCH, J.-L. FILLAUT, D. ASTRUC, *Synlett* **1992**, 57.
 - 48 V. MARVAUD, D. ASTRUC, *Chem. Commun.* **1997**, 773.

- 49 V. MARVAUD, D. ASTRUC, *New J. Chem.* **1997**, 21, 1309.
- 50 V. SARTOR, L. DJAKOVITCH, J.-L. FILLAUT, F. MOULINES, F. NEVEU, V. MARVAUD, J. GUITTARD, J.-C. BLAIS, D. ASTRUC, *J. Am. Chem. Soc.* **1999**, 121, 2929.
- 51 a) S. RIGAUT, M.-H. DELVILLE, D. ASTRUC, *J. Am. Chem. Soc.* **1997**, 119, 1132; b) S. RIGAUT, M.-H. DELVILLE, J. LOSADA, D. ASTRUC, *Inorg. Chim. Acta* **2002**, 334, 225; c) D. ASTRUC, in *Electron Transfer in Chemistry* (Ed.: V. BALZANI), Vol. II, Wiley-VCH, Weinheim, **2001**, pp. 714–803.
- 52 F. MOULINES, B. GLOAGUEN, D. ASTRUC, *Angew. Chem. Int. Ed. Engl.* **1992**, 28, 458.
- 53 G. R. NEWKOME, X. LIN, J. K. YOUNG, *Synlett* **1992**, 53.
- 54 C. VALÉRIO, E. ALONSO, J. RUIZ, J.-C. BLAIS, D. ASTRUC, *Angew. Chem. Int. Ed.* **1999**, 38, 1747.
- 55 C. VALÉRIO, F. MOULINES, J. RUIZ, J.-C. BLAIS, D. ASTRUC, *J. Org. Chem.* **2000**, 65, 1996.
- 56 B. GLOAGUEN, D. ASTRUC, *J. Am. Chem. Soc.* **1990**, 112, 4607.
- 57 D. BUCHHOLZ, B. GLOAGUEN, J.-L. FILLAUT, M. COTRAIT, D. ASTRUC, *Chem. Eur. J.* **1995**, 1, 374.
- 58 D. BUCHHOLZ, D. ASTRUC, *Angew. Chem. Int. Ed. Engl.* **1994**, 33, 1637.
- 59 F. MOULINES, L. DJAKOVITCH, R. BOESE, B. GLOAGUEN, W. THIEL, J.-L. FILLAUT, M.-H. DELVILLE, D. ASTRUC, *Angew. Chem. Int. Ed. Engl.* **1993**, 105, 1132.
- 60 a) D. ASTRUC, C. VALÉRIO, J.-L. FILLAUT, J.-R. HAMON, F. VARRET, in *Magnetism, A Supramolecular Function* (Ed.: O. KAHN), NATO ASI Series, Kluwer, Dordrecht, **1996**, p. 1107; b) C. VALÉRIO, *Ph.D. Thesis*, Université Bordeaux I, **1996**.
- 61 C. VALÉRIO, J.-L. FILLAUT, J. RUIZ, J. GUITTARD, J.-C. BLAIS, D. ASTRUC, *J. Am. Chem. Soc.* **1997**, 119, 2588.
- 62 a) I. CUADRADO, M. MORÁN, C. M. CASADO, B. ALONSO, F. LOBETE, B. GARCIA, J. LOSADA, *Organometallics* **1996**, 15, 5278; b) K. TAKADA, D. J. DIAZ, H. ABRUÑA, I. CUADRADO, C. M. CASADO, B. ALONSO, M. MORÁN, J. LOSADA, *J. Am. Chem. Soc.* **1997**, 119, 10763.
- 63 E. ALONSO, C. VALÉRIO, J. RUIZ, D. ASTRUC, *New J. Chem.* **1997**, 21, 1119.
- 64 E. M. M. DE BRABANDER-VAN DEN BERG, E. W. MEIJER, *Angew. Chem. Int. Ed. Engl.* **1993**, 32, 1308.
- 65 C. WÖRNER, R. MÜLHAUPT, *Angew. Chem. Int. Ed. Engl.* **1993**, 32, 1306.
- 66 C. VALÉRIO, J. RUIZ, E. ALONSO, P. BOUSSAGUET, J. GUITTARD, J.-C. BLAIS, D. ASTRUC, *Bull. Soc. Chim. Fr.* **1997**, 134, 907.
- 67 F. MOULINES, L. DJAKOVITCH, M.-H. DELVILLE, F. ROBERT, P. GOUZERH, D. ASTRUC, *J. Chem. Soc., Chem. Commun.* **1995**, 463.
- 68 F. MOULINES, L. DJAKOVITCH, D. ASTRUC, *New J. Chem.* **1996**, 20, 1071.
- 69 V. SARTOR, S. NLATE, J.-L. FILLAUT, F. DJAKOVITCH, F. MOULINES, V. MARVAUD, F. NEVEU, J.-C. BLAIS, *New J. Chem.* **2000**, 24, 351.
- 70 S. NLATE, J. RUIZ, D. ASTRUC, *Chem. Commun.* **2000**, 417.
- 71 S. NLATE, J. RUIZ, V. SARTOR, R. NAVARRO, J.-C. BLAIS, D. ASTRUC, *Chem. Eur. J.* **2000**, 6, 2544.
- 72 a) B. MARCINIEC, in *Applied Homogeneous Catalysis with Organometallic Compounds* (Eds.: B. CORNILS, W. A. HERRMANN), VCH, Weinheim, **1996**, Vol. 1, Chap. 2.6; b) L. N. LEWIS, J. STEIN, K. A. SMITH, in *Progress in Organosilicon Chemistry* (Eds.: B. MARCINIEC, J. CHOJNOWSKI), Gordon and Breach, Langhorne, USA, **1995**, p. 263.
- 73 K. H. PANNEL, H. SHARMA, *Organometallics* **1991**, 10, 954.
- 74 P. JUTZI, C. BATZ, B. NEUMANN, H. G. STAMMLER, *Angew. Chem. Int. Ed. Engl.* **1996**, 35, 2118.
- 75 J. B. FLANAGAN, S. MARGEL, A. J. BARD, F. C. ANSON, *J. Am. Chem. Soc.* **1978**, 100, 4248.
- 76 J. RUIZ, D. ASTRUC, *C. R. Acad. Sci. Paris*, t. 1, Série II c, **1998**, 21.
- 77 R. L. COLLINS, *J. Chem. Phys.* **1965**, 42, 1072.
- 78 S. J. GREEN, J. J. PIETRON, J. J. STOKES, M. J. HOSTETLER, H. VU, W. P. WUELFING, R. W. MURRAY, *Langmuir* **1998**, 14, 5612.
- 79 C. B. GORMAN, J. C. SMITH, M. W. HAGER, B. L. PARHURST, H. SIERZPUTOWSKA-GRACZ, C. A. HANEY, *J. Am. Chem. Soc.* **1999**, 121, 9958.
- 80 R. MURRAY, in *Molecular Design of Electrode Surfaces* (Ed.: R. MURRAY), Wiley, New York, **1992**, p. 1.

- 81 P. J. DANDLIKER, F. DIEDERICH, M. GROSS, B. KNOBLER, A. LOUATI, E. M. STANFORD, *Angew. Chem. Int. Ed. Engl.* **1994**, 33, 1739.
- 82 G. R. NEWKOME, R. GÜTHER, C. N. MOOREFIELD, F. CARDULLO, L. ECHEGOYEN, F. PÉREZ-CORDERO, H. LUFTMANN, *Angew. Chem. Int. Ed. Engl.* **1995**, 34, 2023.
- 83 H.-F. CHOW, I. Y.-K. CHAN, D. T. W. CHAN, R. W. M. KWOK, *Chem. Eur. J.* **1996**, 2, 1085.
- 84 P. J. DANDLIKER, F. DIEDERICH, J. P. GISSELBRECHT, A. LOUATI, M. GROSS, *Angew. Chem. Int. Ed. Engl.* **1996**, 34, 2725.
- 85 J. ISSBERNER, F. VÖGTLE, L. DE COLA, V. BALZANI, *Chem. Eur. J.* **1997**, 3, 706.
- 86 C. B. GORMAN, B. L. PARKHURST, W. Y. SU, K. Y. CHEN, *J. Am. Chem. Soc.* **1997**, 119, 1141.
- 87 D. K. SMITH, F. DIEDERICH, *Chem. Eur. J.* **1998**, 4, 2353.
- 88 a) C. BOSSARD, S. RIGAUT, D. ASTRUC, M.-H. DELVILLE, G. FÉLIX, A. FÉVRIER-BOUVIER, J. AMIELL, S. FLANDROIS, P. DELHAËS, *J. Chem. Soc., Chem. Commun.* **1993**, 333; b) J. RUIZ, C. PRADET, F. VARRET, D. ASTRUC, *Chem. Commun.* **2002**, 1108.
- 89 Redox potentials of the six cathodic monoelectronic reductions of C₆₀: A. XIE, E. PÉREZ-CORDERO, L. ECHEGOYEN, *J. Am. Chem. Soc.* **1992**, 114, 3978.
- 90 a) For reports on other ferrocene dendrimers, see ref. [9], which reviews dendrimers of the Madrid group, and: S. ACHAR, C. E. IMMOOS, M. G. HILL, V. J. CATALANO, *Inorg. Chem.* **1997**, 36, 2314; R. DESCHENAUX, E. SERRANO, A.-M. LEVELUT, *Chem. Commun.* **1997**, 1577; C.-F. SHU, H.-M. SHEN, *J. Mater. Chem.* **1997**, 7, 47; C. M. CARDONA, A. E. KAIFER, *J. Am. Chem. Soc.* **1998**, 120, 4023; C. KÖLLNER, B. PUGIN, A. TOGNI, *J. Am. Chem. Soc.* **1998**, 120, 10274; b) R. SCHNEIDER, C. KÖLLNER, I. WEBER, A. TOGNI, *Chem. Commun.* **1999**, 2415; c) E. G. OOSTEROM, R. J. VAN HAAREN, J. N. H. REEK, P. C. J. KAMER, P. W. N. M. VAN LEEUWEN, *Chem. Commun.* **1999**, 1119; B. DARDEL, R. DESCHENAUX, C.-O. TURRIN, J. CHIFFRE, D. DE MONTAUZON, J.-C. DARAN, A.-M. CAMINADE, E. MANOURY, G. BALAVOINE, J.-P. MAJORAL, *Macromolecules* **2000**, 33, 7328; M. MOSBACH, W. SCHUHMAN, Patent No. DE 19917052, **1999**, CA 133: 293175; J. IPATSCHI, R. HOSSEINZADEH, P. SCHLAF, *Angew. Chem. Int. Ed.* **1999**, 38, 1658; M. EVEN, E. SERRANO, *Macromolecules* **1999**, 32, 5193; H. C. YOON, M.-Y. HONG, H.-S. KIM, *Anal. Chem.* **2000**, 72, 4420; H. C. YOON, M.-Y. HONG, H.-S. KIM, *Anal. Biochem.* **2000**, 282, 121; M. VALENTINI, P. S. PREGOSIN, H. RUEGGER, *Organometallics* **2000**, 19, 2551; T. D. MCCARLEY, C. J. DUBOIS JR., R. L. MCCARLEY, C. M. CARDONA, A. E. KAIFER, *Polym. Prepr. (Am. Chem. Soc., Div. Polym. Chem.)* **2000**, 41, 674; C. CARDONA, T. D. MCCARLEY, A. E. KAIFER, *J. Org. Chem.* **2000**, 65, 1857; R. DESCHENAUX, *Chimia* **2001**, 55, 139; B. ALONSO, E. ALONSO, D. ASTRUC, J.-C. BLAIS, L. DJAKOVITCH, J.-L. FILLAUT, S. NIATE, F. MOULINES, S. RIGAUT, J. RUIZ, V. SARTOR, C. VALÉRIO, *Advances in Macromolecules* (Ed.: G. NEWKOME), JAI Press Inc., Stamford, CT, **2001**, Vol. 5, pp. 89–127.
- 91 a) Y. WANG, C. CARDONA, A. E. KAIFER, *J. Am. Chem. Soc.* **1999**, 121, 9756; b) A. E. KAIFER, M. GOMEZ-KAIFER, *Supramolecular Electrochemistry*, Wiley-VCH, Weinheim, **1999**.
- 92 C. B. GORMAN, *Adv. Mater.* **1997**, 9, 1117.
- 93 R. M. CROOKS, M. ZHAO, L. SUN, V. CHECHIK, L. K. YEUNG, *Acc. Chem. Res.* **2001**, 34, 181.
- 94 Y. XIA, J. A. ROGERS, K. E. PAUL, G. M. WHITESIDES, *Chem. Rev.* **1999**, 99, 1823.
- 95 a) S. MARCEN, M. V. JIMENEZ, I. T. DOBRINOVICH, F. J. LAHOZ, L. A. ORO, J. RUIZ, D. ASTRUC, *Organometallics* **2002**, 21, 326; b) V. MARTINEZ, J.-C. BLAIS, D. ASTRUC, *Org. Lett.* **2002**, 4, 651.

13

Charge-Transfer Effects on Arene Structure and Reactivity

Sergiy V. Rosokha and Jay K. Kochi

Abstract

Arenes spontaneously form intermolecular 1:1 complexes with a wide variety of electrophiles, cations, acids, and oxidants that are all sufficiently electron-poor to be classified as electron acceptors. Spectral, structural, and thermodynamic properties of these donor/acceptor associates are described within the context of the Mulliken charge-transfer (CT) formulation. The quantitative analyses of such CT complexes provide the mechanistic basis for understanding arene reactivity in different thermal and photochemical processes.

13.1

Introduction

Arenes have historically played a pivotal role in the development of modern organic chemistry, in large part stemming from their π -electronic structures comprised of cyclic arrays of conjugated double bonds. The latter are especially critical to the facile formation of molecular (1:1) complexes with a wide variety of rather common reagents, such as Brønsted and Lewis acids, organic and inorganic cations and oxidants, molecular and ionic electrophiles, etc., all of which are readily recognized as being relatively electron-poor or -deficient, and are thus hereinafter referred to generally as electron acceptors [1–4]. Thermodynamically, such intermolecular complexes of arenes (ArH) and electron acceptors (A) run the gamut from extremely stable and readily isolable in crystalline form to highly labile with lifetimes on a par with molecular collisions [5]. From a mechanistic point of view, these interactions are tantamount to the efficient organization of the reactant arene and the electron acceptor within the prereactive complex [ArH, A] prior to (bimolecular) reaction. For example, in biochemical systems, such assemblies (derived from multiple weak intermolecular interactions) can be dominant, as in enzyme/substrate complexes, antigen/antibody binding, etc., for the variety of regio- and stereospecific transformations [6]. At the other extreme, intermolecular interactions of chromophoric (aromatic) functionalities play an important role in the design of nanomolecular devices such as electronic switches, sensors, etc. [7, 8].

Owing to the inextensible range of complex stabilities extant with various ArH/A combinations, it is important to develop an analytical methodology that is universally applicable and capable of identifying the intermolecular interactions accurately and reliably. As such, in

this chapter we initially explore how the electronic transitions specifically arising from intermolecular interactions of arenes with various electron acceptors provide a comprehensive basis for intermolecular complex formation according to Mulliken [9]. The quantitative treatment of the *static* properties of intermolecular arene complexes is then followed by the mechanistic analysis of aromatic reactivity that proceeds from Mulliken's formulations of intermolecular complexes as *dynamic* precursors to electron transfer based on Marcus–Hush theory [10, 11].

In Section 13.2, a short presentation of the Mulliken formulation provides the theoretical background for understanding the spectral and thermodynamic characteristics as well as charge distributions in intermolecular complexes. Section 13.3 presents the general structural features of intermolecular complexes and focuses more specifically on the structural changes in the arene donor upon complexation. Such changes lead to arene activation (critical to organometallic catalysis), which is described in Section 13.4. Finally, Section 13.5 illustrates how the recognition of intermolecular complexes as crucial intermediates creates the mechanistic basis for understanding arene reactivity in different thermal and photochemical processes. As a result, we emphasize how this unified approach can lead to spectral, structural, and thermodynamic properties, and consequently the reactivity of a wide variety of arene associates, from very weakly bonded encounter complexes to stable organometallic derivatives.

13.2

Mulliken's Quantitative Description of Intermolecular (Charge-Transfer) Complexes

According to Mulliken [9], arenes are classified as electronic donors (D) in measure with their degree of electron-rich character, as evaluated by their ionization potential (IP, gas phase) or oxidation potential (E°_{ox} , solution) [12]. The intermolecular interaction of the arene donor (D) and electronic acceptor (A) spontaneously leads to the electron donor/acceptor or EDA complex, i.e.



13.2.1

Short Theoretical Background

Intermolecular complexes are generated by the linear combination of the principal van der Waals ($\psi_{D,A}$) and dative ($\psi_{D^+A^-}$) states, so that the ground-state (Ψ_{GS}) and excited-state (Ψ_{ES}) wavefunctions in the two-state or charge-transfer (CT) model can be expressed as [13]:

$$\Psi_{\text{GS}} = a\psi_{D,A} + b\psi_{D^+A^-} \quad (2)$$

$$\Psi_{\text{ES}} = b\psi_{D,A} - a\psi_{D^+A^-} \quad (3)$$

The energies of the ground (E_{GS}) and excited (E_{ES}) states that are obtained by solving the secular determinant by the variation method (and constraining the mixing coefficients to the normalized $a^2 + b^2 = 1$) can be expressed as [13]:

$$E_{GS} = (E_{D,A} + E_{D^+A^-})/2 - (\Delta_{DA}^2 + 4H_{DA}^2)^{1/2}/2 \quad (4)$$

$$E_{ES} = (E_{D,A} + E_{D^+A^-})/2 + (\Delta_{DA}^2 + 4H_{DA}^2)^{1/2}/2 \quad (5)$$

and the product of the mixing coefficients is:

$$|ab| = |H_{DA}|/(E_{ES} - E_{GS}) \quad (6)$$

The Coulomb integrals $\int \psi_{D,A} H \psi_{D,A}$ and $\int \psi_{D^+A^-} H \psi_{D^+A^-}$ represent the energies $E_{D,A}$ and $E_{D^+A^-}$ of the van der Waals and dative states, respectively. The energy gap is $\Delta_{DA} = E_{D^+A^-} - E_{D,A}$ and the electronic coupling matrix element is given by the resonance integral $\int \psi_{D,A} H \psi_{D^+A^-} = H_{DA}$.

The optical or charge-transfer transition ($h\nu_{CT}$) stems from electron promotion from the ground to the excited state of the complex, and it follows from Eqs. (4) and (5), that

$$h\nu_{CT} = E_{ES} - E_{GS} = (\Delta_{DA}^2 + 4H_{DA}^2)^{1/2} \quad (7)$$

Most importantly, the spectral characteristics of the charge-transfer (CT) absorption band also provide a quantitative measure of the electronic coupling element in the intermolecular complex, i.e. [14–16]:

$$H_{DA} = 0.0206(v_{\max}\Delta\nu_{1/2}\epsilon_{\max})^{1/2}/r \quad (8)$$

where v_{\max} and $\Delta\nu_{1/2}$ are the maximum and the width (in cm^{-1}), respectively, of the charge-transfer band, ϵ_{\max} is the extinction coefficient ($\text{M}^{-1}\text{cm}^{-1}$), and r is the donor/acceptor separation (\AA) in the complex [17].

While the Mulliken description above is based on the valence-bond formalism, complex formation can alternatively be presented in (equivalent) molecular orbital or MO terms [18]. Thus, charge-transfer bonding and antibonding orbitals are formed as the result of HOMO/LUMO interactions of the donor and acceptor orbitals, and the mixing coefficients refer to the relative participation of donor and acceptor orbitals in the complex wavefunction. Accordingly, the energies of the initial and final (diabatic) states are substituted by the corresponding Coulomb integrals $\int \psi_D H \psi_D$ and $\int \psi_A H \psi_A$, which represent the electron energies of the donor and acceptor orbitals, respectively, and the coupling element H_{DA} is given by the resonance (exchange) integral $H_{AD} = \int \psi_D H \psi_A$, representing the electronic interaction energy in the donor/acceptor dyad. Although the MO approach is less suitable for the consideration of reaction dynamics [19], it often allows a clearer description of the ground-state and optical properties of the intermolecular (charge-transfer) complex, as readily depicted by the simple energy (orbital) diagram in Chart 1, and it will also be employed (interchangeably) hereafter, as appropriate.

13.2.2

Quantitative Evaluation of Arenes as Electron Donors

Donor/acceptor interactions in charge-transfer (CT) complexes are determined primarily by the symmetry and the energetics of the frontier orbitals (HOMO and LUMO) [20]. A

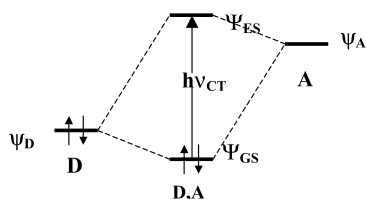


Chart 1

quantitative classification of arene ligands according to their electron-donor and -acceptor strengths is generally based in the gas phase on the (vertical) ionization potential (IP) and the electron affinity (EA), respectively. In solution, the appropriate measure is based on the oxidation (E°_{ox}) and reduction (E°_{red}) potentials. As such, IP and E°_{ox} relate to the energetics of the conversion of an arene (ArH) to its cation radical (ArH^+), whereas EA and E°_{red} relate to the formation of the acceptor anion radical (A^-). Owing to the high reactivities of the ion radicals of most aromatic compounds, the reversible oxidation and reduction potentials are not generally accessible. However, this problem is partially alleviated by the electrochemical measurement of the irreversible anodic and cathodic waves, E_p^a and E_p^c , respectively, which are readily obtained from linear sweep or cyclic voltammograms (CV) [21]. Since the values of E_p^a and E_p^c contain contributions from kinetic terms ($E^\circ = \beta E_p + \text{constant}$), any comparison with the values of the E° is necessarily restricted to a series of structurally related donors [22].

An alternative measure of the electron-donor properties is the ionization potential (IP), which is experimentally determined from photoelectron spectra in the gas phase. The values of IP differ from the oxidation potential E°_{ox} by (cation) solvation, ΔG_s (i.e. $E^\circ_{\text{ox}} \cong \text{IP} + \Delta G_s$) [22]. When the variations in ΔG_s are minor, the values of IP such as those listed in Table 1 can be adequate measures of the electron-donor properties of organic compounds applicable to a particular solvent. This generalization is especially tenable for a series of related compounds [22]. Nonetheless, the global plot of the extensive data [4] indicates that the electron-donor property (i.e. HOMO energy) is consistently revealed in the trend of the gas-phase (ionization) potentials relative to the solution-phase oxidation potentials, despite large differences in structural types. Such a correlation suggests that a similar conclusion pertains to the electron-donor properties of organic anions, for which gas-phase potentials are more difficult to measure consistently. Although the same limitations apply to the use of E_p^c as those described above for the anodic counterpart, the general trend shows that gas-phase electron affinities also generally reflect the trend in the reduction potentials measured in solution (i.e. $E^\circ_{\text{red}} \cong \text{EA} + \Delta G_s$) for the large variety of acceptors included in Table 2 [4]. Because of their use as photochemical quenchers, the enhanced values of the reduction potential for the excited singlet and triplet acceptor species A^* are also listed in Table 2 [4].

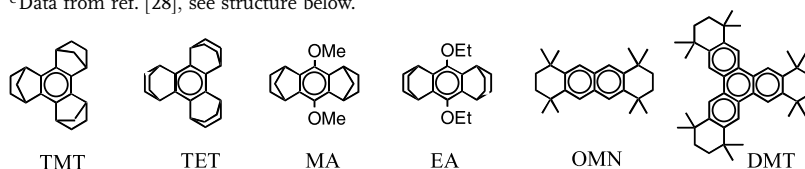
13.2.3

Spectral (UV/vis) Probe for the Formation of CT Complexes

The most characteristic spectroscopic feature of CT complexes is a new absorption band in their electronic (UV/vis/NIR) spectra that is not seen in the individual spectra of either the

Tab. 1. Oxidation potentials and ionization potentials of various classes of arenes^a

Donor ^b	E°_{ox}	IP	Donor ^b	E°_{ox}	IP
Methylbenzenes			Methoxy(hydroxy)benzenes		
Benzene (BEN)	2.62	9.24	Phenol	1.04	8.50
Toluene (TOL)	2.25	8.82	Anisole	1.76	8.22
o-Xylene (o-XY)	2.16	8.56	(MA) ^c	1.16	
Mesitylene (MES)	2.11	8.39	(EA) ^c	1.30	
Durene (DUR)	1.84	8.03	Polycyclic aromatic hydrocarbons		
Pentamethylbenzene (PMB)	1.71	7.92	Naphthalene (NAP)	1.54	8.14
Hexamethylbenzene (HMB)	1.62	7.85	Anthracene (ANT)	1.09	7.45
(TMT) ^c	1.50		(DMT) ^c	1.43	
(TET) ^c	1.55		(OMN) ^c	1.34	

^a E°_{ox} in V vs SCE, IP in eV, data from ref. [4].^b The acronym in parentheses will be used hereinafter.^c Data from ref. [28], see structure below.

uncomplexed donor or the acceptor. Such absorption bands are universally observed for arene associates with organic and inorganic acceptors, for both weak as well as strong molecular complexes, and even in the case of short-lived collision complexes with $K_{\text{CT}} \ll 1$ [3, 4, 23, 24].

As is apparent from Eq. (7), the energy of the electronic transition in CT complexes is determined as the sum of the two terms, the difference in the energy of the diabatic states (Δ_{DA}) and the electronic coupling element (H_{DA}). Depending on their relative values, there can be two limiting cases represented by weak complexes with $H_{\text{DA}} \ll \Delta_{\text{DA}}$ and strong complexes with $\Delta_{\text{DA}} \ll H_{\text{DA}}$.

In a weak complex, the wavefunction Ψ_{GS} for the ground state basically describes a no-bond (or initial) state (D, A), in which the (final) charge-transfer state (D^+ , A^-) does not play

Tab. 2. Reduction potential and electron affinity of (ground-state and excited) arene acceptors^a

Ground-State Acceptor	E°_{red}	EA	Excited Acceptor ^b	E°_{red}
2,6,9,10-Tetracyanoanthracene	−0.45		2,6,9,10-Tetracyanoanthracene (s)	2.82
9,10-Dicyanoanthracene	−0.98		9,10-Dicyanoanthracene (s)	2.88
1,2,4,5-Tetracyanobenzene	−0.65	1.6	1,2,4,5-Tetracyanobenzene (s)	3.83
1,4-Dinitrobenzene	−0.69	2.00	1,4-Dinitrobenzene (t)	2.6
Picric acid	−0.51		2-Phenylpyrrolinium (s)	2.9

^a E°_{red} in V vs. SCE, EA in eV, data from ref. [4].^b Singlet (s) and triplet (t) states.

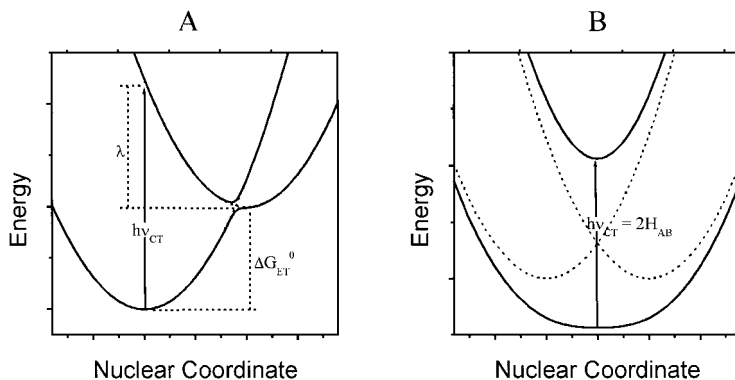


Fig. 1. Optical transitions in charge-transfer complexes in the weak (A) and strong (B) interaction limits.

a significant role, i.e. with mixing coefficients $b \ll a$. The ratios of the mixing coefficients a/b for the no-bond and dative functions are inverted in the excited state. According to Mulliken [9], the optical CT transition ($h\nu_{CT}$) derives from an intracomplex transfer of a single electron from the donor to the acceptor (see Chart 1). As such, the photoexcitation of the CT absorption band of the electrically neutral EDA complex generates the ion-radical pair [25]: $[D, A] \xrightarrow{h\nu_{CT}} [D^+, A^-]$, where the asterisk denotes an electronically and vibrationally excited system. The donor and acceptor components in the Franck–Condon (FC) excited state have the same nuclear coordinates as those in the ground state, and any nuclear relaxation (bond length and angle changes, solvent reorganization, etc.) generates a vibrationally equilibrated excited state. In accordance with Eq. (7), when $H_{DA} \ll \Delta_{DA}$, the energy of the transition is determined primarily by the energy difference of the diabatic states, Δ_{DA} [26], and $h\nu_{CT} \approx \Delta_{DA} = \Delta G_{ET}^0 + \lambda$, as illustrated in Figure 1.

The energy difference ΔG_{ET}^0 between the vibronically equilibrated reactant and product states can be considered as the difference between the IP of the donor and the EA of the acceptor (in the gas phase) or between the corresponding electrochemical potentials (in solution). For a set of structurally related arene donors in the same solvent, a linear (Mulliken) correlation is usually observed experimentally between the donor strength and the CT energy (due to the relatively small changes in λ), i.e.:

$$\text{Mulliken correlation: } h\nu_{CT} = \text{IP} - \text{EA} + \text{constant} \quad (9)$$

Eq. (9) is applicable when a common acceptor is employed [or vice versa for the electron affinities (EA) of a series of acceptors interacting with a common donor], as predicted by Mulliken [9] and as illustrated in Figure 2.

With increasing electronic interaction between the donor and the acceptor, H_{DA} plays a more important role than Δ_{DA} in determining the energy of the CT transition. Such effects are manifested in a deviation of the Mulliken slope from linearity when donors with a wide range of IPs are considered [23b]. (If donors in a narrower IP range are taken, this effect is

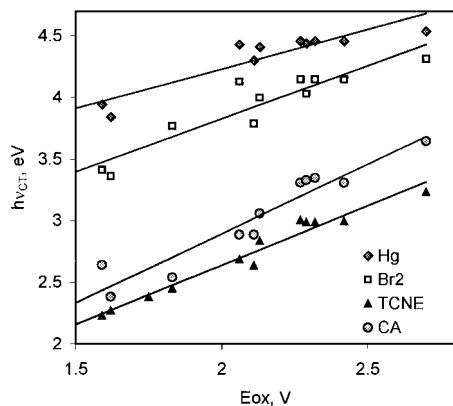


Fig. 2. Mulliken plot for CT complexes of series alkylbenzene donors with different acceptors (acceptors: Hg = $\text{Hg}(\text{O}_2\text{CCF}_3)_2$, Br_2 = bromine, TCNE = tetracyanoethylene, CA = chloroanil). Data from refs. [23a, 23g].

seen as a decrease of the Mulliken slope with increasing values of H_{DA} or acceptor strength [18]). An increased electronic coupling interaction also results in a corresponding increase in the contribution of the dative wavefunction in the CT ground state. Therefore, the mixing coefficient b^2 approaches a^2 , especially for those complexes in which the difference in the redox potentials of the donor and the acceptor is small. Thus, the extent of electron transfer from the donor to the acceptor (which is equal to the difference $a^2 - b^2$) during the photoexcitation becomes smaller. Finally, for strong complexes close to the isergonic point, the absorption is better described as a bonding/antibonding (MO) rather than as a charge-transfer transition.

The spectral behavior of *strong* CT complexes is illustrated by the interaction of the NO^+ cation with a series of arenes. The UV/vis electronic spectra consist of two bands [27, 28], which are assigned to optical transitions from the bonding orbital (high-energy band, $h\nu_{\text{H}}$) and from the arene HOMO (low-energy band, $h\nu_{\text{L}}$) to the antibonding orbital. From the relationship of $h\nu_{\text{H}}$ to the sum of Δ_{DA} and H_{DA} in Eq. (7), it is possible to calculate the electronic coupling elements for a number of complexed arenes (based on $h\nu_{\text{H}}$ and the difference of the arene and nitrosonium potentials $E_{\text{ArH}}^0 - E_{\text{NO}}^0$, taken as Δ_{DA}). Thus, Figure 3C presents a plot of these high H_{DA} values as a function of E_{ox}^0 , with a maximum observed near the isergonic point: $E_{\text{ArH}}^0 \approx E_{\text{NO}}^0 = 1.48$ vs. SCE.

As E_{ArH}^0 approaches the isergonic point, the value of $4H_{\text{DA}}^2$ parallels Δ_{DA}^2 , and their sum remains more or less constant, thus accounting for the invariance of $h\nu_{\text{L}}$ with E_{ArH}^0 . In contrast, the low-energy band ($h\nu_{\text{L}}$) corresponds to the transition from the non-interacting arene orbital to the antibonding MO, and its energy can be written as [28]: $h\nu_{\text{L}} = (\Delta_{\text{DA}}^2 + 4H_{\text{DA}}^2)^{1/2}/2 + \Delta_{\text{DA}}/2$. Since the term $(\Delta_{\text{DA}}^2 + 4H_{\text{DA}}^2)^{1/2}$ is nearly constant for different arenes, the changes in $h\nu_{\text{L}}$ are mainly determined by the $\Delta_{\text{DA}}/2$ term. In other words, $h\nu_{\text{L}}$ decreases linearly with decreasing values of E_{ArH}^0 (Figure 3B).

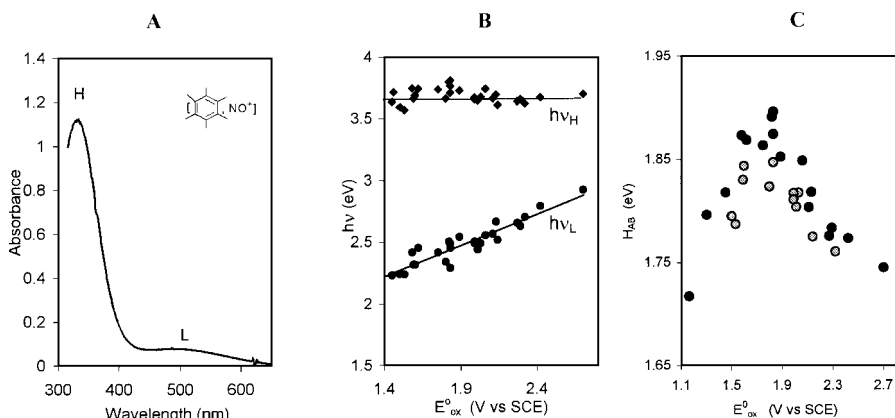


Fig. 3. (A) Typical charge-transfer spectrum of an arene/nitrosonium complex. (B) Variation of the CT transition energy of the high-energy ($h\nu_H$) and low-energy ($h\nu_L$) bands with the oxidation potential of the arene. (C) Dependence of the electronic element H_{AB} (gray points correspond to complexes with sterically hindered donors) on the arene donor strength. Data from ref. [28].

13.2.4

IR Spectroscopic Studies of Charge-Transfer Complexation

The degree of charge transfer in an intermolecular complex is theoretically described as the square of the mixing coefficient. From Eq. (6), together with the normalization $a^2 + b^2 = 1$, we identify the contribution of the dative (D^+ , A^-) state as:

$$b^2 = 1/2 - [1 - 4H_{DA}^2/(\Delta_{DA}^2 + 4H_{DA}^2)]^{1/2}/2 \quad (10)$$

Electron depopulation of the donor and concomitant population of the acceptor in the complex results in a lowering of the vibrational frequencies in the IR spectra of the donor and acceptor moieties. Additionally, complex formation can decrease the symmetry of the donor/acceptor dyad and can lead to increased IR intensity or the appearance of new bands. For example, in halogen/alkylbenzene complexes, the stretching frequencies of the halogens are lowered, as seen in the shift of chlorine band from 557 cm^{-1} in free chlorine to 530 cm^{-1} in the benzene complex, to 527 cm^{-1} in the toluene complex, and to 524 cm^{-1} in the *p*-xylene complex. Increases in the intensity of some of the arene bands are also clearly seen [23b].

In the case of weak complexes with small H_{DA} and/or high Δ_{DA} (large donor/acceptor HOMO-LUMO gap), the value of the charge-transfer contribution, b^2 , is small (e.g. for the benzene complex [BEN, I_2], $b^2 = 0.02$ is determined from the IR band shift [29]). This makes the correlation between the experimental and theoretically predicted values rather unreliable. The most pronounced changes are observed in strong complexes that lie relatively close to the isergonic point, as illustrated by NO^+ /arene complexes. Thus, the N–O stretching frequencies in such complexes approximate that of nitric oxide (1876 cm^{-1}) rather than that of free NO^+ (2272 cm^{-1}), especially in complexes with strong donors such as hexamethylbenzene and pentamethylbenzene [27]. Since the acceptor is a simple diatomic cat-

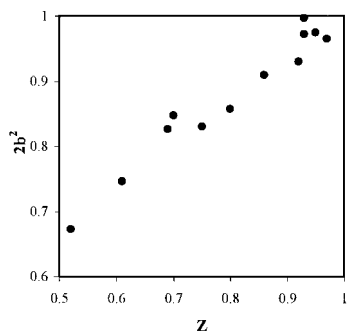


Fig. 4. Correlation of the experimentally determined values of the degrees of charge-transfer (Z) in nitrosonium/arene complexes with the calculated mixing coefficients c_b^2 based on H_{DA} and Δ_{DA} . Data from ref. [28].

ion, the changes in ν_{NO} represent an ambiguous (experimental) measure of the degree of charge transfer (designated as Z) from the aromatic donor to NO^+ [27]:

$$Z = (\nu_{NO^+}^2 - \nu_C^2) / (\nu_{NO^+}^2 - \nu_{NO}^2) \quad (11)$$

where the subscript NO^+ represents the (uncomplexed) cation, C is the complex, and NO the (completely) reduced nitric oxide. Theoretically, the degree of charge transfer can be viewed as the excess charge residing on the NO^+ moiety in the CT complex, $2b^2$ [28]. The calculated values of $2b^2$ based on H_{DA} and Δ_{DA} (obtained from UV/vis and electrochemical data) [28] are plotted against the experimental Z values in Figure 4, and the linear correlation confirms the validity of the CT formalism in correctly predicting the changes in the degree of charge transfer with the arene donor strength.

13.2.5

Thermodynamics of Charge-Transfer Complexation

One of the principal measures of donor/acceptor binding in CT complexes is the formation constant, K_{CT} , which is related to the free energy of complex formation $\Delta G^\circ_{CT} = -2.3RT \log(K_{CT})$. The formation constant is usually determined by absorption spectroscopy, according to the commonly utilized Benesi–Hildebrand treatment [30]. The value of K_{CT} is quantitatively evaluated from the graphical plot of the absorbance change (A_{CT}) as the donor is progressively added to a solution of the acceptor (or vice versa). Relatively strong binding is typically indicated by experimental values of $K_{CT} > 10 \text{ M}^{-1}$. When K_{CT} lies in the range $1 < K_{CT} < 10 \text{ M}^{-1}$, the complex is considered to be weak. Finally, at the limit of very weak donor/acceptor associations with $K_{CT} \ll 1$, the lifetime of the complex can be of the order of that of a molecular collision, and these are referred to as contact CT complexes [24].

The free-energy changes that accompany CT complex formation, ΔG°_{CT} , include several factors, such as electrostatic interactions, entropy changes, etc. In terms of the CT formalism, the energy gain upon complex formation arises from the energy differences of the non-

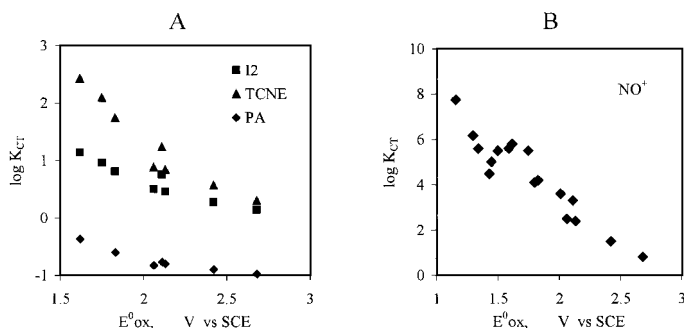


Fig. 5. Typical dependence of the formation constants of arene complexes with different acceptors on the oxidation potential of the arene. Data from refs. [23, 28]. I_2 = iodine, TCNE = tetracyamethylene; PA = picric acid.

interacting donor and acceptor orbitals, and that in the complex and can be expressed as:

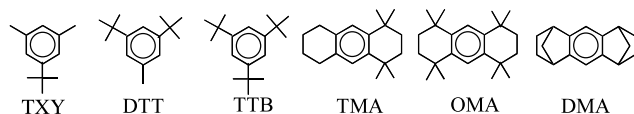
$$\Delta E_{DA} = (\Delta_{DA}^2 + 4H_{DA}^2)^{1/2}/2 - \Delta_{DA}/2 \quad (12)$$

Eq. (12) allows changes in the stability of CT complexes consisting of a single acceptor with a series of similar donors (or vice versa) to be evaluated, since the other factors (e.g. entropy, solvation, etc.), are more or less constant for related aromatic compounds. Eq. (12) can be approximated as $\Delta E = H_{DA}^2/\Delta_{DA}$ when $\Delta_{DA}^2 \gg H_{DA}^2$ for strongly endergonic and/or weakly interacting systems. Arene complexes with bromine and iodine are examples of such systems [23]. Thus, an increase in the donor ability of the arene results in a decrease in Δ_{DA} and an increase in ΔE_{DA} , and a corresponding increase in the formation constants with increasing donor ability of the alkylbenzenes (Figure 5). Similar dependences are observed for arene complexes with other acceptors, as seen in the free energies of complex formation for the CT complexes of different alkylbenzenes with TCNE, chloranil, ICl, and 1,3,5-trinitrobenzene, which are linearly related to those of iodine [23b]. The presence of bulky substituents on the benzene ring, as in encumbered arenes, results in a substantial decrease in the formation constant of the CT complex (Table 3) [31]. As such, steric hindrance inhibits the close approach of the donor to the acceptor to ensure effective orbital interaction, and results in lower H_{DA} values. As can be seen in Table 3, the energy of the CT bands in each series remains roughly constant, which implies that the corresponding Δ_{DA} values are also constant. On the other hand, the H_{DA} value for the complex with mesitylene can be estimated to be ~ 0.4 eV (based on spectral data from Table 3 and $r = 3.5$ Å [31]), while for the mono- and di-*tert*-butyl analogues, H_{DA} is less than 0.25 eV and 0.15 eV, respectively. In other words, steric hindrance (diminishing H_{DA}) is a dominant factor relative to donor strength in determining the changes in Δ_{DA} . As a result, the values of K_{CT} for complex formation of chloranil with mesitylene and durene are substantially higher than that with the more electron-rich hexaethylbenzene [31].

In the limit of strongly coupled complexes close to the isergonic region, $\Delta_{DA}^2 \ll 4H_{DA}^2$, and this approximation leads to the qualitative conclusion that ΔE_{DA} and H_{DA} are strongly

Tab. 3. The effect of steric hindrance on the formation constant for the EDA complexes of chloranil (CA) with alkyl-substituted benzenes^a

Arene donor	$E^\circ_{ox},$ V vs SCE	$K_{CT},$ M^{-1}	$h\nu_{CT},$ eV	$\epsilon_{CT},$ $M^{-1}cm^{-1}$	Arene donor	$E^\circ_{ox},$ V vs SCE	$K_{CT},$ M^{-1}	$h\nu_{CT},$ eV	$\epsilon_{CT},$ $M^{-1}cm^{-1}$
MES	2.11	0.80	2.87	1500	DUR	1.83	1.40	2.61	1600
TXY ^c	2.09	0.29	2.90	650	TMA ^c	1.84	0.36	2.62	300
DTT ^c	2.08	0.18	2.88	240	OMA ^c	1.84	<0.01	b	b
TTB ^c	2.10	<0.01	b	b	DMA ^c	1.51	<0.01	b	b

^a Data from ref. [35].^b No new bands.^c See structure below.

coupled since the stabilization energy of complex formation is largely determined by the donor/acceptor electronic interaction energy $H_{DA} = \int \Psi_D H \Psi_A$. Such a conclusion predicts that the electronic exchange (H_{DA}) between the donor and acceptor orbitals in the CT complex should play a major role in the experimental free-energy change (ΔG_{CT}), and this is confirmed experimentally by the close relationship between the relative stability of the CT complexes and the electronic interaction term H_{DA} in the case of strongly coupled $[ArH, NO^+]$ complexes [28]. Furthermore, the changes in ΔG_{CT}° in such a series are determined by the second term, $\Delta_{DA}/2$, since the first term in Eq. (12) is nearly constant for NO^+ complexes with the series of alkylbenzenes. This explains the experimental observation of the linear dependency of ΔG_{CT}° on E°_{red} [28], which is qualitatively similar to that observed for weak complexes (Figure 5).

Consideration of the spectral and thermodynamic properties of arene CT complexes thus indicates that they are reasonably described within the framework of recent developments of the Mulliken formalism, in the case of both weak and strong complexes in the highly endergonic and nearly isergonic regions. Accordingly, let us now consider the structural consequences attendant upon charge transfer from the donor to the acceptor in such complexes.

13.3

Structural Features of Arene Charge-Transfer Complexes

The donor/acceptor properties and the electronic coupling interactions determine the redistribution of electron density between the aromatic donor and the electron acceptor upon complexation. Significant changes in structure and reactivity of the coordinated arene can be rationalized in terms of spectral and thermodynamic properties within the framework of the CT formalism. This section is devoted to a consideration of the structural effects of arene coordination (in terms of donor/acceptor bond distance and type of bonding, distortion of arene planarity, expansion of the aromatic ring, and π -bond localization).

13.3.1

Bonding Distance of the Donor/Acceptor Dyad in Arene Complexes

The bond distance is the most commonly used measure to gauge the strength of intra- or intermolecular bonds between two nuclei. In the case of intermolecular CT complexes, the donor/acceptor separation is determined by the balance between the HOMO-LUMO (bonding) electronic interaction and the repulsion of filled orbitals. Strong CT interactions can result in significant bond shortening relative to the separation determined by the purely van der Waals contact. For example, the interplanar distance of $d = 3.42 \text{ \AA}$ between hexamethylbenzene and chloranil in their mixed-stack CT crystals is shortened by 0.2 \AA compared to the intermolecular distance $d = 3.62 \text{ \AA}$ in pure crystals of hexamethylbenzene [2]. The intermolecular separation of bromine from the ring plane of benzene in the 1:1 complex is 0.5 \AA shorter than that predicted from the van der Waals radii [32, 33]. Even greater shortening (of about 1 \AA) of the donor/acceptor separation relative to the sum of the van der Waals radii is observed in strongly coupled complexes of alkyl-substituted benzenes with NO^+ , in which the distance between the nitrogen atom and the aromatic ring is $\sim 2.1 \text{ \AA}$ [28].

In different types of complexes, the shortening of the donor/acceptor separation with increasing donor ability of the arene (due to enhancement of the $H_{\text{DA}}/\Delta_{\text{DA}}$ ratio) determines the gain in energy upon complex formation. Thus, the distance between gallium and the aromatic ring in $[\text{ArH}, \text{Ga}^+]$ complexes varies from $d = 2.76 \text{ \AA}$ for benzene to $d = 2.42 \text{ \AA}$ for the hexamethylbenzene complex. A similar trend is observed in π -complexes of transition metals. For example, in the 1:1 complexes of arenes with niobium(0), the Nb/ArH distance is decreased by 0.01 \AA from $d = 1.860 \text{ \AA}$ in the toluene to $d = 1.850 \text{ \AA}$ in the mesitylene complex, as the arene donor strength is increased. Similar effects are observed when arene complexes with metals of different acceptor strengths are compared. For example, the distance between the arene ligand and the chromium center is reduced by 0.015 \AA in the benzene complex $[(\text{BEN})_2\text{Cr}^{\text{I}}]\text{Br}$ ($d = 1.597 \text{ \AA}$), as compared to the corresponding $[(\text{BEN})_2\text{Cr}^0]$ complexes with $d = 1.612 \text{ \AA}$ [2].

The balance between van der Waals repulsion and electronic coupling depends on the stereochemistry. Thus, in complexes of chloranil and TCNE with encumbered hexaalkyl-substituted benzenes (such as hexaethylbenzene and its multiply annulated analogues), the interplanar distance is larger [31], and H_{DA} and K_{CT} are lower, than those in the corresponding complexes with mesitylene and durene, in spite of the weaker donor ability of the latter. On the other hand, sterically encumbered donors with van der Waals cavities of sufficient size can allow small acceptors such as the NO^+ cation to closely approach the benzenoid ring. The distance between the nitrogen atom and the arene ring in nitrosonium complexes with hexaethylbenzene (2.08 \AA) is nearly the same as that in the hexamethylbenzene complex (2.09 \AA) [28], and values of H_{DA} and K_{CT} for the complexes with hindered donors are only slightly lower than those for complexes with relatively unhindered analogues [28].

Organic ligands in transition metal complexes frequently penetrate the coordination sphere of the d-metal to such an extent that the ligand-to-ligand distance is less than the sum of the van der Waals radii. In such cases, steric repulsion between ligands can overcompensate the distance-shortening effects of charge transfer, and eventually cause an increase in the arene-metal distance as the donicity of the arene ligand increases. For exam-

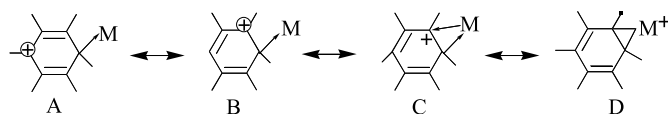
ple, the Ru^{2+} –arene distance in the bis(benzene) complex (1.713 Å) is shorter than that in the corresponding bis(mesitylene) complex ($d = 1.726$ Å) [2].

13.3.2

Relationship Between Hapticity and Charge Transfer in Arene Complexes

Topological classification of metal–arene complexes in terms of hapticity was originally proposed by Cotton [35] as the basis for distinguishing organometallic complexes and their chemistry, but it was never intended to characterize the chemical bonding between the metal and the ligand. As a ligand, benzene has six carbons and six π -electrons accessible for metal coordination and bond formation. The vast majority of metal/arene complexes exhibit η^6 -coordination with equal metal–carbon distances and equal contributions of all π -orbitals to the coordination bonding [2]. In contrast, arene ligands of lower hapticity exhibit aromatic π -orbitals that are no longer equivalent. As a consequence, the orbital symmetry of the benzene ring is distorted up to the point of complete loss of aromaticity, and the arene ligands become quite reactive. As such, η^1 - and η^2 -complexes represent the most interesting substrates for the study of metal–ligand bonding, exhibiting the most pronounced charge-transfer effects, although such reactive complexes are difficult to isolate for X-ray crystallographic analysis [2].

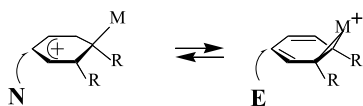
In spite of the large difference between the η^1 - and η^2 -complexes from a structural point of view, their electronic configurations are closely related since two electrons are involved in the coordination bond in both types of complexes. The resonance structure C betrays the facile interconversion between these coordination types [2], i.e.:



Scheme 1

η^1 -Coordination leads to polarization of the π -electrons of the aromatic ligand, whereas η^2 -coordination does not necessarily lead to a polar electronic configuration. Because polarized structures are expected to predominate in the complexes containing metal and arene ligands of very different donor/acceptor strengths, the coordination type depends strongly on the relative donor/acceptor strengths of the arene ligand and the metal center. The transition from η^2 - to η^1 -coordination with increasing acceptor strength is observed in the series of arene complexes with different organic, inorganic, and organometallic acceptors. For example, the molecular complex between durene and CBr_4 as the σ -acceptor features a bridging bromine between neighboring ring carbons of the durene, with carbon–bromine distances of 3.26 and 3.34 Å. Moreover, in most Ag^I complexes with arenes, the Ag^I lies in a bridging position between two carbon atoms with equal C– Ag^I distances of about 2.5 Å. Moderately stronger acceptors such as Cu^I , Ni^0 , Hg^{II} , etc. still prefer η^2 -coordination. For example, in $\mu\text{-}\eta^2$ Ni^0/BEN , Cu^+/BEN , and $\text{Hg}^{2+}/\text{HMB}$ complexes, the distances between the bridging

metals and the closest carbon atom in the aromatic ring are 2.005 and 2.021 Å (to Ni⁰), 2.081 and 2.105 Å (to Cu^I), and 2.56 and 2.58 Å (to Hg^{II}). In contrast, strong electron acceptors such as Al(C₆F₅)₃, SiEt₃⁺, Br⁺, and Cl⁺ form exclusively η^1 -coordinated arene complexes. Similarly, strong organometallic acceptors such as perfluoroaryl-coordinated Pd^{II} or Pt^{II} form mostly η^1 -complexes, while, in similar complexes, the weaker Mo(CO)₃ acceptor shows a clear indication of η^2 -coordination with Mo–C distances of 2.776(4) and 2.840(4) Å for *ipso*- and *ortho*-coordination, respectively. A similar dependence of coordination type on the relative donor/acceptor strengths is observed for a variety of complexes. For example, bivalent d-metals from Cr^{II} to Ni^{II} show η^1 -coordination with the mesitylene group, while Re^I, Rh^I, Ir^I, and Ni⁰ form η^2 -coordinated complexes with the electron-acceptor hexafluorobenzene acting as Lewis base. In many cases, η^1 - and η^2 -coordinated isomers can be very close in energy, and thus exhibit fast rates of η^1 - η^2 interconversion in solution, which can be shifted by changing the relative donor–acceptor strengths of the complex. Dual arene reactivity toward both electrophiles as well as nucleophiles is possible. Thus, the more polarized η^1 -isomer with a positive charge residing on the benzene ring shows enhanced reactivity toward nucleophiles, while the η^2 -isomer exhibits high electron density at localized double bonds and is thus susceptible to electrophilic attack [2].



Scheme 2

13.3.3

Effect of Charge Transfer on the Structural Features of Coordinated Arenes

13.3.3.1 Expansion of the Arene Ring

In the framework of MO theory, both electron detachment from the benzene (π -bonding) HOMO and the addition of an electron to the (π^* -antibonding) benzene LUMO will lead to a decrease in the average bond order in the arene due to loss (or annihilation) of one bonding electron. Consistent with Pauling's direct relationship between bond order and bond length [35], expansion of the arene ring is observed both when the arene acts as an electron donor (and suffers from electron deficiency) or is an electron acceptor (with partial population of the antibonding orbital). However, the changes in the benzene bond lengths upon one-electron oxidation or reduction are calculated to be only about 0.01 Å due to the involvement of six C–C bonds with twelve π -bonding electrons [2]. Therefore, the vast majority of organometallic structures are not suitable models for detecting electron deficiencies or partial cation-radical character in an arene ligand. However, recent advances in the use of low-temperature X-ray diffractometers (with up to 0.001 Å precision) have enabled neutral arenes and their cation (anion) radicals to be distinguished on the basis of differences in their average C–C bond distances. Highly precise X-ray structures clearly reveal significant ex-

pansions of the aromatic rings in arene complexes with inorganic acceptors that show substantial degrees of charge transfer. For example, the average bond length (d_{av}) in crystalline complexes of hexamethylbenzene with the NO^+ cation is 1.417(2) Å, as compared to 1.411(2) Å in the uncomplexed donor. A similar ring expansion with $d_{av} = 1.417(2)$ Å is found for CT complexes of hexamethylbenzene with SbCl_3 [2].

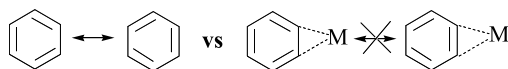
The degree of charge transfer upon complexation, as is apparent from Eq. (10), is related to the relative donor/acceptors strengths of the reagents and their electronic coupling element. In contrast to the (strongly coupled) alkylbenzene complexes with nitrosonium ion, much lower degrees of charge transfer can be expected in complexes with weaker organic acceptors. Furthermore, van der Waals repulsion does not allow two relatively bulky organic molecules to approach each other to within less than $\sim 3.0\text{--}3.5$ Å, and therefore H_{DA} cannot be very high. As a consequence, ring expansion can hardly be detected in most of these CT complexes. (Even with a precision of 0.002 Å, X-ray crystallography does not allow a degree of charge transfer in arenes of less than 10 % to be detected). The hexamethylbenzene/chloranil complex incorporates an arene moiety with $d_{av} = 1.409(2)$ Å [2].

Many organometallic complexes with arene ligands can show degrees of ring expansion that widely exceed those for organic and inorganic acceptors. An average C–C bond length of 1.422 Å is measured for the $[(\text{HMB})\text{TiCl}_3]\text{AlCl}_4$ and $[(\text{HMB})\text{Mn}(\text{CO})_2\text{Cl}]$ complexes. Similarly, $[(\text{HMB})\text{Cr}(\text{CO})_3]$ and $[(\text{HMB})_2\text{Fe}][\text{C}(\text{CN})_3]_2$ show significant ring expansions in the hexamethylbenzene ligand ($d_{av} = 1.423$ Å in both cases) [2]. Extreme bond elongations to $d_{av} = 1.429$ Å and 1.430 Å are found in two symmetrically independent molecules of the ruthenium complex $[(\text{HMB})\text{RuCl}_2(\text{py})]$ [2]. According to Pauling [35b], such long bond distances reveal a charge transfer of approximately 1.4 electrons between the hexamethylbenzene ligand and the metal center [2]. Such a significant redistribution of charge leading to a substantial electron deficiency in the arene ligand is expected to have striking consequences on the reactivity of the metal-coordinated arene up to the point of complete electrophilic/nucleophilic umpolung of its substitution behavior.

13.3.3.2 π -Bond Localization in the Arene Ring

Localization of π -bonds (also termed “double-bond fixation”) is an important structural feature frequently observed upon arene coordination to a metal center. To rationalize this effect, the formation of covalent (σ) bonds between the metal and particular carbon atoms of the arene ring is commonly invoked. However, this cannot explain all the unusual bond distances observed and is not generally applicable to the analogous findings with organic acceptors. Analysis based on the CT concept allows a comparative treatment of all types of donor/acceptor complexes, and predicts a close relationship between the degree of bond localization and the donor/acceptor strengths of the complexed partners.

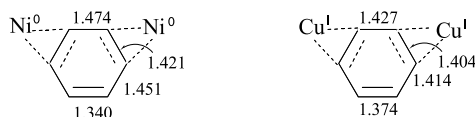
The most pronounced effect of bond localization is observed in the η^2 -complexes due to a loss of equivalence of the mesomeric structures in the benzene ring, i.e.:



Scheme 3

However, η^2 -coordination alone does not result in any degradation of the delocalized electronic configuration, and the above model involves bond localization only in the case of a significant degree of charge transfer between the aromatic ligand and the metal center. For example, in very weak [DUR, CBr₄] and [BEN, Ag⁺]ClO₄[−] complexes, very low degrees of charge transfer occur, and only subtle changes in the geometry (i.e. double-bond localization, and sp²/sp³ rehybridization) of the arene can be detected. Additionally, a bridging arene positioned between two acceptors is frequently observed, which leads to $\mu\text{-}\eta^2(1,2):(4,5)$ complexes. In these complexes, the two metal centers induce opposite changes in the geometry of the benzene ring, which annihilate each other. Stronger metal acceptors (e.g. Mo⁰ and Pt^{II}) more clearly promote the formation of localized double bonds in the η^2 -coordinated benzene ring. Bond contraction of two non-coordinated π -bonds to lengths of just 1.37 Å and 1.35 Å was found in substituted benzene ligands coordinated to Mo⁰ and Pt^{II}, respectively. These distances correspond to bond orders of 1.7 and 1.9. When stronger arene donors, such as naphthalene or anthracene, are coordinated to Ru^I or Ni⁰ centers, the non-coordinated C(α)–C(β) bond clearly approaches the standard value of 1.34 Å for a normal C=C double bond [2].

Localized double bonds, in turn, represent attractive targets for further attack by a second electrophilic center, which explains the frequent observation of $\mu\text{-}\eta^2(1,2):\eta^2(3,4)$ complexes. Such (1,2):(3,4) coordination results in cumulative effects on the geometry of the benzene ring and the strength of the metal–carbon bond (as opposed to an annihilative effect in the (1,2):(4,5) compounds mentioned above). For example, $\mu\text{-}\eta^2(1,2):\eta^2(3,4)$ coordination in the Ni⁰ complex leads to M–C bonds that are close in length to a single σ -bond [2]. It should be noted that such an effect involving the relocation of roughly 0.5 electrons within the aromatic ring is connected with the acceptor strength of nickel, since the bond-length distribution in the isoelectronic copper complex is quite different [2].



Scheme 4

In most η^1 - and η^2 -coordinated complexes, the arene ligand acts as the Lewis base and electron donor, whereas the metal center acts as the Lewis acid and electron acceptor. Thus, a (formal) two-electron donation and (actual) charge transfer occurs in the same direction from the arene to the metal. However, when the acceptor strength of the arene is higher than that of the metal, coordination and charge transfer occur in opposite directions. For example, hexafluorobenzene donates two electrons in coordinating to a metal center. However, its complexes with metals having medium donor/acceptor properties (e.g. Rh^I, Ni⁰, Re^I, Ir^I) exhibit substantial (back-) charge transfer from the metal to the arene that strengthens the bonding in these $\sigma(\eta^2)$ -complexes. As the result, the arene ligand shows a clear cyclohexadienyl structure, the fluorine atoms at the *ipso* carbons deviate from the plane of the ring by as much as 48°, and the metal–carbon bonds are even shorter than those of

standard $M-C(sp^3)$ bonds (as expected for a strained three-membered metal-carbon ring system) [2].

13.3.3.3 Loss of Planarity of the Arene Ring and the Transition from π - to σ -Binding

The planar structure of the six-carbon ring is a general characteristic of undistorted aromatic donors, and any loss of planarity due to either substituents or a folding of the six-carbon ring disrupts the aromaticity.

Bending of an *ipso* substituent out of the aromatic plane occurs in parallel with the interchange from π - to σ -bonding, and is observed in different types of arene complexes with various organic, inorganic, and organometallic acceptors. This results in a significant variation in chemical reactivity. Generally, the $\pi \rightarrow \sigma$ transition occurs with increasing acceptor strength. It results in a positive charge on the aromatic ring when accompanied by complete charge transfer from the aromatic ring to the Lewis acid. For example, in weak π -complexes of Ag^I with arenes, no deviation of the *ipso* substituents out of the plane is observed (bending angle $\alpha \approx 0$) [2]. Complexes of Cu^I , $SiEt_3^+$, and $Al(C_6F_5)_3$ show small deviation angles of $\alpha = 7, 8$, and 9° respectively, which are symptomatic of an increase in the σ -character in the coordination. Bending angles of $\alpha = 42$ and 55° have been determined by X-ray crystallographic studies of crystalline σ -complexes of Br^+ and Cl^+ with hexamethylbenzene [36]. Such a continuous transition from σ - to π -bonded complexes is presented in Figure 6.

From analysis of structural data for a wide range of donor/acceptor interactions between Lewis acids and arenes [2] (from the weak π -complexes of Ag^I , Cu^I , Ni^{II} , and Al^{III} , to stronger π -complexes with Co^{II} , Si^{IV} , and Cr^{II} , to intermediate (π/σ) complexes of Pt^{II} , and to pure σ -complexes with Br^+ and heptamethylbenzenium), it can be concluded that the transition from π - to σ -coordination in η^1 -complexes is accompanied by several effects: (i) a shortening of the distance between the Lewis acid and *ipso*-carbon atom of the arene from a van der Waals contact to a *bona fide* covalent bond; (ii) deviation of the *ipso*-substituent out of

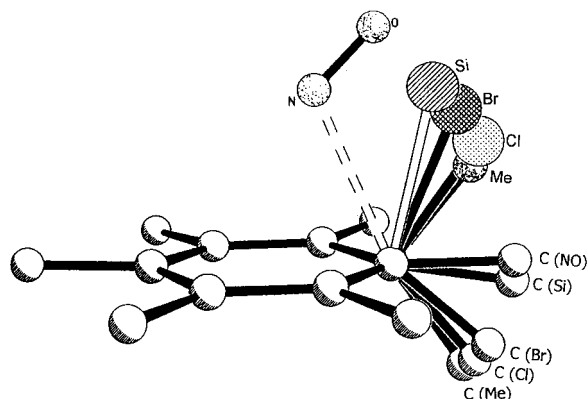
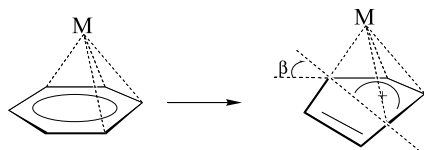


Fig. 6. Superposition of the X-ray structures of hexamethylbenzene σ -complexes with various electrophiles (as indicated) showing the continuous transition from the heptamethylbenzenium σ -complex to the hexamethylbenzene/nitrosonium π -complex. Data from ref. [36].

the plane of the aromatic ring (due to a transition from sp^2 to sp^3 hybridization); (iii) redistribution of the bond lengths in the benzene ring, i.e. elongation of the 1,2-bond to the standard distance of 1.50 Å for a $C(sp^2)-C(sp^3)$ single bond and partial localization of the 2,3-double bond, and (iv) an increase in the degree of charge transfer, as in the chloronium and bromonium complexes with hexamethylbenzene, in which the positive charge of the inorganic component is completely transferred to the arene.

Similar effects are observed in η^2 -complexes; Ag^I and Hg^{II} coordinated to arenes exhibit bending angles of $\alpha \approx 5^\circ$ (which is symptomatic of high π -character of the complex and a low degree of CT). On the other hand, in rhenium, rhodium, iridium, and nickel complexes, arenes exhibit bending angles of up to 45° [2].

In its extreme case, the CT interaction in arene/metal complexes also affects the planarity of the arene ring itself. Various degrees of ring folding are observed in η^4 -coordinated complexes of benzene with metal centers, ranging from folding angles of $\beta = 0^\circ$ in alkaline metal salts, to $\beta = 15^\circ$ in lanthanide complexes, and to $\beta = 30-35^\circ$ in the early transition metal complexes (e.g. with titanium, zirconium). The highest degree of folding is found in the iron and ruthenium complexes ($\beta = 40^\circ$). Interestingly, arene complexes with late transition metals such as cobalt ($\beta = 35^\circ$) and nickel ($\beta = 20-25^\circ$) show lower folding angles [2].



Scheme 5

In most η^6 -coordinated d-metal complexes, the six-carbon ring of benzene remains more or less planar, and its distortion is only manifested in the various degrees of bending of the substituents out of the ring plane. However, significant folding of the arene ring to a boat shape is observed in complexes of benzene with tantalum. Interestingly, the degree of folding depends on the oxidation state of the metal: 20° for Ta^{II} and 25° for Ta^{III} complexes [2]. The better acceptor, Ta^{III} , induces a stronger folding due to a greater degree of charge transfer from the benzene to the tantalum center, and consequently a higher degree of σ -character in the arene–metal bond.

13.4

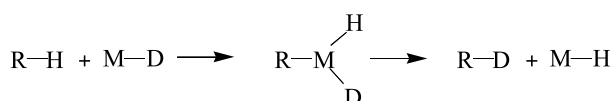
Charge-Transfer Activation of Coordinated Arenes

Redistribution of electron density in CT complexes results in a modification of the chemical properties of coordinated arenes, and this effect is widely used in organometallic catalysis [2]. To demonstrate the relationship between charge transfer in arene complexes and their reactivity, we focus our attention on carbon–hydrogen bond activation, nucleophilic/electrophilic umpolung, and the donor/acceptor properties of arenes in a wide variety of organometallic reactions.

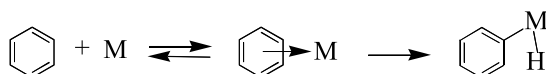
13.4.1

Carbon–Hydrogen Bond Activation

Arene C–H bond activation by transition metal derivatives has been utilized for a variety of chemical transformations, including H/D exchange and various substitution reactions, such as silylation, carboxylation, phenylimine formation, etc. These reactions may occur by direct coupling of the aryl ligand and the substituent when both are attached to the metal center, or by insertion of functional groups into the metal–carbon bond of the arene ligand [2]. The C–H bond activation in aromatic compounds has been frequently compared with metal-catalyzed activation of hydrogen leading to H/D exchange with metal deuterides (M–D), i.e.:

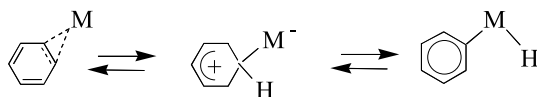
**Scheme 6**

However, this simple model does not explain the (kinetically) enhanced reactivity of arenes relative to alkanes, considering the higher ($D_{\text{C-H}}$) bond energy of arenes, i.e. $D_{\text{C-H, benzene}} = 111 \text{ kcal mol}^{-1}$ vs. $D_{\text{C-H, alkane}} \approx 95 \text{ kcal mol}^{-1}$. Many more examples of metal-activated cleavage of C–H bonds are known for aromatic compounds than for alkanes [37]. To account for this difference, arene/metal coordination is proposed [38], although experimental evidence for such intermediate complexes and their structural features is lacking.

**Scheme 7**

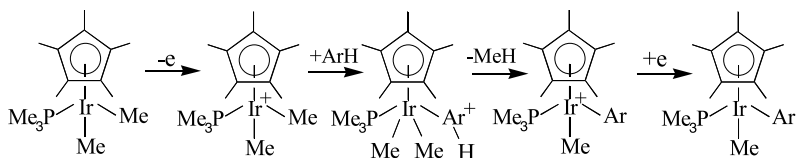
The first instance of metal/arene $\pi(\eta^2)$ -coordination prior to C–H bond activation was observed for the rhodium complex $\text{Cp}^*\text{Rh}(\text{PMe}_3)(\text{H})(\text{C}_6\text{H}_5)$ by ^1H NMR spectroscopic measurement of benzene/toluene exchange and reversible interconversion of *para*- and *meta*-tolyl isomers [34]. The observation of an equilibrium between the rhodium η^2 -complexes with polycyclic arenes and the corresponding (η^1) aryl hydrido metal complexes (which can be tuned by variation of the arene, the metal center, and other metal ligands [2]) supports the pre-equilibrium complexation of arene and metal centers as a prerequisite for C–H bond activation. However, a lack of understanding still persists regarding the mechanism of the interconversion η^2 -coordinated π -complexes and aryl hydrido σ -complexes, which formally represents a hydrogen-atom transfer between two tautomeric structures. Insight into this mechanism can be gained using the established CT character of the metal–arene bond. Thus, a two-step process can be conceived involving an initial charge transfer from the π -

ligated arene to the metal center resulting in the formation of the σ -complex with delocalized positive charge on the arene ring, which then readily transfers a proton to the electron-rich metal center.



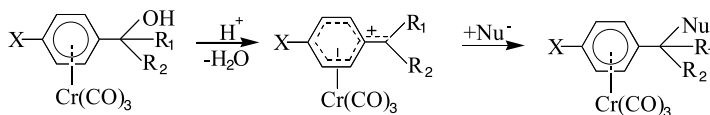
Scheme 8

An interesting example of C–H bond activation is the ferrocenium (1e-oxidant) catalysis of monomethylaryliridium complexes [39], in which the oxidized (17-electron) iridium complex is coordinated to the arene substrate in a $\pi(\eta^2)$ fashion. Complete charge transfer from the arene to the metal (strong acceptor) takes place upon coordination and results in the formation of the σ -arenium complex. The latter can readily transfer a proton to a methyl ligand to yield methane and the oxidized monomethyl complex, which is finally reduced by the original dimethyliridium complex to complete the ET chain process [39]:



Scheme 9

Coordination to transition metals activates benzylic as well as aromatic centers, which become targets for either nucleophilic or electrophilic attack [2]. For example, under acidic conditions, a carbocation is generated, which can then react with a nucleophile, i.e.:

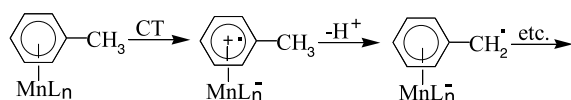


Scheme 10

Coordination to a $\text{Cr}(\text{CO})_3$ center results in substantial stabilization of the carbocation, which is commonly explained either in terms of interaction of the filled d-orbitals of chromium with the empty p-orbital of the benzylic carbon or by chromium (η^7)-coordination of the entire benzylic moiety (with a delocalized positive charge and partial double-bond character of the exocyclic C–C bond) [2]. Both representations are based on the prediction that

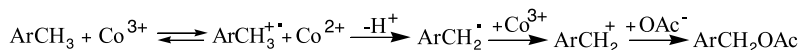
the $\text{Cr}(\text{CO})_3$ group acts as an electron donor in its interaction with a benzylic (carbocationic) acceptor.

Since benzylic hydrogens in $(\text{arene})\text{Cr}(\text{CO})_3$ complexes are more acidic than those in the corresponding free arene, the $\text{Cr}(\text{CO})_3$ group is frequently considered to be an electron acceptor capable of stabilizing carbanions [2] (which can then be trapped by various electrophiles). Such an effect is commonly explained as the stabilizing effect induced by the delocalization of the negative charge onto the chromium moiety [2], i.e. the $\text{Cr}(\text{CO})_3$ group acts as an electron acceptor, and complete CT generates an exocyclic double bond and a negatively charged η^5 -coordinated chromium center. Enhanced rates of deprotonation of benzylic hydrogen have also been found in η^6 -coordinated $\text{Mn}(\text{CO})_3^+$ and FeCp^+ complexes, as well as in η^2 -coordinated Os^{II} complexes. Based on the enhanced acidity of benzylic centers in aromatic cation radicals [40], a CT scheme can be formulated [2]. In the extreme case, this considers a complete electron transfer from the arene to the metal acceptor, resulting in the formation of a cation-radical ligand, which is readily deprotonated at the benzylic position



Scheme 11

This reaction scheme is applicable to C–H bond activation by strong electron acceptors. For example, the formation of benzyl acetate from toluene using Co^{III} as the oxidant has been shown to occur via the toluene cation radical [41]:



Scheme 12

The ET mechanism is proposed on the basis of the high value of $\rho = -2.4$ obtained from the Hammett plot, as well as the observation of benzyl chloride and chlorotoluene as the main products when the oxidation is carried out in the presence of high concentrations of LiCl [41]. Similarly, activation of benzylic C–H bonds by other strong oxidants such as Mn^{III} or Pb^{IV} has been suggested to occur through an initial electron transfer, especially in the case of aromatic substrates with low ionization potentials [42]. However, there have been no reports of complex formation between the metal and the arene prior to ET, and no such reactive complex has been isolated and characterized by X-ray crystallography.

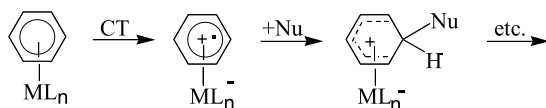
13.4.2

Nucleophilic/Electrophilic Umpolung

The majority of arene functionalizations are based on electrophilic aromatic substitution, i.e. the electron-rich π -system of the arene acts as the Lewis base and is readily attacked by elec-

trophiles (or Lewis acids) such as the cationic nitronium and halonium acceptors [43]. Owing to the electron-rich character of arenes, nucleophilic substitution is generally not favored, but it can be achieved by attaching both electron-withdrawing substituents (such as nitro, cyano, etc.) and good leaving groups (such as chloro, sulfonato, etc.) to the arene substrate [44]. The simultaneous presence of both types of groups promotes nucleophilic substitution according to an addition/elimination mechanism, whereby the electron-withdrawing substituents induce electron deficiency in the aromatic ring to such a degree that addition of the nucleophile becomes feasible.

Activation of an aromatic substrate to nucleophilic addition can also be achieved by coordination of the arene ring to an electron-withdrawing metal center. Moreover, arene/metal complexes can be more effective because: (i) the donor/acceptor properties of the metal complexes can be varied to a much greater extent than those of organic substituents, and (ii) nucleophilic substitution may be carried out with a wide variety of arenes and is not limited to just those bearing electron-withdrawing substituents. Analysis of the reactivity data of coordinated arenes towards nucleophiles in a variety of organometallic complexes indicates that the nucleophile/electrophile umpolung of the metal-ligated arenes can be readily explained in terms of a strong CT interaction between the arene and the metal. This is best demonstrated in the extreme case of complete electron transfer from the arene to the metal center, which leads to an aromatic cation radical that readily reacts with variety of nucleophiles [2], e.g.:

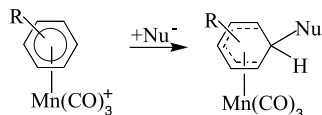


Scheme 13

Such a charge transfer from the ligated arene can lead to: (a) nucleophilic addition or substitution, (b) electron transfer, and (c) proton elimination/transfer, thus revealing the close relationship between all of these processes. The reactivity of the arene ligands towards nucleophiles in (arene) ML_n complexes depends on the electrophilicity of the metal fragments $[ML_n]$, this increasing in the order $[Cr(CO)_3] < [Mo(CO)_3] \ll [FeCp]^+ < [Mn(CO)_3]^+$ [2]. For example, in (arene) $FeCp^+$, which is widely used for synthetic purposes, a chloro or nitro substituent on the arene is readily substituted by such nucleophiles as amides, enolates, thiolates, alkoxides, and carbanions [45].

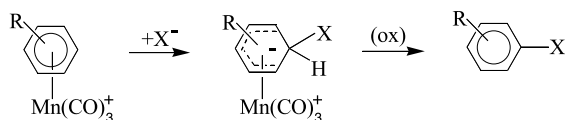
It is generally accepted that the addition of the nucleophile occurs initially at a position *ortho* to the leaving group. In fact, in the reaction of $[(C_6H_5Cl)FeCp]^+$ with relatively stable carbanions such as $CH(COR)_2^-$, the *ortho* adduct can be isolated [46]. Subsequent migration of the nucleophile can result in formation of the *ipso* adduct, which then loses chloride [46c]. Analogous reaction mechanisms have been formulated for substitution reactions involving (arene) $Cr(CO)_3$ and (arene) $Mn(CO)_3^+$ complexes. In such a way, $[(C_6H_5X)Cr(CO)_3]$ ($X = Cl, F$) reacts with carbanions, amines, and thiolates [2, 47]. The use of organometallic nucleophiles such as carbonylmetallates $M(CO)_n^-$ ($M = Fe, W$, etc.) leads to bimetallic complexes [2].

Synthetically useful reactions of (arene) $\text{Mn}(\text{CO})_3^+$ complexes with such nucleophiles as methoxide, benzenethiolate, azide, various amines, and anilines are also noteworthy. These complexes have also been extensively studied with regard to nucleophilic addition reactions resulting in thermally stable cyclohexadienyl complexes [2].



Scheme 14

Grignard reagents and enolates are especially suitable for such nucleophilic additions. The resulting products are of synthetic interest since oxidation leads to rapid release of the metal group, and the free, functionalized arenes are readily obtained:



Scheme 15

Here, either $\text{X} = (\text{H}_2\text{C}(\text{O})\text{-R}')^-$ and $\text{ox} = \text{Jones' reagent}$ or $\text{X} = \text{CN}^-$ and $\text{ox} = \text{Ce}^{\text{IV}}$. It has been emphasized that the addition of nucleophiles to (arene) $\text{Mn}(\text{CO})_3^+$ complexes does not occur through an initial ET from the nucleophile to the metal center [2]. This represents an additional advantage since such redox reactions frequently lead to the decomposition of the metal complex, a typical example being the reductive deligation of bis(arene) Fe^{2+} complexes [48]. On the other hand, intramolecular charge transfer from the arene to the metal not only induces an electron deficiency in the arene ring (which is critical for effective attack of the nucleophile), but it also results in an attenuation of the electrophilicity of the metal center so as to avoid undesired ET reactions of the metal with the nucleophile.

13.4.3

Modification of the Donor/Acceptor Properties of Coordinated Arene Ligands

Charge redistribution between the arene and the acceptor moiety upon complexation results in significant changes in their donor/acceptor properties. For example, charge transfer from an arene to an acceptor converts the aromatic compound from an electron-rich donor to an electron-poor acceptor. Furthermore, the complete charge transfer from hexamethylbenzene to the bromonium ion upon formation of the bromoarene σ -complex leads to a delocalized positive charge on the arene ring. As a result, such positively charged σ -complexes readily react with a variety of nucleophiles and can be stabilized and crystallized only in the presence of such anions as SbCl_6^- and PF_6^- or similar (very weakly nucleophilic) counter-

anions. However, X-ray crystallographic studies clearly reveal that even such weak nucleophiles exhibit strong interactions with the positively charged arenium σ -complex, as evidenced by unusually short intermolecular distances. In crystalline complexes of bromohexamethylbenzenium hexafluoroantimonate, there is a close contact between a fluorine and the carbon atom in the position *para* to the bromine atom, with a shortened F–C distance of 3.066 Å, as compared to the sum of the van der Waals radii of 3.17 Å [2]. In these crystals, the fluorine atoms of hexafluoroantimonate act as electron donors that bond to a positively charged hexamethylbenzene moiety.

Similar structural effects are known with organometallic complexes. Thus, upon coordination to a strong acceptor, the donor ability of hexamethylbenzene is attenuated, and it will then be capable of forming CT complexes with other (even weaker) donors. For example, the hexafluorophosphate salt of [(HMB)₂, Fe^{II}] forms complexes with durene, as established by the observation of new CT absorption bands [2]. The crystal structure of the complex shows alternating stacks of durene with [(HMB)₂, Fe^{II}], in which the interplanar distance between durene and hexamethylbenzene is $d = 3.65$ Å. This close separation and the absorption spectrum of the complex point to substantial CT interactions between durene as the donor and hexamethylbenzene, which acts as an acceptor owing to its high electron deficiency induced by coordination to the electron-poor iron(II) center.

Complete electron transfer from arenes results in aromatic cation radicals, which differ dramatically in their donor/acceptor properties. As such, cation radicals can interact with the parent donor. The resulting (CT) interaction accounts for the self-association (π -dimerization) of aromatic donors with their corresponding cation radicals and results in the formation of charge-resonance (CR) complexes or π -mers [49].



Scheme 16

Analogous processes also occur between arenes and their anion radicals.

The formation of ion-radical dimers (π -mers) in solution can be identified spectroscopically by a new broad (CR) absorption band in the NIR region that is absent in the spectrum of either the neutral arene or its ion-radical component (Table 4) [49]. For different aromatic

Tab. 4. Electronic spectra of various (monomer and dimer) cation radicals^a

Arene donor (ArH)	Absorption band, λ (nm)		Arene donor (ArH)	Absorption band, λ (nm)	
	monomer ArH ⁺	dimer ^b (ArH) ₂ ⁺		monomer ArH ⁺	dimer ^b (ArH) ₂ ⁺
BEN	555	920	NAP	575	1050
HMB	476,508	1351	ANT	680	>900
DTP ^c	460	>800	PYR	500	1400

^aFrom ref. [49] and references therein.

^bAdditional CR band that is absent in the monomer.

^c1,3-*p*-Tolylpropane.

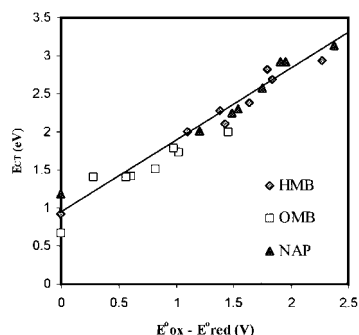


Fig. 7. Mulliken plots for CT complexes of hexamethylbenzene (HMB), octamethylbiphenylene (OMB), and naphthalene (NAP) with various acceptors. Points on the ordinate at $E^0_{ox} - E^0_{red} = 0$ represent the band energies of the charge-resonance (CR) complexes between these donors and their cation radicals. Data from ref. [49].

compounds, this spectral band can be satisfactorily included into the Mulliken plot to describe the interchangeability of the CT and CR energies of a parent arene donor with a series of different types of electron-deficient acceptors (Figure 7). The successful isolation and X-ray crystallographic characterization of such ion-radical dimers provides the basis for the estimation of structural changes during dimerization, in comparison with those occurring during CT formation. For example, the octamethylbiphenylene system, in which both the monomeric cation radical $OMB^{+\cdot}$ and the dimeric cation radical $(OMB_2)^{+\cdot}$ are well characterized (as are the neutral OMB and its CT complexes with various acceptors), represents the best basis for such a comparison. The average C–C bond length, d_{av} , within the aromatic rings of the neutral OMB donor is 1.405 Å, while in the cation radical it is 1.415 Å. In the CT complexes of OMB with TCNE and TCNQ, the value of d_{av} is 1.408 Å, while in $(OMB_2)^{+\cdot}$ it is 1.410 Å. Thus, d_{av} is 0.3 pm longer in CT complexes than in the neutral OMB donor, and in $(OMB_2)^{+\cdot}$ the average bond length is intermediate between that in the neutral OMB and that in its cation radical [49]. The infinite stacks contain dimeric units of $(OMB_2)^{+\cdot}$ with an interplanar separation of 3.41 Å, which corresponds to a tight van der Waals contact between a pair of identical octamethylbiphenylene moieties.

If the substituents on an aromatic compounds prevent the close approach of the cation radical to its neutral counterpart (due to steric hindrance), π -mer formation is inhibited. Such effects can clearly be seen on comparing 2,3,6,7-tetramethylnaphthalene (TMN) and its hindered analogue OMN. Spectrophotometric studies show that the tetramethylnaphthalene forms the dimeric $(TMN)_2^{+\cdot}$ cation radical, as characterized by a very broad absorption band at 1150 nm and the formation constant $K_{dimer} = 490 \text{ M}^{-1}$ at -10°C . In contrast, dimer formation is not observed with the hindered cation radical $OMN^{+\cdot}$. The fact that relatively few ion-radical dimers are known is associated with the opposing requirements for their formation. On the one hand, the cation radical should be relatively stable, which is usually the case with encumbered donors (for which steric hindrance prevents close contact between the radicals), while on the other hand they should be able to approach each other in order for electronic interaction to be appreciable.

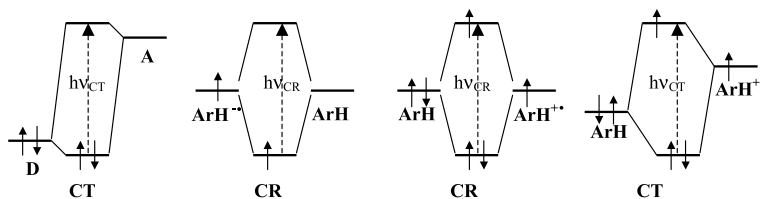


Chart 2

The enhanced acceptor properties of aromatic cation radicals ($\text{ArH}^{+\bullet}$) suggest that they should form CT complexes with the parent arene (ArH) as well as with different arene donors (ArH'). However, in mixed $\text{ArH}^{+\bullet}/\text{ArH}'$ systems, the (partial) reduction of the cation radical leads to the formation of homomolecular dimers. Moreover, the same symmetry and energy of the interacting orbitals favors the ion-radical interaction with the neutral parent, better stabilizing the (homomolecular) dimer and promoting the redox process $\text{ArH}^{+\bullet} + \text{ArH}' \rightarrow \text{ArH} + \text{ArH}'^{+\bullet}$, even if the electron transfer is formally endergonic. We thus conclude that heteromolecular complex formation takes place only when such an ET process is precluded. Indeed, the only known example of a heteronuclear cation-radical/neutral donor complex hitherto found (and characterized spectroscopically and by X-ray crystallography) is that of the hindered $\text{OMN}^{+\bullet}$ cation radical, which is not prone to forming homomolecular π -mers [50]. The qualitative MO diagrams describing CR complex formation and their relationship with the CT complexes are presented in Chart 2. In all cases, the driving force for complex formation derives from the resonance interaction between various HOMO/LUMO, SOMO/LUMO, and HOMO/SOMO combinations of donor/acceptor pairs. It should be noted, however, that CR complexes are symmetrical (isergonic) systems. The position of the absorption band is determined either by the reorganization energy or by the orbital interaction (see Figure 2). ESR measurements indicate complete delocalization of the unpaired electron in the π -mers: $(\text{OMB}_2)^{+\bullet}$ and $(\text{TMN})_2^{+\bullet}$. The average bond length found in $(\text{OMB}_2)^{+\bullet}$ (which is half the sum of those extant in the neutral and isolated cation-radical) supports such a conclusion.

13.5

CT Complexes as Critical Intermediates in Donor/Acceptor Reactions of Arenes

The basic principles describing the effects of CT complexes on the energy profile along the reaction coordinate stem from the theory of electron transfer. Redox processes may occur: (i) as ground-state thermal reactions, (ii) by direct irradiation of the CT band, and (iii) upon photoexcitation of one of the redox partners followed by diffusional complex formation [4, 24], as depicted in Chart 3.

Combination of Mulliken's formalism with the Marcus quadratic representation [10] of the initial and final (diabatic) states allows the energy profile of the ET reaction coordinate to be constructed. As illustrated in Figure 8, an increase in H_{AB} results in (i) a lowering of the ET barrier, (ii) a stabilization of the precursor and successor (CT) complexes, and (iii) a shift of their positions along the reaction coordinate (i.e. the charge is partially transferred from the

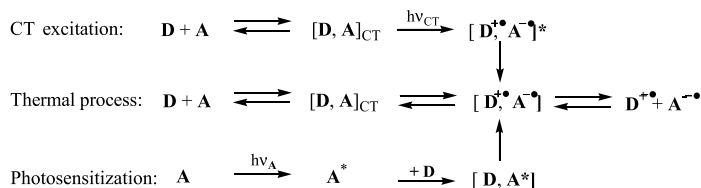


Chart 3

donor to the acceptor to induce the changes in their nuclear configuration). Finally, when the electronic coupling element $H_{\text{DA}} \geq \lambda/2$, the system becomes delocalized with zero energy of activation for electron transfer. In the framework of the Robin–Day classification of mixed-valence systems [51], this change corresponds to the transition from Class I ($H_{\text{DA}} = 0$, non-interacting redox centers) to Class II ($0 < H_{\text{DA}} < \lambda/2$) to Class III ($H_{\text{DA}} \geq \lambda/2$) [13].

Let us now consider how donor/acceptor interactions in the CT (precursor) complexes affect the dynamics of various ET processes and lead to the formation of successor complexes and finally to the free ion radicals, as well as the follow-up reactions leading to new stable products.

13.5.1

Effects of the Donor/Acceptor Interaction on the ET Dynamics of Arene Donors

13.5.1.1 Steric Control of the Inner/Outer-Sphere Electron Transfer

Historically, the development of ET theory has been based on inorganic systems, in which the (metal-ion) redox centers are surrounded by coordinated ligands [52]. In those cases in which no new metal–ligand bonds are formed or bond breakage is observed, the interaction between the redox centers is weak (usually $H_{\text{DA}} < 200 \text{ cm}^{-1}$), and such reactions are conventionally designated as outer-sphere (OS) electron transfer [52, 53].

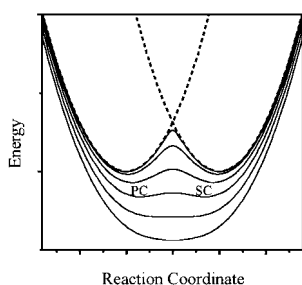


Fig. 8. Typical profiles of the potential-energy surfaces for electron-transfer in the isergonic region (for $\lambda = 1.8 \text{ eV}$). The dotted lines represent the diabatic (non-interacting) states ($H_{\text{DA}} = 0$). Adiabatic states (solid lines) are presented with the values of the electronic coupling element H_{DA}

progressively increasing from top to bottom, 0.1, 0.3, 0.6, 0.9, 1.2, 1.5 eV, and show (i) a lowering of the energy of the adiabatic states, (ii) a shift of the minimum of the precursor complex (PC) toward that of successor state (SC), and (iii) a lowering of the (activation) barrier for electron transfer.

If ligands are involved in the formation of discrete intermediates or if metal ions become ligand-bridged, the process is designated as inner-sphere (IS) electron transfer [52]. In these cases, the electronic interaction between the redox centers is increased substantially, and leads to a lowering of the activation barrier (and hence to increased rates) for the ET reaction [13, 15, 53].

Since such a chemically based differentiation between OS/IS has often proved to be ambiguous in organic reactions [53], we prefer a more general definition of inner/outer-sphere ET based primarily on the degree of the donor/acceptor electronic coupling [24]. According to this classification, *outer-sphere* ET implies weak coupling ($H_{AB} \ll \lambda$), and it is described theoretically by the classical Marcus formulation [10], in which the activation barrier is determined by the reorganization energy λ and the free energy change ΔG_{ET} , i.e.:

$$\Delta G^\ddagger = \lambda(1 + \Delta G_{ET}/\lambda)^2/4 \quad (13)$$

which predicts the characteristic (quadratic) dependence of the rate constant on the driving force ΔG_{ET} . As the donor/acceptor interaction becomes appreciable relative to λ (usually when $H_{AB} > 200 \text{ cm}^{-1}$), a substantial change in the ET reaction profile occurs. For example, for the isergonic process $\Delta G^\ddagger = (\lambda - 2H_{AB})^2/4\lambda$, and such an *inner-sphere* ET process is accompanied by significant deviations from Marcus behavior.

This definition implies the possibility of a continuous transition between outer-sphere and inner-sphere ET processes, and the kinetics can be directly related to the experimental properties of the precursor (CT) complexes as measured by X-ray crystallography, UV/vis/NIR spectroscopy, etc. Arene donors are especially well suited for the demonstration of such a changeover, since (i) the oxidation and reduction potentials (which are important for the free-energy correlation) can be easily tuned over a wide range by varying the substituents, without significant changes in the size and orientation of redox centers, and (ii) their steric encumbrance can be readily modulated by the introduction of bulky substituents at the aromatic ring to allow control of the electronic interaction without affecting the driving force.

Electron transfer (ET) to photoactivated quinone acceptors from a series of unhindered, partially hindered, and heavily hindered aromatic donors (with matched E_{ox}° values) can be examined kinetically by laser flash photolysis [54]. The second-order rate constants for electron transfer from hindered donors such as hexaethylbenzene depend strongly on the temperature, solvent polarity, and salt effect, and they follow the free-energy correlation predicted by Marcus theory (Figure 9A). Moreover, no spectroscopic or kinetic evidence for the formation of the encounter complexes (exciplexes) with photoactivated quinones prior to electron transfer is observed. In contrast, electron transfer from non-hindered (or partially hindered) donors such as hexamethylbenzene, mesitylene, and di-*tert*-butyltoluene, is associated with temperature-independent rate constants that are up to 10^2 times greater than those predicted by Marcus theory and are poorly correlated with the accompanying free-energy changes (Figure 9).

Such a rate constant behavior is ascribed to an inner-sphere ET process. Most importantly, there is unambiguous spectroscopic and kinetic evidence for the formation of encounter complexes $[ArH, Q^*]$ between the arene and the photoexcited (quinone) acceptor prior to electron transfer [54].

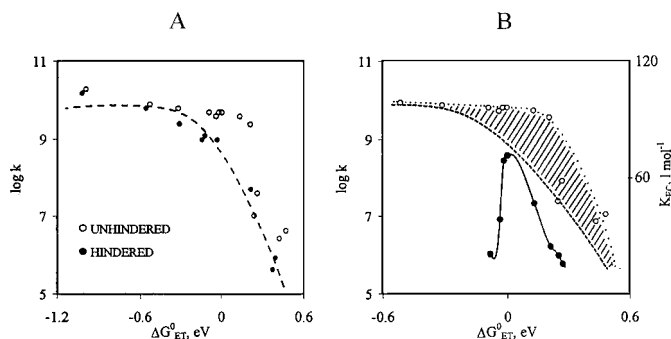


Fig. 9. (A) Free-energy dependence of the second-order rate constant ($\log k$) for electron transfer from hindered and unhindered arene donors to photoactivated quinones. The dashed line represents the best fit of the data points of the hindered donors to the Marcus correlation. (B) Superposition of (A) and the free-energy dependence of the formation product (K_{EC}) for encounter complexes of unhindered arenes with photoactivated quinones showing coincidence of the maximum of encounter complex formation and the maximum deviation of the ET rate constants of the unhindered donors from the classic Marcus (outer-sphere) behavior. Data from ref. [54].



Scheme 17

As illustrated in Figure 9B by the superposition of the Marcus-type plots and the free-energy dependence of the formation constant K_{EC} , the greatest deviations (from the Marcus curve) are observed for donor/acceptor couples that form the strongest encounter complexes (as gauged by their formation constants K_{EC}). On the basis of the absorption and emission data, an electronic coupling element of $H_{DA} \approx 0.15$ eV (1000 cm^{-1}) has been determined for similar complexes (exciplexes) [55]. Even higher values (~ 0.5 eV) can be estimated for H_{DA} in CT complexes of the same donors and ground state (unexcited) chloranil. In contrast, the CT complexes are not detected for similar ground-state pairs involving hindered donors [54, 56]. Such strong electronic couplings account for the substantial lowering of the inner-sphere ET barrier (compare Figure 8) and increased rate constants for unhindered donors.

13.5.1.2 Thermal and Photochemical ET in Strongly Coupled CT Complexes

An increase in the electronic coupling interaction results in the disappearance of the ET barrier and complete delocalization of the transferred electron between the donor and the acceptor. Such effects have been extensively studied for *intramolecular* ET in bridged intervalence compounds [57]. As regards *intermolecular* systems, the only spectrally and structurally characterized system has been that of NO^+ /arene complexes [28].

The NO^+ cation is an efficient oxidant (1.48 V vs. SCE) for various electron-rich arenes [53], and the intermolecular (CT) complexes $[\text{ArH}, \text{NO}^+]$ with alkylbenzenes have been characterized in detail [27]. However, the recent observation [4b, 28] of structurally and spectroscopically similar complexes with electron-rich arenes has led to a more detailed consideration of the role of CT complexes in NO^+ /arene redox processes [28].

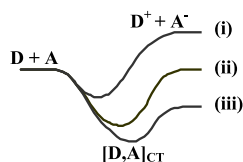


Chart 4

The reorganization energy for the (cross) ET reactions of NO^+ /arene pairs is about 2.5 eV (as evaluated from the self-exchange rates of aromatic donors and the NO^+ acceptor) [28].



Scheme 18

Since the measured values of H_{DA} of ca. 1.4–1.8 eV exceed $\lambda/2$, these CT complexes belong to the Robin–Day Class III category, in which there is complete delocalization of the electron between the donor and the acceptor. As such, there is only one potential minimum on the pathway between the $\{\text{ArH} + \text{NO}^+\}$ reactants and the $\{\text{ArH}^{+\bullet} + \text{NO}^\bullet\}$ products [28]. The free-energy change along the reaction coordinate for the redox transformation in the (i) endergonic, (ii) isergonic, and (iii) exergonic regions of driving force are qualitatively depicted in Chart 4.

The reversible (temperature-modulated) equilibrium between the CT complex and the ET products is shown in Figure 10. This process can be designated as:

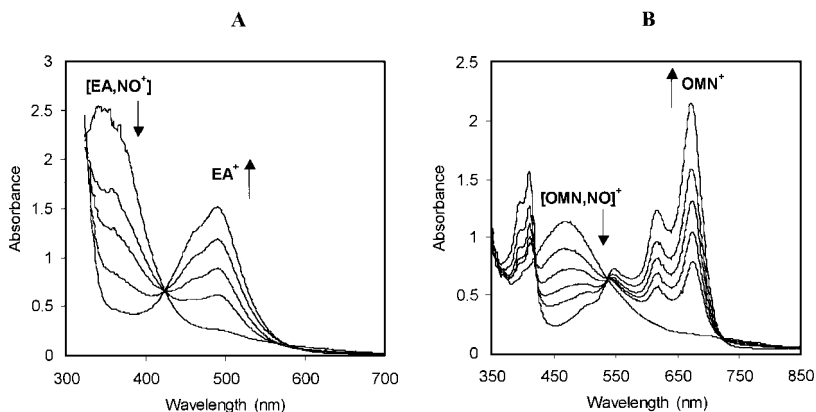


Fig. 10. Temperature modulation of the reversible complexation/electron transfer between aromatic donors and NO^+ . (A) Increase of $\text{EA}^{+\bullet}$ at (bottom to top): -44°C , -10°C , 3°C , 20°C , and after

argon bubbling (to remove NO). (B) Increase of $\text{OMN}^{+\bullet}$ at (bottom to top): -90°C , -30°C , -10°C , 0°C , 20°C and after argon bubbling. Data from ref. [28].

No activation (energy) barrier separates the donor and the acceptor from the ET products (and vice versa). The electron transfer in Scheme 18 is not a kinetic process, but is dependent on the thermodynamics, whereby electron redistribution is concurrent with complex formation. Accordingly, the rate-limiting activation barrier is simply given by the sum of the energy gain from complex formation and the driving force for electron transfer, i.e.:

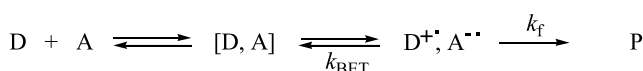
$$\Delta G_{\text{ET}}^{\ddagger} = \Delta G_{\text{CT}} + \Delta G_{\text{ET}}^{\circ}. \quad (14)$$

Nitrosonium/arene complexes also provide an opportunity for the consideration of photochemical processes in Class III systems. Due to the strong electronic interaction, the charge-transfer complex is characterized by comparable values of the mixing coefficients, $b \approx a$ (especially near the isergonic point) [28]. In contrast to the weak CT complexes with $b \ll a$, in which the ground state is close to the (diabatic) reactant and excited product states, no appreciable electron redistribution from the donor to the acceptor occurs in Class III complexes upon optical transition. Laser flash-photolysis experiments show high efficiencies for the formation of aromatic cation radicals upon direct photoexcitation of $[\text{ArH}, \text{NO}^+]$, with quantum yields for the caged radical pair close to unity. Similarly, the quantum yields of free cation radicals are found to be nearly 0.70 in complexes with hexamethylbenzene, 0.60 with pentamethylbenzene, 0.4 with durene, and 0.1 with *p*-xylene [58]. Such results can be explained in terms of the population of the antibonding orbital of the complex, which results in a sharp decrease in the NO/arene binding. In addition, owing to the sizable extent of CT from the arene to NO^+ in the ground state, the nuclear configuration (both in the ground and Franck–Condon excited states) corresponds to that of the arene cation radical and nitric oxide. No nuclear rearrangement of the arene and nitric oxide (nor of the solvent) is needed for the relaxation of the excited state to the solvent-caged radical pair. Such a dissociation proceeds via a practically (barrierless) transition on the vibration timescale of 10^{-13} – 10^{-14} s. The high efficiency of formation of the radical pair is reflected in microsecond kinetics and results in regeneration of the initial $[\text{ArH}, \text{NO}^+]$ complex [58].

13.5.2

Electron-Transfer Paradigm for Arene Transformation via CT Complexes

Thermal and/or photochemical electron transfer within the CT (precursor) complex generates the ion pair $\{\text{D}^+, \text{A}^-\}$ as caged or freely diffusive ion-radicals. Most important from a synthetic point of view are the processes by which highly reactive ion-radicals undergo further irreversible transformation resulting in new (thermodynamically stable) products. In other words, the formation of the (precursor) CT complex and electron transfer act in tandem as a coupled set of pre-equilibria. The resultant ion-radical pair can undergo a subsequent (irreversible) transformation (with rate constant k_f) or back ET (k_{BET}), which represent the basis for the ET paradigm and drive the coupled equilibria towards the products (P) [4], i.e.:



Scheme 19

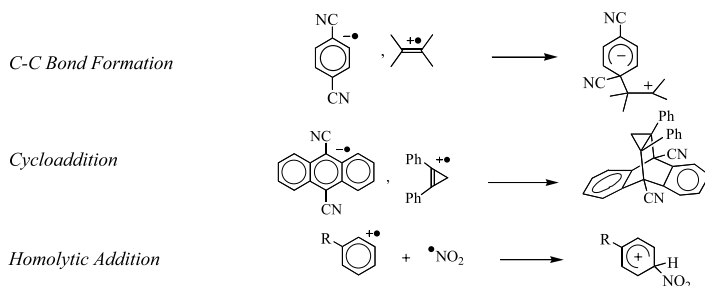
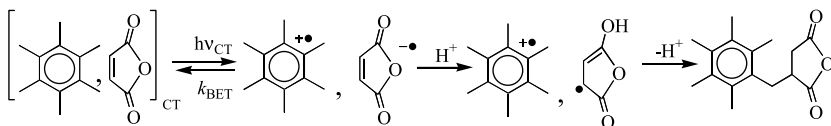


Chart 5

If $k_f > k_{\text{BET}}$, the overall transformation can occur rapidly despite unfavorable driving forces for the electron transfer itself. Only follow-up reactions with high k_f can compete with back electron transfer. Different kinds of such unimolecular processes can drive the equilibria toward the final product. A representative example is the mesolytic cleavage of the C–Sn bond in the radical cation resulting from the oxidation of benzylstannane by photoexcited 9,10-dicyanoanthracene (DCA). This is followed by the addition of the benzyl radical and the tributyltin cation to the reduced acceptor DCA^- [59]. In the arene/nitrosonium system, $[\text{ArH}, \text{NO}^+]$ complexes can exist in solution in equilibrium with a low steady-state concentration of the ion-radical pair. However, the facile deprotonation or fragmentation of the arene cation radical in the case of bifunctional donors such as octamethyl(diphenyl)methane and bicumene can result in an effective (ET) transformation of the arene donor [28, 59]. Another pathway involves collapse of the contact ion pair $[\text{D}^+, \text{A}^-]$ by rapid formation of a bond between the cation radical and anion radical (which effectively competes with the back electron transfer), as illustrated by the examples in Chart 5 [59].

Bimolecular reactions of the ion-radical pair can also effectively compete with the back electron transfer if either component undergoes a rapid reaction with an additive that is present during the ET activation. In NO^+ /arene systems, the introduction of oxygen rapidly oxidizes even small amounts of nitric oxide to compete with back ET and thus successfully effect aromatic nitration [60]. In a related example, the CT complex of hexamethylbenzene and maleic anhydride reaches a photostationary state with no productive reaction. However, if irradiation is carried out in the presence of an acid, the anion radical in the resulting contact ion-radical pair is readily protonated, and the redox equilibrium is driven toward coupling (in competition with the back ET) to yield the photoadduct [59], i.e.:



Scheme 20

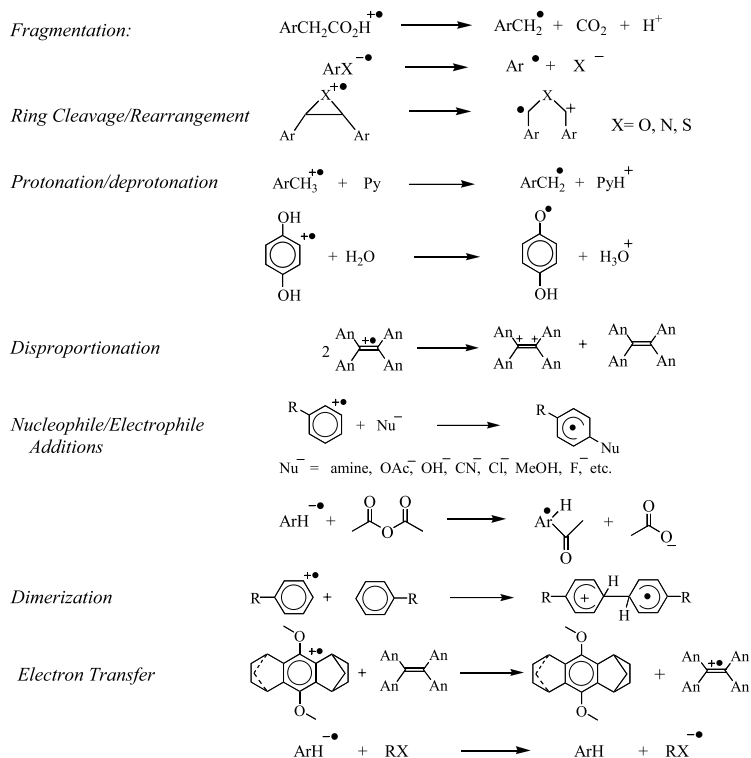


Chart 6

Generally, highly reactive aromatic ion-radicals can undergo a variety of other uni- and bi-molecular processes that compete effectively with back ET and lead to an overall transformation, some examples of which are illustrated in Chart 6 (with Ar representing an aryl group) [59].

The aforementioned examples reveal that a wide variety of aromatic transformations can proceed from the CT complex. If the (CT/ET) pre-equilibria are fast relative to the follow-up process, the overall second-order rate constant $k_2 = K_{\text{CT}}K_{\text{ET}}k_f$. In this kinetic regime (especially in the strongly endergonic ET range), the ion-radical pair may not be experimentally observed in a thermally activated adiabatic process, and the applicability of the ET paradigm is difficult to establish. However, photochemical (laser) activation by the deliberate irradiation of the CT absorption ($h\nu_{\text{CT}}$) will lead to the spontaneous generation of the ion-radical pair, which is experimentally observable when the time resolution of the laser pulse exceeds that of the follow-up processes (k_f and k_{BET}). The relationship between the thermal and photochemical generation of the ion-radical pair is illustrated in Figure 11, and this provides a basis for the experimental demonstration of the viability of the electron-transfer paradigm through comparison of the thermal/photochemical reactions with (thermal) rate constant/CT band energy correlations.

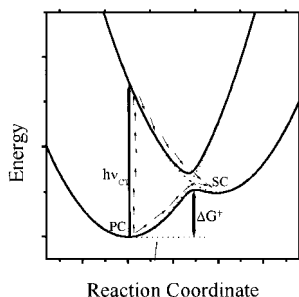


Fig. 11. Graphical relationship between the photochemical and thermal pathways for the CT transformation of the precursor complex (PC) to the successor complexes (SC).

The close relationship between the thermal and photochemical (ET) pathways via CT complexes can also be seen from a consideration of oxidative C–C cleavage in benzopinacol donors, which readily form vividly colored CT complexes with various acceptors such as chloranil (CA), DDQ, and NO^+ [59]. Thus, benzopinacol/CA solutions are stable (at 23 °C) in the dark. However, irradiation of the CT band leads to a slow bleaching of the color with concomitant formation of the retopinacol product. With a stronger acceptor, such as DDQ ($E_{\text{red}}^\circ = 0.6 \text{ V vs. SCE}$), the cleavage of the benzopinacols can also be achieved by thermal means. For example, the CT complex formed upon mixing tetraanisylpinacol and DDQ bleaches within minutes (in the dark) to afford the retopinacol products in quantitative yield [59].

Identical pre-equilibrium CT complexes of various substituted pyridinium salts with organoborates such as BMe_4^- as electron donors are observed in both the thermal and photochemical methyl transformations. Both processes proceed through the radical pair, in which rapid scission of one Me–B bond in the oxidized BMe_4^\cdot generates a methyl radical and BMe_3 . This is followed by the coupling of pyridine and methyl radicals within the solvent cage. Moreover, the spectral characteristics show: (i) a red shift of the CT bands with increasing E_{red}° of the pyridinium acceptor and a blue shift with increasing E_{ox}° of the organoborates, and (ii) that the process with *N*-methylisoquinolinium/ BMe_4^- is slow, but that the methyl-transfer reaction between BMe_4^- and 3-cyano-*N*-methylpyridinium (with the highest E_{red}°) occurs instantaneously. On the other hand, the yellow mixture of 4-phenylpyridinium cation (with relatively low E_{red}°) and BMe_4^- persists for prolonged periods without reaction [59].

The same features are observed in the osmylation of arene donors. Thus, osmium tetroxide spontaneously forms complexes with arenes, and the systematic spectral shift in the CT bands parallels the decrease in the arene IP [59]. The same osmylated adducts are obtained thermally on leaving mixtures to stand in the dark or upon irradiation of the CT bands at low temperature. Time-resolved spectroscopy establishes that irradiation of the CT band of the anthracene/osmium tetroxide complex leads directly to the radical-ion pair $\{\text{ANT}^+, \text{OsO}_4^{\cdot-}\}$, which then collapses to the osmium adduct (with a rate constant $k \sim 10^9 \text{ s}^{-1}$) in competition with back ET [59].

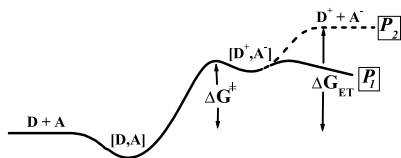


Chart 7

Such examples indicate the applicability of the CT/ET paradigm in describing a variety of aromatic transformations. In the case of a (highly) endergonic process, the involvement of the electron-transfer step in the reaction pathway can be ambiguous. The objection against such a step is often based on the high ET reaction barrier due to Marcus reorganization energy and/or an unfavorable driving force. However, the development of Marcus–Hush theory in the strong interaction range has indicated that the donor/acceptor electronic coupling can result in: (i) a substantial lowering of the barrier to electron transfer, and (ii) a stabilization (lowering in energy) of the adiabatic (CT) precursor and successor complexes relative to the diabatic (non-interacting) reactant and product states, as illustrated in Chart 7 [61].

Because the electronic distribution and nuclear configuration of the donor and the acceptor in the (Class II) successor complexes are similar to those of the free donor/acceptor product (i.e. radical pair), it is reasonable to suggest that products can originate directly from the successor complex (pathway P_1). Such a reaction, which includes an electron-transfer step, does not necessarily proceed via a pair of free ion radicals, and the effective activation energy can be even lower than that required by pathway P_2 . When the follow-up reaction involves the coupling of radicals, the reaction directly proceeding from the (ET) successor complex state can be kinetically favorable (since it excludes diffusional processes).

13.5.3

Electron-Transfer Activation of Electrophilic Aromatic Substitution

Electrophilic aromatic substitution represents one of the most important applications of the transformation of an arene via a CT (precursor) complex. The process is considered to proceed via an (encounter) π -complex between the electrophile (E^+) and the aromatic substrate (ArH), which collapses in a single rate-limiting step to the Wheland intermediate or σ -complex [43, 44], i.e.:



Scheme 21

The focal point in this mechanism is the activation process that leads to the well-established Wheland intermediate. In order to address the mechanism of the activation of π -complexes, we first recognize that most electrophiles (such as NO^+ and NO_2^+ , various nitrating agents, halogens, carbocations, diazonium cations, sulfur trioxide, lead(IV), mercu-

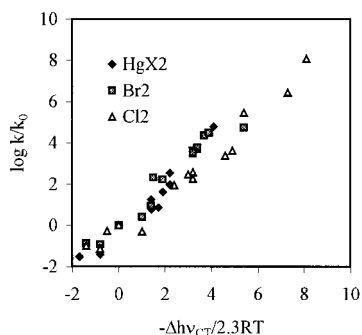


Fig. 12. Linear correlations of the relative reactivity of arenes in electrophilic substitution reactions ($\log k/k_0$) with the optical transition energies in the accompanying CT complexes. Data from ref. [62b].

ry(II), and thallium(III) salts, etc.) are excellent electron acceptors, as judged by their E_{red}° , as well as by their ability to oxidize a variety of donors to the corresponding cation radicals [4]. Furthermore, the various arenes are electron donors, as reflected by their relatively easy oxidation in solution. As a consequence, the π -complex in Chart 7 is more accurately described as an electron donor/acceptor or CT complex between the electrophile and the aromatic nucleophile. The CT absorption bands are visible indications of their strong MO interaction that precedes the transformation [4]. The application of the ET paradigm to electrophilic aromatic substitution is based on (i) the observation of CT interactions between electrophiles and aromatic donors, (ii) the coincidence of the products of the CT photochemical and thermal reactions, and (iii) the quantitative correlations of the second-order rate constants with the CT transition energies for halogenation, mercuriation, thallation, etc. (Figure 12) [62]. Accordingly, let us take halogenation, nitration, and nitrosation with various electrophilic agents as typical examples to elucidate the importance of CT complexes and ET activation as the fundamental steps leading to the Wheland intermediate.

13.5.4

Structural Pre-organization of the Reactants in CT Complexes

Aromatic hydrocarbons are known to spontaneously form weak 1:1 molecular CT complexes with halogens [30, 62]. The recent (low-temperature) refinement of their structure reveals the *highly structured* pre-equilibrium complex shown in Figure 13A [32], in which the axially symmetric Br₂ is poised specifically over a single (C–C) center of benzene. Its pre-reactive character is revealed by the spontaneous transformation of the crystalline [C₆H₆, Br₂] complex into an equimolar mixture of bromobenzene and hydrogen bromide. Further (structural) delineation of electrophilic aromatic bromination has been provided by the isolation and X-ray crystallographic analysis of the σ -adduct or Wheland intermediate with hexamethylbenzene as the arene under similar reaction conditions (see Figure 13B) [36]. (Note that the highly unstable σ -adduct of benzene is unlikely to be isolable owing to its facile α -proton loss.) Such structural studies taken together provide an unequivocal pathway for electrophilic aromatic bromination, in which the key steps are:

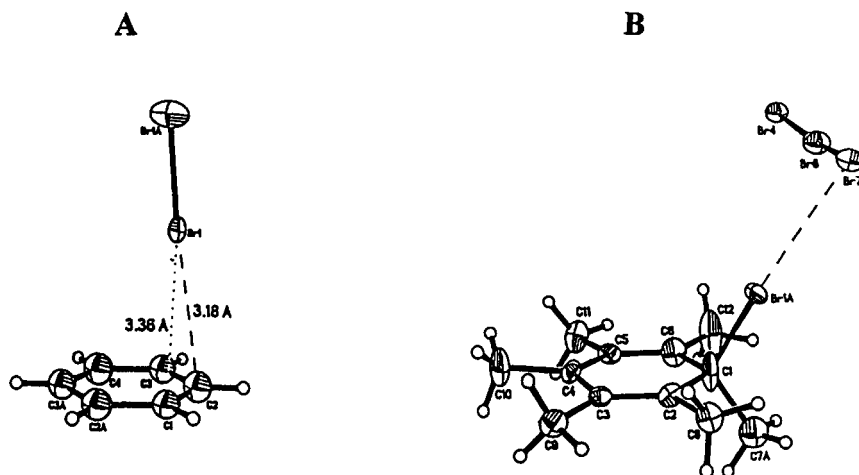
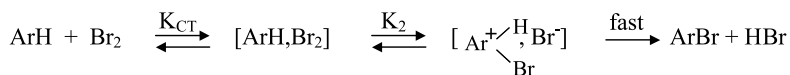


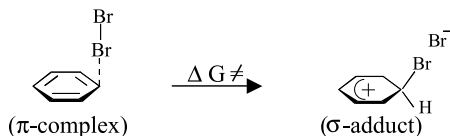
Fig. 13. (A) ORTEP diagram of the pre-equilibrium complex of benzene and bromine showing the pertinent charge-transfer π -bonding. (B) Molecular structure of the σ -adduct (or Wheland inter-

mediate) derived from the bromine interaction with hexamethylbenzene to emphasize the least-motion transformation from the π -complex in A. Data from ref. [32].



Scheme 22

Most relevant is the structural information provided by the pre-equilibrium π -complex in its transformation to the critical σ -adduct. Thus, the composite of the ORTEP structures in Figures 13 A and B represents a close to ideal least-motion study, i.e.:

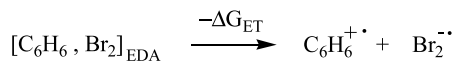


Scheme 23

Even more striking is the regioselective transformation of the highly structured toluene π -complex, with bromine situated specifically over the *ortho* and *para* positions to afford the same isomeric (product) mixture of *o*- and *p*-bromotoluenes as that obtained in solution [63]. As close as these pre-equilibrium intermediates are structurally akin to the (ordered) transition states for electrophilic bromination, it is important to emphasize that they are formed essentially upon bimolecular collision with no activation energy, and the donor/acceptor binding is in accord with the Mulliken formulation.

The continuous transition from π - to σ -coordination in the complexes with different acceptors, as presented in Figure 6, implies the ready transformation of one into the other. The

formation of the σ -complex can be presented as an ET process in which the CT complex leads to the reduced acceptor Br_2^- , i.e.:



Scheme 24

However, the driving force for the ET step ($\Delta G_{\text{ET}} = 60 \text{ kcal mol}^{-1}$ is taken as the difference between the redox potentials of benzene and Br_2) is clearly too endergonic to be consistent with the facile bromination of benzene. However, such an evaluation of the driving force could be valid if electron transfer leads to the *ion-pair* state. Furthermore, the quantitative measurement of the CT absorption leading to the formation of the CT complex $[\text{C}_6\text{H}_6, \text{Br}_2]$ indicates the donor/acceptor electronic coupling interaction to be $H_{\text{DA}} \sim 0.5 \text{ eV}$. As such, the ion radicals $\text{C}_6\text{H}_6^{+\cdot}$ and $\text{Br}_2^{\cdot-}$ are born as a contact (inner-sphere) ion pair, in which the energy is substantially lowered due to the radical-ion interaction, so that the driving force is much more favorable than that simply calculated from the values of E_{ox}° and E_{red}° .

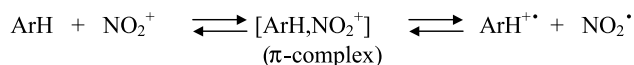
13.5.5

CT Complexes in Aromatic Nitration and Nitrosation

Due to very fast rates of aromatic nitration with the NO_2^+ cation, an independent experimental study of the reactive intermediates pertaining to the ET paradigm is not readily forthcoming. However, such a kinetic restriction is overcome by the use of nitronium ion carriers (NO_2Y) such as nitric acid, acetyl nitrate, N_2O_5 , *N*-nitropyridinium, tetranitromethane, etc., as milder nitrating agents [59]. The latter form colored complexes with arenes, in which the energy of the CT bands corresponds to the predictions of Mulliken theory [9]. Thermal and photochemical reactions of these complexes result in identical isomeric mixtures of aromatic nitration products. Moreover, the thermal nitration of various arenes shows a strong rate dependence on the donor/acceptor strength of the nitrating agent and ArH . These observations support ET activation as a viable mechanistic basis for aromatic nitration. Furthermore, analysis of the products from toluene nitration yields isomeric compositions of *o*-, *m*-, and *p*-nitrotoluene that are singularly invariant over a wide range of substrate selectivities (k/k_0 based on the benzene reference [64]) with different nitrating agents (ranging from the very reactive NO_2^+ to the relatively unreactive *p*-MeOPy NO_2^+). In other words, there is a complete decoupling of the product-forming step from the rate-limiting activation of electrophilic aromatic nitration. Such a clear violation of the reactivity/selectivity principle can only arise when there is at least one reactive intermediate such as the (successor) ion-radical pair, as predicted by the ET paradigm.

In order to combine the CT/ET pathways with essentially diffusion-controlled rates [64] of nitration by NO_2^+ , and the understanding of the dramatically lower reactivity of the struc-

turally related [65] nitrosonium (NO^+) cation [66], let us consider the corresponding reaction profiles constructed in the framework of the ET paradigm. While the reduction potentials of NO^+ and NO_2^+ are comparable in different solvents [67], there is a large difference between NO^+ and NO_2^+ in terms of the magnitudes of their reorganization energies, which differ by a factor of 2, i.e.: $\lambda_{\text{NO}_2} = 140 \text{ kcal mol}^{-1}$ and $\lambda_{\text{NO}} = 69 \text{ kcal mol}^{-1}$, largely as a result of the requisite bending of ONO attendant upon the reduction of the almost linear (triatomic) cation [67]. In order to follow through with the comparison to NO^+ , let us consider the corresponding ET process, viz.:



Scheme 25

Since the temporal course of ET cannot readily be followed owing to the high reactivity of NO_2^+ , we rely on the comparison of the reorganization energy to draw some broad estimates of the electron coupling element for the pre-equilibrium intermediate in Scheme 25. If we take H_{DA} to be the same as that for NO^+ as a first approximation, the ET potential-energy profile will consist of a double potential minimum consisting of a separate precursor (PC) π -complex $[\text{ArH}, \text{NO}_2^+]$ and successor (SC) complex $[\text{ArH}^{+\cdot}, \text{NO}_2^\cdot]$, both with progressively shallower minima (and higher barriers separating them) as the electronic coupling element H_{DA} decreases. In the limit with $H_{\text{DA}} \approx 0$, a single barrier separates the non-interacting reactant state $\{\text{ArH} + \text{NO}_2^+\}$ and the final state $\{\text{ArH}^{+\cdot} + \text{NO}_2^\cdot\}$. In other words, as a result of the large λ_{NO_2} , electron transfer with NO_2^+ cannot progress via a single pre-equilibrium π -complex like that with NO^+ , and the typical cross-section of the potential energy surface includes a pair of pre-equilibrium π -intermediates (PC and SC). As a consequence of the different potential-energy profiles, with a double minimum for NO_2^+ and a single minimum for NO^+ (Chart 4), the rate of electron transfer to NO_2^+ is significantly faster than that to NO^+ , despite the larger magnitude of λ_{NO_2} relative to λ_{NO} , since Chart 8 shows that the activation energy for overall electron transfer is simply given as $\Delta G^\ddagger_{\text{ET}} = \Delta G^\circ_{\text{ET}}$. The pre-equilibrium formation of CT complexes is common to both aromatic nitrosation and nitration, which are known to occur via the active electrophilic species NO^+ and NO_2^+ , respectively [68]. As such, the interconversion of the π -complex to the σ -adduct (like that for bromination) represents the critical activation step, i.e.:

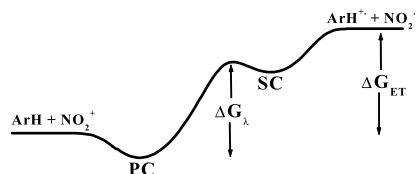
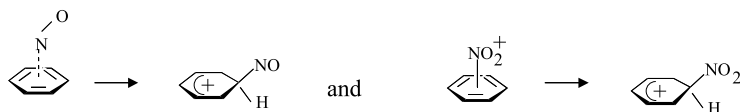


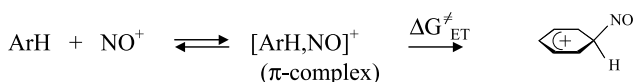
Chart 8



Scheme 26

The least-motion study of such (direct or one-step) transformations cannot readily account for the fact that NO_2^+ moiety must overcome the sizable (reorganization) penalty for ONO bending. Such a significant reorganizational obstacle is conceptually circumvented by decoupling the step involving reorganization from the step leading to the σ -adduct in Scheme 26. Indeed, ET activation as presented in Charts 4 and 8 for NO^+ and NO_2^+ , respectively, satisfies the two-step criterion, since reorganization is implicit in ET and it is separate from σ -adduct formation.

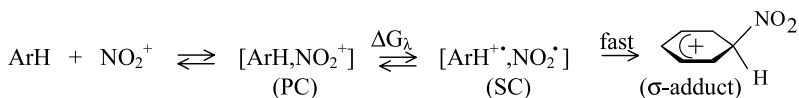
As applied to aromatic nitrosation, the activation process is:



Scheme 27

where the overall activation barrier (ΔG^\ddagger) is evaluated from Eq. (14) [69]. Thus, slow electron transfer, coupled with the subsequent slow deprotonation of the σ -adduct [70], is responsible for aromatic nitrosations, which are by and large limited to only the most active (electron-rich) arene donors [71].

The corresponding two-step activation of aromatic nitration involves an additional intermediate, the successor complex (SC) = $[\text{ArH}^+, \text{NO}_2^-]$, which largely takes on the burden of the NO_2^+ reorganization in the separate ET transformation of the precursor complex (PC) = $[\text{ArH}, \text{NO}_2^+]$. As such, the subsequent (spontaneous) collapse of SC directly to the σ -adduct considerably facilitates the ET pathway for nitration [72] since it entirely by-passes the slow (energy-intensive) step leading from the SC or $[\text{ArH}^+, \text{NO}_2^-]$ to the separated (non-interacting) ion-radical pairs $\{\text{ArH}^+ + \text{NO}_2^-\}$, i.e.:



Scheme 28

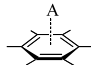
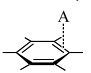
The activation barrier for such a direct collapse of the ion-radical pair is substantially less than ΔG_{ET} (see pathway P_1 in Chart 7) and leads to very fast nitration rates [73]. (The latter underscores the caveat that the viability of ET mechanisms cannot be pre-judged [67] solely by the value of ΔG_{ET}).

Formation of the Wheland intermediate from the ion-radical pair as the critical reactive intermediate is common to both nitration and nitrosation processes. The nitrosoarenes (unlike their nitro counterparts) are excellent electron donors, as judged by their low E_{ox}^0 as

compared to the parent arene [74]. As a result, nitrosoarenes are also better Brønsted bases [75] than the corresponding nitro derivatives, and this marked distinction readily accounts for the large differentiation in the deprotonation rates of their respective conjugate acids (i.e. Wheland intermediates). In the case of aromatic nitration with NO_2^+ , deprotonation is fast and occurs with no kinetic (deuterium) isotope effect. The slower rates of formation of the radical pair leading to Wheland intermediates, together with slower rate of the deprotonation of these intermediates, results in a dramatic difference between the rate of nitration and that of nitrosation.

13.6

Concluding Summary

Arenes are electron donors by virtue of the ease with which they form intermolecular complexes with a variety of electrophiles, cations, acids, and oxidants that are all sufficiently electron-poor to be generally classified as electron acceptors (A). Three structural features are common to all arene complexes that have been isolated and subjected to X-ray crystallographic analysis, namely: (i) their π -structure, either as the axially symmetric  or the asymmetric  forms, (ii) their inner-sphere character, such that the separation of the acceptor (A) from the aromatic plane is less than the sum of their van der Waals radii, and (iii) the significant enlargement of the aromatic chromophore with average bond distances between ring carbons that can approach those extant in the corresponding arene cation radicals.

Charge transfer as depicted by Mulliken provides a single unifying basis for predicting arene reactivity based on the spectral, structural (both molecular and electronic), and thermodynamic properties of their intermolecular complexes, from stable organometallic derivatives to non-bonded collision complexes with very short lifetimes.

References

- 1 a) S. SCHEINER (Ed.), *Molecular Interaction: From van der Waals to Strongly Bound Complexes*, Wiley, New York, 1997; b) P. HOBZA, R. ZAHRAJNÍK, *Intermolecular Complexes*, Elsevier, New York, 1988; c) H. RATAJCZAK, W. J. ORVILLE-THOMAS, *Molecular Interaction*, Wiley, New York, Vol. 1, 1980; d) R. A. MARCUS, *Angew. Chem. Int. Ed. Engl.* **1993**, 32, 1111; e) N. SUTIN, *Acc. Chem. Res.* **1968**, 1, 255; f) See also the unusual number (3) of thematic issues of *Chem. Rev.* that have been issued in the last dozen years: viz. **1988** (vol. 88), **1994** (vol. 94), and **2000** (vol. 100).
- 2 S. M. HUBIG, S. V. LINDEMAN, J. K. KOCHI, *Coord. Chem. Rev.* **2000**, 200–202, 831, and refs. cited therein.
- 3 a) R. FOSTER, *Organic Charge-Transfer Complexes*, Academic Press, New York; b) G. BRIEGLEB, *Electronen-Donator-Acceptor Komplexe*, Springer, Berlin, 1961.
- 4 a) J. K. KOCHI, *Angew. Chem. Int. Ed. Engl.* **1988**, 27, 1227; b) R. RATHORE, J. K. KOCHI, *Adv. Phys. Org. Chem.* **2000**, 35, 193.
- 5 M. J. TAMRES, R. L. STRONG, *Molecular Association*, Vol. 2 (Ed.: R. F. FOSTER), Academic Press, New York, 1979, p. 332ff.
- 6 R. BOYER, *Concepts in Biochemistry*, Brooks/Cole, Monterey, CA, 1999. See also: F. GUTMANN, C. JOHNSON, H. KEYZER, J. MOLNAR, *Charge-Transfer Complexes in Biological Systems*, Dekker, New York, 1977.
- 7 a) B. L. FERINDA, W. F. JAGER, B. DE LANDE, *Tetrahedron* **1993**, 49, 8267;

- b) L. FABRIZZI, A. POGGI, *Chem. Soc. Rev.* **1995**, 198; c) W. B. DAVIS, W. A. SWEC, M. A. RATHER, M. R. WASIELEWSKI, *Nature* **1998**, 396, 60; d) J.-M. TOUR, J. SCHUMM, D. L. PEARSON, *Macromolecules* **1994**, 27, 2348; e) D. K. DAS-GUPTA, in *Introduction to Molecular Electronics* (Eds.: M. C. PETTY, M. R. BRYCE, D. BLOOR), Edward Arnold, London, 1995, pp. 47–71.
- 8 a) H. MEIER, *Angew. Chem.* **1992**, 104, 1425; *Angew. Chem. Int. Ed. Engl.* **1992**, 31, 1399; b) M. TAKESHITA, S. F. SOONG, M. IRIE, *Tetrahedron Lett.* **1998**, 39, 7717; c) D. PHILP, J. F. STODDART, *Angew. Chem.* **1996**, 108, 1242; *Angew. Chem. Int. Ed. Engl.* **1996**, 35, 1154.
- 9 a) R. S. MULLIKEN, W. B. PERSON, *Molecular Complexes*, Wiley, New York, 1969; b) R. S. MULLIKEN, *J. Am. Chem. Soc.* **1952**, 74, 811.
- 10 a) R. A. MARCUS, *J. Chem. Phys.* **1957**, 26, 867; b) R. A. MARCUS, *Discuss. Faraday Soc.* **1960**, 29, 21; c) R. A. MARCUS, *J. Phys. Chem.* **1963**, 67, 853; d) R. A. MARCUS, *J. Chem. Phys.* **1965**, 43, 679.
- 11 a) N. S. HUSH, *Z. Electrochem.* **1957**, 61, 734; b) N. S. HUSH, *Trans. Faraday Soc.* **1961**, 57, 557.
- 12 See: J. K. KOCHI, in *Comprehensive Organic Synthesis*, Vol. 7 (Eds.: B. M. TROST, I. FLEMING, S. V. LEY), Pergamon, New York, chapter 7.4, p. 849ff.
- 13 N. SUTIN, *Prog. Inorg. Chem.* **1983**, 30, 441. See also: N. SUTIN, *Adv. Chem. Phys.* **1999**, 106, 7, and B. S. BRUNSCHWIG, N. SUTIN, *Coord. Chem. Rev.* **1999**, 187, 233.
- 14 a) N. S. HUSH, *Prog. Inorg. Chem.* **1967**, 8, 391; b) N. S. HUSH, *Electrochim. Acta* **1968**, 13, 1005.
- 15 a) M. D. NEWTON, in *Electron Transfer in Chemistry* (Ed.: V. BALZANI), Wiley-VCH, Weinheim, 2001, vol. 1, p. 3; b) B. S. BRUNSCHWIG, N. SUTIN, in *Electron Transfer in Chemistry* (Ed.: V. BALZANI), Wiley-VCH, Weinheim, 2001, vol. 2, p. 583.
- 16 C. CREUTZ, M. D. NEWTON, N. SUTIN, *J. Photochem. Photobiol. A: Chem.* **1994**, 82, 47.
- 17 a) Spectral bandwidths are given as full width at half maximum (fwhm); b) For a discussion of the intermolecular separation parameter r , see Newton in ref. [15a].
- 18 For the application of MO-LCAO methodology to charge-transfer complexes see, e.g. a) R. L. FLURRY, *J. Phys. Chem.* **1965**, 69, 1927; b) R. L. FLURRY, *J. Phys. Chem.* **1969**, 73, 2111; c) R. L. FLURRY, *J. Phys. Chem.* **1969**, 73, 2787.
- 19 S. SHAIK, A. SHURKI, *Angew. Chem. Int. Ed.* **1999**, 38, 586.
- 20 a) I. FLEMING, *Frontier Orbitals and Organic Chemical Reactions*, Wiley, New York, 1976; b) V. F. TRAVEN, *Frontier Orbitals and Properties of Organic Molecules*, Ellis Horwood, New York, 1992; c) G. KLOPMAN, *J. Am. Chem. Soc.* **1968**, 90, 223; d) K. FUKUI, *Acc. Chem. Res.* **1971**, 4, 57; e) K. FUKUI, *Angew. Chem. Int. Ed. Engl.* **1982**, 21, 801; f) W. L. JORGENSEN, L. SALEM, *The Organic Chemist's Book of Orbitals*, Academic Press, New York, 1973.
- 21 a) C. MANN, K. BARNES, *Electrochemical Reactions in Nonaqueous Systems*, Dekker, New York, 1970; b) K. YOSHIDA, *Electrooxidation in Organic Chemistry*, Wiley, New York, 1984; c) A. J. BARD, L. R. FAULKNER, *Electrochemical Methods*, Wiley, New York, 1980.
- 22 J. O. HOWELL, J. M. GONCALVES, C. AMATORE, L. KLASINC, R. M. WIGHTMAN, J. K. KOCHI, *J. Am. Chem. Soc.* **1984**, 106, 3968.
- 23 a) R. KEEFER, L. J. ANDREWS, *J. Am. Chem. Soc.* **1950**, 72, 4677; b) L. J. ANDREWS, R. M. KEEFER, *Molecular Complexes in Organic Chemistry*, Holden Day, San Francisco, 1964; c) R. E. BUCKLES, J. P. YUK, *J. Am. Chem. Soc.* **1953**, 75, 3048; d) F. R. MAYO, J. KATZ, *J. Am. Chem. Soc.* **1947**, 69, 1339; e) J. E. DUBOIS, F. GARNIER, *Spectrochim. Acta* **1967**, 23A, 2279; (f) S. FUKUZUMI, J. K. KOCHI, *J. Am. Chem. Soc.* **1981**, 103, 2783; g) S. FUKUZUMI, J. K. KOCHI, *J. Org. Chem.* **1981**, 46, 4116.
- 24 S. M. HUBIG, J. K. KOCHI, in *Electron Transfer in Chemistry* (Ed.: V. BALZANI), Wiley-VCH, Weinheim, 2001, vol. 2, p. 618.
- 25 a) E. F. HILINSKI, J. M. MASNOVI, C. AMATORE, J. K. KOCHI, P. M. RENTZEPIS, *J. Am. Chem. Soc.* **1983**, 105, 6167; b) K. WYNNE, C. GALLI, R. HOCHSTRASSER, *J. Chem. Phys.* **1994**, 100, 4797.
- 26 J. F. ENDICOTT, in *Electron Transfer in Chemistry* (Ed.: V. BALZANI), Wiley-VCH, Weinheim, 2001, vol. 1, p. 238.
- 27 E. K. KIM, J. K. KOCHI, *J. Am. Chem. Soc.* **1991**, 113, 4962.

- 28 S. V. ROSOKHA, J. K. KOCHI, *J. Am. Chem. Soc.* **2001**, 123, 8985.
- 29 W. B. PEARSON, in *Spectroscopy and Structure of Molecular Complexes* (Ed.: J. YARWOOD), Plenum Press, New York, 1973, p. 1.
- 30 H. A. BENESI, J. H. HILDEBRAND, *J. Am. Chem. Soc.* **1949**, 71, 2703.
- 31 R. RATHORE, S. V. LINDEMAN, J. K. KOCHI, *J. Am. Chem. Soc.* **1997**, 119, 9393.
- 32 A. V. VASILYEV, S. V. LINDEMAN, J. K. KOCHI, *New J. Chem.* **2002**, 26, 582.
- 33 A. V. VASILYEV, S. V. LINDEMAN, J. K. KOCHI, *Chem. Commun.* **2001**, 909.
- 34 W. D. JONES, F. J. FEHER, *J. Am. Chem. Soc.* **1982**, 104, 4240.
- 35 a) F. A. COTTON, *J. Am. Chem. Soc.* **1968**, 90, 6230; b) L. PAULING, *The Nature of the Chemical Bond*, Cornell University Press, Ithaca, NY, 1960.
- 36 S. M. HUBIG, J. K. KOCHI, *J. Org. Chem.* **2000**, 65, 6807.
- 37 a) D. F. McMILLEN, D. M. GOLDEN, *Ann. Rev. Phys. Chem.* **1982**, 33, 493; b) A. E. SHILOV, G. B. SHUL'PIN, *Chem. Rev.* **1997**, 97, 2879; c) See also: R. C. WEAST (Ed.), *CRC Handbook of Chemistry and Physics*, 70th ed., CRC Press, Boca Raton, FL, 1989, p. 206.
- 38 G. W. PARSHALL, *Acc. Chem. Res.* **1975**, 8, 113.
- 39 P. DIVERSI, S. IACOPONI, G. INGROSSO, F. LASCHI, A. LUCCHERINI, C. PINZINI, G. UCCELLO-BARRETTA, P. ZANELLO, *Organometallics* **1995**, 14, 3275.
- 40 a) J. M. MASNOVI, S. SANKARARAMAN, J. K. KOCHI, *J. Am. Chem. Soc.* **1989**, 111, 2263; b) V. D. PARKER, Y. ZHAO, Y. LU, G. ZHENG, *J. Am. Chem. Soc.* **1998**, 120, 12720.
- 41 E. I. HEIBA, R. M. DESSAU, W. J. KOEHL, JR., *J. Am. Chem. Soc.* **1969**, 91, 6830.
- 42 A. E. SHILOV, *Activation of Saturated Hydrocarbons by Transition Metal Complexes*, Reidel, Dordrecht, 1984, p. 21.
- 43 R. TAYLOR, *Electrophilic Aromatic Substitution*, Wiley, New York, 1990.
- 44 J. MARCH, *Advanced Organic Chemistry*, Wiley, New York, 1992, p. 641 and references therein.
- 45 D. ASTRUC, *Topics Curr. Chem.* (Eds.: W. A. HERRMANN), Springer Verlag, Berlin, **1991**, 160, 47.
- 46 a) R. G. SUTHERLAND, L. R. CHOWDHURY, A. PIORKO, C. C. LEE, *Can. J. Chem.* **1986**, 64, 2031; b) R. C. CAMBIE, S. J. JANSSEN, P. S. RUTLEDGE, P. D. WOODGATE, *J. Organomet. Chem.* **1992**, 434, 97; c) R. M. MORIARTY, U. S. GILL, *Organometallics* **1986**, 5, 253.
- 47 M. F. SEMMELHACK, in *Comprehensive Organometallic Chemistry II* (Eds.: E. W. ABEL, F. G. A. STONE, G. WILKINSON), vol. 12, Pergamon, Oxford, 1995, p. 979.
- 48 a) R. E. LEHMANN, J. K. KOCHI, *J. Am. Chem. Soc.* **1991**, 113, 501; b) D. ASTRUC, *Synlett* **1991**, 369.
- 49 a) J. K. KOCHI, R. RATHORE, P. LE MAGUERES, *J. Org. Chem.* **2000**, 65, 6826; b) P. LE MAGUERES, S. V. LINDEMAN, J. K. KOCHI, *J. Chem. Soc., Perkin Trans. 2* **2001**, 1180.
- 50 P. LE MAGUERES, S. V. LINDEMAN, J. K. KOCHI, *Org. Lett.* **2001**, 2, 3567.
- 51 M. B. ROBIN, P. DAY, *Adv. Inorg. Chem. Radiochem.* **1967**, 10, 247.
- 52 H. TAUBE, *Electron-Transfer Reactions of Complex Ions in Solution*, Academic Press, New York, 1970.
- 53 a) L. EBERSON, *Electron Transfer Reactions in Organic Chemistry*, Springer-Verlag, New York, 1987; b) L. EBERSON, S. S. SHAIK, *J. Am. Chem. Soc.* **1990**, 112, 4484; c) J. K. KOCHI, *Acta Chem. Scand.* **1990**, 44, 409; d) D. ASTRUC, *Electron Transfer and Radical Processes in Transition Metal Chemistry*, VCH, New York, 1995; e) S. F. NELSEN, in *Electron Transfer in Chemistry* (Ed.: V. BALZANI), Wiley-VCH, Weinheim, 2001, vol. 1, p. 342.
- 54 S. M. HUBIG, R. RATHORE, J. K. KOCHI, *J. Am. Chem. Soc.* **1999**, 121, 617.
- 55 I. R. GOULD, R. H. YOUNG, L. J. MUELLER, A. C. ALBRECHT, S. FARID, *J. Am. Chem. Soc.* **1994**, 116, 8188.
- 56 S. M. HUBIG, R. RATHORE, J. K. KOCHI, *J. Am. Chem. Soc.* **1997**, 119, 11468.
- 57 a) C. CREUTZ, *Prog. Inorg. Chem.* **1983**, 30, 1; b) For a recent organic application, see: S. V. LINDEMAN, S. V. ROSOKHA, D. SUN, J. K. KOCHI, *J. Am. Chem. Soc.* **2002**, 124, 843.
- 58 a) T. M. BOCKMAN, Z. J. KARPINSKI, S. SANKARARAMAN, J. K. KOCHI, *J. Am. Chem. Soc.* **1992**, 114, 1920; b) S. M. HUBIG, J. K. KOCHI, *J. Am. Chem. Soc.* **2000**, 122, 8279.
- 59 See ref. [4] and refs. therein.
- 60 a) E. K. KIM, J. K. KOCHI, *J. Org. Chem.* **1989**, 54, 1692; b) S. BROWNSTEIN,

- E. GABE, F. LEE, A. PIOTROWSKI, *Can. J. Chem.* **1986**, *64*, 1661.
- 61 S. V. ROSOKHA, J. K. KOCHI, *J. Org. Chem.* **2002**, *67*, 1727.
- 62 a) ref. [30]; b) S. FUKUZUMI, J. K. KOCHI, *J. Am. Chem. Soc.* **1981**, *103*, 7240; c) See also: S. FUKUZUMI, in ref. [23]; d) For a review, see L. J. ANDREWS, R. M. KEEFER, in ref. [23b].
- 63 P. B. D. DE LA MARE, *Electrophilic Halogenation*, Cambridge University Press, 1976.
- 64 G. A. OLAH, R. MALHOTRA, S. C. NARANG, *Nitration: Methods and Mechanisms*, VCH, New York, 1989.
- 65 a) H. FEUER (Ed.), *Chemistry of the Nitro and Nitroso Groups*, Wiley, New York, 1969; b) S. CHOWDHURY, H. KISHI, G. W. DILLOW, P. KEBARLE, *Can. J. Chem.* **1989**, *67*, 603.
- 66 D. L. H. WILLIAMS, *Nitrosation*, Cambridge University Press, 1988; cf. J. H. ATHERTON, R. B. MOODIE, D. R. NOBLE, *J. Chem. Soc., Perkin Trans. 2* **1999**, 699, *ibid.* **2000**, 229.
- 67 T. LUND, L. EBERSON, *J. Chem. Soc., Perkin Trans. 2* **1997**, 1435.
- 68 E. D. HUGHES, C. K. INGOLD, R. I. REED, *Nature* **1946**, *158*, 448, as reviewed in C. K. INGOLD, *Structure and Mechanism in Organic Chemistry*, 2nd ed., Cornell University Press, Ithaca, New York, 1969, pp. 320ff.
- 69 The stepwise activation process for ΔG_{ET} is:
- $$[\text{ArH}, \text{NO}]^+ \xrightleftharpoons{K_{ET}} \text{ArH}^{++} + \text{NO}^\bullet$$
- $$\rightleftharpoons \text{cyclohexadienyl cation with NO and H}, \text{ etc.}$$
- Note that, in this treatment, the energy of the pair of radicals $\{\text{ArH}^{++} + \text{NO}^\bullet\}$ is more or less equivalent to that of the σ -adduct, as previously established experimentally by their simultaneous observation by time-resolved spectroscopy. See S. M. HUBIG, J. K. KOCHI, *J. Am. Chem. Soc.* **2000**, *122*, 8279.
- 70 To account for the sizable deuterium kinetic isotope effect in aromatic nitrosation, see: E. BOSCH, R. RATHORE, J. K. KOCHI, *J. Org. Chem.* **1994**, *59*, 2529–2536.
- 71 Electron-rich arenes yield the most stable cation radicals, as indicated by their enhanced values of K_{ET} . Thus, the enhanced yields of arene cation radicals from electron-rich arenes will correlate with faster nitrosation rates.
- 72 a) Independent time-resolved (ps) spectroscopic studies have established the facile (homolytic) coupling of the arene cation radical (ArH^{++}) with NO_2^\bullet to form the σ -adduct, the second-order process of which occurs at diffusion-controlled rates. See: E. K. KIM, T. M. BOCKMAN, J. K. KOCHI, *J. Am. Chem. Soc.* **1993**, *115*, 3091; b) It is important to emphasize that the electron-transfer mechanism for aromatic nitration in Scheme 28 merely differs quantitatively from that originally proposed by Perrin [72c], in that the successor complex $[\text{ArH}^{++}, \text{NO}_2^\bullet]$ and not a pair of radicals $\{\text{ArH}^{++} + \text{NO}^\bullet\}$ is considered to be the reactive intermediate. For a quantitative delineation of this (kinetic) distinction, see: (c) C. L. PERRIN, *J. Am. Chem. Soc.* **1977**, *99*, 5516.
- 73 It is important to emphasize that the chemical behavior of the successor complex $[\text{ArH}^{++}, \text{NO}_2^\bullet]$ in Class II systems is more like that of the pair of free radicals $\{\text{ArH}^{++}$ and $\text{NO}_2^\bullet\}$. The extent to which the NO_2^\bullet moiety in the successor complex is already bent (i.e. substantially) will further facilitate collapse to the σ -adduct. In this regard, the successor complex in Class II systems is very different from the Class III pre-equilibrium complex $[\text{ArH}, \text{NO}]^+$, which exhibits ion-radical behavior only upon separation to the free $\{\text{ArH}^{++}$ and $\text{NO}^\bullet\}$ species [61].
- 74 E. BOSCH, J. K. KOCHI, *J. Org. Chem.* **1994**, *59*, 5573.
- 75 R. G. PEARSON, in *Nucleophilicity* (Eds.: J. M. HARRIS, S. P. McMANUS), *Adv. Chem. Ser.* **215**, American Chemical Society, Washington DC, 1987.

14

Oxidative Aryl-Coupling Reactions in Synthesis

Guillaume Lessene and Ken S. Feldman

Abstract

The oxidant-mediated coupling of electron-rich arene rings has served over several decades as a valuable procedure to access biaryl units. The complex mixtures of isomers that often plagued the earliest studies have gradually given way to synthetically useful product distributions upon application of more selective coupling protocols. Continual advances in the nature of the oxidant (and its attendant ligands) and more precisely defined reaction conditions have led to increasing levels of control upon C–C bond formation. Chemoselective (C–C *vs.* C–O bond formation with phenols; suppression of product oxidation), regioselective (*o-o'*, *vs.* *o-p'* *vs.* *p-p'* C–C bond formation), and, more recently, stereoselective (atropisomer-selective) biaryl bond formation can now be achieved in many well-defined systems. A survey of the more recent advances in these areas is presented.

14.1

Introduction

The biaryl moiety is a prominent structural feature in numerous naturally occurring and biologically active molecules. Strategies to achieve efficient syntheses of these essential structures have therefore been the focal point of much attention in recent years. Among all of the available methods, the venerable oxidative coupling of arenes, and, in particular, of phenols, is of special interest in view of the presumed reliance on this chemistry in the biosynthesis of these types of compounds. Therefore, biomimetic syntheses of biaryl fragments by oxidative coupling of diaryl precursors have been the goal of many studies within this field.

Considering the broad variety of substrates that take part in oxidative aryl coupling, the challenge has always been, and still is, achieving selectivity upon C–C bond formation. Whereas evolutionary pressures can be brought to bear in order to engineer an enzyme catalyst to promote formation of a single product, the *in vitro* mimicry of this reaction's specificity must address several issues, including over-oxidation, chemoselectivity, regioselectivity, and, finally, stereoselectivity. By examining both the history of this chemistry and the current state of the art of oxidative coupling reactions, some appreciation of how these different problems have been overcome can be realized.

The oxidative coupling of phenols has been known since the 19th century, but seminal studies carried out by Pummerer [1–8], who identified a phenolic radical as an intermediate of the reaction, initiated the modern age of mechanistic understanding in this area. It was then demonstrated that this radical mechanism also occurs in Nature, to produce complex biaryl-containing phenolics [9, 10].

Initially, the potent oxidizing agent potassium ferricyanide was used in this chemistry [11]. Anodic oxidation was examined concurrently as a synthetic tool [12] and later as an analytical method for demonstrating the existence of the phenoxyl radical [13, 14] in the course of mechanistic studies on these couplings. In addition to the earlier methods, phenolic oxidations using dioxygen, halogens, enzymes, etc., also were reported sporadically. The introduction of vanadium complexes (VOCl₃ [15], VOF₃ [16]) and later of thallium [17] and lead reagents [18] offered more reliable reactions and partially solved problems such as over-oxidation and regioselectivity of C–C bond formation between aryl rings. With the use of these reagents, and also by electrochemical methods, it also became possible to utilize phenol ethers in coupling reactions.

More recently, a new class of non-metallic oxidation reagents has been reported – the hypervalent iodine complexes [19]. Phenyliodine(III) diacetate (PIDA) and phenyliodine(III) bis(trifluoroacetate) (PIFA) have proven to be very efficient reagents that give rise to higher regioselectivity than other oxidants in some reactions and, more importantly, offer a mild and non-toxic alternative to the heavy metals.

A broad range of biaryl structures, as is often encountered in various classes of naturally occurring compounds, such as alkaloids, lignans, and tannins, can be prepared by oxidative aryl coupling. Oxidative couplings have also been used to build non-natural skeletons, such as the binaphthol derivatives that play an important role in asymmetric synthesis.

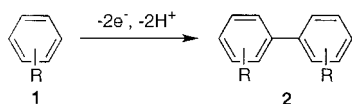
A large number of reviews have previously been published in the field of oxidative coupling reactions [11, 20–26]. In this chapter, current thinking on the different mechanisms involved in these types of reactions and the most recent developments in this field will be presented. Although the period of time between the earliest attempts, which resulted in non-selective and low-yielding reactions, and the more advanced approaches leading to mild, efficient, and regioselective Ar–Ar bond formation is quite significant (almost a century), most of the progress has been made only over the past two decades. The last few years have seen a real acceleration in methodological advances, especially in the area of stereoselection upon biaryl bond formation. Therefore, an important part of this chapter is devoted to the issues of atropisomerism and stereoselection that arise during the formation of a complex biaryl system. In addition, the latest work on catalytic systems that promote enantioselective biaryl coupling reactions is highlighted.

14.2

Mechanistic Overview

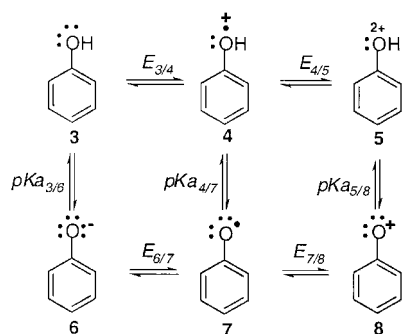
The oxidative coupling of two aryl units **1** leads formally to a loss of two electrons and two protons (Scheme 1).

Two different mechanisms are conceivable for the electron-transfer portion of this transformation: two “single-electron” transfers or one “two-electron” transfer. Moreover, when dealing with phenolic compounds, the pH (protonation state of the phenol) can also influ-



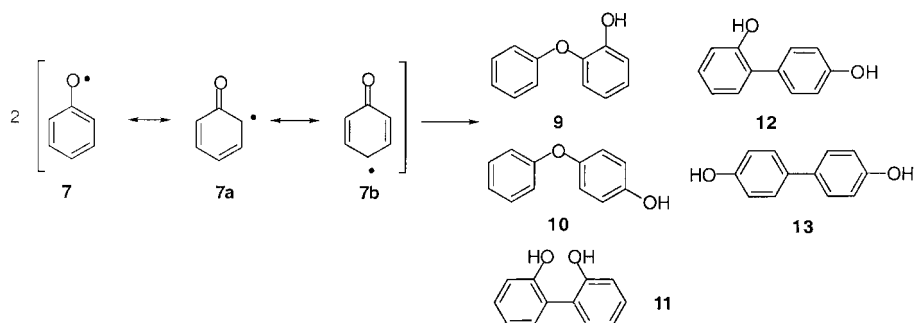
Scheme 1. The essentials of biaryl formation by oxidative coupling of arenes.

ence the mechanistic pathway taken. A mechanistic matrix (Scheme 2) underscores the different states of oxidation/protonation of a phenol unit, and illustrates how each component can be involved in the reaction. Identifying the initial oxidized aryl unit is important for understanding the coupling reaction.



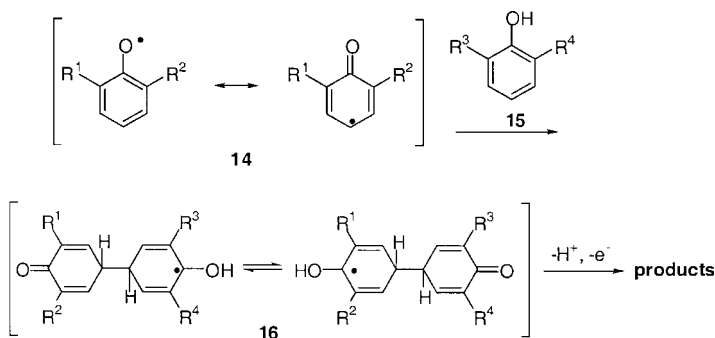
Scheme 2. A comprehensive schematic for phenol oxidation/deprotonation.

The first and most simplistic way of considering the coupling reaction was presented by Pummerer, who described the coupling of two radicals **7**. The mesomeric structures **7a** and **7b** of this intermediate help to rationalize the poor selectivity achieved when reagents such as potassium ferricyanide are used. The calculated electron density within **7** shows that coupling can occur via the oxygen atom (products **9** and **10**) as well as at the *ortho* and *para* positions of the aryl ring (products **11–13**, Scheme 3). However, substituents on the aromatic ring influence the choice of coupling position through steric and electronic effects. Thus, judicious selection/placement of substituents can limit the number of isomers obtained.



Scheme 3. Phenoxy radical coupling possibilities.

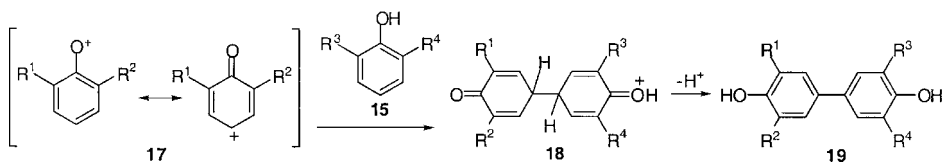
Generally, when two different aryl units are involved in a coupling reaction, the oxidation potentials of the two units will be different. In another mechanistic variant, the more easily oxidized phenol **14** can react with the other unperturbed aromatic unit **15** to furnish a “biaryl” radical **16**, which then oxidizes further, deprotonates, and finally tautomerizes to give the product biaryl (Scheme 4).



Scheme 4. Coupling of a phenoxy radical with an intact phenol.

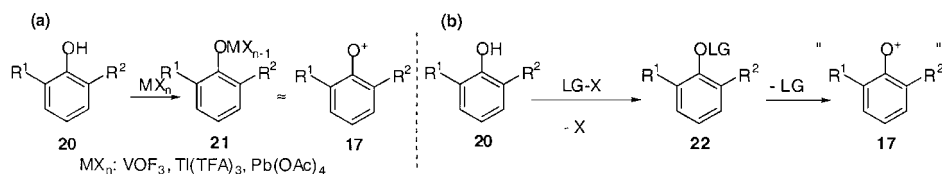
Oxidants that operate according to this one-electron oxidation mechanism include potassium ferricyanide in alkaline solution, cobalt, copper complexes with dioxygen, and some enzymes.

More involved studies of the oxidation of plant phenols [27], as well as the introduction of thallium and hypervalent iodine complexes and the use of electrochemical methods, have emphasized the importance of another intermediate involved in oxidative coupling reactions, namely the phenoxonium ion **8** [28–30]. Due to its ionic nature, reaction through an oxonium ion can improve the regioselectivity of bond formation and lead to fewer unwanted products (for example, no coupling via the oxygen atom). The coupling reaction can then be viewed as an electrophilic aromatic substitution between **17** and a nucleophilic aromatic unit **15** (Scheme 5).



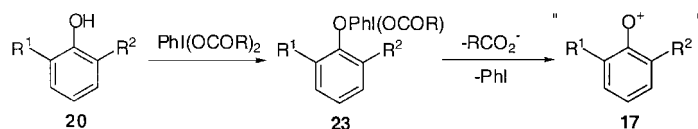
Scheme 5. Phenoxonium ion coupling chemistry.

Vanadium, thallium, and lead complexes might involve **17** or a metal-bound equivalent **21** as an intermediate, although mechanistic details remain obscure for most metal-based systems (Scheme 6a). Phenol derivatives bearing a leaving group on the alcohol, e.g. **22**, may also follow this mechanistic pathway involving a phenoxonium ion or an equivalent thereof. Hypervalent iodine reagents are commonly used in this context, as they have the advantage of being very efficient, mild, and non-toxic (Scheme 6b) [31].



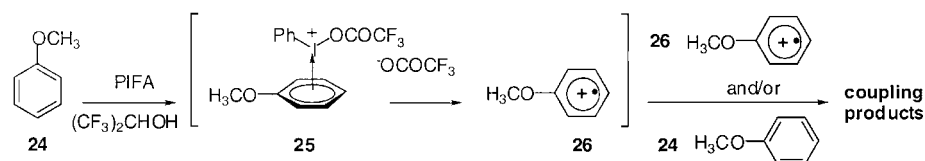
Scheme 6. Phenoxonium cation generation.

The question as to whether the reactive intermediate is the phenol–metal/leaving group complex **21/22** or the free phenoxonium ion **17** has been studied in the particular case of hypervalent iodine. Pelter and co-workers presented permissive evidence in support of a mechanism involving the free oxonium species **17** (Scheme 7): $\text{PhI}(\text{OAc})$ is an extremely good nucleofuge, no transfer of chirality is observed when homochiral hypervalent iodine compounds are used, and calculations made on the cation species correctly predict the regioselectivity of the substitution reaction [32, 33].



Scheme 7. Phenoxonium ion generation using hypervalent iodine precursors.

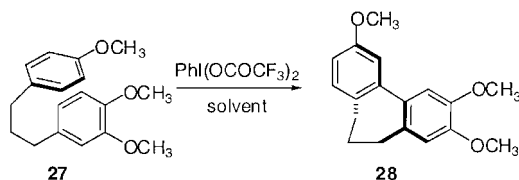
Biaryl formation through oxidative coupling of phenol ethers has also been explored. Although vanadium and lead complexes are known to effect these transformations [34], thallium reagents give the best results [35–37]. More recently, Kita and co-workers have developed the efficient oxidative coupling of phenol ethers using hypervalent iodine reagents activated by $\text{BF}_3 \cdot \text{Et}_2\text{O}$ [38, 39]. The formation of a single electron transfer (SET) complex **25** is proposed to occupy a central role in the mechanism of these reactions (Scheme 8) [40]. Coupling then occurs between two cation radicals **26** or between the cation radical **26** and a neutral phenol ether molecule **24** [41].



Scheme 8. Hypervalent iodine-mediated phenyl methyl ether oxidative coupling.

It is difficult to make generalizations about the oxidative coupling of arenes, given the number of possible mechanisms. Factors that influence the reaction course include the oxidation potential of each aryl unit, the substitution pattern, the solvent system, and the oxidation reagents themselves. Optimization then becomes a case-by-case effort in order to obtain the best selectivities and the best yields. Nevertheless, results over the last decade have

Tab. 1. PIFA-mediated intramolecular biaryl formation.



Solvent	Temp. (°C)	Yield of 28 (%)	
		No $\text{BF}_3 \cdot \text{Et}_2\text{O}$	Containing $\text{BF}_3 \cdot \text{Et}_2\text{O}$
$(\text{CF}_3)_2\text{CHOH}$	25	63	63
$\text{CF}_3\text{CH}_2\text{OH}$	−40	65	84
CH_3CN	−40	46	73
CH_2Cl_2	−40	25	91

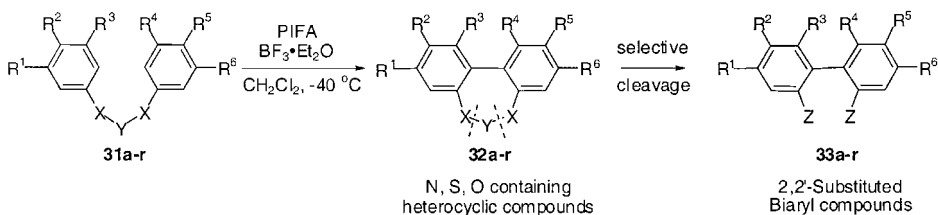
demonstrated that thallium, vanadium, lead, copper, and hypervalent iodine are the most general and reliable reagents for this kind of biaryl-forming reaction.

14.3

Oxidative Coupling Reactions with Hypervalent Iodine Reagents

In recent years, hypervalent iodine reagents have found increasingly broad application in a wide variety of reactions [31, 42, 43]. The oxidative coupling of phenols and phenol ethers is one important field in which these reagents have clearly been used to good advantage. Phenol ethers display only modest reactivity towards hypervalent iodine reagents, but Kita and co-workers have developed conditions under which they participate readily in such reactions [41, 44]. The key appears to be enhancing the electrophilicity of the iodine reagent by activation with $\text{BF}_3 \cdot \text{Et}_2\text{O}$ (Table 1). These conditions can be applied to a large range of phenol ether substrates (Table 2).

Table 3 shows the application of these intramolecular biaryl-forming conditions to the indirect synthesis of acyclic biaryls using a temporary tether strategy (Scheme 9). Silaketal tethers ($\text{Y} = \text{SiR}_2$ and $\text{X} = \text{O}$, **31a–f**) react efficiently to give the biaryl unit. A sulfide derivative ($\text{Y} = \text{S}$, $\text{X} = \text{CH}_2$, **31g**) led to many oxidized products, but sulfoxides ($\text{Y} = \text{SO}$,



Scheme 9. Removable tether strategy for biaryl formation.

Tab. 2. Substituent effects on the PIFA-mediated intramolecular oxidative cyclization of α,ω -biaryls.

29a-m **30a-m**

R^1	R^2	R^3	R^4	R^5	n	X	Yield 30 (%)
OCH ₃	H	OCH ₃	OCH ₃	H	1	CH ₂	91
	–OCH ₂ O–		–OCH ₂ O–	H	1	CH ₂	91
OCH ₃	OCH ₃	OCH ₃	OCH ₃	H	1	CH ₂	99
OCH ₃	OCH ₃	OCH ₃	OCH ₃	OCH ₃	1	CH ₂	92
OCH ₃	OCH ₃	OCH ₃	OTBS	H	1	CH ₂	75
OCH ₃	H	OCH ₃	OCH ₃	H	2	NCOCF ₃	89
OCH ₃	OCH ₃	OCH ₃	OCH ₃	H	2	NCOCF ₃	68
OCH ₃	OCH ₃	OCH ₃	OCH ₃	OCH ₃	2	NCOCF ₃	52
	–OCH ₂ O–		–OCH ₂ O–	H	1	NCOCF ₃	94
OCH ₃	OCH ₃	OCH ₃	OCH ₃	H	1	NCOCF ₃	85
OCH ₃	OCH ₃	OCH ₃	OCH ₃	OCH ₃	1	NCOCF ₃	85
OCH ₃	OCH ₃	OCH ₃	OTBS	H	1	NCOCF ₃	64
OCH ₃	OCH ₃	OCH ₃	OAc	H	1	NCOCF ₃	60

$X = \text{CH}_2$, **31h–k**) and sulfones ($Y = \text{SO}_2$, $X = \text{CH}_2$, **31l,m**) participated effectively in the oxidative coupling reaction. Dibenzyl ethers ($Y = \text{O}$, $X = \text{CH}_2$, **31n–r**) were also coupled in fair to good yields. Cleavage of the temporary tether subsequently delivers the acyclic biaryls **33a–r**.

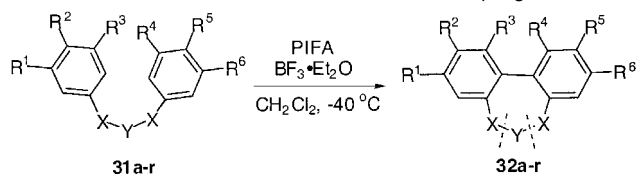
Recently, Kita and co-workers also applied the optimized PIFA/ $\text{BF}_3 \cdot \text{Et}_2\text{O}$ conditions to intermolecular coupling reactions [39]. Thus, several phenol ethers undergo dimerization through oxidative coupling in very good yields (Table 4). Apparently, the reaction leads to a single biaryl regioisomer. No reaction is observed when the ring is substituted by the electron-withdrawing group NO_2 (substrate **34d**).

For the coupling of binaphthyl compounds, the authors note that 0.55 equivalents of PIFA and a temperature below 0°C are necessary conditions to obtain the best yields (Table 5). Carbon–carbon bond formation occurs between the most highly oxygenated aryl rings of the naphthyl units.

The hypervalent iodine reagents PIFA and PIDA have also been used in the synthesis of naturally occurring structures, primarily the amaryllidaceae alkaloids and related species. Work by White's group showed the feasibility of this method for the synthesis of 6a-epipretazettine and (–)-codeine [45, 46]. In the early 1990s, Rama Krishna and co-workers demonstrated that PIDA can promote the oxidative phenolic coupling of diaryl substrates **38a–e** to deliver cyclohexadienones **39a–e**, respectively, in consistent 30 % yields for all of the substrates examined (Scheme 10) [47].

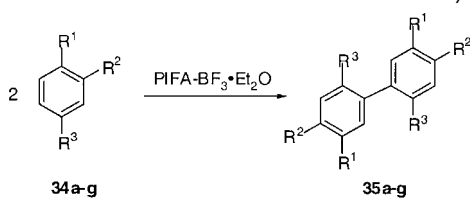
Kita and co-workers elaborated upon these earlier studies by examining substrates bearing a strategically placed nitrogen atom as a route to members of the amaryllidaceae alkaloid

Tab. 3. Substituent effects in the PIFA-mediated coupling of various linked biaryls.

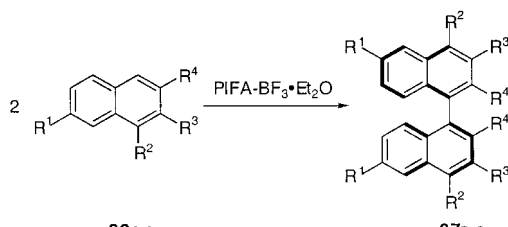


31	R ¹	R ²	R ³	R ⁴	R ⁵	R ⁶	X	Y	Yield 32 (%)
a	OCH ₃	OCH ₃	H	H	OCH ₃	OCH ₃	O	Si ⁱ Bu ₂	56
b		–OCH ₂ O–	H	H		–OCH ₂ O–	O	Si ⁱ Bu ₂	69
c	OCH ₃	OCH ₃	H	H		–OCH ₂ O–	O	Si ⁱ Bu ₂	46
d	OCH ₃	OCH ₃	H	H	OCH ₃	OCH ₃	O	Si ⁱ Bu ₂	81
e		–OCH ₂ O–	H	H		–OCH ₂ O–	O	Si ⁱ Bu ₂	89
f	OCH ₃	OCH ₃	H	H		–OCH ₂ O–	O	Si ⁱ Bu ₂	83
g	OCH ₃	OCH ₃	H	H	OCH ₃	OCH ₃	CH ₂	S	–
h	OCH ₃	OCH ₃	H	H	OCH ₃	OCH ₃	CH ₂	SO	73
i		–OCH ₂ O–	H	H		–OCH ₂ O–	CH ₂	SO	71
j	OCH ₃	OCH ₃	H	H		–OCH ₂ O–	CH ₂	SO	59
k	OCH ₃	OCH ₃	OCH ₃	H	OCH ₃	OCH ₃	CH ₂	SO	42
l	OCH ₃	OCH ₃	H	H	OCH ₃	OCH ₃	CH ₂	SO ₂	78
m		–OCH ₂ O–	H	H		–OCH ₂ O–	CH ₂	SO ₂	72
n	OCH ₃	OCH ₃	H	H	OCH ₃	OCH ₃	CH ₂	O	85
o		–OCH ₂ O–	H	H		–OCH ₂ O–	CH ₂	O	80
p	OCH ₃	OCH ₃	H	H		–OCH ₂ O–	CH ₂	O	51
q	OCH ₃	OCH ₃	OCH ₃	H	OCH ₃	OCH ₃	CH ₂	O	50
r	OCH ₃	OCH ₃	OCH ₃	OCH ₃	OCH ₃	OCH ₃	CH ₂	O	38

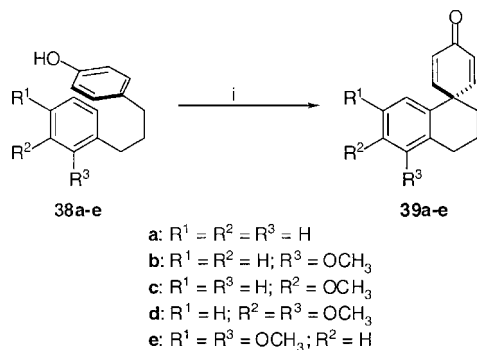
Tab. 4. Intermolecular PIFA-mediated oxidative aryl coupling.



34	R ¹	R ²	R ³	Time (h)	Yield 35 (%)
a	OCH ₃	OCH ₃	OCH ₃	1.5	92
b	OCH ₃	OCH ₃	CH ₃	1.5	93
c	OCH ₃	OCH ₃	Br	1.5	97
d	OCH ₃	OCH ₃	NO ₂	24	–
e	OCH ₃	CH ₃	OCH ₃	1.5	92
f	OCH ₃	Br	OCH ₃	1.5	91
g	Br	OCH ₃	H	3	72

Tab. 5. PIFA-mediated binaphthyl formation from substituted naphthyl ethers.


36	R ¹	R ²	R ³	R ⁴	Time (h)	Yield 37 (%)
a	H	H	H	OCH ₃	3	91
b	H	H	OCH ₃	OCH ₃	1.5	61
c	Br	H	H	OCH ₃	1.5	98
d	H	OCH ₃	H	H	3	94
e	OCH ₃	H	H	OCH ₃	3	82



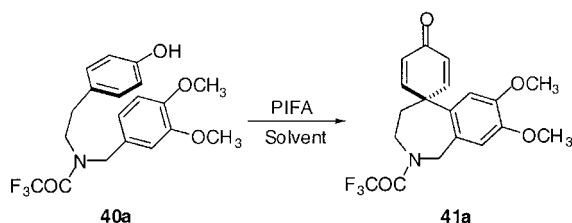
Reagents: i) PIDA, CH₃CN, reflux, 4hrs, 30%

Scheme 10. Cyclohexadienone formation from PIDA-mediated oxidative coupling of phenolic substrates.

family. In 1996, they described an exploration of the coupling of norbelladine derivative **40a** to afford tricyclic compound **41a**, an intermediate in the synthesis of amaryllidaceae alkaloids [22]. Apparently, the reactions only proceeded efficiently in (CF₃)₂CHOH at -40 °C using PIFA (see Table 6) [48]. Other solvents (CH₃CN, benzene, CH₂Cl₂, etc.) gave unsatisfactory results.

Subtle effects on the coupling efficiency exerted by the nitrogen substituent were uncovered. No Ar-Ar coupling products were observed with NCH₃ or unprotected nitrogen (Table 7).

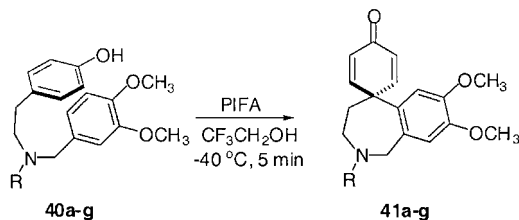
Further substrate variants were explored in order to ascertain the effect of the phenoxy substituents on coupling efficiency (Table 8). The subtle influence of remote substituents is again illustrated by these results, with both more electron-rich (R¹ = R² = TBDMS, **40j**) and more electron-deficient (R¹ = CH₃, R² = Ac, **40n**) analogues performing less satisfactorily than the parent dimethoxy ether **40a**.

Tab. 6. Solvent effects in the PIFA-mediated oxidative coupling of phenolic substrates.

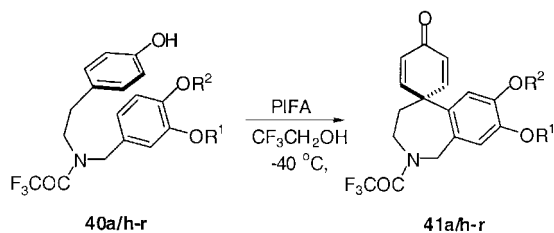
<i>Solvent</i>	<i>Yield (%)</i>	<i>Solvent</i>	<i>Yield (%)</i>
(CF ₃) ₂ CHOH	70	Et ₂ O	30
CF ₃ CH ₂ OH	61	DMF	18
CH ₃ CN	50	THF	15
C ₆ H ₆	44	C ₆ H ₅ CH ₃	14
CH ₂ Cl ₂	30	—	—

Finally, reactions with O-protected phenol **40** were studied, but only silyl ethers (**40s–u**, R = TMS, TBDMS) afforded the cyclohexadienone product **41** in good yield. Other protecting groups primarily yielded the biaryl coupling product **42** (Table 9).

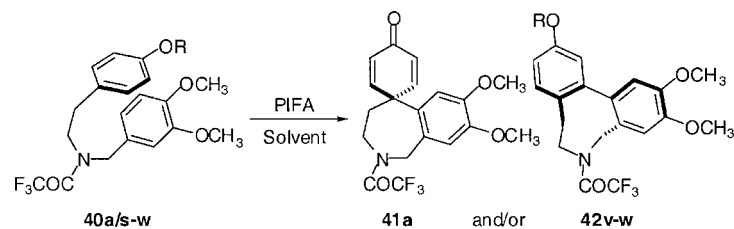
The authors proposed a mechanistic explanation for these different behaviors. For the case of the free phenol cyclization precursor **40a**, an ionic mechanism via intermediate **44** leads to the nucleophilic intramolecular *para* substitution product **41a** (Scheme 11). For the O-protected derivatives **40s–w**, an alternative mechanism leads to the formation of the cation radical **45**, which then participates in an intramolecular cyclization to deliver an activated

Tab. 7. Effect of remote nitrogen substituents on the PIFA-mediated coupling of phenolic substrates.

40	<i>R</i>	<i>Yield 41 (%)</i>
a	COCF ₃	61
b	CO ₂ ^t Bu	49
c	CO ₂ (CH ₂) ₂ TMS	54
d	CO ₂ Et	48
e	COC ₆ F ₅	50
f	CH ₃	—
g	H	—

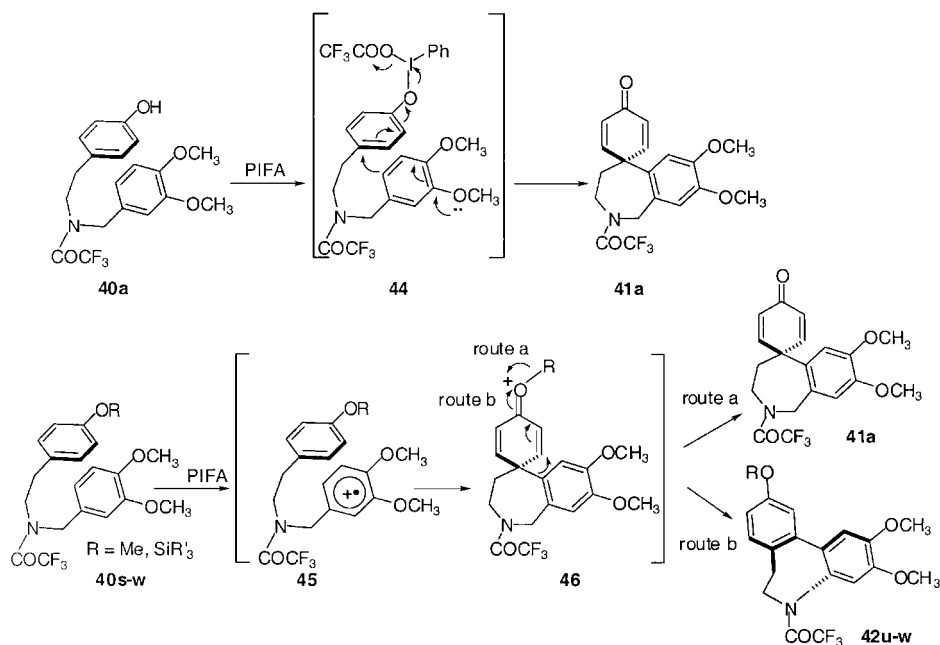
Tab. 8. Effect of various ether substituents on the PIFA-mediated coupling of phenolic substrates.

40	R ¹	R ²	Yield 41 (%)
a	CH ₃	CH ₃	61
h		–CH ₂ –	56
i	TBDMS	CH ₃	42
j	TBDMS	TBDMS	42
k	CH ₃	TBDMS	35
l	PhCH ₂	CH ₃	49
m	CH ₃	^t BuCO	32
n	CH ₃	CH ₃ CO	37
o	CH ₃ CO	CH ₃	Trace
p	H	CH ₃	19
q	CH ₃	H	Trace
r	H	H	Trace

Tab. 9. Effect of phenol ether substitution and solvent variation on the PIFA-mediated oxidative coupling of polyether substrates.

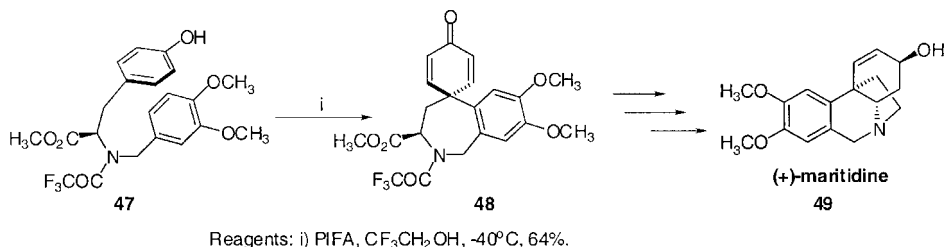
40	R	Solvent	Time	41a (%)	42 (%)
a	H	CF ₃ CH ₂ OH	5 min	61	–
s	TMS	CF ₃ CH ₂ OH	30 min	57	–
t	TBDMS	CF ₃ CH ₂ OH	4.5 h	66	–
u	TBDPS	CF ₃ CH ₂ OH	4 h	23	12
v	PhCH ₂	CF ₃ CH ₂ OH	24 h	–	48
w	CH ₃	CF ₃ CH ₂ OH	30 min	–	47
w	CH ₃	(CF ₃) ₂ CHOH	1 h	–	42
w	CH ₃	CH ₃ CN	3.5 h	33	23
w	CH ₃	CH ₂ Cl ₂	24 h	22	–

dienone intermediate **46**. This species proceeds towards the cyclohexadienone product **41a** in the case of $R = \text{TMS}$ or TBDMS (route a). In the case of $R = \text{CH}_3$ or PhCH_2 in poorly nucleophilic solvents, the reaction follows route b (1,2-aryl shift) to afford the biaryl compounds **42u-w** (Scheme 11).

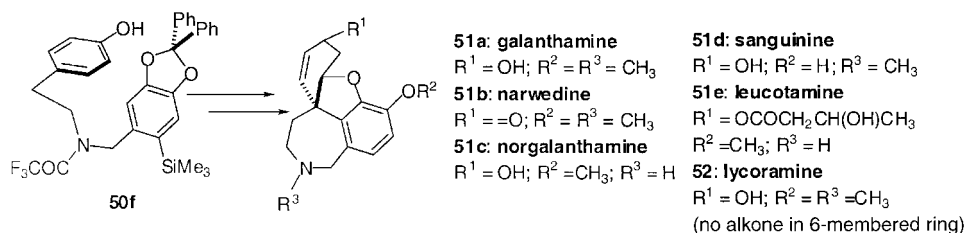


Scheme 11. Mechanistic speculation on the different pathways taken by phenolic and phenyl ether substrates in the PIFA-mediated oxidative coupling reaction.

The first application of this methodology in natural products synthesis involved the preparation of an essential intermediate **48** for the synthesis of (+)-maritidine (**49**) (Scheme 12) [38, 48, 49]. Other complex systems of the same family have been synthesized according to analogous strategies (Scheme 13). These oxidative phenolic coupling reactions encounter the problem of regioselectivity upon C–C bond formation. Incorporation of R_3Si - and CPh_2



Scheme 12. An approach to maritidine using PIFA-mediated aryl coupling.



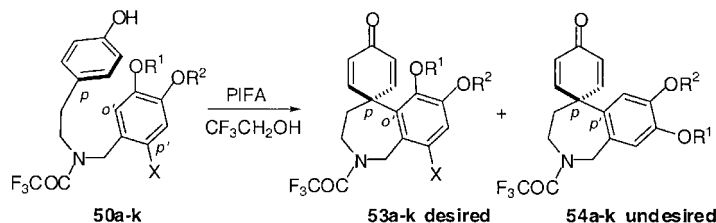
Scheme 13. Galanthamine-type alkaloids targeted by oxidative coupling methodology.

protecting groups (e.g. **50f**) was found to give the desired regioselectivity in the highest yield (Table 10). Exclusive *p-p'* coupling to deliver the undesired isomer **54** was obtained when the *p'* position was not blocked.

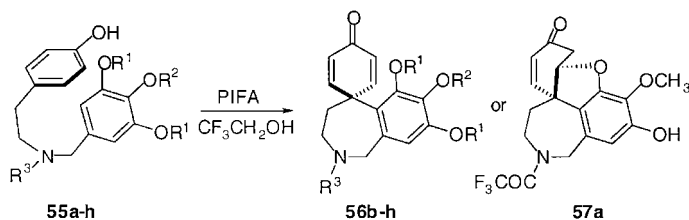
Very recently, Node and co-workers improved the efficiency of this particular oxidative phenolic coupling in the context of a synthesis of (\pm)-galanthamine (**51a**) [50]. By using a trialkoxyarene as one of the aryl units, they were able to obtain yields of **56b** of up to 90 % when the nitrogen was protected with a formyl group and the donor aryl's oxygen atoms were capped by benzyl moieties (Table 11). These authors were even able to isolate an interesting narwedine-type product **57a** in low yield.

A similar kind of strategy, as developed by Kita, has also been successfully applied in a diversity-oriented synthesis of galanthamine-like molecules (Scheme 14) [51]. The

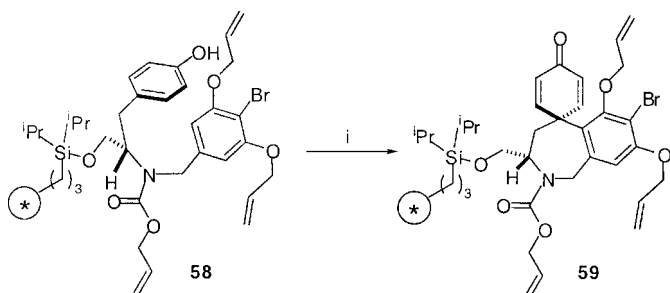
Tab. 10. Regiochemical control in the PIFA-mediated oxidative coupling of unsymmetrically substituted biaryl substrates.



Substrate				Isolated Yield (%)	
50	R^1	R^2	X	53 (<i>p-o'</i>)	54 (<i>p-p'</i>)
a	CH ₃	CH ₃	SPh	0	0
b	CH ₃	CH ₃	TMS	0	26
c	—CH ₂ —		Br	6	2
d	—CH ₂ —		SPh	0	0
e	—CH ₂ —		TMS	32	0
f	—CPh ₂ —		TMS	36	9
g	—C(CH ₃) ₂ —		TMS	46	12
h	—CPh ₂ —		H	0	60
i	—C(CH ₃) ₂ —		H	0	55
j	—CPh ₂ —		TES	37	0
k	—CPh ₂ —		TBS	28	0

Tab. 11. A higher-yielding PIFA-mediated oxidative cyclization approach to galanthamine-type alkaloids.

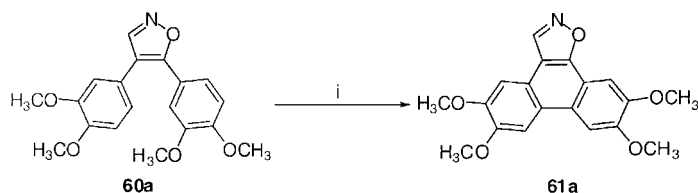
55	R ¹	R ²	R ³	Temp (°C)	Time (min)	Product	Yield (%)
a	H	CH ₃	COCF ₃	−20	20	57a	12
b	Bn	Bn	CHO	−40	120	56b	90
c	CH ₃	CH ₃	CHO	−40	15	56c	95
d	Bn	CH ₃	CHO	−40	60	56d	82
d	Bn	CH ₃	CHO	r.t.	15	56d	85
e	Allyl	CH ₃	CHO	−40	30	56e	48
f	MOM	CH ₃	CHO	−40	10	56f	43
g	CH ₃	CH ₃	COCF ₃	−40	120	56g	75
h	Bn	CH ₃	COCF ₃	−40	60	56h	53

Reagents: i) PIFA, (CF₃)₂CHOH-CH₂Cl₂, 23 °C⊙ = 500-600 micron
1% polystyrene**Scheme 14.** PIFA-mediated, solid-phase synthesis of galanthamine analogue precursors.

tris(allyl)-protected precursor **58** was cyclized under standard conditions. Pelish and co-workers took good advantage of the selectivity and the mildness of the hypervalent iodine reagent to perform the coupling without affecting the resin connection or other parts of the molecule.

In 1999, Dominguez and co-workers showed that phenanthro[9, 10-*d*] fused isoxazoles **61** and related pyrimidines **63** could be obtained from the biaryl isoxazoles **60** and biarylpyrimidines **62**, respectively, with PIFA as the oxidant [52]. This reagent proved to be the most efficient and afforded product mixtures from which the desired biaryl product could be iso-

lated most easily as compared to other oxidants (thallium tris(trifluoroacetate) (TTFA) 42–72 %, RuO_2 71 %, VOF_3 49–69 %, FeCl_3 80 %) (Scheme 15 and Table 12).



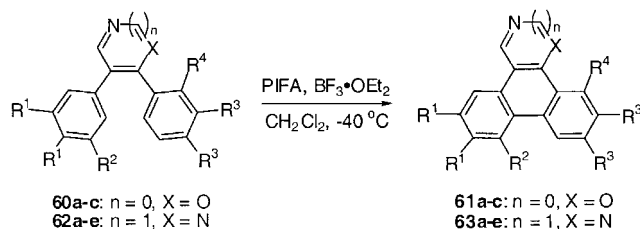
Reagents: i) PIFA (1.1 eq.), $\text{BF}_3 \cdot \text{OEt}_2$, CH_2Cl_2 , -40°C , 85%.

Scheme 15. Isoxazole-appended phenanthrene synthesis by PIFA-mediated oxidative cyclization.

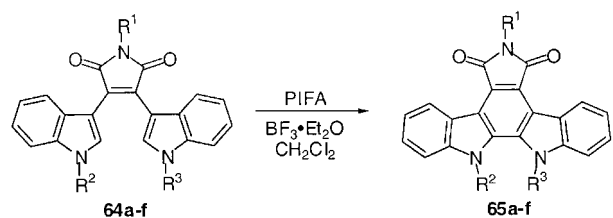
The authors pointed out the interesting fact that the coupling reaction between simple unsubstituted phenyl groups (**60b** and **62b**) forms the expected biaryl product only in the case of the pyrimidine link (e.g. **63b**). This observation suggests that the pyrimidine heterocycle but not the isoxazole analogue can provide sufficient stabilization for the putative radical cation intermediate.

These results prompted Faul and co-workers to investigate the intramolecular coupling of bis(indole)maleimides **64** to prepare indolo[2, 3-*a*]carbazoles **65** [53]. Modest yields were obtained, but the strategy nevertheless proved to be successful (Table 13). It is noteworthy that in the case of **64c**, the reaction proceeded in a slurry in solvents such as Et_2O or toluene and

Tab. 12. Isoxazole and pyrimidine synthesis by PIFA-mediated oxidative cyclization.



Substrate	R^1	R^2	R^3	R^4	Product	Yield (%)
60a	OCH_3	H	OCH_3	H	61a	85
60b	H	H	H	H	—	—
60c	H	H	OCH_3	H	61c	80
60d	OCH_3	H	OCH_3	OCH_3	61d	61
62a	OCH_3	H	OCH_3	H	63a	74
62b	H	H	H	H	63b	23
62c	H	H	OCH_3	H	63c	81
62d	OCH_3	H	OCH_3	OCH_3	63d	51
62e	OCH_3	OCH_3	OCH_3	H	63e	88

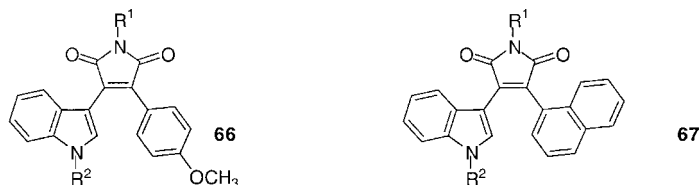
Tab. 13. Carbazole synthesis by PIFA-mediated oxidative cyclization of bis(indole)maleimides.


Substrate	R^1	R^2	R^3	Yield 65 (%)
64a	H	CH ₃	H	56
64b	H	CH ₃	CH ₃	30
64c	H	(CH ₂) ₃ OBn	H	37
64d	H	(CH ₂) ₃ OBn	CH ₃	30
64e	CH ₃	H	H	15
64f	H	H	H	0

that the commonly used solvent CF₃CH₂OH led to decomposition of the starting materials (Table 14). No reaction was observed in the case of 6-mono-substituted indoles (6-Cl, 6-F). Maleimides **66** and **67** (Figure 1) were not as reactive, and did not lead to the expected cyclization products.

Tab. 14. Solvent effects in the synthesis of bis(carbazole) **65c** from bis(indole) precursor **64c**.

Solvent	Yield 65c (%)
CH ₃ CN	20
CF ₃ CH ₂ OH	Decomp.
DMF	Decomp.
Et ₂ O	50
Toluene	40
THF	Decomp.

**Fig. 1.** Unreactive maleimide derivatives in the PIFA-mediated oxidative cyclization reaction.

14.4

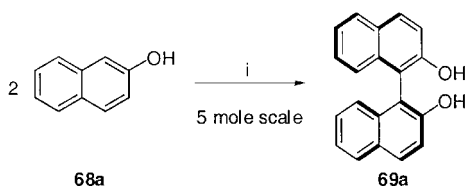
Other Reagents for the Oxidative Coupling Reaction

14.4.1

Iron(III)

Iron complexes remain in current use even though they were among the first reagents tested in the laboratory oxidative coupling of arenes. Despite the low selectivities described in the early papers, some groups have recently reported results that suggest that higher levels of regiochemical control can be attained.

For example, the synthesis of racemic binaphthyl moieties using iron reagents has been greatly improved from the initial Pummerer report [54]. Bjørnholm and co-workers presented a way of preparing binaphthol on a large scale in a minimal amount of solvent (THF) (Scheme 16) [55].



Reagent: i) $\text{FeCl}_3 \cdot 6\text{H}_2\text{O}$ 1.6 eq., THF $\sim 6 \text{ mol.L}^{-1}$, 60%.

Scheme 16. Large-scale iron(III)-mediated oxidative dimerization of 2-naphthol (**68a**).

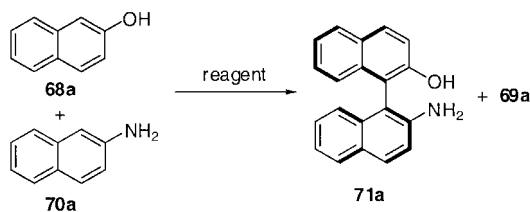
Reagent solubility is an issue in all of the syntheses involving iron-mediated oxidative coupling. The precedent cited in Scheme 16 uses THF as a good solvent for both $\text{FeCl}_3 \cdot 6\text{H}_2\text{O}$ and 2-naphthol. As a means of circumventing these solubility issues, Ding and co-workers devised a two-phase protocol for running the oxidative coupling reaction, whereby the iron reagent is dispersed in water [56]. Very high yields have been obtained with this method (Table 15).

The same authors subsequently reported the cross-coupling reactions between 2-naphthol (**68a**) and 2-naphthylamine (**70a**) [57]. The selectivity in favor of formation of the unsymmetrical product **71a** was good (Table 16). The authors rationalized this selectivity in favor of the cross-coupling product in terms of the formation of a pre-addition complex **72** between the naphthol and the naphthylamine (Figure 2). This explanation was later challenged by Smrcina and co-workers, who suggested that the energy levels of the molecular orbitals of the reaction components are the important factors for predicting the outcome of the reaction [58, 59].

The oxidative coupling reaction performed under these heterogeneous conditions is much more efficient than in the homogeneous case. The proposed mechanism involves an electron transfer to the surface of the iron reagent from the 2-naphthol. High concentrations of the radicals trapped at the surface may account for the high yields observed. These findings are related to Toda's work on coupling reactions with FeCl_3 in the solid state [60]. In 1997, Ras-

Tab. 15. Survey of iron(III) sources used in the two-phase oxidative dimerization of 2-naphthol (**68a**).

Oxidants	Fe ³⁺ : 68a	Temp. (°C)	Time (h)	Yield 69a (%)
FeCl ₃ ·6H ₂ O	2:1	50	1	95
FeCl ₃ ·6H ₂ O	1:1	50	1	90
FeCl ₃ ·6H ₂ O	1:2	50	1	85
FeCl ₃ ·6H ₂ O	1:2	50	1	80 ^a
FeCl ₃ ·6H ₂ O	2:1	r.t.	55	90
FeCl ₃ ·6H ₂ O	1:4	50	24	40
NH ₄ FeCl ₄ ·6H ₂ O	2:1	50	1	95
Fe(NO ₃) ₃ ·9H ₂ O	2:1	50	1	95
Fe(SO ₄) ₃ ·9H ₂ O	4:1	50	3	96
Fe(SO ₄) ₃ ·9H ₂ O	4:1	50	1	75
NH ₄ Fe(SO ₄) ₂ ·12H ₂ O	2:1	50	3	92
NH ₄ Fe(SO ₄) ₂ ·12H ₂ O	2:1	50	1	80

^a Conducted under an N₂ atmosphere.Tab. 16. Oxidative coupling of 2-naphthol (**68a**) and 2-naphthylamine (**70a**) by various iron(III) sources.

Fe ³⁺ : 72	T (°C)	time (h)	71a (%)	69a (%)
4:1	55	6	82	14
4:1	55	3	79	13
4:1	r.t.	6	71	14
2.2:1	55	3	71	19
4:1 ^a	55	3	63	19
4:1 ^b	55	3	31	23
4:1 ^b	55	3	42	30
4:1 ^b	55	3	57	18
4:1 ^c	55	5	39	39
4:1 ^d	55	3	78	20

^a Ultrasound (25 kHz) was employed;^b Fe₂(SO₄)₃·9H₂O, NH₄Fe(SO₄)₂·12H₂O and NH₄FeCl₄·6H₂O were the oxidants used;^c The reaction was performed in the solid state;^d **68a** and **70a** were added separately to the aqueous FeCl₃ solution.

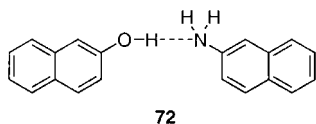


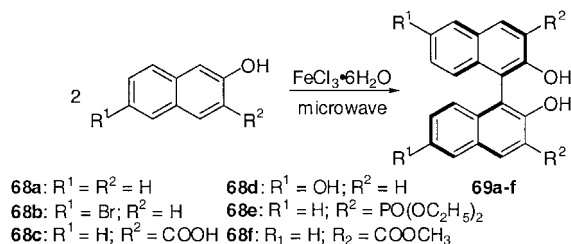
Fig. 2. A 1:1 complex between 2-naphthol (**68a**) and 2-naphthylamine (**70a**).

mussen reported an improvement of this procedure by performing the solid-state reaction in a ball mill to afford the binaphthol **69a** in 87 % yield from 2-naphthol [61]. Additional advances have also been achieved by the use of microwave irradiation in order to promote the solid-state reaction [62]. Several substituted 2-naphthols **68a–f** have been subjected to these conditions (Table 17).

Bushby has examined the FeCl_3 -mediated oxidation of hexyl-protected (Hex) phenol ether units in the preparation of triphenylene-based liquid crystals [63]. This strategy allows the formation of unsymmetrically substituted products **75a–l** (Table 18) [64]. The use of methanol in the work-up is critical in order to obtain the products in good yield. If the protecting group on the phenol component is isopropyl (**74m**), the coupling reaction occurs to give the unprotected phenols **76a–c** directly (Scheme 17) [65].

In a recent paper, the same authors showed that iron(III) chloride can mediate the oxidative coupling of substituted aryl ethers with an observed regioselectivity that depends on the substitution pattern [66]: *meta*-substituted phenol ethers **77** led to polymers (Scheme 18a) whereas *para*-substituted phenol ether **79** gave predominantly biphenyl structures (Scheme 18b). *ortho*-Substituted phenol ether **81** provided a dimer with the Ar–Ar bond at a position *para* to one of the methoxy substituents (Scheme 18c).

Tab. 17. Microwave-assisted oxidative dimerization of 2-naphthol derivatives by iron(III).

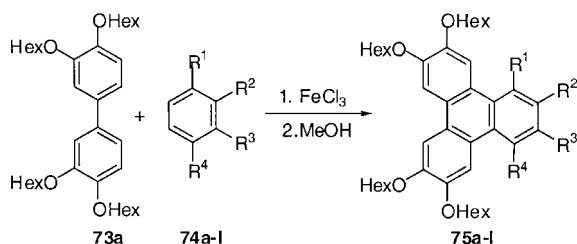


naphthol	Heating ^a	Microwave ^b	Microwave ^c
68a	70 °C, 1 h, 42 %	280 W, 30 s, 55 %	40 W, 30 s, 96 %
68b		280 W, 20 s, 76 %	40 W, 20 s, 95 %
68c		280 W, 100 s, 34 %	40 W, 100 s, 85 %
68d	70 °C, 1 h, >3 %	140 W, 140 s, 3 %	40 W, 140 s, 40 %
68e	70 °C, 1 h, 5 %	140 W, 140 s, 10 %	40 W, 140 s, 62 %
68f		140 W, 140 s, 34 %	40 W, 140 s, 84 %

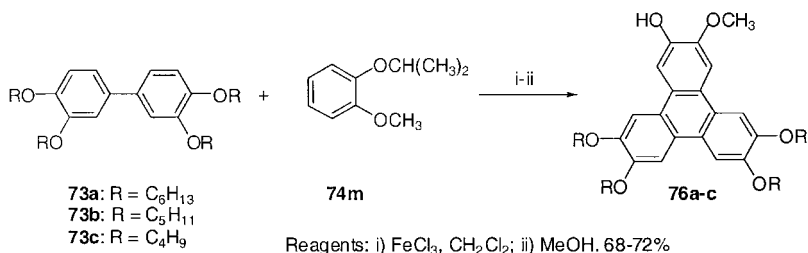
^aOil bath;

^bIrradiation with a commercial microwave oven;

^cIrradiation in a resonance cavity.

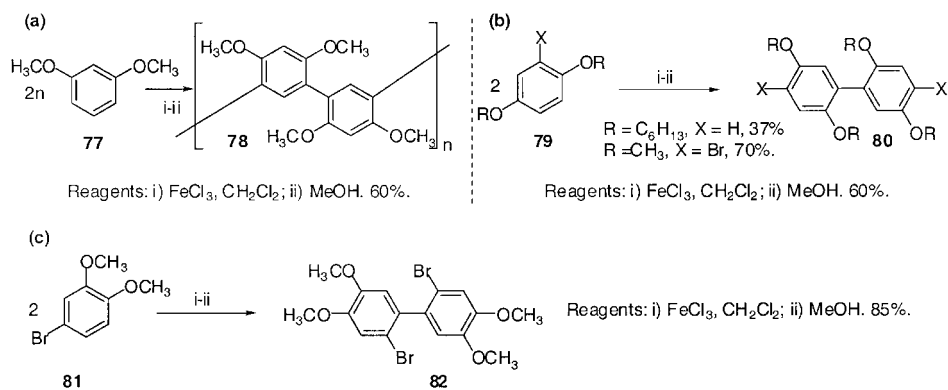
Tab. 18. Synthesis of triphenylenes **75** by oxidative coupling of biphenyl and phenyl ether components.

74	R ¹	R ²	R ³	R ⁴	Reactant Ratio (73a:74)	Yield (%)
a	H	CH ₃	CH ₃	H	xylene solvent	43
b	H	C ₆ H ₁₃	C ₆ H ₁₃	H	dihexylbenzene solvent	35
c	H	CH ₃	OCH ₃	H	1:12	63
d	H	CH ₃	OC ₆ H ₁₃	H	1:12	48
e	H	H	OCH ₃	H	1:9	5
f	H	Br	OCH ₃	H	1:12	40
g	H	–O–o–C ₆ H ₄ O–	H	H	1:6	25
h	CH ₃	CH ₃	OCH ₃	H	1:12	31
i	CH ₃	OCH ₃	CH ₃	H	1:12	40
j	OC ₆ H ₁₃	H	H	OC ₆ H ₁₃	1:4	13
k	CH ₃	OC ₆ H ₁₃	OC ₆ H ₁₃	H	1:2	73
l	F	OCH ₃	OCH ₃	H	1:3.5	67

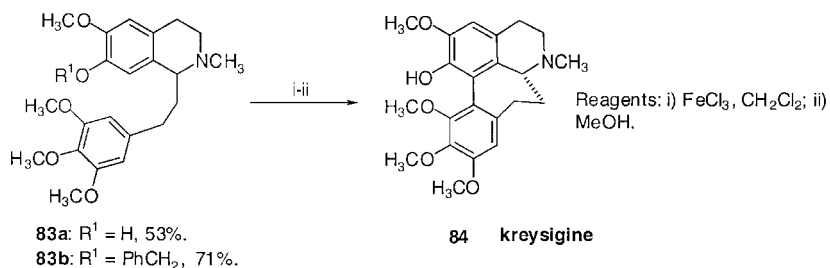
**Scheme 17.** Preparation of phenolic triphenylenes from phenyl isopropyl ether substrates and iron(III).

Some natural products have been synthesized by means of oxidative coupling promoted by iron reagents. In 1995, Herbert and co-workers reported the formation of the alkaloid kreysigine (**84**) by intermolecular oxidative coupling of diaryl substrates **83a/b** with iron(III) chloride followed by methanol work-up [67]. The yield for the free phenolic compound **83a** was 53 %, whereas the benzyl-protected analogue **83b** presumably cyclizes and then debenzylates, in an overall yield of 71 % (Scheme 19).

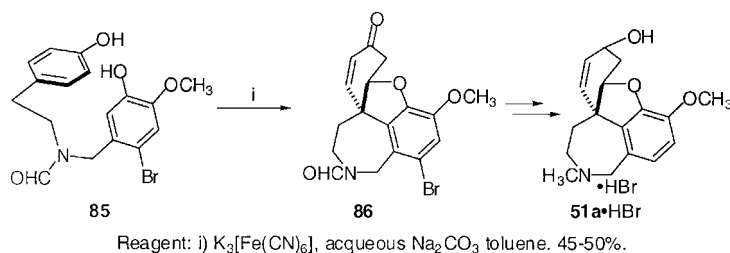
Galanthamine (**51a**) has also been targeted by an iron-mediated coupling strategy [68]. The reagent used was potassium ferricyanide and this procedure afforded the expected product **86** in 45–50 % yield on a 12 kg scale (Scheme 20). The bromine atom on **85** prevents the “wrong” regioisomer from forming. Evidently, this reaction is less efficient than the hyper-



Scheme 18. Iron(III)-mediated oxidative coupling of simple dimethoxyphenols.



Scheme 19. An approach to the synthesis of kreysigine by iron(III)-mediated intramolecular oxidative coupling.



Scheme 20. Large-scale route to galanthamine featuring an iron(III)-mediated oxidative cyclization.

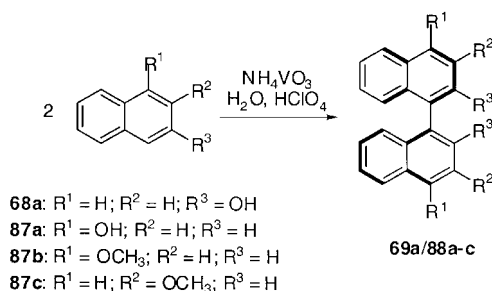
valent iodine version developed by Node (see Section 14.3) [50]. However, the reagents are inexpensive and the reaction is run in a mixture of toluene/aqueous Na_2CO_3 , conditions suitable for the large-scale synthesis of this interesting anti-Alzheimer's drug.

14.4.2

Vanadium, Thallium, and Lead

The coupling of 2-naphthol to give 2,2'-binaphthol has served as a testing ground for many oxidation protocols. For example, binaphthol has been prepared using vanadium reagents

Tab. 19. Vanadium-mediated oxidative dimerization of naphthol derivatives.

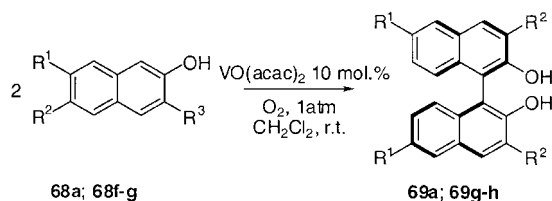


Substrate	Temp.	Time	Product	Yield (%)
68a (5 mM)	0–5 °C	3 min	69a	15
87a (2 mM)	r.t.	20 h	88a	78
87a (0.05 mM)	r.t.	20 h	88a	55
87b (1 mM)	r.t.	5 min	88b	95
87c (1 mM)	Reflux	2 h	88c	50
87c (1 mM)	r.t.	2 h	88c	65
87c (0.02 mM)	r.t.	2 h	88c	70

as well as the iron-based reagents discussed in the preceding section. Ammonium metavanadate in perchloric acid affords the coupled compounds **69a** and **88a–c** in good yields, as reported by Hazra and co-workers (Table 19) [69].

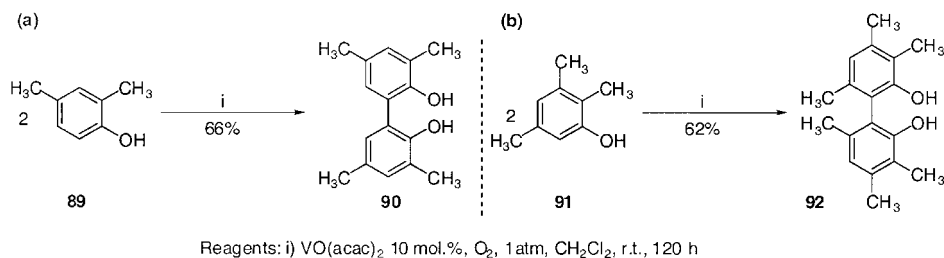
Recently, Uang and co-workers have published a catalytic version of this oxidative coupling [70]. Their goal was to minimize the amount of toxic vanadium used. Dioxygen has been found to be the reagent of choice to oxidize V(IV) to V(V) without interfering with the coupling reaction itself. Except for **68f**, with which the reaction is fairly inefficient, yields of coupled products are high (Table 20).

Tab. 20. Vanadium-mediated dimerization of various 2-naphthol derivatives.



naphthol	R^1	R^2	R^3	Time (h)	Product	Yield (%)
68a	H	H	H	24	69a	92
68f	H	H	CO_2CH_3	120	69f	35
68g	H	OCH_3	H	9	69g	76
68h	Br	H	H	24	69h	90

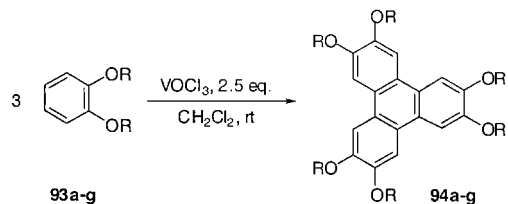
Oxidative coupling of simple monocyclic phenolic units is not as efficient by this method. Phenol itself does not undergo the reaction. Compounds **89** and **91**, however, lead to the desired *ortho-ortho* coupling products, **90** and **92**, respectively, in moderate yields (the starting phenol or decomposition products are also present at the end of the reaction) (Scheme 21).



Scheme 21. Vanadium(IV)-mediated dimerization of simple phenol derivatives.

In 1999, Kumar and co-workers published a new application of the reagent VOCl₃ to the synthesis of triphenylene structures by oxidative coupling. In the presence or absence of concentrated H₂SO₄, the reaction of phenol ethers **93** afforded moderate yields of the desired compounds **94** (Table 21) [71, 72]. The authors showed that 2.5 equiv. of VOCl₃ in CH₂Cl₂ at room temperature are the optimal conditions for this remarkable trimerization. Changes in the amount of reagent (higher or lower), other solvents, and/or lower temperatures led to

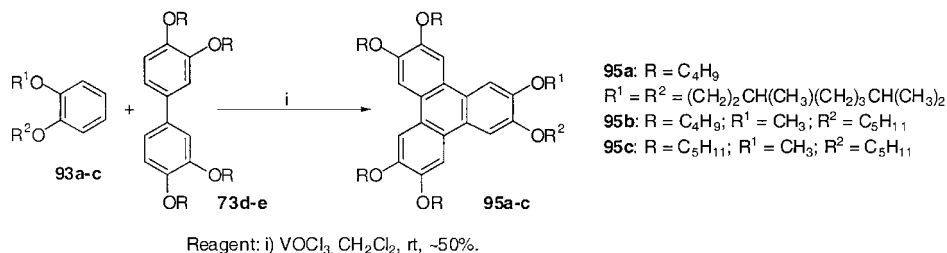
Tab. 21. VOCl₃-mediated trimerization of catechol ethers.



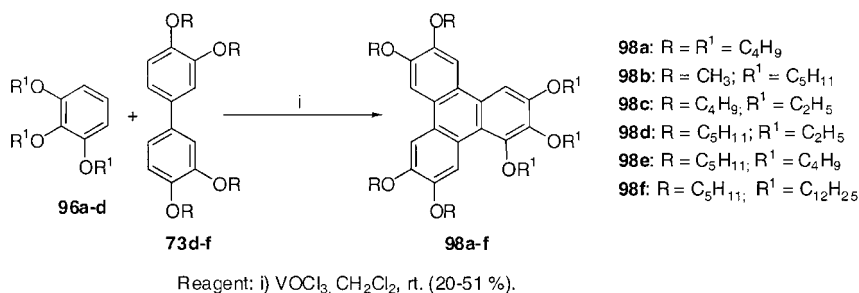
93	R	Yield (%)
a	C ₃ H ₇	53
b	C ₄ H ₉	86
b	C ₄ H ₉	79 ^a
c	C ₅ H ₁₁	85
c	C ₅ H ₁₁	83 ^a
d	C ₉ H ₁₉	56
e	C ₁₀ H ₂₁	70
f	C ₁₁ H ₂₃	70
g	(CH ₂) ₂ CH(CH ₃)(CH ₂) ₃ CH(CH ₃) ₂	65

^a In the presence of 0.4 % of H₂SO₄.

lower yields of the trimeric product **94**. Unsymmetrical triphenylene derivatives **95a–c** can be obtained in 50 % yield by applying this procedure to the biaryl substrates **93a–c** (Scheme 22). Related structures, such as heptaalkoxytriphenylenes **98**, could also be formed in similar yields (20–51 %) (Scheme 23).



Scheme 22. Triphenylene synthesis by VOCl_3 -mediated oxidative coupling of catechol ethers with biphenyls.



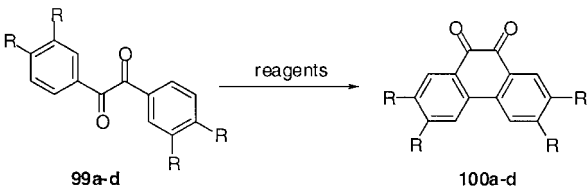
Scheme 23. Triphenylene synthesis by VOCl_3 -mediated oxidative coupling of trialkoxybenzenes with biphenyls.

Oxidative coupling was used to form alkyl- and alkoxy-substituted phenanthrenedione products **100a–d** (Table 22) [73]. These compounds can be obtained by other methods, albeit in much lower yields. In this instance, oxidative coupling proceeds even with carbonyl-substituted arenes, and VOF_3 gives much better results than thallium- or palladium-mediated coupling procedures.

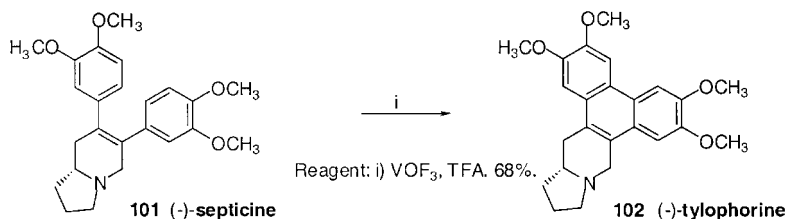
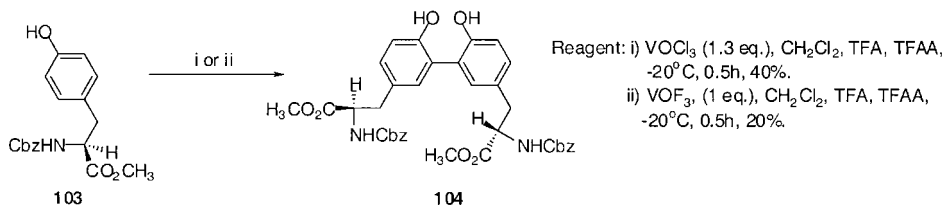
The use of VOF_3 in a mixture of CH_2Cl_2 and TFA allowed Comins and co-workers to complete the total synthesis of tylophorine (**102**), first in racemic form and then as a chiral compound [74, 75]. The oxidative cyclization of septicine (**101**) leads directly to tylophorine in 68 % yield (Scheme 24).

Syntheses of members of the biphenomycine family of antibiotics rely on the oxidative coupling of tyrosine derivatives. Edwards and co-workers have shown that VOCl_3 or VOF_3 can create the biaryl bond of **104** in yields of 40 % and 20 %, respectively, from the simple tyrosine derivative **103** (Scheme 25) [76].

Lead tetraacetate has shown its usefulness in the total synthesis of natural compounds. In a paper describing the preparation of several bioactive biphenyls such as magistophorenes

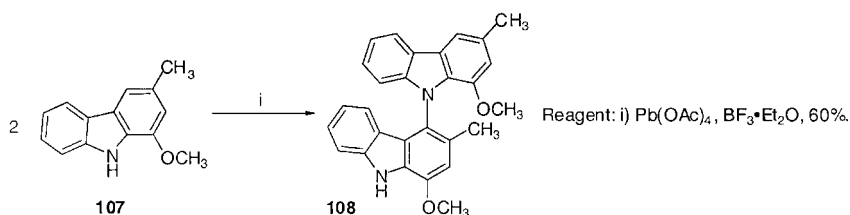
Tab. 22. Oxidative cyclization of benzil derivatives mediated by several oxidants.


99	R	Reagent/solvent	Yield 100 (%)
a	OCH ₃	VOF ₃ /CH ₂ Cl ₂	23
a	OCH ₃	VOF ₃ /(Cl ₂ CH) ₂	88
b	O- <i>i</i> -C ₅ H ₁₁	VOF ₃ /CH ₂ Cl ₂	82
c	OC ₆ H ₁₃	VOF ₃ /CH ₂ Cl ₂	86
d	OC ₁₀ H ₂₁	VOF ₃ /CH ₂ Cl ₂	91
d	OC ₁₀ H ₂₁	Tl ₂ O ₃ /CH ₂ Cl ₂	36
d	OC ₁₀ H ₂₁	Pd(OAc) ₂ /AcOH	0

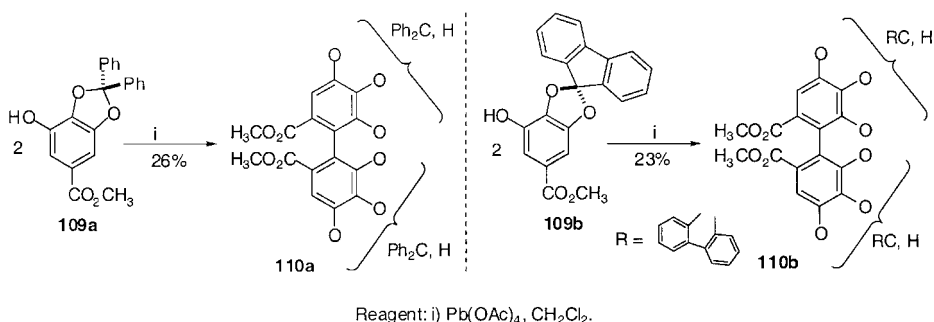
**Scheme 24.** The synthesis of tylophorine by vanadium(V)-mediated oxidative cyclization of septicine.**Scheme 25.** Oxidative coupling of a protected tyrosine substrate promoted by vanadium(V) reagents.

A/B (**206a/b**, Scheme 51) and alkaloids such as murrastifoline F (**108**), the results of Bringmann and co-workers emphasize the fact that the various oxidants are not interchangeable [77]. Thus, an interesting Pb(IV)-mediated homocoupling of the *O*-protected alkaloid murrayafoline A (**107**) provided murrastifoline F (**108**) in 60 % yield. Other oxidants (PIFA, VOF₃) failed in this reaction (Scheme 26).

Feldman and co-workers used lead tetraacetate to generate the biaryl products **110a,b** in a preparative study of the coupling reaction of methyl gallates **109a,b**, respectively, for the synthesis of members of the ellagitannin family (Scheme 27) [78]. The outcome of this reaction is strongly influenced by the substitution pattern on the ring. In the case of the sim-

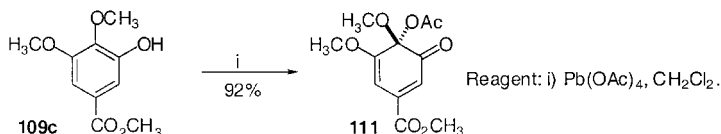


Scheme 26. The synthesis of murrastifoline by lead(IV)-mediated oxidative dimerization of murrayafoline.



Scheme 27. Lead(IV)-mediated oxidative dimerization of gallic acid derivatives.

ple methyl ether-protected gallate derivative **109c**, the product of the reaction is a quinone ketal **111** (Scheme 28). The bulkier protecting groups in **109a,b** favor nucleophilic attack on a putative “phenoxonium ion” intermediate from another aryl unit rather than acetate trapping.



Scheme 28. Lead(IV)-mediated oxidation (Wessely reaction) of a simple gallic acid derivative without biaryl formation.

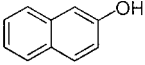
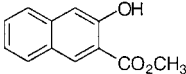
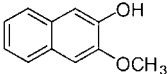
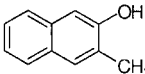
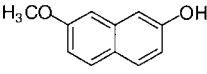
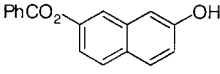
14.4.3

Copper(II)

Copper/amine complex-mediated oxidative coupling has received a lot of attention, especially in the binaphthol field after the work of Brussee [79, 80] and Feringa [81]. This reagent combination permits high yielding, clean, and regioselective oxidative homocoupling of many 2-naphthol derivatives. Cross-coupling reactions can also be performed.

Few examples of cross-coupling between differently substituted 2-naphthols were known when Hovorka and co-workers investigated this reaction in more detail. Anaerobic condi-

Tab. 23. Copper(II)/amine-mediated cross-coupling of variously substituted 2-naphthol derivatives.

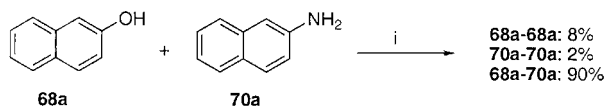
		
68a	68f	68g
		
68h	68i	68j

Substrates	T (°C)	t (min.)	Yield (%)	Selectivity 69 (%)		
68a/68f	50	30	97	f-f (5)	f-a (91)	a-a (4)
68f/68j	41	120	93	f-f (12)	f-j (88)	j-j (0)
68f/68i	50	110	95	f-f (5)	f-i (92)	i-i (3)
68f/68g	23	5	85	f-f (5)	f-g (89)	g-g (6)
68f/68h	23	120	80	f-f (5)	f-h (81)	h-h (14)
68a/68i	23	1440	80	a-a (25)	a-i (48)	i-i (27)

tions and the use of *tert*-butylamine or ethylamine in methanol allowed good selectivities for the unsymmetrical compounds (Table 23) [82].

These authors speculated that this high selectivity in favor of the cross-coupling product stemmed from the preferential formation of an intermediate radical from the electron-rich component [83, 84]. This radical would then react with the anion derived from the more electron-deficient species. Coupling between partners having similar electron density (e.g. **68a** and **68i**) resulted only in a statistical ratio of products. These authors also showed that the amine base could be substituted by NaOMe without affecting the reactivity or the regioselectivity. A significant observation from this work was that either the conditions are suitable and the reaction is fast and gives mainly the cross-coupling product, or the reaction is slow and gives mixtures of homo- and hetero-coupling products.

Research by Vyskocil and co-workers extended the naphthol cross-coupling reaction to mixtures of 2-naphthols and naphthylamines (Scheme 29) [85, 86]. In general, good selectivity in favor of cross-coupling over homo-coupling was observed.



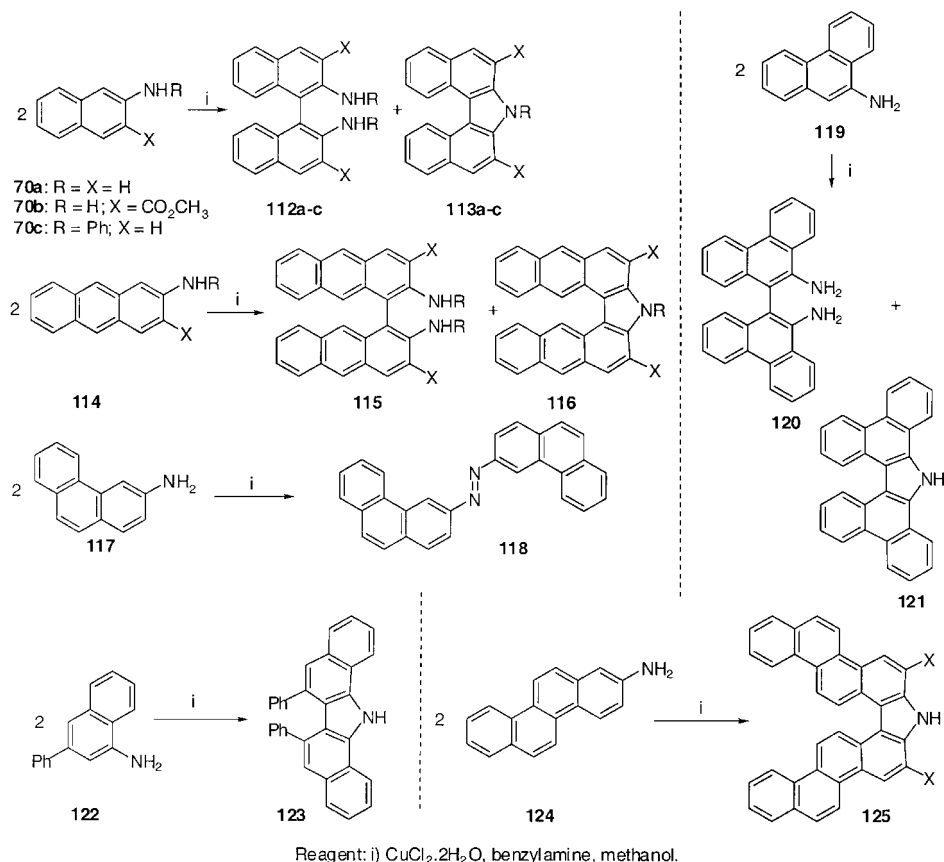
Reagent: i) CuCl₂, benzylamine, MeOH.

Scheme 29. Selective cross-coupling of 2-naphthol (**68a**) and 2-naphthylamine (**70a**) mediated by copper(II) and an amine base.

In a comprehensive study of these cross-coupling reactions with 2-naphthol derivatives, and as a response to Ding's advances on the same transformation using iron reagents [57], Vyskocil and co-workers presented a rational explanation for the outcomes of the different

reactions [58, 59]. The ease of oxidation of each molecule is the deciding factor. In general, **68f**, which is least prone to generate a radical cation by one-electron oxidation, acts as an acceptor towards the intermediate radical cation formed from either **68a**, **70a**, **70b**, or **70c**. Similarly, simple 2-naphthol (**68a**) most probably participates as the radical cation component when it is combined with **70a** because **68a** is now the most easily oxidized species present. These considerations are related to the energy levels of the SOMO, HOMO, and LUMOs of these compounds. Examining the system from this MO perspective allows rationalization of the outcome of the reaction.

In a very recent paper, Vyskocil and co-workers focused on the homocoupling of aryl amines (Scheme 30) [87]. Although these electron-rich units were expected to follow the same reactivity patterns as their oxygenated counterparts, notable differences in the product distributions were seen. For example, formation of carbazoles **113a–c**, **116**, **121**, **123**, **125** was observed from oxidative coupling of naphthylamines **70a–c**, **114**, **119**, **122**, and **124**, respectively (Scheme 30 and Table 24).

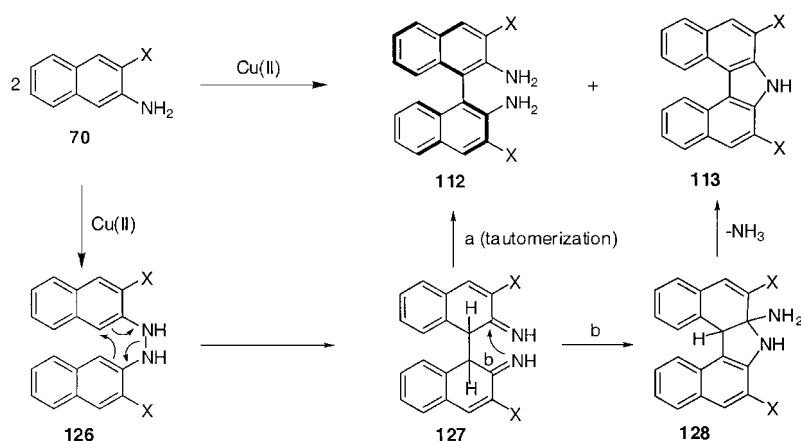


Scheme 30. Survey of copper(II)/amine-mediated oxidative dimerizations of various aryl amines.

Tab. 24. Product distributions from the copper(II)/amine-mediated oxidative dimerizations of the aryl amines indicated above.

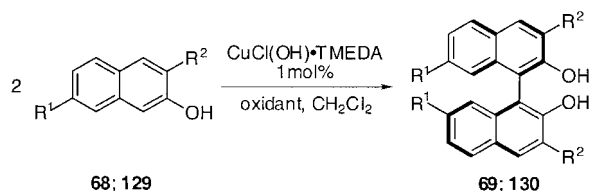
Substrate	Diamine (%)	Carbazole (%)	Other (%)
70a	112a (58)	113a (~1)	–
70b	112b (26)	113b (21)	–
70c	112c (45)	113c (3)	–
114	115 (43)	116 (39)	–
117	–	–	118 (87)
119	120 (2)	121 (78)	–
122	–	123 (25)	–
124	–	125 (85)	–

The results seem to indicate that arylamines do not follow the same mechanism that presumably underlies the coupling of oxygen-substituted aryls. According to the authors, N–N dimerization (**70** → **126**) is a competitive pathway that is favored with hindered substrates. This N–N coupling can eventually lead to both the C–C coupled product (path a) and the carbazole product (path b). The ratio depends upon the structure of the starting material (Scheme 31).

**Scheme 31.** Proposed mechanism for both carbazole and binaphthyl formation upon exposure of naphthylamine derivatives to copper(II) and an amine base.

The use of only catalytic amounts of copper reagent in this oxidative coupling has also been described. Smrcina and co-workers showed that a catalytic cycle could be sustained by using AgCl as a stoichiometric oxidant for copper (see Section 14.6.4) [88]. Nakajima and Koga have improved the turnover of the reaction by using the complex CuCl(OH)·tetramethylethylenediamine (TMEDA) (1 mol %) and dioxygen as the oxidant [89]. This procedure provides a simpler and more efficient coupling reaction and affords the binaph-

Tab. 25. Copper(II)-catalyzed oxidative dimerizations of substituted 2-naphthol derivatives.

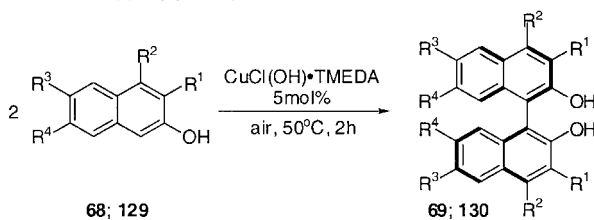


Substrates	<i>R</i> ¹	<i>R</i> ²	Oxidant	Time (h)	Temp.	Product	Yield (%)
68a	H	H	O ₂	8.5	0 °C	69a	90
68h	H	CH ₃	O ₂	1	r.t.	69h	92
68i	CH ₃ O	H	O ₂	1.5	r.t.	69i	96
68f	H	CO ₂ CH ₃	O ₂	96	reflux	69f	99 ^a
129	9-phenanthrol		O ₂	0.5	r.t.	130	79
68a	H	H	Air	20	0 °C	69a	96
68h	H	CH ₃	Air	1	r.t.	69h	96
68i	CH ₃ O	H	Air	2	r.t.	69i	95
68f	H	CO ₂ CH ₃	Air	144	reflux	69f	99 ^a
129	9-phenanthrol		Air	1.5	r.t.	130	77

^a Reaction was performed in CH₃OH.

thol compound in very high yield (Table 25). This protocol was later modified by removing the solvent and performing the reaction in the solid state (Table 26) [90]. Compared to oxidative coupling involving iron (Section 14.4.1) or vanadium (Section 14.4.2), this procedure offers some advantages. The catalytic character is clearly an improvement over the iron

Tab. 26. Copper(II)-catalyzed, solid-state oxidative dimerizations of substituted 2-naphthol derivatives.



Substrates	<i>R</i> ¹	<i>R</i> ²	<i>R</i> ³	<i>R</i> ⁴	Yield (%)
68a	H	H	H	H	92
68h	CH ₃	H	H	H	88
68f	CO ₂ CH ₃	H	H	H	93
68b	H	H	Br	H	92
68i	H	H	H	OCH ₃	92
129	-CH=CH-CH=CH-		H	H	89

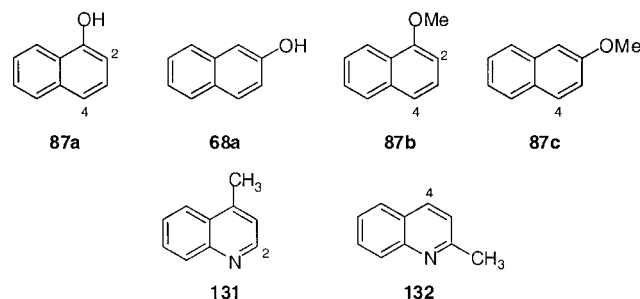
methods that require an excess of the reagent to drive the reaction to completion. Copper-based reagents are also less toxic than their vanadium analogues. Furthermore, the yields are more consistently high for the oxidative coupling of phenol derivatives. Nakajima et al.'s aerobic conditions (Table 26) are a simple and efficient way of creating the binaphthol unit.

14.4.4

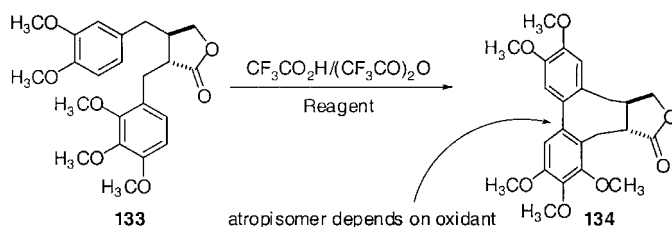
Electrochemical Methods

In principle, electrochemistry should be an effective method for initiating oxidative aryl coupling. It is easy to set the electrode to the right oxidation potential. However, this approach has not received a great deal of attention because of problems such as the formation of films around the electrodes that suppress the electrochemical reduction step. In 1993, Osa and co-workers published an electrocatalytic version of oxidative aromatic coupling. By using a 2,2,6,6-tetramethyl-1-piperidinyloxy- (TEMPO-) modified graphite felt, they succeeded in coupling naphthols and methyl quinolines with high conversions and high current efficiencies (Table 27) [91, 92].

Tab. 27. Electrocatalytic oxidative coupling of naphthalene and quinoline derivatives.



Substrates	Coupling	Current Efficiency (%)	Isolated yield of biaryl (%)
87a	2-2'	92	11
	2-4'		36
	4-4'		44
68a	4-4'	96	99
87b	2-2'	93	7
	2-4'		38
	4-4'		50
87c	4-4'	94	97
131	2-2'	92	95
132	4-4'	91	94

Tab. 28. Survey of oxidants for the intramolecular cyclization of stegane precursors.

Oxidant	Eq.	Time	Yield 134 (%)
$\text{RuO}_2 \cdot 2\text{H}_2\text{O}$	2	18 h	98
Ti_2O_3	0.52	30 min	73
$\text{Mn}(\text{OAc})_3 \cdot 2\text{HO}_2\text{O}$	1.9	15 min	84
$\text{Ce}(\text{OH})_4$	4.8	3 h	72
V_2O_5	4.8	5 d	87
Re_2O_7	1.9	3 h	98
$\text{Fe}(\text{OH})(\text{OAc})_2$	3.8	5 h	62
Co_3O_4	9.5	3 d ^a	78
$\text{CF}_3\text{CO}_2\text{Ag}$	14	1 d	86
CrO_3	3.8	6 d	71
$\text{Rh}_2\text{O}_3 \cdot 5\text{H}_2\text{O}$	4.8	14 d	39
IrO_2	4.8	16 d	77
Pr_2O_{11}	11.6 ^b	64 h	74
SeO_2	5	8 h	70
TeO_2	10	2 d	80
$\text{Cu}(\text{OAc})_2 \cdot \text{H}_2\text{O}$	3.8	1 d	22

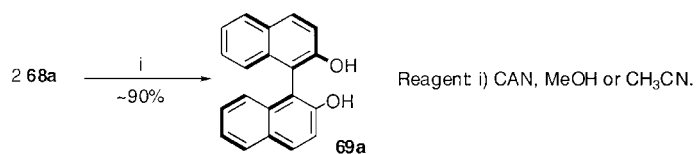
^a ultrasound;^b 11.6 eq. of PrO_2 .

14.4.5

Other Metals

Robin and Planchenault have studied oxidation procedures for non-phenolic biaryl coupling in extensive research directed toward stegane synthesis [93, 94]. This comprehensive study explored commonly used oxidizing reagents such as thallium and vanadium, as well as other metals ranging from ruthenium to tellurium (Table 28). The authors concluded that the intramolecular oxidative coupling of stegane precursor **133** was best accomplished with either ruthenium or rhenium reagents. However, changing the substitution pattern on the aryl rings led to different results: methylenedioxy-protected compounds gave better results with thallium, manganese, and cerium.

Titanium- and cerium-based reagents have been used to prepare binaphthol structures [95, 96]. Jiang showed that treatment of 2-naphthol (**68a**) with cerium(IV) ammonium nitrate (CAN) leads to the biaryl product **69a** in yields of around 90 % (Scheme 32). Cross-coupling of differently substituted naphthols can be accomplished using the same reagents, albeit in lower yields.

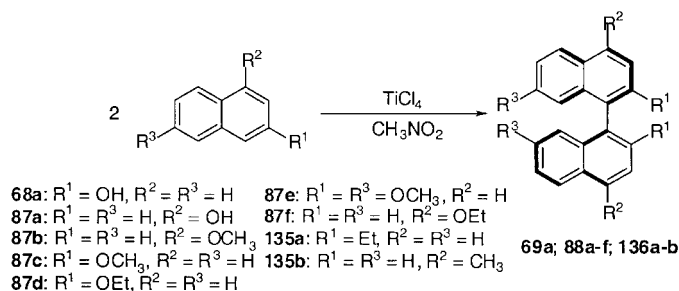


Scheme 32. Cerium(IV)-mediated oxidative dimerization of 2-naphthol.

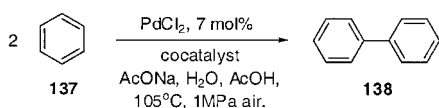
Doussot was the first to use TiCl₄ to generate binaphthalene structures from naphthalene precursors. For a large number of substrates, the reaction afforded the desired compounds in good to high yields (Table 29). These last two methods feature two new reagents for performing oxidative aryl couplings. Both use a stoichiometric (or greater) amount of oxidant, although it is worth noting that the titanium method is applicable to non-oxygenated substrates (**135a,b**).

Methods involving palladium-mediated oxidative coupling have been explored for the combination of non-phenolic aromatic units and for benzene itself. Mukhopadhyay and co-workers have shown that in the presence of a co-catalyst, a catalytic amount of PdCl₂ promotes the coupling between two benzene molecules in the presence of oxygen (air or dioxygen pressure) (Table 30) [97]. The co-catalysts and the presence of oxygen in solution prevent the formation of palladium black and aid in the regeneration of Pd²⁺. Although the mechanism of this reaction is extremely complex due to the number of components employed, the authors suggest that the μ -peroxocobalt(III) species **139** is formed initially, which then reacts

Tab. 29. Titanium(IV)-mediated oxidative dimerization of naphthol and naphthalene derivatives.

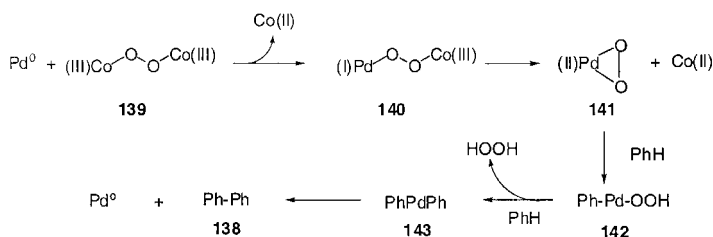


Substrate	TiCl ₄ (eq.)	Temp. (°C)	Time (h)	Product	Yield (%)
87d	2	50	0.8	88d	70
87c	2	50	1	88c	60
87e	1	20	18	88e	40
68a	1	40	4.5	69a	60
135a	1	20	48	136a	33
87f	2	20	1	88f	85
87b	1	20	18	88b	45
87a	1	20	18	—	—
135b	1	20	48	136b	30

Tab. 30. Palladium(II)-mediated dimerization of benzene in the presence of various co-catalysts.

Zr(OAc) ₄ (mol %)	Co(OAc) ₂ (mol %)	Mn(OAc) ₂ (mol %)	Acac (mol %)	Yield (%)
0	1.8	1.8	3.1	83
2.0	0	1.8	3.1	76
2.0	1.8	0	3.1	79
2.0	1.8	1.8	0	82
2.0	1.8	1.8	3.1	89

with palladium(0) to lead to the palladium(II)-peroxo complex **141** (Scheme 33). This complex inserts into a C–H bond of the benzene ring to furnish intermediate **142**, which, after insertion into another benzene C–H to yield **143**, undergoes reductive elimination to afford the biphenyl product **138**.

**Scheme 33.** Possible mechanistic course of the Pd(II)/Co(III)-mediated dimerization of benzene.

Reaction of methyl benzoate (**144**) with a palladium acetate/heteropolyacid mixture has been studied by Lee and coworkers [98]. They showed that aryl–aryl coupling occurs mainly at the 2-2' positions in the presence of various heteropolyacids (HPA; e.g. H₃PMo₁₂O₄₀, H₅PMo₉V₃O₄₀, H₅PMo₁₀V₂O₄₀, etc.) (Scheme 34). The selectivity in favor of the 2-2' coupling product is between 53 and 84 %, but the conversions are low (0.48 to 6.93) due to deactivation of the catalyst. The observed selectivity can be rationalized in terms of formation of the σ -palladium complex **146** with stabilization by the carbonyl group (Figure 3).

**Scheme 34.** Regioselective palladium(II)-mediated dimerization of methyl benzoate.

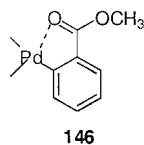
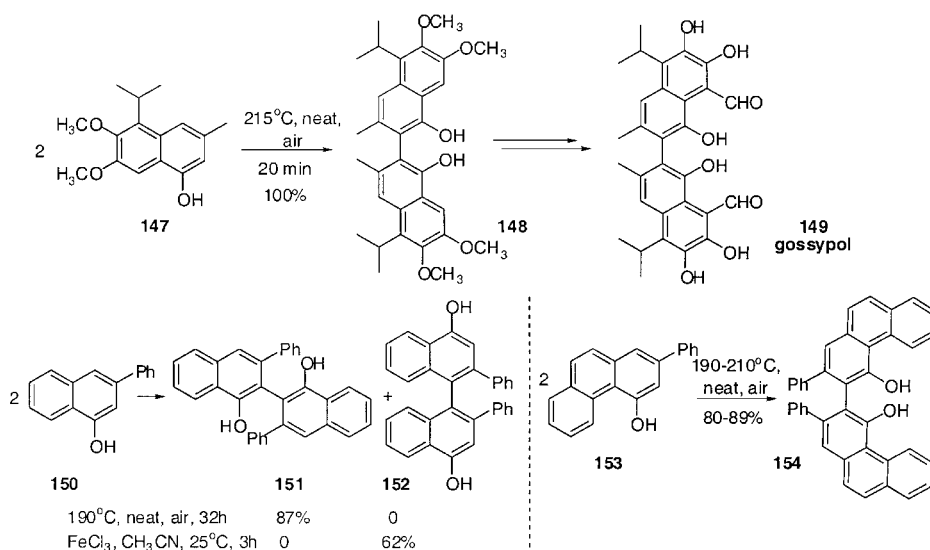


Fig. 3. The putative *ortho*-palladated benzoate intermediate in the dimerization of methyl benzoate.

14.4.6

Non-Metal Mediated Methods

Wulff and co-workers observed that the oxidative dimerization of **147** can be accomplished extremely efficiently when it is melted in a sealed tube in the presence of air, to furnish the biaryl product **148**, a precursor to the natural compound gossypol (**149**) (Scheme 35) [99]. The same reaction with iron(III) chloride gives low yields and a less clean product distribution. It is interesting to note that in the case of 3-phenyl-1-naphthol (**150**), the regioselectivity of the iron(III) chloride-mediated oxidation is completely different from that observed with O₂ as the oxidant, with the *para*-*para*-coupled product **152** being favored. This air oxidation procedure is also applicable to phenanthrol units (e.g. **153** → **154**), giving similarly high yields.



Scheme 35. Oxygen- and iron(III)-mediated dimerization of naphthol and phenanthrol derivatives.

Horseradish peroxidase (HRP) has also been used in an enzymatic process to create aryl-aryl bonds, especially for the synthesis of diiodotyrosine derivatives in a possibly biomimetic transformation [30, 100]. Here again, the regioselectivity of bond formation is an important issue and, depending on both the conditions and the substrate, C-C or C-O-coupling can occur. The effect of substituents *ortho* to the alcohol group has been studied by Sih and co-

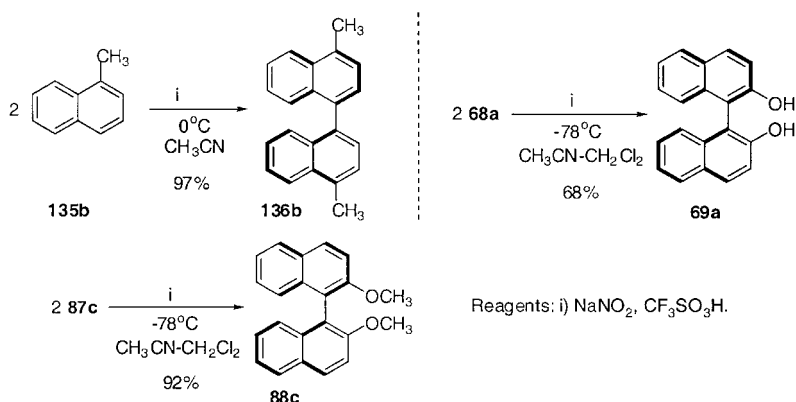
Tab. 31. Horseradish peroxidase-mediated oxidative dimerization of substituted tyrosine derivatives.

Substrate	X	pH	Cosolvent	Enz/Sub. (units/ μ mol)	Time (min)	156 (%)	157 (%)
155a	F	6	CH ₃ CN	6	40	56	
155b	Br	9	CH ₃ CN	6	40		40
155c	I	9	CH ₃ CN	6	60		75
155d	OCH ₃	9	–	1	10		48
155e	OMs	9	CH ₃ CN	6	40		35
155f	Cl	9	–	1	40	43	
155f	Cl	9	–	0.1	20		30

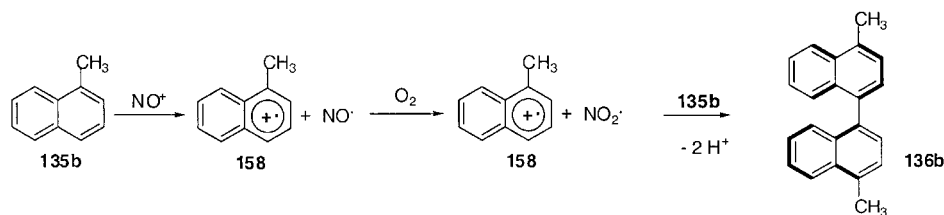
workers [100]. Except in the case of fluorine substitution (**155a**), the coupling of **155** is usually driven towards the C–C-bonded product **157** (Table 31). The chloride-substituted species **155f** represents a case where the enzyme/substrate ratio can influence the selectivity for C–C versus C–O bond formation.

The efficiency of HRP for the coupling of iodotyrosine derivatives has also been studied by Eickhoff, who extended the chemistry to include the formation of biaryl linkages between small peptides in low yields (5–6 %) [30]. Biaryl-containing peptide libraries were also prepared by HRP oxidative coupling of appropriate phenolic precursors.

An interesting use of NO⁺ as an oxidizing agent has been published by Tanaka and co-workers [101]. It was shown that 1-methylnaphthalene (**135b**) can be homocoupled in high yield using a mixture of NaNO₂ and CF₃SO₃H in acetonitrile. 2-Methoxynaphthalene (**87c**) and 2-naphthol (**68a**) were also coupled in high yields at –78 °C (Scheme 36).

**Scheme 36.** NO⁺-mediated dimerization of naphthalene derivatives.

It is noteworthy that naphthalene itself does not react efficiently (6 %) under these conditions and that 1-naphthol is too reactive, even at $-78\text{ }^{\circ}\text{C}$. Steric hindrance is also an important factor that tends to lower the yields and the regioselectivity. The removal of an electron from the aromatic ring by NO^+ triggers the coupling reaction. Oxygen is also involved in the proposed mechanism (Scheme 37).



Scheme 37. Proposed mechanistic course of the NO^+ -mediated dimerization of 1-methylnaphthalene.

14.5

Phase-Supported Oxidants

14.5.1

Reagents Supported on Inorganic Materials

A dispersion of copper sulfate on alumina has been studied by Sakamoto and co-workers for the oxidative dimerization of 2-naphthol derivatives [102, 103]. This heterogeneous reagent leads to the formation of binaphthols in very high yields (Table 32). These results show that the particular heterogeneous conditions indicated are favorable for the coupling of 2-naphthols. In related work, Lakshmi and co-workers have shown that Cu^{2+} -exchanged montmorillonite is an efficient supported copper reagent for the oxidative dimerization of naphthols (Table 32) [104]. Compared to all other methods of binaphthol formation, these supported phases certainly offer practical advantages. The products formed are easily isolated from the solid phase, which can be reactivated and reused.

One-electron oxidation of the naphthol substrate by copper(II) sulfate and coupling of the derived cation radicals seem to be the central steps of this reaction. The presence of dioxygen in the mixture may be important for the reactivation of the copper catalyst (oxidation of Cu(I) to Cu(II)).

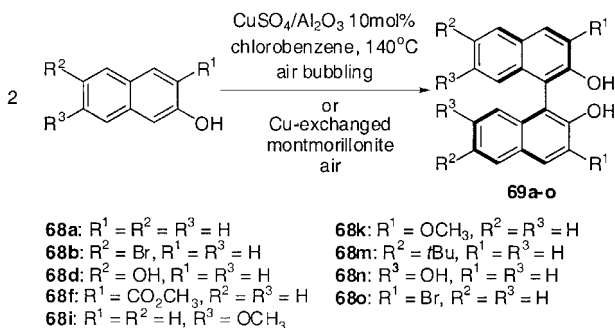
Iron(III) chloride has also been dispersed onto alumina and montmorillonite to perform the same kind of reaction [104, 105]. In a study of these reagents, Li and co-workers showed that similar yields could be obtained in very short reaction times (Table 33).

Zeolites (crystalline aluminosilicates) supporting oxidizing metals (Fe or Cu) have been introduced by Garcia and co-workers [106]. In particular, they showed that FeMCM-41 affords binaphthol from 2-naphthol as virtually the only product. Unfortunately, this compound is trapped in the zeolite pores and the isolated yields are lower than expected.

14.5.2

Polymer-Supported Hypervalent Iodine Reagents

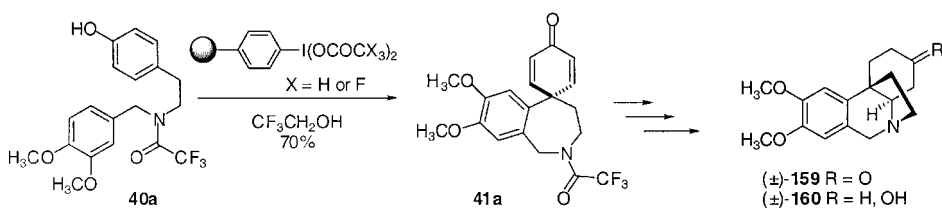
Ley and co-workers studied the applicability of immobilized phenyliodine(III) bis(acetate) as an oxidative coupling reagent in an effort to develop orchestrated multistep syntheses using

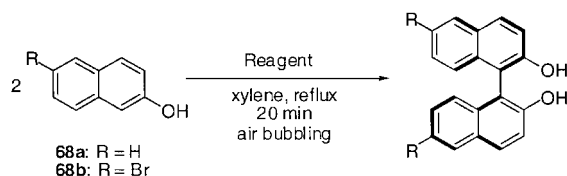
Tab. 32. Alumina and montmorillonite-supported copper(II)-mediated oxidative dimerization of 2-naphthol derivatives.

Substrate	Time (h)	Yield (%)	
		Al_2O_3	montmorillonite
68a	8	97	95
68b	2	98	91
68m	4	98	98
68n	15	93	40
68i	8	97	91
68k	18	41 ^a (94) ^b	—
68f	8	Trace(20) ^c	—
68o	8	d	—
68d	8	e	—

^a Hexyl acetate used as solvent;^b at 160 °C for 8 h in hexyl acetate, $CuSO_4/68k = 2$;^c At 160 °C, $CuSO_4/68f = 2$;^d No reaction;^e Complex mixture of products obtained.

polymer-supported species [107–109]. They successfully applied this strategy in the synthesis of the alkaloids (±)-oxomaritidine (**159**) and (±)-epimaritine (**160**) (Scheme 38). The use of polymer-supported PIFA led to similar yields as those achieved with polymer-supported PIDA in this oxidative coupling reaction. This interesting extension of hypervalent iodine chemistry furnished the coupled products in yields comparable to those achieved using the

**Scheme 38.** Polymer-supported hypervalent iodine-mediated oxidative cyclization of a maritidine precursor.

Tab. 33. Supported iron(III)-mediated oxidative dimerization of 2-naphthol (**68a**) and its 6-bromo analogue (**68b**).

Catalyst (equiv.)	Substrate	Time (min)	Yield (%)
FeCl ₃ /Al ₂ O ₃ (0.2)	68a	20	90
FeCl ₃ /Al ₂ O ₃ (2.0)	68a	10	94 ^a
FeCl ₃ /Al ₂ O ₃ (0.2)	68b	10	91
Fe ³⁺ /mont. (0.2)	68a	180	93
Fe ³⁺ /mont. (0.2)	68b	50	98
FeCl ₃ /SiO ₂ (0.2)	68a	150	98
FeCl ₃ /SiO ₂ (0.2)	68b	180	98

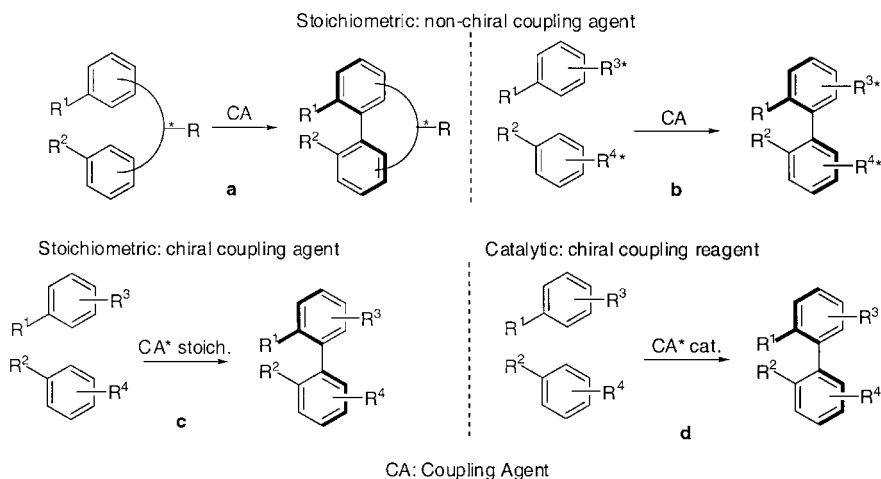
^a Carried out in toluene at 60 °C under nitrogen.

homogeneous version of the reaction (see Section 14.3), with the environmental advantage of a recoverable phase-supported reagent.

14.6

Control of Atropisomerism

In some instances of biaryl formation, *ortho,ortho'* substituents are sufficiently sterically encumbering to restrict rotation about the Ar–Ar linkage. These systems display axial chirality, and the process of atropisomerism through Ar–Ar bond rotation becomes important [110, 111]. Controlling the atrop-selectivity of an oxidative coupling reaction is a key criterion for success in many natural products synthesis endeavors. Such control in biosynthesis is implied, of course, by the existence of single diastereomers of the many biaryl-containing natural principles, and consequently in vitro mimicry of this stereochemical feature is a central element of many biomimetic approaches to natural product targets. To date, two distinct ways of achieving such control have been explored. On the one hand, stereochemical information can be transferred from resident chirality in the precursor. The existing stereogenic center(s) can be incorporated within a backbone element of the structure or can be attached via a removable tether to the molecular core (Scheme 39a). Other related approaches introduce a stereochemical bias by attaching a chiral auxiliary directly to one (or both) of the aryl rings (Scheme 39b). A conceptually distinct strategy for fixing atropisomer stereochemistry upon Ar–Ar bond formation involves the use of a chiral oxidation reagent (Scheme 39c). More interestingly, a catalytic version of these asymmetric reactions can also be envisaged (Scheme 39d). Many publications have appeared recently detailing progress on the first cases (chiral information built into the starting material). In addition, very interesting work relating to the second category (chiral oxidants) and, most recently, catalytic enantioselective couplings have been described.



Scheme 39. Strategies for the asymmetric oxidative coupling of aryl units.

14.6.1

Transfer of Chiral Information via the Molecular Backbone

The ellagitannins [112, 113], natural compounds belonging to the hydrolyzable tannin group of secondary plant metabolites, possess a hexahydroxydiphenoyl (HHDP) moiety **161** of (*S*) absolute configuration (Figure 4; for example, tellimagrandin II (**162**)). Therefore, they represent suitable targets for exploring oxidative coupling using this strategy.

Feldman and co-workers, after screening a wide range of oxidants and protective groups on 3,4,5-trihydroxylated benzoyls, demonstrated the ability of lead tetraacetate [78] to mediate the coupling between two diphenylmethyl ketal-protected galloyl moieties attached to a glucose-derived substrate. The stereoselectivity observed upon oxidative coupling in this biomimetic synthesis was thought to follow from the postulate originally proposed by Schmidt [114] and later refined by Haslam [115], which suggests that the stereochemical outcome of the reaction will be directed by the mutual orientation of the galloyl rings in the most stable conformation of the sugar/digalloyl precursor. The synthesis of a model system **164** (Scheme 40), combined with molecular modeling studies on a simplified model of the digalloyl coupling precursor **163** (e.g. **163a**), provided results consistent with this postulate [78, 116]. It is worth noting that in this example the coupling is not regioselective (with no consequence for

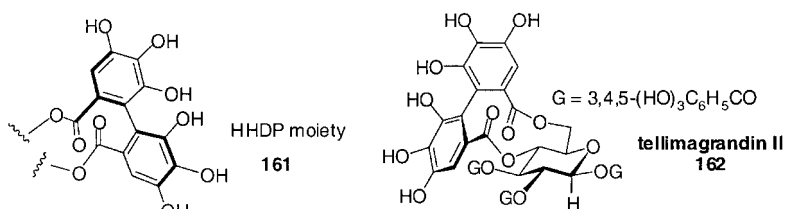
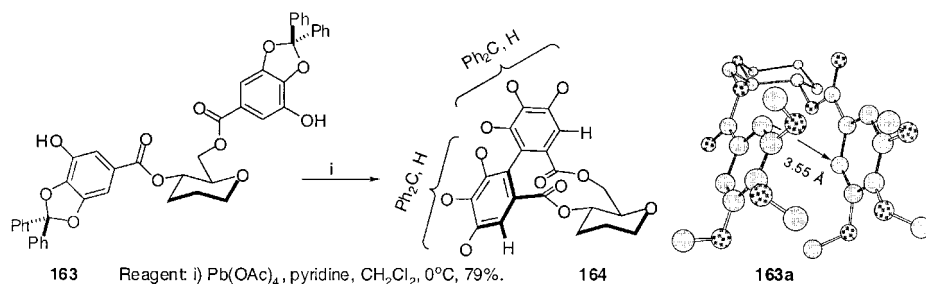


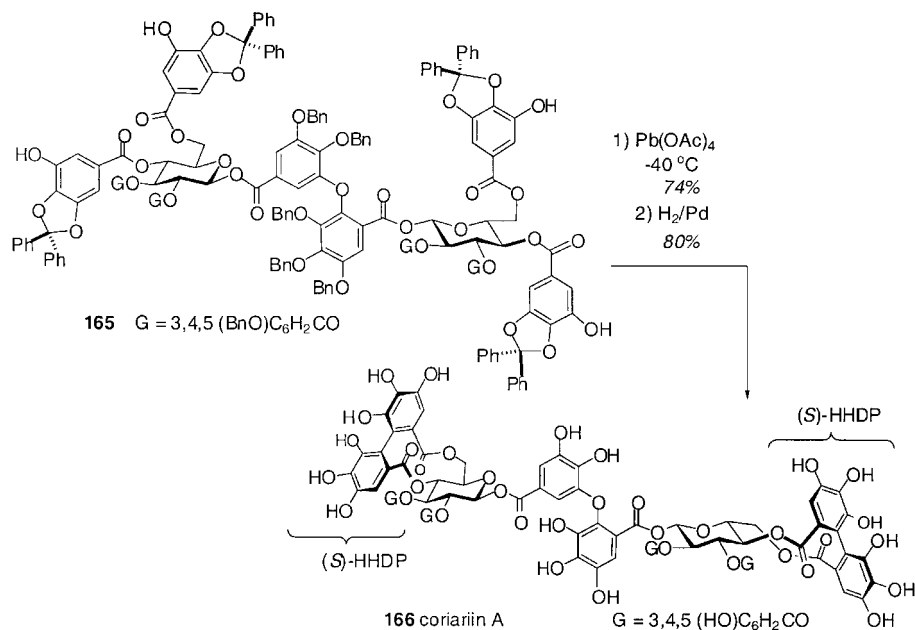
Fig. 4. Examples of (*S*)-hexahydroxydiphenoyl units.



Scheme 40. Stereoselective lead(IV)-mediated oxidative cyclization of a digalloyl pyranose substrate.

the synthesis itself as the protecting groups will be removed), although each regioisomeric biaryl is formed with the (*S*)-configuration.

More complex ellagitannins, such as the natural compounds tellimagrandin I (**162**) [117], sanguini H-5 [18], pedunculagin [118], and coriariin A (**166**) (Scheme 41) [119, 120] have also been synthesized by the lead tetraacetate oxidative coupling procedure, with the same favorable stereoselective (*S*)-biaryl bond formation.



Scheme 41. Application of the lead(IV)-mediated oxidative coupling of galloyl phenols to the synthesis of coriariin A.

Lignans represent another class of compounds that have attracted a lot of attention due to their potent antitumor activities [121]. Molecules such as steganone (**167**), steganol (**168**)

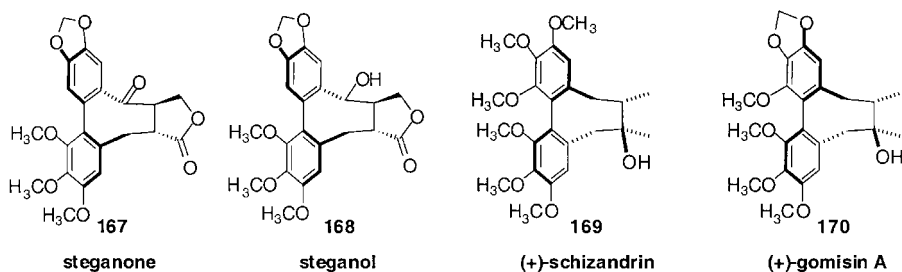


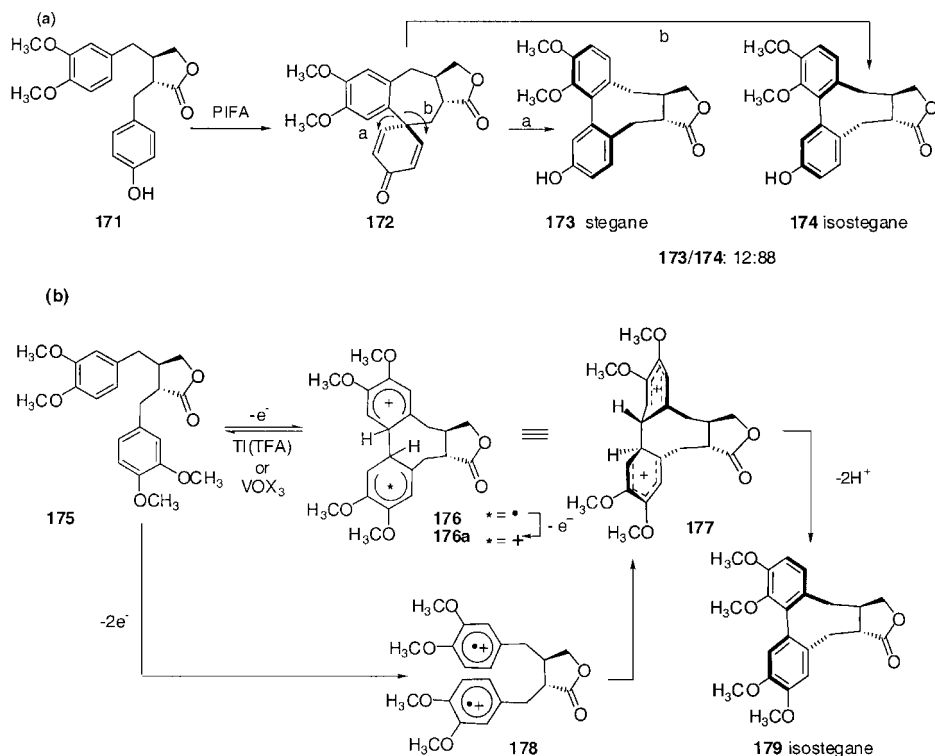
Fig. 5. Examples of stegane-type lignans.

[122, 123], schizandrin (**169**), and gomisin-A (**170**) [124] contain biaryl structures as part of a dibenzocyclooctadiene unit (Figure 5), making them compelling targets for biaryl oxidative coupling methodologies.

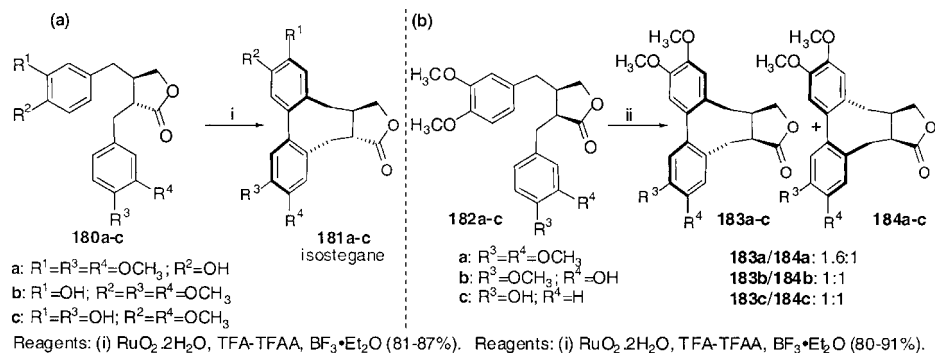
The control of atrop-selectivity upon oxidative coupling has been more challenging in these cases due to the fact that the energy barrier between the two atropisomers is rather low. The natural molecules themselves are sometimes actually present in the two forms (e.g. (+)-schizandrin and (+)-isoschizandrin). In some instances, the non-natural atropisomer is found to be the major coupling product under kinetic control of the reaction, even if the precursor bears the natural stereogenic centers on the butyrolactone moiety [111]. For a *para*-substituted phenol precursor such as **171**, the mechanism of oxidative coupling involves the formation of a spirodienone intermediate **172**. The subsequent rearrangement of this species to the biaryl products **173** and **174** then occurs with migration of the indicated C–C bond in one of two directions (a or b), leading to a mixture of atropisomers usually favoring the non-natural configuration shown in **174** (Scheme 42a) [125]. Buckleton and co-workers have proposed another mechanism for non-phenolic substrates such as **175**. In this case, they hypothesized that either one “two-electron” oxidation (**175** → **178**) or two “one-electron” steps (**175** → **176** → **176a**) can lead to the dication **177**, which then forms the biaryl **179** by proton loss (Scheme 42b). Buckleton posits that the interactions between bridgehead hydrogens (away from each other in intermediate **177** (Scheme 42)) favor the isostegane-like series [37].

Ward, Pelter, and co-workers have documented the efficacy of in situ generated ruthenium tetrakis(trifluoroacetate) (following the work of Robin and Landais) [126, 127] as a useful reagent for the synthesis of a large number of stegane-like molecules [123]. In the *trans*-fused butyrolactone series **180**, single diastereomers **181** are usually obtained (Scheme 43a). If *cis*-fused butyrolactones **182** are used as precursors, the biaryl products are formed as a mixture of atropisomers **183** and **184** (Scheme 43b).

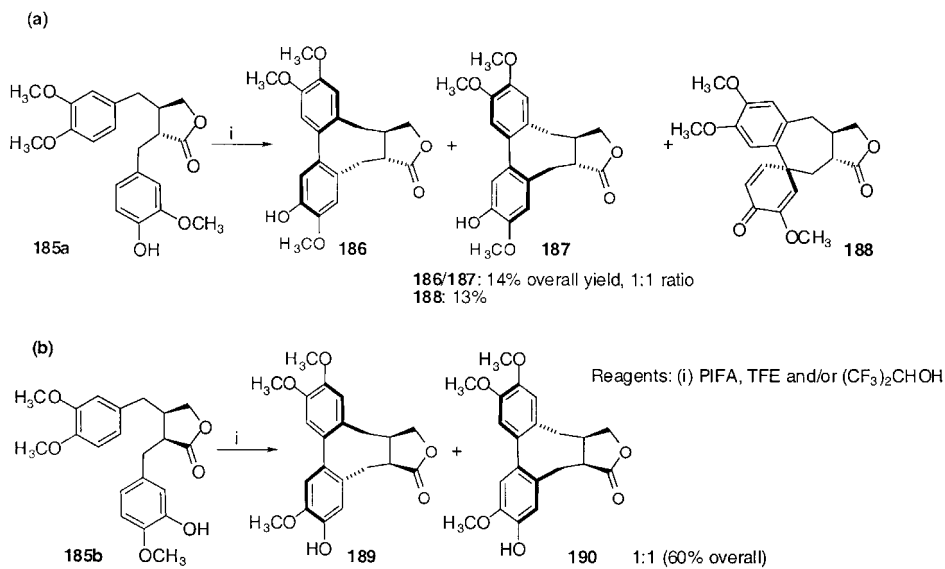
In parallel studies to the ruthenium-based work, Ward and co-workers have also shown that PIFA (Scheme 44) [122, 128] and 2,3-dichloro-5,6-dicyano-1,4-benzoquinone (DDQ) (Scheme 45) [122, 129, 130] are effective reagents for coupling the phenolic precursors **185a,b**. Yields are generally lower than in the fully methylated case (spirodienone products **188** can be formed when a hydroxyl group is present at the *para* position of the 2-benzyl group of **185a**) and unbiased mixtures of atropisomers **186/187** and **189/190** are obtained.



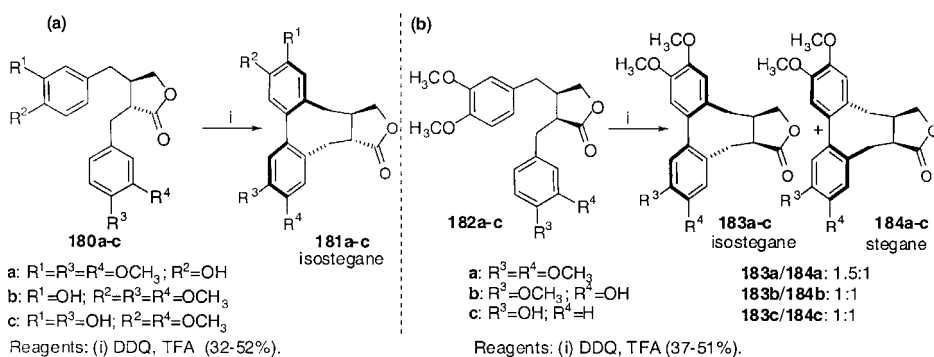
Scheme 42. Mechanistic considerations in the PIFA-mediated oxidative coupling of a *trans*-butylolactone stegane precursor.



Scheme 43. Ruthenium(IV)-mediated oxidative cyclization of *trans*- and *cis*-butylolactone stegane precursors.



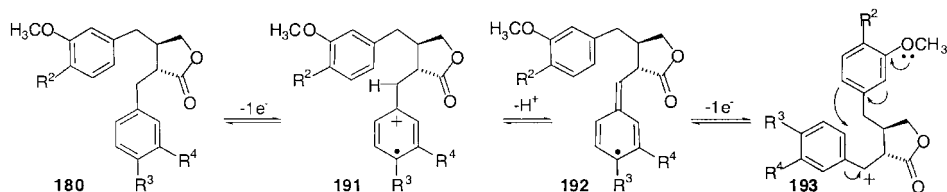
Scheme 44. PIFA-mediated oxidative cyclization of *trans*- and *cis*-butylolactone stegane precursors.



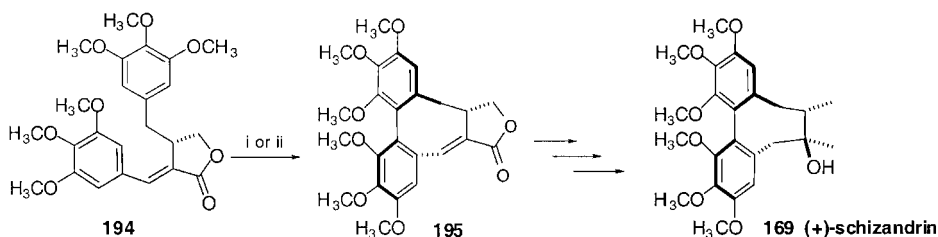
Scheme 45. DDQ-mediated oxidative cyclization of *trans*- and *cis*-butylolactone stegane precursors.

The DDQ-mediated transformations of **180a–c** are oxidative couplings that may actually proceed through nucleophilic capture of a benzylic cation (or an equivalent thereof) **193** by the adjacent aryl ring. Initial one-electron aryl oxidation (**180** \rightarrow **191**) followed by proton loss (**191** \rightarrow **192**) and subsequent one-electron removal may precede benzyl cation **193** formation, as shown in Scheme 46 [129].

Further examples of oxidative aryl coupling within this family of lignan precursors include the preparation of (+)-schizandrin (**169**) and (+)-gomisin A (**170**) (Figure 5), as published by Tanaka and co-workers. In this instance, the key Ar–Ar coupling step with **194** was realized using either ruthenium tetrakis(trifluoroacetate) or iron perchlorate (Scheme 47) [124, 131–133]. As pointed out by the authors, this result was noteworthy as this simple



Scheme 46. Possible involvement of a benzylic cation (or equivalent) in the DDQ-mediated oxidative cyclization of a *trans*-butyrolactone stegane precursor.



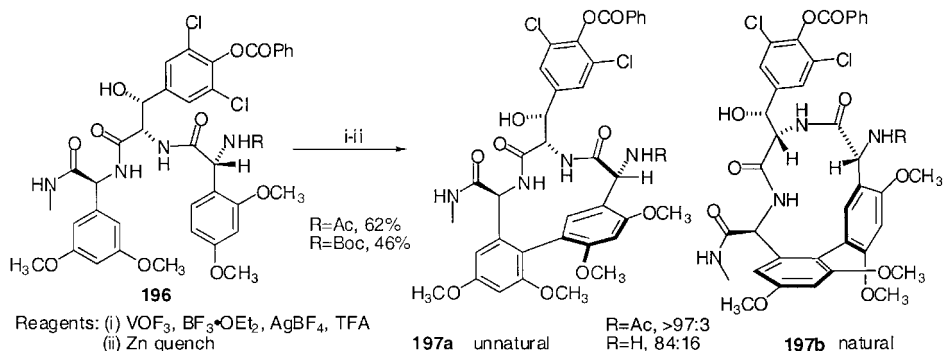
Reagents: (i) $\text{Fe}(\text{ClO}_4)_3 \cdot 6\text{H}_2\text{O}$, $\text{CF}_3\text{COOH} \cdot \text{CH}_2\text{Cl}_2$ (1:10), rt (90%)
 (ii) $\text{Ru}(\text{OCOCF}_3)_4$, CF_3COOH , $\text{BF}_3 \cdot \text{Et}_2\text{O}$, CH_2Cl_2 , rt (91%)

Scheme 47. Iron(III)- and ruthenium(IV)-mediated oxidative cyclization of an unsaturated stegane precursor en route to the natural product schizandrin.

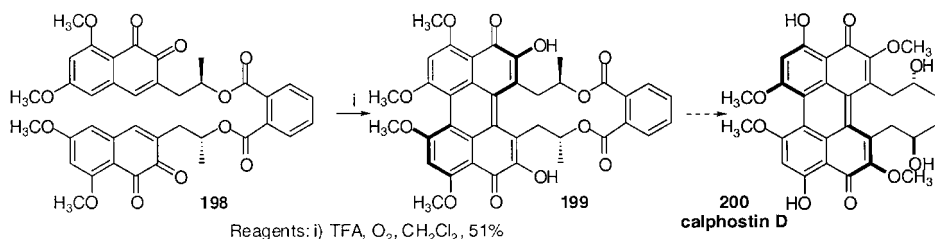
iron(III) reagent had never previously been reported to promote oxidative coupling. Luckily, in this example, the atropisomer generated upon Ar–Ar bond formation matches that required for the natural compound, thus allowing the synthesis to proceed without an equilibration step.

These examples illustrate one important point: whereas oxidative arylic coupling is the natural (biosynthetic) pathway for linking two aryl units, it cannot be assumed that reproducing the reaction *in vitro* will furnish the same stereochemical outcome. This same issue of atrop-selectivity upon biaryl coupling was addressed by Evans and co-workers in an attempted biomimetic synthesis of **197**, the M(5-7) unit of vancomycin [134, 135]. The more stable, natural isomer **197b** is obtained only as a minor component in this kinetically controlled Ar–Ar coupling reaction (Scheme 48). However, subsequent thermal equilibration leads to a preponderance of the desired compound.

Some natural compounds offer a chiral structural backbone that biases the outcome of the oxidative coupling of appended aryls (e.g., the ellagitannins). It was plausible to suppose, therefore, that two aryl units could be linked by a non-natural chiral tether to induce atrop-selective coupling upon exposure to an appropriate oxidant. In one of their attempts to realize the total synthesis of calphostin D (**200**) [136], Merlic and co-workers showed that, in the presence of dioxygen in trifluoroacetic acid (TFA), the precursor **198** affords the coupled compound **199** as a single diastereoisomer. Unfortunately, the relative configuration was incorrect for the calphostin target (Scheme 49).



Scheme 48. Vanadium(V)-mediated biomimetic oxidative cyclization of the precursor to a vancomycin fragment.



Scheme 49. Oxygen-mediated oxidative cyclization of a putative calphostin D precursor.

14.6.2

Oxidative Coupling of Two Chiral Molecules

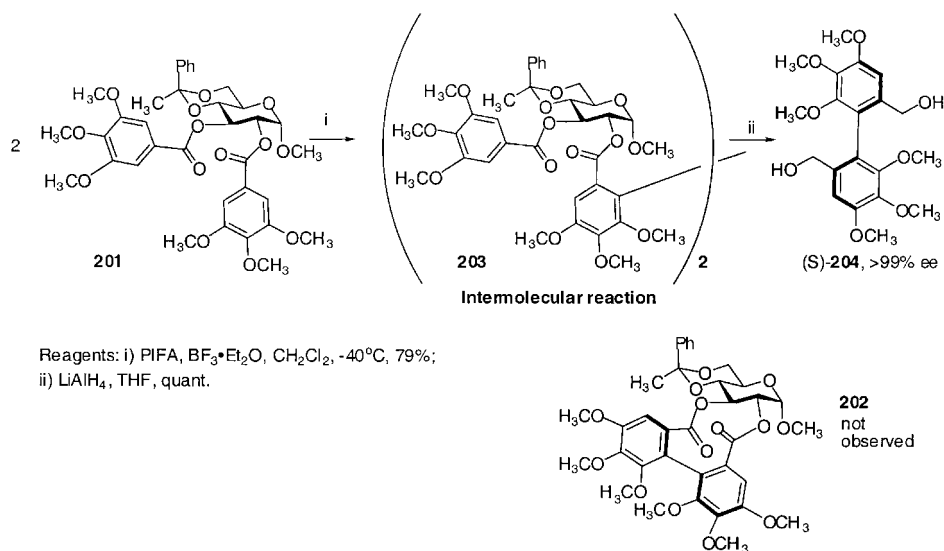
A serendipitous use of a chiral auxiliary in atrop-selective biaryl bond formation has recently been published by Kita and co-workers [39, 137]. With diaryl substrate **201**, which is related to precursors of the ellagitannins (see Section 14.6.1), PIFA-mediated oxidative coupling did not lead to the expected ellagitannin structure **202** (Scheme 50). Rather surprisingly, this reaction proceeds with intermolecular Ar–Ar bond formation. The chiral glucose framework efficiently transfers stereochemical information, but not in a intramolecular closure.

Bringmann and co-workers have shown that modest control of atrop-selectivity can be achieved upon oxidative intermolecular coupling (dimerization) of the chiral phenol **205** [77]. In the synthesis of magistophorenes A and B (**206a/b**), the chiral precursor **205** afforded both isomers with a slight preference for the “B” series when exposed to di-*tert*-butyl peroxide (DTBP) (Scheme 51).

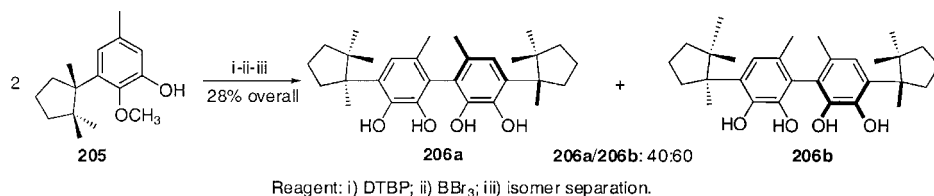
14.6.3

Stoichiometric Chiral Oxidation Reagents

The use of a chiral reagent for the oxidative coupling of naphthols has received much attention as the product chiral binaphthols are widely used in asymmetric synthesis [138]. The well-known oxidative coupling of 2-naphthol by dioxygen in the presence of a copper com-



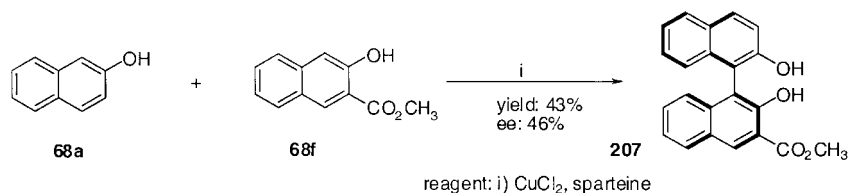
Scheme 50. Unexpected intermolecular coupling of a digalloylated glucose precursor promoted by PIFA.



Scheme 51. Di-*tert*-butyl peroxide-mediated oxidative dimerization of a chiral phenol precursor to the magistophorenes.

plex and an amine has been extended to an asymmetric version by prospecting among the wide range of commercially available chiral amines. Following work initiated by Brussee [79, 80], Smrcina and co-workers have demonstrated that in the case of **207** and the chiral amine mediator sparteine, the reaction is an actual enantioselective oxidative coupling, whereas in other cases the enantiomeric excesses result from second-order asymmetric transformations or diastereoselective crystallizations (Scheme 52) [88].

The observed atrop-selection can be rationalized in terms of the intermediacy of a complex containing square-planar copper. A transition state superimposed on this rigid framework



Scheme 52. Enantioselective cross-coupling of naphthols in the presence of the chiral amine sparteine and copper(II).

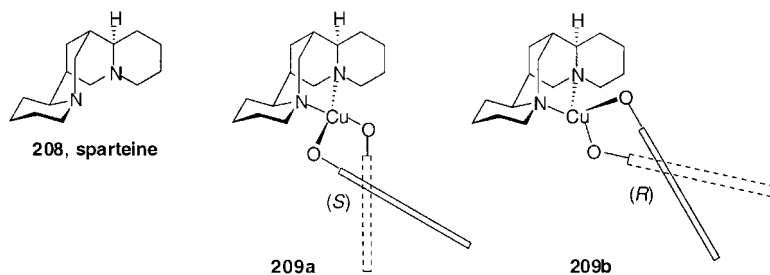


Fig. 6. Rationale for the observed sense of asymmetric induction upon cross-coupling of 2-naphthol (**68a**), as mediated by copper(II) and sparteine.

leads, according to modeling, to a preference for the (*S*)-configuration in the product. Figure 6 depicts two intermediates that highlight the role of sparteine (**208**) in inducing asymmetry into the biaryl-coupling step.

In 1994, Osa and co-workers reported a very interesting means of obtaining chiral binaphthol based on electrocatalytic synthesis [139]. This work required the coating of the electrode with a poly(acrylic acid) (PAA) layer bonded via an amide connection to 4-amino-2,2,6,6-tetramethylpiperidin-1-yloxy [91, 92]. (–)-Sparteine (**208**) was used as both the mediator and as a chiral agent (present in a stoichiometric amount) in the anolyte compartment. The yields and enantiomeric excesses obtained were excellent (Table 34). The complexity of

Tab. 34. Sparteine-mediated electrocatalytic asymmetric oxidative dimerization of 2-naphthol and derivatives.

Substrate	Product	Isolated Yield	ee (%) ^a
		94	99
		92	94
		91	98

^a Measured by chiral HPLC.

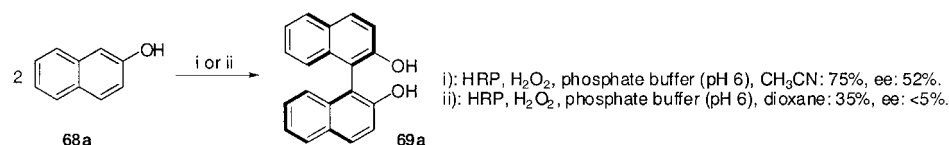
the system and the heterogeneous nature of the components make mechanistic inquiry into the origins of asymmetric induction a daunting challenge.

14.6.4

Catalytic Enantioselective Oxidative Coupling

The most intriguing work in the field of asymmetric oxidative aryl coupling has been directed towards finding catalytic enantioselective reactions. The main goal in these studies has been the synthesis of chiral binaphthyl units as an improvement over stoichiometric chiral reagent enantioselective syntheses.

Horseradish peroxidase (HRP) as a biocatalyst has been separately studied by Sridhar and Schreier [140, 141]. Unfortunately, contrasting results were reported. Sridhar claimed to have coupled naphthol derivatives with noticeable enantioselection, whereas Schreier et al. did not observe any significant asymmetric induction upon Ar–Ar bond formation (Scheme 53). A problem of ee measurement technique was cited by the latter author to explain the ee observed by Sridhar et al. ($[\alpha]_D$ versus chiral HPLC).

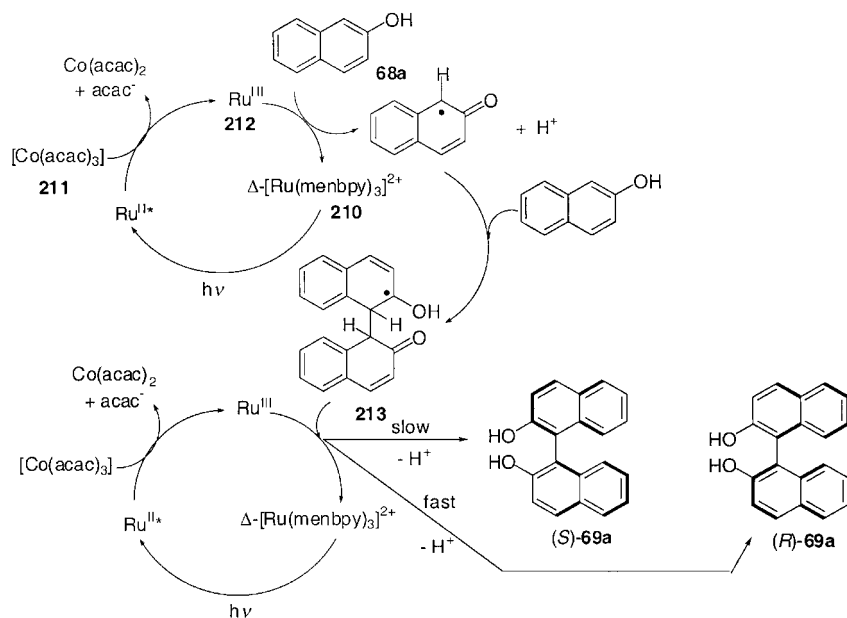


Scheme 53. Horseradish peroxidase-mediated asymmetric oxidative dimerization of 2-naphthol (**68a**).

Photocatalytic enantioselective oxidative aryl coupling reactions have been investigated by two different groups. Both studies involved the use of ruthenium-based photocatalysts [142, 143]. In 1993, Hamada and co-workers introduced a photostable chiral ruthenium tris(bipyridine)-type complex (Δ -[Ru(menbpy) $_3$] $^{2+}$) **210** possessing high redox ability [143]. The catalytic cycle also employed $Co(acac)_3$ **211** to assist in the generation of the active (Δ -[Ru(menbpy) $_3$] $^{3+}$) species **212**. The authors suggested that the enantioselection observed upon binaphthol formation was the result of a faster formation of the (*R*)-enantiomer from the intermediate **213** (second oxidation and/or proton loss), albeit only to a rather low extent (ee : 16 %) (Scheme 54).

The results of a recent study published by Katsuki and co-workers include improvements in the enantiomeric excess of binaphthol formation using chiral (NO)Ru(II)-(salicylidene) ethylenediamino (salen) complex **214** (Figure 7) [142]. The reaction was conducted under aerobic conditions so that dioxygen generated the active ruthenium reagent (Scheme 55). Yields of binaphthol as high as 95 % were realized.

Coupling attempts conducted with (*R,S*)-**214** led to lower enantioselection upon C–C bond formation, an observation that points to the significant role played by the relative configuration (*R,R*) of the binaphthyl and ethylenediamine units in promoting asymmetric induction. This complex was found to be the most efficient among several different structural variations. Solvent effects on this transformation were also studied (Table 35), with toluene and chlorobenzene giving the best results. Low solubility of the catalyst (diethyl ether and diiso-



Scheme 54. Putative mechanism for the ruthenium(III)-mediated enantioselective photocatalytic oxidative dimerization of 2-naphthol (68a).

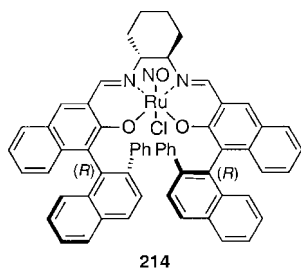
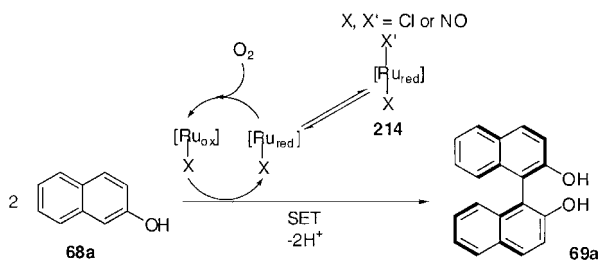


Fig. 7. Katsuki's pre-catalyst for the enantioselective oxidative dimerization of 2-naphthol (68a).



Scheme 55. Mechanistic outline of the oxidative dimerization of 2-naphthol (68a) by catalyst 214.

Tab. 35. Solvent effects in the enantioselective oxidative dimerization of 2-naphthol (**68a**) by (*R,R*)-**214**.

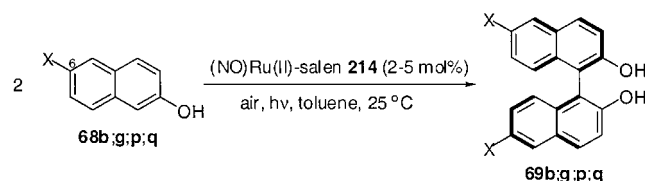
Solvent	Yield (%)	% ee ^a	configuration
Toluene	72	65	<i>R</i>
C ₆ H ₅ Cl	82	62	<i>R</i>
CH ₂ Cl ₂	95	56	<i>R</i>
CH ₃ Cl	33	42	<i>R</i>
ⁱ Pr ₂ O	65	8	<i>R</i>
Et ₂ O	43	61	<i>R</i>
THF	Trace	54	<i>R</i>
CH ₃ CN	No reaction	–	–

^a Measured by chiral HPLC.

propyl ether) or poisoning (acetonitrile and THF) are the suspected reasons for the poor performance in some other solvents.

This transformation has also been applied to other binaphthyl derivatives, and, curiously, it was observed that substitution at the C6 position of the naphthol precursors **68** influences the observed enantioselectivity (Table 36). Electron-withdrawing groups enhance the enantioselectivity but give lower yields, whereas electron-donating groups increase the yields but reduce the enantioselectivity.

Studies have also focused on vanadium-based asymmetric catalysts in addition to these photocatalytic systems. A catalytic achiral version of an oxidative coupling reaction was published in 1999 by Uang and co-workers (see Section 14.4.2) [70]. They developed an air-stable complex (VO(acac)₂) that can be used in catalytic quantities in the presence of dioxygen as a re-oxidant. The promising results obtained led to an investigation of chiral versions of this reagent, and the initial reports document that such a reaction was possible with complexes

Tab. 36. Scope of the asymmetric oxidative dimerization of 2-naphthol derivatives by **214**.

Substrate	X	mol % 2	Yield (%)	% ee ^a	Configuration
68b	Br	2	30	71	<i>R</i>
68b	Br	5	77	69	<i>R</i>
68p	PhC≡C	2	45	71	<i>R</i>
68p	PhC≡C	5	93	68	<i>R</i>
68g	OCH ₃	2	73	33	<i>R</i>
68q	CO ₂ CH ₃	2	Trace	–	–

^a Measured by chiral HPLC.

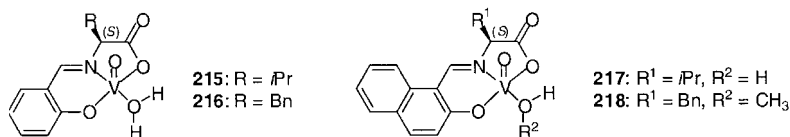


Fig. 8. Amino acid-based vanadium(IV) oxidative coupling pre-catalysts.

215–218 prepared from vanadium(IV) and (*S*)-valine or (*S*)-phenylalanine derivatives (Figure 8) [144].

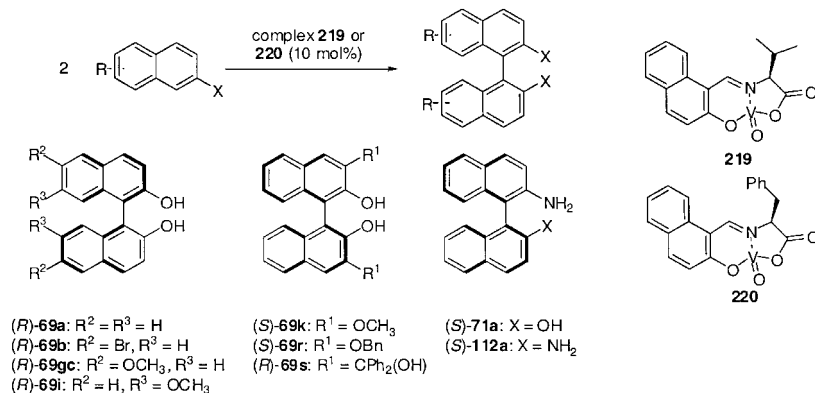
Complex **218**, in the presence of chlorotrimethylsilane (TMSCl) as a promoter, was found to be the most useful and gave the highest enantioselectivity and best yield in this reaction. Dichloromethane, chloroform, and 1,2-dichloroethane proved to be the best solvents for optimizing enantioselectivity. A limited survey of substituents suggested that this catalyst was not particularly sensitive to the electron demand of the aryl system, although steric effects may be important (Table 37, entry 4).

Almost simultaneously, Hon and co-workers published a similar study employing chiral vanadyl complexes **219** and **220** [145]. Although this work was somewhat broader in terms of the range of substitution patterns studied on both the complexes and the naphthol precursors, qualitatively the same kind of results regarding the yields and the enantioselectiv-

Tab. 37. Enantioselective oxidative dimerization of 2-naphthol derivatives mediated by chiral vanadium complex **218**.

Entry	naphthol	Time (h)	Yield (%)	ee (%) ^a
68a		24	82	51
68i		24	91	51
68b		24	50	51
68f		69	trace	—

^a Measured by chiral HPLC.

Tab. 38. Enantioselective dimerization of 2-naphthol (and 2-naphthylamine) derivatives promoted by vanadium complexes **219** and **220**.

Catalyst	Solvent	Time (days)	Product	Yield (%)	ee (%) ^a
219	CCl ₄	9	69a	94	62
219	CCl ₄	7	69b	97	52
220	CH ₂ Cl ₂	3	69g	100	39
220	CCl ₄	6	69i	86	58
219	toluene	15	69k	75	56
219	CCl ₄	8	69r	91	68
220	CCl ₄	15	69s	98	35
219	anisole	11	71a	74	33
219	CH ₂ Cl ₂	11	112a	48	10

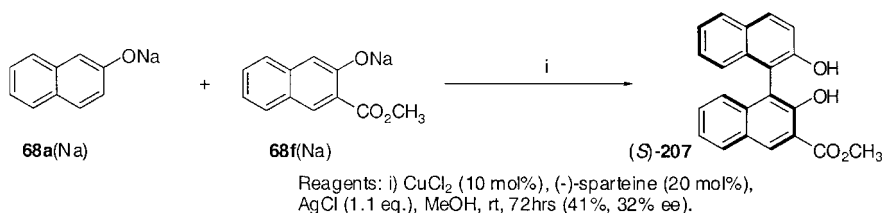
^a Measured by chiral HPLC.

ities were obtained (Table 38). X-ray structural analysis of complex **219**, and examination of the *ee* dependence of the product (*R*)-binaphthol on the *ee* of complex **219**, suggested that a monomeric V(IV) species mediates the reaction. The couplings with aminonaphthalene (**71a** and **112a**) led to lower yields and lower enantioselectivities than with the phenolic analogues.

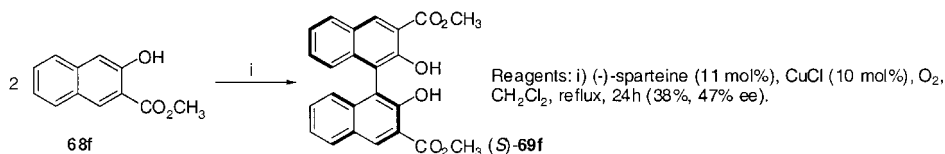
A catalytic version of the copper(II)-mediated stoichiometric chiral amine naphthol oxidative couplings has been developed as an extension of the successful achiral version. Smrcina and co-workers first carried out such a reaction in order to obtain information on the mechanism of their stoichiometric amine reactions. They obtained the biphenyl product (*S*)-**207** in 41 % yield with a modest enantiomeric excess (32 % *ee*) (Scheme 56) [88].

Nakajima and co-workers have carried out extensive investigations into the influence of different chiral diamine-copper complexes on the oxidative dimerization of naphthols [146–148]. As emerged from Smrcina's work, the inclusion of an ester moiety on the naphthol precursor is an important factor for optimizing the enantioselectivity. After establishing a catalytic cycle with TMDA as the base and showing that sparteine gave promising results (Scheme 57), they focused their work on other chiral diamines (Table 39) [147].

The results from this chiral amine survey indicated that the secondary nitrogen in the pyrrolidine ring and the tertiary nitrogen in the side chain of the catalyst **221** are necessary

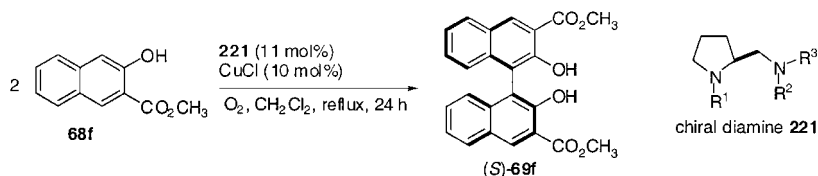


Scheme 56. Enantioselective cross-coupling of 2-naphthol catalyzed by copper(II)/sparteine.



Scheme 57. Enantioselective oxidative dimerization of naphthol derivative **68f** in the presence of a copper(I) pre-catalyst and sparteine.

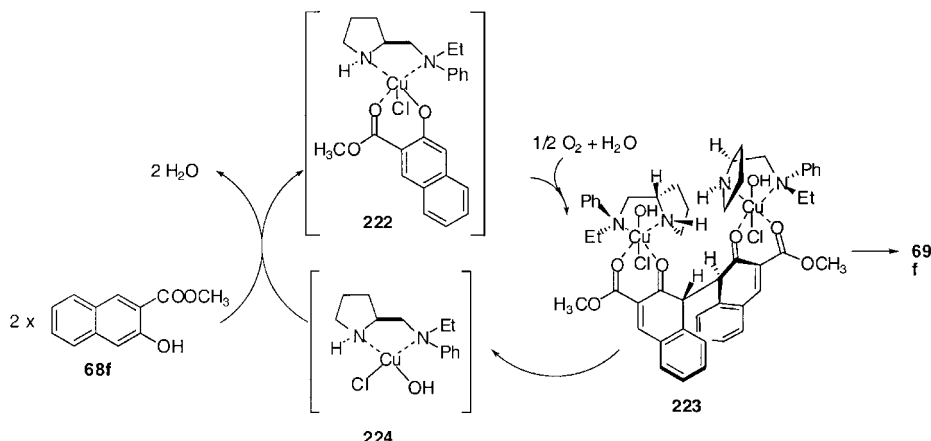
Tab. 39. Survey of pyrrolidine substituent effects on the enantioselective oxidative dimerization of **68f** mediated by a copper(I) pre-catalyst.



Chiral diamine 221				(S)-69f	
221	R¹	R²	R³	Yield (%)	ee (%)^a
a	CH ₃		–(CH ₂) ₄ –	79	2
b	CH ₃	Ph	H	77	4
c	H	H	H	11	0
d	H		–(CH ₂) ₄ –	82	31
e	H	Ph	H	74	30
f	H	Ph	CH ₃	76	59
g	H	4-CH ₃ OC ₆ H ₄			
h	H	4-CF ₃ C ₆ H ₄			
i	H	1-naphthyl			
j	H	2-naphthyl			
k	H	Hex			
l	H	Ph	Et	78	70
m	H	Ph	CH ₂ Ph	87	65
n	H	Ph	Ph	66	12

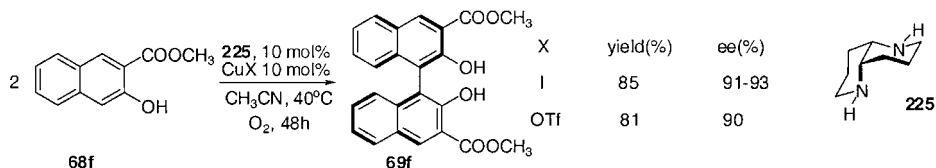
^a Measured by chiral HPLC.

for good asymmetric induction. These data show that the *N*-ethylaniline derivative **221l** is the best candidate. The authors have proposed a mechanistic explanation for the observed asymmetric induction that involves the formation of a diketone/copper-diamine complex **223**. Chirality transfer then depends on minimizing unfavorable steric interactions between the appendages of the chiral auxiliaries (Scheme 58).



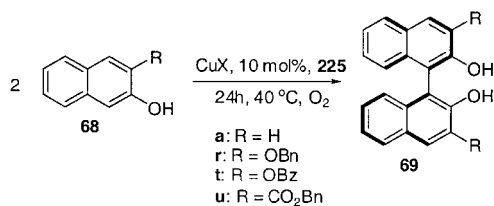
Scheme 58. Mechanistic speculation on the copper/chiral pyrrolidine-mediated oxidative dimerization of **68f**.

In the same vein, Koslowski and co-workers have published a study using chiral 1,5-diazadecalin complex **225**, a species that directs binaphthol formation with excellent enantioselectivity [149]. The use of CuI or Cu(OTf) as a copper source in this procedure contributes to the excellent yields (85 %) and high enantiomeric excesses (~90 %) (Scheme 59). Substituents on the nitrogens of **225** or changes in the copper source resulted in lower yields and/or lower enantioselectivities. Other naphthol substrates have been subjected to these conditions, but both the yields and enantioselectivities were diminished, showing the importance of the ester moiety with regard to the efficiency of the reaction (Table 40).



Scheme 59. The effect of the copper source on the enantioselectivity of the dimerization of **68f**, as mediated by chiral amine **225**.

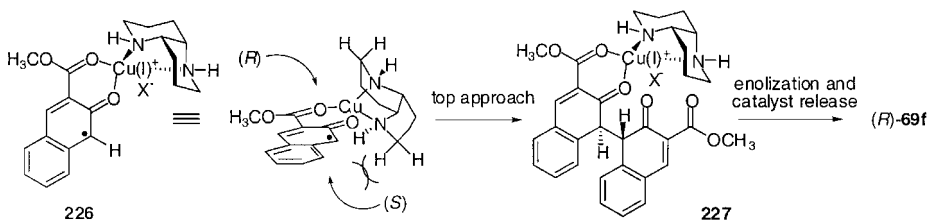
The authors have initiated a mechanistic inquiry into this reaction, and unlike Nakajima, they propose that Ar–Ar bond formation proceeds through a radical addition of one aryl moiety with its unperturbed partner. This speculation extended to a model explaining the

Tab. 40. Substituent effects on the enantioselective oxidative dimerization of 2-naphthol derivatives mediated by copper salts and chiral amine **225**.

Substrate	Cu Source	Solvent	Yield (%)	ee (%) ^a
68a	CuCl	CH ₂ Cl ₂	80 ^b	13
68t	CuCl	CH ₃ CN/(ClCH ₂) ₂	NR	ND
68r	CuCl	(ClCH ₂) ₂	77 ^c	38
68u	CuI	CH ₃ CN/(ClCH ₂) ₂	79	90

^a Measured by chiral HPLC;^b Using air at rt for 5 d.^c Using air at rt for 24 h.

sense of stereoselection (Scheme 60). Complex **226** favors approach of the second unit of **68f** from the less hindered face of the Cu-complexed aryl radical, leading preferentially to the (*R*)-biaryl product **69f**.

**Scheme 60.** Mechanistic speculation on the origins of enantioselection upon oxidative dimerization of **68f** in the copper/**225** system.

14.7

Conclusion

From the recent work published on oxidative aryl coupling reactions, it is clear that at least some of the issues highlighted in the introduction have found solutions. Studies detailing either the chemo-, regio-, or stereoselectivity of biaryl bond formation show that by using the tools of organic and inorganic chemistry, it is now possible to achieve a biomimetic approach to biaryl synthesis in a more efficient way. Further progress should lead to the development of even more selective and general methods that more closely approximate the success with which nature fashions the link between two aromatic units.

References

- 1 R. PUMMERER, F. FRANFURTER, *Ber. Dtsch. Chem. Ges.* **1914**, 47, 1472.
- 2 R. PUMMERER, E. CHERBULIEZ, *Ber. Dtsch. Chem. Ges.* **1914**, 47, 2957.
- 3 R. PUMMERER, F. FRANFURTER, *Ber. Dtsch. Chem. Ges.* **1919**, 52, 1416.
- 4 R. PUMMERER, E. CHERBULIEZ, *Ber. Dtsch. Chem. Ges.* **1919**, 52, 1392.
- 5 R. PUMMERER, *Ber. Dtsch. Chem. Ges.* **1919**, 52, 1403.
- 6 R. PUMMERER, D. MELAMED, H. PUTTFARCKEN, *Ber. Dtsch. Chem. Ges.* **1922**, 55, 3116.
- 7 R. PUMMERER, H. PUTTFARCKEN, P. SCHOPFLOCHER, *Ber. Dtsch. Chem. Ges.* **1925**, 58, 1808.
- 8 R. PUMMERER, F. LUTHER, *Ber. Dtsch. Chem. Ges.* **1928**, 61, 1102.
- 9 D. H. R. BARTON, T. COHEN, *Festschr. Arthur Stoll* **1957**, 117.
- 10 H. ERDTMAN, C. A. WACHTMEISTER, *Festschr. Arthur Stoll* **1957**, 144.
- 11 B. S. THYAGARAJAN, *Chem. Rev.* **1958**, 57, 439.
- 12 F. FICHTER, E. BRUNNER, *Bull. Soc. Chim. Fr.* **1916**, 19, 281.
- 13 F. J. VERMILLION JR., I. A. PEARL, *J. Electrochem. Soc.* **1964**, 111, 1392.
- 14 L. PAPOUCHADO, R. W. SANDFORD, G. PETRIE, R. N. ADAMS, *J. Electroanal. Chem.* **1975**, 65, 275.
- 15 M. S. BAINS, J. C. ARTHUR JR., O. HINOJOSA, *J. Am. Chem. Soc.* **1969**, 91, 4673.
- 16 S. M. KUPCHAN, A. J. LIEPA, *J. Am. Chem. Soc.* **1973**, 95, 4062.
- 17 M. A. SCHWARTZ, B. F. ROSE, B. VICHNUVAJJALA, *J. Am. Chem. Soc.* **1973**, 95, 612.
- 18 K. S. FELDMAN, A. SAMBANDAM, *J. Org. Chem.* **1995**, 60, 8171.
- 19 C. SZÁNTAY, G. BLASKÓ, M. BÁRCZAI-BEKE, P. PECHY, G. DÖRNYEI, *Tetrahedron Lett.* **1980**, 21, 3509.
- 20 C. H. HASSALL, A. I. SCOTT, in *Recent Developments in the Chemistry of Natural Phenolic Compounds* (Ed.: W. D. OLLIS), Pergamon Press, New York, 1961, p. 119.
- 21 H. MUSSO, *Angew. Chem. Int. Ed. Engl.* **1963**, 2, 723.
- 22 W. I. TAYLOR, A. R. BATTERSBY, *Oxidative Coupling of Phenols*, Vol. 1, Marcel Dekker, Inc., New York, 1967.
- 23 O. C. MUSGRAVE, *Chem. Rev.* **1969**, 69, 499.
- 24 M. SAINSBURY, *Tetrahedron* **1980**, 36, 3327.
- 25 W. J. MIJS, C. R. H. I. DE JONGE, *Organic Syntheses by Oxidation with Metal Compounds*, Plenum Press, New York, 1986.
- 26 D. A. WHITING, in *Comprehensive Organic Synthesis*, Vol. 3 (Eds.: B. M. TROST, G. PATTENDEN), Pergamon, Oxford, 1991, p. 659.
- 27 W. A. WATERS, *J. Chem. Soc. B* **1971**, 2026.
- 28 A. RIEKER, E.-L. DREHER, H. GEISEL, M. H. KHALIFA, *Synthesis* **1978**, 851.
- 29 J. S. SWENTON, K. CARPENTER, Y. CHEN, M. L. KERNS, G. W. MORROW, *J. Org. Chem.* **1993**, 58, 3308.
- 30 H. EICKHOFF, G. JUNG, A. RIEKER, *Tetrahedron* **2001**, 57, 353.
- 31 R. M. MORIARTY, O. PRAKASH, *Org. React.* **2001**, 57, 327.
- 32 A. PELTER, R. WARD, *Tetrahedron* **2001**, 57, 273.
- 33 A. PELTER, A. HUSSAIN, G. SMITH, R. S. WARD, *Tetrahedron* **1997**, 53, 3879.
- 34 G. BRINGMANN, S. TASLER, H. ENDRESS, J. KRAUS, K. MESSER, M. WOHLFARTH, W. LOBIN, *J. Am. Chem. Soc.* **2001**, 123, 2703.
- 35 A. MCKILLOP, A. G. TURRELL, D. W. YOUNG, E. C. TAYLOR, *J. Am. Chem. Soc.* **1980**, 102, 6504.
- 36 E. C. TAYLOR, J. G. ANDRADE, G. J. H. RALL, A. MCKILLOP, *J. Am. Chem. Soc.* **1980**, 102, 6513.
- 37 J. S. BUCKLETON, R. C. CAMBIE, G. R. CLARK, P. A. CRAW, C. E. F. RICKARD, P. S. RUTLEDGE, P. D. WOODGATE, *Aust. J. Chem.* **1988**, 41, 305.
- 38 Y. KITA, M. EGI, T. TAKADA, H. TOHMA, *Synthesis* **1999**, 885.
- 39 H. TOHMA, H. MORIOKA, S. TAKIZAWA, M. ARISAWA, Y. KITA, *Tetrahedron* **2001**, 57, 345.
- 40 Y. KITA, H. TOHMA, K. HATANAKA, T. TAKADA, S. FUJITA, S. MITOH, H. SAKURAI, S. OKA, *J. Am. Chem. Soc.* **1994**, 116, 3684.
- 41 Y. KITA, M. GYOTEN, M. OHTSUBO, H. TOHMA, T. TAKADA, *J. Chem. Soc., Chem. Commun.* **1996**, 1481.

- 42 P. J. STANG, V. V. ZHDANKIN, *Chem. Rev.* **1996**, 96, 1123.
- 43 A. VARVOGLIS, *Tetrahedron* **1997**, 53, 1179.
- 44 T. TAKADA, M. ARISAWA, M. GYOTEN, R. HAMADA, H. TOHMA, Y. KITA, *J. Org. Chem.* **1998**, 63, 7698.
- 45 J. D. WHITE, G. CARAVATTI, T. B. KLINE, E. EDSTROM, K. C. RICE, A. BROSSI, *Tetrahedron* **1983**, 39, 2393.
- 46 J. D. WHITE, W. K. M. CHONG, K. THIRRING, *J. Org. Chem.* **1983**, 48, 2300–2302.
- 47 K. V. RAMA KRISHNA, K. SUJATHA, R. S. KAPIL, *Tetrahedron Lett.* **1990**, 31, 1351.
- 48 Y. KITA, T. TAKADA, M. GYOTEN, H. TOHMA, M. H. ZENK, J. EICHHORN, *J. Org. Chem.* **1996**, 61, 5857.
- 49 Y. KITA, M. ARISAWA, M. GYOTEN, M. NAKAJIMA, R. HAMADA, H. TOHMA, T. TAKADA, *J. Org. Chem.* **1998**, 63, 6625.
- 50 M. NODE, S. KODAMA, Y. HAMASHIMA, T. BABA, N. HAMAMICHI, K. NISHIDE, *Angew. Chem. Int. Ed.* **2001**, 40, 3060.
- 51 H. E. PELISH, N. J. WESTWOOD, Y. FENG, T. KIRCHHAUSEN, M. D. SHAIR, *J. Am. Chem. Soc.* **2001**, 123, 6740.
- 52 R. OLIVERA, R. SAN MARTIN, S. PASCUAL, M. HERRERO, E. DOMINGUEZ, *Tetrahedron Lett.* **1999**, 40, 3479.
- 53 M. M. FAUL, K. A. SULLIVAN, *Tetrahedron Lett.* **2001**, 42, 3271.
- 54 R. PUMMERER, A. RIECHE, E. PRELL, *Ber.* **1926**, 59, 2159.
- 55 H.-J. DEUBEN, P. FREDERIKSEN, T. BJØRNHOM, K. BECHGAARD, *Org. Prep. Proc. Int.* **1996**, 28, 484.
- 56 K. DING, Y. WANG, L. ZHANG, Y. WU, *Tetrahedron* **1996**, 52, 1005.
- 57 K. DING, Q. XU, Y. WANG, J. LIU, Z. YU, B. DU, Y. WU, H. KOSHIMA, T. MATSUURA, *J. Chem. Soc., Chem. Commun.* **1997**, 693.
- 58 S. VYSKOCIL, M. SMIRCINA, M. LORENC, V. HANUS, M. POLASEK, P. KOCOVSKY, *J. Chem. Soc., Chem. Commun.* **1998**, 585.
- 59 M. SMIRCINA, S. VYSKOCIL, B. MACA, M. POLASEK, T. A. CLAXTON, A. P. ABBOTT, P. KOCOVSKY, *J. Org. Chem.* **1994**, 59, 2156.
- 60 F. TODA, K. TANAKA, S. IWATA, *J. Org. Chem.* **1989**, 54, 3007.
- 61 M. O. RASMUSSEN, O. AXELSSON, D. TANNER, *Synth. Commun.* **1997**, 27, 4027.
- 62 D. VILLEMEN, F. SAUVAGET, *Synlett* **1994**, 435.
- 63 N. BODEN, R. J. BUSHBY, Z. LU, *Liquid Crystals* **1998**, 25, 47.
- 64 N. BODEN, R. J. BUSHBY, A. N. CAMMIDGE, G. HEADDOCK, *Synthesis* **1995**, 31.
- 65 R. J. BUSHBY, Z. LU, *Synthesis* **2001**, 5, 763.
- 66 N. BODEN, R. J. BUSHBY, Z. LU, G. HEADDOCK, *Tetrahedron Lett.* **2000**, 41, 10117.
- 67 R. B. HERBERT, A. E. KATTAH, A. E. MURTAGH, P. W. SHELDRAKE, *Tetrahedron Lett.* **1995**, 36, 5649.
- 68 L. CZOLLNER, W. FRANTSITS, B. KÜENBURG, U. HEDENIG, J. FRÖHLICH, U. JORDIS, *Tetrahedron Lett.* **1998**, 39, 2087.
- 69 B. HAZRA, S. ACHARYA, R. GHOSH, A. PATRA, A. BANERJEE, *Synth. Commun.* **1999**, 29, 1571.
- 70 D.-R. HWANG, C.-P. CHEN, B.-J. UANG, *J. Chem. Soc., Chem. Commun.* **1999**, 1207.
- 71 S. KUMAR, S. K. VARSHNEY, *Liquid Crystals* **1999**, 26, 1841.
- 72 S. KUMAR, S. K. VARSHNEY, *Synthesis* **2001**, 305.
- 73 B. MOHR, V. ENKELMANN, G. WEGNER, *J. Org. Chem.* **1994**, 59, 635.
- 74 D. L. COMINS, L. A. MORGAN, *Tetrahedron Lett.* **1991**, 32, 5919.
- 75 D. L. COMINS, X. CHEN, L. A. MORGAN, *J. Org. Chem.* **1997**, 62, 7435.
- 76 A. G. BROWN, P. D. EDWARDS, *Tetrahedron Lett.* **1990**, 31, 6581.
- 77 G. BRINGMANN, S. TASLER, *Tetrahedron* **2001**, 57, 331.
- 78 K. S. FELDMAN, S. M. ENSEL, *J. Am. Chem. Soc.* **1994**, 116, 3357.
- 79 J. BRUSSEE, A. C. A. JANSEN, *Tetrahedron Lett.* **1983**, 24, 3261.
- 80 J. BRUSSEE, J. L. G. GROENENDIJK, J. M. TE KOPPELE, A. C. A. JANSEN, *Tetrahedron* **1985**, 41, 3313.
- 81 B. FERINGA, H. WYNBERG, *Bioorg. Chem.* **1978**, 7, 397.
- 82 M. HOVORKA, J. GÜNTEROVA, J. ZAVADA, *Tetrahedron Lett.* **1990**, 31, 413.
- 83 M. HOVORKA, R. SCIGEL, J. GÜNTEROVA, M. TICHY, J. ZAVADA, *Tetrahedron* **1992**, 48, 9503.
- 84 M. HOVORKA, J. ZAVADA, *Tetrahedron* **1992**, 48, 9517.
- 85 M. SMIRCINA, M. LORENC, V. HANUS, P. KOCOVSKY, *Synlett* **1991**, 231.
- 86 M. SMIRCINA, S. VYSKOCIL, J. POLIVKOVA, J. POLAKOVA, P. KOCOVSKY, *Collect. Czech Chem. Commun.* **1996**, 61, 1520.

- 87 S. VYSKOCIL, M. SMRCINA, M. LORENC, I. TISLEROVA, R. D. BROOKS, J. J. KULAGOWSKI, V. LANGER, L. J. FARRUGIA, P. KOCOVSKY, *J. Org. Chem.* **2001**, 66, 1359.
- 88 M. SMRCINA, J. POLAKOVA, S. VYSKOCIL, P. KOCOVSKY, *J. Org. Chem.* **1993**, 58, 4534.
- 89 M. NOJI, M. NAKAJIMA, K. KOGA, *Tetrahedron Lett.* **1994**, 35, 7983.
- 90 M. NAKAJIMA, S.-i. HASHIMOTO, M. NOJI, K. KOGA, *Chem. Pharm. Bull.* **1998**, 46, 1814.
- 91 Y. KASHIWAGI, H. ONO, T. OSA, *Chem. Lett.* **1993**, 81.
- 92 Y. KASHIWAGI, H. ONO, T. OSA, *Chem. Lett.* **1993**, 257.
- 93 D. PLANCHENAULT, R. DHAL, J.-P. ROBIN, *Tetrahedron* **1993**, 49, 5823.
- 94 D. PLANCHENAULT, R. DHAL, J.-P. ROBIN, *Tetrahedron* **1995**, 51, 1395.
- 95 P. JIANG, S. LU, *Synth. Commun.* **2001**, 31, 131.
- 96 J. DOUSSOT, A. GUY, C. FERROUD, *Tetrahedron Lett.* **2000**, 41, 2545.
- 97 S. MUKHOPADHYAY, G. ROTHENBERG, G. LANDO, K. AGBARIA, M. KAZANCI, Y. SASSON, *Adv. Synth. Catal.* **2001**, 343, 455.
- 98 S. H. LEE, K. H. LEE, J. S. LEE, J. D. JUNG, J. S. SHIM, *J. Mol. Cat. A* **1997**, 115, 241.
- 99 J. BAO, W. D. WULFF, J. B. DOMINY, M. J. FUMO, E. B. GRANT, A. C. ROB, M. C. WHITCOMB, S.-M. YEUNG, R. L. OSTRANDER, A. L. RHEINGOLD, *J. Am. Chem. Soc.* **1996**, 118, 3392.
- 100 Y.-A. MA, Z.-W. GUO, C. J. SIH, *Tetrahedron Lett.* **1998**, 39, 9357.
- 101 M. TANAKA, H. NAKASHIMA, M. FUJIWARA, H. ANDO, Y. SOUMA, *J. Org. Chem.* **1996**, 61, 788.
- 102 T. SAKAMOTO, H. YONEHARA, C. PAC, *J. Org. Chem.* **1994**, 59, 6859.
- 103 T. SAKAMOTO, H. YONEHARA, C. PAC, *J. Org. Chem.* **1997**, 62, 3194.
- 104 M. L. KANTAM, P. L. SANTHI, *Synth. Commun.* **1996**, 26, 3075.
- 105 T.-S. LI, H.-Y. DUAN, B.-Z. LI, B. B. TEWARI, S.-H. LI, *J. Chem. Soc., Perkin Trans. 1* **1999**, 291.
- 106 E. ARMENGOL, A. CORMA, H. GARCIA, J. PRIMO, *Eur. J. Org. Chem.* **1999**, 1915.
- 107 S. V. LEY, A. W. THOMAS, H. FINCH, *J. Chem. Soc., Perkin Trans. 1* **1999**, 669.
- 108 S. V. LEY, O. SCHUCHT, A. W. THOMAS, P. J. MURRAY, *J. Chem. Soc., Perkin Trans. 1* **1999**, 1251.
- 109 H. TOGO, G. NOGAMI, M. YOKOYAMA, *Synlett* **1998**, 534.
- 110 E. L. ELIEL, S. H. WILEN, L. N. MANDER, *Stereochemistry of Organic Compounds*, Wiley, New York, 1994.
- 111 G. BRINGMANN, R. WALTER, R. WEIRICH, in *Methods of Organic Chemistry (Houben Weyl)*, Vol. E 21a (Eds.: G. H. HELMCHEN, J. MULZER, E. SCHAUMANN), Thieme, Stuttgart, 1995, p. 567.
- 112 S. QUIDEAU, K. S. FELDMAN, *Chem. Rev.* **1996**, 96, 475.
- 113 K. KHANBABAEI, T. VAN REE, *Synthesis* **2001**, 1585.
- 114 O. T. SCHMIDT, *Fortschr. Chem. Org. Naturst.* **1956**, 13, 70.
- 115 E. HASLAM, *Plant Polyphenols*, Cambridge University Press, Cambridge, 1989.
- 116 K. S. FELDMAN, S. M. ENSEL, *J. Am. Chem. Soc.* **1993**, 115, 1162.
- 117 K. S. FELDMAN, S. M. ENSEL, R. D. MINARD, *J. Am. Chem. Soc.* **1994**, 116, 1742.
- 118 K. S. FELDMAN, R. S. SMITH, *J. Org. Chem.* **1996**, 61, 2606.
- 119 K. S. FELDMAN, M. D. LAWLOR, K. SAHASRABUDHE, *J. Org. Chem.* **2000**, 65, 8011.
- 120 K. S. FELDMAN, M. D. LAWLOR, *J. Am. Chem. Soc.* **2000**, 122, 7396.
- 121 S. M. KUPCHAN, R. W. BRITTON, M. F. ZIEGLER, C. J. GILMORE, R. J. RESTIVO, R. F. BRYAN, *J. Am. Chem. Soc.* **1973**, 95, 1335.
- 122 R. S. WARD, D. D. HUGHES, *Tetrahedron* **2001**, 57, 5633.
- 123 R. S. WARD, D. D. HUGHES, *Tetrahedron* **2001**, 57, 4015.
- 124 M. TANAKA, C. MUKAIYAMA, H. MITSUHASHI, M. MARUNO, T. WAKAMATSU, *J. Org. Chem.* **1995**, 60, 4339.
- 125 A. PELTER, P. SATCHEWELL, R. S. WARD, K. BLAKE, *J. Chem. Soc., Perkin Trans. 1* **1995**, 2201.
- 126 Y. LANDAIS, J.-P. ROBIN, *Tetrahedron Lett.* **1986**, 27, 1785.
- 127 J.-P. ROBIN, Y. LANDAIS, *J. Org. Chem.* **1988**, 53, 224.
- 128 R. S. WARD, A. PELTER, A. ABD-EL-GHANI, *Tetrahedron* **1996**, 52, 1303.
- 129 A. PELTER, R. S. WARD, R. VENKATESWARLU, C. KAMAKSHI, *Tetrahedron* **1991**, 47, 1275.

- 130 A. PELTER, R. S. WARD, D. M. JONES, P. MADDOCKS, *J. Chem. Soc., Perkin Trans. 1* **1993**, 2631.
- 131 M. TANAKA, H. MITSUHASHI, T. WAKAMATSU, *Tetrahedron Lett.* **1992**, 33, 4161.
- 132 M. TANAKA, C. MUKAIYAMA, H. MITSUHASHI, T. WAKAMATSU, *Tetrahedron Lett.* **1992**, 33, 4165.
- 133 M. TANAKA, Y. IKEYA, H. MITSUHASHI, M. MARUNO, T. WAKAMATSU, *Tetrahedron* **1995**, 51, 11703.
- 134 D. A. EVANS, C. J. DINSMORE, *Tetrahedron Lett.* **1993**, 34, 6029.
- 135 D. A. EVANS, C. J. DINSMORE, D. A. EVRARD, K. M. DeVRIES, *J. Am. Chem. Soc.* **1993**, 115, 6426.
- 136 C. A. MERLIC, C. C. ALDRICH, J. ALBANEZE-WALKER, A. SAGHATELIAN, J. MAMMEN, *J. Am. Chem. Soc.* **2001**, 66, 1297.
- 137 M. ARISAWA, S. UTSUMI, M. NAKAJIMA, N. G. RAMESH, H. TOHMA, Y. KITA, *J. Chem. Soc., Chem. Commun.* **1999**, 469.
- 138 R. NOYORI, *Asymmetric Catalysis in Organic Synthesis*, Wiley, New York, 1994.
- 139 T. OSA, Y. KASHIWAGI, Y. YANAGISAWA, J. M. BOBBITT, *J. Chem. Soc., Chem. Commun.* **1994**, 2535.
- 140 M. SRIDHAR, S. K. VADIVEL, U. T. BHALERAO, *Tetrahedron Lett.* **1997**, 38, 5695.
- 141 M. M. SCHMITT, E. SCHÜLER, M. BRAUN, D. HÄRING, P. SCHREIER, *Tetrahedron Lett.* **1998**, 39, 2945.
- 142 R. IRIE, K. MASUTANI, T. KATSUKI, *Synlett* **2000**, 1433.
- 143 T. HAMADA, H. ISHIDA, S. USUI, Y. WATANABE, K. TSUMURA, K. OHKUBO, *J. Chem. Soc., Chem. Commun.* **1993**, 909.
- 144 C.-Y. CHU, D.-R. HWANG, S.-K. WANG, B.-J. UANG, *J. Chem. Soc., Chem. Commun.* **2001**, 980.
- 145 S.-W. HON, C.-H. LI, J.-H. KUO, N. B. BARHATE, Y.-H. LIU, Y. WANG, C.-T. CHEN, *Org. Lett.* **2001**, 3, 869.
- 146 M. NAKAJIMA, K. KANAYAMA, I. MIYOSHI, S.-i. HASHIMOTO, *Tetrahedron Lett.* **1995**, 36, 9519.
- 147 M. NAKAJIMA, I. MIYOSI, K. KANAYAMA, S.-i. HASHIMOTO, *J. Org. Chem.* **1999**, 64, 2264.
- 148 M. NAKAJIMA, *Yakugaku Zasshi* **2000**, 120, 68.
- 149 X. LI, J. YANG, M. C. KOZLOWSKI, *Org. Lett.* **2001**, 3, 1137.

15

Oxidative Conversion of Arenols into *ortho*-Quinols and *ortho*-Quinone Monoketals – A Useful Tactic in Organic Synthesis

Stéphane Quideau

Abstract

The oxidative activation of arenes is a powerful and versatile synthetic tactic that enables dearomatization to give useful synthons. Central to this chemistry are hydroxylated arenes or arenols, the phenolic functions of which can be exploited to facilitate the dearomatizing process by two-electron oxidation. Suitably substituted arenols can hence be converted, with the help of oxygen- or carbon-based nucleophiles, into *ortho*-quinone monoketals and *ortho*-quinols. These 6-oxocyclohexa-2,4-dienones are ideally functionalized for the construction of many complex and polyoxygenated natural product architectures. Today, the inherent and multiple reactivity of arenol-derived *ortho*-quinone monoketals and *ortho*-quinols species is finding numerous and, in many cases, biomimetic applications in modern organic synthesis.

15.1

Introduction

ortho-Quinols and *ortho*-quinone monoketals are cyclohexa-2,4-dienone derivatives **1a–d** bearing one or two singly-bonded oxygen functions at their tetrahedral 6-position (Figure 1). Strictly speaking, *ortho*-quinols are 6-hydroxy-substituted cyclohexa-2,4-dienones **1b**, while derivatives **1c/d** of their 6,6-dihydroxy variants can be viewed as derivatives of *ortho*-quinone monohydrates **1e**. *ortho*-Quinone monoketals are diether derivatives **1c** (R = alkyl) of these monohydrates.

An abundance of information on the various preparation modes and reactivity features of all types of *ortho*-quinol derivatives can be found in the literature on the chemistry of cyclohexadienones [1, 2]. A few review articles have also been dedicated to the specificities of their chemistry and uses in organic synthesis [3–6]. This chapter specifically addresses the oxidative dearomatization of hydroxylated arenes (i.e. arenols) as a versatile and powerful tactic for the preparation of *ortho*-quinol derivatives, utilization of which continues to attract more and more adepts engaged in the various facets of modern organic and bioorganic synthesis. This first section is intended to aid the reader in putting the chemistry of *ortho*-quinol derivatives in their general organic and bioorganic context (Section 15.1). A brief overview of today's most commonly employed oxidative methods for dearomatizing arenols (Section

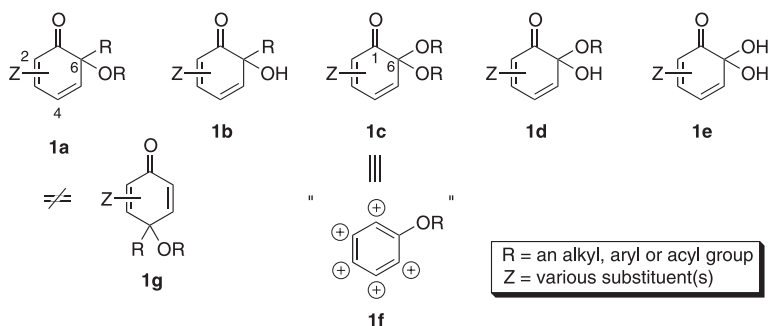


Fig. 1

15.2) is followed by a presentation of contemporary applications of *ortho*-quinols and *ortho*-quinone monoketals in natural products synthesis (Section 15.3).

15.1.1

How to Prepare *ortho*-Quinols and *ortho*-Quinone Monoketals

ortho-Quinone monoketals are traditionally considered and often used in synthesis as monoprotected, “blocked” or “masked” forms of *ortho*-quinones. Direct nucleophilic addition to one carbonyl function of *ortho*-quinones **2a** or cycloaddition with *ortho*-quinone methides **2b** can, in principle, lead to all types of *ortho*-quinol derivatives (Figure 2), but these addition processes are only of preparative value with the most stable *ortho*-quinones [7–9]. Partial hydrolysis of *ortho*-quinone bisketals to monoketals can constitute an alternative methodology (Section 15.2.1), but an adequate level of regioselectivity for preparative purposes is difficult to achieve and the method is again limited to the most stable species [5, 10, 11]. Hence, considerations of all the available possibilities inevitably point to the direct dearomatization of suitably substituted arenols as the most promising route to *ortho*-quinone monoketals and *ortho*-quinols.

Reductive alkylation of 2-methoxybenzoates [12–14], carbon alkylation of the alkali metal salts of arenols [15–19], and sigmatropic rearrangements such as the Claisen reaction of allyl

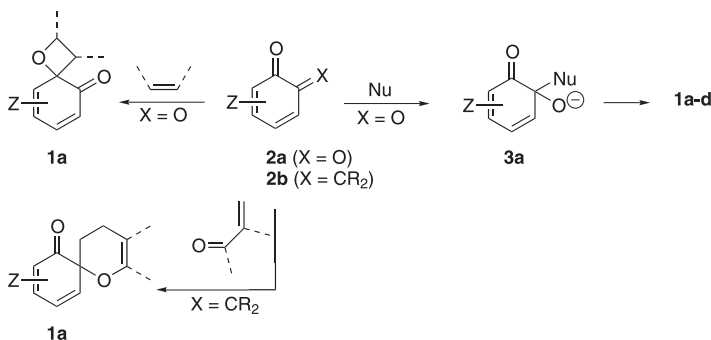


Fig. 2

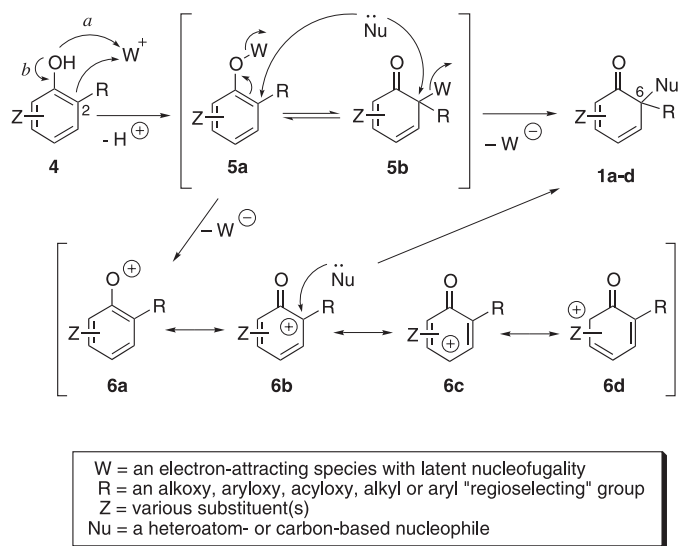


Fig. 3

and propargyl aryl ethers [17, 20] and the Moffat–Olofson reaction of arenoxysulfonium ylides [21–26] are, when directed toward substituted positions, dearomatizing reactions that offer direct routes to cyclohexa-2,4-dienones. Their implementation in the preparation of *ortho*-quinol derivatives has remained limited [27]. Nevertheless, other avenues are available for arenols because their electron-richness makes them ideal candidates for oxidative dearomatization processes [28].

Arenols **4** and their conjugate arenolate bases are both (a) oxygen- and (b) carbon-based nucleophiles, which react with a wide range of electrophilic reagents (Figure 3). Their reactions with soft electrophiles can lead directly to cyclohexadienone derivatives; this is the case, for example, with electrophilic halogenation, which effectively occurs at the electron-rich carbon centers (**4** → **5b**) [29, 30].

Reactions with harder electrophilic reagents do not usually mediate immediate dearomatization, since the electrophilic attack occurs predominantly at the oxygen center (**4** → **5a**). However, when these reagents are equipped with a core atom or a chemical function whose nucleofugality can be turned on, subsequent dearomatizing bond-forming processes can be achieved with (**5a** → **1a–d**) or without (**5a** → **6** → **1a–d**) the help of an appropriate electron-displacing species (Nu). As alluded to above, the key to an efficient preparation of *ortho*-quinols and *ortho*-quinone monoketals does not simply reside in the ability to dearomatize the starting arenol, but in the capacity to control the attack of the electron-displacing species at the substituted 2-position. A regiocontrolling device is necessary to prevent competition from *para* attack, which would lead to cyclohexa-2,5-dienone systems. One can envisage several solutions for this requisite. Non-oxidative pericyclic reactions, such as the Claisen sigmatropic [3,3] rearrangement, are mechanistically well suited for imposing both dearomatization and *ortho*-selective bond formation [27]. Another solution requires the presence of an electron-releasing group at the substituted 2-position of the starting arenol (e.g. R = alkoxy).

Such a substituent often suffices to ensure regioselective introduction of an electron-rich species at this position, even when it is the most hindered locus (Figure 3). This is particularly appropriate for reactions following an ionic-type mechanism with intermolecular delivery of the nucleophile (Nu). Thus, 2-alkylarenols **4** can be transformed by *oxidative nucleophilic substitution*, through intermediates **5** or **6**, into 6-carbo-6-oxocyclohexa-2,4-dienone *ortho*-quinol derivatives using an oxygen-based nucleophile, whereas 2-alkoxyarenols can similarly react with either carbon- or oxygen-based nucleophiles to furnish either 6-carbo-6-oxo- or 6,6-dioxocyclohexa-2,4-dienone derivatives **1a–d**.

15.1.2

Why Bother with *ortho*-Quinols and *ortho*-Quinone Monoketals?

15.1.2.1 Synthetic Reactivity of *ortho*-Quinols and *ortho*-Quinone Monoketals

ortho-Quinone monoketal and *ortho*-quinol cyclohexa-2,4-dienones **1a–d** have been less utilized in synthesis than their *para* cross-conjugated cyclohexa-2,5-dienone counterparts **1g** (Figure 1). The *ortho* and *para* quinonoids do share several reactivity features, but the chemistry of *ortho* species is often more capricious and demands some special considerations. The difference between the linear and the experimentally more stable cross-conjugated systems cannot alone account for the reactivity differences observed between *ortho* and *para* compounds [2, 31]. *ortho*-Quinone monoketals and *ortho*-quinols do exhibit additional reactivity features due to the vicinal positioning of their oxygen functions. This arrangement of electronegative oxygen atoms weakens the bearing C₁–C₆ bond, and the dienone system is predisposed toward dimerization as it can behave both as a dienic and as a dienophilic partner in Diels–Alder cycloaddition. The preparation conditions and substitution pattern must be carefully chosen in order to avoid premature ring-opening, dimerization, or rearomatization events (Section 15.3). *ortho*-Quinone monoketals are masked forms of *ortho*-quinones in which one carbonyl unit is protected as a ketal function. The two vicinal oxygen functions and the two conjugated carbon–carbon double bonds are thus clearly differentiated from one another (see **1c**, Figure 1). In comparison to the reactivity of *ortho*-quinones, that of the linearly conjugated enone system of their monoketals is attenuated for easier control in synthetic manipulations. Another particularly interesting feature of these synthons is their electrophilic reactivity. These quinone ketals are indeed susceptible to direct and conjugate attacks by various types of nucleophiles (Section 15.3.3) [6], in contrast to their aromatic parents, which are more readily transformed through electrophilic aromatic substitution. *ortho*-Quinone monoketals can be viewed as masked aryl cation intermediates (see **1f**, Figure 1), allowing synthetic operations formally equivalent to an otherwise non-trivial nucleophilic aromatic substitution of their parent arenes. *ortho*-Quinone monoketals do share this reactivity feature with their *para* counterparts [32, 33], but substitution is conceivable at the five *sp*² ring carbons depending on the type of nucleophilic attack (see **1f**, Figure 1). Conversion into quinone ketals constitutes a means of rendering arenols amenable to further ring transformations, including carbon–carbon bond-forming events by nucleophilic attack. A last but not least feature of *ortho*-quinol derivatives paradoxically resides in the structural motif that is the principal cause of the complications encountered in their synthetic uses, that is their adjacent oxygenated ring carbons. It is not always trivial to introduce such functionalities on a pre-established cyclic hydrocarbon network. The various possibilities

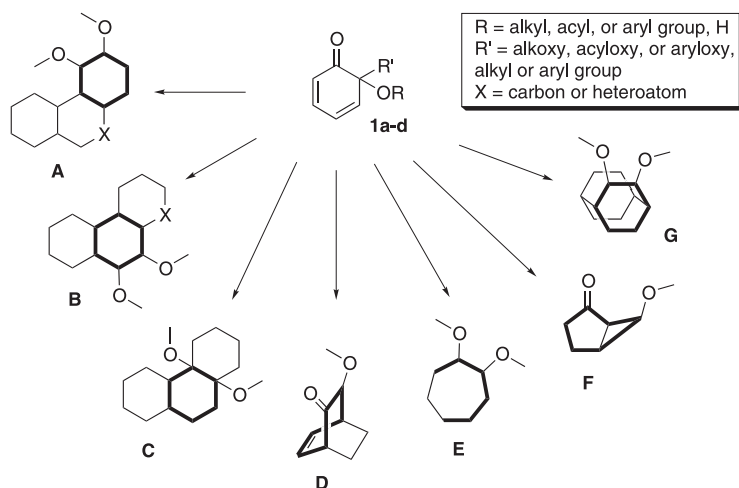


Fig. 4

available for the rapid elaboration of complex structural architectures from *ortho*-quinol derivatives make them ideally functionalized synthons for the construction of polyoxygenated carbo- and heteropolycyclic skeleta (Figure 4).

15.1.2.2 Biosynthetic Implications of *ortho*-Quinols and *ortho*-Quinone Monoketals

Many natural products display structural motifs biosynthetically derived from *ortho*-quinol precursors, and some even feature *ortho*-quinol moieties in their final structural arrangement [1, 6]. Asatone (7) and related neolignans can be put forward as classic examples of complex natural products derived from cyclodimerization of oxidatively activated simple phenol precursors (Figure 5); biomimetic syntheses of 7 have accordingly been accomplished by anodic oxidation (Section 15.2.1) and by Pelter oxidation (Section 15.2.2) of the naturally occurring phenol 9 [34, 36].

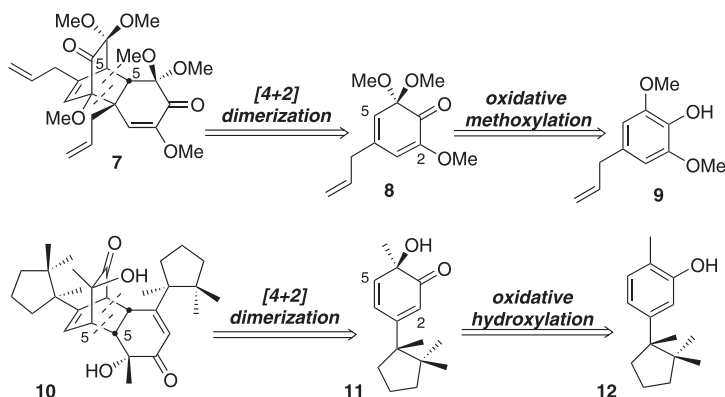


Fig. 5

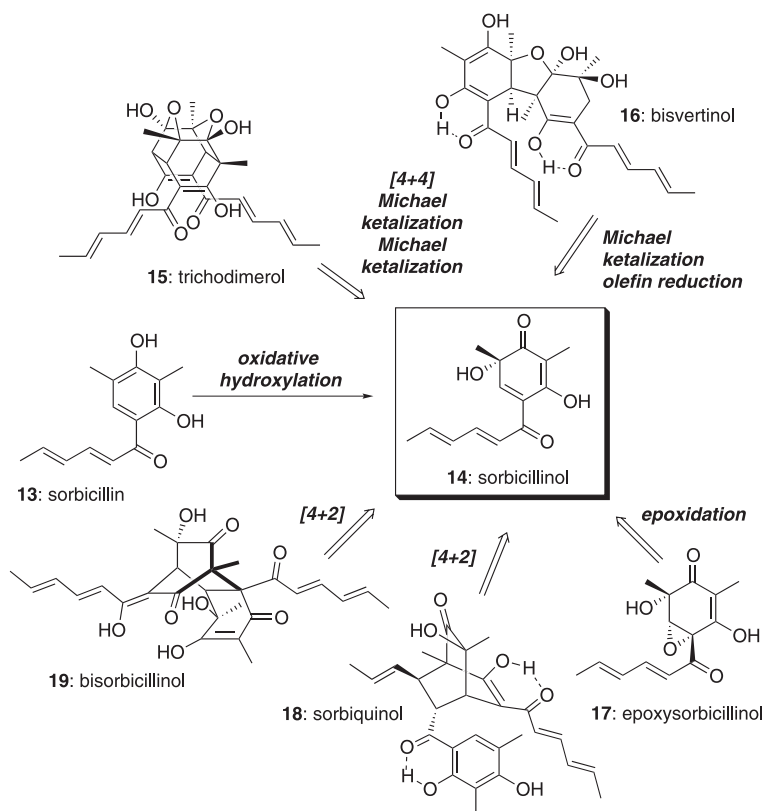


Fig. 6

A series of new examples has recently emerged in the literature. Aquaticol (**10**), an unusual cuparane-type bis-sesquiterpene isolated from the medicinal plant *Veronica anagallis-aquatica*, can be derived from a Diels–Alder cyclodimerization of the *ortho*-quinol **11**, itself derived from an enantiospecific oxidative hydroxylation of (–)- δ -cuparene (**12**) (Figure 5) [37, 38]. Sorbicillinoid members of the vertinoid polyketide class of natural products also present the same chemical filiation inasmuch as they appear to originate biosynthetically from the sorbicillinol (**13**)-derived *ortho*-quinol **14** (Figure 6) (Section 15.3.3) [39, 40].

Scyphostatin (**20**) was isolated in 1997 as a potent inhibitor of neutral sphingomyelinase (N-SMase) [41, 42]. Synthetic studies on this therapeutically important molecule are currently in progress (Section 15.3.3) [43, 44]. Its structure features an epoxycyclohexenone moiety, which could conceivably be made through an oxidative dearomatization approach (Figure 7).

The humulones **23a–d** have been known for many years, but they can still be considered as a topical family of natural products (Figure 8). Found in hop resins and brewing hops, these natural *ortho*-quinols aroused early interest because of their antibiotic and tuberculostatic properties. Oxidative dearomatizing hydroxylation of their phenolic parents **24a–d** was used in their synthesis [1].

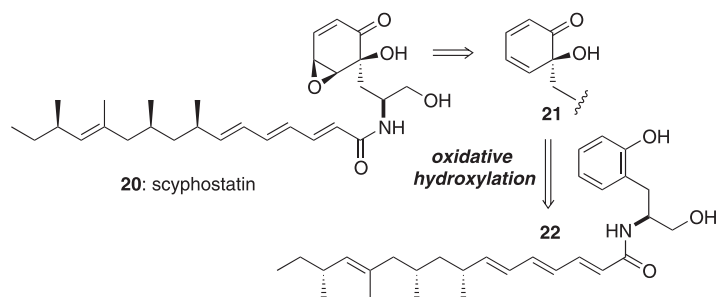


Fig. 7

In addition to the aforementioned prominent biosynthetic implications of *ortho*-quinol derivatives, one can also propose their more discrete roles in the construction of natural products that feature motifs resulting from C–C and C–O phenolic couplings. Numerous alkaloids, lignans, and polyphenolic tannins can be envisaged as stemming from such coupling processes, traditionally said to derive from phenoxy radical combinations. Since two-electron oxidation of phenols can produce *ortho*-quinone derivatives, including monoketals, that are capable of efficiently undergoing selective bond formation, the role of quinone monoketals in biosynthetic scenarios cannot be disregarded. It was the application of this concept in the natural products synthesis arena that allowed Feldman and co-workers to achieve striking advances in complex ellagitannin synthesis [45–50] (see Chapter 14). Generally speaking, the oxidative dearomatization of arenols to give *ortho*-quinols and *ortho*-quinone monoketals, and their synthetic manipulation by cycloadditions (Section 15.3.1) or by nucleophilic attacks (Section 15.3.3) constitutes a tactic that is unequivocally better adapted to regio- and stereoselective bond formation than synthetically disappointing phenoxy radical coupling processes [33, 47, 51].

15.1.2.3 Biomechanistic Implications of *ortho*-Quinols and *ortho*-Quinone Monoketals

Many reasons for studying the chemistry of *ortho*-quinol derivatives lie in their implications in the biomechanisms of naturally occurring compounds [6]. Their putative involvement in the metabolism of α -tocopherol (i.e. vitamin E) [52–54], and in the mode of action of the in-

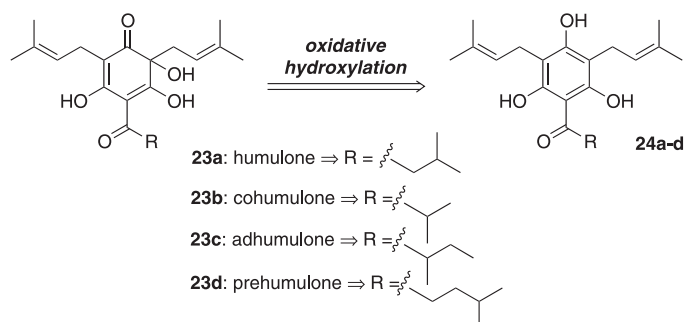


Fig. 8

tercalating antitumor agent *N*-2-methyl-9-hydroxyellipticinium acetate [55, 56], are just a couple of illustrations of their biological significance [57]. In these and other biomechanisms, in which one-electron oxidation of phenol units has often been claimed to be the central chemical event, two-electron oxidation alternatives leading to arenoxenium species and quinone derivatives, including monoketals, can again be invoked. In the same line of thought, one may be puzzled by the biological dichotomy apparently expressed by catecholic arenols (i.e. 2-hydroxyphenols) in natural systems. Many medicinal virtues of such arenols, well exemplified by numerous plant polyphenols, have been attributed to antioxidant-like, radical-scavenging activities due to the ease of one-electron oxidation to phenoxy radicals. Further oxidation gives rise to highly reactive *ortho*-quinones that are probably better known for their toxicity than for their medicinal activity [58]. As blocked *ortho*-quinones, *ortho*-quinone monoketals might instead express an intermediate level of chemical reactivity better suited for the specific molecular interactions that underlie the therapeutic properties of natural phenols under oxidative conditions.

Study of the oxidation chemistry of exifone (**25a**) constitutes a perfect illustration of the above statement [59, 60]. This pyrogallol benzophenone (Adlone®) was commercialized in France for the treatment of cognitive disorders in the elderly, but it was withdrawn from the market because of its hepatotoxicity, which was attributed to its 3,4-quinone metabolite **26a**. Fleury and co-workers found that blocking of **26** in the form of 1,4-benzoxazin-8-one *ortho*-quinols such as **28** led to a twenty-fold decrease in toxicity, together with a five-fold activity enhancement (Figure 9) [59, 60].

15.2

Oxidative Dearomatization of *ortho*-Substituted Arenols

15.2.1

Anodic Oxidation

Anodic oxidation can be used to dearomatize 2-substituted arenols. The outcome of such an electrochemical transformation is extremely sensitive to the reaction conditions used,

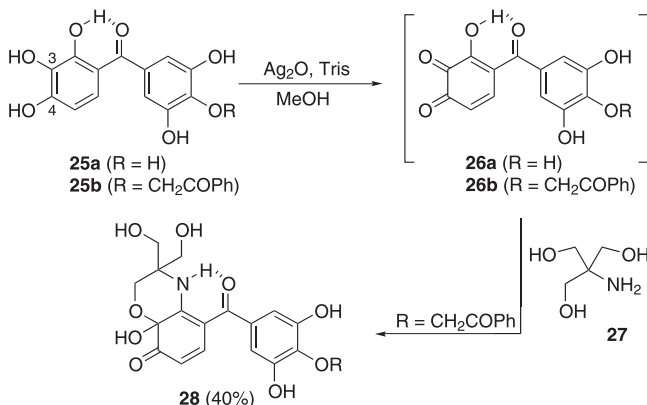


Fig. 9

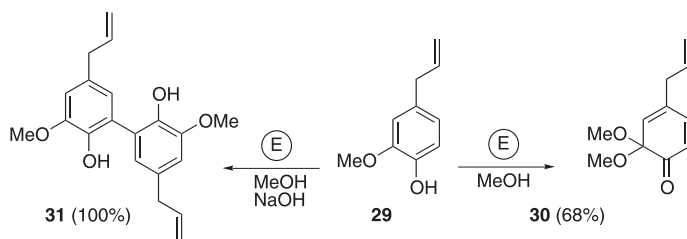


Fig. 10

viz. the applied potentials, the reaction medium, and the type of substituents on the aromatic ring [35, 36, 61, 62]. Neutral conditions appear to favor the formation of cationic intermediates such as **6** through two-electron oxidation (Figure 3). These phenoxenium ions can be rapidly quenched in MeOH to furnish *ortho*-quinone monoketals such as **1c** (Figure 3, R = Nu = OMe), but electrolysis of the same starting phenols in a basic medium at a lower oxidation potential predominantly gives dimers resulting from phenoxy radical coupling [35, 36, 62–64]. Such divergent behavior of arenols has been clearly delineated by Yamamura and co-workers, who showed, *inter alia*, that eugenol (**29**) is converted to the *ortho*-quinone monoketal **30** in 68 % yield when electrolyzed in MeOH at a constant current (90 mA, 0.56 mA cm^{-2} , +750–780 mV *vs.* SCE) using a platinum anode and LiClO_4 as the supporting electrolyte (Figure 10) [36]. However, **29** dimerized to give the biaryl compound **31** in quantitative yield when the electrolysis was performed at a lower oxidation potential (21 mA, 1.5 mA cm^{-2} , +200–220 mV *vs.* SCE) in the presence of NaOH (Figure 10) [36].

The electrooxidative methoxylation of aryl methyl ethers in methanolic KOH is another electrochemically-induced dearomatizing technique that is worth recalling here for comparison purposes [6]. Its mechanistic unfolding is different from that of the oxidative nucleophilic substitution of free arenols (Figure 3) since it involves radical cation intermediates leading to quinone bisketals as primary electrochemical products. Their hydrolysis to give quinone monoketals has been well developed by Swenton and co-workers [5, 10, 11]. This method, referred to herein as the Swenton oxidation, has demonstrated its utility for preparing *para*-quinone monoketals, but *ortho* analogues are harder to produce in this way. Nevertheless, successful experimentation has been described for naphthoquinone monoketals, which are less reactive than benzoquinones because their 4,5-double bond is part of an aromatic ring (Figure 11). Of particular note is the regioselective acid-catalyzed formation of the linearly conjugated system **34**, which is invariably favored over the formation of the cross-conjugated regioisomer **35**. This preference has been attributed to differences in charge stabilization of the cationic intermediates leading to these monoketals [10].

Electrooxidative activation is just one of the tools with which synthetic organic chemists can effect the dearomatization of arenols and their ethers to give cyclohexa-2,4-dienone derivatives. Other methods are based on the utilization of oxidizing reagents that mediate the oxidative nucleophilic substitution of 2-substituted arenols in the presence of appropriate nucleophilic species. These reagents are for the most part all based on metals (Section 15.2.2) or halogens (Section 15.2.3).

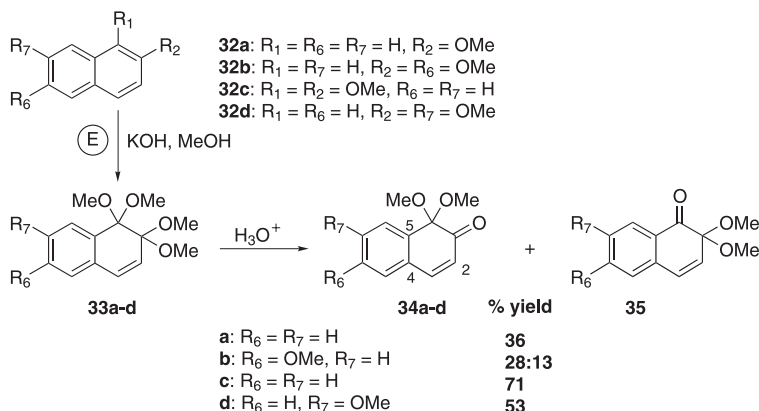


Fig. 11

15.2.2

Metal-Based Oxidative Activation

Metal-based reagents are often used to promote one- and two-electron oxidations of arenols. Radical-mediated C–O coupling reactions of aryloxy radicals can, of course, lead to *ortho*-quinol derivatives, but the preparative value of such an approach is poor and essentially limited to intramolecular cases. For example, certain bis-phenols such as **36a–c** have been spiroannulated in good yields by diradical C–O coupling under favorable one-electron oxidation regimes (Figure 12) [65–67].

Oxidative nucleophilic substitution is, however, a more versatile technique and a much better choice for target-oriented synthesis (Sections 15.1.1 and 15.1.2.2). In 1950, Wessely and co-workers examined the use of lead tetraacetate (LTA) in acetic acid to determine the structure of phenols and, in doing so, they developed their oxidative acetoxylation reaction, referred to herein as Wessely oxidation (Figure 13) [68–76]. If both an *ortho*- and a *para*-position are available to accommodate the entry of the acetoxy nucleophile, *ortho* products often predominate even when the *ortho* position is already occupied by a resident alkyl (e.g. **40** → **41a/b**) or alkoxy group (Figure 13) [69, 74].

Phenols with a free *ortho* position can also give rise to *ortho*-quinone diacetates such as **39a** and **41b**, in addition to or instead of *ortho*-quinol acetates such as **41a** [1, 6]. Phenols bearing a 2-methoxy group are particularly prone to regioselective Wessely oxidation to give 6-

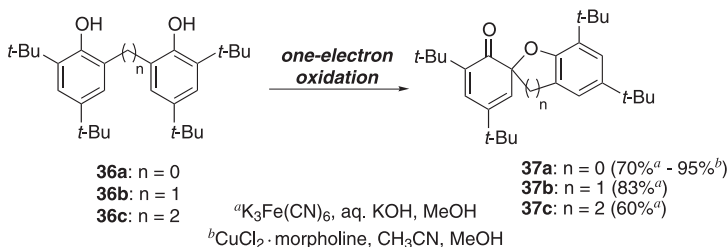


Fig. 12

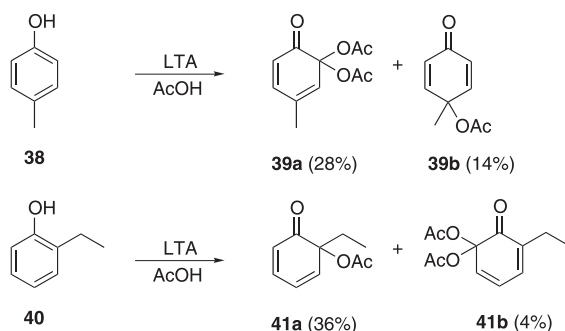


Fig. 13

acetoxy-6-methoxycyclohexa-2,4-dienone derivatives such as **43a/b**, which can be isolated in good yields (Figure 14) [71, 76].

Thallium triacetate [77], and later, thallium trinitrate (TNN) in alcoholic solutions were found to mediate similar transformations of arenols into either *para*- or *ortho*-quinol derivatives. In particular, McKillop and collaborators extensively studied the use of TNN in MeOH to oxidize 4- and a few 2-substituted phenols; this reaction is referred to herein as the McKillop oxidation (Figure 14) [78, 79]. As expected from Andersson's observations (Section 15.3.1), the 5-methoxylated *ortho*-quinone dimethyl monoketal **45a** is stable, but the aldehyde **42a** gave rise to the Diels–Alder dimer **46** under the conditions of the McKillop oxidation. Interestingly, the same aldehyde furnished a non-dimerizing *ortho*-quinol acetate **43a** under the conditions of the Wessely oxidation (Figure 14). We made similar observations when comparing the oxidative methoxylation of 2-methoxyphenols with our oxidative acetoxylation (Section 15.2.3) [80], thus confirming the role of a 6-acetoxy group in the resistance of cyclohexa-2,4-dienones to undergo $[4\pi+2\pi]$ cyclodimerization (Section 15.3.1).

Many other metals have been used over the years to generate *ortho*-quinone monoketals and *ortho*-quinol derivatives [6], but the venerable Wessely oxidation remains to this day the most commonly used metal-based method. For the generation of *ortho*-quinols by selec-

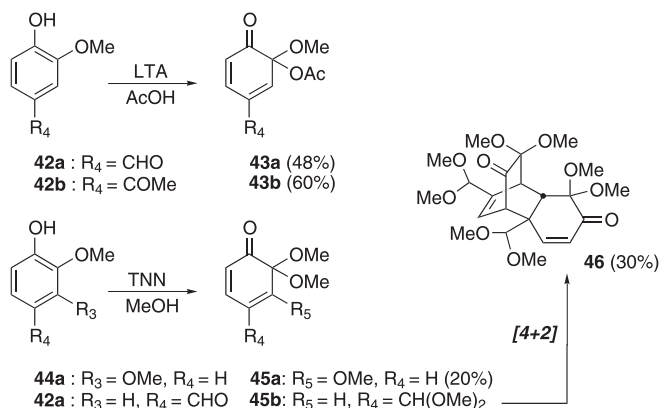


Fig. 14

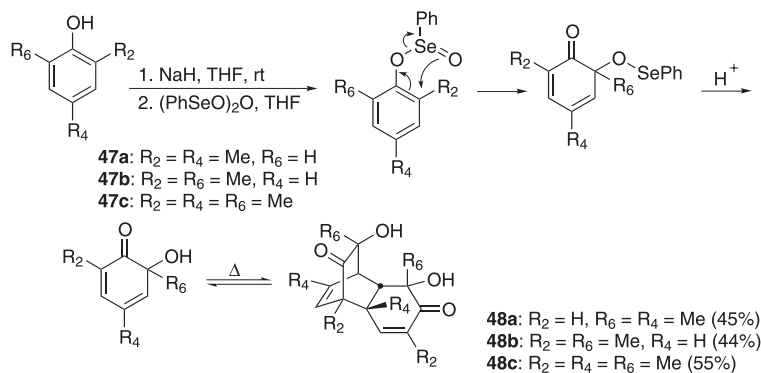


Fig. 15

tive *ortho*-hydroxylation of 2-substituted arenols such as **47a–c**, one should not forget the selenium-based Barton oxidation, in which oxygenation at the *ortho* position is ensured by intramolecular delivery from the diphenylseleninic anhydride following reaction of the latter with the phenolate anion (Figure 15) [81, 82]. Acid hydrolysis furnished *ortho*-quinols that spontaneously dimerized to give bicyclo[2.2.2]octenones **48a–c**. Pyrolysis of such dimers can be used to regenerate the *ortho*-quinol parents in situ [180].

15.2.3

Halogen-Based Reagents

Various electrophilic and oxidizing halogen-based reagents such as bromine, *N*-bromosuccinimide, ammonium tribromides, and polyvalent iodine species, have been used to generate *ortho*-quinol derivatives [6]. For example, the use of phenyltrimethylammonium tribromide is exemplified in Biali's ongoing investigation of chemical modifications of calixarenes [83, 84]. This oxidizing system is used to generate various mono- to tris(spirodienone) derivatives such as **50** from calix[*n*]arenes such as the spherand-type **49** (Figure 16).

The two halogen-based methods that continue to attract organic chemists the most for the oxidative activation of arenols are the Adler oxidation and the Pelter oxidation (vide infra);

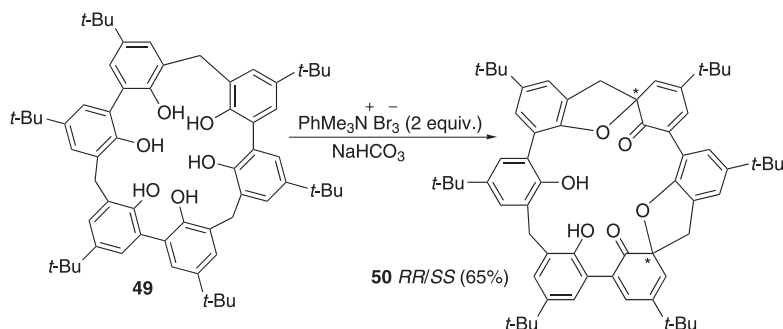


Fig. 16

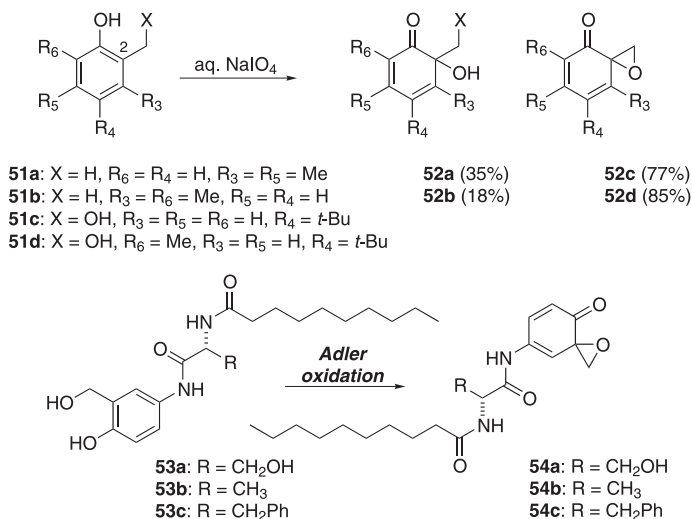


Fig. 17

both methods rely on polyvalent iodine reagents [6]. The Adler oxidation is based on the use of sodium periodate (NaIO₄) or periodic acid (HIO₄) in water, aqueous alcohols, or acetic acid. Initially developed for the determination of phenolic hydroxyl groups in lignins, this oxidation can be used to perform *ortho*-oxygenation of 2-substituted arenols, thus furnishing *ortho*-quinols such as **52a/b** or their ethers and esters, and it is particularly efficient in promoting the spirocyclization of 2-hydroxymethylphenols **51c/d** (Figure 17) [85–96]. This intramolecular version of the Adler oxidation was recently used by Giannis and co-workers to synthesize active spiroepoxide analogues **54a–c** of scyphostatin (**20**) (Figures 7 and 17) [43, 97, 98].

The other method relies on the use of a hypervalent iodine(III) reagent [99–104]. Following in the footsteps of Wessely, Siegel, and Antony [105] first compared the use of LTA to that of phenyliodonium(III) diacetate (PIDA) in acetic acid in performing the oxidative acetoxylation of various alkylphenols. Curiously, they only obtained *para*-quinol acetates with PIDA, whereas LTA gave *ortho*-quinol acetates from the same starting phenols. In 1988, Pelter and co-workers reinvestigated the use of PIDA to oxidize phenols in MeOH and thus introduced the PIDA-mediated oxidative methoxylation of phenols, referred to herein as the Pelter oxidation [106–108]. In 1987, Tamura [109] had reported the use of another less nucleophilic hypervalent iodine reagent, phenyliodonium(III) bis(trifluoroacetate) (PIFA), to promote the oxidative alkoxylation of arenols. Tamura's and Pelter's applications of this oxidative nucleophilic substitution of arenols were essentially limited to the production of *para*-quinone dialkyl monoketals, but numerous other workers have since successfully applied it to the preparation of various *ortho*-quinone monoketals (Section 15.3) [6]. The mechanistic details of the reaction are still under investigation, for they raise an interesting question embedded in the scheme of Figure 3, *viz.* does the reaction follow a concerted or a stepwise pathway? This was also a much debated question with regard to the Wessely and Adler oxidations that follow similar mechanisms [1, 6, 87, 110]. Both routes are driven by the reduc-

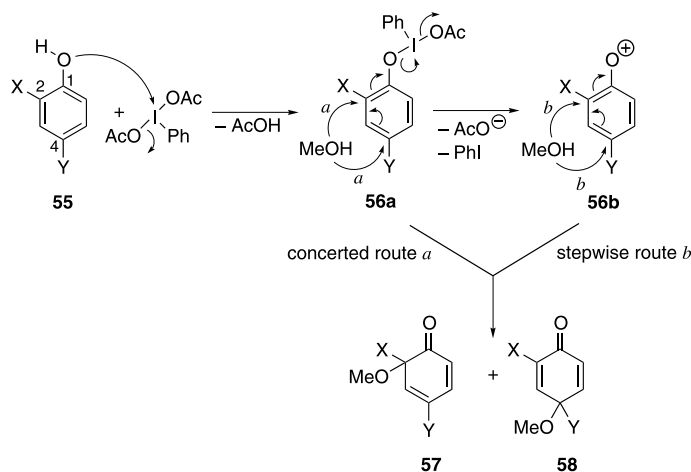


Fig. 18

tive conversion of trivalent iodine into monovalent iodine and first imply the formation of the aryloxyiodonium(III) species **56a**, which can then either undergo direct nucleophilic attack (route *a*) or dissociate to furnish a solvated phenoxenium cation **56b** (route *b*) (Figure 18). Pelter and collaborators recently concluded that the process is most likely to proceed via a phenoxenium ion of type **56b** (route *b*) on the basis of the following arguments: (1) the phenyliodonium(III) group is an extremely powerful nucleofuge with a leaving ability about 10^6 times that of the triflate group; (2) Mulliken charge semiempirical calculations of a series of 2- and 4-substituted phenoxenium cations predict the observed regiochemistry of the nucleophilic attack with accuracy (*vide infra*), and (3) reactions performed on 2-alkoxyphenols in a chiral environment displayed a complete lack of stereochemical control [108, 111]. As alluded to above, and demonstrated many times experimentally, the regiochemistry of the methanol attack (i.e., *ortho*-**57** vs. *para*-**58**) depends more on the electronic nature of the ring substituents than on their steric demand.

Arenols bearing a strong electron-releasing group capable of stabilizing a positive charge at C-2 (e.g. X = OMe) selectively undergo nucleophilic attack at C-2 regardless of the steric situation at C-4 (e.g. Y = H, Me), as well as at C-6. Alkylphenols such as 2,3-dimethylphenol, 3,5-dimethylphenol, 2-benzyl- and 4-benzylphenol, and 2,4,6-tri-*tert*-butylphenol show a net preference for attack at C-4 [108].

The *ortho*-quinol acetates used in our own investigations have been prepared by a modification of the Pelter oxidation. Oxidative methoxylation of 2-methoxyarenols according to Pelter, as well as Tamura, Adler, and McKillop oxidations, affords 6,6-dimethoxycyclohexa-2,4-dienones such as **60**, which are particularly prone to dimerization through Diels–Alder cycloaddition (Figure 19). In agreement with Wessely's early observations, 6-acetoxy analogues of the same starting arenols often do not spontaneously dimerize (Section 15.3.1) and hence can participate in other chemistries [80, 112]. Our oxidative acetoxylation is conveniently performed by simply treating a solution of 2-methoxyarenols such as **59** with PIDA in CH_2Cl_2 to generate non-dimerizing *ortho*-quinol acetates such as **62** in high yield (Figure

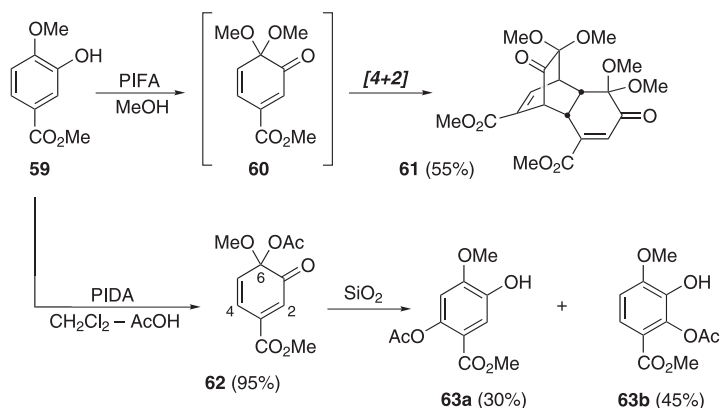


Fig. 19

19). It is not necessary to add acetic acid to the reaction medium; the PIDA reagent suffices for regioselective delivery of the acetate group [112].

The above oxidative nucleophilic substitutions are primarily used to introduce an oxygen-based nucleophile in order to convert arenols into *ortho*-quinone dialkyl monoketals and *ortho*-quinol acetates. Our own investigations into the synthetic utility of arenol dearomatization [113] led us to contemplate the possibility of introducing a carbon-based nucleophile. We ventured to find reagents that would promote the oxidative activation of 2-alkoxynaphthols such as **64a/b** in the presence of masked nucleophiles (Figure 20). Conditions needed to be found that would unveil their nucleophilic power *in situ*, and in a timely fashion to ensure chemo- and regioselective carbon–carbon bond formation at the 2-position. This goal

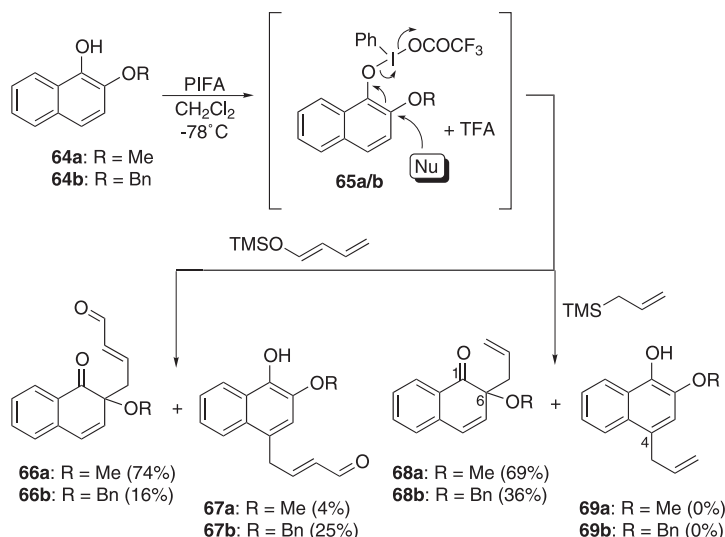


Fig. 20

was achieved by using PIFA as a non-nucleophilic oxidizing agent in the presence of oxidation-sensitive allylsilane or 1-trimethylsilyloxybuta-1,3-diene as soft carbon nucleophiles [113, 114]. The trifluoroacetic acid (TFA) released during the oxidation step generates an acidic medium that is certainly propitious to the requisite cleavage of the Si–C and Si–O bonds. The naphthalenone **68a** had previously been synthesized by Adler oxidation of 2-allylnaphthol in a pitiful yield of 0.53 % [115]. In the present case, the 2-methoxy group acts as a powerful regioselector aiding in the elaboration of the carbon–carbon bond; no C-4 adduct **69a** is observed. An unfortunate loss of selectivity is observed with the 2-benzyloxynaphthol **64b**, however, probably because of the greater steric demand of the phenyl group. There exist a few other approaches for the preparation of *ortho*-quinol derivatives besides those that can be grouped within the aforementioned three main categories. Our recent review on this topic constitutes a source of leading references for these subsidiary methods [6].

15.3

Synthetic Applications of *ortho*-Quinols and *ortho*-Quinone Monoketals

The predisposition of *ortho*-quinols and *ortho*-quinone monoketals toward aromatizing rearrangement and dimerization is at the origin of the difficulties that surround their manipulations in organic synthesis (Section 15.1.2.1) [1, 2]. Aromatization through a methyl 1,2-shift was, for example, the cause of failure of the *ortho*-quinol-based route initially adopted by Wood and co-workers in their recent synthesis of epoxysorbicillinol (**17**; Figure 6) [116]. We have already noted that *ortho*-quinol acetates are less inclined to undergo dimerization than *ortho*-quinone dialkyl ketals, as well as free *ortho*-quinols, but that they are quite sensitive to rearomatizing acetate shifts [117–119]. We experienced this rearrangement chemistry ourselves when submitting certain *ortho*-quinol acetates such as **62** to silica gel chromatography (vide supra). Pericyclic [3,3]- and “pseudopericyclic” [3,5]sigmatropic acetate shifts furnished the phenols **63a** and **63b**, respectively (Figure 19) [6, 80].

It is nevertheless possible to bridle the reactivity of *ortho*-quinols and *ortho*-quinone monoketals for rapid elaboration of structural complexity and diversity in a pertinent manner for target-oriented synthesis. Some remarkable accomplishments have been highlighted in several review articles [3, 5, 6, 120]. Among the most significant ones, one can cite rearrangements of bicyclo[2.2.2]octenone cycloadducts into decalins, ring-contractions to polyquinanes, ring-expansions to tropolones, intramolecular cycloadditions to isotwistanes, cationic annulations to benzofurans, and nucleophilic additions to biaryls, enediyne units, and benzannulated heterocycles of various sizes.

15.3.1

Diels–Alder Cycloadditions

The ability of the cyclohexa-2,4-dienone unit of *ortho*-quinone monoketals and other *ortho*-quinol derivatives to react as either a diene or a dienophile component in $[4\pi+2\pi]$ cycloadditions is arguably their principal virtue in organic synthesis, and paradoxically it is also the principal reason why it is often difficult to exploit them in synthesis; they often dimerize faster than they can combine with another π -system partner. Adler, Andersson, and co-workers have extensively studied the behavior of *ortho*-quinols in Diels–Alder cycloadditions,

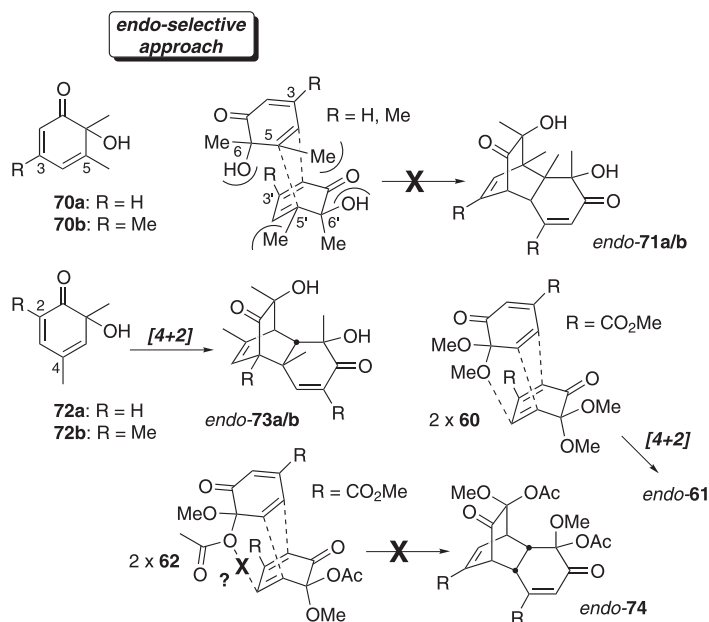


Fig. 21

and observed that systems bearing substituents at their 5-position do not dimerize as readily [85–93, 95, 121]. A substituent at this locus can apparently interfere with the geminal C-6 groups of the other unit in their *endo*-selective “back-to-back” mutual approach, which is observed in all reported cases [1, 6]. Thus, for example, 6-hydroxy-5,6-dimethyl- (**70a**) and 6-hydroxy-3,5,6-trimethylcyclohexa-2,4-dienone (**70b**) do not dimerize, whereas 6-hydroxy-4,6-dimethyl- (**72a**) and 6-hydroxy-2,4,6-trimethylcyclohexa-2,4-dienone (**72b**) do (Figure 21) [85, 94, 95]. An explanation for the exclusive and regioselective participation of the 4,5-double bond as the 2π partner in these dimerizations can be found in a report by Houk [122], who calculated that both the HOMO and the LUMO of 1-substituted electron-deficient dienes possess slightly higher atomic coefficients at the sp^2 -carbon center remote from the carbonyl group, that is C-5 in the dimerizing cyclohexa-2,4-dienone units [79]. Other calculations made on 1-substituted and 1,4-disubstituted dienes did not allow any clear-cut interpretation and hence brought the debate round to the influence of secondary orbital interactions [122–124]. The regioselectivity in Diels–Alder dimerizations of *ortho*-quinol derivatives still awaits theoretical clarification.

This tendency toward spontaneous dimerization was further elaborated for *ortho*-quinone monoketals by Liao, who concluded that electron-withdrawing and/or small groups at the 4-position of 6,6-dimethoxycyclohexa-2,4-dienones tend to facilitate self-dimerization, whereas electron-releasing and/or large groups at their 2- and/or 4-positions, as well as small electron-releasing groups at their 5-position, have the reverse effect [125]. A bromide in the 4-position is particularly efficient at retarding self-dimerization [126]. Liao and co-workers also suggested that one methoxy group in *ortho*-quinone dimethyl ketals participates in sec-

ondary interactions in *endo*-selective transition states and thus enhances the propensity of these cyclohexa-2,4-dienone derivatives to self-dimerize (e.g. **60** → *endo*-**61**, Figures 19 and 21) [125]. A downward modulation of this orbital control with 6-acetoxy analogues (e.g. **62**, Figure 21) could be the cause of their resistance toward dimerization. Furthermore, the 6-acetate carbonyl must be critical to this protecting effect, since many *ortho*-quinol acetates tend to dimerize upon deacetylation [93, 94, 127, 128]. This acetoxy group effect still remains to be clarified, notwithstanding it constitutes a useful control that can be exerted in carefully planned synthesis, as exemplified in the recent synthetic studies towards “bisorbicillinoid” natural products (Section 15.3.3).

Liao and his co-workers have spent the last twenty years investigating [4+2] cycloaddition reactions with “masked” *o*-benzoquinones, or “MOBs” as they named them, and they remain today the frontrunners in unveiling the possibilities of using *ortho*-quinone monoketals in Diels–Alder reactions [6]. Their investigations demonstrated that numerous dienophiles, *inter alia* methyl vinyl ketone, acrylates, allyl, homoallyl crotyl, and cinnamyl alcohols, cyclopentadiene, acyclic dienes, and, more recently, even [60]fullerenes can react inter- or intramolecularly with *ortho*-quinone dimethyl monoketals such as **76** to furnish bicyclo[2.2.2]octenones [125, 129–133]. In all cases, the cycloadditions are regiospecific and proceed with high diastereoselectivity, irrespective of the electronic demand and position of substituents on the 6,6-dimethoxycyclohexa-2,4-dienone core; only the chemical yields are affected [6]. Furans behave in a somewhat unusual manner as electron-rich dienophiles with these quinone monoketals [134, 135]. Cintas and collaborators have also investigated the cycloaddition of furans with the *ortho*-quinone monoketal **76a** [136]. Acceleration of the reaction was achieved under ultrasonic irradiation, and the same stereochemical and regiochemical selectivities as those of the thermally-induced reaction were observed (Figure 22).

Here again, the cycloaddition is *endo*-selective, with only regioisomers **79** being formed, and, when using 2- and/or 3-substituted furans, only the unsubstituted furan double-bond reacts in these inverse electron-demand Diels–Alder processes [134–136]. Indoles, pyrroles, and thiophenes can also be made to react as dienophiles with *ortho*-quinone monoketals

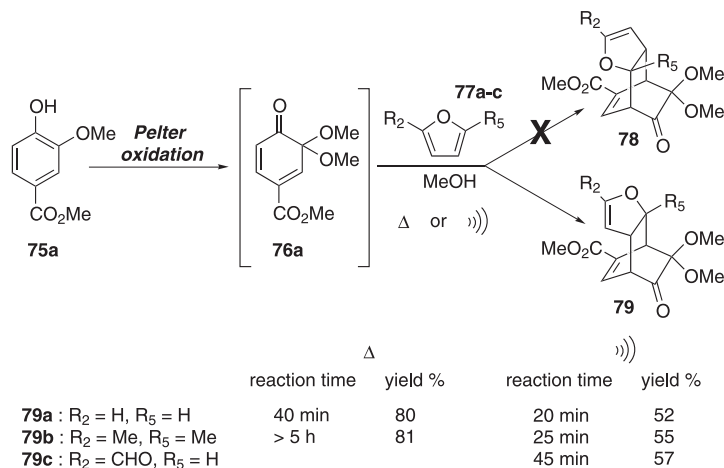


Fig. 22

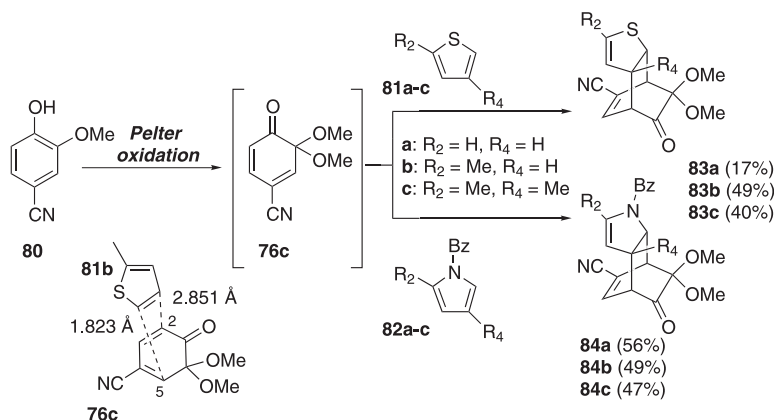


Fig. 23

76a–c bearing an electron-withdrawing group at their 4-position [136, 137]. The same regio- and stereochemical outcomes as those of reactions with furans are observed with these other aromatic species (Figure 23). Supporting evidence for these selectivities was also provided by calculations performed at the *ab initio* RHF/3-21G* level, which indicated asynchronous but still concerted low-energy transition states featuring shorter distances between a heteroatom-bearing sp² center of the aromatic units and the C-5 carbon center of cyclohexadienone unit (e.g. 81b + 76c, Figure 23) [137, 138].

An intriguing dichotomy was revealed in the reactivity of indole (85) with ketals 76a–c (Figure 24). At room temperature, only the Diels–Alder adducts 86a–c are obtained in good yields, but at reflux temperature, only rearomatized Michael-type 1,6-adducts 87a–c are observed [139].

Arjona and Plumet recently contributed to the study of the use of non-aromatic enol and thioenol ethers as dienophiles with inverse electronic demand [140]. Cycloadditions using 76a also proved to be *endo*-selective and regioselective (Figure 25). The regioisomers obtained were those having the heteroatom of the dienophile component adjacent (*ortho*) and *anti* to the carbonyl function, rather than *ortho* and *anti* to the dimethyl ketal function, as in the

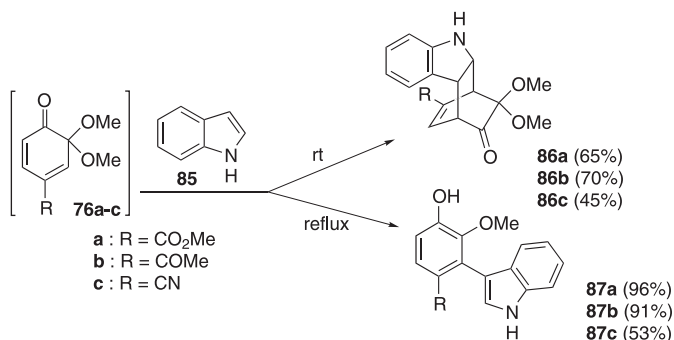


Fig. 24

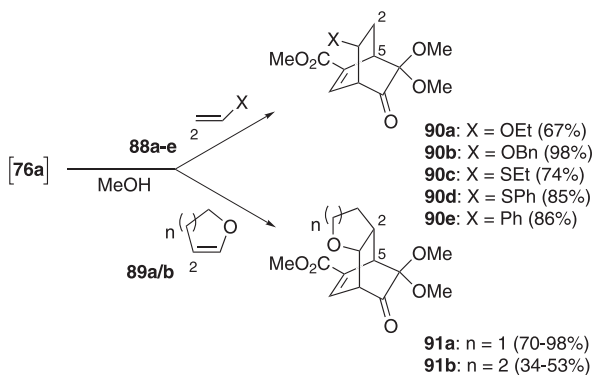


Fig. 25

furan-, pyrrole-, thiophene-, and indole-derived bicyclo[2.2.2]octenones (Figures 22–24). These regiochemical observations are corroborated by those reported in Liao's series of papers on the Diels–Alder reactivity between electron-rich dienophiles, such as benzyl vinyl ether **88b**, dihydrofuran **89a**, dihydropyran **89b**, phenyl vinyl sulfide **88d**, and styrene **88e**, and *ortho*-quinone monoketals derived from eight different 2-methoxyphenols (Figure 25) [141, 142].

Calculations performed at the HF/3-21G level indicated smaller energy gaps between the HOMOs of the aforementioned electron-rich dienophiles and the LUMOs of the quinone ketals, as can be expected for inverse electron-demand Diels–Alder reactions under FMO control [141]. Regiochemical controls observed with quinone ketals such as **76a** were well corroborated by the relative magnitudes of the atomic coefficients of the frontier orbitals. The highest coefficients at C-5 of the quinone ketal LUMO and at C-2 of the electron-rich alkenes would indeed promote bond formation between these centers. The results of calculations on other quinone ketals were, however, rather vague [141].

Numerous applications of the Diels–Alder reaction of *ortho*-quinone monoketals and *ortho*-quinols in natural products synthesis have been reported over the years [6]. The following few recent examples have been selected with the aim of illustrating the usefulness of the cycloaddition of *ortho*-quinol derivatives to give bicyclo[2.2.2]octenones, for these formidable strategic synthons can be further transformed in many ways to give various polycyclic architectures. Liao's group has added a couple of notches to its already remarkable record in the field. They described a total synthesis of the norsesquiterpenoid (\pm)-eremopetasidione **97** [143], the key steps of which were the Diels–Alder reaction of the quinone ketal **93** with ethyl vinyl ketone, followed by a Cope rearrangement of the resulting bicyclo[2.2.2]octenone system **94** (Figure 26).

The first total synthesis of (\pm)-pallascensin **103** was also reported by Liao's group [144] and features an intramolecular Diels–Alder reaction initiated by a regioselective oxidative alkoxylation of 2-methoxy-4-methylphenol **98** using the allylic alcohol **99** in the presence of PIDA. Vinylation of the resulting bicyclo[2.2.2]octenone **100**, followed by ring-expansion through an ionic 1,3-allylic shift gave the bicyclo[4.2.2]decenone **102**, which was further transformed into (\pm)-**103** (Figure 27).

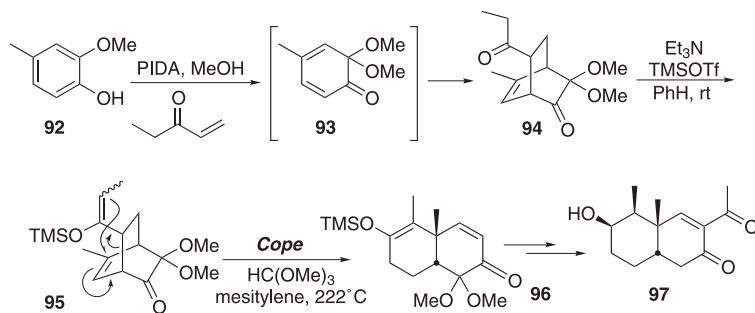


Fig. 26

Rodrigo and co-workers have made some progress towards viridin (**109**) [145]. After suffering a few setbacks due to a capricious installation of the C-10 methyl group, they managed to build the pentacyclic core of **109** from the tricyclic *ortho*-quinone monoketal **105** (Figure 28). This unit behaved both as a diene to furnish the desired pentacyclic fused system **106**, and as a dienophile to furnish **107**. The latter could be converted to the target **108** by a Cope rearrangement. A similar approach was used in their synthesis of (\pm)-xestoquinone and derivatives [146, 147].

The convenient generation of bicyclo[2.2.2]octenones through the use of *ortho*-quinol derivatives in Diels–Alder reactions recently inspired Wood and co-workers in their studies toward the total synthesis of CP-263,114 (**110**) [148]. They relied on the Wessely–Yates tandem oxidative acetoxylation/intramolecular Diels–Alder sequence to build bicyclo[2.2.2]octenones such as **114** en route to advanced isotwistane intermediates such as **111b**, which could eventually be fragmented to furnish the carbocyclic core of **110** (i.e. **111a** \rightarrow **110**, Figure 29) [149–153].

Photochemical transformations of bicyclo[2.2.2]octenones derived from Diels–Alder reaction of spiroepoxycyclohexa-2,4-dienones **116** have been exploited by Singh's group in their synthetic studies towards triquinane **119** and oxa-triquinane **121**, protoilludane **120**, and oxa-sterpurane **122** frameworks (Figure 30) [120, 154]. Spiroepoxycyclohexa-2,4-

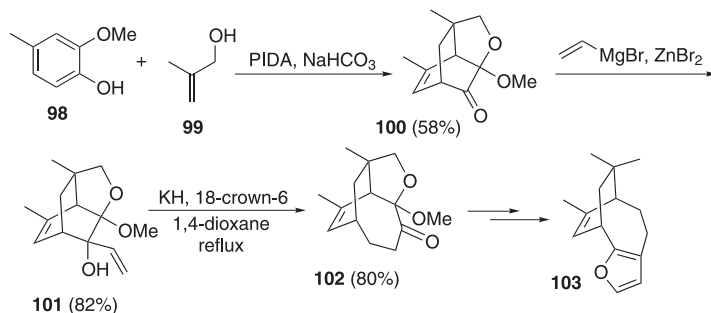


Fig. 27

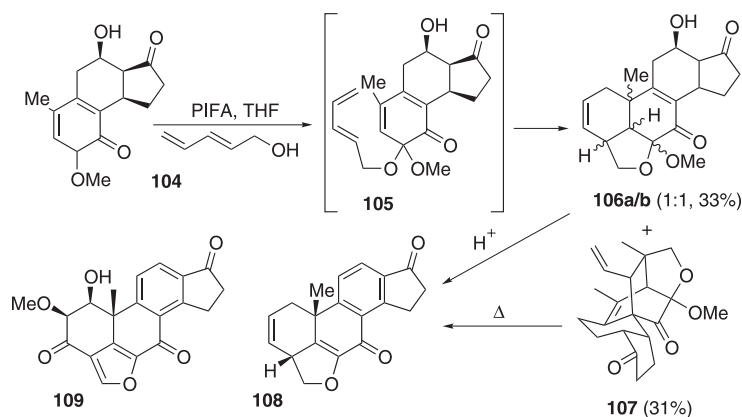


Fig. 28

dienones **116** are cyclic *ortho*-quinol ethers that can easily be generated by Adler oxidation of 2-hydroxymethylphenols **115**. Formal total syntheses of the triquinane (\pm)-coriolin have been achieved through 1,2-acyl shift as a result of oxa-di- π -methane rearrangement of bicyclo[2.2.2]octenones **117** upon triplet oxidation [155, 156]. Oxa-triquinanes **121** and oxa-sterpuranes **122** can be constructed in a stereoselective manner by modulation of the chemical reactivity of photochemically excited bicyclo[2.2.2]octenones [157]; triplet excitation of the β,γ -enone system furnishes **121**, whereas its singlet excitation induces a 1,3-acyl shift to give **122**.

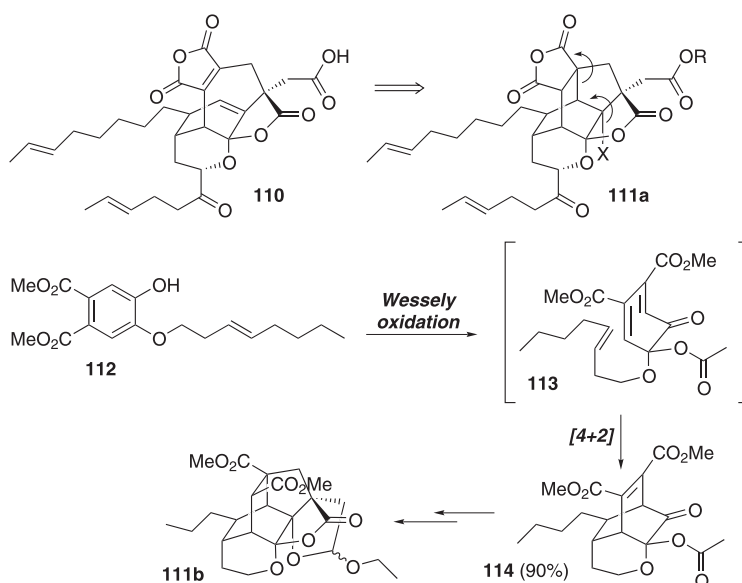


Fig. 29

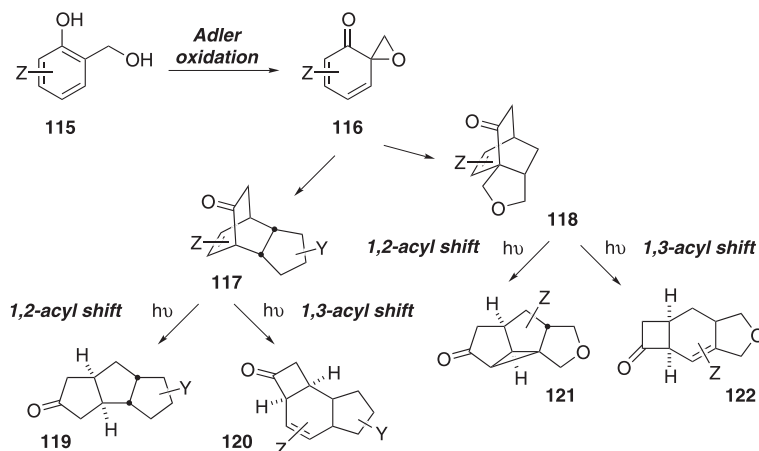


Fig. 30

15.3.2

Photochemical Rearrangements

Cyclohexa-2,4-dienones are particularly sensitive to photochemically-induced transformations. Seminal investigations by Barton and co-workers [158, 159] have demonstrated the facile thermally reversible photoisomerization of these linearly conjugated cyclohexadienones into dienyl ketenes, which can evolve into hexadienoic acid derivatives in the presence of a protonic nucleophile (NuH) (e.g. **126**, Figure 31) [160, 161]. Reaction conditions favoring the π^*,n excitation state as the lowest excited state are best for initiating such a ring-opening event. Under certain conditions allowing the π^*,π excitation path to be followed, bicyclo[3.1.0]hexenones can be produced directly (e.g. **134**, Figure 33), as first observed by Hart and co-workers [160–162]. Early on, *ortho*-quinol acetates were used as substrates to study the photochemical behavior of cyclohexa-2,4-dienones [158, 159], and numerous examples have been described by Quinkert and co-workers [160, 163, 164]. In contrast to the photolytic ring-opening of cyclohexa-2,4-dienones bearing two carbon substituents at their 6-position, *ortho*-quinol acetates of type **123** only led to diene ketenes with the (5*E*)-configuration (Figure 31).

This stereochemical preference is attributed to a stereoelectronic promotion of the C6–C7 bond into a pseudoaxial orientation due to a stabilizing interaction between the corresponding σ orbital and the antibonding $\pi^*_{\text{C=O}}$ orbital in the photoexcited cyclohexadienone **124** (Figure 31). Quinkert additionally invoked a through-space interaction between the two polar carbonyl groups to rationalize the conformational preference leading to the (5*E*)-geometry [160]. From a general viewpoint, different primary and several secondary photoproducts can be obtained under different reaction conditions from differently substituted starting *ortho*-quinol acetates. Of particular note is the possibility of building seven-membered rings from *ortho*-quinol acetates such as **127a–c** bearing a side chain with a 2-oxo group at the 6-position (Figure 32). The presence of a bulky substituent at the 4-position increases the deviation from planarity of the nucleophilically-trapped primary photoproduct **128a–c**. This deviation

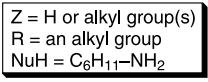


Fig. 31

favors the intramolecular aldol-type reaction that produces the seven-membered rings **130a–c** (Figure 32). Other inter- and intramolecular applications of this nucleophilic trapping of ketenes to the synthesis of macrolides and photochemically modifiable ionophores (e.g. **131** \rightarrow **132**, Figure 32) have also been described by Quinkert and co-workers [160, 164].

Liao and Wei took advantage of the possibility of photochemically rearranging cyclohexa-2,4-dienones into bicyclo[3.1.0]hexenones in their approach to synthetically useful cyclopentenones such as **135** [6, 160–162]. This approach was based on the acid-catalyzed cyclopropane ring-opening of bicyclo[3.1.0]hexenones such as **134**, as generated photochemically from non-dimerizing *ortho*-quinone monoketals such as **133** (Figure 33) [165].

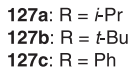


Fig. 32

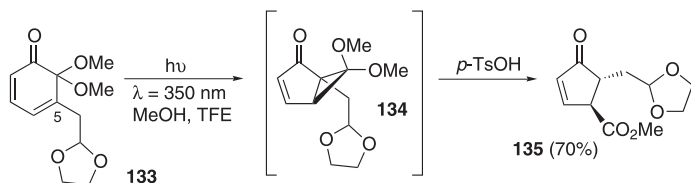


Fig. 33

15.3.3

Nucleophilic Substitutions and Additions

One of the most attractive features of the chemistry of *ortho*-quinol derivatives is the fact that they are amenable to carbon–carbon bond formation by both substitution and addition reactions. These electrophilic entities are typical Michael acceptors, but direct 1,2-additions to their carbonyl group and vinylogous nucleophilic substitutions of their ketal unit are also possible [6]. Elegant synthetic applications of direct additions of lithium acetylides have been described by Danishefsky and Magnus in their total synthesis of the enediyne-containing aglycon calicheamicinone [166–170]. The putative biosynthetic oxidative dearomatization of the natural hexaketide sorbicillin (13) to give the *ortho*-quinol intermediate 14 (Figure 6) has inspired chemists in their synthetic plans towards the dodecaketide “bisorbicillinoids”, as referred to by Nicolaou [171]. Barnes-Seeman and Corey accomplished a remarkable enantioselective total synthesis of the pentacyclic trichodimerol (15) in only two steps from sorbicillin (13) [172]. This phenol was submitted to Wessely oxidation to furnish the two *ortho*-quinol acetates 136a and 136b in 73 % yield. Racemic 136a was separated from 136b and resolved chromatographically. Careful deacetylation of (*S*)-136a induced an astonishing cascade of nucleophilic addition events leading to the target (–)-15, having no less than eight stereogenic centers, six of which are quaternary (Figure 34).

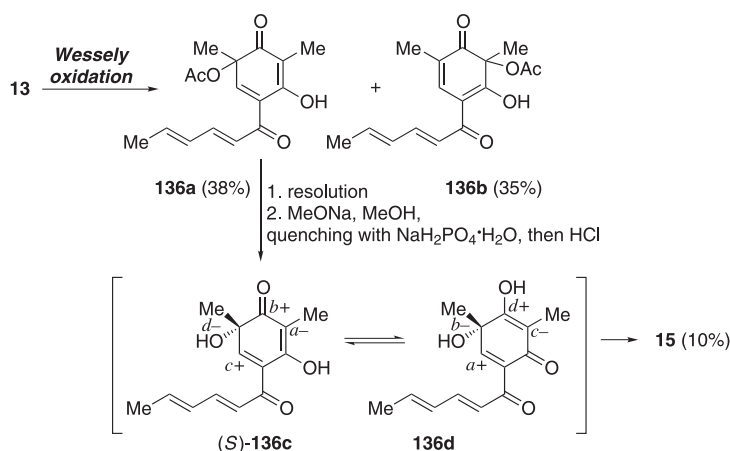


Fig. 34

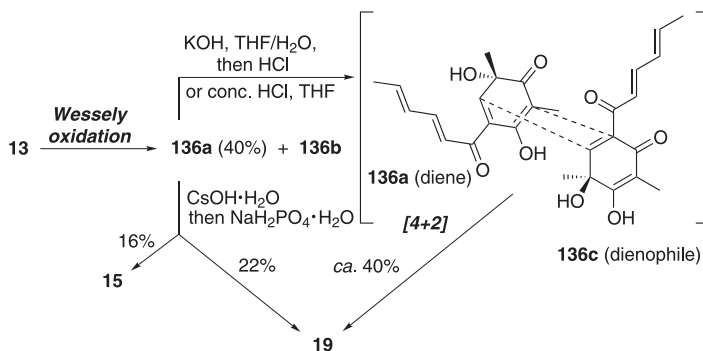


Fig. 35

A mechanistic description of this $[4+4]$ dimerization implies the participation of **136c** and its cyclohexa-2,5-dienone tautomer **136d**. An initial intermolecular Michael addition (connectivity *a*) is followed by a first ketalization (*b*), an intramolecular Michael addition (*c*), and a second and final ketalization (*d*). Nicolaou and co-workers utilized a similar approach in their synthesis of bisorbicillinoids [40, 171, 173]. The Wessely oxidation was also used to dearomatize **13** to give **136a**, which was then slowly dimerized in the presence of $\text{CsOH} \cdot \text{H}_2\text{O}$ in MeOH to furnish **15** in 16 % yield, together with bisorbicillinol (**19**) in 22 % yield (Figure 6). Better yields of the $[4+2]$ *endo*-cycloadduct **19** were obtained by treating **136a** with either solid KOH in aqueous THF or with concentrated HCl in THF (Figure 35). A rather intriguing observation was that the *ortho*-quinol acetate **136a** did not undergo any dimerization, even when heated in benzene or acetic acid for several hours. Deacetylation and acidification of the reaction medium are required to unleash the reactivity of the quinolic system (Section 15.3.1).

ortho-Quinone monoketals and, in particular, *ortho*-quinol acetates continue to demonstrate their utility in biaryl synthesis [6]. Hoshino has shown that various *N*-acyl and *N*-methanesulfonyl-1,2,3,4-tetrahydro-7-methoxyisoquinolin-6-ols **137a** can be transformed into noraporphine **139a** and phenanthrene **140a** derivatives following their conversion to the corresponding *ortho*-quinol acetates **138a** through an apparent vinylogous $\text{S}_{\text{N}}2'$ -type substitution at their C-2 center (Figure 36) [174]. In contrast, regioisomeric 6-methoxyisoquinolin-7-ols **137b** prefer to undergo 1,3-acetate shifts to furnish cyclohexa-2,5-dienone derivatives **138c**, which can then undergo ring-opening rearomatization to give **140b**. Therefore, an electron-releasing alkyl group on the isoquinoline nitrogen (e.g. $\text{R} = \text{Me}$) appears to be necessary to direct the system toward biaryl bond formation by acid-catalyzed Michael-type 1,6-addition at the C-5 center of **138b** to furnish **139b** [174].

In unbiased systems reacting in an intermolecular fashion, *ortho*-quinone monoketals usually behave as Michael 1,4-acceptors. This reactivity feature has been exploited for the rapid and convergent synthesis of fused aromatic polycycles and their quinonoid derivatives. Anionic annulation of phthalides with *ortho*-quinone monoketals was first proposed by Mitchell and Russell for the preparation of linearly fused anthracyclines [175, 176]. Mal and co-workers applied this strategy to the synthesis of benz[*a*]anthraquinone motifs **145a–d** present in angucycline natural products (Figure 37). Dimethyl ketals **142a–c** were generated by means of Pelter oxidation [177].

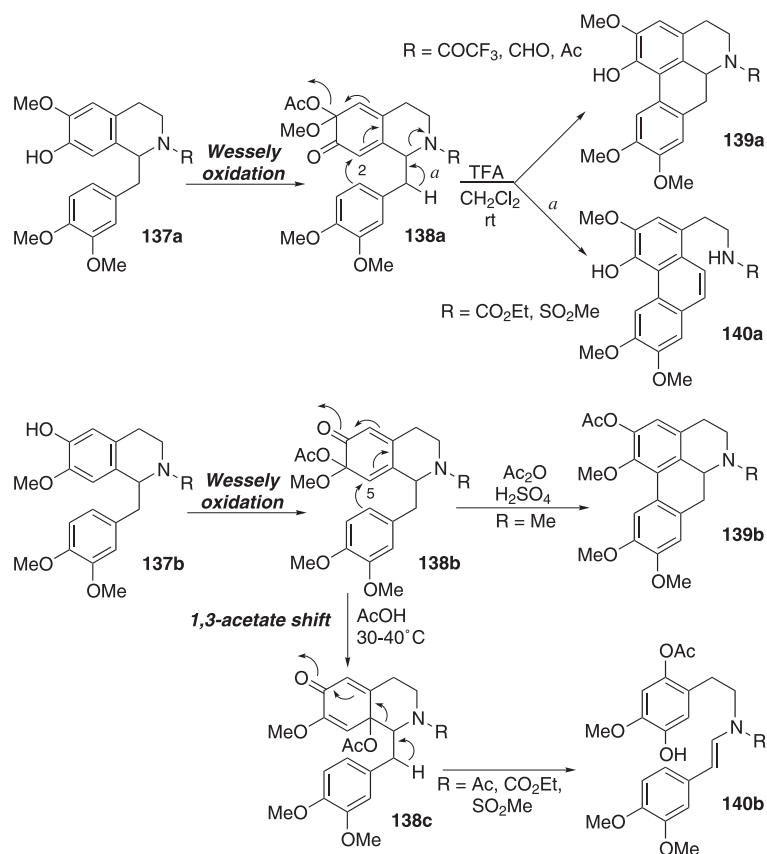


Fig. 36

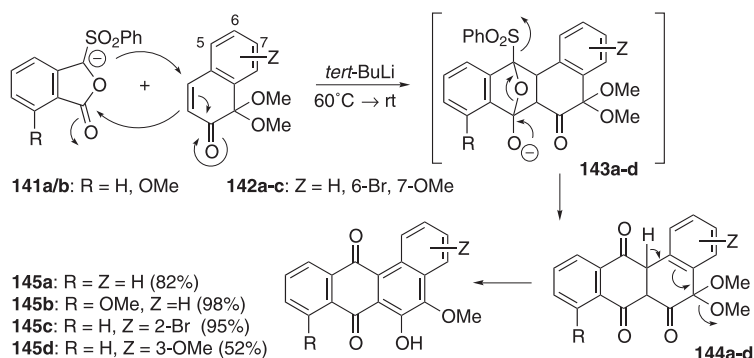


Fig. 37

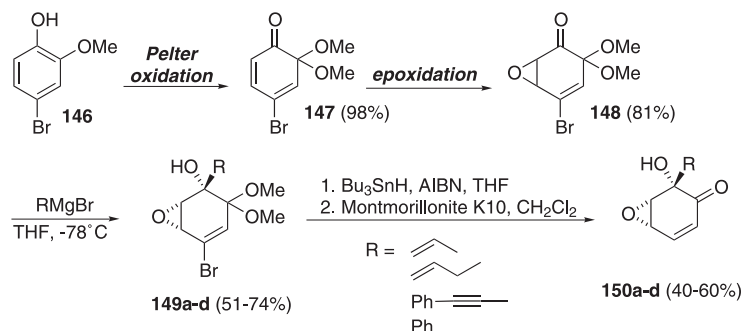


Fig. 38

Regioselective heteroatom–carbon bond formation is another item in the panoply of reactions available with *ortho*-quinol derivatives. The general trends of their electrophilic behavior with respect to both hard and soft heteroatom- as well as carbon-based nucleophiles have been summarized previously [6]. Epoxidation of their double bonds is another example of a heteroatom–carbon bond-forming process. Analogues of scyphostatin (**20**, Figure 7) have been prepared by epoxidation of **147**, which was derived from 4-bromoguaiacol (**146**) by Pelter oxidation; the bromide substitution effect first described by Liao and co-workers (Section 15.3.1) was judiciously exploited to prepare an otherwise unstable *ortho*-quinone monoketal (Figure 38) [44, 126].

Our synthetic studies using *ortho*-quinol acetates have also taken us into the realm of carbon–heteroatom bond formation and notably concern regioselective benzannulation reactions. Intramolecular conjugate 1,4-additions to the enone system of *ortho*-quinol acetates were carried out to build benzannulated five- to seven-membered ether rings, indoles, quinolines, and their oxo derivatives (Figure 39) [112, 113, 178]. The starting 2-methoxyphenols **151a–c** and **154a–c** were tethered with a protected nucleophilic center and submitted to PIDA-mediated oxidative acetoxylation to furnish the acetates **152a–c** and **155a–c** in excellent yields. The silyl-protected *ortho*-quinols **152a–c** and **155a,b** were then treated with a source of fluoride ions (i.e. TBAF = tetrabutylammonium fluoride) to induce cyclization, which was followed by aromatization with concomitant loss of the 6-acetoxy group. The cyclization of *N*-benzylated acetates such as **155c** was promoted by the action of a base (e.g. potassium *tert*-butoxide in THF). All observed cyclizations followed an *exo*-trig mode.

Applications of this benzannulation tactic can be anticipated in the synthesis of polyoxygenated polycyclic alkaloids and heterocyclic terpenoids. Work is currently in progress in our laboratory aimed at constructing the polyoxygenated tetracyclic core of *Amaryllidaceae* alkaloids such as lycorine (**157**). The stable bis(*ortho*-quinol acetate) Tsoc-protected secondary amine **159** has been subjected to the TBAF-mediated deprotection–cyclization conditions in the hope of inducing the formation of both the strategic N–C and C–C bonds in a domino fashion by taking advantage of an electrophile–nucleophile switch of reactivity of the eastern *ortho*-quinol moiety (Figure 40). The heterocyclization occurred, but led only to the indole product **160** [178].

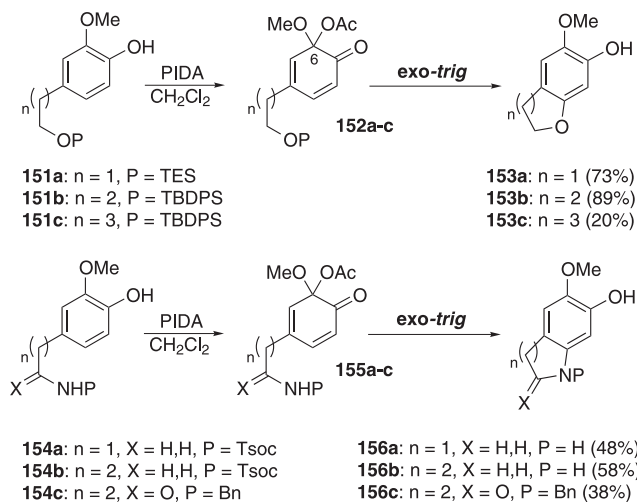


Fig. 39

The last example of this section serves to demonstrate that the oxidative conversion of arenols into *ortho*-quinol derivatives is not only a useful tactic to activate the aromatic nucleus toward further structural elaboration, but that it can also constitute the key reaction enabling the formation of strategic bonds. Cox and Danishefsky provided us with a glowing illustration of such synthetic applications in their recent report on the synthesis of lactonamycin (**161**) [179]. A tetracyclic model **164** of this natural antibiotic was constructed by a Wessely oxidation applied in an intramolecular fashion to the phenolic acid **162** (Figure 41).

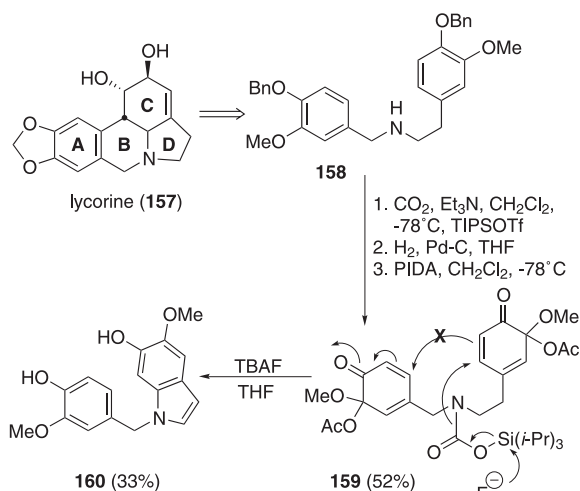


Fig. 40

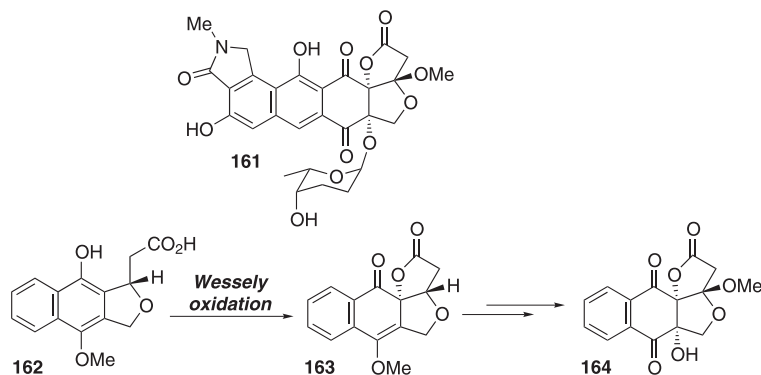


Fig. 41

15.4

Conclusion

The prime objective of writing this chapter was to demonstrate that the oxidative conversion of simple 2-substituted hydroxylated aromatic molecules into *ortho*-quinone monoketals or other *ortho*-quinol derivatives constitutes a powerful tactic for the rapid elaboration of structural complexity and diversity in organic synthesis. The concepts of this tactic are certainly well anchored in fifty years of research in the field of phenol oxidation chemistry, but its synthetic applications have long been thwarted by the difficulties encountered in working with highly reactive *ortho*-quinol derivatives. Subtle electronic and steric effects are often the keys to their high-yielding formation and controlled utilization in various types of chemical reactions. Today, *ortho*-quinol derivatives can be efficiently transformed by regioselective nucleophilic additions and substitutions, by photochemical ring-opening and ring-contracting rearrangements, and by Diels–Alder cycloadditions into versatile bicyclo[2.2.2]oct-5-en-2-one synthons. The increasing number of reports on successful utilizations of *ortho*-quinone monoketals and other *ortho*-quinols is certainly testament to their emerging prominent role in organic synthesis and, in particular, in natural products synthesis. May this chapter be a convincing compilation of examples from the flourishing chemistry of these 6-oxocyclohexa-2,4-dienone derivatives.

Acknowledgements

The author thanks the Délégation Régionale à la Recherche et à la Technologie pour l'Aquitaine, the Conseil Régional d'Aquitaine, the Centre National de la Recherche Scientifique (CNRS), and the Centre de Recherche en Chimie Moléculaire (CNRS, Fédération d'Unités FR1981) for their financial aid. The author also thanks his collaborators, Dr. Denis Deffieux and Dr. Laurent Pouységu, for their help and continuous support.

References

- 1 A. J. WARING, in *Advances in Alicyclic Chemistry*, Vol. 1 (Eds.: H. HART, G. J.

KARABATSOS), Academic Press, New York and London, 1966, pp. 129–256.

- 2 B. MILLER, in *Mechanisms of Molecular Migrations*, Vol. 1 (Ed.: B. S. THYAGARAJAN), Wiley, New York, 1968, pp. 247–313.
- 3 S. FUJITA, *Yuki Gosei Kagaku Kyokaishi* 1982, 40, 307–320.
- 4 J. S. SWENTON, *Acc. Chem. Res.* 1983, 16, 74–81.
- 5 J. S. SWENTON, in *The Chemistry of Quinonoid Compounds*, Vol. 2, Part 2 (Eds.: S. PATAI, Z. RAPPOPORT), John Wiley, New York, 1988, pp. 899–962.
- 6 S. QUIDEAU, L. POUYSÉGU, *Org. Prep. Proc. Int.* 1999, 31, 617–680.
- 7 For a recent example of an *ortho*-quinone methide-based cycloaddition approach to an *ortho*-quinol aryl ether, see: G. G. QIAO, K. LENGHAUS, D. H. SOLOMON, *J. Org. Chem.* 1998, 63, 9806–9811.
- 8 R. MAGNUSSON, *Acta Chem. Scand.* 1960, 14, 1643–1653.
- 9 R. MAGNUSSON, *Acta Chem. Scand.* 1958, 12, 791–792.
- 10 M. G. DOLSON, J. S. SWENTON, *J. Am. Chem. Soc.* 1981, 103, 2361–2371.
- 11 D. R. HENTON, K. ANDERSON, M. J. MANNING, J. S. SWENTON, *J. Org. Chem.* 1980, 45, 3422–3433.
- 12 A. G. SCHULTZ, *Chem. Commun.* 1999, 1263–1271.
- 13 A. G. SCHULTZ, J. P. DITTAMI, F. P. LAVIERI, C. SALOWEY, P. SUNDARARAMAN, M. B. SZYMULA, *J. Org. Chem.* 1984, 49, 4429–4440.
- 14 J. M. HOOK, L. N. MANDER, M. WOOLIAS, *Tetrahedron Lett.* 1982, 23, 1095–1098.
- 15 B. MILLER, *J. Org. Chem.* 1970, 35, 4262–4264.
- 16 B. MILLER, *J. Am. Chem. Soc.* 1965, 87, 5115–5120.
- 17 D. Y. CURTIN, R. J. CRAWFORD, *J. Am. Chem. Soc.* 1957, 79, 3156–3159.
- 18 D. Y. CURTIN, R. J. CRAWFORD, M. WILHELM, *J. Am. Chem. Soc.* 1958, 80, 1391–1397.
- 19 D. Y. CURTIN, D. H. DYBVIG, *J. Am. Chem. Soc.* 1962, 84, 225–232.
- 20 J. ZSINDELY, H. SCHMID, *Helv. Chim. Acta* 1968, 51, 1510–1514.
- 21 M. G. BURDON, J. G. MOFFAT, *J. Am. Chem. Soc.* 1965, 87, 4656–4658.
- 22 M. G. BURDON, J. G. MOFFAT, *J. Am. Chem. Soc.* 1967, 89, 4725–4735.
- 23 M. G. BURDON, J. G. MOFFAT, *J. Am. Chem. Soc.* 1966, 88, 5855–5864.
- 24 K. E. PFITZNER, J. P. MARINO, R. A. OLOFSON, *J. Am. Chem. Soc.* 1965, 87, 4658–4659.
- 25 J. P. MARINO, K. E. PFITZNER, R. A. OLOFSON, *Tetrahedron* 1971, 27, 4181–4194.
- 26 R. A. OLOFSON, J. P. MARINO, *Tetrahedron* 1971, 27, 4195–4208.
- 27 For a recent and elegant use of the Claisen rearrangement for the construction of complex *ortho*-quinol intermediates in the total synthesis of morellin natural products, see: K. C. NICOLAOU, J. LI, *Angew. Chem. Int. Ed. Engl.* 2001, 40, 4264–4268, and references cited therein.
- 28 S. QUIDEAU, K. S. FELDMAN, *Tetrahedron* 2001, 57, ix–x.
- 29 K. OMURA, *J. Org. Chem.* 1996, 61, 7156–7161, and references cited therein.
- 30 E. J. COREY, L. F. HAEFELE, *J. Am. Chem. Soc.* 1959, 81, 2225–2227.
- 31 Recent density functional theory (DFT) calculations have suggested that cyclohexa-2,4-dienones and cyclohexa-2,5-dienones have essentially the same heat of formation, see: D. SANTORO, R. LOUW, *J. Chem. Soc., Perkin Trans. 2* 2001, 645–649.
- 32 D. J. HART, P. A. CAIN, D. A. EVANS, *J. Am. Chem. Soc.* 1978, 100, 1548–1557.
- 33 D. A. EVANS, P. A. CAIN, R. Y. WONG, *J. Am. Chem. Soc.* 1977, 99, 7083–7085.
- 34 L. KÜRTI, L. SZILAGYI, S. ANTUS, M. NOGRADI, *Eur. J. Org. Chem.* 1999, 2579–2581.
- 35 A. NISHIYAMA, H. ETO, Y. TERADA, M. IGUCHI, S. YAMAMURA, *Chem. Pharm. Bull.* 1983, 31, 2834–2844.
- 36 A. NISHIYAMA, H. ETO, Y. TERADA, M. IGUCHI, S. YAMAMURA, *Chem. Pharm. Bull.* 1983, 31, 2820–2833.
- 37 B.-N. SU, Q.-X. ZHU, Z.-J. JIA, *Tetrahedron Lett.* 1999, 40, 357–358.
- 38 B.-N. SU, L. YANG, K. GAO, Z.-J. JIA, *Planta Medica* 2000, 66, 281–283.
- 39 N. ABE, O. SUGIMOTO, K.-i. TANJI, A. HIROTA, *J. Am. Chem. Soc.* 2000, 122, 12606–12607.
- 40 K. C. NICOLAOU, G. VASSILIKOGIANNAKIS, K. B. SIMONSEN, P. S. BARAN, Y.-L. ZHONG, V. P. VIDALI, E. N. PITISINOS, E. A. COULADOUROUS, *J. Am. Chem. Soc.* 2000, 122, 3071–3079.

- 41 M. TANAKA, F. NARA, K. SUZUKI-KONAGAI, T. HOSOYA, T. OGITA, *J. Am. Chem. Soc.* **1997**, *119*, 7871–7872.
- 42 S. SAITO, N. TANAKA, K. FUJIMOTO, H. KOGEN, *Org. Lett.* **2000**, *2*, 505–506.
- 43 C. ARENZ, M. GARTNER, V. WASCHOLOWSKI, A. GIANNIS, *Bioorg. Med. Chem.* **2001**, *9*, 2901–2904.
- 44 K. A. RUNCIE, R. J. K. TAYLOR, *Org. Lett.* **2001**, *3*, 3237–3239.
- 45 K. S. FELDMAN, M. D. LAWLOR, K. SAHASRABUDHE, *J. Org. Chem.* **2000**, *65*, 8011–8019.
- 46 K. S. FELDMAN, M. D. LAWLOR, *J. Am. Chem. Soc.* **2000**, *122*, 7396–7397.
- 47 K. S. FELDMAN, K. SAHASRABUDHE, S. QUIDEAU, K. L. HUNTER, M. D. LAWLOR, in *Plant Polyphenols 2: Chemistry, Biology, Pharmacology, Ecology*, Vol. *Basic Life Science* 66 (Eds.: G. G. GROSS, R. W. HEMINGWAY, T. YOSHIDA), Kluwer Academic/Plenum Publishers, New York, NY, **1999**, pp. 101–125.
- 48 S. QUIDEAU, K. S. FELDMAN, *J. Org. Chem.* **1997**, *62*, 8809–8813.
- 49 K. S. FELDMAN, S. QUIDEAU, H. M. APPEL, *J. Org. Chem.* **1996**, *61*, 6656–6665.
- 50 S. QUIDEAU, K. S. FELDMAN, *Chem. Rev.* **1996**, *96*, 475–503.
- 51 D. J. BENNETT, F. M. DEAN, G. A. HERBIN, D. A. MATKIN, A. W. PRICE, M. L. ROBINSON, *J. Chem. Soc., Perkin Trans. 1* **1980**, 1978–1985.
- 52 D. F. BOWMAN, F. R. HEWGILL, B. R. KENNEDY, *J. Chem. Soc. (C)* **1966**, 2274–2279.
- 53 D. R. NELAN, C. D. ROBESON, *J. Am. Chem. Soc.* **1962**, *84*, 2963–2965.
- 54 P. SCHUDEL, H. MAYER, R. RÜEGG, O. ISLER, *Chimia* **1962**, *16*, 368–369.
- 55 V. K. KANSAL, S. FUNAKOSHI, P. MANGENEY, B. GILLET, B. GUITTET, J. Y. LALLEMAND, P. POTIER, *Tetrahedron* **1985**, *41*, 5107–5120.
- 56 G. PRATVIEL, J. BERNADOUD, T. HA, G. MEUNIER, S. CROS, B. MEUNIER, B. GILLET, E. GUITTET, *J. Med. Chem.* **1986**, *29*, 1350–1355.
- 57 S. ITOH, M. OGINO, Y. FUKUI, H. MURAO, M. KOMATSU, Y. OHSHIRO, T. INOUE, Y. KAI, N. KASAI, *J. Am. Chem. Soc.* **1993**, *115*, 9960–9967.
- 58 J. L. BOLTON, M. A. TRUSH, T. M. PENNING, G. DRYHURST, T. J. MONKS, *Chem. Res. Toxicol.* **2000**, *13*, 135–160.
- 59 M. LARGERON, A. NEUDORFFER, M.-B. FLEURY, *J. Chem. Soc., Perkin Trans. 2* **1998**, 2721–2727.
- 60 M. LARGERON, H. DUPUIS, M.-B. FLEURY, *Tetrahedron* **1995**, *51*, 4953–4968.
- 61 H. EICKHOFF, G. JUNG, A. RIEKER, *Tetrahedron* **2001**, *57*, 353–364, and references cited therein.
- 62 S. TORII, in *Electroorganic Syntheses: Methods and Applications, Part I: Oxidations*, VCH, Tokyo, **1984**, pp. 97–152.
- 63 M. IGUCHI, A. NISHIYAMA, Y. TERADA, S. YAMAMURA, *Chem. Lett.* **1978**, 451–454.
- 64 M. IGUCHI, A. NISHIYAMA, Y. TERADA, S. YAMAMURA, *Tetrahedron Lett.* **1977**, 4511–4514.
- 65 D. G. HEWITT, *J. Chem. Soc. (C)* **1971**, 2967–2973.
- 66 V. V. KARPOV, M. L. KHIDEKEL, *Zhur. Org. Khim.* **1968**, *4*, 837–844.
- 67 E. MÜLLER, R. MAYER, B. NARR, A. RIEKER, K. SCHEFFLER, *Liebigs Ann. Chem.* **1961**, *645*, 25–36.
- 68 F. WESSELY, G. LAUTERBACH-KEIL, F. SINWEL, *Monatsh. Chem.* **1950**, *81*, 811–818.
- 69 F. WESSELY, F. SINWEL, *Monatsh. Chem.* **1950**, *81*, 1055–1070.
- 70 F. WESSELY, J. KOTLAN, F. SINWEL, *Monatsh. Chem.* **1952**, *83*, 902–914.
- 71 F. WESSELY, J. KOTLAN, *Monatsh. Chem.* **1953**, *84*, 291–297.
- 72 F. WESSELY, J. KOTLAN, W. METLESICS, *Monatsh. Chem.* **1954**, *85*, 69–79.
- 73 W. METLESICS, E. SCHINZEL, H. VILISEK, F. WESSELY, *Monatsh. Chem.* **1957**, *88*, 1069–1076.
- 74 F. TAKACS, *Monatsh. Chem.* **1964**, *95*, 961–977.
- 75 F. WESSELY, J. SWOBODA, V. GUTH, *Monatsh. Chem.* **1964**, *95*, 649–670.
- 76 F. WESSELY, M. GROSSA, *Monatsh. Chem.* **1966**, *97*, 571–578.
- 77 E. HECKER, R. LATTRELL, *Angew. Chem.* **1962**, *74*, 652.
- 78 A. MCKILLOP, D. H. PERRY, M. EDWARDS, S. ANTUS, L. FARKAS, M. NÓGRÁDI, E. C. TAYLOR, *J. Org. Chem.* **1976**, *41*, 282–287.
- 79 S. ANTUS, M. NÓGRÁDI, E. BAITZ-GACS, L. RADICS, H.-D. BECKER, B. KARLSSON, A.-M. PILOTTI, *Tetrahedron* **1978**, *34*, 2573–2577.
- 80 S. QUIDEAU, M. A. LOONEY, L. POUYSÉGU, S. HAM, D. M. BIRNEY, *Tetrahedron Lett.* **1999**, *40*, 615–618.

- 81 D. H. R. BARTON, S. V. LEY, P. D. MAGNUS, M. N. ROSENFELD, *J. Chem. Soc., Perkin Trans. 1* **1977**, 567–572.
- 82 D. H. R. BARTON, P. D. MAGNUS, M. N. ROSENFELD, *J. Chem. Soc., Chem. Commun.* **1975**, 301.
- 83 K. AGBARIA, O. ALEKSIUK, S. E. BIALI, V. BÖHMER, M. FRINGS, I. THONDORF, *J. Org. Chem.* **2001**, 66, 2891–2899.
- 84 K. AGBARIA, S. E. BIALI, *J. Org. Chem.* **2001**, 66, 5482–5489.
- 85 G. ANDERSSON, *Acta Chem. Scand.* **1976**, B 30, 64–70.
- 86 G. ANDERSSON, *Acta Chem. Scand.* **1976**, B 30, 403–406.
- 87 E. ADLER, G. ANDERSSON, E. EDMAN, *Acta Chem. Scand.* **1975**, B 29, 909–920.
- 88 G. ANDERSSON, P. BERTSSON, *Acta Chem. Scand.* **1975**, B 29, 948–952.
- 89 E. ADLER, K. HOLMBERG, *Acta Chem. Scand.* **1974**, B 28, 465–472.
- 90 E. ADLER, K. HOLMBERG, *Acta Chem. Scand.* **1974**, B 28, 549–554.
- 91 E. ADLER, K. HOLMBERG, L.-O. RYRFORS, *Acta Chem. Scand.* **1974**, B 28, 888–894.
- 92 H.-D. BECKER, T. BREMHOLT, E. ADLER, *Tetrahedron Lett.* **1972**, 4205–4208.
- 93 E. ADLER, K. HOLMBERG, *Acta Chem. Scand.* **1971**, 25, 2775–2776.
- 94 E. ADLER, J. DAHLEN, G. WESTIN, *Acta Chem. Scand.* **1960**, 14, 1580–1596.
- 95 E. ADLER, *Angew. Chem.* **1957**, 69, 272.
- 96 E. ADLER, S. HERNESTAM, *Acta Chem. Scand.* **1955**, 9, 319–334.
- 97 C. ARENZ, A. GIANNIS, *Angew. Chem. Int. Ed. Engl.* **2000**, 39, 1440–1442.
- 98 C. ARENZ, A. GIANNIS, *Eur. J. Org. Chem.* **2001**, 1, 137–140.
- 99 A. VARVOGLIS, *Synthesis* **1984**, 709–726.
- 100 A. VARVOGLIS, *Hypervalent Iodine in Organic Synthesis*, Academic Press, San Diego, **1997**.
- 101 A. VARVOGLIS, *Tetrahedron* **1997**, 53, 1179–1255.
- 102 P. J. STANG, V. V. ZHDANKIN, *Chem. Rev.* **1996**, 96, 1123–1178.
- 103 G. F. KOSER, in *The Chemistry of Functional Groups* (Eds.: S. PATAI, Z. RAPPOPORT), Wiley, New York, **1983**, pp. 721–811.
- 104 D. F. BANKS, *Chem. Rev.* **1966**, 66, 243–266.
- 105 A. SIEGEL, F. ANTONY, *Monatsh. Chem.* **1955**, 86, 292–300.
- 106 A. PELTER, S. ELGENDY, *Tetrahedron Lett.* **1988**, 29, 677–680.
- 107 A. PELTER, S. M. A. ELGENDY, *J. Chem. Soc., Perkin Trans. 1* **1993**, 1891–1896.
- 108 L. KÜRTI, P. HERCZEGH, J. VISY, M. SIMONYI, S. ANTUS, A. PELTER, *J. Chem. Soc., Perkin Trans. 1* **1999**, 379–380.
- 109 Y. TAMURA, T. YAKURA, J.-I. HARUTA, Y. KITA, *J. Org. Chem.* **1987**, 52, 3927–3930.
- 110 A. J. FATIADI, *Synthesis* **1974**, 229–272.
- 111 A. PELTER, R. S. WARD, *Tetrahedron* **2001**, 57, 273–282.
- 112 S. QUIDEAU, L. POUYSÉGU, M. A. LOONEY, *J. Org. Chem.* **1998**, 63, 9597–9600.
- 113 S. QUIDEAU, L. POUYSÉGU, M. OXOBY, M. A. LOONEY, *Tetrahedron* **2001**, 57, 319–329.
- 114 S. QUIDEAU, M. A. LOONEY, L. POUYSÉGU, *Org. Lett.* **1999**, 1, 1651–1654.
- 115 B. MILLER, W.-O. LIN, *J. Org. Chem.* **1978**, 43, 4441–4446.
- 116 J. L. WOOD, B. D. THOMPSON, N. YUSUFF, D. A. PFLUM, M. S. P. MATTHÄUS, *J. Am. Chem. Soc.* **2001**, 123, 2097–2098.
- 117 F. WESSELY, W. METLESICS, *Monatsh. Chem.* **1954**, 85, 637–653.
- 118 E. ZBIRAL, O. SAIKO, F. WESSELY, *Monatsh. Chem.* **1964**, 95, 533–534.
- 119 G. WELLS, A. SEATON, M. F. G. STEVENS, *J. Med. Chem.* **2000**, 43, 1550–1562.
- 120 V. SINGH, *Acc. Chem. Res.* **1999**, 32, 324–333.
- 121 E. ADLER, S. BRASEN, H. MIYAKE, *Acta Chem. Scand.* **1971**, 25, 2055–2069.
- 122 K. N. HOUK, *J. Am. Chem. Soc.* **1973**, 95, 4092–4094.
- 123 O. EISENSTEIN, J. M. LEFOUR, N. T. ANH, R. F. HUDSON, *Tetrahedron* **1977**, 33, 523–531.
- 124 I. FLEMING, J. P. MICHAEL, L. E. OVERMAN, G. F. TAYLOR, *Tetrahedron Lett.* **1978**, 15, 1313–1314.
- 125 C.-C. LIAO, C.-S. CHU, T.-H. LEE, P. D. RAO, S. KO, L.-D. SONG, H.-C. SHIAO, *J. Org. Chem.* **1999**, 64, 4102–4110.
- 126 C.-H. LAI, Y.-L. SHEN, C.-C. LIAO, *Synlett* **1997**, 1351–1352.
- 127 W. METLESICS, W. WESSELY, *Monatsh. Chem.* **1957**, 88, 108–117.
- 128 K. HOLMBERG, *Acta Chem. Scand.* **1974**, B 28, 857–865.
- 129 Y.-K. CHEN, R. K. PEDDINTI, C.-C. LIAO, *Chem. Commun.* **2001**, 1340–1341.
- 130 C.-F. YEN, R. K. PEDDINTI, C.-C. LIAO, *Org. Lett.* **2000**, 2, 2909–2912.

- 131 C.-S. CHU, T.-H. LEE, P. D. RAO, L.-D. SONG, C.-C. LIAO, *J. Org. Chem.* **1999**, *64*, 4111–4118.
- 132 D.-S. HSU, P. D. RAO, C.-C. LIAO, *Chem. Commun.* **1998**, 1795–1796.
- 133 P. D. RAO, C.-H. CHEN, C.-C. LIAO, *Chem. Commun.* **1998**, 155–156.
- 134 P. D. RAO, C.-H. CHEN, C.-C. LIAO, *Chem. Comm.* **1999**, 713–714.
- 135 C.-H. CHEN, P. D. RAO, C.-C. LIAO, *J. Am. Chem. Soc.* **1998**, *120*, 13254–13255.
- 136 M. AVALOS, R. BABIANO, J. L. BRAVO, N. CABELLO, P. CINTAS, M. B. HURSTHOUSE, J. L. JIMÉNEZ, M. E. LIGHT, J. C. PALACIOS, *Tetrahedron Lett.* **2000**, *41*, 4101–4105.
- 137 M.-F. HSIEH, R. K. PEDDINTI, C.-C. LIAO, *Tetrahedron Lett.* **2001**, *42*, 5481–5484.
- 138 C.-H. LAI, S. KO, P. D. RAO, C.-C. LIAO, *Tetrahedron Lett.* **2001**, *42*, 7851–7854.
- 139 M.-F. HSIEH, P. D. RAO, C.-C. LIAO, *Chem. Comm.* **1999**, 1441–1442.
- 140 O. ARJONA, R. MEDEL, J. PLUMET, *Tetrahedron Lett.* **1999**, *40*, 8431–8433.
- 141 S.-Y. GAO, S. KO, Y.-L. LIN, R. K. PEDDINTI, C.-C. LIAO, *Tetrahedron* **2001**, *57*, 297–308.
- 142 S.-Y. GAO, Y.-L. LIN, P. D. RAO, C.-C. LIAO, *Synlett* **2000**, 421–423, and references cited therein.
- 143 D.-S. HSU, P.-Y. HSU, C.-C. LIAO, *Org. Lett.* **2001**, *3*, 263–265.
- 144 W.-C. LIU, C.-C. LIAO, *Chem. Commun.* **1999**, 117–118.
- 145 F. E. S. SOUZA, R. RODRIGO, *Chem. Commun.* **1999**, 1947–1948.
- 146 H. S. SUTHERLAND, K. C. HIGGS, N. J. TAYLOR, R. RODRIGO, *Tetrahedron* **2001**, *57*, 309–317.
- 147 R. CARLINI, K. HIGGS, C. OLDER, S. RANDHAWA, R. RODRIGO, *J. Org. Chem.* **1997**, *62*, 2330–2331.
- 148 J. T. NJARDARSON, I. M. McDONALD, D. A. SPIEGEL, M. INOUE, J. L. WOOD, *Org. Lett.* **2001**, *3*, 2435–2438.
- 149 P. YATES, H. AUKSI, *Can. J. Chem.* **1979**, *57*, 2853–2863.
- 150 P. YATES, T. S. MACAS, *Can. J. Chem.* **1988**, *66*, 1–10.
- 151 N. K. BHAMARE, T. GRANGER, T. S. MACAS, P. YATES, *J. Chem. Soc., Chem. Commun.* **1990**, 739–740.
- 152 N. K. BHAMARE, T. GRANGER, C. R. JOHN, P. YATES, *Tetrahedron Lett.* **1991**, *32*, 4439–4442.
- 153 P. YATES, N. K. BHAMARE, T. GRANGER, T. S. MACAS, *Can. J. Chem.* **1993**, *71*, 995–1001.
- 154 V. SINGH, B. SAMANTA, *Tetrahedron Lett.* **1999**, *40*, 1807–1810.
- 155 V. SINGH, B. SAMANTA, V. V. KANE, *Tetrahedron* **2000**, *56*, 7785–7795.
- 156 V. SINGH, B. SAMANTA, *Tetrahedron Lett.* **1999**, *40*, 383–386.
- 157 V. SINGH, S. Q. ALAM, *Bioorg. Med. Chem. Lett.* **2000**, 2517–2519.
- 158 D. H. R. BARTON, G. QUINKERT, *J. Chem. Soc.* **1960**, 1–9.
- 159 D. H. R. BARTON, *Helv. Chim. Acta* **1959**, *7*, 2604–2616.
- 160 G. QUINKERT, S. SCHERER, D. REICHERT, H.-P. NESTLER, H. WENNEMERS, A. EBEL, K. URBAHNS, K. WAGNER, K.-P. MICHAELIS, G. WIECH, G. PRESCHER, B. BRONSTERT, B.-J. FREITAG, I. WICKE, D. LISCH, P. BELIK, T. CRECELIUS, D. HÖRSTERMANN, G. ZIMMERMANN, J. W. BATS, G. DÜRNER, D. REHM, *Helv. Chim. Acta* **1997**, *80*, 1683–1772, and references cited therein.
- 161 G. QUINKERT, *Angew. Chem. Int. Ed. Engl.* **1972**, *11*, 1072–1087.
- 162 J. GRIFFITHS, H. HART, *J. Am. Chem. Soc.* **1968**, *90*, 5296–5298, and references cited therein.
- 163 G. QUINKERT, E. KLEINER, B.-J. FREITAG, J. GLENNEBERG, U.-M. BILLHARDT, F. CECHE, K. R. SCHMIEDER, J. W. BATS, G. ZIMMERMANN, G. DÜRNER, D. REHM, E. F. PAULUS, *Helv. Chim. Acta* **1986**, *69*, 469–537.
- 164 G. QUINKERT, U.-M. BILLHARDT, H. JAKOB, G. FISCHER, J. GLENNEBERG, P. NAGLER, V. AUTZE, N. HEIM, M. WACKER, T. SCHWALBE, Y. KURTH, J. W. BATS, G. DÜRNER, G. ZIMMERMANN, G. KESSLER, *Helv. Chim. Acta* **1987**, *70*, 771–861.
- 165 C.-C. LIAO, C.-P. WEI, *Tetrahedron Lett.* **1991**, *32*, 4553–4556.
- 166 I. CHURCHER, D. HALLET, P. MAGNUS, *J. Am. Chem. Soc.* **1998**, *120*, 10350–10358.
- 167 I. CHURCHER, D. HALLET, P. MAGNUS, *J. Am. Chem. Soc.* **1998**, *120*, 3518–3519.
- 168 S. J. DANISHEFSKY, M. D. SHAIR, *J. Org. Chem.* **1996**, *61*, 16–44.
- 169 J. N. HASELTINE, M. P. CABAL, N. B. MANTLO, N. IWASAWA, D. S. YAMASHITA, R. S. COLEMAN, S. J. DANISHEFSKY, G. K.

- SCHULTE, *J. Am. Chem. Soc.* **1991**, *113*, 3850–3866.
- 170 M. P. CABAL, R. S. COLEMAN, S. J. DANISHEFSKY, *J. Am. Chem. Soc.* **1990**, *112*, 3253–3255.
- 171 K. C. NICOLAOU, R. JAUTELAT, G. VASSILIKOGIANNAKIS, P. S. BARAN, K. B. SIMONSEN, *Chem. Eur. J.* **1999**, *5*, 3651–3665.
- 172 D. BARNES-SEEMAN, E. J. COREY, *Org. Lett.* **1999**, *1*, 1503–1504.
- 173 K. C. NICOLAOU, K. B. SIMONSEN, G. VASSILIKOGIANNAKIS, P. S. BARAN, V. P. VIDALI, E. N. PITSINOS, E. A. COULADOUROS, *Angew. Chem. Int. Ed. Engl.* **1999**, *38*, 3555–3559.
- 174 O. HOSHINO, L. SUZUKI, M. H. OGASAWARA, *Tetrahedron* **2001**, *57*, 265–271, and references cited therein.
- 175 A. S. MITCHELL, R. A. RUSSELL, *Tetrahedron* **1997**, *53*, 4387–4410.
- 176 A. S. MITCHELL, R. A. RUSSELL, *Tetrahedron Lett.* **1993**, *34*, 545–548.
- 177 D. MAL, H. N. ROY, N. K. HAZRA, S. ADHIKARI, *Tetrahedron* **1997**, *53*, 2177–2184.
- 178 S. QUIDEAU, L. POUYSÉGU, A.-V. AVELLAN, D. K. WHELLIGAN, M. A. LOONEY, *Tetrahedron Lett.* **2001**, *42*, 7393–7396.
- 179 C. COX, S. J. DANISHEFSKY, *Org. Lett.* **2000**, *2*, 3493–3496.
- 180 For recent uses of the thermally-induced retro-Diels–Alder reaction of bicyclo[2.2.2]octenones to give *ortho*-quinols, see: V. SINGH, U. SHARMA, V. PRASANNA, M. PORINCHU, *Tetrahedron* **1995**, *51*, 6015–6032.

16

Molecular Switches and Machines Using Arene Building Blocks*Hsian-Rong Tseng and J. Fraser Stoddart***Abstract**

The “top-down” approach to device construction currently utilized by solid-state physicists and electronic engineers faces increasing challenges from the intrinsic limitations of the materials themselves. A potential solution to this rapidly emerging problem is the “bottom-up” approach, starting from the smallest components of materials, namely molecules. A molecular-level machine is an assembly of a distinct number of molecular components that can be induced to produce mechanical movements. Similarly, a molecular switch is a molecule that can be stimulated to undergo reversible switching between discrete states. Undoubtedly, the best means of stimulating molecular-level machines and switches are through the action of photons and electrons. Thus, appropriate designs need to incorporate both electrochemically and photochemically active components into the molecules to drive the mechanical and switching processes. A working platform for these molecular-level machines and switches can be created around mechanically interlocked systems. This chapter relates a few case histories that have been inspired by the desire to construct unique molecular switches and motors, using molecules that contain certain ubiquitous arene building blocks.

16.1**Introduction**

The past decade has witnessed a rapidly growing, almost obsessive, interest in molecular switches and motor-molecules that remind us of our computers and our cars. Perhaps it is little wonder that those technological triumphs, which have so changed our lifestyles on many parts of the planet during the latter half of the twentieth century have started to capture the imaginations of scientists and engineers educated and trained in how to make, measure, and model a much smaller world built up of atoms and molecules. Surely it is only natural for these scientists and engineers to ask themselves – can we make switches and motors down at the molecular level and, if we can, what could be the technological implications and consequences? These questions, which were not so long ago dismissed as somewhat academic and esoteric, have all of a sudden become rooted in the highly fashionable practice we call nanoscience and the endless speculation we embrace under the umbrella of nanotechnology. The reason for all the interest and excitement is many-fold. On the

one hand, molecular scientists look at the revolution that has visited the life sciences in the last two decades with the rapidly growing realization that living systems consist, in large measure, of a collection of biomolecular switches and motors that are very closely integrated, one with another in such an awesome way that life itself is not only sustained but also promulgated. On the other hand, molecular scientists are curious to see what they might find out about materials and function if they break away from pursuing the traditional disciplines within gas, solution, and solid-phase chemistry, and begin to explore the new frontiers beyond the molecule between states and across boundaries.

This chapter describes some examples of research that has been inspired by the desire to do something different with arene building blocks that are plentiful in their supply – and, it turns out, rich in their potential for the construction of molecular switches and motors [1].

16.2

From Self-Assembling [2]Catenanes to Electronic Devices

Our first case history starts with the establishment of a recognition motif between π -electron-rich and -deficient arene building blocks within the context of host–guest chemistry. Donor–acceptor interactions lead (Figure 1a) to the π -electron-rich macrocycle, bis(*paraphenylene*)-34-crown-10 (BPP34C10) (**1**) accommodating the π -electron-deficient dicationic guest **2**²⁺ and forming [2] a 1:1 complex [**1**⊃**2**]²⁺, both in solution and in the solid state. The donor–acceptor roles can be reversed [3] to give (Figure 1b) a 1:1 complex [**4**⊃**3**]⁴⁺ between the π -electron-rich 1,4-dimethoxybenzene (**3**) and the π -electron-deficient tetracationic cyclophane **4**⁴⁺. During the past 15 years, these noncovalent interactions between π -electron-deficient and π -electron-rich components in recognition sites have been exploited in our laboratories to self-assemble [2]catenanes. A [2]catenane is a molecule composed of two interlocked macrocyclic components. The two macrocycles are not linked covalently to each other; rather, a mechanical bond holds the two components together, preventing their dissociation.

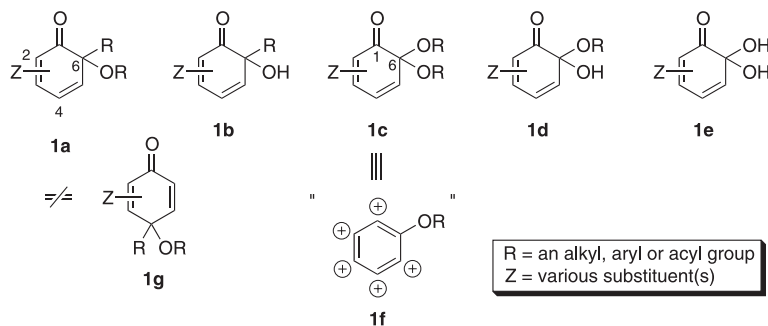


Fig. 1. Two complementary π -electron-donor/acceptor recognition systems, [**1**⊃**2**]²⁺ and [**4**⊃**3**]⁴⁺.

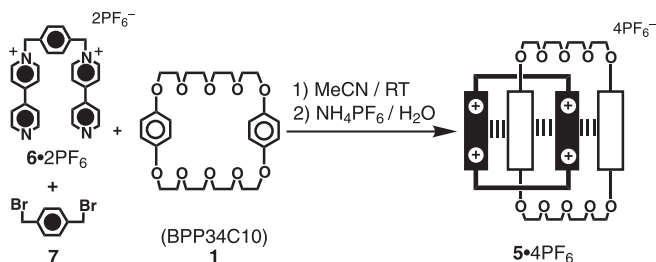


Fig. 2. The template-directed synthesis of the [2]catenane 5·4PF₆.

As shown in Figure 2, the template-directed synthesis of a [2]catenane 5·4PF₆, which relies on donor–acceptor interactions for the initial self-assembly of its component pieces prior to the formation of the mechanical bond, proceeds [4] in 70 % yield when equimolar amounts of 6·2PF₆ and 1,4-bis(bromomethyl)benzene (7) are reacted together in the presence of an excess of BPP34C10 (1). This [2]catenane is composed of a π -electron-deficient tetracationic cyclophane interlocked with a π -electron-rich macrocyclic polyether. In addition to its having a mechanical bond, $[\pi \cdots \pi]$ stacking interactions [5] between the complementary aromatic units, $[C-H \cdots O]$ hydrogen bonds [6] between α -bipyridinium hydrogen atoms and polyether oxygen atoms, and $[C-H \cdots \pi]$ interactions [7] between the hydrogen atoms on the hydroquinone (HQ) ring and the *p*-phenylene spacer in the tetracationic cyclophane hold the two macrocyclic components together and also control their relative movements in solution.

On the basis of the same kinds of π -electron donor–acceptor interactions, and in collaboration with the Balzani group in Bologna, a more complicated (supramolecular) system has been built [8] from three components. Two components behave as hosts with differing π -donor/ π -acceptor capabilities, and the other component fulfils the role of an itinerant guest with redox-controllable π -donor/ π -acceptor properties. Three distinct states can be accessed (Figure 3) by electrochemical manipulation of the guest's π -donor/ π -acceptor properties in the presence of the two hosts, namely the π -electron-donating macrocyclic polyether, 1,5-dinaphtho-38-crown-10 (DN38C10) (8) and the π -electron-accepting tetracationic cyclophane 4⁴⁺. The guest is tetrathiafulvalene (TTF) (9), which is known to exist in three stable oxidation states, namely TTF(0), TTF⁺, and TTF²⁺. The three-component mixture functions as a three-pole system by controlling the oxidation state of the TTF unit. The TTF is (i) uncomplexed in its TTF⁺ state, (ii) complexed with the π -electron-accepting tetracationic cyclophane 4⁴⁺ in its TTF(0) state, and (iii) complexed with the π -electron-donating macrocyclic polyether 8 in its TTF²⁺ state. The reversible electrochemical processes were monitored by absorption spectroscopy. The results show that complexation/decomplexation occurs rapidly on the experimental time-scale.

The [2]catenane 10⁴⁺, incorporating a TTF unit in its π -electron-rich macrocyclic ring, has been self-assembled [9a, 9b] using the template-directed synthetic strategy (Figure 4). The bis(hexafluorophosphate) salt 6·2PF₆ was treated with 1,4-bis(bromomethyl)benzene (7) in the presence of the macrocycle 11 to obtain 10·4PF₆, which was isolated in a yield of 23 % after counterion exchange. X-ray crystallography revealed (Figure 5) that the TTF unit resides preferentially inside the cavity of the tetracationic cyclophane in the solid state. This observation is consistent with the absorption spectrum of 10·4PF₆ in MeCN. It shows a band at

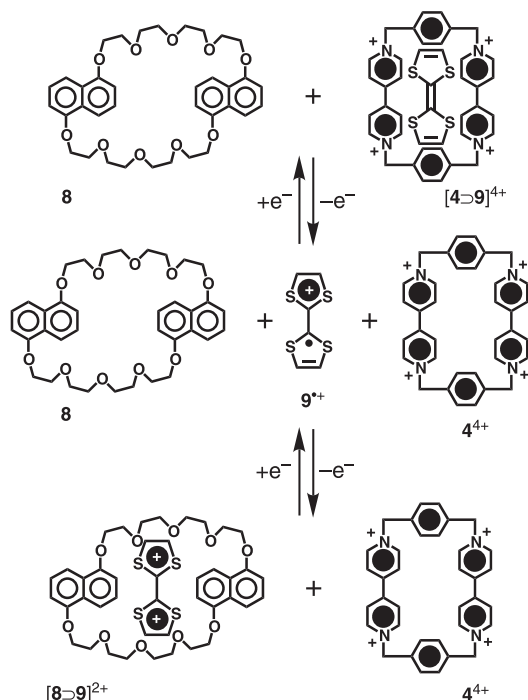


Fig. 3. A three-pole supramolecular switch.

850 nm (curve **a** in Figure 6), corresponding to a charge-transfer (CT) interaction between the TTF unit and the bipyridinium units. The circumrotation of the macrocyclic polyether component through the cavity of the tetracationic cyclophane can be reversibly induced by oxidizing and then reducing the TTF unit. Upon addition of one equivalent of $\text{Fe}(\text{ClO}_4)_3$, the TTF unit is oxidized (from A to B in Figure 6) to its radical cation. Circumrotation of the macrocycle occurs as a result of electrostatic repulsion between this monocationic unit and the two dicationic bipyridinium units. This circumrotation can be monitored by observing the changes in the absorption spectrum. The CT band, centered at 850 nm, gradually dis-

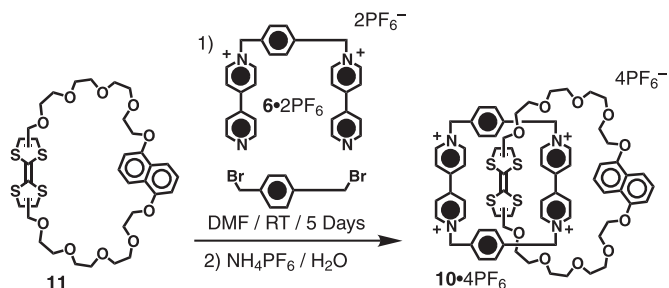


Fig. 4. The template-directed synthesis of the [2]catenane **10**•4PF₆.

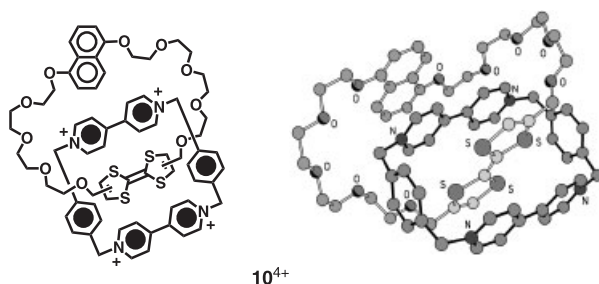


Fig. 5. The X-ray crystal structure of the [2]catenane 10^{4+} .

appears and is replaced by a new CT band, centered at 515 nm (curves **b** and **c** in Figure 6), arising from the 1,5-dihydroxynaphthalene (DNP) ring system and the surrounding bipyridinium units. Again, upon addition of a second equivalent of $\text{Fe}(\text{ClO}_4)_3$, the monocationic (TTF^{+}) unit is oxidized (from B to C in Figure 6) to its dication (TTF^{2+}). The absorption spectrum shows a similar CT band centered at 515 nm (curve **d** in Figure 6), suggesting that the DNP ring system still resides inside the cavity of the tetracationic cyclophane. Upon addition of two equivalents of ascorbic acid, the TTF^{2+} dication is reduced back to its neutral state (from C to A in Figure 6) and the macrocyclic polyether once again circumrotates through the cavity of the tetracationic cyclophane, returning to the original state of the [2]catenane. Absorption spectroscopy corroborates this sequence of events by showing the same band (curve **e** in Figure 6) at 835 nm as that present in the starting [2]catenane $10\cdot 4\text{PF}_6$. The circumrotation of the macrocyclic polyether component through the cavity of the tetracationic cyclophane can also be induced electrochemically. In cyclic voltammetry

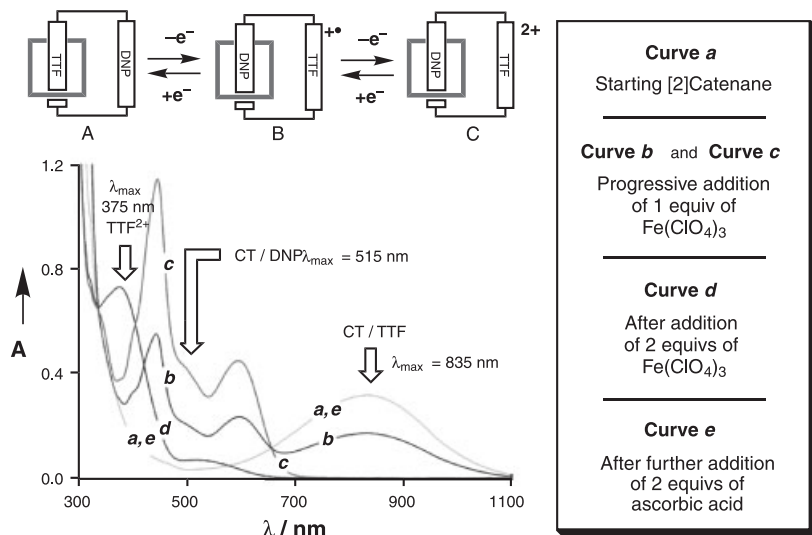


Fig. 6. The absorption spectra of the redox processes of the [2]catenane $10\cdot 4\text{PF}_6$.

(CV) experiments [9a, 9b], the bielectronic oxidation process occurs on the TTF unit at +0.80 V *vs.* saturated calomel electrode (SCE), and the oxidation of the DNP ring system is strongly displaced toward +1.60 V *vs.* SCE, compared to that of the free crown ether (+1.17 V *vs.* SCE). The dramatic increase in the oxidation potential of the DNP ring system indicates that it is encircled by the tetracationic cyclophane after the oxidation of the TTF unit.

The dimiristoylphosphatidyl (DMPA) salt of the switchable [2]catenane **10**⁴⁺ forms [9c] a stable Langmuir–Blodgett (LB) monolayer at the air–water interface. The monolayers can be transferred onto an Au(111) surface and have been studied [9d] by scanning tunneling spectroscopy. The current/voltage behavior of the resulting materials is dictated by the redox state of the TTF unit and by the co-conformation of the [2]catenane. No current is detected between –0.5 V and 0.0 V when the TTF unit is initially in its neutral state and located inside the cavity of the tetracationic cyclophane. However, relatively high tunneling currents are obtained when the TTF unit is initially in the oxidized state and located alongside the cavity of the tetracationic cyclophane.

In collaboration with the Heath group at UCLA, the [2]catenane **10**-4DMPA has been introduced [9e] into electronically reconfigurable molecular switches. By employing the LB technique, monolayers of the DMPA salt of the switchable [2]catenane were transferred onto a parallel arrangement of aligned *n*-type polysilicon wires, supported by a SiO₂ substrate. The 7 μm wide wires were deposited onto the substrate by direct chemical vapor deposition. A second set of wires, perpendicular to the first, was then deposited onto the monolayer through a contact shadow mask, using an electron beam deposition technique. These wires were composed of a layer of Ti (5 nm) and Al (100 nm) and had a width of 10 μm. A typical device is illustrated graphically in Figure 7. In this illustration, an Al/Ti wire overlays six polysilicon wires, forming a linear array of six junctions. A section of these junctions is magnified in Figure 7, which shows the two perpendicular wires sandwiching a film of the DMPA anion lying on top of a monolayer of switchable [2]catenane molecules. By alternating the voltage pulses between +2 V and –2 V, and reading the resistance at 0.1 V, switching between the two states of the [2]catenane is observed. The remnant molecular signature of the device, which is shown in Figure 8, was measured by varying the writing voltage in 40 mV steps and reading the device at –0.2 V. The hysteresis between the open and closed states of the catenane-based switch is evident in this signature. This electronically recon-

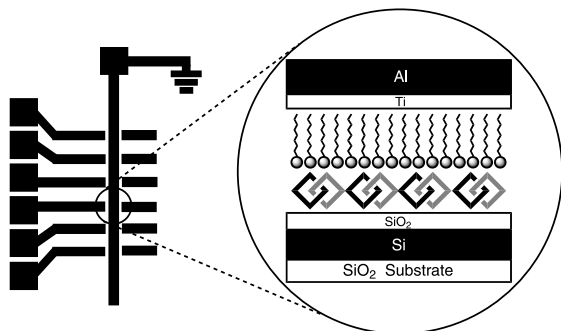


Fig. 7. The electronically reconfigurable molecular devices based on the [2]catenane **10**-4DMPA.

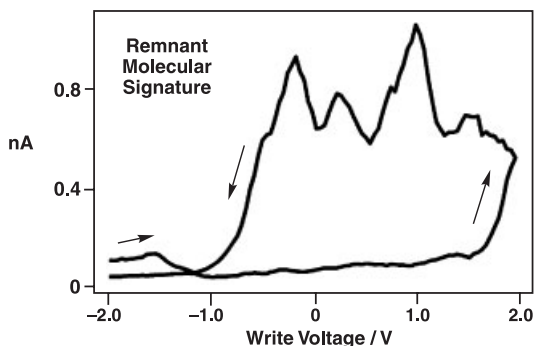


Fig. 8. The remnant molecular signature of the [2]catenane device, measured by varying the write voltage in 40 mV steps and by reading the device at -0.2 V.

figurable bistable catenane-based switch might be useful for generating random access memory.

16.3

A Hybrid [2]Catenane Switch

In collaboration with the Sauvage group in Strasbourg, we have been successful in combining [10] metal–ligand and π -electron donor–acceptor interactions to produce (Figure 9) a [2]catenane $[12\cdot\text{Cu}]^{5+}$ that is capable of chemical switching. The threaded complex $[14\supset 13\cdot\text{Cu}]^{3+}$ was formed by mixing equimolar amounts of $\text{Cu}(\text{MeCN})_4\text{PF}_6$, the dication 13^{2+} , and the phenanthroline-containing macrocycle **14**. Treating the threaded complex

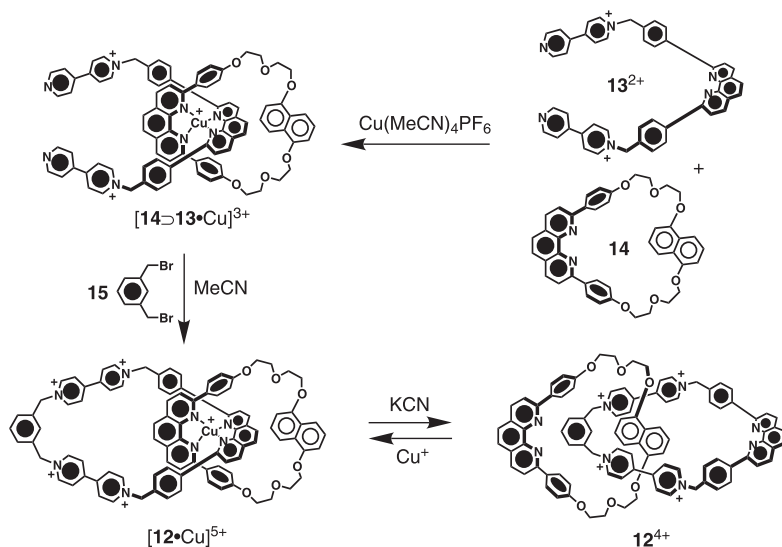


Fig. 9. The synthesis and chemical switching of a hybrid [2]catenane.

$[14 \supset 13\text{-Cu}]^{3+}$ with 1,3-bis(bromomethyl)benzene (**15**) under high dilution conditions in refluxing MeCN, gave the [2]catenane $[12\text{-Cu}]^{5+}$ in 40 % yield. This hybrid molecular switch possesses two different recognition modes, namely (i) coordination of Cu(I) by two phenanthroline ligands and (ii) π -electron donor–acceptor interactions between the DNP ring system and the two bipyridinium units. Since the coordination interaction is the stronger, the stable state of the molecular switch is the [2]catenane $[12\text{-Cu}]^{5+}$, in which the Cu(I) ion is complexed by the two phenanthroline ligands in a tetrahedral coordination geometry. Removal of the Cu(I) ion, however, by the addition of KCN, affords the [2]catenane 12^{4+} , which undergoes a topological change to allow its π -electron-rich DNP ring system to be sandwiched between its two π -electron-deficient bipyridinium units. Thus, non-covalent donor–acceptor interactions dominate the molecular geometry in the demetalated system. The chemically driven co-conformational change between the [2]catenanes $[12\text{-Cu}]^{5+}$ and 12^{4+} was confirmed by ^1H NMR spectroscopy.

16.4

A Self-Complexing Molecular Switch

Our next case history takes what we have learnt about donor–acceptor interactions between arene building blocks in interlocked molecules and exploits that knowledge base in a more conventional intramolecular arena. The self-complexing compound 16^{4+} (Figure 10) incorporates [11] a linear polyether thread intercepted by a DNP ring system, which is co-

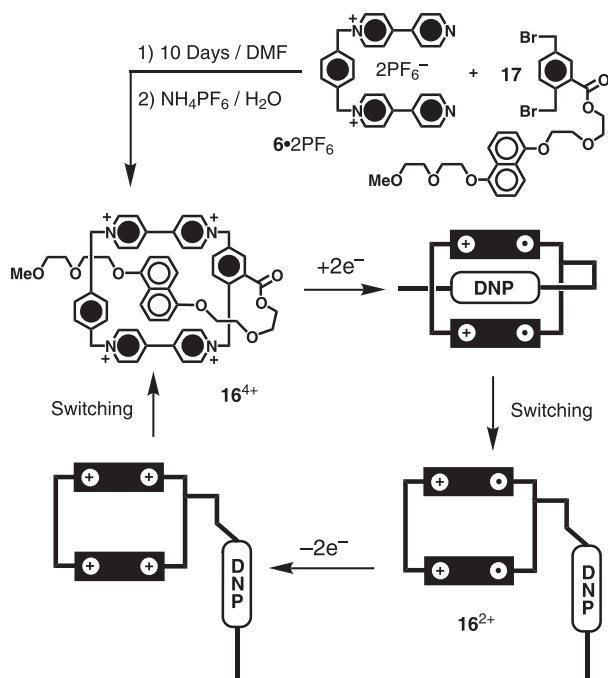


Fig. 10. The synthesis and switching of the self-complexing compound 16^{4+} .

valently bound to one of the phenylene spacers of the tetracationic cyclophane by means of an ester linkage. In solution, the DNP ring system threads through the cavity of the cyclophane. The conformation is stabilized by π - π stacking interactions between the complementary π -electron-rich DNP ring system and the two π -electron-deficient bipyridinium units in the tetracationic cyclophane. By reacting the dication **6**·2PF₆ with the DNP-containing dibromide **17**, the self-complexing macrocycle **16**⁴⁺ was obtained in 24 % yield. The absorption spectrum of the macrocycle **16**⁴⁺, recorded in MeCN at 298 K, shows a band centered at 515 nm, corresponding to the CT interaction between a DNP ring system and the sandwiching bipyridinium units. The absorption increases linearly with the concentration, suggesting that this compound exists only in the self-complexing form. The compound also functions as an electrochemically driven molecular switch. After electrochemical reduction of each bipyridinium unit of the cyclophane, the DNP-containing side chain is ejected from the cyclophane's cavity. This dramatic conformational change is reversible by means of the electrochemical redox process. The switching process was monitored by CV and indeed proved to be reversible.

16.5

Pseudorotaxane-Based Supramolecular Machines

The recognition of different π -donating arene guests with a common π -accepting host has been subjected to control by metal ion crown ether recognition in the next case history to be described. The 18-crown-6 derivative **18**, which bears a DNP ring system [12], is a ditopic compound that can act (Figure 11) as a host for alkali metal (e.g., K⁺) cations as well as a

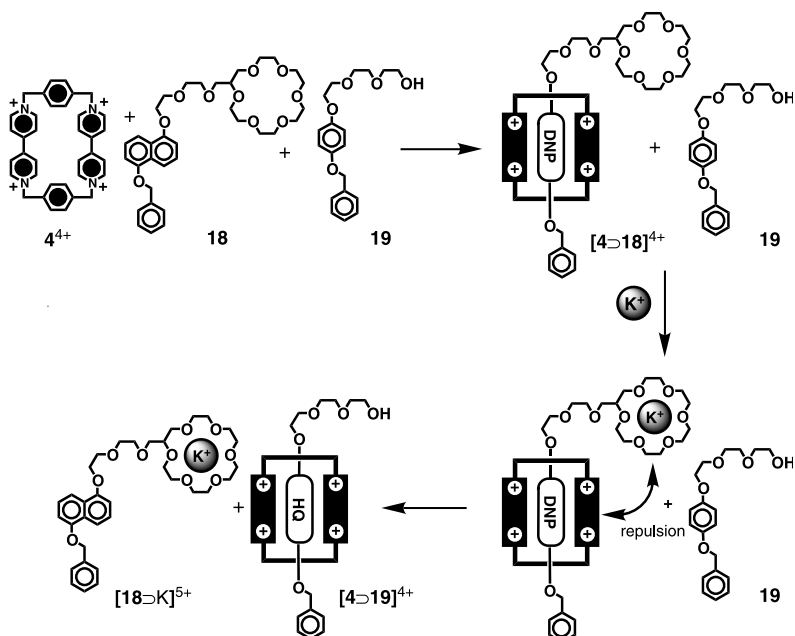


Fig. 11. The chemically controlled competition between two thread-like species **18** and **19** for the cavity of a tetracationic cyclophane **4**⁴⁺.

guest for the tetracationic cyclophane 4^{4+} , in the latter case forming a [2]pseudorotaxane $[4 \supset 18]^{4+}$. In MeCN, the 1:1 complex $[4 \supset 18]^{4+}$ is not affected by the presence of the HQ-containing thread **19**. Upon addition of K^+ ions to a solution of [2]pseudorotaxane $[4 \supset 18]^{4+}$ in MeCN, it disassembles, presumably as a result of electrostatic repulsions between the bound K^+ ion and the 4^{4+} tetracation. The cavity of the tetracationic cyclophane is then free to complex with the neutral thread **19**, forming the [2]pseudorotaxane $[4 \supset 19]^{4+}$. Since the exchange of guests causes the color of the solution to change from purple to reddish-orange, this multicomponent system can also be regarded as a metal-controlled chromophoric molecular switch. The exchange processes occurring in this supramolecular system can also be monitored by ^1H NMR spectroscopy.

16.6

[2]Rotaxanes and Molecular Shuttles

A [2]rotaxane is a molecule composed of macrocyclic and dumbbell-shaped components. The macrocycle encircles the rod-like portion of the dumbbell-shaped component and is mechanically trapped by two bulky stoppers. Thus, the two components cannot dissociate from one another, even though they are not covalently bound to each other. Moreover, if there are two degenerate recognition sites located on the dumbbell-shaped component of the [2]rotaxane, a co-conformational equilibrium state, in which the macrocyclic component can shuttle back and forth along the rod-like portion of the dumbbell, can result. Such a molecule constitutes a molecular shuttle [13]. The first molecular shuttle, **21**· 4PF_6 , was reported [13a] in 1991. Reaction of equimolar amounts of the dication **6**· 2PF_6 and 1,4-bis(bromomethyl)benzene (**7**) in the presence of the dumbbell-shaped compound **20** and AgPF_6 gave **21**· 4PF_6 in 32 % yield (Figure 12). In this molecule, there are two degenerate HQ rings (labeled A and B in Figure 13) located on the dumbbell-shaped component, between which the tetracationic cyclophane can shuttle back and forth. Both the ^1H and ^{13}C NMR spectra of the molecular shuttle **21**· 4PF_6 show temperature-dependent behavior in a range of deuterated solvents. For this degenerate system, we would expect to observe two sets of signals due to the HQ rings – one set due to the protons on the encircled HQ ring,

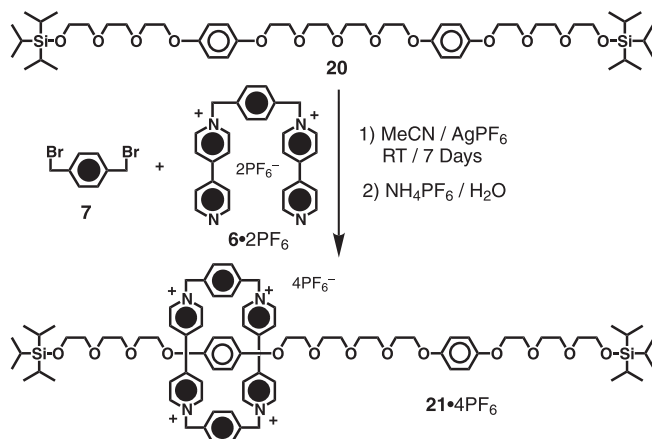


Fig. 12. The template-directed synthesis of the molecular shuttle **21**· 4PF_6 .

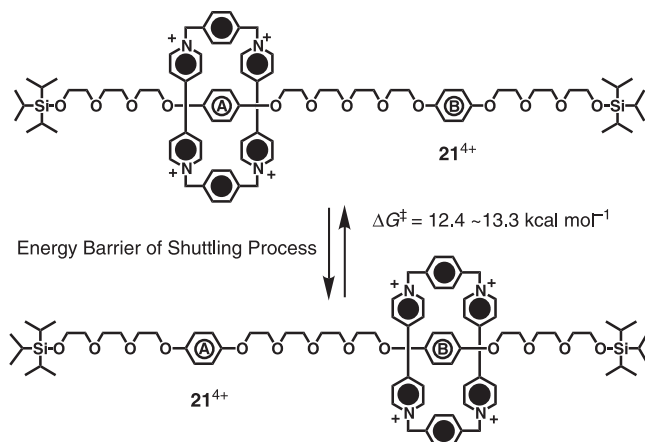


Fig. 13. The shuttling process and energy barrier for the passage of the tetracationic cyclophane between the two degenerate recognition sites, A and B, in the [2]rotaxane 21^{4+} .

and another set arising from the protons on the free HQ ring. Indeed, at room temperature in $[D_6]$ acetone solution, the signals of the HQ protons are merged into the baseline between $\delta = 3.5$ and $\delta = 6.5$, suggesting that the shuttling process in the molecular shuttle $21 \cdot 4PF_6$ is slow on the 1H NMR time-scale at room temperature. Cooling the solution of $21 \cdot 4PF_6$ in $[D_6]$ acetone to 223 K in an effort to further slow down the shuttling process allowed two sets of peaks to be observed at $\delta = 6.38$ and $\delta = 3.8$, corresponding to the protons on the free and encircled HQ rings, respectively. When the same sample was warmed up to 413 K in $[D_6]$ DMSO, only one set of proton signals was observed at $\delta = 5.16$ because of the rapid shuttling process. By monitoring the various signal coalescences with different 1H NMR probes in both the dumbbell and macrocycle components, the energy barrier (ΔG^\ddagger) to the shuttling process was determined [13a, 13e] to be in the range 12.4–13.3 kcal mol $^{-1}$.

It is also possible to control the shuttling process within a non-degenerate molecular shuttle. By incorporating two recognition sites with different π -electron-donor/acceptor abilities into the dumbbell-shaped component, the macrocycle can be located preferentially on one of the two different recognition sites. The macrocycle can then be enticed to reside on the other recognition site by altering the π -electron-donor/acceptor ability of the original recognition site. The [2]rotaxane 22^{4+} constitutes [14] a chemically and electrochemically switchable molecular shuttle. The synthesis of [2]rotaxane $22^{4+} \cdot 4PF_6$ is illustrated in Figure 14. The bis(hexafluorophosphate) salt $6 \cdot 2PF_6$ was treated with 1,4-bis(bromomethyl)benzene (7) in the presence of the dumbbell-shaped compound 23, which incorporates both benzidine and biphenol recognition sites. The chemically and electrochemically controllable switching relies upon the π - π stacking and $[C-H \cdots O]$ interactions between the complementary units in the recognition sites. As expected, the [2]rotaxane 22^{4+} exhibits translational isomerism, with the tetracationic cyclophane located preferentially (84:16 in MeCN at $-44^\circ C$) on the more π -electron-rich benzidine ring. Two translational isomers could also be detected by absorption spectroscopy. The absorption spectrum recorded in MeCN shows two

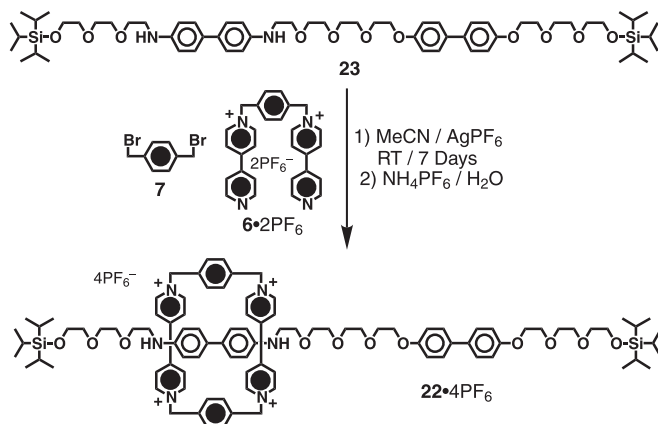


Fig. 14. The template-directed synthesis of the [2]rotaxane $22 \cdot 4PF_6$.

bands, centered on 490 and 690 nm, corresponding to the CT interactions between the tetracationic cyclophane and the biphenol and benzidine units, respectively.

The [2]rotaxane 22^{4+} can be switched (Figure 15) by controlling the pH. Upon addition of an excess of trifluoroacetic acid, the benzidine unit becomes protonated, generating the [2]rotaxane $[22 \cdot 2H]^{6+}$. The tetracationic cyclophane moves away from this newly generated dicationic unit because of electrostatic repulsion. In this case, the absorption spectrum lacks the 690 nm band, confirming the deprotonation of the benzidine unit and the relocation of the cyclophane to the biphenol unit. The [2]rotaxane $[22 \cdot 2H]^{6+}$ can be subsequently deprotonated by the addition of pyridine, regenerating the [2]rotaxane 22^{4+} .

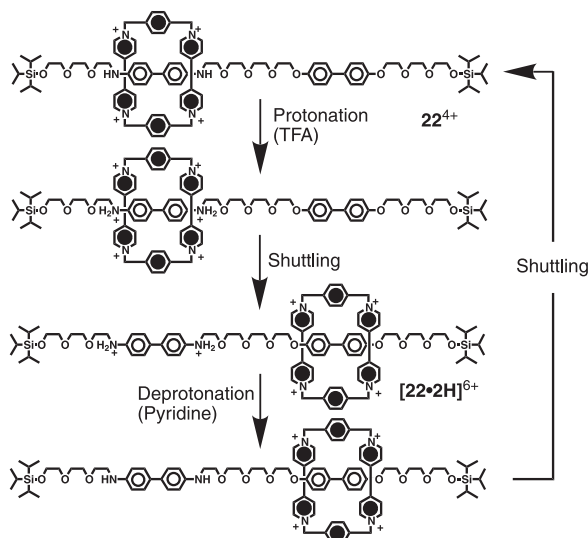


Fig. 15. The acid/base-controllable switching of the [2]rotaxane $22 \cdot 4PF_6$.

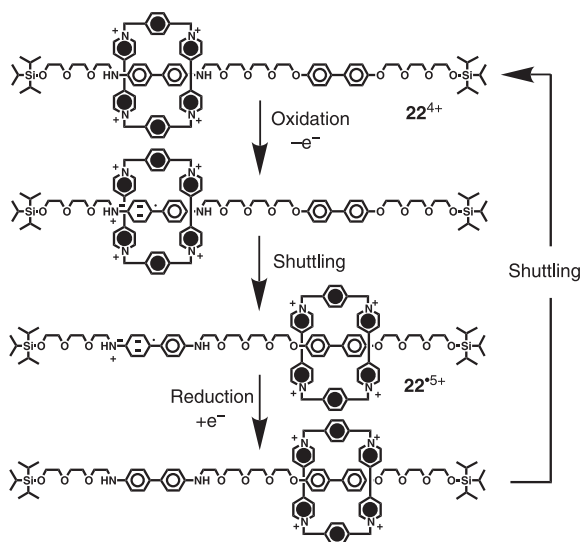


Fig. 16. The redox-controllable switching of the [2]rotaxane **22**·4PF₆.

Cyclic voltammetry shows that the [2]rotaxane **22**⁴⁺ can also undergo electrochemical switching (Figure 16) by a monoelectronic oxidation process to give the radical pentacationic species **22**^{•5+}. On oxidation, the benzidine unit is converted to its monocationic radical state, generating an electrostatic repulsion, which causes the tetracationic cyclophane to move to the biphenol unit in [2]rotaxane **22**⁴⁺. This redox procedure is completely reversible.

The amphiphilic molecular shuttle **24**·4PF₆ was synthesized [15a] by using the dumbbell-shaped compound **25** as the template for the formation of the encircling tetracationic cyclophane (Figure 17) from its precursor **6**·2PF₆ and 1,4-bis(bromomethyl)benzene (**7**). The molecular shuttle **24**·4PF₆ was isolated as an analytically pure, brown solid after column chromatography using a solution of NH₄PF₆ in Me₂CO as the eluent. Spectroscopic studies indicated the presence of the two stable translational isomers, **24**·4PF₆-Green and **24**·4PF₆-Red, in the isolated product. The visible absorption spectrum recorded in Me₂CO showed a broad CT band centered at 805 nm, which is characteristic of the co-conformation (**24**·4PF₆-Green) containing the TTF unit located inside the cavity of the tetracationic cyclophane, and a CT band observed as a shoulder at 540 nm, which results from the DNP ring system encircled by the tetracationic cyclophane in the other co-conformation (**24**·4PF₆-Red). The ¹H NMR spectrum recorded at 298 K in [D₆]acetone also indicated the presence of two co-conformational isomers, slowly interconverting on the ¹H NMR timescale. The ratio of the two translational isomers was estimated by integration of the two different SMe resonances to be approximately 1:1. By means of preparative thin-layer chromatography, it is possible to isolate the translational isomer (**24**·4PF₆-Red), in which the tetracationic cyclophane encircles the DNP ring system. Allowing the solution of the red translational isomer **24**·4PF₆-Red to stand at room temperature for 24 h results in the formation of the “original” brown solution containing a mixture of the two translational isomers. By employing a first-order kinetic treatment, a rate constant of $2 \times 10^{-5} \text{ s}^{-1}$ was obtained for this slow shuttling pro-

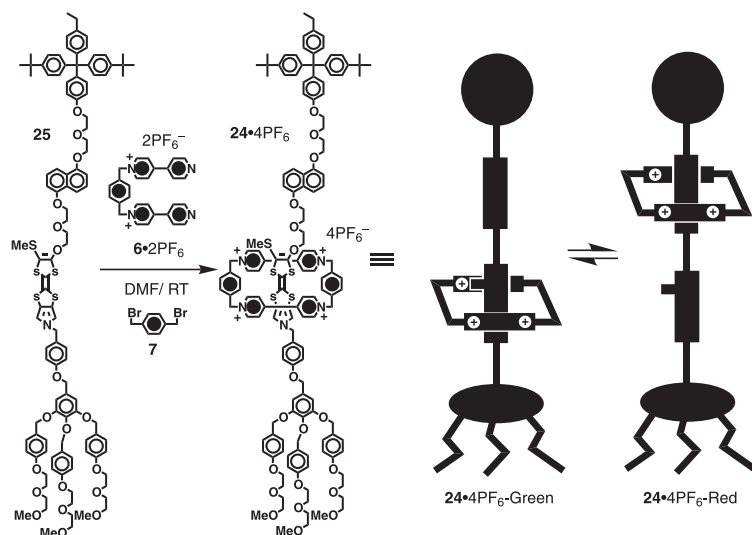


Fig. 17. The synthesis of the slow-shuttling [2]rotaxane **24-4PF₆**.

cess of the tetracationic cyclophane between the two recognition sites. The corresponding free energy of activation (ΔG^\ddagger) for this isomerization is 24 kcal mol^{-1} . This new amphiphilic, bistable [2]rotaxane **24-4PF₆** has been assessed [15b] for its ability to self-organize into an LB monolayer as a prelude to its incorporation into devices (Figure 18).

Two [2]rotaxanes, **[26-H]·3PF₆** and **[27-H]·3PF₆**, incorporating both dialkylammonium and bipyridinium recognition sites have been self-assembled [16] as outlined in Figure 19. Treatment of the bis(hexafluorophosphate) salts **[28-H]·2PF₆** and **[29-H]·2PF₆** with the benzylic bromide **30** in the presence of dibenzo-24-crown-8 (**31**) gave the [2]rotaxanes **[26-H]·3PF₆** and **[27-H]·3PF₆**, respectively, after counterion exchange. In both [2]rotaxanes, the crown ether ring is located preferentially around the dialkylammonium recognition site as a result of a combination of $[\text{N}^+-\text{H}\cdots\text{O}]$ and $[\text{C}-\text{H}\cdots\text{O}]$ hydrogen bonds between the

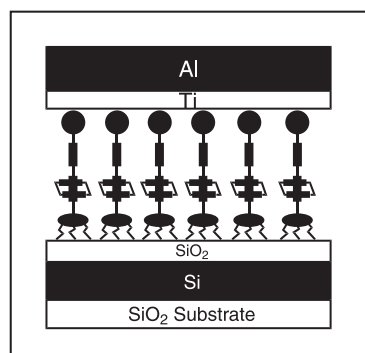


Fig. 18. A [2]rotaxane **24-4PF₆**-based molecular device.

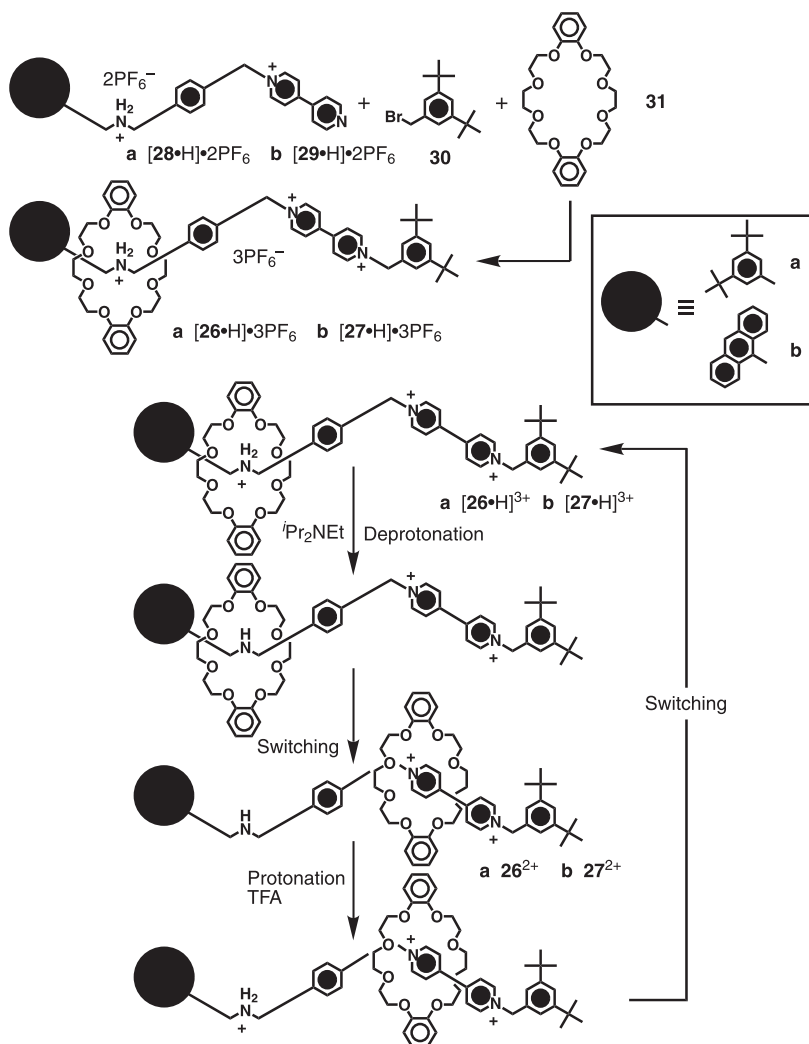


Fig. 19. The acid/base-controllable switching of the [2]rotaxanes **[26-H]·3PF₆** and **[27-H]·3PF₆**.

polyether oxygen atoms and the $-\text{CH}_2\text{NH}_2^+\text{CH}_2-$ units in **[26-H]³⁺** and **[27-H]³⁺**. However, upon addition of *i*Pr₂NEt to the solutions of **[26-H]·3PF₆** or **[27-H]·3PF₆**, the dialkylammonium recognition sites are deprotonated and the hydrogen bonds between the crown ether and the dumbbells are destroyed. As a result, the crown ether ring moves to encircle the bipyridinium recognition sites, giving **26·2PF₆** and **27·2PF₆**, respectively. Upon addition of trifluoroacetic acid, protonations restore the dialkylammonium recognition sites and the crown ether ring moves back from the bipyridinium recognition sites to the dialkylammonium recognition sites. The case history outlined in this section has demonstrated how the concept of a molecular shuttle can be transformed into molecular abacus-like switches

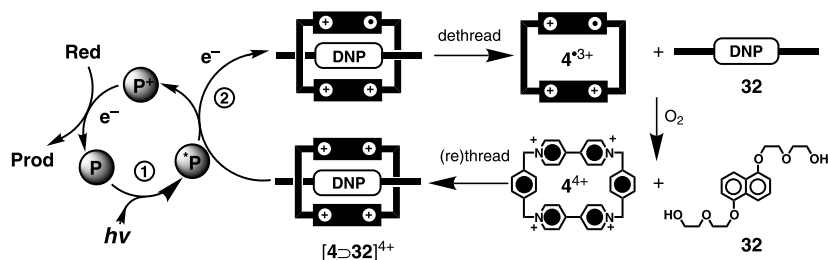


Fig. 20. The photochemically induced dethreading of the pseudorotaxane $[4 \supset 32]^{4+}$.

that can be both chemically and electrochemically driven. The next section describes how very similar kinds of switches and machines have been designed and operated photochemically in collaboration with the Balzani group and, in the case of the solid-state systems, with the Zink group at UCLA.

16.7

The Evolution of Photochemically Driven Molecular Switches

The [2]pseudorotaxane $[4 \supset 32]^{4+}$ can behave [17a] as a photochemically driven molecular switch (Figure 20) in aqueous solution. When the thread-like compound **32** is added to the tetrachloride salt of the tetracationic cyclophane 4^{4+} , it forms the [2]pseudorotaxane $[4 \supset 32]^{4+}$ in aqueous solution. Next, the deoxygenated solution of the [2]pseudorotaxane $[4 \supset 32]^{4+}$ is irradiated in the presence of an external electron-transfer photosensitizer (**P**, 9-anthracene-carboxylic acid) and a sacrificial reductant (**Red**, triethanolamine). It should be noted that the photosensitizer must (i) be able to absorb light efficiently (Process 1 in Figure 20) and (ii) have a sufficiently long-lived excited state (**P***) so that its irradiation in the presence of the [2]pseudorotaxane $[4 \supset 32]^{4+}$ will lead to the transfer of an electron to one of the bipyridinium units of the cyclophane (Process 2 in Figure 20). The related fast back electron transfer from the reduced cyclophane to the oxidized photosensitizer is prevented by the presence of the sacrificial reductant (**Red**). As a consequence, the π - π stacking interactions, which hold the 1:1 complex $[4 \supset 32]^{4+}$ together, are seriously impaired, resulting in dethreading of the [2]pseudorotaxane. This process can be monitored by the disappearance of the CT band between the DNP ring system and the cyclophane, and the appearance of the fluorescence of the DNP ring system in the “free” **32**. If oxygen is allowed to enter the aqueous solution, the reduced cyclophane 4^{3+} is re-oxidized and the [2]pseudorotaxane $[4 \supset 32]^{4+}$ is re-formed.

The same concept has been demonstrated [17b] in the solid state by two different approaches, affording supramolecular machines. In the first system (Figure 21), the supramolecular machines are physically trapped in a rigid, nanoporous, and optically transparent matrix by condensation of a sol-gel silica framework around the [2]pseudorotaxane $[4 \supset 32]^{4+}$, photosensitizer (**P**), and sacrificial reductant (**Red**). The XeCl laser-induced fluorescent emission of the dethreaded DNP ring system in component **32** is monitored. The dethreading process was found to be roughly an order of magnitude slower in the gel than in solution. This reduced rate of dethreading probably results from the stabilization in-

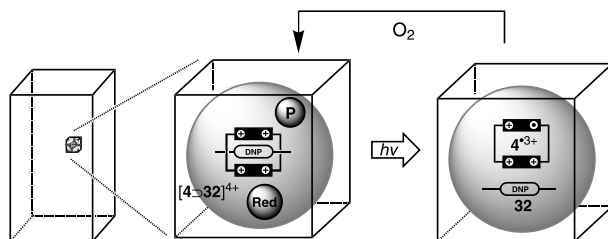


Fig. 21. Supramolecular machines in an interior pore of a sol-gel monolith.

teraction between the negatively charged pore walls of the silicate matrix and the positively charged components of the supramolecular machine. In the second system (Figures 22 and 23), the [2]pseudorotaxanes $[4\supset 33]^{4+}$ are tethered onto the surface of a silica film. In this case, the monobenzylated DNP derivative **33** is attached to sol-gel films (Step 2 in Figure 22) that are pre-functionalized by treating the surface silanol groups with isocyanatopropyltriethoxysilane (Step 1 in Figure 22). After capturing the tetracationic cyclophane 4^{4+} , the derivatized films were allowed to perform three threading and dethreading redox cycles in an aqueous solution containing the photosensitizer (**P**) and the sacrificial reductant (**Red**; here ethylenediaminetetraacetate was applied).

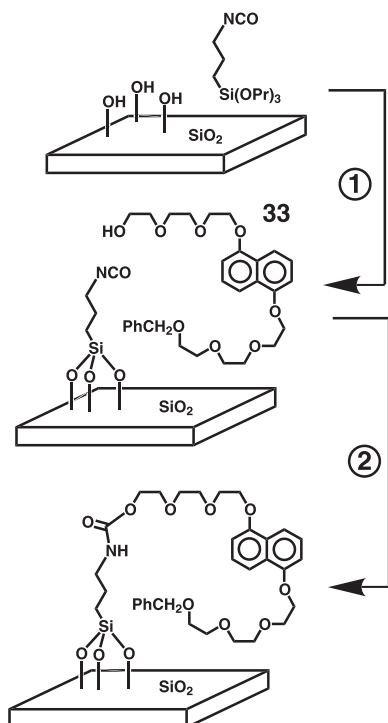


Fig. 22. The two-step procedure to anchor the thread **33** onto the surface of a sol-gel film.

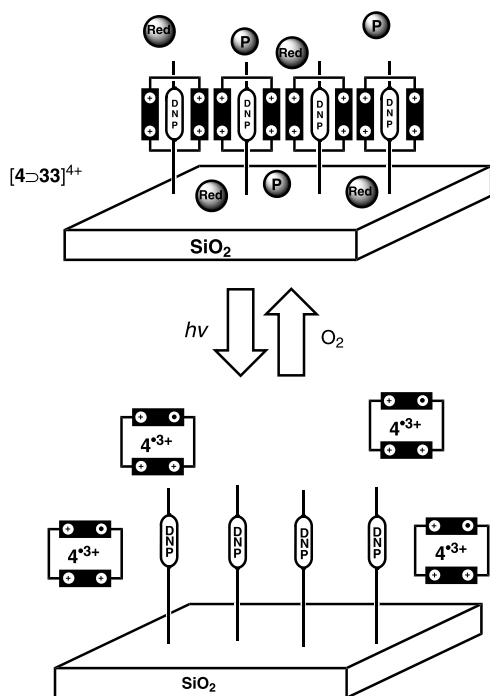


Fig. 23. Supramolecular machines in action on a sol-gel surface.

The design of photochemically driven supramolecular machines can be improved by incorporating the photoactive component (**P**) into either the thread or the cyclophane in order to increase the efficiency of the electron-transfer process. [2]Pseudorotaxanes containing metal-complex photosensitizers can be regarded as “light-fueled” motors. A photoactive metal complex has been incorporated (Figure 24) into both the thread and the ring components [18, 19] in separate experiments. The [2]pseudorotaxane [8>34]⁴⁺ incorporates [18a] the 1,5-dinaphtho-38-crown-10 [1/5-DN38C10] (**8**) and the photoactive ruthenium complex containing thread **34**⁴⁺. The threading and dethreading motions of the [2]pseudorotaxane [8>34]⁴⁺ can be triggered (Figure 24a) by irradiation with visible light and oxygenation of the solution, respectively. Photoirradiation induces intramolecular single electron transfer from the metal complex **P** to the adjacent bipyridinium unit. As a result, the π - π stacking interactions between the crown ether **8** and the thread **34**⁴⁺ are destroyed. The competing back electron transfer is blocked by the presence of the reductant (**Red**). Upon introduction of oxygen into the reaction mixture, the bipyridinium unit is oxidized and complexation between **8** and **34**⁴⁺ is restored. The mechanical motions exhibited by this supramolecular machine can be monitored by the intensity of the fluorescence associated with the free crown ether **8**. Similarly, the [2]pseudorotaxane [35>36]⁴⁺ incorporates [18b] a photoactive rhenium complex containing cyclophane **35**⁴⁺ and a DNP-containing thread **36**. The threading and dethreading processes involving this [2]pseudorotaxane [35>36]⁴⁺ can also be triggered (Figure 24b) by irradiation with visible light and oxygenation of the solution,

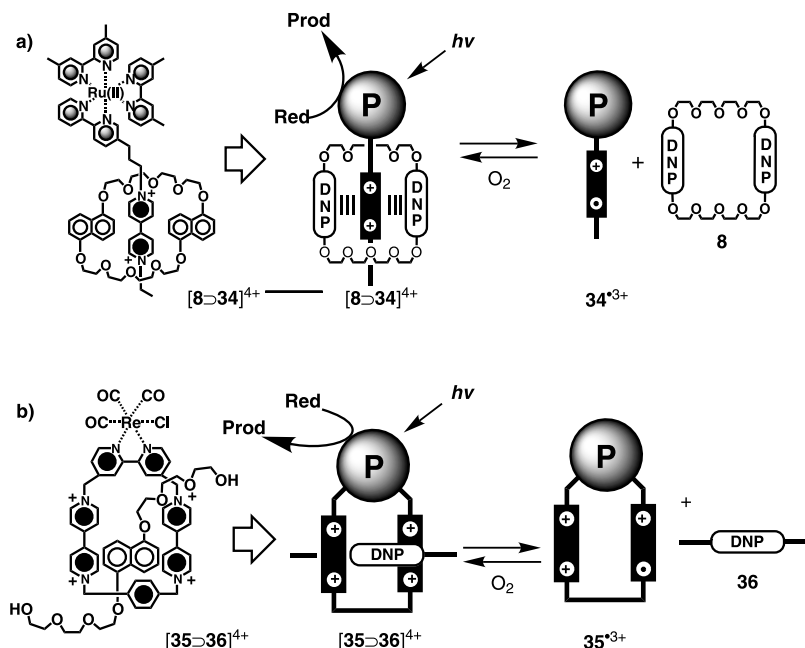


Fig. 24. Photocontrollable molecular machines based on the [2]pseudorotaxanes $[8 \supset 34]^{4+}$ and $[35 \supset 36]^{4+}$.

respectively. Photoirradiation induces intramolecular single electron transfer from the ruthenium metal complex **P** to an adjacent bipyridinium unit of the cyclophane. As a consequence, the π - π stacking interactions between the cyclophane 35^{4+} and the thread **36** are destroyed. The competing back electron transfer is blocked by the presence of the reductant (**Red**). Upon introduction of oxygen into the reaction mixture, the bipyridinium unit is oxidized and complexation between the cyclophane 35^{4+} and the thread **36** is restored. The mechanical motions exhibited by this supramolecular machine can be monitored by the intensity of the fluorescence associated with the free DNP-containing thread **36**.

Following the evolution of these photochemically driven supramolecular machines, a molecular machine was reported [19] in the form of a molecular-level abacus. It was designed in the shape of the [2]rotaxane **37**·6PF₆, composed of the π -electron-donating macrocyclic polyether BPP34C10 (**1**) and a dumbbell-shaped component **38**·6PF₆, which contains (i) a photoactive Ru(II)-polypyridine complex as one of its stoppers, (ii) a *p*-terphenyl-type ring system as a rigid spacer, (iii) 4,4'-bipyridinium and 3,3'-dimethyl-4,4'-bipyridinium units as two different π -electron-accepting stations, and (iv) a tetraarylmethane group to act as the second inert stopper. The [2]rotaxane **37**·6PF₆ was synthesized (Figure 25) by a thermodynamically driven slippage reaction between the dumbbell **38**·6PF₆ and BPP34C10 (**1**). The mechanical properties of this molecular shuttle were characterized by cyclic voltammetry. The stable translational isomer is the one in which the BPP34C10 component encircles the 4,4'-bipyridinium unit, in keeping with the fact that this unit is a much better π -electron acceptor than the 3,3'-dimethyl-4,4'-bipyridinium unit. Two strategies have been employed in order to

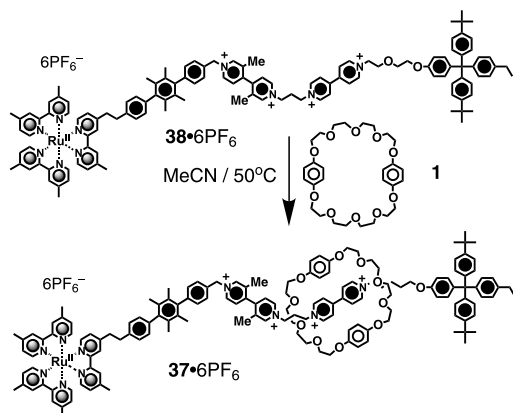


Fig. 25. The synthesis of the [2]rotaxane **37**·4PF₆ by the slippage approach.

obtain the photoinduced abacus-like movement of the BPP34C10 ring between the two stations.

An intramolecular mechanism, which is illustrated in Figure 26, is based on the following four operations: (a) Destabilization of the stable translational isomer: a photoinduced electron transfer from the photoactive stopper **P** to the A₁ station (Step 1), which is encircled by the BPP34C10 ring, in order to destabilize the π - π stacking interaction between the ring component and the A₁ station. (b) Ring displacement: the BPP34C10 moves from the reduced A₁ to A₂ (Step 2) as a result of destabilization of the π - π stacking interactions between the ring component and the A₁ station. This step competes with the back electron transfer process from the reduced A₁ to the oxidized photoactive unit P⁺ (Step 3). (c) Electronic reset:

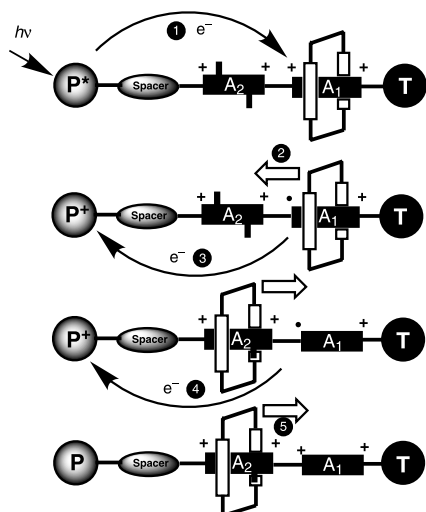


Fig. 26. Intramolecular mechanism.

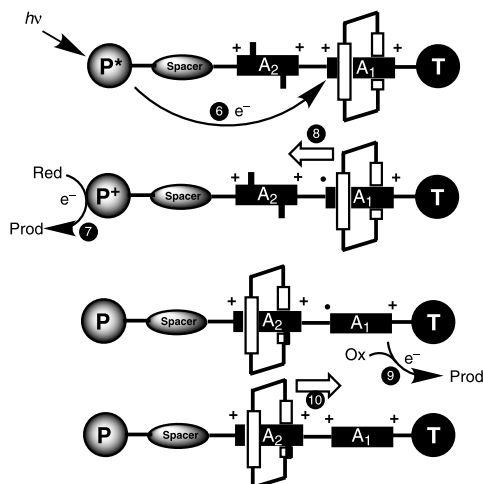


Fig. 27. Sacrificial mechanism.

a back electron transfer process from the uncomplexed reduced A_1 to P^+ (Step 4) takes place with consequent restoration of the electron-acceptor character to the A_1 station. (d) Nuclear reset: back movement of the BPP34C10 from the A_2 to the A_1 station (Step 5). Unfortunately, in this mechanism, the back electron transfer process (Step 2) is faster than the ring displacement process (Step 3). Therefore, the intramolecular mechanism does not allow this system to behave as a molecular-level abacus. Figure 27 illustrates an alternative sacrificial mechanism, which is based on the following four operations: (a) Destabilization of the stable translational isomer (Step 6); this is the same as Step 1 mentioned in the intramolecular mechanism. (b) Ring displacement: after scavenging of the oxidized photoactive unit, a suitable reductant **Red** is added to the solution to react with the oxidized photoactive unit P^+ (Step 7). The back electron transfer reaction is thus quenched and the BPP34C10 ring moves from the reduced A_1 to A_2 (Step 8). (c) Electronic reset: the electron-acceptor power of the A_1 station can be restored by oxidizing the reduced A_1 with a suitable oxidant **Ox** (Step 9). (d) Nuclear reset (Step 10). Experiments have shown [19] that the photochemically driven switching of this molecular-level abacus-like system can be successfully accomplished in solution by means of this sacrificial mechanism.

16.8

Chemically Switchable Pseudorotaxanes

We have developed a number of these supramolecular machine-like systems in collaboration with the Balzani group, and have used them to perform logic functions. An example is presented in the next section. Figure 28 illustrates the chemical switching [20a] of the [2]pseudorotaxane $[8 \rightarrow 39]^{2+}$, which incorporates a π -electron-deficient unit (diazapyrenium dication) in its thread-like component 39^{2+} and two π -electron-rich units (DNP) in the crown ether 1/5-DN38C10 (**8**). Since the thread-like component 39^{2+} forms adducts

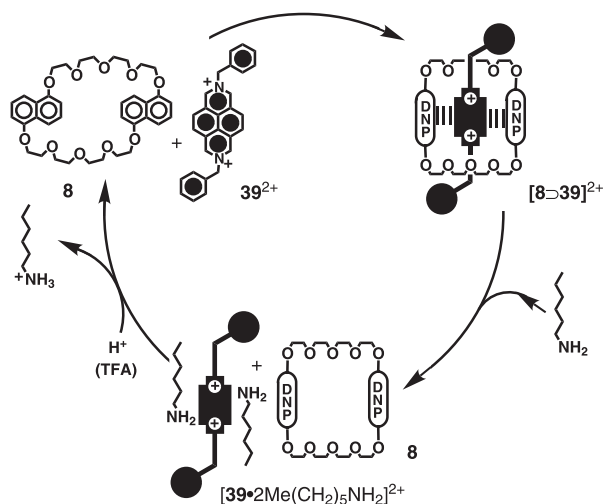


Fig. 28. Amine/acid-controlled dethreading/rethreading cycle of [2]pseudorotaxane $[8 \supset 39]^{2+}$.

$[39 \cdot 2\text{Me}(\text{CH}_2)_5\text{NH}_2]^{2+}$ with *n*-hexylamine, addition of this amine induces the dethreading of [2]pseudorotaxane $[8 \supset 39]^{2+}$. This process is quantitatively reversible upon the addition of trifluoroacetic acid (TFA). The changes in the absorption and fluorescence spectra allow the on/off switching to be easily monitored.

The same phenomenon was probed [20b] in the chemical switching (Figure 29) of the [2]catenane 40^{4+} . It incorporates BPP34C10 and a tetracationic cyclophane, comprising a bipyridinium and a diazapyrenium unit. X-ray crystallographic analysis revealed that the BPP34C10 exclusively encircles the diazapyrenium ring system in the solid state. The ^1H NMR spectrum ($[\text{D}_6]\text{acetone}$, 193 K) of the [2]catenane 40^{4+} shows the signals for two co-conformations in a ratio of 96:4. The major isomer corresponds to the same co-conformation

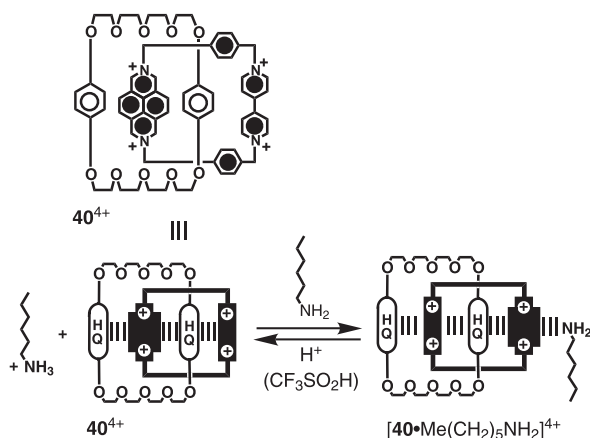


Fig. 29. A chemically switchable [2]catenane 40^{4+} .

as that observed in the solid state. The diazapyrenium unit is located inside the cavity of the BPP34C10 and the bipyridinium unit is positioned “alongside”. Since *n*-hexylamine can form adducts $[40\text{-Me}(\text{CH}_2)_5\text{NH}_2]^{4+}$ with the diazapyrenium ring system, the equilibrium between the two co-conformations can be displaced in favor of the isomer having the diazapyrenium ring system alongside the cavity of BPP34C10. The differential pulse voltammogram (MeCN, 298 K) of the [2]catenane 40^{4+} shows two peaks at -0.31 mV and -0.57 mV *vs.* SCE for the monoelectronic reduction of the alongside bipyridinium unit and of the inside diazapyrenium ring system, respectively. After the addition of *n*-hexylamine, the first peak shifts by -60 mV to a potential that corresponds to the monoelectronic reduction of a bipyridinium unit encircled by the BPP34C10. Similarly, the second peak shifts by -20 mV to a potential that is associated with the monoelectronic reduction of a diazapyrenium ring system interacting with *n*-hexylamine. Protonation of *n*-hexylamine occurs upon addition of $\text{CF}_3\text{SO}_3\text{H}$. As a result, the adducts formed between the *n*-hexylamine and the diazapyrenium unit of the [2]catenane are destroyed, restoring the original equilibrium between the two co-conformations associated with [2]catenane 40^{4+} .

16.9

Molecule-Based XOR Logic Gate

The chemical dethreading and rethreading actions of a [2]pseudorotaxane can be used to perform logic operations at the supramolecular level [21]. The [2]pseudorotaxane $[41 \supset 39]^{2+}$ shows an exclusive OR (XOR) gate with the corresponding truth table shown in Figure 30. This logic gate can be controlled by the consecutive additions of $\text{CF}_3\text{SO}_3\text{H}$ and tributylamine, the two different input signals, and the result can be read by monitoring the fluo-

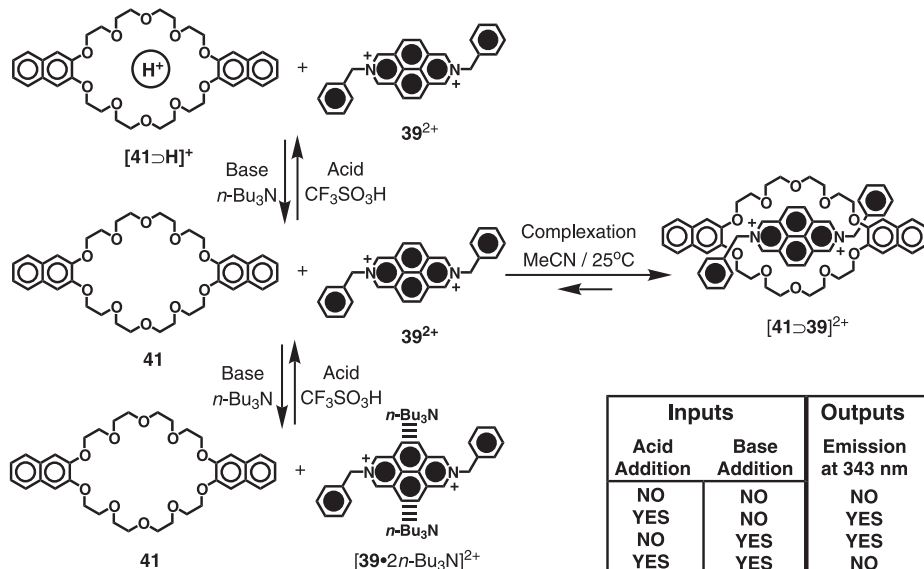


Fig. 30. A molecule-based logic gate controlled by acid/base inputs.

rescence associated with the 2,3-dihydroxynaphthalene ring system, the output signal. In its free form, the macrocyclic polyether **41** shows a fluorescent band at 343 nm. In MeCN, the 343 nm fluorescence band of **41** is quenched as a result of the formation of a strong π - π stacking complex, namely the [2]pseudorotaxane [**41** \supset **39**] $^{2+}$ (Input: NO/NO, Output: NO). Upon addition of CF₃SO₃H, the [2]pseudorotaxane [**41** \supset **39**] $^{2+}$ dissociates as a result of the formation of the fluorescent complex [**41**·H] $^{1+}$ (Input: YES/NO, Output: YES). Similarly, the addition of tributylamine to the solution of the [2]pseudorotaxane [**41** \supset **39**] $^{2+}$ induces the release of the fluorescent macrocycle **41** and the formation of the charge-transfer complex [**39**·2*n*Bu₃N] $^{2+}$ (Input: NO/YES, Output: YES). However, the simultaneous addition of CF₃SO₃H and tributylamine to the solution of the [2]pseudorotaxane [**41** \supset **39**] $^{2+}$ does not change the complexation between macrocycle **41** and diazapyrenium **39** $^{2+}$ (Input: YES/YES, Output: NO).

16.10

Conclusions

This collection of case histories gives little more than a flavor for how we have used arene building blocks in our research to construct molecular switches that are already finding their way into electronic devices. Hopefully, they will give the reader a feeling for the opportunities that we believe now exist to assemble molecular machinery on a grander and grander scale from readily available arene building blocks. However, many issues remain to be tackled, not least of all, how the motor-molecules that have been shown to operate incoherently in solution can be made to run cooperatively in unison on surfaces and inside solids.

References

- 1 For reviews and monographs on molecular switches and machines, see: a) J. F. STODDART, *Chem. Aust.* **1992**, 59, 576–577 and 581; b) M. GÓMEZ-LÓPEZ, J. A. PREECE, J. F. STODDART, *Nanotechnology* **1996**, 7, 183–192; c) M. GÓMEZ-LÓPEZ, J. F. STODDART, *Bull. Soc. Chim. Belg.* **1997**, 106, 491–500; d) V. BALZANI, M. GÓMEZ-LÓPEZ, J. F. STODDART, *Acc. Chem. Res.* **1998**, 31, 405–414; e) L. FABBRIZZI, M. LICCHELLI, P. PALLAVICINI, *Acc. Chem. Res.* **1999**, 32, 846–853; f) M. IRIE, *Chem. Rev.* **2000**, 100, 1685–1716; g) Y. YOKOYAMA, *Chem. Rev.* **2000**, 100, 1717–1739; h) G. BERKOVIC, V. KRONGAUZ, V. WEISS, *Chem. Rev.* **2000**, 100, 1741–1753; i) B. L. FERGING, R. A. VAN DELDEN, N. KOUMURA, E. M. GEERTSEMA, *Chem. Rev.* **2000**, 100, 1789–1816; j) V. BALZANI, A. CREDI, F. M. RAYMO, J. F. STODDART, *Angew. Chem. Int. Ed.* **2000**, 39, 3348–3391; k) T. R. KELLY, J. P. SESTELO, *Structure and Bonding* **2001**, 99, 19–54; l) L. RAEHM, J.-P. SAUVAGE, *Structure and Bonding* **2001**, 99, 55–78; m) A. R. PEASE, J. F. STODDART, *Structure and Bonding* **2001**, 99, 189–236; n) C. BUSTAMANTE, D. KELLER, G. OSTER, *Acc. Chem. Res.* **2001**, 34, 412–420; o) A. N. SHIPWAY, I. WILLNER, *Acc. Chem. Res.* **2001**, 34, 421–432; p) A. R. PEASE, J. O. JEPPESEN, J. F. STODDART, Y. LUO, C. P. COLLIER, J. R. HEATH, *Acc. Chem. Res.* **2001**, 34, 433–444; q) R. BALLARDINI, V. BALZANI, A. CREDI, M. T. GANDOLFI, M. VENTURI, *Acc. Chem. Res.* **2001**, 34, 445–455; r) A. HARADA, *Acc. Chem. Res.* **2001**, 34, 456–464; s) C. A. SCHALLEY, K. BEIZAI, F. VÖGTLE, *Acc. Chem. Res.* **2001**, 34, 465–476; t) J.-P. COLLIN, C. DIETRICH-BUCHECKER, P. GAVIÑA, M. C. JIMENEZ-MOLERO, J.-P. SAUVAGE, *Acc. Chem. Res.*

- 2001, 34, 477–487; u) V. AMENDOLA, L. FABBRIZZI, C. MANGANO, P. PALLAVICINI, *Acc. Chem. Res.* **2001**, 34, 488–493; v) S. SHINKAI, M. IKEDA, A. SUGASAKI, M. TAKEUCHI, *Acc. Chem. Res.* **2001**, 34, 494–503; w) B. L. FERLINGA, *Acc. Chem. Res.* **2001**, 34, 504–513; x) T. R. KELLY, *Acc. Chem. Res.* **2001**, 34, 514–522; y) F. M. RAYMO, *Adv. Mater.* **2002**, 14, 401–414; z) B. L. FERLINGA (Ed.), *Molecular Switches*, Wiley-VCH, Weinheim, **2001**.
- 2 B. L. ALLWOOD, H. SHAHRIARI-ZAVAREH, N. SPENCER, J. F. STODDART, D. J. WILLIAMS, *J. Chem. Soc., Chem. Commun.* **1987**, 1064–1066.
 - 3 B. ODELL, M. V. REDDINGTON, A. M. Z. SLAWIN, N. SPENCER, J. F. STODDART, D. J. WILLIAMS, *Angew. Chem. Int. Ed. Engl.* **1988**, 27, 1547–1550.
 - 4 a) P. R. ASHTON, T. T. GOODNOW, A. E. KAIFER, M. V. REDDINGTON, A. M. Z. SLAWIN, N. SPENCER, J. F. STODDART, C. VICENT, D. J. WILLIAMS, *Angew. Chem. Int. Ed. Engl.* **1989**, 28, 1396–1399; b) P. L. ANELLI, P. R. ASHTON, R. BALLARDINI, V. BALZANI, M. DELGADO, M. T. GANDOLFI, T. T. GOODNOW, A. E. KAIFER, D. PHILP, M. PIETRASZKIEWICZ, L. PRODI, M. V. REDDINGTON, A. M. Z. SLAWIN, N. SPENCER, J. F. STODDART, C. VICENT, D. J. WILLIAMS, *J. Am. Chem. Soc.* **1992**, 114, 193–218.
 - 5 For accounts and reviews on [C–H···O] hydrogen bonds, see: a) G. R. DESIRAJU, *Acc. Chem. Res.* **1991**, 24, 290–296; b) G. R. DESIRAJU, *Acc. Chem. Res.* **1996**, 29, 441–449; c) T. STEINER, *Chem. Commun.* **1996**, 727–734; d) I. BERGER, M. EGLI, *Chem. Eur. J.* **1997**, 3, 1400–1404; e) K. N. HOUK, S. MENZER, S. P. NEWTON, F. M. RAYMO, J. F. STODDART, D. J. WILLIAMS, *J. Am. Chem. Soc.* **1999**, 121, 1479–1487; f) F. M. RAYMO, M. D. BARTBERGER, K. N. HOUK, J. F. STODDART, *J. Am. Chem. Soc.* **2001**, 123, 9264.
 - 6 For accounts and reviews on [$\pi \cdots \pi$] stacking interactions, see: a) C. A. HUNTER, J. K. M. SANDERS, *J. Am. Chem. Soc.* **1990**, 112, 5525–5534; b) M. H. SCHWARTZ, *J. Inclusion Phenom.* **1990**, 9, 1–35; c) J. H. WILLIAMS, *Acc. Chem. Res.* **1993**, 26, 539–598; d) C. A. HUNTER, *Angew. Chem. Int. Ed. Engl.* **1993**, 32, 1584–1586; e) C. A. HUNTER, *J. Mol. Biol.* **1993**, 230, 1025–1054; f) T. DAHL, *Acta Chem. Scand.* **1994**, 48, 95–116; g) F. COZZI, J. S. SIEGEL, *Pure Appl. Chem.* **1995**, 67, 683–689; h) C. G. CLAESSENS, J. F. STODDART, *J. Phys. Org. Chem.* **1997**, 10, 254–272.
 - 7 For accounts and reviews on [C–H··· π] stacking interactions, see: a) M. OKI, *Acc. Chem. Res.* **1990**, 23, 351–356; b) M. C. ETTER, *J. Phys. Chem.* **1991**, 95, 4601–4610; c) M. J. ZAWOROTKO, *Chem. Soc. Rev.* **1994**, 23, 282–288; d) M. NISHIO, Y. UMEZAWA, M. HIROTA, Y. TAKEUCHI, *Tetrahedron* **1995**, 51, 8665–8701; e) M. NISHIO, Y. UMEZAWA, M. HIROTA, Y. TAKEUCHI, *The [C–H··· π] Interaction*, Wiley-VCH, New York, **1998**.
 - 8 P. R. ASHTON, V. BALZANI, J. BECHER, A. CREDI, M. C. T. FYFE, G. MATTERSTEIG, S. MENZER, M. B. NIELSEN, F. M. RAYMO, J. F. STODDART, M. VENTURI, A. J. P. WHITE, D. J. WILLIAMS, *J. Am. Chem. Soc.* **1999**, 121, 3951–3957.
 - 9 a) M. ASAKAWA, P. R. ASHTON, V. BALZANI, A. CREDI, C. HAMERS, G. MATTERSTEIG, M. MONTALTI, A. N. SHIPWAY, N. SPENCER, J. F. STODDART, M. S. TOLLEY, M. VENTURI, A. J. P. WHITE, D. J. WILLIAMS, *Angew. Chem. Int. Ed.* **1998**, 37, 333–337; b) V. BALZANI, A. CREDI, G. MATTERSTEIG, O. A. MATTHEWS, F. M. RAYMO, J. F. STODDART, M. VENTURI, A. J. P. WHITE, D. J. WILLIAMS, *J. Org. Chem.* **2000**, 65, 1924–1936; c) C. L. BROWN, U. JONAS, J. A. PREECE, H. RINGSDORF, M. SEITZ, J. F. STODDART, *Langmuir* **2000**, 16, 1924–1930; d) M. ASAKAWA, M. HIGUCHI, G. MATTERSTEIG, T. NAKAMURA, A. R. PEASE, F. M. RAYMO, T. SHIMIZU, J. F. STODDART, *Adv. Mater.* **2000**, 12, 1099–1102; e) C. P. COLLIER, G. MATTERSTEIG, E. W. WONG, Y. LUO, K. BEVERLY, J. SAMPAIO, F. M. RAYMO, J. F. STODDART, J. R. HEATH, *Science* **2000**, 289, 1172–1175.
 - 10 D. B. AMABILINO, C. O. DIETRICH-BUCHECKER, A. LIVOREIL, L. PÉREZ-GARCÍA, J.-P. SAUVAGE, J. F. STODDART, *J. Am. Chem. Soc.* **1996**, 118, 3905–3913.
 - 11 P. R. ASHTON, R. BALLARDINI, V. BALZANI, S. E. BOYD, A. CREDI, M. T. GANDOLFI, M. GÓMEZ-LÓPEZ, S. IQBAL, D. PHILP, J. A. PREECE, L. PRODI, H. G. RICKETTS, J. F. STODDART, M. S. TOLLEY, M. VENTURI, A.

- J. P. WHITE, D. J. WILLIAMS, *Chem. Eur. J.* **1997**, *3*, 152–170.
- 12 a) M. ASAKAWA, P. R. ASHTON, S. IQBAL, J. F. STODDART, N. D. TINKER, A. J. P. WHITE, D. J. WILLIAMS, *Chem. Commun.* **1996**, 483–486; b) M. ASAKAWA, S. IQBAL, J. F. STODDART, N. D. TINKER, *Angew. Chem. Int. Ed. Engl.* **1996**, *35*, 976–978.
 - 13 a) P. L. ANELLI, N. SPENCER, J. F. STODDART, *J. Am. Chem. Soc.* **1991**, *113*, 5131–5133; b) P. R. ASHTON, R. A. BISSELL, N. SPENCER, J. F. STODDART, M. S. TOLLEY, *Synlett* **1992**, 914–918; c) P. R. ASHTON, R. A. BISSELL, R. GÓRSKI, D. PHILP, N. SPENCER, J. F. STODDART, M. S. TOLLEY, *Synlett* **1992**, 919–922; d) P. R. ASHTON, R. A. BISSELL, N. SPENCER, J. F. STODDART, M. S. TOLLEY, *Synlett*, **1992**, 923–926; e) P. L. ANELLI, M. ASAKAWA, P. R. ASHTON, R. A. BISSELL, G. CLAVIER, R. GÓRSKI, A. E. KAIFER, S. J. LANGFORD, G. MATTERSTEIG, S. MENZER, D. PHILP, A. M. Z. SLAWIN, N. SPENCER, J. F. STODDART, M. S. TOLLEY, D. J. WILLIAMS, *Chem. Eur. J.* **1997**, *3*, 1113–1135.
 - 14 R. A. BISSELL, E. CÓRDOVA, A. E. KAIFER, J. F. STODDART, *Nature* **1994**, *369*, 133–137.
 - 15 a) J. O. JEPPESEN, J. PERKINS, J. BECHER, J. F. STODDART, *Angew. Chem. Int. Ed.* **2001**, *40*, 1216–1221; b) Y. LUO, C. P. COLLIER, J. O. JEPPESEN, K. A. NIELSEN, E. DEIONNO, G. HO, J. PERKINS, H.-R. TSENG, T. YAMAMOTO, J. F. STODDART, J. R. HEATH, *ChemPhysChem* **2002**, in press.
 - 16 a) P. R. ASHTON, R. BALLARDINI, V. BALZANI, M. GÓMEZ-LÓPEZ, S. E. LAWRENCE, M.-V. MARTÍNEZ-DÍAZ, M. MONTALI, A. PIERSANTI, L. PRODI, J. F. STODDART, D. J. WILLIAMS, *J. Am. Chem. Soc.* **1997**, *119*, 10641–10651; b) P. R. ASHTON, R. BALLARDINI, V. BALZANI, I. BAXTER, A. CREDI, M. C. T. FYFE, M. T. GANDOLFI, M. GÓMEZ-LÓPEZ, M.-V. MARTÍNEZ-DÍAZ, A. PIERSANTI, N. SPENCER, J. F. STODDART, M. VENTURI, A. J. P. WHITE, D. J. WILLIAMS, *J. Am. Chem. Soc.* **1998**, *120*, 11932–11942.
 - 17 a) R. BALLARDINI, V. BALZANI, M. T. GANDOLFI, L. PRODI, M. VENTURI, D. PHILP, H. G. RICKETTS, J. F. STODDART, *Angew. Chem. Int. Ed. Engl.* **1993**, *32*, 1301–1303; b) S. CHIA, J. CAO, J. F. STODDART, J. I. ZICK, *Angew. Chem. Int. Ed.* **2001**, *40*, 2447–2451.
 - 18 a) P. R. ASHTON, V. BALZANI, O. KOCIAN, L. PRODI, N. SPENCER, J. F. STODDART, *J. Am. Chem. Soc.* **1998**, *120*, 11190–11191; b) P. R. ASHTON, R. BALLARDINI, V. BALZANI, E. C. CONSTABLE, A. CREDI, O. KOCIAN, S. J. LANGFORD, L. PRODI, J. A. PREECE, E. R. SCHOFIELD, N. SPENCER, J. F. STODDART, S. WENGER, *Chem. Eur. J.* **1998**, *4*, 2413–2422.
 - 19 P. R. ASHTON, R. BALLARDINI, V. BALZANI, A. CREDI, R. DRESS, E. ISHOW, O. KOCIAN, J. A. PREECE, N. SPENCER, J. F. STODDART, M. VENTURI, S. WENGER, *Chem. Eur. J.* **2000**, *6*, 3558–3574.
 - 20 a) R. BALLARDINI, V. BALZANI, A. CREDI, M. T. GANDOLFI, S. J. LANGFORD, S. MENZER, L. PRODI, J. F. STODDART, M. VENTURI, D. J. WILLIAMS, *Angew. Chem. Int. Ed. Engl.* **1996**, *35*, 978–981; b) V. BALZANI, A. CREDI, S. J. LANGFORD, F. M. RAYMO, J. F. STODDART, M. VENTURI, *J. Am. Chem. Soc.* **2000**, *122*, 3542–3543.
 - 21 A. CREDI, V. BALZANI, S. J. LANGFORD, J. F. STODDART, *J. Am. Chem. Soc.* **1997**, *119*, 2679–2681.

Index

a

- ab initio* calculations 41
- absolute configuration 373
- absorption spectroscopy 443, 576
- acceptor 439
- acenaphthenone 28
- acentricity 198
- acepentalene 38, 42
- acepentalene metal complex 42
- acepentalenediide 42
- acetal 306
- acetamide 130
- acetic anhydride 12
- acetyl nitrate 472
- acetylcholine esterase 73
- acetylene 171, 172
- Acetylene Chemistry 213
- acetylenic ether 265
- acetylenic molecular scaffolding 213
- Acetylenic scaffolding 196
- σ -acetylide complex 208
- acetylsalicylic acid 11
- acid 475
- acid-catalyzed cyclization 353
- acridine 142
- acridone 358
- acrylonitrile 320
- activation of saturated hydrocarbons 477
- Acyclic Diyne Metathesis (ADIMET) 217
- acyloxacarbene 259
- adamantane 8
- addition/elimination mechanism 456
- adenosine receptor antagonists 76
- Adler oxidation 550, 560
- aggregate 243
- aggregation 235
- aggregation-induced planarization 239
- agrochemical 92, 117, 364
- air–water interface 235
- alcohol 405
- aldol 20
- aldol trimerization 20
- alizarin 12
- alkaline metal salt 452
- alkaloid 66, 290, 366, 503, 516, 545, 566
- alkaloid lignan 480
- 1-alkenylboranes 54
- 1-alkenyl halides 88
- alkenyne 54
- alkoxide 375, 406
- alkoxo complex 152
- p*-alkoxybenzyl bromide 409
- alkoxycarbene 259
- 6-alkylaminopurine nucleoside 76
- alkyl migration 256
- alkylidene 218
- alkyllithium 336, 349
- alkyl-substituted benzene 446
- alkyne 53, 252
- alkyne cyclotrimerization 250
- alkyne metathesis 218
- β -alkynylamines 90
- all-carbon core 196
- allenic structure 241
- allograft rejection 66
- allotropes of carbon 181
- allylamine 129
- 243-allyl dendrimer 421
- allylsilane 554
- aluminosilicate 515
- Alzheimer 74
- amaryllidaceae alkaloid 485
- amide 108, 129, 337, 339, 406
- amido complex 109
- amidoferrocenyl dendrimer 426
- amination 116
- amine 405, 457

- aminocarbene 259
- aminonaphthalene 531
- aminophosphine ligand 96
- aminophosphines 381
- 3-aminopyridazine 74
- aminopyridine 73
- ammonia surrogate 132, 147
- ammonium metavanadate 500
- ammonium tribromide 550
- analgesic 139
- ancistrobrevine B 61
- o*- and *p*-dichlorobenzenetricarbonylchromium 374
- androgen 321
- aniline 113, 115, 298, 457
- aniline complex 315
- aniline purple 12
- anilinetropone 148
- anionic Fries rearrangement 334
- anisole 298, 306, 324, 390
- anisoletetricarbonylchromium 372
- annelation 18, 185
- annulation 280
- annulene 6, 13, 18, 189, 278
- [12]annulene 204
- [18]annulene 204
- anodic oxidation 546
- Anson–Bard equation 424
- antagonists of the CRH receptor 74
- anthracene 6, 12, 187, 450, 468
- 9-anthracene-carboxylic acid 589
- anthracycline 280, 286, 564
- anthracyclinone 286
- anthranilate 358
- antiallergic drug 56
- anti-Alzheimer's drug 499
- antiaromatic 33
- anti-aromaticity 5, 17, 39
- antibacterial agent 73
- antibiotic 91, 285, 502, 544
- anti-epileptic drug 358
- antigen/antibody binding 435
- anti-HIV alkaloid 61
- anti-inflammatory property 67, 139, 388
- anti-malaria property 65
- anti-MRSA activity 91
- anti-neoplastic agent 76
- antioxidant 546
- antitumor agent 138, 285, 519, 546
- anxiety 74
- aquaticol 544
- arachidoic acid 67
- arene building blocks 575
- arene cation radical 478
- arene donor 461
- arene donor strength 443
- arene planarity 445
- arene–metal bond 452
- arene–metal distance 446
- (arene)chromium complex 63
- areneselenolate 378
- arenetricarbonylchromium complexes 368
- arenol 539, 546
- arenoxenium 546
- arenoxysulfonium ylide 541
- aripiprazole 137
- aromatic 5
- aromatic carbanionic chemistry 331
- aromatic carbon–nitrogen bond 108
- aromatic cation radical 458
- aromatic chromophore 475
- aromatic C–N bond formation 129
- aromatic donor 464
- aromatic ether complex 419
- aromatic ion-radical 467
- aromatic nitration 466, 472
- aromatic polyester 99
- aromatic steroid 385
- aromatic–aromatic coupling 54
- aromaticity 5, 39
- aromatization 171, 172
- aromatization energy 255
- arthritis 11, 67
- aryl amine 506
- aryl bromide 113
- aryl chloride 13, 55, 84, 93, 124
- aryl dialdehyde 60
- aryl ether 541
- aryl halides 107
- aryl piperazine 120
- N*-Arylpiperazine 136
- aryl sulfide 108
- aryl tosylate 121
- aryl triflate 56, 111, 115
- arylamine 107
- arylamine material 143
- α -arylamino acid 386
- aryl–aryl cross coupling 332, 344
- arylated tetraethynylethenes 198
- arylation 138, 380, 388
- arylation of primary alkylamine 138
- arylboron compounds 53
- arylcarbene–chromium 250
- arylcyclopropene 268
- arylferrocene 63
- o*-arylhydroxylamine 374
- aryloxy carbene 259
- arylphosphines 379

- arylpiperazine 381
- 3-arylpyrrole 89
- arylvinamidinium salt 89
- asatone 543
- ascorbic acid 578
- aspirin 11
- Astruc 1, 400
- Asymmetric Catalysis 538
- asymmetric catalyst 529
- asymmetric cross-coupling 121
- asymmetric induction 527
- asymmetric synthesis 64, 188, 524
- asymmetric tandem addition 306
- atomic force microscopy (AFM) 242
- atropisomerism 64, 79, 480, 517
- Au(111) surface 579
- average valence 4
- axial chirality 63, 70, 79
- axially chiral biaryl 63
- azacrown ether 146
- azaindole 73
- azathioxanthone 358
- azide 406, 457
- azobenzene 142
- azole 129, 132
- azulene 6
- b**
- back electron transfer 466, 589, 594
- Baeyer 4
- ball-milling procedure 98
- Balzani 576
- Barton oxidation 550
- Barton 550, 561
- base catalyst 321
- base-catalyzed isomerization 189
- bay-region diol epoxide 58
- 9-BBN 414
- Benesi–Hildebrand treatment 443
- benz[a]anthraquinone 564
- benzamide 130
- benzannulation 250, 251, 277, 566
- benzazocinone 360
- 1,2-benzazulene 175
- benzene 1, 169, 472
- benzene homologation 278
- benzenethiolate 457
- benzenoid aromaticity 199
- benzenoid spacer 211
- benzidine 584
- benzimidazole 139
- benzoazocinone 361
- benzo[c]phenanthridine alkaloid 58
- benzocyclobutene 12
- benzofuran 374, 375, 377
- benzo-fused heterocycle 378
- benzoic acid derivative 334
- benzopinacol 468
- benzopyrazole 107
- o-benzoquinone 556
- benzothiophene 137
- benzotriazole 134
- benzoxepine 270
- benzyl acetate 455
- benzyl complex 11
- benzyl radical 466
- benzyl silane 347
- benzyl thiolate 382
- benzylation activation 404
- benzylstannane 466
- Bergman cyclization 171, 186
- Berthelot 169, 171, 177, 192
- biaryl derivative 53, 273, 479
- biaryl P,N ligand 136
- biaryl quinone 273
- biaryl synthesis 534, 564
- biarylloxazole 492
- biarylpyrimidine 492
- bicumene 466
- bicyclic hydrocarbon 177
- bicyclo[2.2.2]octenone 558
- bimetallic activation 380
- binaphthalene 64
- binaphthol 108, 480
- 2,2'-binaphthol 499
- binaphthyl 485
- binaphthyl ligand 148
- binaphthylphosphine 108
- BINAP 112, 115, 116
- BINAP-ligated palladium 113
- bioactive biphenyl 502
- biocatalyst 527
- biologically active chemical 56
- bioluminescence 72
- biomimetic approach 534
- biomimetic synthesis 479, 518, 523
- bioorganic synthesis 539
- biosynthesis 479
- biosynthetic oxidative dearomatization 563
- biphenol 584
- biphenomycine 502
- biphenylene 12, 185
- bipyridinium 577, 581
- birefringence 231
- bis(alkyne) 265
- 1,3-bis(bromomethyl)benzene 581
- 1,4-bis(bromomethyl)benzene 576
- bis(indole)maleimide 493

- bisorbicillinoids 564
- bis(*paraphenylene*)-34-crown-10 575
- blood platelet 11
- blood vessel 11
- bond elongation 449
- bond length 448
- bond localization 449
- π -bond localization 445, 449
- bond order 448
- borane 8
- borazine 6
- bowl-shaped aromatic 176
- bow-type hydrocarbon 182
- bridged aromatic hydrocarbon 187
- bridging bromine 447
- bromine 550
- 9-bromoanthracene 146
- bromobenzene 470
- 3-bromochromone 89
- 4-bromomethylpyridine 410
- N*-bromosuccinimide 550
- bromothiophene 118
- bromotoluene 471
- bronchospasm 68
- Brønsted acid 435
- Brønsted base 475
- Buchwald 13, 84, 95, 112
- Buckminsterfullerene 206
- bulky phosphine 95
- Bunz 14, 217
- 1-butyl-3-methylimidazolium tetrafluoroborate 83
- butyrolactone 520
- γ -butyrolactone 377
- C**
- C₆₀ 430, 434
- C₂₀-fullerene 32, 44
- cable-like structure 242
- calicene 37
- calicheamicin 186
- calixarene 11, 18, 550
- calphostin 523
- calphostin D 523
- carbamate 129, 130, 341
- carbamoyl migration 352
- carbanion 383
- carbapenems 91
- carbazole 57, 69, 147, 284, 506, 507
- carbazole alkaloid 57
- carbene 172
- carbene complex 251
- carbene insertion 174
- carbocation 469
- carbohydrate chemistry 140, 262
- carboline 139
- α -carboline 136
- carbon nanotube 11, 18, 245
- carbon-carbon bond formation 53, 383
- carborane 8, 387
- carboxylic acid 339
- carbyne 209, 218
- carcinogenic amine 140
- carcinogenic polynuclear aromatic hydrocarbon 58
- cardiovascular disease 71
- carotenoid 198
- catalytic electron-transfer reaction 428
- catalytic enantioselective coupling 517
- catalytic enantioselective oxidative coupling 527
- catalyzed hydrosilylation 420
- catechol 374, 501
- [2]catenane 575
- C-C bond formation 479
- C-C coupling on supports 87
- cerium(IV) ammonium nitrate (CAN) 306, 510
- C-H acidity 251
- C-H activation 405
- C-H bond activation 453
- charge transfer 449, 475
- charge-transfer band 437
- charge-transfer complex 465, 476
- charge-transfer (CT) interaction 577
- charge-transfer effect 240
- charge-transfer π -bonding 471
- charge-transfer transition 437
- chelating ligand 112
- chelating phosphine 116, 159
- chelation 256
- chelilutine 59
- chemical switching 595
- chemical vapor deposition 579
- chemosensor 146
- Chinese herbal medicine 57
- chiral aluminum catalyst 100
- chiral amine 525, 533
- chiral biaryl 387
- chiral binaphthol 524, 526
- chiral diamine-copper complex 531
- chiral ferrocene 364
- chiral glucose framework 524
- chiral HPLC 526
- chiral oxidation 517, 524
- chiral plane 273
- chiral reagent 524
- chiral ruthenium tris(bipyridine) 527
- chiral vanadium complex 530
- chloranil 444, 463, 468
- 4-chloroanisole 126

- chloroarene-Cr(CO)₃ 378
- chlorobenzene 55
- chlorobenzenetricarbonylchromium 372
- chlorocarbonylferrocene 409, 412
- chlorocarbonylmetallocene 417
- chloropyridine 123, 126
- 4-chloropyridine 343
- 4-chlorotoluene 128
- chromium carbene complex 252
- chromium template 253
- chromophore 102, 142, 146, 196, 198, 200
- chrysene 58, 282
- cine* S_NAr 393
- circular structure 177
- circulatory trouble 11
- circulene 8
- circumrotation 577
- circumtriindene 27
- cis*-decalin complex 311
- cis-trans* photoisomerization 215
- Claisen reaction 540
- clausenamine A 57
- cleavage of aryl ether 406
- C–N bond 382
- cobalt template 251
- cobaltocene 403
- (–)-codeine 485
- colchicine 290
- collision complex 439
- Collman's reagent 391
- combinatorial methodology 84
- combinatorial synthesis 381
- η^2 -complex 298, 447
- σ -complex 451, 469
- conducting polymer 99
- conformational change 582
- conjugated alkadiene 53
- conjugated diene 53
- conjugated material 212
- conjugated molecular rods 196
- conjugated polymer 107, 209, 212, 219, 225, 235, 244
- contact ion pair 466
- coordinated arene 452
- coordinating solvent 256
- η^1 -coordination 447
- Cope rearrangement 558
- copper reagent 482, 507
- copper sulfate on alumina 515
- copper/amine complex 504
- copper-mediated coupling 184
- copper-mediated reaction 108
- corannulene 9, 176
- Corey 563
- coriariin A 519
- Coronene 9
- Corriu 344
- corticotropin 74
- coumarin 90
- counterion exchange 587
- CO 374
- CpFe⁺ group 401
- CpFe⁺(η^6 -aniline) 401
- CpFe⁺(η^6 -arene) salt 402
- CpFe^I(η^6 -C₆Me₆) 403
- p*-cresol 321
- cross-coupling 53, 95, 97, 108, 120, 214, 272, 365
- crotonaldehyde 320, 323
- 18-crown-6 55, 116, 374, 582
- crown ether 579, 588
- CT absorption 467
- CT band 589
- CT complex 443, 452
- CT formalism 443
- cumulene 189
- N*-cumyl carboxamide 333
- cuparane 544
- cuparenol 544
- cyclic arrangement 310
- cyclic ketone 20
- cyclic voltammetry 403, 414, 424, 578
- cyclization 304, 310
- cycloaddition 331, 347
- [2 + 2] cycloaddition 174, 253
- [3 + 2 + 1] cycloaddition 251
- cycloaddition reaction 251, 311
- cycloallene 171, 174
- cycloaromatization 186
- cyclobutadiene 7
- cyclobutadiene complex 184
- cyclocarbonylation 280
- cycloheptatrienyl anion 7
- cyclohexa-2,4-dienone 539
- cyclohexadiene 370, 387, 392
- η^4 -cyclohexadiene complex 370
- η^5 -cyclohexadienyltricarbonylchromium anionic species 369
- cyclohexadienone 254, 485, 561
- cyclohexadienyl 403, 450, 457
- cyclohexadienyl anion 297
- cyclohexadienyl cation 298
- cyclohexadienyloxo ligand 406
- cyclohexanone 26
- cyclohexatriene 1, 6
- cyclohexene 306
- cyclohexenone 299, 306
- cyclooctatetraene 7, 13
- cyclooctyne 219

cyclooxygenase 68
 cyclopentadiene 32
 cyclopentadienide 32
 cyclopentadienyl anion 6, 32
 cyclopentadienyl cation 6, 32
 η^5 -cyclopentadienyl iron 366
 cyclopentenone 320, 562
 cyclophane 8, 11, 17, 171, 275, 277, 575
 cyclophane 187,
 cyclophynes 191
 cyclopropane 251, 265
 cyclopropenyl anion 7
 cyclopropylamine 139
 cyclosporin 66
 cyclotrimerization 22
 Cypridina luciferin 72
 cytokine activity 76

d

damaged DNA 139
 damirones A and B 138
 Danishefsky 563
 daunomycinone 286, 296
 D¹BPF 120
 DDQ 468
 De Gennes 421
 de Meijere 14, 32
 dearomatization 297, 300, 370, 539
 deboronation 345
 debromination reaction 188
 decaalkylation 416
 decaallylferrocene 424
 decacyclene 27
 decacyclopropylferrocene 35
 decadehydrocorannulene 45
 decaferrocenyl dendrimer 424
 decaisopropyl cyclopentadienyl cobalt 413
 decalin 310
 decamethylferrocene 35, 426
 decarbonylation 261
 degree of charge transfer 443
 dehydroannulene 177
 dehydrobenzoannulene 183
 dehydro[14]annulene 185
 dementia 74
 demethoxylation 390
 dendrimer 11, 18, 100, 145, 279, 412, 431
 dendritic construction 412
 dendritic core 278, 411
 dendritic effect 426
 dendritic polyamine 428
 dendron 209
 density functional theory (DFT) 29, 569
 11-deoxydaunomycinone 286
 deoxyjacarubein 358
 deprotonation 403
 derivatized electrode 427
 desilylation 360
 detoxification treatment 57
 device 400, 587
 Dewar 1
 diabatic state 439
 diacetylene 176
 diamagnetic susceptibility 6
 diaryl 479
 diaryl amine 358
 diaryl nitrile 353
 diaryl phosphite 358
 diaryl selenide 378
 diaryl sulfone 358
 diarylalkyne 221
 diarylamine linkage 144
 diarylamine 115
 diarylethyne 281
 diazine 337
 diazocyclopentadiene 37
 diazonium cation 469
 dibenzazepinone 358
 dibenzocyclooctadiene 520
 dibenzo-18-crown-6 376
 dibenzofulvene 172
 dibenzofuran 281, 390
 dibenzophosphorinone 358, 359
 dibenzopyranones 353
 dibenzthiepinone 359
 1,1'-dibromoferrocene 143
 dichlorobenzene 376
 o-dichlorobenzene 405
 2,3-dichloro-5,6-dicyano-1,4-benzoquinone (DDQ) 520
 Diederich 9, 14, 196
 Diels–Alder
 Diels–Alder cycloaddition 554
 Diels–Alder cyclodimerization 544
 Diels–Alder reaction 6, 53, 99, 289, 311, 326, 331, 544
 dienophile 313, 556
 diethyl carboxamide 333
 differential pulse voltammogram 596
 diffusional complex 460
 diffusional process 469
 dihapto-coordinated arene 298
 dihydroanisole 299
 dihydroazulene 200
 dihydronaphthalene 302, 325
 1,2-dihydronaphthalene 299
 1,5-dihydroxynaphthalene (DNP) 578
 3,7-dihydroxytropolone 62

- 2,6-diisopropylphenyl imidazolium 124
 π -dimerization 458
 dimerization of 2-naphthol 528
 1,4-dimethoxybenzene 575
 dimethylacetylene dicarboxylate 326
 dimethylaniline 200
 dimethyl-*N*-carboxy anhydride 378
 diode 245
 diospyrin 62
 dioxygen 480, 482
 diphenylhydrazone 136
 diphenylmethane 389
 diphenylseleninic anhydride 550
 directionality 406
 disconnection approach 363
 di-*tert*-butyl peroxide (DTBP) 524
 ditopic compound 582
 divergent synthesis 421
 dodecaallylation 406
 dodecahedrane 45
 donicity 446
 donor/acceptor interaction 449, 451, 461, 575
 donor/acceptor separation 446
 Dötz 14, 250
 Dötz reaction 13, 250, 252
 double functionalization 369, 387
 DPPF 112, 116, 129, 152
 DPPP 117
 drug development 108
 drug-resistant bacteria 61
 dumbbell 588
 durene 411, 412, 446, 458
 dye 12
 dyestuff 146
- e**
 early transition metal chemistry 148, 452
 effective conjugation length 212
 electrical conductivity 209
 electrocatalytic synthesis 526
 electrochemical manipulation 576
 electrochemical method 480
 electrochemical oxidation 118
 electrochemical sensing 141
 electrochemical study 201, 204, 206
 electrochemical switching 586
 electrochemical time scale 427
 electrochemical transformation 546
 electrochemical wave 145
 electrocyclic reactions 6
 electrocyclization 172, 254
 electrode modifier 146
 electroluminescence 245
 electron acceptor 435, 475
 electron affinity 438
 14-electron amido complex 154
 electron beam deposition 579
 19-electron complex 403, 408, 428
 electron density 445
 electron donor 437, 475
 electron reservoir 403, 430
 electron transfer 18, 289, 405, 428, 431, 436, 480
 458, 465, 476, 592
 electron-deficient alkyne 255
 electron-deficient carbene 251
 electronic application 107
 electronic coupling 437, 461, 469, 473
 electronic device 70
 electronic property 210
 electronic switch 435
 electronic transition 439
 electron-rich arene 478
 electron-rich molecule 403
 electrooxidative methoxylation 547
 electrophilic addition 302
 electrophilic aromatic bromination 470
 electrophilic aromatic substitution 330, 363, 455,
 469, 477
 electrophilic halogenation 541
 electrophilic reagent 541
 electrophilic substitution 6, 315
 electrophilic/nucleophilic umpolung 449
 electroreduction 410
 electrostatic interaction 443
 ellagitannin 518, 523
 emeraldine 141
 enamine 110, 318
 enantiofacial discrimination 324
 enantioselective catalysis 273
 encounter complex 462
 encumbered arene 444
 endohedral incorporation 50
 enediyne 563
 energy migration 241
 enhanced nucleophilic substitution 368
 enolate 457
 entropy change 443
 enyne 285
 enzyme 435, 480
 enzyme catalyst 479
 enzyme cyclooxygenase 67
 ephedrine 380
 (\pm)-epimaritine 516
 6a-epipretazettine 485
 epoxidation 566
 epoxycyclohexenone 544
 EPR 428
 erectile dysfunction 71

estradiol 320
 estrone 13
 ET dynamics 461
 ET mechanism 455
 ET paradigm 467
 ether sulfonamide 360
 ethynylbenzene 177
 2-ethynyltolane 180
 eugenol 547
 excimer 235
 exciplex 463
 exifone 546
 exponential growth 143

f
¹⁹F NMR spectroscopy 381
 Faraday 1
 fast electron transfer 427
 Fe^I complex 403
 Fe^I dendrimer 428
 Fe^I sandwich 428
 Feldman 15, 479
 ferrocene 6, 8, 17, 223, 401
 ferrocene derivative 185
 ferrocenium 6, 426
 ferrocenyl dendrimer 424
 ferrocenylsilylation 421
 Fischer-type carbene complex 257
 five-membered carbocycle 32
 flash vacuum pyrolysis 174
 flexible coils 229
 flow reactor 99
 fluorenone 147
 fluorescence 201, 210, 225, 240, 591, 596
 fluorescent emission 589
 fluorination 92
 fluorine 450
 fluoroalkene 92
 4-fluoroanisole 381
 fluoroarene 374
 fluoroarene-Cr(CO)₃ 374, 377
 fluorobenzene complex 380
 food mutagen 140
 Franck–Condon 440
 fredericamycin A 286, 288
 free-energy change 443, 464
 free-energy correlation 462
 Friedel–Crafts reaction 352
 Fries rearrangement 352
 Fu 13, 84
 fullerene 6, 11, 18, 32, 100, 176, 185, 192
 fulvene 32, 37
 fulvenyl tetrafluoroborate 37
 furan 118, 323, 337, 556

3-furylcarbene complex 284
 fuschine 12
 Fused Heterocycle 283
 fused polycyclic aromatic 60

g

galactose 83
 galanthamine 498
 (±)-galanthamine 491
 gallic acid 504
 gallium 446
 galloyl phenol 519
 gastrointestinal ulceration 67
 gel phase 242, 243
 geodesic dome 27
 glucosamine 83
 glucose 83, 518
 glycoside 290
 glycosylamine 138
 gnididione sesquiterpenoid 338
 gomisin-A 520
 (+)-gomisin A 522
 gramine 341
 graphite 192
 graphyne 180
 Grignard cross-coupling 348
 Grignard reagent 64, 457
 Grubbs 218, 222
 Grubbs ring-closing metathesis 361
 guanosine 140

h

H. Taube 16
 H/D exchange 453
 H-1-antihistaminic norastemizole 138
 haloalkene 53
 haloalkyne 53, 265
 halogen 469, 480
 halogenation 470
 halogen-exchange reaction 92
 halogenoarene 405
 halonitrobenzenes 330
 halopyridine 79, 343
 Hammett plot 455
 hapticity 447
 haptotropic metal migration 272
 hard carbanion 405
 Harman 15, 297
 Hartwig 13, 14, 107
 Heck reaction 87, 180
 helicity 277, 282
 hemilabile ligand 136
 hepatitis B virus 57
 heptamethylbenzenium 451

- Herrmann 218
 heteroaromatic 189
 heteroaromatic amine 111
 heteroaromatic directed *ortho* metalation 337
 heteroaromatic halide 108
 heteroaryl benzoic acid 65
 heteroaryl halide 53
 heteroarylboron compound 53
 heteroatom–carbon bond formation 566
 heterobiaryls 344
 heterocycle 116, 262, 346, 353, 358, 405
 heterocyclic carbene 124
 heterocyclic chemistry 364
 heterocyclization 566
 heterogeneous catalyst 129
 heteromolecular complex 460
 heteropolyacid 512
 heteropolycyclic skeleta 543
 heterosteroid 289
 hexaalkylation 408
 hexaalkynylbenzene 10
 hexabenzaldehyde star 410
 hexa(butadiynyl)benzene 180
 hexacarbonylmolybdenum 280
 hexadienyne 174
 hexaethylbenzene 403, 462
 hexaethynylbenzene 177
 hexaferrocene star 408
 hexafluorobenzene 448
 hexafunctionalization 406
 hexahexylbenzene 408
 hexaiodo derivative 409
 hexametallic redox catalyst 410
 hexamethylbenzene 403, 406, 442, 458, 462, 471
 hexasilane 409
 high-spin states 141
 hindered biaryl bond 61
 Hippocrates 11
 history 1
 HIV protease inhibition 61, 71
 Hoffmann 10
 hole-transport properties 141, 146
 homoaromaticity 7, 17
 homogeneous catalysis 13, 82, 433
 hop 544
 Hopf 14
 hopping mechanism 427
 Horseradish peroxidase (HRP) 513, 527
 host–guest chemistry 575
 Hückel 7, 16, 32
 Hückel aromaticity 205
 Hückel theory 33, 39
 humulone 544
 hydrazine 129
 hydrazones 353
 hydride reduction 306
 hydroboration 53, 410
 hydroelementation 409
 hydrogen bromide 470
 β -hydrogen elimination 155
 hydrogen migration 174
 hydrogenation 299
 hydrogen-shift 176
 hydrophenanthrenone 304
 hydrophilic phase 82
 hydroquinone 265, 275, 576
 hydrosilylation 409
p-hydroxybenzaldehyde 410
 hydroxybiphenyl 374
 2-hydroxychrysene 58
 hydroxyitraconazole 137
 hydroxylamine ether 353
 hydroxylated arene 539
 2-hydroxymethylphenol 551
 hydrozirconation 409
 hypervalent iodine(III) reagent 480, 551
 hypervalent iodonium 97
 hysteresis 579
- i**
- I-B antiarrhythmic agent 375
 imidazole 108, 378
 imidazolium ligand 218
 imidazopyrazinone 72
 imine 129, 132
 α -imino ester 387
 immobilization 263
 immobilization of ketone 87
 immunoglobulin E antibody 56
 immunomodulator 76
 immunosuppressive activity 65
 1-indanone 22
 indazole 71
 indene 256
 indenyllithium 388
 indole 107, 133, 284, 341, 365, 382, 556, 566
 indolenine 340
 indolocarbazole 290
 indolo[2, 3-*a*]carbazole 493
 infectious disease 91
 inhibitors of inositol monophosphatase 62
 inner-sphere (IS) electron transfer 462
 insertion 254
 interchain interaction 240
 intermolecular interaction 435
 interstrand cross-link 140

intramolecular amination 112
 intramolecular charge transfer 457
 intramolecular ET 463
 intramolecular *ipso* S_NAr 379
 intramolecular relaxation 428
 iodobenzene 62
 iododesilylation 272, 358
 iodoferrocene 63
 iodonium tetrafluoroborate 60
 iodotyrosine 514
 ion radical 461
 ionic liquid 83
 ionization potential 403, 436
 ionophore 562
 ion-radical interaction 460
 ion-radical pair 440, 465, 474
ipso addition of MeO^- 372
ipso nucleophilic aromatic substitution 369, 372
ipso S_NAr 380
ipso S_NAr mechanism 382
ipso substitution 383
 IR spectroscopic study 442
 iron complex 406
 iron(III) chloride 497, 515
 iron(III) source 496
 isobenzene 171, 172
 isochromane 61
 isoflavone 89
 isolobal analogy 10
 isoquinoline 343
 isoquinoline alkaloid 58
 isostegane 520
 isotropic melt 235, 239
 isotropic phase 234
 isotwistane 554, 559
 isoxazole 492
 iterative procedure 417

j

J. Loschmidt 16
 Jahn–Teller-active species 403
 Jones' reagent 457
 Jutzi 424

k

Karsted catalyst 420
 Kekulé 1, 9, 330
 kekulene 9
 ketal 262, 542
 ketalization 564
 ketone arylation 121
 Kochi 15, 435

korupensamines A–D 61
 kreysigine 498

l

L-alanine 386
 lactam 129, 130
 lactonamycin 567
 lactone 377
 Ladenburg 1, 4
 lamellar phase 242
 Langmuir–Blodgett (LB) monolayer 579
 Langmuir–Blodgett technique 235
 lanthanide complex 452
 large ferrocenyl dendrimer 421
 large phosphine 158
 laser flash photolysis 462, 465
 late transition metal amide 156
 lavendamycin 110
 layered hydrocarbon 191
 lead reagent 480
 lead tetraacetate 502, 518, 548
 leucotamine 491
 Lewis acid-catalyzed reaction 148
 Lewis acid 260, 318, 435, 451, 456
 Lewis base 448, 455
 library synthesis 108
 ligand-exchange reaction 402
 light-driven molecular switch 196
 light-emitting diode 211, 225, 228, 244
 lignan 545
 lignin 551
 linear conjugation 213
 linker 86, 381
 (\pm)- α -lipoic acid 87
 5-lipoxygenase 68
 liquid crystalline material 99, 188
 liquid-crystalline texture 231
 lithiation 369
 lithium acetylide 563
 lithium phenylacetylide 375
 localized mixed-valence complex 408
 logic function 594
 logic gate 596
 Loschmidt 1
 Loschmidt replacement 9
 low-temperature X-ray 448
 lycoramine 491
 lycorine 566

m

macrocycle 205, 208, 224, 575, 584
 macrocyclization 204, 277
 macrolide 562

- macromolecule 141
 - magistophorenes A and B 502, 524
 - magnetic material 146
 - magnetic ring current 6
 - magnetic susceptibility 5, 41
 - Magnus 563
 - makaluvamine C 138
 - malaria 12
 - MALDI-TOF mass spectrum 421
 - maleic anhydride 466
 - maleimide 494
 - manganese complex 372
 - Marcus formulation 462
 - Marcus theory 462
 - Marcus–Hush theory 436, 469
 - marine antitumor antibiotics 186
 - marine source 70
 - (+)-maritidine 490
 - materials chemistry 218
 - materials science 141, 184, 345
 - McKillop oxidation 549
 - measurements of aromaticity 17
 - mechanical motion 592
 - mechanical property 244
 - mechanism 149
 - Meijer 417
 - membrane reactor 99
 - memory 580
 - mercuriation 470
 - Merrifield resin 129, 346
 - mesitylboronic acid 76
 - mesitylene 413, 444, 462
 - [2.2]metacyclophane 277
 - metal amido complex 107
 - metal oxide support 129
 - metal-based nucleophile 391
 - metal-catalyzed activation of hydrogen 453
 - metal-centered star 407
 - metal-containing nanostructure 184
 - metal-halogen exchange 343
 - metallabenzene 18
 - metallacyclobutadiene 218
 - metallodendrimer 400, 417
 - metalloporphyrin 18
 - metalloproteinase-13 inhibitor 91
 - metathesis 217
 - methoxide 457
 - methoxide anion 382
 - 2-methoxybenzoate 540
 - 3-methoxycyclohexene 299
 - 6-methoxytetrahydroquinoline 374
 - methyl acrylate 320
 - methyl benzoate 512
 - methyl gallate 503
 - N*-methylmaleimide 320, 326
 - N*-methylpyrrole 306
 - methyl quinoline 509
 - methyl radical 468
 - m*-fluorotoluenetricarbonylchromium 374
 - Michael acceptor 305, 316, 317, 563
 - Michael reaction 311, 564, 417
 - Michael–aldol ring-closure 314
 - michellamine 61
 - microorganism 59
 - microwave irradiation 87, 497
 - mild hydride donor 303
 - Mills–Nixon effect 9
 - Mitsunobu reaction 270
 - mixed valence 4, 426, 461
 - mixed-valence Fe^{II}/Fe^{III} complex 426
 - modified electrode 427
 - Moffat–Olofson reaction 541
 - molecular abacus 588
 - molecular anisotropy 231
 - molecular battery 426, 430
 - molecular electronics 177
 - molecular machine 592
 - molecular nitrogen 380
 - molecular orbital theory 5
 - molecular photochemical switch 196
 - molecular rotor 80
 - molecular scaffolding 196
 - molecular shuttle 583, 584
 - molecular signature 580
 - molecular solid 102
 - molecular switch 199, 574, 581, 582
 - molecular torsion 241
 - molecular wire 225
 - monoelectronic reduction 434
 - monophosphine complex 158
 - monosubstituted benzene 364
 - montmorillonite 515
 - morpholine 128, 378
 - Mössbauer spectroscopy 426, 428, 431
 - motor-molecule 574
 - Mulliken 436, 475
 - Mulliken theory 472
 - multilayer diode 244
 - murrayastifoline F 503
 - murrayafoline A 503
- n**
- N,O ligand 148
 - nalidixic acid 73
 - nanocable 242
 - nanomolecular device 435
 - nanoparticle 245
 - nanoribbon 243

- nanoscience 574
 nanoscopic assembly 400
 nanotechnology 574
 nanowire 242
 naphthalene 174, 298, 302, 324, 450
 naphthalene chromium tricarbonyl 272
 naphthohydroquinone 251
 2-naphthol 495, 505, 514
 naphthoquinone 260, 285, 547
 naphthylamine 505
 2-naphthylamine 495
 narwedine 491
 natural antibiotic 567
 natural product synthesis 273, 353, 490, 540, 558
 naturally occurring phenol 543
 NaY zeolite 129
 near-IR 213
 Negishi 344
 Negishi cross-coupling 335
 nematic phase 231, 235
 neolignan 543
 Newkome 412
 N–H activation 107
 nickel catalyst 250
 Nicolaou 61, 563
 niobium(0) 446
 nitrate 410
 nitrating agent 472
 nitration 470
 nitric acid 472
 nitric oxide 442, 465
 nitrile 387
 144-nitrile dendrimer 417
 nitrite 410
 nitro chemistry 363
 nitrogen fixation 135
 nitrogen heterocycle 136
 nitrogen nucleophile 382
 nitronium ion 472
 N-nitropyridinium 472
 nitrosation 470
 nitrosoarene 475
 nitrosonium ion 449
 nitrosonium/arene complex 465
 NMR chemical shift 5
 NO⁺ acceptor 464
 nonaallylation 414, 418
 non-benzenoid aromatic 178
 noncovalent interaction 575
 nonlinear optical material 99, 146
 nonlinear optical property 198
 noraporphine 564
 norbelladine 487
 norbornene 142
 norbornenyl cation 8
 norcaradiene 176
 norgalanthamine 491
 norsesquiterpenoid 558
 nuclear configuration 461
 nuclear rearrangement 465
 nucleobase 140
 nucleophilic addition 540
 nucleophilic aromatic substitution 363, 368, 369
 nucleophilic reaction 369, 402
 nucleophilic substitution 405, 456
 nucleophilic/electrophilic umpolung 452, 455
 nucleoside 139
- o**
- octafunctionalization 411
 octamethylbiphenylene 459
 octamethyl(diphenyl)methane 466
 oligophenylene 251
 oligoquinane 32, 38
 one-electron oxidation 515, 548
 one-electron oxidation mechanism 482
 optical CT transition 440
 optical micrograph 231
 optical microscopy 234, 235
 optical property 235, 240
 optoelectronic application 102
 optoelectronic device 196
 optonics 196
 organic acceptor 449
 organic blue emitter 244
 organic electrophile 53
 organic semiconductor 225
 organoborane 54, 97
 organoborate 468
 organoboron compound 53
 organofluorine chemistry 92
 organolead 97
 organomagnesium 349
 organometallic acceptor 448
 organometallic dendron 419
 organometallic dianion 391
 organosilicon chemistry 433
 organozinc 62, 349
 ortho metalation 342
 ortho-coordination 448
 ortho-hydroxylation 550
 ortho-metalation 59
 ortho-quinol 539, 558
 ortho-quinone 539
 ortho-quinone methide 540
 ortho-quinone monoketal 556, 558
 [Os]-anisole chemistry 310
 [Os]-bound naphthalene 326

[Os]-phenol complex 318
 osmium tetraoxide 468
 outer-sphere (OS) electron transfer 461
 oxasteroid 289
 oxasterpurane 560
 oxa-sterpurane 559
 oxa-triquinane 559, 560
 oxazoline 337
 oxcarbazepine 358
 oxetane ring 143
 oxidant 475
 oxidation potential 35, 436, 482
 oxidative acetoxylation 559
 oxidative acetylenic coupling 197
 oxidative activation 539
 oxidative addition 54, 95, 97, 150, 160
 oxidative aryl-coupling 479
 oxidative C–C cleavage 468
 oxidative coupling 58, 479
 oxidative dimerization of 2-naphthol 495
 oxidative hydroxylation 544
 oxidative nucleophilic substitution 542, 547
 oxime 374
 oxindole 358
 (\pm)-oxomaritidine 516
 oxonium 306
 oxonium ion 482
 o-xylene 412

P

P,N ligand 122, 148
 P,O ligand 123, 136
 pagodane 8, 46
 palladium acetate 116
 palladium alkoxide 109
 palladium amide 109
 palladium amido complex 152
 palladium catalysis 13, 53, 178
 palladium complex 18, 108
 palladium particle 129
 palladium-catalyzed amination 96, 107
 palladium-mediated oxidative coupling 511
 palladium(II)-peroxo complex 512
 (\pm)-pallescensin 558
 pantherinine 70
 Pasteur 5
 Pauling 5, 448
 Pauson–Khand reaction 13
 Pd-catalyzed allylic alkylation 383
 Pd-catalyzed cross-coupling 196
 PE spectra 49
 pedunculagin 519
 Pelter oxidation 543, 550, 564, 566
 pentaammineosmium(II) 298
 pentaaryl cyclopentadienyl cation 33
 pentachlorocyclopentadienyl cation 33
 pentacyclic trichodimerol 563
 pentacyclopropylcyclopentadiene 35
 pentacyclopropylcyclopentadienyl cation 34
 pentaerythritol 279
 pentafulvalene 37
 pentaisopropylcyclopentadienyl cation 33
 pentalene metal complex 39
 pentalenediide 40
 pentamethylbenzene 442
 1,2,3,4,5-pentamethylcobaltocenium 416
 pentamethylcyclopentadienyl 34, 412
 1,2,3,4,5-pentamethylrhodocenium 416
 peptide 514
 peptidomimetics 139
 perchlorination 48
 pericyclopropylated hydrocarbon 37
 perfluoroaryl 448
 pericyclic reaction 541
 periodic acid 551
 Perkin 12
 perylene dye 147
 PHANEPOS 114
 pharmaceutical industry 65
 pharmacophore 290
 phase-supported oxidant 515
 phase-transfer catalysis 135, 376, 257, 377, 388
 phenanthrene 6, 60, 175, 279, 564
 phenanthrenedione 502
 phenanthridines 346
 phenanthrol 513
 9-phenanthrol 353
 phenanthroline 580
 phene 5
 phenol 298, 318, 324, 479
 η^2 -phenol complex 323
 phenol dendron 419
 phenol derivative 255
 phenol ether 485
 phenol precursor 543
 phenolate anion 550
 phenolic compound 58
 phenolic coupling 545
 phenolic radical 480
 phenolic triphenylene 498
 phenoxenium ion 547
 phenoxide 390
 phenoxonium ion 482, 504
 phenoxy radical 545, 546
 phenoxyl radical 480
 phenylalanine 59, 530
 phenylamine 381
 phenylboronic acid 54

- phenylene 17
- p*-phenylene 576
- [*n*]phenylene 185
- 1,3-phenylene diamine 142
- p*-phenylene diamine 144
- phenylene spacer 582
- p*-phenylene unit 100
- phenyliodine(III) bis(trifluoroacetate) (PIFA) 480
- phenyliodine(III) diacetate (PIDA) 480
- phenyliodonium(III) bis(trifluoroacetate) (PIFA) 551
- phosphabenzene 265
- phosphaphenanthrene 265
- phosphine 108
- phosphine oxide 128
- phosphino ether ligand 121, 143
- phosphorus heterocycle 17
- photoactivated quinone 462
- photoactive metal complex 591
- photocatalytic system 529
- photochemical irradiation 382
- photochemical process 465
- photochemical ring-opening 568
- photocyclization 60, 280
- photoelectron spectra 438
- photoexcitation 441, 460
- photoisomerization 561
- photolytic arene exchange 401
- photosensitizer 589
- photovoltaic cell 225
- phthalocyanin 10
- piperazine 116, 119, 140, 381
- piperazines 137
- piperidine 128, 140, 382
- Plant Polyphenols 570
- plastic laser 225
- pleiadannulene 9
- poisonous snakebite 57
- polarized structure 447
- polyacetylene 209
- poly(acrylic acid) (PAA) 526
- polyallyl dendrimer 421
- polyamine 146
- polyaniline 107, 141, 144
- polyaromatic hydrocarbon 17
- polyaromatic system 99
- polyaryl 345
- poly(aryleneethynylene) 231
- polybranching reaction 413
- polybromobenzene 119
- polycationic dendrimer 417
- polycondensation 226
- polycyclic arene 282
- polycyclic aromatic alkaloid 70
- polycyclic aromatic hydrocarbon 20
- polycyclic benzenoid arene 253
- polycyclic benzenoid 60
- polycyclic hydrocarbon 177
- polycyclic system 310
- poly(dialkyl*paraphenyleneethynylene*) 217
- polyene 53
- polyether 576, 581
- polyferrocenium dendrimer 426
- polyfunctionalized aromatic 250
- polyhedral borane 17
- polyimide 99
- poly(iminoarene)s 143
- poly(*m*-aniline) 142
- polymer catalyst 99
- polymer chemistry 53, 99, 188
- polymer science 219
- polymer-bound isocyanide 382
- polymeric arylamine 141
- polymerization 148, 210, 216
- polymer-supported hypervalent iodine reagent 515
- polymer 92, 212, 427
- poly(*paraphenyleneethynylene*)s 219
- polyphenolic tannin 545
- poly(phenylene) 178
- polypyridine 410
- polyquinane 554
- polyradical 141
- polysilicon wire 579
- polystyrene-based resin 84
- polysubstituted aromatics 332
- polysubstituted benzene 364
- polythiophene 238
- porphycen 10, 18
- porphyrin 10, 18, 66
- potassium ferricyanide 480
- PPV 244
- primary amine 128
- prochiral aromatic molecule 324
- prodigiosin alkaloid 65
- prodigiosine 67
- propargyl ether 265
- propynylated aromatic 221
- prostaglandin 11, 67
- protected hydrazines 132
- protein kinase inhibitor 352
- protoilludane 559
- proton reservoir 403
- pseudoephedrine 380
- pseudorotaxane 582
- [2]pseudorotaxane 595
- PtBu₃ 95
- P(*t*Bu)₃ 124

- purine 76
 - pyrazolyl ring 324
 - pyridine 116, 211, 342, 337, 468
 - pyridyl halide 126
 - pyridyl triflate 118
 - pyridylphenol 70
 - pyrimidine 492
 - pyrogallol 546
 - pyrone 61
 - pyrrole 66, 89, 133, 337, 339, 556
 - pyrroleboronic acid 66
 - pyrrolidine 378, 381, 382, 531
 - pyrrolidinone 91
 - pyrrolylcarbene 283
- q**
- quadrant analysis 324
 - quadratic coupling 241
 - quantum mechanical methods 50
 - Quideau 15
 - quinine 12
 - p*-quinodimethane 188
 - quinoline 337, 343
 - quinone 273
 - quinone acceptor 462
 - o*-quinone methide complex 318, 323
 - quinonoid 542
- r**
- radialene 205, 208, 216
 - radical addition 533
 - radical process 431
 - radical scavenger 59
 - radical-scavenging activity 546
 - raloxifene 137
 - Raman scattering 212
 - recognition mode 581
 - recognition site 575, 587
 - recycling of the catalyst 82
 - redox potential 472
 - redox process 582
 - redox properties 99
 - redox sensors 426
 - redox-active dendrimer 417
 - redox-stable metallocene dendrimer 430
 - reductant 426, 428
 - reductive cyclization 60
 - reductive elimination 54, 97, 109, 152
 - remote metalation 332
 - Reppe 170
 - resin-bound palladium catalyst 83
 - resin-bound thiourea 83
 - resonance energy 6
 - resorcarene 11
 - retro-Diels–Alder reaction 39, 573
 - retro-Mannich 341
 - rhodium-catalyzed hydroformylation 90
 - rhombic distortion 403, 428
 - rigid rod 229
 - rigid-rod polymer 99
 - ring current 17
 - ring folding 452
 - ring-closing metathesis 66
 - ring-closure 311
 - Robin–Day classification 461
 - Robustaflavone 57
 - rod-like hydrocarbon 177
 - Rose 15, 368
 - rotamer 241
 - [*n*]rotane 208
 - [2]rotaxane 583
 - ruthenium complex 449, 452
 - ruthenium tetrakis(trifluoroacetate) 520
 - ruthenium-based photocatalyst 527
- s**
- sacrificial reductant 589
 - salicylaldehyde 12
 - salt effect 462
 - sandwich complex 44, 428
 - sanguinine 491
 - scanning tunneling spectroscopy 579
 - Schiff-base anion 386
 - schizandrin 520, 523
 - (+)-schizandrin 522
 - Schrock 218, 248
 - Schrödinger 5
 - scorpionate ligand 324
 - Scott 14, 20
 - scyphostatin 544, 551, 566
 - secondary amine 115
 - selenium 550
 - self-assembled monolayer 235
 - self-assembly 576
 - self-association 458
 - self-exchange rate 464
 - Semmelhack 13
 - sensor 146, 225, 435
 - septicidin 138
 - septicine 502
 - sesquiterpene 38, 544
 - seven-membered ring 562
 - shuttling process 584
 - Siegel 9
 - sigmatropic rearrangement 540
 - signal processing 198
 - silaketal 484
 - silicon 367

- silver trifluoromethanesulfonate 306
 silyl ether 488
 silylacetylene 268
 single electron transfer (SET) 483
 single-electron oxidation 427
 single-electron reductant 420
 single-electron reduction 403
 single-point energy calculation 29
 Slater 5
 smectic liquid-crystalline state 235
 smectic phase 231
 Smiles reaction 379
 S_NAr 372
 Sniekus 15, 330
 $S_{NR}1$ Mechanism 363
 sodium channel blocker 375
 sodium periodate 551
 sol-gel methodology 263
 sol-gel silica 589
 solid support 346
 solid-phase amination 119
 solid-phase chemistry 382
 solid-phase synthesis 84, 381, 492
 solid-state ordering 244
 solid-state reaction 98, 497
 solid-supported aryl halide 119
 solvation 444
 solvatochromicity 247
 solvent cage 468
 solvent effect 527
 solvent polarity 462
 solvent reorganization 440
 solvent-caged radical pair 465
 Sondheimer 189
 Sonogashira 196
 Sonogashira coupling 360
 sorbicillin 563
 sorbicillinol 544
 sparteine 525
 Speir's reagent 409
 spherical aromaticity 17
 sphingomyelinase 544
 spicamycin 138
 spin-coating 244
 spiroannulated cyclopentadiene 37
 spiroconjugation 38
 spirocyclization 551
 spirodienone 520
 spiroepoxide 551
 stabilized carbanion 383, 406
 π - π stacking interaction 582, 589
 stannylacetylene 268
 stealthins A and B 59
 stegane precursor 510
 steganol 519
 steganone 519
 stereogenic spirocenter 286
 sterically hindered alkyl monophosphines 160
 steroid 13, 251, 288, 321
 Stille 344
 Stille reaction 87
 Stoddart 15
 strained arene 252
 strong reductant 403
 styrene 170
N-substituted aniline complex 318
 substituted arene 251
 substituted naphthalene 347
 successor complex 469
 succinimide 311
 sugar 259, 286
 sulfonamide 337, 364
 sulfone 485
 sulfonylurea herbicide 338
 sulfoxide 484
 sulfoximine 129, 132
 sulfur trioxide 469
 superoxide 404
 supramolecular chemistry 431
 supramolecular machine 589
 Suzuki 14, 344
 Suzuki reaction 53
 Swenton oxidation 547
- t**
 tandem addition 303
 tandem electrophilic/nucleophilic addition 325
 tannin 480, 518
 Taube 3, 15
 T-cell proliferation 67
 TCNE 444, 459
 TCNQ 459
tele-meta S_NAr 394
 tellimagrandin II 518
 template-directed synthesis 576, 583
 terminal alkyne 260
 terpene 259
 terpenoid 566
 terpenin 56
 tetraazacyclophane 146
 tetracyclone 189
 tetraethynylethene 196
 tetrahydropyrroloquinoline 137
 tetralin 174, 310, 314, 390
 α -tetralone 28, 30
 tetramethylnaphthalene 459
 2,2,6,6-tetramethyl-1-piperidinyloxy- (TEMPO-) 509

- tetranitromethane 472
 tetraphenylmethane 102
 tetrathiafulvalene (TTF) 576
 thallation 470
 thallium reagent 480
 thallium triacetate 549
 thallium trinitrate 549
 theory of resonance 5
 thermal phase behavior 99
 thermocyclization 174
 thiaazepine 360
 Thiele 4, 32, 37
 thin film 242
 thin-film formation 239
 thin-film transistor 225
 thiocarbamate 347
 thiocarbene 259
 thiol 405
 thiolate 377, 406
 thiophene 4, 60, 118, 184, 199, 222, 337, 556
 thiophenol 349
 thioxanthone 358, 366
 third-order nonlinear optical properties 212
 threaded complex 580
 time-resolved fluorescence 240
 tocopherol 545
 tolane 281
 toluene 301, 413
 toluene cation radical 455
 topological change 581
 torsional coupling 241
 Tp ligand 323
 TPPTS ligand 82
 transfer hydrogenation 148
 transfer of chiral information 518
 $\pi \rightarrow \sigma$ transition 451
 transition metal catalyst 53
 translational isomers 586
 translocation 357
 transmetalation 54, 64, 97
 trialkoxyarene 491
 triarylamine 107, 145
 triarylamine polymer 143
 triazene 178
 triazine 117
 tributyltin cation 466
 tricarbonylchromium tripod 374
 trifluoroacetamide 380
 trifluoroacetic acid 60
 trifluoromethanesulfonic acid 60, 301
 trifluoromethylated compounds 92
 α -(trifluoromethyl)-styrene 92
 trifluoromethyl-substituted building block 92
 trifoliaphane 192
 1,2,3-trimethoxybenzene 384
 trimethylsilyl alkyne 272
 trimethylsilylarene 144
 trimethylsilylation 410
 trimethylsilylethyne 185
 2-trimethylsilyloxyfuran 306
 1,3,5-trinitrobenzene 444
 triphenylene 501
 triple-branching reaction 419
 triplet oxidation 560
 tripodal amine 412
 triquinane 38, 559
 tris(pyrrolyl)phosphine 381
 tris(*tert*-butyl)benzene 403
 tris-annulated benzene 20, 22, 23
 tropolone 554
 tropylium 13
 truxone 21
 tryptamine 341
 tryptophol 341
 tuberculostatic property 544
 tungsten carbyne 219
 tunneling current 579
 two-electron oxidation 539
 two-phase catalysis 82
 tylophorine 502
 tyrosine 502
- U**
- Ullmann coupling 108
 unactivated aryl halide 120, 136
 uranocene 44
 UV/vis spectroscopy 237, 441
- V**
- valence-bond formalism 437
 van der Waals contact 446
 vanadium complex 480
 vancomycin 61, 523
 veratrole 384, 387
 veratroletricarbonylchromium 395
 vertinoid polyketide 544
 vibronic fine structure 238
 vinyl carbene 253
 vinyl ketene 256
 vinylacetylene 170
 vinylborane 54
 vinylcarbene chromium 250
 vinylheptafulvene 200
 vinylidene carbene 170, 176
 vinylogous nucleophilic substitution 563
 viridin 559
 vitamin E 59, 265, 285, 545
 vitamin K 265, 285

Vögtle 417
Vollhardt 9, 13, 185, 250
von Ragué Schleyer 7

w

wave mechanics 5
weak π -complex 451
weak nucleophile 458
Wessely oxidation 548, 563, 567
Wessely reaction 504
Wheland intermediate 469, 475
Williamson coupling 410

x

xanthone 358, 366
Xantphos 159
xestoquinone 559
xylenes 302
p-xylylene 188

y

ynamine 265

z

zeolite 515